

**FOURTH INTERNATIONAL
KIMBERLITE
CONFERENCE**

PERTH 1986

**EXTENDED
ABSTRACTS**

**Geological Society of Australia
ABSTRACTS**

Number 16





Digitized by the Internet Archive
in 2018 with funding from
University of Alberta Libraries

G. Pearson

**FOURTH INTERNATIONAL
KIMBERLITE CONFERENCE
EXTENDED ABSTRACTS**

**GEOLOGICAL SOCIETY OF AUSTRALIA
ABSTRACTS SERIES
NUMBER 16**

**Perth, Western Australia,
August 11th - 15th, 1986.**

Geological Society of Australia Incorporated
Office Bearers 1986 - 1987

President	D. M. Boyd
Vice-Presidents	J. B. Waterhouse, I. R. Johnson
Hon. Secretary	A. P. Belperio
Hon. Treasurer	J. W. Hunt
Hon. Administrative Officer	D. H. Probert
Hon. Editor (Journal)	R. W. LeMaitre
Hon. Editor (Special Publications)	G. Fleming

All Extended Abstracts in this volume have been reproduced by the camera-ready method from authors' contributions. Papers presented at the Conference have been selected from brief preliminary abstracts by the Programme and Publications Subcommittee, with the assistance of the Editorial Panel. There has been no editing of the Extended Abstracts by the Programme and Publications Subcommittee, and they have not been subject to review. Accordingly, the Programme and Publications Subcommittee and its associated Editorial Panel take no responsibility for any errors and omissions, or for the opinions stated by the Authors.

Compiled by C. B. Smith

Published by the
Organising Committee of the Fourth International Kimberlite Conference
under the sponsorship of the
Geological Society of Australia Incorporated,
Challis House, 10 Martin Place, Sydney

Additional copies and other volumes associated with the conference
may be purchased from the Geological Society of Australia

FOURTH INTERNATIONAL KIMBERLITE CONFERENCE

INTERNATIONAL ADVISORY COMMITTEE

Dr. F. R. Boyd (USA)
◊ Prof. J. B. Dawson (UK)
Dr. J. Ferguson (Australia)
◊ Dr. J. J. Gurney (South Africa)
◊ Mr. J. B. Hawthorne (South Africa)
Dr. J. Kornprobst (France)
◊ Prof. H. O. A. Meyer (USA)
◊ Dr. R. H. Mitchell (Canada)
◊ Dr. P. H. Nixon (UK)
Prof. N. V. Sobolev (USSR)

CONFERENCE ORGANISING COMMITTEE

Dr. A. F. Trendall (Chairman)
Prof. P. G. Harris (Vice Chairman)
Dr. G. P. Gregory (Treasurer)
Mr. J. D. Lewis (Secretary)
Dr. W. J. Atkinson (alternate Mr. C. B. Smith)
Dr. R. V. Danchin (alternate Mr. J. Stracke)
Dr. L. R. Davidson
Dr. J. Ferguson
Mr. M. Gunn
Dr. A. J. A. Janse
Mr. W. D. Jones
Dr. R. T. Pidgeon
Dr. J. R. Ross

PROGRAMME AND PUBLICATIONS SUBCOMMITTEE

Dr. J. R. Ross (Chairman)
Dr. L. R. Davidson
Prof. P. G. Harris
Mr. C. B. Smith

EDITORIAL PANEL

Dr. A. L. Jaques (Section I)
Dr. J. Ferguson (Section II)
Prof. D. H. Green (Section III)
Dr. S. Y. O'Reilly (Section IV)
Dr. R. V. Danchin (Section V)
Dr. A. J. A. Janse (Section VI)

ACKNOWLEDGEMENT OF SUPPORT

The Organising Committee of the Fourth International Kimberlite Conference expresses its sincere thanks to the many persons, companies and other bodies that have assisted the organisation of this Conference. These include:-

Principal Sponsor: Geological Society of Australia Incorporated

Co-Sponsors: Bureau of Mineral Resources, Geology and Geophysics
Commission on Experimental Petrology
Geological Society of Australia (WA Division)
International Association of Geochemistry and
Cosmochemistry
International Association of Volcanology and Chemistry
of the Earth's Interior
University of Western Australia
Western Australian Department of Mines

Particular appreciation is recorded of the assistance received from the following sources:

ANZ Bank
Argyle Diamond Mines Pty Limited
Ashton Exploration Joint Venture
Ashton Mining Pty Ltd
Australian Airlines (formerly Trans Australia Airlines)
BP Minerals Australia
BP Minerals International
The Broken Hill Proprietary Company Ltd
CRA Exploration Pty Limited
Murdoch University
QANTAS Airways Limited
Stockdale Prospecting Ltd
UNESCO
Western Australian Institute of Technology
Western Mining Corporation Ltd

In addition, the Programme and Publications Subcommittee wishes to acknowledge the invaluable assistance of the following people in the preparation of this volume:

Mrs. S. Yap (CRA Exploration Pty Limited)
Mrs. J. E. Hall (CRA Exploration Pty Limited)
Ms S. M. Mead (Western Mining Corporation)
Mrs J. H. Thom
Mr. T. Dods
Mr. D. Smart
Ms M. T. Muggeridge

FOURTH INTERNATIONAL KIMBERLITE CONFERENCE

EXTENDED ABSTRACTS VOLUME

C O N T E N T S

	Page
Introduction	2
Section I WHAT ARE WE CONCERNED WITH?	5
Descriptive lithology, mineralogy, petrology and geochemistry of kimberlite and closely related rocks and their constituent minerals - excluding xenoliths and xenocrysts. Invited review by Professor R. H. (Roger) Mitchell	
Section II WHEN AND WHERE DO THEY OCCUR?	103
Their distribution in geologic space and time; their tectonic setting and regional occurrence; possible causes of observed distribution patterns. Invited review by Professor J. B. (Barry) Dawson	
Section III HOW DO THEY FORM?	151
Upper mantle processes, magma genesis, ascent and eruption. Invited review by Professor D. H. (David) Egglar	
Section IV WHAT IS THE NATURE OF THE UPPER MANTLE AND THE LOWER CRUST?	219
Descriptive lithology, mineralogy, petrology and geochemistry of xenoliths and xenocrysts; physical and chemical conditions within the upper mantle and lower crust. Invited review by Dr. B. (Ben) Harte	
Section V DIAMONDS	359
All aspects of diamond research, including inclusions in diamonds. Invited review by Dr. J. J. (John) Gurney	
Section VI DIAMOND EXPLORATION	431
Exploration for primary and alluvial deposits of diamonds, including: concepts, exploration technology, evaluation procedures and case histories. Invited review by Dr. W. J. (Warren) Atkinson	
Special Invited Lecture: "The constitution and evolution of the mantle", by Professor A. E. Ringwood	487
Biographies	493
Author Index	511

INTRODUCTION

This Conference has continued the tradition of the three preceding International Kimberlite Conferences in providing a forum for the presentation and discussion of papers on kimberlites and related rocks. Topics discussed include their characteristics, occurrence, mantle source, genesis, mineralogy, diamond content and exploration.

The technical sessions and papers have been organised into six sections in accordance with a structure which addresses a number of basic questions relating to kimberlites and closely related rocks. These questions include some areas of research not well represented at previous conferences as well as the more traditional areas of kimberlite research.

This volume is organised into the same six sections and each commences with an abstract of an invited review paper. This review is followed by the poster and oral papers in that section, presented in alphabetical order of first authors. Poster papers, being an important feature of the Conference, carry equal weight with oral papers. Please note that some papers will not be presented by the first author and the Programme and Information volume should be consulted to relate the Extended Abstract to the papers listed in the detailed programme.

Section I, "What are we concerned with?", is essentially descriptive, dealing with the lithology, mineralogy, petrography and geochemistry of kimberlites, lamproites and related rocks such as olivine melilitites, carbonatites and nephelinites. It includes papers dealing with nomenclature, classification and definitions of these rocks. Descriptions include details of macrocryst mineral species and xenoliths, but papers where the xenoliths and xenocrysts are the main descriptive focus are included in Section IV.

Section II, "When and where do they occur?", deals with the distribution of kimberlitic rocks in geologic space and time, and their relationship to structure on both local and global scales. Processes within the upper mantle, and the processes of magma genesis, ascent and eruption that lead to emplacement of kimberlites and related rocks, are described in Section III.

Section IV, "What is the nature of the upper mantle and lower crust?" includes descriptions of xenoliths and xenocrysts, papers on physical and chemical conditions within the upper mantle and lower crust, and on superimposed changes caused by the processes of metasomatism, magma generation and emplacement. Papers dealing with mantle fabrics and isotope geochemistry are included here.

Section V, "Diamonds", includes papers describing diamond morphology and occurrence, mineral inclusions within diamond, trace element and isotope studies, and diamond genesis. Exploration for and evaluation of both alluvial and primary sources of diamond are covered in Section VI, "Diamond Exploration", which includes methods and case histories, and descriptions of alluvial diamond deposits.

An invited lecture by Professor A. E. Ringwood, entitled "The constitution and evolution of the mantle", is to be given at a special meeting of the Western Australian Division of the Geological Society of Australia and held in conjunction with the 4th International Kimberlite Conference, and an extended abstract of that paper is included in this volume. It addresses the static constitution and dynamics of the mantle, their possible influence on kimberlite genesis, and also considers the processes that give rise to the sub-continental lithosphere. This overview of the mantle is designed to provide a framework for the more specific reviews that head Sections III and IV.

The previous three International Kimberlite Conferences have featured content which reflected the geographic venue of the Conference and the topics being most actively researched at the time. Traditionally, mantle nodule descriptions have formed a major part of the proceedings, reflecting their abundance in the African kimberlites that have historically provided much of the material for research work. The discoveries in Australia of diamond in lamproite has renewed interest in the petrographic nature of the host rock itself, and created controversy as to the relationships between kimberlite and lamproite. It has focussed more attention on diamond exploration.

Table 1 shows a breakdown of papers submitted to the past and present International Kimberlite Conferences, with all papers being notionally allocated to the sections being used in the Fourth Conference. It shows an increasing interest in research relating to diamonds and a substantial increase in exploration oriented papers in the Fourth Conference that may reflect the deliberate structure of its programme. The proportion of descriptive papers in Sections I and IV has decreased.

Table 1
COMPARISON OF INTERNATIONAL KIMBERLITE CONFERENCE PAPERS
SUBDIVIDED BY SECTION
(expressed as a percentage of the total papers)

<u>Conference</u>	<u>No. of Papers</u>	<u>Sections</u>					
		I	II	III	IV	V	VI
1st IKC	95	29	7	14	47	2	0
2nd IKC	133	25	18	17	34	6	0
3rd IKC	136	26	5	26	33	8	2
4th IKC	156	20	10	15	29	15	11

The programme of the Fourth International Conference is expected to include a total of 158 papers, and a total of 156 abstracts are included in this volume. Following the decision to have no concurrent sessions, the programme has been divided into 73 oral papers and 85 poster papers on the basis of content. The geographic subdivision of these papers, on a basis of the affiliations of the 245 authors and co-authors, is given in Table 2. A total of 17 countries are represented.

Table 2
GEOGRAPHICAL BREAKDOWN OF FOURTH IKC PAPERS BY AUTHOR

Australia	72	Norway	2
Botswana	2	South Africa	32
Brazil	1	Swaziland	1
Canada	14	UK	20
China	7	USA	55
France	3	USSR	18
India	4	West Germany	7
Japan	4	Zimbabwe	1
New Zealand	2	TOTAL	245

I. WHAT ARE WE CONCERNED WITH?

Descriptive lithology, mineralogy, petrology and geochemistry of kimberlites and closely related rocks and their constituent minerals - excluding xenoliths and xenocrysts.



PHOTOMICROGRAPH OF KIMBERLITE FROM THE KIMBERLEY MINE
(BIG HOLE), SOUTH AFRICA

CONTENTS OF SECTION I

	Page
REVIEW PAPER	
The nature of kimberlites R. H. MITCHELL	9
The Cummins Range carbonatite, Western Australia R. L. ANDREW, M. N. RICHARDS, A. L. JAQUES, J. KNUTSON and R. TOWNEND	12
Chemical and textural variations of mica in the Nickila Lake and Upper Canada Mine kimberlites, Ontario, Canada M. ARIMA, R. L. BARNETT and R. KERRICH	15
The bearing of brucite on serpentinisation reactions in kimberlite and on dolomite in the mantle G. W. BERG	18
Geology and volcanology of the Argyle (AK1) lamproite diatreme G. L. BOXER, V. LORENZ and C. B. SMITH	21
Geology, petrology and geochemistry of the Bow Hill lamprophyre dykes, Western Australia D. C. FIELDING and A. L. JAQUES	24
Geochemical and microprobe studies of diamond-bearing ultramafic rocks from central and south India A. K. GUPTA, K. YAGI, J. LOVERING and A. L. JAQUES	27
The Cross diatreme: A kimberlite in a young orogenic belt D. C. HALL, H. HELMSTAEDT and D. J. SCHULZE	30
Alkalic ultramafic magmas in north-central Montana, USA: genetic connections of alnoite, kimberlite and carbonatite B. C. HEARN	33
Geochemistry of porphyritic kimberlites in Mengyin County, Shandong Province and in Fuxian County, Liaoning Province, China G. HE and Y. ZHAO	36
Carbonatites and their patterns of REE distribution in Erdaobian and Boshan areas, China G. HE, Z. SHANGUAN and Y. ZHAO	39
The statistical classification of kimberlite garnet by divisive cluster analysis and multiple discriminant analysis B. C. JAGO and R. H. MITCHELL	42
F-rich micas in the West Kimberley lamproites; contrasts with kimberlites and other micaceous alkaline ultramafic intrusions A. L. JAQUES	45
Mineralogy and Petrology of the Argyle lamproite pipe, Western Australia A. L. JAQUES, G. BOXER, H. LUCAS and S. E. HAGGERTY	48
Geochemistry of the Argyle lamproite pipe A. L. JAQUES, S-S. SUN and B. W. CHAPPELL,	51
Diamond-bearing alkaline intrusions from Wandagee, Carnarvon Basin, Western Australia I. D. KERR, A. L. JAQUES, H. LUCAS, S-S. SUN and B. W. CHAPPELL	54
Kimberlite carbonates: a carbon-oxygen stable isotope study M. D. KIRKLEY, H. S. SMITH and J. J. GURNEY	57
The nature of iron in kimberlitic ilmenites and chromites H. LUCAS, M. T. MUGGERIDGE and D. M. McCONCHIE	60

	Page
Oxide minerals in Chicken Park kimberlite, North Colorado M. E. McCALLUM	63
The kimberlites of Guinea, West Africa H. O. A. MEYER and R. A. MAHIN	66
Oxide and silicate minerals in the kimberlites of Minas Gerais, Brazil H. O. A. MEYER, S. E. HAGGERTY and D. P. SVISERO	69
The nomenclature and origin of the noncumulate ultramafic rocks and the systematic position of kimberlites E. A. K. MIDDLEMOST	72
Mineralogy of micaceous kimberlites from the New Elands and Star Mines, Orange Free State, South Africa R. H. MITCHELL and H. O. A. MEYER	75
Kimberlite olivines A. E. MOORE	78
Ultramafic xenoliths from Vajrakarur kimberlites, India C. E. NEHRU and A. K. REDDY	81
Kimberlite as a variety of lamprophyre N. M. S. ROCK	84
Lamproites from the Luangwa Valley, Eastern Zambia B. H. SCOTT-SMITH, E. M. W. SKINNER and P. E. LONEY	87
The petrology of kimberlites, related rocks and associated mantle xenoliths from the Kuruman Province, South Africa S. R. SHEE, J. W. BRISTOW, P. B. S. SHEE and D. R. BELL	90
Peculiarities in the fluid and melt compositions of the lamproites and kimberlites based on the study of inclusions in olivines A. V. SOBOLEV, N. V. SOBOLEV, C. B. SMITH and J. DUBESSY	93
A comparative study of fluid and melt inclusions, their compositions, time-space relations, genesis and tectonic control B. M. VLADIMIROV and L. V. SOLOVYEVA	95
Geology and economic evaluation of the Mt Weld carbonatite, Laverton, Western Australia G. C. WILLETT, R. K. DUNCAN and R. A. RANKIN	97
LIL-bearing Ti-Cr-Fe oxides in Chinese kimberlites J. ZHOU	100

ROGER H. MITCHELL

Dept. of Geology, Lakehead University, Thunder Bay, Ontario, Canada

Kimberlites are complex hybrid rocks containing minerals that may be derived from (1) the fragmentation of upper mantle xenoliths (2) the megacryst or discrete nodule suite and (3) the primary phenocryst and groundmass minerals that crystallized from the kimberlite magma itself. The contribution to the overall mineralogy of kimberlite from each of these sources varies widely and significantly influences the petrographic character of the rocks. Further modal variations result from differentiation processes. Recognizing this complexity kimberlites are defined as follows:

Kimberlites are a clan of volatile-rich (dominantly CO₂) potassic ultrabasic rocks. Commonly they exhibit a distinctive inequigranular texture resulting from the presence of macrocrysts (0.5-10 mm), and in some instances megacrysts (>10 mm) set in a fine grained matrix. The megacryst-macrocryst assemblage consists of rounded anhedral crystals of magnesian ilmenite, Cr-poor titanian pyrope, olivine, Cr-poor clinopyroxene, phlogopite, enstatite and Ti-poor chromite. Olivine is the dominant member of the macrocryst assemblage. The matrix minerals include second generation euhedral primary olivine and/or phlogopite, together with perovskite, spinel (titaniferous magnesian aluminous chromite, titanian chromite, members of the magnesian ulvöspinel-ulvöspinel-magnetite series), diopside (Al- and Ti-poor), monticellite, apatite, calcite and primary late-stage serpentine (commonly Fe-rich). Some kimberlites contain late-stage poikilitic eastonitic phlogopites. Nickeliferous sulphides and rutile are common accessory minerals. The replacement of early-formed olivine, phlogopite, monticellite and apatite by deuteric serpentine and calcite is common. Evolved members of the clan may be devoid of, or poor in, macrocrysts and composed essentially of calcite, serpentine and magnetite, together with minor phlogopite, apatite and perovskite (Mitchell 1986).

Compositional data and textural observations suggest that the cryptogenic macrocrystal olivine population consists of a mixture of xenocrysts (Iherzolite/harzburgite-derived) and several batches of resorbed phenocrysts. Depending upon the presence or absence (<5% vol.) of macrocrysts, kimberlites may be termed macrocrystal or aphanitic varieties respectively.

Currently kimberlites are described, and classified in part, on the basis of their groundmass modal mineralogy. Five varieties based upon the predominance of diopside, monticellite, phlogopite, calcite and serpentine are recognized by Skinner and Clement (1979). Groundmass olivine is considered to be ubiquitous and subdivisions are not made upon the basis of olivine content. In some highly differentiated kimberlites, apatite, perovskite or spinel may be present in more than accessory quantities and in such cases are included in the descriptive name.

Current textural-genetic classifications of kimberlites (Clement 1982, Clement and Skinner 1985) recognize the existence of crater, diatreme and hypabyssal facies kimberlites. Their relationships are illustrated in figure 1. Rocks from each facies can be described according to the terminology outlined in figure 2. Of particular importance is the description of the groundmass as uniform or segregationary. In the case of diatreme facies rocks the presence of pelletal lapilli appears to be a characteristic diagnostic feature. In figure 2 the term "autolithic" is used in the original sense of referring to fragments of an earlier generation of kimberlite found within a younger kimberlite and not to rounded or ball-shaped inclusions of kimberlite termed "nucleated autoliths". The latter are better termed globular segregations (Clement 1982, Mitchell 1986).

Bona fide kimberlite lavas are unknown, the only current candidate being a small flow at the Igwisi Hills, Tanzania (Dawson 1980). Pyroclastic kimberlites are known from craters in Tanzania and Botswana and as xenoliths in diatremes. Epiclastic kimberlites preserved in craters represent reworked pyroclastics and material derived from country rocks deposited in crater-lakes. They consist of a complex sequence of alluvial fan and lacustrine deposits. The volume of kimberlite pyroclastics appears to be small and they are confined to craters and thinly-bedded tuff rings and small cones. Complex stratovolcanoes are not formed. Lava lakes are absent. Hydrovolcanism may have played a dominant role in the formation of crater-facies kimberlites.

Diatremes are vertical cone-shaped bodies that range from 300-2000 m in axial length. Maximum diameters are approximately 1000 m. Diatremes are filled primarily with tuffisitic kimberlite breccias containing a heterogeneous assemblage of locally-derived clasts, autoliths, pelletal lapilli and mantle-derived xenoliths. Some country rock xenoliths appear to have descended within the diatreme. Central conduits filled with hypabyssal kimberlite are absent. There is little evidence of tuffisitization and diatremes appear to have been emplaced passively without regard to the local structure at relatively low temperatures.

Diatremes are gradational with depth into "root zones" (Clement 1982). These irregular bodies (figure 1) consist of several batches of hypabyssal kimberlite. Their emplacement has been controlled by the local structure. Root zones are believed to develop by a variety of subsurface processes including hydraulic fracturing and wedging, stoping, intermittent explosive and/or implosive brecciation and rock bursting (Clement 1982, Mitchell 1986). With depth root zones are transitional into dikes (figure 1) which may represent feeders to the system.

Diatreme-root zone relationships suggest that explosive volcanism or simple fluidization does not play a significant role in diatreme emplacement. Embryonic pipe modification by fluidization (Clement 1982) or hydrovolcanism (Mitchell 1986) are preferable processes.

Hypabyssal kimberlites also form dike swarms and sill complexes, the latter commonly exhibiting differentiation and segregation features.

The megacrysts are primarily Cr-poor titanian pyrope (0-3% Cr₂O₃, 0-1.5% TiO₂), magnesian ilmenite (3-23% MgO), subcalcic to calcic diopside, and enstatite, together with lesser quantities of iron-rich olivine (Fo = 88-78) and zircon. Coexisting megacrysts define regular trends in their Ca/Ca + Mg and Mg/Mg + Fe ratios suggesting formation from a differentiating magma. Megacrysts are regarded as being mantle-derived xenocrysts or high pressure phenocrysts (Dawson 1980, Mitchell 1986).

Macrocrysts include olivine (see above), phlogopite and Ti-poor spinels. Phlogopite and spinel may represent intermediate pressure phenocrysts (lower crust-uppermost mantle).

Important primary groundmass phases include olivine (Fo = 93-85), phlogopite, diopside, spinel, perovskite, monticellite, apatite, calcite and serpentine. Only phlogopite and spinel show extensive compositional variation. Phlogopites range from TiO₂(0-6%)-bearing varieties to TiO₂-poor phlogopite, tetra-ferriphlogopite and eastonitic phlogopite. Spinel exhibit two compositional trends. Trend 1 found in serpentine-calcite-monticellite kimberlites is from titanian magnesian aluminous chromite to magnesian ulvospinel-magnetite and appears to be unique to kimberlites. Trend 2 is from titanian magnesian chromite to Ti-magnetite and is a Cr- and Mg-rich variant of spinel compositional trends found in lamprophyres, and alkali basalt. A similar trend is found in lamproites.

Kimberlites are alumina-poor volatile-rich potassic ultrabasic rocks (Table 1). It is not possible to identify unequivocally the composition of primitive kimberlite magma as lavas are unknown and most bulk compositions are biased as a result of contamination or by the presence of significant amounts of xenocrystal (macrocrystal) olivine. Rocks free of crustal contamination can be recognised by Clement's (1982) contamination index (C.I. = SiO₂ + Al₂O₃ + Na₂O/MgO + 2H₂O).

The trace element geochemistry of kimberlite (Table 2) is dominated by significant contents of compatible elements (Co, Cr, Ni, Sc) and incompatible elements (REE, Th, U, Nb, Zr, Sr, Rb). Only the latter may provide information regarding the sources of kimberlites in the mantle. Rare earth element distribution patterns are light REE enriched suggesting formation of the magma by either small degrees (0-2%) of melting of a cryptically metasomatized source or large degrees (1-10%) of melting of a patently metasomatized source.

In terms of their Sr, Nd and Pb isotopic composition kimberlites form two groups (Smith 1983). Isotopic group I (equivalent to serpentine-calcite-monticellite kimberlites) have Sr and Nd isotopic compositions suggesting derivation from a source that was undifferentiated or slightly depleted relative to the bulk earth composition. Isotopic group II (equivalent to micaceous or phlogopite kimberlites) appear to have been derived from an ancient light REE- and Rb-enriched source. Such kimberlites are apparently a unique magma type. Stable isotopic studies suggest that groundwater has played a significant role during the emplacement of kimberlites.

References

- CLEMENT, C.R. 1982. A comparative geological study of some major kimberlite pipes in the Northern Cape and Orange Free States. Ph.D. Thesis (2 vols.) Univ. Cape Town.
- CLEMENT, C.R. & SKINNER, E.M.W. 1985. A textural genetic classification of kimberlite. Trans. Geol. Soc. S. Africa (in press).
- DAWSON, J.B. 1980. Kimberlites and Their Xenoliths. Springer Verlag. New York.
- MITCHELL, R.H. 1986. Kimberlites: Mineralogy, Geochemistry and Petrology. Plenum Publication Corp. Inc. New York.
- SKINNER, E.M.W. & CLEMENT, C.R.C. 1979. Mineralogical classification of South African kimberlites. Proc. 2nd Internat. Conf. Vol. 1, 129-139.
- SMITH, C.B. 1983. Pb, Sr and Nd isotopic evidence for sources of African Cretaceous kimberlite. Nature 304, 51-54.

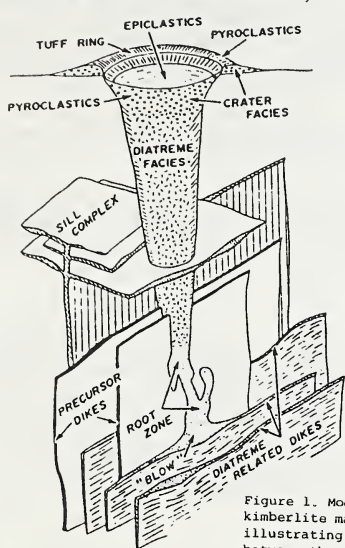


Figure 1. Model of an idealized kimberlite magmatic system illustrating the relationships between the different facies. (after Mitchell 1986)

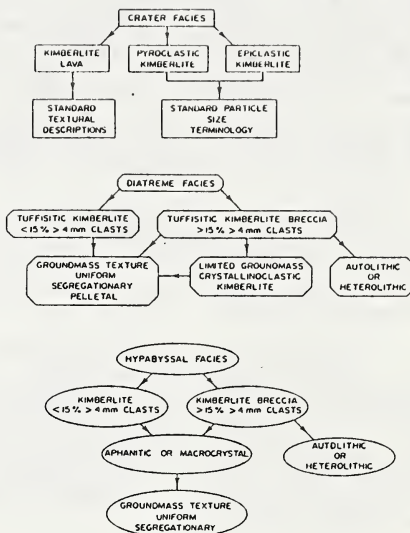


Figure 2. Textural genetic classification of kimberlites, after Clement (1982) and Clement & Skinner (1985).

Table 1. Average major element compositions of kimberlite.

	1	2	3	4	5	6	7	8	9
SiO ₂	35.2	31.1	33.21	36.36	34.03	30.18	30.00	27.64	27.03
TiO ₂	2.32	2.03	1.97	0.98	1.52	3.39	1.52	1.65	1.47
Al ₂ O ₃	4.4	4.9	4.45	5.13	3.37	2.48	2.45	3.17	2.46
Cr ₂ O ₃	-	-	0.17	0.22	0.20	0.22	0.25	0.14	0.15
Fe ₂ O ₃	-	-	6.78	-	4.58	3.92	5.98	5.40	5.53
FeO	9.8*	10.5*	3.43	7.71*	3.78	8.68	2.99	2.75	1.71
MnO	0.11	0.10	0.17	0.16	0.16	0.19	0.16	0.13	0.10
MgO	27.9	23.9	22.78	17.43	25.39	27.53	28.57	24.31	25.53
CaO	7.6	10.6	9.36	11.16	9.45	9.65	10.12	14.13	13.56
Na ₂ O	0.32	0.31	0.19	0.42	0.48	0.25	0.18	0.23	0.12
K ₂ O	0.98	2.1	0.79	1.52	1.60	1.82	0.46	0.79	0.34
P ₂ O ₅	0.7	0.7	0.65	0.55	1.12	0.51	0.65	0.55	0.46
CO ₂	3.3	7.1	4.58	n.d.	5.08	7.39	n.d.	10.84	11.12
H ₂ O ⁺	7.4	5.9	8.04	n.d.	7.25	3.70	n.d.	7.89	10.15
H ₂ O	-	-	2.66	n.d.	0.99	-	n.d.	0.24	-
	100.30	99.24	99.23	81.64	99.01	99.91	83.33	99.36	99.73
No.	-	-	(25)	(80)	(11)	(41)	(14)	(63)	(229)

1-2, kimberlite and micaceous kimberlite (Dawson 1980); 3-4 Lesothon and S. Africa kimberlites (Gurney & Ebrahim, Lesotho Kimberlites, 200-294, 1973); 5 S. Africa (Muramatsu, Geochem. J. 17, 71-86, 1983); 6 Holsteinsborg, Greenland (Scott, Proc. 2nd. Internat. Kimb. Conf. 1, 190-205, 1979); 7 Shandong and Liaoning, China (Zhang & Liu, Geochem. J. 17, 209-221, 1983); 8 Siberia (Ilupin & Lutts, Sov. Geol. 6, 61-73, 1971); 9 Alakit region, Siberia (Ilupin et al., Geochem. Internat. 11, 357-370, 1974).

Table 2. Average trace element content of kimberlite (after Mitchell 1986)

Li	29	Ge	0.5*	Sb	-	Yb	(1.2)
Be	1.6*	As	-	Te	-	Lu	(0.16)
B	(36)*	Se	0.15*	I	-	Hf	5.6
F	2774	Br	-	Cs	2.2*	Ta	11
P	(3880)	Rb	73	Ba	1100	W	-
S	1687	Sr	851	La	(150)	Re	0.069*
Cl	202	Y	(22)	Ce	(200)	Os	1.34*
Sc	14	Zr	184	Pr	(22)	Ir	0.003*
Ti	(11800)	Nb	141	Nd	(85)	Pt	(0.19)*
V	100	Mo	1.7*	Sm	(13)	Au	0.012*
Cr	893	Ru	0.065*	Eu	(3.0)	Hg	(0.008)*
Mn	(1160)	Rh	0.0071	Gd	(8.0)	Tl	(0.219)*
Co	65	Pd	0.0081*	Tb	(1.0)	Pb	15.3
Ni	965	Ag	0.134*	Oy	-	Bi	(0.024)*
Cu	93	Cd	(0.073)	Hg	(0.55)	Th	17
Zn	69	In	-	Er	(1.45)	U	3.1
Ga	5.7*	Sn	5.4*	Tm	(0.23)		

Values in parentheses from Muramatsu (1983).
* = unreliable data or inadequate data base.

R.L. Andrew¹, M.N. Richards², A.L. Jaques³, J. Knutson³ and R. Townend⁴

1. CRA Exploration Pty. Limited, P.O. Box 175, Belmont, Western Australia, 6104.

2. CRA Exploration Pty. Limited, P.O. Box 254, Norwood, South Australia, 5067.

3. Bureau of Mineral Resources, G.P.O. Box 378, Canberra, A.C.T. 2601.

4. RDG, 52 Murray Road, Welshpool, Western Australia, 6106.

The Cummins Range carbonatite, discovered by CRAE in 1978, lies on the southern margin of the Kimberley craton at the junction of the Proterozoic Halls Creek and King Leopold Mobile Zones (latitude 19° 07'S, longitude 127° 10'E). The carbonatite complex intrudes Precambrian metasediments and granite gneisses as a zoned, vertical stock. In plan, the complex has the shape of an asymmetrical rhomb with dimensions of 1.7 x 1.8 km and a surface area of 18.6 ha. The complex is deeply weathered and exposure is very poor, being limited to a few isolated low mounds of silicified limonitic collapse breccia in the centre of the intrusive. Elsewhere the complex is covered by a blanket of aeolian sand 0.5 - 1.5 m thick. Although surface expression is very poor, the complex is easily recognised by a marked 4900 nT bullseye magnetic anomaly.

The margins of the complex have not been intersected with drilling but airborne and ground magnetic data indicate that the contacts are sharp and vertical to steeply dipping with strike directions of 040° or 140°, parallel to the two Proterozoic Mobile Zones. This suggests that the emplacement of the complex was controlled by major basement fractures.

The complex is of late Proterozoic age. An age of 905 ± 2 Ma has been obtained from the Rb-Sr method on phlogopite - whole rock and phlogopite-apatite separates with an initial ⁸⁷Sr/⁸⁶Sr ratio of 0.7030 ± 0.0002 (Sun and others, this volume). This date is in agreement with the 854 ± 57 Ma age obtained by the K-Ar method on pyroxenes, but differs from the 1012 ± 3 Ma age obtained by U-Pb dating of zircons (Pidgeon and others, this volume). The U content of these zircons is very low but the ²⁰⁸Pb and Th contents were high, distinguishing them from zircons in kimberlites and basic metamorphic rocks.

Drilling has revealed that the intrusion consists of three broadly concentric zones. A small central carbonatite plug is surrounded by an inner zone of carbonated, mica-rich, altered pyroxenite, now largely composed of amphibole, which passes into an outer zone of unaltered pyroxenite. The exception to this concentric pattern is a 300 x 500 m satellite body of carbonated, mica and amphibole-rich rock on the eastern side of the complex. This satellite body may also have at its core a small carbonatite plug, thus explaining the anomalous alteration pattern. The inner, strongly altered and carbonated zone with abundant amphibole is cut by numerous carbonatite intrusions. The carbonatite intrusives are steeply dipping and have a discontinuous ring-dyke or cone-sheet morphology with variable thickness up to 60 m. The altered pyroxenite (amphibolite) passes outwards into unaltered pyroxenite as the density of ring dykes and cone sheets decreases. The unaltered pyroxenite occupies more than half of the complex and may, in fact, be a composite body. Two other major rock types have been recognised within the complex: a silicified, limonite-rich collapse breccia and chlorite schist. The breccia is interpreted as being the weathering product of the central carbonatite plug and of the larger carbonatite dykes. The chlorite schist is thought to represent Precambrian basement rafted into the complex during intrusion.

The carbonatites include both sovite and beforosite. They range from massive to laminated, coarse grained, equigranular textured types containing abundant apatite and variable amounts of phlogopite, magnetite and clinopyroxene to finer grained, more recrystallised types with marked foliation and lineation containing abundant alkali amphibole and chlorite. Sulphide-rich vugs and veins up to several centimetres wide containing pyrite, pyrrhotite, chalcopyrite and occasionally, barite and fluorite are common. Other phases occurring as accessories in the carbonatite plug and dykes include zircon, sphene, baddeleyite, monazite, aeschynite, pyrochlore, columbite and allanite.

The carbonated, altered, mica-and amphibole-rich pyroxenite varies greatly in its mineralogy, grain size and texture. It commonly consists of granular, pale green clinopyroxene (mainly diopside) and coarse mica (dark, turbid biotite cores enclosed by phlogopite) rimmed and replaced to varying extents by linedated, fibrous alkali amphibole (dominantly richterite), chlorite and calcite intergrown with the same suite of accessory minerals found in the carbonatite. Additional accessory minerals are ilmenite, bastnaesite and thorianite. The relative proportions of mineral phases and degree of carbonate alteration vary greatly. The calc-alteration is first recognised by an increase in interstitial carbonate and minor replacement of pyroxene by amphibole. This advances to a stage where microveins of carbonate form in cleavage planes of the mafic minerals, interstitial carbonate becomes commoner and pyroxene is replaced by amphibole and chlorite. As alteration intensifies, pyroxene is completely replaced by amphibole and chlorite, the density of microveining increases and the original pyroxenite textures are destroyed by the dominance of interstitial carbonate which constitutes most of the matrix. In extremely altered rocks, the concentration of carbonate increases to a level where the rock is classified as a carbonatite.

The unaltered pyroxenite is also characterised by variable mineralogy, grain size and texture. The pyroxenite ranges from clinopyroxenite to micaceous clinopyroxenite composed of granular, dominantly diopsidic pyroxene, mica (dominantly phlogopite), magnetite, apatite, calcite and dolomite with accessory baddeleyite, sphene, ilmenite, monazite, zircon, zirconolite, pyrite, pyrrhotite and chalcopyrite. The accessory minerals tend to be more abundant in the pegmatitic phases of the pyroxenite.

The pyroxenes show a wide compositional range from diopside through salite, ferro-augite, augite and aegirine; all are characterised by low Al and very low Cr contents. The micas lie in the range Mg 85 - 45, have moderate Ti and Al contents (1-2% TiO₂, 10-14% Al₂O₃), very low Cr and low Ba, Na and F (up to 0.5% BaO, 1% Na₂O, 3% F). In weathered zones the micas become hydrated, and are hydrobiotites or, less commonly, vermiculites. The amphiboles are alkali-rich, ranging from sodic-calcic (richterite) compositions with moderate Al contents (6-8% Al₂O₃) to strongly pleochroic, mauve coloured, sodic amphibole (magnesian riebeckite) with lower Mg/(Mg + Fe), very low Al and higher F contents. The carbonate phases range in composition from calcite through magnesian calcite to dolomite with Fe and Mn dolomite occurring as minor phases. The pyrochlore is commonly uraniferous and, in some samples, Ba-rich.

The Cummins Range complex exhibits a wide range of bulk compositions which reflect the varying modal proportions of specific phases such as apatite. The silicate rocks of the Cummins Range complex have a range of agpaitic indices (0.88-2.1) and K₂O contents commonly exceed Na₂O. Like carbonatites elsewhere the Cummins Range rocks are strongly enriched in P, Sr, Zr, Nb, Ta, Th, U and LREE. Zr and Nb contents, for example, range from 700 and 200 ppm respectively in the pyroxenite to 5000 ppm Zr and 1400 ppm Nb in baddeleyite-rich zones, whereas some of the coarser grained carbonatites contain less than 10 ppm Zr. Rb abundances are low in all Cummins Range rocks whereas Sr varies with the modal proportion of apatite, reaching 1.27% SrO in an apatite-rich carbonatite. Sr and Nd isotopic data indicate that the Cummins Range carbonatite was derived from mantle sources with near-chondritic Rb/Sr and Sm/Nd ratios (Sun and others, this volume), and it is suggested that the Cummins Range carbonatite may be related to the Bow Hill lamprophyre dyke swarm in the East Kimberley region (Fielding and Jacques, this volume), which is of comparable age.

The oxidised zone over the complex is of particular interest because it hosts LREE, Nb, U and P mineralisation. Weathering has involved leaching, dissolution and silicification of carbonates and alteration of the silicate minerals to clays. These processes have resulted in the physical concentration of resistant minerals such as monazite, apatite, zircon and pyrochlore to levels many times greater than in the primary rock types. Element concentrations in the enriched zone can reach 3.8% Ce, 3.1% La, 431 ppm Eu, 0.39% Nb, 350 ppm Y and 120 ppm U. This style of physical concentration has also been noted at the Sukulu carbonatite, Uganda (Reedman, 1984) at Mrima Hill, Kenya (Deans, 1966) and at Magnet Cove, Arkansas (Rose et al. 1958). Secondary monazite may also be present.

ACKNOWLEDGEMENTS

We wish to thank the management of CRA Exploration Pty. Limited for permission to publish this abstract. We would like to thank all those geologists who have worked on, or contributed to, the Cummins Range Project. ALJ and JK publish with the permission of the Director, Bureau of Mineral Resources, Canberra.

REFERENCES

- DEANS, T., 1966. Economic mineralogy of African carbonatites. In Tuttle, O. and Gittins, J. "Carbonatites", Interscience, New York.
- FIELDING, D. C. & JAQUES, A. L. Geology, petrology and geochemistry of the Bow Hill lamprophyre dykes, Western Australia (this volume).
- PIDGEON, R. T., SMITH, C. B. & FANNING, M., 1986. The ages of kimberlite and lamproite emplacement in Western Australia, (this volume)
- REEDMAN, J. H., 1984. Resource of phosphate, niobium, iron and other elements in residual soils over the Sukulu carbonatite, Southeastern Uganda. Econ. Geol., 79, 716-724.
- ROSE, H. J., BLADE, L. V. and Ross, M., 1958. Earthy monazite at Magnet Cove, Arkansas. Am. Mineralogist, 43, 935-997.
- SUN, S.-S., McCULLOCH, M. T. & JAQUES, A. L. Isotopic evolution of the Kimberley Block, Western Australia (this volume).

M. Arima,¹ R.L. Barnett,² and R. Kerrich²

1. Geological Institute, Yokohama National University,
Hodogaya-ku, Yokohama, 240 Japan.
2. Department of Geology, University of Western Ontario,
London, Ontario, N6A 5B7 Canada.

Introduction

Micaceous kimberlites occur at Nickila Lake (NL) and the Upper Canada Mine (UCM) near Kirkland Lake in the Archean Abitibi greenstone belt, Superior province. K-Ar age determinations indicate the emplacement age of 151 Ma for the UCM kimberlite dyke (Lee and Lawrence, 1968) and that of 147 Ma for the NL kimberlite diatreme (Arima et al., 1986). Both kimberlites contain abundant phenocryst and xenocryst micas together with mica-bearing nodules. In this study we report various chemical and textural features of mica in the kimberlites.

UCM kimberlite

One of the striking features in this kimberlite is an occurrence of Ba-rich phlogopite in a pargasite-diopside-chromite nodule. The phlogopite is characterized by its high BaO, Na₂O, Cr₂O₃ and low TiO₂ contents (Table 1, Fig. 1-b). Relatively high Cr₂O₃ is also evident in coexisting pargasite and diopside (Table 1). Comparing to Ba-rich micas previously reported from mafic-ultramafic alkalalic volcanic rocks (summarized by Gaspar and Wyllie, 1982; Barnett et al., 1984), the UCM Ba-phlogopite contains higher Cr₂O₃ and Na₂O. The pargasite is compositionally similar to amphibole of upper mantle origin (Dawson and Smith, 1982). Fine grained diopside neoblasts are present along the grain boundary of pargasite and phlogopite. Textural relations and chemistry of minerals suggest that the nodule is mantle origin. Phlogopite could be a principle carrier of BaO in the upper mantle.

In the UCM kimberlite, abundant mica phenocrysts typically exhibit dark brown core (up to 21 wt.% FeO_T) with a corroded outline (type 1 groundmass mica of Smith et al., 1978) which is mantled by euhedral to subhedral pale brown phlogopite. X-ray intensity distribution scan reveal the core and mantle domains of the mica have a chemically sharp and distinct interface. Mantle domain of the mica has composition similar to that of pale brown phenocryst phlogopite (type 2 mica of Smith et al., 1978) (Table 1, Fig. 1-b). In the type 1 micas, core domains of several different grains show a wide range of chemical variation especially in TiO₂ and FeO_T (Fig. 1-b). Type 2 micas exhibit a wide compositional range and most grains of the mica are uniform in composition, excepting some large grains in which Cr₂O₃ content decreases from core to margin with concomitant increases in FeO_T, TiO₂, and BaO, and decrease in MgO. Textural and chemical relations between mantle and core domains of the type 1 mica suggest a resorption of Fe-rich biotite xenocryst and overgrowth of type 2 mica prior to or during kimberlite emplacement. Additionally the sporadic occurrence of low TiO₂ phlogopite with reverse pleochroism (Table 1, Fig. 1-b) mantled by pale brown phlogopite compositionally identical to type 2 mica suggests micas of several different origins were introduced into the UCM kimberlite magma prior to or during the crystallization of type 2 phenocryst phlogopite.

NL kimberlite

The NL kimberlite is dominated by tuffisitic breccia facies containing a wide variety of incorporated nodules from the upper mantle and crust. Despite extensive alteration which obscured the original features of the kimberlite, the relatively fresh hypabyssal kimberlite fragment suggests that the diatreme is related to micaceous kimberlite magmatism. In the fragment, poikilitic phlogopite phenocrysts occur together with diopside, olivine, Mg-chromite and Mg-titanomagnetite spinels, calcite, apatite, perovskite, and serpentine. The phlogopite in the fragment contains higher BaO (up to 1.5 wt.%) and FeO_T than phlogopites in the tuffisitic facies (Table 1, Fig. 1-a). Ti-phlogopite also occurs in veinlet networks infiltrating a deformed ultramafic nodule incorporated in the fragment. The textural relations indicate that the deformation, transgranular fracturing, and neoblast formation of endopside predate

Table 1. Analyses of minerals in the NL and UPC kimberlite

	1	2	3	4	5	6	7	8	9
SiO ₂	39.72	45.76	52.53	-	36.22	38.55	42.20	41.47	41.75
TiO ₂	0.00	0.02	0.11	0.13	3.06	3.22	0.11	3.04	2.19
Al ₂ O ₃	15.01	10.95	3.32	12.89	16.32	13.77	10.19	9.17	11.76
Cr ₂ O ₃	1.06	2.05	2.40	53.25	0.08	0.00	0.00	0.09	0.21
FeO _T	2.09	2.84	2.44	17.18	20.31	6.54	5.24	8.79	5.98
MnO _T	0.05	0.14	0.19	0.12	0.36	0.00	0.06	0.09	0.00
MgO	24.78	19.45	15.89	13.79	10.14	22.34	25.28	22.23	23.40
CaO	0.00	10.34	22.26	-	0.00	0.00	0.00	0.00	0.00
Na ₂ O	2.01	4.73	1.14	-	0.46	0.21	0.14	0.16	0.23
K ₂ O	6.79	0.06	0.04	-	10.09	10.58	10.07	10.07	10.12
BaO	4.27	0.16	0.01	-	0.23	0.31	0.20	0.39	0.00
Total	95.78	97.05	100.33	97.36	97.27	95.52	93.49	95.54	95.64

1-4; phlogopite, amphibole, clinopyroxene, and chromite in a Ba-phlogopite nodule incorporated in the UCM kimberlite respectively.

5-6; type 1 and type 2 mica in UCM kimberlite respectively.

7; reverse pleochroism phlogopite in UCM kimberlite.

8-9; phlogopite in hypabyssal fragment and in tuffisitic facies in NL kimberlite, respectively.

the veinlet formation. Veinlet phlogopites present along fractures of olivine and endiopside grains and connect with a kelyphite rim mantling a Cr-garnet. The kelyphite rim consists of Cr-rich phlogopite, Mg-Al spinel, and Cr-rich serpentine-like phase. The kelyphitic phlogopite is richer in Cr₂O₃ (2.5 wt.%) and Al₂O₃ (15 wt.%) than the veinlet phlogopite (0.75 wt.% Cr₂O₃ and 13.5 wt.% Al₂O₃) present in endiopside grains. The veinlet phlogopite associated with olivine has composition similar to groundmass mica of the host kimberlite fragment. The veinlet and kelyphitic phlogopites were probably formed simultaneously by the local scale equilibration during the infiltration of kimberlite liquid into the nodule.

Distinct variety of mica with comparable composition to type 1 mica (core domain) occurs in a salite-hornblende-apatite-ilmenite nodule in the NL kimberlite tuffisitic facies (Fig.1-b, B). Compositions of clinopyroxene, amphibole, and ilmenite in this nodule suggest that this nodule is a lower crustal origin. The mica shows relatively high Al₂O₃ (no tetrahedral site deficiency) and low Cr₂O₃ which are characteristics of type 1 mica, mica from alkali lamprophers (Rock, 1986), and mica of lower crustal metamorphic rocks. Although an igneous origin of type 1 mica derived from intrusive precursor to kimberlite has been suggested (Smith et al., 1978), type 1 mica could alternatively be of lower crustal metamorphic origin, incorporated into the kimberlite magma.

References

- Arima, M., Barnett, R.L., Hayatsu, A., and Kerrich, R., 1986, A new kimberlite occurrence at Nickila Lake, Abitibi greenstone belt: petrology, geochemistry, and isotopic characteristics. GAC/MAC Ann. Meeting Abst. p. 42.
- Barnett, R.L. Arima, M., Blackwell, J.D., Winder, C.G., Palmer, H.C., and Hayatsu, A., 1984, The picton and verty lake ultramafic dikes: Jurassic magmatism in the St. Lawrence platform near Belleville, Ontario. Can. J. Earth Sci. v. 21, p. 1460-1472.
- Dawson, J.B., and Smith, J.V., 1982, Upper-mantle amphiboles: a review. Min. Mag., v. 45, p. 35-46.
- Gaspar, J.C., and Wyllie, P.J., 1982, Barium phlogopite from the Jacupiranga carbonatite, Brazil. Amm. Mineral. v. 67, p. 997-1000.
- Lee, H.A., and Lawrence, D.E., 1968, A new occurrence of kimberlite in Gauthier township, Ontario. Geol. Surv. Canada, paper 68-22, p. 1-16.
- Rock, N.M.S., 1986, The nature and origin of lamprophers: a overview. in Fitton, J. G., and Upton, B.B.J., eds. Proceedings of the Conference on Alkali Igneous Rocks, Edinburgh, Geol. Soc. London.
- Smith, J.V., Brennesholtz, R., and Dawson, J.B., 1978, Chemistry of micas from kimberlites and xenoliths - I. Micaceous kimberlites. Geochim. Cosmochim. Acta v. 42, p. 959-971.

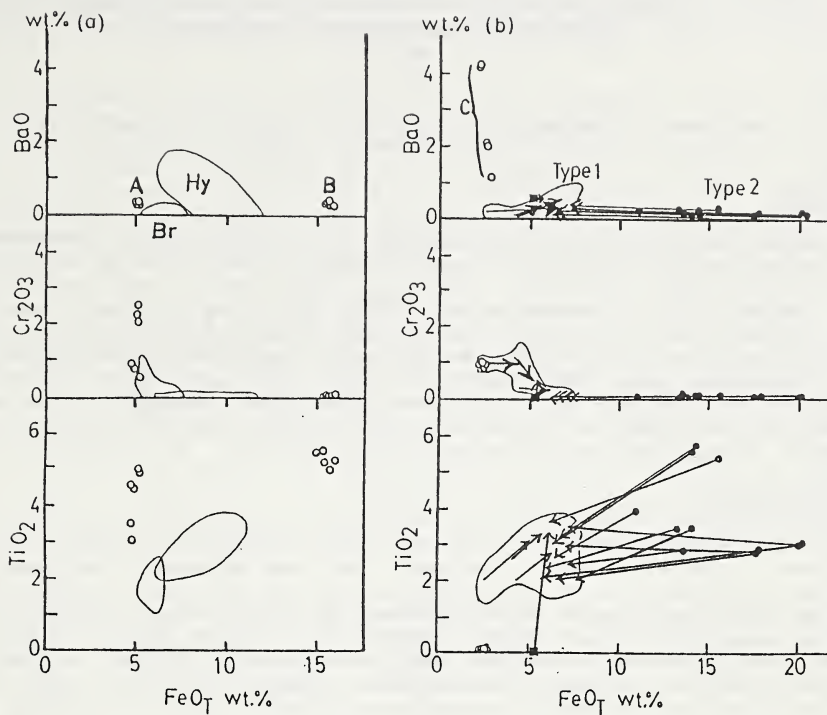


Fig. 1. Plots of BaO , Cr_2O_3 , and TiO_2 against FeO_T for phlogopites from NL kimberlite (a) and UCM kimberlite (b). Solid circle = dark core of type 1 mica, solid square = reverse pleochroism phlogopite, open circle = mica from nodules; A = veinlet phlogopite nodule, B = apatite-amphibole-clinopyroxene nodule, C = Ba-phlogopite nodule. Hy and Br indicate phlogopite from hypabyssal fragment and tuffisitic facies respectively. Arrow indicates core-mantle or core-margin relations.

The results summarised in Tables 1a and 1b indicate an association between freshness and brucite, which is considerably strengthened when samples with $\leq 0,23\%$ brucite are classified as "brucite absent". If the overall association is accepted, concentrations of less than about 0,25% of brucite thus appear to be of little diagnostic value.

The experimental studies of Hemley et al. (1977) demonstrate that the formation of brucite in a serpentinising system is favoured by relatively low availability of H_2O , SiO_2 and CO_2 . Abundance of these components leads respectively to (a) dissolution of brucite, (b) formation of serpentine instead of brucite, and (c) formation of magnesite. Thus the general association of brucite with freshness and its absence or paucity in altered kimberlites is consistent with the combined experimental data and the petrographic assessments that fresh kimberlites were serpentinised predominantly isochemically by a restricted volume of water, in contrast to altered kimberlites.

The loss of $Mg(OH)_2$ in solution during open-system serpentinisation must lower the MgO/SiO_2 ratios in altered kimberlites. With few exceptions the MgO/SiO_2 ratios of altered kimberlites are indeed less than 1, while fresh brucite-carrying kimberlites have MgO/SiO_2 ratios in the range 1,08 to 1,23. However, where not a consequence of shale-contamination, low MgO/SiO_2 ratios of altered kimberlites are thought generally to be a consequence of brucite-removal, rather than a primary characteristic of the kimberlite prior to its alteration. Kresten (1973) emphasised that the removal of $Mg(OH)_2$ in solution occurs during alteration and is required to stabilise some minerals such as talc which is common in kimberlites. An abundance of primary low MgO/SiO_2 -minerals such as phlogopite will on the other hand also inhibit the formation of brucite, as observed by Malkov (1974). Only one micaceous kimberlite was found in the present survey to contain brucite (Jag K-9: 0,43% brucite).

An extensively serpentinised non-micaceous kimberlite classified as "altered" but having a low Sr isotope ratio of 0,704 (Barrett and Berg, 1975, Sample DiB 3) was found to contain 3,5% brucite. This indicates that in contrast to other altered kimberlites serpentinisation of DiB 3 was isochemical leaving an undisturbed Sr isotope relation.

Peridotites

In 8 out of the 10 peridotite nodules studied brucite occurs in concentrations from 0,14 to 0,43 wt. % which is substantially less than would be present if they had been serpentinised isochemically. This suggests that relatively large volumes of serpentinising fluids have carried $Mg(OH)_2$ out of many samples and bulk-rock chemistries of peridotites will reflect deficient MgO/SiO_2 ratios; this aspect is not pursued in the present work. Where larger amounts of brucite (0,72 and 5,22 wt. %) were found in the peridotites, it occurs predominantly in characteristic black nodules of up to about 4mm in cross section. When unaltered these nodules consist of brucite intergrown with calcite on a 20 micron scale in typical decompression textures. Replacement of the intergrowth by serpentine is evident to varying degrees, and is almost complete in the specimen carrying 0,72 wt. % of brucite. In this nodule minor magnetite occurs in the replacement serpentine. The black grains are strongly deformed where the host peridotite is sheared, but the decompression-textures do not appear to be deformed.

The brucite/calcite intergrowths are interpreted to represent dolomite from the mantle, metamorphosed by decompression upon emplacement, by a reaction represented in a simplified form as



by Harker (1974), the MgO being hydrated to brucite. Direct formation of brucite from dolomite without intermediate periclase has also been postulated in some metamorphic rocks (Deer et al., 1962) and this would better explain the undisturbed decompression textures observed in the present study. Emplacement appears to have been too rapid for the dolomite to be consumed by the silicate-carbonate reactions reviewed by Wyllie et al. (1983).

The abundance, distribution and mode of origin of the inferred dolomite in the mantle remains speculative. Replacement by serpentine may be responsible for the brucite calcite intergrowths not having been reported previously. An estimate of the distribution of dolomite in samples from the mantle may be possible if the "Wavy 2-4mm lenticles of dull-brown near isotropic glass (?) ..." consisting mainly of chrysotile,

which are reported in about a third of the nodules studied by Boyd and Nixon (1978), represent completely serpentinised brucite/calcite intergrowths.

CONCLUSIONS

Carmichael et al. (1974) suggested that stable isotope measurements should help clarify the role of ground water in the alteration of kimberlites. Surprisingly, the fresh and altered kimberlites studied here could not be distinguished on the basis of bulk hydrogen isotope determinations, which overlap in a range of $\delta D = 78 - 104$ (Berg, Clayton and O'Neil, in prep.). Subject to an appropriate original mineralogy, brucite appears to offer a more reliable indicator of the extent of ground water circulation which affected a kimberlite, and the presence of brucite is recommended as an additional criterion of acceptability when selecting kimberlites for detailed geochemical study.

The presence of dolomite in the mantle source of kimberlite has long been suggested on the basis of experimental petrology (e.g. Wyllie, 1978; Eggler, 1978), but these authors noted the absence of more direct evidence apart from a single inclusion of dolomite in a garnet reported by McGetchin and Besancon (1973). The brucite/calcite intergrowths described here may contribute to fill this gap.

REFERENCES

- BARRETT D.R. and BERG G.W. 1975. Complementary petrographic and strontium isotope ratio studies of South African kimberlites. *Physics and Chemistry of the Earth* **9**, 619-635.
- BERG, G.W. 1982. The geochemistry of some kimberlites from the type area in Kimberley, South Africa, in relation to models of kimberlite petrogenesis. Public communication and unpagged abstract, Third International Kimberlite Conference, Clermont Ferrand, France.
- BERG G.W. and ALLSOPP H.L. 1972. Low $^{87}\text{Sr}/^{86}\text{Sr}$ ratios in fresh South African kimberlites. *Earth and Planetary Science Letters* **16**, 27-30.
- BOYD J.R. and NIXON P.H. 1978. Ultramafic nodules from the Kimberley pipes, South Africa. *Geochimica et Cosmochimica Acta* **42**, 1367-1382.
- CARMICHAEL I.E., TURNER T.J. and VERHOOGEN J. 1974. *Igneous Petrology*. McGraw Hill Inc., 739 pp.
- DEER W.A., HOWIE R.A. and ZUSSMAN J. 1962. *Rock-forming Minerals*, Vol. 5, Non-silicates. London, Longmans Green & Co., 371 pp.
- EGGLER D.H. 1978. The effect of CO_2 upon partial melting of peridotite in the system $\text{Na}_2\text{O}-\text{CaO}-\text{Al}_2\text{O}_3-\text{MgO}-\text{SiO}_2$ to 35 Kbar, with an analysis of melting in a peridotite- $\text{H}_2\text{O}-\text{CO}_2$ system. *American Journal of Science* **278**, 305-343.
- HARKER A. 1974. *Metamorphism*. 362 pp. Chapman and Hall.
- HEMLEY J.J., MONTOYA J.W., SHAW D.R. and LUCE R.W. 1977. Mineral equilibria in the $\text{MgO}-\text{SiO}_2-\text{H}_2\text{O}$ system: II Talc-antigorite-forsterite-anthophyllite-enstatite stability relations and some geologic implications in the system. *American Journal of Science* **277**, 353-383.
- KRESTEN P. 1973. Differential thermal analysis of kimberlites. In Nixon P.H. ed, *Lesotho Kimberlites*, pp. 269-279. National Development Corporation, Maseru.
- MALKOV B.A. 1974. Brucite in kimberlite. *Doklady Akademii Nauk SSSR, Earth Science Section* **215**, 157-160.
- McGETCHIN T.R. and BESANCON J.R. 1973. Carbonate inclusions in mantle-derived pyrope. *Earth and Planetary Science Letters* **18**, 408-410.
- MITCHELL R.H. 1978. Mineralogy of the Elwin Bay kimberlite, Somerset Island, N.W.T., Canada. *American Mineralogist* **63**, 45-57.
- WYLLIE P.J. 1978. Mantle fluid compositions buffered in peridotite- $\text{CO}_2-\text{H}_2\text{O}$ by carbonates, amphibole, and phlogopite. *Journal of Geology* **86**, 687-713.
- WYLLIE P.J., HUANG W.L., OTTO J. and BYRNES A.P. 1983. Carbonation of peridotites and decarbonation of siliceous dolomites represented in the system $\text{CaO}-\text{MgO}-\text{SiO}_2-\text{CO}_2$ to 30 Kbar. *Tectonophysics* **100**, 359-388.
- ZINCHUK N.N., MELNIK I.M. and KHARKIV A.D. 1973. Features of the composition and genesis of brucite from Yakutian kimberlites. *Doklady Akademii Nauk SSSR* **269**, 449-454.

G. L. Boxer¹, V. Lorenz² and C. B. Smith³

1. Argyle Diamonds Mines Ltd, Kununurra, Western Australia

2. University of Mainz, West Germany

3. CRA Exploration Pty Limited, Western Australia

The diamondiferous Argyle (AK1) olivine lamproite diatreme is located in the East Kimberley region of Western Australia, at latitude 16° 14' S and longitude 128° 23' E. The diatreme is located near the eastern margin of the north north east trending Halls Creek Mobile Zone. This Mobile Zone contains Archaean (?) and Lower Proterozoic sediments and volcanics metamorphosed and strongly deformed at ca 1920 Ma, intruded by mafic plutons and late stage granites at ca 1800 Ma (Bofinger, 1967; Hancock and Rutland, 1984). Later movements on structures within this Mobile Zone produced deposition of sediments in fault controlled basins during the Middle and Upper Proterozoic and Phanerozoic. In addition sinistral wrench faulting continued from the Proterozoic to at least past Upper Devonian. The country rocks immediately surrounding the AK1 diatreme are predominantly quartzites and siltstones of Lower to Middle Proterozoic age belonging to the Revolver Creek Formation and Carr Boyd Group. Dating by whole rock Rb-Sr and mica Rb-Sr and K-Ar methods (Pidgeon et al this volume) give Argyle an intrusion age of 1200 ± 50 Ma, which is contemporaneous with the Middle Proterozoic dates obtained by Bofinger (1967) for the adjacent Carr Boyd Group country rock sediments.

The diatreme has an elongate shape in plan (Fig. 1), with a length of 2 km and a width varying from 150 to 500 m. The surface area is ca. 50 ha. The body was emplaced along a pre-existing fault, but the present shape results from post-intrusion faulting plus regional tilting of 30° to the north. As a result of the tilting the northern end of the diatreme represents a shallower erosion level than the southern. The form of the diatreme is variable in cross section (Fig. 1), bowl-shaped in the north but essentially steep dipping in the south.

The main rock type in the diatreme is a quartzose tuff, with a lesser amount of younger quartz-free tuff and minor late-stage intrusive dykes of olivine lamproite. Accidental inclusions of quartz grains comprise a significant proportion of the quartzose tuffs. The main tuff type is a lapilli ash tuff with lesser amounts of coarse ash and fine ash tuffs. The olivine lamproite dykes intrude all areas of the diatreme and lamproite flows may possibly be present. Epiclastic rocks (now quartzites) occur interbedded and locally intermixed with the pyroclastic rocks. The predominant juvenile clast type is altered, glassy and microcrystalline, lacks vesicles, has a blocky and equant shape and contains quartz xenocrysts. These clasts have probably formed by rapid chilling caused by magma contact with water. The presence of accretionary and armoured lapilli indicate wet eruption conditions. Bedding is either absent, or poorly developed in the tuffs, although plane parallel bedding and low-angle cross-bedding suggestive of base surge eruptions are present in the central and northern areas of the diatreme. The massive units, lacking bedding, result from enlargement of the crater by collapse and consequent mass flows (lahars) of unconsolidated material down the sides of the crater onto the crater floor. Such debris flow units constitute the dominant rock type.

Syn-sedimentary deformation and water escape structures indicate that abundant water was enclosed in the deposits and subsequently driven out by subsidence and compaction under the load of superincumbent tuffs. The accidental quartz grains in the quartzose tuffs have been derived from the surrounding country rocks, likely to have been poorly cemented at the time of the volcanicity. Groundwater would have been present in the pore spaces of these sands and sandstones, and in fractures in the fault zone into which the diatreme was emplaced. All the above evidence favours a phreatomagmatic eruption process, caused by interaction of rising lamproite magma with groundwater. Removal and eruption of country rock by this process from levels below the vent led to subsidence downward slumping of the crater deposits and creation of a deepening diatreme as the phreatomagmatic eruptions progressed. The downturning and downfaulting of the country rock adjacent to the diatreme contacts (Fig. 2) and the presence of bedded tuff, often with steep dips, at deep levels of the diatreme, support this subsidence hypothesis.

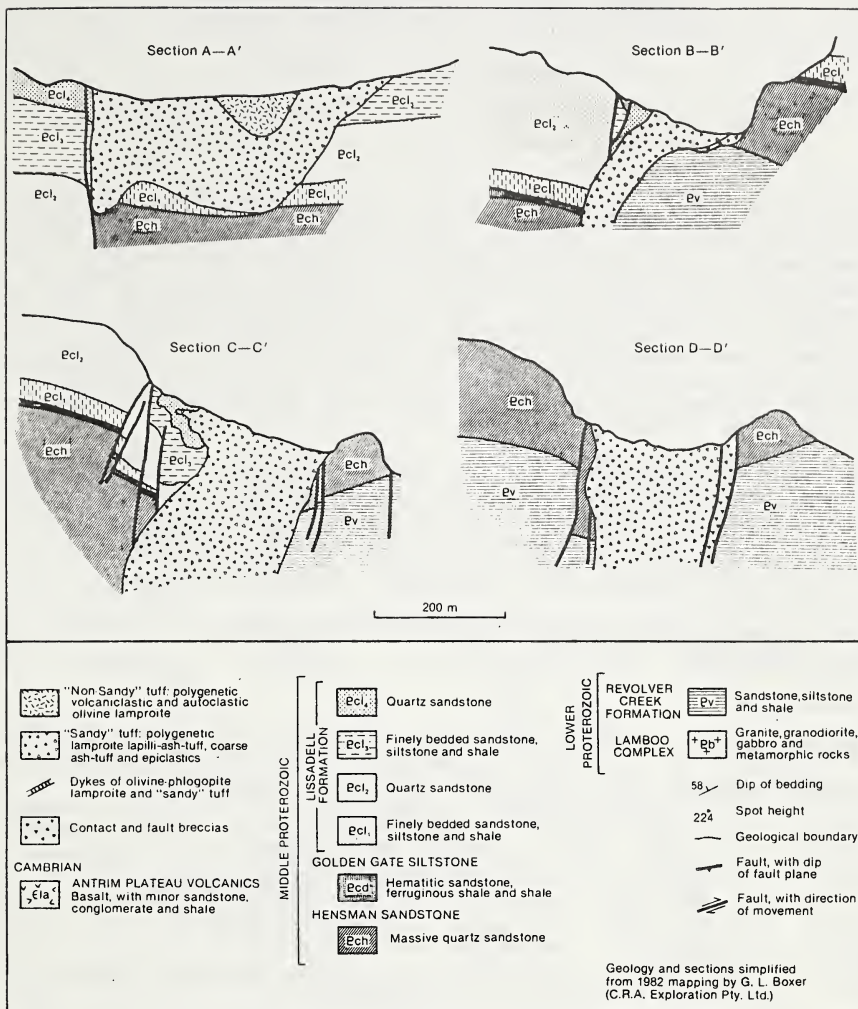


Fig. 2 Cross sections through the Argyle Pipe

REFERENCES

BOFINGER, V. M., 1967. Geochronology in the East Kimberley area of Western Australia. PhD thesis, Australian National University, unpublished.

HANCOCK, S. L. & RUTLAND, R. W. R., 1984. Tectonics of an early Proterozoic geosuture: the Halls Creek orogenic sub-province, northern Australia. *Jour. Geodynamics*, Vol. 1 p. 387-432.

PIDGEON, R. T., SMITH, C. B. & FANNING, M., 1986. The ages of kimberlite and lamproite emplacement in Western Australia. This volume.

LORENZ, V., 1986a. On the growth of maars and diatremes and its relevance to the formation of tuff-rings. *Bull. volcanol.*, in press.

LORENZ, V., 1986b. Maars and diatremes of phreatomagmatic origin, a review. *Trans. Geol. Soc. S. Afr.*, in press.

GEOLOGY, PETROLOGY AND GEOCHEMISTRY OF THE
BOW HILL LAMPROPHYRE DYKES, WESTERN AUSTRALIA

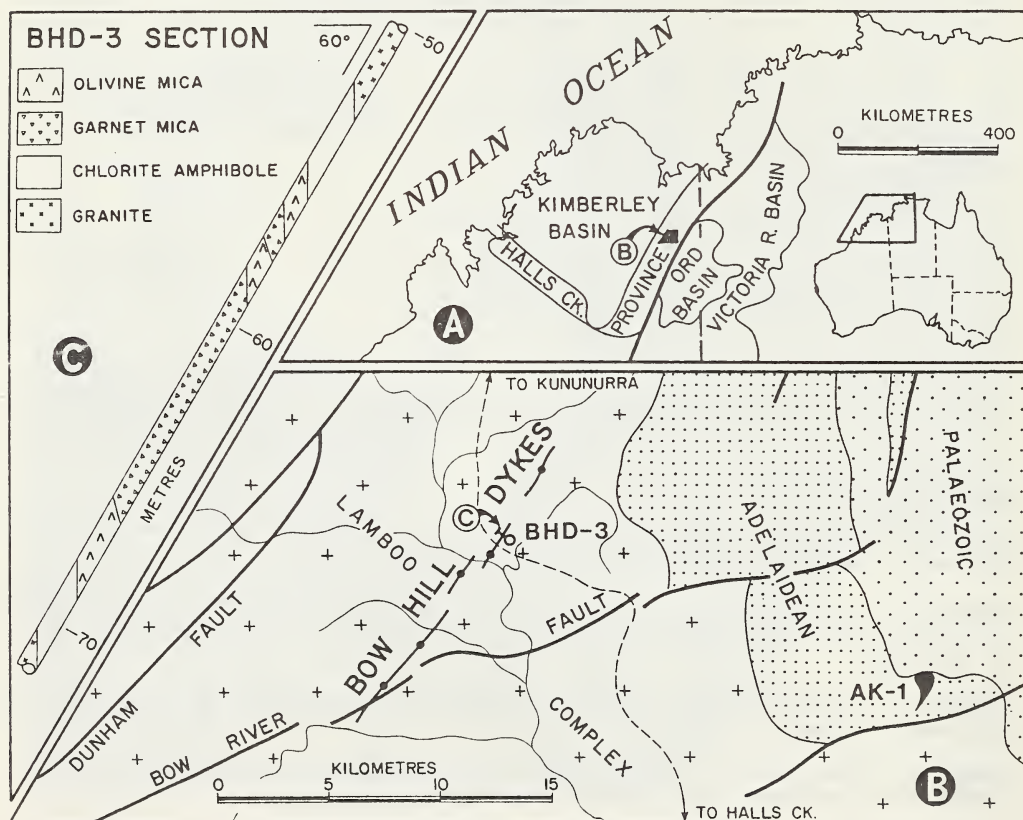
D.C. Fielding¹ and A.L. Jaques²

1. CRA Exploration Pty Ltd, Kununurra, Western Australia, 6743.

2. Bureau of Mineral Resources, GPO Box 378, Canberra, ACT, 2601.

The Bow Hill dykes, a swarm of micaceous ultramafic and mafic lamprophyres, occur at long. 128° 13' E, lat. 16° 43' S, some 125km SW of Kununurra and 22 km W of the Argyle (AK1) pipe, in the East Kimberley region of Western Australia (Fig. 1). They were discovered by the Ashton Joint Venture in 1980 after detrital andradite garnet and lamproitic chromite were recovered in routine stream sediment sampling (Atkinson et al 1984). The suite intrudes Early Proterozoic Bow River Granite of the Lamboo Complex. Rb-Sr and K-Ar dating of phlogopites suggest an emplacement age for the dykes of 815 Ma (Pidgeon et al this volume). However, this age is approximately 100 my younger than obtained by Rb-Sr based on whole rock samples with the initial ratio (0.7057) defined by clinopyroxene separates (Sun et al this volume).

Eight individual dykes ranging in thickness from a few cms to 13m and up to 2 km long are emplaced en-echelon over a strike length of 19 km. The strike direction is NNE and sub-parallel to the major structures within the Halls Creek Mobile Zone such as the Dunham Fault (Fig. 1). Exposures are poor and the dykes deeply weathered. The dykes are surrounded by a marked fenite zone up to several meters wide in which chlorite and alkali amphibole are conspicuous. Alteration farthest from the dykes



consists of sericitisation of feldspar and replacement of mica in the granite by chlorite. Closer to the contact alteration is more intense with extensive development of alkali amphibole, in most cases pale magnesio-arfvedsonite. In the most strongly altered zones the granite is cut by numerous veinlets composed of strongly zoned clinopyroxene, alkali amphibole and alkali feldspar (see below), and alkali amphibole and chlorite are widespread.

Three main rock types are present in the dykes: 1) fine-grained ultramafic contact zone rocks at the margins of the dykes containing abundant chlorite, sodic amphibole, alkali feldspar and, commonly, alkali pyroxene; 2) ultramafic olivine-phlogopite lamprophyre, and 3) garnet-phlogopite pegmatite. The olivine-phlogopite lamprophyre consists of abundant coarse serpentinitised olivine and large plates of pleochroic mica together with granular to prismatic clinopyroxene and lesser amounts of carbonate, apatite, dark red brown perovskite, spinel, trace rutile and Mn-ilmenite, and richteritic amphibole, commonly replacing pyroxene. The ultramafic olivine-phlogopite lamprophyre grades into and in places is cut by segregation veinlets containing abundant prismatic diopside strongly zoned to green aegirine-augite together with apatite, calcite, clinozoisite and sphene. These rocks are petrologically similar to those found at the contact and in veins some of which, in addition to the zoned pyroxene and epidote, contain abundant interstitial alkali feldspar. The garnet-phlogopite pegmatites, which are in places banded, occur both near the margins and in the inner portions of the dykes. The relative proportions of the garnet-phlogopite pegmatite and olivine-phlogopite lamprophyre are uncertain: drilling showed that in one dyke the pegmatite occupied the entire central portion of the dyke and and comprised nearly half of the dyke (Jaques et al 1986). The pegmatites are coarsely crystalline and composed of abundant phlogopite up to 4 mm long and large (up to 1 cm) anhedral, poikilitic garnet which displays spectacular zoning from dark red-brown melanite cores through to colourless andradite rims. Other phases present include diopsidic clinopyroxene, carbonate, apatite, clinozoisite, sphene, and richteritic amphibole.

Microprobe analyses show the olivines are highly magnesian ($Mg_{92-92.8}$). The micas show a wide range of compositions from rare Ti-rich biotite cores (Mg_{62-66} , 6 wt % TiO_2) to more typical Al-rich phlogopite (13-15 wt % Al_2O_3 , Mg_{89-76}) with variable TiO_2 contents (0.2-3.6 wt %) to thin rims of tetraferriphlogopite with low Ti and Al. The pyroxenes range from Na-Al-poor diopside microphenocrysts to aegirine-augite (up to 6 wt % Na_2O). The spinels range from titaniferous chromite with up to 55 wt % Cr_2O_3 through to more abundant Mg-poor titaniferous magnetite. Ilmenite is a late-formed accessory and contains up to 12 wt % MnO. The groundmass garnets show a wide range in composition and zoned from melanite-schorlomite cores with up to 14 wt % TiO_2 and appreciable Zr and Nb to andradite rims with less than 1 wt % TiO_2 . The amphibole is pale to colourless richterite with up to 1.6 wt % K_2O .

Macrocryst minerals recovered from concentrates include chrome spinel, garnet, chrome diopside, and rare enstatite. The chrome spinels range in composition from magnesian aluminous chromite (up to 40 wt % Al_2O_3) through to magnesiochromite with up to 60 wt % Cr_2O_3 . The garnets are dominantly chrome pyropes (2-6 wt % Cr_2O_3) and calcic pyrope almandines belonging to Dawson and Stephens (1975) cluster groups 9 and 3. The chrome diopsides contain up to 1.8 wt % Cr_2O_3 and have moderate Al_2O_3 contents (1.5-3 wt %). No diamond was recovered in the bulk sampling program.

The Bow Hill dykes show a wide range in composition. The olivine phlogopite lamprophyres are ultrabasic (40-44 wt % SiO_2) and rich in MgO (20-22 wt %) with high Ni and Cr contents (900-1300 ppm). They are mildly peralkaline and contain a little nepheline, leucite and acmite in their CIPW norm. The garnet-phlogopite pegmatites are poorer in MgO (15-5 wt %) and richer in CaO (13-25 wt %) and Al_2O_3 (7-10 wt %). All have high K_2O/Na_2O ratios (5-20) with K_2O contents ranging up to 5.5 wt % in the olivine phlogopite lamprophyres.

The Bow Hill dykes, particularly the garnet-phlogopite pegmatites, are enriched in incompatible elements, particularly Ba, Rb, Ti, Nb, and F. Trace element abundance ranges in the olivine-phlogopite lamprophyres are: Ba = 2500-3000 ppm, Rb = 250-350 ppm, and Zr and Nb = 70-130 ppm, whereas comparable ranges in the garnet-phlogopite pegmatites are: Ba = 4500-5500 ppm, Sr = 500-3000 ppm, and Zr and Nb = 40-1000 ppm. F contents lie in the range 0.4 to 0.65 wt %. Features of the Bow Hill dykes are their

very low Zr/Nb ratios and very high Rb/Sr ratios in the olivine phlogopites (both near 1). Zr contents decrease from olivine-phlogopite lamprophyre to the garnet-mica pegmatite, reflecting crystallisation of Zr-rich garnet. The Bow Hill dykes are strongly enriched in LREE (200-700x chondrites) and have highly fractionated REE patterns with very low abundances of Sc (10-25) and HREE (3-5x chondrites) similar to kimberlites.

Both kimberlites (Maude Creek, Devil's elbow) and lamproites (Argyle, Lissadell Road dykes) are known from the East Kimberley region (Atkinson et al 1984; Jaques et al 1986). The Bow Hill dykes display petrologic and geochemical differences to both, notably in the association of fenite and the presence of sodic amphibole and pyroxene, melanitic-andraditic garnet, sphene, and clinozoisite. The dykes have many of the petrologic features of ultramafic lamprophyres (Rock 1986), particularly aillikites rather than alnoites since melilite is lacking, but are not as silica undersaturated. They are also richer in MgO and K₂O and have higher K/Na ratios than is typical of most ultramafic lamprophyres, and therefore lie between micaceous kimberlite and ultramafic lamprophyre. The Bow Hill dykes, nevertheless, possess many of the features of ultramafic lamprophyres and, like them, are considered to have affinities with lamprophyre-carbonatite suites. In particular, similarities in age and Nd isotopic composition (Bow Hill ϵ_{Nd} at 900 Ma = +2, Sun et al this volume) suggest that the Bow Hill dykes may be related to the Cummins Range carbonatite (Andrews et al this volume) which lies some 350km to the south at the intersection of the Halls Creek and King Leopold Mobile Zones. The distribution and form of the Bow Hill dykes i.e. en-echelon dykes parallel to major structures, indicates a strong structural control by earlier (early Proterozoic) left-lateral faults and suggests emplacement in a tensional environment. Such an environment may have been generated locally during reactivation of the older fundamental fractures or, alternatively, the reactivation might be associated with limited crustal extension at the eastern and northern margins of the Kimberley craton.

ACKNOWLEDGEMENTS

We thank CRAE Pty Ltd for permission to publish, B.W. Chappell for the INAA analyses, and C.B. Smith for his interest. ALJ publishes with the permission of the Director, Bureau of Mineral Resources.

REFERENCES

- ATKINSON W.J., HUGHES F.E. and SMITH C.B. 1984. A review of the kimberlitic rocks of Western Australia. In Kornprobst J. ed, *Kimberlites 1: Kimberlites and Related Rocks*, pp. 195-224. Elsevier, Amsterdam.
- DAWSON J.B. and STEPHENS W.E. 1975. Statistical analysis of garnets from kimberlites and associated xenoliths. *Journal of Geology* 83, 589-607.
- JAQUES A.L., LEWIS J.D. and SMITH C.B. 1986. The kimberlitic and lamproitic rocks of Western Australia. *Geological Survey of Western Australia Bulletin* 132.
- ROCK N.M.S. 1986. The nature and origin of ultramafic lamprophyres: alnoites and allied rocks. *Journal of Petrology* 27, 155-196.

Alok K. Gupta¹, Kenzo Yagi², J. Lovering³ and A. L. Jaques⁴

1. Department of Geology and Geophysics, University of Allahabad, U. P. India
2. Department of Geology, Hokkaido University, Sapporo, Japan
3. Department of Geology, University of Melbourne, Victoria, Australia
4. Petrology Division, Bureau of Mineral Resources, Canberra, Australia

INTRODUCTION

There are five kimberlite bodies in and around Lattavaram (14°55'30"N, 77°17'30"E) and Wajrakharur, and one near Muligiripalli (14°51'N, 77°18'30"). Wajrakharur is located 9 km NNE of Lattavaram, whereas Muligiripalli lies 15 km west of Wajrakharur. All these localities are in Anantapur district of Andhra Pradesh, south India.

An ultramafic intrusive, allegedly containing diamond occurs at Chelima (15° 26' N, 78° 42' E) also in south India.

There are three kimberlite pipes near Panna (24°40'N, 80°12'E) in the state of Madhya Pradesh, central India: (1) one at Majhgawan, 20 km south of Panna, (2) one at Hinota about 3.5 km northwest of Majhgawan and (3) the third one occurring 65 km south of Majhgawan.

Kimberlites from Wajrakharur, Anantapur District

Of the three pipes present in Wajrakharur, one lies just north of Wajrakharur village (P-1, areal extent: 1010x180m², oval-shaped, trending N60°E). The second one (P-2, areal extent 180x70m², sickle shaped) is located in the same village. The third one (P-6, not exposed; projected areal extent 240x260 m²) is situated 2 km west of the first one (P-1). Two pipes are located at a distance of 1 km (P-3) and 1.6 km (P-4) east of Lattavaram village. One of the pipes (P-3, crescent-shaped, trend, E-W) has an areal extent of 120x40m². Both these pipes often include large megacrysts of olivine (up to 10 cm and 6 cm) and granitic xenoliths. The pipe at Muligiripalli is massive and extended over an area of 240x45m² and trend N75°E (P-5).

The chemical analyses of these ultramafic pipes are given in Tables 1 and 2. Detailed studies on the Wajrakharur kimberlites are in progress, but the analyses of the opaque phases (P-1) show that this pipe is characterised by two types of chromian spinels. The first is Mg-rich [Mg/(Mg + Fe) = 0.6] with high Cr content [Cr/(Cr + Al) = 0.79] and low concentration of Ti and without Fe³⁺ appears to be a mantle product, whereas the other one (a titaniferous chromite, poor in Mg, Al and enriched in Fe) presumably crystallised later in the kimberlitic melt. The Mg-rich ilmenite present as xenocryst in P-1, is a high pressure product. Two garnet xenocryst in P-1, is a high pressure product. Garnet xenocrysts occur in P-1 and P-6. Most are chrome pyropes belonging to garnet cluster group 9 of Dawson and Stephens but some Ti-pyropes (group 1) are also present.

The Lattavaram kimberlite is characterised by the presence of phenocrysts of olivine (Fa_{7.26-9.53}), phlogopite (MgO:26.63%, FeO:7.88%, TiO₂:1.69%) and chromian spinel [(Mg_{0.52+0.03} Fe_{0.49+0.03})(Cr_{1.37+0.08} Al_{0.47+0.03} Ti_{0.07+0.02})O₄] set in a groundmass of ankerite, perovskite, phlogopite, diopside and magnetite.

The Muligiripalli kimberlite contains phenocrystal olivine (Fa_{15.04-16.15}) and phlogopite (FeO:10.15%, TiO₂:1.97%, MgO:23.23%) in a groundmass of clinopyroxene (salite to diopside), K-richterite (K₂O/Na₂O ratio = 13), perovskite, calcite, phlogopite and serpentine. Studies of Kushiro and Erlank (1970) indicate that in presence of garnet, K-richterite is not stable even at 1000°C and 20 kb. It is noteworthy that garnet is absent from the Muligiripalli rock. The assemblage K-richterite, phlogopite + diopside + calcite noted in this pipe may be a low pressure product and is represented under higher pressures by the assemblage, olivine + enstatite + garnet + diopside₂ + fluid (containing H₂O, CO₂, K₂O, etc; Erlank and Rickard, 1977).

Majhgawan Pipe, Madhyapradesh

The Majhgawan pipe (7) occurs as a funnel-shaped body intruding into Kaimur sandstone, and was emplaced 910-940 (+30) Ma. The pipe is elliptical in cross section, trending N 30° E covering a distance of 360m, with a maximum width of 235m.

The pipe is characterised by serpentine (pseudomorphous after olivine), phenocrystal phlogopite (FeO:5.24-5.29; MgO:21.86; TiO₂:5.69-7.46%, MgO:21.20-21.86%) in a groundmass of rutile, titanomagnetite, calcite, phlogopite and serpentine. Reference to the study of Buddington and Lindsley (1964) suggests that the titanomagnetite with 15 mole % ulvospinel with ilmenite intergrowth, crystallised at 550°C under FMQ buffer. It is concluded that the talc and the carbonate phase present in the groundmass was formed by reaction between forsteritic olivine with a CO₂ and H₂O-rich vapour phase, under near surface condition at a temperature of 450 ±25°C. The chemistry of the Majhgawan pipe is summarised in Tables 1 and 2.

Chelima Dyke

The ultramafic dyke at Chelima trends WNW-ESE and intrudes a rock sequence of Upper Precambrian quartzite and shale intercalated with limestone, dolomite and cherts. Based on ancient workings within the pipe, it is speculated that the dyke was mined for diamond in the past (Sen and Rao, 1967).

A compositional plot of the Chelima dyke in a MgO-Al₂O₃-FeO diagram shows that it lies in the lamproite field, whereas the other ultramafic rocks under investigation plot in the kimberlite field. Major and minor element chemistry of the rocks are summarised in Tables 1 and 2. Bergman and Baker (1984) also consider the Chelima dyke to be carbonated lamproite.

The dyke from Chelima is characterised by phenocrystal olivine (now altered to serpentine), phlogopite (FeO:7.25-11.41%, TiO₂:4.60-5.44%) and chromium spinel set in a groundmass of rutile, serpentine, ankerite (CaO:25.08-29.29%, FeO: 7.48-8.43%, MgO:13.30-17.38%), phlogopite and pyrite. Crystallisation of primary serpentine in the groundmass is considered to be due to a reaction between talc and magnesite at a temperature of 350° ±25°C under near surface condition.

Composition of volatile phase in the kimberlites and the lamproite

Textural studies indicate that the carbonate phase in all the Indian kimberlites precipitated at a late stage. Experimental studies of Eggler and Wendlandt (1979) on an average kimberlite composition under 55 kb in presence of a volatile with variable CO₂/(CO₂+H₂O) suggests that such a late stage precipitation of the carbonate phases should take place when this ratio is 0:1. Study of Kerrick on stability or serpentine suggests that in cases of Indian kimberlites, the ratio of CO₂/(CO₂+H₂O) in the volatiles might have been 0.05 so that serpentine could crystallise in the groundmass at a late stage.

P-T and fO₂ conditions of crystallisation

Thermodynamic calculation based on partitioning of Mg and Fe between olivine and chromian spinel in the Lattavaram kimberlite (P-3) suggests a temperature of equilibration between 1090 and 1220°C. This temperature range corresponds to the solidus of an average kimberlite composition (Eggler and Wendlandt, 1979) at pressures between 52-60 kb. The intersection of the Lesotho geotherm (Boyd, 1973) with the solidus of an average kimberlite composition (Eggler and Wendlandt, 1979) occurs at 52 kb and 1130°C, which is within the temperature range calculated for the Lattavaram kimberlite. The point of intersection of the CCO buffer line with the FMQ and MW buffer was considered by Rosenhauer et al (1977) to be the diamond facies region. When the temperature range of 1090-1220°C is plotted in this diamond facies region, the fO₂ condition of crystallisation is estimated to be between 10⁻⁷ and 10⁻⁸ bar.

Petrogenetic model

If a lherzolitic mantle (containing 50-60% olivine, 10-15% orthopyroxene, 25-30% clinopyroxene and 10 to 15% garnet, all in volume percentage) is assumed for peninsular India, then using the REE partition coefficients given by Frey et al (1978), it is estimated from thermodynamic calculation (Haskin, 1982) that 1.1 to 1.5% melting of such mantle materials can account for the observed abundance of La, Ce and Nd in the alkali-rich liquid fraction of the ultramafic rocks. The liquid crystallised during the ascent of the crystal-fluid mush. Most of the phenocrysts represent pre-fluidised product from the mantle.

REFERENCES

- BUDDINGTON, A. F. & LINDSLEY, D. H., 1964. Iron-titanium oxide minerals and synthetic equivalents. *J. Petrol.* 5, 310-337.
- BERGMAN, S. C. & BAKER, N. R., 1984. A new look at the Proterozoic dyke from Chelima and Andra Pradesh, India: diamondiferous lamproite? *Geol. Soc. America Abstracts*, 444.
- EGGLER, D. H. & WENDLANDT, R. F., 1979. Experimental studies on the relationship between kimberlite magmas and partial melting of peridotite. In: kimberlites, diatremes and diamonds, their geology, petrology and geochemistry (ed. F. R. Boyd, H. O. A. Meyer). *Am. Geophys. Union.* 1, 330-358.
- ERLANK, A. J. & RICKARD, R. S., 1977. Potassic richterite-bearing peridotite from kimberlite and evidence to provide upper mantle metasomatism. *Abstr. 2nd Internat. Kimberlite Confer. held at Santa Fe, USA.*
- FREY, F. W., GREEN, D. H. & ROY, S. D., 1978. Integrated models of basalt petrogenesis: a study of quartz tholeiites to olivine melilitites from south eastern Australia utilising geochemical and experimental petrological data. *J. Petrol.* 19, 463-513.

Table 1
Chemical analyses of Indian kimberlites
from Anantapur district

	1	2	3	4	5	7	8
SiO ₂	43.22	33.40	32.95	39.30	34.16	33.69	40.08
TiO ₂	1.44	2.47	4.45	1.41	4.52	6.04	5.21
Al ₂ O ₃	5.01	5.78	3.59	3.57	3.74	3.28	3.99
Fe ₂ O ₃	4.47	8.48	7.38	4.88	12.99	-	-
FeO	2.94	2.90	5.83	4.49	-	10.98	9.76
MnO	0.20	0.20	0.19	0.14	0.19	0.11	0.11
MgO	15.70	17.38	20.63	29.44	20.51	24.40	15.93
CaO	20.07	17.41	12.05	7.11	12.68	3.78	7.51
Na ₂ O	0.12	0.74	0.32	0.21	0.43	0.11	0.06
K ₂ O	0.04	1.70	1.12	0.92	1.11	0.86	2.41
P ₂ O ₅	0.90	0.95	0.86	0.42	0.91	2.65	1.41
SO ₃	<0.01	0.19	0.16	0.03	0.18	1.66	0.11
BaO	0.08	0.32	0.18	0.14	0.18	3.05	0.17
Cr ₂ O ₃	0.10	0.14	0.15	0.21	0.13	0.17	0.07
NiO	0.06	0.06	0.11	0.17	-	-	-
Rb ₂ O	<0.01	0.02	0.01	0.01	-	-	-
SrO	0.07	0.17	0.12	0.06	-	-	-
ZrO ₂	0.03	0.04	0.07	0.02	7.20	8.12	11.94
I.L.	5.77	7.25	9.93	7.74	-	-	-
Sum	100.22	99.60	100.10	100.27	98.93	98.90	98.76

Table 2
Trace element geochemistry
of kimberlites and a lamproite

	3	5	7	7	8
Sc	10	19	21	23	18
V	82	237	55	80	93
Co	85	85	70	73	68
Ni	1357	779	1059	1017	538
Cu	54	114	42	91	33
Zn	79	79	80	84	72
Rb	106	147	76	80	137
Sr	680	996	1835	2035	1223
Y	14	23	35	48	41
Zr	147	388	1079	1033	958
Nb	87	138	214	214	237
La	417	778	410	382	1721
Ce	116	239	826	801	563
Nd	43	105	361	347	235
Ca	7	13	15	27	13
Th	13	21	15	*	27
Pb	9	13	41	353	6

3, 5, 7 and 8 refer to pipe 3 and 5 in and around Wajrahur; 7 and 8 designate pipes in Majhawan and Chelima, respectively

1, 2, 3, 4 and 5 represent pipes P₁, P₂, P₃, P₄ and P₅ respectively
7: Majhawan pipe, 8: Chelima dyke. I.L.: ignition loss

D.C. Hall, H. Helmstaedt, and D.J. Schulze

Dept. of Geological Sciences, Queen's University
Kingston, Ontario, Canada K7L 3N6

The Cross kimberlite is one of about forty diatremes located along the western edge of the Paleozoic carbonate platform in the Front and Main ranges of the Rocky Mountains in southeastern British Columbia, Canada. The Cross diatreme is the only one of this group that has been recognized as a kimberlite (Roberts et al., 1980). It outcrops on a steep south-facing slope at an elevation of 2200 m, and has an exposed diameter of approximately 70 m. It has intruded carbonates of the Permo-Carboniferous Rocky Mountain Group that, in the vicinity of the diatreme, are generally flat-lying. The contacts are steeply dipping, and although the wall rocks show no evidence of thermal alteration, the carbonate beds are locally distorted along the eastern margin. The diatreme appears to have been deformed together with the country rocks, which are part of the Bourgeau thrust sheet.

Phlogopite separates have been dated by the Rb/Sr method and have yielded an Upper Permian age (Smith, 1983). Thus the diatreme is older than the deformation which formed the Rocky Mountains, and suggests that it has been thrust eastwards relative to the mantle and basement through which it intruded. Palinspastic reconstruction suggests that the horizontal displacement may be in excess of 100 km (Norris, 1965).

Throughout, the kimberlite consists of phlogopite and serpentinized olivine macrocrysts in a matrix of calcite, serpentine, and fine-grained (<120 microns) opaque oxides (rutile, ilmenite, and spinel), sulphides, and apatite. Fresh olivine has not been observed. Serpentinized olivine relics commonly possess carbonated cores. Xenoliths of serpentinized peridotite and sedimentary rock are common, as are spinel xenocrysts. Also observed, although not as abundant, are garnet lherzolite and glimmerite xenoliths, and garnet xenocrysts.

Several kimberlite phases have been recognized. The central portion of the outcrop is occupied by a friable, tuffisitic kimberlite breccia. The eastern and western extremities contain massive kimberlite. A phlogopite-rich, sub-vertical dyke, approximately 20 cm wide, has intruded the central breccia. The northern margin of the outcrop contains massive kimberlite which is distinctly red-spotted, due to hematite staining.

The eastern massive phase (EMP) is a serpentine-calcite macrocrystic kimberlite. Phlogopite macrocrysts have ragged margins, and are rimmed by very fine-grained opaque oxides. The cores of some micas are biotite, which are sharply transitional to the phlogopite rim. Groundmass spinels are zoned and may be rimmed by ilmenite or sulphide, which also occur as discrete grains. Skeletal rutile grains are common. Serpentinized peridotite xenoliths are abundant in this phase.

The western massive phase (WMP) is also a serpentine-calcite macrocrystic kimberlite, however phlogopite macrocrysts are more abundant, and the occurrence of biotite cores is widespread. Narrow rim zones exhibit reverse pleochroism. Groundmass opaque grains are predominantly ilmenite and skeletal rutile. Zoned spinels and sulphides also occur. Ilmenite also occurs as rims on rutile and spinel. Serpentinized peridotite xenoliths are not as common as in the EMP.

The central breccia (CB) is a calcite tuffisitic kimberlite breccia. Fragments of shale, limestone, and kimberlite locally comprise up to 50% of the rock volume. Relics of olivine possess thin talc rims. Phlogopite macrocrysts are virtually absent. Groundmass opaque minerals are predominantly rutile and sulphide. Ilmenite is absent. Spinels are rare, and are commonly rimmed by rutile or sulphide.

The dyke (D1) is a phlogopite-serpentine macrocrystic kimberlite. Macrocrysts are more abundant than in the EMP and WMP. Phlogopite macrocrysts are short and stubby, and many have biotite cores. Reversely pleochroic rims occur on some grains. Groundmass opaque grains are predominantly skeletal rutile and zoned spinel. Ilmenite occurs as discrete grains and as rims on spinel, and may in turn be rimmed by sulphide. Xenoliths are virtually absent, although spinel xenocrysts are moderately abundant.

The hematite-stained, red-spotted phase (RSP) is a opaque-mineral-rich serpentine macrocrystic kimberlite. Phlogopite macrocrysts are euhedral, and biotite cores are rare. Reversely pleochroic rims are absent. Weathering has produced many small hematite patches, generally less than 2 cm in diameter. These are mainly associated with peridotite xenoliths and olivine macrocrysts, but also partially replace the groundmass. Groundmass opaque grains are predominantly rutile and zoned spinel. Ilmenite and sulphide are rare. Rutile occurs as discrete grains and as rims on spinel, and may itself be rimmed by spongy magnetite haloes.

Eroded material down-slope contains boulders of a friable, phlogopite-serpentine tuffitic kimberlite breccia (BB). Clasts consist primarily of sedimentary fragments, as well as serpentinized peridotite xenoliths. Unlike the CB, this breccia contains abundant, spherical kimberlite accretionary pellets averaging 2 cm in diameter. Most of these pellets accreted on nuclei of sedimentary xenoliths. Accretionary kimberlite growth also occurs on olivine relics. In sharp contrast to the CB, phlogopite macrocrysts are abundant. Both the macrocrystic and groundmass phlogopite commonly possess reversely pleochroic rims. Groundmass opaque grains are predominantly ilmenite, which also rims rutile. Spinel is not common, and sulphide is observed only in the cores of olivine relics.

Large accretionary pellets up to 6 cm in diameter occur in boulders of massive kimberlite (ARP) that are similar in appearance to the EMP but are not found in outcrop. The pellets accreted on nuclei of serpentinized peridotite xenoliths. The pelletal phase is a phlogopite-calcite macrocrystic kimberlite. Macrocrysts are not as abundant as in the host phase. Phlogopite is abundant in the groundmass, and is reversely pleochroic. Opaque grains in the groundmass are predominantly skeletal rutile. Zoned spinel and ilmenite are also abundant, but sulphides are virtually absent. The ilmenite is commonly rimmed by rutile.

The dark, strongly pleochroic cores of mica macrocrysts are mainly biotites ($mg=0.30-0.88$) with low chromium contents (<0.3 wt.% Cr₂O₃) and a wide range of titanium contents (1.8-5.2 wt.% TiO₂). These resemble the Type I micas noted in several South African kimberlites by Smith et al. (1978), who suggested that they may be derived from a related precursor intrusion. Pale phlogopite rims on the dark cores have a restricted mg (0.83-0.88), and are chrome-free. Pale mica macrocrysts that lack biotite cores, and pale, normally pleochroic groundmass grains are more magnesium-rich ($mg=0.88-0.90$) and contain >0.6 wt.% Cr₂O₃. Reversely pleochroic micas, which are found as rims on some macrocrysts and in the groundmass of the ARP pellets and the BB kimberlite, are characterized by low silica contents, and partial substitution of barium for potassium.

Ilmenites are magnesium-poor (<1.2 wt.% MgO) and manganese-rich (2.4-10.4 wt.% MnO). Calculated ferric iron contents are low. Niobium is detected, but has not been determined quantitatively. Thus, they are not typical of kimberlite ilmenites as defined by Mitchell (1979), but they are compositionally similar to ilmenites from carbonatites and carbonate-rich rocks in kimberlites (Gaspar and Wyllie, 1984). Rutile contains detectable niobium and tantalum.

Zoning is common in the fine-grained groundmass spinels. All are aluminum-poor. A compositional trend extends from titaniferous magnesian chromite towards magnesian ulvospinel - magnetite (Fig. 1). The latter occur both as rims on the former, and as discrete grains. This trend is similar to that developed in the groundmass spinels of the Koidu kimberlite dykes in Sierra Leone (Tompkins and Haggerty, 1985). In the D1 kimberlite, the latter stages of this trend are accompanied by magnesium depletion. Mantles of magnesian titaniferous magnetite are developed on the spinels in the ARP, RSP, and D1 kimberlite.

Spinel of separate kimberlite phases are distinguishable by their Mg and Al contents. Within each phase, the number of Mg and Al ions per formula unit is relatively invariant (with the exception of the Mg depletion noted in D1), despite the increases in Fe and Ti, and the decrease in Cr. Thus, in a Mg vs. Al cation-cation plot, the spinels of each phase occupy a restricted field. These fields are slightly overlapping, and define an overall trend of decreasing Mg as Al decreases (Fig.2), which suggests that the several phases of the diatreme may represent separate intrusions drawn from a single fractionating source.

References

Gaspar, J.C. and Wyllie, P.J. 1984. The alleged kimberlite-carbonatite relationship: evidence from ilmenite and spinel from Premier and Wesselton Mines and the Benfontein Sill, South Africa. *Contributions to Mineralogy and Petrology* 85, 133-140.

Mitchell, R.H. 1977. The alleged kimberlite-carbonatite relationship: additional contrary mineralogical evidence. *American Journal of Science* 279, 570-589.

Norris, D.K. 1965. Stratigraphy of the Rocky Mountain Group in the southeastern cordillera of Canada. *Geological Survey of Canada Bulletin* 125.

Roberts, M.A., Skall, M. and Pighin, D.L. 1980. Diatremes in the Rocky Mountains of southeastern B.C., (abstract). *Canadian Institute of Mining Bulletin* 73, 74-75.

Smith, C.B. 1983. Rubidium - strontium, uranium - lead and samarium - neodymium isotopic studies of kimberlite and selected mantle-derived xenoliths. Unpublished Ph.D. thesis, University of the Witwatersrand, Johannesburg.

Smith, J.V., Brennesholtz, R. and Dawson, J.B. 1978. Chemistry of micas from kimberlites and xenoliths - I. Micaceous kimberlites. *Geochimica et Cosmochimica Acta* 42, 959-971.

Tompkins, L.A. and Haggerty, S.E. 1985. Groundmass oxide minerals in the Koidu kimberlite dikes, Sierra Leone, West Africa. *Contributions to Mineralogy and Petrology* 91, 245-263.

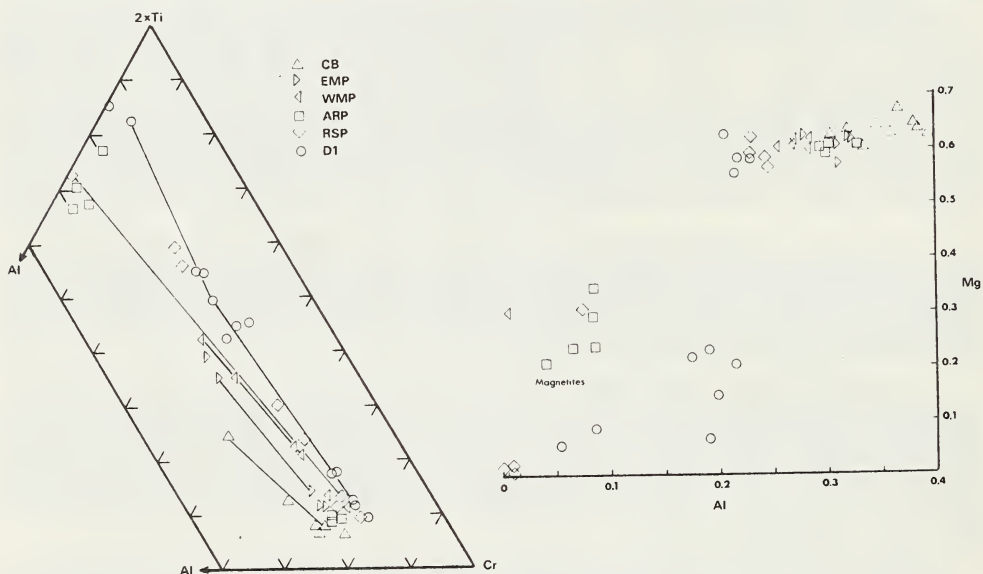


Figure 1 (left). Al-Cr-(2xTi) plot of groundmass spinel compositions. The tie lines connect cores (lower right) to rims (upper left) of selected analyses. Some analyses are omitted for clarity.

Figure 2 (right). Mg vs. Al cation-cation plot of groundmass spinel compositions, based on four oxygens per formula unit. Symbols as for Fig. 1. The aluminum-poor spinels (<0.1 Al p.f.u.) are magnetites.

B. Carter Hearn, Jr.

U.S. Geological Survey, 959 National Center, Reston, VA 22092, USA

The extent of genetic relationships among kimberlites, carbonatites, alnoites, and other rare alkalic igneous rocks continues to be an important field of research and speculation. Compositions of groundmass spinels have been cited as definitive indicators for separating true kimberlites from alnoitic and other non-kimberlitic rocks (Mitchell, 1986). Igneous rocks and related breccia-facies occurrences in a stable cratonic setting in the Missouri River Breaks area of north-central Montana provide geochemical evidence for a continuum of compositions between alnoitic rocks and kimberlitic rocks (here referred to as kimberlites) that are closely similar to true kimberlites in contents of major and trace elements, including the rare earths (REE), and contain groundmass spinels that are transitional between alnoitic and true kimberlitic spinels. In addition, the Missouri Breaks rocks provide evidence for late-stage carbonatitic derivatives that have similarities to isolated carbonate-rich mica peridotite intrusions in east-central Montana. All of the occurrences are known or inferred to have been emplaced during the middle Eocene, 46 to 51 Ma, following a longer span of mafic alkalic and felsic alkalic igneous activity from late Cretaceous to middle Eocene time in several nearby igneous centers, and preceding the 27 Ma old lamproite at Smoky Butte 120 km to the southeast (Marvin et al, 1980).

Diatremes and intrusions in the Missouri River Breaks area consist of alnoite (ALN) (= turjaite, melilite-bearing), monticellite peridotite (MoP) (melilite-free), carbonate-rich mica peridotite (CMiP), kimberlite (KI) (phlogopite-calcite-serpentine KI), and rare carbonatite (CAR), which tend to show a continuum of major- and trace-element compositions. Ranges of MgO content (ALN, 10-25; MoP and CMiP, 19-31; KI 23-32 wt percent) overlap, as do the fields of major-element oxides versus MgO, except for CaO and SiO₂ which show adjacent but offset ALN and MoP-CMiP fields. The Williams Ranch KI values plot close to or within most MoP oxide fields, but have higher K₂O (fig. 1) and P₂O₅. Compositional trends among intrusions and within single intrusions suggest that the major control is the addition/subtraction of Fo 80-90 olivine, with subsidiary control attributable to shallow-level fractionation of phlogopite, Fe-Ti oxide, nepheline, and apatite. Montana KI and MgO-rich MoP-CMiP values plot within the general KI compositional fields defined by African, Russian, and several United States KI (Dawson, 1978; Fesq et al, 1975; Danchin et al, 1975), except for higher K₂O in Montana KI. However, the higher K₂O is similar to K₂O in phlogopite-rich African KI such as New Elands (Dawson, 1978). In Montana CAR, only Al₂O₃, Na₂O, TiO₂, and P₂O₅ are similar to some ALN.

Trace elements versus MgO also show overlapping ranges for ALN and MoP-CMiP, and for MoP-CMiP and KI, although KI tends to have higher abundances of Cs, Hf, and U than MoP-CMiP. Cr and Co are positively correlated with MgO, while many magmaphile elements show poorly defined negative correlation with MgO. The ranges of trace-element abundances of the Montana samples are similar to ranges defined by the general compositions of African, Russian, and United States KI (Mitchell and Brunfelt, 1975; Fesq et al, 1975). REE patterns for ALN, MoP, and KI are all light REE-enriched, steep, and nearly linear (La 120-600X, Lu 2-10X chondrite), with KI in the higher part of the ranges (fig. 2). CAR and CMiP patterns are also linear, more strongly light REE-enriched, and slightly steeper (La 500-1000X, Lu 4-7X chondrite). The REE abundances of Montana ALN, MoP, CMiP, CAR, and KI are all in the general world-wide KI range (Mitchell and Brunfelt, 1975; Fesq et al, 1975), but are lower than some carbonate-rich, evolved KI such as de Bruyn, South Africa (Fesq et al, 1975) (fig. 2).

The overlapping ranges of major, trace, and rare-earth elements among Montana ALN, MoP, CMiP, KI and CAR suggest a close genetic relationship by processes of magma generation and fractionation, and further suggest that the MgO-rich members are transitional to or equivalent to true kimberlites. Montana KI and some CMiP, in keeping with the continuity of ranges of chemical compositions, have groundmass spinel compositions (Table 1) that are also intermediate between those typical of alnoitic rocks and those in kimberlites from elsewhere. The mineralogical variability within

rocks classified as true kimberlites suggests that their groundmass mineralogical characteristics may overlap with other alkalic ultramafic rocks. The wide variations in late-stage conditions of emplacement, diatreme formation, and crystallization may be more important than initial differences in composition in determining the development of mineralogical characteristics of true kimberlite. The existence of a wide spectrum of related magmas of kimberlitic affinity, reinforced by the occurrences of diamond in lamproitic rocks, indicates that rock types other than kimberlite could have economic potential.

TABLE 1: Cation ratios of groundmass spinels

	Mg/(Mg + Fe)	Cr/(Cr + Al)	Ti/(Ti + Cr + Al)
Williams Ranch KI			
FeCr spinel	0.2 - 0.5	0.6 - 0.7	0.07 - 0.2
MgCr Usp magnetite	0.1 - 0.3	0.1 - 0.8	0.78 - 0.96
Macdougall Springs CMiP			
FeCr spinel	0.25 - 0.45	0.60 - 0.85	0.05 - 0.40
MgCr Usp magnetite	0.2 - 0.3	0.2 - 0.4	0.5 - 0.6

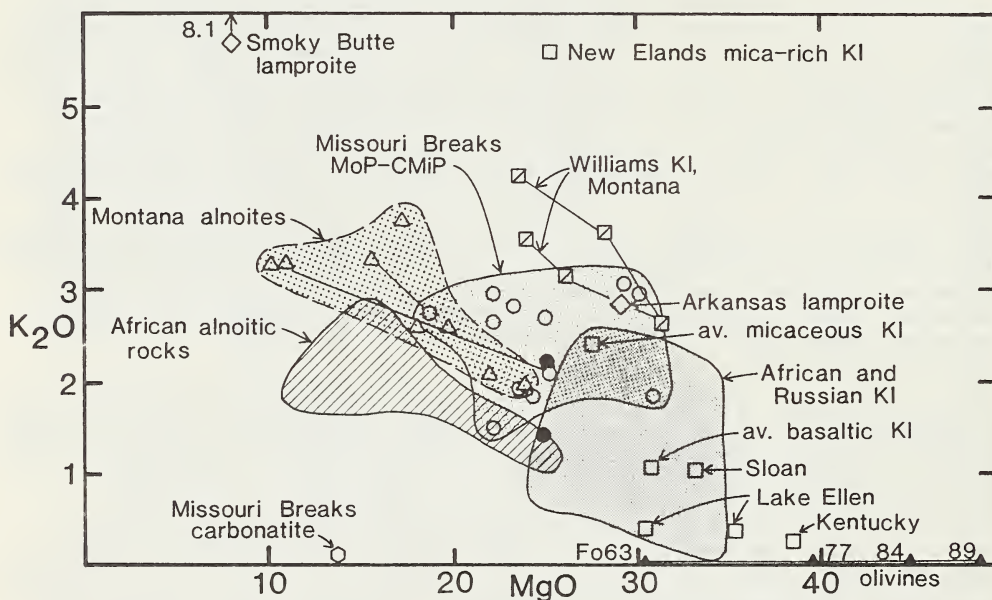


Fig. 1 K_2O - MgO variation for Montana rocks in comparison with African alnoitic rocks and African and Russian kimberlites (Dawson, 1978; Danchin et al, 1975; Fesq et al, 1975); kimberlites from the Sloan pipe, Colorado, Lake Ellen, Michigan, and Elliott County, Kentucky, USA; and lamproites from Smoky Butte, Montana, and Prairie Creek, Arkansas, USA. Olivine compositions from Fo 63 to 89 are shown on the MgO axis. Lines connect samples from the same intrusions. Triangles: Missouri Breaks alnoites; open circles: Missouri Breaks monticellite peridotites (MoP) and carbonate-rich mica peridotites (CMiP); closed circles: east-central Montana CMiP; squares: kimberlites (KI); diamonds: lamproites; hexagon: Missouri Breaks carbonatite dike.

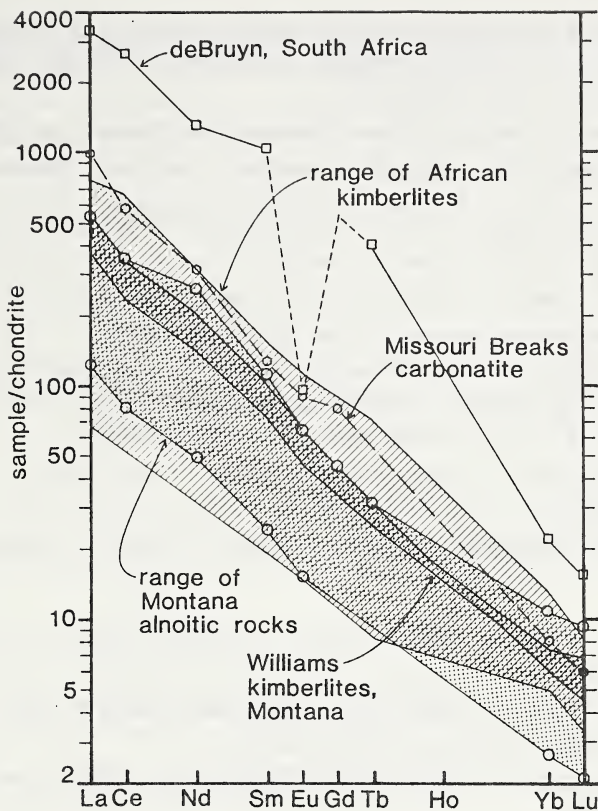


Fig. 2 Ranges of chondrite-normalized rare-earth element patterns for Montana alnoitic rocks (includes alnoites, monticellite peridotites, and carbonate-rich mica peridotites), Montana kimberlites, and a Missouri Breaks carbonatite, in comparison with the range of African kimberlites and the enriched de Bruyn kimberlite, South Africa (Fesq et al, 1975; Mitchell and Brunfelt, 1975).

DANCHIN R.V., FERGUSON J., MACIVER J.R., and NIXON P.H. 1975. The composition of late stage kimberlite liquids as revealed by nucleated autoliths. In Ahrens L.H., Dawson J.B., Duncan A.R., and Erlank A.J., eds, *Physics and Chemistry of the Earth*, Vol 9, pp. 235-245. Pergamon Press, Oxford.

DAWSON J.B. 1978. *Kimberlites and Their Xenoliths*. 252 pp. Springer-Verlag, Berlin.

FESQ H.W., KABLE E.J.D., and GURNEY J.J. 1975. Aspects of the geochemistry of kimberlites from the Premier Mine, and other selected South African occurrences with particular reference to the rare earth elements. In Ahrens L.H., Dawson J.B., Duncan A.R., and Erlank A.J., eds, *Physics and Chemistry of the Earth*, Vol 9, pp. 687-707.

MARVIN R.F., HEARN B.C.JR., MEHNERT H.H., NAESER C.W., ZARTMAN R.E., and LINDSEY D.A. 1980. Late Cretaceous-Paleocene-Eocene igneous activity in north-central Montana. *Ischron/West* 29, 5-25.

MITCHELL R.H. 1986. *Kimberlites: Mineralogy, Geochemistry, and Petrology*. 220 pp. Plenum Publishing, New York.

MITCHELL R.H., and BRUNFELT A.O. 1975. Rare earth element geochemistry of kimberlite. In Ahrens L.H., Dawson J.B., Duncan A.R., and Erlank A.J., eds, *Physics and Chemistry of the Earth*, Vol 9, pp. 671-686. Pergamon Press, Oxford.

GEOCHEMISTRY OF PORPHYRITIC KIMBERLITES IN MENGYIN COUNTY, SHANDONG PROVINCE, AND IN FUXIAN COUNTY, LIAONING PROVINCE, CHINA.

HE GUANZHI¹ AND ZHAO YUNLONG²

¹Institute of Geology, State Seismological Bureau, Beijing, China.

²Beijing Institute of Uranium Geology, Beijing, China.

Recently, the facts of open pit mining of kimberlite pipes suggest that for the kimberlite pipes in Mengyin county, Shandong province, four phenomenons are found in depth of 45-50 meters in open pit:

1. The kimberlite pipes are in irregular form;
2. The veins extending from the intruded into the wall rocks (the Archean hornblende-biotite gneisses are 2216-2545 m. y.). These kimberlite veins are connected with other veins on the surface.
3. The thickness of kimberlite-breccia on the margin of kimberlite pipes decreases;
4. In these kimberlite pipes, content of diamond and pyrope increases with depth.

Kimberlite pipe in Fuxian county, Liaoning province, exhibits following phenomena:

1. The wall rock (quartzite) of kimberlite has been baked evidently;
2. The kimberlite pipe dips at north;
3. On the excavated surface of kimberlite pipe, some veins intruded also the wall rock,

Thus, these kimberlite pipes are normal intrusive not the products of explosion.

In Mengyin and Fuxian areas, Porphyritic kimberlites contain the less exotic materials (include xenocrysts of wall rock and that from the deep crust), their chemical composition, as we analysed, is as follows: $\text{SiO}_2=30.07-37.54\%$, $\text{Al}_2\text{O}_3=1.47-5.05\%$, $\text{MgO}=23.77-35.1\%$, $\text{MnO}=0.21-0.1\%$, $\text{P}_2\text{O}_5=0.14-1.94\%$, $\text{K}_2\text{O} (0.09-2.85)\% > \text{Na}_2\text{O} (0.04-0.32)\%$; $\text{CO}_2=1.26-6.5\%$, $\text{H}_2\text{O}^+=6.8-12.8\%$; P_2O_5 , H_2O^+ and CO_2 higher than those in ultrabasic rocks, but different in relatively low TiO_2 content, and $\text{K}_2\text{O} > \text{Na}_2\text{O}$.

The chemical analysis indicates: the porphyritic kimberlites in Mengyin have REE₅ value of 0.044-0.15%, but the porphyritic kimberlites in Fuxian have their REEs value of 0.034-0.1%.

The neutron activation analysis of rare-earth and trace elements of porphyritic kimberlites in Mengyin and Fuxian counties shows: Ce=107-267 ppm, Th=15.5-38.4 ppm, Tb=0.037-0.38 ppm, Eu=2.6-4.04 ppm, Sc=8.17-17.5 ppm, Co=15.2-92 ppm, Sm=8.9-13 ppm, Lu=0.07-0.13 ppm, U=0.9-2.3 ppm, Yb=0.88-2.5 ppm, Nd=36.5-104 ppm, La=92.6-155 ppm.

This fact suggests: Sc, Co, Th is close to that of kimberlites in other parts of the world. The REEs are higher than those in ultramafic rocks and chondrites. The studied porphyritic kimberlites are relatively rich in light REEs, La/Yb=91-171. Therefore, the results of neutron activation and X-fluorescence analysis indicate that for the porphyritic kimberlites in Fuxian county, the light REEs are lower than that in Mengyin county.

According to the published data (Laul, J. C., et al., 1973, 1975), Sm/Nd ratio is 0.305 in chondrite. But the Sm/Nd ratio detected in most samples of porphyritic kimberlites is higher than that in chondrites. The Sm/Nd ratio (0.277-0.303) detected in several samples is close to that in chondrites.

All this indicates that the original kimberlitic magma chamber was located in the depth of 150-250 km and deeper in the upper mantle, and most intruded magma has been contaminated by crustal materials on its way up to the surface.

REE distribution in these porphyritic kimberlite is of a normal pattern (Fig. 1). Many samples of porphyritic kimberlites show no depletion in Eu. This fact is also found in the kimberlites from South Africa (Fieremans, M., et al., 1982). It suggests that there is no evidence of fractionation.

At the same time, the result of neutron activation analysis shows: In porphyritic kimberlites, the REEs content is highest in perovskite, and the light REEs especially concentrate in it; La, Nd, Tb and Lu are of positive value in the magnochromites, but Ce, Eu and Yb are depleted; the Nd, Tb and Lu are of positive value in the pyropes, the La, Sm and Yb are depleted; the La, Nd, Tb and Lu are of positive value in the phlogipites, and Ce, Sm and Yb are depleted. These results are determined in these minerals for REE distribution patterns.

Of course, REEs depletion is related with the mineral crystal lattice and crystal defect in these minerals, and related with the fractionation of REE. But, the possibility of REEs heterogeneity in mantle minerals can not be excluded.

A pattern of REE distribution of kimberlite-carbonatite is shown Fig. 2. It is seen that the REEs in kimberlite-carbonatite are lowest than that in porphyritic kimberlites.

Study of the porphyritic kimberlites by fission track method suggests that element uranium occurs mainly in perovskite, reaching 30-50 ppm; less

in iron colloid minerals and serpophites, reaching 15ppm; and little in ferrocalcites, apatites and on cleavage face of phylogopites, reaching <10 ppm. But uranium is not found in pyropes, no altered olivines, antigorites and enstenites (xenoliths).

The fact indicates that the kimberlitic magma in the process of its upwelling and intrusion has absorbed uranium by the above minerals. Of course, the possibility of existence of uranium in small amount in the upper mantle is not excluded.

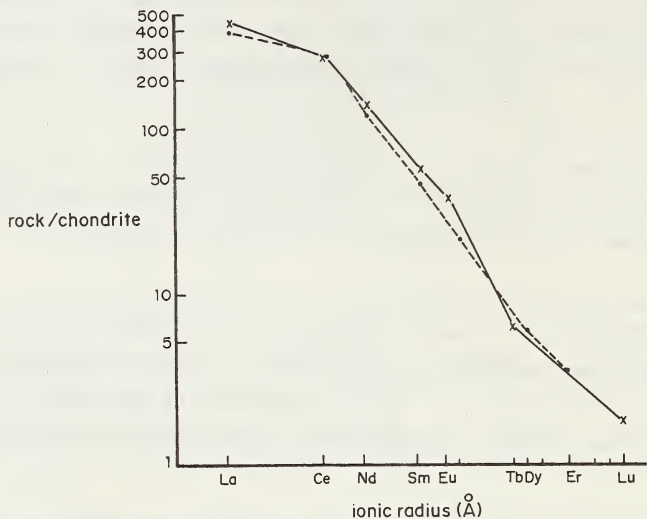


Fig. 1 A pattern of REE distribution in porphyritic kimberlite.
 x—neutron activation analysis; x—fluorescence analysis.

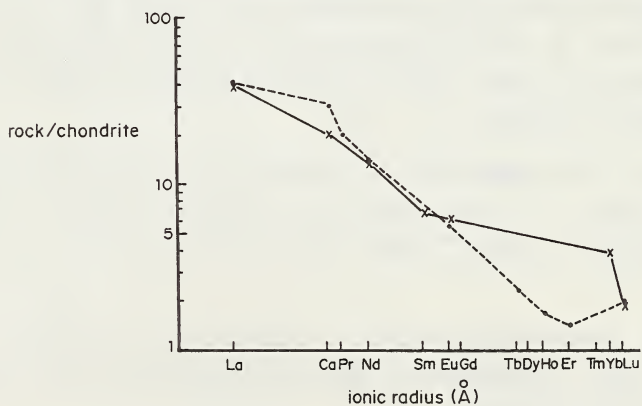


Fig. 2 A pattern of REE distribution in kimberlite-carbonatite.
 x—neutron activation analysis; x—fluorescence analysis.

CARBONATITES AND THEIR PATTERNS OF REE DISTRIBUTION IN ERDAOBIAN AND BOSHAN AREAS, CHINA.

HE GUANZHI, SHANGUAN ZHIGUAN¹ AND ZHAO YUNLONG²

¹Institute of Geology, State Seismological Bureau, Beijing, China.

²Beijing Institute of Uranium Geology, Beijing, China.

Carbonatite has been found in Erdaobian area of Zhangbei county, Hebei province. The carbonatite occurs in the form of a pipe with its long axis trending to N60-70°W, 200 m in width, and 300 m in length. It emplaced in the Tertiary Hannuoba basalt.

The Hannuoba basalt is distributed on the northern side of deep Chicheng-Shangyi fault zone. This deep fault zone extends in NW-NWW direction. Thus, the long axis of this carbonatite body is orientated principally in consistence with the Chicheng-Shangyi deep fault zone. To southwest of this deep fault zone, some ultrabasic rock bodies may be seen, they have been emplaced in the Archean metamorphic rocks.

Fresh carbonatite rock is grey-brown, and white, loose after weathering. Major minerals of this carbonatite body are calcite, has grained or radial texture; its accessory minerals are enstatite, chrom diopside, garnet, zircon, picotite, ilmenite and magnetite; but no apatite is found. Study of this carbonatite body indicates that it belongs to a calcite carbonatite type.

At the same time, in this carbonatite body some xenoliths are found, there are basalt and augite-peridotite. These xenoliths are oval or rounded, some xenoliths have 10-15 cm diameter or more.

Carbonatite has also been found in the vicinity of Boshan city, Shandong province, such as in Badao village, Dongshima and Xishima areas. Among them, one carbonatite pipe is found in Badao village, its long axis extends in N15°W direction 80 m in width, and 200 m in length. It has been emplaced in cambrian periodic limestone. In the eastern part of the pipe, carbonatite shows linear flow structure EW trend and dipping south at 65-80°. This carbonatite body is of a biotite-carbonatite type, locally contains hornblende rich biotite-granite, basalt and andesite breccia (xenoliths). Major minerals of this carbonatite pipe are calcite; and their accessory minerals are biotite (vermiculated), feldspar and quartz (xenocryst), enstatite, diopside, zircon (or baddeleyite), magnetite and olivine.

The clusters of carbonatite veins occur in Dongshima and Xishima areas southwest of Boshan city. These veins trend to N55°E, dip to NW at 8-20°, each vein is 10-40 cm wide. They have been emplaced in cambrian periodic limestone. They also contain many xenoliths, such as hornblende-biotite

garnet xenoliths. Major minerals of these carbonatite bodies are calcite, biotite, apatite, augite, zircon and magnetite.

The age of Boshan carbonatite bodies is determined to be 123-135 m.y. and Erdaobian carbonatite body is nearly late Tertiary.

Chemical composition of carbonatite in Boshan area, as we analysed, is as follows: $\text{TiO}_2=0.62-0.67\%$, $\text{MgO}=2.21-8.16\%$, $\text{Na}_2\text{O}=0.45-1.45\%$, $\text{K}_2\text{O}=1.75-4.85\%$, $\text{P}_2\text{O}_5=2.9-6.4\%$ and $\text{F}^-=0.2-0.3\%$.

Stable isotope analysis of Erdaobian shows: for two samples of fresh carbonatite, $\delta^{13}\text{C} = -7.3\%$, $\delta^{18}\text{O} = +8.5\%$; $\delta^{13}\text{C} = -5.7\%$, $\delta^{18}\text{O} = +10.1\%$; The data fall in a range of mantle carbonatitic magma. For other nine samples of carbonatite, $\delta^{13}\text{C} = -9.4--11.8\%$, $\delta^{18}\text{O} = +22.3--23.1\%$; these values are close to stable isotope value ($\delta^{13}\text{C} = -7.5--11.1\%$, $\delta^{18}\text{O} = +19.6--22\%$) incalcite from basalts (wall rock). It indicates that some carbonatitic magma came from mantle, but their major components (calcite) may be come from basaltic magma, in form of its product of late differentiation. otherwise, stable isotope analysis shows $\delta^{18}\text{O} = +5.6\%$ in enstatite, $\delta^{18}\text{O} = +5.6\%$ in chrom diopside, $\delta^{18}\text{O} = +4.1\%$ in picotite; These facts show that the carbonatitic magma in Erdaobian area came from mantle.

In Boshan area, the stable isotope analysis of carbonatites show $\delta^{13}\text{C} = +0.1\%$, $\delta^{18}\text{O} = +11.2\%$; $\delta^{13}\text{C} = -1.9\%$, $\delta^{18}\text{O} = +14.16\%$; $\delta^{13}\text{C} = -5.64\%$, $\delta^{18}\text{O} = +9.64\%$. These values indicate: $\delta^{13}\text{C} = -5.64\%$ is fitted to mantle carbonatite, but the rest values indicate that the carbonatite has been contaminated by the crustal materials on its way up to the surface.

The neutron activation analysis shows: the Erdaobian carbonatite is relatively poor in REE, the average value of four samples is as follows: La=1.05 ppm, Ce=2.3 ppm, Nd=1.33 ppm, Sm=0.38 ppm, Lu=0.12 ppm, Tb=0.07ppm, Yb=0.27 ppm, Lu=0.05 ppm. But the Boshan carbonatite is relatively rich in REE, especially in LREE. The range of REE is: La=336-1184 ppm, Ce=694-2240 ppm, Nd=254-1186 ppm, Sm=13.5-51.7 ppm, Lu=12.3-22.1 ppm, Tb=1.66-60.4ppm, Yb=3.74-6 ppm, Lu=0.18-0.68 ppm. Sm/Nd=0.286 and La/Yb=3.89 are in Erdaobian; the Sm/Nd=0.11-0.204 and La/Yb=56-316.58 are in Boshan. These Sm/Nd ratio shows: Sm/Nd ratio in Erdaobian carbonatite is about the same as chondrites Sm/Nd ratio (0.305), therefore, the carbonatite might come from mantle; Sm/Nd ratio in Boshan carbonatite is more lower than that in chondrites, therefore, the carbonatite might come from deep crust; because it is very rich in LREE. Thus, it may be related to alkaline rock (such as aegirinite).

REE distribution in Boshan carbonatite is of a normal pattern(Fig.1), it is not depleted in Eu, there is no evidence for fractionation. But REE

distribution in Erdaobian carbonatite is of a abnormal pattern, Ce and Yb are positive value, the La and Tb are depleted (Fig.2).

Therefore, Erdaobian carbonatite is REE-poor carbonatite; and Boshan carbonatite is a REE-rich carbonatite.

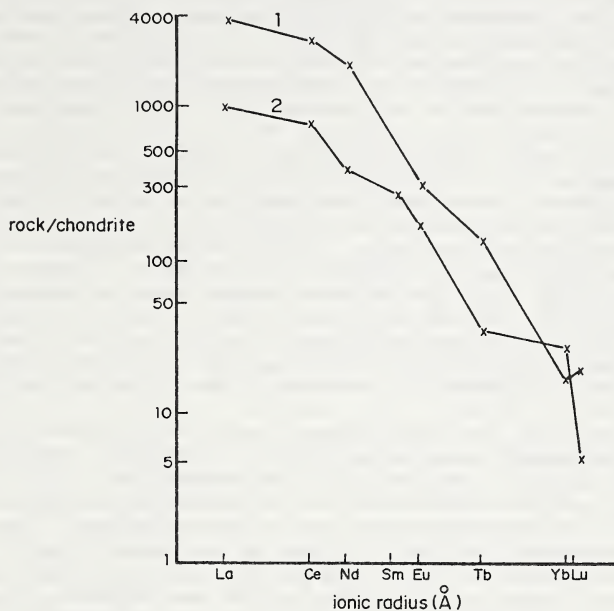


Fig. 1 A pattern of REE distribution in carbonatite from Boshan area, Shandong province. x--neutron activation analysis

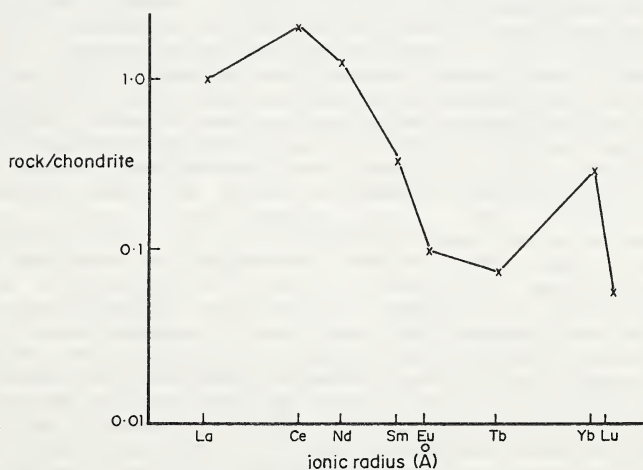


Fig. 2 A pattern of REE distribution in carbonatite from Erdaobian area, Hebei province. x--neutron activation analysis.

THE STATISTICAL CLASSIFICATION OF KIMBERLITE GARNET
BY DIVISIVE CLUSTER ANALYSIS AND MULTIPLE DISCRIMINANT ANALYSIS

BRUCE C. JAGO AND ROGER H. MITCHELL
LAKEHEAD UNIVERISTY, THUNDER BAY, CANADA

Garnet concentrates from eight Somerset Island kimberlites have been classified into statistically significant, compositionally coherent groups of garnet using TWINSpan, a divisive cluster analysis technique and multiple discriminant analysis (MDA). This scheme for classifying garnet from kimberlite and associated ultrabasic xenoliths is a preferred alternative to agglomerative cluster analysis and non-statistical cluster fusion used by Dawson and Stephens (1976) and Danchin and Wyatt (1979), as it embodies a purely statistical approach. The sample base used in this classification scheme included only garnet in kimberlite concentrate and is believed to be random and representative at the present level of erosion as each intrusion is relatively petrographically simple. On average each population tested was comprised of 225 samples. Mitchell (1978, 1979), Dawson (1980) and Jago (1982) concluded that the diverse sample base of other schemes has led to some confusion and misclassification of new samples, (especially Group 1 and Cr-poor Group 9 garnet) and to considerable compositional overlap between discrete groups of garnet characteristic of one kimberlite or kimberlite province with those in another.

TWINSpan computes the classification by repeated dichotomization (division) of the sample population (Fig. 1) through reciprocal averaging (Hill 1973), a gradient scaling technique. This method classifies both samples and variables, ultimately generating groups of like samples with a characteristic suite of variables. The sample/variable classification is given in an ordered two-way table. The example illustrated in Fig. 2 shows that each cluster is characterized by a suite of variables which are ordered (5) to (1) according to their relative contribution to the characterization of one group compared to the other.

Multiple discriminant analysis (MDA) (Pearce 1974) was chosen to test the statistical significance of the fusion of garnet clusters as it can monitor simultaneously the changes in several variables in an statistical analysis and order the variables according to their ability to contribute to the variation between test groups. Although MDA can not be used directly as a classification tool, the method outlined by Klecka (1975) can 1) determine at what level of statistical significance a prior classification of data into two or more subsets falls, 2) the role of each variable contributing to the statistical analysis, 3) into which subset a misclassified case belongs and 4) the rate or percent overall correct case classification of existing subsets.

The principal advantage of TWINSpan is the linear dependence of computer time to the amount of data analysed, in contrast to other methods in which time requirements rise to the second or third higher order of the number of samples. In addition, TWINSpan does not store zero values of the data matrix, nor does it produce or store a secondary matrix of sample similarities. Although the method may generate any number of clusters, the statistically optimum number of clusters generated is not determined by TWINSpan but by multiple discriminant analysis. This is favoured over Danchin and Wyatt's (1979) scheme, as their centroid method of calculation is prone to reversals and the combination of statistically non-similar clusters and Dawson and Stephens' (1976) scheme, which used the rate of change in the number of clusters generated to determine the optimum number of clusters. Both methods ultimately used petrogenetic similarity as a final criteria although this can be highly subjective as it is based upon an a priori knowledge of sample paragenesis.

Our two-level classification scheme illustrated in Fig. 1 initially generates, from a random population of garnet and raw oxide data (TiO₂, Al₂O₃, Cr₂O₃, FeO, MgO, CaO), 'X' clusters of garnet. Using MDA, these are combined at a minimum 95% confidence level and 90% correct case classification to form 'Y', statistically significant, compositionally coherent groups of clusters. This is termed the 'Primary Aggregation Level' (PAL). Each of the 'Y' groups is then disaggregated at the 'Primary Disaggregation Level' (PDL) and the constituent clusters processed by MDA to determine, if within each, there exist 'Z' statistically significant, compositionally coherent subgroups of clusters. Each of the 'Z' subgroups is then tested for compositional variation trends using correlation analysis. Garnet in individual subgroups can then be plotted on multivariate diagrams

TWINSPAN in conjunction with MDA typically generated groups of garnets which lie along three major compositional variation trends, generally comprising six sub-groups. Figures 3, 4 and 5 illustrate an example of our method applied to Nord, one of eight test populations. Solid lines on these figures depict sub-group boundaries defined by a large number of data points, while dashed lines define boundaries which are constrained by relatively few points. Trend 1 garnets are characterized by relatively Ca- and Cr-poor (av. CaO=4.91, av. Cr₂O₃=1.16 wt.%) and Ti-rich compositions and are divided at 'PDL' into relatively Mg-rich, Ti-poor (Trend 1A) and Mg-poor, Ti-rich (Trend 1B) subgroups. Both in general demonstrate a moderate to strong negative correlation between Fe+Ti and Mg at relatively constant CaO. Possible source parageneses include dunite, Cr-poor garnet lherzolite, websterite, pyroxenite and mono- and poly-mineralic macrocrysts. Trend 2 garnets lie along a parallel compositional variation trend to Trend 1 but, in comparison are Ca- and Cr-rich (av. CaO=5.13, av. Cr₂O₃=3.83 wt.%) and may contain up to 1.48 wt.% TiO₂. The compositional variation trend of Trend 2A is similar to Trend 1 in contrast to Trend 2B which exhibits little correlatable variation in major and minor elements and may plot within a relatively restricted compositional range on the Ca-rich side of Trend 2A. Source parageneses include Dawson and Stephens' (1976) Group 11 garnets, Cr-rich macrocrysts, harzburgite and granular and porphyroclastic garnet +/- chromite lherzolite, the latter group dominating. However, lherzolitic garnet is not separated naturally into two groups which are compositionally similar to Trends 2A and 2B suggesting that some other source may be important. Although Nord does not demonstrate the relationship, Trend 3 is composed of Mg-Ti-rich, Ca-poor (Trend 3A) and Mg-Ti-poor, Ca-rich (Trend 3B) subgroups. Overall, it is characterized by the highest CaO and Cr₂O₃ contents (av. CaO=6.09, av. Cr₂O₃=6.87 wt.%) of all groups whilst major and minor elements demonstrate a positive correlation between Mg and Ti and Ca and Cr and a negative correlation between Mg+Ti and Ca. Trend 3, in contrast to its orientation depicted on Fig. 3, may be orientated subparallel to Trends 1 and 2. Trend 3 garnets are compositionally most similar to Dawson and Stephens' (1976) Groups 10 and 11 macrocrysts, but may include rare Cr-rich lherzolite, harzburgite and Cr-poor knorrrigitic garnets.

Trend 1 garnet using Dawson and Stephens' (1976) classification is dominated by Group 1 macrocrysts. Ti-rich compositions characteristic of Trend 1B on average contain a higher proportion of rare Group 2 macrocrysts and a significant component of Cr-poor Group 9 garnet. Trend 2A is dominated by Cr-poor Group 9 and lesser Cr-rich Group 9 garnet while Cr-rich Group 9 characterizes Trend 2B. Trends 3A and 3B are dominated by Ti-poor, Cr-rich Group 9 garnets although Trend 3B may also contain a significant component of relatively Ti-rich Group 11 garnets.

REFERENCES

Dawson, J.B. and Stephens, W.E. (1976) Statistical classification of garnets from kimberlite and associated xenoliths-Addendum. *Journal of Geology*, 84, 495-496.

Dawson, J.B. (1980) Kimberlites and their xenoliths. Springer-Verlag, New York.

Danchin, R.V. and Wyatt, B.A. (1979) Statistical cluster analysis of garnets from kimberlites and their xenoliths. Cambridge Kimberlite Symposium II, Extended Abstract Volume, 22-27.

Hill, M.O. (1973) Reciprocal averaging: an eigenvector method of ordination. *Journal Ecology*, 61, 237-249.

Jago, B.C. (1982) Mineralogy and petrology of the Ham kimberlite, Somerset Island, N.W.T., Canada. M.Sc. Thesis, Lakehead University, Thunder Bay, Ontario.

Klecka, W.R. (1975) Discriminant analysis. In, *Statistical Package for the Social Sciences*, 2nd Edition (N.H. Nie, C.H. Hull, J.G. Jenkins, K. Steinbrenner and D.H. Bent, eds.), McGraw-Hill, New York, 434-462.

Mitchell R.H. (1978) Mineralogy of the Elwin Bay kimberlite, Somerset Island, N.W.T., Canada. *American Mineralogist*, 63, 47-57.

Mitchell, R.H. (1979) Mineralogy of the Tunraq kimberlite, Somerset Island, N.W.T., Canada. In, *Kimberlites, Diatremes, Diamonds: Their Geology, Petrology and Geochemistry*. (F.R. Boyd and H.O.A. Meyer, eds.) American Geophysical Union Special Paper SP0024, 161-171.

Pearce, J.A. (1976) Statistical analysis of major element patterns in basalts. *Journal Petrology*, 17, 15-43.

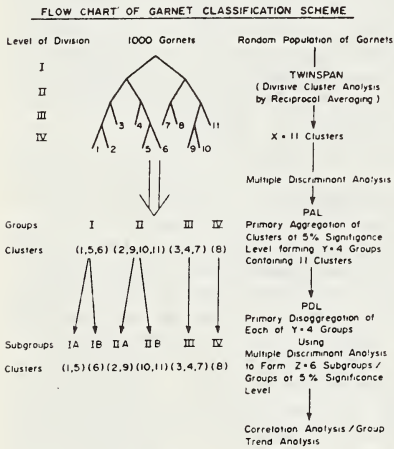


Figure 1

EXAMPLE ORDERED TWO-WAY TABLE

VARIABLES	SAMPLE NUMBERS								
	GROUP 1				GROUP 2				
MgO	1	3	5	7	9	2	4	6	8
FeO	5	5	5	5	5	5	5	5	5
Al ₂ O ₃	4	4	4	4	4	2	2	2	2
Cr ₂ O ₃	3	3	3	3	3	1	1	1	1
TiO ₂	2	2	2	2	2	1	1	1	1

Figure 2

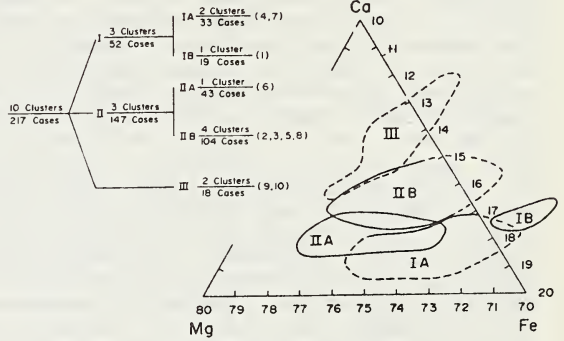


Figure 3

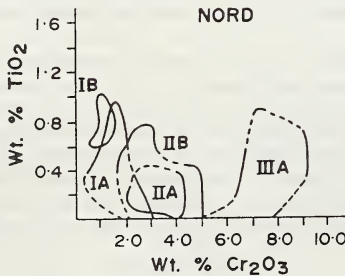


Figure 4

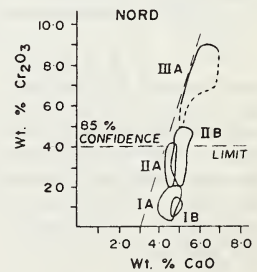


Figure 5

F-RICH MICAS IN THE WEST KIMBERLEY LAMPROITES; CONTRASTS WITH
KIMBERLITES AND OTHER MICACEOUS ALKALINE ULTRAMAFIC INTRUSIONS

A.L. Jaques

Bureau of Mineral Resources, GPO Box 378, Canberra, ACT 2601.

Mica is a ubiquitous phenocryst and/or groundmass phase in many alkaline ultrabasic rocks, particularly those belonging to the ultrapotassic suite, and clearly plays an important role in their petrogenesis. Previous studies have shown that micas from kimberlites, lamprophyres, lamproites and other potassic volcanics have a wide range of compositions, particularly in terms of their Ti and Al contents (Bachinski and Simpson 1984; review). Experimental studies have shown that phlogopitic mica is a near liquidus phase in a spectrum of hydrous potassic liquids over a wide range of temperature, pressure, oxygen fugacity, and volatile contents indicating that a number of variables control or influence the stability and composition of mica crystallising in mafic and ultramafic melts. Studies have shown, for example, that Ti solubility increases with temperature and oxygen fugacity and decreases with pressure (Tronnes et al 1985). Both bulk composition and the composition of the fluid phase also influence mica composition and stability, with the latter likely to be strongly influenced by the halogen content of the fluid phase. Jaques et al (1984) proposed that F plays a major role in the petrogenesis of lamproites by 1) combining with high H₂O contents (low CO₂) in the source region to yield silica-saturated rather than strongly undersaturated partial melts, and 2) enhancing the stability of phlogopite to higher T. This paper presents data on the halogen content of mica from the West Kimberley lamproites and various other ultrapotassic rocks including micaceous kimberlites from southern Africa with a view to establishing the importance of F in the petrogenesis of the lamproite suite in contrast to kimberlite. The data show that F (and Ti) contents are higher in lamproite micas than kimberlites, commonly by up to an order of magnitude.

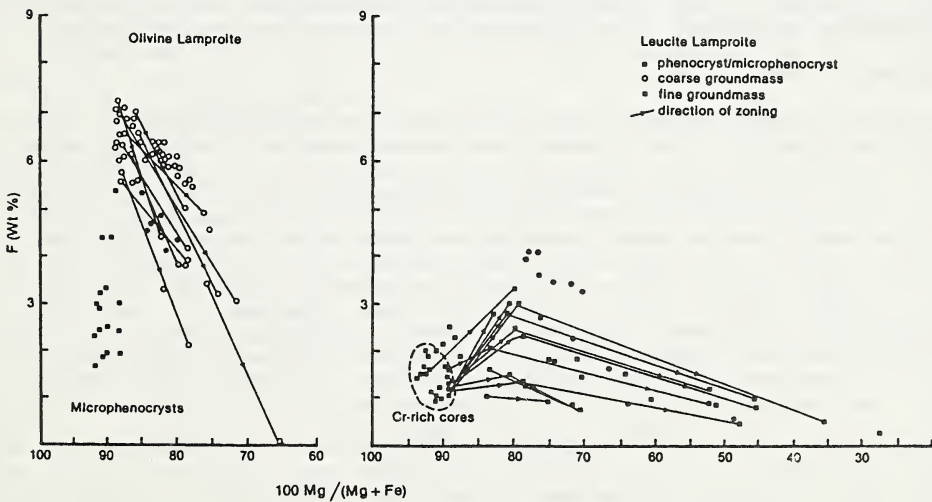


Fig. 1. Variation of F content in mica from the West Kimberley lamproites (after Jaques et al 1986).

Data from nearly 500 whole rock analyses of the West Kimberley lamproites indicate that bulk rock F contents range from 0.2 to 0.8 wt % F with most containing 0.4 to 0.6 wt % (Jaques et al 1986). Cl contents are low (av. 120-150 ppm) and F/Cl ratios high, averaging 41 in olivine lamproite and 17 in leucite lamproite. Phlogopites from the West Kimberley lamproites show a wide range in 100Mg/(Mg+Fe) ratios (92-27) and in Ti (1-12.2 wt % TiO₂) and Al contents (1-12.8 wt % Al₂O₃; Mitchell 1981; Jaques et al 1984, 1986; this work). F contents are high, typically 2 to 4 wt % and ranging up to 7 wt % (maximum value = 7.14 wt %) in Ti-rich (5-7% TiO₂) phlogopite in olivine lamproites from Ellendale (Ellendale 9). The suite exhibits a broad correlation of F with TiO₂ content whereas phenocrysts typically show zoning trends of an initial increase in F with Ti content followed by a decrease (Fig. 1). Microphenocrysts and groundmass micas show a decrease in F with decreasing Mg/(Mg+Fe) whereas mantles on Cr-rich cores in phenocrysts commonly show an initial increase in F followed by a decrease with Mg/(Mg+Fe) as shown in Fig. 1. Apparent partition coefficients between phlogopite and melt, estimated from average F contents in phenocrysts and/or microphenocrysts and whole rock F contents, range from 10-12 (9.5-12.7) in F-rich phenocrysts in olivine lamproite to much less than 10 (4-10) in the more F-poor phenocrysts in the more evolved leucite lamproites. An olivine-leucite lamproite from Oscar containing fresh glass has an apparent phlogopite-melt partition coefficient of 12.5. Cl contents in phenocryst and microphenocryst phlogopites are typically very low (<100 ppm) and slightly higher in Fe-enriched rims and late crystallising groundmass flakes (150-250 ppm). F/Cl ratios are typically higher than the bulk rocks. In addition to mica F is also hosted in potassic richterite which in leucite lamproites commonly contains 1-2 wt % F. Where phlogopite and potassic richterite co-exist the mica, which crystallised first, invariably contains more F.

The Argyle lamproites (Atkinson et al 1984) are also characterised by high F contents with the magmatic rocks containing 0.29 to 0.56 wt % F (Jaques et al 1986, this volume). Groundmass micas in these rocks (where present) contain up to 1.6 wt % F (typically 0.6-1.4 wt %). Cl contents are low, typically 200 ppm or less.

Data from other lamproite suites show that lamproites generally have high F contents, e.g. Leucite Hills = 0.06-0.71 (Kuehner et al 1981). Microprobe analyses (Foley et al in press; this work) show that the high bulk rock F contents are reflected in their mica compositions. Magmatic olivine lamproites from Prairie Creek, Arkansas contain phlogopite with 4-6 wt % F and 4-7 wt % TiO₂. Phenocryst micas from Leucite Hills lamproites exhibit a wide range in F contents which correlate with Ti content, and extend from comparatively low values (1 wt % F, 2 wt % TiO₂) to high values (4 wt % F, 4-5 wt % TiO₂) comparable to the mid-range of those found in the West Kimberley lamproites. Coarse micas in the Hills Pond peridotite, Kansas, have high Ti (5-6 wt % TiO₂) but low F contents (0.6-0.8 wt %) and comparatively low Mg/(Mg+Fe).

Data on halogen contents in kimberlite have been given by Paul et al 1976 and Wedepohl and Muramatsu (1979). The data show a large range with the highest values (up to 0.72 wt % F) reported from the central Indian kimberlites. The value given by Paul et al (1976) for average kimberlite excluding central India (0.165 wt %) is very similar to the mean value of 0.19 wt % given by Wedepohl and Muramatsu (1979). Data on the F contents of mica in kimberlites have been given by Paul et al (1976), Smith et al (1978, 1981), and Delaney et al (1980). Smith et al (1981) suggested that most unaltered micas which crystallised from unaltered kimberlites are low in Cl (< 0.05 wt %) and contain moderate F (0.6-1 wt %). New data obtained for phenocryst and microphenocryst phlogopite ('type II') in micaceous kimberlites from southern Africa (De Beers, Newlands, Loxton, Dornkloof Sover, Southern Fissures, Bellsbank) support this view. The kimberlite micas typically have higher Al (11-15% Al₂O₃), lower Ti (<4% TiO₂), and substantially lower F (<1%) contents than mica in the olivine lamproites. Some of the highest F contents (0.8-0.9%) were found in rare Ti-rich (3-4% TiO₂) biotite ('type I') cores. For example, in the Dornkloof Sover dyke biotite cores (Mg₆₆) with 0.8-0.9 wt % F are rimmed by phlogopite (Mg₈₀) with similar F contents (0.4-0.5 wt %) to that of the phlogopite phenocrysts (0.4-0.5 wt %). Cl contents in most of the kimberlitic micas are low (typically 0.02-0.06 wt %) although systematically higher contents (0.05-0.15 wt %) were found in several of the kimberlites examined (De Beers, Benfontein Sill, Newlands). New whole rock F data for 4 of the kimberlites (Finsch = 0.04 wt %, Loxton = 0.24 wt %, Newlands = 0.12 wt %, and Dornkloof Sover = 0.09 wt %) are all lower than typically found in lamproites.

The data indicate that the F content of early crystallised micas reflect the F contents of their host rock. Lamproites have high F contents and lamproitic mica are F-rich; Ti- and F-rich micas appear to be characteristic of lamproites. Kimberlites generally have lower F contents and their micas are much less F-rich, commonly by an order of magnitude. Micas from other potassic lamprophyres appear to have F contents between kimberlites and lamproites. These differences in F contents are inferred to reflect differences in the F content of their mantle sources and it is suggested that the F contents in ultrapotassic rocks and their early-formed micas are a measure of the degree of metasomatic enrichment of their source regions. F in the source regions of such rocks is inferred to be held mainly in mica. High F contents in the melt result in an enhanced stability of mica at high T and P, as confirmed by experimental studies by Foley et al (in press) and thus have a significant bearing on the crystallisation of the magma.

REFERENCES

- ATKINSON W.J., HUGHES F.E. and SMITH C.B. 1984a. A review of the kimberlitic rocks of Western Australia. In Kornprobst J. ed, **Kimberlites 1: Kimberlites and Related Rocks**, pp. 195-224. Elsevier, Amsterdam.
- BACHINSKI S.W. and SIMPSON E.L. 1984. Ti-phlogopites of the Shaw's Cove minette: a comparison with micas of other lamprophyres, potassic rocks, kimberlites and mantle xenoliths. **American Mineralogist** 69, 41-56.
- DELANEY J.S., SMITH J.V., CARSWELL D.A. and DAWSON J.B. 1980. Chemistry of micas in kimberlites and xenoliths -II. Primary- and secondary-textured micas from peridotitic xenoliths. **Geochimica et Cosmochimica Acta** 44, 857-872.
- FOLEY S.F., TAYLOR W.R. and GREEN D.H. in press. The role of fluorine and oxygen fugacity in the genesis of the ultrapotassic rocks. **Contributions to Mineralogy and Petrology**.
- JAQUES A.L., LEWIS J.D. and SMITH C.B. 1986. The kimberlitic and lamproitic rocks of Western Australia. Geological Survey of Western Australia Bulletin 132.
- JAQUES A.L., LEWIS J.D., SMITH C.B., GREGORY G.P., FERGUSON J., CHAPPELL B.W. and McCULLOCH M.T. 1984. The diamond-bearing ultrapotassic (lamproitic) rocks of the West Kimberley region, Western Australia. In Kornprobst J. ed, **Kimberlites 1: Kimberlites and Related Rocks**, pp. 225-254. Elsevier, Amsterdam.
- KUEHNER S.M., EDGAR A.D. and ARIMA M. 1981. Petrogenesis of the ultrapotassic rocks from the Leucite Hills, Wyoming. **American Mineralogist** 66, 663-677.
- MITCHELL R.H. 1981. Titaniferous phlogopites from the leucite lamproites of the west Kimberley area, Western Australia. **Contributions to Mineralogy and Petrology** 76, 243-251.
- PAUL D.K., BUCKLEY F. and NIXON P.H. 1976. Fluorine and chlorine geochemistry of kimberlites. **Chemical Geology** 17, 125-133.
- SMITH J.V., BRENNESHOLTZ R. and DAWSON J.B. 1980. Chemistry of micas from kimberlites and xenoliths-I. Micaceous kimberlites. **Geochimica et Cosmochimica Acta** 42, 959-971.
- SMITH J.V., DELANEY J.S., HERVIG R.L. and DAWSON J.B. 1981. Storage of F and Cl in the upper mantle: geochemical implications. **Lithos** 14, 133-147.
- TRONNES R.G., EDGAR A.D. and ARIMA M. 1985. A high pressure-high temperature study of TiO₂ solubility in Mg-rich phlogopite: implications to phlogopite chemistry. **Geochimica et Cosmochimica Acta** 49, 2323-2329.
- WEDEPOHL K.H. and MURAMATSU Y. 1979. The chemical composition of kimberlites compared with the average composition of three basaltic magma types. In Boyd F.R. and Meyer H.O.A. eds, **Kimberlites, Diatremes, and Diamonds: Their Geology, Petrology, and Geochemistry**, pp. 300-312. American Geophysical Union Washington, D.C.

A.L. Jaques¹, G. Boxer², H. Lucas³, and S.E. Haggerty⁴

1. Bureau of Mineral Resources, GPO Box 378, Canberra, ACT, Australia, 2601
2. Argyle Diamond Mines, Kununurra, Western Australia, 6743
3. CRA Exploration Pty Ltd, P.O. Box 175, Belmont, Western Australia, 6104
4. Dept of Geology, University of Massachusetts, Amhurst, MA 01003, USA

PETROGRAPHY

The richly diamondiferous Precambrian Argyle lamproite pipe in the East Kimberley region of Western Australia has been described by Atkinson et al (1984a,b) and Boxer et al (this volume). The pipe is composed of olivine lamproite volcanoclastic rocks intruded by olivine (-phlogopite) lamproite dykes. The volcanoclastic lamproites consist of two basic types: polygenetic lapilli ash tuffs and ash tuffs ('sandy tuffs') composed of juvenile fragments of olivine lamproite with abundant accidental, rounded quartz grains and fragments of disaggregated country rock sandstone, and largely monogenetic olivine lamproite lapilli tuff, hyaloclastite, and autobreccia of hydroclastic origin ('non-sandy tuff'). The juvenile clasts range from dense, blocky, poorly vesiculated, porphyritic types to highly vesiculated vitric clasts including pumice and fiamme. Many of the vitric lapilli are cored, typically by altered olivine macrocrysts, and many contain quartz grains and lithic fragments.

All the juvenile clasts contain two generations of olivine which is now entirely altered to talc+carbonate+sulphide or serpentine-septechlorite+magnetite - anhedral to resorbed macrocrysts up to 5 mm and smaller euhedral phenocrysts and microphenocrysts. The phenocrysts and microphenocrysts commonly contain tiny inclusions of chrome spinel, and in the vitric clasts, exhibit skeletal forms, particularly hopper types. The former olivine crystals are set in a groundmass which in the vitric clasts contains only tiny spinel euhedra in a serpentinous base (former glass and palagonite) whereas dense porphyritic types contain spinel, former leucite (now K-feldspar+talc+smectite), phlogopite, apatite, and oxide phases. The lamproite dykes consist of altered olivine, phlogopite, spinel, apatite, K-feldspar, and oxide phases.

MINERALOGY

Mica is characterised by low Al and high Ti contents (2-9 wt % Al_2O_3 and TiO_2) and moderate enrichment in Fe (9-14% FeO, $Mg/(Mg+Fe) < 0.8$). Most have low Cr, Na and Ba, and moderate F contents (<0.2 wt % Cr_2O_3 , up to 0.6 wt % BaO and 2 wt % F). The Argyle micas are typical of lamproite micas but show less variation than, and are more Fe-rich than, the majority of the West Kimberley micas (Jaques et al 1986).

Chrome spinel is the most common macrocryst phase recovered in Argyle concentrates. The macrocryst spinels are distinguished from the groundmass spinels by their larger size, irregular shape, and uniformly magnesian, Ti-poor (<1 wt % TiO_2) compositions which range from magnesian aluminous chromite through to magnesiochromite with up to 67 wt % Cr_2O_3 . The groundmass spinels are mostly titaniferous magnesiochromites (TMC) and titaniferous chromites (TC) containing 3-4 wt % TiO_2 , 50-60 wt % Cr_2O_3 , and 5-15 wt % MgO but rare grains of titaniferous aluminous magnesiochromite (TMAC, 14 wt % Al_2O_3 , 16 wt % MgO) also occur as discrete groundmass grains and as inclusions in olivine. Individual grains are zoned from cores of TMAC or TMC through more Al-poor, Fe-rich TMC or TC to rims enriched in titanomagnetite. The evolutionary trend of the Argyle groundmass spinels is therefore one of decreasing Al and Mg and increasing Cr and Fe^{2+} followed by increasing Fe^{2+} , Ti and Fe^{3+} . The trend toward titaniferous magnetite is much less marked than shown by spinels from the West Kimberley lamproites.

Ilmenite occurs as ragged, irregular anhedral up to 200 um across of late-stage primary origin in the groundmass of many of the magmatic rocks and in the juvenile clasts where it ranges in modal abundance from 1 to 10 vol. %. MnO contents are high (3-8 wt %) and MgO and Cr_2O_3 contents low (<1 wt % and <0.5 wt %). Sphene is widespread in the groundmass where it occurs as granular subhedra and rims on ilmenite. Compositions are close to stoichiometric with low Al, Fe and Na but variable amounts of

Sr. Anatase and rutile occur as discrete granules and granular aggregates, commonly in association with Mn-ilmenite. Compositions show variable amounts of Nb (up to 2.5 wt % Nb₂O₅) and subordinate Fe. A number of other phases are present mostly occurring as groundmass phases of probable secondary origin. These include ZrTiFe-silicate and LaCe-titanate; zircon is also present. Sulphide phases include pentlandite, pyrrhotite, chalcopyrite, pyrite, sphalerite, and galena.

Priderite occurs as small euhedral crystals in the groundmass of juvenile clasts and in magmatic lamproite where it is commonly associated with ovoid blebs of carbonate in association with Mn-ilmenite and rutile. The priderites show several unusual compositional features: 1) high V contents (1.3-1.5 wt % V₂O₃), 2) high Ce₂O₃ contents (0.4-2.7 wt %; Table 1, 1-4), 3) K:Ba ratios vary widely between grains and some are strongly zoned (Table 1, 2-3), and 4) end-member K-priderite is present in some rocks (Table 1, 4). The V-Ce-priderite is comparable with a similar phase described by Mitchell and Haggerty (in press) from a Type 2 kimberlite at New Elands, South Africa (Table 1, 9).

Priderite (confirmed by X-ray analysis) was also found as a 0.5 mm grain in heavy mineral concentrate from the pipe. It is also end-member K-priderite but unlike the groundmass grains contains some 9 wt % Cr₂O₃ and substantially lower contents of Ce₂O₃ and Fe with V below detection limits (Table 1, 5). Chromian-armalcolite is present (Table 1, 6), enclosed within the K-Cr-priderite grain. The assemblage is interpreted as an upper mantle xenocryst.

An as yet unidentified opaque titanate (Table 1, 7) with a composition similar to mannardite-redledgeite series (Ba.H₂O)(V,Cr)₆O₁₆ occurs in association with talc replacing olivine. This phase is very similar (Table 1, 8) in the A-formula Ba site to a minor phase reported from the Benfontein kimberlite-carbonatite sills by Scatena-Wachel and Jones (1984) with the exception that the small cation B-formula site is dominated by Fe³⁺ rather than Cr and V.

Table 1. Electron microbeam analyses of LIL-titanates.

	1	2	3	4	5	6	7	8	9	10
SiO ₂	0.19				0.00		0.83	1.9-3.6	0.19	0.37
TiO ₂	71.47	76.67	71.97	81.29	72.66	76.77	53.64	51-54	78.47	71.90
ZrO ₂	0.01	0.10	0.07	0.10	0.19	0.51	0.04	0.4-0.5	0.06	0.01
Al ₂ O ₃	0.00	0.00	0.00	0.00	1.02	0.88	0.02	1.0-1.7	0.00	0.04
Cr ₂ O ₃	0.00	0.00	0.00		9.06	9.12	3.49		0.00	8.38
V ₂ O ₃	1.36	1.66	1.50	1.32	0.00		5.35		1.65	
Fe ₂ O ₃								15.6-16.1	7.10	
*FeO	7.98	7.37	8.39	6.48	3.32	6.16	5.49			4.38
MgO	0.01	0.00	0.00	0.00	0.96	5.59	0.63	2.1-3.4	0.53	1.23
MnO	0.04	0.01	0.05	0.00	0.00	0.06	0.00		0.00	0.00
CaO	0.00	0.50	0.54	0.33	0.00	0.00	0.00	1.3	0.34	0.54
SrO					0.00					
BaO	11.07	5.66	12.09	0.94	0.93		20.82	16.1-16.7	1.19	0.83
Na ₂ O	0.04				0.03		0.08		0.00	0.48
K ₂ O	4.65	6.24	3.52	7.40	9.33		0.00		9.63	9.39
Nb ₂ O ₅					0.17	0.21		1.6		
Y ₂ O ₃					0.00					
La ₂ O ₃	0.00	0.00	0.00	0.00	0.00		0.00			
Ce ₂ O ₃	2.24	1.14	2.69	0.39	0.29		3.97	0.5	0.70	
Other					0.22+		#			
Total	99.06	99.35	100.82	98.25	98.18	99.30	94.36	94-96	99.86	97.55

*Fe as FeO, +Ta₂O₅, #Sc present in spectral scans

Rare chrome diopside and enstatite, and very rare garnet have been recovered from concentrates. The chrome diopsides are Mg-rich, very poor in Al_2O_3 and Na_2O (commonly < 1 wt %), and have high Ca/(Ca+Mg) ratios, and belong to Stephens and Dawson group 5. The enstatites also have very low Al contents. The garnets are almandine-pyrope, titanian and chrome pyrope belonging to Dawson and Stephens cluster groups 3, 1 and 9. The chrome pyropes are calcium-saturated, contain up to 6 wt % CaO and Cr_2O_3 , and are similar to those recovered from the West Kimberley lamproites (see Jaques et al 1986).

DISCUSSION

The Argyle macrocryst assemblage, like that of the West Kimberley lamproites, is dominated chrome spinel and diamond. The compositions of the spinels, pyroxenes and garnets in the two provinces are similar and the chrome spinels and pyroxenes are compositionally similar to the phases observed in rare altered peridotite xenoliths recovered from the Argyle pipe (O'Neill et al this volume). A feature of the xenoliths and xenocrysts is their highly refractory chemistry and this suggests that both provinces are underlain, at least in part, by reduced, refractory (olivine-rich, garnet and pyroxene-poor) peridotite.

The K-Cr-priderite discovered in the Argyle concentrate is very similar to the phase (Table 1, 10) reported by Jones et al (1982) in their study of metasomites from the Bultfontein kimberlite. The association and composition of armalcolite is very similar to the LIMA settings at Bultfontein and Jagersfontein (Haggerty et al 1983; Haggerty, 1983), and it is noteworthy that it too bears the depletion signature of substantial Cr_2O_3 (9 wt %). The discovery of LIL-titanate of similar composition to phases found in metasomites from the Kaapvaal craton provides the first direct evidence of LIL enrichment of the lithosphere beneath the Kimberley craton. Such enrichments have previously been proposed on the basis of the lamproite geochemistry and isotopic constraints (Jaques et al 1984, this volume; Nelson et al 1986). The high Cr contents in LIL-titanates from Argyle and several localities in South Africa are interpreted to indicate similar histories for the Kaapvaal and Kimberley cratons, viz. LIL enrichment of a previously depleted (refractory) subcontinental lithosphere.

ACKNOWLEDGMENTS

We thank CRAE Pty Ltd and Argyle Diamond Mines Pty Ltd permission to publish information and C.B. Smith for his interest and support of the project. ALJ publishes with the permission of the Director, Bureau of Mineral Resources.

REFERENCES

- ATKINSON W.J., HUGHES F.E. and SMITH C.B. 1984a. A review of the kimberlitic rocks of Western Australia. In Kornprobst J. ed, *Kimberlites 1: Kimberlites and Related Rocks*, pp. 195-224. Elsevier, Amsterdam.
- ATKINSON W.J., SMITH J.B. and BOXER G.L. 1984b. The discovery and geology of the Argyle diamond deposits, Kimberley, Western Australia. *Australasian Institute of Mining and Metallurgy, Darwin Conference, 1984*, pp. 141-149.
- HAGGERTY S.E. 1983. The mineral chemistry of new titanates from the Jagersfontein kimberlite, South Africa: Implications for metasomatism in the upper mantle. *Geochimica et Cosmochimica Acta* 47, 1833-1854.
- HAGGERTY S.E., SMYTH J.R., ERLANK A.J., RICKARD R.S. and DANCHIN R.V. 1983. Lindsleyite (Ba) and mathiasite (K): two new chromium-titanates in the crichtonite series from the upper mantle. *American Mineralogist* 68, 494-505.
- JAQUES A.L., LEWIS J.D. and SMITH C.B. 1986. The kimberlitic and lamproitic rocks of Western Australia. *Geological Survey of Western Australia Bulletin* 132.
- JAQUES A.L., LEWIS J.D., SMITH C.B., GREGORY G.P., FERGUSON J., CHAPPELL B.W. and McCULLOCH M.T. 1984. The diamond-bearing ultrapotassic (lamproitic) rocks of the West Kimberley region, Western Australia. In Kornprobst J. ed, *Kimberlites 1: Kimberlites and Related Rocks*, pp. 225-254. Elsevier, Amsterdam.
- JONES A.P., SMITH J.V. and DAWSON J.B. 1982. Mantle metasomatism in 14 veined peridotites from the Bultfontein mine, South Africa. *Journal of Geology* 90, 435-453.
- NELSON D.R., McCULLOCH M.T. and SUN S-S. 1986. The origins of ultrapotassic rocks as inferred from Sr, Nd and Pb isotopes. *Geochimica et Cosmochimica Acta* 50, 231-245.
- SCATENA-WACHEL D.E. and JONES A.P. 1984. Primary baddeleyite (ZrO_2) in kimberlite from Benfontein, South Africa. *Mineralogical Magazine* 48, 257-161.

GEOCHEMISTRY OF THE ARGYLE LAMPROITE PIPE

A.L. Jaques¹, S-S. Sun¹, and B.W. Chappell²

1. Bureau of Mineral Resources, GPO Box 378, Canberra, ACT, 2601, Australia.
2. Geology Dept, Australian National University, P.O. Box 4, Canberra, ACT, 2600.

Major and trace element (including REE) abundances have been determined by XRF and INAA, and Sr and Nd isotopic ratios have been measured for the three major rock units ('sandy tuffs' = ST, 'non-sandy tuffs' = NST, and olivine-phlogopite lamproite dykes = OPLD) recognised in the Argyle (AK1) pipe (Atkinson et al 1984a,b; Boxer et al this volume; Jaques et al this volume). The aims of the study were to chemically characterise the Argyle lamproite, examine the chemical relationships between the various units and to compare the chemistry of the Argyle lamproite with lamproites from the West Kimberley (Jaques et al 1984, 1986a,b; Fraser et al 1985; Nelson et al 1986).

Geochemical study of the Argyle pipe is complicated by several factors. Firstly the bulk of the rocks are pyroclastics and the juvenile clasts are dominantly fine (lapilli and ash). Secondly, all three units have undergone low temperature alteration; olivine is totally altered to talc/serpentine, and smectite and secondary titanates (sphene, anatase) are widespread. Thirdly, the ST are polygenetic and show the effects of addition of large amounts of quartz from the country rocks; whole rock compositions of ST lie along mixing lines between country rock quartzite and lamproite approximating NST compositions. All ST data quoted for comparison with the other units refer to the least contaminated ST, i.e. those with the lowest SiO₂ (60-62 wt %) and highest MgO (12-15 wt %) contents.

Several significant observations emerge from the major element geochemistry. All three units have high contents of K₂O (4-6 wt %) and TiO₂ (2-4 wt %) and high K₂O/Na₂O (>25) and K₂O/Al₂O₃ (> 0.75) ratios typical of lamproites. Unlike the West Kimberley lamproites the Argyle rocks are generally not perpotassic. All except oxidised surface samples are magnesian and have high Mg/(Mg+Fe²⁺) ratios (0.76-0.86) consistent with mantle derivation. The NST are the most magnesian containing up to 25 wt % MgO and show the least variation in Mg/(Mg+Fe). Analyses of several of the larger lapilli in ST with petrologic features resembling OPLD show them to be similar to the more Mg-poor OPLD. CaO contents of the Argyle lamproites show a wide range from low values (4-5 wt %) typical of the West Kimberley olivine lamproites to comparatively high values which are attended by high CO₂ contents (5-12 wt %). The Argyle lamproites have very low Na₂O contents (commonly < 0.2 wt %) which probably reflect both low primary values and the effects of leaching; oxidised surface samples are almost totally leached of alkalis. Contents of P₂O₅ and F are high (1-1.5 wt % and up to 0.6 wt % respectively).

The Argyle lamproites are strongly enriched in the incompatible elements K, Rb, Sr, Ba, Pb, Th, U, Ti, Zr, Nb, Ta, Hf, and P, a feature typical of lamproites and micaceous kimberlites. NST and OPLD samples typically contain 300-400 ppm Rb and 750-1250 ppm Sr, and have high Rb/Sr ratios (0.2-0.35). The ST show a much wider range of abundances and abundance ratios but those with the highest juvenile component have ratios similar to the NST and OPLD. Although similar in terms of their Rb/Sr ratios the Argyle lamproites are much less enriched in Rb and Sr than the West Kimberley lamproites. Ba contents in the Argyle rocks show a wide range, probably reflecting secondary alteration, with average values of 1000-1500 ppm. This contrasts markedly with the very high Ba contents of the West Kimberley lamproites which are typically > 5000 ppm (Jaques et al 1984). Pb contents show a large variation reflecting secondary sulphides, especially galena. Th and U contents and Th/U ratios in the NST and OPLD are similar (Th/U = 7-8) and lower than in the West Kimberley lamproites.

Ni and Cr contents are high, particularly in the NST which average 1000 ppm Ni and 1400 ppm Cr: Ni contents in the less Mg-rich OPLD range down to 500 ppm. V (av. 100 ppm), Sc (12-15 ppm) and Y (av. 20-22) contents are low and similar in both the NST and OPLD. Zr and Nb contents are high averaging 630 ppm Zr and 190 ppm Nb in the NST and 840 ppm Zr and 240 ppm Nb in the OPLD. The ST have lower abundances as a result of the included quartz. The NST and OPLD have similar low Zr/Nb and Ti/Zr

ratios (av. 3.3-3.5, 26-27) whereas the ST have slightly higher Zr/Nb and slightly lower Ti/Zr ratios. Hf and Ta contents are high in both the NST and OPLD, the latter having distinctly higher Hf contents (av. 27 ppm cf 18 ppm). Hf/Ta ratios in the most juvenile-rich ST and NST are similar (1.5-2.2) whereas the OPLD extend to slightly higher ratios (2.4).

All three units are strongly enriched in LREE and have highly fractionated REE patterns with low abundances of HREE. La abundances in the NST lie in the range 267-416x chondrites (av. 115 ppm) and abundances are slightly higher in the OPLD (310-470x chondrites, av. 129 ppm) and much lower in the ST. HREE abundances in the NST and OPLD lie in the range 5-7x chondrites whereas the ST with higher proportions of country rock fragments extend to higher values (10x). The NST and OPLD have similar high La/Yb ratios (NST = 76-100, av. 99; OPLD = 65-123, av. 90) whereas the ST have La/Yb ratios which extend from values which overlap the magmatic rocks to much lower ratios (<50).

Trace element data show that the NST and OPLD have very similar abundances and abundance ratios of incompatible elements whereas the ST show a much wider range of abundances due to the inclusion of varying amounts of accidental fragments. On incompatible element ratio plots (e.g. Ti/Zr vs Zr/Nb) the ST form a field which overlaps all or part of the other two units. The similarity between all three units in the Argyle pipe is clearly shown on plots of incompatible element abundances normalised to mantle abundances. The patterns are strikingly similar with abundances of incompatible elements in the OPLD some 15 to 30% higher than the NST whereas abundances in the ST are some 10 to 60% lower than the NST. The higher abundances in the OPLD rocks is attributed largely to a more differentiated character of the OPLD which contain some 10% (relative) more FeO (Fe as FeO) and about 10% less MgO than the NST. A more fractionated character is consistent with their lack of diamonds compared to the pyroclastic units (Atkinson et al 1984a). The low abundances of the ST reflect the dilution effects of incorporation of variable amounts of material derived from the country rocks. Features of the normalised plots are marked negative anomalies in K, Sr, and P. Similar negative relative anomalies in these elements are exhibited by the West Kimberley lamproites but absolute abundances are much higher. In particular the Argyle lamproites lack the marked overabundance of Ba and Rb shown by the West Kimberley lamproites.

In contrast to the trace element data which strongly suggests that the pyroclastic and magmatic rocks are comagmatic, small differences are apparent in initial Nd isotopic compositions between the NST and the OPLD and clasts in the ST. The NST have initial ϵ_{Nd} values at the time of emplacement (1178 Ma, Sun et al this volume) in the range -3.6 to -4.0 whereas the OPLD have slightly less radiogenic values in the range -4.6 to -5.3. Sr isotopic systematics in at least some of the NST appear to have been disturbed whereas whole rock $^{87}Sr/^{86}Sr$ ratios in the OPLD and magmatic clasts of OPLD-type in the ST are consistent with an initial $^{87}Sr/^{86}Sr$ ratio of 0.7063 defined by apatite concentrates (Sun et al this volume). These small differences in isotopic composition might be due to contamination of the OPLD by Archean crustal materials but the high REE and Sr contents of the lamproites should render them relatively immune to the effects of crustal contamination. A more likely explanation is that these differences reflect small heterogeneities in their source regions, such as are observed within individual fields in the West Kimberley (Jaques et al 1986a), and/or small differences in magma generation processes such as slightly differing degrees of partial melting or reaction with wall-rocks.

Although the style of enrichment is very similar (the same elements are involved) the degree of enrichment in incompatible elements exhibited by the Argyle lamproites is much less than that shown by the West Kimberley lamproites. This is evident in the much lower abundances, particularly of Ba and La, and lower Ba/La, Th/U, La/Nb, and La/Ta, and higher K/Rb and K/Ba ratios in the Argyle rocks. The level at which the West Kimberley lamproites are enriched relative to the Argyle rocks is not uniform. Ti and K abundances in the Argyle rocks are approximately 0.8x those in the Ellendale olivine lamproites whereas Rb and Zr abundances are approximately 0.6x and La and Th abundances approximately 0.3x those in the Ellendale olivine lamproites. Nevertheless, both lamproites suites appear to have been formed by similar processes and model calculations suggest that both lamproite suites could have been derived from the same type of enriched lithosphere sources formed >2000 Ma. This enrichment is inferred to have been superimposed on a formerly depleted, refractory peridotite as evidenced by

the very low Al, Ca, Na, Y, Sc and V abundances in the lamproites themselves and by the refractory nature of the peridotitic xenoliths and xenocrysts (Jaques et al 1984, this volume; O'Neill et al this volume). The discovery of large-ion-lithophile element enriched titanates in the Argyle concentrates (Jaques et al this volume) is consistent with metasomatic enrichment of the source. The presence of eclogitic xenocrysts in concentrates from the pipe and the dominance of eclogitic paragenesis inclusions including pyroxenes with very high K contents in Argyle diamonds (Hall and Smith 1984; Jaques et al this volume) suggests that eclogitic sources are also involved.

ACKNOWLEDGMENTS

We thank CRAE Pty Ltd and Argyle Diamond Mines Pty Ltd for drill core material, G. Boxer for assistance and advice in sample selection, and C.B. Smith for his interest in the study. ALJ and S-SS publish with the permission of the Director, Bureau of Mineral Resources.

REFERENCES

- ATKINSON W.J., HUGHES F.E. and SMITH C.B. 1984a. A review of the kimberlitic rocks of Western Australia. In Kornprobst J. ed, **Kimberlites 1: Kimberlites and Related Rocks**, pp. 195-224. Elsevier, Amsterdam.
- ATKINSON W.J., SMITH J.B. and BOXER G.L. 1984b. The discovery and geology of the Argyle diamond deposits, Kimberley, Western Australia. **Australasian Institute of Mining and Metallurgy**, Darwin Conference, 1984, pp. 141-149.
- FRASER K.J., HAWKESWORTH C.J., ERLANK A.J., MITCHELL R.H. and SCOTT-SMITH B.H. 1985. Sr, Nd and Pb isotope and minor element geochemistry of lamproites and kimberlites. **Earth Planetary Science Letters** 76, 57-70.
- HALL A.E. and SMITH C.B. 1984. Lamproite diamonds - are they different?. In Glover J.E. and Harris P.G. eds, **Kimberlite Occurrence and Origin: A Basis for Conceptual Models in Exploration**, pp. 167-212. Geology Department and University Extension, University of Western Australia, Publication No. 8.
- JAQUES A.L., CHAPPELL B.W., SUN S-S., LEWIS J.D. and SMITH C.B. 1986a. The West Kimberley lamproites: intraplate volcanism of extreme character. (Abstr.) **International Volcanological Congress, New Zealand**. p. 171.
- JAQUES A.L., LEWIS J.D. and SMITH C.B. 1986b. The kimberlitic and lamproitic rocks of Western Australia. **Geological Survey of Western Australia Bulletin** 132.
- JAQUES A.L., LEWIS J.D., SMITH C.B., GREGORY G.P., FERGUSON J., CHAPPELL B.W. and McCULLOCH M.T. 1984. The diamond-bearing ultrapotassic (lamproitic) rocks of the West Kimberley region, Western Australia. In Kornprobst J. ed, **Kimberlites 1: Kimberlites and Related Rocks**, pp. 225-254. Elsevier, Amsterdam.
- NELSON D.R., McCULLOCH M.T. and SUN S-S. 1986. The origins of ultrapotassic rocks as inferred from Sr, Nd and Pb isotopes. **Geochimica et Cosmochimica Acta** 50, 231-245.

DIAMOND-BEARING ALKALINE INTRUSIONS FROM WANDAGEE,
CARNARVON BASIN, WESTERN AUSTRALIA

I.D. Kerr⁴, A.L. Jaques², H. Lucas¹, S-S. Sun²
and B.W. Chappell

1. CRA Exploration Pty Ltd, P.O. Box 175, Belmont, WA 6104.
2. Bureau of Mineral Resources, GPO Box 378, Canberra, ACT 2601.
3. Geology Dept, Australian National University, Canberra, ACT 2600.
4. 182 Mica St, Broken Hill, New South Wales, 2880.

Reconnaissance stream-sediment sampling and aeromagnetic surveys led to the discovery in 1978 by CRA Exploration Pty Ltd of 16 small kimberlite-like diatremes and associated sills and dykes in the vicinity of Wandagee Hill in the northern Carnarvon Basin of Western Australia (Atkinson et al 1984; Jaques et al 1986). Subsequent exploration by Stockdale Prospecting Ltd located an additional diatreme and a number of sills and dykes. A total of 22 bodies, 14 diatremes and 8 sills and dykes, are now known from the Wandagee area where they form an elongate N-S belt some 50 km long and 15 km wide at the eastern margin of the Wandagee Ridge, a basement horst which separates the Merlinleigh sub-basin to the east from the overlapping Gasgoyne sub-basin to the west. The Merlinleigh sub-basin, a half-graben filled with up to 6 km of mainly Permian sediments, forms part of the Carnarvon Basin which is a Phanerozoic trough infilled with terrestrial and marine clastic sediments and developed at the western margin of the continent prior to breakup of Gondwanaland (Veevers, 1981). The Wandagee bodies intrude Permian (Artinskian) black shales and siltstones. U-Pb dating of zircon indicates a Jurassic (160 ± 10 Ma) age of emplacement (Atkinson et al 1984; Pidgeon et al, this volume) which is consistent with stratigraphic relations and coincides with the early rift phase of the breakup. The diatremes range in size from 1 to 14 ha and are covered by up to 160 m of late Cretaceous (Aptian) sediments and Recent deposits. They are steep-sided, pipe-shaped bodies filled with decomposed tuffs and tuff-breccias which locally are weakly bedded. The Wandagee tuffs are therefore assigned to the lower part of the crater zone in the kimberlite pipe model of Hawthorn (1975). The sill and dykes range in thickness from 1 to 15 m, and are composed of dark, massive, porphyritic picrite.

PETROLOGY

The sills and dykes are highly porphyritic picrites containing abundant olivine phenocrysts and microphenocrysts (Mg_{92-87}), subordinate olivine macrocrysts (Mg_{92-90}) and diopside micropenocrysts set in a groundmass crowded with a felt-like mass of Ti-Al salite prisms and granular spinel. The largely cryptocrystalline, interstitial base is composed mainly of Al-rich serpentine but alkali feldspar is discernable in places and apatite is present in coarser grained rocks. Also present, particularly in abundant segregation, vesicles and veinlets filled with calcite is analcime, mauve titansalite, biotite, kaersutite, and skeletal Ti-magnetite. The pyroxenes and spinels exhibit a wide range of compositions. The pyroxenes range from diopside cores with low TiO_2 (< 0.7 wt %), Al_2O_3 (1-2 wt %) and Na_2O (0.2-0.3 wt %) and moderate Cr_2O_3 (up to 1 wt %) to rims of Ti- and Al-rich salite (up to 3 wt % TiO_2 , 8 wt % Al_2O_3) with higher Na (up to 0.9 wt % Na_2O) and negligible Cr. The mauve brown variolitic pyroxenes in the segregation patches extend to more Ti- and Al-rich compositions (up to 5 wt % TiO_2 and 11 wt % Al_2O_3). The spinel compositions range from titaniferous aluminous chromite (TMAC) with up to 60% Cr_2O_3 through Mg-poor titaniferous chromite (TC) and titaniferous chromian magnetite (TCM) to titaniferous magnetite (TM) containing up to 19 wt % TiO_2 . Individual grains are typically zoned from TMAC and TMC cores to TCM and TM rims.

The highly altered tuffs are composed of juvenile lapilli and coarse ash together with accidental lithic fragments, particularly pyritic shale. The juvenile clasts which are commonly cored by altered olivine, 0.5-5 mm across, or less commonly phlogopites, consist of phenocrysts and micro-phenocrysts of former olivine and magnesian Al-rich phlogopite in an altered groundmass of serpentine and carbonate containing sub- to euhedral spinels. The spinels in the tuffs also exhibit a wide

range of compositions from Cr and Al-rich types (TMAC with up to 50 wt % TiO₂ and 16 wt % Al₂O₃) towards more Fe³⁺- and Ti-rich compositions i.e. aluminous TC and TCM and TM with up to 15 wt % TiO₂. Compared to the spinels in the picrite dykes and sills those in the tuffs are richer in Mg and Al and, thus more like spinels found in kimberlite (Haggerty 1976).

Concentrates from the Wandagee bodies have yielded magnesio-chromite, chrome diopside, garnet, picroilmenite, olivine, kimberlitic mica and zircon, and extremely rare diamond. The chromites are rich in Mg and Cr (Cr/(Cr+Al) = 0.7-0.77), and have high TiO₂ contents (up to 5 wt %). The chrome diopsides are rich in Ca, poor in Al, Na, and Ti, and contain up to 2 wt % Cr₂O₃. The garnets belong mainly to Dawson and Stephens (1975) cluster groups 1, 9, and 11 and, with rare exception, fall well within the Ca-rich field on CaO-Cr₂O₃ diagrams (Gurney 1984) discriminating garnets from lherzolite and garnets from diamond inclusions. The picroilmenite has moderate to high MgO contents (8-20 wt %).

Microxenoliths of dunite with coarse or granular texture are common. Also present are small xenoliths of crustal metamorphics derived from the Precambrian basement including sillimanite, garnet, biotite, feldspar-quartz granulite and hornblende-plagioclase-quartz-garnet granulites.

CHEMISTRY

The picrites have uniformly high MgO contents (21-28%), are very rich in normative olivine and range from slightly undersaturated to barely saturated. They have low contents of Na₂O and K₂O (av. 1 wt %) with Na₂O/K₂O ratios near 1. The picrites have comparatively low levels of enrichment in incompatible elements; Ba = 200-800 ppm, Rb = 10-30 ppm, Sr = 100-600 ppm, Zr = 75-200 ppm, Nb = 30-60 ppm, Ta and Hf = 2-3 ppm. They have moderate K/Rb (200-300) ratios and low Rb/Sr (av. 0.05), Th/U (3-4), and Zr/Nb (2-3) ratios. The Wandagee picrites have strongly fractionated REE patterns with LREE enrichments of 90-120x chondrites and low abundances of HREE (3-4x). Similar abundances of LREE are found in both kimberlite and highly undersaturated basalts but the very low abundances of HREE is more typical of kimberlite (Fesq et al 1975; Nixon et al 1981). Sr and Nd isotope data indicate that the picrites have been derived from mantle with Nd and Sr isotopic ratios close to 'bulk earth'.

Chemical data on the tuffs is hindered by their fragmental nature and highly altered state. Analyses of the groundmass in the juvenile clasts by microprobe using a defocused beam gave compositions broadly similar to, although less Mg-rich than, the picrites (Atkinson et al 1984). This suggests that the Wandagee tuffs might be closer in chemistry to the picrites than is suggested by the differences in their mineralogy and mineral chemistry. An important observation is that neither contain perovskite indicating that they are not strongly silica undersaturated.

DISCUSSION

The mineralogy and chemistry of the picrites suggest affinities with undersaturated basaltic rocks. The lower abundances of incompatible elements in the Wandagee picrites may be interpreted in terms of larger degrees of partial melting under comparatively shallow depths compared to kimberlites (cf Frey et al 1977). Nd and Sr isotopic ratios in the Wandagee rocks are similar to those in group I (non-micaceous) kimberlite (Smith 1983) and undersaturated basaltic rocks whose generation is believed to include involvement of the convecting mantle (e.g. McDonough et al, 1985). The microxenoliths and the nature of the xenocryst garnets and pyroxenes indicate the presence of depleted garnet lherzolite beneath the Wandagee region. The presence of rare diamond indicates that at least some of the Wandagee pipes have tapped mantle within the diamond stability field. The Wandagee rocks therefore add to the spectrum of volcanic rocks now known to host diamond. However, the rarity of diamond in the Wandagee intrusives suggest that they are largely derived from depths above the diamond stability field and are therefore unlikely to host diamond at economic grades. The Wandagee intrusions are interpreted as having been derived by small to moderate degrees of partial melting, involving interaction of depleted, refractory lherzolite of the subcontinental lithosphere with diapiric mantle derived from the convecting asthenosphere. This model is similar to the models of Nixon et al

(1981) for kimberlites and McDonough et al (1986) for alkali basalts. The upwelling of the asthenosphere is inferred to have been generated in response to rifting processes associated with the break up of Gondwanaland .

ACKNOWLEDGEMENTS

We thank CRA Exploration Pty Ltd for permission to publish, and C.B. Smith for his help in initiating the study. ALJ and S-S.S publish with the permission of the Director, Bureau of Mineral Resources.

REFERENCES

- ATKINSON W.J., HUGHES F.E. and SMITH C.B. 1984. A review of the kimberlitic rocks of Western Australia. In Kornprobst J. ed, **Kimberlites 1: Kimberlites and Related Rocks**, pp. 195-224. Elsevier, Amsterdam.
- FESQ H.W., KABLE E.J.D. and GURNEY J.J. 1975. Aspects of the geochemistry of kimberlites from the Premier mine and other selected South African occurrences with particular reference to the rare earth elements. **Physics and Chemistry of the Earth** 9, 687-709.
- FREY F.A., FERGUSON J. and CHAPPELL B.W. 1977. Petrogenesis of South African and Australian kimberlite suites. (Abstract). **Second International Kimberlite Conference, Santa Fe** (unpagged).
- HAGGERTY S.E. 1976. Opaque mineral oxides in terrestrial igneous rocks. In Rumble D. ed, **Reviews in Mineralogy - Volume 3, Oxide Minerals**, pp. 101-300. Mineralogical Society of America.
- HAWTHORNE J.B. 1975. Model of a kimberlite pipe. **Physics and Chemistry of the Earth** 9, 1-15.
- GURNEY J.J. 1984. A correlation between garnets and diamonds in kimberlites. In Glover J.E. and Harris P.G. eds, **Kimberlite Occurrence and Origin**, pp. 143-166. Geology Department and Extension, University of Western Australia, Publication No 8.
- JAQUES A.L., LEWIS J.D. and SMITH C.B. 1986. The kimberlitic and lamproitic rocks of Western Australia. **Geological Survey of Western Australia Bulletin** 132.
- MCDONOUGH W.F., MCCULLOCH M.T. and SUN S-S. 1985. Isotopic and geochemical systematics in Tertiary-Recent basalts from southeastern Australia and implications for the evolution of the sub-continental lithosphere. **Geochimica et Cosmochimica Acta** 49, 2051-2067.
- NIXON P.H., ROGERS, N.W., GIBSON I.L. and GREY A. 1981. Depleted and fertile mantle xenoliths from southern African kimberlites. **Annual Reviews of Earth and Planetary Sciences** 9, 285-309.
- SMITH C.B. 1983. Pb, Sr and Nd isotope evidence for sources of southern African Cretaceous kimberlite. **Nature** 304, 51-54.
- VEEVERS J.J. 1981. Morphotectonics of rifted continental margins in embryo (East Africa), youth (Africa-Arabia) and maturity (Australia). **Journal of Geology** 89, 57-82.

KIRKLEY M.B., SMITH H.S. and GURNEY J.J.

Geochemistry Department, University of Cape Town, South Africa

Wide variations in $\delta^{13}\text{C}$ and $\delta^{18}\text{O}$ values of kimberlite carbonates have been reported by several workers (e.g. Kobelski et al., 1979). Some of these variations are interpreted here to be the result of primary magmatic fractionation processes. Others are the result of secondary mixing and exchange processes.

Standard of Comparison

Fresh hypabyssal kimberlite, that is representative of pipes in the Kimberley District of South Africa, is readily available from the Wesselton mine. Hence the Wesselton kimberlite was chosen as a standard for comparison with other kimberlite occurrences. Carbonates from the Wesselton kimberlite define the carbon and oxygen isotope fields shown in Figs. 1, 2 and 3 where the isotope compositions of carbonates from other occurrences are illustrated. Wesselton samples containing significant quantities (>1 vol%) of carbonate as a replacement product in microxenoliths have been excluded from the suite because the isotopic composition of oxygen in this type of carbonate can be shown to be contaminated by oxygen from the precursor minerals.

Isotope Contamination by Host Rock Assimilation

Carbonates from Group II (micaceous) kimberlites display a range of $\delta^{13}\text{C}$ and $\delta^{18}\text{O}$ values that flank the Wesselton field and extend to values approaching those of sedimentary carbonates (Fig. 1). Carbonates from Finsch, Bellsbank and Swartruggens have ^{13}C - and ^{18}O -enriched isotope signatures relative to the Wesselton field. These three Group II kimberlites intrude the thick Precambrian Chuniespoort Group dolomites (Transvaal System). Carbonate from a Group I (non-micaceous) kimberlite that intrudes dolomite, the Toxteth occurrence near Kuruman, was found to be similarly enriched in ^{13}C and ^{18}O . Assimilation of sedimentary carbonate host rock has

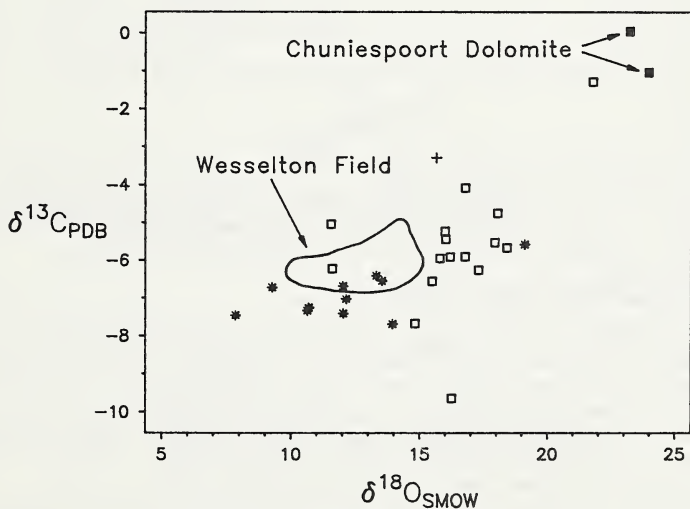


Figure 1. Stable isotope composition of carbonates from Group II kimberlites. Squares represent carbonates from Finsch, Bellsbank and Swartruggens. The cross represents carbonate from the Group I Toxteth occurrence. Stars represent carbonates from Group II kimberlites which do not intersect dolomite.

apparently allowed ^{13}C and ^{18}O enriched CO_2 to mix with kimberlite volatiles thus changing the stable isotope compositions of kimberlite groundmass carbonate. One sample from the Newlands kimberlite, an occurrence which does not intersect dolomite, plots with the Finsch group. This sample may be ^{18}O enriched as a result of low temperature meteoric water alteration.

Isotope Fractionation Through Magmatic Differentiation

Carbonates from the Benfontein Middle sill have carbon and oxygen isotope compositions that overlap those from Wesselton. Lower sill carbonates however are relatively depleted in ^{18}O and enriched in ^{13}C such that they exhibit isotopic signatures similar to those of carbonatite carbonates (Fig. 2). The isotopic trend defined by Middle sill/Lower sill carbonates is similar to that which developed through differentiation of the carbonatites of Laacher See, West Germany (Taylor et al, 1967). TiO_2 enrichment in Lower sill groundmass titanomagnetites is consistent with the hypothesis that the Lower sill represents a later differentiate of the Benfontein magma relative to the Middle sill. These data support the hypothesis that kimberlites can differentiate to carbonatitic compositions in terms of carbon and oxygen isotope values.

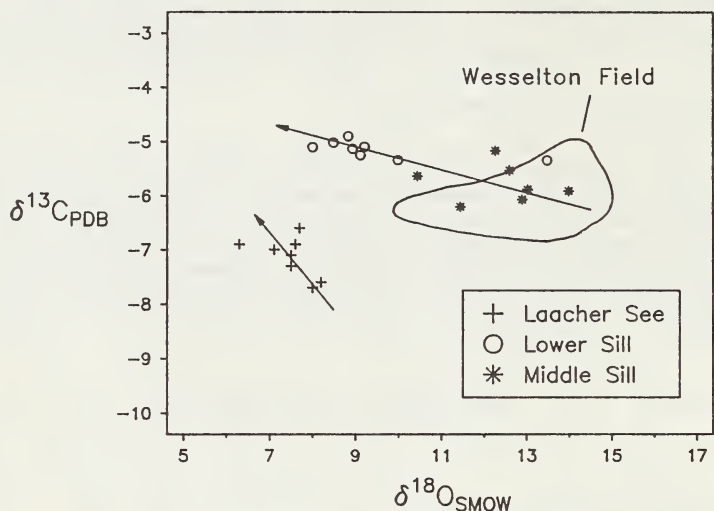


Figure 2. $\delta^{13}\text{C}$ - $\delta^{18}\text{O}$ relationship between carbonates from the Middle sill and Lower sill at Benfontein, compared with Laacher See carbonatites (Taylor et al., 1967). Arrows indicate differentiation trends.

Isotope Fractionation Between Vapor and Liquid

Carbonates with isotope compositions similar to those at Wesselton are conspicuously absent in the Monastery kimberlite. Carbonates from the Monastery kimberlite groundmass and from carbonatized xenoliths have isotopic signatures that are ^{13}C enriched by 2 to 4 per mil relative to the Wesselton average (Fig. 3). Such ^{13}C enrichment may be a function of ^{13}C being fractionated into CO_2 vapor, as has been shown to occur in basalt systems (Pineau et al., 1976; Javoy et al., 1978), and suggests that the Monastery volatiles were particularly enriched in CO_2 .

Calcite inclusions found in ilmenite megacrysts from Monastery have ^{13}C enriched signatures similar to the kimberlitic calcites. Petrographically these inclusions appear to be primary and armoured against alteration by the enclosing megacryst. The isotopic similarities between these carbonate occurrences at Monastery imply that the kimberlite and megacryst systems had similar CO_2 -rich compositions. This supports a close genetic relationship between kimberlite and megacryst liquids and implies that CO_2 enrichment is a function of the Monastery source area.

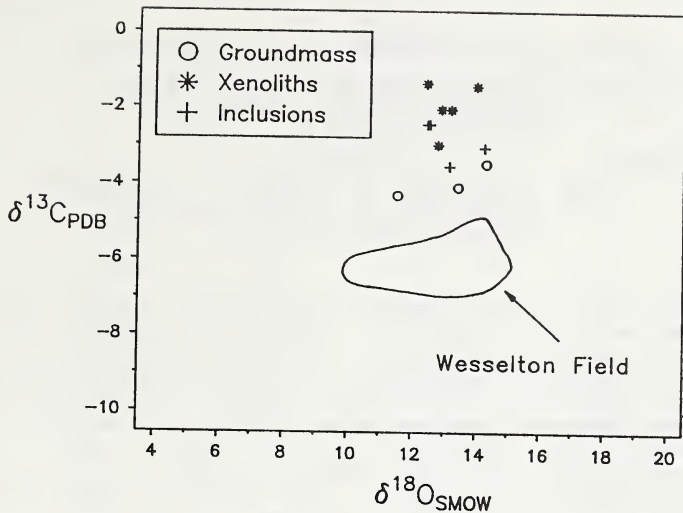


Figure 3. ^{13}C enrichment exhibited by groundmass carbonate from the Monastery kimberlite, carbonatized xenoliths, and calcite inclusions in ilmenite megacrysts.

References

- JAVOY M., PINEAU F. and IYAMA I. 1978. Experimental determination of the isotopic fractionation between gaseous CO_2 and carbon dissolved in tholeiitic magma. *Contributions to Mineralogy and Petrology* 67, 35-39.
- KOBELSKI B.J., GOLD D.P. and DEINES P. 1979. Variations in stable isotope compositions for carbon and oxygen in some South African and Lesothan kimberlites. In Boyd F.R. and Meyer H.O.A. (eds.): *Kimberlites, Diatremes, and Diamonds: Their Geology, Petrology, and Geochemistry*; Proceedings of the Second International Kimberlite Conference Volume 1. American Geophysical Union: Washington D.C., pp 252-271.
- PINEAU F., JAVOY M. and BOTTINGA Y. 1976. $^{13}\text{C}/^{12}\text{C}$ ratios of rocks and inclusions in popping rocks of the Mid-Atlantic Ridge and their bearing on the problem of deep-seated carbon. *Earth and Planetary Science Letters* 29, 413-421.
- TAYLOR H.P., FRECHEN J. and DEGENS E.T. 1967. Oxygen and carbon isotope studies of carbonatites from the Laacher See District, West Germany and the Alno District, Sweden. *Geochimica Cosmochimica Acta* 31, 407-430.

THE NATURE OF IRON IN KIMBERLITIC ILMENITES AND CHROMITES

H.Lucas¹, M.T.Muggeridge² and D.M.McConchie²

1. C.R.A. Exploration Pty. Ltd.
21 Wynyard Street
Belmont, 6104, W.A.
2. Department of Geology
University of Western Australia
Nedlands, 6009, W.A.

INTRODUCTION

For kimberlites and petrogenetically similar rocks, data on the total concentration of iron in ilmenites and chromites, its crystallographic site distribution, and the ferrous/ferric ratio may be useful in identifying potentially diamondiferous lithologies and distinguishing them from other igneous suites. Conventional chemical analytical methods permit the accurate determination of total iron in these minerals, but distribution data depend heavily on the analytical method used and the assumptions adopted. The resulting lack of reproducibility within and between laboratories is unacceptable if the value of the analyses to exploration is to be fully realised.

In this study, ilmenite and chromite grains are used to compare various analytical procedures. The accuracy of each procedure is evaluated by comparing the indirectly obtained ferrous/ferric ratio data with data obtained by Mössbauer spectroscopy. Mössbauer spectroscopy enables the direct determination of the ferrous/ferric ratio for each crystallographic site and the discrimination of any secondary ferruginous phases incorporated in the mineral examined and, because it uses the solid mineral grains, there is no risk of altering the oxidation state of the iron during chemical dissolution. The spectra obtained by Mössbauer analysis are a direct response to the number of iron atoms in each electronic configuration and hence, determinations of site occupancies and oxidation states do not depend on assumptions such as mineral stoichiometry and the absence of lattice defects.

Ilmenite and chromite grains were selected for analysis, on the basis of their apparent freedom from inclusions and alteration rims, using a binocular microscope. The selected grains were boiled in 40% HF for 1 hr and subsequently in acid oxalate to remove surface contaminants. Each selected grain was then sectioned and analysed with an electron microprobe using wavelength dispersion procedures (EPMA), with a scanning electron microscope using energy dispersion procedures (SEM), and by Mössbauer spectroscopy; the FeO and Fe₂O₃ content of large grains were also analysed by standard wet chemical methods. For both EPMA and SEM analyses, determination of the ferrous/ferric ratio was made for ilmenite using the Boyd molecular proportions method (Boyd, 1971), and for chromite using the method of Fisher (1972).

PRELIMINARY RESULTS AND DISCUSSION

For ilmenites and chromites, agreement between EPMA and SEM analytical data for major components is generally reasonable (e.g., Table 1) although some MgO determinations for ilmenites reveal differences between the methods as high as 20%. However, agreement between EPMA and SEM methods on the ferrous/ferric ratio is usually poor with differences of the order of 50% being common. The disagreement arises because although the difference between the total iron contents determined by each method is small, partitioning of the iron between divalent and trivalent forms by any indirect method

(e.g., the method of Boyd, 1971) will reflect the cumulative errors in determinations of all components used in the calculation.

TABLE 1

Comparison of EPMA and SEM analytical data
for representative ilmenite and chromite grains **

COMPONENT	ILMENITE		CHROMITE	
	EPMA	SEM	EPMA	SEM
SiO ₂	0.00	0.00	0.02	0.00
TiO ₂	49.90	52.29	1.09	1.17
Al ₂ O ₃	0.22	0.00	6.18	6.11
V ₂ O ₃	0.00	0.32	0.17	0.15
Cr ₂ O ₃	1.33	1.42	61.29	61.00
Fe ₂ O ₃	10.25	6.63	2.59	3.09
FeO	27.98	33.23	14.61	15.09
MnO	0.29	0.36	0.33	0.55
MgO	9.28	7.53	12.05	11.82
CaO	0.06	0.00	0.00	0.00
NiO	0.00	0.00	0.13	0.00
*Total Fe	37.20	39.44	16.94	17.87
#FeO/Fe ₂ O ₃	2.73	5.01	5.64	4.88

* Total Fe is expressed as %FeO

The direct ferrous/ferric ratio determined by Mössbauer spectroscopy is 2.70 for the ilmenite and 4.26 for the chromite

**Ilmenite compositions are means of 4 (SEM) and 2 (EPMA) analyses
Chromite compositions are means of 4 (SEM) and 3 (EPMA) analyses

Thus for the ilmenite in Table 1, the difference between the ferrous/ferric ratios calculated from each analysis is largely a reflection of the cumulative differences between the MgO and TiO₂ contents determined by each method.

Mössbauer data for the ilmenite show a ferrous/ferric ratio which is in excellent agreement with the ratio obtained using EPMA. Wet chemical analysis of the ilmenite yields a ferrous/ferric ratio (1.55) which agrees with neither the EPMA data nor the SEM data although the wet chemically determined total iron concentration (37.78) agrees well with both. The ferrous/ferric ratio determined by wet chemical analysis is lower than that determined by EPMA or SEM methods possibly because difficulties in dissolving many rock materials cause wet chemical determinations of ferrous/ferric ratios to err in favour of Fe₂O₃ (e.g., Bancroft *et al.*, 1977) no matter how careful the analyst. However, despite the possible bias in wet chemical determinations of ferrous/ferric ratios, the results obtained to date are in better agreement with the EPMA and Mössbauer data than are determinations based on SEM analyses.

For the chromite, ferrous/ferric ratios determined by EPMA and by SEM frequently disagree with each other and in some grains both differ from the Mössbauer data. Where the Fe₂O₃ concentration is much lower than the FeO concentration, slight differences in the Fe₂O₃ content determined by each procedure will be magnified in the calculated ferrous/ferric ratio, but this observation cannot explain the difference in the first place. There are three possible explanations for the disagreement between the procedures:-

1. Two of the three procedures are inaccurate. This explanation is unlikely in view of the data for ilmenites.

2. Finger's calculation method is unsatisfactory. This explanation is also unlikely because no assumption used in the method appears to be sufficiently erroneous to account for the discrepancies.
3. The differences between the EPMA and SEM data reflect the same cumulative errors that affect the ilmenite analyses and data from both differ from Mössbauer data because the Mössbauer examines whole grains including inclusions which are usually avoided during electron beam point analyses. This explanation is supported by a) high standard deviations between individual point analyses, b) the presence of unidentified platy contaminants noted during crushing, and c) the presence of traces of hematite in the Mössbauer spectra of some chromites. Calculations show that because the ferric iron content of the chromites is so low, as little as 1.5% contaminant hematite could fully account for the difference between the Mössbauer data and data derived by electron beam methods.

CONCLUSIONS

Compositional data for chromites and ilmenites have been used by several authors (e.g., Boyd and Nixon, 1973; Singhvi et al., 1974; Haggerty, 1975; Sobolev et al., 1975) to provide an insight into the origin of kimberlite pipes and to distinguish kimberlitic ilmenites and chromites from those with other origins.

Almost all these studies require knowledge of ferrous/ferric ratios but this study raises some major questions as to the usefulness of some analytical techniques. SEM data appear to be good for overall comparisons but cumulative errors encountered in assessing ferrous/ferric ratios may make this method unsatisfactory for more complex studies. Wet chemical analyses are probably unsuitable due to their tendency for bias in favour of trivalent iron, and although Mössbauer probably gives the best ferrous/ferric ratios it is not suited to routine analyses. Probably the best routine analytical method is EPMA, but its use raises the question of whether bulk grain compositions (including alteration rims zones and inclusions) are more useful or less useful in petrogenetic analysis than the composition of the most alteration and inclusion free part of the grain. Either approach involves assumptions which require careful consideration in relation to both what to analyse and how.

REFERENCES

- Bancroft, G.M., Sham, T.K., Riddle, C., Smith, T.E. and Turek, A., 1977: Ferric/Ferrous-iron ratios in bulk rock samples by Mössbauer spectroscopy - the determination of standard rock samples G-2, GA, W-1, and Mica-Fe. *Chem. Geol.*, 19, 277-84.
- Boyd, F.R., 1971: Enstatite-ilmenite and diopside-ilmenite intergrowths from the Monastery Mine. *Carnegie Inst. Yearbook*, 70, 134-8.
- Boyd, F.R., and Nixon, P.H., 1973: Origin of the ilmenite-silicate nodules in kimberlites from Lesotho and South Africa. In P.H. Nixon (ed.) *Lesotho Kimberlites*, p.254-268.
- Finger, L.W., 1972: The uncertainty in the calculated ferric iron content of a microprobe analysis. *Carnegie Inst. Yearbook*, 71, 600-603.
- Haggerty, S.E., 1975: The chemistry and genesis of opaque minerals in kimberlites. *Phys. Chem. Earth*, 9, 295-307.
- Singhvi, A.K., Gupta, D.K., Gokhale, K.V.G.K. and Rao, G.N., 1974: Mössbauer spectra of ilmenites from primary and secondary sources. *Phys. Stat. Sol.*, 23, 321-324.
- Sobolev, N.V., Pokhilenko, N.P., Lavreutev, Yu. G., and Usova, L.V., 1975: Distinctive features of the composition of chrome spinels in the diamonds and kimberlites of Yakutia. *Sov. Geol. Geophys.*, 16, 1-16.

OXIDE MINERALS IN CHICKEN PARK KIMBERLITE
NORTHERN COLORADO

M.E. McCallum

Department of Earth Resources
Colorado State University, Fort Collins, Colorado 80523, U.S.A.

Hypabyssal phases of the Chicken Park kimberlite complex in the State Line District of northern Colorado are characterized by high concentrations of ilmenite, spinel, and perovskite, and minor amounts of rutile. Total oxide content locally exceeds 20 volume percent. Spinel and ilmenite occur primarily as macrocrysts (> 1 mm) and microcrysts (< 1 mm) (grains of probable xenocrystic and/or very early phenocrystic origin), and as euhedral or corroded anhedral grains in the kimberlite groundmass. Titanomagnetite commonly rims ilmenite, chromian spinel and perovskite, occurs as reduction "exsolution" lamellae along {0001} planes in some macrocrystic-microcrystic ilmenite, and as atollis surrounding many groundmass spinels. Perovskite occurs predominantly as euhedral to subhedral crystals in the groundmass, but also is an important component (intergrown with titanomagnetite) of reaction mantles rimming many ilmenite grains. Rutile is found as tiny acicular to rod-like inclusions in the outer parts of serpentinized olivine macrocrysts and as small irregular "intergrowths" with perovskite in ilmenite reaction mantles.

Picroilmenites dominate the opaque mineral macrocryst-microcryst suite, and their generally rounded, corroded and mantled nature is distinctive from most of the typically small (< 0.1 mm), euhedral to subhedral "lath" or rhombohedral platelet groundmass ilmenites. The groundmass ilmenites are characterized by enrichment in manganese and iron (1.0-8.2 wt.% MnO and 35 to 41 wt.% FeO) and low MgO (0.5 to 6.0 wt.%) (Table 1, analyses 17 and 18). Macrocrystic-microcrystic ilmenites (Table 1, analyses 13-16) generally are MnO poor (< 1.0 wt.%) and contain 10-21 wt.% MgO; low MgO (< 12 wt.%) grains tend to be enriched in iron, and some high Fe₂O₃ (17-21 wt.%) varieties are enriched in Cr₂O₃ (1.0-3.6 wt.%). Ilmenite with reduction "exsolution" lamellae of spinel generally have lower MgO and higher FeO contents (Table 1, analyses 11 and 12) but exhibit a rather wide range of compositions. Many ilmenite grains show a core to rim enrichment in MgO and depletion in FeO.

Spinel is abundant in the groundmass as small (most < 0.05 mm) compositionally simple euhedral grains of titanomagnetite, Mg-titanomagnetite (as much as 12.5 wt.% MgO), and local Ti-Mg-chromites (Table 1, analyses 3-5). Zoned groundmass spinel grains tend to be somewhat larger (most 0.03-0.13 mm), and exhibit a generally consistent trend from Cr-Al-rich and Ti-Mn-poor cores (28-60 wt.% Cr₂O₃, 5-20 wt.% Al₂O₃, 0.3-7.0 wt.% TiO₂ and 0.2-0.5 wt.% MnO) to mantles and rims that are progressively enriched in TiO₂ and MnO (as much as 12.3 and 1.5 wt.% respectively) and depleted in Cr₂O₃ and Al₂O₃ (as little as 0.23 and 0.61 wt.% respectively) (Table 1, analyses 1 and 2; Fig. 1, B-E). Zoned crystals with highly chromian cores (> 45 wt.% Cr₂O₃) exhibit intermediate zones that are more aluminous than adjacent core and rim (Fig. 1, B). These zones are comparable in composition to cores of the generally smaller, less chromian, zoned spinel crystals (Fig. 1, C-E) which apparently nucleated during the same period of crystallization. Atoll textured or skeletal spinels occur as discrete forms or as "mantles" on chromite or Cr-titanomagnetite cores. These spinels typically are manganese titanomagnetites (Table 1, analysis 6; Fig. 1, E), and are compositionally similar to most of the smallest (< 0.02 mm) euhedral-anhedral titanomagnetite grains in the groundmass and to many of the reaction mantle spinels rimming earlier formed groundmass and xenocrystic(?) oxide minerals (Table 1, analyses 7 and 8; Fig. 1, H and I). Titanomagnetite reduction "exsolution" lamellae in ilmenite macrocrysts and microcrysts are chemically similar to associated reaction mantle spinels (Table 1, analyses 7-10; Fig. 1, H and I) although the lamellae generally are less enriched in MnO (0.1-2.1 vs. 0.5-3.6 wt.%), more enriched in FeO (37-52 vs. 25-37 wt.%), and exhibit a greater range of Fe₂O₃, TiO₂ and MnO values. Rare xenocrysts of aluminous chromite (Fig. 1, A) are compositionally similar to Al-chromite grains in spinel peridotite xenoliths recovered from the district, and are rimmed by manganese titanomagnetite. Some tiny (< 0.002 mm) opaque grains in serpentinized olivine macrocrysts give energy dispersive x-ray patterns that are consistent with magnetite.

Euhedral to subhedral, groundmass perovskite crystals range from about 0.05-0.13 mm in diameter and generally are zoned, the larger grains exhibiting more pronounced chemical variations. Cores typically contain in excess of 2.5 wt.% REE (Ce, Nd and La the major contributors), but rim totals generally are less than 0.5 wt.% (Table 1, analyses 19 and 20). Na_2O content, which may exceed 0.50 wt.% in cores, also decreases towards rims (commonly by about one half). FeO systematically increases from core to rim (about 0.9-1.2 vs. 1.1-1.7 wt.%) and Nb_2O_5 also is slightly more enriched in rims (0.36-0.44 vs. 0.44-0.52 wt.%). Perovskite in reaction mantles of ilmenite grains is chemically similar to rims of groundmass euhedra, although FeO contents tend to be somewhat higher (locally exceed 2 wt.%).

The small size of the rutile grains (generally less than 0.002 mm wide although acicular crystals may exceed 0.02 mm in length) present difficulties in obtaining accurate chemical analyses. However, partial analyses indicate that the rutiles are chromian, and low totals may in part indicate the presence of Nb which has been reported from kimberlite rutiles elsewhere (e.g. Mitchell, 1979).

The Chicken Park kimberlite oxide mineral assemblage reflects crystallization from a Ti-rich liquid that became progressively more enriched in Fe and Mn as Al-Mg-Cr spinels and microilmenite formed. Most microilmenite crystallized early in the mantle although more magnesian rims on some grains probably were added during magma ascent. Reduction "exsolution" of titanomagnetite lamellae in microilmenite also occurred early as indicated by extensive resorption of these grains and involvement of the lamellae in reaction mantles of perovskite and titanomagnetite. Variable chemistry of the lamellae apparently reflects changes in f_{O_2} and T during the reduction exsolution process, and this information will be useful in providing data on the redox state of the upper mantle under northern Colorado.

The earliest groundmass spinels were Al-deficient aluminous-magnesian chromites that were subsequently partially resorbed and rimmed by titaniferous-aluminous-magnesian chromite which also nucleated as discrete crystals. Ilmenite was no longer crystallizing at this point and the residual melt became progressively enriched in Ti along with Fe^{3+} and Mn which favored the formation of chromian titanomagnetite and eventually manganian titanomagnetite (Fig. 1). These phases occur as progressive growth rims on zoned spinels, as small discrete crystals and as reaction mantles on ilmenite grains. Perovskite crystallization was initiated by increased Ca levels in the melt. Accompanying increases in CO_2 content favored the transport of Mn and Nb-REE, the former concentrated in late stage, euhedral, Mn-rich ilmenites and titanomagnetites, the latter in perovskites, particularly the euhedral to subhedral groundmass grains. Some late stage Mn-ilmenites also have significant enrichment in Nb. The final oxide phase to crystallize was manganian titanomagnetite that occurs as atolls, skeletal and tiny groundmass crystals, and as rims and/or reaction mantles on spinel, ilmenite and perovskite crystals. Irregular grains of rutile "intergrown" with perovskite in reaction mantles appear to be replacing the perovskite and if so, would also be very late stage. Variations in compositions of zoned crystal sequences and reaction mantles reflect changes in cation activities along with redox conditions and temperature.

REFERENCE

MITCHELL, R.H., 1979, Mineralogy of the Tunraq kimberlite, Somerset Island, N.W.T., Canada. In: F.R. Boyd and H.O.A. Meyer (eds.), *Kimberlite, Diatremes and Diamonds*, Vol. 1, pp. 161-171. American Geophysical Union, Washington.

Research supported by the South African CSIR and Department of Geochemistry, University of Cape Town.

Table 1. Representative Chemical Compositions of Oxide Minerals from Chicken Park Kimberlite.

wt. %	Zoned spinels				Unzoned spinels			Atoll spinel	Reaction mantle spinels		"Exsolution" lamellae spinels in ilmenite macrocrysts	
	core	1 rim	2 core	2 rim	3	4	5		6	7	8	9
TiO ₂	0.29	8.26	4.48	8.69	6.24	7.41	9.20	7.90	11.43	21.45	29.11	23.72
Al ₂ O ₃	8.81	1.88	16.95	2.24	8.36	10.88	6.41	3.41	4.46	1.16	1.06	1.07
Cr ₂ O ₃	56.45	3.27	34.34	4.91	13.04	8.32	0.40	0.84	4.55	0.50	0.98	3.02
FeO	14.77	26.03	16.96	25.38	23.28	20.89	25.70	28.58	30.79	46.04	49.81	49.34
Fe ₂ O ₃	6.55	50.75	12.52	48.87	38.66	39.93	47.97	51.90	40.34	26.39	12.14	19.02
MnO	0.47	0.61	0.44	0.68	0.73	0.67	0.68	0.90	0.95	2.02	0.85	0.38
MgO	11.87	7.81	13.88	8.68	9.54	11.99	9.22	6.09	6.83	1.96	4.73	2.12
	99.21	98.61	99.57	99.45	99.85	100.09	99.58	99.62	99.35	99.52	98.68	98.67
wt. %	Ilmenite macrocrysts with spinel "exsolution" lamellae		Ilmenite macrocrysts		Mantled ilmenite microcrysts		Euhedral ilmenites		Zoned perovskites			
	11	12	13	14	15	16	17	18	19		20	
	core	rim	core	rim	core	rim	core	rim	core	rim	core	rim
TiO ₂	55.28	53.55	59.89	52.23	56.43	57.45	54.14	52.81	55.65	56.00	55.39	54.86
Al ₂ O ₃	0.62	0.07	0.09	0.38	0.07	0.00	0.01	0.00	0.27	0.24	0.00	0.00
Cr ₂ O ₃	0.11	0.31	0.09	0.29	0.22	0.14	0.20	0.22	0.00	0.03	0.00	0.03
FeO	26.88	29.73	15.48	26.64	21.94	21.62	36.64	38.75	1.06	1.34	1.40	1.74
Fe ₂ O ₃	4.68	5.74	3.22	8.70	4.91	2.99	0.51	0.17	*	*	*	*
MnO	0.39	0.95	0.66	0.20	0.63	0.97	3.19	7.74	0.05	0.00	0.04	0.09
MgO	12.61	9.81	21.13	11.28	15.81	16.29	4.92	0.25	0.13	0.08	0.14	0.08
CaO	0.00	0.03	0.07	0.04	0.00	0.06	0.09	0.37	39.38	40.87	38.42	40.57
Na ₂ O	n.a.	n.a.	n.a.	n.a.	n.a.	n.a.	n.a.	n.a.	0.40	0.23	0.39	0.17
Nb ₂ O ₅	n.a.	n.a.	n.a.	n.a.	n.a.	n.a.	n.a.	n.a.	0.42	0.45	0.41	0.52
REE	n.a.	n.a.	n.a.	n.a.	n.a.	n.a.	n.a.	n.a.	2.59	0.23	2.57	0.51
	100.57	100.19	100.63	99.76	100.01	99.52	99.70	100.31	99.95	99.47	98.76	98.57

n.a. - not analyzed. * all Fe as FeO. Electron microprobe analyses obtained at the University of Cape Town, South Africa, and the U.S. Geological Survey, Denver, Colorado.

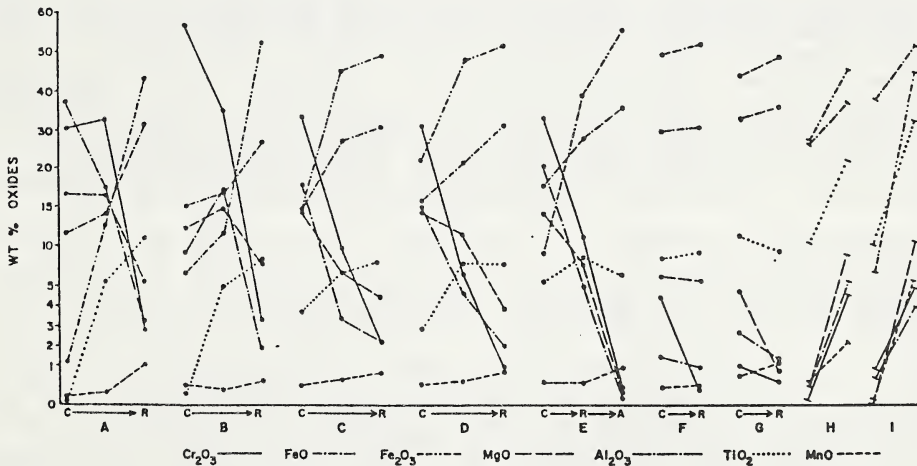


Fig. 1. Major element variations in spinels. A: Red-brown aluminous chromite macrocryst (derived from spinel peridotite xenolith) with titanomagnetite rim (R). B-D: Zoned spinels with chromian cores (C) and titanomagnetite rims (R). E: Zoned chromian spinel with titanomagnetite atoll (A). F and G: Small (> 0.04 mm), euhedral, groundmass titanomagnetites. H: General compositional range of titanomagnetite reaction rims on ilmenite. I: General compositional range of titanomagnetite "exsolution" lamellae in ilmenite.

Department of Earth and Atmospheric Sciences, Purdue University
West Lafayette, IN 47907, USA

The most extensive field of kimberlites in West Africa occurs in south-central Guinea, but in spite of their discovery in 1952 by Soguinex and later considerable work by Russian geologists in the 1960's (Vladimirov et al., 1971) little information is available in the scientific literature. About 20 small kimberlite pipes and numerous dikes have been emplaced into Archaean basement rocks consisting mostly of granitic gneisses and quartzitic schists, possibly of Dahomeyan or Birrimian age. Extensive dolerite magmatism occurred about 180 Ma ago and this predates the kimberlitic events. The kimberlite dikes are often oriented almost E-W, but other trends such as 055° and 115° are present. Dikes vary in width from thin stringers or veins (cms), to proper dikes 3 m thick. Dikes may occur "en echelon" or in groups of 3 or more, and extend for 2-3 km. The pipes are relatively small, resembling more the "blows" of South Africa. The largest pipe, Antochka, is roughly 5.2 ha in size. In some instances numerous veins and stringers are localized and form kimberlite stockworks. Clusters of pipes occur, for example at Banankoro, and often it appears that pipes have originated at the intersection of dikes. The absolute age of the kimberlitic magmatism is unknown, but is younger than the 180 Ma age of the dolerites which are often cross-cut by the kimberlite dikes. The kimberlites have undergone erosion since emplacement and probably represent root zone facies.

Unfortunately, many of the pipes, dikes and associated alluvial deposits have been ravaged by the local miners. This together with the thinness of many dikes, the extensive and deep weathering makes sampling at present difficult. Nevertheless, samples from the Antochka and Droujba pipes have been examined as well as heavy mineral concentrate immediately above or close to other pipes and dikes. Kozlov (1966) reports that most dikes consist of an olivine macrocryst-bearing kimberlite sometimes rich in groundmass-mica, whereas the pipes are formed from brecciated kimberlite. The minerals in both types of kimberlite appear to be similar, but differ in modal percentage. Koslov comments that clinopyroxene is present in the kimberlite groundmass of both dikes and pipes, but this mineral was not identified in the present study.

The Droujba kimberlite consists of large (0.5 cm) macrocrysts of olivine, ilmenite and rare pyrope garnet (<1.2 cm) set in a fine grained groundmass of phlogopite, spinel, calcite, serpentine and minor perovskite and some sulfides. Small euhedral (0.5 mm) olivines are scattered throughout the groundmass. The Antochka kimberlite is somewhat similar although mica appears to be smaller and less abundant. Autoliths were observed in one pipe as well as xenoliths of granulite, presumably derived from the lower crust. It is reported that all the kimberlites contain diamond, but the dikes appear to be richer in this mineral than the pipes. Ilmenite is the most abundant and characteristic tracer mineral in the Guinean kimberlites and may form megacrysts up to 3 cms in size.

Phlogopite in the Droujba kimberlites occurs in three distinct ways: 1) as light brownish microphenocrysts (TiO_2 2-4 wt.%; Al_2O_3 14-17 wt.% and FeO_T 5-7.5 wt.%) with colorless rims (TiO_2 < 1 wt.%; Al_2O_3 10-14 wt.% and FeO_T 2-5 wt.%), 2) as laths with colorless cores similar in compositional range to the brownish microphenocrysts, but having orange rims of tetraferriphlogopite (TiO_2 and Al_2O_3 < 1 wt.%, FeO_T 12-18 wt.%), and 3) as small groundmass micas with high Al_2O_3 contents of between 16 and 19 wt.%, TiO_2 < 2.5 wt.% and FeO_T 3 to 5.5 wt.% (Table 1). No zoning was observed in the groundmass micas. Cr_2O_3 contents are low (<0.2 wt.%) in all micas although the cores of the brown and colorless microphenocrysts appear on average to be higher than the rims. In general the micas do not contain inclusions of spinel suggesting much of the groundmass mica crystallized later than the spinel and ilmenite, a feature which may explain the low TiO_2 content of the phlogopite. Phlogopites similar to the brownish and colorless microphenocrysts have been noted in chlorite-phlogopite intergrowths from Koidu, Sierra Leone by Tompkins and Haggerty (1984); however, compositionally the core and rims are reversed. Phlogopite in the Antochka kimberlite is fairly uniform in composition (TiO_2 2-3 wt.%, Al_2O_3 11.5-14.5 wt.% and FeO_T 5.5-7 wt.%) (Table 1) and appears to be similar to Type-II groundmass micas of Smith et al. (1978).

Spinels are common in both the Droujba and Antochka kimberlites and are generally < 0.25 mm in size. Most are euhedral to subhedral, but those larger than 0.1 mm are usually embayed or corroded. Atoll spinels are common in Droujba, but are absent in Antochka. Compositionally the spinels range from aluminous magnesian chromites (Cr_2O_3 >48 wt.%, Al_2O_3 3-15 wt.% and MgO 12-15 wt.%) to titanian chromites (TiO_2 6-12 wt.%) to ulvospinel-magnetite (Table 2). This trend (AMC-TMC-Usp Mag) has been observed also in spinels from kimberlites at Bellsbank (Boctor and Boyd, 1982), Zagadochnaya (Rozova et al., 1982) and Koidu (Tompkins and Haggerty, 1984) and corresponds to Trend 2 of Mitchell (1986).

The least evolved and rarest of the spinels at Droujba is a translucent red aluminous magnesian chromite (TiO_2 < 1 wt.%) which is zoned towards an opaque rim containing less Al_2O_3 and Cr_2O_3 and more TiO_2 than the red core (Table 2). The most evolved spinels in the Droujba kimberlite are the groundmass and outer mantles of the atoll spinels, these are mostly ulvospinel-magnetite with up to 1.5 wt.% MnO. The atoll cores are generally titanian magnesian chromites and form the intermediate section of Trend 2. The cores show variation in mg (0.2-0.5) and depletion in Al and Cr as Ti increases. In contrast to Droujba, the Antochka kimberlite contains an abundance of the translucent red-brown least evolved AMC spinels. These, similar to those in the Droujba kimberlite are mantled by opaque rims consisting of the more highly evolved ulvospinel-magnetite members (Table 2).

Olivine (\sim Foggo) from the Droujba pipe is typically kimberlitic as is the garnet (Cr_2O_3 \sim 2 wt.%; CaO \sim 4 wt.%; MgO 22-23 wt.%). As far as is known no group 10 garnets (Dawson and Stephens, 1975) have been reported to date from Guinea.

Ilmenite, the most ubiquitous mineral in Guinean kimberlites has varying MgO contents from 8 to 20 wt.%, and Cr_2O_3 0.3-1.6 wt.%. In the Droujba kimberlite groundmass ilmenites have slightly lower Cr_2O_3 and higher MnO contents than macrocrysts (Table 3).

There is a similarity between the occurrences of kimberlite in Guinea and those in Sierra Leone (Grantham and Allen, 1960; Tompkins and Haggerty, 1984) and Liberia (Haggerty, 1982). In the three regions dikes seem to predominate over pipes, which are all relatively small. There are also petrographic and mineralogical similarities between the kimberlites of Guinea and Sierra Leone in that they consist predominantly of macrocrystal olivine and ilmenite in a groundmass of small second generation olivine, phlogopite, serpentine and calcite. The minerals also are comparable in their chemistries. The third major kimberlite field in West Africa, that of Mali, close to Guinea, appears to be somewhat different in that pipes seem to be much more common than dikes.

References

- BOCTOR N.Z. & BOYD F.R. 1982. Petrology of kimberlite from the DeBruyn and Martin Mine, Bellsbank, South Africa. *Am. Mineral.*, **67**, 917-925.
- DAWSON J.B. & STEPHENS W.E. 1975. Statistical analysis of garnets from kimberlites and associated xenoliths. *J. Geol.*, **83**, 589-607.
- GRANTHAM D.R. & ALLEN J.B. 1960. Kimberlite in Sierra Leone. *Overseas Geol. Miner. Resour.*, **8**, 5-25.
- HAGGERTY S.E. 1982. Kimberlites in Western Liberia: An overview of the geological setting in a plate tectonic framework. *J. Geophys. Res.*, **81**, 10811-10826.
- KOSLOV I.T. 1966. The geology and petrography of kimberlites in Guinea. *Soviet Geol.*, **6**, 113-125.
- ROZOVÁ Y.V., FRANTSESON E.V., PLESHAKOV A.P., BOTOVA M.M. & FILIPOVA L.P. 1982. High iron chrome spinels in kimberlites of Yakutia. *Int. Geol. Rev.*, **24**, 1417-1425.
- SMITH J.V., BRENNESHOLTZ R. & DAWSON J.B. 1978. Chemistry of micas from kimberlites and xenoliths, I. Micaceous kimberlites. *Geochim. Cosmochim. Acta*, **42**, 959-971.
- TOMPKINS L.A. & HAGGERTY S.E. 1984. The Koidu kimberlite complex, Sierra Leone: Geological setting, petrology and mineral chemistry. *Proc. 3rd Int. Kimb. Conf.*, Vol. I, 81-105.
- VLADIMIROV B.M., TVERDOKHLEBOV V.A. & KOLESNIKOVA T.P. 1971. Geology and petrography of igneous rocks from the southwestern Guinea-Liberian shield. *Acad. Sci. U.S.S.R. Siberian Branch*, 242 pp. (In Russian).

Table 1: Representative analyses of Phlogopite, Olivine and Garnet.

	Mica						Olivine		Garnet		
	1	2	3	4	5	6	7	8	9	10	11
SiO ₂	38.1	38.8	38.3	38.1	40.1	39.3	40.6	40.6	43.2	44.0	42.6
TiO ₂	3.01	0.49	1.08	3.36	0.26	2.42	0.04	0.02	0.69	0.34	0.48
Al ₂ O ₃	15.2	13.5	17.2	15.8	0.92	13.7	0.00	0.00	19.9	21.3	20.2
Cr ₂ O ₃	0.01	0.02	0.07	0.02	0.00	0.7	0.04	0.00	2.18	0.83	3.56
FeO*	6.48	4.87	3.75	5.60	15.7	6.72	11.6	7.35	8.11	7.62	7.52
MgO	21.0	27.8	24.6	22.9	26.7	23.0	47.9	51.1	22.7	21.3	21.9
CaO	0.01	0.00	0.00	0.00	0.00	0.00	0.02	0.04	4.37	4.12	4.36
MnO	0.06	0.00	0.09	0.11	0.07	0.14	0.19	0.07	0.24	0.38	0.30
NiO	0.11	0.06	0.03	0.08	0.01	0.03	0.28	0.42	0.00	0.00	n.d.
Na ₂ O	0.02	0.00	0.39	0.00	0.02	0.36	0.09	0.04	0.06	0.12	n.d.
K ₂ O	10.0	8.34	10.1	10.6	9.95	9.32	0.00	0.01	0.00	0.00	n.d.
	94.0	93.9	95.6	96.6	93.7	95.1	100.8	99.6	101.4	99.6	100.9

* All iron expressed as FeO. 1-5,7-10 Droujba; 6 Antochka; 11 Bafateya;
1 and 2 - core and rim microphenocryst, 3 - groundmass, 4 and 5 - core and rim
(tetraferriphlogopite).

Table 2: Representative analyses of spinels in Guinean kimberlites.

	1	2	3	4	5	6	7	8	9	10
TiO ₂	7.83	8.08	5.41	6.36	3.65	1.10	7.26	2.81	2.04	2.93
Al ₂ O ₃	0.43	5.94	1.98	4.80	1.15	3.35	1.49	0.02	9.47	0.92
Cr ₂ O ₃	2.94	15.3	2.25	44.4	1.13	62.7	0.95	1.92	54.1	0.66
FeO _T	74.7	54.6	72.2	29.2	77.6	18.8	78.0	87.0	20.0	72.0
MgO	6.18	13.7	11.3	14.7	10.8	12.8	6.05	2.57	15.0	16.5
CaO	0.15	0.13	0.09	0.02	0.04	0.00	0.79	0.33	0.12	0.46
MnO	1.93	0.74	1.32	0.84	1.01	0.24	1.43	0.92	0.34	1.18
	94.2	98.5	94.6	100.3	95.4	99.0	96.0	95.6	101.0	94.7
Fe ₂ O ₃ *	52.5	40.0	60.2	-	66.7	-	56.8	64.4	-	71.8
FeO*	27.5	18.6	18.1	-	17.6	-	26.9	29.0	-	7.32
	99.5	101.5	100.7	-	102.8	-	101.7	102.0	-	101.8

FeO_T All iron as FeO; * Based on 4 oxygen and 3 cations.

1-7 Droujba; 8-10 Antochka

1,2 - groundmass; 3 - mantle on ilmenite; 4,5 - core and rim of atoll;
6,7 - core and rim of red aluminous magnesian chromite; 8 - groundmass
9,10 - core and rim of red aluminous magnesian chromite

Table 3: Representative analyses of ilmenites.

	1	2	3	4	5	6	7	8	9	10
TiO ₂	49.7	51.5	59.5	58.4	51.5	53.5	50.3	49.3	50.9	49.4
Al ₂ O ₃	1.29	0.73	0.05	0.14	0.63	0.79	0.63	0.64	0.53	0.50
Cr ₂ O ₃	0.56	0.66	0.39	0.25	1.57	0.77	0.68	0.41	0.71	0.30
FeO _T	36.0	25.3	20.8	22.9	33.7	29.1	38.3	39.3	35.3	39.5
MgO	12.5	20.5	17.6	15.7	11.6	14.6	10.1	9.62	11.2	9.75
CaO	0.05	0.02	0.08	0.06	0.03	0.05	0.02	0.02	0.02	0.01
MnO	0.25	0.83	1.71	1.55	0.21	0.33	0.18	0.20	0.23	0.30
	100.4	99.5	100.1	99.0	99.3	99.1	100.2	99.5	98.9	99.8

1-4 Droujba; 5,6 - Fenaria dike; 7,8 - Banankoro pipes 3 and 4;
9,10 Bafateya dike. All megacrysts except 3 and 4 which are groundmass phases.

HENRY O. A. MEYER¹, STEPHEN E. HAGGERTY² AND DARCY P. SVISERO³

1. Department of Earth and Atmospheric Sciences, Purdue University, West Lafayette, IN 47907
2. Department of Geology, University of Massachusetts, Amherst, MA 01003
3. Instituto de Geociencias, Universidade de Sao Paulo, Sao Paulo, Brasil

Several intrusions in the region of Coromandel, Minas Gerais, have been reported to be kimberlites on the basis of the heavy mineral contents (i.e. pyrope garnet, magnesian ilmenite) of weathered rock and overlying soils. In view of the presence of several other types of alkalic rock (e.g. carbonatites) in the region it is important to establish the true identity of the possible kimberlites. Accordingly, a detailed examination of groundmass phases, particularly spinels, has been undertaken on a number of the intrusions from which fresh, relatively unaltered rock has been obtained. For example, the rocks constituting the Limeira I and Indaia I intrusions consist of numerous irregular macrocrysts of olivine, Mg-ilmenite, rare phlogopite and clinopyroxene set in a fine grained groundmass of calcite, serpentine, spinels, perovskite, monticellite and apatite.

Olivine (Fog2-86) varies in size between 5 and 0.25 mm and may be angular, especially the larger grains, or display euhedral hexagonal shapes, usually those <1 mm. Some olivines contain Mg-ilmenite, and also consist of compound grains. Olivine probably constitutes 30 to 35% of the rock (Table 1). Mg-ilmenite (~13 wt.% MgO) is ubiquitous and ranges between 1 and 0.1 mm. Most grains are rounded but in detail have ragged margins due to replacement by perovskite and spinel. Pseudomorphs of calcite, monticellite and serpentine after phlogopite macrocrysts up to 1.5 mm in length are present. Rare remnant cores of mica occur in some of the pseudomorphs (Table 1). The groundmass perovskite is often euhedral with rhombic or rectangular shapes (<0.05 mm), and apatite is present as laths up to 0.25 mm long. Spinel is generally <0.04 mm in size, angular and/or rounded.

In contrast to the above rocks those constituting the Limeira II and Indaia II intrusions are much finer grained and consist of olivine macrocrysts, generally between 0.5 and 0.05 mm in size, and some small Mg-ilmenites (<0.25 mm) with little or no alteration to perovskite at the margin. The groundmass has a flow texture in which euhedral perovskite (<0.01 mm), spinels and apatite are randomly scattered throughout the very fine grained felty aggregate of thin lath shaped crystals of clinopyroxene composition (Table 1). In Indaia II small plates of phlogopite occur that poikilitically enclose numerous crystals of the groundmass (Table 1).

Spinel in both Limeira I and Indaia I are usually small, somewhat less than 0.04 mm in size, and show varying shapes from rectangular to irregular or rounded. No atoll spinels are observed. Angular orange-red spinels that are aluminous magnesian chromites are rare. They probably represent fragments from disaggregated spinel peridotites that occur as xenoliths in both intrusions. The groundmass spinels in Limeira I have Al₂O₃ < 2 wt%, MgO between 11 and 14 wt%, and TiO₂ 6 to 19 wt%. In some instances cores of spinels have higher Cr₂O₃ than the rims (40 vs. 1 wt%), whereas TiO₂ and FeO_T are higher in the rims. Similar compositional variations occur in the spinels in Indaia I (Table 2). When plotted in the reduced spinel prism (Haggerty, 1976; Mitchell, 1986) the overall trend for Limeira spinels is from titanian chromites to magnesian ulvospinel-ulvospinel-magnetite (MUM) at a fairly constant Mg/(Mg+Fe) of 0.3. Indaia I spinels show a similar trend, but a slightly higher Mg/(Mg+Fe) of 0.4. Comparable trends, but at Mg/(Mg+Fe) between 0.5 and 0.7 are to be observed in the Jos (Mitchell and Meyer, 1980), Green Mountain (Boctor and Meyer, 1979) and Benfontein (Boctor and Boyd, 1981) kimberlites. In the Wesselton (Shee, 1984) and De Beers (Pasteris, 1982) spinels in different kimberlite events although having similar trends vary in Mg/(Mg+Fe). The absence of aluminous and for the most part chrome-rich spinels, and the dominance of MUM type which plot close to the Mg₂TiO₄ (qandilite)-Fe₂TiO₄ (ulvospinel) apex of the condensed spinel prism suggests crystallization from a highly evolved magma. A feature of the spinels in support of this suggestion are the relatively high MnO contents (>1 wt%) a feature also noted for spinels in the Green Mountain kimberlite. Also noted in the Green Mountain kimberlite, and in kimberlites

from the Premier Mine and Lesotho are reaction rims of perovskite on the Mg-ilmenite. MUM spinels in kimberlites are usually confined to serpentine, calcite, monticellite and diopside kimberlites and the first three minerals are major components in Limeira I and Indaia I rocks. Mica is notably absent in the groundmass, and MUM spinels usually do not occur in micaceous kimberlites, particularly in the Group II variety (Smith, 1983; Mitchell, 1986).

In contrast to the spinels in Limeira I and Indaia I those in Limeira II and Indaia II are small, irregular and have cores corresponding to titanian magnesian chromites. These cores are replaced in whole or part by mantles of titanomagnetite containing minor ulvospinel. These spinels appear to be highly evolved and contain MnO between 1 and 2 wt% (Table 2). In the reduced prism the spinels plot close to the Fe-rich side of the diagram in view of the high Fe/(Fe+Mg) of 0.9. A compositional gap appears to be present between the cores and mantles. The overall trend is somewhat similar to that observed in spinels from Bellsbank kimberlite (Boctor and Boyd, 1982) and to the later part of the Zagadochnaya kimberlite (Rozova et al., 1982) although the Brazilian spinels have higher Fe/(Fe+Mg).

Most kimberlites with spinels that display this trend (Trend 2; Mitchell, 1986) are micaceous and it has been suggested the spinel trend results from crystallization of phlogopite which removes Al and Mg. However, in the case of Indaia II the mica is a late stage phase and poikilitically encloses both spinel and groundmass clinopyroxene. The trend for spinels in Limeira II and Indaia II is also mirrored by spinels in the Matinha intrusion, also in Minas Gerais. This rock is a petrographic variant of those from both Limeira and Indaia in that macrocrysts of olivine of various sizes, and rare phlogopite, are set in a felty groundmass of lath shaped pyroxene (Table 1), spinel and perovskite. Some intersertal glass is present. Apart from the absence of flow texture in Matinha, plus its coarser groundmass nature, the rock is akin to that of Limeira II and Indaia II. These latter rocks are different to those of Limeira I and Indaia I in that they are much finer grained, show flow texture, have a groundmass of clinopyroxene in which late stage mica is present, and also have a different evolutionary spinel trend. This trend from titanian magnesian chromites to ulvospinel-titanomagnetites is not unique to kimberlites, and has analogs in other types of rock, e.g. lamproites (Mitchell, 1986a,b) and other alkaline rocks (Haggerty, 1976).

Outcrops of the Japecanga intrusion, in the Coromandel area of Minas Gerais, are deeply weathered and associated minerals are extensively altered. Spinel (0.01 to 0.02 mm) form the dominant opaque oxide (1-2%) but show extensive modification to fretted hematite, oriented intergrowths of magnesioferrite and possibly hydrated ferric oxide (e.g. goethite). Remnants of gray, Cr-rich spinel cores, mantled by Mg-rich titanomagnetite is the prevalent association (Table 2) and is thus analogous to the overall spinel trends in the Limeira and Indaia intrusions and is more typical of kimberlites than other alkaline rocks. Although composite analyses of altered intergrowths yield consistently low analytical totals, it is nonetheless evident that spinel core compositions are most unusual (Table 2), being high in MnO (up to 5 wt.%) with moderate Cr₂O₃ (13-26 wt.%), reflecting an evolved and carbonate-rich magma source. Spinel rims are depleted in MnO and are either titanomagnetites or magnesian-titanomagnetites.

Discrete ilmenite grains (1-5 mm) from eluvial soils are rounded and remarkably unaltered with MgO contents in the range 7.5 to 11 wt.% and Cr₂O₃ between 0.2 and 2.7 wt.%. Trace but significant amounts of Nb and Zr are present (Table 1), and high Fe³⁺ are consistent with kimberlites having a carbonate affinity (e.g. Tompkins and Haggerty, 1985).

Although these Brazilian rocks have been termed pseudo-kimberlites, the mineralogy and composition of certain groundmass phases are comparable with kimberlites from other worldwide localities. However, in detail some chemical signatures (e.g. MnO contents of some spinels) and petrographic features (e.g. Limeira II, Matinha) suggest these intrusions were derived from possibly highly evolved carbonate-rich magmas. It is conceivable these Brazilian rocks may be a link between those exemplified by the Group II (Smith, 1983) serpentine-calcite-monticellite kimberlites and others similar to the carbonate kimberlite sill of Benfontein.

Xenoliths in Limeira I are dunites and harzburgites of which some are metasomatized with the formation of spinel and associated phlogopite and diopside. This style of metasomatism is identical to that found in metamatites in the Kaapvaal craton of southern Africa (e.g. Erlank et al., 1982). The subcratonic lithosphere beneath Minas Gerais is, therefore, depleted and in a similar manner to the Kaapvaal craton has been subsequently enriched. Although spinel peridotite xenoliths are common, no garnet-bearing varieties have been yet observed from this region of Minas Gerais. Perhaps this is a reflection of the tectonic setting of these intrusions within an ancient mobile zone and is also a clue to the highly evolved nature of the rocks.

References

- BOCTOR N.Z. & BOYD F.R. 1981. *Contrib. Mineral. Petrol.*, **76**, 253-259.
 - - - - & - - - - 1982. *Am. Mineral.*, **67**, 917-925.
 - - - - & MEYER H.O.A. 1979. *Proc. Second Int. Kimb. conf.*, vol. 1, 217-228.
 ERLANK A.J., ALLSOPP H.L., HAWKESWORTH C.J. & MENZIES M.A. 1982. *Terra Cognita*, **2**, 261-263.
 HAGGERTY S.E. 1976. In "Oxide Minerals". *Revs. in Min.*, Vol. 3, Min. Soc. Am., D.C.
 MITCHELL R.H. 1986a. *Kimberlites: Mineralogy, geochemistry and petrology*. Plenum, NY
 - - - - 1986b. *Geol. Soc. S. Africa Trans* (in press).
 - - - - & MEYER H.O.A. 1980. *Can. Mineral.*, **18**, 241-250.
 PASTERIS J.D. 1982. *Am. Mineral.*, **67**, 244-250.
 ROZOVA Y.V., FRANTSESSON E.V., PLESHAKOV A.P., BOTOVA M.M. & FILIPOVA L.P. 1982. *Int. Geol. Rev.*, **24**, 1417-1425.
 SHEE S.R. 1984. *Proc. Third Int. Kimb. Conf.*, Vol. 1, 59-73.
 SMITH C.B. 1983. *Nature*, **304**, 51-54.
 TOMPKINS L.A. & HAGGERTY S.E. 1985. *Contrib. Mineral. Petrol.*, **91**, 245-263.

Table 1: Representative analyses of silicates and ilmenite

	Macrocrysts							Groundmass			
	1	2	3	4	5	6	7	8	9	10	11
	Olivine		Pyx.	Mica		Ilmenite		Monti.	Pyroxene		Mica
SiO ₂	41.2	39.9	(52)	42.5	0.23	-	-	36.7	52.8	51.9	39.4
TiO ₂	0.00	0.00	0.07	1.64	49.1	50.3	42.7	0.19	1.61	2.20	6.56
Al ₂ O ₃	0.00	0.00	2.77	10.2	0.49	0.08	0.04	0.00	2.25	1.90	10.4
Cr ₂ O ₃	0.00	0.00	0.31	0.23	1.46	0.24	2.65	0.32	0.08	0.06	0.10
FeO	8.51	13.2	1.67	6.41	36.1	36.5	43.4	3.27	5.76	6.11	5.51
MgO	50.6	46.4	17.8	24.0	12.3	10.8	7.77	24.0	13.9	15.0	21.2
CaO	0.04	0.08	25.7	0.00	0.18	0.00	0.00	33.4	20.6	21.2	0.04
MnO	0.12	0.12	0.06	0.02	0.59	0.41	0.39	0.33	0.16	0.11	0.13
NiO	0.31	0.12	-	0.00	0.00	-	-	0.06	0.00	0.00	0.00
Na ₂ O	0.11	0.00	-	0.35	0.00	-	-	0.00	1.72	0.89	0.21
K ₂ O	0.01	0.03	-	10.10	0.00	-	-	0.10	0.69	0.55	9.45
TOTAL	100.9	99.8	(100)	95.5	100.5	98.8*	97.9†	98.3	99.6	99.9	93.0

* Includes 0.28 ZrO₂ and 0.14 Nb₂O₅. † Includes 0.25 ZrO₂ and 0.63 Nb₂O₅.
 1,3 - Limeira I; 2,4,5,8 - Indaia I; 6,7 - Japocanga; 9,11 - Indaia II; 10 - Matinha

Table 2. Representative Spinel Analyses

	Limeira I		Indaia I		Limeira II			Japocanga	
					Core	Margin		Core	Margin
TiO ₂	17.3	11.3	14.3	22.8	3.37	12.3	10.6	10.2	21.9
Al ₂ O ₃	0.97	1.40	1.03	0.79	4.38	0.54	0.39	2.94	1.94
Cr ₂ O ₃	6.09	0.14	14.5	10.3	41.0	1.14	7.01	13.5	0.18
Fe ₂ O ₃ *	34.9	51.5	32.1	22.8	18.9	45.2	43.4	33.0	26.2
FeO*	27.4	20.7	22.4	21.8	24.0	33.7	32.0	23.1	42.6
MgO	11.8	12.2	13.2	18.4	6.52	4.50	4.78	8.00	5.21
CaO	0.34	0.48	0.21	0.69	0.27	0.56	0.40	-	-
MnO	1.10	1.12	1.13	1.17	1.05	0.95	1.05	4.5	0.95
TOTAL	99.9	98.8	98.9	98.8	99.5	99.0	99.5	95.2	99.0

mg 0.263 0.245 0.314 0.438 0.221 0.097 0.107 0.213 0.123

* Calculated on basis of 4 oxygen and 3 cations

THE NOMENCLATURE AND ORIGIN OF THE NONCUMULATE ULTRAMAFIC
ROCKS AND THE SYSTEMATIC POSITION OF KIMBERLITES

Eric A. K. Middlemost

Department of Geology & Geophysics, University of Sydney, NSW, Australia

In most discussions of the systematics of igneous rocks, the kimberlites are omitted, or considered in a perfunctory manner. This is mainly because they are rare and their geochemical and petrographic characteristics set them apart from the more common igneous rocks. It is convenient to visualise igneous rocks as occupying a discrete field within multidimensional compositional space; and just as the Hertzprung-Russell diagram portrays the various types of stars and defines the stellar "main sequence", so in a similar manner the Total Alkali Silica (TAS) diagram portrays the broad spectrum of diverse igneous rocks and specifies the common rocks of the igneous main sequence. The compositions of the rocks that belong to the igneous main sequence range from the picobasalts and basalts through to the rhyolites, trachytes and phonolites. Most of the terms and concepts used in igneous petrology were developed in order to describe and account for the origin and evolution of the rocks of the main sequence. The trends in magmatic differentiation that characterise the rocks of the main sequence, together with the criteria conventionally used to define these trends, are often inapplicable to rocks outside the main sequence. A close examination of the low-silica igneous rocks reveals that, when compared to the rocks of the main sequence, they are in many ways dissimilar to normal volcanic or plutonic rocks.

An investigation of the concept of the plutonic and volcanic associations reveals that the rocks of the volcanic association are products of volcanic activity at, or very near, the surface of a planet; whereas the rocks of the plutonic association (Kennedy & Anderson 1938:25) usually "comprise the great, subjacent stocks and batholiths" and typically comprise the granites and granodiorites of the continental crust. The peridotites of the upper mantle are dissimilar to crustal plutonic rocks as they evolved over long eons of time in a high temperature essentially static environment where annealing generated granular rocks in which the minerals have a high degree of inter-facial stability. It is proposed that the mantle rocks as a group belong to an ultraplutonic association. Included in this new association are rocks such as dunite, that are essentially solid residues left after partial melting, and a variety of peridotites. The latter have experienced one or more periods of partial melting, and periods of incompatible element enrichment caused by deep-mantle degassing and/or the reflux of previously subducted lithospheric materials. Another proposal is that the root name peridotite, should only be used to describe plutonic or ultraplutonic rocks: because, whereas it is proper to use this term to name rocks of these associations, it is contrary to conventional petrographic practice to use it to describe volcanic or quasi-volcanic rocks of similar composition. It would also be consistent with the foregoing discussion to accept the nomenclature introduced by Bogatkov et al. (1981:30), and give all the volcanic and quasi-volcanic rocks that contain between 25 and 41% SiO₂, and less than 4.0% (Na₂O + K₂O) the root, or family name picrite. Irrespective of whether or not one recalculates their major element compositions on a H₂O⁺ and CO₂ free basis, most kimberlites plot within the compositional field proposed for the picrite family on the TAS diagram.

In the preceding discussion the term quasi-volcanic was used to characterize rocks that have volcanic affinities but belong to the diatremic association (Harris et al. 1981:30). Such rocks usually occur in minor intrusions, dykes or pipes, and their structures and textures often indicate that they were injected as pipe-surge, or fluidized, systems. During emplacement these systems are characteristically composed of magmaclasts (i.e. fragments of partly or completely congealed magma), xenoclasts (i.e. xenoliths and xenocrysts) and a propellant phase. Before congealment part of the propellant phase may escape; however in many diatremic rocks part of it is trapped in carbonates and late-stage magmatic and/or secondary hydrous silicate minerals. The H₂O⁺ and/or CO₂ contents of the diatremic rocks are normally

significantly higher than those of the rocks of the main sequence. In brief, it is argued that volatile components are a part of the very nature of the diatremic rocks, and it is thus inappropriate to recalculate the major element compositions of these rocks on a H₂O and CO₂ free basis. The lamprophyres are pre-eminent among the rocks of the diatremic association. In orthodox classifications of igneous rocks they occupy an extensive range that embraces many families and even clans of rocks. The ordinary lamprophyres are part of the main sequence of rocks and they are essentially shoshonites; the alkaline lamprophyres are essentially potassic tephrites; whereas the melilitic lamprophyres occur well outside the main sequence and are essentially picrites and foidites. It is proposed that the rocks of the diatremic association and the lamprophyres are synonymous; and as the lamproites and kimberlites are members of the diatremic association, they are thus also members of the lamprophyric association.

In the preceding discussion it was stated that the range of the melilitic lamprophyres extended from the picritic field into the foiditic field. On the extended TAS diagram the foidite domain is expanded into the low-silica field, and the new boundary lines are placed at 35% SiO₂ and 4% total alkali. In order to understand the nature of the low-silica rocks and the relationship between the picrites and foidites one has to take cognisance of the fact that these rocks contain less SiO₂ than both the normal upper mantle rocks, and the common igneous rock-forming silicate minerals of the crust. A high content of non-silicate minerals is found in the picritic rocks that grade into the non-silicate clan of rocks.

Most of the rocks of the lamprophyric association are usually regarded as being potassic, however it is difficult to apply this term in a systematic way to an association of rocks that ranges in composition from picrites to shoshonites. Zanettin (1984:20) has recently proposed that volcanic rocks are sodic when Na₂O - 1.5 > K₂O, and potassic when Na₂O - 1.5 < K₂O. These criteria are absurd, as they imply that all volcanic rocks that contain less than 1.5% Na₂O, and most that contain less than 1.8 Na₂O, are potassic, even if Na₂O is strongly enriched relative to K₂O. This absurdity explains why Le Maitre (1984:250) classified 83% of the picrobasalts as potassic rocks, yet the mean Na₂O and K₂O values of these rocks were 1.44% and 0.51% respectively. There is clearly a need for precisely defined terms to describe the alkaline character of the rocks that plot within the picrobasalt, tephrite, picrite and foidite fields of the extended TAS diagram. It is proposed that the general term potassium-dominant should be used to describe all igneous rocks in which K₂O exceeds Na₂O; and the term perpotassic should be used to describe igneous rocks that contain significant amounts of potassium relative to Na₂O or another oxide such as MgO. There is no simple way of defining perpotassic using a K₂O/Na₂O ratio because this ratio tends to change with magmatic differentiation. If one wishes to use the K₂O/Na₂O ratio to define the term perpotassic one has to change the limits set on the ratio as one proceeds from one domain to the next on the TAS diagram. One might choose a limiting ratio as low as 1.2 in the picrobasalt field, but increase it to 2.5 in the phonotephrite field as it contains many leucite-bearing rocks. It is proposed that the use of the term perpotassic should normally be restricted to the rocks on the low-silica side of the main sequence, and it should be defined by using a K₂O versus MgO diagram (cf. Figure 1). In this diagram the lamproites are observed to be perpotassic (i.e. above line AB); whereas the kimberlites, and most of the lamprophyres, plot between the lamproites and the normal hyperalkalic rocks of the main sequence.

An elegant method of illustrating the alkaline character of igneous rocks is to plot their Al, Na and K abundances on a triangular diagram (cf. Figure 2). This diagram enables one to explore changes in the Na/Al, K/Al and K/Na ratios, and in the peralkaline tendency, of the rocks being studied. The kimberlites and lamproites occupy discrete fields on the Al-Na-K diagram; with the lamproites being quite unique in that they are normally peralkaline with remarkably high K/Al ratios. It is proposed that, either the K₂O versus MgO, or the Al-Na-K diagrams, should be used to separate the lamproites from the kimberlites.

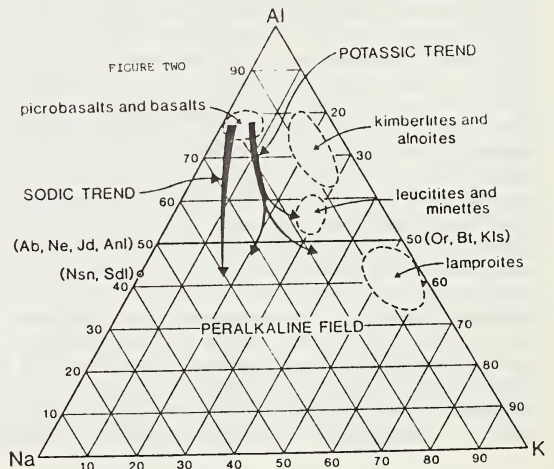
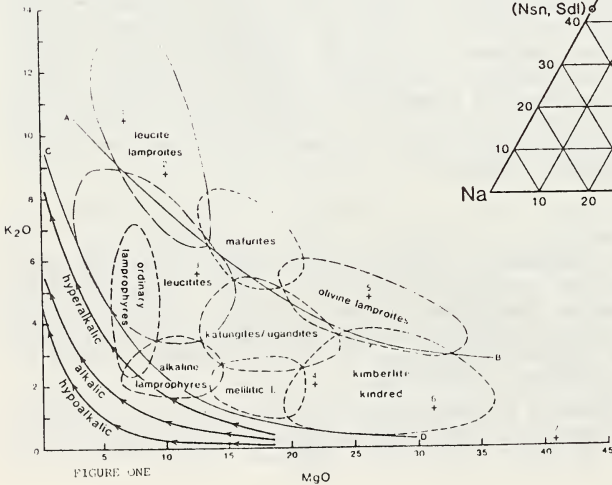
When one studies the origin of a suite of main sequence igneous rocks one is able to use one of a number of standard variation diagrams: they enable one to

relate the various rocks to each other by differentiation processes that operate at pressures lower than those anticipated in the source region. However, when one considers the origin of rocks outside the main sequence, such as foidites and picrite, one discovers no generally accepted indices of magmatic differentiation. In order to remedy this difficulty a general differentiation index (GDI) is proposed. The GDI is equal to the sum of the differences between the major oxides of a particular rock, and the oxides of a hypothetical ideal upper mantle rock. It is demonstrated that this index is a valuable aid in the difficult search for primary foiditic, picritic and tephritic magmas.

It is concluded that the kimberlites are potassium-dominant picrites of the lamprophyric association; and they characteristically carry phlogopite and a variety of ultraplutonic xenoclasts: whereas the lamproites are a suite of peralkaline, perpotassic tephrites, phonotephrites and tephriphonolites that belong to the lamprophyric association, and they are readily defined on a K_2O versus MgO diagram. The nature and origin of the magmatic component in the olivine lamproites and kimberlites is examined and discussed.

References

Bogatikov, O.A., Mikhailov, N.P. & Gonshakova, V. (eds) (1981) Classification and Nomenclature of Magmatic Rocks, Nedra, Moscow, USSR.
 Harris, P.G., Kennedy, W.Q. & Scarfe, C.M. (1970) Volcanism versus plutonism - the effect of chemical composition, in Newall, G. & Rast, N. (eds) Mechanism of Igneous Intrusion, Geol. J., Spec. Issue, 2, 187-200.
 Kennedy, W.Q. & Anderson, E.M. (1938) Crustal layers and the origin of magmas, Bull. Volc., Serie II, Tome III, 23-41.
 Le Maitre, R. (1984) A proposal by the IUGS subcommission on the systematics of igneous rocks for a chemical classification of volcanic rocks based on the total alkali silica (TAS) diagram, Australian J. Earth Sci., 31, 243-55.
 Zanettin, B. (1984) Proposed new chemical classification of volcanic rocks, Episodes, 7(4), 19-20.



ROGER H. MITCHELL¹ & HENRY O.A. MEYER²

1-Department of Geology, Lakehead University, Thunder Bay, Ontario, Canada P7B 5E1
2-Department of Geosciences, Purdue University, W.Lafayette, Indiana 47907, U.S.A.

Micaceous kimberlites occur at the New Elands and Star Mines, Orange Free State, South Africa. At New Elands there occur three east-west striking dikes which cross-cut an approximately north-south trending system of thin dikes. The Star Mine consists of three sub-parallel dikes named the Burns, Wynandsfontein and New Star dikes.

Kimberlites at both localities are predominantly fine grained hypabyssal phlogopite kimberlites that in some examples contain abundant macrocrystal olivine. Megacrystal (> 10 mm) micas, magnesian ilmenite and Ti-pyroxene are absent. Micro-xenoliths of eclogite and harzburgite occur in the Star dikes.

In the New Elands dikes microphenocrystal (0.2-1.5 mm) micas occur in three petrographically and compositionally distinct types; 1. colorless-to-pale brown titanian phlogopite ($mg = 0.87-0.96$, $FeO_T = 2.4-6.5\%$, $TiO_2 = 0.15-2.44\%$, $Cr_2O_3 = 0.1-1.0\%$), 2. fluid inclusion-rich brown titanian phlogopite ($mg = 0.85-0.91$, $FeO_T = 4.1-6.8\%$, $TiO_2 = 1.14-3.5\%$, $Cr_2O_3 = 0.18-0.84\%$) and 3. rare olive green titanian magnesian biotite ($mg = 0.56-0.61$, $FeO_T = 15.4-17.6\%$, $TiO_2 = 1.71-4.28\%$, $Cr_2O_3 = 0.05\%$). Complex mantling and zoning with respect to TiO_2 , Cr_2O_3 and FeO_T are characteristic. Continuous zoning is commonly from colorless or pale brown cores to darker brown margins relatively richer in TiO_2 and FeO_T . The pattern of discontinuous mantling is varied and mantles that are normally or reversely zoned relative to the core composition are equally common. Boundaries between the cores and mantles are well-defined and are sub-parallel in the case of multiple overgrowths. The relationships suggest that the mantles are epitaxial overgrowths rather than passive reaction mantles formed by interactions between the microphenocrysts and the late stage groundmass fluids.

At the Star Mine microphenocrystal micas are pale brown relatively low Cr_2O_3 (< 0.5%) low TiO_2 (0-0.8%), low FeO_T (2.5-4.2%) titanian phlogopites and relatively higher Cr_2O_3 (0.96-1.39%), TiO_2 (1.59-2.10%) and FeO_T (4.30-5.39%) darker brown titanian phlogopites. Complex mantling and zoning similar to that observed in the New Elands kimberlites is characteristic.

Groundmass micas (0.01-0.15 mm) form a dense interlocking mass of euhedral-to-subhedral tabular crystals. Commonly they are continuously zoned either from colorless cores to brown margins or from brown cores to colorless margins. All types are titanian phlogopites ($mg = 0.87-0.96$, $FeO_T = 2.41-7.8\%$, $TiO_2 = 0.15-2.59\%$, $Cr_2O_3 = 0.1-1.0\%$). In the New Elands kimberlites the groundmass micas commonly exhibit reaction rims of red tetraferriphlogopite, although at the Star Mine such rims are found only in the Wynandsfontein dike.

Representative compositions of the micas are given in Table 1. The paragenesis and composition of mica in the New Elands and Star kimberlites are similar. The presence of reverse and normally zoned and mantled crystals of different composition in close proximity is interpreted as suggesting that the bulk of the micas have not crystallized in-situ. The simplest explanation of the mica compositional variation and mantling is that they represent the products of crystallization of several batches of kimberlite magma of broadly similar but slightly different composition. Incorporation of crystals derived from one batch of magma into another will result in the development of epitaxial mantles, these mantles representing the composition of the current liquidus phlogopite. Concentration of crystals derived from different batches of magma at different stages of crystallization together with batch mixing and hybridization results in the observed heterogeneous mica population. These mica-rich dikes were probably emplaced as a crystal-rich slurry produced by the flushing out of a differentiated continuously replenished magma chamber. Only the outermost Fe-rich margins of the crystals and the tetraferriphlogopites probably crystallized in-situ. This interpretation of the mica population implies that the "groundmass" micas in these micaceous kimberlites are in reality small microphenocrysts. Direct comparison of the whole rock composition of such micaceous

kimberlites with those of rocks derived from other magmas e.g. lamproites, is thus considered to be inappropriate.

Spinel in the New Elands dikes are Ti-poor ($< 0.5\% \text{TiO}_2$) magnesian aluminous chromites that exhibit a considerable range in their Cr/ Cr+Al (0.56-0.86) and Mg/ Mg+Fe (0.55-0.72) ratios.

All of the Star dikes contain compositionally uniform titanian magnesian chromites (Mg/ Mg+Fe = 0.39-0.50, Cr / Cr+Al = 0.90-0.95) that are poor in Al_2O_3 ($< 1\%$). Titaniferrous magnesian magnetite (Mg / Mg+Fe = 0.8-0.9) exhibiting a wide range in Ti / Ti+Cr+Al ratios (0.39-0.95) occurs only in the Burns dike. The absence of Ti-rich spinels in other dikes is attributable to their resorption during the later stages of crystallization of the groundmass. Representative compositions are given in Table 2.

Fresh olivines are present only in the Star dikes. The largest crystals have magnesian cores (mg = 0.92-0.94) that are zoned towards relatively Fe-rich margins (mg = 0.91-0.93). Smaller crystals have compositions that are similar to these rims (mg = 0.90-0.91). The overall compositional range is thus very limited (mg = 0.90-0.94). Second generation euhedral groundmass olivine is absent.

In the New Elands dikes garnets are found as macrocrystal phases (in heavy mineral concentrates) and as an apparently primary groundmass phase. Macrocrystal garnets are all believed to be xenocrysts derived from eclogitic, lherzolitic and harzburgitic sources. The population consists of calcium pyrope almandine (29%), chrome pyrope (29%) and low calcium chrome pyrope (42%), classified as group 3, 9 and 10 garnets by the Dawson and Stephens (1975) garnet classification scheme. Set in the calcite-chlorite rich groundmass are small (100-500 μm) brown euhedral Zr-rich garnets (Table 3). In the Star kimberlites xenocrystal garnets derived from eclogitic and lherzolitic sources are present. In the groundmass of the Burns dike there exists an apparently primary Ti-rich Zr-free garnet (Table 3).

Primary euhedral partially resorbed microphenocrysts of Al-poor ($< 0.5\% \text{Al}_2\text{O}_3$), Cr-poor ($< 0.2\% \text{Cr}_2\text{O}_3$) diopside occur in the New Elands kimberlites.

Other minerals present as minor late stage primary groundmass minerals in both the New Elands and Star dikes include perovskite, pyrite, rutile, apatite, calcite and K-Ba-V-titanates belonging to the hollandite group of minerals. The titanates occur as stellate clusters of reddish-brown prisms. In the New Elands dikes they are a previously unrecognized V and Ce-rich hollandite (Table 3), related to priderite and mannardite (Mitchell and Haggerty 1986). In the Star dike there occurs a V-free Cr-bearing Ba-rich hollandite (Table 3).

This study confirms and extends previous works (Smith et al. 1978, Mitchell 1986) which have suggested that each micaceous kimberlite contains a characteristic assemblage of micas and that their general trend of evolution is towards Ti and Fe enrichment coupled with Cr_2O_3 depletion, and ultimately to the development of tetraferriphlogopite. Spinel compositional trends are similar to those determined for other micaceous kimberlites and are identical to those observed in lamproites. (Mitchell 1985).

The New Elands and Star kimberlites belong to a province of micaceous kimberlites which are isotopically different to the commoner serpentine-calcite-monticellite kimberlites. These isotopic group II (Smith 1983) kimberlites differ in their mineralogy to the isotopic group I kimberlites in containing primary microphenocrystal diopside, hollandite group minerals and Zr- and Ti-rich garnets in addition to their complex mica assemblages. Group II kimberlites also lack Ti-pyrope and magnesian ilmenite megacrysts, second generation groundmass olivines, monticellite and poikilitic eastonitic phlogopites. Spinel compositional trends are different in each kimberlite isotopic group. Geochemical and mineralogical evidence thus both support the hypothesis that the two varieties of kimberlite are derived from different sources in the mantle. There is no mineralogical evidence to support any relationship to each other by simple differentiation processes at high or low pressure.

The presence of hollandite group minerals and spinels similar in composition to those found in lamproites does not demonstrate any genetic relationship between lamproites and micaceous kimberlites. The hollandites are unlike priderite and the spinels are similar to those found in wide variety of other rock types. Importantly none of the characteristic minerals of lamproites e.g. potassian titanian richterite, leucite, sanidine, sodic titanian tetraferriphlogopite, wadeite etc. (Mitchell 1985) are

found in isotopic group II micaceous kimberlites.

It is suggested that the micaceous kimberlites of the Barkly West, Boshof and Winburg districts may represent a third distinct class of mantle-derived diamond-bearing magmas.

References

DAWSON, J.B. & STEPHENS, W.E. 1975. Statistical analysis of garnets from kimberlites and associated xenoliths. *J. Geol.* 83, 589-607.
 MITCHELL, R.H. 1985. A review of the mineralogy of lamproites. *Geol. Soc. S. Africa. Trans.* 88, in press.
 MITCHELL, R.H. 1986. Kimberlites: Mineralogy, Geochemistry and Petrology. Plenum Pub. Corp. Ltd. New York.
 MITCHELL, R.H. & HAGGERTY, S.E. 1986. A new K-Ba-V-titanate related to priderite from the New Elands kimberlite, South Africa. *N. Jahrb. Mineral.* in press.
 SMITH, C.B. 1983. Pb, Sr, and Nd isotopic evidence for sources of African Cretaceous kimberlites. *Nature* 304, 51-54.
 SMITH, J.V., BRENNESHOLTZ, R. & DAWSON, J.B. 1978. Chemistry of micas from kimberlites and xenoliths I. Micaceous kimberlites. *Geochim. Cosmochim. Acta* 42, 959-971.

Table 1. Representative compositions of micas from the New Elands and Star Mines.

	1	2	3	4	5	6	7	8	9	10	11	12	13
SiO ₂	41.16	40.80	41.75	39.95	38.06	41.27	40.20	39.69	42.53	39.55	40.41	40.97	40.63
TiO ₂	0.47	1.63	1.78	3.25	3.96	1.69	2.21	0.49	0.18	0.07	1.93	1.94	0.53
Al ₂ O ₃	12.16	11.57	11.72	12.81	11.64	11.48	9.12	0.26	12.54	10.63	11.57	10.95	0.30
Cr ₂ O ₃	0.84	0.08	0.46	0.30	0.13	0.52	0.12	0.13	0.68	0.07	1.28	0.15	0.09
FeO _T	2.54	5.72	4.35	6.32	17.05	4.27	10.39	17.61	2.01	10.50	4.76	7.82	17.39
MnO	0.00	0.06	0.03	0.07	0.19	0.07	0.14	0.15	0.04	0.11	0.00	0.11	0.07
MgO	26.05	22.99	23.93	22.11	14.69	24.50	22.61	24.99	25.43	20.23	24.51	24.02	24.89
CaO	0.00	0.00	0.00	0.00	0.00	0.07	0.00	0.00	0.00	0.00	0.00	0.00	0.05
Na ₂ O	0.13	0.08	0.18	0.34	0.29	0.18	0.21	0.25	0.28	0.32	0.00	0.09	0.00
K ₂ O	10.30	10.31	10.70	10.41	9.68	10.31	10.54	9.67	10.26	9.60	10.10	11.13	9.95
NiO	0.13	0.07	0.21	0.29	0.00	0.11	0.05	0.04	0.18	0.02	0.00	0.00	0.13
	93.78	93.22	95.11	95.85	95.69	94.45	95.59	93.83	95.03	94.10	94.56	97.18	94.03

* FeO_T = total iron expressed as FeO. Compositions 1-8 New Elands, 9-13 Star. 1, 2, 9, 10 colorless-to-brown microphenocrysts; 3, 4 fluid inclusion-rich microphenocrysts; 5 Ti-magnesian biotite; 6, 7, 11, 12 groundmass micas; 8, 13 tetraferriphlogopite

Table 2. Representative compositions of spinels from the New Elands and Star Mines.

	1	2	3	4	5	6	7	8	9	10	11	12	13
TiO ₂	0.43	0.27	0.40	2.47	3.40	2.06	3.79	2.55	3.19	7.74	7.61	8.11	8.19
Al ₂ O ₃	6.90	15.42	22.66	2.69	3.12	2.96	3.25	3.35	3.47	1.18	0.48	0.25	0.07
Cr ₂ O ₃	64.17	62.79	43.67	58.17	57.47	58.82	57.42	59.87	58.04	9.71	3.59	1.68	0.61
FeO*	14.87	15.42	19.63	22.48	22.54	22.11	23.57	20.83	22.94	69.40	75.48	77.98	78.33
MnO _T	0.21	0.23	0.59	0.56	0.42	0.46	0.46	0.39	0.39	0.71	0.65	0.93	0.73
MgO	13.77	13.89	13.51	13.20	13.14	12.37	12.90	13.89	12.94	6.38	5.80	5.71	5.52
	100.41	99.89	101.0	99.57	100.1	98.48	101.4	100.9	101.9	95.12	93.61	94.65	93.46
Fe ₂ O ₃ ⁺	-	-	-	-	-	-	-	-	-	46.13	52.93	54.70	54.95
FeO	-	-	-	-	-	-	-	-	-	27.88	27.84	28.75	28.87
										99.83	99.49	100.3	99.16

*Total iron expressed as FeO. + Fe₂O₃ and FeO calculated from stoichiometry. 1-9 chromites; 1-3 New Elands, 4-5 New Star, 6-7 Wynandsfontein, 8-9 Burns; 10-13 titaniferous magnesian magnetites, Burns.

Table 3. Representative compositions of garnet and K-Ba-titanates.

	1	2	3	4	
SiO ₂	23.44	28.43	0.37	0.69	
TiO ₂	13.92	25.46	75.73	70.01	
ZrO ₂	14.40	0.00	0.08	-	1. Zr-rich garnet, New Elands.
Al ₂ O ₃	0.00	0.37	0.00	1.30	2. Ti-rich garnet, Star.
Cr ₂ O ₃	0.12	0.14	0.50	1.66	3. K-Ba-V-titanate, New Elands.
Fe ₂ O ₃	14.14	5.98	3.52	5.50	4. Ba-K-Cr-titanate, Star.
V ₂ O ₅	-	-	4.51	0.00	
Ca ₂ SiO ₇	-	-	1.52	-	
MnO	0.10	0.83	0.17	-	
MgO	2.35	3.79	0.94	0.00	
CaO	30.08	34.43	0.00	1.56	
Na ₂ O	1.06	0.95	0.00	0.00	
K ₂ O	-	-	8.69	3.27	
BaO	-	-	3.92	14.41	
	99.21	99.86	99.95	98.40	

INTRODUCTION

Olivine dominates the phenocryst assemblage in kimberlites. Compositional variation of this phase should therefore mirror evolutionary paths of the host magma. Also, it has been suggested (e.g. Bailey, 1984) that kimberlites are hybrid rocks, significantly contaminated by dissociated mantle xenoliths. A study of kimberlite olivines should place constraints on the proportion of such exotic material present. This in turn has important bearing on the chemical character of kimberlite magmas. Of particular concern is whether the high bulk rock MgO content that characterizes kimberlites reflects an originally very MgO-rich magma or substantial contamination of a highly refined incompatible-rich magma by xenocrystic olivines.

Extremely fresh kimberlite samples were collected for study from the Letseng-la-terai kimberlite, Lesotho, the deBeers and Newlands pipes in the Kimberley area, and two pipes from the Gibeon district, Namibia. These represent kimberlite clusters on an East - West transect across southern Africa. According to the classification of Smith (1983), the Newlands pipe belongs to the Type II group of kimberlites, while the others studied fall into his type I group. For comparative purposes, a study was also made of olivines in a very fresh sample from the Hamilton Branch kimberlite, U.S.A.

PETROGRAPHY

Between two and six thin sections were examined for each of the kimberlites studied. In these samples, virtually all of the olivines occur as discrete grains. Orthopyroxene, garnet and other mantle-derived minerals are extremely rare or absent in the thin sections studied, either as discrete grains or as intergrowths with olivine.

Superficial examination of the thin sections suggests that kimberlite olivines group into two dominant populations: (i) Large grains with rounded margins (macrocrysts) and (ii) small euhedral to subhedral crystals. In some of the specimens studied (e.g. de Beers), many though not all, of the large olivines show undulose extinction or sub-grain optical domains indicating recrystallization. In such cases however, both undulose extinction and sub-grain crystallographic domains also occur in some of the associated euhedral olivines of the second population. In contrast, in the Newlands kimberlite, both types of olivine are entirely strain free. In all samples, some of the large rounded olivines extinguished parallel to long edges, possibly relict rational crystal faces.

To place constraints on the possible occurrence of two distinct olivine populations in kimberlites, longest axes of all grains greater than 0,25mm were measured in two thin sections (total area roughly 1800mm²) from the deBeers kimberlite and four thin sections (total area roughly 3600mm²) from the Newlands sample. Surprisingly, these data suggest a continuous size variation rather than two distinct populations. (Fig. 1)

CHEMISTRY

In each kimberlite sample studied, olivines were subjectively divided according to decreasing size into four groups: (i) Large, (ii) Intermediate-sized, (iii) small and (iv) micro-olivines. The first two categories would include the macrocrysts, while the euhedral to subhedral olivines would fall into the third and fourth.

Between 70 to 100 electron microprobe analyses of olivines were made in each of the kimberlites studied. At least two analyses (centre and edge) were made of individual olivines. The olivines from the different pipes have a fairly consistent pattern of chemical variation, broadly similar to that illustrated by the deBeers kimberlite. (Fig. 2)

Collectively, the centres of the large majority of the olivines define a single continuous field characterized by decreasing Mg/(Mg + Fe) associated with a slight sympathetic decrease in Ni. In general, the large and intermediate sized olivines are Mg-rich relative to small olivines and micro-olivines, although there is some overlap in the chemical fields of these different size groups. Edge compositions of all the olivines tend to be relatively Mg-poor, and define a field characterized by sharply decreasing Ni.

In addition to the olivines constituting the dominant chemical field described above, there are rare individuals characterized by distinctly higher Fe and lower Ni contents. Most of the olivines with this distinctive chemical signature are rounded macrocrysts although some small euhedral olivines and micro-olivines may also be markedly Fe-rich and Ni-poor. This chemically distinct group of olivines has been recognised in all of the kimberlites studied, including the north American Hamilton Branch pipe.

DISCUSSION

The petrographic and chemical data presented suggest that most kimberlitic olivines belong to a single size and chemical population. As the euhedral olivines are undoubtedly cognate phenocrysts, any model for the origin of kimberlite magmas which requires that a substantial proportion of the olivines are xenocrysts must provide compelling evidence to substantiate such an exotic origin.

An alternative interpretation of the data presented is that the greater majority of kimberlite olivines are cognate phenocrysts. If valid, this would indicate an extended period of crystallization of the phase in the kimberlite magma, with the Mg-rich macrocrysts being the earliest formed crystals. Rounding of the macrocrysts may simply reflect their longer exposure to fluidization processes during magma ascent. Several lines of evidence lend support to this interpretation:

1. Orthopyroxene and pyrope xenocrysts are extremely rare in kimberlites. These phases would be expected to be more common if a substantial proportion of the olivines in kimberlites are derived from disaggregated mantle xenoliths.
2. A. Harwood (kimberlite symposium, University of Cape Town, 1986) recognizes a temperature-related sequence of primary fluid inclusions in euhedral olivines in kimberlites. His initial data indicate that macrocryst olivines have primary fluid inclusions matching high temperature inclusions in the euhedral olivines. This suggests co-magmatic crystallization of these olivines.
3. Egglar and Wendlandt (1978) show that a rock corresponding to an average Lesotho kimberlite composition will have a liquidus temperature of 1450°C if the CO₂/(CO₂ + H₂O) ratio is 0.5. This temperature closely matches the maximum palaeogeotherm temperatures recorded in mantle xenoliths from the Lesotho kimberlites (Nixon and Boyd, (1973), which presumably set minimum temperatures for the entraining magma. Much lower liquidus temperatures would be appropriate to kimberlites if a significant portion of the olivines are xenocrysts.

The origin of the Fe-rich and Ni-poor olivines that characterize all of the kimberlites studied is speculative, though appears to be intimately related to the processes responsible for kimberlite genesis. Chemically, they are analogous to the high iron, low nickel olivines described from olivine melilitites in Southern Africa (Moore and Erlank, 1979), possibly pointing to a genetic link between the two rock types.

Acknowledgements : Julian Hobbs is thanked for his critical comments, and Diana Evans for typing the abstract.

References

- Bailey D.K. (1984) *Developments in Petrology* IIA (323-33). Elsevier.
Egglar D.H. and Wendlandt R.F. (1978) *Carnegie Inst. Wash. Yb* 77 (751-6)
Moore A.E. and Erlank A.J. (1979) *Contrib. Min. Pet.* 70 (391 - 405)
Nixon P.H. and Boyd F.R. (1973) *Lesotho kimberlites* (48 - 56)
Smith C.B. (1983) *Nature* 304 (51 - 54)

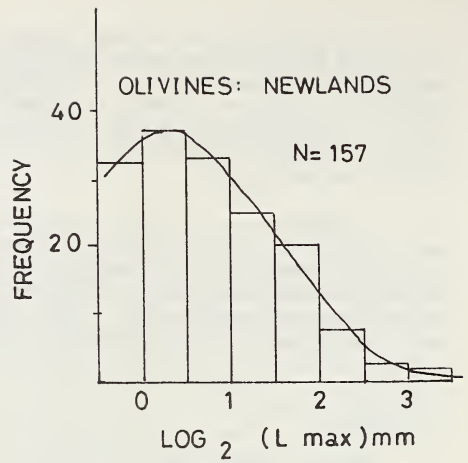
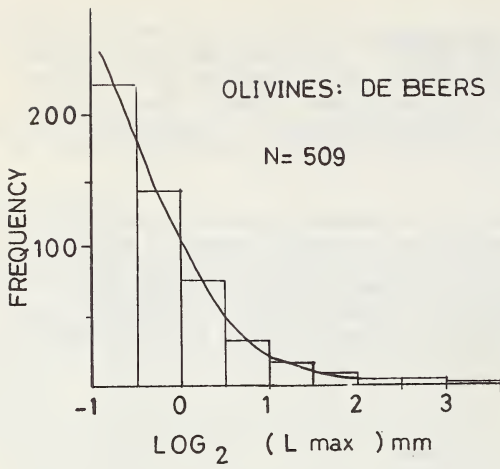


Fig 1. Histograms of longest axes (L max) for all olivines greater than 0,5mm in two thin sections (total area = 1800mm²) from the deBeers kimberlite, and for thin sections (total area = 3600mm²) from the Newlands pipe.

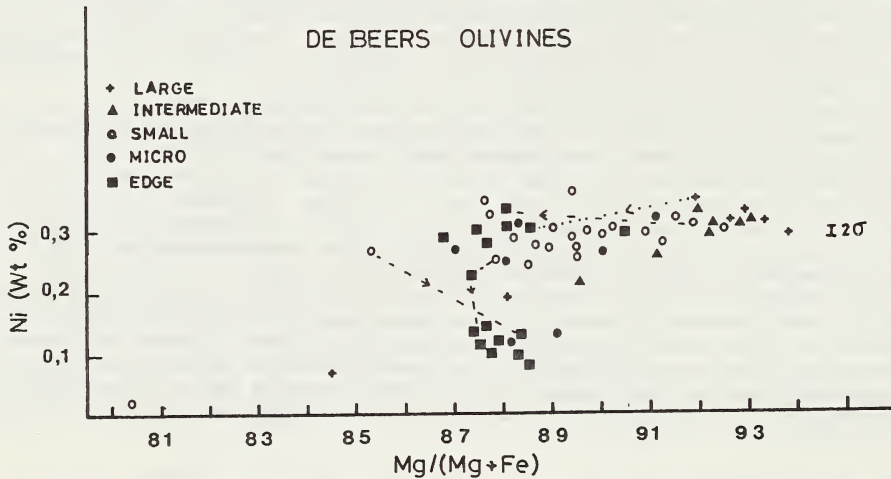


Fig 2. Mg/(Mg + Fe) - Ni plot for olivines from the deBeers kimberlite. Olivines are subjectively divided according to size into four groups : 1) Large (crosses); 2) Intermediate (triangles); 3) Small (open circles); 4) micro (solid circles). Squares denote edge compositions of all olivines. Dotted lines show core to margin variation for individual olivines. Note that with the exception of rare Fe-rich and Ni-poor grains, centres of all olivines analysed define a continuous field. Although there is some compositional overlap for the different size groups, the largest olivines are in general Mg-rich and the smallest crystals Mg-poor.

INTRODUCTION

The Vajrakarur diamond bearing kimberlite pipes have been described for their physical setting, age, general mineralogical, petrological and chemical characteristics by several earlier authors, including Reddy (1986a, 1986b). To date, eight pipes have been indentified and some dated at 840-1150 million years (Paul et. al., 1975). While kimberlite is the most dominant rock type, a few of these pipes are lamproites. Crustal xenoliths and megacrysts of a variety of minerals are present in all the pipes. Xenoliths of mantle origin are present in some of them only. Pipes 1, 3, 4 and 6 are kimberlites (1 and 6 brecciated); 2 and 5 are phlogopite-rich lamproites; 7 and 8 are recent finds.

PRESENT INVESTIGATION AND ITS SCOPE

The ultramafic xenoliths obtained from deep pits and bore holes are the focus of the present study. From scores of samples collected, a total of 32 reasonably fresh samples have been studied. Many of them are from pipe 3, the smallest of the well developed pipes. A detailed investigation of the mineral chemistry of these samples, using an automated ARL SEMQ electron microprobe has yielded data which are used in interpreting the PT conditions of equilibration of the ultramafic xenoliths. These data points define the proterozoic geotherm in the southern part of India and place constraints on the minimum depth of origin of the kimberlites and lead to a better understanding of the occurrence of diamonds in the pipe rocks of Vajrakarur area.

PETROGRAPHY AND MINERALOGY

Among the different varieties of ultramafic xenoliths present in the area the most common are the garnet lherzolites and garnet harzburgites. Eclogites are rare and mostly confined to pipe 3. Olivine orthopyroxenites, wehrlites and related olivine cpx rocks are also rare. Texturally, most xenoliths are coarse-grained and granoblastic with 120° triple junctions. Shearing is present only occasionally. Detailed accounts are given by Reddy (1986a, 1986b) and Ganguly and Bhattacharya (in press).

Olivine (altered to serpentine), orthopyroxene, clinopyroxene and garnet are the most abundant minerals. Spinel (chromite, ilmenite, magnetite and titanomagnetite) are common accessories along with lesser amounts of perovskite, rutile, richterite, and apatite. All the major minerals plus spinel and ilmenite occur as megacrysts. The kimberlites and lamproites have fragments of all the major and minor minerals mentioned above and are highly altered and have abundant carbonates.

The mineral compositions from the different xenoliths are broadly similar but have distinctive characteristics of their own from each of the xenolith groups. A summary of this information is presented in Fig. 1. Olivines in all the olivine-bearing xenolith types are essentially similar (Fo₈₄₋₉₄ with low Cr₂O₃ values). Those in the kimberlites are lower in Fo (to Fo₇₈). Orthopyroxenes from lherzolites and harzburgites are similar. Cr₂O₃ values of orthopyroxenes are higher than those in co-existing olivines; NiO is the reverse. The Ca, Mg, Fe values as well as the Al₂O and Na₂O contents of the cpx of lherzolites and eclogites are broadly similar. Garnets from lherzolites and harzburgites are comparable. Garnets in eclogites are variable; there are two

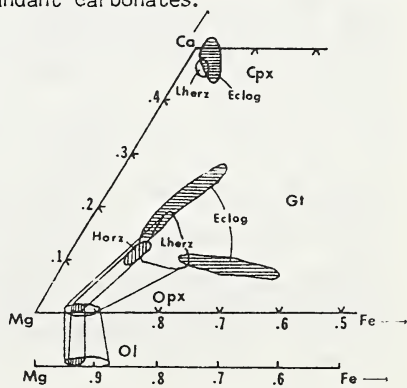


Fig. 1: Mineral data

types, the Ca-rich and the Ca-poor varieties. The later belong to a higher PT regime. Cr_2O_3 in garnets is variable (1 to 5 wt %). Values up to 10 wt % have been noted from some garnet megacrysts.

Iron-titanium oxide minerals are represented by chromite, ilmenite, magnetite and titanomagnetite. Ilmenites are mostly present in lherzolites and kimberlite matrix. Titanomagnetites are confined to kimberlites. Most ilmenites are high in MgO (14 to 19 wt %) and have variable Cr_2O_3 content (<1 to 7 wt %). Some of the ilmenites are zoned with Mg-rich rims. Ilmenites from the kimberlite matrix are intimately intergrown with titanomagnetite and have rims of perovskite. The one ilmenite analyzed from an eclogite was very poor in Cr_2O_3 .

Chromites are mostly confined to lherzolites and the kimberlite matrix. The data are plotted in Fig. 2. Those from the lherzolites define a trend of iron enrichment coupled with Cr/(Cr + Al) enrichment. In contrast, the chromites in the kimberlite matrix are variable from one pipe to another. Those from pipe 3 kimberlite matrix define a parallel trend to the pipe 3 lherzolite chromite trend but extend to slightly lower Mg/(Mg + Fe) ratio and much lower Cr/(Cr + Al) ratio. Chromites from pipe 2 lamproite are extremely poor in Mg/(Mg + Fe) and moderately rich in Cr/(Cr + Al). Chromites from pipe 5 lamproite span a large Mg/(Mg + Fe) ratio but are confined to the intermediate values of the Cr/(Cr + Al) ratio. No diamonds are reported from pipes 2 and 5.

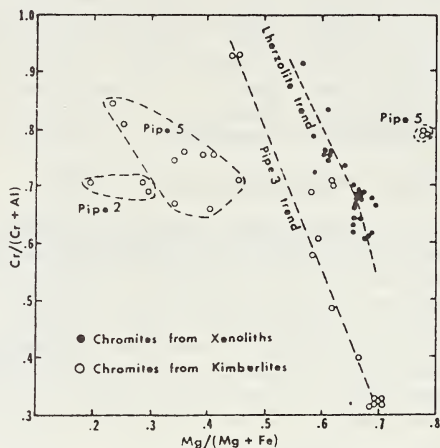


Fig. 2: Chromite trends

THE VAJRAKARUR GEOTHERM

Several geothermometric and geobarometric calculations for garnet peridotites have been evaluated by Finnerty and Boyd (1984). Following the equations of Lane and Ganguly (1980) and Perkins et. al., (1981) for Al-opx/gt equilibrium data, the gt-opx thermometer (modification of Lee and Ganguly, 1984, Ganguly, personal communication), and the gt-cpx thermometer of (Ganguly 1979), the mineral compositional data are used to solve simultaneously for the PT condition of each xenolith sample. In the case of the eclogites (and samples without opx) the gt-cpx PT trajectory is calculated and its intersection with the geotherm established from the other samples, is taken as a reasonable estimate of the PT value of the sample. The PT values and the resulting geotherm are shown in Fig. 3.

From a total of 32 samples studied data sets of 21 samples are used to define the Vajrakarur geotherm. Also included are data from Ganguly and Bhattacharya (in press) on nine xenolith samples and three from Akella et. al., (1979). The excellent linear fit of all the PT values of the xenoliths indicates a steady state thermal condition in the mantle beneath south India during the Proterozoic time. This geotherm is in general agreement with the geotherm proposed by Ganguly and Bhattacharya (in press) for the proterozoic of India and Lesotho.

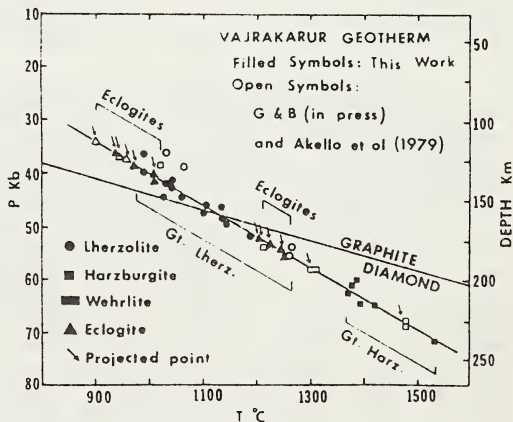


Fig. 3: The Vajrakarur Geotherm

The garnet lherzolite samples occupy an extended PT regime along the geotherm from about 40 kb, 1050°C all the way up to 55 kb 1275°C. Most harzburgites occupy the highest PT portion of the geotherm. The eclogites occupy two regions, one at the low PT and the other at intermediate PT. The low PT samples represent the lowest PT values from the Vajrakarur xenoliths. The intermediate ones are nearly coincident with lherzolites. There is an apparent sparsity of samples between the PT regimes of eclogites and lherzolite groups on one hand, and the harzburgite group on the other. The significance of these gaps is uncertain. In Vajrakarur, garnet harzburgites are at higher PT regimes than garnet lherzolites. This apparent discrepancy may be due to mantle heterogeneity. Some of the Vajrakarur harzburgites do fall in the PT regime of the lherzolites.

Interestingly, the graphite-diamond transition curve (Kennedy and Kennedy 1977) passes through the intermediate PT cluster of eclogites (which is also the high end of the lherzolite group). Most Vajrakarur harzburgites plot in the diamond stability field. Using these data it is possible to develop garnet compositional criteria that could be used as diagnostic of diamond incidence in the Vajrakarur pipes.

CONCLUSIONS

The PT regime of the ultramafic xenoliths from Vajrakarur, India are determined using $opx \pm cpx \pm$ garnet assemblage geothermometers and geobarometers. The values define a linear geotherm similar to the ones from parts of south Africa and suggest a steady state in the mantle in south India during the Proterozoic. Heterogeneity of the mantle is indicated by the PT regimes of garnet harzburgites, garnet lherzolites and the two different types of eclogites. The compositional properties of garnets in the different xenolith varieties may be used as diagnostic for PT regimes which in turn can help in determining the likelihood of diamond occurrence in the pipe rocks. PT regimes of the xenoliths indicate that the kimberlites containing diamonds must have originated at depths of about 225 km and temperatures near 1500°C.

ACKNOWLEDGEMENTS Thanks are due to Shri D.P.Dhondial, Director General, Geological Survey of India, for permitting Dr. Ajit K. Reddy to work on this project in USA and publish the results. Partial financial support from the City University of New York Research Foundation, for this research project, is gratefully acknowledged. Thanks are also due to Dr. M. Prinz (American Museum of Natural History) for extending the electron microprobe facilities and to Mr. M. Weisberg, Mr. N. Chatterjee, Mr. Y. Fei and Mrs. F. Cohen for their technical assistance.

REFERENCES

- Akella, J., Rao, P.S., McCalister, R.H., Boyd, F.R., and Meyer, H.O.A. 1979. Mineralogic studies on the diamondiferous kimberlite of Vajrakarur area, southern India. In Boyd, F.R. and Meyer, H.O.A. (eds). *American Geophysical Union*. Washington, 172-177.
- Finnerty, A.A., and Boyd, F.R. 1984. Evaluation of thermobarometers for garnet peridotites. *Geochimica et Cosmochimica Acta* 48, 15-27.
- Ganguly, J. 1979. Garnet and clinopyroxene solid solutions and geothermometry based on Fe-Mg distribution coefficient. *Geochimica et Cosmochimica Acta* 43, 1021-1029.
- Ganguly, J., and Bhattacharya, P.K. (in press). Xenoliths in proterozoic kimberlites from southern India. Petrology and geophysical implications in Nixon, P.H., (ed), **Mantle Xenoliths**
- Kennedy, C.S., and Kennedy, G.C. 1976. The equilibrium boundary between graphite and diamond. *Journal of Geophysical Research*, Vol 81, 14, 2467-2470.
- Lane, D.L., and Ganguly J. 1980. Al_2O_3 Solubility in orthopyroxene in the system $MgO-Al_2O_3-SiO_2$. A reevaluation, and mantle geotherm. *Journal of Geophysical Research* 85, B12, 6963-6972.
- Paul, D.K., Rex, D.C., and Harris, P.G. 1975. Chemical characteristics and K-Ar ages of Indian kimberlites. *Geological Society of America* 86, 364-366.
- Perkins, D., III, Holland, T.J.B., and Newton, R.C. 1981. The Al_2O_3 content of enstatite in equilibrium with garnet in the system $MgO-Al_2O_3-SiO_2$ at 15-40 Kbar and 900°-1600°C. *Contributions to Mineralogy and Petrology* 78, 99-109.
- Reddy, A.K., 1986a. Petrology and geochemistry of Vajrakarur kimberlites. *Records of Geological Survey of India* (in press).
- Reddy, A.K., 1986b. Kimberlite and lamproite rocks of Vajrakarur area, Andhra Pradesh. *Journal Geological Society of India* (in press).

Nicholas M. S. Rock

Dept. Geology, University of Western Australia, Nedlands, Perth 6009, WA.

Kimberlites have often been compared, classified or confused with lamprophyres. The framework in Figure 1 may help to clarify both their respective affinities and differences, by reappraising kimberlite as a 'family' of rock-types within the lamprophyre 'clan'. Kimberlites must be varieties of lamprophyres, not vice-versa, because: (i) micaceous kimberlites are frequently described as 'lamprophyric' (e.g. Skinner & Clement 1979), but relatively few lamprophyres as 'kimberlitic'; (ii) lamprophyre is a less restrictive, purely descriptive term with no type-locality; (iii) lamprophyre has historical precedence (Von Gumbel 1874 versus Lewis 1888).

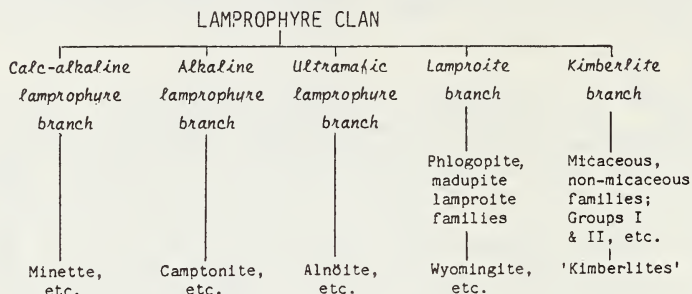


Fig. 1. The lamprophyre 'clan', with kimberlite considered as one of the 'branches'. Definitions of other 'branches' and 'families' after Streckeisen (1979), Mitchell (1986) and Rock (1987).

JUSTIFICATION FOR GROUPING KIMBERLITES AND OTHER LAMPROPHYRES TOGETHER

Figure 1 unites a coherent grouping of petrologically distinctive rocks, distinguished from other igneous rocks not least by having crystal-laden fluid rather than essentially liquid parent magmas. Contemporaneous kimberlites coexist with other lamprophyres in several areas. All rock-types in Figure 1 also share the following features in common: (1) They occur as minor intrusions, with diatremes and dykes more widespread than sills and lavas very rare. (2) They are emplaced explosively from great depths, commonly yielding fluidised explosion-breccias, intrusion breccias, tuffs or pyroclastics. (3) They have high contents of alkalis (especially K), H_2O , CO_2 , F, Cl, P, Ba, Sr, Rb, Zr, Th, Nb and LREE, typical of highly evolved alkaline rocks, with V, Cr and Ni contents ranging between levels typical of basic and ultrabasic rocks, while Ti, Y and HREE levels lie near or below MORB (Fig. 2). (4) Carbonate minerals are usually abundant, and partly primary. (5) At least one hydrous mafic mineral is present (especially phlogopite, but also serpentine, amphiboles). (6) Typical olivine compositions are Fe_{30-94} . (7) Cognate orthopyroxenes are absent. (8) Varied crustal and mantle-derived xenolith and megacryst suites are abundant. (9) The mineralogy is a hybrid, often disequilibrium mixture of macrocryst, phenocryst and groundmass phases, variously formed by magmatic crystallisation, partial or 'arrested' resorption of liquidus phases, autometasomatism, or incorporation of foreign materials. (10) Whole-rock compositions bear little relation to parent magmas.

COMPARISONS BETWEEN KIMBERLITES AND OTHER LAMPROPHYRE VARIETIES

Kimberlites are most similar to ultramafic lamprophyres and least similar to alkaline lamprophyres. Olivine-lamproites, ultramafic lamprophyres and kimberlites may grade into one another petrologically, being among few igneous rocks to carry rutile, perovskite and $Ba\pm Fe^3$ -rich micas. Phlogopite-free kimberlites are the least 'lamprophyric', but they in turn violate the definition of kimberlite itself as a "potassic" rock-type (Clement *et al.* 1984).

Although calc-alkaline lamprophyre whole-rock compositions and felsic mineralogy differ greatly from kimberlites, many minette phlogopites match secondary phenocryst or macrocryst rims, "Type II" groundmass phlogopites, and unzoned pre-fluidisation phenocrysts in kimberlites (Bachinski & Simpson 1984).

Some lamproites are sufficiently similar to kimberlites to have been confused: e.g. Prairie Creek (USA) and Chelima (India). Lamproites show the following specific links with kimberlites (additional to those of other lamprophyres): (a) They are the only terrestrial igneous rocks carrying armalcolite, diamond or potassium richterite. (b) Lamproite mafic mineralogy mirrors MARID xenoliths in kimberlites.

Figure 2b shows how close ultramafic lamprophyres and kimberlites are in average composition. Many 'kimberlites' and 'mica-peridotites' are really ultramafic lamprophyres. Indeed, ultramafic lamprophyres may be expressions of 'kimberlite magmatism' in tectonic regimes which preclude true kimberlites (e.g. oceanic islands). The two types show the following additional mutual links: (a) Exceptionally low SiO_2 and Al_2O_3 contents combined with high $[MgO+CaO]$ and K_2O . (b) Unusual mineralogy (e.g. microilmenite, monticellite). (c) Absence of feldspars. (d) Overlapping mafic mineral compositions. (e) Frequent association with carbonatitic rocks. (f) Associated fenite-like metasomatism.

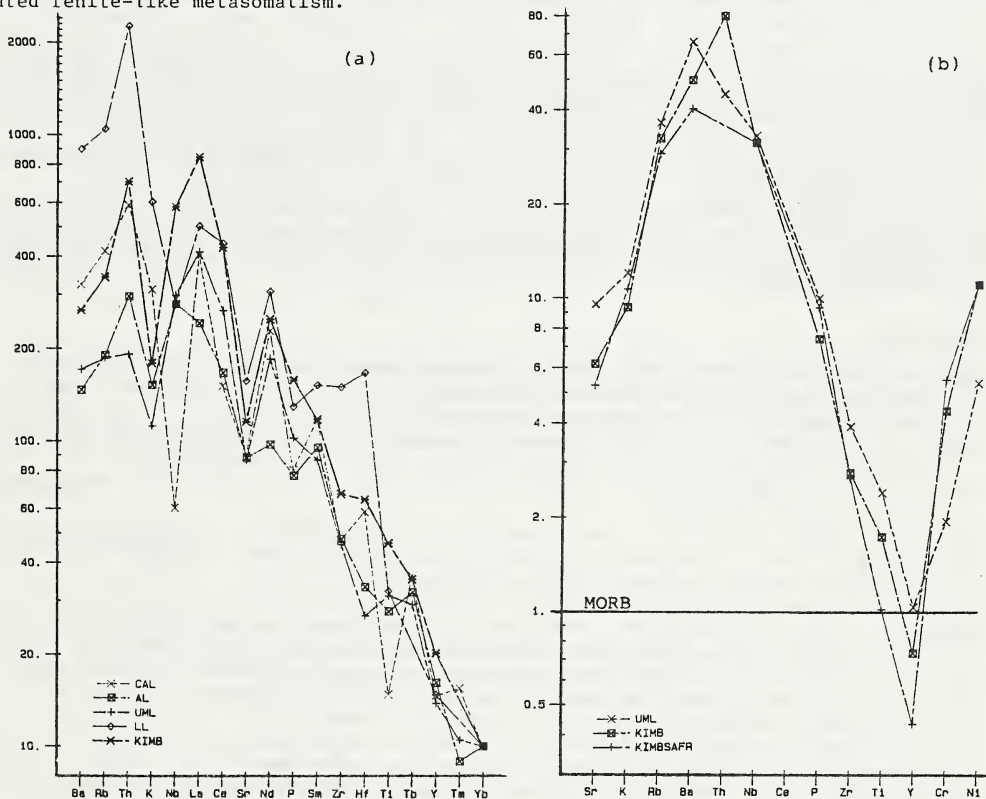


Fig. 2. Comparisons of mean minor and trace element geochemistry for kimberlites and other lamprophyres. Data from Rock (1987), Wedepohl and Muramatsu (1979). CAL = 754 calc-alkaline lamprophyres; AL = 563 alkaline lamprophyres; UML = 245 ultramafic lamprophyres; LL = 293 lamproites; KIMB = 670 kimberlites. KIMBSAFR = 11 South African kimberlites.

Fig. 2a. Chondrite-normalised 'spidergrams'. Element order and normalising values from Thompson et al. (1984).

Fig. 2b. MORB-normalised 'spidergrams'. Element order and normalising values from Pearce (1982).

This can be readily adapted from the kimberlite definition of Clement et al. (1984); underlined phrases are quoted verbatim:

"Lamprophyres are volatile-rich, alkalic, ultrabasic to mesotype igneous rocks which occur as small volcanic pipes, dykes, and sills. They are often emplaced explosively, generating associated breccias, tuffs and/or pyroclastics. They have a distinctively inequigranular texture resulting from the presence of phenocrysts and, often, macrocrysts set in a finer-grained matrix. They carry at least one hydrous or carbonate mineral as a prominent primary, phenocrystal and/or groundmass constituent - alkali or calcic amphibole, carbonate (commonly calcite, also ankerite, breunnerite, dolomite), phlogopite-biotite or serpentine. Additionally, phenocrysts and groundmass may include several of the following minerals: apatite, clinopyroxene (commonly diopside, titan-augite), ilmenite (Mg and/or Mn-rich), melanite-andradite garnet (sometimes Zr-rich), melilite, monticellite, olivine (F₀₈₀₋₉₅), perovskite, spinels (often Mn-rich), and sulphate minerals (baryte etc.) Rare silicates of alkalis or Ba with Fe, Ti and/or Zr (wadeite etc.) or alkali sulphide minerals (e.g. bartonite) may be present. Feldspars (albite, Ba-Fe-K-feldspar, plagioclase), feldspathoids (analcime, nepheline, sodalite group) or minor quartz sometimes occur in the groundmass only. Mafic minerals typical of basic or ultrabasic rocks (e.g. forsteritic olivine, diopside, phlogopite), commonly coexist with minerals typical of highly evolved rocks (quartz, albite, orthoclase, aegirine, alkali amphiboles). Most macrocrysts are anhedral, mantle-derived mafic minerals which include olivine, phlogopite, picroilmenite, chromian spinel, magnesian garnet, clinopyroxene (commonly chromian diopside), orthopyroxene (commonly enstatite) and amphibole (commonly kaersutite). Macrocrysts of mantle-derived anorthoclase, sanidine, apatite and corundum may also occur. The macrocrysts and relatively early-formed matrix minerals are commonly altered by deuteric processes (mainly serpentinization and carbonatization). Phenocrysts and other matrix phases, however, may be strikingly euhedral (panidiomorphic) and fresh. Lamprophyres commonly contain inclusions of upper mantle-derived ultramafic rocks. Variable quantities of crustal xenoliths and xenocrysts may also be present. Some lamprophyres may contain diamond but only as a very rare constituent".

References

- BACHINSKI S.W. and SIMPSON E.L. 1984. Ti-phlogopites of the Shaw's Cove minettes: a comparison with micas of other lamprophyres, potassic rocks, kimberlites and mantle xenoliths. *American Mineralogist* 69, 41-56.
- BOYD F.R. and MEYER H.A.O. 1979. Kimberlites, diatremes and diamonds: their geology, petrology and geochemistry. American Geophysical Union, Washington.
- CLEMENT C.R., SKINNER E.M.W. and SCOTT SMITH B.H. 1984. Kimberlite redefined. *Journal of Geology* 92, 223-228.
- LEWIS H.C. 1888. The matrix of the diamond. *Geological Magazine* 5, 129-131.
- MITCHELL R.H. 1986. A review of the mineralogy of lamproites. *Transactions of the Geological Society of South Africa* (in press).
- PEARCE J.A. 1982. Trace element characteristics of lavas from destructive plate boundaries. In Thorpe R.S. ed, *Andesites*, pp. 525-548. Wiley, New York.
- ROCK N.M.S. 1987. The nature and origin of lamprophyres: an overview. In Fitton, J.G. and Upton, B.G.J. eds, *The Alkaline Rocks - a review symposium*. Special Publication, Geological Society of London (in press).
- SKINNER, E.M.W. & CLEMENT C.R. 1979. Mineralogical classification of Southern African kimberlites. In Boyd and Meyer (1979, qv), pp. 129-139.
- STRECKEISEN A. 1979. Classification and nomenclature of volcanic rocks, lamprophyres, carbonatites and melilitic rocks. *Geology* 7, 331-5.
- THOMPSON R.N., MORRISON M.A., HENDRY G.L. and PARRY S.J. 1984. An assessment of the relative roles of crust and mantle in magma genesis, an elemental approach. *Philosophical Transactions of the Royal Society, London* A310, 549-90.
- VON GUMBEL C.W. 1874. *Die palaeolithischen Eruptivgesteine des Fichtelgebirges*. Franz, Munich.
- WEDEPOHL K.H. and MURAMATSU K. 1979. The chemical composition of kimberlites compared with the average composition of three basaltic magma types. In Boyd and Meyer (1979, qv), pp. 300-312.

B.H. Scott Smith¹, E.M.W. Skinner² and P.E Loney³

¹ 670 Montroyal Boulevard, North Vancouver, B.C. V7R 2G3, Canada

² Geology Department, De Beers Consolidated Mines Ltd, P.O. Box 47, Kimberley 8301
South Africa

³ De Beers Prospecting Botswana Ltd., P.O. Box 90, Lobatse, Botswana

INTRODUCTION

Kimberlite-like intrusions were found in the Luangwa Valley of Eastern Zambia during the early 1960's. They are located along the Kapamba River, a tributary of the Luangwa River, approximately 150km west-north-west of Chipata. The occurrences (some of which yielded rare diamonds) were initially referred to as kimberlites, although differences from kimberlites elsewhere were noted. Subsequently, however, one of the authors (EMWS) recognised their lamproitic character.

GEOLOGY

The Kapamba bodies lie within a downfaulted, north-east trending graben which is contained within the Irumide tectonic belt (1355 my). The Luangwa graben is considered to be a south-westward extension of the East African Rift system. The Kapamba intrusions cut through upper Karoo sediments and are thus younger than 250 my in age.

The Kapamba occurrences comprise fourteen single, or groups of small, pipe-like bodies and an associated suite of dykes. Together they form a north-west to south-east trending province approximately 25km long. Many of the pipes form distinct topographic features and exposure is fairly good. Most of the pipes are approximately circular in shape and range in size up to 45 hectares.

The geology of the pipes is variable, and often complex, and numerous rock types are present. They include magmatic rocks (with some autolithic breccias) and crater-facies rocks which vary from massive to well bedded (including some cross- and graded-bedding). In some pipes only crater-facies material is found, while in others significant (up to 200m) outcrops of magmatic material occur.

PETROGRAPHY

Crater-facies rocks

These rocks are mostly fragmental composed of juvenile lapilli, single grains of quartz and feldspar and a few xenoliths. The juvenile lapilli have a porphyritic texture, with olivines set in fine-grained or glassy groundmass. The olivines comprise abundant phenocrysts which occur as multiple-growth aggregates and anhedral, rounded or subhedral macrocrysts. The nature of the matrix of the lapilli varies between pipes and even within a single thin section. The matrix includes microphenocrysts of phlogopite, or clinopyroxene and leucite, set in a glassy base. Vesicles may be present. The other main constituents are individual, angular grains of quartz and lesser amounts of feldspar. Where these xenocrysts are abundant, the rocks resemble sandstones. Most of the xenolithic material is derived from the country rock sediments. The fine matrix of the crater-facies rocks is composed of brown indiscernible clayey material. The crater-facies rocks are broadly similar, but differ with respect to: (1) fragment or grain size, (2) variation in proportion of dark juvenile and leucocratic xenolithic material, (3) absence or nature of bedding, (4) variation in olivine content, (5) degree of alteration, (6) megascopic and macroscopic colour.

Magmatic Rocks

The magmatic rocks, which occur within the pipe-like intrusions, are often fairly fresh and have porphyritic textures. The olivines are fresher, but otherwise similar to those described from the juvenile lapilli. The macrocrysts may show some detailed euhedralism resulting in serrate margins. The abundance of macrocrysts varies. Two main

varieties of groundmass occur. The first type is very fine-grained and displays a distinct segregatory texture with orange-brown, phlogopite-rich and grey, clinopyroxene-rich areas. This groundmass type usually also contains leucite, amphibole, oxide minerals and apatite. These minerals are set in a glassy base. The second type of groundmass has uniform textures, is medium-grained and is composed of leucite, clinopyroxene, phlogopite, amphibole, sanidine, opaque minerals, apatite and glass. The leucite may be either isotropic or replaced by a mosaic of low birefringent mineral(s) and sometimes may also be brown and somewhat turbid indicating some alteration. The phlogopite has a distinctive orange-brown colour and occurs only as late-stage, interstitial, poikilitic grains. The amphibole displays yellow to pink pleochroism.

Dyke Rocks

The dyke rocks are coarser grained and have a non-porphyrific texture. They are altered but primary constituents include olivine phenocrysts, clinopyroxene, leucite and sanidine.

Discussion

The magmatic rocks at Kapamba are classified as lamproites based on their mineralogy, textures, the colour and pleochroism of the phlogopite and amphibole (after Scott Smith and Skinner 1984 or Mitchell in press). A variety of mineralogical types are present which include clinopyroxene-olivine-phlogopite, clinopyroxene-leucite, clinopyroxene, and phlogopite-leucite lamproites. It is important to note that the phlogopite occurs only as a groundmass mineral and no phenocrysts are present. Such lamproites would be termed madupitic by Mitchell (in press). An overview of the mineralogy of the Kapamba province suggests that generally the rocks become more evolved to the south-east, with decreasing amounts of olivine and the increasing abundance of leucite. The juvenile lapilli are best termed glassy-olivine lamproite. The crater-facies rocks include both pyroclastic and epiclastic varieties. The former are interpreted as comprising mostly lapilli tuffs but ash deposits and slightly welded, juvenile lapilli-rich tuffs are also present.

MINERAL CHEMISTRY

Phlogopites are similar in composition to groundmass or madupitic micas in other lamproites being titaniferous (5 - 9.5 wt.% TiO_2) and poor in alumina (4 - 11.5 wt.% Al_2O_3). Some of the phlogopites, however, do have higher Mg/(Mg+Fe) atomic ratios (0.83 - 0.65), FeO (7 - 14 wt.%) and BaO (0.9 - 4.1 wt.%) contents than is typical of other lamproites. Olivines range in composition with Mg/(Mg+Fe) ratios of 0.820 to 0.935. The cores of the most of the xenocrysts fall in the range 0.905 to 0.925. The compositions of the cores of the phenocrysts differ from each of the intrusions analysed, but together fall in the range 0.880 to 0.915 and are less magnesium than most of the xenocrysts. The rims of all the olivines show very restricted compositions suggestive of late-stage overgrowths or equilibration. The clinopyroxenes are diopsides which are zoned. The zoning, higher FeO and, more significantly, higher Al_2O_3 contents distinguish them from most other lamproitic clinopyroxenes, but their compositions do not extend into the fields of clinopyroxenes from other potassic rocks. Amphiboles are titanian potassic richterite which have higher Na_2O and Al_2O_3 contents than typical of most lamproites. Spinel is mostly titanomagnetite with some cores of titaniferous, magnesian-chromite. They are similar to those in other lamproites. Leucite appears to have been replaced by a mixture of sanidine and sodium aluminosilicates, mostly with compositions closely resembling analcite. The replacement by analcite has been noted in other lamproites and is considered to be a secondary process. Groundmass feldspar is Fe-bearing sanidine as found in other lamproites. Perovskites have high Na_2O and SrO, features typical of lamproitic perovskites.

Discussion

Some of the mineral compositions are very similar to those found in lamproites elsewhere, but there are some significant differences which, in many cases, are evident in the more evolved varieties. These differences may reflect the Kapamba 'signature', because each lamproite province is characterised by certain minerals having different

compositions. Minerals from Kapamba which have compositions that can be distinguished from other lamproites, however, also begin to approach those found in other potassic rocks (South-west Uganda and the leucitites of New South Wales and Western Italy). Although not documented here, the mineral compositions vary between each of the Kapamba intrusions examined. Using mineral chemistry to assess their relative degree of evolution suggests that the intrusions become more evolved from north-west to the south-east of the province.

WHOLE-ROCK GEOCHEMISTRY

The whole-rock compositions of some of the Kapamba rocks support the classification of these rocks as lamproites. The most notable feature of these data is the variable alkali content. Some samples have high K_2O contents (± 5 wt.%) and high K_2O/Na_2O ratios (3 to 5), as is the case in other lamproites. Other samples, however, have high Na_2O contents (± 4 wt.%) and low K_2O/Na_2O ratios (0.3 to 0.4) which are very different from lamproites. Primary mineral compositions cannot account for this variation. The only feature which might explain this variation is the secondary replacement of leucite by analcite. It does not appear to be related to late-stage enrichment of the magmas represented by the rocks examined. It seems more likely that the high Na_2O values have resulted from some other process, such as the interaction with groundwater (Gupta and Fyfe 1975).

HEAVY MINERAL CONCENTRATES

The nature of the heavy mineral concentrates from the different intrusions is extremely variable. Some pipes yield abundant garnets which have peridotitic compositions with the majority being chrome pyropes. Spinel may also occur in some pipes and are magnesian chromites. Rare chrome diopside also occurs. Some of the pipes are diamondiferous but none are economic.

CONCLUSIONS

The Kapamba intrusions are classified as lamproites according to their petrography, mineral chemistry and whole-rock geochemistry. They therefore represent another province of diamond-bearing lamproite.

The geology and petrography of the Kapamba pipes suggest that they comprise craters predominantly infilled with pyroclastic, lapilli tuffs and intruded by younger, magmatic lamproite which appear to have formed an extrusive, ponded lava lake-type body. This model is similar to those of other lamproites. Mineral and whole-rock geochemistry suggests that the intrusions generally become relatively more evolved from the north-west to the south-east of the province.

The compositions of some of the minerals, usually those from the more evolved varieties, display distinct differences from data for lamproites elsewhere. These features, however, are not extreme enough to preclude their classification as lamproites. They may rather reflect the 'signature' of the Kapamba lamproite province. These variations, however, indicate a similarity with other potassic rocks including South-west Uganda, which is notable because the Kapamba province occurs within, what is considered to be, a south-westerly extension of the East African Rift.

REFERENCES

- Gupta A.K. and Fyfe W.S. 1975. Leucite survival: the alteration to analcime. *Canadian Mineralogist* 13, 361-363.
- Mitchell R.H. In press. A review of the mineralogy of lamproites. *Transactions of the Geological Society of South Africa* 88, number 2.
- Scott Smith B.H. and Skinner E.M.W. 1984. A new look at Prairie Creek, Arkansas. In Kornprobst J. ed., *Proceedings of the Third International Kimberlite Conference, Volume 1 - Kimberlites and related rocks. Developments in Petrology* 9, 255-283.

S.R. Shee¹, J.W. Bristow², P.B.S. Shee², D.R. Bell¹⁻³

1. Geology Dept., AARL, Box 106, Crown Mines, 2025, R.S.A.
2. Geology Dept., DBCM Ltd., Box 47, Kimberley, R.S.A.
3. Present Address: Geological and Planetary Sciences, California Institute of Technology, Pasadena, California, 91125, U.S.A.

INTRODUCTION

The Kuruman province comprises some twelve kimberlites and related rock occurrences, emplaced as dykes and pipes in the vicinity of the town of Kuruman in the northern Cape Province, R.S.A. These bodies intrude early Proterozoic Ghaap Plateau dolomites and overlying Asbestos Hills Banded Ironstones of the Griqualand West Sequence, towards the inferred north-western margin of the Kaapvaal craton (~ 2 500 m.y.). All are apparently barren of diamonds. The four occurrences dated thus far (Elston, Zero, Bathlaros and Riries) have emplacement ages of ~ 1 600 m.y. (Bristow et al., - this conference) establishing this province as the oldest yet documented. These rocks provide a unique opportunity to study the Kaapvaal upper mantle lithologies, processes and thermal structures of late Proterozoic age.

This paper describes the petrography and matrix mineral chemistry of the four dated intrusives. In addition a suite of mantle-derived peridotites from the Zero kimberlite have been studied with the aim of establishing the pressure - temperature regime under which they last equilibrated. The geochronology, isotopic characteristics and whole-rock geochemistry of these occurrences are described and discussed in a companion paper by Bristow et al. (this conference).

PETROGRAPHY

All four of the above localities are classified as hypabyssal-facies intrusions. Elston and Zero are petrographically similar, being rich in macrocrystic olivines, with a groundmass dominated by carbonate and variable phlogopite together with minor spinel, perovskite, probable monticellite, apatite and ilmenite laths. Heavy mineral concentrates are dominated by chromian spinels and garnet with minor clinopyroxene and rare ilmenite. Subcalcic (G10) garnets (Dawson and Stephens, 1975) with compositions similar to pyropes included in diamonds are abundant.

The Bathlaros kimberlite occurs as macrocrystic and aphanitic varieties with altered olivine macrocrysts and phenocrysts set in a groundmass of phlogopite, calcite, serpentine, apatite, spinel, perovskite, ilmenite laths, minor clinopyroxene and possible amphibole. Matrix mineral chemistry and whole-rock geochemistry indicate that the Bathlaros kimberlite is chemically more evolved than Elston and Zero. Heavy mineral concentrates from Bathlaros consist predominantly of chromian spinel; few other heavy minerals typical of most kimberlites are present.

The Riries dyke consists of altered olivine phenocrysts plus ilmenite and phlogopite macrocrysts set in a groundmass of phlogopite, ilmenite, carbonate, spinel and secondary quartz. Petrography and matrix mineral chemistry suggest that Riries is not a kimberlite but a lamprophyric rock. Heavy mineral concentrates from Riries consist of ilmenite and chromian spinel.

The character of the intrusions changes from east to west in the order Elston and Zero (kimberlite), Bathlaros (evolved or marginal kimberlite) and Riries (lamprophyre).

MATRIX MINERAL CHEMISTRY

Matrix phlogopites and spinels were analysed in the Zero and Bathlaros kimberlites, and Riries parakimberlite.

Phlogopite

Figure 1 is a plot of wt.% TiO₂ versus 100(Mg/Mg+Fe). Shown on the diagram for comparative purposes is the compositional field for matrix phlogopites from the Wesselton kimberlite, Kimberley (Shee, 1986). The micas from the Kuruman occurrences show little compositional overlap with those from Wesselton. The matrix micas show a trend of increasing titanium contents and decreasing 100(Mg/Mg+Fe) ratios in the order Zero, Bathlaros and Riries which confirms the petrographic variations in these intrusions noted above. The Bathlaros micas are mantled by late stage pleochroic colourless - red-brown tetraferriphlogites with low 100(Mg/Mg+Fe) ratios and very low titanium and aluminium contents. These overgrowths probably formed under conditions of higher oxygen fugacity.

Spinel

The spinels in Elston consist of subhedral to euhedral chromites (0.08 mm in size) mantled by thick rims of chromium-poor titanomagnetite. Euhedral titanomagnetite crystals (0.04 mm in size) are also present. The spinels at Bathlaros are relatively large (up to 0.2 mm) euhedral microphenocrysts which occur singly or form aggregates with other spinel or perovskite grains. Some of these spinels have chromium-rich cores mantled by titanium and chromium-poor magnetite mantles. Spinel from Riries are euhedral chromites mantled by titanomagnetite mantles and unzoned titanomagnetites. The compositional variations of the spinels from these localities are shown in Figure 2. Those from Elston are most similar to matrix spinels from Wesselton (Shee, 1984, 1986). Spinel from Bathlaros and Riries have lower chromium and magnesium contents substantiating the more evolved nature of these occurrences.

Ilmenite

Euhedral ilmenite laths (up to 0.1 mm in length) are rare constituents of the Elston and Bathlaros kimberlites but are more abundant in the Riries lamprophyre. The compositions of the laths in Elston are unusual for kimberlitic groundmass ilmenite in being chromium-poor and highly manganese (0.1 - 0.2 wt.% Cr₂O₃, 13 - 18 wt.% MnO). The magnesium levels are not much lower than normal (12 - 15 wt.% MgO) but iron contents are noticeably low (13 - 16 wt.% FeO). Euhedral ilmenites from Riries are iron-rich (> 46 wt.% FeO) with low magnesium, chromium and manganese contents (all < 0.5 wt.%).

MANTLE XENOLITHS

The Zero kimberlite contains an abundant and lithologically diverse suite of mantle-derived xenoliths. Eclogitic and peridotitic rock types are present in approximately equal proportions. The following peridotite types are present in decreasing order of abundance: chromium spinel harzburgite, garnet harzburgite, garnet lherzolites and aluminium spinel lherzolite. Garnet websterites, orthopyroxenites and phlogopite-clinopyroxenite are also present. The metasomatic assemblages phl + Ti-chromite + cpx and ilm + phl occur as variable equilibrated additions to the above peridotitic hosts confirming the diversity of metasomatic processes in the evolution of subcontinental lithosphere. Other assemblages present are rare large (> 1 cm) ilmenite nodules probably of the Cr-poor megacryst suite and large olivine nodules (1 - 6 cm) sometimes with enstatite, chromite, clinopyroxene and emerald green uvarovite-bearing garnet inclusions.

The garnet peridotites contain a significant proportion (± 50%) of subcalcic garnet-bearing harzburgites some of which have diamond-inclusion type G10 garnets. The orthopyroxenes in these garnet harzburgites have high aluminium contents (> 1 wt.% Al₂O₃) and geobarometric calculations indicate equilibration at relatively shallow pressures (< 40 Kbars at 1050°C) in the graphite stability field. Some garnet harzburgites with no modal clinopyroxene are calcium saturated i.e. > 5 wt.% CaO in the garnet and > 1 wt.% CaO in the orthopyroxenes. These rocks typically yield high calculated temperatures and pressures of equilibration i.e. 1200 - 1360°C at 50 - 55 kbars. Thermobarometric calculations on other garnet peridotites suggest correlation of high temperatures with deformation textures and Ti-enriched mineral compositions. These calculations will allow construction of a thermal profile of the southern African subcratonic mantle at 1600 m.y. for comparison with "geotherms" inferred for 1200 m.y. (Premier) and Jurassic - Cretaceous kimberlites.

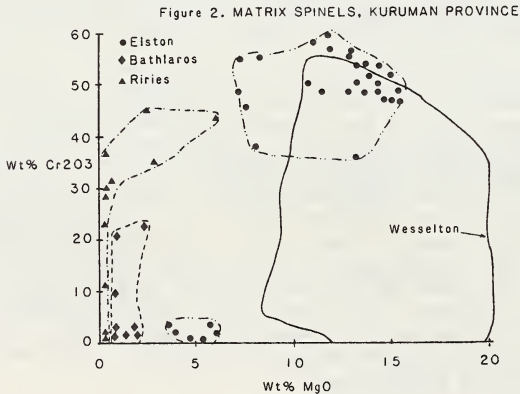
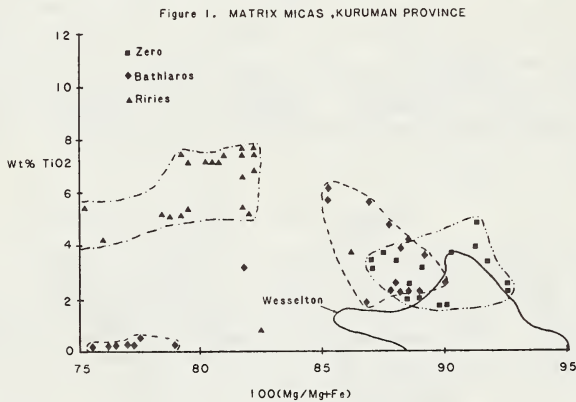
CONCLUSIONS

Kimberlites and related rocks near Kuruman have emplacement ages of 1600 m.y. establishing this province as the oldest yet documented. The petrographic character of the intrusions changes from east to west in the order Elston and Zero (kimberlite), Bathlaros (evolved or marginal kimberlite) and Riries (lamprophyre). The compositions of the matrix phlogopites, spinels and ilmenite from these intrusions confirms the petrographic variation.

An extensive suite of mantle-derived xenoliths exists at Zero. Garnet harzburgites with subcalcic G10 garnets yield relatively shallow pressures of equilibration. High temperatures and pressures are recorded in deformed peridotites and in calcium saturated garnet harzburgites.

REFERENCES

- BRISTOW, J.W., SMITH, C.B., ALLSOPP, H., SHEE, S.R. and SKINNER, E.M.W. (1986). Setting, geochronology and geochemical characteristics of 1600 m.y. kimberlites and related rocks from the Kuruman Province, South Africa. Proceed. 4th Kimberlite Conf., Perth, Australia. Abstract.
- DAWSON, J.B. and STEPHENS, W.E. (1975). Statistical classification of garnets from kimberlites and associated xenoliths. *J. Geol.*, 83, p. 589-607.
- SHEE, S.R. (1984). The oxide minerals of the Wesselton Mine kimberlites, Kimberley, South Africa. Kornprobst, J., Ed., *Kimberlites: 1 Kimberlites and Related Rocks. Develop. in Petrology*, 11A. Elsevier, Amsterdam. 466 pp.
- SHEE, S.R. (1986). The petrogenesis of the Wesselton Mine kimberlites, Kimberley, South Africa. PhD thesis (Unpubl.), University of Cape Town.



PECULIARITIES IN THE FLUID AND MELT COMPOSITIONS OF THE LAMPROITES
AND KIMBERLITES BASED ON THE STUDY OF INCLUSIONS IN OLIVINES

A. V. Sobolev¹, N. V. Sobolev², C. B. Smith³ and J. Dubessy⁴

1. Vernadsky Geochemistry Institute, Academy of Sciences of the USSR, Moscow, USSR
2. Institute of Geology and Geophysics, Siberian Division of Academy of Sciences of the USSR, Novosibirsk, USSR
3. CRA Exploration Pty Limited, 21 Wynyard Street, Belmont, Western Australia
4. CREGU, Nancy, France

The discovery and study of the province of diamondiferous ultrapotassic lamproites in Western Australia (Atkinson et al, 1984) has posed a series of problems, which firstly include the following:

the relationship between the various lamproite types and between lamproite and kimberlite;

the conditions of their formation and crystallisation, and the composition of the original lamproite melt and fluid content.

The present contribution deals with the results of direct determination of both the melt and fluid compositions, the liquidus assemblage and crystallisation temperature in olivine lamproites from the Ellendale field (pipes 11, 9, 4, 7) and in diopside-olivine-leucite lamproite from Mt. Cedric, as established from study of magmatic inclusions. The results of studying inclusions in olivine lamproite from the Ellendale 11 pipe were published earlier (Sobolev et al, 1985). For comparison, we have also worked on typical diamondiferous kimberlite from Udachnaya kimberlite pipe, Yakutia, USSR, and lamproitic rock of the hypabyssal facies from Prairie Creek, Arkansas, USA, described by Scott Smith and Skinner (1984). In most cases small (less than 0.5mm) second generation olivines (olivine-2) were studied and found in all cases to be of Fo₆₇₋₉₃ composition.

The primary inclusions (trapped during crystallisation) in olivine-2 from olivine lamproites from Western Australia are represented by partially crystallised melt, fluid, chromite, orthopyroxene and a combination of the above-mentioned phases. Microprobe analysis of crystallised melt inclusions shows the presence of calcilite, microilmenite, apatite, perovskite, phlogopite, K-richterite, residual glasses and probable fluorite (from optics). From microthermometric data (20 determinations) fluid inclusions are represented by practically pure CO₂ (triple point -56.5 to -58.3°C) of various density ($\rho = 0.88 - 0.20 \text{ g/cm}^3$). No additional phases such as liquid H₂O or reactionary phases around the fluid inclusions were observed up to 2000 x magnification. The position of inclusions within olivine crystals, and their composition, are indicative of simultaneous crystallization of olivine-2, orthopyroxene, chromespinel and possibly, clinopyroxene, from a melt saturated in fluid whose major component was CO₂ (Sobolev et al, 1985).

Inclusions in olivine-2 from kimberlite are represented mainly by decrepitated (exploded) melt and fluid inclusions and chromite. The scarce primary fluid inclusions are also represented by CO₂ (the temperature of the triple point was -56.5 to -58.0°C from 10 determinations) with maximum density 0.75 g/cm³. Similar fluid inclusions have been fixed also in olivine-2 from lamproitic rocks from Prairie Creek. From 4 determinations they are characterised by a triple point within the temperature range -56.6 to 57.5°C, $\rho = 0.85 \text{ g/cm}^3$.

The high temperature microscopic study of melt inclusions in olivines from olivine lamproites of Ellendale field has been carried out in an atmosphere of extra pure helium. From 55 runs only 5 show a homogenisation of small (5-15 microns) melt inclusions at 950 - 1050°C. In all the remaining cases the inclusions were decrepitated at 650 - 800°C or were found to be decrepitated in natural conditions. A distinct visible melting of the hermetic melt inclusions has been established to take place at a temperature from about 600°C. At 800°C the melt has a low viscosity as evidenced by a visible sudden rapid movement of the fluid phase inside the inclusions.

The composition of a melt at the moment of trapping, estimated from the compositions of quenched homogenised melt inclusions, is close to typical leucite lamproite, but with higher concentration of Na_2O (up to 2.4 wt %), BaO (up to 3.3 wt %) and exceptionally high concentration of F (up to 1.4 wt %). Evaluation of the crystallisation temperature of olivine-2 obtained by homogenisation of the melt inclusions (950-1050°C) permits one to estimate the pressure of crystallisation of the association of subphenocrysts by the use of syngenetic inclusions of highest density ($\rho = 0.88 \text{ g/cm}^3$) and P-V-T of pure CO_2 . The pressure thus evaluated was up to 5 kbars. This is the minimum estimation as one cannot exclude a denser fluid when carrying out further examination.

The study of the composition of the fluid inclusions in olivines from both lamproite and kimberlite rocks was carried out using the Raman microprobe technique (Touray et al, 1985). In order to fix H_2O we used the technique of heating the inclusions up to 350°C (Sobolev, Clocciatti, Dameincourt, 1985). It has been found that the fluid inclusions of all the studied rocks consist of CO_2 (90-95% mole), N_2 (up to 3.5 mol %) and CO (up to 2.5 mol %) occur as trace components of fluid from Australian lamproites. The upper limit of H_2O contents for the fluid phase has been fixed to be below 5% mol for lamproites (3 analyses) and below 7 mol % for kimberlites (2 analyses). Thus the partial pressure of H_2O in magmatic fluid seems to be not higher than 0.5 kbars. Such contents of H_2O cannot explain an exceptionally low temperature for lamproite melt. It seems that the essential role here belongs to the HF- component.

Thus from the reported data it may be concluded that olivine-2 from olivine lamproite had crystallised together with orthopyroxene, chromspinel and, possibly, clinopyroxene from a melt similar in composition to coexisting leucite lamproite at a temperature of about 1000°C and a pressure of near 5 kbars. The major component of the fluid, as also for kimberlite, was CO_2 . The variations in CO_2 concentrations in kimberlitic and lamproitic rocks may be explained rather by the difference in the CaO concentration in the magmas and the possibility or impossibility of CO_2 bonding in magmatic or early-postmagmatic calcite.

In conclusion, one must stress the exceptional activity of F in lamproite melt in the Upper Mantle conditions that has to be taken into account when postulating a hypothesis on lamproite rock formation.

REFERENCES

- ATKINSON, W. J., HUGHES, F. E. & SMITH, C. B., 1984. A review of the kimberlitic rocks of Western Australia; in Kornprobst, J. (Ed), Kimberlites. 1: Kimberlites and Related Rocks, pp.195-224, Elsevier, Amsterdam.
- SCOTT SMITH, B. H. & SKINNER, E. M. W., 1984. Ibid. pp.255-284.
- SOBOLEV, A. V., CLOCCIATTI, R., DAMEINCCURT, P., 1983. C. R. Acad. Sci. Paris. v.296.
- SOBOLEV, A. V. et al 1985. In Russian. Doklady Acad. Sci. USSR, V.284, pp.196-201.
- TCURNAR, J. C. et al 1985. Scanning Electron Microscopy, pp.103-118.

KIMBERLITE AND KIMBERLITE-LIKE ROCKS, THEIR COMPOSITIONS,
TIME-SPACE RELATIONS, GENESIS AND TECTONIC CONTROL

B. M. Vladimirov and L. V. Solovjeva

Institute of the Earth's Crust, Siberian Branch of the USSR Ac. Sci, Irkutsk, USSR

Rocks termed at present as kimberlites do not represent a united genetic group. According to the geological characteristics of their manifestations in the crust, their natural associations, chemical features and mineral compositions, they may be subdivided into five individual groups. They are (1) kimberlites from localised complexes, (2) kimberlite-like lamprophyres related to K-rich basalts, (3) kimberlite-like basanites associated with alkaline-ultramafic carbonatite-bearing complexes, (4) kimberlite-like mafic and ultramafic volcanites related to olivine-alkaline basalts, (5) kimberlite-like peridotitic breccias from alpine-type hyperbasic complexes.

Kimberlites from localised complexes (proper kimberlites) are discovered only on ancient platforms within their Archaean-Lower Proterozoic cratons, i.e. in those parts of the continents where the mantle substance was differentiated to great depths and the thick lithosphere was formed. In different epochs kimberlites penetrated into the crust, as a rule, at final stages of tectono-magmatic activity. Within individual cycles their intrusion was preceded or accompanied by intrusion of magmas of varying petrochemical types. They were tholeiite-basaltic magmas, or alkaline-ultramafic magmas, or alkaline-basaltic ones. In the kimberlite-productive cycles standard sets of magmatic rocks associations are absent. Within a tectono-magmatic cycle kimberlites may be associated with tholeiitic basalts, alkaline basalts and alkaline-ultramafic rocks. They also occur autonomously, without any connections with other types of magmatic rocks.

The nature of the time/space relations between kimberlite and other types of igneous rocks formed within the same tectonic cycle indicates a distinct genetic singularity of kimberlite magmatism. Thick tectonosphere, low-gradient thermal regime of primary magmatic chambers, low melting degree of the initial substance, high rates of the melts rising to the surface without delays in intermediate reservoirs beginning with 120 km depth are necessary for origination of kimberlites and their penetration into the upper portions of the crust. According to the current thermal and geodynamic models of continental and oceanic rifting, as well as to the models of island arc and continental margin formation, the above conditions are not realised. These conditions are in line with the geological data. Classic types of kimberlites are not found in the systems mentioned above.

The specific petrochemical and geochemical characteristics of kimberlite is well seen from the coefficients: Si/Mg, Ca/Ca+Mg, Ni/Co, Cr/V, Ni/V, Na/K, Li/Rb, K/Rb, Sc/V. In total they are ultramafic (not alkaline) rocks slightly oversaturated with alumina. To judge from their texture, structure and mineralogical features, they are holomelanocratic volcanites forming small bodies of pipe and vein facies. Direct transitions and connections with rocks of other genetic associations are not established. All the above-mentioned indicate genetic independence of kimberlite magmas.

All the kimberlite-like rocks cannot be identified with proper kimberlites. They converge with the latter according to some features.

The kimberlite-like basanites from alkaline-ultramafic complexes show maximum convergence with kimberlites in their texture and structure, rock-forming minerals, petrochemical and geochemical features. However, such high-pressure minerals as Cr-rich garnet, chromite, magnesian subcalcic endiopsides and diamonds are absent in them. Unlike kimberlites, they often contain phenocrysts of titanaugite, aegerine-augite, fassaite. In the matrix alkaline amphiboles and feldspathoids are present. Judging from the fact that deep-seated xenoliths are represented as spinel lherzolite and metamorphic eclogites (very rare), the primary magmas producing these associations were formed in the spinel-garnet mantle zone. These rock manifestations are controlled by continental rift zones, mobile belts and margins of platforms.

Kimberlite-like mafic and ultramafic volcanites from associations of alkaline olivine basalts strongly differ from kimberlites in their petrochemical, geochemical and mineralogical features, but they are rather close to them in deep-seated nodule composition. Among the nodules, together with prevailing spinel lherzolite, spinel-garnet and garnet varieties are present. Sometime, in their composition uvarovite-pyrope with knorringite mineral admixture are present. High-chromic and at the same time low-calcic knorringite-pyropes do not occur in them. Unlike deep-seated nodules from kimberlites, garnet lherzolites and harzburgites from kimberlite-like rocks do not contain magnesian and ferromagnesian endiopsides, as well as diopsides with low aluminium content and at the same time with high Na_2O content. Phenocrysts of the above clinopyroxene varieties are absent in kimberlite-rocks. Ultramafic xenoliths are widely distributed in the kimberlite-like rocks of this series. They consist of minerals with high ferrugineity (augites, salite-augites, bronzites, chrysolites) and related typochemical phenocrysts. This type of kimberlite-like rocks is confined to continental rifts, subductive zones of median massifs and marginal platform structures.

The kimberlite-like rocks from associations with K-rich alkaline basalts are identical to kimberlites by suites of high-pressure minerals, but, as well as the above group of rocks, differ from them in their mineralogical, petrochemical and geochemical features.

GEOLOGY AND ECONOMIC EVALUATION OF THE MT. WELD
CARBONATITE, LAVERTON, WESTERN AUSTRALIA

G. C. Willett, R. K. Duncan, R. A. Rankin

Union Oil Development Corporation

INTRODUCTION

The Mt. Weld carbonatite lies approximately 35 km. southeast of Laverton township and intrudes an Archean volcanosedimentary sequence within the Eastern Goldfields Province of the Yilgarn Block of Western Australia. Discovery of the carbonatite followed from an airborne magnetometer survey carried out by the Bureau of Mineral Resources, Canberra in 1966. A pronounced magnetic anomaly indicated the presence of a large circular feature (approx. 4 km. in diameter) lying beneath a surficial cover of alluvium and horizontally bedded lacustrine sediments.

Drilling of this feature by geologists of the Utah Development Company confirmed the presence of a carbonatite (Appleby et al., 1973; Cawsey et al., 1974).

K/Ar and Sr⁸⁷/Sr⁸⁶ isotopic dating of the carbonatite gave post-Archean ages of 2,064 ± 40 m. yrs. (Amdel, 1973) and 2,020 ± 17 m. yrs. respectively (Collerson, 1982).

Intrusion of the Proterozoic carbonatite near Mt. Weld appears spatially and tectonically related to the deep-seated long-active Laverton tectonic zone. Drilling of the host Archean sequence in the vicinity of the carbonatite intersected weathered aphanitic basic volcanics, serpentinites (some members amygdaloidal) and rarely, acid to intermediate volcanics. Rare carbonatite dyking was encountered up to 5 kms. from the intrusion (Hallberg, 1985).

Exploration by Union Oil (1981-85) led to the discovery of significant deposits of residual apatite within the regolith of the carbonatite. These deposits are currently being evaluated as a source of raw material for local fertiliser manufacture.

GEOLOGY OF THE CARBONATITE

Wallrock Alteration

An annulus of brecciated glimmerite approximately 0.5 km. in width, encloses a sovitic pipe. This annulus is a zone of lower density altered country rock, the glimmerite consisting of a fine grained felted matrix of "ferri-biotite".

It would appear that the wallrock alteration was one of alkali metasomatism under oxidising conditions associated with brecciation and assimilation (xenoliths).

Subsequent carbonate invasion of the brecciated wallrock, veined and pervaded the felted biotite matrix introducing calcite, dolomite and accessory phases such as apatite, pyrochlore, barite, magnetite, ilmenite and sulphides. Minor chloritic and riebeckitic alteration was associated with the invasion of carbonate.

Primary Carbonatite

Sovite is the dominant carbonate-rich variety of carbonatite with rauhaugite, calcitic rauhaugite and dolomitic sovite present as subdominant rock types. Locally apatite or biotite may dominate the carbonate phase forming a phosphorite or glimmerite.

Relict cumulate textures are discernible in some of the sovites and rauhaugites. Primary carbonate occurs as subidiomorphic to rounded grains forming the cumulate phase with minor apatite, biotite, carbonate and magnetite present as an intercumulate. Fine dense schillers of iron oxide cloud the primary carbonate and enhance the cumulate texture.

Large elongate and branching carbonate grains comprise the primary cumulate phase in some sovites. Such textures are reminiscent of the "harrisitic cumulates" first

described by Wadsworth (1960) for rocks in the Rhum intrusive and later referred to as "harrisitic spinifex" by Nesbitt (1971) when describing skeletal olivine in Archean ultramafic rocks. Donaldson (1974), when discussing these textures for olivine cumulates in the slowly cooled Rhum intrusive, attributed their formation to crystallising under conditions of magma supersaturation.

Rare spherulitic and orbicular textures are present in the intrusive. They arise from the tangential arrangement of biotite laths about calcite grains in olivine sovite (Mariano, 1981) or contain olivine, apatite and biotite cores rimmed by magnetite in a calcitic matrix (Bartram, 1973).

Similar spherulitic and orbicular structures have been described for the Sokli (Finland) and Vvorijarvi (U.S.S.R.) carbonatites by Lapin and Vartiainen (1983). They postulate that segregation of the initial melt into phoscoritic and carbonatitic fractions of limited mutual miscibility combined with the difference in density and viscosity of each fraction gave rise to these structures.

Associated with the primary cumulate rocks (subidiomorphic, harrisitic and orbicular varieties) are medium grained granular sovites and rauhaugites. In contrast with the cumulate rocks, carbonate is usually free of iron oxide schillers. Secondly, these rocks exhibit marked flow alignment of grains and flow layering of minerals. Apatite and biotite, in particular, form elongate (prismatic and tabloid) crystals which are strongly aligned.

Granular sovite and rauhaugite may be seen replacing primary cumulate carbonatite. These rocks do not appear to be the products of recrystallisation because they exhibit magmatic textures (grain alignment and flow layering) and contain accumulations of apatite, magnetite, biotite and pyrochlore relative to the primary carbonatite. Thus it would appear that accumulations of apatite-magnetite-biotite-pyrochlore precipitated out of the primary cumulate carbonatite and formed a denser "crystal mush" that was subsequently injected into crystallised carbonatite. Layering of minerals is produced by their mutual segregation and concentration in the near vertical plane of magma flow.

Conditions appear to have been reducing during crystallisation of the carbonatite. The presence of pyrite with magnetite, crystallisation of olivine with high fayalite contents, presence of Fe^{2+} in dolomite and the occasional presence of primary salite would suggest this (Mariano, 1981). Minimal late stage alkali buildup and alteration is indicated by fibrous riebeckite and aegirine in late veining and interstices, and the development of "ferri-biotite" rims on phenocrystal biotite. Accessory finer grained "ferri-biotite" is also present.

Late veining also carries calcite, dolomite and trace quantities of barite, magnesiocrocidolite, strontianite and fluorite. Polycrystalline apatite and monazite appear to be contemporary with magnesiocrocidolite in some examples.

Regolith of the Carbonatite

Regolith development of the carbonatite was a complex process involving weathering of the primary carbonatite, development of a lateritised residuum and formation of a soil horizon.

The base of the regolith is defined simply as the limit of weathering. Partway up through the weathering profile a natural division occurs in which accumulations of residual minerals (residual zone) are superceded by a supergene minerals assemblage (supergene zone).

Formation of the residual zone resulted from the leaching and removal of carbonate minerals en masse by circulating groundwater. Concentration, by volume reduction, of primary minerals such as apatite, magnetite, ilmenite, Nb-rutile, remnant silicates, zircon and baddeleyite occurred. Concurrent ferruginisation of the residual zone led to the present laterites.

The supergene zone is characterised by insoluble ferric iron oxides with adsorbed Nb, Ta, Ti, V and Cr, aluminous oxides, clays, crandallite group minerals, secondary

phosphates, REE oxides and manganiferous wads. Residual primary minerals are rare.

Extreme conditions of lateritic weathering appear to have prevailed for the supergene zone over a prolonged period causing the degradation of resistant minerals and oxidation of metal ions. Florencite pseudomorphs after pyrochlore, leaching of Nb and Ta from pyrochlore and their reprecipitation in goyazite and florencite, and the complete degradation of magnetite to hematite and maghemite are examples. The formation of cerianite (Ce⁴⁺) and fractionation of LREE from HREE throughout the regolith are further indications.

ECONOMIC EVALUATION OF THE REGOLITH

Drilling of the regolith outlined an extensive sheet of residual apatite mineralisation covering most of the carbonatite. A geostatistical study of this resource by Gregory (1984) gave a global estimate of:

250 ± 37 million tonnes (precision @ 95%) @ 18% P₂O₅
using a cutoff grade of 10% P₂O₅ as apatite.

Not all this apatite-bearing rock is considered potential ore for fertiliser manufacture. Some material will be too costly to extract from the ground and other material is contaminated with iron, aluminium and magnesium. Studies underway are aimed at quantifying the amount of "ore grade and quality" material suitable for exploitation as a principal source of rock phosphate for fertiliser manufacture in Western Australia.

REFERENCES

- AMDEL, 1973. Laboratory report no. AN 3799/73 ed. A. W. Webb.
- APPLEBY, W. R., and ALEXANDER, C., 1973. Report on progress of exploration on the Mt. Weld Complex, Laverton, Western Australia. Utah Development Co. Report no. 219.
- BARTRAM, G. D., 1973. Petrological descriptions of core samples from Mt. Weld carbonatite. Report no. 1621, Delta Petrological Services, Perth.
- CAWSEY, A. L., and APPLEBY, W. R., 1974. Report on exploration Mt. Weld complex, Laverton District, Western Australia. Utah Development Co. Report no. 248.
- COLLERSON, K. D., 1982. Age and strontium isotope systematics of the Mt. Weld carbonatite, Western Australia. Commissioned report to Union Oil Development Corp.
- DONALDSON, C. H., 1974. Olivine crystal types in harrisitic rocks of the Rhum pluton and Archean spinifex rocks. Geol. Soc. Am. Bull., 85, 1721-1726.
- GREGORY, C. M., 1984. Mt. Weld Project geostatistical study. Report of Utah Development Co.
- HALLBERG, J. A., 1985. Geology and mineral deposits of the Leonora-Laverton area, Northeastern Yilgarn Block, Western Australia. Hesperian Press, Western Australia.
- LAPIN, A. V., and VARTIAINEN, H., 1983. Orbicular and spherulitic carbonatites from Sokli and Vvorijarvi. Lithos, Vol. 16, 53-60.
- MARIANO, A. N., 1981. Characterisation of selected drill core from the Mt. Weld carbonatite complex, Laverton Western Australia. Confidential report to Molycorp Inc.
- NESBITT, R. W., 1971. Skeletal crystal forms in the ultramafic rocks of the Yilgarn Block, Western Australia: evidence for an Archean ultramafic liquid. Spec. Publs. geol. Soc. Aust., 3, 331-347.
- WADSWORTH, W. J., 1960. The layered ultrabasic rocks of south-west Rhum, Inner Hebrides. Phil. Trans. R. Soc., Ser. B, 244, 21-64.

Zhou Jianxiang

Institute of Mineral Deposits, CAGS, 26 Baiwanzhuang Road, Beijing, China

The purpose of this contribution is to provide an overview of the LIL-bearing Ti-Cr-Fe oxides. Also discussed is the chemistry of the precipitational environment which differs from that normally conceived to be present in the upper mantle.

LIL stands for large ion lithophile elements. It includes K, Ba, Ca, Sr, Na, REE, Rb, Pb and U. LIL-bearing Ti-Cr-Fe oxides have been discovered in a few Chinese kimberlites (Zhou et al, 1980, 1982, 1984; Dong et al, 1983). They are crichtonite series, yiemengite, Cr-priderite and so on. The LIL elements, K, Ba, Ca, Sr, REE and Na in these minerals are in significant concentrations, from 1 wt % oxide to 8 wt % oxides. Because of structural flexibility, these mineral are also repositories for refractory elements, such as Ti, Cr, Nb, Zr and Al. Few kimberlite bodies which contain so many LIL-bearing Ti-Cr-Fe oxides have been discovered in the other parts of the world. Only one example, the Jagersfontein kimberlite, South Africa which has a very similar Ba-specific assemblage has been described (Haggerty, 1975; Smyth et al, 1978; Jones et al, 1982). The kimberlites with LIL-bearing Ti-Cr-Fe oxides are similar to others in mineral assemblage. The main rock-forming minerals are olivine, phlogopite and the accessory minerals are diamond, pyrope, chromite, ilmenite, Cr-picroilmenite, perovskite, Cr-diopside, apatite, zircon and magnetite.

The following species of crichtonite have been recognised: (1) mathiasite, K member of crichtonite; (2) lindsleyite, Ba member of crichtonite; (3) lovingite, Ca member of crichtonite. Mathiasite is more common than others and it exhibits some degree of solid solution towards lovingite or lindsleyite (Fig. 1). Although compositional variation or zoning within individual crichtonites is not common, there is a little difference compositionally among grains. A few other mineral inclusions with very high ZrO₂ or K₂O (unidentified) in crichtonite have been found. Major elements in order of decreasing abundance are as follows (by oxide weight percent): TiO₂ 53-60 wt %, Cr₂O₃ 16-20 wt %, FeO 7-11 wt %, ZrO₂ 4-5 wt % and MgO about 4 wt %. These are the small cations occupying the M-formula position in AM₂O₃₈. Other elements in this position are Mn, Al, Nb and so on, but their total content is less than 2 wt %. The large radius cation position is occupied by K₂O, CaO, BaO, SrO, Na₂O and REE, their contents varying in each member of crichtonite (Table 1). More than 30 crichtonite xenocrysts have been analysed, but the pure K, Ba, Ca members have not been found. These crichtonites are named according to the dominant A-site cation in this paper. The contents of small radius cations, such as Fe²⁺, Fe³⁺, Al, Cr, Ti, Mg and Zr, of crichtonites in Chinese kimberlites are different from other members of the crichtonite series, especially for Cr₂O₃, Zr₂O and Nb₂O₅ contents. These crichtonites as high pressure reservoirs for refractory and LIL elements in the upper mantle may be important for understanding the dynamics of fluid movements and mantle metasomatism (Haggerty, 1983).

Yiemengite (K, Ba) (Cr, Ti, Fe, Mg)₁₂O₁₉ in chemical formula and crystal structure is similar to magnetoplumbite which occurs in products of secure radioactive waste disposal. So yiemengite and above crichtonites may have a direct application to such secure disposal, because they all have structural flexibility in hosting large and small cations and they are highly refractory. Typical yiemengite contains K₂O 3.38 wt %, BaO 3.03 wt %, Cr₂O₃ 37.18 wt %, TiO₂ 29.57 wt %, FeO 17.77 wt %, MgO 5.69 wt % as the major oxides. Other oxides present are CaO 0.13 wt %, SrO 0.12 wt %, ZrO₂ 0.04 wt %, Al₂O₃ 1.08 wt %, Nb₂O₅ 1.03, V₂O₅ 0.01 wt %. X-ray study shows it must be a hexagonal symmetry, P63/mmc. Cell parameters are a = 5.81 Å, c = 22.94 Å. Yiemengite usually is a homogeneous discrete single crystal. Sometimes a rim of decomposition products around yiemengite is found. Yiemengite was metasomatised and replaced by combinations of subhedral chromite and Cr-priderite (Fig. 2). These chromites contain relatively high titanium (TiO₂ about 6 wt %) and low alumina (Al₂O₃ 2 wt %). They are enriched in magnesium-ulvospinel with minor magnesioferrite. This is indicative of somewhat lower f_{o2} conditions (Haggerty 1983).

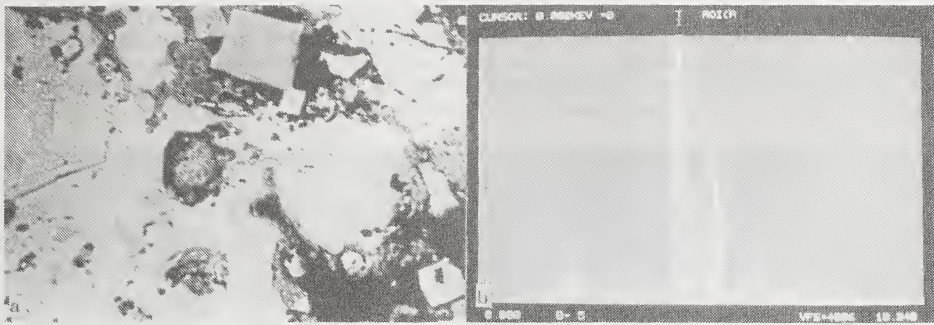


Fig. 1 (a) Backscattered electron image (composition) of crichtonite, illustrating the solid solution of mathiasite (dark grey) and loveringite (light grey); note the subhedral chromite which is a product of decomposition of crichtonite; (b) Energy dispersive spectrum of loveringite, showing higher CaO content

Cr-priderite intergrows with yiemengite. It differs in small cations from priderite $(K, Ba)_2(Ti, Fe)_6O_{13}$ which is described by Post (1982). The small cation position in Cr-priderite is dominated by titanium (65.02 wt % TiO_2), followed by chromium (14.23 wt % Cr_2O_3). Iron concentration is about 3.19 wt % FeO. The large cation position is dominated by potassium (5.91 wt % K_2O) and barium (8.52 wt % BaO). So Cr-priderite is distinguished also from priderite in Arkansas, United States.

Table 1

Representative analyses of Cr-priderite (PR-1, PR-2), yiemengite (YM-1, YM-2), mathiasite (MA-1), lindsleyite (LI-1), loveringite (LO-1) and chromite (CR-1).

All samples come from kimberlites in Shandong Province, China.

The analyses were done at the BRGM electron microprobe facility in France.

	PR-1	PR-2	YM-1	YM-2	CR-1	LI-1	MA-1	LO-1
K_2O	5.91	5.79	3.38	3.27	0.03	0.85	1.19	0.81
CaO	0.01	0.03	0.13	0.13	0.02	0.46	0.62	1.42
BaO	8.52	7.64	3.03	2.93	0.09	2.95	1.85	1.67
Na_2O	0.27	0.19	0.01	0.05	0.00	0.05	0.05	0.09
SrO	0.00	0.00	0.12	0.00	0.00	0.77	0.40	0.56
TiO_2	65.02	64.99	29.57	29.72	5.81	57.45	59.43	60.36
ZrO_2	0.00	0.00	0.04	0.00	0.00	4.26	4.79	4.65
Cr_2O_3	14.23	13.38	37.18	37.02	54.97	17.70	15.71	16.75
Al_2O_3	0.22	0.21	1.08	1.11	1.77	0.48	0.62	0.66
V_2O_5	0.00	0.00	0.01	0.00	0.00	0.00	0.00	0.26
FeO	3.19	3.21	17.77	17.85	25.07	8.05	9.36	7.48
MgO	0.50	0.47	5.69	5.72	10.73	3.76	4.08	4.02
MnO	0.04	0.06	0.22	0.19	0.35	0.02	0.14	0.13
Nb_2O_5	2.37	2.09	1.03	1.23	0.00	3.97	2.60	1.40
Tr_2O_3	-	-	-	-	-	1.00	1.00	1.00
Total	100.29	98.51	99.26	99.21	98.84	100.86	100.66	100.24

These LIL-bearing Ti-Cr-Fe oxides are also associated with several other highly incompatible element-rich phases: (1) Cr-bearing picroilmenite with Cr_2O_3 4-8 wt % and MgO 10-15 wt %; (2) Ti-bearing chromite with TiO_2 about 5 wt %; (3) Cr-bearing pyrope with Cr_2O_3 about 5-10 wt %; (4) Other rare minerals and unidentified mantle minerals.

This association of LIL-bearing oxides described here is indicative of a highly alkalic environment. Considering other LIL-bearing oxides discovered in Jagersfontein Kimberlites (Haggerty, 1983) and Western Australian leucite-lamproites, the role of alkalis in the mantle and the origin of alkalic rocks in general has thus taken on a new dimension. On the other hand, this association of LIL-bearing oxides is also enriched in refractory and incompatible elements. It shows clearly that these minerals precipitate in residual liquids during crystallisation or fractionate into liquids

during partial melting. In a word, these mineral chemistries are sufficiently diagnostic to warrant consideration for the existence of very specific conditions in some regions of the upper mantle. It is concluded that the refractory and LIL-bearing oxides association resulted from metasomatism by the introduction of liquids enriched in above elements into harzburgites or peridotites (Haggerty, 1983).

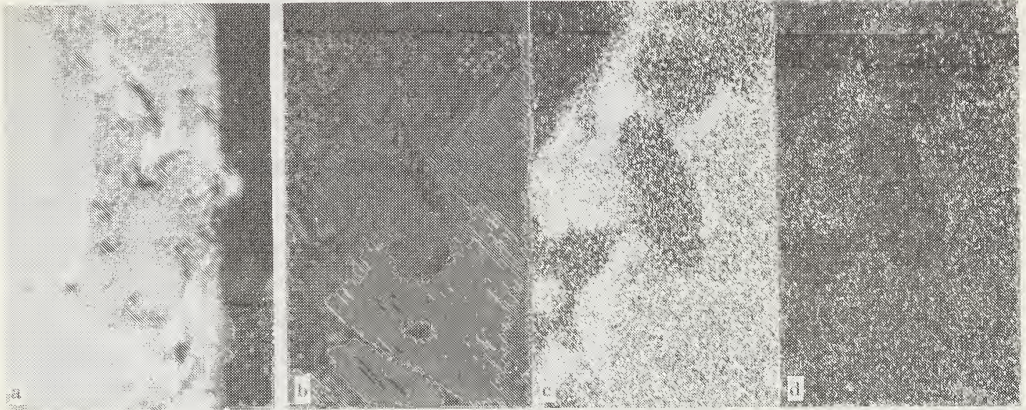


Fig. 2 (a) Reflected light photomicrograph taken under oil-immersion objectives, partial decomposition of yiemengite containing subcubic spinels (dark grey) and Cr-priderite (white) in the rim; (b) Backscattered electron image (composition); (c) Ti K X-ray image; (d) K K X-ray image. (b)-(d) in the same area, showing the intergrowth of yiemengite, chromite and Cr-priderite.

This study was supported by the Institute of Mineral Deposits, CAGS and Seventh Geological Team of Shandong Province. Prof S. E. Haggerty provided very helpful materials and ideas. This study has benefitted from collaboration with Dr. Z. Johan, Dr. D. Ohnenstetter on the electron microanalysis of LIL-bearing oxides. To all I express my gratitude. I wish also to thank the organisers, the editors and the reviewers of the 4th IKC, especially Prof. Peter Harris, Dr. Alec Trendall, Mr. J. D. Lewis and Dr. J. R. Ross.

REFERENCES

- DONG, Z., ZHOU, J., LI, Q. and PENG, Z., 1983. Yiemengite, $K(Cr, Ti, Fe, Mg)_{12}O_{10}$, a new mineral from Chinese kimberlites. *Kexue Tongbao (Bul. Sci.)* 29, 920-923.
- HAGGERTY, S. E., 1975. The chemistry and genesis of opaque minerals in kimberlites. *Physics and Chemistry of the Earth* 9, 295-307.
- HAGGERTY, S. W., 1983. The mineral chemistry of new titanates from the Jagersfontein kimberlite, South Africa: Implications for metasomatism in the upper mantle. *Geochimica et Cosmochimica Acta* 47, 1833-1854.
- HAGGERTY, S. E., ERLANK, A. J. & GREY, I. E., 1986. Metasomatic mineral titanate complexing in the upper mantle. *Nature* 6056, 761-763.
- JONES, A. P., SMITH, J. V. & DAWSON, J. B., 1982. Mantle metasomatism in 14 veined peridotites from the Bultfontein Mine, South Africa. *Journal of Geology* 90, 435-453.
- POST, J. E., VON DREELE, R. B. & BUSECK, P. R., 1982. Symmetry and cation displacements in hollandites: structure refinements of hollandite, cryptomelane and priderite. *Acta Cryst.* 38, 1056-1065.
- SMITH, J. R., ERLANK, A. J. & RICHARD, R. S., 1978. A new Ba-Sr-Cr-Fe titanate mineral from a kimberlite nodule (abstr). *EOS Amer. Geoph. Union* 59, 394.
- ZHOU, J., 1980. Microanalysis techniques of mineral and their geological application (in Chinese). *Geological Review* 6, 547-551.
- ZHOU, J., ZHOU, K., FANG, Y. & YANG, G., 1982. A preliminary study of ilmenites from kimberlites by electron probe. *Bulletin of IMD, CAGS.* 3, 103-114.
- ZHOU, J., 1984. Mathiasite in kimberlite of China. *Acta Miner. Sinica* 3, 193-198.

II. WHEN AND WHERE DO THEY OCCUR?

**Their distribution in geologic space and time;
their tectonic setting and regional occurrence;
possible causes of observed distribution patterns.**



GLOBAL KIMBERLITE AND LAMPROITE DISTRIBUTION. CONTINENTAL REASSEMBLY IS A 180 Ma FIT FROM HURLEY AND SMITH (1980)

	Page
REVIEW PAPER	
Distribution of kimberlites and associated rocks in space and time: Relationship to tectonic processes J. B. DAWSON	107
A review of radiometric dating methods applicable to kimberlites and related rocks H. L. ALLSOPP, C. B. SMITH, J. W. BRISTOW, R. BROWN, J. D. KRAMERS and O. G. GARVIE	109
Setting, geochronology and geochemical characteristics of 1600my kimberlites and related rocks from the Kuruman Province, South Africa J. W. BRISTOW, C. B. SMITH, H. L. ALLSOPP, S. R. SHEE, and E. M. W. SKINNER	112
Geological setting, petrography and petrogenesis of olivine melilitites on the Natal Coast, South Africa E. A. COLGAN and H. L. ALLSOPP	115
Kimberlites and the mantle sample - can we decode their geotectonic message? H. HELMSTAEDT and D. J. SCHULZE	118
A review of the geology of some kimberlites in China S. HU, P. ZHANG and G. WAN	121
Kimberlites and their ultramafic xenoliths from western Kenya M. ITO	124
Magsat anomalies, crustal magnetisation, heat flow and kimberlite occurrences in Australia B. D. JOHNSON, M. A. MAYHEW, S. Y. O'REILLY, W. L. GRIFFIN, F. ARNOTT and P. J. WASILEWSKI	127
A catalogue of kimberlite occurrences M. T. MUGGERIDGE	130
Heavy minerals in kimberlites from Tanzania - the neglected craton P. H. NIXON and E. CONDLIFFE	133
The ages of kimberlite and lamproite emplacement in Western Australia R. T. PIDGEON, C. B. SMITH and C. M. FANNING	136
The influence of the regional structure of the Rhodesia craton on the distribution of kimberlites in Botswana and Zimbabwe D. A. PRETORIUS	139
Alkalic ultrabasic dykes of the south east Yilgarn margin, West Australia J. V. A. ROBEY, J. W. BRISTOW, M. R. MARX, J. JOYCE R. V. DANCHIN and F. ARNOTT	142
New occurrences of kimberlite in Brazil D. P. SVISERO and H. O. A. MEYER	145
The distribution pattern of kimberlites and their cognate rocks in Shandong, China G. WAN	148

DISTRIBUTION OF KIMBERLITES AND ASSOCIATED ROCKS IN SPACE AND TIME:
RELATIONSHIP TO TECTONIC PROCESSES

J. B. Dawson

Department of Geology,
University of Sheffield,
Sheffield, S1 3JD, U.K.

In this review kimberlites are those low-volume, ultrabasic, ultrapotassic rocks that conform to the definition by Clement et al. (1984). Stricter definitions on both petrographic and chemical criteria (Rock, 1986) has enabled some occurrences of rocks previously referred to as 'kimberlitic' to be reclassified as 'ultrabasic lamprophyres'. Included within the review are occurrences of lamproite (i) because olivine lamproite from the U.S.A. (the Praire Creek 'kimberlite') and olivine- and leucite-lamproites in N.W. Australia contain diamonds, and hence originate in the same depth-zone in the upper mantle as kimberlites; and (ii) because both kimberlites and lamproites belong to a geochemically unique group of rocks characterised by high-alkali, high-potassic, high LILE values combine with high Mg, Ni and Cr contents, together with low Al. The overlap is particularly marked between Group II kimberlites and olivine lamproites (Dawson, in press).

A new kimberlite province is now known in N.E. China, and new individual kimberlites have been reported from the U.S.A. (Lake Ellen), Brazil and southern Africa; all these occurrences confirm previous observations that kimberlites are mainly confined to the old, stable cratons. The intrusion of diamond-bearing lamproites of Precambrian and late-Tertiary age on the Kimberley Craton of N.W. Australia, again substantiates earlier observations that the older cratons are prone to repeated intrusion of material from the deeper parts of the upper mantle (Dawson, 1980).

Occurrences previously held to be kimberlite but now discredited include several from eastern Canada and the eastern U.S.A.; the only occurrence in Argentina; the occurrences in eastern Sweden at Kalix and Alno; and on the Taimyr peninsula of the USSR.

The distribution of lamproites (Bergman, in press) is likewise confined mainly to cratonic areas, although others (e.g. E. Australia, S.E. Spain) are not. Significantly, coeval lamproites occur within a swarm of Group II kimberlite dykes at Swartruggens, S. Africa (Skinner & Scott Smith, 1979) reinforcing an earlier observation of a similar relationship between kimberlites and fitzroyites in the Seguela area of the Ivory Coast.

Kimberlite magmatism took place in W. Africa, S. Africa (Premier Mine) and in India in the Precambrian; and the presence of diamonds in Precambrian sediments (of both Archaean and Proterozoic age) and in Phanerozoic basal conglomerates overlying Precambrian terranes is perhaps indicative of the presence of more Precambrian kimberlites that have been either removed by later erosion or blanketed by later sedimentary cover. Cambrian kimberlites are known in W. Greenland, and others occur in the Silurian (USSR), the Devonian (USSR, U.S.A.), Upper Triassic (Swaziland), the Permian (eastern U.S.A.), Upper Jurassic (USSR; S. Africa), in the Cretaceous (S. Africa, Angola, W. Africa and Brazil), and the Eocene (Tanzania). Even accounting for enhanced possibility of recognition of relatively young activity compared with older magmatism (due to decreased chance of subsequent sediment burial), the Upper Jurassic/Cretaceous activity was the major epoch of kimberlite intrusion.

Most phases of kimberlite activity were accompanied by coeval igneous activity of a very limited nature. Coeval rock-types vary from locality to locality but include lamprophyres, lamproites, nepheline syenites and carbonatites.

Known lamproites range in age from Proterozoic (Chelima, India; W. Greenland; Argyle W. Australia), Palaeozoic, Mesozoic (Kansas, U.S.A.; S. Africa), but most are Tertiary (e.g. N.W. Australia, Highwood Mountains, U.S.A.) and Gaussberg (Antarctica) is of Recent age (Bergman, in press).

Various hypotheses have been proposed to place kimberlite activity in its contemporary tectonic framework. Much current work tends to associate kimberlite magmatism with crustal thinning linked with major plate movements; certainly, the Mesozoic activity

in Liberia, Angola, S. Africa and Brazil is contemporaneous with the opening of the S. Atlantic. Evidence for linking it with hot spot activity is less obvious.

References

- Bergman, S.C. (in press). Lamproites and other potassium-rich igneous rocks: a review of their occurrence, mineralogy and geochemistry. In: Fitton, J.G. & Upton, B.G.J. eds. Alkaline igneous rocks. Geol. Soc. London, Spec. Publ.
- Clement, C.R., Skinner, E.M.W. & Scott Smith, B.H. (1984). Kimberlite redefined. J. Geol., 92, 223-228.
- Dawson, J.B. (1980). Kimberlites and their xenoliths. Springer, Berlin.
- Dawson, J.B. (in press). The kimberlite clan: relationship to olivine- and leucite-lamproites, and inferences for upper mantle metasomatism. In: Fitton, J.G. & Upton, B.G.J., eds. Alkaline igneous rocks. Geol. Soc. London, Spec. Publ.
- Rock, N.M.S. (1986). The nature and origin of ultramafic lamprophyres: alsoites and allied rocks. J. Petrol. 27, 193-227.
- Skinner, E.M.W. & Scott, B.H. (1979). Petrography, mineralogy and geochemistry of kimerlite and associated lamprophyre dykes near Swatuggens, Western Transvaal, R.S.A. De Beers Kimberlite Symposium II, unpagged.

A REVIEW OF RADIOMETRIC DATING METHODS
APPLICABLE TO KIMBERLITES AND RELATED ROCKS

H L Allsopp¹, C B Smith², J W Bristow³, R Brown⁴, J D Kramers⁵ and O G Garvie⁶

¹ BPI Geophysics, Univ. Witwatersrand, Johannesburg, RSA, (deceased 24.3.86)

² Max Planck Institut fur Chemie, Mainz, West Germany

³ Dept. Geology, DBCM, Box 47, Kimberley, RSA

⁴ BPI Geophysics, Univ. Witwatersrand, Johannesburg, RSA

⁵ Dept. of Geology, Univ. of Zimbabwe, Harare, Zimbabwe

⁶ Geology Dept., AARL, Box 106, Crown Mines, RSA

INTRODUCTION

Because of the compositional diversity of kimberlites, no simple dating method can be applied to all occurrences. Furthermore, the altered nature of many kimberlites, at least as far as surface exposures are concerned, diminishes the usefulness of some methods. Dating of diatreme facies (as opposed to hypabyssal facies) kimberlites may also present difficulties because of the presence of contaminants of crustal derivation that may not be isotopically reset during eruptive events.

Rb-Sr METHODS

Phlogopite mica is present in many kimberlites and notably in Group II types. In general two distinct types of mica are present, viz. fine grained groundmass phlogopite and coarser grained phenocrysts and/or xenocrysts. The latter two mica types (here considered together as macrocrysts) are easier to date by virtue of their larger size and higher Rb-Sr ratios. Mineral separation and cleaning is considerably less difficult compared to groundmass mica, and the macrocrysts tend to contain much lower common Sr and consequently more radiogenic Sr. Commonly, a model age from one analysis of macrocrystic mica is sufficient to constrain the emplacement age.

Refinement of the Rb-Sr dating technique in the Bernard Price Institute Isotope Laboratory has led to successful dating of many previously undated kimberlites and related rocks. This has been achieved in part by the development of a mild acid-leaching procedure which significantly reduces the common Sr component originating from carbonates that commonly invade and adhere to mica platelets. Detailed leaching tests on a full range of fresh to altered mica from one locality have shown that the leaching does not remove significant amounts of Rb or radiogenic Sr (Fig. 1) even in the case of moderately altered micas. However isochron representation of Rb-Sr mica data may represent mixing lines (between hypothetically pure mica and carbonate - Allsopp and Barrett, 1975). Consequently the analysis of low-Rb components such as fresh whole rock or primary minerals such as clinopyroxene is advantageous (Smith et al., 1985). The dating of 1 mg samples, with ages as young as 20 m.y., is feasible by the Rb-Sr method. A problem with some kimberlites, that is not alleviated by leaching, is the presence of minor amounts of crustal biotite. At New Elands, biotite is present in the kimberlite and has not been isotopically reset, resulting in anomalously old ages if not completely removed from analysed samples (Smith et al., 1985).

K-Ar METHODS

K-Ar dating of kimberlite whole rocks and micas is also quite feasible, though Ar loss may be a serious problem, especially with altered samples (Fitch and Miller, 1983). The $^{40}\text{Ar}/^{39}\text{Ar}$ (Smith et al., 1985; Allsopp and Roddick, 1984) provides a method of monitoring Ar-loss. Laser heating Ar-Ar techniques may also have important implications for mica dating, particularly in respect of small sample sizes (see Sutter and Hartung, 1984). Anomalously old mica xenocrysts may present problems to both K-Ar and Rb-Sr dating, though are considered important insofar as mantle studies are concerned.

Zircon is rare or absent in most kimberlites, but where present is useful material for dating by the conventional U-Pb method. (Davis, 1977; Pidgeon, unpubl. data). Very low U and Pb abundances present problems to conventional U-Pb techniques. The U content of kimberlite zircons is particularly low (<10 ppm) and consequently reasonably large sample sizes, exceptionally high precision, and low blank levels are pre-requisites for the application of this method. The ^{238}U - ^{206}Pb ages have generally been regarded as the most reliable, but difficulties arise in that such ages may reflect Pb-loss; the concordia approach is thus preferred but in view of blank considerations substantial sample quantities are required. Some published ^{238}U - ^{206}Pb ages for kimberlites may be unreliable on account of the above considerations. In general U-Pb zircon ages show good agreement with age data obtained by other techniques though some results obtained by Davis may be about 5% too high.

Kimberlitic zircons have been dated by means of the ANU Ion probe, SHRIMP (Bristow, 1986; Kinny et al., this conference). The low U contents present problems to automatic peak selection but, given careful monitoring and sufficient counting times, good results may be obtained.

Perovskite is a common groundmass component of most kimberlites and related rocks. Separation of this commonly very fine grained mineral is, however, difficult. Almost pure perovskite separates can be obtained by dissolution of kimberlite in HF, followed by magnetic separation of perovskite from other insoluble heavy minerals. This procedure is not deleterious to the reliability of the results provided that the perovskite is fresh, with euhedral to rounded morphology. Perovskite characterized by anhedral, skeletal morphology (commonly with "atoll" structures) apparently do not give reliable results. Th-Pb ages on perovskites are also feasible and provide an additional check on data reliability.

FISSION TRACK METHODS

The fission track method has been applied successfully to both kimberlitic zircons (Naeser and McCallum, 1977; Haggerty et al., 1983) and apatites. Kimberlitic zircon tend to be strongly refractory and etching of tracks is much more difficult than is the case with crustal zircons. Also the low U abundance of these zircons results in fewer tracks to count and hence poorer precision. To some extent this is overcome by the large size of kimberlitic zircons which allows analyses of a greater number of samples from a single grain. In the case of apatites, ages have been obtained from both primary matrix apatite and from apatite obtained from xenoliths contained in intrusions. The ages of apatite in xenoliths are reset and though only limited data are thus far available the method appears to have wide application (see Naeser, 1971; Gleadow and Edwards, 1978). An advantage of this method is that alteration does not have particularly adverse effects, and samples from surface exposures may be used. A disadvantage is that fission tracks may be annealed, particularly in apatites, by subsequent thermal events adjacent to or affecting the kimberlite or related rock intrusions. Consequently fission track ages may not necessarily represent true emplacement ages and must be interpreted with caution.

CONCLUSION

Emplacement ages of kimberlites and related alkalic rock types may be determined by a wide variety of techniques, though in terms of routine procedures Rb-Sr mica dating is probably the most commonly used technique; zircons are a rare component of most kimberlites and separation of perovskite in sufficient amounts for U-Pb analysis is exceedingly difficult. Mild-acid leaching procedures have been shown to greatly improve the success of Rb-Sr mica dating, even on altered samples. Finally it should be emphasized that careful petrographic inspection of any mineral or specimen considered for dating is essential.

REFERENCES

Allsopp, H L and Barrett, D R (1975). Rb-Sr determinations on South African kimberlite pipes. Phys. Chem. Earth, 9, 605-617.

- Allsopp, H L and Roddick, J C (1984). Rb-Sr and ^{40}Ar - ^{39}Ar age determinations on phlogopite micas from the pre-Lebombo Group Dokolwayo kimberlite pipe. Spec. Publ. geol. Soc. S. Afr., 13, 267-271.
- Bristow, J W (1986). Updating dating down under. Nuclear Active, 34, 12-15.
- Davis, G L (1977). The ages and uranium content of zircons from kimberlites and associated rocks. Carnegie Inst. Washington Yearbook, 76, 631-635.
- Fitch, F J and Miller, J A (1983). K-Ar age of the east peripheral kimberlite at De Beers Mine, Kimberley, RSA. Geol. Mag., 120, 505-512.
- Gleadow, A J W and Edwards, A C (1978). Fission track age of a basic inclusion from the Kayrunnera kimberlitic breccia pipe. J. geol. Soc. Australia, 25, p. 359.
- Haggerty, S E, Raber, E and Naeser, C W (1983). Fission track dating of kimberlitic zircons. Earth Planet. Sci. Lett., 63, 41-50.
- Naeser, C W (1971). Geochronology of the Navajo-Hopi diatremes, Four Corners Area. J. Geophys. Res., 76, 4978-4985.
- Naeser, C W and McCallum, M E (1977). Fission track dating of kimberlitic zircons. Abstr. Sec. Int. Kimb. Conf., Sante Fe, New Mexico.
- Smith, C B, Allsopp, H L, Kramers, J D, Hutchinson, G and Roddick, J C (1985). Emplacement ages of Jurassic-Cretaceous South African kimberlites by the Rb-Sr method on phlogopite and whole-rock samples. Trans. geol. Soc. S. Afr., 88 (2), in press.
- Sutter, J F and Hartung, J B (1984). Laser microprobe ^{40}Ar / ^{39}Ar dating of mineral grains in-situ. Scanning Electron Microscopy, IV, 1525-1529.

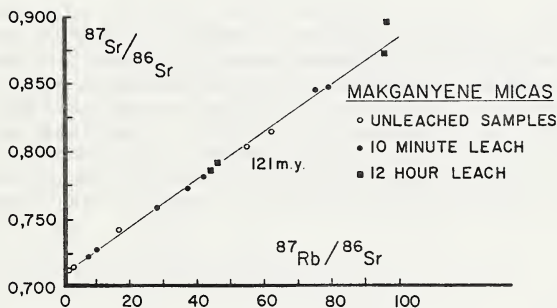


FIGURE 1

J W Bristow¹, C B Smith², H L Allsopp³, S R Shee⁴ and E M W Skinner¹

¹ Geology Dept., DBCM Ltd., Box 47, Kimberley 8300, RSA.

² Max Planck Instit. fur Chemie, Mainz, W. Germany.

³ B.P.I. Geophysics, Univ. of the Witwatersrand, Johannesburg 2000, RSA.

⁴ Geology Dept., AARL, Box 106, Crown Mines 2025, RSA.

INTRODUCTION

Recent radiometric dating of kimberlites and related alkaline intrusions (in particular Elston, Zero, Bathlaros, and Riries) from the Kuruman district of the northern Cape, South Africa (Fig. 1), has shown that these intrusions are approximately 1600 m.y. old and thus represent the oldest known kimberlites yet documented. Though known of for many years the Proterozoic age of these alkalic rocks was previously not suspected. Drilling and trenching of these localities has exposed material suitable for a wide range of petrographic, mineralogical, geochemical and isotopic studies. In addition the Zero kimberlite was found to contain an excellent suite of mantle xenoliths including peridotites, eclogites and metasomatized rocks (see Shee et al., this conference). The geological setting, geochronology, and major and trace element and isotope chemistry are reported in this paper.

GEOLOGICAL SETTING

The Kuruman intrusives include kimberlites (*sensu stricto*), marginal kimberlites, and alkalic rocks distinct from kimberlites and referred to as lamprophyres (see Shee et al., this conference). They are present in the form of small eroded pipes and dykes and are located near the inferred western edge of the Kaapvaal craton (>2500 m.y.) adjacent to the younger Kheis Belt (~1800 m.y.) of the northern Cape Province. The pipes and dykes intrude early Proterozoic Ghaap Plateau dolomites and overlying Asbestos Hills Banded Ironstones of the Griqualand West Sequence. Outcrops of these intrusives are typically weathered and the rocks tend to be extensively carbonatized. Xenoliths of dolomite are common along with other crustal inclusions. Zero contains abundant mantle inclusions.

GEOCHRONOLOGY

The majority of the Kuruman kimberlites contain phlogopite mica, which may be present as both a macrocryst and groundmass phase. In view of this, phlogopite was separated from a number of the intrusives for Rb-Sr dating purposes. Ages have been obtained for four intrusions represented by three kimberlites (Bathlaros, Zero and Elston) and a phlogopite rich lamprophyre (Riries). The results are presented in Table 1 and indicate an overall age slightly higher than 1600 m.y. A possible age progression may be present from west (Elston) to east (Riries) though this is by no means unequivocal, particularly as some of the data are only model ages.

TABLE 1

Locality	Age	Comments
Elston kimberlite	~ 1674	Rb-Sr mica model age
Bathlaros kimberlite	~ 1649	Rb-Sr mica isochron
Zero kimberlite	~ 1635	Rb-Sr mica model age
Riries lamprophyre	~ 1606	Rb-Sr mica model age

WHOLE ROCK CHEMISTRY

Eight of the freshest kimberlite samples obtained from a borehole drilled into the Bathlaros kimberlite have been analysed for major and trace elements. Abbreviated averages of these analyses are presented in Table 2; average analyses of Group I and II kimberlites, and lamproites are included for comparison (Shee, 1986). Inspection of Table 2 shows that the average Bathlaros kimberlite is broadly similar to the average Group I kimberlite. Some exceptions are present, notably in TiO_2 , Fe_2O_3 , CaO, Sr, Nb and Ba. Nb and Ba are particularly enriched in Bathlaros, relative to Group I and II kimberlites and lamproites. Differences in TiO_2 , Fe_2O_3 and CaO may be due to fractionation effects. Reasons for the extreme enrichment in Nb and Ba are presently not clear. However the possibility of contamination with dolomite xenoliths and carbonatization of the intrusives affecting some major and trace element abundances cannot be excluded. Also a point that should be noted is that average Ba data presented for Group I kimberlites is probably not a true reflection of the actual value. The reported value is probably too high due to bias introduced by the presence of altered samples in the data set.

TABLE 2

	SiO ₂	TiO ₂	Al ₂ O ₃	Fe ₂ O ₃	MgO	CaO	Na ₂ O	K ₂ O	Rb	Sr	Y	Sr	Nb	Ba
K	31.9	2.6	2.5	10.4	30.0	6.9	0.3	1.4	73	771	14	323	389	2926
GI	30.3	1.9	2.9	8.6	29.6	10.1	0.4	1.3	77	1186	16	318	171	1399
GII	36.1	1.0	3.2	8.2	27.3	6.6	0.2	3.1	141	1023	16	286	98	1392
LAMP	50.0	5.2	6.9	7.5	11.2	3.5	0.5	8.2	399	1150	16	1100	157	10865

Key :- K = Bathlaros kimberlite, Kuruman Province; GI = Group I kimberlite;
GII = Group II kimberlite; Lamp = lamproite.

ISOTOPE CHEMISTRY

Presently available isotopic data suggest that the Kuruman kimberlites have initial-Sr and initial-Nd ratios which were enriched relative to Bulk Earth at 1600 m.y. As such, and in spite of significant age differences, the Kuruman kimberlites appear to show similarities to the Jurassic-Cretaceous Group II kimberlites of southern Africa which have been equated (isotopically) with derivation from an enriched lithosphere (Smith, 1983). On this basis, southern African kimberlites emplaced at 1600 m.y. and the Jurassic-Cretaceous appear to represent magmas tapped from a source characterized by an enrichment in Sm/Nd and Rb/Sr. Data for the Kuruman kimberlites are in contrast to data for the Premier (~ 1200 m.y.), Zimbabwe (~ 500 m.y.) and younger Group I kimberlites which have isotopic ratios compatible with derivation from an asthenospheric-type source (Smith, 1983). The isotopic data obtained from Kuruman do, however, to some extent contradict petrographic and geochemical data which suggest that these rocks are close to Group I kimberlites. Additional isotopic analyses presently in progress should resolve this and it is possible that the alteration (carbonatization) referred to above is effectively masking many of the original primary petrographic characteristics of these rocks.

CONCLUSION

Kimberlites and related rocks from the Kuruman Province of South Africa have been dated at 1600 m.y. and presently represent the oldest documented kimberlite province. The location of these intrusions near the inferred margin of the Kaapvaal craton is considered significant in that previously the oldest known kimberlites (Premier Group) had been documented near the craton centre. The recognition of 1600 m.y. old kimberlites in southern Africa means that four major periods, viz. 1600 m.y. (Kuruman), 1200 m.y. (Premier), 500 m.y. (Zimbabwe) and 240-80 m.y. (Southern Africa), of kimberlitic and related alkalic magmatism have been recognized on the subcontinent (see Allsopp *et al.*, 1985; Smith *et al.*, 1985).

Ongoing studies of the Kuruman intrusives and their associated mantle xenoliths will provide important information on regional geological events, and mantle processes and compositions at, and prior to 1600 m.y.

REFERENCES

Allsopp, H L, Bristow, J W and Skinner, E M W (1985). The Rb-Sr geochronology of the Colossus kimberlite, Zimbabwe. *Trans. geol. Soc. S. Afr.*, 88 (2), in press.

Shee, S R (1986). The petrogenesis of the Wesselton Mine kimberlites, Kimberley, South Africa. Ph.D. thesis (unpubl.), Univ. of Cape Town.

Shee, S R, Bristow, J W, Shee P B S and Bell, D R (1986). The petrology of kimberlites, related rocks and associated mantle xenoliths from the Kuruman Province, South Africa. *Proceed. 4th Kimb. Conf.*, Perth, Australia. Abstract.

Smith, C B (1983). Pb, Sr and Nd isotopic evidence for sources of southern African Cretaceous kimberlites. *Nature*, 304, 51-54.

Smith, C B, Allsopp, H L, Kramers, J D, Hutchinson, G and Roddick, J C, (1985). Emplacement ages of southern African Jurassic - Cretaceous kimberlites by the Rb-Sr method on phlogopite and whole rock samples. *Trans. geol. S. Afr.*, 88(2), in press.

Acknowledgement : K Fraser is thanked for providing some isotopic data for Bathlaros.



FIGURE 1

GEOLOGICAL SETTING, PETROGRAPHY AND PETROGENESIS OF OLIVINE MELILITITES
ON THE NATAL COAST, SOUTH AFRICA

E.A. Colgan¹ and H.L. Allsopp²

1. Geology Department, De Beers Consolidated Mines Ltd., P.O. Box 47, Kimberley, R.S.A.
2. BPI Geophysics, University of the Witwatersrand, Johannesburg, R.S.A. (Deceased 24/03/1986).

INTRODUCTION

Six olivine melilitite intrusions are present in Northern Natal. They occur to the northeast of Eshowe which is approximately 100 km north of Durban (Fig. 1). The closest known alkaline intrusives to these occurrences occur to the north and southwest and are represented by the Dokolwayo kimberlite, nephelinite lavas that occur at the base of the Lebombo basalts and the Griqualand East kimberlite province.

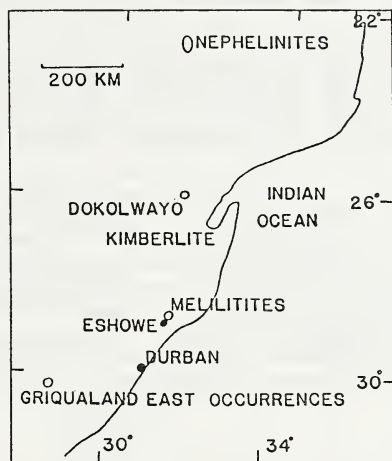


FIG. 1

GEOLOGICAL SETTING

The Eshowe melilitites occur at the junction of the Archaean Kaapvaal craton and the Upper Proterozoic Natal Mobile Belt. Two melilitites intrude the craton and four intrude a zone of mobile belt metamorphic sequences overthrust on to the craton (Mathews, 1981). The region has been affected by extensional tectonics recurring along the same zone of approximately north-south oriented weakness. This tectonism is believed to have been initiated in the Palaeozoic with the formation of the Pan African Mozambique Belt and culminated in the Cretaceous with Gondwana fragmentation. The Eshowe melilitites intrude an area of tilted and step-faulted horst and graben structures that developed in response to two different styles of Gondwana fragmentation: east-west extension and northeast-southwest transpression. The structural development of the region is associated with the extensional and transpressional forces interacting with pre-existing crustal structures found within the Kaapvaal craton, the Natal Mobile Belt and the Mozambique Belt.

GEOLOGY AND PETROGRAPHY

The intrusions consist of four dykes; Tembani Ranch, Emtilombo, Ndundulu and Umgoya and two pipes; Cowards Bush and Nqoleni. The dykes, in general, occur on uplifted horsts while the pipes occur in a graben structure. The level of preservation of the occurrences probably reflects differential rates of erosion. Surface exposures of the melilitites are rare and where present are extremely weathered.

The dykes vary from 30 cm up to 2 m in width and they trend in two directions: Ndundulu strikes approximately 80° while the remaining three trend approximately 120°. These strike directions may reflect some structural control by the underlying basement. Both pipes are small. Cowards Bush is 1.2 ha in area and is irregular elliptical in outline while Nqoleni is 0.5 ha in area and is circular.

Cowards Bush and Nqoleni consist of single intrusions that are, in general, texturally consistent. Both pipes comprise xenolith-rich, fluidised tuffisitic melilitite breccia that is texturally similar to diatrema-facies, tuffisitic kimberlite breccia. The most conspicuous features of the rock type are the abundance of country rock xenoliths, the fragmental, disrupted nature, and the close packing of the larger constituents. Minor differences in mineralogy and texture between the two occurrences are evident.

Little is known about the petrography of Ndundulu and Umgoya dykes, as they are extremely weathered. Tembani Ranch dyke, a narrow anastomosing intrusion, is a fine-grained porphyritic hypabyssal rock. This consists of altered olivine, melilitite and minor phlogopite phenocrysts and rare clinopyroxene macrocrysts set in a finer-grained groundmass of altered melilitite laths and accessory phlogopite, clinopyroxene, apatite, perovskite and opaque spinels. The groundmass minerals have a uniform distribution, although, small irregular 'pools' of isotropic serpentine (?) are locally present.

The Emtilombo dyke (Fig. 2) is mineralogically similar, but texturally more complex than the Tembani Ranch dyke. Five textural varieties are present: one variety is a fluidised, hypabyssal-facies, globular segregationary melilitite breccia and four are textural and mineralogical variants of a macrocrystic hypabyssal melilitite.

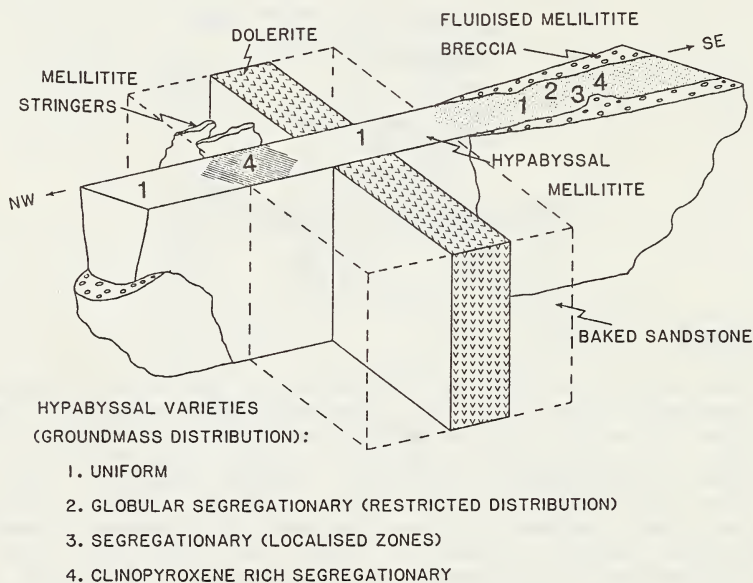


FIG. 2 EMTILOMBO DYKE

The textures and to some extent the mineralogy, reflect the emplacement history of the dyke. The nature of the sandstone country rock appears to have influenced the mode of intrusion. It is envisaged that a single magmatic pulse was associated with simultaneous fluidisation of magma at the dyke contacts. It seems probable the driving mechanism for the fluidisation was the incorporation of additional volatiles, in the form of water, from the country rock. This, in association with volatiles present in the magma led to a fluidised, subsurface intrusion. The country rock in the vicinity of

the dolerite dyke (?) is baked. This would have driven out much of the original contained water prior to the intrusion of the melilitite and no fluidised melilitite breccia is present in this area.

CHEMISTRY

Bulk chemistry, matrix mineral and concentrate mineral compositions of the Eshowe occurrences are broadly similar to olivine melilitites of Namaqualand, R.S.A. (Moore 1979) and to the Norseman dykes, Australia (Robey et. al., 1986). Subtle differences are, however, apparent. Bulk analyses of the Eshowe rocks, for example, suggest a more magnesian parent magma and olivine tends to have higher Fo contents, with most of the grains ranging from Fo₈₃ to Fo₈₅. These and other variations can probably be related to different regional settings and source area characteristics. Chemical compositions and trends of the various minerals (xenocrysts, macrocrysts, phenocrysts and groundmass), such as the complex chemical zonation found in some olivine phenocrysts, have important implications for the evolutionary trend of the parental magma to the Eshowe melilitites, during its ascent to surface.

DISCUSSION

Rb-Sr phlogopite age measurements show that the Eshowe melilitites were emplaced approximately 80 m.y. ago. In regional terms, intrusion of the melilitites followed major basaltic volcanism and rift tectonics. Consideration of the timing and nature of alkaline magmatism along the South African east coast suggests a close relationship between the tectonic development and associated mantle processes operating in the region. Broadly speaking there is a cycle of (i) limited alkaline magmatism (ii) voluminous basalt and felsic magmatism (iii) transitional alkaline basalt magmatism and finally (iv) minor alkaline magmatism (Eshowe olivine melilitites) in the region (Bristow pers. comm.). This cycle reflects early (\pm 200 m.y.) sodic and potassic magmatism (the Lebombo nephelinites and Dokolwayo kimberlite) and a final phase (\pm 80 m) of sodic magmatism (the Eshowe melilitites). Chemical and isotopic data suggest that the cycle was initiated by mantle metasomatism and subsequently controlled by the interaction of a varying thermal regime and extensional tectonics leading to continental rifting. These processes resulted in progressive attenuation of the crust in the cratonic and overthrust cratonic region into which the Eshowe melilitites were subsequently emplaced. This attenuation is considered to have an important bearing on the formation of melilitites rather than other types of alkalic rocks in the region.

CONCLUSION

The Eshowe melilitites provide evidence of alkaline ultrabasic magmatism associated with crustal attenuation, rifting and finally continental fragmentation. Overall it is suggested that these rocks represent part of a major magmatic cycle; this magmatism probably developed in response to metasomatic mantle enrichment (see Bristow et. al., 1984) and was a key factor in the fragmentation of eastern Gondwanaland.

REFERENCES

- BRISTOW J.W., ALLSOPP H.L., ERLANK A.J., MARSH J.S. and ARMSTRONG R.A. 1984. Strontium Isotope Characterization of Karoo Volcanic Rocks. In *Petrogenesis of the Volcanic Rocks of the Karoo Province*. Spec. Publ. No. 13 Geol. Soc. S. Afr. pp 295-329.
- MATHEWS P.E. 1981. Eastern or Natal sector of the Namaqua-Natal mobile belt in southern Africa. In *Precambrian of the Southern Hemisphere*. pp 705-715. Ed. Hunter. Publ. Elsevier, Amsterdam.
- MOORE A.E. 1979. The Geochemistry of the Olivine Melilitites and Related Rocks of Namaqualand-Bushmanland, South Africa. Ph.D. thesis (Unpubl.) Univ. Cape Town, 383 pp.
- ROBEY J.v.A., BRISTOW J.W., MARX M.R., JOYCE J.J., DANCHIN R.V. and ARNOT F. 1986. Alkalic ultrabasic dykes of the south-east Yilgarn margin, west Australia. This Conference.

H. Helmstaedt and D.J. Schulze

Dept. of Geological Sciences, Queen's University, Kingston, Canada, K7L 3N6

Although studies of kimberlites and their mantle-derived inclusions still convey contradictory geotectonic messages (the models of diamond genesis by Haggerty (1986) and Schulze (1986) are two recent examples), geotectonic information derived from such studies should ultimately fit into compatible upper mantle models that can be integrated with those from other Earth science disciplines. Tectonic aspects of kimberlites and related rocks involve their local and regional structural settings, their larger-scale geotectonic controls, the physical processes controlling kimberlite formation in the upper mantle, and the ascent through the lithosphere. Inclusion studies (involving xenoliths, megacrysts, and diamonds thought to have equilibrated under upper mantle conditions) yield information about the composition, physical conditions of formation, textures, and structures of small isolated samples that are combined to obtain a picture of the composition, physical conditions, structure, and origin of the lithospheric column traversed by the kimberlite. Viewed in this context, geotectonic bits of information from kimberlite and inclusion studies can be divided into those contributing to the understanding of processes of upper mantle formation and those monitoring later modifications of the mantle. As the mantle evolves continuously, such categories naturally are end members of a continuous spectrum of processes. However, the division makes sense for diamondiferous kimberlite provinces on Precambrian shields, where the subcontinental lithosphere, from which most of the mantle sample was derived, was assembled in Early Precambrian times, whereas the kimberlite eruptions and other intraplate magmatism were triggered by distinctly later events.

For the southern African craton, where Archean isotopic signatures have survived in xenoliths as well as in diamond inclusions (e.g. Kramers, 1979; Richardson et al., 1984; Richardson et al., 1985), the origin of the lithospheric section traversed by the kimberlites becomes a problem of Archean tectonics. If integrated with current models based largely on rocks from Archean granite-greenstone and granulite-gneiss terrains, xenolith studies will lead to a much improved understanding of Archean tectonic processes.

Opinion amongst students of Archean rocks has long been divided as to whether the evolution of the Archean lithosphere can be explained in terms of plate tectonic processes (e.g. Kroner, 1981). Two of the major arguments against Archean plate interactions have been the apparent absence from the Archean rock record of ophiolites and eclogites (e.g. McCall, 1981), the presence of which in Phanerozoic orogenic belts is commonly accepted as evidence for sea-floor spreading and subduction, respectively. Many workers, however, have accepted that the mafic volcanic sequences of greenstone belts originate in proto-oceanic (e.g. Windley, 1976) or marginal basin settings (e.g. Tarney et al., 1976), and evidence for the occurrence of complete or partial ophiolite assemblages in Archean greenstone belts from South Africa, Wyoming, and northwestern Canada was presented by de Wit and Stern (1980), Harper (1986), and Helmstaedt et al. (1986). Whereas this supports Archean sea-floor spreading, arguments for Archean subduction have been of a more theoretical nature (e.g. Nisbet and Fowler, 1983), as surface occurrences of eclogites of undisputed Archean age have not been reported. Workers on mantle nodules from kimberlites, however, have found that the origin of a number of xenolith and xenocryst types can be explained by subduction of oceanic lithosphere. These include certain eclogites and grosopydites which may have been derived from subducted metabasites and rodingites (e.g. Helmstaedt and Carmichael, 1978; Walker, 1979; Ater et al., 1984; MacGregor, 1985), alkremites, derived from Al-rich sediments (Exley et al., 1983) or black wall-chlorite alteration around metaserpentinites (this paper), grossular inclusions in diamonds (Sobolev et al., 1984), peraluminous garnet-kyanite rocks, derived from pelitic sediments (Helmstaedt and Hall, 1985), diamondiferous low-Ca garnet harzburgites and dunites, derived from graphite-bearing metaserpentinites (Schulze, 1986), and green garnets related to wehrlites, derived from uvarovite-bearing serpentinites (Schulze, this volume). Such nodules, if indeed of Archean age, represent part of the complimentary mantle sample of rocks exposed in Archean shields and constitute direct evidence for subduction in the Archean rock record.

Although it is still a matter of debate whether the higher heat loss from the Archean Earth required "faster spreading" or "more ridge" (Hargraves, 1986), it is likely that the Archean was characterized by relatively fast spreading rates and subduction of relatively young oceanic lithosphere (e.g. Abbott and Hoffman, 1984; Abbott, 1984). As such conditions would favour relatively shallow or low-angle subduction, we propose that the Archean lithosphere beneath the southern African craton was formed by lateral underplating of subducted oceanic lithosphere. In a regional plate tectonic synthesis, Light (1982) showed that the Zimbabwean and Kaapvaal cratons may have been separated by more than 1000 km of oceanic crust and that this crust was subducted beneath the Kaapvaal craton. To explain the presence of Archean subducted rocks among the mantle sample from kimberlites of the Kaapvaal craton, we envisage that this and earlier subduction zones were shallow-dipping and that the entire craton was repeatedly underplated by oceanic lithosphere.

The post-Archean evolution of the continental lithosphere involves a change from a regime of rapid spreading and predominantly shallow, low-angle subduction to more normal plate tectonics. Low-angle subduction, the dominant process during the formation of the Archean lithosphere, became an exception, restricted to episodes of rapid plate convergence and/or subduction of low-density crust. As it can be shown that such episodes have preceeded some of the major kimberlite events within and on the margins of stable cratons (Helmstaedt and Gurney, 1982), low-angle subduction is held responsible for the intraplate processes that modified the upper mantle, controlled kimberlite distribution, and eventually triggered the kimberlite eruptions. The post-Archean metasomatic overprint recognized in many upper mantle nodules and the formation of the megacryst suite may be related to these episodes.

References:

- Abbot, D.H. and Hoffman, S.E., 1984. Archean plate tectonics revisited. 1. Heat flow, spreading rate and the age of subducting lithosphere and their effects on the origin and evolution of continents. *Tectonics* 3, 429-448.
- Abbott, D.H., 1984. Archean plate tectonics revisited. 2. Paleo-sea level changes, continental area, oceanic heat loss and the area-age distribution of the ocean basins. *Tectonics* 3, 709-722.
- Ater, P.C., Eggler, D.H., and McCallum, M.E. 1984. Petrology and geochemistry of mantle xenoliths from Colorado-Wyoming kimberlites: Recycled ocean crust? In Kornprobst, J., ed., *Kimberlites, II: The Mantle and Crust-Mantle Relationships*, Elsevier, Amsterdam, pp. 309-318.
- DeWit, M.J. and Stern, C.R., 1980. A 3500 My ophiolite complex from the Barberton greenstone belt, S.A. Extended abstracts 2nd International Archean Symposium, Perth. Geological Society of Australia, pp. 85-86.
- Exley, R.A., Smith, J.V., and Dawson, J.B., 1983. Alkremite, garnetite and eclogite xenoliths from Bellsbank and Jagersfontein, South Africa. *American Mineralogist* 68, 512-516.
- Haggerty, S.E., 1986. Diamond genesis in a multiply-constrained model. *Nature* 320, 34-38.
- Hargraves, R.B., 1986. Faster spreading or more ridge in the Archean? *Geology*, in press.
- Harper, G.D., 1986. Dismembered Archean ophiolite, Wind River Mountains, Wyoming (USA). *Ophioliti*, in press.
- Helmstaedt, H. and Carmichael, D.M., 1978. Are grosspydites metarodingites? Implications for upper mantle models based on xenoliths from some diamondiferous kimberlites. XI Meeting Intern. Mineralogical Association., Novosibirsk, Abstracts and Programs.

- Helmstaedt, H. and Gurney, J.J. 1984. Kimberlites of southern Africa - are they related to subduction processes? In Kornprobst, J., ed., Kimberlites, : I Kimberlites and Related Rocks, Elsevier, Amsterdam, pp. 425-434.
- Helmstaedt, H. and Hall, D.C. 1985. Subducted refractory carbon as source material for diamond formation in the upper mantle - evidence from peraluminous xenoliths in kimberlites. All-Union Conference "Native elements formation in the endogenic processes", Yakutsk, USSR, Abstracts vol. IV, 19-20.
- Helmstaedt, H., Padgham, W.A., and Brophy, J.A., 1986. Multiple dikes in the Lower Kam Group, Yellowknife greenstone belt: Evidence for Archean sea-floor spreading. *Geology*, in press.
- Kramers, J.D. 1979. Lead, uranium, strontium, potassium and rubidium in inclusion-bearing diamonds and mantle-derived xenoliths from southern Africa. *Earth and Planetary Science Letters* 42, 58-70.
- Kroner, A. 1981. Ed., *Precambrian Plate Tectonics*, Elsevier, Amsterdam, 781 pp.
- Light, M.P.R., 1982. The Limpopo mobile belt: A result of continental collision. *Tectonics* 1, 325-342.
- MacGregor, I.D. 1985. The Roberts Victor eclogites: Ancient oceanic crust? *Geological Society of America, Abstracts with Programs* 17, p. 650.
- McCall, G.J.H., 1981. Progress in research into the early history of the Earth: A review, 1970-1980. *Geological Society of Australia Special Publication* 7, 3-18.
- Nisbet, E.G. and Fowler, C.M.R., 1983. Model for Archean plate tectonics. *Geology* 11, 376-379.
- Richardson, S.H., Gurney, J.J., Erlank, A.J. and Harris, J.W. 1984. Origin of diamonds in old enriched mantle. *Nature* 310, 198-202.
- Richardson, S.H., Erlank, A.J. and Hart, S.R. 1985. Kimberlite-borne garnet peridotite xenoliths from old enriched subcontinental lithosphere. *Earth and Planetary Science Letters* 75, 116-128.
- Schulze, D.J., 1986. Calcium anomalies in the mantle and a subducted metaserpentinite origin for diamonds. *Nature* 319, 483-485.
- Schulze, D.J., 1986. Green garnets and wehrlites from Kimberley, South Africa. Extended abstract, this volume.
- Sobolev, N.V., Yefimova, E.S., Lavrent'yev, Yu.G. and Sobolev, V.S. 1984. Dominant calcsilicate association of crystalline inclusions in placer diamonds from southeastern Australia. *Doklady Akademii Nauk SSSR* 274, 397-401.
- Tarney, J., Dalziel, I.W.D., and de Wit, M.J., 1976. Marginal basin 'Rocas Verdes' complex from S. Chile: A model for Archean greenstone belt formation. In Windley, B.F., ed., *The Early History of the Earth*, pp. 131-146. John Wiley, London.
- Walker, D.A., 1979. Textural and compositional studies of eclogites from the Roberts Victor kimberlite, South Africa. M.Sc. thesis, Oxford University, unpublished.
- Windley, B.F., 1976. New tectonic models for the evolution of Archean continents and oceans. In Windley, B.F., ed., *The Early History of the Earth*, pp. 105-111. John Wiley, London.

Hu Siyi¹, Zhang Peiyuan², Wan Guodong³

¹Sino-British Cooperation Brigade, ²Ministry of Geology and Mineral Resources, Beijing, ³Shandong Bureau of Geology and Mineral Resources

Extended Abstract

A. INTRODUCTION.

The kimberlites of Mengyin in Shandong Province, of Hebi in Henan Province and of Fuxian in Liaoning Province are only three of a number of kimberlite provinces that are known in China. These three groups of kimberlites have been studied intensively in the last decade and they are considerably better documented than are most other groups in China. Many small kimberlite dykes also occur in Zhenyuan in Guizhou Province and there are some intrusions in the Yanbei area of Shanxi Province and in the Jingshan area of Hubei Province that may be either kimberlites or related rocks. In the Yuanshui river in Hunan Province diamonds and pyropes have been found in alluvials, (these are also known as the Changde diamond deposits), and in the Bachu area of the Xinjiang Uighur Autonomous Region. To date no kimberlites have been found in either of these areas, (see Fig.).

The three kimberlites provinces reviewed occur on the Sino-Korean craton which is of Archaean age. The Yangzi and Tarim cratons, on which the Guizhou kimberlites and the Bachu mineral anomalies occur respectively, were formed in the Proterozoic. The Sino-Korean craton is mostly covered by Palaeozoic and younger sediments, some of which contain diamonds. This, and the possible early Palaeozoic age of some of the kimberlites described in this paper, present interesting problems to the diamond geologist.

B. MENGYIN KIMBERLITES.

The Mengyin kimberlites are located in Mengyin County of Shandong Province. They comprise 47 groups of dykes and 11 small pipes, the first of which were found in 1965 by a heavy mineral survey. An open pit mine has been developed around two small pipes, referred to as Shengli 1, and it is possible that one or more of the other pipes will be mined in the future. The dykes trend between 15° and 35° and in most cases dip steeply to the west. Their strike parallels the major Tanlu fault zone, (see Fig.), that separates the Archaean basement of western Shandong from the Proterozoic rocks in the eastern part of the province. Individual dykes have a strike length of up to several hundred metres, the maximum being 1.4kms, and an average thickness of 20 to 40cms although the maximum width is 3m. The Mengyin kimberlites can be divided geographically into three fields which are called, from SW to NE, Changmazhuang, Xiyu and Peli. The three kimberlite fields are arranged in sinistral en echelon pattern. The Changmazhuang and Xiyu fields have small clusters of pipes at their centers. The pipes are irregular in outline with strong structural control in the NNE and NW joint directions of the Archaean gneiss country rock. The largest pipe, Hongqi 6 in the Xiyu field, measures 220m by 90m and has a surface area of 1.98 ha. The pipes decrease in size with depth and their roots have been shown by extensive drilling to be dykes, which also trend in a NNE direction. It is estimated that there has been between 1km and 1.5kms of erosion since kimberlite emplacement.

Age determination using the K-Ar method on whole rock kimberlite samples and on phlogopites give two groups of ages. Whole rock determinations suggest a late Mesozoic age of 77 to 88 m.y., while the phlogopites give a possible range of 234 to 554 m.y.

C. HEBI KIMBERLITES.

The Hebi kimberlites lie to the west of Hebi City in Henan Province, (see Fig). They were found in 1971 by a combination of detailed geological mapping and indicator mineral prospecting. There are 79 bodies in this kimberlite province. Most of them are dykes, some are sills but no pipes have been found to date. The kimberlites occur in a belt

that trends between 5° and 15° and measures 20kms by 6.5kms. This belt is 25kms to the west of, and parallel to a major NNE striking fault zone, the Taihang Mountain fracture. The dykes are several tens of metres long and 10 to 15cms wide. The longest individual dyke has a strike length of 800m. Both the dykes and the sills are intruded into marls, dolomites and limestones of Cambrian and Ordovician ages. The sills occur in a marl at the boundary between Lower Ordovician dolomite and Middle Ordovician limestone. The age of these bodies has not been established radiometrically but they contain abundant igneous xenoliths, which are thought to be of late Mesozoic and early Cenozoic age, suggesting kimberlite emplacement in the early Cenozoic.

D. FUXIAN KIMBERLITES.

The Fuxian kimberlites occur mainly in the Toudaogou area of Fuxian county, Liaoning Province, (see Fig.), and were found in the early 1970's by both ground magnetic surveys and heavy mineral sampling. Most kimberlites are pipe-like in outline and there is one dyke that joins two of the smaller pipes. The individual bodies trend at 70° to 80°. Most of the kimberlites occur in a downwarp at a fault intersection and are located on the eastern side of the Tanlu fault zone, where the country rock is Proterozoic sandstones overlain by Paleozoic sediment. The pipes have irregular outlines and often have faulted contacts. Pipe 50 is one of the largest pipes in the province and has a length of 275m in an E-W direction and a maximum width of 60m. The area at surface is 0.64 ha. and at 80m depth is nearly 1.00 ha. Pipe 50 contains some good quality diamonds and there is a placer deposit in a stream that drains the pipe, in which the quality of the stones is even better. The Fuxian kimberlites have been dated radiometrically using the K-Ar method on whole rock kimberlite and phlogopites. The latter datings give an age of 350 to 450m.y.

E. PETROLOGY AND MINERALOGY.

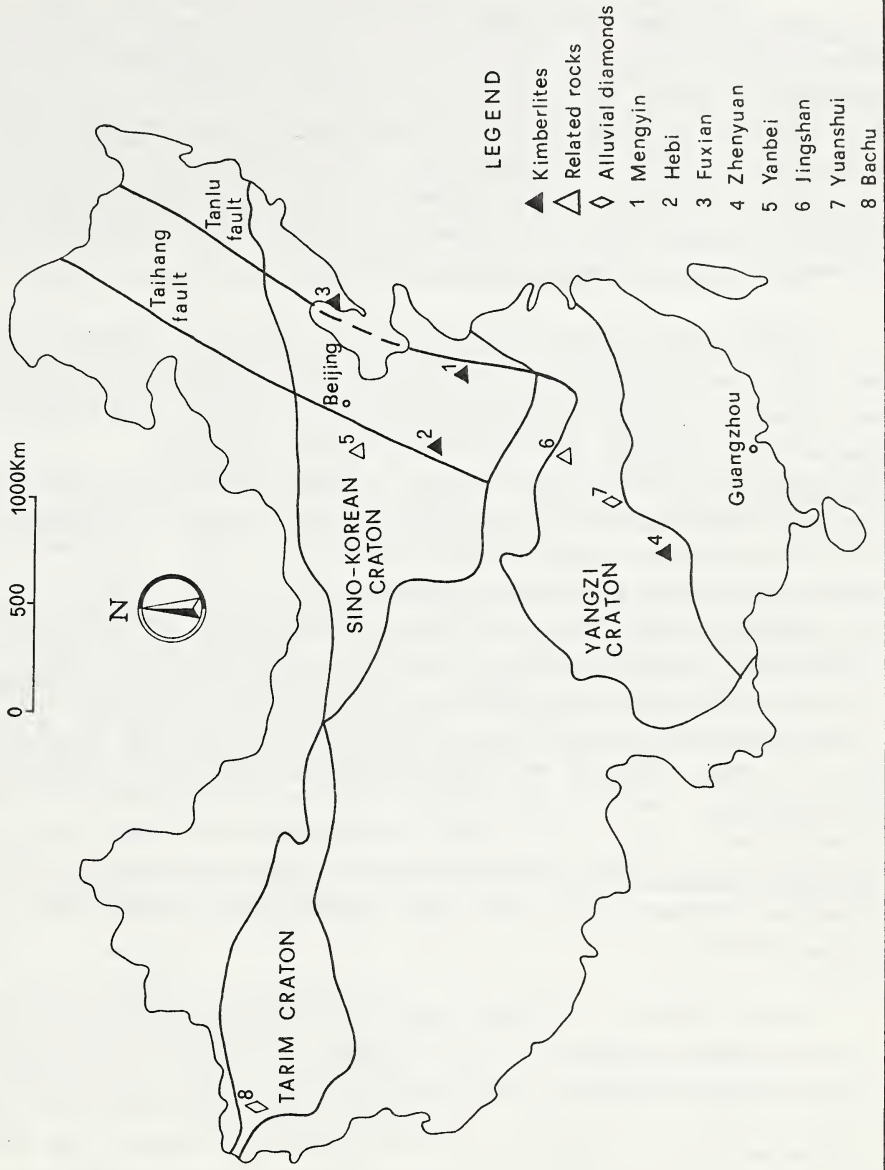
Most of the kimberlites described in this paper are magmatic varieties which are, in other parts of the world, usually associated with the root zones of kimberlite pipes. Macrocystic kimberlite and kimberlite breccia are the most frequently found rock types although a few examples of tuffisitic kimberlite have been found, such as the Hongqi 23 body in the Mengyin province. It is possible therefore, that some of the intrusions have been eroded to the level of the diatreme-root zone transition.

Mantle and lower crustal xenoliths have been found in some of the kimberlites and differences between the nodule suites from various locations have been noted. In the Mengyin kimberlites there are peridotites, dunites, eclogites and pyrope nodules, while in the Hebi kimberlites there are peridotites and pyrope nodules. The Fuxian kimberlites contain xenoliths of peridotite, dunite, an olivine-augite rock and nodules of phlogopite glimmerite.

Mineralogically, the Mengyin, Hebi and Fuxian kimberlites are ilmenite-poor when compared with many kimberlites in other parts of the world and ilmenite is only rarely found at Mengyin and Fuxian and has never been recovered from the Hebi kimberlites. Pyrope and chromite are the most common heavy minerals found. The chromite content of some Chinese kimberlites can be very high, often exceeding the pyrope content, another feature that is unusual in kimberlites from elsewhere.

With the exception of those in Hebi province, all the other kimberlites discussed are diamond bearing to some extent. Some of the Mengyin and Fuxian kimberlites are economically diamondiferous.

THE DISTRIBUTION OF SOME KIMBERLITES IN CHINA



LEGEND

- ▲ Kimberlites
- △ Related rocks
- ◇ Alluvial diamonds
- 1 Mengyin
- 2 Hebi
- 3 Fuxian
- 4 Zhenyuan
- 5 Yanbei
- 6 Jingshan
- 7 Yuanshui
- 8 Bachu

Masahiro Ito

Laboratory of Geology, College of General Education, Nagoya University, Japan

Three western Kenya kimberlites, Y1B1, Y1B3 and YA17, were found in the Nyanzian greenstone belt to the north of Winam Gulf by exploration-drillings. The localities are as follows; Y1B1 Hole, 34°11.2'E, 0°4.7'S, Y1B3 Hole, 34°14.0'E, 0°3.1'S and YA17 Hole, 34°30.9'E, 0°9.5'N. Though the western Kenya kimberlites were intruded into the Archean rocks of $(2.71 \pm 0.34) \times 10^3$ Ma (Yanagi et al., 1981), their exact age of intrusions can not be defined. However, owing to alignment of these western Kenya kimberlite-localities parallel to Kavirond Rift, these kimberlite magmatism may be correlated with the rifting followed by Tertiary to Recent volcanic activities.

The drill-cores are about 140 to 220 metres long and are composed of a very thin soil layer, laminated tuffaceous silt and sand and yellow-green to dark green kimberlites. Two or three thin horizons concentrating ultramafic xenoliths were found and are sometimes overlain by weakly laminated kimberlite poor in xenoliths.

Y1B1 kimberlite: Macrocrysts are olivine, pyroxene, phlogopite and small amounts of amphibole, opaque minerals and non-chromian garnet. The matrix is composed of cryptocrystalline serpentine, opaque minerals, perovskite, calcite, titaniferous andradite and saponite. Small-sized autoliths were found commonly in thin sections.

YA17 kimberlite: Macrocrysts are olivine, natrolite and/or thomsonite and small amounts of phlogopite and opaque minerals. The matrix is composed mainly of saponite, diopside, natrolite, thomsonite, opaque minerals, calcite and small amounts of perovskite, titaniferous andradite, pectolite, amphibole, cancrinite and apatite. Druses or veins of natrolite and/or thomsonite were found, commonly associated with calcite and diopside.

Y1B3 kimberlite: The drill-core specimens are intensely weathered. This kimberlite is mineralogically similar to YA17 kimberlite rather than Y1B1 kimberlite.

Ultramafic xenoliths: Garnet-free harzburgite, dunite and phlogopite-bearing hornblende were found. Harzburgite and dunite contain secondary-textured amphibole, phlogopite and opaque minerals.

Chemical compositions of major and trace elements of western Kenya kimberlites and their ultramafic xenoliths are shown in Table 1. Y1B1 kimberlite from the deep part of the drill-core shows lower K_2O and Na_2O contents than those from the shallow part. YA17 kimberlite shows fairly low K_2O and high Na_2O contents. High CaO and CO_2 contents of the shallow part of Y1B1 kimberlite are derived clearly from calcite. High contents of Rb, Sr, Y, Zr, Nb, Pb and Ba and low contents of Co and Ni are characteristically shown for the shallow part of the Y1B1 drill-core. The chemical features of major and trace elements of YA17 kimberlite are similar to those of the shallow part of the Y1B1 drill-core. These differences in major and trace elemental abundances may result from low temperature alteration at the saponite stage.

The source of macrocrysts of olivine, phlogopite and amphibole in western Kenya kimberlites will be discussed by comparison with the chemistry of these minerals in ultramafic xenoliths. Relatively low NiO and CaO contents together with wide spread in MgO/(MgO+FeO) ratios are considered to be diagnostic of olivine phenocrysts.

Three compositional types(I, II, III) of phlogopite are identified especially owing to their TiO₂ and Cr₂O₃ contents as shown in Fig. 1. Type I phlogopites are poor in TiO₂ with variable contents of Cr₂O₃, FeO and Al₂O₃, type II rich in TiO₂ and FeO with relatively high Al₂O₃ and low Cr₂O₃ contents, and type III rich in TiO₂, Cr₂O₃ and Al₂O₃ with relatively high FeO contents. Since the phlogopites of type I and type II are similar in chemistry to phlogopites from ultramafic xenoliths, these phlogopite macrocrysts are considered to be discrete ultramafic rocks. Type III phlogopites including the rim part of zoned phlogopites may have crystallized in the kimberlite magma.

Amphibole macrocrysts comprise titanian edenite, edenite, edenitic hornblende, magnesio-katophorite and richterite. All of these amphiboles are considered to be discrete ultramafic rocks, owing to their chemistry similar to those in ultramafic xenoliths together with metasomatic ultramafic microxenoliths; titanian edenite in hornblendite, edenitic hornblende in harzburgite, magnesio-katophorite in dunite and edenite, magnesio-katophorite and richterite in the metasomatic ultramafic microxenoliths.

The values of $\delta^{13}\text{C}_{\text{PDB}}$ and $\delta^{18}\text{O}_{\text{SMOW}}$ of the calcite macrocryst and the matrix carbonate of the yellow-green kimberlites(shallow parts of the drill-core) are slightly heavier than those of the matrix carbonate of dark green kimberlite(deep parts of the drill-core). This suggests some meteoric-hydrothermal water interaction during the diatreme emplacement. These values of the western Kenya kimberlites are heavier than those of the kimberlites from other localities(Kobelski, B. J. et al., 1979).

References

- Kobelski, B. J., Gold, D. P. and Deines, P. O., 1979, Variations in stable isotope compositions for carbon and oxygen in some South African and Lesothan kimberlites. In Boyd, F. R. and Meyer, H. O. A.(ed.): Kimberlites, diatremes, and diamonds: Their geology, petrology, and geochemistry. Proceedings 2nd International Kimberlite Conference 1, American Geophysical Union. pp. 252-271.
- Yanagi, T. and Suwa, K., 1981: Rb-Sr radiometric dating on Precambrian rocks in the western part of Kenya. 6th Preliminary Report of African Studies, Nagoya University, 163-172.

Table 1. Chemical compositions of western Kenya kimberlites.

(wt.%)	1	2	3	4	5
SiO ₂	30.10	35.49	39.33	41.48	41.86
TiO ₂	1.60	0.73	1.72	0.05	0.02
Al ₂ O ₃	3.95	2.42	5.25	0.80	0.48
Fe ₂ O ₃	7.34	6.00	6.59	1.74	0.84
FeO	4.05	5.34	5.40	5.56	6.29
MnO	0.22	0.20	0.20	0.12	0.12
MgO	21.39	33.68	17.70	44.24	46.56
CaO	11.68	3.49	11.58	0.49	0.25
Na ₂ O	1.33	0.47	3.36	0.26	0.17
K ₂ O	2.03	0.30	0.94	0.14	0.06
P ₂ O ₅	0.74	0.18	0.70	0.01	0.00
H ₂ O(+)	3.73	6.46	4.18	2.54	1.43
H ₂ O(-)	2.24	2.20	3.12	1.36	0.67
CO ₂	8.75	2.54	0.73	0.45	0.34
Total	99.15	99.50	100.80	99.24	99.09

(ppm)					
Cr	630	626	610	1800	1000
Co	45	66	43	76	84
Ni	475	980	330	1900	2000
Cu	0	0	0	0	0
Zn	66	60	74	36	34
Br	0	0	0	0	0
Rb	29	3	26	0	0
Sr	900	230	610	26	12
Y	20	5	17	0	1
Zr	185	65	150	11	7
Nb	29	0	2	0	0
Mo	2	2	3	1	1
Pb	12	7	7	3	3
Th	12	7	8	1	1
Ba	485	196	740	27	6
Ga	5	2	7	2	6

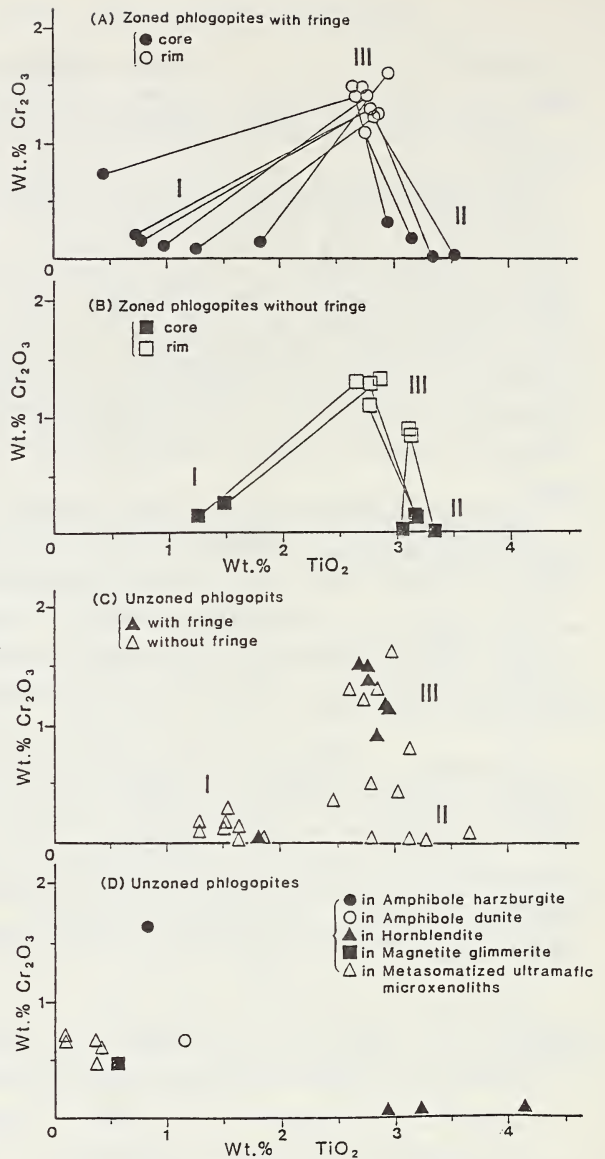


Fig. 1. Cr₂O₃ vs. TiO₂ for phlogopites in the western Kenya kimberlites and their ultramafic xenoliths.

1: Yellow-green Y1B1 kimb. (shallow part), average of 2 samples.

2: Dark green Y1B1 kimb. (deep part), average of 5 samples.

3: Dark grayish green YA17 kimb. (shallow & deep parts), average of 5 samples.

4: Harzburgite in Y1B1 kimb.

5: Harzburgite in YA17 kimb.

MAGSAT ANOMALIES, CRUSTAL MAGNETISATION, HEAT FLOW AND
KIMBERLITE OCCURRENCES IN AUSTRALIA

B.D. Johnson¹, M.A. Mayhew², Suzanne Y. O'Reilly¹, W.L. Griffin³,
F. Arnott⁴ and P.J. Wasilewski⁵

- ¹ School of Earth Sciences, Macquarie University, North Ryde,
NSW 2113, Australia
- ² Earth Sciences Division, National Science Foundation,
Washington DC 20550, USA
- ³ Mineralogisk-Geologisk Museum, Sars Gate 1, 0562 Oslo, Norway
- ⁴ Stockdale Prospecting Ltd, 60 Wilson Street, South Yarra,
VIC 3141, Australia
- ⁵ NASA/Goddard Space Flight Center, Greenbelt MD 20771, USA

INTRODUCTION

The Magsat map of Australia (Johnson and Mayhew, 1985) shows a good correlation between large scale tectonic structures and crustal source magnetic anomalies observed at satellite altitudes. The Precambrian cratonic blocks coincide with large positive magnetic anomalies, the largest of which is situated over the Gawler Block in South Australia. The tectonically active southeastern part of Australia is marked by low relief magnetic anomalies. The boundary between the cratonic blocks and this southeastern part of Australia is marked by a steep gradient in the anomaly field.

MAGSAT INVERSION

Inversion techniques have been applied to the Magsat data (Mayhew and Johnson, in preparation) to obtain an equivalent layer solution comprising a horizontal distribution of average vertical magnetisation for a crustal layer of constant thickness. The inversion results have a spatial resolution of the order of 100 kms and reveal features that are not easily seen in the magnetic field observed at 300-400 kms elevation. Since the earth's magnetic field inclination varies considerably through the latitude range of Australia, it is useful to compute the "reduced to the pole" magnetic anomaly from the equivalent layer solution using a vertical direction for the magnetisation.

In reality, the thickness of the magnetic layer varies from place to place largely as a function of vertical temperature gradients. In regions where the temperature gradient is high, the Curie point geotherm for magnetite is reached at depths within the continental crust. However, in regions of shallow temperature gradient, the Curie point geotherm is reached at levels below the base of the crust. We have previously argued that the mantle is essentially non-magnetic (Wasilewski et al, 1977) and therefore in such regions the thickness of the magnetic crust may be defined by the crust-mantle boundary.

XENOLITH-DERIVED GEOTHERMS

Appropriate mineral assemblages from xenoliths in basaltic and kimberlitic host rocks provide pressure and temperature measurements which can be used to define vertical temperature profiles for crustal and upper mantle depths. A range of such vertical temperature profiles, for contrasting lithospheric environments, can be used to transform the magnetic anomaly inversion results (for a constant thickness assumption) into more realistic magnetisations for a magnetic crust of variable thickness.

O'Reilly and Griffin (1985) derived a vertical temperature profile for southeastern Australia which has much higher temperatures at any given pressure than conventional continental or oceanic geotherms. The Curie point for magnetite is reached at a depth of only 12 km and substantiates the interpretation that the subdued magnetic anomalies of southeastern Australia are at least in part due to a relatively thin magnetic crust.

The combined interpretation of the Magsat crustal anomaly field and the geothermobarometry results leads to an exciting possibility whereby a heat-flow model for Australia may be derived which can be used to predict temperature at any location and depth. This enables the interpolation of the sparse surface heat-flow data and avoids the anomalies due to circulating artesian waters.

In addition, because P and T are constrained at depth, there is no necessity to assume arbitrarily a steady-state conductive heat-flow model which may result in misleading extrapolation of heat-flow production to high pressures. Construction of a xenolith-derived geotherm for eastern Australia, for example, predicts that there is a small field where diamond would be stable. This contrasts with the extrapolated steady-state geotherm prediction that the temperature is too high for diamond stability at all pressures.

CONCLUSION

This integrated petrological and geophysical investigation of the crust of Australia is particularly significant in the search for diamond-bearing kimberlites as it could identify likely areas for exploration targeting.

REFERENCES

- BRANSON J.C., MOSS F.J. and TAYLOR F.J. 1976. Deep crustal reflection seismic test survey, Mildura, Victoria, and Broken Hill, N.S.W. **Bureau of Mineral Resources Report 193.**
- CULL J.P. 1982. An appraisal of Australian heat-flow data. **BMR Journal of Australian Geology and Geophysics**, 7, 11-21.
- FINLAYSON D.M., CULL J.P. and DRUMMOND B.J. 1984. Upper mantle structure from the Trans-Australian Seismic Refraction data. **Journal of the Geological Society of Australia**, 21, 447-458.
- JOHNSON B.D. and MAYHEW M.A. 1985. Interpretation of satellite magnetometer data (abstract). **Exploration Geophysics**, 16(2/3), 238-240.
- MAYHEW M.A. and JOHNSON B.D. (in preparation). An equivalent layer magnetization model for Australia based on Magsat data. Manuscript to be submitted to **Earth and Planetary Science Letters**,
- O'REILLY S.Y. and GRIFFIN W.L. 1985. A xenolith-derived geotherm for southeastern Australia and its geophysical implications. **Tectonophysics**, 111, 41-63.
- POWELL C.McA. 1984. Terminal fold-belt deformation: relationship of mid-Carboniferous megakinks in the Tasman fold belt to coeval thrusts in cratonic Australia. **Geology**, 12, 546-549.
- SCHACKLEFORD P.R.J. 1978. The determination of crustal structure in the Adelaide Geosyncline using quarry blasts as seismic sources. Unpublished M.Sc. Thesis, University of Adelaide.
- VEEVERS J.J. 1984. **Phanerozoic Earth History of Australia**, Oxford University Press, 418 pp.
- WASILEWSKI P.J., THOMAS H.H. and MAYHEW M.A. 1977. The Moho as a magnetic boundary. **Geophysics Research Letters**, 6, 541-544.

FIGURES

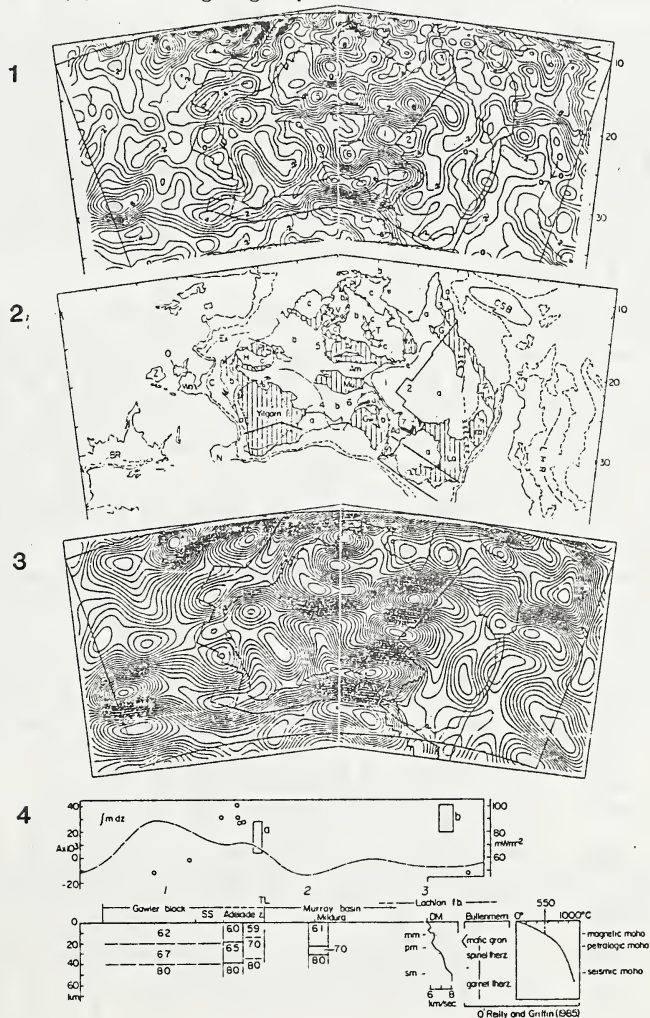
Fig. 1 Magnetisations derived from inversion of Magsat crustal magnetic anomalies for a 40 km uniform thickness equivalent layer. Contours are at an interval of 0.1 A/m. Dots indicate locations of dipoles forming the equivalent layer. Heavy lines indicate a) the Tasman Line as drawn by Powell (1984)

onshore and the continent-ocean boundary (Veevers, 1984) offshore western Australia.

Fig. 2 Sketch map of major structural units in Australia for comparison with Fig. 1. Ruled areas represent areas of exposed crystalline rocks, blank areas sedimentary cover. Numbers are positions of magnetisation anomalies indicated on Fig. 1.

Fig. 3 Reduced to the pole magnetic field calculated for an altitude of 325 km using a vertical magnetisation direction and the equivalent layer magnetisation intensities shown in Fig. 1.

Fig. 4 Crustal section across the Gawler Block, the Adelaide zone, the Murray Basin, and the Lachlan Fold Belt. Crustal seismic layering with P-wave velocities indicated from Finlayson et al (1984), Schackelford (1978) and Branson et al (1976). At lower right are geotherm and lower crust/upper mantle lithologies inferred from xenolith studies (O'Reilly and Griffin, 1985). Above is profile of heat flow determinations (Cull, 1982) (scale on right). Grouped determinations indicated by boxes (a) enclosing a group along the craton margin and (b) enclosing a group in the Lachlan Fold belt.



M. T. Muggeridge

Department of Geology, University of Western Australia, Nedlands, WA 6009, Australia

Since the first affirmed discoveries of kimberlite in the 1870's, and especially over the last 25 years, a wealth of literature has been published describing various aspects of individual occurrences, groups of occurrences or world-wide distribution of this rock. At least 700 individual kimberlite bodies are on public record. Recently many features of closely related rocks, such as lamproite and alnoite, have received increased attention. Information derived from mantle nodules, which are often present as xenoliths within kimberlite and similar rocks, is important for research into upper mantle conditions. With the ever-increasing volume of available data, many researchers face the problem of assimilating the new material and reviewing the total data bank on kimberlites and related types. It is likely that less obvious, but meaningful and diagnostic, data groupings are being overlooked. This paper discusses a systematic method of tabulating essential information on individual occurrences of these rocks in order to provide a convenient catalogue which can be readily adapted to a personalized computer database.

A sample of the reference catalogue is given in Table 1 (see Fig. 1 for relevant localities). Kimberlites and related rocks are listed primarily according to country of origin. Tabulated information on district and precise location is shown. The lists also indicate a kimberlitic body's membership of clusters, fields and provinces where clearly defined in the literature. Latest accepted petrological classifications and radiometric and/or geological ages are an essential component. Where known, grade and economic status are given. Additional information, such as relation to craton and nature and age of craton, basement and country rock, is included. This classification incorporates data on significant minerals and xenoliths, beyond the scope of similar previously published tables (e.g. Dawson 1980), and includes a summary of relevant published references on each occurrence.

The catalogue has been developed in database format on an Apple Macintosh computer system using Microsoft File, a programme that allows interactive addition, re-ordering and re-sizing of information fields at any stage during data entry and comprehensive sorting of records on one or more of these fields. These features are powerful tools, facilitating extension of the catalogue to include new information and reshuffling of data to permit its presentation in numerous different sequences. In order to optimize these characteristics, data entered into the catalogue have been consistently formatted. This ensures that re-ordering of the database, or searching for specific information within it, is done efficiently. Much of the information is coded to conserve space. However, further coding has been avoided for presentation purposes and to minimize time-consuming reference to keys. In the catalogue database, information on an individual kimberlite province, field, cluster or body constitutes a single record, and the data are partitioned into several fields each representing a different geological or geographical parameter. Reference to Table 1 shows that common information, such as "Country", is repeated from one record to another. This is so that a record displaced from its initial position during database re-ordering still has all the data needed to characterize it, either for immediate clarity or further sorting. Sorting a database on a variety of parameters is a means by which data can be studied and assessed in detail from many viewpoints. The application has great potential for kimberlitic rocks, where useful ordering of data on some individual parameter(s), e.g. "body type" and "grade", can be achieved (see Table 2), and there is the distinct possibility of disclosing interesting, perhaps subtle, data correlations that have hitherto gone unnoticed.

In summary, apart from providing a condensed reference system on kimberlites and related lithologies this catalogue, if used as a computer database, is designed to permit easy correlation between, and integration of, data belonging to any of the fields of information listed.

DAWSON J.B. 1980. Kimberlites and their xenoliths. Springer Verlag, NY, 252 pp.

P.H. Nixon and E. Condliffe

Dept. of Earth Sciences, University of Leeds, Leeds LS2 9JT, U.K.

There are over 400 kimberlites in Tanzania (Wilson, 1982), including Mwadui, the largest pipe in the world. Published data are scarce reflecting the poor outcrop, sediment-filled craters and the unexcavated nature of the deposits. There have been few published petrographic data even from Mwadui, the only significant producer, since the pioneering study of Edwards and Howkins (1966). Few xenoliths have been described and appear to be rare although Williams (1932) illustrates eclogites from the Shinyanga District some of which could be grosspyritic (Reid et al., 1976), and Boyd and Nixon (1970) give an analysis of a 'hot' subcalic clinopyroxene discrete nodule from a heavy mineral concentrate. Here, we extend the study of concentrates from Kimberlites, with a view to determining the chemical and petrological nature of the Tanzania Craton and to assess its similarities or differences with respect to the much studied Kaapvaal Craton of southern Africa.

The samples are mostly in the size range 1-5mm, and are from a dozen or so kimberlites, mostly in the Mwadui area and to the south (Fig. 1). They are here treated together except where a significant local trend is observed.

The compositions of the silicates (Fig. 2) show broadly similar distribution fields to those observed in southern Africa kimberlites, an understanding of which enables an interpretation to be attempted. Clinopyroxenes and garnets are abundant, orthopyroxenes less so and olivines are absent. The main oxides are ilmenites and spinels.

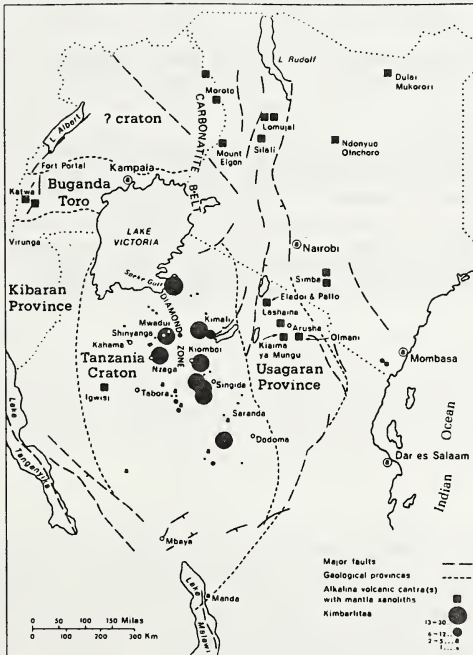


Fig. 1. Tectonic map of East Africa after Nixon (in press) showing the outline of the Tanzanian Craton and major faults together with the distribution of kimberlites. Data mainly from Geological Survey sources, Williams (1939) and Edwards and Howkins (1966).

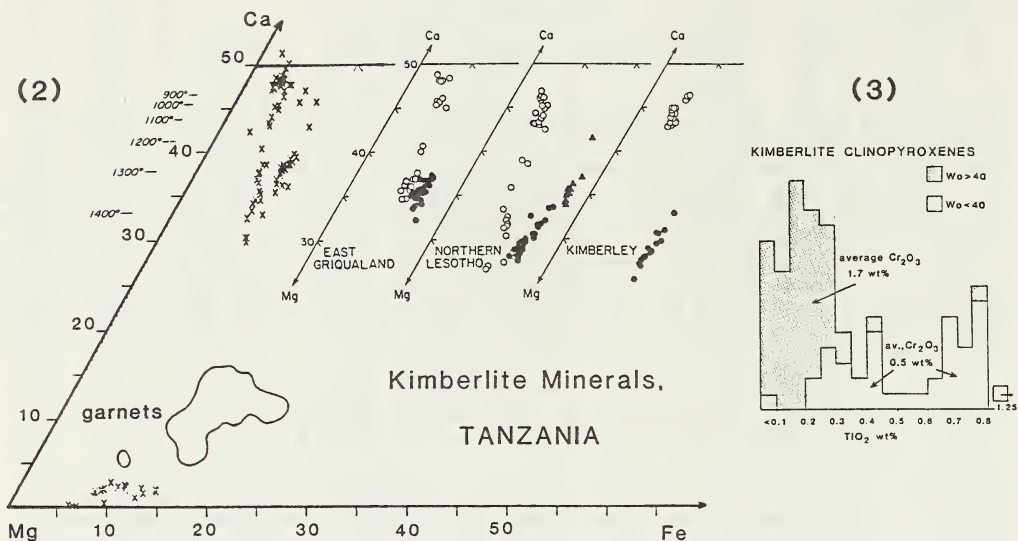


Figure 2. Range of compositions of silicate minerals in Tanzania kimberlite heavy mineral concentrates. The clinopyroxenes are compared with those from East Griqualand, northern Lesotho and Kimberley in southern Africa (see Boyd and Nixon, 1980, and references therein). The open circles are cpx compositions from garnet lherzolites; the close circles are from discrete nodules and the triangles from cpx intergrowths with ilmenite mostly lamellar). The garnet field excludes almandine varieties from the basement rocks. Orthopyroxenes are shown at the bottom of the diagram; olivines are absent.

Figure 3. Compositions of clinopyroxenes in Tanzania kimberlite heavy mineral concentrates.

Clinopyroxenes

Bright green Cr-rich and dark green Cr-poor diopsides are common, the former are calcic and Ti-poor and are similar to those of low temperature garnet lherzolite xenoliths. The latter are subcalcic and show a bimodal Ti distribution (Fig. 3). This is tentatively ascribed to derivation from high-temperature lherzolites (cf. the sheared xenoliths from Thaba Putsoa, Lesotho; Nixon and Boyd, 1973) and discrete nodules (megacrysts). Chromium values, however, are similar in both subgroups. Besides lower Ti the calcic clinopyroxenes are also depleted in Fe relative to the subcalcic types.

Orthopyroxenes

The chemical depletion is mirrored in the orthopyroxenes which range from enstatite to more fertile bronzite, the latter being relatively calcic and thought to have been in equilibration with the subcalcic ('hot') clinopyroxenes. Limited data indicate that the orthopyroxenes define PT points within the diamond stability field.

Garnets

Garnets with 70-80% pyrope typify the Tanzania concentrates. Purple low Ti Cr-rich varieties are similar to those from depleted lherzolites. Subcalcic Cr-rich pyropes (knorringite-rich) similar to those found as diamond inclusions are present. Several Cr garnets ($\text{Cr}_2\text{O}_3 > 6 \text{ wt}\%$) are also rich in $\text{TiO}_2 (> 0.4 \text{ wt}\%)$. These may be part of the high-temperature lherzolite or discrete nodule (megacryst) suite. The latter are brown to red and usually range up to 1+ wt% TiO_2 and 2 wt% Cr_2O_3 .

Ultra pyrope-rich (85% py) types may be from alkmmites. Orange almandine-rich garnet with variable grossularite may be from basement granulites and from disaggregated eclogites (see comparable analysis in Reid et al., 1975).

Spinel

Inclusions in garnets typified by a pipe in the Nzega area show the following ranges, wt% analyses MgO, 9.2 - 12.2; Al₂O₃ 12.1 - 14.6; Cr₂O₃, 55.4 - 58.4; FeO, 15.8 - 17.5 and negligible calculated Fe₂O₃. Discrete grains from Mwadui range to high values of Cr₂O₃ (62 wt%) and low Al₂O₃ similar to those found in diamond inclusions and subcalcic garnet harzburgites.

Ilmenites

These commonly show rinds of pimply perovskite. Compositional ranges of ilmenite vary to over 6 wt% Cr₂O₃ and 14 wt% MgO. Typical values are around 0.5 wt% Cr₂O₃ and 9 wt% MgO but pipes may have ilmenites showing a distinctive signature e.g. Mabuki, which shows a direct variation from about 1 to 3 wt% Cr₂O₃ and 4 to 9 wt% MgO.

Additional minerals observed and in most cases analysed include titaniferous magnetite, richterite amphibole, tremolite, zircon, phlogopite and apatite.

It is concluded that there are many similarities between the depleted lithosphere of Tanzania and southern Africa and that an ultradepleted basal layer exists. The effects of enrichment or metasomatism (phlogopite, richterite) were observed but the extent is unknown. The high temperature suite of inclusions, particularly those of the discrete nodule suite (subcalcic low Cr diopside, Ti pyrope, bronzite, ilmenite and zircon) can be matched with those erupted through the Kaapvaal Craton but there are differences in detail. We thank Williamsons Mine for assistance and samples.

BOYD, F.R. and NIXON, P.H. 1970. Kimberlite diopsides Carnegie Inst. Washington, Yearbk 68, 324-329.

BOYD, F.R. and NIXON, P.H. 1980. Discretenodules from the kimberlites of East Griqualand, southern Africa. Carnegie Inst. Washington Year Book 79, 296-302.

EDWARDS, C.B. and HOWKINS, J.B. 1966. Kimberlites in Tanganyika with special reference to the Mwadui occurrence. Econ. Geol. 61, 537-554.

NIXON, P.H. (in press) Chapter 17. Africa-Arabia plate. Kimberlite xenoliths and their cratonic setting. In (ed. P.H. Nixon) Mantle Xenoliths, Wiley & Sons, Chichester.

NIXON, P.H. and BOYD, F.R. 1973. The petrogenesis of the granular and sheared ultrabasic nodule suite in kimberlites in Lesotho Kimberlites (ed. P.H. Nixon). Lesotho National Development Corp. pp. 48-56.

REID, A.M., BROWN, R.W., DAWSON, J.B., WHITFIELD, G.G. and SIEBERT, J.C. 1976. Garnet and pyroxene compositions in some diamondiferous eclogites. Contr. Mineral. Petrol., 58, 203-220.

WILLIAMS, A.F. 1932. The Genesis of the Diamond. 2 vols. Benn Ltd., London.

WILLIAMS, G.J. 1939. The kimberlite province and associated diamond deposits of Tanganyika Territory. Dept. Lands and Mines, Geological Division, Bull. No. 12. 41pp. Dar es Salaam.

WILSON, A.N. (1982). Diamonds from birth to eternity. Gemmological Inst. Amer. 450pp.

R. T. Pidgeon¹, C. B. Smith² and C. M. Fanning³

1. West Australian Institute of Technology, Bentley, WA

2. CRA Exploration Pty Limited, 21 Wynyard Street, Belmont, WA

3. Australian Mineral Development Laboratories, Frewville, SA

INTRODUCTION

The purpose of this paper is to report new zircon U-Pb, Rb-Sr, K-Ar and fission track age determinations for kimberlite and associated rocks from the north-west of Western Australia and to discuss the significance of the results together with previous age determinations on lamproites (Jaques et al, 1984). The locations of the investigated pipes are shown on Figure 1. Age determinations on these pipes are described below.

THE WANDAGEE M142 PIPE

A zircon U-Pb age of 160 ± 10 Ma was determined for this pipe. This age is interpreted as the time of crystallisation of the zircon and also as the time of emplacement of the pipe in the middle Jurassic. This accords with local geological constraints.

THE SKERRING KIMBERLITE PIPE

U-Pb measurements on zircons from this pipe indicate an age of 802 ± 10 Ma. These zircons have uranium contents of 5 ppm which are the lowest uranium contents in zircons known to the authors. There is no isotopic or morphological evidence for the presence of inherited lead in the clear, rounded zircons which are typical of kimberlites; the measured age is interpreted as dating the crystallisation of the zircons. This is also interpreted as the age of emplacement of the kimberlite although independent evidence is not presently available to confirm this interpretation.

THE PTEROPUS CREEK KIMBERLITE PIPE

A fission track age zircon of 510 ± 30 Ma and a zircon U-Pb age of 810 ± 20 Ma have been determined for this pipe. There are a number of possible explanations for the discrepancy between the two ages. One possibility is that the zircon U-Pb age dates the crystallisation of the zircon whereas the fission track age dates the emplacement of the kimberlite 510 ± 30 Ma ago. Another explanation is that the zircon U-Pb age of 810 ± 20 Ma is essentially the age of emplacement of the pipe and the fission track age is dating a later resetting - for example the heating associated with the extrusion of the Antrim Plateau lavas. The coincidence of Skerring and Pteropus Creek zircon U-Pb ages is presently interpreted as favouring the second explanation.

THE BOW HILL LAMPROPHYRE

K-Ar age determinations on phlogopites from this pipe range from 804 to 826 Ma with a mean age of ca 815 Ma. Rb-Sr measurements for the phlogopites yield model ages within the range 769 to 841 Ma for a postulated $R_i = 0.705$, and 752 to 819 Ma ($R_i = 0.710$) in approximate agreement with the K-Ar age. However, a Rb-Sr isochron regression treatment suggests a reset age of ca 570 Ma ($R_i = 0.766$) for the phlogopites not recorded by K-Ar systematics. The general agreement between K-Ar and Rb-Sr model ages suggests emplacement of the lamprophyre at ca 800-815 Ma with a younger, ca 570 Ma indistinct overprint.

THE ARGYLE AK1 LAMPROITE

At the time of this report no zircons have been recovered from this lamproite and dating has relied on Rb-Sr - K-Ar measurements on whole rock and phlogopite samples. Rb-Sr whole rock systems of the sandy tuff unit suggest an imprecise age of 1100 ± 300 Ma for the pipe. A better estimate of the age is provided by an isochron age of $T045 \pm 150$ Ma for samples of lamproite drill core. Rb-Sr measurements on phlogopites from three samples of the drill core yield consistent ages of ca 1147 ± 20 Ma with an R_i of ca 0.707 (based on isochron regression and model age calculations). K-Ar ages for the

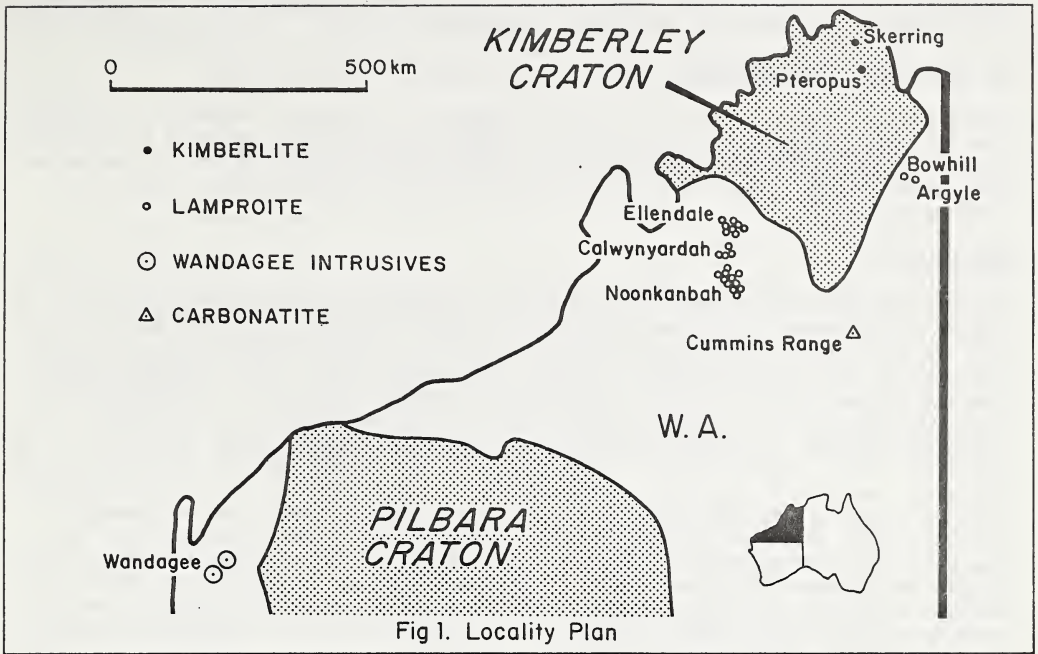


Fig 1. Locality Plan

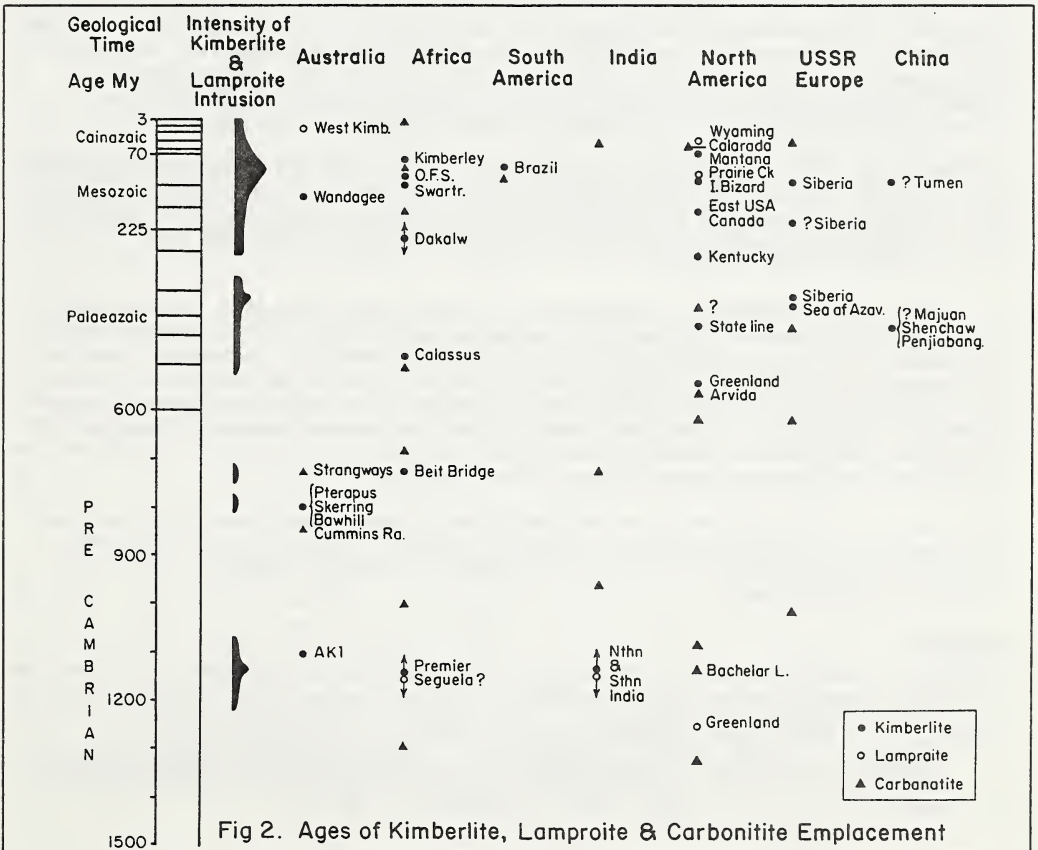


Fig 2. Ages of Kimberlite, Lamproite & Carbonatite Emplacement

phlogopites are slightly older ranging from 1224 \pm 12 Ma to 1253 \pm 26 Ma, but anomalously low K contents indicate that these ages are probably too old.

THE WEST KIMBERLEY LAMPROITES

Jaques et al (1984) reported K-Ar and Rb-Sr ages for 14 separate lamproite intrusions from the Fitzroy area of the West Kimberley region. The results showed a transition in ages of emplacement from 20-22 Ma in the Ellendale area to 18-20 Ma in the Noonkanbah area further south. These early Miocene pipes are the youngest primary sources of diamonds yet found.

CONCLUSIONS

The age determinations presented in this paper indicate a long, possibly episodic, history of emplacement of kimberlitic rocks in the Kimberleys of Western Australia (Fig. 2). The first recognised kimberlitic events were at ca 1200 Ma and ca 810 Ma; these follow long after and therefore were not related to the intense metamorphism, granitic and basic to ultramafic magmatism of the King Leopold and Halls Creek Mobile Zones (which concluded at about 1800 Ma) and the basic magmatism of the Carson Volcanics (1760 Ma). Widespread eruption of tholeiitic basalt across Northern Australia in the Cambrian (Antrim Plateau basalt) also cannot be related in time to any Australian kimberlitic activity. Post-Cambrian igneous activity in the Kimberley is restricted entirely to the west where there is a possible date of 357 Ma (Bennett & Gellatly, 1970) on some acid volcanics (Spielers volcanics, Oscar Range Inlier) and some dolerites were emplaced in the Triassic. Again, there is a big difference in age between this magmatism and the Miocene lamproite emplacement in the West Kimberley. Whereas in South Africa and in Siberia kimberlites appear to have been emplaced just prior to and just after major periods of flood basalt activity, no such relationship exists in the Kimberley of Western Australia.

Comparison of the periods of emplacement of the kimberlitic rocks with the timing of major structural events in the Kimberley (Fig. 2) also shows no apparent relationship. The Miocene lamproites of the West Kimberley were emplaced some 150 My after the Triassic/Jurassic period of transcurrent faulting, and there is no known phase of tectonism within 100 My of the Pre-Cambrian lamproites and kimberlites.

At Wandagee in the Carnarvon Basin, emplacement of the Jurassic kimberlitic diatremes and sills was towards the end of a period of rifting and tensional conditions, just prior to crustal separation of Australia from the Indian plate during the Cretaceous. Acid and alkaline volcanic activity also occurred offshore during the late Carboniferous or early Permian.

On a global scale, kimberlitic rocks appear to have been emplaced at certain specific ages (Fig. 2). A peak of such activity occurred during the Cretaceous and is well represented in Africa, South America, USSR and North America. Curiously it has not yet been recorded in Australia. However, the Cretaceous peak may be part of a broader cycle encompassing activity ranging from the Triassic (or even Carboniferous) upwards. The Miocene lamproites of the West Kimberley and the Jurassic bodies of Wandagee and South Australia (Terowie, Eurelia), effectively belong to this cycle. Palaeozoic age kimberlites have not yet been described from Australia.

The other major global peak is at ca 1200 My and is represented in Africa, India and North America (including Greenland). Argyle coincides with this cycle. The only recorded overseas analogue of the ca 800 My bodies of Western Australia is the Beit Bridge body in Zimbabwe.

REFERENCES

- BENNETT, R. & GELLATLY, D. C., 1970. Rb-Sr age determinations of some rocks from the West Kimberley Region, Western Australia. B. M. R. Aust. Rec. 1970/20 (unpubl).
- JAQUES, A. L., WEBB, A. W., FANNING, C. M., BLACK, L. P., PIDGEON, R. T., FERGUSON, J., SMITH, C. B. & GREGORY, G. P., 1984. The age of diamond-bearing pipes and associated leucite lamproites of the West Kimberley region, Western Australia. B. M. R. J. Aust. Geol. & Geophys., 9, pp.1-8.

THE INFLUENCE OF THE REGIONAL STRUCTURE OF THE RHODESIA CRATON ON THE
DISTRIBUTION OF KIMBERLITES IN BOTSWANA AND ZIMBABWE

D.A. Pretorius

Economic Geology Research Unit, University of the Witwatersrand
1 Jan Smuts Avenue, 2001 Johannesburg, South Africa

Alluvial diamonds were discovered in 1903 in what was then Southern Rhodesia. In the following ten years, search for the sources of these Somabula diamonds resulted in the discovery of the Colossus kimberlite field housing four pipes and one kimberlitic sill and the Clare Field containing six pipes, one sill, and one fissure (Fig. 1). Later prospecting resulted in the finding of nine further kimberlitic bodies, bringing the total so far located up to 22, six of which have been proved to contain diamonds. Of these six, only one, the River Ranch pipe, is of possible economic interest. Up to the end of 1979, the total recorded production of diamonds from Zimbabwe was a relatively-insignificant 20 000 carats, of which 95 per cent had been recovered from the Somabula Field, in which the alluvial diamonds have been derived from the weathering and reworking of detrital stones in Karoo-age sediments (Table I).

Exploration in Zimbabwe led to the conclusion that its potential for economically-viable deposits of diamonds was poor. In the latter half of the 1960's, very significant discoveries of diamondiferous kimberlites were made south of the Makgadikgadi Pans in Botswana, to the southwest of the region containing the Somabula, Colossus, and Clare fields. Consequent investigations culminated in the delineation of the Orapa kimberlite field, containing two productive pipes, Orapa and Letlhakane, out of a total of, at least, 29 kimberlitic bodies. Production from the first-rank Orapa pipe commenced in 1971 and, to the end of 1985, a little under 50 million carats had been recovered. The lesser Letlhakane pipe started producing in 1977 and had yielded over 4 million carats to the end of 1985 (Table I).

The limited exposures of the Precambrian rocks in northeastern Botswana indicate that this segment of the territory is an integral part of the long-recognized Rhodesia Craton of which the classic Archean granite-greenstone terrane of the central region of Zimbabwe constitutes the shield. The investigations, the results of which are summarized in this abstract, have had as their goals: (i) the definition of the extent and geometry of the Rhodesia Craton; (ii) the identification of the distribution pattern, if any, of kimberlites on the craton; and (iii) the delineation of structural controls, if any, on the localization of the Orapa, Colossus, Clare, and other kimberlite fields.

The tectonic nuclei of Southern Africa are constituted by the Kaapvaal and Rhodesia cratons in which Archean granite-greenstone basements are exposed. These cratons are surrounded by centripetally-overthrust terranes in which the oldest, regional, metamorphic imprints are of the order of 2000 Ma. Kimberlites occur in equal abundance in cratonic and overthrust terranes, but diamond-bearing varieties are preferentially developed on the cratons, where they are present in both the shield and the platform regions. Up to 1970, diamond production came essentially from the Kaapvaal Craton, with comparatively very small quantities only emanating from the Rhodesia Craton. Discoveries in Botswana, within the last two decades, have resulted in substantial changes in the distribution-patterns of production.

Gravimetric, aeromagnetic, and borehole-drilling investigations, carried out in Botswana in the past ten years have contributed substantially to an unravelling of the subsurface geology and structure beneath the extensive cover of Quaternary Kalahari formations in the central segment of Southern Africa. As a result, it is now possible to define the boundaries of the Rhodesia Craton, its extent and shape, and its first-order structures. This crustal fragment is a classic chelonic craton, ovoid in shape, with a long axis at least 1 500 km long, in a northeasterly direction, and a short axis of the order of 600 km long, in a northwesterly direction. It is distinctly asymmetrical, along the northeasterly axis, about the point of maximum tectonic elevation of the craton, with the longer segment of the axis extending southwestwards from central Zimbabwe into central Botswana.

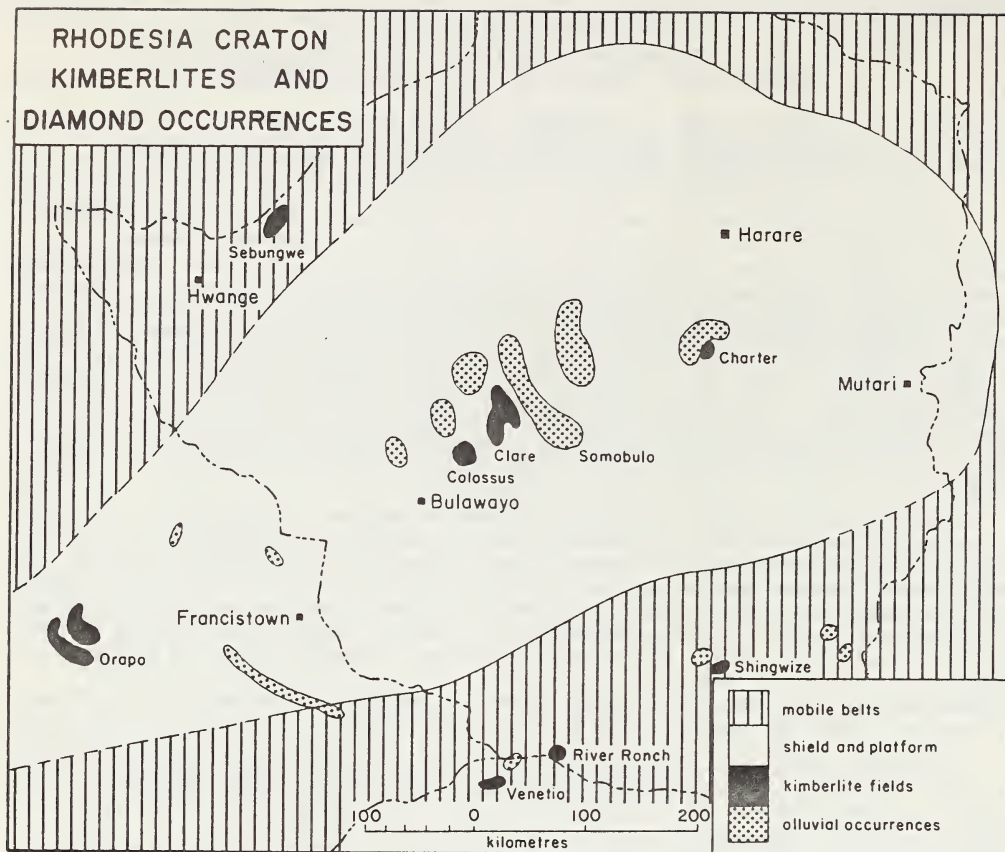


Figure 1 : The shield and platform of the Rhodesia Craton, with their enveloping mobile belts of metamorphic terrane. Kimberlite fields are aligned along ENE-to-NE trends along the spine of the craton and on the north-eastern flanks.

TABLE I
DIAMOND PRODUCTION FROM THE RHODESIA CRATON
ZIMBABWE AND BOTSWANA : 1905-1985

Country	Source of Diamonds	Carats
Botswana	Orapa Pipe	49 878 839
Botswana	Letlhakane Pipe	4 160 389
Zimbabwe	Somabula Alluvials	19 185
Zimbabwe	Colossus Pipe	144
Zimbabwe	Wessels Sill	81
Zimbabwe	Other Sources	227
Total Production from Rhodesia Craton		54 058 865

The Rhodesia chelonic craton shows a typical concentric pattern of alternating upwarps and downwarps wrapping around the point of maximum tectonic elevation. The upwarps are characterized by gravity lows and the downwarps by gravity highs, indicative of uplifted and depressed Archean granitic basement, respectively. The aeromagnetic field over Botswana also clearly indicates a curvilinear fabric on the southwestern portion of the craton, concave towards the central region of Zimbabwe.

Kimberlites are sporadically distributed over the whole of the Rhodesia Craton, but there is a distinctly greater number on the longer southwestern segment of the crustal fragment. Diamond-bearing pipes also are known only within the western portion of the craton. Because of the turtle-backed shape of the chelonic craton, there is a quaquaversal regional plunge radially away from the point of maximum tectonic elevation. As there is progressively decreasing uplift down the regional plunge, the degree of erosion of kimberlite pipes also diminishes down the plunge. Consequently, factors responsible for the development of larger volumes of alluvial diamonds become less favourable from central and southwestern Zimbabwe into central Botswana, while factors inclining towards the preservation of the uppermost portions of pipes are enhanced along the same trend.

Kimberlite pipes were preferentially intruded along upwarps, distinguished by elevated basement and gravity lows. In addition to the concentric upwarps, the north-easterly-trending spine of the chelonic craton also represents an axis of extensive arching. Four clusters of diamond-bearing kimberlite pipes - Orapa in Botswana and Colossus, Clare, and Charter in Zimbabwe - are located on the spinal upwarp, where this is intersected by different concentric upwarps. Other diamondiferous clusters, such as River Ranch in southern Zimbabwe and Venetia in the northwestern Transvaal occur on concentric upwarps. Employing concepts developed from these structural observations, a target-area was selected in east-central Botswana, in which subsequent exploration has indicated the presence of the Gope 25 diamond-bearing kimberlite pipe.

J. v.A. Robey¹, J.W. Bristow¹, M.R. Marx², J. Joyce², R.V. Danchin² and F. Arnot²

¹. Geology Department, De Beers Consolidated Mines Limited, P.O. Box 47, Kimberley, 8300, R.S.A.

². Stockdale Prospecting, 60 Wilson Street, South Yara V3141, Australia.

INTRODUCTION

In 1979 Stockdale Prospecting Ltd. recovered kimberlitic ilmenites from reconnaissance loam samples taken in the Fraser Range area some 100 km east of Norseman. Subsequent detailed follow-up sampling, ground magnetic surveys and core drilling showed the primary source of these ilmenites to be two dykes, named AN1 and AN10.

This paper details the petrological, geochemical and geochronological studies undertaken on fresh drill core from the AN10 dyke.

REGIONAL GEOLOGY

The dykes are situated some 10 km SE and 70 km E of Norseman respectively. This area straddles the margin between the south-eastern edge of the Archaean Yilgarn craton and the adjacent Proterozoic Fraser Range belt.

AN10 is intruded through an Archaean section of granites dated at approximately 2615 m.y. Greenstone belts occur further to the west. Early Proterozoic unmetamorphosed basic to ultrabasic dykes of the Widgiemooltha Dyke Suite occur within the Archaean of this area.

In contrast the Proterozoic section through which AN1 is intruded consists of garnet gneisses of the Mount Andrew Migmatite Complex with basic and acid granulites and gneisses of the Fraser Complex occurring further to the east. Rocks of both these complexes range in age from 1210 m.y. to 1680 m.y. Deformed basic to ultrabasic bodies of a noritic affinity are widespread within the gneisses and granulites of the Fraser belt. They have not been accurately dated but are thought to be early Proterozoic and are probably correlated to the Widgiemooltha dykes.

PETROLOGY

The AN1 dyke strikes east-northeast and based on the ground magnetic anomaly is 600 m in length and vertical. Dyke widths determined in two drill intersections vary from 1 to 10 m.

The AN10 dyke, further to the west, strikes west-northwest and based on the surface ilmenite anomaly, is probably an en echelon set 10 km in length. A dyke width of 1 m was calculated from an intersection between 62 and 65 m in an angled drill hole. Fresh core was recovered from this intersection.

Petrography

Detailed petrography has shown the AN10 dyke to consist of abundant olivine and phlogopite phenocrysts plus rarer olivine and ilmenite macrocrysts, set in a fine-grained groundmass of clinopyroxene and phlogopite with subordinate amounts of interstitial serpentine, calcite and nepheline as well as discrete perovskite, spinel, ilmenite and apatite grains. Schorlomite garnet occurs in the contact samples.

Olivines occur as rare, large macrocrysts (4 mm in size) and smaller (< 1 mm) phenocrysts with complex euhedral to subhedral shapes. All the olivines are totally serpentinised and carbonatised.

High Mg, low Cr ilmenite macrocrysts occur up to 6 mm in size and correlate in composition with those in the surface ilmenite anomaly. Smaller matrix ilmenites tend to be poorer in Mg.

Phlogopite phenocrysts commonly consist of a weakly pleochroic core surrounded by a highly pleochroic mantle that is similar in pleochroism to interstitial groundmass phlogopite. The compositions of the mantle and groundmass phlogopites are enriched in Al_2O_3 and TiO_2 but depleted in FeO relative to core compositions.

Diopside clinopyroxene occurs as acicular to tabular grains intimately intergrown with groundmass phlogopite, serpentine, calcite and nepheline.

Perovskites are relatively coarse and may occur intergrown with phlogopite, spinel and ilmenite.

Spinel is titanomagnetite with very low Cr_2O_3 .

Serpentine and nepheline occur as interstitial groundmass minerals.

Spheroidal structures composed of calcite and amphibole occur throughout the specimens. These are considered to represent completely digested country rock microxenoliths as similar mineral associations are observed in partly replaced microxenoliths.

Within 10 cm of either contact schorlomite garnet occurs as red-brown, subhedral, poikilitic clots up to 1 mm in size. These are zoned with low-Ti cores and high-Ti rims.

The AN10 dyke is classified petrographically as an olivine lamprophyre probably of alnoitic affinity.

Whole Rock Geochemistry

Samples from across the AN10 dyke were analysed by XRF for major and trace elements. Results presented in Table 1 indicate that the rock is strongly undersaturated and magnesium-rich and shows strong similarities to rocks of the alnoite-melilitite-nephelinite series.

Geochronology

A relatively large number of mica separates were prepared from several specimens across the AN10 dyke. These were carefully cleaned and inspected and the freshest material analysed for Rb, Sr and Sr isotope ratios. The data are plotted in Fig. 1 on a conventional isochron diagram which yields an age of 849 ± 9 m.y. with an initial $^{87}Sr/^{86}Sr$ ratio of .7036.

CONCLUSION

The AN10 and AN1 dykes were located by routine heavy mineral exploration for kimberlites. Both dykes produced strong surface anomalies of Mg-rich ilmenite.

Drilling provided fresh core from AN10 on which petrological studies were undertaken. The dykes are olivine lamprophyres similar to the alnoite-melilitite-nephelinite suite of rocks. Dating of micas suggest an emplacement age of 849 m.y. from a mantle source isotopically slightly depleted relative to Bulk Earth.

The criteria reviewed suggest that the alkalic ultrabasic dykes located near Norseman represent a previously unrecognised phase of late Proterozoic alkalic magmatism and that they are not associated with the early Proterozoic ultrabasic intrusives found in the general area.

REFERENCES

- CLEMENT C.R. 1982. A comparative geological study of some major kimberlite pipes in the Northern Cape and Orange Free State, 2 vols. Unpubl. PhD thesis, University of Cape Town, Cape Town.
- MOORE A.E. 1979. The geochemistry of olivine melilitites and related rocks of Namaqualand-Bushmanland, South Africa, 2 vols. Unpubl. PhD thesis, University of Cape Town, Cape Town.

ROCK N.M.S. 1986. The nature and origin of ultramafic lamprophyres: Alnoites and allied rocks, Journal of Petrology, vol. 27, Part 1, 155-196.

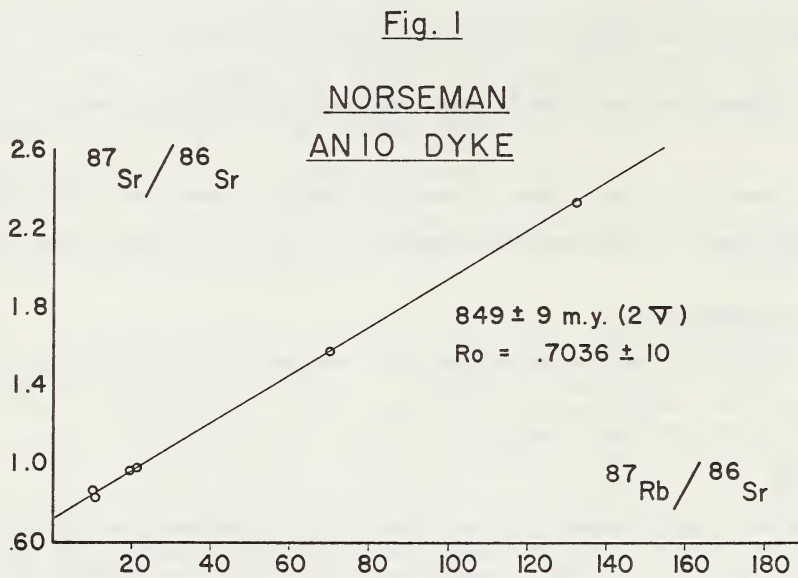


TABLE 1

	<u>1</u>	<u>2</u>	<u>3</u>	<u>4</u>	<u>5</u>
SiO ₂	36.90	35.07	34.42	34.53	41.61
TiO ₂	6.24	6.12	3.25	2.06	1.12
Al ₂ O ₃	6.24	5.95	9.84	2.97	3.72
Fe ₂ O ₃	15.10	18.12	13.58	10.38	9.45
MnO	.18	.23	.26	.18	.22
MgO	17.30	16.58	16.35	33.80	31.43
CaO	14.70	13.33	17.10	12.50	7.58
Na ₂ O	.50	1.60	2.25	.39	.24
K ₂ O	1.34	1.65	2.25	1.40	3.59
P ₂ O ₅	1.50	1.35	1.60	1.79	1.03

All data normalised volatile free and all Fe as Fe₂O₃.

- 1: Average of 4 samples from the AN10 dyke, this study.
- 2: Average Namaqualand melilitite-nephelinite (Moore, 1979).
- 3: Average of 55 melilitite-rich alnoites (Rock, 1986).
- 4: Average Group 1 kimberlite (Clement, 1983).
- 5: Average Group 2 kimberlite.

*Darcy P. Svisero: Institute of Geosciences, University of São Paulo
Caixa Postal 20.899, São Paulo, Brazil.

Henry O.A. Meyer: Department of Geosciences, Purdue University
West Lafayette, Indiana 47907, USA.

During the last decade considerable exploration activity directed towards finding new deposits of diamond and kimberlites has been underway in Brazil. For various and obvious reasons companies have not always reported their discoveries and it is rumored that there are in excess of 300 kimberlites, or kimberlitic-like intrusions, throughout Brazil (Svisero et al. 1979). Currently known ones are in Minas Gerais, Piauí and Rondônia States (Svisero et al. 1984). However, it is emphasized that because of the extensive tropical weathering the identification of several of the intrusions as kimberlitic is based on the presence of Mg-ilmenite, and pyrope garnet in heavy mineral concentrates of weathered rock and overlying soils. Based on similar studies, as well as examination of fresh rock in some instances, new occurrences of kimberlites are reported herein for the States of Piauí, Mato Grosso and Santa Catarina (Fig. 1).

In Piauí State the kimberlites of Redondão and Belmonte have been previously described. In this report we present data on the Açude kimberlite which is one in a field of several other possible kimberlites remote from Belmonte and Redondão. Geological reconnaissance shows that the body is a diatreme intrusive in reddish arenites of the Cabeças Formation, the Devonian member of the Parnaíba Basin. The intrusion is located near a dam 15 km south of Ipiranga do Piauí, not far from Picos, the main town in eastern Piauí State. Despite the arid climate, the kimberlite is weathered, with limonitic concretions dispersed over its surface. The material presently available from Açude is extensively weathered but appears to consist of serpentinized olivine macrocrysts in a fine grained groundmass in which only calcite, perovskite and opaques remain. One or two larger (0.5 mm) grains of Mg-ilmenite with reactions rims of perovskite are present. Macrocrysts (~ 1 cm) of garnet and Mg-ilmenite have been analyzed, plus a dark green clinopyroxene megacryst (> 1 cm). Garnet is typically kimberlitic and contains MgO ~ 22 wt%, FeO ~ 7 wt%, CaO ~ 5 wt% and Cr₂O₃ ~ 3 wt%. Ilmenite contains up to 16 wt% MgO and lamellar intergrowths with silicate (now serpentinized) occur. The pyroxene megacryst is compositionally equivalent to low-Cr pyroxene megacrysts from kimberlites in Lesotho, South Africa and Colorado. For example, Al₂O₃ < 3 wt%, TiO₂ and Cr₂O₃ both < 1 wt% and Na₂O < 2 wt%. Ca/(Ca+Mg) is $^{20}0.35$ which falls in the range of low-Cr pyroxene megacrysts from Monastery and Letseng.

In southeast Mato Grosso State, several possible kimberlite intrusions occur, mostly in difficult-to-reach places along the headwaters of the Batovi, Coliseu and Jatobá rivers. One of these intrusions (Batovi kimberlite), located 50 km north of Paranatinga, is intrusive in arkosic arenites of the Diamantino Formation the topmost member of the Proterozoic Alto Paraguai Group. Although weathered the rock is grey-green in color and fine grained with irregularly shaped macrocrysts (~ 3 mm) of serpentinized olivine (?), ilmenite and garnet. The groundmass is completely altered except for some perovskite, spinels and small Mg-ilmenites that are compositionally similar to the larger macrocrysts (8-13 wt% MgO). Garnets have Cr₂O₃ and CaO contents of 1.2 and 5.5 wt% respectively with high MgO (20²3 wt%) and low FeO (9 wt%). The spinels are generally low in TiO₂ and Al₂O₃ (both < 10 wt%), and MgO (< 12 wt%) but have high FeO (36-67² wt%) and variable Cr₂O₃ (2-40 wt%). The very high FeO and very low Cr₂O₃ spinels are mostly magnetites whereas those rich in Cr₂O₃ are mostly low-titanian magnesian chromites. Similar spinels occur in several kimberlites worldwide.

Surrounding the city of Lajes in Santa Catarina State are numerous diatremes intrusives in the Paleozoic-Mesozoic sediments of the southeast

border of the Paraná Basin. The most conspicuous is Janjão, near the Lajes airport, weathered on the surface and surrounded by pale yellowish arenites of the Permian Passa Dois Formation. Geophysical surveys (magnetometry, radiometry and gammaspectrometry) have revealed dimensions of 200 x 50 meters for the Janjão diatreme, with the main axis oriented N40E (Svisero et al. 1985). Preliminary study of minerals from Janjão and three other diatremes in the area (Pandolfo, Ipiranga and Cará) suggest possible kimberlitic affinity but at this date considerably more data are required to verify this suggestion. For example, Janjão diatreme contains Mg-ilmenites ($MgO \sim 4$ wt%), garnets (Cr_2O_3 1-2 wt%, CaO 4-7 wt%, MgO 20-22 wt% and $FeO \sim 7$ wt%), Cr-spinel, magnetite, zircon and numerous clinopyroxenes. Compositionally the clinopyroxenes are similar to the pyroxene megacrysts from kimberlite except that they (Janjão) have much higher contents of Al_2O_3 (~ 6 wt% versus < 1 wt%). In this respect they have similarity with the megacrysts from alkali basalts. Pyroxenes in the Cará, Ipiranga and Pandolfo are similar to those from Janjão.

In summary, the present data indicates that at least two new kimberlite fields and possibly a third exists in Brazil. Furthermore, during this study at least five more intrusions in the Coromandel area of western Minas Gerais State have been identified as containing kimberlitic-type minerals.

REFERENCES

- SVISERO D.P., MEYER H.O.A. and TSAI H.M. 1979. Kimberlites in Brazil: An Initial Report. In Boyd F.R. and Meyer H.O.A. eds, Kimberlites, Diatremes and Diamonds: Their Geology, Petrology and Geochemistry, pp. 92-100, AGU, Washington.
- SVISERO D.P., MEYER H.O.A., HARALYI N.L.E. and HASUI Y. 1984. A Note on the Geology of Some Brazilian Kimberlites. *Journal of Geology* 92, 331-338.
- SVISERO D.P., HARALYI N.L.E. and SHCEIBE L.F. 1985. Magnetometry, Radiometry and Gammaspectrometry at Janjão Diatreme, Lajes, SC. Proceedings of Second Southern Brazilian Symposium on Geology, pp. 261-272 (In Portuguese).
- *Sponsored by FAPESP and CNPq.



Fig. 1 - Location of kimberlite intrusions and detrital diamond occurrences in Brazil.

The Distribution Pattern of
Kimberlites and Their Cognate Rocks in Shandong, China

Wan Guodong
Shandong Bureau of Geology and Mineral Resources

Extended Abstract

INTRODUCTION.

The co-existence of kimberlites and cognate rocks is a common phenomenon. The study of the regional distribution patterns of kimberlites and their cognate rocks is an important way of predicting and prospecting for diamond deposits. Some research projects have been conducted in Shandong, China to select target areas for primary diamond deposits. Some diamondiferous kimberlites and related basic dykes, (distributed in an E-W direction), have also been found in Liaoning and Guizhou Provinces in China and these are thought to have been emplaced during the Silurian and Carboniferous. Some cognate rocks are found in the area surrounding the Liaoning kimberlite field and these will be studied in the future. The kimberlites in Guizhou, which lie at the contact between an upwarp axis and a syncline, are associated with dykes and sills of mica-peridotite containing minor diamond. We will take the western Shandong platform as an example to illustrate the regional distribution pattern of the kimberlites and their cognate xenoliths.

A. THE KIMBERLITES NEAR MENG YIN.

The kimberlites in Meng Yin occur near the centre of the western Shandong platform. Three kimberlite zones, consisting of 11 pipes and dozens of dykes, have been found, all containing diamond. Most of them are surrounded by Archaean gneiss and the dykes trend in a NNE direction. The depth of erosion is estimated to be more than 1km and only the root zones are preserved. The kimberlites are characterised by having little microilmenite, but abundant microchromite, ($Cr_2O_3 > 54\%$), and perovskite. This mineralogy is the result of the initial crystallisation of chromite, (caused by its higher lattice energy compared with that of ilmenite), and a consequent removal of iron from the magma, making the mass crystallisation of ilmenite difficult. Later, large quantities of perovskite crystallised as well as certain transitional minerals between microchromite and microilmenite, such as the new mineral of yimengite, which suggests that the magma forming the kimberlites in this region may have had a higher temperature and deeper source than magmas which form kimberlites with a higher microilmenite content.

B. THE COGNATE ROCKS.

The cognate rocks of the kimberlites in Meng Yin, Shandong are distributed on the fringe of the western Shandong platform, Fig. 1, a distance of 30kms from the centre of kimberlite emplacement. Some glimmerites and carbonatites occur in the north, (Laiwu and Zibo areas), and some lamprophyres and olivine glimmerite breccias are found in the south, (Xuecheng and Zaochuang areas). They are mostly in the form of sills and dykes, occasionally of pipes. Chemically, they belong to the subalkaline and ultrabasic rock groups. The main constituent minerals of these rocks are Fe-phlogopite, calcite, aegerine-augite, apatite and titanomagnetite. Calcite is the chief member of the carbonates and no nepheline occurs, which indicates the very high initial temperatures and deep source of the parent magmas.

C. RELATIONSHIP OF KIMBERLITES AND COGNATE ROCKS.

Both kimberlites and cognate rocks show similar patterns of rare earth elements, which belong to the "Ce-rich" and "Y-depletion" trends and implies that both are cognate products formed under high pressure. It can be seen from Fig. 2 that HREE contents in these rocks are low, with smooth and gentle curves, indicating an undifferentiated source region of garnet-lherzolite, (the unmelted garnet has been found in some nodules). On the La/Sm - La diagram, the points for both the kimberlites and the cognate rocks show an oblique line pattern that implies they were produced by partial melting. H_2O is greater than CO_2 in the kimberlites, whereas CO_2 is greater than H_2O in the cognate rocks; the ratio of H_2O/CO_2 controlled the differentiation path of the magma.

D. AGES OF THE INTRUSIONS.

The K-Ar isotopic ages for the cognate rocks range between 123 and 126Ma. Large quantities of volcanic breccia with a confirmed early Cretaceous age have been found in a carbonatite pipe in Boshan County. Also, clasts of volcanic rock with an early Cretaceous age have been found in thin sections of a kimberlite that cross-cuts a 113Ma old diabase dyke. The diabase formed somewhat later than the ultrabasic rocks. Both the kimberlites and the cognate rocks are controlled by the structures on the western Shandong platform which began to uplift in the Triassic period. Prof. Li Siguang suggested that the Meng Yin kimberlites may be related to the Tanlu fault, which is of Mesozoic age. However, the isotopic age data of the kimberlites are variable: the K-Ar method gives an age of 77 to 88Ma, whereas the Sm-Nd method and the K-Ar method from mica give ages of 400 to 500Ma, perhaps resulting from the presence and interference of the xenocrysts from deep sources in the kimberlites. This remains to be studied in the future. Based on the field geological relationships and the isotopic data available, I consider the kimberlites were formed in the Cretaceous and are contemporaneous with the cognate rocks.

E. CONCLUSIONS.

It is suggested that the liquid produced by the partial melting under high temperature and pressure in the mantle was separated into two parts: one part was kimberlite magma under high P and T which then ascended and was emplaced into the centre of the platform forming the pipes and dykes; the other part was the residual magma which, due to the decrease of pressure, was emplaced obliquely into the structures on the fringe of the platform, forming sills, dykes and a few pipes. Because the cognate rocks are more abundant than the kimberlites, the distribution patterns of the cognate rocks can be used for predicting and searching for diamondiferous kimberlites. This "central distribution pattern" is very similar to those in South Africa and Siberia.

COMPARATIVE DISCUSSION.

In Western Australia, by comparison, the lamproites, kimberlites and their cognate rocks, which are their fractionation products, are distributed on the fringe of the Kimberley block, where some new rock types have also been found. Some other kimberlites are distributed on the margins of the Australian continent. This could be related to the structure of the blocks where the lamproites and kimberlites occur, such that even at depths of 300-400kms the asthenosphere cannot have been touched. Therefore the large scale geology of the region must be taken into account when using a distribution pattern to predict and search for a diamondiferous kimberlite.

REFERENCES

- KHAIN, V. E., 1978. Evolution of more general theory of global tectonics from plate tectonics. *Geotectonics* 3.
- KUSKOV, O. L., 1978. Stability of carbonates in the terrestrial mantle. *Geochemistry* 12, 1813-1920.
- PERCHUK, L. L., VAGANOR, V. I. Petrochemical and thermodynamics. Evidence on the origin of kimberlites. *Contrib. Mineral Petrol.*, 72 2 219-227.
- MILASHEV, V. A., 1973. The world kimberlite provinces. 1.

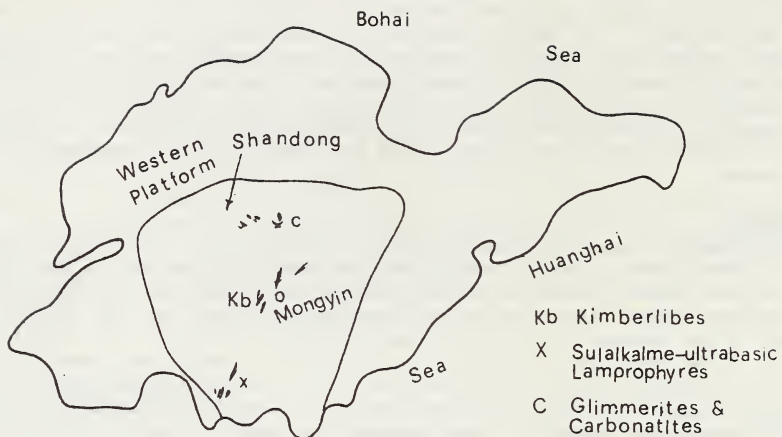


Fig1. The Distribution of Kimberlites & Their Cognate Rocks in Shandong, China.

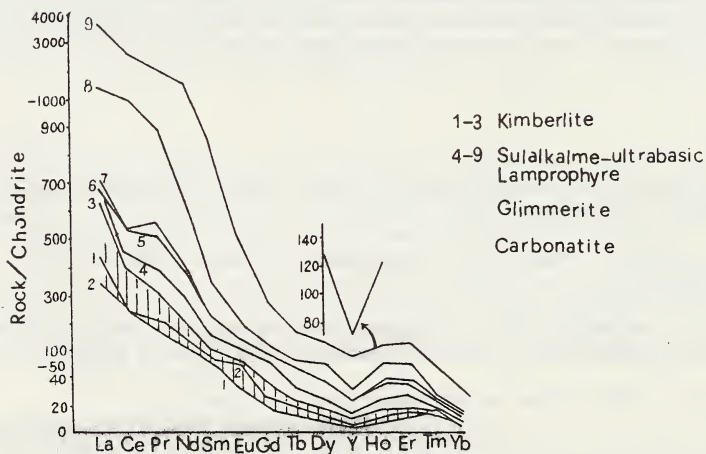


Fig2. REE Distribution Pattern of Kimberlites & Their Cognate Rocks in Shandong, China.

	Page
REVIEW PAPER	
Kimberlites: How do they form? D. H. EGGLE	155
Co-existing carbonatitic, ultramafic and mafic melts in the lithosphere; evidence from spinel lherzolite xenoliths, NW Spitzbergen H. E. F. AMUNDTSEN	160
Solubility of CO ₂ in kimberlitic and carbonatitic melts G. P. BREY and L. KOGARKO	163
Nodule associations from ouachitite and camptonite lamprophyres, Western Otago and South Westland, New Zealand C. G. BRODIE and A. F. COOPER	164
The origin of kimberlite pipes: an interpretation based on a synthesis of geological features displayed by Southern African occurrences C. R. CLEMENT and A. M. REID	167
High pressure melting experiments on an aphanitic kimberlite from the Wesselton Mine, Kimberley, South Africa A. D. EDGAR, M. ARIMA, D. K. BALDWIN, D. R. BELL, S. R. SHEE, E. M. W. SKINNER and E. C. WALKER	170
The genesis of lamproitic magmas in a reduced, fluorine-rich mantle S. F. FOLEY	173
Kimberlite/lamproite petrogenesis: geochemical and isotope evidence from North America, South Africa and Western Australia K. J. FRASER and C. J. HAWKESWORTH	176
Role of sulfides in the evolution of mantle rocks of basic and ultrabasic composition and in the emergence of kimberlite bodies V. K. GARANIN, G. P. KUDRYAVTSEVA and A. N. KROT	178
Peridotite melting to GPa and genesis of primary mantle-derived magmas D. H. GREEN, T. J. FALLOON, G. P. BREY and K. G. NICKEL	181
Speculations concerning the importance of metasomatic melt migration in the formation of pyroxenite sheets in garnet-peridotite xenoliths from Matsoku, Lesotho B. HARTE	184
Heteromorphism and crystallisation paths of katungites, Navajo volcanic field, Arizona, USA A. W. LAUGHLIN, R. W. CHARLES and M. J. ALDRICH	187
Iron-oxides in pisolite-like clasts in Ellendale lamproite intrusions D. M. McCONCHIE and C. B. SMITH	190
Experimental study of amphibole and phlogopite stability in metasomatized peridotite under water-saturated and water-undersaturated conditions K. MENGEL and D. H. GREEN	193
Ultrapotassic magmas: end-products of subduction and mantle recycling of sediments? D. R. NELSON, M. T. McCULLOCH and A. E. RINGWOOD	196
Evolution of minette, lamproite and mafic phonolite magmas in the Highwood Mountains Province, Montana, USA: geochemical and mineralogical evidence H. E. O'BRIEN, A. J. IRVING and I. S. McCALLUM	199
Contrasting Group 1 and Group 2 kimberlite petrology: towards a genetic model for kimberlites E. M. W. SKINNER	202

CONTENTS OF SECTION III (cont'd)

	Page
Volcanology of the Ellendale diatremes C. B. SMITH and V. LORENZ	205
Melting and subsolidus phase relation of mantle peridotite up to 25 GPa E. TAKAHASHI, E. ITO and C. M. SCARFE	208
The role of reduced C-O-H fluids in mantle partial melting W. R. TAYLOR and D. H. GREEN	211
Genesis and migration of kimberlites and other low-SiO ₂ , high-alkali magmas P. J. WYLLIE	214
Experimental investigation of the lamproite formation V. N. ZYRYANOV	217

David H. Egglar

Pennsylvania State University

LITHOSPHERIC OR ASTHENOSPHERIC SOURCE REGIONS?

Several continents but particularly southern Africa contain Archean cratons that have subcontinental upper mantle (SCUM) roots extending to depths of at least 170-190 km beneath craton and about the 140 km beneath mobile belts bordering cratons. Those estimates derive from maximum paleodepths of major-element-depleted peridotites and depths of "kinks" in paleogeotherms (Boyd and Gurney, 1986). Cratonic SCUM contains xenolithic diamonds of Archean (3.2-3.3 b.y.) age (Richardson et. al., 1984) and yields low-Ca garnets, inferred to represent disaggregated garnet harzburgites, that are associated with the Archean diamonds (Boyd et. al., 1985; Boyd and Gurney, 1986). Uninflected SCUM paleotemperatures, whether in Archean or Cretaceous, range from 900-1200C (Boyd and Gurney, 1986), but inflected paleotemperatures (Cretaceous) range up to about 1400C.

In southern Africa, at least, diamondiferous kimberlites occur on the craton. Kimberlites occur off-craton as well but are joined by other alkalic magmas, of somewhat younger age, such as carbonate-rich kimberlite, ultrabasic lamprophyre, nephelinite, alnoite, melilitite, and carbonatite (Moore, 1979; McIver and Ferguson, 1979).

SCUM has seen repeated metasomatism of its cold, old, depleted harzburgite. Isotopic systematics in diamond inclusions record an enrichment event perhaps 300 m.y. older than Archean diamond growth (Richardson et. al., 1984). Most peridotite xenoliths from southern Africa have lower $^{143}\text{Nd}/^{144}\text{Nd}$ and higher $^{87}\text{Sr}/^{86}\text{Sr}$ than Bulk Earth and incompatible element contents unreasonably high for depleted harzburgite; model Nd ages of indicated metasomatism are in the range 1.0-1.4 b.y. (Hawkesworth et. al., 1983). Karoo basalts have similar isotopic signatures (Hawkesworth et. al. 1983). Other cratons have seen similar long-term metasomatism that creates SCUM reservoirs for subsequent magmatism (e.g., Superior Province of Canada, Bell et. al., 1982 and Wyoming Province, Dudas et. al., 1986).

Smith (1983) delineated type I and type II kimberlites, with isotopic signatures slightly depleted relative to Bulk Earth and enriched, respectively. Model Nd ages for type II samples (DM) cluster at 0.88 and 1.05 b.y. Model ages and $^{147}\text{Sm}/^{144}\text{Nd}$ of samples do not correlate, suggesting that the kimberlites do in fact represent rather large degrees of melting of metasomatized sources. Type I kimberlites, with a distinctively asthenospheric isotopic signature, in fact are as enriched or more enriched than Type II in REE, HFSE, and Sr (Erlank et. al., 1986), their lower contents of Rb, Ba, and K presumably reflecting lower modal phlogopite. Thus type I kimberlites appear to have as enriched a source as Type II but with an enrichment age close to the age of kimberlite magmatism. In detail, trace element patterns prevent any direct linkage of kimberlite source regions and metasomatism that produced enriched garnet peridotite, K-richrichterite peridotite, or MARID suites (Erlank et. al., 1986).

Diamondiferous lamproites from Western Australia are similar to Type II kimberlites in $^{143}\text{Nd}/^{144}\text{Nd}$ (and in model ages: 0.9-1.3 b.y.) but have even higher $^{87}\text{Sr}/^{86}\text{Sr}$ (M.T. McCulloch et. al., 1983), implying enriched sources.

Is there any asthenospheric contribution to kimberlite or lamproite generation? Asthenosphere certainly underlies the region of kimberlite generation, at depths that have been estimated from 180 to 400 km, and may diapirically rise (H.W. Green and Gueguen, 1974), perturbing temperatures of "kinked" geotherms, providing heat for generation of kimberlite melts, and possibly contributing to the porphyroclastic textures observed in peridotite xenoliths (Dawson, 1985). Asthenospheric melts may cause the "precursory" Fe-Ti metasomatism that produces ilmenite-bearing peridotites (Ehrenburg, 1982), or marginal zoning on grains in porphyroclastic peridotites (Smith and Boyd, 1986).

There have been repeated suggestions that kimberlites represent mixtures of high-temperature asthenospheric melts and carbonate-rich lithospheric melts. Such models have severe geochemical problems, because essentially all the budget of incompatible elements must come from the lithosphere. Moreover, type I kimberlites, with high Nd contents, show isotopically no evidence of long-term LREE-enrichment and thus cannot have come from a long-term carbonate-rich lithospheric reservoir.

Maximum depths of generation of kimberlite melts presumably exceed deepest paleodepths of entrained xenoliths, i.e., about 200 km. Temperatures of generation must exceed the kimberlite solidus, 1200C (Eggler and Wendlandt, 1979) but plausibly are as high as the Eggler-Wendlandt liquidus, 1500C, where four-phase peridotite is essentially on the liquidus. The hottest paleotemperatures of xenoliths also approach 1500C. Sources probably contain four-phase peridotite + magnesite + phogopite + minor phases containing important incompatible elements. The f_{O_2} of such a carbonate-bearing source cannot be lower than EMCD (enstatite-magnesite-olivine-diamond) and plausibly is at EMCD. Any fluids present at such conditions are primarily H₂O with minor CO₂. There is no necessity, however, for any fluid to be present at all and certainly none is present after melting commences. In fact, entry of fluids, CH₄-H₂O or H₂O-CO₂, into lithosphere from asthenosphere is unlikely because asthenosphere is probably partially melted.

In the model of Wyllie (1980), kimberlite generation actually begins with crack propagation at about 80 km depth near a postulated "blip" in the peridotite solidus. In the other principle model of peridotite melting (Olafsson and Eggler, 1983; Eggler, 1986), the solidus kinks in the same pressure region, although for different reasons, and peridotite diapirs (or melts that equilibrate with peridotite) may or may not freeze as they pass through that region, depending on CO₂/H₂O ratio. In Wyllie's model, cracks form by fluid release and propagate back into the deeper region of kimberlite generation.

KIMBERLITE FROM LITHOSPHERE BASE TO CRUST

Once kimberlite is generated at about 200 km, it probably rises fairly quickly through the lithosphere. Spera (1984) calculates ascent rates of 0.4-7 km/hr for alkali basalts, based on criteria including fracture annealing and xenolith sizes.

Dissolution rates of peridotite minerals suggest rates of about 10km/hr (Kuo and Kirkpatrick, 1985). Spera (1984) calculates higher ascent rates (40-100 km/hr) for kimberlites, as do others (less than 36 km/hr for 10-cm-sized xenoliths - Harris, 1985; 15-25 km/hr from exsolution features in clinopyroxenes - McCallister et. al., 1979; 40-70 km/hr from kinetic data on coarsening of olivine neoblasts - Mercier, 1979). (Preservation of diamonds may not be a criterion of ascent rate, in as much as diamonds can survive

hours to months unless they actually oxidize, and in as much as no kimberlites that actually contain diamond-indicator garnets fail to contain diamonds - Gurney, 1985).

Ascent velocities even as low as 1 km/hr require ascent of kimberlites via fractures as opposed to diapirs (Spera, 1984). Lithospheric fractures plausibly extend to within about 2 km of the surface, the typical vertical extent of diatremes (Dawson, 1985). Individual fractures extend down to the 150-200 depth range, based on occurrences such as the predominance of eclogite xenoliths in the Roberts Victor but not in nearby pipes and the occurrence of completely different megacryst assemblages in pipes only a few km apart in the Colorado-Wyoming Front Range (Eggler et. al., 1979). Although there is a general myth that kimberlites ascending these fractures represent "subequal portions of solid, melt, and vapor" (Spera, 1984), kimberlites in fact contain relatively small amounts of mantle-derived macrocrysts or xenoliths (Clement et. al., 1984). Moreover, having begun their life without fluid (see above), they are unlikely to evolve fluid during mantle ascent unless they in fact freeze in their narrow conduits ("heat death" of Spera, 1984). Although Spera (1984), like McGetchin and Ullrich (1973), calculated ascent rates assuming melt-fluid mixtures, magma fracture alone can propagate cracks at km/hr rates (Spence and Turcotte, 1984).

Major changes in kimberlite phase equilibria would be expected at about 80 km depth due largely to the instability of dolomite in equilibrium with peridotite assemblages (e.g., Wyllie, 1978; Eggler, 1978). The kimberlite solidus would deviate (fall lower in temperature) from the peridotite solidus, and enstatite could no longer crystallize from kimberlite magma. (The abundance of olivine and rarity of enstatite as macrocrysts or phenocrysts in kimberlite presumably reflect absence of the high-pressure crystallization of enstatite and low-pressure crystallization of olivine). Depending on temperature and CO₂/H₂O, some magmas could freeze and evolve fluid.

No convincing evidence exists for extensive assimilation by kimberlite magmas in the upper mantle, at least those that reach the crust, nor for crystallization except possibly olivine macrocrysts or microphenocrysts.

KIMBERLITES IN THE UPPER CRUST

Kimberlites undergo tremendous modification in the crust from high temperature magmas to the apparently low temperature rocks observed (matrices of phlogopite, carbonate, serpentine, diopside, and monticellite - Clement et.

al., 1984). Assimilation also occurs, producing anomalously high-SiO₂, high-Al₂O₃, and high Na₂O kimberlites (Clements et. al., 1984). Details of crystallization are unclear, including how much crystallization of the observed matrices is subsolidus or hydrothermal or both.

Many kimberlite dikes culminate in diatreme pipes, with crater-facies epiclastic and tuffaceous kimberlite at their tops and root zones at their bases, for a total extent of about 2.5 km. Some dikes do not vent, however, and root zones may be intruded by separate hypabyssal kimberlites (Dawson, 1985). Although expansion of exsolved gas can account for the implied high ascent velocities and fluidization, Clement (1982) has ascribed much of the brecciation to magmatic stoping and fracturing. He postulates that pipes develop by explosive breaching of the surface from only 0.5 km and that diatremes represent downward extension of the fluidized system, incorporating early magmatically-brecciated rocks.

COEXISTING CARBONATITIC, ULTRAMAFIC AND
MAFIC MELTS IN THE LITHOSPHERE: EVIDENCE FROM
SPINEL LHERZOLITE XENOLITHS, NW SPITSBERGEN

H.E.F. Amundsen

Mineralogisk-Geologisk Museum,
Sars gt. 1, 0562 OSLO 5, Norway

Abundant xenoliths of lower crust and upper mantle material occur in Quaternary volcanic centres on NW Spitsbergen. Xenolith P/T data indicate a thin (27 km) continental crust and high geothermal gradient (9kb/950°C - 17kb/1150°C; Amundsen et al., 1987). Spinel lherzolite xenoliths contain quenched liquids representing three different origins: 1) Melts introduced into the lherzolite material shortly prior to or during eruption; 2) Melts formed by incipient fusion of the lherzolite assemblage; 3) Trapped melts associated with amphibole + apatite + phlogopite.

Shortly prior to or during eruption, Ti, Na, K, P - rich basaltic melt (L_B) infiltrated the lherzolite material along cracks and grain boundaries. L_B locally carries abundant immiscible droplets of ($H_2O + CO_2$) - rich ultramafic silicate melt (L_U) and Mg - rich carbonatite melt (L_C). During quenching both L_U and L_C crystallized spherulitic ankerite + dolomite + magnesite, leaving a residual H_2O - rich ultramafic silicate melt (eg 58.0% SiO_2 , .03% TiO_2 , .08% Al_2O_3 , .02% Cr_2O_3 , 3.9% FeO, 26.9% MgO, .22% NiO, .38% CaO, .07% Na_2O , .08% K_2O , 10.2% LOI) in droplets of L_U . Some samples show infiltration of L_U alone.

Melts formed by incipient fusion of the lherzolite assemblage (L_B^*) typically occur surrounding corroded spinel grains, or are associated with breakdown of amphibole + phlogopite. $L_U + L_C$ commonly occur as immiscible droplets in these melts, indicating that incipient fusion may have been promoted by introduction of $L_U + L_C$ alone, shortly prior to or during eruption. L_U showing this mode of occurrence ranges from carbonate - bearing (Fig.1) to carbonate free.

Amphibole + apatite + phlogopite occur in some lherzolites, either evenly distributed or concentrated in amphibole - rich selvages. Trapped melts are ubiquitous in these samples, occurring both interstitially in large (up to 1 mm) polygonal cavities, and as rounded inclusions in lherzolite phases and in amphibole. L_U and Mg to Ca - rich L_C both show this mode of occurrence, and petrographic evidence indicates that they are residual after crystallization of the hydrous phases. L_U in these samples is compositionally similar to L_U in the infiltrating fluid assemblages, but is usually carbonate - free and may contain small amounts of Al, Ca, K and up to 3% NiO (eg 53.3% SiO_2 , .11% TiO_2 , 4.7% Al_2O_3 , .12% Cr_2O_3 , 8.9% FeO, 21.4% MgO, 2.1% NiO, 1.0% CaO, .06% Na_2O , .28% K_2O , 7.9% LOI). Similar trapped fluids also occur in several anhydrous lherzolites.

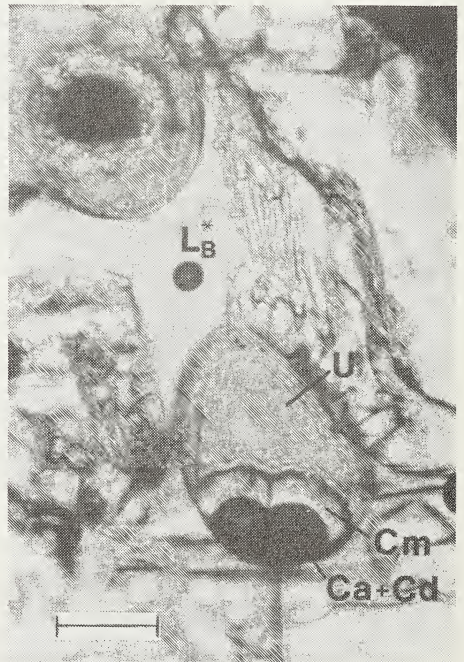


Fig. 1: Droplets of carbonatebearing L_U in L_B^* in incipiently melting lherzolite. U = Ultramafic glass; Ca = ankerite; Cd = dolomite; Cm = Magnesite. Scale bar = .05 mm.

Modification of the infiltrating melts by resorption of lherzolite phases, and fractional crystallization of $Cpx + Ol + Sp$, make direct comparisons between L_B and host basalts (basanites - hawaiiites) difficult. However, host basalts resemble L_B with regard to Ti, Al, Na, K, P, and they themselves contain scattered, apparently immiscible, droplets of $L_U + L_C$. Both L_U and L_C have much lower densities than L_B , and $L_U + L_C$ occur alone in several xenoliths, infiltrating along cracks and grain boundaries, as immiscible droplets in partial melts or as inclusions in minerals, indicating that gravitational separation of immiscible liquids has occurred at depth both prior to and during the eruption. It seems unlikely that the assemblage of melts infiltrating the xenoliths could have migrated any significant distance without separating. This suggests the existence of a homogeneous "protomelt", which unmixed into immiscible $L_B + L_U + L_C$, at some stage during upwards migration. It seems likely that the host basalt at some stage originated by gravitational separation from an assemblage of melts similar to that infiltrating the xenoliths. The onset of immiscibility, and subsequent liquid fractionation, may be the prerequisite factor triggering explosive alkaline volcanism.

Reconstruction of the protomelt by reintegrating the melt assemblage infiltrating xenoliths is not straightforward. However, $L_U + L_C$ constitute up to 30 - 50% of the infiltrating melts, indicating a strongly undersaturated protomelt with kimberlitic or lamproitic affinities (rich in Mg, Ni, CO_2 , H_2O).

Coexisting L_B (or L_B^*) + $L_U + L_C$ define a previously unknown field of liquid immiscibility, occurring in primitive ($CO_2 + H_2O$)-rich magma compositions under upper mantle P/T conditions. This field covers a range of compositions, which include ultramafic lamprophyres, kimberlites, carbonatites and some alkaline basalts. Petrographic evidence shows that L_U may contain considerable amounts of L_C - component and (to a lesser extent) vice versa, indicating closure of the immiscibility - field along the $L_U - L_C$ boundary, most likely with increasing T and/or P. Coexisting $L_B^* + L_U + L_C$ from two representative samples are plotted in the pseudoternary Greig - diagram of Weiblen and Roedder (1973) in figure 2.

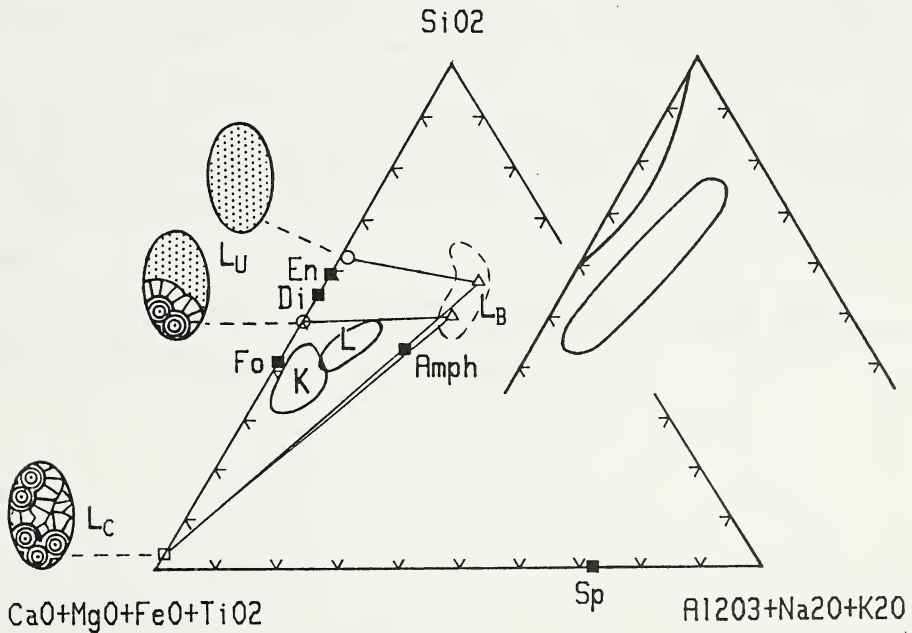


Fig. 2: Pseudoternary Greig diagram showing coexisting $L_B^* + L_U + L_C$ from two representative samples ($L_U - L_C$ tielines omitted); stippled outline shows compositions of L_B and L_B^* coexisting with $L_U + L_C$. Also shown are compositional fields for ultramafic lamproites from western Australia (L) and Kimberlites (K). Inserted figure shows two - liquid fields occurring in the system leucite-fayalite - SiO_2 (Weiblen and Roedder 1978) for comparison.

Major and minor elements and volatiles are strongly fractionated between the co-existing liquids: Ti, Al, Na, K, P are partitioned into L_B (or L_B^*); Mg, Ni, $H_2O + CO_2$ are partitioned into L_U ; Mg, Fe, Ca, show variable partitioning into L_C . The strong partitioning of incompatible elements into L_U has important implications for storage and migration of Ni (and other siderophile elements ?) in the upper mantle. The existence of ultramafic melts, resembling high degrees of melting of residual mantle material, in apparent equilibrium with an amphibole lherzolite assemblage, puts a new perspective on interpretations of komatiites. Formation of such melts could be linked to relatively low - T processes in a ($CO_2 + H_2O$) - rich primitive mantle.

Mass balance calculations, combined with constructed immiscibility fields, show that introduction of basanite (L_B) + $L_U + L_C$, with subsequent crystallization of amphibole + apatite + phlogopite, may account for the observed association of these phases and trapped liquids. Thus, the presence of amphibole + apatite + phlogopite in these lherzolites may be due to interaction between mantle wallrock and kimberlitic liquids, migrating up from a deeper source in the underlying mantle. A similar origin has been proposed for amphibole - apatite rich xenoliths from Kiama, Australia (eg Wass et al., 1980).

The NW Spitsbergen lherzolite xenoliths show that both carbonate - silicate and silicate - silicate immiscibility are important processes under upper mantle P/T - conditions, and suggest a genetic link between introduction of kimberlitic liquids in the upper mantle and the generation of carbonatites and alkaline basalts.

References:

- Amundsen, H.E.F., Griffin, W.L. and O'Reilly, S.Y. (1987) The lower crust and upper mantle beneath northwestern Spitsbergen: evidence from xenoliths and geophysics. In prep.
- Wass, S.Y., Henderson, P and Elliot, C.J. (1980) Chemical heterogeneity and metasomatism in the upper mantle - evidence from rare earth and other elements in apatite - rich xenoliths in basaltic rocks from eastern Australia. Roy.Soc.Lon. A, 297, pp 333-346.
- Weiblen, P.W. and Roedder, E. (1973) Petrology of melt inclusions in Apollo samples 15598 and 62295, and of clasts in 67915 and several lunar soils. Proc.Fourth Lunar Sci. Conf., Geochim.Cosmochim.Acta Suppl.4, Vol.1, pp681-703. Pergamon Press.

¹Max-Planck-Institut für Chemie, Saarstrasse 23, D-6500 Mainz, F.R.Germany;
²Vernadski Institute, Akademia Nauk USSR, Moscow, USSR

The solubility of CO₂ was measured as a function of pressure at liquidus temperatures in complex kimberlitic, olivine melilititic and carbonatitic compositions. The chosen compositions were characterized by (in wt.-%) 35.9% SiO₂, 35% MgO, 8.7% CaO in the kimberlitic composition and ranged between 39 to 5% SiO₂, 13 to 28% CaO at app. 16% MgO in olivine melilitic and carbonatitic compositions. CO₂ solubility in kimberlite increases from 5.7 wt.-% at 20 kb to 9.8 wt.-% at 30 kb and 11.9 wt.-% at 40 kb. There seems to be no increase from 40 to 50 kb. The solubility of CO₂ at 20 kb is lower in kimberlite than in the Ca-rich olivine melilitite of similar SiO₂ content, at 30 kb it is however very similar. This is probably due to preferred complexing of a carbonate molecule with Ca at lower pressures while at higher pressures Mg is equally well suited. CO₂ solubility increases at 30 kb from 9 wt.-% for the olivine melilitite composition to 37 wt.-% for the carbonatitic composition and is linearly dependent on the CaO content of the melt. An increase from 10 to 30 kb raises the CO₂ solubility by 6 wt.-%, independent of composition.

The CO₂-saturated liquidus temperatures for the kimberlite composition chosen range from 1460°C at 20 kb to 1690°C at 50 kb with olivine as the liquidus phase from 20 - 40 kb and olivine and orthopyroxene at 50 kb. It has been shown (Brey, 1976; Eggler and Wendlandt, 1977) that in systems with both CO₂ and H₂O garnet, magnesite and possibly clinopyroxene come close to the liquidus of kimberlitic compositions in addition to olivine and orthopyroxene. This may also be true for pure CO₂ systems at higher pressures. Thus kimberlites may indeed be partial melting products of a peridotitic mantle (see also Wyllie, 1980).

In the series of compositions from olivine melilitite to carbonatite the liquidus phases change at 30 kb from garnet + clinopyroxene to clinopyroxene only, then to olivine + clinopyroxene and finally to periclase for the carbonatitic composition. The field of periclase expands dramatically at lower pressures to SiO₂-richer compositions. Periclase is the liquidus phase at 5 kb for a composition with 23 wt.-% SiO₂. Carbonatitic melts generated at depth in a peridotitic mantle with CO₂ as the only volatile species will, on ascent, immediately crystallize periclase, become SiO₂-rich by fractional crystallization and cannot reach the earth's surface. This is only possible in the additional presence of H₂O since water expands the stability of silicates towards carbonatitic compositions.

REFERENCES

- BREY, G.P. 1976. Ph.D. Thesis, Australian National University, Canberra, unpub.
EGGLER, D.H. and WENDLANDT, R.F. 1977. Extended Abstracts, **Second International Kimberlite Conference**.
WYLLIE, P.J. 1980. *J. Geophys. Res.* 85, B12, 6902-6910.

NODULE ASSOCIATIONS FROM OUACHITITE AND CAMPTONITE LAMPROPHYRES,
WESTERN OTAGO AND SOUTH WESTLAND, NEW ZEALAND

C.G. Brodie and A.F. Cooper
Geology Department, University of Otago, Dunedin, New Zealand

The Alpine dyke swarm of western South Island, New Zealand comprises a suite of highly alkaline lamprophyres with associated tinguaitite, trachyte and carbonatite differentiates (Cooper 1986). Intrusion of dykes, sills and diatremes occurred in late Oligocene-early Miocene times along tension joints and shears related to the propagation of the Alpine Fault plate boundary through southern New Zealand. In an area centred on Haast River, felsic and carbonatitic differentiates occur, and many dykes carry nodules of gabbro, and varieties of syenite. Seismic profiling suggests a subjacent shallow magma chamber. Elsewhere lamprophyres carry mantle-derived nodules and have risen directly from the melt zone without appreciable crustal fractionation.

High pressure nodule-bearing lamprophyres range between end-member feldspar-free ouachitite and feldspar-bearing camptonite. Mineralogically they are composed of olivine (Fo_{76-82}), tiansalite, kaersutite, titanphlogopite or titan-biotite, titanomagnetite or ilmenite, apatite, calcite and occasional perovskite with minor interstitial analcime, sodalite or alkali feldspar in ouachitite and plagioclase in camptonite.

Chemically both lamprophyre types are highly alkaline ultrabasic rocks with marked degrees of undersaturation expressed normatively by high ne, common lc, and, when calculated on a volatile-free basis, cs. Nodule-bearing dykes have high Cr, Ni and Mg values suggesting near primitive melts. As with other members of the swarm lamprophyres exhibit highly fractionated REE patterns with $(La/Yb)_N$ in the range 14.8 to 46.2. Enrichment in large ion lithophile (Th, Ba, Rb, Sr) and high field strength (Ti, Ta, Nb) incompatible elements, together with the REE data, indicates similarity to within-plate alkaline rocks. Lamprophyres are thus chemically equivalent to hydrated and carbonated nephelinites with ouachitites approaching melilite-nephelinite and camptonite transitional to nepheline basanite.

Nodules of inferred high pressure origin in ouachitites and camptonites can be divided into three main types: Cr-diopside series, Al-augite series, and amphibole-apatite series. Megacrysts of pargasite-kaersutite, clinopyroxene (ranging from endiopside, through titanaugite and tiansalite, to sodian ferrosalite), olivine, biotite, and titanomagnetite occur in many dykes, but it is often unclear as to whether such crystals are comagmatic or xenocrystic.

Cr-diopside series nodules have a textural variation ranging from coarse equant to porphyroclastic, with minerals typically showing effects of deformation in the kink banding of olivine and orthopyroxene. In order of abundance nodules comprise spinel harzburgite, spinel lherzolite and wehrlite. Typically olivine (Fo_{90-93}) and a low Ca-Al enstatite (En_{89-92}) dominate, with minor chrome diopside and Cr-spinel or chromite ($Cr/Cr + Al$ 0.55 to 0.80). Cr-diopside occurs as discrete grains and as a component of intergrowths with spinel. The symplectites being interpreted as forming by exsolution from orthopyroxene. Titanian chromian magnesio-hastingsite (dissimilar in composition to the amphibole of the host ouachitite) and phlogopite occur by partial replacement of Cr-diopside, indicating metasomatic alteration of lherzolite at depth. One composite nodule shows a phlogopite-Tr-Cr-magnesio-hastingsite-bearing lherzolite intruded by a vein of pargasite-diopside-phlogopite-apatite-calcite. Lherzolite phases show a progressive decrease in Mg towards the vein over a distance of 1.5cm (e.g. olivine Fo_{91} is replaced by Fo_{84}). Vein mineral chemistry is totally dissimilar to that of the host ouachitite suggesting an episode of diffusion, related to magma intrusion, postdating the pargasite-phlogopite metasomatic alteration of lherzolite, but predating entrainment of the nodule.

Comparison of amphibole- and phlogopite-free Cr-diopside series nodules with similar examples worldwide (Frey and Green 1974; Frey and Prinz 1978) shows typical enrichment in MgO , Cr, Ni and Cu and low concentrations of Al_2O_3 , CaO , Na_2O , Sr, Ba, Sc,

Nb, Zn and Zr. This chemical signature is compatible with either refractory partial melt residues, or upper mantle fractional crystallization cumulates. The residual hypothesis is preferred.

A variety of mineral geothermometers give estimated temperatures of equilibration ranging from 800° to 1000°C. Pressure estimates are difficult to make, the only constraint being the pressure range 7.5 to 20kb determined for the experimental stability of spinel lherzolite (Green and Ringwood, 1967).

Al augite nodules range in size up to 25cms. They have a variable modal mineralogy spanning all fields in the amphibole-olivine-clinopyroxene classification plot. Nodules are commonly layered with grain morphology suggesting adcumulus growth, but with textures variously modified by deformation and metamorphic recrystallization. Minerals are typically more Fe-rich than equivalent Cr-diopside nodule phases, with olivine (Fo₇₃₋₈₁) having slightly higher CaO contents (up to 0.18 wt%). Clinopyroxene is dominantly a low-Cr Al-augite, richer in jadeite and tschermakite components but poorer in Ti than in the host ouchitite. Exsolution lamellae of ilmenite, titanomagnetite and amphibole are prominent. Amphibole, typically a titanian pargasite, occurs as discrete grains, as lamellae in augite, and as an interstitial phase poikilolithically enclosing augite and olivine. Within a single nodule all forms are compositionally identical. A titanphlogopite (Mg 0.830 to 0.783) occurs in several nodules. Oxides and sulphides are most abundant in amphibole-rich lithologies where combinations of ilmenite (with up to 5.5 wt% MgO), titanomagnetite, hercynite-rich spinel, pyrite and chalcopyrite occur. A single composite nodule shows a dykelet of augite hornblendite of low Mg intrusive into a pargasite peridotite.

Within the Al-augite group, nodules with lowest Mg/Mg + ΣFe (total range 0.685-0.886) are broadly enriched in Al₂O₃, TiO₂, CaO, Na₂O, K₂O, Nb, Zr, Sc, Ba, V, Cr, Ga, Rb, Sr and Y relative to the Ni-MgO₃ rich varieties.² Compositional trends do not parallel low pressure fractionation trends within the dyke swarm but are interpreted to reflect proportions of cumulate phases augite, pargasite, and olivine.

In terms of P-T conditions of formation magnetite-ilmenite geothermometry suggest temperatures of 1100±50°C, but again pressure is not well constrained. The Al^{VI}/ΣAl ratio and jadeite-Ca tschermak content of the clinopyroxene (Thompson 1974) do however suggest equilibration in the range 8-16kb. Amphibole-apatite series nodules are typically small (~2cms) with a heterogeneous, occasionally loosely packed, cumulate texture. Modal proportions are variable but the sequence of crystallization is typically apatite, a pale green sodian ferrosalite containing appreciable acmite, titanomagnetite, biotite, pargasite-kaersutite (Mg 0.44 to 0.52), and sphene. Disaggregated xenocrystic fragments from such nodules, together with Fe-rich orthopyroxene (Mg 0.685 to 0.605) and olivine (minimum Fo₇₂) are common throughout the dyke swarm and are overgrown by groundmass or phenocryst phases resulting in reverse zoning. P-T constraints of amphibole-apatite crystallization are difficult to determine. The presence of sphene constrains the upper pressure limit to 22kb (Hellman and Green 1979). K-Al^{VI} contents of amphibole (Best 1970) suggest pressure lower than those of the garnet lherzolite stability field, a feature these amphiboles share with those from Al-augite nodules. Moreover, Al^{VI}/ΣAl values of coexisting amphibole and clinopyroxene from both amphibole-apatite and Al-augite nodules have similar ratios, displaced to high Al^{VI} values compared to coexisting pairs from alkali gabbro nodules and the phenocryst/groundmass areas of host lamprophyres. On the basis of experimental synthesis high Al^{VI} in both amphibole and clinopyroxene is inferred to indicate high pressure crystallization. The absence of plagioclase and the mineral chemistry of both amphibole-apatite and Al-augite group parageneses suggest derivation from the upper mantle.

In marked contrast to the LIL and LREE enriched character of the dykes Nd-Sr isotope ratios indicate derivation of magmas from a mantle source which has experienced long-term depletion in Nd and Sr. Isotope ratios ²⁰⁶Pb/²⁰⁴Pb (19.19-20.59), ²⁰⁷Pb/²⁰⁴Pb (15.64-15.71) and ²⁰⁸Pb/²⁰⁴Pb (39.03-44.22) indicates high radiogenic Pb requiring unrealistically high values of ²³⁸U/²⁰⁴Pb at the time of lamprophyre generation (Barreiro 1983). Isotope ratios are interpreted as suggesting LREE and incompatible element enrichment of the mantle source, with a timing, constrained by the

Pb data, of no more than 200 my. This petrogenetic scheme is supported by various lines of petrographic, mineralogical and geochemical evidence, including the introduction of amphibole/phlogopite into the lherzolite and the interaction of lherzolite mineralogy with cross-cutting amphibole-rich veinlets. Amphibole-apatite parageneses have been observed elsewhere as occurring interstitially, as intrusive veins, and as partial replacement of lherzolite lithologies (Wass 1979). While such relationships have not been observed in the Alpine dyke swarm the atypical early precipitation of apatite, and the Na-Fe enriched composition of amphibole and clinopyroxene suggest crystallization from a fractionated magma or fluid which might also be capable of producing metasomatism of the required chemical signature. Although amphibole apatite series nodules may have crystallized in any or all three metasomatic-magmatic events inferred petrographically (*viz* initial hydration/carbonation of the mantle, magmatism resulting in Al-augite cumulates, or the late Oligocene-early Miocene phase of lamprophyre genesis), the lack of deformation suggests an origin late in this sequence.

It is envisaged that magmas originating by partial melting of hydrated and carbonated garnet lherzolite rose to higher levels of the mantle fractionating en route to produce the cumulate members of Al-augite series lithologies. As a consequence of the shape of the peridotite solidus (Olafsson and Eggler 1983) such differentiated magmas would interact with mantle lherzolite at lower pressures, perhaps precipitating phases of the amphibole-apatite series nodules and causing metasomatic alteration of the country rock peridotite. In the late Oligocene-early Miocene rise of volatiles along the newly developed fracture system of the Alpine Fault plate boundary triggered a metasomatic-melting event producing small volumes of primary lamprophyre magma. These magmas incorporated fragments of variously metasomatized and depleted wall rock peridotite (Cr-diopside series nodules) together with crystalline products of earlier magmatism (Al-augite and amphibole-apatite series nodules) and rose into the crust. Locally lamprophyre magmas stagnated in the crust and fractionated to felsic and carbonatitic differentiates, elsewhere they intruded directly to higher levels preserving their primitive compositions.

REFERENCES

- Best, M.G. 1970. Kaersutite-peridotite inclusions and kindred megacrysts in basanitic lavas, Grand Canyon, Arizona. *Contributions to Mineralogy and Petrology* 27, 25-44.
- Barreiro, B. 1983. An isotopic study of Westland dike swarm, South Island, New Zealand. *Carnegie Institution of Washington Yearbook* 82, 471-475.
- Cooper, A.F. 1986. A carbonatitic lamprophyre dike swarm from the Southern Alps, Otago and Westland. In Smith, I.E.M., ed., *Cenozoic Volcanism in New Zealand*. *Royal Society of New Zealand Bulletin* 23, 313-336.
- Frey, F.A. and Green, D.H. 1974. The mineralogy, geochemistry and origin of lherzolite inclusions in Victorian basanites. *Geochimica et Cosmochimica Acta* 38, 1023-1059.
- Frey, F.A. and Prinz, M. 1978. Ultramafic inclusions from San Carlos, Arizona: petrologic and geochemical data bearing on their petrogenesis. *Earth and Planetary Science Letters* 38, 129-176.
- Green, D.H. and Ringwood, A.E. 1967. The stability fields of aluminous pyroxene peridotite and garnet peridotite and their relevance in upper mantle structure. *Earth and Planetary Science Letters* 3, 151-160.
- Hellman, P.L. and Green, T.H. 1979. The role of sphene as an accessory phase in the high pressure partial melting of hydrous mafic compositions. *Earth and Planetary Science Letters* 42, 191-201.
- Olafsson, M. and Eggler, D.H. 1983. Phase relations of amphibole, amphibole-carbonate, and phlogopite-carbonate peridotite: petrologic constraints on the asthenosphere. *Earth and Planetary Science Letters* 64, 305-315.
- Thompson, R.N. 1974. Some high pressure pyroxenes. *Mineralogical Magazine* 39, 768-787.
- Wass, S.Y. 1979. Fractional crystallization in the mantle of late stage kimberlitic liquids - evidence in xenoliths from the Kiama area, N.S.W., Australia. In Boyd, F.R. and Meyer, H.O.A., eds., *The Mantle Sample: inclusions in kimberlites and other volcanics*. *Proceedings of the Second International Kimberlite Conference* 2, 366-373.

C R Clement¹ and A M Reid²

¹ Geology Department, De Beers Consolidated Mines Limited, Kimberley

² Department of Geology, University of Cape Town

INTRODUCTION

Synthesis of information from numerous occurrences indicates that kimberlite pipes are characterised by distinctive root, diatreme and crater zones. These zones are defined by specific contact and internal geological features and by differences in the nature of the infilling material (Hawthorne 1975, Clement, 1982). In this paper a theory of pipe formation is proposed which takes this geological complexity into account and stresses the important contributions of a number of interrelated, precursor, subsurface, genetic processes to the development of kimberlite pipes.

ROOT ZONES

A distinguishing feature of root (hypabyssal) zones is pronounced pipe irregularity in the form of: rapid changes in the dip and strike of contacts; local, low-angle, outward-dipping contacts; splitting of root zones into two or more discrete channels; blocky or serrated pipe contacts; pronounced elongation of the pipes or parts thereof along one or more preferred directions; non-vertical pipe axes; local transitions to partially dyke-like character; and subsurface dome-like or less regular appendages. This morphological irregularity of root zones is commonly related to joint set patterns and other discontinuities in the country rocks.

A second intrinsic feature of root zones is the occurrence of contact breccias which have been formed more or less in situ and consist of monolithological wall rock fragments with, or more commonly, without interstitial kimberlite. Explosion, intrusion and fluidisation breccias occur. Explosion breccias, devoid of kimberlitic material, are the most common form of contact breccia and occur primarily under overhangs (outward-dipping contacts) of country rock. Such contact breccias reach 50m in width and some persist vertically for many tens of metres. They consist of angular fragments (5-50cm) which have not been substantially displaced, as discrete breccia masses or relative to each other, after fragmentation. Minor slumping of the breccias may have occurred. Secondary minerals occur locally in voids between the breccia fragments. Fluidisation breccias also occur under overhangs and, similarly, have not been significantly displaced since their formation. They are kimberlite-free and consist (apart from minor secondary material) of locally derived wall rock. However, unlike explosion breccias, they consist predominantly of moderately to well-rounded "pebbles" or "cobbles". Intrusion breccias are relatively rare and reflect penetration of kimberlite magma along discontinuities in the wall rocks of pipes to produce country-rock/kimberlite "stockworks" of limited size (up to 30m in width). Partial or complete detachment of angular wall rock blocks at contacts by magmatic intrusion is an associated feature.

Root zones are further characterised by complex internal geology. Commonly several (up to 20 plus) discrete kimberlite and kimberlite breccias (terminology of Clement, 1982; Clement and Skinner, in press), separated by sharp or gradational contacts, are present. Although they may differ considerably in respect of petrographic features such as texture, mineralogy and xenolith content and character these intrusions all reflect non-violent emplacement of kimberlite magma. Relatively slow crystallisation is indicated by commonly extensive and complex deuteric alteration of phenocrysts, by widespread, similarly complex, metasomatism of xenocrysts and crustal xenoliths by kimberlite magma/residual fluids and by the hypabyssal (subvolcanic) nature of the intrusions. Bulk composition determinations of these intrusions commonly indicate extremely high levels of volatile constituents relative to most other ultrabasic rocks.

DIATREME ZONES

Classical views of the nature of kimberlite pipes reflect the well known morpho-

logical features of the diatreme zones. The main features of the latter are: regular shapes (inverted truncated cones); steep (80° - 85°) joint-bounded, smooth contacts (rare but in some instances extensive contact breccias do occur); vertical axes; and considerable vertical extent (up to ~ 2 km). Typically diatreme zones contain tuffitic kimberlite breccias (Clement, 1982, Clement & Skinner, in press) which consist of abundant, small (mainly microscopic to 5cm across), angular, generally unaltered country rock xenoliths, complex assemblages of juvenile lapilli, mantle-derived xenoliths, discrete or broken kimberlite minerals and xenocrysts from mantle and crustal sources. These components are set in a matrix which consists in considerable part of minerals formed by vapour - phase crystallisation (or minerals which are the products of vapour condensates). Primary matrix mineralogical character is, however, commonly masked by extensive secondary alteration.

Huge down-raftered masses of country rock (floating reefs) commonly occur in peripheral locations in diatreme zones. Many of these masses are extensively brecciated, are devoid of kimberlite and closely resemble some root zone contact breccias (eg. kimberlite-free explosion breccias). Other floating reefs occur as competent down-raftered masses.

CRATER ZONES

Preserved examples of crater zones rarely exceed 300m in depth. They are rudely circular and have relatively flat (50° - 70°) contacts. The surrounding wall rocks are commonly brecciated and the craters contain complex assemblages of pyroclastic and epiclastic kimberlite.

MODEL OF FORMATION

Root zone features - notably the complex morphology, the number, hypabyssal character, internal contact relationships and distribution (in relation to relative ages) of discrete intrusions (and contact breccias), the occurrence, at different stratigraphic levels, of contact breccias (commonly under overhangs that appear to be breached arches) and the presence of blind extensions (which may show several of the above features) - suggest that kimberlite pipes are initiated by intermittent, subsurface, upward-migrating processes. It is proposed that these processes lead eventually to irregular embryonic "pipes" that have developed upwards, from depths of 2-3km, to within 500m of surface and are bounded by extensively brecciated wall rocks. Existing root zones are interpreted as remnants of such embryonic pipes.

It is considered that the genetic processes that are consistent with root zone features and are responsible for root zone (and hence embryonic pipe) formation and upward migration involve all or combinations of the following: hydraulic fracturing and wedging, magmatic stoping and intrusion brecciation, explosive and/or implosive brecciation, spalling, slumping and, possibly, rock bursting from temporarily free faces. Certain kimberlite-free contact breccias imply explosive brecciation resulting from the sequential release of PAV energy through the processes of second boiling and subsequent decompression, as proposed by Burnham (1985). Some similar breccias may reflect implosion of volatiles (previously rammed into the country rocks) due to pressure release caused, for example, by temporary withdrawal of magma. An additional possibility is that some kimberlite-free contact breccias reflect subsurface explosive interaction between rising magma and relatively deep, local, reservoirs of meteoric water. Such interaction seems unlikely, due to pressure constraints, at depths of 2-3km below the paleosurface. It may, however, have occurred, in some instances, near the tops of embryonic pipes (in near-surface environments).

The original presence of extended root zones (embryonic pipes) is indicated by rare, preserved, contact breccias within diatreme zones, by the nature of brecciated floating reef masses (interpreted as detached, down-slumped, contact breccia), by transitional morphological relationships between diatreme and root zones, by the occurrence of breached arches at different (successive) levels in the root zone remnants of embryonic pipes, by transitions between diatreme facies and hypabyssal facies kimberlites and, less directly, by the shallow nature of crater zones. The upward extension of embryonic pipes is considered to be terminated by explosive outburst (formation of craters). Explosive breakthrough is probably accompanied by

depressurisation-induced authigenic brecciation of the margins of the upper parts of embryonic pipes (extending and intensifying previously formed contact breccias).

The formation of diatreme zones is ascribed to the development, following explosive outburst, of vapour-liquid-solid fluidised systems. The fluids involved are believed to consist primarily of exsolved CO₂ and H₂O, a situation consistent with the geochemical character of kimberlites. However, the fluidising fluids may be contaminated by meteoric water in many instances. Due to rapid depressurisation and attendant vapourisation and adiabatic expansion, these systems are believed to have evolved rapidly down embryonic pipes. Diatreme zones reflect the partial to complete incorporation, into these downward-migrating fluidised systems, of the breccia "envelopes" surrounding the embryonic pipe columns (plus other slumped or plucked country rock blocks and floating reefs). The diatreme zones thus contain complex assemblages of juvenile lapilli (autoliths, pelletal and less regularly-shaped lapilli) and xenolithic material. More or less regular-shaped diatreme conduits, commonly bounded by joint planes, are formed. The fluidisation events are considered to be short-lived and to wane rapidly from "lean-phase fluidisation" (capable of considerable pneumatic transport of solids) to "bubbling bed" (quiescent fluidised bed) systems, prior to rapid quenching.

Following the cessation of explosive outburst, the concomitant deposition of pyroclastic material and deflation accompanying final (interstitial) consolidation (vapour-phase crystallisation), cyclical deposition of epiclastic kimberlite (derived from ejectamenta surrounding the crater) occurs. An unresolved problem is the extent to which phreatomagmatic activity, resulting in pyroclastic outflow (base surge) and other pyroclastic deposits, plays a role in the formation of crater zones. Lorenz (pers. comm.) postulates that certain bedded units in the Orapa and Jwaneng craters (Botswana) are pyroclastic flows (probably base surge deposits). However, detailed studies which unambiguously confirm the occurrence of such material have not been undertaken at these (or other) localities. Phreatomagmatic activity may play a role in the development of the crater zones of kimberlite pipes. However, any theory which ascribes the formation of the pipes in toto primarily to this eruptive mechanism ignores (amongst other things); the genetic implications of the root zones, the petrographic nature of diatreme-facies kimberlite and the potential of magmas such as kimberlite to exsolve abundant juvenile volatiles on entering low-pressure regimes.

Irregularities in pipe morphologies and internal textural and mineralogical variations in part reflect multiple genetic events within major pipes. The genetic cycle outlined above may be repeated several (many) times, at varying intervals. Geological complexity may be further enhanced by interrupted (incomplete or aborted) or overlapping intrusive-explosive cycles and by variations in the nature, intensity, depth (relative to the paleosurface) and duration of specific formational/emplacement processes, during repeated cycles of subvolcanic-volcanic activity.

Secondary (post-volcanic activity) alteration, particularly along the diatreme contacts, results in volume adjustments (increases) within pipes. These volumetric increases cause slicken-siding along contacts and minor thrust faulting, particularly near surface, within the pipes.

REFERENCES

- Burnham, C W, 1985. *Economic Geology*, 80, 6, 1515-1522.
- Clement, C R, 1982. Unpublished Ph.D. Thesis, University of Cape Town.
- Clement, C R and Skinner E M W. In Press. *Geological Society of Southern Africa*.
- Hawthorne, J B, 1975. *Physics and Chemistry of the Earth*, 9, 1-15. Pergamon Press, Oxford.

A.D. Edgar⁽¹⁾, M. Arima⁽¹⁾, D.K. Baldwin⁽¹⁾, D.R. Bell⁽²⁾, S.R. Shee⁽³⁾,
E.M.W. Skinner⁽⁴⁾ and E.C. Walker⁽¹⁾

- (1) Department of Geology, University of Western Ontario, London, Canada N6A 5B7.
(2) Department of Geology, California Institute of Technology, Pasadena, CA 91125.
(3) Anglo American Research Laboratories, Johannesburg, S. Africa.
(4) Geology Department, DeBeer Consolidated Mines Limited, Kimberley, S. Africa.

Phase relations of an aphanitic kimberlite from the Wesselton mine, Kimberley, South Africa have been determined at 10-40 K bar and 1000-1525°C. This kimberlite is fine-grained with low macrocrystic olivine content which distinguishes it from other macrocrystic Type I kimberlites from the same locality. From this study, crystallization paths in the aphanitic kimberlite at depth can be compared with those inferred from its petrography and some suggestions made as to the source material for this unusual kimberlite.

PETROGRAPHY AND GEOCHEMISTRY

The petrography and geochemistry of aphanitic and macrocrystic Wesselton kimberlites (Shee 1984) indicate that the aphanitic varieties can be distinguished by olivine microphenocrysts in a groundmass of calcite, monticellite, ilmenite, spinel, perovskite, apatite, serpentine and rare phlogopite. Xenocrysts of olivine and phlogopite and xenoliths only occur in trace amounts. Whole rock analyses indicate Mg/Mg + Fe, K/K + Na and Ca/Ca + Mg ratios range from 0.80-0.86, 0.13-0.81 and 0.24-0.29 respectively. Olivine microphenocrysts have Mg/Mg + Fe of 0.83-0.95. Groundmass monticellites have Mg/Mg + Fe of 0.92-0.94, spinels have chromite-rich cores and titanomagnetite-rich rims.

EXPERIMENTAL METHODS

Experiments were done in a 1.27 cm piston-cylinder apparatus in Fe-soaked Pt, Pt and Ag₅₀Pd₅₀ capsules. Pressures and temperatures are considered accurate to ±0.5 K bar and ± 5°C respectively. Runs were buffered at f_{O_2} s equivalent to $\Delta QFM \ll NNO$ buffers by the graphite furnaces used (Brey and Green 1975). Experiments were done with no added volatiles ($X_{CO_2} = CO_2 / (CO_2 + H_2O) \text{ mol.} = 0.24$) and with CO_2 added as $Ag_2C_2O_4$ at $X_{CO_2} = 0.52$. Identification of products was made optically, by X-ray diffraction and by electron microprobe.

RESULTS

Results of experiments at $X_{CO_2} = 0.24$ (Fig. 1a) show that olivine, clinopyroxene, spinel, monticellite, perovskite and calcite are primary crystalline phases. Quench and primary phases were distinguished by their morphology and/or composition. Olivine is on the liquidus up to 40 K bar with spinel and clinopyroxene as additional phases at 5-65°C and 60-135°C below the liquidus respectively. At slightly greater than 40 K bar the "spinel in" curve intersects the liquidus (Fig. 1a) resulting in olivine + spinel as the liquidus assemblage. Calcite is the primary carbonate about 70°C subliquidus at 35 K bar to >300°C at 10 K bar. Below about 13 K bar, 1000-1250°C monticellite occurs with olivine + spinel + perovskite + calcite. Clinopyroxene is absent in all runs with monticellite, suggesting some type of reaction relationship. Distinction between primary and quench perovskite is difficult but appears to lie at temperatures below "calcite in" curve (Fig. 1a).

The effect of increasing CO_2 to $X_{CO_2} = 0.52$ is shown in Fig. 1b. In these runs identification is more difficult due to the abundance of fine-grained quench products. The liquidus is at a slightly higher temperature and the olivine + spinel + calcite near liquidus assemblage gives way to clinopyroxene + olivine + spinel + calcite at slightly greater than 35 K bar. The incoming of clinopyroxene occurs near the liquidus at 35 K bar decreasing to >100°C below the liquidus at 20 K bar. In contrast to the lower X_{CO_2} experiments (Fig. 1a), calcite occurs in all runs presumably due to the higher a_{CO_2} . As clinopyroxene increases with decreasing temperature, dolomite crystallizes as a second carbonate phase possibly caused by the depletion of Ca in residual liquids. Below the "dolomite in" curve, olivine is rare or absent. The nature of the products of these runs does not permit unequivocal identi-

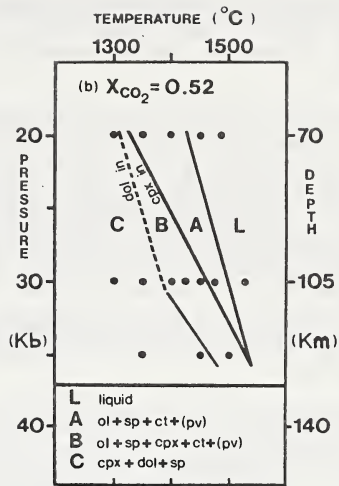
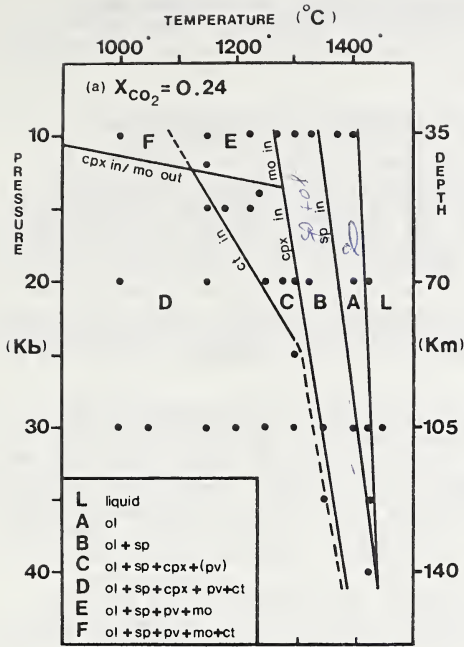


Fig. 1. Experimental results (a) $X_{CO_2} = 0.24$. No added volatile (b) $X_{CO_2} = 0.52$. Abbreviations -- ol-olivine, sp-spinel, cpx-clinopyroxene, pv-perovskite, mo-monticellite, ct-calcite, dol-dolomite. Brackets indicate phase may or may not be present.

fication of either of these carbonates as primary.

Analyses of olivines show Mg/Mg + Fe of 0.90-0.98. These ratios do not differ appreciably between runs done with Fe-soaked and non Fe-soaked Pt capsules suggesting that Fe loss to the Pt was not a major problem. Clinopyroxene, although difficult to analyse due to its fine grain size, appears to be fassaite with high CaO and Al[IV]. Monticellite has Mg/Mg + Fe ranging from 0.82-0.94. Perovskite analyses generally have low totals, possibly due to the presence of high Nb and REE contents (c.f. Shee, 1984; Mitchell, 1984). Although most spinel analyses are semiquantitative due to their fine-grain size, they appear to be aluminous magnesioferrite (Mg/Mg + Fe = 0.32-0.50) and rare aluminous magnesiochromite (Mg/Mg + Fe = 0.54-0.58).

DISCUSSION

These experiments can be used to indicate the possible polybaric crystallization path of the aphanitic kimberlite, to compare this path with that inferred from its petrography, to compare the mineral chemistry of the experimental and natural products, and to draw some implications as to the source material of this magma. Mineralogically, the basic differences between the experiments and the rock are the occurrence of clinopyroxene exclusively in the experiments, and ilmenite and phlogopite occurring exclusively in the rock.

The assemblage of olivine and olivine + spinel close to the liquidus between 10-40 K bar in low X_{CO_2} runs (Fig. 1a) is in accordance with their occurrence as early-formed microphenocrysts in the rock. The conditions under which the kimberlite began its rapid ascent are constrained by the results at low X_{CO_2} (Fig. 1a). The moderate temperature gap between the "spinel in" and "clinopyroxene in" curves; the antipathy between clinopyroxene and monticellite-bearing assemblages, with the latter restricted to the lower P-T range of the experiments, and the absence of clinopyroxene in the rock suggest that ascent may have begun at $>1400^{\circ}C$ at >140 km. At depths of about 35 km and $<1250^{\circ}C$ quasi-isobaric crystallization may have begun with clinopyroxene reacting out to form monticellite. At this stage, the kimberlite "took off" aided by the now enriched volatile residual liquid.

The petrography does not indicate the reaction producing monticellite which occurs in the groundmass with spinel and olivine. There is little evidence of spinel being resorbed as implied by a reaction such as clinopyroxene + spinel + $L^1 \rightarrow$ olivine + monticellite + L^{11} . Lack of close association of olivine and monticellite in the

rock suggests a reaction $\text{clinopyroxene} + \text{L}^1 \rightarrow \text{monticellite} + \text{L}^{11}$. This seems unlikely as the liquid compositions would be improbably different. Based on the topology of Fig. 1a, the most feasible reaction is $\text{clinopyroxene} + \text{L} \rightarrow \text{monticellite} + \text{olivine}$.

Liquidus to near liquidus carbonates occur as calcite in low X_{CO_2} and as calcite + dolomite in high X_{CO_2} runs (Fig. 1). The presence of carbonates is well established in high pressure experiments on comparable compositions (Eggler and Wendlandt, 1979; Wyllie, 1980). The apparent contradiction between the presence of calcite as a late-stage groundmass mineral associated with serpentine in the rock and its high pressure stability may be resolved if the aphanitic kimberlite consolidated at $>10000^\circ\text{C}$; temperatures comparable to those suggested for other kimberlites (McMahon et al. 1979).

The presence of minor groundmass phlogopite and its absence in the experiments is likely due to our inability to detect this mineral near the solidus in such a low K_{20} composition.

Variations in the mineral chemistry in the rock and in the experiments may be due to the unrealistically high f_{O_2} in the experiments which is similar to that used for peridotite compositions (Olafsson and Eggler 1983) but slightly higher than that suggested for the Benfontein Kimberlite (McMahon et al. 1979). The Mg/Mg + Fe ratios for olivines in the experiments exceed those in the rock. Assuming appreciable Fe-loss to the Pt-capsules does not occur, then the high f_{O_2} might result in a shift in the equilibrium of $\text{Fe}^{2+} \rightarrow \text{Fe}^{3+}$ causing low Fe olivines. Similarly the Cr-poor, Al-rich spinels in the experiments might result from high f_{O_2} stabilizing Fe^{3+} , thus reducing Cr in the octahedral site in spinels. The characteristic spinel chemistry in kimberlites is formed under polybaric f_{O_2} conditions, not duplicated in the experiments.

The source material for the aphanitic kimberlite is difficult to determine based only on this study. However, by comparison with other experimental studies and from the chemistry of the aphanitic and macrocrystic varieties, some generalizations can be made. The greater degree of SiO_2 - undersaturation and higher normative spinel in the aphanitic relative to the macrocrystic kimberlite at Wesselton, and to the composition used in Eggler and Wendlandt's (1979) experiments makes derivation of the aphanitic from the macrocrystic, or any more SiO_2 -enriched kimberlite improbable. The absence of orthopyroxene under either X_{CO_2} conditions and the relatively low pressure at which olivine is no longer a liquidus phase under the higher X_{CO_2} conditions suggests that the aphanitic Wesselton kimberlite was not derived from a carbonated lherzolite source. Whether such high X_{CO_2} experiments are justified depends on whether the aphanitic kimberlite represents a "degassed" magma.

REFERENCES

- BREY, G. and GREEN, D.H. 1975. The role of CO_2 in the genesis of olivine melilitite. *Contributions to Mineralogy and Petrology* 49, 93-103.
- EGGLER, D.H. and WENDLANDT, R.F. 1979. Experimental studies on the relationship between kimberlite magmas and partial melting of peridotite. In Boyd, F.R. and Meyer, H.O.A. eds. *Kimberlites, Diatremes and Diamonds: Their Geology, Petrology and Geochemistry*. American Geophysical Union, 331-338.
- McMAHON, B.M., HAGGERTY, S.E. and BENCE, R.J. 1979. Oxide mineral chemistry and oxygen fugacities of the Benfontein Sills, South Africa. *Extended Abstracts, Kimberlite Symposium II*, Cambridge.
- MITCHELL, R.H. 1984. Mineralogy and origin of carbonate-rich segregations in a composite kimberlite sill. *Neues Jahrbuch Mineralogie Abhandlung* 150, 185-197.
- OLAFASSON, M. and EGGLER, D.H. 1983. Phase relations of amphibole, amphibole-carbonate, and phlogopite-carbonate peridotite: petrologic constraints on the asthenosphere. *Earth and Planetary Science Letters* 64, 305-315.
- SHEE, S.R. 1984. The oxide minerals of the Wesselton mine Kimberlite, Kimberley, South Africa. In Kornprobst, J. ed. *Kimberlite I: Kimberlites and Related Rocks*, Elsevier, 59-73.
- WYLLIE, P.J. 1980. The origin of kimberlite. *Journal Geophysical Research* 85, 6902-6910.

S.F.Foley

Geology Department, University of Tasmania, Hobart, Australia, 7001.

Lamproites include a range of compositions which have high Mg-number, Ni and Cr, and carry mantle-derived ultramafic nodules, and thus appear to represent little-modified mantle-derived liquids. These range in SiO₂ content from about 40 wt% to at least 51 wt%, and experimental work has indicated that leucite lamproites as silica-rich as 55 wt% could be in equilibrium with mantle minerals at high pressures [Barton and Hamilton 1982]. Petrogenetic models must explain this range of apparently primary magmas, which may be greater than 10 wt% SiO₂ within a single volcanic field, such as the West Kimberley region of Western Australia.

Previous experimental studies on lamproites, kimberlites and other mafic alkaline rocks have emphasised the importance of volatile constituents. These have shown that a range of SiO₂ contents may be attributed to variation in the H₂O/CO₂ ratio, with more siliceous melts resulting from a higher H₂O/CO₂ ratio. However, most lamproites, both silica-rich and silica-poor, have high H₂O but low CO₂ contents, so that the H₂O/CO₂ ratio does not appear to be the controlling factor of the composition of most lamproite suites.

With the aid of experimental results, the discussion of volatile effects is extended to include fluorine and methane. Fluorine contents are high in lamproites [0.3-0.8 wt%], and the presence of methane is compatible with the survival of diamonds in a carbon-bearing, but CO₂-poor mantle.

In simple system experimental studies, fluorine has been shown to increase the stability of mica so that melt compositions will be rich in K₂O and MgO due to the control of melting by residual phlogopite to greater temperatures than in water-rich, fluorine-free conditions [Foley et al. 1986a].

For a water-bearing mantle, the maximum fO₂ stability of diamonds can be modelled by the 'CW buffer' [carbon (as graphite or diamond) + H₂O], which lies midway between IW and MW for temperatures and pressures likely to exist in the mantle. Fluid compositions at CW are dominated by water [~90%], and CH₄ increases with decreasing fO₂ from CW towards IW, where CH₄ > H₂O [Taylor, this volume].

Foley et al. [1986b] developed the hypothesis that the range of lamproite primary magma compositions can be explained simply by pressure variation in melting of a reduced mica-harzburgite mantle with fO₂ between CW and IW due to the effects of the major volatile components H₂O, CH₄ and HF. The effect of all these components on melt structure is to expand the liquidus phase volume of the least polymerised phase, which promotes the production of silica-rich melts such as leucite lamproites. The range in silica content of primary magmas down to those of typical olivine lamproites [40-42 wt%] may correspond to increasing pressure, which is known to cause generation of melts with lower silica contents. Both fluorine and water cause a decrease in the viscosity of the melt, and thus will increase the flow rate of melts in the mantle, facilitating the escape of low-degree melts.

The oxygen fugacity of lamproitic magmas at the time of phenocryst crystallisation can be estimated from the compositions of chrome-spinels occurring as inclusions in olivine phenocrysts, thereby avoiding any weathering effect on measured whole-rock oxidation state. Estimates of fO₂ by this method range from MW to above NNO for different lamproites [Foley 1985]. The proposition of a reduced source thus requires oxidation during magma ascent, which can be achieved by dissociation of ~0.1 wt% H₂O (driven by diffusive loss of H₂) for oxidation between CW and NNO during ascent. This amount of dissociation will be lower still if carbon species are involved in the oxidation.

In order to test the model for lamproite genesis outlined above, high pressure liquidus experiments with reduced volatile mixtures were undertaken on two lamproite compositions spanning the range of silica contents characteristic of primary lamproites [table 1]. The olivine lamproite composition is a likely primary magma composition for the West Kimberley region (estimated by A.L.Jaques). The leucite lamproite is the Gausberg olivine leucitite, which does not differ greatly from leucite lamproites of the West Kimberley region.

Experimental assemblies consisted of an outer Pt or AgPd capsule enclosing two graphite capsules which contained the sample and an iron-wustite mixture respectively. Volatiles were added as a mixture of $Al_4C_3 + Al(OH)_3$ (producing $CH_4 + H_2O$ with residual Al_2O_3) between the graphite capsules, and as distilled water in the sample capsule. The iron-wustite mixture did not buffer the vapour composition at IW (discussed elsewhere by Foley and Taylor), but served to prevent oxidation beyond the H_2O -maximum on the carbon saturation curve [=CW]. Vapour compositions were analysed by mass spectrometer and found to be dominated by water with minor methane, indicating fO_2 just below CW [see Taylor this volume]. Several runs with $CH_4 > H_2O$ enable comparison of charges with variable H_2O/CH_4 vapours. Charges generally did not quench well to glass, and contained disseminated graphite from methane breakdown. Discrimination between primary and quench micas was not difficult due to the large, well-formed nature of primary crystals.

Experimental results and implications

Figure 1 depicts liquidus diagrams for olivine lamproite and leucite lamproite compositions with water-rich fluid compositions at fO_2 just below CW. For the olivine lamproite, garnet does not appear in any of the experiments, and clinopyroxene is restricted to well below the liquidus. This is consistent with models for lamproite genesis in a geochemically depleted mantle. Orthopyroxene does not appear at the liquidus at the pressures studied, but its stability field is greatly increased above 30 kbar, indicating that it probably reaches the liquidus between 45 and 55 kbar. At the changeover from olivine to orthopyroxene as the liquidus mineral, there will be a unique point at which mica also becomes a liquidus phase. This point represents the pressure-temperature conditions at which olivine lamproite may have formed by melting of a phlogopite harzburgite; it is interpreted to lie between 45 and 55 kbar, which is consistent with the occurrence of diamonds in many olivine lamproites.

For the leucite lamproite, orthopyroxene is the liquidus phase at and above 25 kbar, but does not appear at 20 kbar. The phase relations of the leucite lamproite can also be interpreted to indicate an origin by melting of mica harzburgite. Once again, there should theoretically be a unique pressure for a primary magma at which mica reaches the liquidus, below which olivine appears as the liquidus phase. It is considered unlikely that the olivine field would remain narrower than $25^\circ C$ over 5 kbar, which is required for it to fall between the points determined at 15-20 kbar and 1100-1125 $^\circ C$. The appearance of mica at the liquidus over this pressure range can be reconciled with the mica harzburgite melting model by either of the following: [i] the composition studied is not primary, but has crystallised, and subsequently lost, a small amount of olivine at high pressure; or, [ii] the experiments may contain more water than in natural melting conditions. In the latter case the leucite lamproite may represent a primary liquid, but may fall within the phlogopite liquidus phase field at its pressure of origin due to excess H_2O expanding the liquidus phase field of phlogopite. In either case, it is clear that the pressure at which multiple saturation in mica, olivine, and orthopyroxene occurs cannot be much greater than 20 kbar, as constrained by the inflection in the liquidus in figure 1b. These results are taken to support the hypothesis of Foley et al. [1986b] that olivine lamproite and leucite lamproite may both be derived from mica harzburgite in reduced conditions with variation in pressure as the major control on melt composition.

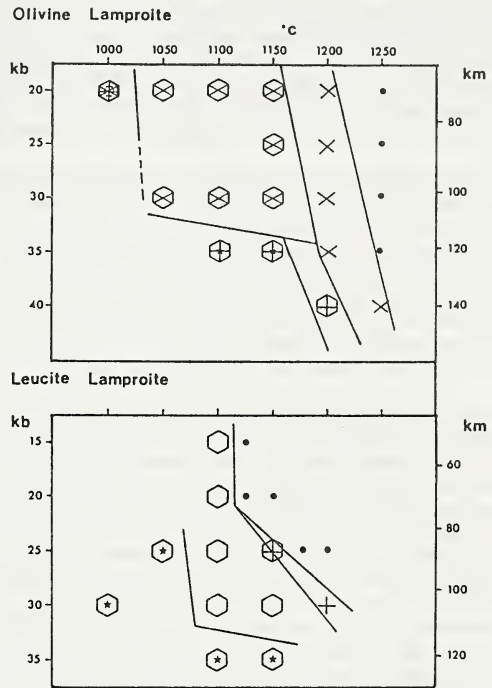
Several experiments had higher measured CH_4/H_2O vapour compositions, and thus oxygen fugacity closer to IW. Under these conditions, all phases are stable to higher temperatures due to the decreased water activity. Mica stability is increased despite the lower water activity since the F/OH ratio of mica is increased. Production of

lamproitic melts from mica harzburgite may also be possible under these very reduced conditions, but further experiments are required to verify this and to ascertain the pressures involved.

Table 1 : Starting compositions used in the experiments (wt %)

Figure 1 : Experimental results with H₂O-rich, reduced fluids

	Olivine Lamproite	Leucite Lamproite
SiO ₂	43.78	51.37
TiO ₂	3.86	3.45
Al ₂ O ₃	4.49	9.95
FeO	8.67	6.05
MnO	0.17	0.09
MgO	23.79	8.03
CaO	5.08	4.67
Na ₂ O	0.58	1.67
K ₂ O	5.08	11.76
P ₂ O ₅	1.64	1.50
BaO	1.75	0.63
SrO	0.15	0.23
ZrO ₂	0.15	0.14
Cr ₂ O ₃	0.17	0.10
NiO	0.13	0.03
F	0.53	0.33



● = liquid only, X = olivine, ○ = mica,
 + = orthopyroxene, o = clinopyroxene,
 * = rutile, I = ilmenite.

References

- Barton, M., Hamilton, D.L. [1982] Mineral Mag 45, 267-278
 Foley, S.F. [1985] Tschermsk Min Petr Mitt 34, 217-238
 Foley, S.F., Taylor, W.R., Green, D.H. [1986a] Contrib Mineral Petrol 93, 46-55
 Foley, S.F., Taylor, W.R., Green, D.H. [1986b] Contrib Mineral Petrol, in press

K.J. Fraser and C.J. Hawkesworth

Department of Earth Sciences, The Open University, Milton Keynes,
MK7 6AA, England

Major, trace element and isotope results are reported for lamproites from the Leucite Hills, Wyoming, W. Australia and Smoky Butte, Montana and Group II kimberlites from Finsch Mine, South Africa. The W. Australia lamproites form more than 100 separate intrusions and grade petrographically from olivine lamproites through leucite bearing olivine-diopside lamproites to leucite lamproite lamproites with phlogopite, diopside and K-richrichterite. The lamproites from Smoky Butte occur in a small (3 km long) area of thin dykes and plugs and they contain armacolite, sanidine, alkali amphiboles and Ti phlogopite. Finsch Mine is a composite intrusion and the rocks are hypabyssal kimberlites containing phlogopite, olivine, diopside, serpentine and calcite.

All samples have low ϵ_{Nd} , implying at least a contribution from old, low Sm/Nd material. However, 2 groups may be recognised on the basis of ϵ_{Sr} values. Smoky Butte lamproites have low ϵ_{Sr} (10 to 19) with very low ϵ_{Nd} = -22 to -26. Despite containing 8% K_2O and 290-380 ppm Nd, they have low Sm/Nd and Rb/Sr consistent with their ϵ_{Nd} and ϵ_{Sr} values. In contrast the W. Australia lamproites and Finsch kimberlites have high ϵ_{Sr} and ϵ_{Nd} ; ϵ_{Sr} = 118 to 228, ϵ_{Nd} = -10 to -19 and ϵ_{Sr} = 56 to 110, ϵ_{Nd} = -6 to -7 respectively. The isotope variations cannot readily be explained by crustal contamination processes, rather they indicate that these lamproites and kimberlites were derived from old segments of the subcontinental mantle.

Trace element considerations of the Finsch kimberlite suite exhibit positive correlations between x/Nd vs Sm/Nd, where $x = Th, Ta, La, Ce, Sr, Hf, Zr, Sm, Y$ and Yb . If such trends reflect varying degrees of partial melting they require Nd to be more incompatible than, for example, Th, Ta and La. This is considered unlikely assuming that at least the relative K_D values for basaltic systems are appropriate at the depths of kimberlite genesis², and so the alternative interpretation of a mixing model is preferred. The ubiquitous presence of macrocrystic olivine and the high garnet content in the Finsch concentrate³ all point towards significant entrainment of upper mantle peridotite material within the kimberlites. Such peridotite would hence represent one endmember of the mixing lines, and the depleted and fertile xenoliths of Nixon *et al.*⁴ have trace element ratios consistent with this model. In terms of Ni and Cr contents the Finsch kimberlites Ni = 1063-1544 ppm, are intermediate between peridotites, Ni = 2000-3000 ppm, and primary melts, 400-800 ppm. A strong positive correlation between Ni contents and Sm/Nd ratios suggests that for an average peridotite Ni content of 2000 ppm the Sm/Nd ratio is ~ 0.2 . The Finsch kimberlites Sm/Nd ratios vary between .112 and .166. The low Sm/Nd, 'primary melt', endmember is restricted to Sm/Nd ratios $< .112$ and $> .06$, the latter reflecting the minimum Sm/Nd ratio for all x/Nd 's to be positive. For Sm/Nd $\sim .1$ Ni = 900 ppm, which is high for a primitive melt (i.e. $D = Cl/Co = 2.2$), for Dni values appropriate to basaltic systems, e.g. 4-7. However, there is evidence to suggest that lower Dni values may be applicable to some mantle processes^{5,6}. D = Cl/Co

Assuming Sm/Nd = .1 for the 'melt' endmember and Sm/Nd = .2 for the peridotite endmember then x/Nd values for each component can be estimated. An average Nd content for peridotite is ~ 2 ppm and for the simplest model the 'melt' Nd content must be > 165 ppm and < 4800 ppm. For Nd = 165 ppm then the whole Finsch range can be attributed to mixing of $> 15\%$ melt and $< 75\%$ peridotite. Even with such a high 'peridotite' content the trace element profile of the kimberlite is dominated by that of the melt endmember owing to the disparity in trace element content between peridotite and melt. Petrographic estimation of the peridotite content is difficult as the olivine macrocrysts are rounded and corroded (i.e. partial assimilation) while the orthopyroxene fraction is not present (total assimilation). However, point counting has shown that olivine macrocrysts may constitute up to 45 vol% of the rock.

For $D = Cl/Co$ and using known K_D values¹ for olivine, orthopyroxene, clinopyroxene and garnet, and using $Cl =$ concentration of mineral in melt as inferred above, the source characteristics of the 'melt endmember' (Co) can be estimated. Small degrees of

partial melting of garnet lherzolite with trace element concentrations comparable with those of mantle peridotites can account for the trace element contents of the 'melt' endmember. However, the source to the melt endmember must differ from the entrained peridotites: the Sr and Nd isotopes imply an old enriched source and the high K₂O contents of the kimberlites (0.81, 2.64-4.23 wt %) suggest the presence of a K bearing phase within the kimberlite source. Also in order to maintain a generally increasing degree of incompatibility (i.e. decreasing D) from Yb, Y, Sm, Zr, Hf, Nd, Sr, Ce, La, Ta up to Th requires that at least Th/Nd, Ta/Nd, La/Nd, Ce/Nd and Sr/Nd ratios within the source of the melt endmember are less than those exhibited by either the melt itself and the peridotite endmember.

Mixing is also evident from the Pb isotopes where further data have not substantiated the tentative 1.4 Ga age inferred previously. On a $^{207}\text{Pb}/^{204}\text{Pb}$ vs $^{206}\text{Pb}/^{204}\text{Pb}$ diagram the peridotite endmember could plot close to the Stacey and Kramers⁸ growth curve while the 'melt' endmember would exhibit low $^{206}\text{Pb}/^{204}\text{Pb}$ and $^{207}\text{Pb}/^{204}\text{Pb}$ ratios. The most unradiogenic Finsch sample ($^{207}\text{Pb}/^{204}\text{Pb} = 15.43$, $^{206}\text{Pb}/^{204}\text{Pb} = 17.51$) suggests a minimum age of 2.5 Ga for the 'melt' endmember.

Further trace element considerations reveal something of the nature of the ancient source enrichment events. In many of the Finsch kimberlites high Rb/Sr (and $^{87}\text{Sr}/^{86}\text{Sr}$) ratios occur with low Rb/Ba (< .1) whereas in the remaining samples high Rb/Sr ratios are accompanied by high Rb/Ba - as is also observed in metasomatised PP and PKP mantle xenoliths (Erlank *et al.*, this vol.). High Rb/Sr with high Rb/Ba are attributed to the migration of H₂O rich fluids, while the trend to high Rb/Sr with low Rb/Ba is often characterised by relatively high La, Ta and Ti, and appears to be due to the introduction of small volume partial melts with the stabilisation of melt related phlogopite.

Similar models may be constructed for the less differentiated members of the W. Australia lamproite suite, however subsequent differentiation and sample collection over a wide geographical area combine to obscure original mixing relationships. High Rb/Sr with low Rb/Ba ratios can again be attributed to melt related enrichment processes while low $^{206}\text{Pb}/^{204}\text{Pb} = 17.3 - 17.6$ together with high $^{207}\text{Pb}/^{204}\text{Pb} = 15.7 - 15.8$ requires a complex 3 stage evolution. The lamproites from Smoky Butte, Montana, on the other hand exhibit extremely unradiogenic Pb isotope ratios ($^{206}\text{Pb}/^{204}\text{Pb} = 16.0 - 16.6$) compatible with a 2 stage evolution history and very low Rb/Ba (.01-.004) with high K/Rb (500-900) ratios suggest that amphibole may have been a feature of the source regions.

In the rocks considered here diamonds tend to be restricted to those with more primitive characteristics: Cr > 500 ppm, MgO > 10%, Zr < 850 ppm and Ni > 485 ppm, and it is interesting to speculate whether they originate as xenocrysts from upper mantle peridotite or as xenocrysts from within the enriched 'kimberlitic/lamproitic melt' source which in the case of Finsch Mine would suggest from ages on diamond inclusions a source age of 3.2 Ga.

- 1 Frey, F.A., Green, D.H. and Roy, S.D. (1978). *J. Pet.* Vol. 19, Pt. 3, 463-513.
- 2 Kramers, J.D., Smith, C.B., Lock, N.P., Harmon, R.S. and Boyd, F.R. (1981). *Nature* 291, 53-56.
- 3 Gurney, J.J. and Switzer, G.S. (1973). *Contrib. Mineral. petrol.* 39, 103-116.
- 4 Nixon, P.H. *et al.* (1981). *Ann. Rev. Earth Planet. Sci.* 9, 285-309.
- 5 Bickle, M.J., Ford, C.E. and Nisbet, E.G. (1977). *Earth Planet. Sci. Lett* 37, 97-106
- 6 Hanson, G.N. and Langmuir, C.H. (1978). *Geochim. Cosmochim. Acta* 42, 725-741.
- 7 Fraser, K.J., Hawkesworth, C.J., Erlank, A.J., Mitchell, R.H. and Scott-Smith, B.H. (1985). *Earth Planet. Sci. Lett.* 76, 57-70.
- 8 Stacey, J.S. and Kramers, J.D. (1975). *Earth Planet. Sci. Lett.* 26, 207-221.
- 9 Richardson, S.H., Gurney, J.J., Erlank, A.J. and Harris, J.W. (1984). *Nature* 310, 198-202.

ROLE OF SULFIDES IN THE EVOLUTION OF MANTLE ROCKS OF
BASIC AND ULTRABASIC COMPOSITION AND IN THE EMERGENCE
OF KIMBERLITE BODIES

V.K.Garanin, G.P.Kudryavtseva and A.N.Krot

Department of Geology, Moscow State University, USSR

In kimberlite bodies sulfides occur in diamonds, in xenocrysts of garnet, olivine, zircon, pyroxene, ilmenite, chromespinel, in xenoliths of abyssal rocks of basic and ultrabasic composition and in kimberlite rocks themselves. Such heterogeneity is associated with the different stages in the evolution of mantle rocks and kimberlite melts. Sulfides are represented by magmatic, metasomatic and superimposed hydrothermal minerals. Sulfide nodules are developed in xenocrysts, diamonds and abyssal rocks have a complicated zonal structure. Core of nodules is composed either of quenched sulfide melt based on Fe and Ni or pyrrhotite and pentlandite in various combinations; internal part (outside the core) broken rim is composed of Co-containing pentlandite, external one - of chalcopyrite (Fig.1), sometimes with bornite or djerfisherite (Fig.2). The latter is encountered only in ilmenitic rocks.

In accordance with paragenesis of these minerals, diamond included, a regular evolution of the initial sulfide melt entrapped by minerals is traced (Fig.3). Composition of the initial sulfide melt in minerals of eclogitic paragenesis is extremely poor in Ni (less than 3 mass.%) and enriched with Fe (over 55 mass.%); in minerals of ultrabasic magnesian-ferriperous (ilmenite) series the amount of Ni is greater (from 2,5 to 10 mass.%), while that of Fe is less (from 51 to 56 mass.%); in minerals of ultrabasic magnesian paragenesis the melt is substantially enriched with Ni (20-26 mass.%) and poor in Fe (34-40 mass.%).

For sulfide nodules from diamond and minerals in the relatively rich diamond pipes the availability of non-degraded monosulfide solid solution based on pyrrhotite is characteristic which gives evidence of the quenching conditions in the emergence of productive kimberlite bodies. The amount of sulfide inclusions presented in diamond of the ultrabasic paragenesis is much less than in diamond of the basic paragenesis.

Thus, at crystallization of diamond and mineral the basic and ultrabasic paragenesis there is a successive regular change in the composition of sulfide magmatic melts that have liquated as function of the paragenesis type, P-T conditions of crystallization of mineral association, and of the composition of the host mineral.

Polymictic sulfide systems of various mineral associations are described, and in all types of xenoliths of ultrabasic and basic rocks both in the form of inclusions in minerals and interstitial - in the intergranular space of minerals. Sulfide nodules in minerals of xenoliths are identical by chemical and phase composition with nodules of mineral insets in kimberlites in accordance with type of paragenesis. This fact evidences of the creation of mineral insets as a result of xenoliths disintegration.

Sulfide inclusions in the intergranular space of rock-forming minerals of xenoliths are subdivided into three types:

1. Nodules of pyrrhotite-pentlandite-chalcopyrite composition; 2. The same aggregates but with partial or full replacement of chalcopyrite by djerfisherite and monomineral inclusions of djerfisherite; 3. Oriented silicate-sulfide growths of irregular shape of pyrrhotite-pentlandite-chalcopyrite-olivine composition. The first is the typical example of primary-magmatic sulfide formations. In the second case formation of djerfisherite, very often in close association with amphibole and mica, is connected with the abyssal mantle metasomatism under the influence of fluids rich in S and alkalis over rocks of basic and ultrabasic composition. As a rule, the above refers only to ilmenite rocks rich in K, Ti, Fe, Mg. Superimposed metasomatic mineral association is a much more recent formation. Formation of the third type sulfides is likely to result from disintegration of the basic rock-forming minerals crystallized from the residual silicate-sulfide melt. However, one must

not exclude that such oriented olivine-sulfide growths can be formed as a result of the S-rich kimberlite magma effect over xenoliths of abyssal rocks. Therefore, peculiarities of composition and structure of sulfide minerals are in close connection with the three basic stages in the evolution of ultrabasic rocks and eclogites in kimberlites.

In kimberlite rocks as themselves sulfides are widely developed as well, and are associated with the hydrothermal stage of kimberlite bodies formation. Most typical are as follows: scattered crystals of pyrite

pyrite or pyrite-magnetite pseudomorphs by olivine and diopside, pyrite-sphalerite-galenite-calcite veins. The latter sometimes form thick streaks at the boundary of different phases of kimberlite magmas intrusion. There are several generations of sulfide minerals according to the long-term evolution and multi-stage formation of kimberlite bodies.

REFERENCES

- Barashkov, Yu.P., Marshintsev, V.K., Gotovtsev, V.V. and Leskova, N.V. (1981). Nature of mineral inclusions in kimberlitic olivines (in Russian). In V.V.Koval'sky, Eds., *Mineralogy and geochemistry of Yakutian ultrabasic and basic rocks*, p. 86-106, Yakutsk.
- Boctor, N.Z. and Boyd, F.R. (1980). Ilmenite nodules and associated sulfides in kimberlite from Yakutia, USSR. *Carnegie Inst. Wash. Year-Book* 79, p.302-304.
- Garanin, V.K., Krot, A.N. and Kudryavtseva, G.P. (1984). Primary magmatic mineralization in kimberlites, part I (in Russian). *Proceeding of X Conference young scientists of Geological Faculty*, p.3-95, Moscow.
- Yefimova, E.S. and Sobolev, N.V. Inclusions of sulfides in diamonds and features of their paragenesis (in Russian). *Zapiski Vsesoyuznogo Mineralogicheskogo Obshestva*, 3, p.300-310.



Fig.1. Poly-mineralic sulfide inclusion in zircon. External thin rim is composed of chalcopyrite (1), internal one - of Co-containing pentlandite (2). Core of nodule is unhomogeneous and composed of high nickel pyrrhotite (3) and poor nickel pyrrhotite (4). Back-scattered electron image with composition contrast 350^x

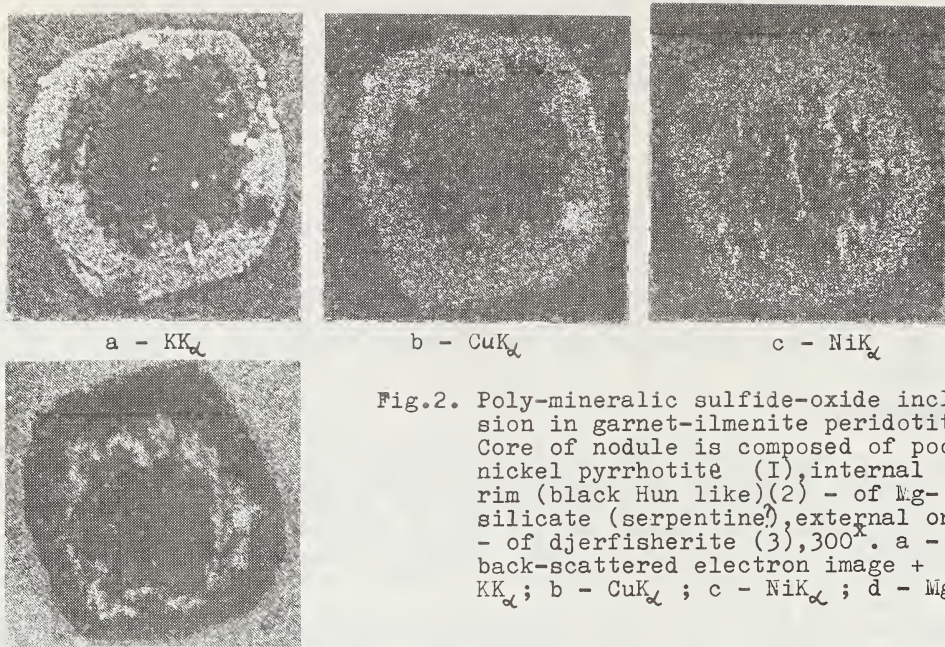


Fig.2. Poly-mineralic sulfide-oxide inclusion in garnet-ilmenite peridotite. Core of nodule is composed of poor nickel pyrrhotite (1), internal rim (black Hun like) (2) - of Mg-silicate (serpentine), external one - of djerfisherite (3), 300 \times . a - back-scattered electron image + KK_{α} ; b - CuK_{α} ; c - NiK_{α} ; d - MgK_{α}

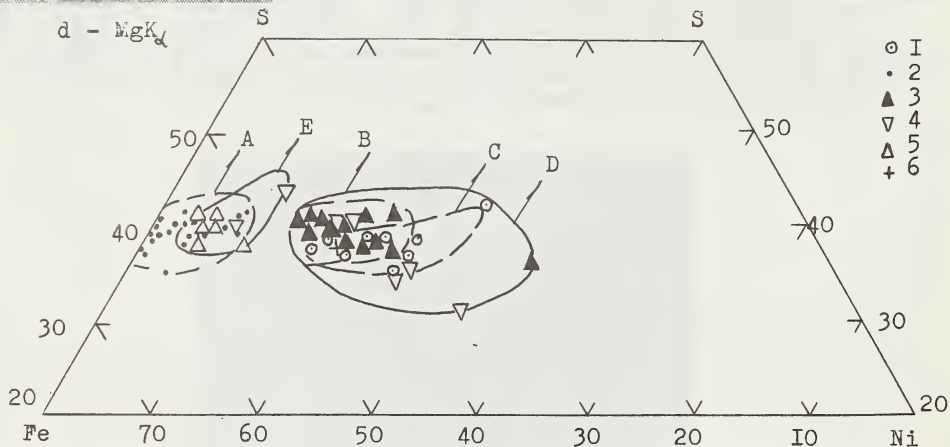


Fig.3. Calculated compositions of primary sulfide melts from inclusions in: 1 - diamonds of basic (eclogitic) paragenesis (by E.S.Efimova and N.V.Sobolev, 1983); 2 - diamonds of ultrabasic paragenesis (by E.S.Efimova and N.V.Sobolev, 1983); 3 - zircon (by V.K.Garanin et.al., 1983); 4 - olivine (by I.P.Barashkov et.al., 1981); 5 - ilmenite (by Boctor and Boyd, 1981); 6 - garnet from ultrabasic (websterite) paragenesis. Lines outline fields of sulfide melt from: A - diamonds of eclogitic paragenesis; B - zircon of ultrabasic (magnesian) paragenesis; C - diamonds of ultrabasic (magnesian) paragenesis; D - minerals of ultrabasic magnesian series of rocks; E - minerals of ultrabasic magnesian-ferrous series of rocks

D.H. GREEN⁺, T.J. FALLOON⁺, G.P. BREY^{*} AND K.G. NICKEL^{*}⁺Department of Geology, University of Tasmania, Box 252C, G.P.O. Hobart, 7001.^{*}Max Planck Inst. für Chemie, Postfach 3060, D6500 Mainz, FRG.

The anhydrous melting behaviour of lherzolite has been studied experimentally from 0-6GPa with emphasis on careful determination of the solidus temperature and the compositional changes of liquids and residual phases as functions of pressure, temperature and degree of partial melting. The lherzolite composition studied (MORB Pyrolite) is suitable as a source composition for modern mid-ocean ridge basalts and as such also approximates to a 'primitive' or most typical source composition for voluminous basaltic, picritic or komatiitic volcanism throughout geological time. The study also enables comparison with parallel melting studies on "Hawaiian pyrolite" (source composition for intraplate 'hot-spot' magmas), on refractory Tinaquillo lherzolite (?source composition for back-arc basin tholeiites) and on K-enriched 'sub-continental' lherzolite (?source composition for high K/Na 'continental' basalts). The solidus of 'MORB Pyrolite' lies ~25°C above Hawaiian pyrolite solidus and essentially coincident with Tinaquillo lherzolite solidus from 0-4GPa. The solidus slope is ~100°C/GPa between 2 and 4 GPa and results in convergence of liquidus and solidus up to 5GPa. This is accompanied by change in melt composition with melts at higher pressures becoming more olivine rich, and at low degrees of melting, more strongly silica undersaturated (fig. 1).

Melting of lherzolite is dominated by cotectic melting of solid solutions and thus the solidus temperature varies smoothly rather than discontinuously as a function of pressure. There is an inflection in the solidus around 1.5GPa, seen in both MORB Pyrolite and Tinaquillo lherzolite compositions. At any pressure the degree of melting increases regularly with increasing temperature. Detailed matching of liquids generated at 0.8 to 2 GPa, ranging from quartz tholeiites to tholeiitic picrites, with the spectrum of natural MORB glasses and aphyric basalts, demonstrates that primary magma production on divergent plate margins on the modern earth requires the existence of tholeiitic picritic (15-35% normative olivine) magmas as well as primary alkali picrites (lower degrees of melting). Primary olivine tholeiites, tholeiites and quartz tholeiites (lower pressures of magma segregation) can also be identified among ocean floor basalt glasses but some of these glasses require more refractory source peridotite compositions than MORB pyrolite and are interpreted as second stage melting of MORB pyrolite. The role of second-stage melting (i.e. a second melting of refractory residue after partial or complete extraction of a first stage melt) is particularly evident near convergent plate margins in the modern earth. In this environment, high magnesia quartz tholeiites or olivine-poor tholeiites (e.g. Tongan fore-arc lavas, Troodos Upper Pillow lavas) are produced from source peridotite resembling Tinaquillo lherzolite composition. Extremely refractory boninite lavas are interpreted as 'third stage melting' of residual harzburgite following access of water-rich fluids in the subduction environments.

In the studies of melting relationships at 5 GPa, the extremely high temperatures of the solidus, permits extensive solid solution between coexisting pyroxenes, and orthopyroxene is eliminated as a residual phase before either garnet or clinopyroxene ('pigeonitic' with 6-7%CaO). Residues from moderate to high degrees of melting at 5 GPa are therefore not harzburgitic but remain lherzolitic in character. On the other hand liquids are rich in both normative olivine and hypersthene components and approach compositions of pyroxenitic komatiites. The melting interval for MORB pyrolite composition at 5 GPa remains >200°C and liquids of pyroxenitic komatiite character (~26% MgO) require high degrees of melting - they are not small melt fractions produced at near-solidus conditions.

Our melting studies confirm the high temperatures, and high degrees of melting [assuming a lherzolite source with 3-4% CaO, Al₂O₃ and Mg[#]=90] required to generate peridotitic komatiite liquids and show that liquids at 1750°C and 1800°C at 5 GPa are not peridotitic komatiite in character but approach pyroxenitic komatiite. The most conservative models for peridotitic komatiite genesis are those requiring the lowest temperatures at depth of magma segregation and thus the coolest model geotherm for

Archaean period. On this basis, the preferred model for Archaean peridotitic komatiite genesis involves multistage or continuous extraction of melt from mantle diapirs ascending at ~1700°C. Dunite xenoliths in kimberlite pipes are possible refractory residues from extraction of such melts. The roles of olivine, chromite and low Ca, low Al orthopyroxene as residual phases imply low pressure [<2 GPa] melt extraction processes for this xenolith type.

In the modern and Phanerozoic Earth, maximum temperatures of primary magmas are ~1450°C, consistent with overall cooling of the Earth through time and changes in patterns of convective heat loss. C-H-O fluids play a key role in modern magma genesis. Deep levels of the Earth's Mantle are at low oxygen fugacities (~IW) and the earth is degassing reduced volatiles dominated by methane + hydrogen. The asthenosphere acts as a fluid-absent zone of partial separating $CH_4 > H_2$ fluids in the deep mantle from H_2O -rich or $H_2O + CO_2$ fluids in the lithosphere. The lithosphere is variable in oxygen fugacity (IW to FMQ) and acts as a lid or seal to melt migration from the asthenosphere, due to stability of pargasitic amphibole + phlogopite. A process of "redox melting" [fig.2] may occur in the peridotite-C-H-O system by interaction of reduced CH_4 -rich fluids with oxidized lithosphere. This process is advanced as an explanation of the association of diamond (precipitated by oxidation of methane) and extremely refractory garnet harzburgite with Fo₉₄ olivine and extremely low-calcium garnets. The fluid-rock interaction produces a kimberlitic or olivine lamproitic melt due to the water-rich character of the fluid on the diamond-fluid saturation surface at P~50-55kb, T~1200°C.

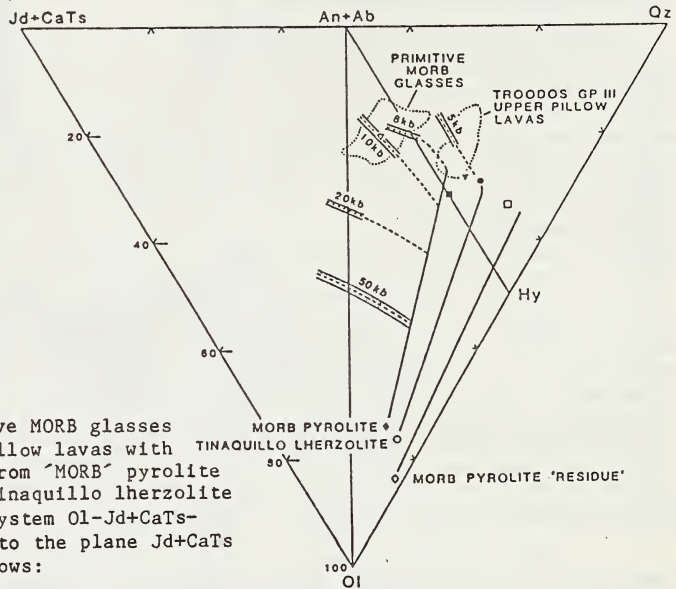


FIG.1 Comparison of primitive MORB glasses and Troodos Gp.III upper pillow lavas with equilibrium partial melts from "MORB" pyrolite at 8, 10, 20 and 50kb and Tinaquillo lherzolite at 5kbar in the normative system Ol-Jd+CaTs-Qz-Di, projected from Di onto the plane Jd+CaTs-Qz-Ol. Symbols are as follows:

- (■) calculated parental composition for the Troodos Gp.III upper pillow lavas.
- (▼) Refractory primitive magma composition identified from glass inclusions in magnesian (Fo₉₄) olivine phenocrysts from Tonga.
- (●) Marianas fore-arc lava
- (□) Cape Vogel boninite parental magma composition
- (▽) Primitive MORB glass DSDP3-18-7-1

==== Ol + Opx + Cpx Cotectic
 - - - - Ol + Opx Cotectic
 ——— Olivine only residual phase

SHIELD UPPER MANTLE

A. OXIDIZED (MW) AT DEPTH
IW \approx MW THROUGH LVZ

B. REDUCED (IW) AT DEPTH
IW \approx MW IN LITHOSPHERE

C. DEEP LITHOSPHERIC
FRACTURES

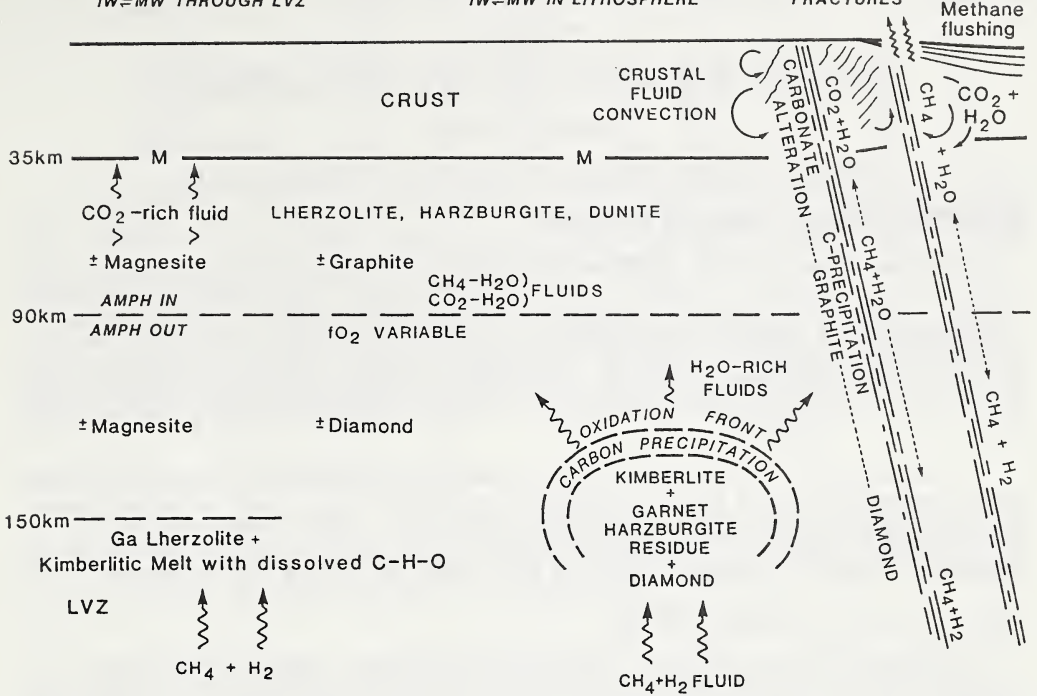


FIG.2 Schematic model for the continental lithosphere beneath Archean/Proterozoic shield regions. The deep mantle is degassing ($\text{CH}_4 + \text{H}_2$) fluids but the intrinsic f_{O_2} of the lithosphere is very variable from FMQ to IW. Different scenarios (A,B,C) illustrate alternative interactions between reduced fluids and the oxidised lithosphere. 'A' suggests a deep, thin asthenospheric layer (partial melting) in which the f_{O_2} change from mantle to lithosphere is accommodated within the fluid-absent melt. 'B' suggests a mechanism of 'redox' melting in which diamond-bearing refractory garnet harzburgite is left as a residue from oxidation of $\text{CH}_4 + \text{H}_2$ to $\text{H}_2\text{O} + \text{C}$ with extraction of water-rich kimberlitic melt. 'C' suggests a role for deep lithosphere fractures in localizing mantle fluid release and interaction of these fluids with oxidised crustal fluids at shallow depths.

SPECULATIONS CONCERNING THE IMPORTANCE OF METASOMATIC MELT MIGRATION IN
THE FORMATION OF PYROXENITE SHEETS IN GARNET-PERIDOTITE
XENOLITHS FROM MATSOKU, LESOTHO

Ben Harte

Grant Institute of Geology, University of Edinburgh, Scotland

Robert H Hunter

Department of Earth Sciences, University of Cambridge, England

METASOMATISM AND MELT INJECTION AT MATSOKU

Many xenoliths show the development of modal and textural inhomogeneities, which vary from discontinuous stringers (~1 mm wide) to layers (2-5 cm wide), in which original garnet peridotite is modified to give garnet + orthopyroxene-rich and/or clinopyroxene-rich material which commonly includes IRPS minerals (ilmenite, rutile, phlogopite and sulphides). Since the petrographic evidence indicates the modification to be occurring in largely solid rock the phenomena are described as metasomatic, even though the infiltrating fluid appears to have been basic-ultrabasic silicate melt (Harte et al., in press).

In association with the obvious metasomatic phenomena noted above, the Matsoku garnet peridotites host a series of discrete pyroxenite sheets (1-16 cm wide), which have the general form of minor magmatic intrusions. These sheets show a number of curious features and it is suggested that they in part may also be the result of an essentially metasomatic process involving melt migration through a solid matrix.

DESCRIPTION OF THE PYROXENITE SHEETS

Although they are generally rich in orthopyroxene and/or clinopyroxene, the pyroxenite sheets often show considerable structural and textural complexity. Lenticles, foliae or seams enriched in olivine, garnet, clinopyroxene or IRPS minerals may occur. Where complete sections are preserved across larger (10-15cm thick) sheets clinopyroxene-rich margins are often present (Fig. 1) and may be accompanied by concentrations of garnet and IRPS minerals. Sometimes a discontinuous selvage of garnet occurs along the contacts of the sheets.

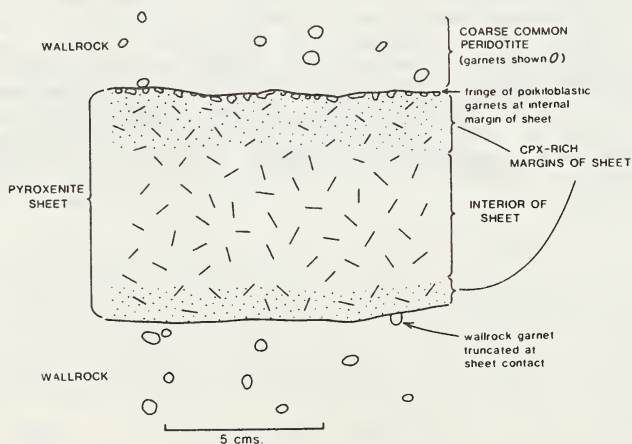


Figure 1
Sketch showing common features of thick pyroxenite sheets

Table 1 illustrates the variety of modal proportions seen in the sheets: with 88 and 171 representing fairly homogeneous sheets; 139CM and 139I respectively representing clinopyroxene-rich margin and clinopyroxene-poor interior of a single sheet; and 137CM and 129CM representing the margins of sheets richer in garnet and ilmenite.

Table 1. Modal Proportions in Pyroxenite Sheets and other rocks

Rock No.	88	171	139CM	139I	137CM	129CM	108M	108H
olivine	18.2	8.0	18.9	17.2	1.2	0.5	19.2	48.0
orthopyroxene	74.9	39.5	39.1	63.6	20.5	47.2	58.9	43.0
clinopyroxene	4.1	42.5	36.0	14.5	56.0	12.1	3.5	3.5
garnet	2.3	8.9	4.5	2.2	19.9	24.2	10.8	5.5
IRPS minerals	0.5	1.1	1.5	2.5	2.4	16.0	7.6	0.0

In one case (LBM 99) a parallel pair of apparently similar garnet selvages are seen crossing layering within a pyroxenite sheet, thereby suggesting multiple injections of melt. Boundaries between layers within sheets are usually gradational. Whilst contacts with host peridotite often appear roughly planar in gross form, they are irregular on the scale of a few mm.

The grain size within the sheets is dominantly below 1mm, and grains show a mixture of granuloblastic and irregular shapes. Garnets are usually poikiloblastic, and pyroxenes frequently show the patchy and sometimes zoned development of fine ilmenite and silicate inclusions. Curious garnet-rich "pools" (Harte et al., 1975, p. 500) are often present in these rocks.

INTERPRETATION OF THE PYROXENITE SHEETS

The above features clearly show that despite their gross intrusive appearance the pyroxenite sheets do not represent the straightforward homogeneous crystallisation products of a silicate liquid. Differential movement of crystals and liquid is clearly indicated in many cases and it is evident that this is not a straightforward plating of early crystals on relatively cool wallrock margins.

Given that many other phenomena in the Matsoku xenoliths appear to result from metasomatic melt migration, the question arises as to what extent such phenomena are responsible for the varied features seen in the pyroxenite sheets. Rock LBM 108M shows textural and modal (Table 1) similarities to some parts of pyroxenite sheets, but also preserves textures suggesting its conversion from a normal garnet peridotite (108H). Thus large garnets are seen in a state of transition to poikiloblastic garnets (see also Fig. 11a of Harte et al., 1975).

One of the most striking features of the sheets, certainly the larger and better preserved ones, is their development of clinopyroxene-rich (+ garnet and IRPS) margins (Fig. 1) in contrast to relatively orthopyroxene-rich and sometimes olivine-rich interiors. The broadly symmetrical nature of this layering is reminiscent of the metasomatic zoning developed where rock units with different chemical potentials (e.g. limestone within pelite) are present during metamorphism. However, such situations involve changes in mineral species, and in the present case the same silicate minerals occur from sheet core to within the host rock. Given the likely order of crystallisation from the melt of olivine, orthopyroxene, clinopyroxene and finally garnet, it is as if the melt has crystallised outwards from the centres of the sheets towards the margins. Obviously with the crystallisation of a sheet-like body of liquid one would expect the temperature gradient to cause crystallisation in the opposite sense. If, however, melt were able to move sideways into the wallrocks, and also from the centre of the sheets into their largely crystalline margins, then concentration of clinopyroxene and garnet towards the margins might be achieved.

Outward migration of melt from within the pyroxenite sheets will be controlled by textural considerations. In order for a fluid to penetrate matrix grains, it must be able to form a continuous framework; all pores must be connected along grain edges. The contiguity of a fluid phase in a matrix of grains in textural equilibrium is controlled by the pore geometry; specifically by the dihedral angle (θ) which occurs at the junction of the fluid (f) and adjacent grains (s). This is controlled by the ratio of intergrain:interphase ($\gamma_{ss}:\gamma_{sf}$) surface energies, and is resolved as $\gamma_{ss} = 2\gamma_{sf}\cos\theta/2$. For values of $\theta < 60^\circ$, the fluid is able to disperse along grain edges. For values of $\theta > 60^\circ$, small proportions of fluid form isolated pockets at grain corners (Beeré, 1975; Park and Yoon, 1985).

Experimental measurements of dihedral angles for relevant fluid-matrix systems are few: Waff and Bulau (1979, 1982) measured values of θ between 30-50° for melts ranging from tholeiite to nepheline basanite in equilibrium with a matrix of olivine; Hunter and McKenzie (in prep.) have measured values of $\theta < 60^\circ$ for dolomitic carbonates in equilibrium with a peridotite matrix at 30kb. Watson (1982) conducted a "melt-infiltration" experiment using a synthetic basaltic composition and an olivine matrix. The fluid became dispersed along the, initially dry, grain edges, thereby experimentally confirming the feasibility of the outward infiltration of the melt.

During the migration of melt from the core of pyroxenite sheets towards the wallrock, changes in grain boundary shape can occur by solution-precipitation or Oswald ripening. In order for a fluid to penetrate along dry grain edges, solution must occur at the grain boundary. If the fluid were initially out of equilibrium (chemical) with the matrix, it would rapidly become saturated in matrix components by dissolution at grain edges. Once the melt has crystallised, its configuration and geometry will no longer be controlled by $\chi_{SS} : \chi_{SF}$ but by the intergrain-boundary energies alone. The grain boundaries of the new mineral assemblage will change shape through solution-precipitation or Oswald ripening to achieve a new minimum-energy configuration. If the new silicates and oxides have intergrain dihedral angles greater than 60°, as many do, then grains of minor phases will be isolated at the corners of principal phases and the original contiguity and geometry of the fluid phase will no longer be conserved. The rocks will have a mineralogy and chemistry that has been modified by infiltration of a fluid, evidence for which will not be present.

The physico-chemical model operating in formation of the pyroxenite sheets requires closer definition, and questions concerning the magnitude of temperature gradients between sheet and wallrock, and the possible repetition of injections of melt into the centres of pyroxenite sheets, require resolution. However, we suggest that the migration of melt, within a crystalline matrix in accordance with the principles of textural equilibration discussed above, may have played an important role in the development of the pyroxenite sheets. The outward infiltration of melt into the cooler margins of the pyroxenite sheets and the adjacent wallrocks may have created the clinopyroxene and garnet rich margins seen in some sheets.

REFERENCES

- BEERÉ W. 1975. A unifying theory of the stability of penetrating liquid phases and sintering pores. *Acta Metallurgica* 23, 131-138.
- HARTE B., COX K.G. and GURNEY J.J. 1975. Petrography and geological history of upper mantle xenoliths from the Matsoku kimberlite pipe. *Physics and Chemistry of the Earth* 9, 477-506.
- HARTE B., WINTERBURN P.A. and GURNEY J.J. In press. Metasomatic and enrichment phenomena in garnet-peridotite facies mantle xenoliths from the Matsoku kimberlite pipe, Lesotho. In Menzies M.A. and Hawkesworth C.J. eds. *Mantle Metasomatism*. Academic Press, London.
- PARK H.-H. and YOON D.N. 1985. Effect of dihedral angle on the morphology of grains in a matrix phase. *Metallurgical Transactions* 16, 923-928.
- WAFF H.S. and BULAU J.R. 1979. Equilibrium fluid distribution in an ultramafic partial melt under hydrostatic conditions. *Journal of Geophysical Research* 84, 6109-6114.
- WAFF H.S. and BULAU J.R. 1982. Experimental determination of near-equilibrium textures in partially molten silicates at high pressures. *Advances in Earth and Planetary Sciences* 12, 229-236.
- WATSON E.B. 1982. Melt infiltration and magma evolution. *Geology* 10, 236-240.

HETEROMORPHISM AND CRYSTALLIZATION PATHS OF KATUNGITES,
NAVAJO VOLCANIC FIELD, ARIZONA, USA

A. W. Laughlin, R. W. Charles, M. J. Aldrich

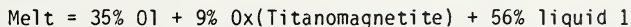
Los Alamos National Laboratory
P.O. Box 1663, MS D462, Los Alamos, New Mexico 87545, USA

A swarm of thin, isochemical but heteromorphic, lamprophyre (katungite) dikes crops out in the valley of Hasbidito Creek in NE Arizona. The dikes, which are generally well exposed, are part of the mid-Tertiary Navajo volcanic field of the Colorado Plateau. In contrast to the minette dikes of the region, these katungites have produced strong thermal effects on the adjacent Triassic sandstone wallrocks which are commonly baked and bleached at the contacts. It is evident that the katungite dikes were emplaced at higher temperatures and were more volatile-rich than the minettes. The few inclusions in the katungite dikes are crustal in origin.

Whole-rock chemical analyses of samples from four of the dikes indicate that the dikes are chemically identical to the katungites of Uganda originally described by Holmes (1937). Like the Ugandan samples, the Arizona katungites are characterized by extreme silica undersaturation and high concentrations of TiO_2 , MgO , CaO , K_2O , and P_2O_5 (Table 1). They are notably enriched in the rare-earth elements, particularly the LREE, and in Ba, U, and Th. Striking characteristics of these isochemical dikes include the wide variability in modal mineralogic compositions (heteromorphism) and the large number of mineral phases present.

We have identified over 20 mineral phases in samples of the Arizona katungites, and as many as 18 phases may occur in a single sample (Table 2). Electron microprobe analyses have been completed on most phases. The major phases are phlogopite (Ph), olivine (Ol), perovskite (Pv), opaque oxides (Ox), \pm melilite (Mel), and \pm clinopyroxene (Cpx). There is an antithetic relationship in the abundances of Mel and Cpx with Mel ranging from 0 to 23% and Cpx from 30 to 0%. Two generations of Cpx can be distinguished; one earlier (ECpx) and one later (LCpx) than the Mel. Minor and trace phases include wollastonite (Wo), nepheline (Ne), apatite (Ap), pectolite (Pe), thomsonite (Th), natrolite (Nat), calcite (Ca), dolomite (Do), tobermorite (To), aenigmatite (Ang), and andradite (Ad). Some of these phases have been identified only in X-ray patterns. The complex and variable mineralogic compositions of these samples reflect both incomplete reactions and differing crystallization histories for individual dikes.

Based upon the modal mineralogies of nine samples of the dikes we recognize four general non-equilibrium assemblages: (1) Ol, Ph, Pv, Ox, ECpx; (2) Ol, Ph, Pv, Ox, Mel; (3) Ol, Ph, Pv, Ox, LCpx; and (4) Ol, Ph, Pv, Ox, Mel, Pe, Th \pm Wo. Comparison of the assemblages with recent experimental results of Arima and Edgar (1983) and Lloyd (1985) shows they represent various combinations of complete and incomplete reactions. Heterogeneous reaction relations were determined by entering the phase compositions determined by electron microprobe into the computer code GENMIX to obtain balanced reactions. A few examples are given below. In all four assemblages Ol and Ox crystallized first at approximately 15 Kb and 1200°C, based upon the 5% H_2O phase diagram of Arima and Edgar (1983). A melt composition based on sample BOL-4-84 (Table 1) with iron as FeO and recalculated to 100% will yield the following reaction (in molar percent):



Liquid 1 will be higher in Al_2O_3 and CaO and lower in MgO and FeO than the original melt. The presence of Ph in all assemblages indicates that nearly isobaric crystallization then occurred with the melt moving from the Ol-Ox-liquid(L) field into the ECpx-Ph-Pv-Ox-Ap-L field. The approximate reaction relation here is:



TABLE 1
MAJOR AND TRACE ELEMENT ANALYSES OF KATUNGITE SAMPLES

	<u>Major Elements (%)</u>					
	Holmes (1937)	AWL-35-83	BOL-4-84	BOL-8-84	BOL-12-84	BOL-13-84
SiO ₂	35.51	33.58	34.37	34.10	32.77	33.69
TiO ₂	4.88	4.74	5.16	4.52	4.74	4.30
Al ₂ O ₃	6.83	6.84	6.53	6.31	6.27	6.62
Fe ₂ O ₃	9.68	5.40	5.57	6.33	7.30	5.51
FeO	2.70	7.56	7.57	6.02	5.07	7.12
MnO	0.22	0.20	0.20	0.18	0.18	0.20
MgO	11.67	16.14	16.55	17.80	15.92	15.56
CaO	16.00	14.25	13.92	11.85	12.37	14.23
Na ₂ O	1.56	1.45	1.16	1.30	1.45	1.42
K ₂ O	3.30	3.26	3.06	2.69	1.98	3.54
H ₂ O ⁺	3.11	4.12	3.77	6.74	9.26	4.91
H ₂ O ⁻	1.31	0.38	0.27	0.59	0.75	0.26
P ₂ O ₅	1.18	1.60	1.52	1.06	1.38	1.70
SrO	0.24	0.23	0.29	0.16	0.18	0.26
S	-	0.21	<0.01	0.16	<0.01	<0.01
Total	100.41*	99.95	99.94	99.80	99.62	99.31

<u>Trace Elements (ppm)</u>					
La	164	182	136	157	178
Ce	335	356	269	338	352
Nd	151	139	116	163	170
Sm	15.6	23.7	18.2	20.4	21.6
Eu	4.99	5.16	3.98	5.15	5.29
Tb	2.28	1.53	1.18	1.53	2.30
Dy	7.11	7.36	5.68	6.14	6.80
Yb	2.66	2.56	2.19	2.54	2.55
Lu	0.282	0.279	0.145	0.250	0.257
Ba	1970	2048	1291	1904	1854
U	5.56	5.15	4.09	4.88	5.40
Cr	566	-	-	-	-
Th	20.2	21.5	16.5	22.4	21.5
Rb	86	117	90.1	97.7	148

* Includes 1.47% CO₂

TABLE 2

MODAL MINERALOGIC COMPOSITION OF KATUNGITE SAMPLES

Mineral	AWL-35-83 %	BOL-1B-84 %	BOL-2A-84 %	BOL-3-84 %	BOL-4-84 %	BOL-8-84 %	BOL-11-84 %	BOL-12-84 %	BOL-13-84 %
Olivine	12	12	12	12	18	6	19	2	16
Phlogopite	30	17	7	35	29	25	39	16	31
Perovskite	7	8	5	7	5	4	4	3	4
Melilitite	23	-	3	13	18	-	8	-	3
Clinopyroxene	Tr	30	25	-	Tr	22	1	20	-
Opaque Oxides	7	7	10	11	7	5	13	8	9
Wollastonite	2	-	-	-	-	-	-	?	?
K-Feldspar	-	-	-	-	-	-	-	Tr	-
Pectolite	3	-	-	3	-	-	Tr	-	3
Natrolite	-	-	-	-	-	-	-	Tr	-
Thomsonite	1	-	-	-	-	-	-	-	-
Andradite	1	-	-	1	-	-	-	-	1
Calcite	2	-	2	-	-	1	-	-	Tr
Dolomite	-	-	-	-	-	Tr	-	-	-
Serpentine	Tr	11	13	Tr	-	17	-	17	Tr
Chlorite	Tr	-	-	-	-	-	-	-	Tr
Hematite	Tr	-	-	-	-	-	-	-	Tr
Tobermorite*	Tr	-	-	-	-	-	-	-	-
Na-Amphibole	-	-	-	-	-	-	-	-	Tr
Aenigmatite*	Tr?	-	-	-	-	-	-	-	-
Apatite	Tr	-	-	-	Tr	1	-	1	Tr
Pyrite	Tr	-	-	-	-	-	-	-	-
Nepheline	-	-	-	-	-	4	-	-	?
Altered Groundmass	10	15	23	18	22	15	16	33	33

*Identified only by x-ray diffraction.

Liquid 2 is a high alkali + water-bearing critical fluid. This reaction may have occurred during ponding of the katungite magma at the base of the crust beneath the Colorado Plateau (~43 km depth). Continued crystallization apparently took place along diverging paths. Some portions of the magma moved rapidly to the surface freezing in the ECpx-Ph-Pv-Ox-Ap equilibrium assemblage along with unreacted Ol. In other cases, ascent was slower and the magma moved into the Ol-Mel-Pv-Ap-Ox-L field. Phlogopite apparently did not react at this point although the ECpx reacted with the liquid to form Mel. As pressure and temperature continued to fall, completed reaction (Mel+L→LCpx) and incomplete reaction (Mel+L→Wo+Pe+Th) assemblages developed. Variable amounts of very late serpentinization of Ol occurred in most samples along with very minor chloritization of Ph. A late-stage, interstitial, low-Ti Ad crystallized in some samples.

REFERENCES

- Arima, M. and Edgar, A. D. 1983. High pressure experimental studies on a katungite and their bearing on the genesis of some potassium-rich magmas of the west branch of the African rift. *Journal of Petrology*, v. 24, 166-180.
- Holmes, A. 1937. The petrology of a katungite. *Geological Magazine*, v. 74, 200-219.
- Lloyd, F. E. 1985. Experimental melting and crystallization of glassy olivine melilitites. *Contributions to Mineralogy and Petrology*, v. 90, 236-243.

IRON-OXIDES IN PISOLITE-LIKE CLASTS
IN ELLENDALE LAMPROITE INTRUSIONS

D.M.McConchie ¹ and C.B.Smith ²

1. Department of Geology
University of Western Australia
Nedlands, 6009, W.A.
2. C.R.A. Exploration Pty. Ltd.
21 Wynyard Street
Belmont, 6104, W.A.

INTRODUCTION

Ferruginous pisolite-like clasts occur sporadically throughout the crater-sequences of many Miocene lamproites (Jaques et al., 1984) in the Ellendale area, Western Australia. Some of these clasts may be a post-intrusion alteration product of primary ferro-silicate minerals, but most are considered to be pisolites formed in the soil horizon and incorporated in the lamproite tuff during its explosive emplacement. Nodules which may be alteration products usually consist of relict ferro-silicate minerals, magnetite and hematite; they are usually silicified and are compositionally similar to adjacent groundmass material (these nodules were excluded from this study). Nodules which may be soil-derived pisolites contain fine quartz and abundant ferrimagnetic and superparamagnetic α -Fe₂O₃.

Unsilicified nodules, which formed in the soil horizon as pisolites, can be used as a guide to the geochronology of lamproite emplacement (Hanstein et al., 1983), and also to give some clue to emplacement temperatures within various parts of the lamproite tuff. In this study we are interested primarily in the palaeotemperature data which can be obtained from these pisolites.

In this study we examine pisolites from the Ellendale 7 lamproite pipe which intrudes Permian Grant Formation sandstone. The lamproite has a champagne glass cross section typical of the Ellendale pipes (Atkinson et al., 1984), with a broad crater measuring 34.7 ha at the surface. The crater contains a sequence of volcanogenic sediments (Jaques et al., 1986) commencing with quartz-rich tuff and passing upwards into younger agglomerates which alternate with lapilli-ash tuffs. A central core of magmatic olivine lamproite has risen up the vent and formed a lava lake within the crater, overlying the tuffs. The tuffs and agglomerates contain abundant clasts of lamproite, lesser amounts of country rock sandstone and siltstone, occasional clasts from crystalline basement (metadolerite, schist) and rare mantle peridotite nodules. Ferruginous pisolites are common both as discrete pellets and as silicified aggregates of pellets. The larger pisolitic nodules contain rounded ferruginous concretions (0.2 - 1.0cm in diameter) set in a silicified fragmental groundmass which texturally resembles the host tuff. The concretions show concentric rings around an ovoid kernel and are cut by radial cracks resembling syneresis cracks. We consider the outer concentric rings to be accretionary iron-oxides which grew around a central core during lateritisation. Subsequent volcanic or epiclastic activity within the

crater incorporated these pisolites within the crater sediments. The core may represent a former ferromagnesian mineral from the lamproite; S.E. Haggerty (pers. comm.) has suggested the rounded clasts are ferruginised olivine crystals, and that the radial cracks are fracture cracks typical of olivine. In contrast, Jaques et al. (1986) describe the apparent pisolites as ferruginised accretionary lapilli or autoliths, implying a primary volcanic origin. In further contrast, J. Elliston (pers. comm.) has suggested the entire "pisolitic" structures are orbicules formed from a gel. However, irrespective of the precise origin of the ferruginous nodules, their physical morphology and their incorporation within the lamproite tuff indicate that they formed either prior to or during tuff emplacement. Hence, they must have experienced, and may have been modified by, thermal events during lamproite tuff emplacement.

DISCUSSION

The ferruginous clasts relevant to this study all contain α -Fe₂O₃ (possibly with adsorbed water) as their only iron-bearing mineral. The Mössbauer spectra of these clasts show either the full 6 line hyperfine splitting of hematite (Isomer Shift relative to natural iron, 0.34-0.42 mm/sec; Quadrupole Splitting, 0.51-0.55 mm/sec; Magnetic Splitting, 490-508 kOe), or a combination of the 2 line quadrupole doublet of superparamagnetic α -Fe₂O₃ (Isomer Shift, 0.36-0.44 mm/sec; Quadrupole Splitting, 0.60-0.68 mm/sec) with the 6 line hyperfine spectrum of hematite.

The superparamagnetic doublet is observed at room temperature only where the iron-oxide crystals are extremely fine (< 200Å, see Kündig et al., 1966). The proportion of superparamagnetic α -Fe₂O₃ in each sample can be assessed by comparing the peak area for the superparamagnetic doublet with the total area of spectral absorption.

Particles of α -Fe₂O₃ fine enough to be superparamagnetic cannot be produced by any natural abrasional process; they must be formed by direct chemical precipitation. Hence, the only way to produce superparamagnetic α -Fe₂O₃ from ferrimagnetic hematite must involve dissolution and reprecipitation. However, superparamagnetic α -Fe₂O₃ will very slowly (over a few million years in laterite profiles) alter to ferrimagnetic hematite under normal lateritisation conditions (Hanstein et al., 1983). The rate of alteration can be increased by ageing at elevated temperatures (about 100°C) in water (Johnston and Lewis, 1983) or by heating the superparamagnetic α -Fe₂O₃ to about 300°C under anhydrous conditions; neither heating nor ageing can reverse the process.

In this study we found that ferruginous clasts near the centre of the lamproite tuff body contained ferrimagnetic α -Fe₂O₃ only, but similar clasts from nearer the margins of the tuff body frequently contained about >50% superparamagnetic α -Fe₂O₃. We also noted that many of the ferruginous clasts in the lamproite tuff were morphologically and compositionally similar to pisolites in laterite near the lamproite pipe and that their Mössbauer spectra were almost identical.

If the superparamagnetic α -Fe₂O₃ containing clasts are heated

at 300°C the superparamagnetic to ferrimagnetic α -Fe₂O₃ ratio decreases until after 10 days no superparamagnetic α -Fe₂O₃ remains. A similar total loss of superparamagnetic α -Fe₂O₃ can be achieved at 350°C after 3 days and at 400°C after 21 hrs. The work of Johnston and Lewis (1983) suggests that in wet environments the transformation would be complete at lower temperatures (92°C for 116 hrs).

CONCLUSIONS

Because the ferruginous clasts must have been present at the time of tuff emplacement, and because the alteration of superparamagnetic α -Fe₂O₃ to ferrimagnetic α -Fe₂O₃ is not reversible without a dissolution stage, the clasts can be used to set some upper limits on temperatures/heating times for various parts of the lamproite tuff body. Hence, we may conclude that, if the tuff was emplaced in a hydrous environment, temperatures near the margins where the superparamagnetic clasts are preserved are very unlikely to have exceeded 100°C for 120 hrs. If emplacement occurred under largely anhydrous conditions then temperatures near the tuff margins cannot have exceeded 300°C for 10 days or 400°C for 21 hrs. Near the centre of the tuff body, where clasts do not contain superparamagnetic α -Fe₂O₃, the above temperature limits may have been exceeded, but by how much is unknown. Ultimately as more ferruginous clasts from various parts of the tuff are examined, it may be possible to establish temperature profiles for the tuff body, but the presently established limits do imply that the lamproite tuff had a low temperature when emplaced, or that cooling was extremely rapid, or that thermal gradients were very high, or some combination of these possibilities.

REFERENCES

- Atkinson, W.J., Hughes, F.E., 1984: A review of the kimberlitic rocks of Western Australia. In *Kimberlites 1: Kimberlites and related rocks*, J. Kornprobst (ed.) Elsevier, Amsterdam, 195-224.
- Hanstein, T., Hauser, U., Mbeshherubusa, F., Neuwirth, W. and Spath, H., 1983: Dating of Western Australian laterites by means of Mössbauer spectroscopy. *Z. Geomorph. N.F.*, 27, 171-190.
- Jaques, A.L., Webb, A.W., Fanning, C.M., Black, L.P., Pidgeon, R.T., Ferguson, J., Smith, C.B., and Gregory, G.P., 1984: The age of the diamond bearing pipes and associated leucite lamproites of the West Kimberley region, Western Australia: *BMR J. Australian Geol. and Geophys.*, v.9, 1-7.
- Jaques, A.L., Lewis, J.D. and Smith, C.B., 1986: The kimberlites and lamproites of Western Australia. *Geol. Survey of W.A. Bull.132*, 268pp (in press).
- Johnston, J.H. and Lewis, D.G., 1983: a detailed study of the transformation of ferrihydrite to hematite in an aqueous medium at 92°C. *Geochim. Cosmochim. Acta*, 47, 1823-1831.
- Kündig, W., Bömmel, H., Constabaris, G. and Lindquist, R.H., 1966: Some properties of supported small α -Fe₂O₃ particles determined with the Mössbauer effect. *Phys. Rev.*, 142, 327-333.

K. Mengel and D.H. Green

Department of Geology, University of Tasmania,
Hobart, Tasmania, Australia 7001

The specific composition of kimberlitic and alkali-basaltic melts enriched in incompatible elements has been interpreted by many authors as a result of metasomatic alteration of the source peridotite. Evidence for metasomatism in the mantle also arises from peridotite xenoliths brought up by these magmas. In such xenoliths, amphibole and phlogopite are the predominant products of metasomatic reactions. These minerals contain large proportions of incompatible elements such as K, Rb, Ba, Cs etc. relative to the anhydrous phases of the peridotite. Their stability at high pressures plays an important role in the formation of highly enriched mafic melts.

High pressure experiments were carried out on a natural peridotite composition (NHD peridotite) which was derived from a suite of spinel harzburgite and lherzolite xenoliths from the Northern Hessian Depression (NW Germany) (Wedepohl, 1985). The normative mineralogy of NHD peridotite is 78 % olivine, 18 % orthopyroxene, 7 % clinopyroxene, 1 % Cr-spinel and 1.5 % phlogopite. From this composition, 60 % olivine was subtracted to avoid the dominance of olivine in the charge products. The starting composition was made from synthetic oxides. Experiments were run in a piston cylinder apparatus using Ag-Pd capsules. The run products were examined by optical methods and all phases except glass and spinel were analyzed by electron microprobe whenever their grain size was large enough ($\geq 3 \mu\text{m}$).

For experiments at water-saturated conditions, 1 % water was added by a microsyringe to approximately 15 mg of the starting mix (NHD peridotite minus 60 % olivine), which is equivalent to 0.4 % water in the original NHD peridotite (no olivine subtracted). These experiments yielded subsolidus assemblages of olivine, orthopyroxene, clinopyroxene, amphibole, phlogopite, spinel (and garnet). The solidus was easily determined by the appearance of glass and textural changes of the charge. It resembles the solidus curves for pyrolite (Green, 1973) and for St. Pauls peridotite (Millhollen et al., 1974) at water-saturated conditions. Amphibole and phlogopite are present above the solidus at 15 and 25 kb. Phlogopite was observed above the solidus at 30 kb, 1030° C. These phases coexist with olivine, orthopyroxene, clinopyroxene, spinel (garnet) and liquid. The compositions of olivine, orthopyroxene, clinopyroxene, amphibole, phlogopite (and garnet) are very similar below and above the solidus at 15 and 25 kb. The K/Na ratio of the amphiboles is lower than that of the starting material and is probably buffered by the occurrence of phlogopite. The composition of the liquids could not be determined because the glass was modified by quench crystallization of olivine and pyroxenes. Unlike comparable experiments on pyrolite (Green, 1976) there is no significant increase in 100 Mg/Mg+Fe (Mg-number) of the residual phases in NHD peridotite when the solidus is crossed (15 and 25 kb). The amount of melt formed near the solidus, thus, cannot exceed a few percent.

For the experiments at water-undersaturated conditions the starting material (NHD peridotite minus 60 % olivine) was presaturated with water (2 %) in large capacity runs at 15 kb, 925° C. The excess water was driven out after the experiments at 450° C. The amount of water remaining in the charge was 0.4 % (equivalent to 0.15 % water in the original NHD peridotite). The large capacity run products consist of 30 % olivine, 30 % orthopyroxene, 21 % amphibole, 3 % phlogopite and 2 % Cr-spinel. All water is exclusively locked in amphibole and phlogopite.

The solidus of NHD-peridotite at water-undersaturated conditions coincides with the disappearance of amphibole. Within the experimental brackets no amphibole was observed above the solidus. The shape of the amphibole breakdown curve resembles that in pyrolite under water-undersaturated conditions (Green, 1973) but it is confined to approximately 2 kb lower pressures. This is probably due to the lower concentrations of alkalis, Ti and Al in NHD peridotite. Phlogopite, however, persists to temperatures of up to 150° C above the solidus (28 kb). The linear shape of the upper stability of phlogopite in NHD-peridotite is similar to that suggested by Wendlandt and Eggler (1980) for a natural peridotite containing 10 % additional phlogopite. Phlogopite is an abundant quench phase at 25 kb, 1200° C and at 28 kb, 1250° C. It occurs as relatively large platelets which cannot be distinguished easily from primary phlogopites at lower temperatures. A clear distinction between primary and quench phlogopite can only be achieved by microprobe analyses. Quenched phlogopites are much higher in Ti and Fe and lower in Cr contents compared to primary phlogopite. The back bending of the amphibole stability curve between 25 and 28 kb leads to a wide P,T field where a liquid (liq 1) coexists with olivine, orthopyroxene, clinopyroxene, spinel (and garnet) and phlogopite. At 25 and 28 kb an increase in Mg-number of olivine, opx, cpx, garnet and phlogopite is observed with increasing temperatures across the solidus. This can be explained by the formation of a melt (Mg-number 70 to 76) by the breakdown of amphibole. At 28 kb the compositions of the residual phases are fairly constant in the phlogopite-present melting interval over a range of more than 100° C. A further increase in Mg-number of residual olivine and orthopyroxene is observed in the phlogopite-absent melting region. At 25 kb, 1200° C and 28 kb, 1250° C the residual clinopyroxenes have lower Mg-numbers and lower Ca/Al-ratios when compared to the phlogopite-present melting region. The compositions of the liquids (glass) in both regions could not be determined directly by microprobe, but it is highly probable that liquids in the phlogopite-present melting interval (liq 1) have a different composition (e.g. lower K/Na-ratios) from those in the phlogopite-absent melting range (liq 2).

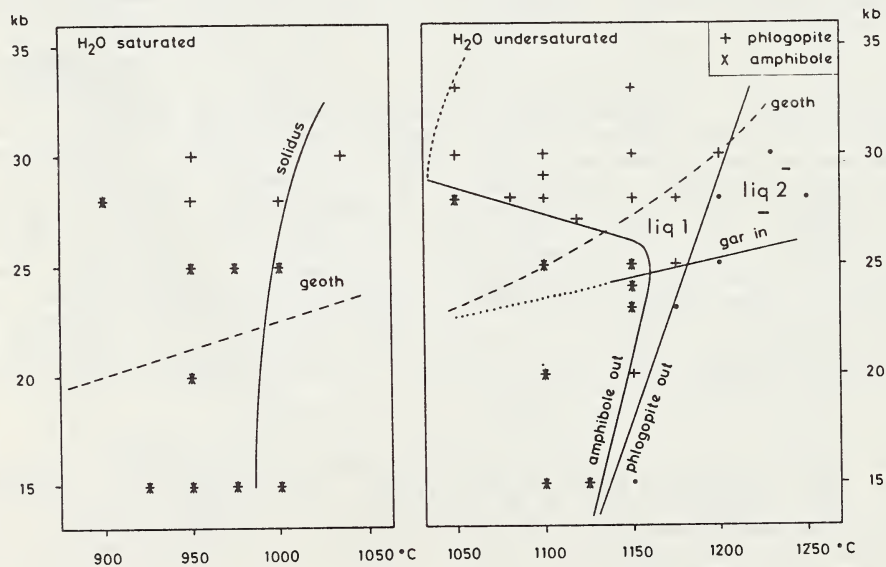


Fig. 1: Stability of amphibole and phlogopite in NHD peridotite under water-saturated and water-undersaturated conditions. Coexisting phases are olivine, orthopyroxene, clinopyroxene, spinel (and garnet).

In an attempt to characterize the nature of these liquids, "sandwich" experiments were carried out at 28 kb, 1250° C and 28 kb, 1195° C. A layer of basanite glass (NHD basanite) containing 4 % water was embedded between two layers of NHD peridotite minus 60 % olivine (presaturated with water). The residual phases in the peridotite layers were directly analyzed by electron microprobe. The glass in the basanite layer was quenched modified as in the non-sandwich experiments. Small amounts of glass are also observed within the upper and the lower peridotite layers. Microprobe analyses from this glass gave significant amounts of P₂O₅. Because there was no P added to the peridotite starting mix, this observation is taken as evidence for a mixing between the melt formed within the peridotite layers and the embedded basanitic melt. Areas of 20 to 50 μm were analyzed in the basanite layer with a scanning electron beam to include quenched phases (mainly clinopyroxene) and to avoid vaporization of the alkalis in the analysis. Each set of area scan analyses represents a compositional spectrum of the basanite layer with a large range of Mg-numbers depending on the amount of quenched phases included in the scan analyses. Within a set of such analyses the Si, Ti, Al, Fe, Mg, Ca and P are correlated with the Mg-number reflecting the proportions of quenched crystals in each area scan. From Mg-number versus oxide plots the composition of the liquid in equilibrium with the peridotite is estimated using the olivine/liquid Mg-Fe K_D of Takahashi and Kushiro (1983) to choose an appropriate Mg-number for the basanite liquid. A sandwich experiment at 28 kb, 1250° C had residual olivine, orthopyroxene, clinopyroxene, garnet and minor spinel in the peridotite layers. At 28 kb, 1195° C phlogopite was stable as an additional residual phase beside these phases. These are the same residual phase assemblages as in experiments at the same conditions where no basanite was added. The composition of the residual phases has changed very little when compared with those in the non-sandwich experiments. Therefore, the composition of the liquids in the non-sandwich experiments cannot be very different from that of the basanite used in the sandwiched layer. The composition of the liquid in the 28 kb, 1195° C experiment (residual phlogopite) as calculated from Mg-number versus oxide plots reveals a greater similarity to that of NHD basanite than the liquid in the 28 kb, 1250° C experiment where all phlogopite has entered the melt. The glass in the latter experiment has a much higher K/Na ratio, reflecting the total consumption of phlogopite. The K/Na ratio of the liquid in the 28 kb, 1195° C sandwich experiment has the same K/Na ratio as NHD basanite and the other alkali basaltic species from the northern Hessian Depression, indicating that the respective melts have formed in the P,T field where phlogopite is a residual phase.

This experimental approach permits the testing of models with low degrees of partial melting of peridotite where direct analyses of the quenched liquid present in the experimental charge are not feasible.

REFERENCES

- GREEN, D. H., 1973. Experimental melting studies on a model upper mantle composition at high pressure under water-saturated and water-undersaturated conditions. *Earth and Planetary Science Letters* 19, 37-53.
- GREEN, D. H., 1976. Experimental testing of "equilibrium" partial melting of peridotite under water-saturated, high pressure conditions. *Canadian Mineralogist* 14, 255-268.
- MILLHOLLEN, G. L., IRVING, A. J. & WYLLIE, P. J., 1974. Melting interval of peridotite with 5.6 per cent water to 30 kilobars. *Journal of Geology* 82, 575-587.
- TAKAHASHI, E. & KUSHIRO, I., 1983. Melting of a dry peridotite at high pressures and basalt magma genesis. *American Mineralogist* 68, 859-879.
- WEDEPCHL, K. H., 1985. Origin of the Tertiary basaltic volcanism of the northern Hessian Depression. *Contributions to Mineralogy and Petrology* 89, 122-143.
- WENDLANDT, R. F. & EGGLEER, D. H., 1980. The origin of potassic magmas: 2. Stability of phlogopite in natural spinel lherzolite and in the system KAlSiO₄-MgO-SiO₂-H₂O-CO₂ at high pressures and high temperatures. *American Journal of Science* 280, 421-458

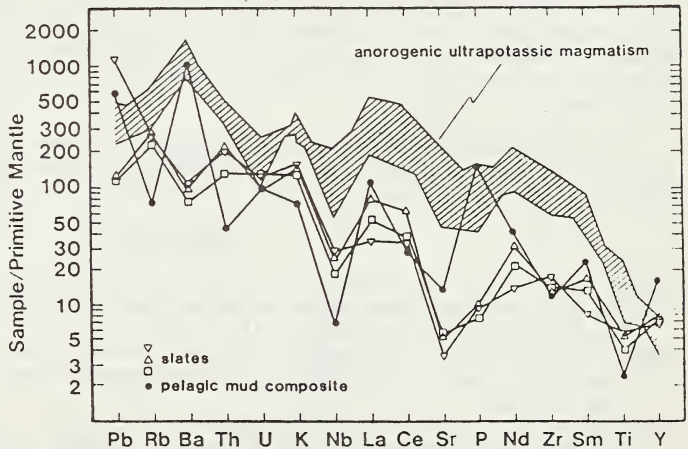
D.R. Nelson, M.T. McCulloch and A.E. Ringwood

Research School of Earth Sciences, Australian National University, Canberra, 2601.

Isotopic studies indicate that some examples of potassic magmatism are derived from ancient, highly enriched (radiogenic $^{87}\text{Sr}/^{86}\text{Sr}$, unradiogenic $^{143}\text{Nd}/^{144}\text{Nd}$) sources, and in an attempt to investigate the origins of these enriched components, we have undertaken a comparative Sr, Nd and Pb isotopic and geochemical examination of potassic magmatism from a number of localities. Diamond-bearing lamproites from Western Australia, leucitites from Gaussberg, high-K alkaline dykes from MacRobertson Land, Enderby Land and Queen Mary Land regions of east Antarctica and madupities, wyomingites and orendites from Leucite Hills, Wyoming, have remarkably similar geochemical characteristics (Fig. 1). All have high Ni and Cr contents and high Mg numbers (each locality averaging $\text{Mg}/(\text{Mg}+\text{total Fe}) > 0.65$ with the exception of Manning Massif, Mt Bayliss and Bunger Hills samples, which have Mg numbers of 0.58, 0.58 and 0.50 respectively) as well as high to extreme abundances of K_2O , TiO_2 , F, Cl, SO_2 , H_2O , P_2O_5 , Ba, LREE, high $\text{K}_2\text{O}/\text{Na}_2\text{O}$, $\text{Fe}^{3+}/\text{Fe}^{2+}$, Th/U, La/Nb and Ba/La ratios, low K/Rb and K/Ba ratios and relatively low abundances of Al_2O_3 , CaO and Na_2O . On a Sr-Nd isotope diagram (Fig. 2), these magmas lie within the "enriched" quadrant, indicating that their sources have had long histories (>1 byrs) of high Rb/Sr and low Sm/Nd (ie; LREE enrichment). Pb isotopic compositions (Fig. 3) indicate multistage histories of U/Pb fractionation, requiring an earlier high U/Pb stage to generate the high $^{207}\text{Pb}/^{204}\text{Pb}$, followed by a low U/Pb stage during which the evolution of $^{206}\text{Pb}/^{204}\text{Pb}$ is retarded.

There are a number of possible mechanisms which could account for these unusual chemical and isotopic properties, the most obvious of which is crustal contamination. However, the extremely high concentrations of Sr, Pb and the REE make these magmas insensitive to bulk contamination processes, requiring the assimilation of substantial amounts of crustal material to account for their isotopic compositions. Because of their extreme degree of LREE-enrichment, bulk assimilation of felsic granulite within the lower continental crust will effectively dilute the incompatible element contents of the magmas and should therefore produce a positive correlation between Nd concentration and eNd. In the case of the Western Australian lamproites, a correlation in the opposite sense was noted by McCulloch et al (1983). Crustal assimilation via specialised mechanisms, such as selective volatile transfer or zone refining, is conceivable but is unable to account for the high Mg numbers and Ni and Cr contents or the presence of mantle xenoliths (and in one case, diamonds). Furthermore, the remarkable similarities of unusual geochemical and isotopic compositions of these magmas from diverse localities are unlikely to be the result of random crustal contamination processes but instead, suggest their derivation by a common mechanism.

Figure 1. Trace element patterns, normalised to estimated primitive mantle abundances, of average potassic magmas (hatched) from Western Australia (McCulloch et al 1983, Nelson et al 1986, Jaques et al 1984, Nixon et al 1984), Priestley Peak and Gaussberg, Antarctica (Sheraton and England 1980, Sheraton 1983, Collerson and McCulloch 1983, Sheraton and Cundari 1980) and Leucite Hills (orendites and wyomingites, from Kuehner et al 1981, Vollmer et al 1984; Th and U data not available) compared with some examples of modern sediments (from Thompson et al 1984).



Petrogenetic models involving small degrees of partial melting of a lherzolitic or harzburgitic mantle source which has been variably "metasomatised" by an incompatible element rich component have been advocated by a number of workers (eg; Jaques et al 1984, Vollmer et al 1984). For example, enrichment events within the subcontinental lithosphere or upper mantle may result in crystallisation of phlogopite and LIL-rich titanates which are later reactivated to produce isotopically evolved ultrapotassic magmatism (cf. Jaques et al 1986). However, these models frequently fail to address the crucial question of the ultimate source of these metasomatic components. Furthermore, the unusual multistage histories of U/Pb fractionation indicated by the Pb isotopic compositions of these magmas, particularly the earlier high U/Pb stage, are not readily explained by models which favour the generation of these "metasomatic" components entirely within the upper mantle or subcontinental lithosphere.

Figure 2. Initial Sr-Nd isotope diagram showing fields for Western Australian lamproites (McCulloch et al 1983), Leucite Hills (Vollmer et al 1984 and analyses of two wyomingites from this study), Gausberg (Collerson and McCulloch 1983) and the Priestley Peak melasyenite at its emplacement age of 482 myrs (initial Sr and age data from Black and James 1983). Initial ϵ_{Nd} values for Manning Massif tristanite (emplacement age; 50 myrs, from Sheraton 1983), Mt Bayliss alkali melasyenite (414 myrs old) and Bunger Hills trachybasalt dyke (Cambrian or younger) are -9.3, -12.3 and <-16.3 respectively. Initial Sr not determined for these samples. Field of mid-ocean ridge basalts shown for comparison.

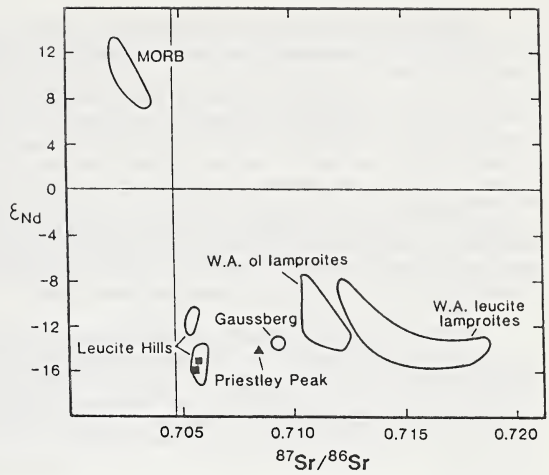
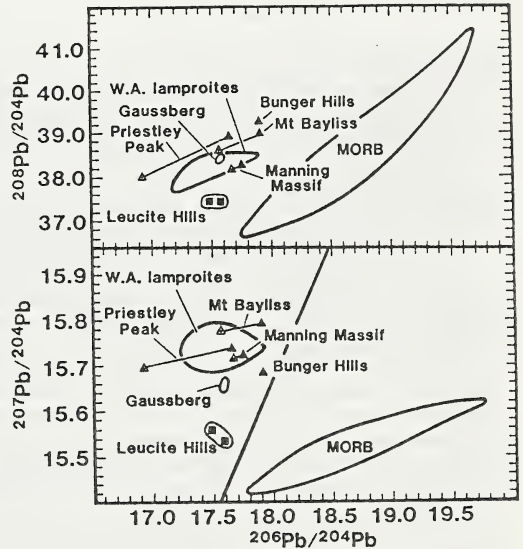


Figure 3. Pb-Pb isotope diagram showing compositions of Western Australian lamproites and Gausberg leucities (from Nelson et al 1986), Leucite Hills and Antarctic dykes (Δ = measured, \triangle = age corrected). Field of mid-ocean ridge basalts for comparison. Corrections to $^{206}Pb/^{204}Pb$ for decay since emplacement are small for the 50 myr old Manning Massif tristanite and because of its low U/Pb, to the Mt Bayliss alkali melasyenite dyke but are considerably larger for the Priestley Peak melasyenite. Age corrections to the measured $^{207}Pb/^{204}Pb$ ratios are within analytical error for the Manning Massif and Mt Bayliss samples. The exact emplacement age of the Bunger Hills trachybasalt dyke is uncertain but is believed to be Cambrian or younger. Its high measured $^{207}Pb/^{204}Pb$ requires a long history (>1 byrs) of high U/Pb and is a feature that predates emplacement. The general features of the Nd and Pb isotopic compositions of the Antarctic dykes are independent of any uncertainty introduced by the age corrections and are similar to those of lamproites from Western Australia and leucites from Gausberg.



We propose that the geochemical and isotopic characteristics of these and possibly other examples of continental potassic magmatism are due predominantly to the involvement of a sedimentary component, and that these magmas represent mixtures of mantle and the fusion products of ancient sediments which have been subducted into the mantle (to depths within the field of diamond stability) and stored for long time periods within the subcontinental lithosphere. A number of other studies (see, for example, Nelson et al 1986 and references cited therein) have argued for the involvement of more recently subducted sediments in the generation of highly potassic magmatism from Italy and Spain, whilst the arlike Ba/La, Ba/Nb and La/Nb ratios of some examples of continental potassic magmatism has been previously pointed out by Thompson et al (1984) and Varne (1985). The high abundances of F, Cl, P_2O_5 , SO_2 and H_2O , high K/Ba and low K/Rb ratios of these examples of continental potassic magmatism, their highly oxidised nature (evidenced by their high Fe^{3+}/Fe^{2+}) and their radiogenic Sr and unradiogenic Nd are readily explained by the involvement of a sedimentary component. By analogy with modern sediments, ancient oceanic sediments will probably have possessed high $^{206}Pb/^{204}Pb$ and $^{207}Pb/^{204}Pb$ due to the contribution of radiogenic Pb from the upper continental crust. Although the U/Pb ratio of modern pelagic oceanic sediments is variable, it is frequently low, and may have been generally lower during the Archean when the lower degree of oxidation of the Earth's atmosphere would favour the less soluble U^{4+} ion over U^{6+} . Ancient sediments therefore probably possessed low U/Pb ratios and the isotopic evolution of Pb would have been severely retarded following its erosion from the continents and deposition in the ocean basins. Hence, the unradiogenic $^{206}Pb/^{204}Pb$ of continental ultrapotassic magmas may be an indication of the time elapsed during sedimentation and storage within the mantle or subcontinental lithosphere, whereas the variation in $^{207}Pb/^{204}Pb$ may reflect the nature and age of the continental provenance.

The presence of diamonds in the Western Australian lamproites provides further support for the involvement of sediment recycling processes, as an extremely wide range of $\delta^{13}\text{C}$ values (including values as low as -34 per mil) have been documented by carbon isotopic studies of diamonds from kimberlites and lamproites (see Ozima et al 1985 and references therein), consistent with an origin of some diamonds from sedimentary sources of carbon. A wide range of $^3\text{He}/^4\text{He}$ ratios were also recently reported by Ozima et al (1985) for diamonds. These authors interpreted the high $^3\text{He}/^4\text{He}$ ratios of some South African examples as indicating that these diamonds had remained closed systems for almost the age of the Earth. However, an alternative interpretation is offered by the recently confirmed high $^3\text{He}/^4\text{He}$ ratios of modern ocean sediments (Ozima et al 1984) and manganese nodules (Sano et al 1985), believed to be carried by interplanetary dust particles. Furthermore, a common mineral assemblage of diamond inclusions, olivine + knorringite-rich garnet + enstatite, has been attributed to recrystallisation of the residue of olivine + chrome spinel + enstatite cumulates within oceanic crust following its hydrothermal alteration and partial melting during subduction into the mantle (Ringwood 1977). These data argue for the involvement of components derived from both subducted sediments and oceanic crust in the formation of diamonds.

Although these examples of continental potassic magmatism are not obviously associated with any known modern or past subduction zones, their unusual multistage Pb isotopic compositions require a significant time period (probably much greater than 1 byrs) to have elapsed between the fractionation events lowering the U/Pb ratio (ie; erosion and sedimentation at the Earth's surface) and subsequent potassic magmatism. As these suites all intrude old Archaean or Proterozoic cratons, their sources are probably stored for long periods within the subcontinental lithosphere. The existence of substantial reservoirs of low U/Pb, enriched mantle components within the subcontinental lithosphere may also account for the generally radiogenic Pb of the MORB and ocean island source reservoirs.

REFERENCES

- BLACK L.P. and JAMES P.R. (1983) Geological history of the Archaean Napier Complex of Enderby Land. In Oliver R.L., James P.R. and Jago J.B. eds, *Proceedings of the 4th International Symposium on Antarctic Earth Science*, pp. 11-15.
- COLLERSON K.D. and McCULLOCH M.T. (1983) Nd and Sr isotope geochemistry of leucite-bearing lavas from Gaussberg, East Antarctica. In Oliver R.L., James P.R. and Jago J.B. eds, *Proceedings of the 4th International Symposium on Antarctic Earth Science*, pp. 676-680.
- JAQUES A.L., LEWIS J.D., SMITH C.B., GREGORY G.P., FERGUSON J., CHAPPELL B.W. and McCULLOCH M.T. (1984) The diamond-bearing ultrapotassic (lamproitic) rocks of the west Kimberley region, Western Australia. In Kornprobst J. ed, *Kimberlites and Related Rocks Vol. 2A*, pp. 225-254. Elsevier, Amsterdam.
- JAQUES A.L., CHAPPELL B.W., SUN S.-S., LEWIS J.D. and SMITH C.B. (1986) The west Kimberley lamproites: intraplate volcanism of extreme character. (Abstr.) *International Volcanological Congress, New Zealand*, p171.
- KUENHER S.M., EDGAR A.D. and ARIMA M. (1981) Petrogenesis of the ultrapotassic rocks from the Leucite Hills, Wyoming. *American Mineralogist* 66, 663-677.
- McCULLOCH M.T., JAQUES A.L., NELSON D.R. and LEWIS J.D. (1983) Nd and Sr isotopes in kimberlites and lamproites from Western Australia: an enriched mantle origin. *Nature* 302, 400-403.
- NELSON D.R., McCULLOCH M.T. and SUN S.-S. (1986) The origins of ultrapotassic rocks as inferred from Sr, Nd and Pb isotopes. *Geochimica et Cosmochimica Acta* 50, 231-245.
- NIXON P.H., THIRWALL M.F., BUCKLEY F. and DAVIES C.J. (1984) Spanish and Western Australian lamproites: aspects of whole rock geochemistry. In Kornprobst J. ed, *Kimberlites and Related Rocks Vol. 2A*, pp. 285-296. Elsevier, Amsterdam.
- OZIMA M., TAKAYANAGI M., ZASHU S. and AMARI S. (1984) High $^3\text{He}/^4\text{He}$ ratio in ocean sediments. *Nature* 311, 448-450.
- OZIMA M., ZASHU S., MATTEY D.P. and PILLINGER C.T. (1985) Helium, Argon and Carbon isotopic compositions in diamonds and their implications in mantle evolution. *Geochemical Journal* 1, 127-134.
- RINGWOOD A.E. (1977) Synthesis of pyrope-knorringite solid solution series. *Earth and Planetary Science Letters* 36, 443-448.
- SANO Y., TOYODA K. and WAKITA H. (1984) $^3\text{He}/^4\text{He}$ ratios of modern marine ferromanganese nodules. *Nature* 317, 520-522.
- SHERATON J.W. (1983) Geochemistry of mafic igneous rocks of the northern Prince Charles Mountains, Antarctica. *Journal of the Geological Society of Australia* 30, 295-304.
- SHERATON J.W. and CUNDARI A. (1980) Leucites from Gaussberg, Antarctica. *Contributions to Mineralogy and Petrology* 71, 417-427.
- SHERATON J.W. and ENGLAND R.N. (1980) Highly potassic mafic dykes from Antarctica. *Journal of the Geological Society of Australia* 27, 1-18.
- THOMPSON R.N., MORRISON M.A., HENDRY G.L. and PARRY S.J. (1984) An assessment of the relative roles of crust and mantle in magma genesis: an elemental approach. *Philosophical Transactions of the Royal Society of London* A310, 549-590.
- VARNE R. (1985) Ancient subcontinental mantle: A source for K-rich orogenic volcanics. *Geology* 13, 405-408.
- VOLLMER R., OGDEN P., SCHILLING J.-G., KINGSLEY R.H. and WAGGONER D.G. (1984) Nd and Sr isotopes in ultrapotassic volcanic rocks from the Leucite Hills, Wyoming. *Contributions to Mineralogy and Petrology* 87, 359-386.

Hugh E. O'Brien, Anthony J. Irving and I. S. McCallum, Dept. of Geological Sciences, University of Washington, Seattle, WA 98195, U.S.A.

INTRODUCTION

Potassic mafic volcanic and intrusive rocks of the Eocene Highwood Mountains province of north-central Montana show mineralogical, textural and chemical evidence for multiple episodes of fractional crystallization and mixing of minette and mafic phonolite magmas at low pressures. Phenocryst compositions and bulk rock REE abundances of the most primitive mafic minette magmas are consistent with their derivation by partial melting of a phlogopite-bearing garnet peridotite mantle. Despite the distinctly different phenocryst assemblages of the minettes and mafic phonolites, the bulk compositions of these two groups overlap significantly (Figure 1). The mineralogical differences evidently result from differences in volatile fugacities during crystallization, implying that low pressure degassing was important.

ROCK TYPES

The Highwood province consists of an older series of quartz-normative latite flows and dikes and a younger series of K-rich, silica-undersaturated minette and mafic phonolite flows, dikes and sills and rare lamproitic dikes. Shonkinite, the phaneritic equivalent of mafic phonolite, forms four major stocks, and fine grained phaneritic equivalents of the minettes occur in several smaller intrusive bodies. The hiatal porphyritic minettes contain phenocrysts of diopside ($mg = 92$, $Al_2O_3 = 1$ wt. %) + phlogopite ($mg = 92$) ± Mg-rich olivine (F089-92) in a sanidine + biotite + salite + oxide groundmass. The seriate porphyritic mafic phonolites contain salite ($mg = 76$, $Al_2O_3 = 4$ wt. %) + pseudoleucite + olivine (F077-60) phenocrysts in a salite + sanidine + oxide ± biotite ± nepheline ± glass matrix. The rare lamproitic rocks contain phenocrysts of phlogopite + diopside + leucite + olivine (now pseudomorphed by talc + serpentine) in a leucite + sanidine + mica + clinopyroxene + oxide matrix, and appear to form a mineralogical link between the minettes and the mafic phonolites. Cumulate xenoliths are common in all magma types, but mantle xenoliths are apparently absent.

GEOCHEMISTRY

Neither major nor trace element abundances serve to discriminate mafic phonolites from minettes. However, the most primitive minettes have slightly higher MgO contents than the corresponding mafic phonolites whereas the latter show slightly more evolved compositions (Figure 1A). The lamproitic dike is chemically indistinguishable from the primitive minettes. The syenite trend (Figure 1A) could be the product of biotite pyroxenite fractionation from primitive mafic phonolite magma, which is consistent with the large bodies of pyroxenite mapped in the field. This figure also shows two trends that converge at $MgO \sim 11.5$ wt. %. Samples plotting on the higher CaO branch represent shonkinites enriched in salite + biotite. The lower CaO branch may represent an olivine control trend. However, even the two most magnesian Highwood samples (missourites) plot on the well defined Sc-CaO curve demonstrating the importance of clinopyroxene fractionation (Figure 1F). Na_2O is incompatible and increases with fractionation (Figure 1B) while K_2O remains essentially constant across a wide range of MgO values (Figure 1C) except for the syenites and trachytes in which sanidine is an important early phase. Ba-Ni plots (Figure 1D) show the same trends suggesting that a K, Ba-rich phase crystallized throughout the fractionation sequence. BaO increases from ~ 0.5 wt. % in phlogopites from primitive minettes to ~ 4.0 wt. % in biotite from more evolved shonkinites suggesting that mica + cpx fractionation was responsible for maintaining a bulk D_{Ba} value of ~ 1.0 . Figure 1E is also consistent with cpx + mica fractionation if the genetically unrelated syenites of Highwood Baldy and the latites are excluded. The presence of plagioclase phenocrysts in these latter rocks suggests they were derived from a distinctly different source region, possibly within the lower crust.

ROLE OF FLUIDS

Early crystallization of F-poor phlogopite and evidence of explosive eruption indicate that a fluid phase (H₂O- and CO₂-rich) played an important role in the petrogenesis of the minettes and lamproitic rocks. However, microphenocrysts of salite and F-rich biotite in minette that crystallized subsequent to dike emplacement and degassing, have the same composition as the salite phenocrysts and interstitial biotite in mafic phonolite. This indicates that conditions during the later stages of minette crystallization were similar to those during mafic phonolite crystallization, i.e., mafic phonolites are essentially outgassed equivalents of minettes.

MAGMA MIXING

The majority of the evolved mafic phonolites and evolved minettes contain mixed phenocryst assemblages which are consistent with periodic mixing between these two magma types. Colorless diopside occurs in the mafic phonolites as separate subhedral xenocrysts, as euhedral to subhedral cores in green salite and as continuous growth bands 20-100 μ m wide within salite. Many mafic phonolites also contain rounded, resorbed phlogopite and/or large (\sim 1 cm), rounded zoned olivine xenocrysts with Mg-rich (Fo_{>87}) cores. The more evolved minettes contain complexly zoned clinopyroxene, salite and olivine (Fo_{<77}) xenocrysts, and resorbed phlogopite rimmed by Ti, Ba-rich biotite. It is possible that mixing of the two major magma types may have initiated eruption of the Highwood volcanics. The presence of diopside and phlogopite xenocrysts in mafic phonolite flows and tuffs is consistent with injection and mixing of a pulse of fluid-rich minette magma into the subvolcanic mafic phonolite magma system causing degassing and triggering explosive eruptions. The rarity of minette flows is consistent with such a model.

CONSTRAINTS ON MANTLE SOURCES

The primitive minettes show marked light REE enrichment (Figure 2), and have relatively high contents of Ba (2000-5000 ppm), Sr (850-1200 ppm), Ni (250-330 ppm) and Cr (500-725 ppm). These features are consistent with residual garnet, mica and clinopyroxene in the source. Furthermore, the compositions of olivine, diopside and phlogopite phenocrysts in the most primitive minettes are very similar to those in phlogopite-garnet lherzolite xenoliths in minettes from The Thumb, NM (Ehrenberg, 1982). Thus, we suggest that the Highwood parental minette magmas were derived by small degrees of partial melting of phlogopite-bearing garnet peridotite mantle.

References

- EHRENBERG S.N. 1982. Petrogenesis of garnet lherzolite and megacrystalline nodules from The Thumb, Navajo volcanic field. *Journal of Petrology* 23, 507-547.
- SCHNETZLER C.C. and PHILPOTTS J.A. 1970. Partition coefficients of rare-earth elements between igneous matrix material and rock-forming mineral phenocrysts-II. *Geochimica et Cosmochimica Acta* 34, 331-340.

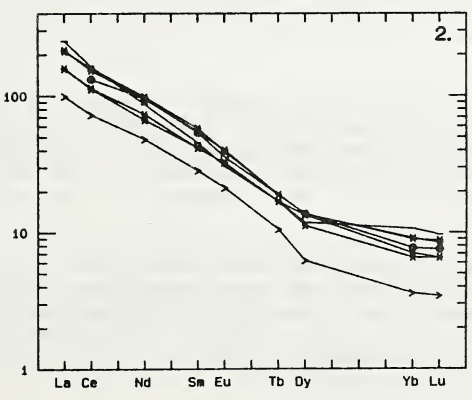
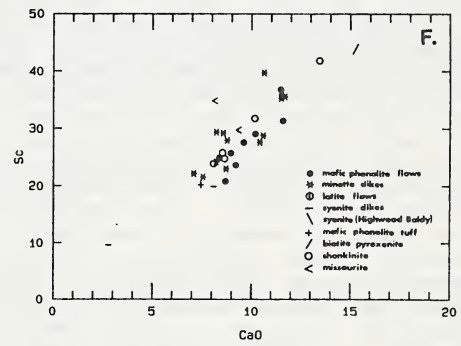
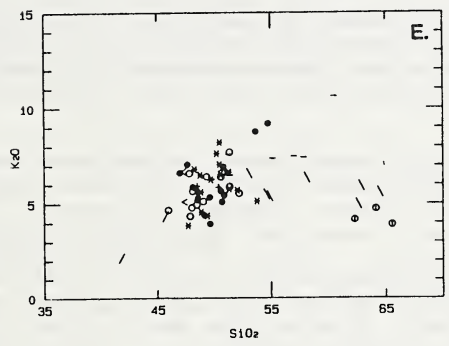
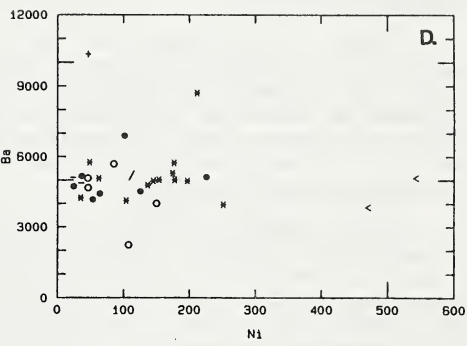
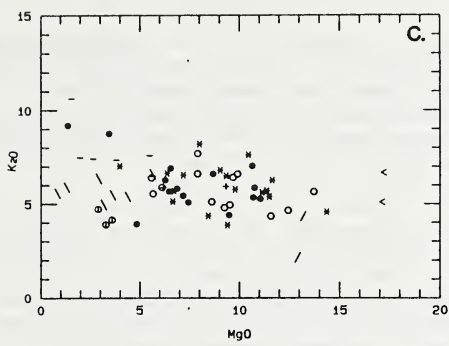
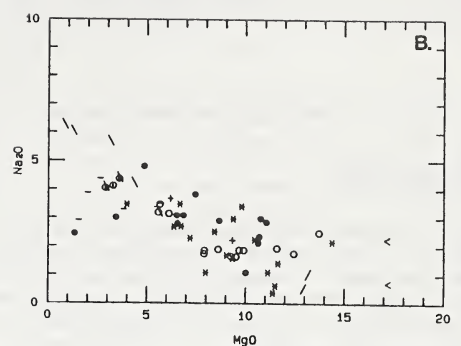
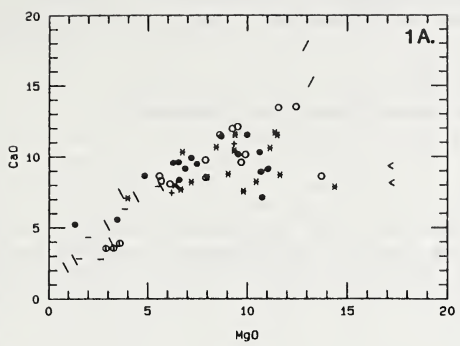


Fig. 1. (A-E) Variation diagrams for selected Highwood whole-rock samples. Compositions determined by ICP emission spectroscopy. Key to symbols for all figures given in 1F.

Fig. 2. Chondrite-normalized REE abundances for 7 Highwood samples (data for one mafic phonolite from Schmetzler & Philpotts, 1970).

CONTRASTING GROUP 1 AND GROUP 2 KIMBERLITE PETROLOGY:
TOWARDS A GENETIC MODEL FOR KIMBERLITES

E.M.W. Skinner

Geology Department, De Beers Consolidated Mines Ltd., Kimberley.

INTRODUCTION

Southern African kimberlites can be subdivided into two distinct groups (termed Group 1 and Group 2, e.g. Smith, 1983) on the basis of differences in distribution, petrography, content of mantle-derived xenocrysts and xenoliths, isotopic character, age and whole-rock geochemistry. The contrasting petrology of the two groups has important implications for models of kimberlite genesis.

CONTRASTING PETROLOGY

To date 162 occurrences out of a total of approximately 840 southern African kimberlites, have been identified as Group 2 varieties. These are distributed within a belt ($\pm 400 \times 1250$ km) extending from Eendekuil (near Sutherland, western Cape) in the south-west to Dokolwayo (Swaziland) in the north-east. Group 1 kimberlites are more widely distributed. Group 2 kimberlites have been identified only in southern Africa.

Broad Petrographic Distinctions

Group 1 kimberlites are characterised by several of the following major (volumetrically abundant) matrix minerals; monticellite, calcite, serpentine and phlogopite. Groundmass spinels and perovskite are typically abundant and relatively coarse-grained. Groundmass ilmenite may be present. Olivine phenocrysts in Group 1's are generally less than 1 mm in size and commonly contain small inclusions of rutile. Olivine xenocryst to phenocryst ratios, in terms of volume, commonly approximate 1:1.

Group 2 kimberlites are nearly always dominated by phenocrysts or groundmass phlogopite with or without diopside. Groundmass spinels and perovskite, if present, are rare and small. Groundmass ilmenite does not occur. Olivine phenocrysts in Group 2's vary considerably in size and abundance relative to xenocrysts. Rutile inclusions in olivine phenocrysts have not been found.

Both xenocryst and phenocryst olivines in several Group 2 kimberlites exhibit pronounced overgrowths. Core compositions of individual xenocrysts and phenocrysts are uniform with respect to both major and minor elements. However populations of both xenocrysts and phenocrysts may exhibit variable compositions (e.g. Fo_{93} to Fo_{87} for xenocryst cores and Fo_{95} to Fo_{89} for phenocryst cores). In contrast overgrowth compositions are always similar irrespective of whether the core is a xenocryst or phenocryst. Overgrowth compositions are uniform with respect to major elements (e.g. Fo_{90}) but Ni, Mn and Ca vary. Nickel typically increases from about 0,4 wt.% (core content) to about 0,55 wt.% at the core - overgrowth boundary. It then decreases rapidly towards the overgrowth rim (e.g. 0,2 wt.%).

Mantle-derived Constituents

Most Group 1 kimberlites carry a full suite (e.g. olivine, ilmenite, garnet, chromite, cpx., opx. and zircon) of mantle-derived xenocrysts although some are devoid of ilmenite. All 'on-craton' Group 2 kimberlites are essentially devoid of ilmenite and zircon xenocrysts. Garnet, chromite and olivine xenocryst populations in 'on-craton' Group 2's appear to be compositionally more homogeneous than these populations in Group 1 varieties.

Olivine xenocrysts are by far the most abundant mantle-derived mineral in both groups of kimberlite. Apart from xenocrystal phlogopite and ilmenite which may reach up to about 4 vol.%, other xenocrysts rarely exceed 1 vol.%. Not only is orthopyroxene very much less abundant than olivine but it is also less abundant than garnet and clinopyroxene. This is surprising in view of the likelihood that the source rocks of kimberlite contain significant proportions of orthopyroxene.

Similar variations in the proportions of peridotite and eclogite xenolith populations are evident for both groups of kimberlite. However, mantle metasomatized peridotites and 'marid'-type xenoliths are rare in Group 2 occurrences.

Smith (1983) maintains that deformed, "hot" peridotites (containing high Ti garnets) are found only in Group 1 kimberlites. He uses this to support his hypothesis that Group 1's are asthenosphere-derived. This argument is, to some extent, supported by the general scarcity of titanium-rich garnets in Group 2 kimberlites (the Dokolwayo kimberlite being a notable exception). Xenolith proportions and heavy mineral suites are commonly poorly correlated in any particular kimberlite. For example, at Roberts Victor, garnets picked out of heavy mineral concentrate are dominated by peridotitic types whereas the xenolith population is mainly eclogitic. Some xenoliths and xenocrysts are isotopically out of equilibrium with the host kimberlite. This is true of both groups of kimberlite. Such xenoliths and xenocrysts have little bearing on the nature of the source rocks. Most xenoliths and many xenocrysts may in fact merely represent higher level mantle constituents picked up by an already well-developed (isotopically and geochemically distinct) kimberlite magma.

Isotopes and Ages

Smith (1983) showed that most Group 1 kimberlites are isotopically slightly depleted relative to Bulk Earth with respect to Sr and Nd. Pb values are relatively radiogenic and variable. In contrast Group 2 kimberlites are isotopically enriched relative to Bulk Earth with respect to Sr and Nd. Pb isotopes are relatively unradiogenic. Group 1's are considered by Smith (1983) to be derived from asthenospheric-like sources whereas Group 2's are thought to be derived from lithospheric sources with an isotopic character indicative of ancient (metasomatic) enrichment.

Group 1 kimberlites range in age from about 1 600 to about 50 million years. In southern Africa most of these fall within the time span from ± 250 to 50 m.y. A vague periodicity of volcanism is evident. In contrast Group 2 kimberlites range in age from about 110 to 200 million years (a time span of only 90 m.y.) and ages increase progressively from Eendekuil to Dokolwayo. It is notable that the 200 m.y. age of Dokolwayo broadly correlates with the opening of the Indian ocean whereas the younger Eendekuil age broadly correlates with the opening of the Atlantic. Group 1 kimberlites do not exhibit well-defined age patterns.

Where Cretaceous kimberlites occur in the same area Group 2's are always older than Group 1's and age differences range from about 5 m.y. (e.g. in the Harts River Valley area) to about 55 m.y. (e.g. in the Swartruggens area).

Whole-rock Geochemistry

Group 2 kimberlites are characterised by higher levels of SiO₂, K₂O, Rb, Ba and LREE but lower CO₂, TiO₂ and Nb compared to Group 1's (Smith et al, in press). Correlations between SiO₂ and CO₂ may reflect different source rock conditions as well as differences in the degree of evolution. Considering the former, if the source peridotite is relatively enriched in CO₂, experimental evidence indicates that the orthopyroxene field is expanded and the resultant melt is relatively undersaturated with respect to silica.

In spite of suggestions by Smith (1983) broad similarities of major element composition and trace element abundance patterns suggest that both groups of kimberlite may perhaps have been generated within the lithosphere with Group 1's being derived from parts of the lithosphere that have not undergone isotopic and other enrichment processes.

Relative deficiencies in TiO₂ and Nb in Group 2's may relate to the evidence provided by xenocryst and xenolith populations which indicates that Group 2's are derived from source rocks that are essentially devoid of ilmenite, rutile and zircon. Deficiencies in TiO₂ may, however, also be consistent with differences in the degree of "evolution" with more highly "evolved" rocks containing higher TiO₂.

The contrasting petrological nature of Group 1 and Group 2 kimberlites allows the development of a new model for kimberlite genesis and emplacement. The main aspects of this model, which requires some fundamental assumptions, are presented below:

- (1) It is assumed that kimberlite volcanism occurs as a result of the introduction of heat or volatile elements from below.
- (2) Kimberlite magmas are initially generated by small degrees of partial melting from isotopically and geochemically distinct lithospheric source rocks. However, melting of the Group 2 source rocks, will be accelerated by the presence of higher proportions of K_2O , Rb, Ba, LREE and H_2O . Smaller amounts of CO_2 relative to H_2O will favour an increased contribution from the orthopyroxene component in peridotite resulting in relatively higher SiO_2 in Group 2 magmas.
- (3) Compositional restrictions with respect to mantle-derived xenocrysts and the absence of Ti-rich xenoliths and xenocrysts indicates that Group 2 kimberlites are derived from a smaller segment of the upper mantle compared with Group 1 kimberlites.
- (4) The fact that Group 2 kimberlites predate Group 1 kimberlites in the same area indicates that, if the genesis of both magmas is initiated by the same or similar volcanic processes, then Group 2 magmas are generated faster and are emplaced sooner than Group 1 kimberlites.
- (5) The almost linear age progression of Group 2's and the apparent association between age and break up of Gondwanaland may indicate that hot-spot activity is more important in respect of the generation of Group 2 magmas. The transfer of heat and associated volatile elements from a stationary hot-spot into the upper moving plate is likely to be more effective where the plate has been preconditioned, by the earlier addition of other incompatible elements.
- (6) The compositional variations exhibited by olivine xenocrysts and phenocrysts may provide valuable clues to processes of genesis and emplacement. Following the model first projected by Clement (1984) it is proposed that early (larger and generally more refractory) olivine phenocrysts crystallise from small pockets of magma. These magma pockets move upwards and subsequently coalesce to form a larger magma diapir which continues to ascend. Olivine xenocrysts (derived from the break-up of peridotitic wall rocks of differing composition) are incorporated into this magma. Both xenocrysts and early phenocrysts exhibiting partial resorption are subsequently armoured by overgrowths of olivine. These, together with smaller phenocrysts, crystallise at constant $Mg/(Mg+Fe)$ but changing Ni content. Uniform overgrowth compositions suggest that equilibrium conditions are attained within the magma (with respect to major elements) but Ni variation probably reflects the greater sensitivity of this element to changing pressure, temperature, wall-rock composition and oxygen fugacity during upward migration.
- (7) Upward movement of the enlarged diapir may be accelerated as a result of the relative increase in volatiles in the residual melt caused by crystallisation of relatively large amounts of late-stage olivine and the incorporation of xenocrysts.
- (8) Decelerated ascent close to surface possibly is caused by loss of energy through degassing as evidenced by large proportions of secondary fluid inclusions in both xenocryst and phenocryst olivines.

REFERENCES

- Clement C.R. 1982. A comparative geological study of some major kimberlite pipes in the northern Cape and Orange Free State. PhD thesis (unpubl.) Univ. Cape Town, 432pp.
- Smith C.B. 1985. Rubidium-strontium, uranium-lead, and samarium-neodymium isotopic studies of kimberlites and related mantle-derived xenoliths. Ph.D thesis (unpubl.), Univ. Witwatersrand, 436pp.
- Smith C.B., Gurney J.J., Skinner E.M.W., Clement C.R., & Ebrahim N. 1985. Geochemical character of southern African kimberlites. A new approach based on isotopic constraints. Trans. Geol. Soc. S. Afr., 88(2) in press.

C. B. Smith¹ and V. Lorenz²

1. CRA Exploration Pty Limited, Western Australia
 2. University of Mainz, West Germany

INTRODUCTION

More than 100 Miocene lamproites occur in the West Kimberley (Jaques et al, 1984), and are spread over a 7500 sq km triangular area from Ellendale to Noonkanbah to beyond Fitzroy Crossing. A few are emplaced into Lower Proterozoic granites and metamorphics of the King Leopold Mobile Zone; the majority intrude Phanerozoic sediments of the Lennard Shelf and Fitzroy Trough, at the north eastern margin of the Canning Basin. Forty eight lamproites occur in the Ellendale Field on the Lennard Shelf (Atkinson et al, 1984), 43 of them aligned with the Oscar Fault (one of the major step faults bounding the Fitzroy Trough) in an elongate belt 40 km long by 10 km across and trending at 305°. The Fitzroy Trough started forming in the Ordovician, with major graben development in the Devonian. Sedimentation continued until the Triassic, during which the early structures were reactivated with strong right lateral and vertical movements on the graben step faults.

DESCRIPTION OF THE DIATREMES

The lamproites range from leucite lamproite, containing variable amounts of phlogopite, diopside, richterite and usually less than 5% modal olivine, to olivine lamproite with no leucite, variable amounts of phlogopite, diopside and richterite and typically about 30% modal olivine. The leucite lamproites typically contain 50 - 55 wt % SiO₂ and would be relatively viscous, compared to the olivine lamproites with usually 35% - 42% wt % SiO₂. H₂O+ contents are high, ranging from 2 wt % to 7 wt % from leucite to olivine lamproite, and CO₂ contents are low usually less than 0.25 wt %. Of the 46 Ellendale occurrences 14 are classifiable as olivine lamproites, 28 are leucite lamproites and 4 are transitional rock types with modal olivine contents of +20% and appreciable quantities of leucite also present.

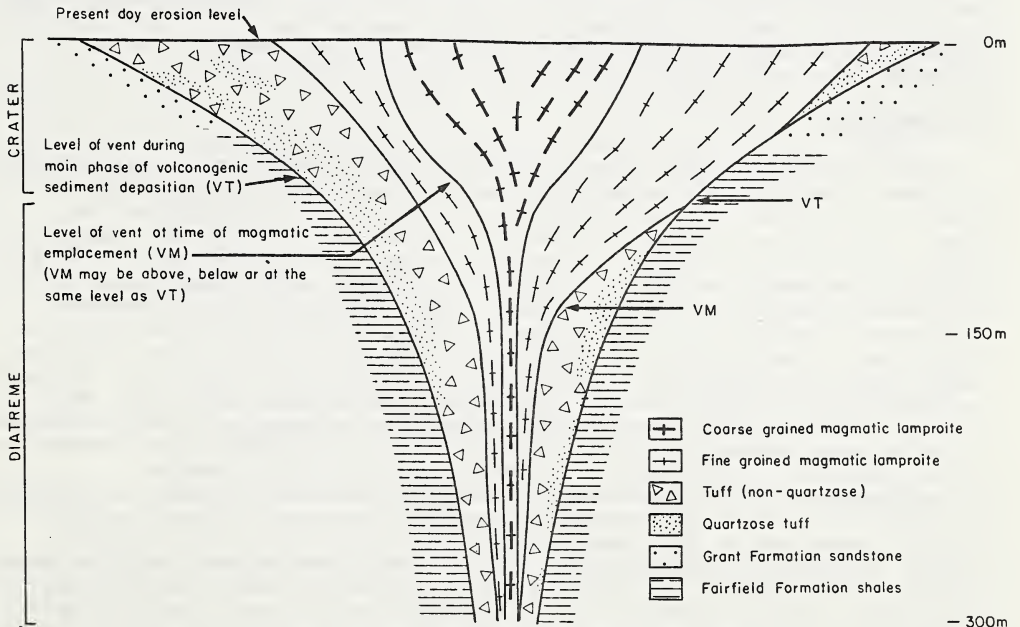


Fig. 1 Model of an Ellendale Lamproite Pipe

Most of the Ellendale diatremes are emplaced into Permian Grant Formation sandstone which overlies Devonian/Carboniferous shales of the Fairfield Formation. The Grant Formation is a good local aquifer. A zone of indurated sandstone often borders the diatremes and can form rocky hills up to 80m high, indicating the minimum amount of post-intrusion erosion that has taken place at Ellendale. Structurally the sandstone is undisturbed adjacent to the contact and preserves its regional subhorizontal disposition. In size the Ellendale diatremes range upwards from less than 1 ha (under 100 metres diameter) to 113 ha (more than 1 km across). About 1/3 of the bodies are larger than 10 ha. Many of the diatremes are elongate in plan view with long axis a little north of west. The typical Ellendale diatreme is champagne-glass shaped, having a narrow feeder vent corresponding to the stem of the glass, overlain by a broad, shallow crater (Fig. 1). In plan view individual bodies are essentially oval or circular but often assume complex shape through the coalescence of adjacent craters. The earliest volcanogenic beds within the crater sequence are often thinly bedded white mudstones and sandstones showing soft-rock deformation structures such as slump folding and microfaulting. Interbedded thin horizons containing juvenile lamproite clasts testify to their volcanogenic nature. They are overlain by varying thicknesses of quartz-rich tuffaceous sandstones and lapilli ash-tuffs. The content of juvenile lamproite lapilli increase upwards, as the quartz sand content decreases, but there are occasional oscillations. The upper (younger) part of the sequence is free of quartz sand and generally massive in texture with bedding evidence restricted to gross changes in grain size, imbrication of clasts, and vague colour differences. Country rock clasts are angular and predominantly composed of Fairfield Group shale, occasional limestone and lesser amounts of Grant Group sandstone. Fossil wood fragments occur, carbonised or silicified, and probably represent Miocene trees growing just outside the crater at the time of the eruptions. They testify to epiclastic deposition. Crystalline basement fragments are rare but include schist, metabasics and granite. This implies that the diatremes extend well down into the Fairfield Group, but the explosive volcanism did not generally reach down the 1000m to the basement.

Final stages in the volcanism show magma rising up the conduit into the centre of the craters where it spread out to form a lava lake or dome. The magmatic lamproite overlies the crater sediments, and may even overlap onto country rock. The base of the magmatic lamproite is highly vesicular and brecciated, and incorporates clasts from underlying crater sediments. The more viscous leucite lamproite shows streaky flow banding, passing downward with increasing brecciation into a lamproite breccia. The upper and central part of the magmatic section is coarser grained than the lower, the junction being a sharp intrusive contact at certain leucite lamproites and yet gradational at olivine lamproite pipes.

VOLCANOGENESIS

At nearly all Ellendale pipes volcanic activity commenced with a phreatomagmatic phase when rising lamproite magma interacted explosively with copious amounts of groundwater from the rather unconsolidated sands/sandstones of the Permian Grant Group. A maar formed and then collapsed due to ejection of juvenile and especially country rock clasts, a diatreme developing underneath. Phreatomagmatic activity at surface led to deposition of many thin pyroclastic beds, mostly of base surge origin, both on the crater rim and within the maar. Continued activity led to repeated subsidence of the diatreme content and associated collapse of the crater rim. Flows of lahars from collapsing crater rim deposits and from sands exposed in the collapsing country rocks within the crater wall accumulated on the crater floor. The interbedded pyroclastic and epiclastic crater floor deposits subsided repeatedly within the diatreme. The explosive activity removed groundwater as steam and a cone of depression formed allowing downward extension of the diatreme (Lorenz, 1986a). When the diatreme had penetrated deep enough into dry mudstones of the Fairfield Formation phreatomagmatic activity ended because of lack of groundwater and magma could then rise non-explosively. The lamproite magma intruded the diatremes and formed lava lakes (olivine lamproites) or lava domes (leucite lamproites) within the initial maar crater. In a number of leucite lamproite pipes early phreatomagmatic eruptions were followed by rise into the maar crater of magma carrying only small microphenocrysts of phlogopite. This was followed by lamproite magma carrying large phlogopite phenocrysts implying that the respective magma batches rose from a stratified magma reservoir which could be the reason for fractionation and variation in diamond grade. The

fractionation process did not separate all the diamond, neither did diamond resorb completely during residence time in the magma reservoir.

COMPARISONS WITH OTHER PHREATOMAGMATIC DIATREMES

With their volcanoclastic deposits and sequence of events the Ellendale pipes are comparable to many other small phreatomagmatic volcanoes. In the Quarternary Eifel volcanic fields many scoria cones are located in initial maars because magma continued to rise when lack of groundwater ended an initial phreatomagmatic phase. In many Cainozoic volcanic fields of Central and Western Europe initial phreatomagmatic maar-diatreme activity was followed by emplacement of a lava lake (Hocheifel and Hegau/Germany, Massif Central/France). In contrast to the basic and ultrabasic magmas which formed lava lakes or scoria cones in initial maars, intermediate and acid magmas formed lava domes in initial maars as e.g. trachyte and phonolite domes in the Massif Central or in the Eifel or many small dacite and rhyolite domes in the Permocarboniferous of Europe. In the initial maars at Ellendale the ultrabasic olivine lamproites formed lava lakes whereas the more viscous leucite lamproites formed lava domes. At Calwinyardah 50 km south of Ellendale phreatomagmatic activity lasted as long as the volcanic activity, with the result that only a maar formed. Restoration of the groundwater table allowed formation of a maar lake and accumulation of fossiliferous lake sediments. This evolution was similar to the present situation in the lakes of the Eifel and Massif Central or Victoria maars.

Concerning the lack of lithification of Permian Grant Group sediments, the volcanicity at many Ellendale pipes, at least initially, resembled areas of syndimentary volcanism where maars and diatremes formed within unconsolidated sediments such as the Carboniferous Midland Valley (Scotland), the Tertiary Limagne graben (France), the Tertiary Hegau-Molasse trough (Germany) and the Permocarboniferous Saar-Nahe trough (Germany). In contrast to those areas the unconsolidated sediments of the Grant Group which formed the aquifer were not very thick, causing an early end to the phreatomagmatic activity followed by non-explosive rise of lamproite magma. The hydrogeological conditions at the site of the syndimentary or early post-depositional Argyle pipe in the East Kimberley were more favourable for continuous supply of groundwater during eruptive activity, with result that this pipe is more evolved and only contains late magmatic lamproite dykes within the thick phreatomagmatic volcanoclastic deposits.

Kimberlite diatremes from southern Africa, mostly cut by erosion at much deeper levels, also erupted phreatomagmatically (Lorenz 1986b). In contrast to the Ellendale pipes most had much longer phreatomagmatic phases, as indicated by the larger diatreme size, implying that hydrogeological conditions were rather favourable in southern Africa. Due to erosion it is unknown if the late kimberlite dykes found in many diatremes have fed lava lakes in the respective maars or if most kimberlite diatremes ended in maars with accumulated lake sediments such as at Orapa and Mwadui.

REFERENCES

- ATKINSON, W. J., HUGHES, F. E. & SMITH, C. B., 1984. A review of the kimberlitic rocks of Western Australia; in Kornprobst, J. (Ed), Kimberlites. 1: Kimberlites and Related Rocks, pp.195-224, Elsevier, Amsterdam.
- JAIQUES, A. L., LEWIS, J. D., SMITH, C. B., FERGUSON, J., CHAPPELL, B. W. & McCULLOCH, M. T., 1984. The diamond-bearing ultrapotassic (lamproitic) rocks of the West Kimberley region, Western Australia; In Kornprobst, J. (Ed), Kimberlites. 1: Kimberlites and Related Rocks, pp.225-254, Elsevier, Amsterdam.
- LORENZ, V., 1986a. On the growth of maars and diatremes and its relevance to the formation of tuff-rings. Bull. Volcanol. in press.
- LORENZ, V., 1986b. Maars and diatremes of phreatomagmatic origin, a review. Trans. Geol. Soc. S. Africa, in press.

Eiichi TAKAHASHI, Eiji ITO and Christopher M. Scarfe*

Institute for Study of the Earth's Interior, Okayama University, Misasa, Tottori-ken, 682-02, Japan

* Permanent Address, Department of Geology, University of Alberta, Edmonton, T6G 2E3, Canada

Melting phase relations and subsolidus mineral paragenesis of fertile peridotite (KLB-1 and PHN-1611) were studied in the pressure range 1 atm to 25 GPa (250 kilobars). The main scope of the present study is two-fold. First is to clarify mineralogy and chemistry of the Earth's deep interior. Second is to study the origin of mantle peridotite, a question to ask from what source material and by what processes the peridotitic nature of the Earth's upper mantle has been established in its early history.

The starting materials are; KLB-1, a fertile spinel lherzolite xenolith with $Mg^*=89$ from the Kilborne Hole Crater, New Mexico, U.S.A. (Takahashi, 1986), and PHN-1611, a sheared garnet lherzolite xenolith with $Mg^*=88$ from Thaba Putsoa kimberlite pipe, Lesotho (Nixon & Boyd, 1973; specimen by the courtesy of F.R. Boyd and P.H. Nixon). A 5000 ton uniaxial split-sphere apparatus of Okayama university (USSA-5000) was employed (Fig. 1) in which eight tungsten carbide cubic anvils (32 mm edge length) are simultaneously compressed and a pressure medium of MgO octahedron is put in the geometric center of the tungsten carbide anvils. High-pressure and high-temperature experiments up to 27 GPa and 2000°C are routinely conducted in the USSA-5000 apparatus (Ito et al., 1984). The size of the MgO pressure medium varies as a function of maximum pressure of the experiments; edge length of MgO octahedron is 18 mm up to 8 GPa, 14 mm up to 14 GPa, 10 mm up to 20 GPa, 7 mm up to 24 GPa and 6 mm up to 27 GPa. Cylindrical graphite heater (4.0 mm OD, 3.0 mm ID and 15 mm long) was used in the experiments below 8 GPa and cylindrical LaCrO₃ heaters of various size were employed at pressures above 8 GPa.

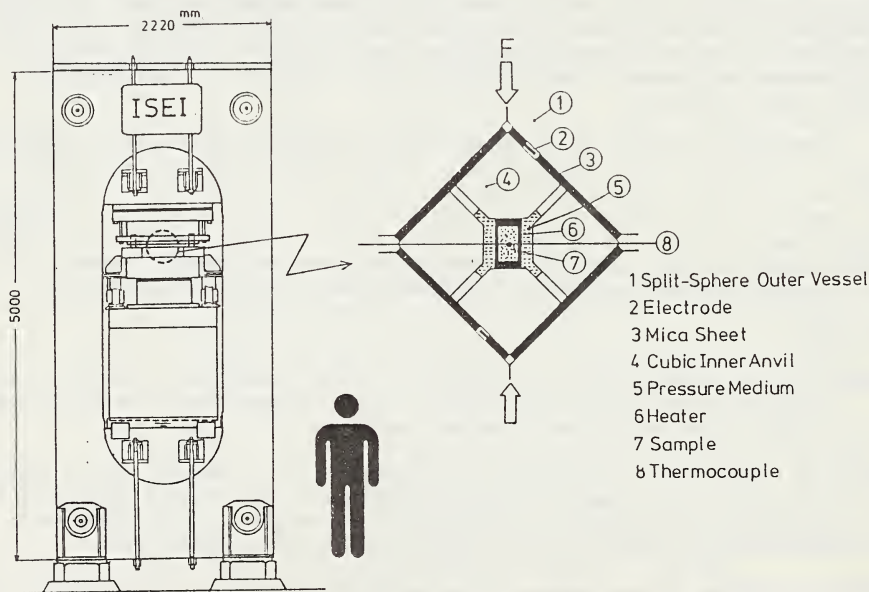


Fig. 1 A whole plan of the uniaxial split-sphere type ultrahigh pressure apparatus (USSA-5000) of Okayama University (left) and a schematic cross-section of the high-pressure vessel with the furnace assembly (right). Eight tungsten carbide cube anvils (32 mm edge length), each with one truncated corner (12 to 1.5 mm edge), are compressed with the aid of the 5000 ton press. After Ito et al. (1984).

Eight subsolidus experiments (60 min long each) were carried out using PHN-1611, along a model adiabatic geotherm beneath the African shield which passes through 1400°C at 200 km depth and 1600°C at 700 km depth. Coexisting phases were identified with X-ray diffractometry and EPMA analysis. Mineral paragenesis in the model mantle is estimated based on these experiments (Fig. 2). In the upper mantle down to 400 km depth, olivine (α -phase), enstatite, diopsidic clinopyroxene and pyropic garnet are the major constituent minerals of peridotite. In the transition layer between 400 and 670 km depth, olivine undergoes successive phase transitions from α to β (modified spinel) and then β to γ (spinel). The amount of majorite component in garnet solid solution increases continuously in the depth range 200 to 500 km (Fig. 3) and eliminates enstatite at about 400 km depth. Diopsidic clinopyroxene survives to about 500 km depth and transforms to an unquenchable phase (Ca-P). In the lower mantle beneath the 670 km discontinuity, magnesian perovskite of Mg_{SiO_3} stoichiometry is the dominant constituent phase (Ito et al., 1984). Minor amount of magnesiowustite ($Mg_{\approx 75}$), Ca-P of either diopsidic or wollastonite-like composition and an unknown aluminous phase (Al-P) are also found to be present.

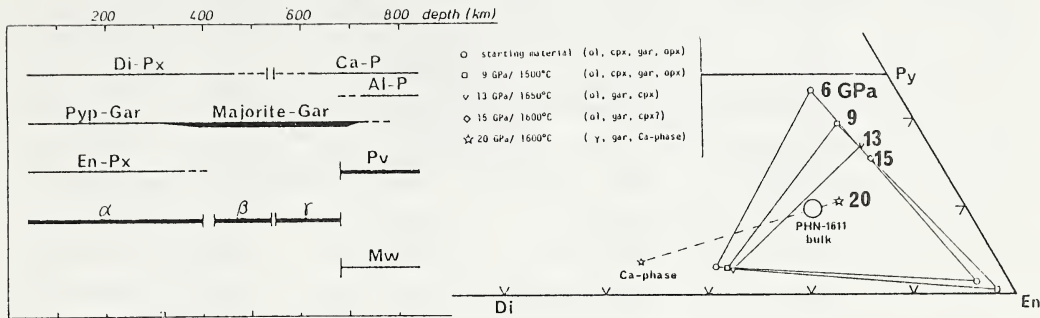


Fig. 2 Mineral paragenesis of mantle peridotite along a model geotherm down to 700 km depth. Dominant phases likely to be present in more than 30 vol% are indicated with heavy lines.

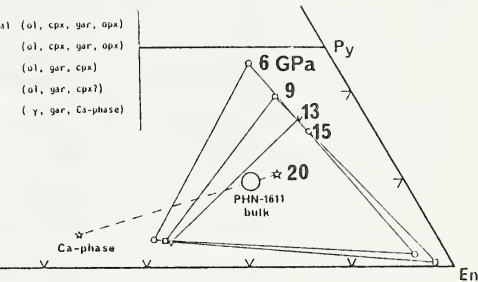


Fig. 3 Composition of garnet and pyroxenes of a peridotite PHN-1611 along a model geotherm. Projection on the plane $(Al_{2O_3}+Cr_{2O_3})-(Mg\cdot Fe\cdot Mn)SiO_3-CaSiO_3$.

Melting phase relations of the mantle peridotite KLB-1 and PHN-1611 were studied in the pressure range from 1 atm to 25 GPa. Phase diagram of KLB-1 up to 14 GPa is shown in Fig. 4 (that of PHN-1611 show similar results). At low pressures, the peridotite has a large melting temperature interval ($>600^\circ C$ at 1 atm), whereas the melting interval contracts to less than about $150^\circ C$ at 14 GPa due to relatively gentle dT/dP slope of liquidus and relatively steep solidus curve. In the pressure range up to 14 GPa, liquidus phase is olivine of $Fo=96\pm 1$. The second mineral to crystallize changes successively; enstatite (1 atm to 3 GPa), pigeonitic clinopyroxene (3 to 7 GPa), garnet of pyrope (at 7 GPa) to majorite (at 14 GPa) compositions.

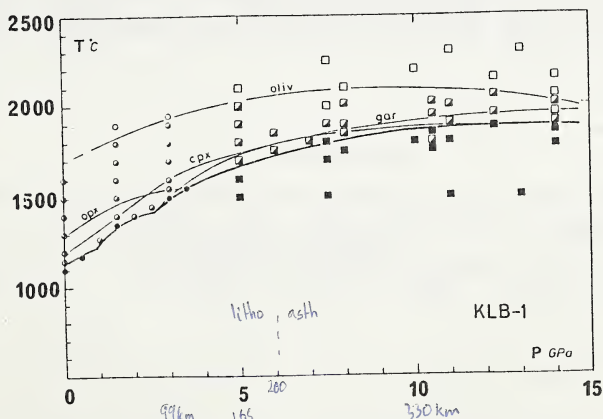


Fig. 4 Melting phase relation of a fertile peridotite KLB-1 under dry conditions up to 14 GPa (after Takahashi, 1986).

Preliminary melting phase relations of the mantle peridotite in the pressure range between 15 and 20 GPa are shown in Fig. 5. The results for the peridotite KLB-1 and PHN-1611 are indistinguishable in the resolution in pressure and temperature of Fig. 5. Olivine appears as a liquidus phase up to about 17 GPa. However, majorite-garnet appears on the liquidus as well as olivine at 16 and 17 GPa runs. At pressures above 18 GPa, β -spinel and majorite garnet coexist on the peridotite liquidus. As noted by Kato & Kumazawa (1986), under slightly hydrous conditions, the liquidus phase is a hydrous phase-B ($Mg_{23}Si_{80}H_6$) coexisting with majorite at 18 to 20 GPa pressure range. In a melting experiment at 25 GPa and $\sim 3000^\circ C$, peridotite PHN-1611 was completely molten, whereas a charge of $(Mg_{0.8} \cdot Fe_{0.2})_2SiO_4$ composition was partially molten and the liquidus phase was perovskite of almost pure $MgSiO_3$ composition.

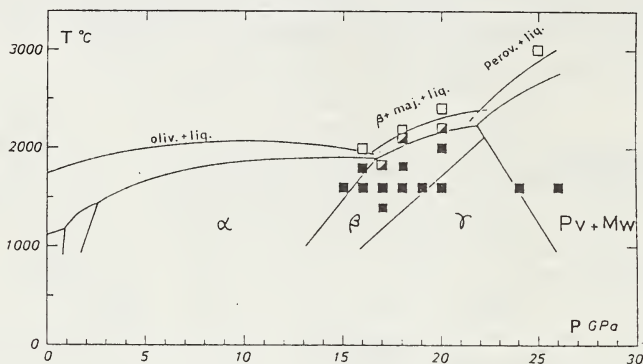


Fig. 5 A preliminary phase relation of peridotites KLB-1 and PHN-1611 up to 25 GPa under dry conditions.

Compositions of partial melts formed near the peridotite solidus were determined by analyzing quenched liquid segregated from the peridotite matrix with a defocused electron beam (50 to 100 μm diam.) by EPMA. MgO content (or normative olivine component) of the peridotite partial melt increases systematically with increasing pressure (hence temperature); olivine tholeiite (1 GPa and $1300^\circ C$, $MgO=9.5$ wt%), picrite (3 GPa and $1550^\circ C$, $MgO=19.5$ %), peridotitic komatiite (5 to 8 GPa, $MgO>30$ %; Takahashi & Scarfe, 1985), and peridotite itself!! (15 to 20 GPa, $MgO=37-40$ wt%).

Based on the following observations; (1) convergence of the liquidus and solidus at pressure >15 GPa, (2) the near solidus partial melt composition very close to the bulk rock at 15-20 GPa, (3) eutectitic melting relation between majorite-garnet and M_2SiO_4 phases at 16-20 GPa, it is proposed that the upper mantle peridotite was generated as an ultrabasic magma (or magmas) by partial melting of primitive earth at great depth during or soon after the accretional stage. Likely candidates for the residue of the Earth's deep melting are majorite garnet (400-600 km depth) and $MgSiO_3$ perovskite (>600 km depth).

REFERENCES

- Ito, E., E. Takahashi and Y. Matsui (1984) *Earth Planet. Sci. Lett.*, **67**, 238-248.
 Kato, T. and M. Kumazawa (1986) *Geophys. Res. Lett.*, **13**, 181-184.
 Nixon, P.H. and F.R. Boyd (1973) in *Lesotho Kimberlite*, 48-56.
 Takahashi, E. (1986) *J. Geophys. Res.* **91**, in press.
 Takahashi, E. and C.M. Scarfe (1985) *Nature*, **315**, 566-568.

W.R.TAYLOR & D.H.GREEN

Geology Dept, University of Tasmania, Hobart 7001

Until very recently, many petrogenetic models were based on the assumption that f_{O_2} -conditions in magma source-regions of the upper mantle were relatively oxidized, lying near the f_{O_2} defined by the synthetic assemblage fayalite-magnetite-quartz (FMQ). This was consistent with the petrogenetic role inferred for oxidized CO_2 - H_2O volatiles and carbonated peridotite. However, if magma generation involving volatile components takes place in a reduced environment, for example at f_{O_2} 's near the iron-wustite (IW) oxygen buffer - as suggested by intrinsic f_{O_2} measurements on mantle-derived minerals - then in the model system "peridotite"-C-O-H, volatiles will be dominantly $CH_4 > H_2O > H_2 > C_2H_6$ mixtures and crystalline carbonates will not be stable relative to diamond or graphite (Taylor, 1986). The nature of mantle melting under reduced conditions is expected to be very different from that occurring in an oxidized environment. This problem may be investigated from both a theoretical and experimental basis.

Using a thermodynamic model for C-O-H fluids at elevated P,T, phase relations in the presence of elemental carbon may be represented on a $\log f_{O_2}$ - X_C diagram of the type devised by Frost (1979) (where X_C = mole fraction of carbon relative to H_2 in the bulk fluid). This diagram may be contoured in terms of species mole fraction or fugacity as illustrated in Fig.1 at 30 kbar, 1600 K for H_2O . The curved line is an isobaric, isothermal slice of the graphite saturation surface that delineates the stability field of graphite and coexisting fluid. Oxidized and reduced fluid-only regions lie, respectively, above and to the left of the saturation curve. These regions are effectively separated by a large graphite + fluid field that extends to very water-rich fluid compositions at GW on the "nose" of the saturation curve (Fig.1). Fluids lying on the upper horizontal portion of the saturation curve are dominantly H_2O - CO_2 mixtures. With increasing X_C the curve intersects the $\log f_{O_2}$ axis at a point on the graphite- CO_2 -CO (GCO) f_{O_2} buffer. With decreasing f_{O_2} fluids progress from $H_2O > CH_4 > H_2$ mixtures to $CH_4 > H_2 > C_2H_6$ mixtures at f_{O_2} 's below IW. Below and to the right of the saturation curve a metastable region exists. Fluids are carbon supersaturated and may only lie in this region if elemental carbon crystallization is suppressed e.g. fails to nucleate. The GCO buffer and the locus of points in P-T- f_{O_2} space defining the maximum water mole fraction (GW) are given by the following equations (applicable over the range 5-50 kbar, 800-1700 K for P[bar] & T[K]):

$$\log(f_{O_2}/\text{bar}) = a + b \ln T + c/T + d(P/T) + e(P/T)^2$$

GCO	2.0815	2.5754E-1	-21060	0.17112	-7.4268E-4
GW	5.0186	-6.5844E-2	-22674	0.12858	-6.6384E-4

Recognizing that melting in the system peridotite-C-O-H will be largely a function of f_{H_2O} , the isobaric, isothermal solidus of graphite peridotite can be

approximated by the intersection of an $f\text{H}_2\text{O}$ contour with the graphite saturation curve (see Fig. 2). Vapour excess melting will then be initiated at minimum $f\text{H}_2\text{O}$'s corresponding to either a reduced condition (point A) or an oxidized condition (point B). In Fig. 2 the stability fields of graphite-bearing and graphite-free peridotite are delineated in qualitative fashion; the lines AY and BX correspond to the solidus of graphite-free peridotite. Provided $f\text{O}_2$ remains above GW, vapour-excess melting of graphite peridotite in the presence of $\text{H}_2\text{O}-\text{CO}_2$ fluids will not differ greatly from the graphite-free case because $f\text{H}_2\text{O}$ and $f\text{CO}_2$ contours extend in more or less parallel fashion from oxidized conditions towards the graphite saturation surface. The same however cannot be said for conditions more reduced than GW. While the reduced portion of the of the diagram mirrors the oxidized part in terms of phase fields, with carbide rather than carbonate as the C-bearing phase, the nature of melts formed at "A", involving $\text{H}_2\text{O}-\text{CH}_4$ fluids, are likely to be very different from melts formed at "B" where $\text{H}_2\text{O}-\text{CO}_2$ fluids predominate.

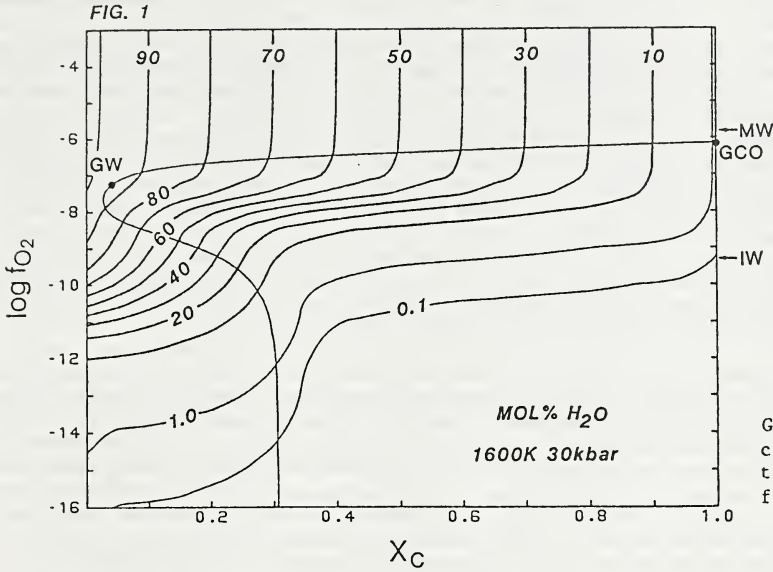
As a first step in evaluating the nature of reduced volatile interactions with silicate melts, experimental liquidus studies were undertaken in the system nepheline-forsterite-silica under conditions of H_2O , CO_2 and CH_4 volatile saturation at 28 kbar to contrast the behaviour of reduced versus oxidized volatiles. Compared to the volatile-absent system, the effect of methane is to expand the Fo phase field relative to En_{ss} (melt depolymerization) and to increase significantly the activity of non-network aluminium (which leads to early appearance of garnet on the liquidus of other compositions). This contrasts with the effect of CO_2 which gives rise to expansion of the En_{ss} phase field and the effect of H_2O -saturation which results in a greater expansion of the Fo field than CH_4 . IR spectroscopic investigations establish the presence of both dissolved oxidized (OH groups) and reduced ("silicon monoxide" units) melt components in the CH_4 -saturated glasses; reduced carbon solubility is <2000 ppm (Taylor & Green, 1986). Melt saturation with C-H fluids dominated by methane results in liquidus depressions comparable to pure CO_2 (i.e. $\sim 100^\circ\text{C}$ at ~ 30 kbar), however, since methane forms no known solid compounds by interaction with silicate minerals over a large $f\text{O}_2$ -range, reduced ($\text{CH}_4 + \text{H}_2$) fluids may be important carriers of C and H from relatively undegassed regions of the mantle into regions depleted of their volatile constituents.

Volatile influx is expected to play a major role in modifying mantle $f\text{O}_2$ environments by direct redox interaction with solid phases in an upper mantle we believe to be largely $f\text{O}_2$ unbuffered or of limited buffer capacity. Redox interactions between reduced fluids ($f\text{O}_2 < \text{IW}$) and oxidized regions of the upper mantle ($f\text{O}_2 \sim \text{MW-FMQ}$) will result in a progressive increase in fluid-phase $f\text{H}_2\text{O}$ which will eventually give rise to partial melting (intersection with the reduced solidus in Fig.2) accompanied by diamond or graphite precipitation (intersection with the carbon saturation surface). Operation of such "redox melting" processes offers a ready explanation for the origin of strongly depleted harzburgites that are prominent constituents in the roots of cratons and important hosts for diamond (Boyd & Gurney,

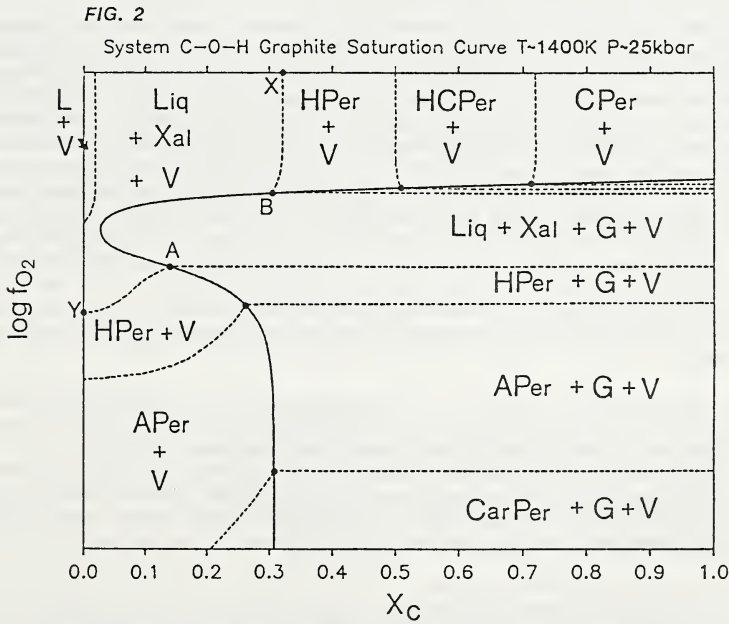
1982). Extensive "flushing" of the pre-cratonic mantle by deep mantle-derived $\text{CH}_4 + \text{H}_2$ fluids may have led to large scale "redox melting" and associated diamond precipitation, thus effectively stripping the pre-cratonic mantle of its basaltic components.

References

Boyd, F.R. & Gurney, J.J. 1982. Rep. Geophys. Lab., Carnegie Inst. Ybk 81, 261-267.
 Frost, B.R. 1979. Am. J. Sci. 279, 1033-1059.
 Taylor, W.R. & Green, D.H. 1986. Geochim. Cosmochim. Acta (submitted).
 Taylor, W.R. 1986. Geol. Soc. Aust. Special Publ. 12, (in press).



Graphite saturation curve contoured in terms of water mole fraction.



Vapour-excess phase relations of graphite-free and graphite-bearing peridotite. CPer = carbonated peridotite; HPer = hydrated peridotite; HCPe = carbonated & hydrated peridotite; APer = anhydrous peridotite; CarPer = carbide peridotite; G = graphite; V = vapour; Xal = anhydrous crystals; Liq = melt. Oxidized solidus = BX; Reduced solidus = AY.

GENESIS AND MIGRATION OF KIMBERLITES
AND OTHER LOW-SiO₂, HIGH-ALKALI MAGMAS

Peter J. Wyllie

Division of Geological and Planetary Sciences
California Institute of Technology
Pasadena, CA 91125, U.S.A.

The only demonstrated way of generating low-SiO₂, high-alkali magmas from peridotite is by the involvement of CO₂ at pressures greater than about 25kbar. CO₂ reacts with peridotite to generate dolomite (magnesite at higher pressures), and melting then occurs at a eutectic between carbonate and silicates. Kimberlite magmas contain juvenile H₂O as well as CO₂. There is abundant evidence in fluid inclusions of mantle nodules for the passage of H₂O and CO₂ through the upper mantle. However, the oxygen fugacity in the mantle at the depths of kimberlite generation may be too low for the existence of carbonate, and for comprehension of kimberlite generation we need to know the phase relationships in the system peridotite-C-H-O-S-K. With low oxygen fugacities at high pressures, C-H-O exists as H₂O with CH₄ or graphite/diamond. Under these conditions, it appears that the peridotite-C-H-O solidus may remain close to that for peridotite-H₂O, with carbonate ions being generated in the melt when CH₄ or graphite/diamond dissolves (Eggler and Baker, 1982; Ryabchikov et. al., 1981; Woermann and Rosenhauer, 1985). Phase relationships in the system peridotite-CO₂-H₂O represent an important limit, for the oxidized condition, and they form the basis for interpretation of relationships in more reduced systems. Location of the solidus for peridotite-CO₂-H₂O is a prerequisite for understanding kimberlite petrogenesis. In the following discussion, the solidus used by Wyllie (1980) for peridotite-CO₂-H₂O is assumed to coincide with that for peridotite-C-H-O deeper than about 170km.

Two experimental determinations of the solidus for peridotite with amphibole and dolomite (Brey et. al., 1983; Olafsson and Eggler, 1983) give results differing from each other, and from other estimated peridotite-CO₂-H₂O phase diagrams based on model systems (Figs. 1A and B). Interpretation of these experimental results in terms of the topology of intersecting stability fields for dolomite, amphibole and phlogopite with the peridotite-vapor solidus indicates that the experiments involve a divergence of about 10kbar for the location of the point on the solidus for peridotite-CO₂, where the solidus drops sharply in temperature as dolomite becomes stable with increasing pressure (points E76 to OE in Fig. 1C). Resolution of the discrepancy between these two results is critical for interpreting magmatic and metasomatic processes in the lithosphere.

There are four levels within the upper mantle where critical changes occur in the physical processes that control the chemistry and mode of migration of the low-SiO₂, volatile-rich magmas. The first critical level, (1), is the depth of the lithosphere-asthenosphere boundary layer, through which the mantle flow regime changes from convective (ductile) to static (brittle). A depth of 200km is commonly adopted for this level in subcratonic mantle, corresponding approximately to the 1200°C isotherm. The two depths where the solidus is intersected by the local geotherm, (2) and (3), limit the depth interval within which magmas can be generated. The fourth level, (4), is the narrow depth interval within which the solidus for peridotite-CO₂-H₂O changes slope, and becomes sub-horizontal, with low dP/dT, as indicated in Fig. 1. The depth of level (4) differs according to different experimental investigators. Levels (2), (3) and (4) are different for lherzolites and harzburgites (Wyllie et. al., 1983); compared with lherzolite, the solidus temperature of harzburgite is higher and therefore the levels (2) and (3) are deeper, and level (4) is also deeper. The depths of levels (1), (2) and (3) vary from place to place and from time to time, as a function of geotherm and local history. Any hypothesis for the generation and transportation of kimberlites must consider the involvement of these four levels.

Subcratonic geotherms calculated from heat flow are consistent with geotherms determined from the mineralogy of mantle nodules from kimberlites, down to about 165 km and 1100°C, where the nodules indicate an inflection in the geotherm, with a shallower segment extending to about 200km and 1400°C. The inflected portion is situated within the lowest 30km of the lithosphere, within the stability field for diamond. The inflected geotherm represents the ambient temperature as a function of depth at the time of kimberlite eruption. The abnormally high temperatures could be caused by local magmatic intrusions, or by local or regional uprise of isotherms, caused by mantle upwelling.

Consider a craton with normal, undisturbed geotherm, composed largely of lherzolite with a concentration of harzburgite in its lower part, between about 170km and 200km depth, along with pods of eclogite (Boyd and Gurney, 1982; Haggerty, 1985). The geotherm intersects the solidus for

lherzolite-CO₂-H₂O at 270km and 185km (levels 2 and 3), but no magma is generated unless volatile components are present or introduced into this depth interval between levels (2) and (3). Assume that a part of the lithosphere is in the early stages of rifting, initiated by an increase in heat flow supplied by a mantle plume from the asthenosphere. Sparse volatile components (C-H-O-S-K) entrained in the rising plume will generate interstitial melt at level (2), 270km, where the lherzolite is transported across the solidus curve. The melt may rise at the same rate as the plume, or percolate upwards faster than the mantle host. As the plume diverges laterally below the asthenosphere-lithosphere boundary, level (1) at 200km, the melt becomes concentrated in layers or chambers in the boundary layer above the plume. This is associated with local uprise of geotherms, and thinning of the lithosphere. Lateral divergence of the asthenosphere transports some of the entrained plume melt, and this penetrates into the lithosphere, forming small dikes or magma chambers.

The magmas entering the depleted lithosphere, both above the plume and laterally beneath the undisturbed craton, remain sealed within the more rigid lithosphere, maintained at temperatures above the solidus for lherzolite-C-H-O. They have no tendency to crystallize nor to evolve vapors unless they reach 10-15km above the asthenosphere-lithosphere boundary. However, the magma from lherzolite coming into contact with harzburgite will react with it, and this could cause precipitation of minerals through magma contamination; this slow process could lead to the growth of large minerals resembling the discrete nodules in kimberlites. Magmas managing to insinuate their way near to level (3), the solidus for lherzolite-C-H-O, will evolve H₂O-rich vapors. Part of the carbon component of the relatively oxidized melt will be evolved in the vapor phase, and exposure to the more reduced lithosphere may cause thermal cracking of the vapor (Haggerty, 1985), with the nucleation of microdiamonds (to join the old macrodiamonds resident in the lower lithosphere through thousands of millions of years). The vapors cause metasomatism in the deep lithosphere. They may also promote crack propagation, permitting rapid uprise of the kimberlite magma. Many intrusions from this level will solidify before rising far (thermal death according to Spera, 1984), but others will enter the crust as kimberlite intrusions (Artyushkov and Sobolev, 1984). Kimberlites may be erupted either from the magma accumulating above the plume, or from the lateral magma chambers in the lithosphere base. These magmas, freed from equilibrium with their peridotite host, are not affected by the phase relationships at level (4). The deep depleted lithosphere, with harzburgite, has been repeatedly invaded and metasomatized by melts from the asthenosphere.

The continued heat flux from the rising plume, and the concentration of hotter magma at the asthenosphere-lithosphere boundary, will promote further thinning of the lithosphere. According to Gliko et. al. (1985), it takes only several million years for lithosphere thickness to be halved when additional heat flow (of appropriate magnitude) is supplied to the base of the lithosphere. The magma near the boundary layer will rise with the boundary layer, either percolating through the newly deformable matrix, or as a series of diapirs, with liquid increasing in amount as the boundary layer rises, extending further above the solidus for peridotite-C-H-O. This magma intersects the shallower solidus for peridotite-CO₂-H₂O at level (4), in the range of 90-70 km depth. Magma chambers may be formed as the magma solidifies, and vapors will be evolved causing metasomatism in the overlying mantle, and causing intermittent crack propagation which releases magmas through the lithosphere. A variety of alkalic magma compositions may be generated at level (4), depending sensitively upon conditions. Magmas rising from this level may include olivine nephelinites, melilite-bearing lavas, and other igneous associations differentiating at shallower levels to carbonatites.

At a later stage of evolution, the magmas rising from the asthenosphere from progressively deeper levels may become too high in temperature to intersect the solidus at level (4), and these may approach the solidus for volatile-free peridotite at shallower levels, yielding basaltic magmas.

REFERENCES.

- ARTYUSHKOV E.V. and SOBOLEV S.V. 1984. Physics of the kimberlite magmatism. In J.Kornprobst, ed, *Kimberlites I*, pp. 309-322. Elsevier, Amsterdam.
- BOYD F.R. and GURNEY J.J. 1982. Low-calcium garnets: keys to craton structure and diamond crystallization. *Carnegie Institute of Washington Year Book* 81, 261-267.
- BREY G., BRICE W.R., ELLIS D.J., GREEN D.H., HARRIS K.L. and RYABCHIKOV I.D. 1983. Pyroxene-carbonate reactions in the upper mantle. *Earth and Planetary Science Letters* 62, 63-74.
- EGGLER D.H. and BAKER D.R. 1982. Reduced volatiles in the system C-O-H: implications to mantle melting, fluid formation, and diamond genesis. In Akimoto S. and Manghnani M. H. eds, *High Pressure Research in Geophysics, Advances in Earth and Planetary Sciences* 12, pp 237-250. Reidel Publishing Co., Dordrecht.

- GLIKO A.O., GRACHEV A.F. and MAGNITSKY V.A. 1985. Thermal model for lithospheric thinning and associated uplift in the neotectonic phase of intraplate orogenic activity and continental rifts. *Journal of Geodynamics Research*, 3, 137-153.
- HAGGERTY S.E. 1985. Diamond genesis in a multiply-constrained model. *Nature*, 320, 34-38.
- OLAFSSON M. and EGGLEER D.H. 1983. Phase relations of amphibole, amphibole-carbonate, and phlogopite-carbonate peridotite: petrologic constraints on the asthenosphere. *Earth and Planetary Science Letters* 64, 305-315.
- RYABCHIKOV I.D., GREEN D.H., WALL W.J. and BREY G.P. 1981. The oxidation state of carbon in the reduced-velocity zone. *Geochemistry International* 1981, 148-158.
- SPERA F.J. 1984. Carbon dioxide in petrogenesis III: role of volatiles in the ascent of alkaline magma with special reference to xenolith-bearing mafic lavas. *Contributions Mineralogy Petrology* 88, 217-232.
- WOERMANN E. and ROSENHAUER M. 1985. Fluid phases and the redox state of the Earth's mantle: extrapolations based on experimental, phase-theoretical and petrological data. *Fortschr. Miner.* 63, 263-349.
- WYLLIE P.J. 1980. The origin of kimberlites. *Journal Geophysical Research* 85, 6902-6910.
- WYLLIE P.J., HUANG W.L., OTTO J. and BYRNES A.P. 1983. Carbonation of peridotites and decarbonation of siliceous dolomites represented in the system CaO-MgO-SiO₂-CO₂ to 30 kbar. *Tectonophysics* 100, 359-388.
- WYLLIE P.J. 1987. Metasomatism and fluid generation in mantle xenoliths: experimental. In Nixon P. H. ed, *Mantle Xenoliths*, Chapter, Wiley, in press.

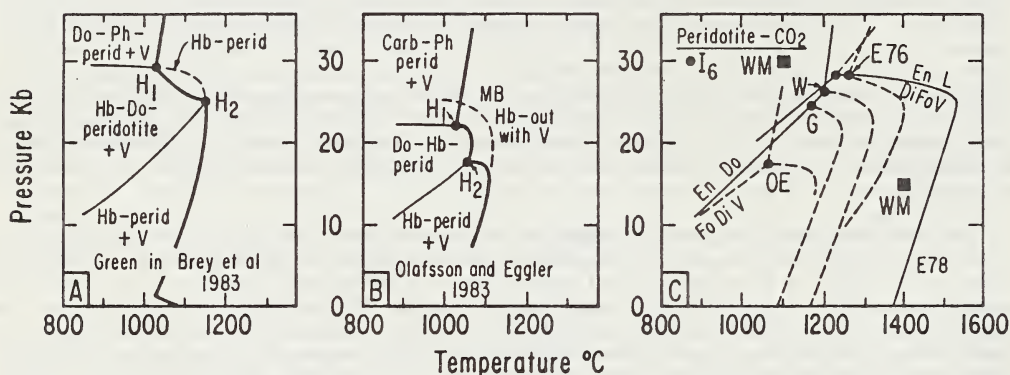


FIG. 1 (A) and (B). Experimentally determined solidus curves for peridotite-CO₂-H₂O. (C). Variety of estimated positions for point I₆ on the solidus for peridotite-CO₂. See Wyllie (1987) for details. G is based on results in Fig. 1A, and OE is based on results in Fig. 1B.

V.N. Zyryanov

Institute of Experimental Mineralogy, USSR Acad.Sci.

Constant scientific and practical interest in lamproites has made us initiate an experimental study of their formation. In our view, lamproites are a product of the fluid-magmatic interaction between mantle material and high potassium deep-seated fluids. To test this assumption we carried out model experiments on the interaction between mantle material and potash fluids in the superheated liquidus region. The liquidus of lamproite was earlier determined as 1125°C at P(H₂O)=1kb by Carmichael (1967) and as 1075°C at P(H₂O)=10kb by Arima & Edgar (1983). Based on these data, experimental conditions were accurately chosen to model the evolution of lamproite melt under decompression. Runs were performed in gas bombs with internal heating. The accuracy of the temperature and pressure control and measurements was 5°C, 50bar, respectively. The starting materials were mixtures of garnet hartzburgite (TYB 237) from Yakutia and alkali basalt (TF-38) from Galapagos in different proportions and the chemical KOH, K₂CO₃, KCl, KPHF·2H₂O of analytical grade. Platinum capsules, 3mm in diameter, were charged with 25mg silicate material and 10mg potash chemical. In runs with K₂CO₃, KCl water was introduced into their composition in amounts of 20wt% of the rock weight. The charged capsules were sealed and loaded in fives into the thick-walled air-tight capsules filled with water. Since water dissociates at high temperature, the presence of water in the outer capsule after the run helped to maintain the water in the fluid at the original level. The capsules in the bombs were held at T=1100°C and P=5kb for 5 hours; after that the pressure was decreased to 2.5kb and one hour later the charges were quenched. The run products consisted of minerals and glass appeared as un cemented tuff. The minerals and glass were analyzed on the Camebax microprobe. The mineral-parageneses observed in the run products are given in Table 1.

Mineral-parageneses of the interaction between mafic-intramafic mixtures and K-fluids

Table 1

TYB 237: TF-38 wt%	KOH	K ₂ CO ₃	KCl	KPHF·2H ₂ O
90:10	Ol+Phl+Mtch+Ks	Ol+Phl+Phl ₁ +Phl ₂ (wolgidite)	Ol+Opx+Cpx+G1 (cedrecite)	Ol+Phl
80:20	Ol+CaOl+Phl+ Mtch+G1 (wolgidite)	Ol+Phl+Phl ₁ +Phl ₂ (wolgidite)	Ol+Cpx+G1 (madupite)	CaOl+Phl+ Phl ₁ +Lar
50:50	Ol+Phl+Ks (fitzroite)	Ol+Phl+Phl ₁ +G1 (fitzroite)	Ol+Opx+Cpx+Phl+ Phl ₁ +KAmf+G1 (wayomingite)	Phl ₁ +Phl ₂

After the minerals and glass were analyzed, the run products were converted into homogeneous glasses by fusing with the three-fold amount of lithium metaborate in carbide glass crucibles over gas burner. The resulting glasses were also analyzed on the microprobe. Their compositions, as normalized to 100%, are given in Table 2. Since the analyses cannot be claimed to correspond fully to the actual compositions because of very high dilution, only the Al₂O₃FeO and K₂O were used to derive the triangle diagram. The analyses showed that K₂CO₃, KCl and KOH fluids are most favorable for the generation of lamproite melts. With increasing basalt content in the mixture or decreasing partial melting, the points for the run products approached those for high-potash rocks from the Leucite Hills and Western Australia. The obtained products differed markedly from natural melts in that they had high magnesium and, consequent-

ly, low silicon.

Run products of the interaction between mafic-ultramafic mixtures and potassium fluids.

Table 2

	KOH			K ₂ CO ₃		
	90:10	80:20	50:50	90:10	80:20	50:50
TYB237: TF-38 wt%	90:10	80:20	50:50	90:10	80:20	50:50
SiO ₂	41.50	42.03	40.50	42.26	42.48	46.20
TiO ₂	0.15	0.24	0.51	0.16	0.17	0.58
Al ₂ O ₃	2.10	3.12	6.84	2.24	3.46	6.10
FeO	5.61	5.39	5.49	6.15	5.84	5.75
MnO	0.09	0.20	0.09	-	0.05	-
MgO	45.59	42.89	33.96	43.95	41.33	27.83
CaO	1.56	2.03	4.52	0.53	1.56	4.27
Na ₂ O	0.07	0.30	0.15	0.10	0.05	-
K ₂ O	3.31	4.76	7.86	4.59	5.52	8.95

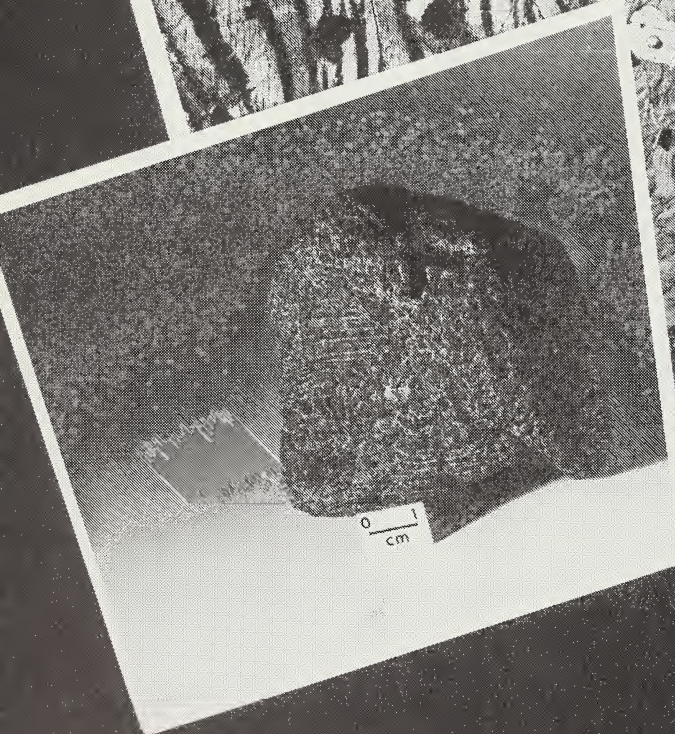
	KCl			KFHF*2H ₂ O		
	90:10	80:20	50:50	90:10	80:20	50:50
SiO ₂	44.21	49.00	48.43	31.89	38.51	41.92
TiO ₂	0.14	0.20	0.95	0.04	0.57	0.13
Al ₂ O ₃	2.12	2.56	5.06	2.17	6.71	4.47
FeO	5.55	5.84	5.14	3.95	4.78	5.07
MnO	0.06	-	-	0.02	0.05	0.01
MgO	44.12	39.03	30.10	37.36	28.69	38.23
CaO	1.74	2.44	6.27	1.63	6.86	1.17
Na ₂ O	0.09	-	-	0.12	0.25	0.11
K ₂ O	1.93	2.64	5.23	22.78	13.53	8.85

The material from the runs with KFHF*2H₂O was the most different from natural lamproites. Despite some discrepancy between bulk compositions of natural lamproites and run products, the mineral-parageneses in the latter were used as the bases for classification. On the whole, all fluids used in the experimentations yielded compositions of enhanced magnesianness (100 Mg/Mg+Fe) which varied within narrow limits (Ol_{91.5-92.2} Opx_{92.4-95.5}; Cpx_{93.6-96.1}; Phl_{89.4-90.1}; KAmf_{90.1-92.7}). By analogy with mineral composition from natural lamproites it can be concluded that run products contained no quench phases. It appears that all the minerals crystallized as a result of decreasing pressure from 5 to 2.5 kb. Unlike natural lamproites, the run products contained no leucite Ti and Zr-bearing minerals. Leucite could be formed from the high-potash glass which however failed to crystallize because of high (20%) water content. Since the charge did not contain Ti and Zr, no priderite or wadite were formed. Their occurrence in natural lamproites indicates that Ti and Zr have redistributed from the substrate into the potash melts.

The present experiments have supported the view that lamproite melt can be formed as a result of the fluid-magmatic interaction between the mantle substance and high-potash fluids. Crystallization of fluid-magmatic mixture resulting in tuff or tuff-breccia structures takes place as the mixture erupts through the overlying rocks, under the continuing interaction with the fluid under decreasing pressure to precede a decrease in temperature.

IV. WHAT IS THE NATURE OF THE UPPER MANTLE AND LOWER CRUST?

Descriptive lithology, mineralogy, petrology and geochemistry of xenoliths and xenocrysts; physical and chemical conditions within the upper mantle and lower crust.



MANTLE XENOLITHS FROM BULLENMERRI AND MT LEURA,
WESTERN VICTORIA, AUSTRALIA

	Page
REVIEW PAPER	
The nature of the upper mantle and lower crust B. HARTE	224
Experimental calibration of geothermobarometers in natural lherzolitic systems at high pressure G. P. BREY and K. G. NICKEL	228
Sub-continental lithosphere beneath Katwe-Kikorongo, SW Uganda G. R. DAVIES and F. E. LLOYD	229
Characterisation of metasomatic processes in peridotite nodules contained in kimberlite A. J. ERLANK, F. G. WATERS, S. E. HAGGERTY and C. J. HAWKESWORTH	232
Subcontinental lithospheric and asthenospheric metasomatism in the region of Jagersfontein, South Africa S. W. FIELD, S. E. HAGGERTY and A. J. ERLANK	235
Olivine barometry in the spinel and garnet stability fields: Precision, accuracy and a basin and range (USA) geotherm A. A. FINNERTY	238
Mantle metasomatism of pyroxenite xenoliths from Kaula Island, Hawaii M. O. GARCIA and A. A. PRESTI	241
The pressure dependence of creep in olivine: Consequences for mantle flow H. W. GREEN, R. BORCH and B. E. HOBBS	244
Chemical and isotopic characteristics of multiply-metasomatised mantle xenoliths from western Victoria W. L. GRIFFIN and S. Y. O'REILLY	247
Source regions for oxides, sulfides and metals in upper mantle: Clues to the stability of diamonds, and the origin of kimberlites and lamproites S. E. HAGGERTY	250
Crustal xenoliths from Southern Africa: Chemical and age variations within the continental crust C. J. HAWKESWORTH, P. VAN CALSTEREN, Z. PALACZ and N. W. ROGERS	253
Megacrysts and deformed nodules from the Jagersfontein kimberlite pipe J. J. HOPS, J. J. GURNEY and B. HARTE	256
Eclogite - garnetite transformations in basaltic and pyrolytic compositions at high pressure and high temperature T. IRIFUNE, W. O. HIBBERSON and A. E. RINGWOOD	259
Polybaric magma mixing in alkalic basalts and kimberlites: Evidence from corundum, zircon and ilmenite megacrysts A. J. IRVING	262
Sm-Nd systematics in eclogites from Siberia E. JAGOUTZ	265
Archaean zircon xenocrysts from the Jwaneng kimberlite pipe, Botswana P. D. KINNY, I. S. WILLIAMS, W. COMPSTON and J. BRISTOW	267
Garnets from West Australian kimberlites and associated rocks H. LUCAS, R. RAMSAY, A. E. HALL, C. B. SMITH and N. V. SOBOLEV	270
Carbon in olivine by nuclear reaction analysis E. A. MATHEZ, J. D. BLACIC, J. BEERY, C. MAGGIORE and M. HOLLANDER	273
Abundances and carbon isotope compositions of trapped fluids in mantle diopsides: implications for mantle recycling models D. MATTEY, C. T. PILLINGER and M. A. MENZIES	276

	Page
Corganites and corgaspinites. Two new types of aluminous assemblages from the Jagersfontein kimberlite pipe P. MAZZONE and S. E. HAGGERTY	279
Sodium in garnet and potassium in clinopyroxene: criteria for classifying mantle eclogites T. E. McCANDLESS and J. J. GURNEY	282
Sm-Nd systematics in eclogite and garnet peridotite nodules from kimberlites: Implications for the early differentiation of the earth M. T. McCULLOCH	285
Chemical and isotopic evolution of the SE Australian subcontinental lithosphere W. F. McDONOUGH and M. T. McCULLOCH	288
Carbonated xenoliths from the Macdougall Springs mica peridotite diatreme: Inferences for upper mantle conditions in north central Montana E. S. McGEE and B. C. HEARN, Jr	291
Ba and LREE enriched mantle below the Archaean crust of Scotland M. MENZIES, A. HALLIDAY, Z. PALACZ, R. HUNTER and C. HAWKESWORTH	294
Garnet-pyroxene and orthopyroxene-clinopyroxene equilibria in the system $\text{SiO}_2\text{-MgO-Al}_2\text{O}_3\text{-CaO-Cr}_2\text{O}_3$ (SMACCR): a new geobarometer K. G. NICKEL	296
Mantle magmatic events indicated by zoned olivine and pyroxene compositional variations in a composite mantle xenolith from Lashaine Volcano, Tanzania J. E. NIELSON	297
Diamond-bearing peridotite xenoliths from the Argyle (AK1) pipe H. St. C. O'NEILL, A. L. JAQUES, C. B. SMITH and J. MOON	300
Petrological constraints on geophysical models for the lower crust, moho and mantle: thermal and seismic interpretations S. Y. O'REILLY, W. L. GRIFFIN and B. D. JOHNSON	303
Mantle-derived argon components in phlogopite from Southern African kimberlites D. PHILLIPS and T. C. ONSTOTT	306
Xenoliths of diamondiferous peridotites from Udachnaya kimberlite pipe, Yakutia N. P. POKHILENKO and N. V. SOBOLEV	309
Composition and age of the lower crust in North Queensland R. L. RUDNICK, I. S. WILLIAMS, S. R. TAYLOR and W. COMPSTON	312
Chemical disequilibrium and diffusion gradients in eclogite xenolith JGG 41: An isothermal model for exsolution reaction V. SAUTTER and B. HARTE	315
Cerium isotopes - new aspects for kimberlite genesis by a new isotopic system D. SCHIER and E. JAGOUTZ	318
Interaction of metasomatic fluids and basaltic melt with mantle xenoliths A. SCHNEIDER	320
Green garnets and wehrlites from Kimberley, South Africa D. J. SCHULZE	323
Evolution of sub-continental mantle and crust: Eclogites from Southern Africa J. W. SHERVAIS, L. A. TAYLOR, G. W. LUGMAIR, R. N. CLAYTON, T. MAYEDA and R. L. KOROTEV	326

	Page
Isotopic and geochemical studies of kimberlite and included xenoliths Craig B. SMITH, H. L. ALLSOPP, J. D. KRAMERS, J. J. GURNEY and E. JAGOUTZ	329
Sr and Nd isotopic systematics of diamond-bearing eclogite xenoliths and eclogitic inclusions in diamond from Southern Africa Craig B. SMITH, J. J. GURNEY, J. W. HARRIS, D. N. ROBINSON, S. R. SHEE and E. JAGOUTZ	332
Compositional heterogeneities in minerals in peridotite nodules D. SMITH and F. R. BOYD	335
Sheared lherzolites from kimberlites of Yakutia N. V. SOBOLEV, N. P. POKHILENKO, D. A. CARSWELL and A. S. RODIONOV	338
Heterogeneity of the upper mantle beneath the Siberian Platform L. V. SOLOVJEVA	340
Ultramafic xenoliths from the Pali-Aike basalts: Implications for the nature and evolution of the subcontinental lithosphere below southern South America C. R. STERN, K. FUTA, S. SAUL and M. A. SKEWES	343
Isotopic evolution of the Kimberley block, Western Australia S-S. SUN, A. L. JAQUES and M. T. McCULLOCH	346
The solubility and diffusivity of carbon in olivine: Implications for carbon in the Earth's upper mantle T. N. TINGLE, H. W. GREEN and A. A. FINNERTY	349
A suggested origin of marid nodules in kimberlites by high pressure crystallisation of lamproitic magma F. WATERS	352
Mantle/crustal xenoliths in Hawaiiite Lavas: The Cima Volcanic Field, California H. G. WILSHIRE and J. S. NOLLER	355

Ben Harte

Grant Institute of Geology, University of Edinburgh, Scotland

GEOPHYSICAL, TECTONIC AND GEOCHEMICAL FRAMEWORK

The major layering of the crust and upper mantle has been largely defined by the discontinuities (Moho, 670km discontinuity, Conrad discontinuity, low velocity zone) revealed by studies of seismic wave velocities. The concept of plate tectonics has enforced a major distinction between a relatively rigid lithosphere (containing the Moho) and an underlying convective asthenosphere. The age and nature of the modern oceanic lithosphere is moderately well constrained by considerations of sea-floor spreading, plate tectonics and obducted slabs of ocean floor. In contrast the construction and origin of the continental lithosphere (crust and mantle), which has evolved through a much longer period of time, remains the complex puzzle which has long excited the deliberations of geoscientists.

Recently, extensive data from seismic reflection experiments have revealed that the lower continental crust is frequently characterised by many, often sub-horizontal, reflectors. Such reflectors occur beneath Archaean and tectonically-young terranes (Smithson, 1986), and there is considerable uncertainty concerning their origin or origins (?small-scale lithological layering, mylonite zones, H₂O-rich layers). Layering of the lower crust by basic intrusions may be an extensive cause of the reflectors and increases speculation concerning the widespread occurrence of underplating. Dipping seismic reflectors in the upper crust often die out in the lower crust, but some (e.g. the Outer Isles Thrust of north-west Scotland) may continue and displace the Moho. Most recently the occurrence of strong reflectors (both dipping and sub-horizontal) has been identified in the upper mantle lithosphere (McGeary and Warner, 1985).

In order to explain the origin of many features of the stable continental lithosphere, it is natural to turn to the processes seen in presently active tectonic regimes. But in endeavouring to interpret features of the continental lower crust and mantle lithosphere, it is often difficult to assess whether extensional or compressive tectonic regimes have had the major influence. Thus basalt injection during rifting, and tectonic imbrication and mylonite formation during continental collision, may both be invoked to explain lower crustal seismic reflectors. Similarly, major aspects of layering of continental lithosphere may be attributed to subduction zone processes (Oxburgh and Parmentier, 1978), whilst recent seismic reflection data from the Basin and Range province (USA) suggest that the Moho is related to Cenozoic magmatism and extension (Klemperer et al., 1986). In general a polygenetic origin of features in the continental lower crust and mantle lithosphere must be expected (Fountain and Salisbury, 1981; Smithson, 1986).

Within cratons, the above uncertainties are compounded by lack of knowledge concerning global tectonic processes in the Archaean. With the prominent exception of komatiite distribution, there is little evidence from exposed Archaean terranes of the higher-than-present-day geothermal gradients which might be expected from abundances of radioactive elements.

Geophysical and geochemical evidence may be adduced to support the concept of layered mantle convection, with the upper convecting layer extending to a depth of about 700km (Richter and McKenzie, 1981). This upper convecting layer may be equated with the asthenospheric reservoir of MORB, which (with its depleted trace element and isotope characteristics) may be broadly viewed as the long term complement to the differentiated continental crust. In addition to the MORB reservoir (asthenosphere), other potential reservoirs with distinct geochemical signatures are: the lower mantle, continental crust, continental mantle lithosphere, oceanic crust and oceanic mantle lithosphere. In explaining the geochemistry of different basalt provinces (oceanic islands, continental alkali basalts, continental flood basalts, arc volcan-

ics) these different reservoirs are tapped to varying degrees by different authors (e.g. Allegre et al., 1983; Hofmann and White, 1982; McKenzie and O'Nions, 1983). The physical position of these reservoirs is not fixed; thus oceanic lithosphere may be partly incorporated in continental lithosphere and recycled to the asthenosphere, whilst continental lithosphere may also return to the asthenosphere. However, the geochemical constraints provided by the identification of these (or other) reservoirs, provides a framework, which can interact with observations on xenolith types in different provinces, to develop an understanding of both upper mantle constitution and basalt genesis (Hawkesworth et al., 1983).

XENOLITHS AND THE NATURE OF THE LOWER CONTINENTAL CRUST AND MOHO

Xenoliths believed to represent the lower continental crust and Moho region are available from igneous rocks erupted in a wide variety of tectonic environments (e.g. convergent plate boundaries, intraplate rifts, stable platforms and cratons) - Kay and Kay (1980). In general the xenoliths reveal dominantly basic lithologies but with widely variable proportions of ultrabasic and metasedimentary rocks.

The basic rocks range from pyroxene-plagioclase rocks, which in some cases may represent little-metamorphosed igneous cumulates, to thoroughly-metamorphic amphibolites, garnet pyroxenites and eclogites (e.g. Wäss and Irving, 1976; Griffin et al., 1979; Upton et al. 1984). When xenoliths from one locality are assembled (by a combination of P-T estimates and wishful thinking) into vertical sections, an interdigitation of basic and ultrabasic rocks across the crust-mantle boundary may be indicated (Griffin et al., 1984; Jackson, 1980). The occurrence of garnet-pyroxene-granulites in the uppermost mantle can be argued if P-T estimates are considered in isolation.

The ages of initial formation of many xenoliths attributed to the lower continental crust are evidently old (e.g. Rogers and Hawkesworth, 1982). However, there is uncertainty concerning the age of the metamorphic mineral assemblages in xenoliths by comparison with their age of eruption; and evidence exists in some cases of metamorphism considerably before eruption (Harte et al., 1981). If P-T estimates from a suite of lower crustal xenoliths all refer to the same time then they may be used to construct fossil geotherms. As might be anticipated such geotherms often indicate relatively high heat flow regimes; again, whether these geotherms pertain to the time of eruption or some preceding compressional or extensional tectonic regime is a moot point. Evidently more data on the ages of these xenoliths and their mineral assemblages is much needed.

XENOLITHS/XENOCRYSTS AND THE NATURE OF THE CONTINENTAL MANTLE LITHOSPHERE

The majority of xenoliths are peridotites, pyroxenites and eclogites. Often the pyroxenites seem to be genetically related to peridotites, but the associations of the eclogites (and also grosspyrites) are less clear. The formation of eclogites from subducted oceanic lithosphere has been suggested (Helmstaedt and Schulze, 1979). The peridotite xenoliths from basaltic hosts are usually non-garnetiferous, whilst those from kimberlitic hosts are garnetiferous; but exceptions occur. Within both spinel-peridotites and garnet-peridotites evidence of initial ages of formation of 1 to 3.5 Ga may be found (e.g. Cohen et al., 1984; Menzies et al., 1985). Recent data from diamond inclusions (Richardson et al., 1984) not only yield evidence of >3 Ga old continental lithosphere, but of geothermal gradients at that time which were similar to those of present-day shields.

Considering the peridotite xenoliths and their relationships the following points may be noted:-

(1) A large proportion of the common coarse or protogranular xenoliths are depleted in basalt constituents. However many of these xenoliths show a secondary LREE enrichment, which may often be relatively recent (e.g. Menzies et al., 1985).

(2) Garnet-peridotite xenoliths from kimberlite pipes are often of two major types: coarse peridotites with low estimated temperatures (<1100°C) of equilibration

and deformed peridotites with high estimated temperatures of equilibration. The cold coarse group are often highly depleted in basaltic constituents, whilst the hot deformed group are usually more fertile and may have trace element and isotope signatures indicative of the MORB asthenosphere reservoir (Richardson et al., 1985). It is debated whether the hot deformed peridotites have 'primary' compositions (Boyd and Nixon, 1975), or secondary compositions caused by interaction with an 'asthenospheric' magma, whose presence is also shown by Cr-poor megacryst suites (Harte, 1983).

(3) In southern Africa the cratonic region mapped at the surface, finds expression in the mantle lithosphere mapped at depth by the distribution of diamonds, low-calcium garnets and the equilibration conditions of high-temperature peridotites (Boyd and Gurney, 1986).

(4) A wide variety of peridotite-pyroxenite xenoliths showing modal metasomatism are found. In many cases this metasomatism appears to be consequent upon the incursion of melts. Several associations of metasomatic nodules and eruptive rocks may be broadly recognised: (a) alkali clinopyroxenite nodules from highly alkaline continental volcanics; (b) kaersutite/pargasite and mica bearing nodules from alkali basalts; (c) ilmenite-rutile-phlogopite-sulphide nodules from kimberlites; (d) richterite and mica bearing nodules from kimberlites. The enriched trace element inventories of such nodules and the longevity of the continental mantle lithosphere endorse it as a potentially important geochemical reservoir.

REFERENCES

- ALLEGRE C.J., DUPRE B., RICHARD P., ROUSSEAU D. and BROOKS C. 1982. Subcontinental versus suboceanic mantle, II. Nd-Sr-Pb isotopic comparison of continental tholeiites with mid-ocean ridge tholeiites, and the structure of the continental lithosphere. *Earth and Planetary Science Letters* 57, 25-34.
- BOYD F.R. and NIXON P.H. 1975. Origins of the ultramafic nodules from some kimberlites of northern Lesotho and the Monastery Mine, South Africa. *Physics and Chemistry of the Earth* 9, 431-454.
- COHEN R.S., O'NIONS R.K. and DAWSON J.B. 1984. Isotope geochemistry of xenoliths from East Africa: implications for development of mantle reservoirs and their interaction. *Earth and Planetary Science Letters* 68, 209-220.
- FOUNTAIN D.M. and SALISBURY M.H. 1981. Exposed cross-sections through the continental crust: implications for crustal structure, petrology and evolution. *Earth and Planetary Science Letters* 56, 263-277.
- GRIFFIN W.L., CARSWELL D.A. and NIXON P.H. 1979. Lower-crustal granulites and eclogites from Lesotho, southern Africa. In Boyd F.R. and Meyer H.O.A. eds, *The Mantle Sample: Inclusions in Kimberlites and other Volcanics*, pp. 59-86. American Geophysical Union, Washington D.C.
- GRIFFIN W.L., WASS S.Y. and HOLLIS J.D. 1984. Ultramafic xenoliths from Bullenmerri and Gnotuk Maars, Victoria, Australia: Petrology of a sub-continental crust-mantle transition. *Journal of Petrology* 25, 53-87.
- HARTE B. 1983. Mantle peridotites and processes - the kimberlite sample. In Hawkesworth C.J. and Norry M.J. eds, *Continental Basalts and Mantle Xenoliths*, pp. 46-91. Shiva, Nantwich.
- HARTE B., JACKSON P.M. and MACINTYRE M. 1981. Age of mineral equilibria in granulite facies nodules from kimberlites. *Nature* 291, 147-148.
- HAWKESWORTH C.J., ERLANK A.J., MARSH J.S., MENZIES M. and van CALSTEREN P. 1983. Evolution of the continental lithosphere: evidence from volcanics and xenoliths in southern Africa. In Hawkesworth C.J. and Norry M.J. eds, *Continental Basalts and Mantle Xenoliths* pp. 111-138.

- HELMSTAEDT H. and SCHULZE D.J. 1979. Garnet clinopyroxene-chlorite eclogite transition in a xenolith from Moses Rock: Further evidence for metamorphosed ophiolites beneath the Colorado Plateau. In Boyd F.R. and Meyer H.O.A. eds, *The Mantle Sample: Inclusions in Kimberlites and other Volcanics*, pp. 357-365. American Geophysical Union, Washington D.C.
- HOFMANN A.W. and WHITE W.M. 1982. Mantle plumes from ancient oceanic crust. *Earth and Planetary Science Letters* 57, 421-436.
- JACKSON P.M. 1980. Petrology of some nodules from kimberlites in northern Lesotho. Unpublished PhD thesis, University of Edinburgh.
- KAY R.W. and KAY S.M. 1980. Chemistry of the lower crust: inferences from magmas and xenoliths. In *Continental Tectonics*, pp. 139-150. National Academy of Sciences, Washington D.C.
- KLEMPERER S.L., HAUGE T.A., HAUSER E.C., OLIVER J.E. and POTTER C.J. In press. The Moho in the northern basin and range province, Nevada, along the Cocorp 40°N seismic reflection transect. *Geological Society of America Bulletin*.
- McGEARY S. and WARNER M.R. 1985. Seismic profiling the continental lithosphere. *Nature* 317, 795-797.
- McKENZIE D.P. and O'NIONS R.K. 1983. Mantle reservoirs and ocean island basalts. *Nature* 301, 229-231.
- MENZIES M., KEMPTON P. and DUNGAN M. 1985. Interaction of continental lithosphere and asthenospheric melts below the Geronimo volcanic field, Arizona, U.S.A. *Journal of Petrology* 26, 663-693.
- OXBURGH E.R. and PARMENTIER E.M. 1978. Thermal processes in the formation of continental lithosphere. *Philosophical Transactions of the Royal Society of London A-288*, 415-429.
- RICHARDSON S.H., GURNEY J.J., ERLANK A.J. and HARRIS J.W. 1984. Origin of diamonds in old enriched mantle. *Nature* 310, 198-202.
- RICHARDSON S.H., ERLANK A.J. and HART S.R. 1985. Kimberlite-borne garnet peridotite xenoliths from old enriched subcontinental lithosphere. *Earth and Planetary Science Letters* 75, 116-128.
- RICHTER F.M. and McKENZIE D.P. 1981. On some consequences and possible causes of layered mantle convection. *Journal of Geophysical Research* 86, 6133-6142.
- ROGERS N.W. and HAWKESWORTH C.J. 1982. Proterozoic age and cumulate origin for granulite xenoliths, Lesotho. *Nature* 299, 409-413.
- SMITHSON S.B. 1986. A physical model of the lower crust from North America based on seismic reflection data. In Dawson J.B., Carswell D.A., Hall J. and Wedepohl K.H. eds, *The Nature of the Lower Continental Crust*, in press. Geological Society of London Special Publication No. 25.
- UPTON B.G.J., ASPEN P. and HUNTER R.H. 1984. Xenoliths and their implications for the deep geology of the Midland Valley of Scotland and adjacent regions. *Transactions of the Royal Society of Edinburgh: Earth Sciences* 75, 65-70.
- WASS A. and IRVING A.J. 1976. *Xenmeg: A catalogue of occurrences of xenoliths and megacrysts in basic volcanic rocks of eastern Australia*, 441pp. Australian Museum, Sydney.

G.P. Brey and K. G. Nickel

Max-Planck-Institut für Chemie, Saarstrasse 23, D-6500 Mainz, F.R.Germany

Important informations about the constitution of the continental lithosphere may be obtained from garnet lherzolite xenoliths sampled by kimberlites. In particular P,T distributions within the deep lithosphere give constraints and boundary conditions for the modelling of the dynamic behaviour of the earth's interior.

The basis of the widely used two-pyroxene thermometer is the exchange of the enstatite component between ortho- and clinopyroxene, well known in the system CaO - MgO - SiO₂ (CMS) up to 60 kb. The direct application to more complex systems may be misleading because of the uncertainties introduced by other important constituents of pyroxenes, but non-idealities may cancel each other in the complex natural system and very simple empirical thermometers and barometers (e.g. Finnerty and Boyd 1984; Brey et al., 1986) may be applicable. The arguments for successful application are however debatable and thus it is necessary to have experimental data to verify or falsify the use of such empirical geothermobarometers.

We thus performed experiments with complex, natural compositions typical for the upper mantle in the range 800 - 1500°C, 25 - 50 kb. Experiments in Fe-bearing systems are problematic because of possible loss or gain of Fe to or from the sample container and the need to demonstrate equilibrium values in systems with several degrees of compositional freedom. In our approach we use single crystal olivines of a composition near equilibrium with the charge and accordingly they do not react with the samples. Within this single crystal olivine we subject starting materials of strongly differing mineralogy/mineral chemistry (natural spinel and garnet lherzolite, synthetic mineral and oxide mixes) to the same P,T condition. For the most important chemical parameters for geothermobarometry (i.e. Al- and Ca-content of pyroxenes) the direction and the coincidence of the approached equilibrium value can be demonstrated.

The obtained data set together with some data from the literature allows to evaluate not only two-pyroxene thermometry and Al-in-orthopyroxene barometry, but also other thermobarometric reactions (e.g. Fe/Mg exchanges garnet-olivine or garnet-orthopyroxene or Cr-solubility in orthopyroxene). The various thermobarometers are currently revised but the preliminary evaluation suggests that pressure-temperature estimates with almost acceptable systematic errors are obtained using the Nickel and Green (1985) barometer in combination with the Wells (1977) thermometer.

Application of these two methods defines groups of low-temperature xenoliths (T < 1100°C) in accord with conductive heat flow geotherms and contrasting groups of high-temperature xenoliths, recording a range of temperatures at near-isobaric conditions. The level of this isobaric 'temperature discontinuity' is different for the different suites/provinces and is interpreted as an expression of the movement of 'kiel-shaped' continents over heat sources (such as upwelling streams of convection cells), resulting in (repeated?) processes of:

- a) lithospheric thinning by thermal erosion involving the generation of magmas and, hence, causing differentiation processes both within the lithosphere and the convecting mantle below and
- b) magmatic underplating, when the continent rests over cooler regions of the convecting mantle and thickens again.

REFERENCES

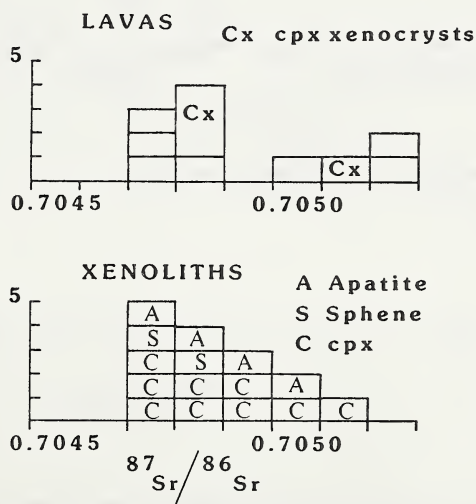
- BREY, G.P., NICKEL, K.G. and KOGARKO, L. 1986. *Contrib. Mineral. Petrol.* 92, 448-455.
FINNERTY, A.A. and BOYD, F.R. 1984. *Geochim. Cosmochim. Acta* 48, 15-27.
NICKEL, K.G. and GREEN, D.H. 1985. *Earth Planet. Sci. Lett.* 73, 158-170.
WELLS, P.R.A. 1977. *Contrib. Mineral. Petrol.* 62, 129-139.

Dept. of Earth Sciences, University of Leeds

Recent K rich mafic volcanics of the western branch of the East African rift system contain hydrous pyroxenites with variable amounts of phlogopite, amphibole, apatite, sphene, perovskite, Fe-Ti oxides and calcite. This study concentrates on the volcanic products and xenoliths from two adjacent craters in the centre of the Katwe-Kikorongo volcanic field, S.W. Uganda, which lies immediately to the north of Lake Albert. Our aim is to ascertain if the xenoliths, which show evidence of both magmatic and metasomatic textures, represent old metasomatised mantle (Lloyd and Bailey, 1975) or are high P/T cumulates from the host magmas.

Highly undersaturated rocks such as the olivine melilitites and clinopyroxene rich kalsilite-nepheline-leucite bearing assemblages in the western rift are notoriously susceptible to low temperature alteration (Taylor et al. 1984). In an effort to minimise the effects of alteration the volcanic rocks were crushed by hand and secondary zeolites and carbonate carefully removed. The majority of rocks prepared in this way contain less than 1% H₂O indicating they are relatively unaltered. In addition clinopyroxene separates were obtained from the few porphyritic lavas to enable us to determine the isotope systematics on unequivocally fresh material. However it should be noted that the clinopyroxenes are always highly zoned and may be surrounded by a reaction zone of melilite, implying a possible xenocrystic origin. Isotope analyses of xenolith material was only carried out on mineral separates.

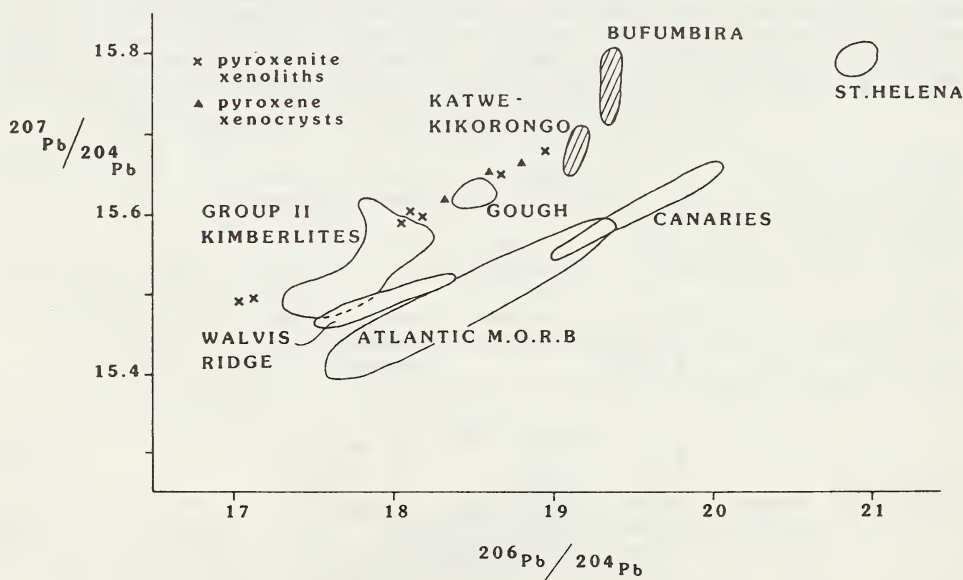
Certain lava samples were split into 2 prior to preparation. The extraction of zeolites and carbonate reduces the measured $^{87}\text{Sr}/^{86}\text{Sr}$, e.g. S23161 0.70531 to 0.70453. Significantly, "cleaned" whole rock samples with H₂O contents greater than 1% yield $^{87}\text{Sr}/^{86}\text{Sr}$ ratios greater than 0.7052. These apparently altered samples will not be considered further in the discussion. Apatite-clinopyroxene and sphene-clinopyroxene mineral pairs establish the xenoliths to be in Sr and Nd isotope equilibrium. The exception is the carbonate which, although having high trace element contents suggesting a magmatic origin ($\text{La}_N = 645$), has a relatively radiogenic $^{87}\text{Sr}/^{86}\text{Sr}$ ratio of 0.70563 indicating a minor crustal contribution. Fig. 1 demonstrates that the $^{87}\text{Sr}/^{86}\text{Sr}$ ratios

FIGURE 1 $^{87}\text{Sr}/^{86}\text{Sr}$ histogram for lavas and xenoliths

of the lavas encompass those of the xenoliths and show a significantly greater range. The $^{143}\text{Nd}/^{144}\text{Nd}$ ratios of the lavas are more radiogenic, >0.51261 , than the xenoliths 0.51255 to 0.51261 . The xenoliths and lavas therefore plot close to the Bulk Earth value on a Sr-Nd isotope diagram being more radiogenic in terms of $^{143}\text{Nd}/^{144}\text{Nd}$ than the nearby Virunga volcanic field (Vollmer and Norry, 1983). Clinopyroxenes separated from the lavas are not in Sr/Nd isotope equilibrium with their hosts. Significantly the $^{87}\text{Sr}/^{86}\text{Sr}$ ratios of the lavas are not consistently more radiogenic implying that the disequilibrium is not simply a consequence of low temperature alteration of the host. REE patterns of clinopyroxenes from the xenoliths and lavas are comparable $(\text{Ce}/\text{Yb})_{\text{N}} = 1 - 1.4$. Perhaps more relevant are the highly variable clinopyroxene-host partition coefficients La; $0.19 - 0.47$ Yb; $0.23 - 0.78$ strongly suggesting that the clinopyroxenes have not all equilibrated with their host magmas and hence that they are xenocrysts originating from disaggregated xenoliths.

The lavas show limited Pb isotope variation, $^{206}\text{Pb}/^{204}\text{Pb}$ 19.09 - 19.19, but are notable for their relatively radiogenic $^{207}\text{Pb}/^{204}\text{Pb}$, 15.65 - 15.7., and $^{208}\text{Pb}/^{204}\text{Pb}$, 39.58 - 40.03, ratios. The data define steeply inclined arrays on Pb/Pb isotope diagrams (Fig. 2) being slightly less radiogenic than the K rich mafic volcanics from Virunga (Vollmer and Norry, 1983). In terms of Sr, Nd and Pb isotope ratios the Katwe-Kikorongo volcanics are less extreme than the Bufumbira rocks. Unlike the Virunga suite, we do have combined major and trace element data and hence can be certain from their high Ni, Cr and MgO contents and low SiO_2 that the Katwe-Kikorongo volcanics have suffered limited fractionation and crustal interaction subsequent to equilibration with their ultrabasic, and presumably, mantle source. The suite shows enriched trace element characteristics ($5\% \text{K}_2\text{O}$, $\text{Zr}/\text{Nb} = 2$, $\text{Rb}/\text{Sr} 0.05 - 0.08$ and $(\text{La}/\text{Yb})_{\text{N}} = 100$) comparable to group I and II kimberlites but not as extreme as lamproites.

FIGURE 2 $^{207}\text{Pb}/^{204}\text{Pb}$ vs $^{206}\text{Pb}/^{204}\text{Pb}$ isotope diagram.



In marked contrast to the lavas, and their Sr and Nd isotope ratios, the xenoliths display significant Pb isotope variation, $^{206}\text{Pb}/^{204}\text{Pb}$ 17.0 - 19.0, and on Pb/Pb isotope diagrams form linear arrays displaced to significantly more radiogenic $^{207}\text{Pb}/^{204}\text{Pb}$ and $^{208}\text{Pb}/^{204}\text{Pb}$ than, for example Atlantic MORB (Fig. 2). In addition $^{206}\text{Pb}/^{204}\text{Pb}$ ratios range to values less radiogenic than MORB and Group II kimberlites (Sun, 1980; Smith,

1983, Fraser et al. 1986). Clinopyroxene from the lavas plot among the xenolith data confirming their xenocrystic origin. The linear array defined by the xenoliths, and the xenocrysts, equate to an age of approximately 1300 My. Due to the partially carbonated nature of the xenoliths, whole rock U/Pb ratios have not been determined. However, u values of the clinopyroxenes increase significantly along the array 1-100. Acceptance of the 1300 My age as of geological significance implies stabilisation of the subcontinental lithosphere during the regional Kibaran crust forming event. Consideration of the Nd isotope systematics of the xenoliths suggest that they can only have been LREE enriched, to their present degree, for an absolute maximum of 900 My. We therefore conclude that, although the xenoliths contain an old component with a relatively high u , the Pb/Pb linear arrays hold no direct age significance and represent, at least in part, mixing arrays.

The subcontinental lithosphere beneath this 5 sq km region of the Katwe-Kikorongo volcanic field is isotopically very heterogeneous and has major and trace element chemistry (K_2O 3.5%, Sr >1000 ppm, Ba >1000 ppm and $(La/Yb)_N > 50$) capable of producing K rich mafic volcanics, such as lamproites and olivine melilitites, even at relatively high degrees of partial melting i.e. >10%. We have shown that the hydrous pyroxenite xenoliths did not originate as high P/T cumulates from their host volcanics, nor do they represent the source materials for these volcanics. Significantly the type of xenolith, magmatic or metasomatic texture, has no control as to their position on the Pb-Pb arrays. We propose that the hydrous pyroxenitic mantle originated from an alkaline magma (basanite), residual fluids from which, caused the observed metasomatism. The xenoliths are therefore analogous to Type II spinel lherzolites. The Katwe-Kikorongo volcanics are derived from similar pyroxenite material, possibly deeper in the subcontinental lithosphere, that lie on an extension of the Pb-Pb mixing arrays. The mantle derived component of the Virunga volcanism originated from an equivalent source.

KRASER, K.J., HAWKESWORTH, C.J., ERLANK, A.J., MITCHELL, R.H. and SCOTT-SMITH, B.H.
1986. E.P.S.L., 76, 57.

LLOYD, F.E. and BAILEY, D.K. 1975. Phys. Chem. Earth, 9, 389.

SMITH, C.B. 1983. Nature 304, 51.

SUN, S.S. 1980. Phil. Trans. R. Soc. 297, 409.

TAYLOR, H.P., TURI, B. and CUNDERI, A. 1984. E.P.S.L. 69, 263.

CHARACTERIZATION OF METASOMATIC PROCESSES IN
PERIDOTITE NODULES CONTAINED IN KIMBERLITE

A.J. Erlank*, F.G. Waters*, S.E. Haggerty** and C.J. Hawkesworth***

*Dept. of Geochemistry, University of Cape Town, Rondebosch, R.S.A.

**Dept. of Geology, University of Massachusetts, Amherst, Mass., U.S.A.

***Dept. of Earth Sciences, Open University, Milton Keynes, U.K.

A comprehensive account has recently been given of a large suite of metasomatised peridotite nodules from the Kimberley pipes, particularly from Bultfontein (Erlank *et al.*, 1986). We present first a summary of the distinguishing characteristics of the metasomatic changes observed in this suite, and then use them as a basis for examining metasomatic changes and styles in materials from other southern African kimberlites. The Kimberley suite is divided into garnet peridotites (GP) which contain no texturally equilibrated or primary (mantle derived) phlogopite, garnet phlogopite peridotites (GPP), which constitute the most abundant peridotites, phlogopite peridotites (PP) and phlogopite K-richterite peridotites (PKP). The latter two groups contain no garnet, while diopside may or may not be present in all four groups. The Cr-titanate minerals, lindsleyite and mathiasite (LIMA) are found only in PKP rocks, together with a new Ba- and Ce-rich Cr-titanate, Nb-Cr rutile and armalcolite (Haggerty *et al.*, 1983, 1986).

Textural, mineralogical, chemical and isotopic data are consistent with an overall metasomatic process that is manifested by the GP-GPP-PP-PKP sequence recognized. The sequence does not imply that all PKP rocks will have formed from GP precursors, but does imply that the PKP suite represents the most highly metasomatised peridotites. The metasomatism can be viewed as one in which H₂O-rich fluids charged with K and other silicate-incompatible elements have migrated upwards in old lithospheric mantle, over a depth interval of some 30 - 50 km within the garnet stability field (Fig. 1) during the past 150 - 90 Ma (Fig. 2). The metasomatism is quantitatively dominated by the introduction of primary phlogopite, with many of the GPP rocks containing ~ 1 % or less phlogopite. At deeper levels garnet appears to be more abundant, and garnet replacement by phlogopite + diopside is common, as manifested also by veins consisting mainly of these two minerals. However phlogopite has replaced all anhydrous silicates throughout the depth range involved. Enstatite, diopside, phlogopite and Cr-spinel together with constituent whole rocks show a well defined decrease in Al₂O₃ content within the GPP-PP-PKP sequence. Although some PKP rocks have formed from garnet-bearing rocks at shallower levels, most PKP rocks formed directly from Al-deficient harzburgitic rocks, with K-richterite replacing all pre-existing silicates, including phlogopite. Veined samples consist dominantly of K-richterite with lesser phlogopite and minor opaque minerals. The acme of metasomatism is represented by the growth of LIMA, and the new Ba and Ce-rich Cr-titanate, from precursor Cr-spinel, in PKP rocks. The latter suite shows highest levels of enrichment in S, Na, K, Rb, Ba, Sr, LREE, Fe, Ti, Zr and Nb (Fig. 3). These enrichments are reflected by associated mineralogical development, for example high Sr contents are found in diopside, K-richterite and particularly LIMA. Chemical and textural distinctions can be made between primary and secondary phlogopite (Fig. 4) and diopside. Nd-isotopic measurements indicate the existence of an ancient (> 1 Ga) enrichment in these sub-cratonic lithospheric mantle samples, and evidence for it is given by low Nd-isotopic ratios in diopside, phlogopite and non-metasomatic garnet from GPP rocks (Richardson *et al.*, 1985).

The obvious similarities between PKP and MARID rocks, and to a lesser extent kimberlite, suggest that they must be related in some way in mantle space and time. Detailed assessment of mineralogical, major and trace element, and isotopic variations indicate that no simple relationships exist between these groups. Isotopic and trace element evidence is consistent with an asthenospheric (hot spot or subduction related?) origin for the fluids that led to the GPP and PP metasomatism (and possibly for the MARID parent magmas). If these fluids can be shown to be unrelated to the host kimberlite formation but are older, then their distribution over a considerable depth interval in the lithospheric mantle below Kimberley assumes a wider significance (Fig. 1). Kimberlites and MARID magmas may owe part of their geochemical signatures to interaction with stockwork-veined metasomatised mantle with linked channelways rich in incompatible elements (Erlank *et al.*, 1986; Waters this volume). It is speculated that the PKP metasomatism may be derived in part from "last gasp" incompatible element-rich

aqueous fluids escaping from crystallizing MARID magmas. One MARID nodule (from Newlands, kindly supplied by L. Daniels) has a thin rind of PKP material, interpreted as wall rock metasomite as depicted in Fig. 1.

The styles of metasomatism recognized in the Kimberley peridotites are also present elsewhere. Replacement of garnet by primary phlogopite, and the close spatial association of phlogopite and diopside with accompanying Cr-spinel (GPP and PP rocks), is common in peridotites from many other localities, including Jagersfontein (coarse peridotites only), Monastery, Lesotho localities such as Kao and Pipe 200, and the Precambrian Premier Kimberlite. We have also confirmed the presence of K-richrichterite in one Monastery and several Kampfersdam and Jagersfontein samples. There is also abundant edenitic and pargasitic amphibole with classic replacement textures in GPP rocks from Jagersfontein; we propose that these be called GPAP rocks, with amphibole being non-richrichteritic. Both PKP and GPAP rocks at Jagersfontein contain examples that are veined; further details are given by Field *et al.*, (this volume).

The southern African kimberlites referred to above are apparently Group I kimberlites with predicted ϵ_{Sr} and ϵ_{Nd} close to bulk earth values. In contrast enriched Group II kimberlites with higher ϵ_{Sr} and lower ϵ_{Nd} values (Smith, 1983) appear to be deficient in metasomatized nodules (M. Skinner, pers. comm.) which is counterintuitive. Thus we have not recognized any primary phlogopite or amphibole in a large suite of peridotites from the Finsch pipe. However, several MARID samples are present in the Newlands Group II kimberlite, including the one described above with a PKP rind.

For present purposes the different styles of metasomatism can be simply assessed in two ways. First we consider critical element abundances in primary phlogopites, the metasomatic mineral common to all suites. As shown by several workers TiO_2 and Cr_2O_3 are useful in this respect and Fig. 4 indicates the distinction that can be made for Kimberley peridotite phlogopites of various kinds. Ranges (in wt. percent) in composition for primary phlogopites from various peridotite types at other localities are as follows: Jagersfontein (0.1-0.9 TiO_2 , 0.3-1.1 Cr_2O_3), Monastery (0.1-0.8 TiO_2 , 0.1-1.0 Cr_2O_3 , R.O. Moore, pers. comm.), Pipe 200 (0.2-0.5 TiO_2 , 0.9-1.1 Cr_2O_3), Newlands (0.2-1.7 TiO_2 , 0.3-1.0 Cr_2O_3), Premier (0.6-1.9 TiO_2 , 0.3-0.8 Cr_2O_3), Matsoku (1.5-1.6 TiO_2 , 0.5-0.8 Cr_2O_3 , B. Harte and J.J. Gurney, pers. comm.). In general there is overlap with primary peridotite phlogopites from Kimberley (Fig. 4) with nearly all samples having < 1.2 % Cr_2O_3 . In detail the Precambrian Premier and the Matsoku micas tend to have higher TiO_2 contents, however taken as a whole all these primary phlogopites are remarkably similar in bulk composition.

Consideration can next be given to silicate-incompatible trace elements by comparison of the mantle normalized diagrams shown in Figs. 3, 5 and 6. In a general sense the enrichment trends are similar, increasing in the sequence GP → GPP → PP and, where present, the PKP and GPAP suites. Furthermore the slopes of the trends are similar with least enrichment for Ti and maximum enrichment for Rb, Nb or K, and with enrichment factors of ~ 100X nominal mantle commonly being reached. In detail, although the enrichment trends for Kimberley and Premier are reasonably similar, they are somewhat different from those shown for Jagersfontein. In the latter the trends from Sr → K → Nb are generally smooth, while in the other two localities the most enriched samples show decreased abundances of Nb and Sr relative to K. Although the trends refer to average abundances, the differences arise from higher Nb contents (up to 53ppm) and lower Zr/Nb ratios (some < 1), and higher Sr abundances (up to 420ppm in PKP and 480ppm in GPAP nodules) in the Jagersfontein samples. Coupled with the apparent greater proportion of GPAP relative to PKP nodules, and with amphibole compositions generally having $Na_2O > K_2O$ (Field *et al.*, this volume) the above comments point to a greater diversity of mantle fluid compositions beneath Jagersfontein as compared with those beneath Kimberley, even though there are obvious similarities in metasomatic style for the respective metasomatic suites (e.g. PKP rocks, LIMA, rutile etc.).

Further work is required on nodules from other pipes (off-craton and on-craton, older and younger, Group I and Group II kimberlites) but the available evidence suggests a general similarity of metasomatic styles in terms of mantle space and time in sub-cratonic lithosphere beneath southern Africa.

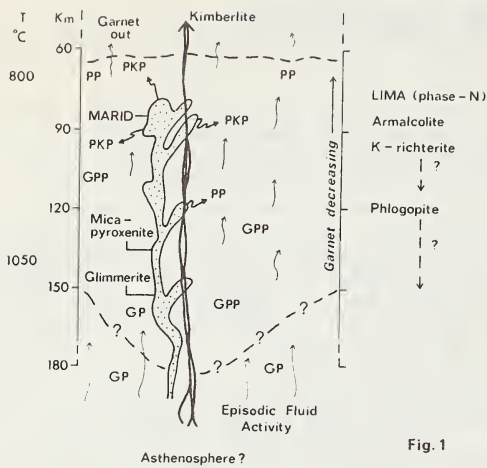


Fig. 1

Fig. 1. Scenario of recent MARID and metasomatic activity in old subcratonic lithosphere beneath Kimberley. Details from Erlank *et al.* (1986).

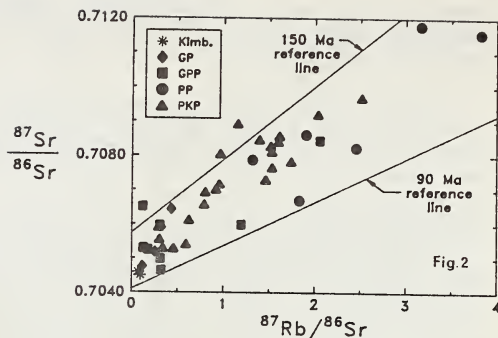
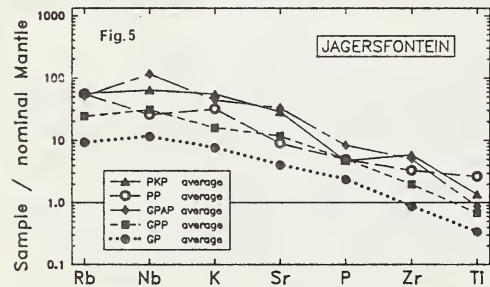
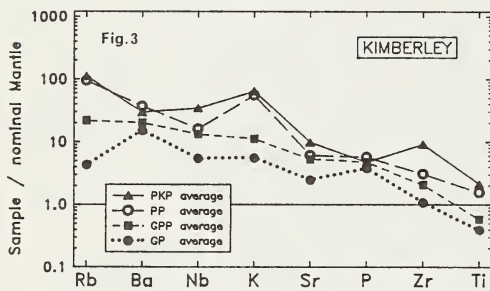


Fig. 2. Rb-Sr isochron diagram. Reference lines indicate recent metasomatic activity and do not necessarily imply any age significance.

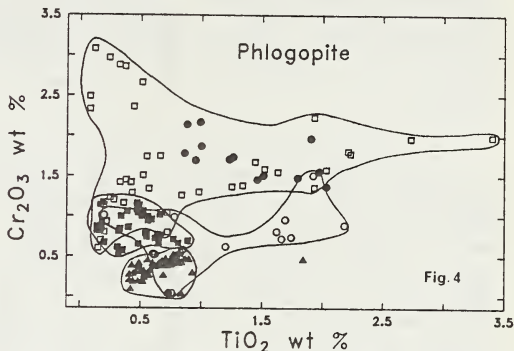
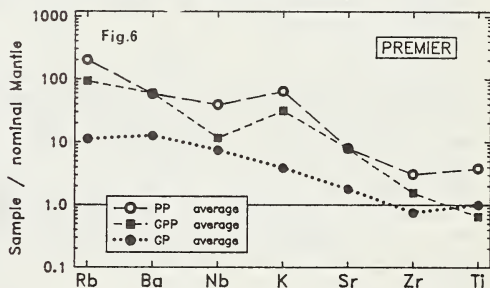


Fig. 4. Kimberley nodules: Closed triangles - PKP; open circles - PP; filled squares - primary GPP; open squares - secondary GPP; filled circles - secondary GP.



REFERENCES

Erlank, A.J., Waters, F.G., Hawkesworth, C.J., Haggerty, S.E., Allsopp, H.L., Rickard, R.S., and Menzies, M. 1986. Evidence for mantle metasomatism in peridotite nodules from the Kimberley pipes, South Africa. In M. Menzies and C.J. Hawkesworth (Eds.): *Mantle Metasomatism*, Academic Press, U.K., in press.

Haggerty, S.E., Smyth, J.R., Erlank, A.J., Rickard, R.S., and Danchin, R.V. 1983. Lindsleyite (Ba) and Mathiasite (K): two new chromium-titanates in the crichtonite series from the upper mantle. *Amer. Mineral.* 68, 494-505

Haggerty, S.E., Erlank, A.J., and Grey, I.E. 1986. Metasomatic mineral titanate complexing in the upper mantle. *Nature*, 319, 761-763.

Jianxiang, Z., Gujie, Y., and Jianhong, Z. 1984. Mathiasite in kimberlite of China. *Acta Mineral. Sinica*, 9, 193-200.

Richardson, S.H., Erlank, A.J., and Hart, S.R. 1985. Kimberlite-borne garnet peridotite xenoliths from old enriched subcontinental lithosphere. *Earth Planet Sci. Lett.* 75, 116-128.

Smith, C.B. 1983. Pb, Sr and Nd isotopic evidence for sources of southern Africa Cretaceous kimberlites. *Nature*, 304, 51-54.

Subcontinental lithospheric and asthenospheric metasomatism
in the region of Jagersfontein South Africa

Stephen W. Field, Stephen E. Haggerty, and *A.J. Erlank
Dept. of Geology, University of Massachusetts, Amherst, Mass., USA.
*Dept. of Geochemistry, University of Cape Town, Rondebosch, RSA.

The Cretaceous Jagersfontein kimberlite is located close to the edge of the Kaapvaal craton, displaced from the Kimberley cluster in the interior of the craton. Historically, the diatreme is of interest because it was at Jagersfontein that the association between diamonds and host rock was first established. Mineralogically, it is one of four localities at which high-pressure alkali titanates of the crichtonite series (lindsleyite-mathiasite) have been recognized along with Nb-Cr-rutile and armalcolite (Haggerty et al., 1983). In addition to the metasomatic oxides, metasomatic silicates, most notably amphiboles and phlogopites, have been identified in peridotite nodules recovered from the diatreme (Johnston, 1983; Harte and Gurney, 1980). The chemistries and textures of these silicates, major targets of this study, can be used to model metasomatic events in asthenospheric and lithospheric peridotites in the upper mantle beneath Jagersfontein. The position of this kimberlite with respect to the Kimberley cluster permits a comparison of metasomatism at the cratonic edge with interior-craton metasomatism. Jagersfontein is, therefore, a potentially important region for modelling the geometry of the subcontinental lithosphere.

Ultramafic xenoliths found at Jagersfontein include garnet lherzolites (ol+opx+gt+>5%cpx), garnet harzburgites (ol+opx+gt+<5%cpx), harzburgites (ol+opx±<5%cpx) and diopsidic-harzburgites (ol+opx+>5%cpx); the latter considered here to be refertilized harzburgites. Petrographic evidence and electron microbeam analyses suggest that the peridotites were subjected to at least two episodes of metasomatism, hereafter referred to as Stage A and Stage B metasomatism.

Phlogopites form two distinct textural and chemical populations (Table 1): large (1.5–2.5mm) grains many of which are intergrown with amphiboles, and fine-grained (<1mm) phlogopites usually found rimming or replacing other silicate minerals. The large phlogopites (Al₂O₃ 12.4–15.1 wt%, MgO 25.3–27.1 wt%, FeO 2.6–3.6 wt%) are considered to have formed during the Stage A metasomatic event along with amphibole. They contain lower Cr₂O₃ (0.3–1.1 wt%) and TiO₂ (0.1–0.9 wt%) (Fig.1) but higher BaO (0.3–3.4 wt%) than their fine-grained counterpart. Stage A metasomatic phlogopites are present in harzburgites and diopsidic-harzburgites but are rare in garnet lherzolites and garnet harzburgites. Fine grained Stage B metasomatic phlogopite is a constituent of most samples. The phlogopites are found in veins or rims, in association with fine-grained Cr-spinels and Cr-diopsides replacing opx, cpx, ol and amphibole. Barium contents are low in these grains (0–0.4 wt%), but TiO₂ (0.5–4.48 wt%) and Cr₂O₃ (0.9–2.2 wt%) are high (Fig.1), compared to stage A metasomatic phlogopites. A correlation is present between phlogopite composition and nodule type. Garnet lherzolite and garnet harzburgite Stage B phlogopites are generally richer in FeO (4.4–6.0 wt%) and lower in MgO (20–23 wt%) than Stage B metasomatic phlogopite (FeO 2.5–4.5 wt%, MgO 25.0–27.0 wt%) in harzburgites and diopsidic harzburgites. Phlogopites in garnet-bearing peridotites are also generally richer in Al₂O₃.

Cr-diopsides are commonly found as small grains with phlogopite replacing cpx, opx, or amphibole. These Cr-diopsides are considered to have formed during the Stage B metasomatic event. They are lower in Al₂O₃ and generally higher in FeO and TiO₂ content than the Cr-diopsides that comprise the original host rock mineralogy. Stage B metasomatic phlogopites are commonly accompanied by fine-grained, Al-rich, Cr-spinel.

Amphiboles are present in garnet lherzolites, garnet harzburgites, harzburgites, and diopsidic-harzburgites and are considered to have formed during the Stage A metasomatic event. They display both equilibrated and non-equilibrated textures. Grains in apparent disequilibrium with their host rock minerals contain inclusions of host rock minerals, usually cpx. Grain boundaries are irregular and diffuse. These amphiboles have varying mineral chemistries and exhibit weak zoning, especially in Cr₂O₃, around the inclusions. Texturally equilibrated amphiboles contain no fragments of other minerals, although they are frequently intergrown with garnet, pyroxene, Cr-spinel, or phlogopite. These amphiboles are chemically homogeneous.

Jagersfontein amphibole chemistries span a wide range of compositions. They are classified, according to Leake (1978), as pargasitic hornblende, edenitic hornblende, Mg-kataphorite, and richterite. Although there are four different classes of amphiboles, there are no distinct groups of amphibole types; the amphiboles define a complete spectrum of compositions that span the four amphibole classification fields. Amphiboles vary gradationally in SiO_2 , Al_2O_3 , Cr_2O_3 , MgO, FeO, and CaO. Silica varies inversely with Al_2O_3 (0.5–12.5 wt%) and a similar relationship exists between FeO (1.2–3.5 wt%) and MgO (19.0–24 wt%) (Fig.2). Aluminum and Cr_2O_3 (0.5–2.5 wt%) contents, however, vary in direct proportion (Fig.3). CaO contents, which range from 5.8–11.0 wt%, vary inversely with $\text{Na}_2\text{O} + \text{K}_2\text{O}$ (3.3–6.6 wt% + 1.0–5.0 wt%). Amphiboles like phlogopites show a correlation between nodule type and composition (Table 2). Garnet lherzolite and garnet harzburgite amphiboles are pargasitic hornblendes and edenitic hornblendes, whereas harzburgite and diopsidic-harzburgite contain Mg-kataphorites and richterites. The edenitic and pargasitic hornblendes are lower in silica (6.30–6.75 cations/23 oxygens) than Mg-kataphorites and K-richterites (6.90–7.85 cations/23 oxygens). Amphiboles in garnet-bearing rocks are mostly richer in FeO (2.0–3.5 wt%) and poorer in MgO (19.0–20.5 wt%) than the Mg-kataphorites and richterites (FeO 1.4–3.0 wt%, MgO 21.0–24.0 wt%). Harzburgite and diopsidic-harzburgite amphiboles contain less Cr_2O_3 (0.5–1.8 wt%) and Al_2O_3 (0.8–6.0 wt%) than garnet lherzolite and garnet harzburgite amphiboles (Cr_2O_3 2.0–2.5 wt%, Al_2O_3 9.0–12.5 wt%). The CaO content of garnet lherzolite and garnet harzburgite amphiboles ranges from 8.0 to 11.0 wt% whereas the CaO content of the harzburgite and diopsidic-harzburgite is usually less than 7.5 wt%. The $\text{CaO}/(\text{CaO} + \text{Na}_2\text{O} + \text{K}_2\text{O})$ ratio of edenitic and pargasitic amphiboles is always higher than that of harzburgite and diopsidic-harzburgite. In general, amphiboles in previously depleted peridotites are richer in SiO_2 , MgO, Na_2O , and K_2O . Amphiboles in the more fertile peridotites are enriched in Al_2O_3 , FeO, and CaO.

Metasomatic mineralogy at Jagersfontein is dominated by amphiboles and phlogopites. Both minerals show continuous trends in mineral chemistries that correlate with peridotite type. Amphibole and phlogopite compositions in part reflect the compositions of their host rock mineralogy. Variations in TiO_2 , BaO, and K_2O suggest variations in the composition of the metasomatizing fluids. The existence of amphibole in garnet lherzolite nodules suggests that at Jagersfontein, asthenospheric material is probably present above 120 km, the lowest reported stability limit for pargasite (Horiya et al., 1974). This is seemingly incompatible with the occurrence of diamonds which are believed to have formed in the lithosphere at depths greater than 150 km (Boyd and Gurney, 1986). Possible explanations for the presence of K-richterite bearing harzburgites, pargasite-edenite bearing garnet lherzolites, and diamonds include: (1) multiple paths of kimberlite intrusion, each bearing a distinct xenolith suite; (2) an irregular asthenospheric-lithospheric boundary; (3) remanent lenses or pockets of asthenospheric rocks within the lithosphere; or (4) diamond nucleation and growth over a limited P-T.

CONCLUSIONS Peridotites in the subcratonic lithosphere and asthenosphere beneath Jagersfontein have been modified by two metasomatic episodes. Stage A metasomatism produced amphiboles and phlogopites characterized by relatively low TiO_2 and Cr_2O_3 contents. Stage B metasomatism produced TiO_2 - and Cr_2O_3 -rich, fine-grained phlogopites, TiO_2 -poor Cr-diopsides, and Al_2O_3 -rich Cr-spinels. Amphibole and phlogopite chemistries span a broad range of compositions reflecting the compositions of the host rock minerals and the compositions of the metasomatizing fluids. The metasomatic mineralogy at Jagersfontein is similar to the metasomatic mineralogy at Bullfontein in the Kimberley district and possibly in other parts of the Kaapvaal craton.

REFERENCES

- Boyd, F.R., Gurney, J.J. 1986. Diamonds and the African Lithosphere. *Science*, 232, 472–477.
- Haggerty, S.E., Smyth, J.R., Erlank, A.J., Rickard, R.S., Danchin, R.V. 1983. Lindsleyite (Ba) and mathiasite (K): two new chromium-titanates in the crichtonite series from the upper mantle, *American Mineralogist*, 68, 494–505.
- Harte, B., Gurney, J.J. 1983. Compositional and textural features of peridotite nodules from the Jagersfontein kimberlite pipe, South Africa, *TERRA cognita*, 2, 256–257.
- Johnston, J. 1973. Petrology and geochemistry of ultramafic xenoliths from the Jagersfontein Mine, O.F.S., South Africa, Extended Abstracts, 1st International Kimberlite Conference,

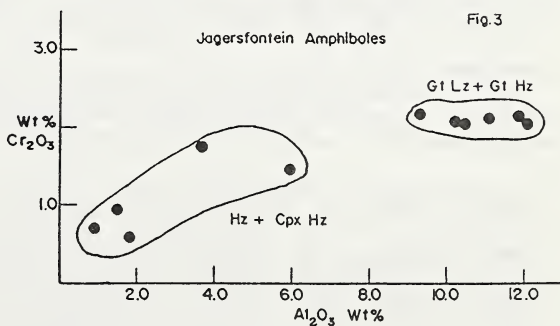
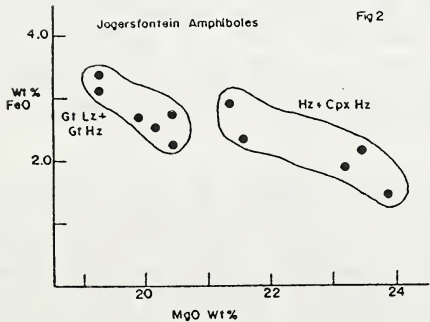
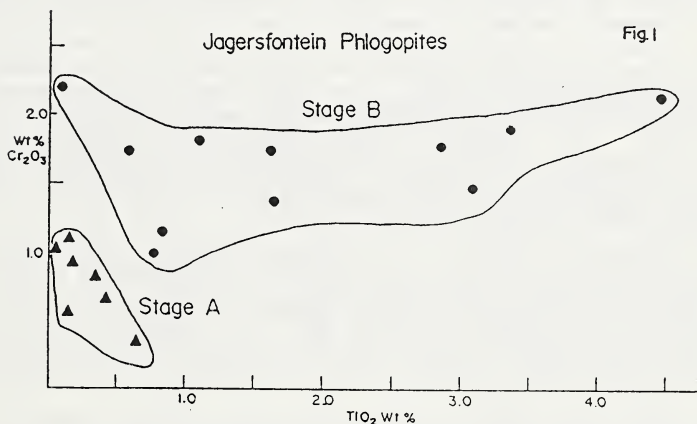
Hariya, Y., Oba, T., Terada, S. 1974, Stability relation of some hydro-silicate minerals at high pressure, Proceedings of the 4th International Conference on High-Pressure, 206-210.
 Leake, B.E. 1978. Nomenclature of Amphiboles, Mineralogical Magazine, 42, 533-563.

TABLE 1 PHLOGOPITE

WT. %	STAGE A		STAGE B	
	276	576	311	236
SiO ₂	40.85	39.97	40.38	39.65
TiO ₂	0.15	0.19	3.37	4.48
Al ₂ O ₃	13.75	15.14	14.78	14.56
Cr ₂ O ₃	0.51	0.92	1.87	2.12
FeO	2.85	3.06	4.26	5.76
MnO	0.03	0.03	0.04	0.07
MgO	27.11	25.40	21.63	20.08
NiO	0.19	0.16	0.19	0.14
CaO	0.00	0.00	0.02	0.03
BaO	1.41	1.93	0.12	0.11
Na ₂ O	1.01	1.02	0.31	0.21
K ₂ O	8.29	7.61	9.07	8.93
Total	96.15	95.43	96.04	96.14

TABLE 2 AMPHIBOLE

GT LZ	GT HZ	HZ	DI HZ
259	576	586	592
46.23	47.67	54.20	55.76
0.34	0.06	0.26	0.30
11.11	10.56	3.70	0.93
2.13	2.03	1.78	0.72
2.55	3.21	2.32	1.88
0.04	0.10	0.09	0.03
20.17	19.85	21.57	23.19
0.12	0.09	0.11	0.07
10.28	8.78	6.97	6.81
0.13	0.04	0.00	0.03
3.93	4.72	5.61	4.10
1.03	0.79	1.54	3.84
98.06	97.90	98.15	97.66



OLIVINE BAROMETRY IN THE SPINEL AND GARNET STABILITY FIELDS:
PRECISION, ACCURACY AND A BASIN AND RANGE (USA) GEOTHERM

Anthony A. Finnerty

Department of Geology, University of California
Davis, California, USA 95616

Experimental calibration of the solubility of Ca in olivine coexisting with ortho- and clinopyroxene revealed a pressure effect (Finnerty and Boyd, 1978) that is useful for barometry in the garnet (*ibid.*) and spinel (Finnerty and Rigden, 1981) stability fields. The pressure effect and the original calibration were quantitatively confirmed by run reversals (Adams and Bishop, 1982). The contribution of $\pm 10^\circ\text{C}$ imprecision in temperature estimation, attainable with thermometers based on the pyroxene miscibility gap (Finnerty and Boyd, 1984), to imprecision in the pressure estimate is ± 1.3 kbar. Calcium in olivine can be analyzed by electron microprobe with precision better than $\pm 5\%$ relative, contributing an additional ± 1.8 kbar to the imprecision of the pressure estimate (± 3.1 kbar total).

The accuracy of thermobarometers, obtained by combining the olivine barometer with a variety of thermometers, was tested by comparing P-T estimates for graphite- and diamond-bearing garnet lherzolite xenoliths from the northern Lesotho suite with stability fields of the two carbon polymorphs. Although the olivine barometer passes this accuracy test in combination with a variety of thermometers for the northern Lesotho suite (e.g. Fig. 1, Wells, 1977, thermometer vs. Finnerty and Rigden, 1981, barometer), it gives acceptable results only in combination with the Wells (1977) thermometer for spinel lherzolite xenoliths from alkali basalt at San Carlos, Arizona, USA. With the other thermometers tested, pressure estimates for some xenoliths are too low for spinel stability, or higher than the upper stability of the analyzed Cr-rich spinel (O'Neill, 1981). Even with the Wells thermometer, pressure estimates several kbar too high for spinel stability were obtained for some xenoliths from eastern China. The minerals in each xenolith are chemically homogeneous, indicating that disequilibrium is not the problem. The accuracy of the olivine barometer will most likely be improved by calibration experiments on compositions that more closely resemble those of the xenoliths.

Inflected geotherms observed for northern Lesotho and other kimberlite localities are not artifacts of the thermometer used (Finnerty and Boyd, 1984). The inflections cannot be artifacts of the barometer either because the inflections persist when the olivine barometer is used (Fig. 1). Although inflected geotherms probably do not characterize average upper mantle, they must be real and are most likely peculiar to sub-cratonic regions in which kimberlite liquid is being formed.

The spinel lherzolite xenolith suite from San Carlos basalt (erupted 5.3 ma ago, Holloway and Cross, 1978) yields a geotherm ranging from 940°C , 12 kbar (40 km) to 1070°C , 26 kbar (85 km), with a slope of $\sim 8^\circ\text{C}/\text{kbar}$ ($3^\circ\text{C}/\text{km}$, Fig. 2). This gradient is similar to the slope of the Ca isopleths for the olivine barometer, but extends over a range much greater than can be attributed to imprecision in P-T estimation, and thus the gradient is significant. The San Carlos locality is near the border between the Colorado Plateau and the Basin and Range province, a region of extension, high heat flow and thin lithosphere. The lower depth limit of the San Carlos geotherm coincides with the 45 km crustal thickness estimated for the Colorado Plateau using Rayleigh wave dispersion and seismic refraction (Keller et al., 1979), and thus it appears that peridotite wall rock was sampled by the ascending magma from depths of 85 km up to the crust-mantle boundary at 40-45 km.

A steep thermal gradient ($\sim 23^\circ\text{C}/\text{km}$) is required between the surface and the shallow depth limit of the San Carlos geotherm. Characteristic geotherms calculated for depths to 30 km, constrained by observed high heat flows and assumed conductive heat transport, from steady state thermomechanical models for the Basin and Range province (Lachenbruch and Sass, 1978) intersect the San Carlos geotherm at the lower pressure limit (Fig. 2, heavy solid lines). The combined geotherm is similar to that which would be expected for a conductive thermal boundary layer overlying a region characterized by heat transport by convection or diapiric uprise (e.g. Schubert,

1979; Oxburgh and Parmentier, 1978). The unusually low shear wave velocity (~4.5 km.sec, Keller et al., 1979) for this region is suggestive of the existence of a small proportion of melt in the uppermost mantle beneath the Basin and Range province, although there is no evidence for a melt phase in the ultramafic xenoliths.

The San Carlos geotherm, geophysical observations and heat flow models are consistent with a model in which a diapir or convective upwelling emplaces hot mantle material against lithospheric crust. Melting induced in the ascending mantle rock by decreasing pressure produces basaltic magma, which transports ultramafic xenoliths to the surface. The thermal gradient in the uppermost mantle is small because heat is transported by mass movement, but is very steep in the overlying conductive crust. Thermal expansion, perhaps coupled with a temperature-induced transition from brittle to ductile rheological behaviour and silicic magmatism in the crust (e.g. Eaton, 1982), causes crustal extension and thinning.

O'Reilly and Griffen (1985) obtained a geotherm for garnet websterite xenoliths from basalts in southeastern Australia. The geotherm is steeper than that for San Carlos (Fig. 2, heavy dashed line), and thus does not require an abrupt change in slope in order to project to a reasonable surface temperature. The authors interpret the Australian geotherm in terms of convective heat transport, related to lithospheric thinning and diking of the crust by magmas, and infer that the seismic Moho coincides with the phase transition from spinel lherzolite to garnet lherzolite. Apparently, very different processes have operated in the Basin and Range province than in southeastern Australia. Thermobarometry of spinel lherzolite xenoliths from southeastern Australia and from other localities within the Basin and Range province and the Colorado Plateau will be needed to confirm the differences between the two regions.

REFERENCES

- ADAMS, G.E. and BISHOP, F.C. 1982. Experimental investigation of Ca-Mg exchange between olivine, orthopyroxene, and clinopyroxene: potential for geobarometry. *Earth and Planetary Science Letters* 57, 241-250.
- EATON, G.P. 1982. The Basin and Range province: Origin and tectonic significance. *Annual Reviews of Earth and Planetary Science* 10, 409-440.
- FINNERTY, A.A. and BOYD, F.R. 1978. Pressure-dependent solubility of calcium in forsterite coexisting with diopside and enstatite. *Carnegie Institution of Washington Yearbook* 77, 713-717.
- FINNERTY, A.A. and BOYD, F.R. 1984. Evaluation of thermobarometers for garnet peridotites. *Geochimica et Cosmochimica Acta* 48, 15-27.
- FINNERTY, A.A. and RIGDEN, S.M. 1981. Olivine barometry: Application to pressure estimation for terrestrial and lunar rocks. *Lunar and Planetary Science* XII, 279-281.
- HOLLOWAY, J.R. and CROSS, C. 1978. The San Carlos alkaline rock association. *Geological Society of America Cordilleran Section Special Paper* No. 2. 171-173.
- KELLER, G.R., BRAILE, L.W. and SCHLUE, J.W. 1979. Regional crustal structure of the Rio Grande rift from surface wave dispersion measurements. In Riecker, R.E. Ed., *Rio Grande Rift: Tectonics and Magnetism*, pp. 115-126. American Geophysical Union, Washington, D.C.
- LACHENBRUCH, A.H. and SASS, J.H. 1978. Models of an extending lithosphere and heat flow in the Basin and Range province. *Geological Society of America Memoir* 152, 209-250.
- O'REILLY, S.Y. and GRIFFIN, W.L. 1985. A xenolith-derived geotherm for southeastern Australia and its geophysical implications. *Tectonophysics* 111, 41-63.
- O'NEILL, H. ST. C. 1981. The transition between spinel lherzolite and garnet lherzolite, and its use as a geobarometer. *Contributions to Mineralogy and Petrology* 77, 185-194.
- OXBURGH, E.R. and PARMENTIER, E.M. 1978. Thermal processes in the formation of continental lithosphere. *Philosophical Transactions of the Royal Society of London A*, 288, 415-429.
- SCHUBERT, G. 1979. Subsolidus convection in the mantles of terrestrial planets. *Annual Reviews of Earth and Planetary Physics* 7, 289-342.
- WELLS, P.R.A. 1977. Pyroxene thermometry in simple and complex systems. *Contributions to Mineralogy and Petrology* 62, 129-139.

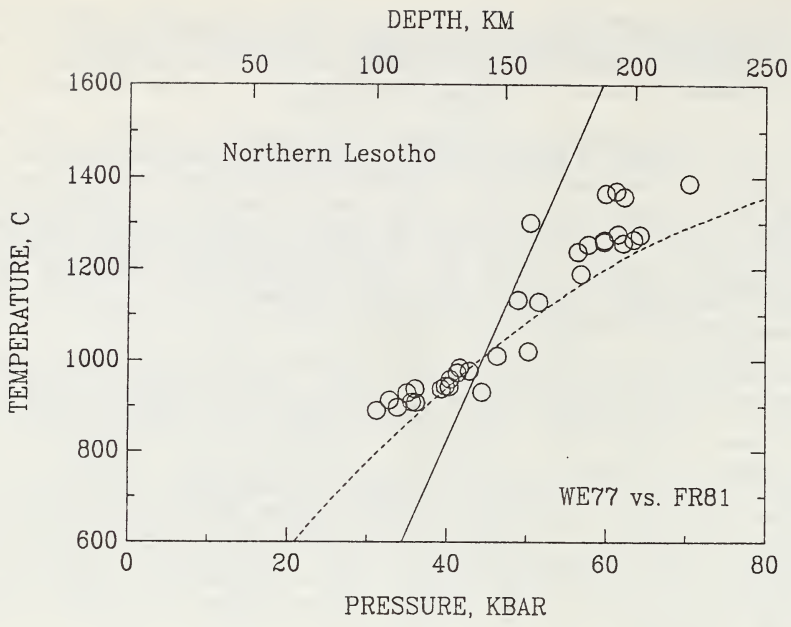


Fig. 1. Geotherm for garnet lherzolite xenoliths from northern Lesotho, southern Africa. Solid line represent the graphite to diamond transition. The dashed line is a calculated conductive geotherm for a cratonic setting.

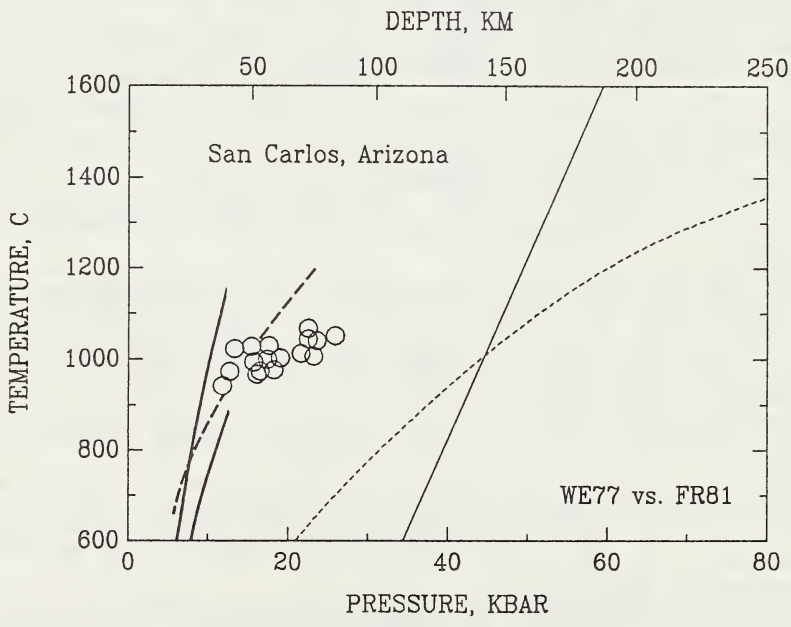


Fig. 2. Geotherm for spinel lherzolite xenoliths from San Carlos, Arizona. Heavy solid lines outline model conductive geotherms for average Basin and Range heat flows. Heavy dashed line represents garnet websterite geotherm for southeastern Australia.

M. O. Garcia and A. A. Presti

Hawaii Institute of Geophysics
University of Hawaii
Honolulu, Hawaii 96822

Both garnet-bearing and non-garnet-bearing pyroxenite xenoliths have been discovered from a new locality in the Hawaiian Islands, Kaula Island (Fig. 1). This tiny, 1 km long, remnant of a tuff cone is located 93 km SW of the island of Kauai (Fig. 2). It contains pyroxenite and ultramafic (spinel lherzolite and dunite) xenoliths in a palagonitized, nephelinite tuff. Xenoliths are abundant and fresh. Compared to the garnet pyroxenites from Salt Lake Crater, Oahu (Hawaii), the Kaula xenoliths are less mafic. They contain little or no olivine (<1 vol. %) and their clinopyroxenes (cpx) have lower Mg #s (72-83 vs. 79-89). Both Salt Lake Crater (Helz, 1979) and Kaula pyroxenites contain glass along fractures within and along the margins of cpx. The Kaula glasses are high Al_2O_3 basalts and are quartz to hypersthene normative (Table 1).

Unlike some glass-bearing mantle xenoliths (e.g. Comin-Chiaramonti et al., 1986), the glass compositions in the Kaula pyroxenites cannot be explained by decompressional melting of phases in the xenoliths. Intrusion of the host nephelinite or any combination of host nephelinite and xenolith phases are inadequate to explain the glass compositions. Mass balance calculations require a K-, P-rich component which is missing from the xenoliths.

Jones et al. (1983) suggested mantle metasomatism as a process to explain the composition of similar glasses from mantle xenoliths from Tanzania. In the absence of a suitable alternative model, mantle metasomatism seems the only plausible explanation for the high K and P contents of the Kaula glasses.

The introduction of the metasomatic fluid occurred prior to the incorporation of the xenolith into the host nephelinite, but after metamorphism of the xenolith. The presence of the glass along fractures within cpx suggests that it was related to or followed a deformational event. The most recent deformational event experienced by the mantle under Kaula Island may be its ascent over the Hawaiian arch. Clague (1986) proposed this process as a mechanism to produce Hawaiian post-erosional volcanism (of which the host nephelinite is an example). Thus, the metasomatism of the pyroxenite xenoliths may have occurred just prior to their incorporation in the host nephelinite.

References

- Clague D.A. 1986. Hawaiian alkaline volcanism. *Journal of Geological Society of London*, in press.
- Comin-Chiaramonti P., Demarchi G., Girardi V.A.V., Princivalle F. and Sinigoi, S. 1986. Evidence of mantle metasomatism and heterogeneity from peridotite inclusions of northeastern Brazil and Paraguay. *Earth and Planetary Science Letters* 77, 203-217.
- Helz R.T. 1979. Glass-bearing pyroxenites from Salt Lake Crater, Oahu. *Hawaii Symposium Abstracts Volume*, 87.
- Jones A.P., Smith J.V. and Dawson J.B. 1983. Glasses in mantle xenoliths from Olmani, Tanzania. *Journal of Geology* 91, 167-178.

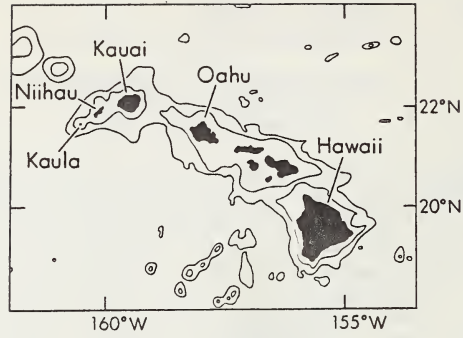


Fig. 1. Bathymetric map of the Hawaiian Islands and nearby seamounts with 1,000 and 2,000 fathom contours. Note oblique trend of Kaula, Niihau and Kauai (NE-SW) to the trend of the Hawaiian Islands (NW-SE).

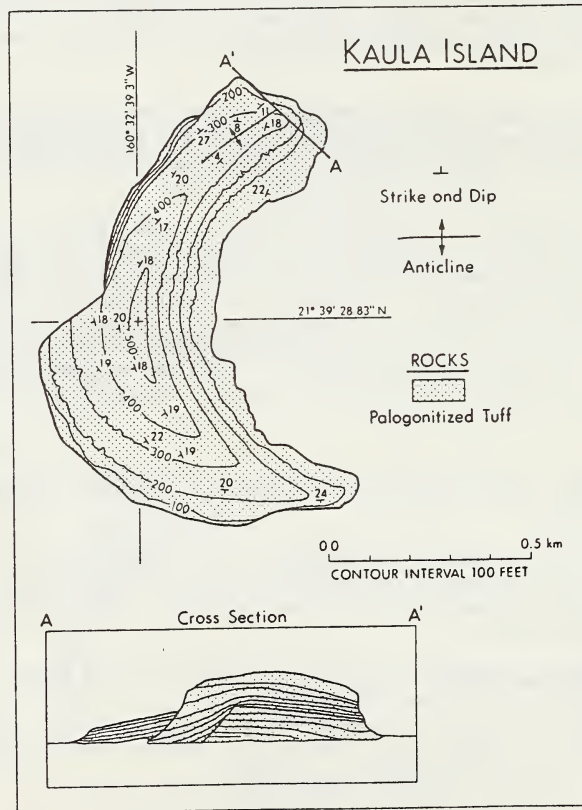


Fig. 2. Geologic map of Kaula Island. Topographic base map from Palmer (1936). Cross section shows depositional anticline exposed at the north end of Kaula Island. Kaula Island consists entirely of palagonitized tuff.

TABLE 1

	Classes		Host
	KA-110	KA-107	Nephelinite
SiO ₂	49.02	47.51	40.95
TiO ₂	0.47	1.06	2.83
Al ₂ O ₃	19.70	18.78	12.02
FeO	10.28	12.17	12.78
MnO	0.30	0.29	0.23
MgO	5.27	6.24	12.82
CaO	12.22	11.22	10.84
Na ₂ O	1.14	1.46	3.76
K ₂ O	0.44	0.74	1.23
P ₂ O ₅	0.34	0.24	0.86
Total	99.18	99.71	98.32
Q	3.1	0.0	-
Or	2.6	4.4	2.8
Ab	9.7	12.4	-
An	47.7	42.7	12.5
Lc	0.0	0.0	3.6
Ne	0.0	0.0	17.5
Di	9.3	9.7	29.5
Hy	12.9	11.2	-
Ol	0.0	4.3	24.2
Mt	2.0	2.3	2.5
Il	0.9	2.0	5.5
Ap	0.8	0.6	2.0
Mg# ¹	47.7	47.8	67.0

¹Based on $\text{Fe}_2\text{O}_3/\text{FeO} = 0.15$

THE PRESSURE DEPENDENCE OF CREEP IN OLIVINE:
CONSEQUENCES FOR MANTLE FLOW

H. W. Green*, R. S. Borch* and B. E. Hobbs†

*University of California, Davis CA 95616 USA

†Division of Geomechanics, CSIRO, Melbourne, AUSTRALIA

Olivine is the most abundant and weakest phase in the uppermost mantle, hence its flow properties control the rheology of the region. While the flow properties of olivine have been studied extensively, previous experiments have been restricted to pressures below 1.6 GPa. Creep of olivine, like most materials at high temperature, is well-described by the power-law creep equation,

$$\dot{\epsilon} = A \sigma^n \exp(-\Delta G^*/RT), \quad (1)$$

where $\dot{\epsilon}$ is the strain-rate, A is a constant, σ is the applied stress, n is a constant usually between 3 and 4, ΔG^* is the activation free energy, R is the gas constant and T is the absolute temperature.

The pressure dependence of creep is presumed to be reflected in the activation volume, ΔV^* , where $\Delta G^* = \Delta E^* + P\Delta V^* - T\Delta S^*$. Extrapolations of the low-pressure data to mantle conditions, when attempted, have generally relied on the assumption that the rate-controlling step in the deformation process is diffusion of oxygen, leading to an estimation that the pressure-dependence of creep is small ($\Delta V^* \sim 10 \text{ cm}^3/\text{mole}$).

We have determined the pressure dependence of steady-state creep of an anhydrous synthetic harzburgite over the pressure range 1-3 GPa in a modified Griggs apparatus using a new liquid cell that greatly reduces uncertainties in friction. We find a strong pressure dependence of the flow stress (Fig. 1), corresponding to an apparent ΔV^* of $25 \text{ cm}^3/\text{mole}$. However, direct determination of ΔH^* as a function of pressure shows that ΔH^* decreases strongly with pressure, hence the pressure-dependence of our data cannot be interpreted in terms of ΔV^* . The positive pressure-dependence of the flow stress, therefore, is a consequence of the stronger decrease in ΔS^* .

PRESSURE DEPENDENCE OF FLOW STRESS

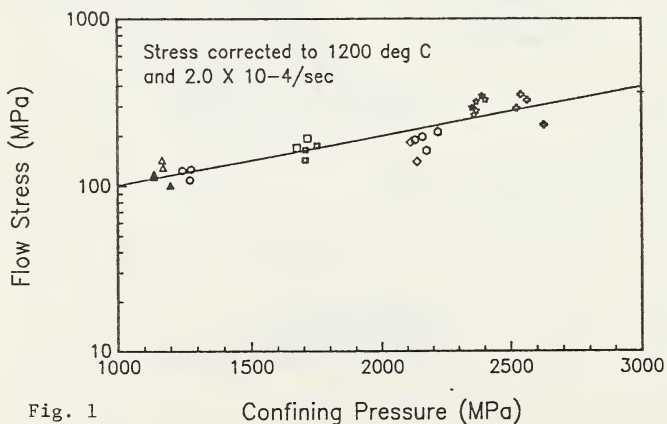


Fig. 1

Confining Pressure (MPa)

Previously, a number of workers have suggested that diffusion kinetics and rheology should scale with the homologous temperature, T/T_m , where T_m is the temperature of melting, or the solidus for solid solutions (c.f. Sammis et al, 1981). Predictive equations from these theories fail to describe our data. We have developed, however, a generalized theory that recaptures both our data and those from simple

systems. Our derivation shows that the pressure dependence of creep precisely follows the pressure dependence of melting. That is, at constant T/T_m , the creep strength is independent of pressure. The line in Fig. 1 is calculated from this relationship using only the data at 1.2GPa.

This discovery provides for the first time a reliable method for extrapolation to mantle conditions. To calculate the strain-rate for a given stress at depth, one needs only the solidus, the geotherm and rheological data at one pressure. The only modification of (1) that is necessary is substitution of the "equivalent temperature", T_{eq} , where

$$T_{eq} = \left(\frac{P}{T_m} \right)^o T_m \quad (2)$$

The superscripts p and o denote, respectively, the pressure of interest and the pressure at which the temperature dependence of creep has been determined. ΔH^* in (1) similarly becomes $^o\Delta H^*$.

Our extrapolation procedure predicts that reduction of the solidus due to trace quantities of volatiles should be reflected in a similar reduction in the strength of the solid. The predicted water-weakening for olivine is comparable to that observed by Chopra and Paterson (1984), and the predicted CO_2 -induced weakening at pressures above 2.8GPa has been confirmed in our laboratory.

Extrapolation of our experimental results to the base of the olivine-bearing mantle using the dry peridotite solidus of Herzberg (1983) and various published suboceanic geotherms, produces an approximately isoviscous mantle between 200 and 400km depth. Our preferred geotherm has, at shallow depths, a slope appropriate for "average" suboceanic mantle and is tied to the olivine-spinel transition at 1725K, 1.3GPa (Lees, et. al., 1983). This geotherm yields at 200-400km, for a stress of 0.1MPa, an effective viscosity of 10^{21} Pa sec and for a stress of 1.0MPa, yields 10^{18} Pa sec (Fig. 2). Of particular interest is the lack of any low-viscosity channel beneath the lithosphere. Similar calculations for H_2O -bearing and CO_2 -bearing mantles yield effective viscosities two to four orders of magnitude lower.

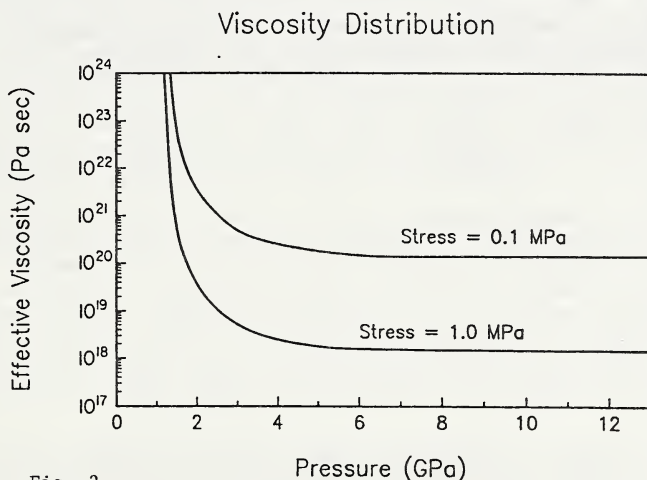


Fig. 2

The ubiquitous association of CO_2 emanations with volcanism (Barnes et al., 1978), the presence of CO_2 -filled fluid inclusions in mantle xenoliths (Roedder, 1965) and the presence of exsolved fluid bubbles in mantle olivine (Green and Gueguen, 1983) indicate that at least those regions of the upper mantle associated with volcanic eruptions should reflect the weakening implied by the CO_2 -related solidus reduction. It is

possible, therefore, that the asthenosphere may be weakened by introduction of carbon. Since our results indicate that carbon distributed throughout the upper mantle would result in a viscosity too low to be compatible with a variety of observations, we suggest that the carbon may be transported directly from the deep mantle or core-mantle boundary in narrow plumes of the sort envisioned by Morgan (1971) and Loper (1985), among others. Previous plume models are initiated by thermal instabilities produced by cooling of the outer core. However, our results imply that exsolution of carbon from the core and dissolution into the silicates also could produce reduction in viscosity and probably an increase in buoyancy.

REFERENCES

- BARNES, I., IRWIN, W.P. and WHITE, D.E. 1978. Global distribution of carbon dioxide discharges and major zones of seismicity. *U. S. Geol. Surv. Water Resour. Invest., Open-file Rep.* 78-39.
- GREEN, H.W. and GUEGUEN, Y. 1983. Deformation of peridotite in the mantle and extraction by kimberlite: A case history documented by fluid and solid precipitates in olivine. *Tectonophysics* 92, 71-92.
- HERZBERG, C.T. 1983. Solidus and liquidus temperatures and mineralogies for anhydrous garnet-lherzolites to 15 GPa. *Phys. Earth Plan. Int.*, 32, 193-202.
- LEES, A.C., BUKOWINSKI, M.S.T. and JEANLOZ, R. 1983. Reflection properties of phase transition and compositional change models of the 670-km discontinuity. *J. Geophys. Res.*, 88, 8145-8159.
- LOPER, D.E. 1985. A simple model of whole-mantle convection. *J. Geophys. Res.*, 90, 1809-1836.
- MORGAN, W.J. 1971. Convective plumes in the lower mantle, *Nature*, 230, 42-43.
- ROEDDER, E. 1965. Liquid CO₂ inclusions in olivine-bearing nodules and phenocrysts from basalts. *Am. Mineral.* 50, 1746-1782.
- SAMMIS, C.G., SMITH, J.C. and SCHUBERT, G. 1981. A critical assessment of estimation methods for activation volume, *J. Geophys. Res.*, 86, 10707-10718.

¹W.L. Griffin and ²Suzanne Y. O'Reilly

¹Geologisk Museum, Sars' gate 1, N-0562 Oslo 5, Norway
²School of Earth Sciences, Macquarie University,
North Ryde, N.S.W. 2113 Australia

Most Cr-diopside spinel lherzolite xenoliths from Bullenmerri and Gnotuk maars, western Victoria, show modal metasomatism, involving introduction of amphibole \pm mica \pm apatite(Cl-CO₂) at the expense of pyroxenes + spinel (Griffin et al. 1984). The microstructural situation of the volatile-bearing phases ranges from obvious replacement rims on spinel, to apparent equilibrium mosaics with olivine + clinopyroxene + orthopyroxene \pm spinel. Similar effects are common in lherzolites from other Victorian localities. The metasomatism is attributed to infiltration of CO₂-rich fluids, which are observed in fluid inclusions (Andersen et al. 1985). Most of the fluid was probably introduced during the intrusion and crystallization of basaltic magmas, now represented by veins of pyroxenite.

Major element compositions of the lherzolites are little affected by the metasomatism, except for the introduction of Fe. Mg/(Mg+Fe) drops markedly (from >90 to <80) while Cr/(Cr+Al) is unaffected; these two "indices of refractoriness" are therefore not correlated, and neither is clearly related to a partial melting event. Na, Ca, Cr and Al contents are essentially controlled by premetasomatic pyroxene/olivine/spinel ratios; Ca may have been introduced in some apatite-rich (ca. 5%) lherzolites.

REE patterns of anhydrous lherzolites range from LREE-depleted ((La/Yb)_N = 0.4) to LREE-enriched ((La/Yb)_N = 30), all at low EREE. These rocks show an inverse correlation of (Nd/Sm) with CaO, and separated clinopyroxenes show a correlation of (Nd/Sm)_N with Nd. This can be modelled as uptake by clinopyroxene of the REE from an infiltrating fluid with (La/Yb)_N > 50. The clinopyroxene-rich rocks are thus less "contaminated" with the LREE-enriched component. Amphibole-rich peridotites are enriched in REE (with (La/Yb)_N = 10), Zr and Ta, with high K/Rb. Mica-rich rocks are enriched in K, Rb, Ba, Ta and Ti, with low K/Rb. Introduction of apatite leads to high EREE (with (La/Yb)_N = 30-50), Sr, U and Th contents. The distribution of trace elements in the peridotites is thus controlled by the crystal chemistry of the metasomatic phases (Fig. 1). The variable distribution of these phases in space and time results in a decoupling of major, minor and trace elements during metasomatism, related mainly to crystal/fluid partitioning. Models involving a "KREEP" or "infiltrating melt" component are clearly oversimplified.

Examination of >2000 lherzolite xenoliths from Bullenmerri and Gnotuk shows that amphibole lherzolite is the most common type; micaceous ones are least common, and "dry" ones are rare. This may reflect their distribution in the mantle, with micaceous selvages on abundant metasomatic veins and pyroxenite dikes, and small relict volumes of "dry" lherzolites, showing various degrees of cryptic metasomatism, within a "matrix" of amphibole lherzolite. The sporadic distribution of apatite in these rock types, and in clinopyroxene+apatite veins, suggests that the introduction of apatite may be independent of the formation of mica and amphibole.

The overall pattern of trace element enrichment in Victorian lherzolites (Fig. 2) reflects the volumetric distribution of the different types of metasomatism. Ni, Cr, V, Sc, Y and Na values are similar to those in depleted mantle xenoliths and the source regions of N-type MORB. Median concentrations of Ba, Th, U, Ta, Nb and LREE range from 2-10x primordial values. The low median values of K and Ti reflect "dumping" of these components in micaceous rocks of limited volumetric abundance. The resulting mantle signature resembles that of calculated source regions for intraplate undersaturated magmas like the Honolulu Series. Similar patterns are seen in other continental and oceanic suites of metasomatized mantle xenoliths

(Dreiser Weiher, Zabargad,, St. Paul's Rocks, Nunivak Is.) where data bases are large enough.

Abundant xenoliths of garnet- and spinel-pyroxenites are products of an older magmatic episode; igneous-textured wehrlite series xenoliths represent a younger (recent?) episode. Both types have metasomatically modified their wall rocks (Griffin et al. 1984; Irving 1980).

The Sr-Nd isotopic compositions of the lherzolites (Fig. 3) spread into the "enriched mantle" field. T_{DM} model ages cluster at 600 ± 120 Ma. At 700 Ma $>1/3$ of the lherzolites have $\epsilon Nd > Dm$; this represents a maximum age for the LREE-enrichment "event". Several of the garnet- and spinel pyroxenites have $\epsilon Sr \approx 150$ and $\epsilon Nd \approx -9$; the rest scatter toward the field occupied by the lherzolites (Fig. 4). This is interpreted as the effect of wall-rock reaction, leading to isotopic equilibration between the small dikes of pyroxenite and the surrounding reservoir of lherzolite. At 300-500 Ma the pyroxenites define a good mixing hyperbola with the lherzolites, most of which have $\epsilon Sr > 0$ at this time (Fig. 4).

Plots of $^{143}Nd/^{144}Nd$ vs. Nd and $^{87}Sr/^{86}Sr$ vs. Sr support this mixing model, and define a second trend for the apatite-bearing lherzolites. The apatite component has a present-day ϵSr and $\epsilon Nd \approx 0$. The isotopic systematics of the lherzolites and pyroxenites suggest at least three "events": (1) intrusion of basaltic magmas 300-500 Ma ago, leading to cryptic and patent metasomatism of the lherzolite wall rocks, and changing their isotopic compositions as well as Rb/Sr and Sm/Nd ratios; (2) introduction of the apatite component with "bulk-earth" isotopic ratios; (3) intrusion of basaltic magmas (parental to the wehrlite series) with $\epsilon Sr = -10$, $\epsilon Nd = 2-5$, leading to some of the scatter around the mixing line resulting from (1) and (2).

The least-modified magmas of (1) have very unradiogenic Nd and unsupported radiogenic Sr. They thus contain a large component from an older, undepleted reservoir. This may be either a deeper primitive mantle, or recycled crustal material. The relatively radiogenic Sr of the lherzolites suggests a similar effect. We suggest that the pyroxenite-forming magmas and their associated fluids may have been derived from the material of a subduction zone during the Paleozoic crustal-accretion event in this region. The apatite component (2) may have a similar origin, but cannot be clearly explained with the present data. Event (3) is probably sub-recent, related to the same general episode of basanitic magmatism which resulted in the Newer Volcanics.

The major metasomatic effects observed in lherzolite xenoliths from Victoria may thus reflect modification of a mantle wedge by fluids (largely sea water?) and melts derived from a subducted plate. Fragments of such a plate may be represented by some compositionally and isotopically unusual xenoliths, such as those found at Delegate.

REFERENCES

- ANDERSEN, T., O'REILLY, S.Y. and GRIFFIN, W.L. 1984. The trapped fluid phase in upper mantle xenoliths from Victoria, Australia: implications for mantle metasomatism. Contributions to Mineralogy and Petrology 88, 72-85.
- GRIFFIN, W.L., WASS, S.Y. and HOLLIS, J.D. 1984. Ultramafic xenoliths from Bullenmerri and Gnotuk maars, Victoria, Australia: petrology of a sub-continental crust-mantle transition. Journal of Petrology 25, 53-87.
- IRVING, A.J. 1980. Petrology and geochemistry of composite ultramafic xenoliths in alkalic basalts and implications for magmatic processes within the mantle. American Journal of Science 280A, 389-246.

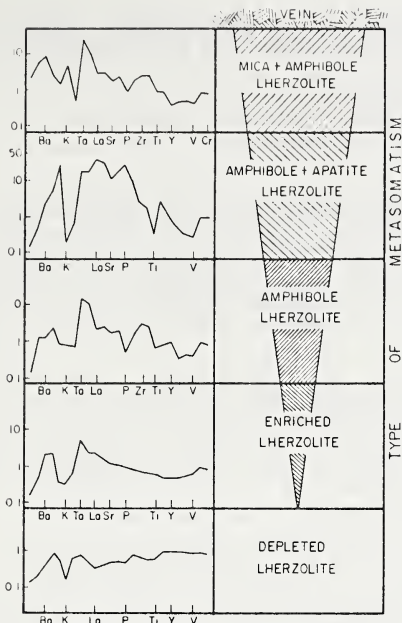


Fig. 1. Correlation of key minor and trace element abundances (normalised to primordial mantle) with type of metasomatism.

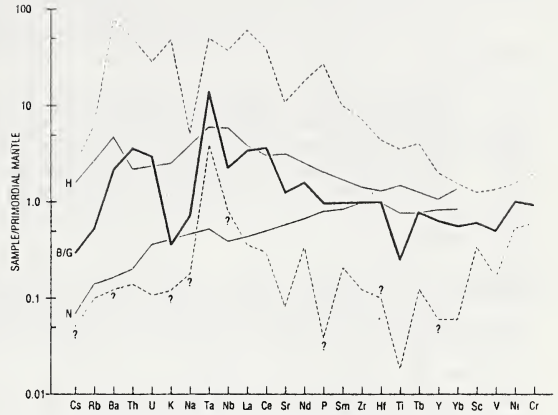


Fig. 2. Dark line: median of minor/trace element abundances in Victorian lherzolites. Stippled field covers range of analyses (n=12-65). H: calculated source region for Honolulu Series magmas. N: calculated source region for N-type MORB.

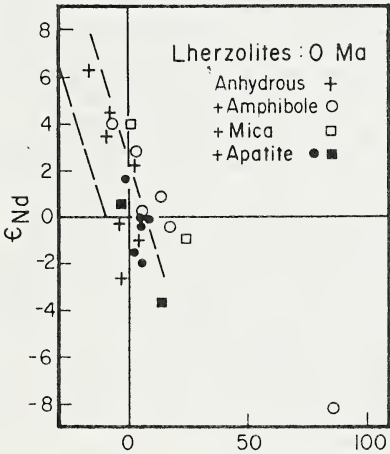


Fig. 3. Sr/Nd isotopic compositions of lherzolites from Bullenmerri/Gnotuk.

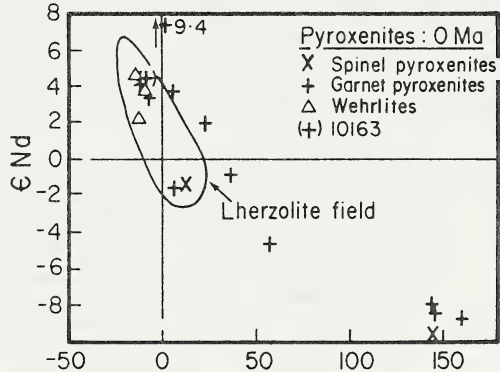


Fig. 4. Sr/Nd isotopic compositions of spinel- and garnet pyroxenite xenoliths from Bullenmerri/Gnotuk. Lherzolite field encloses main cluster of lherzolite values.

Source regions for oxides, sulfides and metals in the upper mantle: Clues to the stability of diamonds, and the origin of kimberlites and lamproites.

Stephen E. Haggerty

Dept. of Geology, University of Massachusetts, Amherst, Mass. USA
4th International Kimberlite Conference.

Although oxides, sulfides and metals are minor components in the upper mantle, these mineral groups provide information on redox conditions, mineral complexing and compositions of metasomatic fluids, liquid immiscibility and diamond genesis, and serve as prospecting and evaluation guides to diamond resource potential. New mineral data from kimberlites, lamproites, metasomatized harzburgites, carbonatites, melilitites, and discrete nodules has broadened the scope for genetic models of these rock types.

Oxides: Lithosphere-derived ultramafic diamonds contain magnesiochromite ($\text{Cr}_2\text{O}_3 > 60 \text{ wt}\%$) with estimated P-40-50 Kb and T-1100-1400°C. Similar compositions are now shown to be present in depleted spinel harzburgites from kimberlites. Metasomatism of these spinels yields a new mineral with a magnetoplumbite ($\text{AM}_{12}\text{O}_{10}$) structure, followed by lindsleyite ($\text{AM}_{21}\text{O}_{38}$), where A = large cations Ba, Ca, Sr, K, Na, and M = small cations, Fe, Ti, Cr, Mg, Zr, REE, in association with Ca-Cr-Zr armalcolite at estimated P-20-25 kb and T-900-1100°C. Priderite and jeppeite are the Cr-depleted, low pressure analogues in lamproites. These minerals imply a continuum between kimberlites and lamproites, differing only in the degree of metasomatic assimilation. Low pressure, high T melt-derived spinels in kimberlites and lamproites are members of the Mg-titanomagnetite series, nucleated on Mg-Al-Cr spinels, underscoring a genetic relationship. Spinels in carbonatites and carbonated kimberlites have higher magnetite components and are, therefore, more oxidized. Wüstite is present as a diamond inclusion and in some kimberlite dikes and sills indicative of low redox conditions. From a global compilation of upper mantle-derived ilmenites (Fig. 1) it is concluded: that ilmenites having $\leq 10 \text{ wt}\%$ MgO and $\leq 0.5 \text{ wt}\%$ Cr_2O_3 are either of low P origin or are derived from the asthenosphere; correspondingly higher values are of lithosphere origin; carbonated ilmenites have high MnO ($\geq 5 \text{ wt}\%$) contents; and lamproites are depleted in ilmenite because of the high alkali affinity for Ti, hence priderite, jeppeite, Ti-phlogopite and titanianrichterite. Rutiles in eclogites and diamond inclusions are close to end-member compositions, whereas metasomatic rutiles and rutiles in MARID suite nodules are typically Nb_2O_5 ($> 2 \text{ wt}\%$), and Cr_2O_3 ($> 2 \text{ wt}\%$) enriched. High Ti contents and large concentrations of silicate-incompatible elements are, therefore, characteristic of metasomatic fluids; high Cr values derive from depleted lithosphere. A single ovoid grain (3 x 2 mm) from heavy mineral concentrates of the Argyle olivine lamproite is an unusual K-Cr-priderite. The grain has an inclusion of Cr-armalcolite, minor Mn-ilmenite along cracks and MnCrMg spinel along grain boundaries in association with talc, phlogopite and titanite (sphene). This priderite is similar in composition to one of two unidentified minerals described as an alteration fringe to microilmenite in a metasomite from Bultfontein. Mineral compositions similar to mannardite-redledgeite series minerals, $(\text{Ba.OH})\text{Ti}_6\text{V}_2\text{O}_{16}$ - $(\text{Ba.OH})\text{Ti}_6\text{Cr}_2\text{O}_{16}$ are recorded for discrete opaque crystals present in an ultramafic clast from an autobrecciated olivine lamproite at Argyle. Dolomite is an associated mineral and both are enclosed in talc, probably after xenocrystic olivine. Analytical data for an unidentified mineral from the Benfontein kimberlite-carbonate sills is similar in large cation Ba concentrations but Fe^{3+} is the dominant small cation replacing Cr and V in the inferred mannardite-redledgeite series. The relationship between BaO and TiO_2 for a variety of LIL-titanates show that two distinct groupings are present, both having negative slopes (Fig. 2). LIMA minerals, K-Cr-priderite from Bultfontein and Argyle, and the possible mannardite-redledgeite minerals from Argyle (dolomite association) and Benfontein (calcite and baddeleyite associated), are Cr + LREE-bearing and form one group. The second mineral grouping is composed of a variety of priderites and these are demonstrably melt-derived. It is tentatively concluded that the K-Ba-titanate field, in which LIMA is present, is typical of metasomatic association.

Sulfides: Low temperature equilibrated assemblages in diamonds, eclogites, and in discrete nodules of olivine, garnet, pyroxene, ilmenite and ilmenite-pyroxene intergrowths, are troilite, pyrrhotite, pyrite, pentlandite and chalcopyrite, with accessory polydymite and hazelwoodite. Bulk compositions conform to monosulfide solid solutions and liquid immiscibility (900-1100°C) is inevitable at upper mantle P-T conditions; carbon solubility may be enhanced and carbon reduction catalytically accelerated, thus accounting for the abundance of sulfides in diamonds. A new sulfide signature is apparent based on Fe/Fe+Ni ratios: eclogitic suite diamonds have the highest values (0.88-0.99), discrete nodules are intermediate (0.77-0.82), and depleted ultramafic diamonds are the lowest (0.59-0.64). Discrete nodules are geochemically fertile and intermediate Fe:Ni ratios are, therefore, asthenospheric. Complex alkali phyllosulfides, in association with pyrrhotite, are present in metasomites, indicating that the fluids were sulfur bearing.

Metals: Increasing recognition of Fe metal in diamonds supports the proposition for growth in a highly reduced lower lithospheric environment. Metallic Fe from the lower crust implies that the upper lithosphere is also highly reduced. However, metasomatism at 75-100 km, and the source regions inferred for carbonatites (~50-70 km) are more oxidizing, suggesting that the lithosphere has an alternating redox potential, more complex than previously modelled.

It is concluded that a genetic relationship exists between kimberlites and lamproites, and between kimberlites and carbonatites; metasomatism is the critical keystone. Oxide, sulfide and metal mineralogies are a reflection of rock types and processes in the upper mantle. Compositional signatures are specific and a more accurate definition of sub-cratonic environments is becoming possible. Opaque mineral stratigraphy for the upper mantle (Fig. 3) establishes the inferred presence of two metasomatic horizons: a phlogopite, K-richterite peridotite (PKP) metasome; and a phlogopite, amphibole, carbonate, zircon metasome. Experimental mineral equilibria place the zones at depths of ~ 60-100 km. Metasomatism is induced from melt stagnation in cool lithosphere and volatile liberation following thermal trauma of asthenospheric proto-melts. Maximum intensities of metasomatism, and development of metasomes, arises at ~ 100 km depth because this lithospheric region is coincident with the thermal blip in the C-O-H peridotite solidus. Rapidly ascending proto-melts from the asthenosphere, intersect the metasomes (which are hydrous and carbonated minimum melts) and lateral flash melting results (Fig. 4). Kinetic energy for alkali explosive volcanism, and the acquisition of silicate incompatible element signatures and high redox states, results directly from metasome assimilation. Geophysical implications for metasomes relate to the seismic low velocity zone and to electrical conductivity anomalies in the upper mantle (Fig. 4). These properties may not be due to partial melting but to attenuations caused by hydrous and carbonated mineralogies.

Evidence for metasomatism in the Kaapvaal craton of southern Africa is unequivocal. The presence of LIMA and magnetoplumbite minerals in China and Africa suggests a comparable metasomatic style, and preliminary data for an equally exotic array of LiL-titanates in olivine lamproites from NW Australia, in association with Ti-phlogopite and K-Ti richterite as essential components, logically implies that all three provinces have undergone similar upper mantle processes of metasomatism. Lamproites are an ultrametasomatic progression from metasomatic kimberlites. Thermal crisis of proto-melts ascending from the asthenosphere into old and cooler lithosphere assures that subcratonic metasomatism is the rule rather than the exception.

UPPER MANTLE SOURCE REGIONS - OPAQUE MINERALS

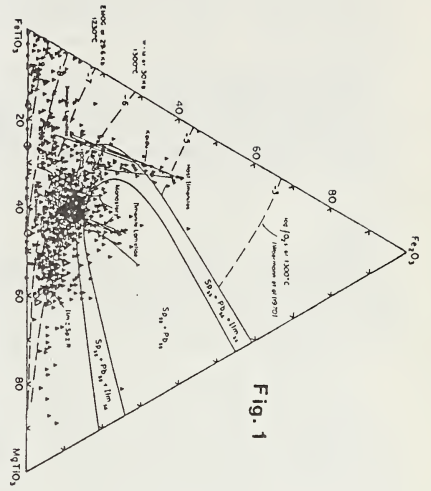


Fig. 1

Km	ROCK TYPES	SPINEL	ILMENITE	RUTILE	TITANATES	METALS & SULFIDES	
						Per, Pel	Mss > Fe-Ni
0-50	Kimb, Lamp Corb	Zoned to Fa ³⁺ +Ti	Mg ²⁺ > Mn	Decomp	Per, Pel	Mss > Fe-Ni	
50-100	MARID + Z + Cc Mesosome		>Mg < Cr	>Nb	Llb LIMA <Cr	Mss > Fe-Ni K-Sulf	
100-150	Hz + Dun	>Cr+Ti	>Mg+Cr	>Nb+Cr	LMA, Y, H Arm K-Cr-Prd	Mss > Fe-Ni K-Sulf	
150-200	Lith Diamond Asth	Vorible	>Mg+Cr	Absent	Fe ⁰ Absent Rare Sulf	Fe ⁰ Absent Rare Sulf	
200-300	Fertile GI LZ	Rare	>Mg+Cr	Absent	Fe ⁰ Absent Rare Sulf	Fe ⁰ Absent Rare Sulf	

Fig. 3

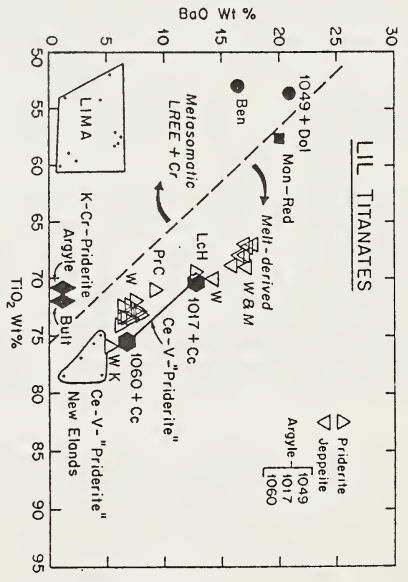


Fig. 2

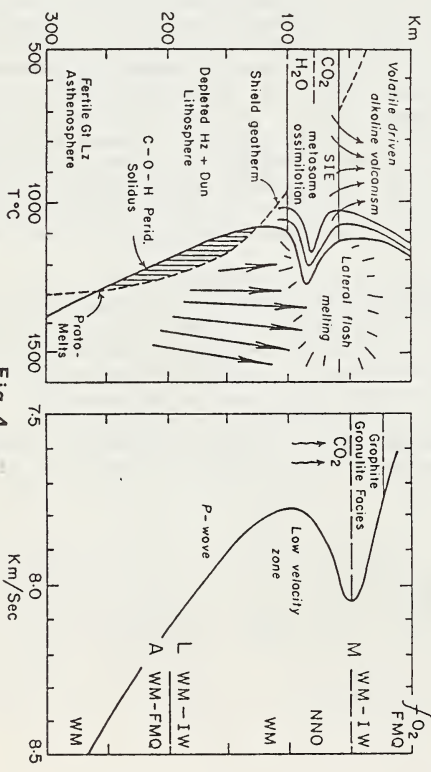


Fig. 4

CRUSTAL XENOLITHS FROM SOUTHERN AFRICA: CHEMICAL AND AGE VARIATIONS
WITHIN THE CONTINENTAL CRUST

C.J. Hawkesworth, P. van Calsteren, Z. Palacz, N.W. Rogers

Department of Earth Sciences, The Open University, Milton Keynes
MK7 6AA, England

The nature of the lower crust may be inferred from its physical properties, but it may only be sampled at surface exposures of rocks which are thought to have crystallised under suitable P/T conditions, or from xenolith suites included in kimberlites and alkali basalts. Heat flow and heat production studies indicate that the lower crust is relatively depleted in U, Th and K, but whether this is a primary or secondary (i.e. metamorphic) feature remains unresolved. In addition models for the evolution of the continental crust are highly sensitive to whether there are significant age differences between upper and lower crustal rocks in different areas.

REGIONAL GEOLOGY AND P/T ESTIMATES

The geology of southern Africa offers a rare opportunity to study the evolution of the continental lithosphere. The surface outcrop preserves a record of major orogenic and magmatic events ranging in age from 3600-30 Ma. Archaean rocks occur in cratonic nuclei surrounded by mobile belts containing varying proportions of new and reworked crustal material. After the last major orogenic episode and the stabilisation of the crust, both the crust and the underlying sub-continental mantle were sampled by wide-spread Karoo magmatism from ~ 190 Ma, as xenoliths in kimberlites emplaced in the Cretaceous, and by mid-Tertiary alkaline volcanism.

Crustal xenoliths have been reported for many of the kimberlite localities in southern Africa. They comprise a cosmopolitan selection of the common rock types exposed on the surface, including a variety of granites, granite gneisses, amphibolites and metasediments, together with basalts and sediments of Karoo age. Of particular interest, however, is a suite of mafic to felsic granulites which preserve temperatures and pressures in the range 550-1000 °C and 4.5-20 kb respectively, and which appear to be restricted to pipes in the younger, Proterozoic belts around the margins of the Archaean¹⁻³. To date no comparable high pressure granulite xenoliths have been reported from the cratonic areas, and the highest pressure rocks in our collection from the Kimberley area still record pressures of less than 10 kb. Available P/T data therefore suggest that mineral equilibration in lower crustal xenoliths took place at deeper levels, and also under lower geothermal gradients, in samples from kimberlite pipes off the craton⁴.

MAJOR, TRACE ELEMENT AND ISOTOPE VARIATIONS

Amphibolite facies xenoliths from southern Africa are characterised by higher SiO₂, alkalis, and lower Fe and Mg than those of granulite facies. A striking feature of xenolith suites is how few acid to intermediate rock types have been reported with granulite facies mineralogy. The mafic granulite xenoliths have high and variable Sr, Ba and Pb, and REE patterns that range from LREE enriched to LREE depleted, but with no significant HREE depletion and common positive Eu anomalies. Thus plagioclase feldspar, rather than garnet, has influenced their trace element compositions, and the present garnet-bearing assemblages are metamorphic rather than igneous. It follows that the petrogenesis of such granulites should be argued on the basis of normative, rather than modal, mineralogy and they have been successfully modelled as cumulates with varying proportions of plagioclase, clinopyroxene and olivine⁵. Such a model interprets the low average Rb/Sr of 0.017 as a primary feature, and for appropriate U and Pb partition coefficients it predicts slightly low μ values consistent with present day Pb isotope ratios.

Radiogenic isotope studies have been carried out on whole rock xenoliths and a selection of separated minerals from four areas: northern Lesotho and eastern Namaqualand in the marginal Proterozoic mobile belts, and Voorspoed and Kimberley within the Kaapvaal craton. The first concern was the extent to which whole rock xenoliths may have interacted with host kimberlite. A large, gneissic xenolith (30 cm diameter) with

a marked alteration rim ~ 1 cm thick, was sawn into sub-samples ranging from 12 to 100 g. At the time of kimberlite emplacement $^{87}\text{Sr}/^{86}\text{Sr}$ in the four sub-samples = 0.7292 - 0.7352 and $^{143}\text{Nd}/^{144}\text{Nd}$ was indistinguishable analytically at 0.51059 ± 2 ($\epsilon_{\text{Nd}} = -38$), even though the host kimberlite had values of 0.7038 and 0.51270^6 . Thus entrainment in the kimberlite appears to have leached material from the outer portions of this xenolith without significantly changing the isotope ratios of even the altered rim.

Figure 1 summarises the present day ϵ_{Sr} and ϵ_{Nd} values of crustal xenoliths from southern Africa and compares them with those of granulite facies rocks world-wide reported by Ben Othman *et al.*⁷, and the Lewisian⁸. Most of the Lesotho and Namaqualand granulite xenoliths are mafic, they tend to have low Rb/Sr but variable Sm/Nd, and hence now form near vertical $\epsilon_{\text{Nd}} - \epsilon_{\text{Sr}}$ trends. In this they are similar to the granulites of the Lewisian, albeit not as old (mid-Proterozoic rather than Archaean), and they contrast with many of the granulites analysed by Ben Othman *et al.* (*ibid.*) which tend to have relative high ϵ_{Sr} .

Also illustrated on Figure 1 is a dashed curve linking the present day ϵ_{Sr} , ϵ_{Nd} values of crustal material of different ages with average Sm/Nd = 0.178 and Rb/Sr = 0.12 following Weaver and Tarney⁹. It emphasises the relatively low inferred Rb/Sr ratios of the Lewisian and south African granulites consistent with models in which the lower crust is characterised by relatively low alkali and heat producing element abundances. The amphibolite facies xenoliths have high ϵ_{Sr} , and particularly striking is the difference in ϵ_{Nd} and ϵ_{Sr} between the amphibolite and granulite facies xenoliths from Lesotho. The former yield Archaean model Nd ages, whereas the best estimate of the age of the latter is $1.4 \pm 0.1 \text{ Ga}^5$.

Pb-isotope analyses on selected Lesotho mafic granulites indicate that while many have low Rb/Sr ratios, these are not accompanied by strikingly low U/Pb or Th/Pb. Present day Pb isotope ratios plot just below the Pb-ore growth curve¹⁰ with $^{206}\text{Pb}/^{204}\text{Pb} = 17.3-17.6$, implying second stage μ values of ~ 4.6 . Thus although the Lewisian and south African granulites arguably have similar low average Sm/Nd and Rb/Sr ratios, they have significantly different U/Pb and Th/Pb, since the Lewisian is characterised by unusually unradiogenic Pb (inferred $\mu \sim 2.6^{11}$).

AGE IMPLICATIONS

The isotope data reveal no significant differences in whole rock ages between granulite and amphibolite facies xenoliths at the same localities, either within the Archaean craton or in the east Namaqualand mobile belt. At Lesotho, however, which is situated on the craton/mobile belt margin, the granulite facies rocks yield Proterozoic ages whereas those from amphibolite facies rocks are Archaean. Only in very localised areas is there any evidence for whole rock age variations with depth in these segments of the continental crust.

Mineral age data in xenoliths are predictably complex, since they reflect the relationship between temperatures in the xenolith source regions and in the host kimberlite, and the blocking conditions for different decay schemes in different minerals. Amphibolite facies xenoliths tend to preserve Rb-Sr biotite ages similar to, and slightly less than biotite ages from the surface terrains. The two analyses on micas from mafic granulites, by contrast, yield biotite ages of 150-200 Ma: much younger than the probable age of metamorphism, but not totally reset at the time of kimberlite emplacement at ~ 90 Ma. Nonetheless garnet from a mafic granulite preserves an Sm-Nd age of 770 Ma consistent with cooling after the metamorphic event at 1000-900 Ma recorded in the surface rocks. These preliminary data suggest that integrated mineral age studies on crustal xenolith suites may yield interesting new information on the thermal regimes, particularly after orogenic events, within the continental lithosphere.

DISCUSSION

Perspectives on the nature of the lower crust differ depending on whether they are based on near surface granulites, or on crustal xenolith suites from either kimberlites or alkali basalts. Although most attention is focussed on those aspects of the lower crust which are in some way chemically unusual, the most obvious being low U/Pb and Rb/Sr which with time will generate relatively unradiogenic Pb- and Sr-isotope ratios.

Mafic xenoliths from south Africa and Lewisian gneisses typify granulites which have distinctive trace element features, but generated by primary and secondary processes respectively. Moreover, in each case the trace element features appear to have been mineralogically determined.

Most studies of mafic granulites have concluded that they are of igneous origin^{2,4}, and the Lesotho rocks have been successfully modelled as liquid compositions and as related cumulates with varying properties of plagioclase, clinopyroxene and olivine⁵. The other way of generating distinctive trace element, and hence isotope ratios in the lower crust is by depletion during granulite facies metamorphism. Heat flow arguments and the many detailed studies on the Lewisian have encouraged speculation that depletion is ubiquitous in the lower crust. However, it is worth noting that most of the granulites analysed by Ben Othman *et al.* do not appear to have been depleted significantly by metamorphic processes, and the same is true of the granulites in the Indian Archaean¹² and of most mafic granulite xenolith suites^{5,13}. Why then does granulite metamorphism sometimes result in the depletion of elements such as Rb, K, and U? The critical reaction appears to be the breakdown of mica in the presence of quartz to form an aluminium silicate, K feldspar and fluid. Rb, Th and U are released into the fluid, whereas K and Ba are partly retained in the K-feldspar, Sr in plagioclase and any amphibole. This is then accentuated for U with the release of more H₂O-rich and of intermediate to acid composition. Basic and/or dry rocks are unlikely to have these trace element ratios changed significantly during granulite facies metamorphism.

- ¹ Jackson, P.M. and Harte B. (1977). 2nd Int. Kimberlite Conf. Extended Abstr.
- ² Griffin, W.L. *et al.* (1979). In: The mantle sample, Eds. F.R. Boyd and H.O.A. Meyer, A.G.U. Washington, D.C., 1977-204.
- ³ Robey, J.A. (1981). Univ. of Cape Town Ph.D.
- ⁴ van Calsteren, P.W. *et al.* Spec. Publ. Geol. Soc. Lond. (in press).
- ⁵ Rogers, N.W. and Hawkesworth, C.J. (1982). Nature 299, 409-413.
- ⁶ Kramers, J.D. *et al.* (1981). Nature 291, 53-55.
- ⁷ Ben Othman, D. *et al.* (1984). Nature 307, 510-515.
- ⁸ Hamilton, J. *et al.* (1979). Nature 277, 25-28.
- ⁹ Weaver, B.L. and Tarney, J. (1984). Nature 310, 575-577.
- ¹⁰ Stacey, J.S. and Kramers, J.D. (1975). Earth Planet. Sci. Lett. 26, 201-221.
- ¹¹ Moorbath, S. *et al.* (1969). Earth Planet. Sci. Lett. 6, 245-256.
- ¹² Allen, P. *et al.* (1983). Mem 9 Geol. Soc. India, 450-461.
- ¹³ Dupuy, C. *et al.* (1979). Phys. Chem. Earth 11, 410-415.

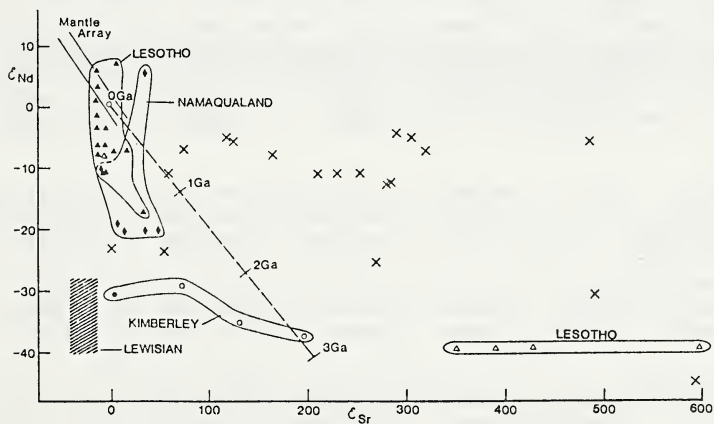


Figure 1 ϵ_{Nd} vs ϵ_{Sr} diagram. Crosses are data from Ben Othman *et al.*⁷, the field for the Lewisian is after Hamilton *et al.*⁸, filled symbols are granulite, open symbols are amphibolite facies rocks.

J.J. HOPS, J.J. GURNEY AND B. HARTE*

Department of Geochemistry, University of Cape Town, South Africa

*Grant Institute of Geology, University of Edinburgh, Scotland

The Jagersfontein kimberlite is a Group 1 kimberlite (Smith, 1984), which hosts abundant deformed peridotite nodules as well as discrete nodules belonging to the Cr-poor megacryst suite. As such it provides an opportunity to evaluate the possible association between the deformed nodules and the Cr-poor megacrysts from a single locality.

Deformed nodules at Jagersfontein can be classified as porphyroclastic or mosaic-porphyroclastic in terms of the classification of Harte (1977). Olivine and orthopyroxene are always the dominant modal phases, with minor amounts of garnet and clinopyroxene. No primary phlogopite, amphibole or spinel is found in these nodules.

Major element mineral chemistry of the deformed peridotites shows that they are generally homogenous. However, the garnets occasionally have rims that are enriched in FeO, TiO₂ and Na₂O and depleted in Cr₂O₃ relative to the grain cores. Porphyroclast and neoblast compositions are usually not distinguishable from each other, but some of the orthopyroxene neoblasts are enriched in Al₂O₃, CaO and Cr₂O₃ relative to the porphyroclasts, suggesting a hotter environment of equilibration.

The Cr-poor megacryst suite at Jagersfontein is represented, in order of decreasing abundance, by garnet, subcalcic clinopyroxene, olivine, orthopyroxene and phlogopite. A significant difference from other documented megacryst localities is the absence of ilmenite and ilmenite-silicate intergrowths. Zircon is also absent.

The megacrysts are homogenous with respect to their major element mineral chemistry and can be distinguished chemically from the minerals in the deformed nodules. The chemical trends defined by the Cr-poor megacrysts are consistent with their derivation by high pressure crystallization of a fractionating melt.

Table 1

Range of chemical parameters of megacrysts and deformed peridotites

	Ca/Ca+Mg	Mg/Mg+Fe	TiO ₂ (wt%)	Cr ₂ O ₃ (wt%)	Na ₂ O (wt%)
GARNET					
Megacryst		75-82	.5-1.2	.4- 1.2	.07-.14
Lherzolite		82-86	.1-1.1	1.7- 6.5	.04-.13
Harzburgite		82	.01-.09	10.1-10.9	n.d.
CLINOPYROXENE					
Megacryst	30-37	85-88	.3- .5	.1- .4	1.4-2.6
Lherzolite	36-43	89-92	.04-.5	.6- 1.6	1.1-2.3
ORTHOPIYROXENE					
Megacryst	1.8-2.9	83-89	.1- .25	<.1	.2-.4
Lherzolite	1.8-2.5	91-93	.05-.2	.1- .4	.1-.3
Harzburgite	1.9	92	n.d.	.34- .36	n.d.
OLIVINE					
Megacryst		85-87			
Lherzolite		89-92			
Harzburgite		92			

*n.d. = not detected

Garnet megacrysts display a wide range in Mg/Mg+Fe and have restricted Ca concentration. In contrast, garnets from the deformed peridotites are more magnesian and have a range in Ca concentration. Subcalcic clinopyroxene megacrysts are Ca-poor and Fe-rich in comparison with the clinopyroxenes from the deformed peridotites. Olivine and orthopyroxene megacrysts are Fe-rich in comparison with olivine and orthopyroxene in the deformed peridotites. The megacrysts are also distinguished by being Cr-poor with respect to the corresponding minerals in the deformed peridotites. Ranges in mineral chemistry are presented in Table 1.

The deformed peridotite nodules yield calculated equilibration temperatures, using the thermometer of Bertrand & Mercier (1986), in the range 1144 to 1341 °C. There is an apparent correlation between temperature of equilibration and texture, in that the nodules at the low temperature end of this range are porphyroclastic whereas those at higher temperatures are mosaic-porphyroclastic. Temperature calculations using the Bertrand & Mercier (1986) thermometer require mineral compositions for coexisting clinopyroxene and orthopyroxene, which render it an unsuitable thermometer for the megacryst suite because, although certain clinopyroxene and orthopyroxene megacrysts may well be in equilibrium, coexisting silicate phases are rare. However, based on the results of a comparative study on the deformed nodules, the temperatures obtained using the Lindsley & Dixon (1976, 20 kbar) or Boyd & Nixon (1973) thermometers, which require only clinopyroxene or orthopyroxene compositions respectively for the temperature calculations, are essentially equivalent to those obtained using Bertrand & Mercier (1986). This suggests comparison between equilibration temperatures obtained using the different thermometers may be valid.

Temperature estimates for the discrete subcalcic clinopyroxene megacrysts, using the thermometer of Lindsley & Dixon (1976, 20kbar), are in the range 1314 to 1442 °C. Subcalcic clinopyroxene megacrysts with garnet inclusions have temperatures in the range 1316 to 1471 °C, and garnet megacrysts with clinopyroxene inclusions have temperatures in the range 1297 to 1413 °C. Orthopyroxene megacrysts yield equilibration temperatures, using the empirical thermometer of Boyd & Nixon (1973), in the range 1190 to 1340 °C.

Calculated equilibration pressures for the deformed peridotites, using the barometer of Nickel & Green (1985), are essentially isobaric at 50 ± 2 kbar. Pressure calculations using the Nickel & Green (1985) barometer require mineral compositions for coexisting garnet and orthopyroxene. Only one garnet megacryst with coexisting orthopyroxene was found, tie-lines were drawn parallel to this coexisting pair from high, intermediate and low temperature discrete orthopyroxene megacrysts to garnet megacrysts and these were then assumed to be in equilibrium. Pressure estimates obtained for these megacrysts are essentially isobaric at 52 ± 1 kbar. This suggests that the deformed peridotites and the megacrysts have equilibrated at essentially similar depths. The large range of temperatures associated with this isobaric pressure reflects a thermal perturbation of the steady-state continental geotherm by an igneous event.

Petrographically similar polyminerallic inclusions are found in garnet megacrysts as well as in garnets from some deformed nodules. These inclusions consist of serpentine, phlogopite, amphibole, aluminous spinel, aluminous clinopyroxene and aluminous orthopyroxene. Similar inclusions have been interpreted by Schulze (1985) as representing high pressure liquids from which the discrete nodules crystallized. However, it is possible that these inclusions represent a secondary product resulting from reaction between garnet and a metasomatic liquid, possibly of kimberlitic affinity.

The spatial association between the deformed nodules and a pegmatitic phase as proposed by Ehrenberg (1979, 1982) and Harte & Gurney (1981) appears to be substantiated by this study of megacrysts and deformed nodules from Jagersfontein.

REFERENCES

- BERTRAND P. and MERCIER J-C.C. 1986. The mutual solubility of coexisting ortho and clinopyroxene: towards an absolute geothermometer for the natural system. *Tectonophysics* 70, 85-113.
- BOYD F.R. and NIXON P.H. 1973. Origin of the ilmenite-silicate nodules in kimberlites from Lesotho and South Africa. In Nixon P.H. ed, *Lesotho Kimberlites*, pp 254-268. Lesotho National Development Corporation, Maseru.
- EHRENBERG S.N. 1979. Garnetiferous ultramafic inclusions in minette from the Navajo volcanic field. In Boyd F.R. and Meyer H.O.A. eds, *The Mantle Sample*, pp 330-344. American Geophysical Union, Washington.
- EHRENBERG S.N. 1982. Petrogenesis of garnet lherzolite and megacrystalline nodules from the Thumb, Navajo volcanic field. *Journal of Petrology* 23, 507-547.
- HARTE B. 1977. Rock nomenclature with particular relation to deformation and recrystallisation textures in olivine-bearing xenoliths. *Journal of Geology* 85, 279-288.
- HARTE B. and GURNEY J.J. 1981. The mode of formation of chromium-poor megacryst suites from kimberlites. *Journal of Geology* 89, 749-753.
- LINDSLEY D.H. and DIXON S.A. 1976. Diopside-enstatite equilibria at 850-1400 °C, 5-35 kbar. *American Journal of Science* 276, 1285-1301.
- NICKEL K.G. and GREEN D.H. 1985. Empirical geothermobarometry for garnet peridotites and implications for the nature of the lithosphere, kimberlites and diamonds. *Earth and Planetary Science Letters* 73, 158-170.
- SCHULZE D.J. 1985. Evidence for primary kimberlitic liquids in megacrysts from kimberlites in Kentucky, U.S.A. *Journal of Geology* 93, 75-79.
- SMITH C.B. 1984. Rubidium-strontium, uranium-lead and samarium-neodymium isotopic studies of kimberlite and selected mantle-derived xenoliths. Unpub. Ph.D., University of Witwatersrand.

ECLOGITE-GARNETITE TRANSFORMATIONS IN BASALTIC AND PYROLITIC COMPOSITIONS
AT HIGH PRESSURE AND HIGH TEMPERATURE

T. IRIFUNE, W.O. HIBBERSON, A.E. RINGWOOD

RESEARCH SCHOOL OF EARTH SCIENCES, THE AUSTRALIAN NATIONAL UNIVERSITY
CANBERRA ACT 2601, AUSTRALIA

Extensive experimental studies have been made in our laboratory on high-pressure phase equilibria in basalt and pyrolite compositions at pressures to 18 GPa and temperatures of 1200 - 1400°C. The compositions studied so far are 1) primitive MORB (Green et al., 1978; Liu, 1980; Irifune et al., 1986), 2) alkali-poor olivine tholeiite (Ringwood, 1967; Irifune et al., 1986), and 3) pyrolite minus olivine (Sun, 1982; Irifune, 1986), as listed in Table 1. Further, a corresponding study on the composition of an eclogitic garnet inclusion in diamond (A1-24; Moore and Gurney, 1985) is currently in progress. We summarize herein these experimental data and discuss the nature of the garnet-eclogite transformation in these compositions. Implications for the constitution of the earth's mantle are also discussed.

High-pressure experiments were carried out using an MA8 type apparatus with truncated split-sphere guide blocks (Ohtani et al., 1986). Seimi-sintered MgO was used as a pressure medium and two sheets of TiC + MgO were used as heaters. Temperature was measured by a Pt-Pt10%Rh thermocouple. Glass and amphibolite with about 1% water were used as starting materials, and the quenching method was employed to identify phases in the run product. Further details of the experimental techniques are given in Irifune and Hibberson (1985) and Irifune et al. (1986).

Figure 1 shows lattice parameters of garnet in basalt and pyrolite compositions as a function of pressure. Electron microprobe analyses revealed that the variations of the garnet lattice parameters below 12 - 13 GPa are due to chemical changes, specifically in Ca contents, in these garnets. The lattice parameters thereafter increase rather rapidly, which is mainly caused by solution of pyroxene in the garnet structure. The lattice parameters level off at pressures above 14 - 16 GPa, indicative of formation of single phase garnetite (\pm stishovite). Formation of garnetite at these pressures is also confirmed by electron microprobe analysis.

Figure 2 depicts the chemical composition change of garnet in the pyrolite minus olivine composition as a function of pressure. Garnet becomes aluminum-deficient with increasing pressure and the numbers of M^{2+} (Ca + Mg + Fe) and Si^{4+} increase in a complementary manner, which indicates substitution of $M^{2+} + Si^{4+}$ for Al^{3+} at high pressure. Further, the sodium contents of garnet increases with increasing pressure, indicative of the coupled substitution of $Na^{+} - Si^{4+}$ for $M^{2+} - Al^{3+}$. Moore and Gurney (1985) denied the possibility of this substitution because of the existence of a negative correlation between Si and Na in high-Na garnet inclusions as shown by the

region of group B garnets in Fig. 3. However, our experimental data show that positive correlations exist between Si and Na and suggest the negative correlation in group B garnet is superficial. Similar variations in chemical compositions of garnets are observed for other bulk compositions.

The Na-rich garnet is considered to be formed at extremely high pressures, above 10 GPa, as seen in Fig.3. The most Al-deficient garnet in group B (A1-24) so far reported is found to be formed at pressures above 14 GPa at 1200 C. As the temperature dependence of the eclogite-garnetite

Table 1. Compositons of starting materials

	(1)	(2)	(3)	(4)
SiO ₂	50.39	47.20	51.78	47.63
TiO ₂	0.57	0.10	0.46	0.88
Al ₂ O ₃	16.08	14.51	11.44	11.29
Cr ₂ O ₃	-	-	0.92	0.20
FeO	7.68	11.81	3.12	10.95
MgO	10.49	12.10	23.14	22.05
CaO	13.05	13.19	9.50	7.10
Na ₂ O	1.87	0.65	0.94	0.48
TOTAL	98.26	99.56	101.30	99.77

(1) DSDP, (2) alkali-poor olivine tholeiite,
(3) pyrolite minus 62 % olivine, (4) A1-24.

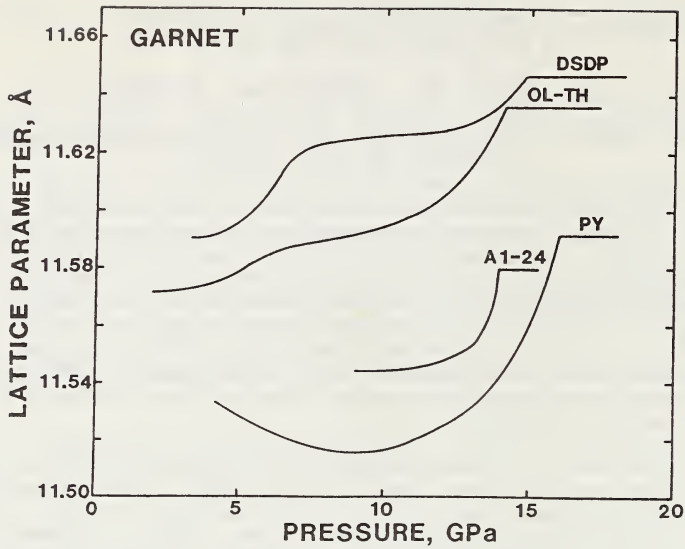


Fig.1 Lattice parameters of garnets in basaltic and pyrolitic compositions as a function of pressure.

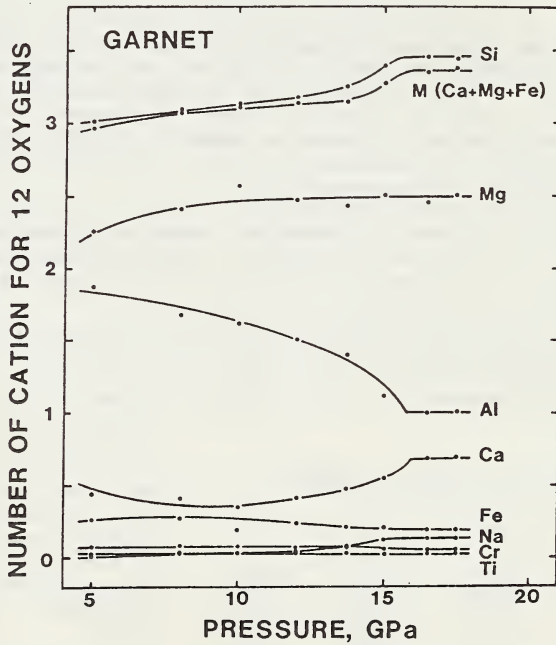


Fig.2 Compositions of garnets in "pyrolite minus olivine" as a function of pressure.

transformation is quite small, in the order of 0.002 GPa/°C (Irifune, 1986), it is evident that this garnet is derived from a depth of at least 400 km and accordingly represents the most deep-seated mantle minerals available to date. On the other hand, the low Na and Si garnet inclusions (group A) are formed at relatively low pressures, below 10 GPa.

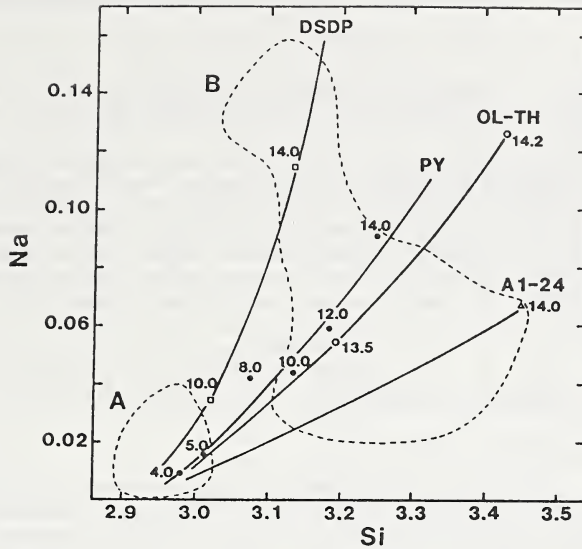


Fig. 3 Correlations between atomic Na and Si in garnets of various starting compositions. Numbers indicate pressure in GPa. Group A represents normal eclogitic inclusion garnets and group B represents garnets containing pyroxenes in solid solution, as described by Moore and Gurney (1985).

Mineralogy and density changes in descending oceanic crust and surrounding mantle are evaluated on the basis of our experimental data. Basaltic materials are substantially denser than surrounding mantle to depths of at least 600 km and possibly throughout the mantle. The results of this study combined with seismological data confirm that it is most unlikely that eclogitic materials comprise a large portion of the upper mantle.

References

- GREEN D.H., HIBBERSON W.O. AND JAUQUES A.L. 1978. Petrogenesis of mid-ocean ridge basalts. In McElhinney M.W. ed, *The Earth, its Origin, Structure and Evolution*, pp. 265-299. Academic Press, London.
- IRIFUNE T. AND HIBBERSON W.O. 1985. Improved furnace design for multiple anvil apparatus for pressures to 18 GPa and temperatures to 2000°C. *High Temperatures-High Pressures* 17, 575-579.
- IRIFUNE T., SEKINE T., RINGWOOD A.E. AND HIBBERSON W.O. 1986. The eclogite-garnetite transformation at high pressure and some geophysical implications. *Earth and Planetary Science Letters* 77, 245-256.
- IRIFUNE T. 1986. An experimental investigation of the pyroxene-garnet transformation in a pyrolite composition and its bearing on the constitution of the mantle. *Physics of the Earth and Planetary Interiors* (submitted).
- LIU L.-G. 1980. The mineralogy of an eclogitic earth mantle. *Earth and Planetary Science Letters* 23, 262-267.
- MOORE R.O. AND GURNEY J.J. 1985. Pyroxene solid solution in garnets included in diamond. *Nature* 318, 553-555.
- OHTANI E., IRIFUNE T., HIBBERSON, W.O. AND RINGWOOD A.E. 1986. High-pressure and high-temperature generation by multiple anvil (MA8) apparatus with the truncated split sphere. In Program with Abstracts, U.S.-Japan Seminar, *High-Pressure Research: Applications in Geophysics and Geochemistry*, pp. 90-91.
- RINGWOOD A.E. 1967. The pyroxene-garnet transformation in the earth's mantle. *Earth and Planetary Science Letters* 2, 255-263.

Anthony J. Irving

Dept. of Geological Sciences,
University of Washington, Seattle, WA 98195, U.S.A.

Megacryst phases enclosed in basanite, minette and kimberlite magmas provide a record of polybaric magmatic evolution during ascent of mantle-derived magmas. Evidence from trace element, isotopic and phase equilibrium data (e.g. Irving and Frey, 1984) implies that some megacrysts (e.g. Al-augite, pyrope garnet in basanites) could be cognate with the host magma, whereas others (e.g. corundum, zircon, anorthoclase in basanites) must be exotic to their hosts. One mechanism for the origin of the latter suite is precipitation from evolved magmas (e.g. nepheline benmoreites and phonolites) followed by mixing with later pulses of more primitive mafic magma. The possibility that some corundum megacrysts are xenocrysts from crustal metamorphic rocks, or are a product of desilication reactions between basanite, minette or kimberlite magmas and crustal rocks, must also be considered.

Corundum and Zircon, Rubyvale, Queensland

A variety of megacryst species including corundum, zircon, anorthoclase, magnetite, ilmenite and pleonaste spinel occur within numerous Tertiary basaltic plugs in the Rubyvale region of central Queensland, Australia (Veevers et al., 1964; Stephenson, 1976), and adjacent alluvial deposits are actively mined for gem sapphire. The very similar geologic settings in southeast Asia (Barr and Macdonald, 1981) and Nigeria (Wright, 1970) imply that much of the world's gem sapphire forms megacrysts in alkalic basalts. The host rocks of four of the Rubyvale plugs (Mts. Leura, Pleasant, Hoy and Ball) are slightly to moderately evolved basanites (Mg/Mg+Fe²⁺ 68.8-58.3). The corundum megacrysts (commonly 1-2 cm across) show multiple compositional zoning, especially in TiO₂ content (as reflected by zones of rutile exsolution). ICP bulk analysis of one megacryst shows minor contents of Fe, Ti (250 ppm), Mn (13 ppm), Cr (4 ppm), V (6 ppm), Sr (0.6 ppm) and Be (0.2 ppm).

Fluid inclusions within the corundums are very distinctive. They form planar arrays transverse to growth zoning, and heating-freezing studies reveal two main types. Type 1 is pure CO₂ (liquid + vapor). Such inclusions also occur in sapphires from minette at Yogo, Montana (Roedder, 1972). More common and associated with the first type are multi-phase inclusions composed of subequal amounts of CO₂ (liquid + vapor) and H₂O containing halite, sylvite and other unidentified daughter minerals. Dissolution studies of the halide salts imply a high total salinity in the H₂O phase (~ 35% NaCl and a similar value for KCl). These Type 2 inclusions remain unhomogenized at temperatures up to 685°C. Taken together the growth zoning, CO₂-rich inclusions, and high inclusion homogenization temperatures suggest a high temperature (and pressure) magmatic origin for the corundum megacrysts. The occurrences of corundum intergrown with anorthoclase at Mt. Leura (Stephenson, 1976) and with sanidine + rutile in alkalic basalt from Loch Roag, Scotland (Upton et al., 1983) support this conclusion.

Zircon megacrysts from Rubyvale lack fluid inclusions. Two crystals analyzed by INAA contain relatively low bulk Hf (0.55-0.60%), U (7-30 ppm), Ta (0.7 ppm) and REE (see Fig. 1). These minor element abundances are quite similar to those in zircons from nepheline syenite pegmatites but much lower than those in zircons from granitoids (Kapustin, 1986; Murali et al., 1983). Taken with the occurrence of corundum in miassic nepheline syenite pegmatites and the experimental evidence for instability of anorthoclase in basalt (Chapman, 1976), these data permit the inference that the Rubyvale megacryst assemblage may have crystallized from phonolitic magma at elevated (probably deep crustal) pressures. High pressure phonolites are known in north Queensland (Irving and Price, 1981) and have been modeled as products of fractional crystallization of basanites. The mechanism by which basanite magma would evolve to a condition of alumina-saturation is not clear, but may involve crystallization under moderate CO₂ and/or halogen partial pressures.

Magnesian ilmenite megacrysts are well known in kimberlites. Preliminary results from INAA of an ilmenite from Monastery Mine, Orange Free State show relatively high contents of REE (0.3-0.5 x chondrites), Ta, Hf (28 ppm) and Sc (22 ppm). Furthermore the LREE abundances in this ilmenite are enriched by an order of magnitude over those expected for equilibrium with the host kimberlite (see Fig. 2), based upon known experimental partition coefficient values (McKay and Weill, 1976; Irving et al., 1978). In contrast data for an ilmenite megacryst from Benfontein are compatible with equilibrium with its host kimberlite (Fujimaki et al., 1984). The Monastery sample apparently crystallized from a liquid (or fluid) more enriched in LREE than the present host kimberlite thus implying magma mixing at this kimberlite pipe. The possibility that zircon megacrysts in kimberlites may have crystallized from evolved liquids and are exotic to their hosts will also require testing.

REFERENCES

- BARR S.M. and MACDONALD A.S. 1981. Geochemistry and geochronology of the late Cenozoic basalts of southeast Asia. *Bulletin of the Geological Society of America* 92, pt. I, 508-512 and Pt. II, 1069-1142.
- CHAPMAN, N.A. 1976. Inclusions and megacrysts from undersaturated tuffs and basanites, east Fife, Scotland. *Journal of Petrology* 17, 472-498.
- FUJIMAKI H., TATSUMOTO M. and AOKI K. 1984. Partition coefficients of Hf, Zr and REE between phenocrysts and groundmasses. *Proceedings of the Fourteenth Lunar and Planetary Science Conference, Part 2, Journal of Geophysical Research* 89, B662-B672.
- IRVING A.J. and FREY F.A. 1984. Trace element abundances in megacrysts and their host basalts: Constraints on partition coefficients and megacryst genesis. *Geochimica et Cosmochimica Acta* 48, 1201-1221.
- IRVING A.J. and PRICE R.C. 1981. Geochemistry and evolution of lherzolite-bearing phonolitic lavas from Nigeria, Australia, East Germany and New Zealand. *Geochimica et Cosmochimica Acta* 45, 1309-1320.
- IRVING A.J., MERRILL R.B. and SINGLETON D.E. 1978. Experimental partitioning of rare earth elements and scandium among armalcolite, ilmenite, olivine and mare basalt liquid. *Proceedings of the Ninth Lunar and Planetary Science Conference*, pp. 601-612. Pergamon.
- KAPUSTIN Y.L. 1986. Trace-element distribution in generations of accessory zircon in pegmatites. *Doklady Earth Science Sections* 277, 153-167.
- McKAY G.A. AND WEILL D.F. 1976. Petrogenesis of KREEP. *Proceedings of the Seventh Lunar Science Conference*, pp. 2427-2447. Pergamon.
- MITCHELL R.H. and BRUNFELT A.O. 1975. Rare earth element geochemistry of kimberlites. In Ahrens L.H. et al. eds., *Physics and Chemistry of the Earth, Volume 9*, pp. 671-685. Pergamon.
- MURALI A.V. et al. 1983. Trace element characteristics, REE patterns and partition coefficients of zircons from different geological environments - a case study on Indian zircons. *Geochimica et Cosmochimica Acta* 47, 2047-2052.
- ROEDDER E. 1972. Composition of fluid inclusions. *United States Geological Survey Professional Paper* 440JJ, 164p.
- STEPHENSON P.J. 1976. Sapphire and zircon in some basaltic rocks from Queensland, Australia. *Abstracts, 25th International Geological Congress* 2, 602-603.
- UPTON B.G.J., ASPEN P. and CHAPMAN N.A. 1983. The upper mantle and deep crust beneath the British Isles: Evidence from inclusions in volcanic rocks. *Journal of the Geological Society of London* 140, 105-121.
- VEEVERS J.J. et al. 1964. The geology of the Emerald 1:250,000 Sheet area, Queensland. *Bureau of Mineral Resources, Geology and Geophysics, Report* 68.
- WRIGHT J.B. 1970. High pressure phases in Nigerian Cainozoic lavas: Distribution and geotectonic setting. *Bulletin Volcanologique* 34, 833-847.

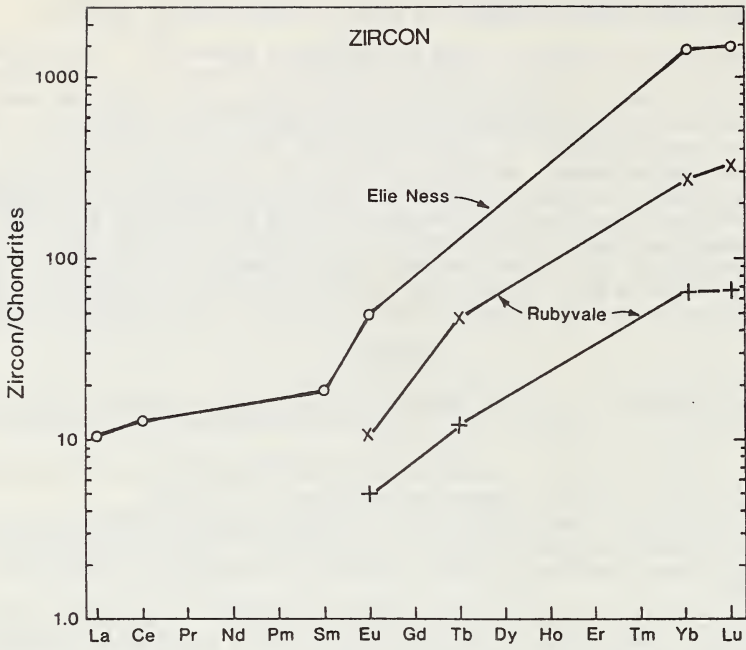


Figure 1. Chondrite-normalized REE data for zircon megacrysts from Rubyvale and Elie Ness, Scotland (Irving and Frey, 1984)

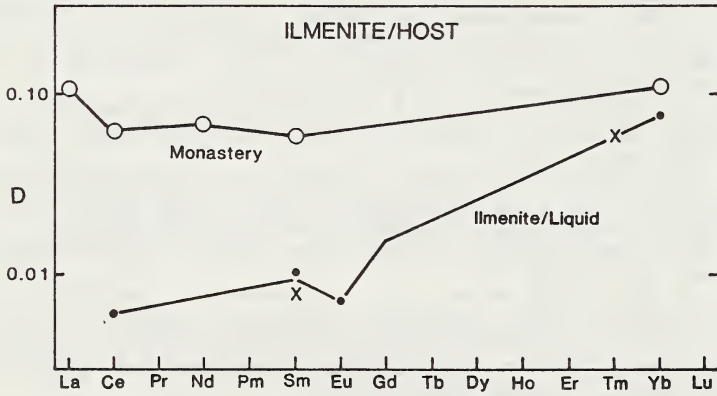


Figure 2. Comparison of ilmenite/host kimberlite REE abundance ratios (using host data from Mitchell and Brunfelt, 1975) with experimentally-determined D values.

E. Jagoutz

Max-Planck-Institut für Chemie, Saarstrasse 23, D-6500 Mainz, F.R.Germany

Gnt, Cpx and, due to high modal abundance, Opx are mainly responsible for the geochemistry of REE, Sr and Pb in terrestrial mantle. K, U, Th, Rb, however, are incompatible to these minerals. The major phases containing REE are Gnt and Cpx, while Opx and Ol contain negligible amounts of LREE. Sr and Pb, on the other hand, do not enter the Gnt structure and are therefore restricted to Cpx. Compatibility and partition of trace elements might drastically change with phase transitions or also with P-T dependent solid solutions of these minerals. For example, Cpx might incorporate Sr, but when this Cpx is transformed into Gnt structure, the Sr is possibly incompatible to this mineral and might be lost. When this Gnt is transformed back into Cpx structure by decompression, we would find an extremely Sr-poor Cpx.

The modal amounts of Cpx and Gnt are temperature and pressure dependent. Firstly, reactions such as $Ts + Wo \rightarrow Gnt$ are frequently observed in eclogites and pyroxenites as exsolution of Gnt from the Cpx. On the other hand, the dissolution of Cpx in Gnt postulated by Ringwood (1967) results in Gnt with a low Al/Si ratio. Sobolev (1974) reported Gnt with an excess silica content in diamond-bearing eclogites from Siberia. Moore and Gurney (1985) also reported garnet inclusions in diamonds with considerable amounts of dissolved Cpx.

Nd and Sr isotopes are measured in a number of eclogites. Sample BD 1934 (Fig. 1) is an eclogite from Tanzania (donated by J.B. Dawson), in which Gnt is exsolved from the pyroxene. The different generations of Gnt have different Nd isotopic compositions. The isochron defined only by the petrographically different Gnt has an apparent age of 1.5 b.y., but the isochron defined by Gnt and Cpx gives an age of 1.75 b.y. The obtained results of sample BD 1934 suggest that this eclogite has a slow cooling history from 1200°C to 800°C with a cooling rate of <5°C/m.y. It might be possible that this age and cooling history represents the incorporation of this eclogite into the lithosphere.

The sample OBNA 0062 (donated by G. Kurat) is an eclogite from Siberia with Gnt exsolution within the Cpx. The distribution of Gnt within the Cpx matrix is shown in Fig. 2. This sample is isotopically heterogeneous on a cm-scale as shown in Fig. 1. The variation (40 ε) of Nd isotopes is greater than observed in the full range of oceanic basalts. The isotopic variation could be caused by an open system. Gnt and Cpx are close to isotopic equilibrium as in the normal high temperature lherzolites, indicating that this sample comes from a temperature range above the closure temperature of Nd diffusion in Cpx. This could well be the asthenospheric mantle.

Another remarkable and puzzling observation is the low Nd and Sm concentration in the Cpx and Gnt of this sample (50 - 75 ppb) and their very depleted Sm/Nd ratio. This depleted character and the low Sm and Nd concentrations possibly indicate that this sample was derived either from a garnetite or an amphibole before converted into an eclogite.

JW 604 is a diamond-bearing eclogite (donated by N.V. Sobolev) with graphite, rutile and disthene. The Gnt of this sample has excess Si indicating that Cpx is dissolved in the Gnt. The different generations of Cpx and Gnt show only slight variations in isotopic composition. The age of equilibration between Gnt and Cpx is about 340 m.y. (Fig. 1), possibly close to the emplacement age of the kimberlite. Sm and Nd concentrations of the minerals from this sample are between 0.5 and 2 ppm and therefore quite normal for eclogitic minerals. On the other hand, the Gnt in this sample is enriched in Nd and Sm relative to the Cpx which is surprising. This could indicate that if Si in the Gnt is in 6fold coordination, the lattice of the Gnt is widened as shown by experimentally measured lattice parameters (Irifune et al. 1986) and the Gnt is more compatible for REE trace elements.

Isotopes results are also reported from subcalcic Gnt separated from diamond-bearing harzburgites and dunites from the Odajanai Mine, Siberia. Gnt has remarkably unradiogenic Nd (-38ε) and unusually high concentrations of Sm, Nd and Sr. From the fact that this Gnt is subcalcic we know that this composition is only stable in a Cpx-free environment like harzburgite. In contrast to the subcalcic garnet from S. Africa, which are found there in mineral concentrates, these Gnts are separated from actual

rocks. The isotopic composition of the Siberian Gnts are very similar to the Gnt from S. Africa as reported by Richardson et al. (1984). Considering the isotopic variations found in these rocks the significance of a model age seems to be questionable. Possibly, the subcalcic Gnts are in reaction equilibrium with the Opx.

The Sm/Nd variations observed in these examples of subsolidus equilibrium between Gnt and pyroxene are bearing important consequences on the isotopic systems. The isotopic signature on basalts and rocks equilibrated with melts gives a volume integrated information which might not be specific for a certain mantle segment.

REFERENCES

IRIFUNE T., SEKINE T., RINGWOOD A.E. and HIBBERSON W.O. 1986. The eclogite-garnetite transformation at high pressure and some geophysical implications. *In press*.
 MOORE R.O. and GURNEY J.J. 1985. Pyroxene solid solution in garnets included in diamond. *Nature* 318, 553-555.
 RICHARDSON S.H., GURNEY J.J., ERLANK A.J. and HARRIS J.W. 1984. Origin of diamonds in old enriched mantle. *Nature* 310, 198-202.
 RINGWOOD A.E. 1967. The Pyroxene-garnet transformation in the Earth's mantle. *Earth Planet. Sci. Lett.* 2, 255-263.
 SOBOLEV, N.V. 1974. *Deep-Seated Inclusions in Kimberlites and the Problem of the Composition of the Upper Mantle*. Izdatel'stvo Nauka, translated 1977 by Amer. Geophys. Union, Washington, D.C.

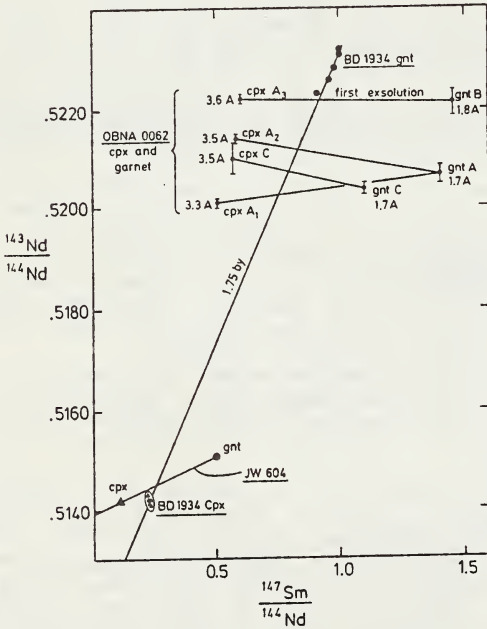


Fig. 1: Nd-isochron of Siberian eclogites.

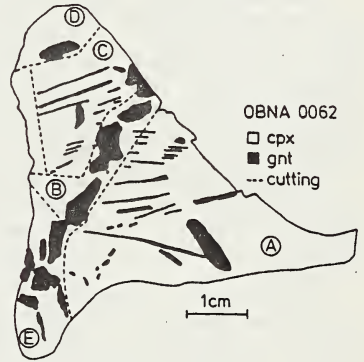


Fig. 2: Garnet distribution of OBNA 0062.

P.D.Kinny¹, I.S.Williams¹, W.Compston¹ and J.W. Bristow²

¹Research School of Earth Sciences, Australian National University, Canberra.

²De Beers Consolidated Mines Ltd., Kimberley.

INTRODUCTION

U-Pb ages of kimberlitic zircon were first obtained by Davis *et al.*, 1976. Results compiled subsequently from over 20 localities in and around the Kaapvaal craton of southern Africa, and others from Brazil (Davis, 1977), all gave ages in the range 94 - 52 Ma, close to the known ages of pipe emplacement as determined by other methods. Davis recognised that as xenocrysts the zircons could be much older than their indicated ages, but might not have retained radiogenic Pb until the temperature dropped in the rising kimberlitic magma prior to eruption. We present here the results of U-Pb dating by ion microprobe of zircons from the Jwaneng pipe in Botswana which show that some zircons have in fact preserved Precambrian ages, although the pipe was emplaced in the late Permian. Two distinct age populations are present, hereafter termed the "old" and "young" zircons. The results are confirmed independently by hafnium model ages measured on the same grains with the ion microprobe, providing direct evidence for the occurrence of deep-seated nodules of Archaean age in the mantle source regions of the Jwaneng kimberlite, as well as others which formed close to the time eruption.

THE JWANENG ZIRCONS

The Jwaneng zircons are typical of those previously described from kimberlites which are believed to be xenocrysts associated with the deep-seated suite of discrete nodules (Kresten *et al.*, 1975). They are rounded megacrysts up to 3mm in diameter with minor surface pitting. Colours range from colourless to honey brown or orange hues. Viewed in section, the crystals show no internal structure other than an abundance of platy and acicular inclusions (rarely over 60µm in length) some of which have been identified as apatite, and, in some instances, fluid inclusions. One grain in particular, J2 9, contains networks and droplets of liquid inclusions of the type illustrated in Kresten *et al.*, 1975, p50. Their alignment in discrete arcuate planes within the crystal indicates a secondary origin related to fracture annealing.

The two age groups are morphologically indistinguishable, but can be identified by differences in their trace element compositions. All grains are typically trace element-poor; low U and Th abundances in particular are consistent with the findings of Ahrens *et al.*, 1967 and later workers. However, as shown in Figure 1, the young grains are markedly richer in U than the old grains and with Th/U averaging 0.2 as compared with values typically in the range 0.4 - 0.5. Additionally, the young grains are considerably poorer in Hf and heavy REE, and higher in Ta content. The latter was identified with the ion-probe during Hf isotopic analyses as present in the zircons in unusually high abundances, though still below detection limits of the CAMECA electron-probe at ANU (~ 100 ppm for Ta).

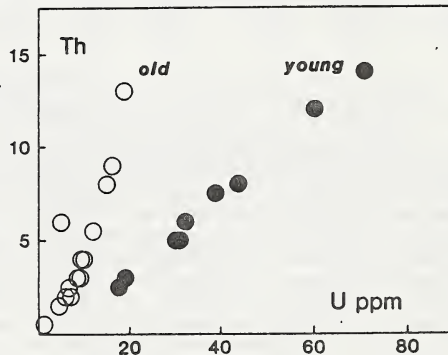


Figure 1: Plot of U vs Th contents of zircons from the Jwaneng kimberlite.

ANALYTICAL METHODS

Fifteen grains selected at random were broken, and fragments mounted in two epoxy discs (J1 and J2) which were polished and a conductive coating applied to their surface. No other prior treatment of samples is required for isotopic analysis by ion microprobe, in which material for analysis is sputtered from an exposed 25µm area within a crystal by a focused beam of oxygen ions. The routine for U-Pb analyses by the ANU ion microprobe SHRIMP has been described in detail by Compston *et al.*, 1984, and in subsequent publications, however the techniques employed for hafnium isotopic analyses have not yet been described. Briefly, Hf isotopes are measured on the electron multiplier as HfO⁺ species. Reduced ratios are corrected for isobaric interferences of YbO, LuO and HfOH, and for mass fractionation by normalizing standard Hf isotopic ratios to values determined by thermal ionization mass spectrometry (Patchett, 1983).

RESULTS

Young zircons : For young zircons which are low in radiogenic ²⁰⁷Pb, the measured ²⁰⁷Pb/²⁰⁶Pb yields a very imprecise estimate of age. On average, 74% of the total ²⁰⁷Pb measured in the young Jwaneng zircons was non-radiogenic, as compared with 19% of the total ²⁰⁶Pb. The ²⁰⁶Pb/²³⁸U age of these grains is consequently the most reliable. The results of the ion-probe U-Pb analyses of nine young grains are given in the lower part of Table 1. Seven of these gave values of ²⁰⁶Pb*/²³⁸U (* radiogenic) which are equal to within the analytical uncertainties. The

weighted mean value, $0.03720 \pm 2 (1\sigma)$, corresponds to an age of 235 ± 2 Ma. This result is very close to a Rb-Sr mica age of ca. 242 Ma (J.W.Bristow, unpubl. data) for a small satellite pipe adjacent to the main DK2 pipe at Jwaneng from which the zircons were derived. It suggests that the Jwaneng kimberlites were emplaced at 235 Ma or soon after. The remaining two grains, J2 1 and J2 6, gave younger $^{206}\text{Pb}/^{238}\text{U}$ ages of 223 ± 3 and 218 ± 3 Ma

respectively (both 1σ). We interpret these results as indicating that those two grains lost a small portion of their accumulated radiogenic Pb recently. The possibility that all of the grains have leaked a little Pb since their time of formation must be considered, because it would imply that 235 ± 2 Ma is not strictly a maximum age for the pipe even if the zircons are xenocrysts. Since the locus of Pb loss from young zircons is approximately parallel with the Concordia curve, the extent to which this may have occurred cannot be determined. However, in this case the effects are probably minor, given the similarity between the majority of zircon $^{206}\text{Pb}/^{238}\text{U}$ ages and the mica age.

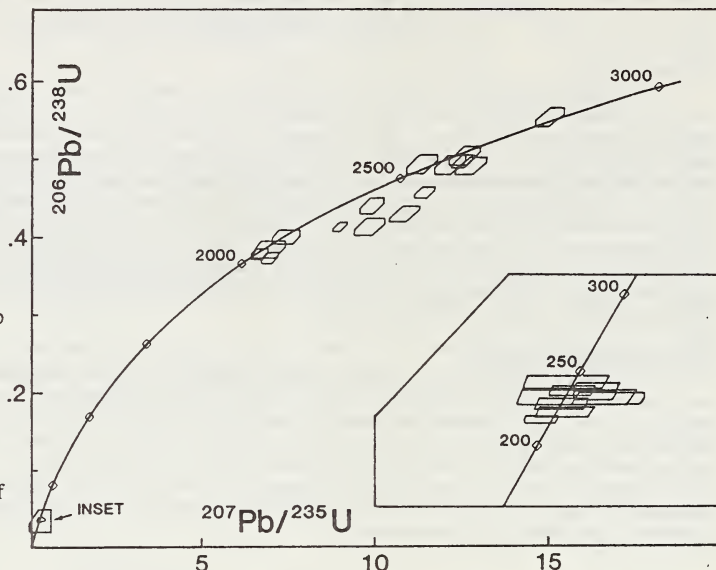


Figure 2: Concordia diagram showing results of U-Pb isotopic analyses of Jwaneng zircons. Error limits, as per Table 1, are 1σ .

Old zircons : Of the fifteen grains analysed, six have preserved much older Pb/Pb and U-Pb ages than those described above, confirming their xenocrystic origin. In order to investigate the extent of any internal isotopic variation, three of the old grains were analysed at three separate locations, and one grain in five areas. The results of these analyses are listed in the upper part of Table 1, and plotted on a U-Pb Concordia diagram in Figure 2. The single analysis of Grain J2 9 has been omitted from Fig.2, because the grain contains less than 1 ppm radiogenic Pb and the analytical uncertainties are much larger than for the other grains. At least one analysed area on each grain gave concordant U-Pb ages. These ranged from 2100 to 2800 Ma. The four grains for which multiple areas were analysed showed contrasting variations in isotopic composition. Three analyses of J1 2 were equal to within error and concordant at 2135 Ma. The results for J1 3 and J2 7 included both concordant and slightly discordant analyses (plotting below the Concordia curve), consistent with closure of the U-Pb systems at 2600 and 2695 Ma respectively, followed by variable minor Pb loss either recently or at the time of pipe emplacement. In contrast, three analyses of J1 1 showed a significant range in $^{207}\text{Pb}/^{206}\text{Pb}$ indicating that this zircon lost Pb in ancient times, in fact as early as 1707 ± 664 Ma (based on the lower intercept with Concordia of a regression line through the three data points). These results indicate that processes causing Pb loss were operative both in the source regions of the zircon xenocrysts and, subsequently, in the pipe itself.

Hafnium data : The isotopic composition of hafnium is modified over time by the addition of ^{176}Hf from the decay of ^{176}Lu . Since Hf substitutes for Zr in the zircon lattice at the percent level, it preserves in the zircon the isotopic composition of the source environment at the time of crystallization, and is well-buffered against post-crystallization disturbances that may affect other isotopic systems. Furthermore, since kimberlitic zircons are highly depleted in REE, correction for subsequent *in situ* decay of ^{176}Lu is negligible. Four zircons from Jwaneng were analysed for Hf, two young and two old grains, and results are shown in Table 2. Whereas both old grains (J2 7 and J2 9) give Archaean Hf model ages, the young grains (J2 11 and J2 12) contain a more evolved Hf isotopic composition, consistent with relatively recent extraction from the mantle.

DISCUSSION

Considering the elevated temperatures ($\geq 1100^\circ\text{C}$) estimated for the source regions of the ilmenite-silicate nodules with which kimberlitic zircons are believed to be associated (Boyd and Nixon, 1973) the preservation of old U-Pb ages implies that the ca 750°C "blocking temperature" assumed for Pb in zircons (eg Mattinson, 1978) is too low, or that factors other than ambient temperature influence the retention capability of kimberlitic zircon for Pb. Certainly, as was pointed out by Davis (1977), the possible influence of accumulated radiation damage on Pb loss from such U-depleted crystals would be minimal.

Collectively, the U-Pb isotopic data for the old zircons are consistent with the following alternatives:

1. Original formation *ca* 2800 Ma followed by variable Pb loss during a single diffusive episode at 2100 Ma,
 2. Formation of different grains at discrete times between 2800 and 2100 Ma, or
 3. Formation of all grains prior to 2800 Ma, with the observed array of nearly-concordant U-Pb ages in different grains reflecting different times at which they began to retain radiogenic Pb.
- The last best explains the Hf model ages of 3.58 ± 0.17 and 3.18 ± 0.15 Ga for J2 7 and J2 9 respectively, which are significantly older than their U-Pb ages, and which are in agreement with Archaean model Sm-Nd and Rb-Sr ages that have been measured on garnet inclusions in diamonds from southern African kimberlites (Richardson *et al.*, 1984).

In the context of previous studies it could be argued that the young zircons represent Precambrian xenocrysts whose U-Pb isotopic systems have been reset to the pipe age. However, several lines of evidence argue for a separate origin close to the time of eruption: the lack of a continuum of U-Pb isotopic compositions between the young and old grains, the differences in trace element composition, and, most conclusively, the difference in Hf isotopic composition.

Table 1: SHRIMP U-Pb isotopic analyses of zircons from the Jwaneng Kimberlite, Botswana. Isotopic ratios are corrected for common Pb (mostly surface Pb) which was determined from the measured $^{208}\text{Pb}/^{206}\text{Pb}$, the expected radiogenic $^{208}\text{Pb}/^{206}\text{Pb}$ for the measured Th/U, and assuming a common $^{208}\text{Pb}/^{206}\text{Pb}$ ratio of 2.2285 (Broken Hill Pb composition). Ages were calculated using $\lambda^{238}\text{U} = 1.55125 \times 10^{-10} \text{ y}^{-1}$, $\lambda^{235}\text{U} = 9.8485 \times 10^{-10} \text{ y}^{-1}$, and $^{238}\text{U}/^{235}\text{U} = 137.88$. 1 σ errors.

Grain - spot	U ppm	Th ppm	232/238	%common 206 Pb	207/206	206/238	207/235	207/206 age [Ma]
J1 1-1	15	8	.555	5.8	.1834 ± 34	.496 ± 8	12.54 ± .32	2684 ± 31
J1 1-2	9	3	.424	7.6	.1974 ± 41	.553 ± 12	15.05 ± .42	2805 ± 34
J1 1-3	17	9	.592	2.2	.1586 ± 28	.412 ± 6	9.01 ± .21	2441 ± 30
J1 2-1	9	3	.423	16.8	.1357 ± 70	.399 ± 9	7.47 ± .42	2173 ± 90
J1 2-2	12	6	.495	8.3	.1288 ± 39	.377 ± 7	6.70 ± .25	2082 ± 53
J1 2-3	10	4	.414	6.5	.1362 ± 41	.372 ± 7	6.99 ± .25	2180 ± 52
J1 3-1	5	2	.435	11.5	.1736 ± 62	.412 ± 11	9.86 ± .44	2593 ± 60
J1 3-2	7	3	.433	7.6	.1675 ± 50	.492 ± 12	11.36 ± .45	2533 ± 50
J1 3-3	6	2	.450	8.4	.1797 ± 50	.491 ± 12	12.17 ± .45	2650 ± 46
J1 3-4	19	13	.726	5.6	.1818 ± 38	.456 ± 7	11.43 ± .30	2669 ± 35
J1 3-5	9	4	.505	8.0	.1641 ± 47	.439 ± 10	9.93 ± .35	2498 ± 48
J1 5-1	5	6	1.342	12.9	.1320 ± 79	.383 ± 11	6.97 ± .49	2125 ± 105
J2 7-1	7	2	.391	8.3	.1817 ± 46	.503 ± 12	12.60 ± .45	2668 ± 42
J2 7-2	7	2	.389	9.7	.1890 ± 50	.490 ± 11	12.77 ± .46	2733 ± 44
J2 7-3	7	2	.400	9.4	.1836 ± 50	.429 ± 10	10.86 ± .45	2686 ± 45
J2 9-1	1	<1	.373	44.7	.1722±464	.586 ± 58	13.9 ± 4.0	2579±465

Grain - spot	U ppm	Th ppm	232/238	%common 206 Pb	207/206	206/238	207/235	206/238 age [Ma]
J1 4A-1	31	5	.180	14.2	.051 ± 7	.0361 ± 6	.255 ± 39	229 ± 4
J2 1-1	31	5	.192	21.2	.053 ± 8	.0352 ± 5	.259 ± 44	223 ± 3
J2 2-1	18	3	.169	33.0	.054 ± 16	.0368 ± 8	.272 ± 88	233 ± 5
J2 3-1	39	8	.205	12.7	.058 ± 6	.0378 ± 5	.304 ± 32	239 ± 3
J2 4-1	33	6	.190	24.6	.064 ± 10	.0366 ± 6	.321 ± 52	232 ± 4
J2 5-1	61	12	.211	13.9	.059 ± 6	.0370 ± 5	.301 ± 30	234 ± 3
J2 6-1	71	14	.207	12.1	.047 ± 5	.0344 ± 4	.225 ± 25	218 ± 3
J2 11-1	44	8	.207	16.1	.052 ± 6	.0375 ± 5	.270 ± 34	237 ± 3
J2 12-1	19	3	.179	26.1	.049 ± 11	.0384 ± 7	.257 ± 67	243 ± 4

Table 2: SHRIMP Hf isotopic analyses of zircons from the Jwaneng Kimberlite, Botswana. Uncertainties in $^{176}\text{Hf}/^{177}\text{Hf}$ and in age are the standard error, based on counting statistics. %HfO₂ and Zr/Hf are from electron-probe analyses. The measured $^{176}\text{Lu}/^{177}\text{Hf}$ was calculated as $0.5 \times ^{176}\text{LuO}^+ / ^{177}\text{HfO}^+$ (as observed for zircon standards). Ages were modelled on an unfractionated chondritic mantle reservoir (Patchett, 1983) using $\lambda^{176}\text{Lu} (\beta^-) = 1.94 \times 10^{-11} \text{ y}^{-1}$.

Grain	%HfO ₂	Zr/Hf	measured $^{176}\text{Lu}/^{177}\text{Hf}$	measured $^{176}\text{Hf}/^{177}\text{Hf}$	initial $^{176}\text{Hf}/^{177}\text{Hf}$	model age [Ga]
J2 7	0.68	167	.00022	.28042 ± 12	.28041	3.58 ± .17
J2 9	0.81	139	.00032	.28070 ± 10	.28068	3.18 ± .15
J2 11	0.51	223	.00001	.28300 ± 14	as measured	-0.20 ± .19
J2 12	0.60	191	.00004	.28286 ± 13	as measured	0.01 ± .18

REFERENCES

- AHRENS L.H., CHERRY R.D. and ERLANK A.J. 1967. Observations on the Th-U relationship in zircons from granitic rocks and from kimberlites. *Geochimica et Cosmochimica Acta* 31, 2379-2387.
- BOYD F.R. and NIXON P.H. 1973. Origin of the ilmenite-silicate nodules in kimberlites from Lesotho and South Africa. In Nixon P.H. ed, *Lesotho Kimberlites*, pp 254-268, LNDC, Maseru, Lesotho.
- COMPSTON W., WILLIAMS I.S. and MEYER C. 1984. U-Pb geochronology of zircons from Lunar breccia 73217 using a sensitive high mass-resolution ion microprobe. *Journal of Geophysical Research* 89 Supplement, B525-534.
- DAVIS G.L., KROGH T.E. and ERLANK, A.J. 1976. The ages of zircons from kimberlites from South Africa. *Carnegie Institute of Washington Yearbook* (1975), 821-824.
- DAVIS G.L. 1977. The ages and uranium contents of zircons from kimberlites and associated rocks. *Carnegie Institute of Washington Yearbook* (1976), 631-635.
- KRESTEN P., FELS P. and BERGGREN G. 1975. Kimberlitic zircons - A possible aid in prospecting for kimberlites. *Mineralium Deposita* 10, 47-56.
- MATTINSON J.M. 1978. Age, origin, and thermal histories of some plutonic rocks from the Salinian Block of California. *Contributions to Mineralogy and Petrology* 67, 233-245.
- PATCHETT P.J. 1983. Importance of the Lu-Hf isotopic system in studies of planetary chronology and chemical evolution. *Geochimica et Cosmochimica Acta* 47, 81-91.
- RICHARDSON S.H., GURNEY J.J., ERLANK A.J. and HARRIS J.W. 1984. Origin of diamonds in old enriched mantle. *Nature* 310, 198-202.

H. Lucas¹, R. Ramsay¹, A. E. Hall¹, C. B. Smith¹ and N. V. Sobolev²

1. CRA Exploration Pty Limited, Belmont, Western Australia

2. Academy of Geological Sciences, Novosibirsk, Siberia

INTRODUCTION

This study is a survey of garnet chemistry from selected kimberlites, olivine lamproites and related rocks in Western Australia. Garnets were selected from heavy mineral concentrates, analysed, classified into Dawson and Stephens (1975) cluster groups (D & S Gp No. 1-12) and plotted on CaO vs Cr₂O₃ diagrams of Sobolev (1964) and Gurney (1984). Comparisons of the garnet types occurring in lamproite and kimberlite, diamondiferous and non-diamondiferous bodies, in different structural settings and of different intrusive ages, were made. The similarities of the Western Australian garnets with non-Australian kimberlite garnet analyses and their implications to the nature of the deep crust and mantle are discussed.

LOCALITIES STUDIED

West Kimberley: Ellendale Pipes

Three diamondiferous, olivine lamproite pipes, Ellendale 4, 7, and 9 were selected for study from the more than 100 Miocene intrusions in the West Kimberley province (Jaques et al 1984). The lamproites intrude the Lennard Shelf and adjacent Fitzroy basin where Upper Palaeozoic and early Mesozoic sediments overly deformed crystalline basement stabilized around 1800 Ma ago. Megacryst minerals occurring with garnet include titaniferous magnesiochromite, chrome-diopside, olivine, orthopyroxene, rutile, corundum, kyanite, staurolite and andalusite. Ellendale 4 and 9 garnet is dominated by crustal almandine which is absent in Ellendale 7 and this probably reflects rock type variability in the crystalline basement. Most of the Ellendale chrome-pyropes analyses (D & S Gp 9) plot within the lherzolitic field of Sobolev (1964) but rare subcalcic chrome-pyrope (D & S Gp 10) was recovered from Ellendale 7 and 9. A wehrlitic garnet (D & S Gp 11) and titanian pyrope (D & S Gp 1 and 2) similar to megacrystal garnets (Nixon and Boyd 1973b) occur in Ellendale 7. Calcic pyrope-almandine (D & S Gp 3 and 6), with elevated Na₂O content suggestive of mantle eclogites, is also present.

East Kimberley: Maude Creek, Argyle, Bow Hill

The East Kimberley region contains kimberlites, lamproites and lamprophyres intruding the 1800 Ma cratonised Halls Creek Mobile Zone or the adjacent eastern margin of the Kimberley Block.

The Argyle olivine lamproite is a richly diamondiferous pipe which intrudes the Halls Creek Mobile Zone and is dated at 1200 Ma (Pidgeon et al, this volume). Macrocryst minerals are rare but magnesiochromite, garnet, chrome-diopside, orthopyroxene and magnesium-ilmenite have been recovered. Almandine of probable crustal origin is the dominant garnet. Of the rare pyropes present, chrome-pyrope is the most common. Titanian pyrope (D & S Gp 1) and calcic pyrope-almandine (D & S Gp 3) do occur but no subcalcic ones have been recovered.

The diamondiferous micaceous Maude Creek kimberlite dyke, with its abundant magnesium-ilmenite and pyrope garnet intrudes the eastern edge of the Kimberley Block. Titanian pyropes (D & S Gp 1 and 2) similar to the Lesotho megacrystal garnets (Nixon and Boyd, 1973b) predominate. Lherzolitic chrome-pyrope (D & S Gp 9 and 11) is also common and several subcalcic chrome-pyropes (D & S Gp 10) were recovered.

West of Argyle is Bow Hill, a non-diamondiferous lamprophyric dyke-swarm (Jaques and Fielding, this volume) intruding the Lower Proterozoic granites of the Halls Creek Mobile Zone and has been dated at 815 Ma (Pidgeon et al this volume). Macrocryst minerals include garnet, chrome-diopside, orthopyroxene and magnesiochromite.

Andradite with significant levels of TiO_2 , Nb_2O_5 and ZrO_2 is the dominant garnet recovered. Chrome-bearing lherzolitic garnets (D & S Gp 9) and calcic pyrope-almandines (D & S Gp 3) of likely crustal origin are also present.

North Kimberley: Skerring and Hadfields Creek

The Skerring pipe 802 Ma (Pidgeon et al this volume) and Hadfields Creek dyke are non-diamondiferous, micaceous kimberlites intruding the north of Kimberley Block. The heavy mineral concentrates are characterized by coarse magnesium-ilmenite and pyrope. Skerring also contains subcalcic diopside, chrome-diopside, rutile, zircon and graphitic intergrowths of silica with ilmenite. Titanian pyrope (D & S Gp 1 and 2), similar to Lesotho megacrystal garnets (Nixon and Boyd, 1973b), is the most common garnet type. Chrome-pyrope analyses from Skerring plot mostly within the lherzolitic field of Sobolev (1964) but the Hadfields Creek analyses are displaced into the wehrlitic field with increasing Cr_2O_3 content. A high-calcium chrome wehrlitic pyrope was recovered from Skerring. Rare subcalcic chrome-pyrope (D & S Gp 10) and few eclogitic garnets (D & S Gp 3 and 6) also occur.

Carnavon Basin: Wandagee

Intruding the Phanerozoic Carnavon Basin to the west of the Pilbara craton are 22 kimberlite-like diatremes, associated picrite sills and dykes (Kerr et al this volume) emplaced at about 160 Ma (Atkinson et al 1984). Two occurrences contain very rare microdiamonds. The macrocryst minerals in the concentrates usually include magnesiochromite, chrome-diopside, garnet, magnesium-ilmenite, magnetite, olivine and zircon. Crustal almandine is common. While chrome-bearing pyropes (D & S Gps 1, 9 and 11) are prevalent their analyses are displaced to higher levels in Sobolev (1964) lherzolitic field because of greater calcium contents.

CONCLUSIONS

Garnets from the selected Western Australian sources appear to be chemically similar to those from non-Australian kimberlites. This implies that similar chemical, pressure and temperature conditions prevail under stable cratons here, as for those elsewhere in the world. Peridotitic garnets (D & S Gps 1, 9 and 11) predominate over mantle derived eclogitic garnets (D & S Gp 3 and 6) in all occurrences studied. This contrasts to the garnet varieties occurring as inclusions in Argyle diamonds where eclogitic garnets are dominant and from Ellendale diamonds where eclogitic and peridotitic varieties occur in approximately equal proportions (Hall and Smith, 1984).

Western Australian kimberlites are characterised by abundant megacrystal, titanian pyrope (D & S Gp 1 and 2) which is rarely recovered from the lamproites. Subcalcic chrome-pyrope from the kimberlites and Ellendale lamproites suggests garnet harzburgite occurs as a widespread component of the mantle but the relative abundance of these garnets can not be related to the diamond content of the occurrences, for example non-diamondiferous Skerring contains subcalcic garnets. The relatively calcic peridotitic garnets from Wandagee support a more fertile mantle in the structurally "off craton" environment. The Bow Hill andradite garnet which is rare or unknown in kimberlites, suggests this lamprophyre may be related to alnoite or melilitite.

Variations in garnet composition within and between the studied occurrences support the vertical and horizontal heterogeneity of the mantle under north-western Australia.

REFERENCES

- ATKINSON W. J. et al 1984. A review of the Kimberlitic Rocks of Western Australia. In Kornprobst J. ed, Kimberlites, Vol 1, pp 195 - 224. Elsevier, Amsterdam-Oxford-New York-Tokyo.
- DAWSON, J. B. & STEPHENS, W. E. 1975. Statistical Analysis of Garnets from Kimberlites and Associated Xenoliths. *Journal of Geology* 83, 580 - 607.

FIELDING, D. C. & JAQUES, A. L. 1986. Geology, petrology and geochemistry of the Bow Hill lamprophyre dykes. This volume.

GURNEY, J. J. 1984. A Correlation Between Garnets and Diamonds in Kimberlites. In Glover, J. E. and Harris, P. G. eds, Kimberlite Occurrence and Origin: A Basis for Conceptual Models in Exploration. The University of Western Australia. Pub. No. 8, 143 - 166.

HALL, A. E. & SMITH, C. B. 1984. Lamproite Diamonds - Are They Different? In Glover, J. E. and Harris, P. G. eds, Kimberlite Occurrence and Origin: A Basis for Conceptual Models in Exploration. The University of Western Australia. Pub. No. 8, 167-212.

JAQUES, A. L., LEWIS, J. D., SMITH, C. B., FERGUSON, J., CHAPPELL, B. W. & McCULLOCH, M. T., 1984. The diamond-bearing ultrapotassic (lamproitic) rocks of the West Kimberley region, Western Australia; In Kornprobst, J. (Ed), Kimberlites. 1: Kimberlites and Related Rocks, pp.225-254, Elsevier, Amsterdam.

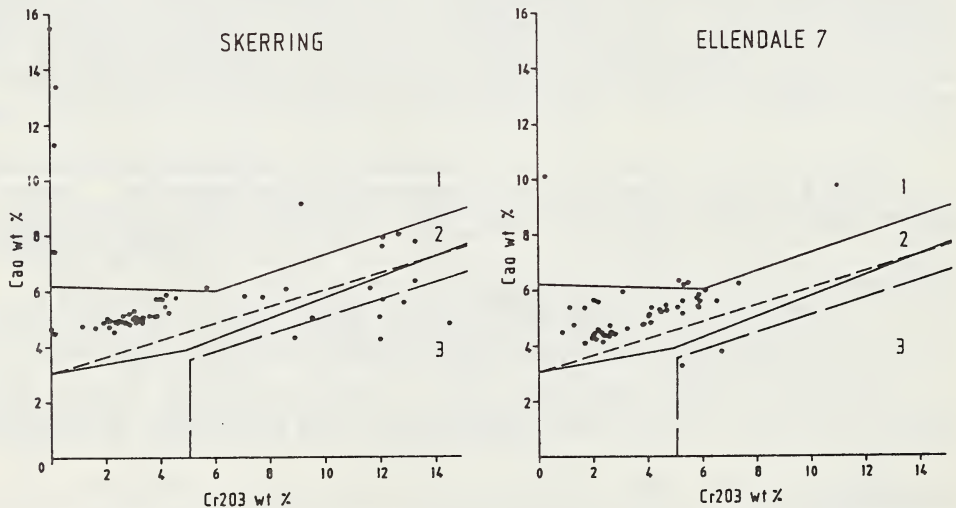
KERR, I., LUCAS, H. & JAQUES, A. L. 1986. Alkali picrites of Wandagee. This volume.

NIXON, P. H. & BOYD, F. R. 1973b. The Discrete Nodule Association in Kimberlites From Northern Lesotho. In Nixon, P. H. ed, Lesotho Kimberlites, Lesotho Natural Development Corporation Maseru, 67-75.

SMITH, C. B. & PIDGEON, R. T. 1986. The ages of the kimberlitic rocks of Western Australia. This volume.

SOBOLEV, N. V. 1977. Deep Seated Inclusions in Kimberlites and the Problem of the Composition of the Upper Mantle. (Transl. D. A. Brown). Boyd, F. R. ed, A G U., Washington.

SCBOLEV, N. V. 1964. The Physiochemical Conditions of Mineral Formation in the Crust and Mantle. Geologiya Geofiziya Novosibirsk 1, 7-22.



Representative plots of CaO vs Cr₂O₃ (wt%) for garnets from SKERRING & ELLENDALE 7

LEGEND • 1 - Wehrlitic field. 2 - Lherzolititic field 3 - Harzburgitic field
 - - - - 85% line Gurney (1984)

E.A. Mathez¹, J.D. Blacic², J. Beery³, C. Maggiore³, and M. Hollander³

(1) Dept. of Geological Sciences, University of Washington, Seattle, WA 98195 U.S.A.

(2) Dept. of Earth and Space Sciences and (3) Dept. of Physics, Los Alamos National Laboratory, Los Alamos, NM 87545 U.S.A.

INTRODUCTION

The possibility that C and H may dissolve in greater than trace amounts in silicates that are nominally volatile-free has important consequences for mantle petrology and mechanics. If, for example, silicates are important reservoirs for C and H, then the stabilities of fluids, graphite, diamond and other volatile-rich phases would depend on the modal mineralogy of the mantle and solubilities of the volatile elements in its constituent phases. In fact, a significant solubility for C in olivine and other minerals has been proposed in a series of papers by F. Freund and coworkers (1,2,3,4,5). In these studies it is argued (1) that C becomes concentrated in near-surface regions of olivine and other materials, reaching concentrations of greater than 2 at.% within about 5000 Å of the crystal surfaces and on the order of 10^3 - 10^4 ppm 1-2 microns below the surface; (2) that these high surface concentrations result from the rapid diffusion of C from the crystal interiors; and (3) that C is present in a truly dissolved state, existing "atomically" (i.e., in the ground state) in both extrinsic cation vacancies and interstitial sites.

These assertions have been disputed in two recent studies. First, Mathez et al. (6) were unable to detect significant concentrations of C in one of two mantle olivine crystals using the same nuclear reaction analysis (NRA) technique employed in the Freund studies. The second crystal was found to contain C, but it was interpreted to represent C in inclusions or cracks rather than in solution. Second, Tsong et al. (7), in a study of the behavior of C on mineral surfaces, attributed the supposed diffusion properties of C to surface contamination. As a consequence of this disagreement, a more detailed study of C solubility in olivine using NRA has been conducted.

NUCLEAR REACTION ANALYSIS

The importance of NRA is that it can be used for in situ microanalysis of trace quantities of certain light elements in solid targets and that for some of these elements distinction can be made between their surface and bulk concentrations. A beam of light ions from an accelerator can be used to create nuclear reactions involving target atoms if the beam energies are sufficient to overcome the coulomb barriers of the nuclei. Nuclear reactions are customarily expressed in a shorthand form such that $j(k,x)y$ describes a reaction in which j is the target nucleus, k the incident particle, x the reaction produce and y the residual nucleus. Useful analytical reactions include $^{12}\text{C}(d,p)^{13}\text{C}$, $^{16}\text{O}(d,\alpha)^{14}\text{N}$, $^{19}\text{F}(p,\alpha)^{16}\text{O}$, $^{11}\text{B}(p,\alpha)^8\text{Be}$ and $^2\text{H}(d,p)^3\text{H}$, where d , p and α indicate a deuteron, proton and alpha particle, respectively. The analytical rationale is that energies of the emitted particles are "characteristic" for specific incident particle energies and that their intensities are proportional to concentrations.

For d - p reactions, the proton spectrum also provides information on the concentration of target nuclei as a function of depth (Fig. 1). The concentration of C in the bulk target is represented by the integrated signal (shaded), excluding that from the surface. In the case of olivine, the bulk signal originates from 2000 Å to 3 microns below the surface. The distinction between surface and bulk concentrations is particularly important in the case of C because most materials readily adsorb C from the atmosphere, and thus their surfaces are severely contaminated.

The experiments were conducted using the Van de Graaff accelerator at Los Alamos National Laboratory. A 1.3 MeV deuteron beam was focused with a superconducting magnet. Although beam diameters of < 20 microns can be achieved, thermal and radiation damage of the olivine limited the minimum beam size to 125 microns. The energy resolution of the entire system is 20 KeV, which corresponds to a depth resolution

(Fig. 1) of $\sim 1700 \text{ \AA}$ in olivine. This means that C concentrations can be determined in individual layers 1700 \AA thick and 125 microns wide.

A major problem of the NRA technique for C analysis is that there is a significant interference in the C proton spectrum from d-p reactions involving Mg and Si. For a typical mantle olivine, Mg and Si account for backgrounds that are equivalent to 700 and 100 ppm at. C, respectively. These important background components contribute significantly to the magnitude of the detection limit, which for olivine is computed at 65 ppm at. from consideration of counting statistics only. An important requirement of the technique is that the analytical surface must be flat over the region of the beam. For rough surfaces, the proton signal from surface C is smeared to lower energies and thus yields an apparent bulk C signal. Some previous studies may have suffered from an incomplete knowledge of the background and problems associated with surface roughness. As a check on accuracy and analytical procedure, a C-bearing diopside glass was analyzed (Fig. 2A). Analysis by NRA indicated a C content of 2.4 at.%, which compares with a concentration of 2.2 % obtained by electron probe. A typical olivine spectrum is shown in Fig. 2B.

RESULTS

Olivine crystals from four different geological environments but of similar compositions (Fog₀₋₉₂) were studied. None of the samples were found to contain C in detectable quantities, i.e., in concentrations $> 65 \text{ ppm at.}$ ($= 37 \text{ ppm wt.}$). The samples include: (a) Four gem-quality crystals from Zabargad Island (Red Sea), Egypt. Fluid inclusions indicate that they crystallized under shallow crustal conditions in the presence of hypersaline fluid (8). (b) Crystals separated from Group 1 spinel lherzolite xenoliths and mantle-derived megacrysts from alkali basalts from the southwest USA. They are believed to have recrystallized in the presence of CO₂-dominated fluids at pressures of 6-8 kb. (c) Two San Carlos megacrysts, one of which was held in contact with graphite and the other with magnesite at 30 kb and 1400°C for 24 hours. The samples were prepared by Trace Tingle as part of a separate study on C solubility. The regions analyzed include those within 100 microns of the contacts between the olivines and C-rich phases. (d) Olivines from two granular garnet lherzolite xenoliths from the Finsch kimberlite pipe, RSA. One of the xenoliths contains diamond, and compositions of coexisting phases from it and other Finsch lherzolites indicate equilibration conditions of $> 50 \text{ kb}$ and $\sim 1130^\circ\text{C}$ (9).

It is concluded that the solubility of C in olivine is negligible under all conditions found in the crust and upper mantle and that analytical problems likely plagued some of the earlier experiments to the extent that their reliability is questionable.

REFERENCES

- (1) Freund, F., H. Kathrein, H. Wengeler, R. Knobel, and H. Heinen, 1980, *Geochim. Cosmochim. Acta*, 44, 1319.
- (2) Freund, F., 1981, *Contrib. Mineral. Petrol.*, 76, 472.
- (3) Wengeler, H., R. Knobel, H. Kathrein, F. Freund, G. DeMortier, and G. Wolff, 1982, *J. Phys. Chem. Solids*, 43, 59.
- (4) Kathrein, H., H. Gonska, and F. Freund, 1983, *Appl. Phys.*, 6, 241.
- (5) Oberheuser, G., H. Kathrein, G. DeMortier, H. Gonska, and F. Freund, 1983, *Geochim. Cosmochim. Acta*, 47, 1117.
- (6) Mathez, E., J. Blacic, J. Beery, C. Maggiore, and M. Hollander, 1984, *Geophys. Res. Lett.*, 11, 947.
- (7) Tsong, I.S.T., U. Knipping, C. Loxton, C. Magee, and G. Arnold, 1985, *Phys. Chem. Mineral.*, 12, 261.
- (8) Clocchiatti, R., D. Massare, and C. Jehanno, 1981, *Bull. Mineral.*, 104, 354.
- (9) Shee, S., J. Gurney, and D. Robinson, 1982, *Contrib. Mineral. Petrol.*, 81, 79.

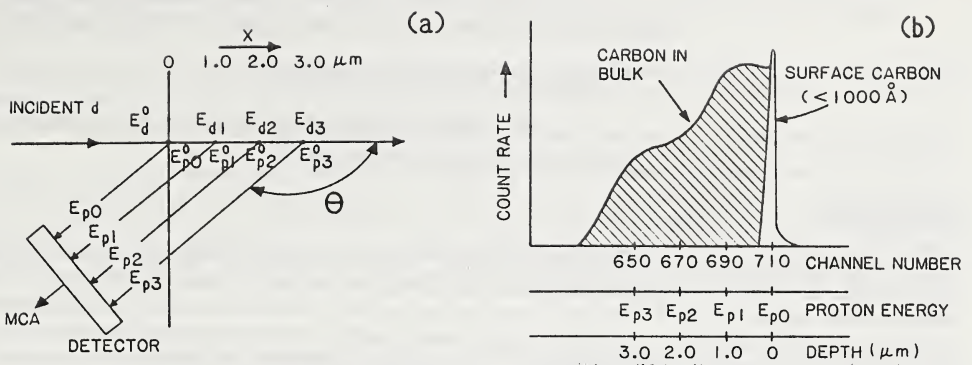


Figure 1. (a) Illustration of the $^{12}\text{C}(d,p)^{13}\text{C}$ nuclear reaction technique. Deuterons of initial energy E_d^0 lose energy as they penetrate the target, acquiring energies of E_{d1} , E_{d2} , and E_{d3} at depths of 1, 2, and 3 microns. Protons produced at corresponding depths have initial energies such that $E_{p1}^0 > E_{p2}^0 > E_{p3}^0$. The proton energies are dependent on deuteron energies at specific depths and the energy inherently released by the nuclear reaction. Protons lose energy as they escape from the target and at the detector possess energies $E_{p0} = E_{p0}^0 > E_{p1} > E_{p2} > E_{p3}$. (b) An idealized proton spectrum from a target containing C in its bulk. Note the correspondence of channel number, proton energy and depth. The complex shape of the spectrum is partly due to the variation with depth of nuclear cross sections of target atoms for deuterons. Modified from ref. (5) and (6).

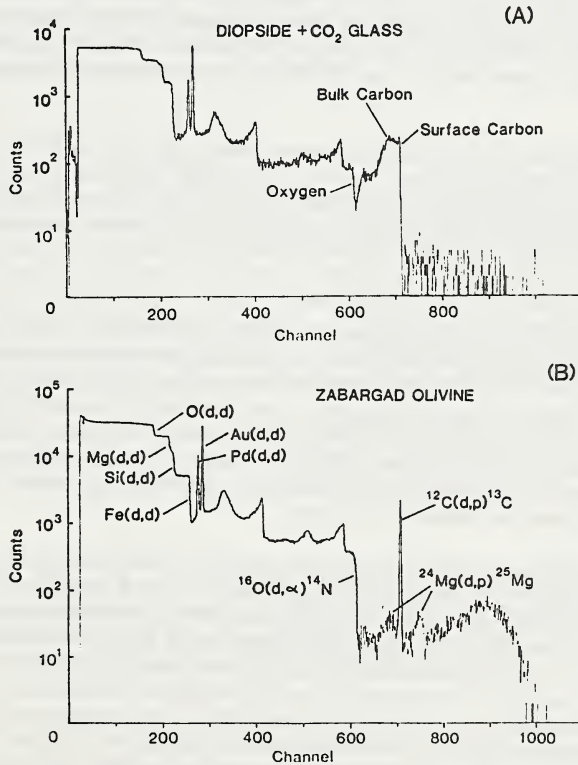


Figure 2. Particle spectra of (a) diopside + CO_2 glass and (b) Zabargad olivine (Fo_{92}). The glass contains 2.2 at. % C. Carbon in the olivine spectrum is atmospheric contamination and within 1000–1400Å of the surface. Most of the background above channel 614 is due to Mg, with a small contribution from Si.

ABUNDANCES AND CARBON ISOTOPE COMPOSITIONS OF TRAPPED FLUIDS IN MANTLE DIOPSIDES: IMPLICATIONS FOR MANTLE RECYCLING MODELS

D.P. Matthey, C.T. Pillinger and M.A. Menzies*

Department of Earth Sciences, The Open University, Walton Hall, Milton Keynes MK7 6AA, U.K.; * Royal Holloway and Bedford New College, Egham, Surrey, U.K.

INTRODUCTION

The stable isotopic compositions of both carbon in CO_2 ($\delta^{13}\text{C} = -9$ to -15% rel. to PDB) and hydrogen in H_2O ($\delta\text{D} = -32\%$ to -46% rel. to SMOW) in back arc basin basalts are different from normal mid-ocean ridge basalts ($\delta^{13}\text{C} = -6.5\%$ and $\delta\text{D} = -80\%$, respectively) [1,2]. This observation provides important evidence for recycling of volatile components from subducted lithosphere and suggests that light element isotope ratios potentially act as sensitive tracers of recycled crustal components in mantle processes. The ubiquitous presence of fluid inclusions in mantle minerals offers a direct means of studying the relationship between mantle volatiles and the petrology and geochemistry of host nodules and magmas. We have used stepped heating, vacuum crushing and high sensitivity mass spectrometry to measure the abundance and isotopic composition of CO_2 in diopsides separated from exceptionally well preserved mantle nodules.

SAMPLE LOCALITIES AND ANALYTICAL TECHNIQUES

Carbon abundances and isotope ratios have been determined on diopsides previously characterised for He, Sr, Nd abundances, and $^3\text{He}/^4\text{He}$, $^{87}\text{Sr}/^{86}\text{Sr}$, $^{143}\text{Nd}/^{144}\text{Nd}$ ratios. Host magmas include kimberlite, carbonatite and a variety of orogenic and anorogenic basaltic hosts from the following localities: 1. Bulfontein, South Africa (micaceous garnet lherzolites in kimberlite host); 2. Bullenmerri Maar, Victoria, Australia (garnet lherzolites in basalt host); 3. Foster Crater, Antarctica (pyroxenites and glimmerites in basanite host); 4. Lashaine, Tanzania (garnet lherzolite, pyroxenite in ankaramite, carbonatite host); 5. Auvergne, France (spinel lherzolite in basanite host); 6. Ichinomegata, Japan (spinel lherzolite in basalt host); 7. Geronimo Volcanic Field, Arizona, USA (spinel lherzolite, pyroxenites in basanite host).

Handpicked diopside grains (5-15 mg) were ultrasonically cleaned in 2M HCl, distilled water and dichloromethane, dried at 110°C , and then degassed in the vacuum system at 150°C to 10^{-6} torr. Carbon was released from the sample by stepped heating in 1 atmosphere of pure oxygen in 100°C steps from 300°C to 1300°C . Carbon isotopes were measured on CO_2 using a triple collector static vacuum mass spectrometer to a precision of better than $\pm 1\%$.

RESULTS

Stepped heating clearly resolves two isotopically distinct carbon components in all the samples. The first component dominates the release profile and is released by oxidation with a maximum release peak at 400°C . This component has a uniform isotopic composition ($-28 \pm 2\%$) and is believed to be surficial organic contamination. A second isotopically distinct component is released at higher temperatures, usually above 800°C . This form of carbon is indigenous and may be derived from a number of possible sites. These include 1) CO_2 (and possibly CO and CH_4) released by the decrepitation of fluid inclusions; 2) molecular CO_2 (or other gaseous carbon species) contained within the diopside lattice; 3) decomposition of carbonate species, existing within the lattice, as veins or as daughter crystals in fluid inclusions; 4) oxidation of reduced carbon (eg. graphite).

Combined pyrolysis/combustion heating experiments suggest that elemental carbon or CO are not present in the samples studied and that CO_2 is the principle species released. The source of this CO_2 is probably from fluid inclusions, or from the lattice. Vacuum crushing experiments confirm that the contents of the pseudo-secondary and secondary fluid inclusions which characterise some samples are pure CO_2 . Other samples do not contain visible fluid inclusions, do not produce CO_2 on vacuum crushing and yet release significant quantities CO_2 at high temperatures ($> 1000^\circ\text{C}$). This carbon must exist as molecular CO_2 (or CO_3^{2-}) within the diopside lattice. In general, the origin of CO_2 released at high temperatures is most likely to be lattice CO_2 , with a variable contribution from fluid inclusions, according to their abundance, size, and dimensions of their host mineral grain. CO_2 from fluid inclusions appears to be released over a wide temperature range, and can partially be masked by the low temperature contamination release (200°C to 600°C). However, carbon released at high temperatures by stepped heating is wholly indigenous, dominantly released from the diopside lattice, and could be closely associated with the crystallisation environment of the diopside.

C-He-REE abundances in diopsides

Carbon abundances, measured by stepped heating or by vacuum crushing can be subject to large errors because of uncertainties as to the efficiency of the extraction technique. Nevertheless, carbon abundances reveal surprisingly good correlations with He and rare earth element (REE) abundances.

Figure 1 is a plot of C versus He for Bullenmerri samples and shows that amphibole bearing xenoliths with elevated $^{87}\text{Sr}/^{86}\text{Sr}$ ratios (0.7040-0.7065) have high C/He ratios; diopsides from anhydrous lherzolites and pyroxenites with lower, uniform $^{87}\text{Sr}/^{86}\text{Sr}$ ratios (0.7037-0.7040) have low C/He ratios. Whereas $^3\text{He}/^4\text{He}$ ratios in diopsides from Bullenmerri are relatively uniform ($R/R_A = 6 - 10$) and are completely decoupled from $^{87}\text{Sr}/^{86}\text{Sr}$ ratios [3], the C/He and carbon isotope ratios indicate that fluids from different sources are associated with hydrous and anhydrous mantle facies.

Carbon versus Nd for all samples is plotted in Figure 2 (note log-log scale) and shows a broad positive correlation. Diopsides hosted by kimberlite from Bulfontein (South Africa) are amongst the most carbon rich (10 ppm to 425 ppm) and have high C/Nd ratios. Diopsides from Bullenmerri (Australia), Auvergne (France), Foster Crater (Antarctica) and Geronimo (Arizona) generally contain less C (1 ppm to 62 ppm) with a range of lower C/Nd ratios. Light REE enriched diopsides (with Sm/Nd ratios < 0.33) are generally carbon rich and light REE depleted diopsides contain less than 3 ppm C which suggests that under certain circumstances CO_2 and the light rare earth elements may be coupled.

C-Nd isotopes in diopsides

Carbon isotopes measured in this study vary from -3‰ to -32‰, but with most data typically falling within the range -8‰ to -12‰. $\delta^{13}\text{C}$ values appear to vary systematically with REE abundances, $^{87}\text{Sr}/^{86}\text{Sr}$ and $^{143}\text{Nd}/^{144}\text{Nd}$ particularly in diopsides from Bulfontein and Bullenmerri. Figure 3 shows a plot of $\delta^{13}\text{C}$ versus $^{143}\text{Nd}/^{144}\text{Nd}$. Carbon in diopsides from Bulfontein varies from -8.5‰ to -13‰ and shows a positive correlation with $^{143}\text{Nd}/^{144}\text{Nd}$. Similar trends are apparent for diopsides from hydrous and anhydrous lherzolites from Bullenmerri, implying that the trace element enrichment events thus preserved are associated with isotopically light carbon.

DISCUSSION

Isotopically variable CO_2 ($\delta^{13}\text{C}$ ranging from -31‰ to -3‰) occurs in mantle environments closely related to active or recent subduction (eg. back arc basins [1], Ichinomegata and Geronimo (Figure 3)) which strongly implicate a sedimentary carbon component derived from the subducted slab. This isotopic variation (approximately 30 ‰) approaches the range in limiting compositions of carbon in pelagic sediments (ie. organic carbon to marine carbonate). Although diamonds display a similar range in carbon isotopes the variation so far observed in diopsides representing subcontinental lithosphere is more restricted (-8‰ to -15‰) and slightly lower than typical MORB $\delta^{13}\text{C}$ values. Fluid compositional heterogeneity found within nodule suites and even within single grains, and decoupling of $^3\text{He}/^4\text{He}$ from solid chemistry and other fluids requires several sources, with at least one source having close affinities with MORB.

A possible interpretation of the C-He-Nd data is that subcontinental lithosphere preserves relict carbon isotope heterogeneity, possibly primordial, but more probably related to ancient subduction events, which has either overwriten, or has been overwriten by, other fluids with MORB-source characteristics.

References:

1. Mathey D.P., Carr R.H., Wright I.P and Pillinger C.T., 1984. Carbon isotopes in submarine basalts. Earth and Planetary Science Letters, 70, 196-206.
2. Poreda, R., 1985. Helium-3 and deuterium in back-arc basalts: Lau Basin and the Mariana Trough. Earth and Planet. Sci. Letts., 73, 244-254.
3. Porcelli, D.R., O'Nions, R.K. and O'Reilly, S.Y., 1986. Helium and strontium isotopes in ultramafic xenoliths. Chem. Geol., in press.

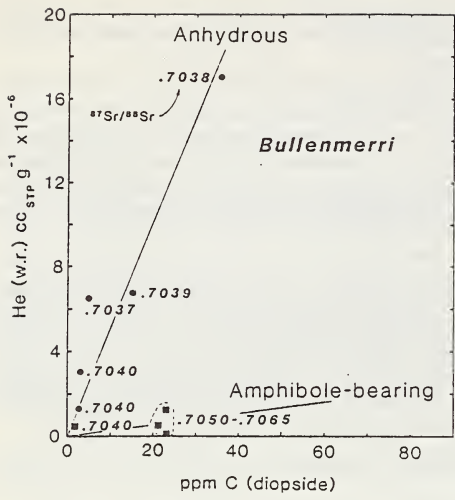


Figure 1

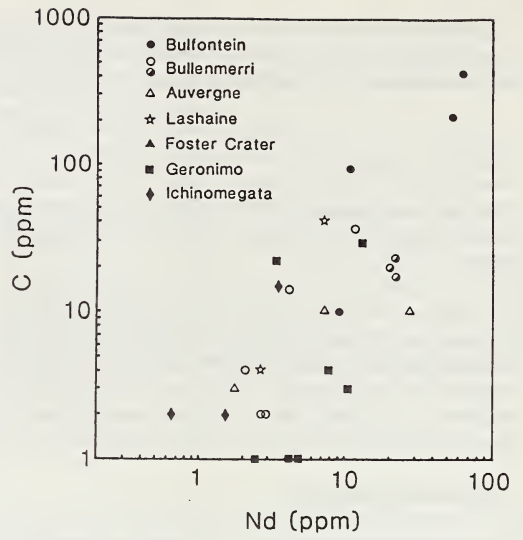


Figure 2

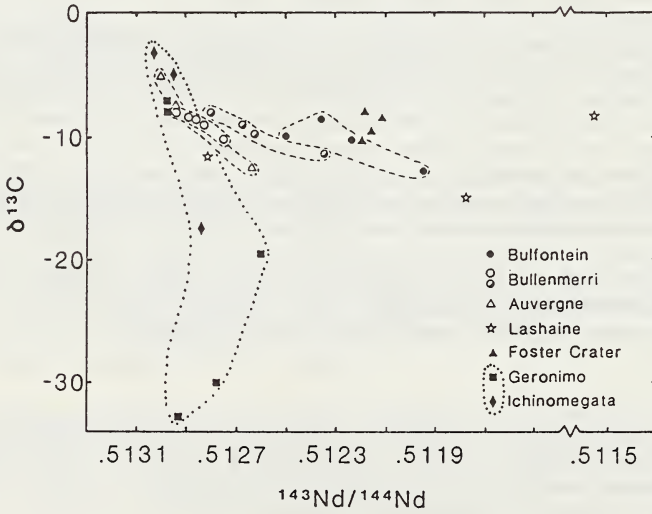


Figure 3

Corganites and corgaspinites: Two new types of aluminous assemblages
from the Jagersfontein kimberlite pipe

Peter Mazzone and Stephen E. Haggerty
Dept. of Geology, University of Massachusetts, Amherst, Mass. USA
4th International Kimberlite Conference

INTRODUCTION. Two new varieties of peraluminous xenoliths related to alkremites have been recovered from the Jagersfontein kimberlite pipe, South Africa. This paper will highlight some of the physical, petrographic and chemical characteristics of these nodules, compare them with alkremite samples, also from Jagersfontein, and provide a tentative working hypothesis concerning their origin.

SAMPLES AND PETROGRAPHY. The present nodule suite consists of 56 samples which can be categorized into 3 groups: a garnet+spinel assemblage (alkremite), a corundum+garnet assemblage (corganite) and a corundum+garnet+spinel assemblage (corgaspinite).

The alkremite nodules are similar to others previously described from Bellsbank and Jagersfontein kimberlites, South Africa^{1,2} and kimberlites from Moses Rock Dike, Utah³. They typically occur as oval nodules (up to 5 cm in length) containing flesh colored garnet and black spinel. The modal abundances of these two minerals are highly variable and rare samples contain >90% spinel while others consist of >90% garnet. Accessory phases may include any combination of clear corundum, brown pleochroic phlogopite and calcite confined to cracks and grain boundaries. In addition, clear anhedral pyroxene grains (usually < 1 mm) enclosing tan pleochroic amphibole, phlogopite and microscopic euhedral green spinels are confined to garnet cores. The corundum bearing corganites and less abundant corgaspinites are similar in size and shape to the alkremites but are easily distinguished from them by the presence of light to dark blue sapphire and rare ruby grains which vary widely in size (up to 1 cm) and abundance (5 to 75%). In many cases the corundum and, more rarely, the spinel grains in these assemblages are confined to discrete layers, with band widths between 1 and 2 cm. Garnet usually comprises 30 to 70% of the mode, may show kelyphite rims, and in a few cases displays extensive alteration to a submicroscopic, optically unidentifiable material. Spinel may vary between 0% (i.e. corganite) and 30% (i.e. corgaspinite) by mode. Accessory phases in these assemblages are similar to those of the alkremite suite, with the exception of amphibole which has not yet been identified in the corundum rich samples. One observation of note is that the pyroxene mineral clusters confined to garnet cores in the alkremite nodules are also present in the corganites and corgaspinites (with the exception of amphibole) and, in these latter assemblages, the pyroxene is usually much coarser (up to 3 mm) and more abundant. Green euhedral spinels within the pyroxenes also attain appreciable sizes (up to 1 mm).

MINERAL CHEMISTRY. Electron microbeam analyses for selected samples are shown in Table 1. All primary minerals are essentially homogeneous based on core and rim analyses of individual grains. Figure 1 shows the Ca-Mg-Fe atomic ratios of garnets, spinels and pyroxenes from the Jagerfontein nodule suite and published alkremite data¹⁻³.

Garnets are chromium-poor pyropes containing nearly constant almandine ($Fe/Fe+Mg+Ca = 0.17-0.19$), and variable grossular ($Ca/Ca+Mg+Fe = 0.16-0.31$). Alkremite (open symbols) garnets tend to cluster near the magnesian-rich part of the scatter, but one garnet grain (JAG ALK-17) lies above the main garnet trend (Fig. 1), and contains an anomalously high grossular content that resembles that of grosspyrite garnets⁵. Corundum grains in the corundum rich assemblages, as well as accessory corundum grains in the alkremites (not shown in Fig. 1) are generally pure, containing 98-99 wt.% Al_2O_3 , minor amounts of FeO (0.5 to 1.0 wt.%), Cr_2O_3 (0.2 to 0.4 wt.%) and TiO_2 (0.2 to 0.6 wt.%). Primary spinels (SP1, Table 1) have variable Cr_2O_3 contents (up to 2.3 wt.% in the alkremites, open symbols, but generally <1.0 wt.% in the corganites and corgaspinites, solid symbols) and are essentially hercynite-bearing pleonastes. The Mg/Mg+Fe ratios of primary spinels are very similar to those of associated garnets ranging between 74 and 80. Brown spinels mantling corundum (SP3, Table 1) are compositionally very similar to primary spinel grains and completely overlap SP1 in Fig. 1. In contrast, green euhedral spinels (SP2, Table 1) contain highly variable Cr_2O_3 contents (1.0 to 10.8 wt.%) with cores being generally richer in Cr_2O_3 than rims. They contain higher Fe_2O_3 contents (calculated), lower FeO, and slightly lower Mg/Mg+Fe ratios than the other spinels and, although some overlap is present, as

a group they define a tail trending toward higher Fe contents on the Ca-Mg-Fe projection.

BULK CHEMISTRY. Bulk rock major element analyses of selected corganite, corgaspinite and alkremite nodules from Jagersfontein as well as calculated bulk rock alkremite compositions^{1,4} are given in Table 2 (total Fe is reported as Fe_2O_3'). The corganites (CG) and corgaspinites (CGS) have a wide compositional spectrum, specifically with respect to SiO_2 (2.41-40.48 wt. %) and Al_2O_3 (21.78-80.67 wt. %). Variations are also evident in Fe_2O_3' (4.17-12.21 wt. %), CaO (1.83-11.62 wt. %) and MgO (7.57-15.56 wt. %). Cr values for all samples are relatively constant and consistently low (0.05-0.29 wt. %). Generally, the corgaspinites contain higher amounts of Al and lower amounts of Si, Ca and Mg than the corganites with no preference of Fe^{3+} for either assemblage. The alkremite data (Table 2) are subdivided into two groups consisting of alkremites (ALK) and spinel-rich alkremites (SP-ALK). The first group (ALK) show variations in SiO_2 (29.5-41.0 wt. %), Al_2O_3 (19.9-34.0 wt. %) and CaO (4.8-10.4 wt. %), but relatively constant Fe_2O_3' (9.1-10.9 wt. %) and MgO (16.4-19.7 wt. %). Cr values are again consistently low (0.1-0.5 wt. %). The spinel-rich alkremite group has very low, but variable SiO_2 (1.0-13.1 wt. %) and relatively high Al_2O_3 (50.6-63.5 wt. %) and MgO (19.6-23.3 wt. %) contents. In addition, this group is characterized by variable Cr_2O_3 contents (0.08-2.5 wt. %). These data are consistent with very high modal spinel (up to 95 %).

Data from Table 2 are presented in Figure 2, together with compositional fields for eclogites and average basalts⁵. The CaO-MgO-total FeO plot (Fig. 2a) shows that most of the Jagersfontein samples fall in the basalt field with relatively constant CaO/FeO ratios and variable MgO; the spinel-rich alkremites plot close to the MgO-FeO join. One calculated alkremite composition¹ conforms with the present alkremite trend, whereas the other⁴ is shifted toward slightly higher MgO contents. An alternate representation expressed as CaO- Al_2O_3 -(FeO+MgO) in Fig. 2b, emphasizes the nature of these extreme bulk compositions relative to basalts and eclogites. Corganites and corgaspinites form a continuous trend, however, from near the Al_2O_3 apex toward the eclogite and basalt fields. In order to obtain a representative bulk composition for the suite, the corganite and corgaspinite, alkremite, and spinel-rich alkremite data were averaged, both as individual groups, and as a single group, thus generating four additional bulk compositions (Table 2). These calculated bulk compositions are too rich in Al and too poor in Ca to correspond to any variety of eclogites. In fact, any combination of group averages yields similar results.

DISCUSSION. Coherence in geochemical data (Fig. 1-2) imply a genetic link among alkremites, corgaspinites and corganites. Cotectic crystallization and subsequent fractionation of garnet and spinel from an aluminous partial mantle melt has been suggested for the production of alkremites¹. Arguments favoring this process are: (1) distinct cumulate textures and (2) only slight enrichment in mantle alumina, from that of average mantle composition⁶, is needed to cause coprecipitation of garnet+spinel in the CMAS system. If this is applicable to the corganite and corgaspinite suite, liquidus corundum+garnet and excessively high temperatures are required⁷. Al-enrichment in the source regions of alkremite "magmas" has been addressed², with subduction of chloritic oceanic crust generating local regions of upper mantle enrichment in Mg and Al. Pelitic sediments are capable of generating strongly peraluminous magmas⁸ and, although plausible, is restrictive. Metasomatic reaction between pyroxenitic melts and peridotite has also been suggested due to the presence of secondary minerals such as kornerepin and chlorite³. An alternate explanation for these peraluminous assemblages is fractional crystallization of feldspathic magmas at the base of the crust. Such liquids are, on rare occasions, capable of crystallizing corundum and spinel at reasonable temperatures and pressures⁹. Early accumulation of these phases would cause a density stratification resulting in layering of corundum followed by spinel. Subsequent metamorphism at higher pressures would stabilize garnet which could produce a garnet-corundum assemblage in the corundum rich layers, and a garnet-spinel assemblage in the spinel layers. Trace element and isotopic data in progress, may help to resolve the genesis of these unusual xenoliths.

REFERENCES. (1) Nixon, P. H. et al., (1978), *Contrib. Mineral. Petrol.*, 65, 341, (2) Exley, R. A. et al., (1983), *Amer. Min.*, 68, 512, (3) Padovani, E. R., and Tracy, R. J., (1981), *Amer. Min.*, 66, 741, (4) Ponomarenko, A. I., (1975), *Dokl. Akad. Nauk. U.S.S.R.*, 225, No. 4, (5) Dawson, J. B., (1980) Kimberlites and their xenoliths, Springer Verlag, Heidelberg, (6) O'Hara, M. J., (1968), *Earth-Sci. Rev.* 4, 69, (7) Gasparik, T., (1984), *Amer. Min.*, 69, 1025, (8) Miller, C. F., (1985) *Jour. of Geol.*, 93, 673, (9) Presnall, D. C. et al., (1978), *Contrib. Mineral. Petrol.*, 66, 203.

TABLE 1. MICROBREM ANALYSES OF SELECTED JAGERSFONTEIN SAMPLES

SiO ₂	JAG 83 CG-5			JAG 80 CG-7		
	SP1	SP2	SP3	SP1	SP2	SP3
SiO ₂	48.84	47.00	47.31	41.51	45.56	45.56
TiO ₂	0.24	0.18	0.22	0.33	0.13	0.22
Al ₂ O ₃	25.05	87.80	98.98	17.11	8.75	61.48
Cr ₂ O ₃	0.03	0.21	0.25	0.35	0.17	2.71
Fe ₂ O ₃	9.09	12.13	0.59	6.37	6.00	9.97
MnO	0.22	0.09	0.11	0.18	0.26	0.12
MgO	15.07	19.02	0.10	21.18	15.24	20.78
NiO	0.02	0.20	0.07	0.01	0.15	0.06
ZnO	0.19	0.01	0.08	0.03	0.06	0.06
CaO	9.95	0.01	18.22	0.02	12.14	0.02
MgO	0.01	0.30	0.59	0.01	0.95	0.05
K ₂ O	0.01	10.31	0.01	0.01	0.01	0.01
Total	100.51	99.84	100.09	96.07	100.00	100.53

SiO ₂	JAG 83 CG-4			JAG 83 CG-3		
	SP1	SP2	SP3	SP1	SP2	SP3
SiO ₂	47.33	47.33	47.33	47.33	47.33	47.33
TiO ₂	0.52	0.24	0.43	0.21	0.05	1.62
Al ₂ O ₃	23.45	98.01	18.11	24.11	14.51	11.42
Cr ₂ O ₃	0.21	0.38	0.28	0.02	0.09	0.37
Fe ₂ O ₃	8.80	0.96	5.24	8.45	0.67	4.29
MnO	0.42	0.24	0.17	0.05	0.09	0.50
MgO	16.50	0.24	20.28	17.30	0.10	22.57
NiO	0.01	0.29	0.35	0.05	0.18	0.14
ZnO	0.01	0.01	0.01	0.01	0.01	0.01
CaO	8.56	0.16	0.19	7.97	0.01	20.00
MgO	0.18	0.01	0.59	0.05	0.20	1.18
K ₂ O	0.01	9.21	0.01	0.01	10.53	0.01
Total	100.23	100.40	96.15	99.90	100.44	98.09

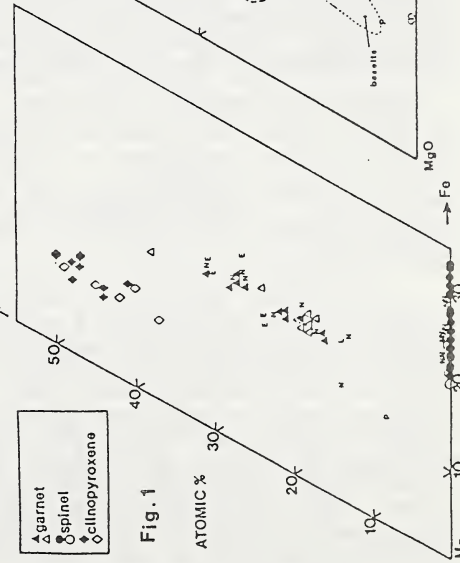


Fig. 1

TABLE 2. WHOLE ROCK MAJOR ELEMENTS OF JAGERSFONTEIN BODILLES

SAMPLE	SiO ₂	TiO ₂	Al ₂ O ₃	Cr ₂ O ₃	Fe ₂ O ₃	MnO	MgO	CaO	H ₂ O	K ₂ O	Σ ₉	TOTAL
JAG 83 CG-4*	33.98	0.28	36.12	0.05	8.14	0.16	13.13	8.32	0.00	0.30	0.06	100.53
JAG 84 EG-6	39.80	0.39	23.84	0.29	12.21	0.21	14.07	9.62	0.00	0.45	0.05	100.74
JAG 80 CG-8	18.69	0.34	59.88	0.19	5.78	0.12	9.53	4.59	0.81	0.35	0.06	99.93
JAG 83 CG-3-2*	15.51	0.25	83.94	0.10	4.80	0.12	9.51	4.35	0.58	0.33	0.06	99.64
JAG 84 EG-4	33.98	0.38	35.23	0.07	9.00	0.16	13.38	8.21	0.00	0.17	0.06	100.62
JAG 83 EG-8*	27.83	0.28	47.11	0.13	7.22	0.15	12.01	5.70	0.00	0.12	0.05	100.60
JAG 85 CG-9	2.41	0.29	80.87	0.10	4.17	0.07	7.57	1.63	2.36	0.34	0.10	99.91
JAG 80 CG-7	35.48	0.29	32.61	0.06	9.26	0.16	13.15	9.22	0.51	0.23	0.07	101.02
JAG 84 EG-8	40.48	0.31	21.78	0.11	10.09	0.21	15.56	10.63	0.44	0.26	0.08	99.95
JAG CG-12	33.02	0.23	31.75	0.03	9.23	0.12	9.40	11.62	0.07	0.08	0.07	100.62
JAO 84 AL68	35.14	0.25	28.75	0.15	10.83	0.17	16.26	8.60	0.00	0.15	0.05	100.35
JAG ALK 7	35.18	0.37	27.05	0.12	9.99	0.14	17.31	9.70	0.01	0.41	0.05	100.31
JAG ALK 9	29.47	0.29	34.00	0.54	10.93	0.29	19.73	4.84	0.00	0.29	0.04	100.42
JAG ALK 10	41.03	0.45	19.94	0.13	11.29	0.52	18.51	7.62	0.14	0.54	0.05	100.22
JAG ALK 11*	35.78	0.26	28.73	0.06	10.44	0.24	18.55	6.38	0.00	0.13	0.05	100.60
JAG ALK 15*	31.98	0.19	35.99	0.22	9.63	0.39	19.56	5.75	0.00	0.13	0.05	100.89
JAG ALK 18	30.72	0.22	32.47	0.11	10.49	0.13	16.49	8.48	0.28	0.24	0.05	99.68
JAG ALK 17	33.99	0.18	28.08	0.16	10.09	0.11	16.35	10.39	0.00	0.10	0.05	100.46
JAG ALK 16	33.73	0.19	30.78	0.30	9.06	0.30	16.79	6.94	0.00	0.12	0.04	100.24
JAG 83 SP-ALK 35	13.12	0.22	51.13	1.10	11.21	0.18	20.53	2.18	0.42	0.11	0.04	100.24
JAG 85 SP-ALK 1*	1.86	0.14	83.00	2.45	8.76	0.08	23.33	0.19	0.29	0.03	0.03	100.16
JAG 83 SP-ALK 13*	11.46	0.47	50.56	0.08	14.23	0.13	19.61	2.25	0.64	0.32	0.06	99.81
JAG 83 SP-ALK 34	0.97	0.17	63.50	2.25	9.11	0.08	23.12	0.20	0.28	0.06	0.04	95.78
CG + CG3 average ¹	28.11	0.30	43.75	0.11	7.99	0.15	11.73	7.40	0.48	0.26	0.06	100.34
ALK average ¹	34.11	0.28	28.31	0.20	10.31	0.25	17.95	7.63	0.05	0.23	0.05	100.35
SP-ALK average ¹	8.85	0.25	57.05	1.47	10.83	0.12	21.65	1.21	0.41	0.13	0.04	100.07
Bulk average ¹	26.78	0.28	40.41	0.38	9.39	0.18	15.69	6.41	0.30	0.23	0.05	100.26
Avg. ahtremitt ²	28.90	0.15	31.84	0.69	6.03	0.21	24.10	2.77	0.07	0.39	NA	56.95
Avg. ahtremitt ³	28.20	0.17	36.80	1.10	10.50	0.23	17.70	5.90	NA	NA	NA	100.60

1 This study
2 From Panomarenko (1975)
3 From Nixon et al. (1978)

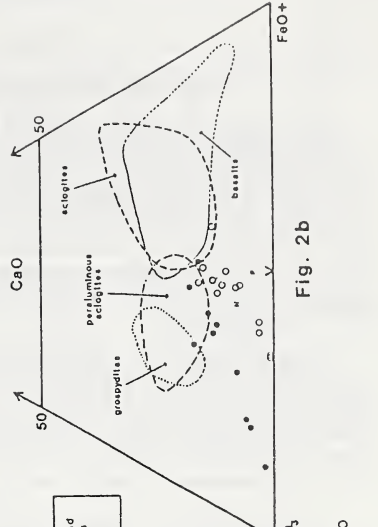


Fig. 2b

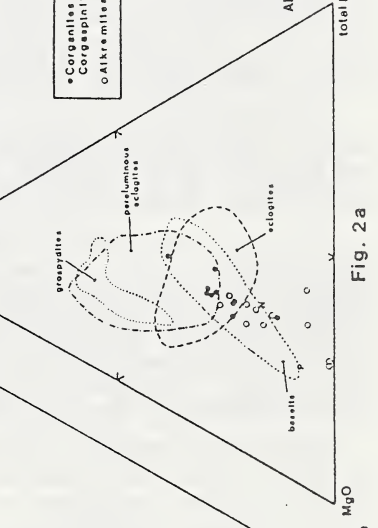


Fig. 2a

SODIUM IN GARNET AND POTASSIUM IN CLINOPYROXENE:
CRITERIA FOR CLASSIFYING MANTLE ECLOGITES

Tom E. McCandless and John J. Gurney

Department of Geochemistry, University of Cape Town, South Africa

MacGregor and Carter (1970) recognized two groups of eclogites at Roberts Victor, based largely on textural differences. Group I eclogites have large, cloudy, subhedral to rounded garnets set in a matrix of clinopyroxene. Some garnets may be poikilobitically enclosed in clinopyroxene, and some clinopyroxene may contain exsolution lamellae. Group II eclogites have an interlocking texture of anhedral garnet and clinopyroxene, and the minerals are less altered than in group I eclogites. Chemically, it was noted that group II clinopyroxenes were lower in K_2O than those in group I eclogites, a feature also noted by Erlank (1970). Garnets also tend to have higher Na_2O content in group I eclogites.

Hatton (1978), in an extensive study of 700 Roberts Victor eclogites, continued to apply the MacGregor and Carter (1970) scheme. He found that although 75% of the eclogites could be regarded as group I, many could not be placed in either category based on texture alone. He relied heavily on the fresh appearance of minerals as a distinguishing criteria, and included eclogites with fresh, unaltered grains in the group II category, though their textures varied.

Several workers have found that eclogitic inclusions in diamond contain potassium-enriched clinopyroxene and sodium-enriched garnet (Sobolev, 1977; Gurney et al., 1979; Tsai et al., 1979; Moore and Gurney, 1985). Similar enrichment occurs in the garnet and clinopyroxene of diamondiferous eclogites, (Reid et al., 1976), and Robinson et al., (1984) suggested that this may be used to classify eclogites.

This investigation returns to the eclogites of Roberts Victor, to demonstrate that sodium in garnet and potassium in clinopyroxene are useful criteria for discriminating two groups of mantle eclogites. Diamondiferous eclogites from several localities are also examined in the light of this new scheme.

A total of 564 garnet and pyroxene microprobe analyses were obtained from polished thin sections of group I, group II, and diamondiferous eclogites. The group I and II eclogites are taken from the suite previously studied by Hatton (1978), and include megacryst-bearing, chrome-rich, and inhomogeneous varieties. The diamondiferous eclogites are from the Roberts Victor, Orapa, Star, Jagersfontein, Newlands, Ardo (Excelsior), Mitchemanskraal, and Sloan 2 kimberlites, with some containing both diamond and graphite. Sixty second counting times were taken for sodium in garnet and potassium in clinopyroxene, to ensure a 0.01% lower limit of detection, with 0.01% 2 sigma.

Based on the original classification of Hatton (1978) the results show that sodium in garnet (Na_2O_{gt}) and potassium in clinopyroxene (K_2O_{cpx}) are significantly enriched in group I eclogites, and depleted in group II eclogites. Sodium in group I garnets averages $0.10 \pm 0.02\%$ Na_2O . In contrast, group II garnets have an average sodium content of $0.05 \pm 0.03\%$ Na_2O (Fig. 1a). Group I clinopyroxenes have an average potassium content of $0.12 \pm 0.03\%$ K_2O , while group II clinopyroxenes average $0.04 \pm 0.05\%$ K_2O (Fig. 1b).

It can be seen from Figs. 1a and 1b that the oxide ranges overlap for the two eclogite groups. For the group I eclogites, low values of Na_2O_{gt} and K_2O_{cpx} are present only in metasomatized nodules (recognized by the presence of abundant secondary phlogopite in the rock; Hatton, 1978). It is possible that sodium has been removed from the garnet during metasomatism or other alteration processes. Potassium depletion in eclogitic clinopyroxene from metasomatism or decompression melting has been reported elsewhere (Switzer and Melson, 1969; Mysen and Griffin, 1973; Reid et al., 1976; McCandless and Collins, this volume). It has also been noted that measured K_2O in clinopyroxene can vary with crystallographic orientation (McCandless and Collins, this volume). The high K_2O_{cpx} and Na_2O_{gt} values in group II eclogites are largely from kyanite-bearing eclogites. These eclogites were classified as group II based on their fresh appearance (Hatton, 1978), while MacGregor and Carter (1970) found that all kyanite-bearing eclogites were group I. On the basis of our proposed criteria, we agree

with the latter. The problems inherent in using texture alone as a criteria for classifying eclogites thus become apparent.

Even with these samples included in their original groups defined by Hatton (1978) however, it is found that 81% of the garnets from group I eclogites have 0.09% or more Na_2O , while 89% of the group II garnets are below this value. For K_2O in clinopyroxene, 94% of the group I clinopyroxenes are at or above 0.08% K_2O , with 76% of the group II clinopyroxenes below this value. When the metasomatized group I and kyanite-bearing group II eclogites are excluded, 91% of the group I garnets have 0.09% or greater Na_2O in garnet, and 96% of garnets in group II eclogites have less than 0.09% Na_2O . For the group I clinopyroxenes, 99% are at or above 0.08% K_2O , and 86% of the group II clinopyroxenes are below 0.08% K_2O .

It is proposed that values of 0.08% K_2O in clinopyroxene and 0.09% Na_2O in garnet can be used as criteria for classifying mantle eclogites. Eclogites with average contents of $\text{K}_2\text{Ocp} > 0.08\%$ or $\text{Na}_2\text{Ogt} > 0.09\%$ are considered as group I, and eclogites below these values are group II. For reasons previously discussed, both values may not be high in a group I eclogite, in which case the presence of either enriched garnet or clinopyroxene is considered significant. By applying these guidelines to the eclogites of at Roberts Victor, 90-100% are correctly placed into a group I or II category. This is a highly successful result. It remains to be shown how widely applicable these criteria will prove to be.

It has been noted that diamondiferous eclogites have K_2O -enriched clinopyroxene and Na_2O -enriched garnet (Robinson et al., 1984; Reid et al., 1976). The average values of these oxides in diamondiferous eclogites are nearly identical to those for group I eclogites. Sodium in garnet is $0.11 \pm 0.02\%$ Na_2O , and potassium in clinopyroxene is $0.10 \pm 0.04\%$ K_2O . Low contents of K_2O present in clinopyroxene are believed to be due to those processes similarly attributed to low values in Rovic group I clinopyroxenes. Thus, based on K_2Ocp alone, only 65% of the diamondiferous eclogites would be classified as group I. In considering Na_2Ogt , however, all of the diamondiferous eclogites are group I, using the cut off limits expressed above. It is believed that all of the diamondiferous eclogites of this study are group I eclogites, based on these results. Conversely, this suggests that group I eclogites formed under conditions similar to those required for diamond genesis.

The application of peridotitic garnet chemistry to evaluate the presence of diamond in kimberlites has been proven (Gurney, 1984). An increasing number of kimberlites are now recognized as having eclogitic diamonds, based on associated mineral inclusions (Otter and Gurney, this volume; Moore and Gurney, 1985, this volume; Rickard et al., this volume) The similar enrichment patterns of K_2O in clinopyroxene and Na_2O in garnet for group I and diamondiferous eclogites has been shown. Group I eclogites, and the garnets and clinopyroxenes derived from them, may therefore be useful tools in the prospecting and evaluation of kimberlites, where the eclogitic diamond paragenesis is important.

REFERENCES

- ERLANK, A. J. 1970. Distribution of potassium in mafic and ultramafic nodules. Carnegie Institute of Washington Yearbook, 68, pp. 433-439.
- GURNEY, J. J. 1984. A correlation between garnets and diamonds in kimberlites. In Glover, J. E. and Harris, P. G., eds, Kimberlite Occurrence and Origin: Conceptual Models in Exploration. University Extension, University of Western Australia, pp. 143-166.
- GURNEY, J. J., HARRIS, J. W., and RICKARD, R. S. 1979. Silicate and oxide inclusions in diamonds from the Finsch kimberlite pipe. In Boyd, F. R., and Meyer, H. O. A., eds, Kimberlites, diatremes and diamonds: their petrology, mineralogy, and geochemistry
- HATTON, C. J. 1978. The geochemistry and origin of xenoliths from the Roberts Victor Mine. Unpublished Phd. Thesis, University of Cape Town.
- MACGREGOR I. D. and CARTER, J. L. 1970. The chemistry of clinopyroxenes and garnets of eclogite and peridotite xenoliths from the Roberts Victor mine, South Africa. Physics of the Earth and Planetary Interiors, 3, pp. 391-397.
- MOORE, R. O. and GURNEY, J. J. Pyroxene solid solution in garnets included in diamonds. Nature, 318, 6046, pp.553-555.
- MYSEN, B. and GRIFFIN, W. L. 1973. Pyroxene stoichiometry and the breakdown of

- omphacite. *American Mineralogist* 53, pp.60-63.
- REID, A. M., BROWN, R. W., DAWSON, J. B., WHITFIELD, G. G. and SIEBERT, J. C. 1976. Garnet and clinopyroxene compositions in some diamondiferous eclogites. *Contributions to Mineralogy and Petrology*, 58, pp. 203-220.
- ROBINSON, D. N., GURNEY, J. J., and SHEE, S. R. 1984. Diamond eclogite and graphite eclogite xenoliths from Orapa, Botswana. In Kornprobst, J. Ed., *Kimberlites II: The Mantle and Crust-Mantle Relationships, Developments in Petrology IIB*, Elsevier, New York, pp. 11-24.
- SOBOLEV, N. V. 1977. Deep-Seated Inclusions in Kimberlite and Problem of the Composition of the Upper Mantle. *American Geophysical Union, Washington*, 279 p.
- SWITZER, G. and MELSON, W. G. 1969. Partially melted kyanite eclogite from the Roberts Victor Mine, South Africa. *Smithsonian Contributions to the Earth Sciences* 1. Smithsonian Institution Press, Washington, D. C. 7p.
- TSAI, H., MEYER, H. O. A. MOREAU, J. and MILLEDGE, H. J. 1979. Mineral inclusions in diamond, Premier, Jagersfontein and Finsch kimberlites, South Africa, and Williamson Mine, Tanzania. In Boyd, F. R. and Meyer, H. O. A., eds, *Kimberlites, Diatremes, and Diamonds: Their Geology, Petrology, and Geochemistry*. American Geophysical Union, Washington, pp. 16-26.

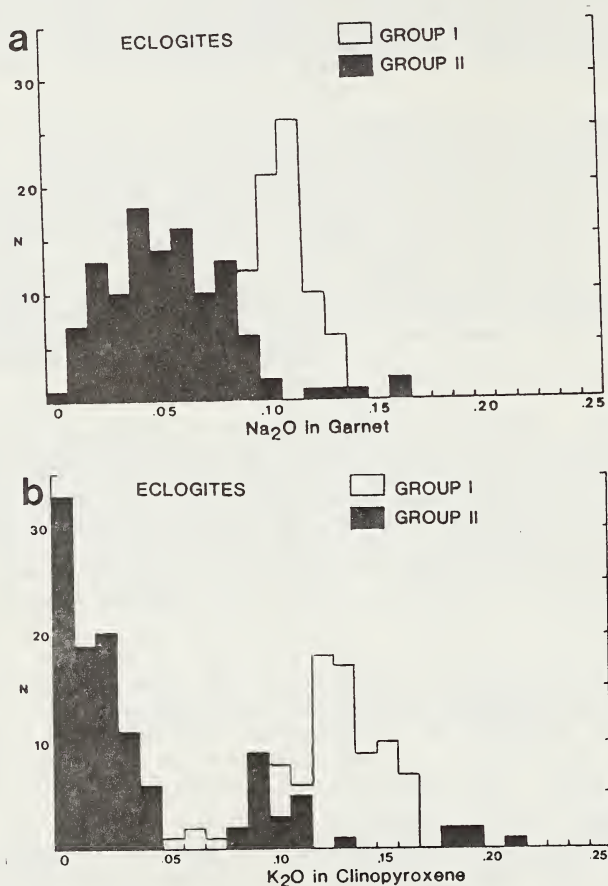


Figure 1. Histograms of (a) Na₂O in garnets and (b) K₂O in clinopyroxenes from Roberts Victor group I and group II eclogites. Values in weight percent.

Sm-Nd SYSTEMATICS IN ECLOGITE AND GARNET PERIDOTITE NODULES FROM KIMBERLITES:
IMPLICATIONS FOR THE EARLY DIFFERENTIATION OF THE EARTH

Malcolm T. McCulloch

Research School of Earth Sciences, ANU, Canberra, ACT, 2601, AUSTRALIA

In this study we report Sm-Nd isotopic data for eclogites from the Roberts Victor pipe in South Africa and Yakutia, U.S.S.R. In addition, a garnet lherzolite has been analyzed from the Mir pipe in the Yakutia province. The isotopic systematics have been examined in co-existing garnet and clinopyroxene. These minerals are strongly LREE depleted (low Nd/Sm) and LREE enriched (high Nd/Sm) respectively and thus enable relatively precise determinations of both the initial neodymium isotopic composition and the most recent time of equilibration of these mineral systems. The garnet-clinopyroxene pairs for the Roberts Victor eclogites define mineral isochron ages of 144 ± 10 Ma and 188 ± 33 Ma (figure 1). The younger mineral age of 144 ± 10 Ma is in reasonable agreement with previous estimates of the intrusion age of the host kimberlite given by Rb-Sr mica ages of ~ 125 Ma, but significantly older than a U-Pb zircon age of 92.2 Ma (Davies et al., 1976). These results are therefore consistent with almost complete isotopic re-equilibration of garnet and clinopyroxene during the kimberlite magmatism. Recent isotopic studies by Richardson et al. (1985) of garnet lherzolites from northern Lesotho also indicate isotopic re-equilibration at the time of kimberlite sampling. Although the Roberts Victor eclogites give similar Sm-Nd mineral isochron ages, the initial $^{143}\text{Nd}/^{144}\text{Nd}$ ratios vary from $\epsilon_{\text{Nd}} = -14.4 \pm 0.3$ to $\epsilon_{\text{Nd}} = +3.7 \pm 0.1$. This range confirms the observation that the xenoliths are unrelated to the host kimberlite and indicates long-term (> 1000 Ma) heterogeneities in the sources for the eclogites. However, the timing of the events which produced these heterogeneities is not well constrained by the Sm-Nd mineral data due to the almost total isotopic re-equilibration of the garnet-clinopyroxene pairs.

A striking feature of the Sm-Nd isotopic data for a garnet lherzolite (M602) and eclogites from Yakutia (Siberia) is that the garnet-clinopyroxene pairs gives ages of 1540 ± 10 Ma, 2600 ± 150 Ma, 1690 ± 50 Ma, 1320 ± 20 Ma and 674 ± 30 Ma respectively (figures 2a,b), which are all much older than the 150 Ma to 440 Ma age estimated for the kimberlite pipes. In addition, the initial $^{143}\text{Nd}/^{144}\text{Nd}$ ratios for the garnet lherzolite and one of the eclogites are substantially higher than CHUR with ϵ_{Nd} values of 24.5 ± 0.2 and 20.1 ± 3.0 respectively. These values are significantly more positive than 'normal' mantle materials (figure 3) and have previously only observed in a garnet lherzolite and an eclogite (McCulloch, 1982 and Jagoutz et al., 1984). In fact, garnet from the garnet lherzolite has a measured value of $\epsilon_{\text{Nd}}(0) = +227$ which is one of the highest values yet reported. The younger eclogites 47639 and 47637 have negative ϵ_{Nd} values of -2.2 ± 0.2 and -5.5 ± 0.2 respectively.

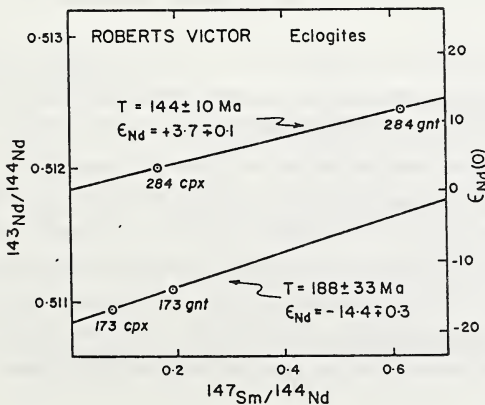


Figure 1. Isochron diagram for co-existing garnet and clinopyroxene from eclogites from Roberts Victor. The mineral ages are only slightly older than the age of the kimberlite host indicating almost complete re-equilibration during kimberlite sampling.

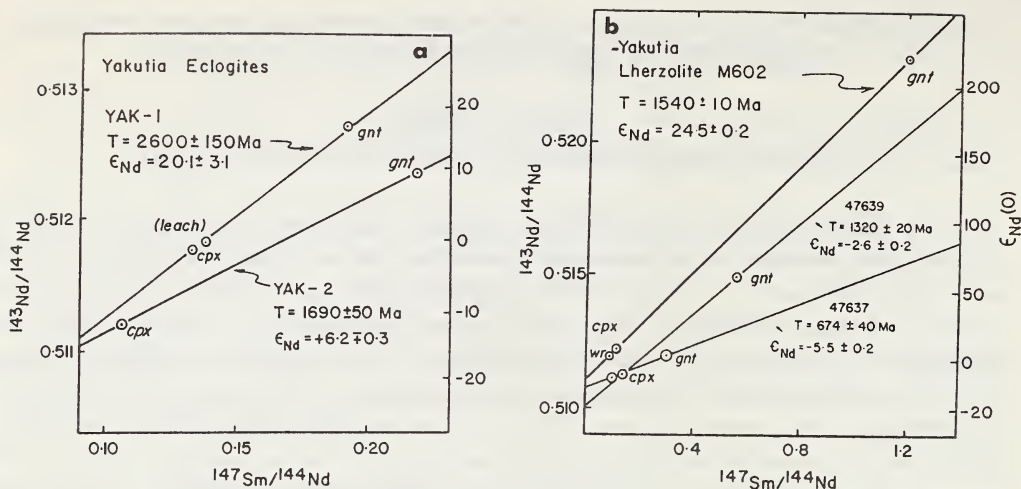


Figure 2. *a*, Sm-Nd internal isochron diagram for the Yakutia 1 and 2 eclogites. The age and initial ratio given by the intersection of co-existing garnet and clinopyroxene represent minimum estimates. Both ages are significantly older than the age of the host kimberlite. *b*, Sm-Nd internal isochron for the garnet lherzolite M602 from the Mir kimberlite pipe and the eclogites 47639 and 47637 from the Yakutia province. The garnet from M602 has an extremely high $^{143}\text{Nd}/^{144}\text{Nd}$ ratio corresponding to $\epsilon_{\text{Nd}}(0) = +227$.

The major difficulty in interpreting these results is ascertaining the effects of isotopic re-equilibration and evaluating whether the nodules have remained as closed isotopic systems. Isotopic re-equilibration is obviously an important process as evidenced by the young ages from Roberts Victor and the wide range of internal isochron ages from Yakutia (2600 Ma to 680 Ma). If the whole rock systems have Sm/Nd ratios less than chondritic, than later isotopic re-equilibration will produce lower ϵ_{Nd} values and of course younger ages (c.f. McCulloch and Black, 1984). This effect is apparent in the Yakutia eclogites where the ϵ_{Nd} values become progressively lower as the internal isochron ages decrease (figure 3). This implies that the highly positive ϵ_{Nd} values of +24.5 and +20.1 for M602 and Yak-1 are *minimum* values. It is also noted that the converse applies to whole rock systems with Sm/Nd ratios greater than chondritic. Assuming that the nodules acted as essentially closed isotopic systems (on a whole-rock scale), the highly positive ϵ_{Nd} values from Yakutia therefore require long-lived strongly LREE depleted sources.

A model to account for these highly positive ϵ_{Nd} values has been proposed by McCulloch (1982) whereby processes similar to those that operated in early Lunar history are envisaged. That is, cumulates precipitating from an early terrestrial magma ocean. To account for the long-lived strongly LREE depleted character observed in the most positive ϵ_{Nd} nodules, it is necessary to form a chemically stratified (or isolated) garnet-rich layer during the crystallisation of the magma ocean early in the earth's history (i.e. prior to 4000 Ma). Independent petrologic evidence (Ohtani, 1985) suggests that a garnet-rich layer with a thickness of ~200 km thickness may have been present in the lower portion of the earth's primitive upper mantle. An alternative mechanism for producing LREE depletions involves the subduction of oceanic lithosphere with LREE depletions. This process has been proposed by Ringwood (1982) as a means of essentially irreversibly differentiating the earth's mantle and involves the conversion of basaltic components of oceanic crust into eclogite and consequently their sinking deep into the earth's mantle (~650km). To

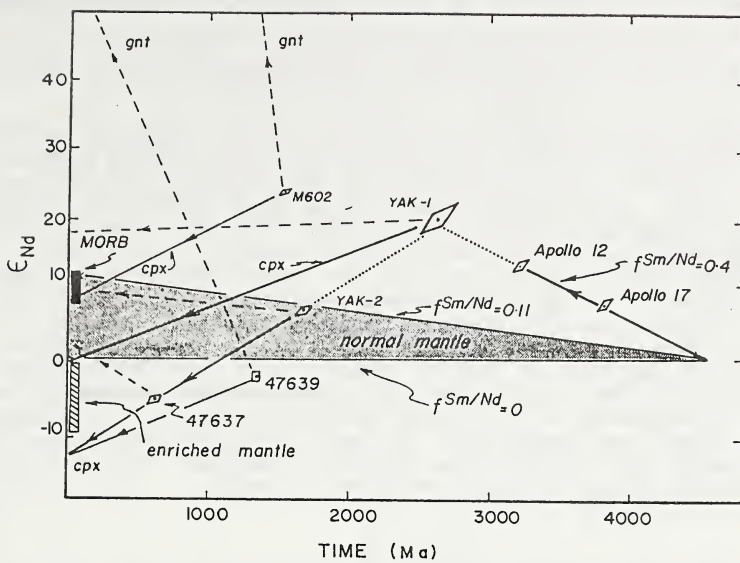


Figure 3. ϵ_{Nd} versus time diagram showing initial ratios and inferred evolutionary history for Yakutia xenoliths. The ϵ_{Nd} values for YAK-1, YAK-2, 47639, 47637 and M602 are given by the intersection of co-existing garnet (broken lines) and clinopyroxene (solid lines). The increase in ϵ_{Nd} values with age is consistent with progressive re-equilibration. The highly positive ϵ_{Nd} values for Yak-1 and M602 indicate that the sources of these xenoliths were probably differentiated in the first 100 to 200 Ma of earth history. Also shown are the ϵ_{Nd} values of the Apollo 12 and 17 Lunar basalts. A similar type of evolutionary history could also account for the highly positive ϵ_{Nd} values found in the Yakutia xenoliths.

satisfy the isotopic constraints the early formed oceanic crust would have to be strongly LREE depleted relative to the bulk mantle. At ~2600 Ma (the oldest Sm-Nd mineral age) these materials were then probably partially melted with the resultant LREE enriched melts ascending into the subcontinental lithosphere where they were trapped and solidified within the eclogite stability field and then finally incorporated in later kimberlite magmatism.

REFERENCES

- DAVIES G.L., KROGH T.E. and ERLANK A.J. 1976. The ages of zircons from kimberlites from South Africa. *Carnegie Institute Inst. Washington Yearbook* 75, 821-824.
- JAGOUTZ E., DAWSON B., HOERNES S., SPETTEL B. and WANKE H. 1984. Anorthositic oceanic crust in the Archaean Earth. In: *Lunar and Planetary Science, XV*, Lunar and Planetary Institute, Houston, 395-396.
- McCULLOCH M.T. 1982. Identification of Earth's Earliest differentiates. Abstracts 5th International Conference on Geochronology Cosmochronology Isotope Geology, Nikko, Japan. 244-246.
- McCULLOCH M.T. and BLACK L.P. 1984. Sm-Nd isotopic systematics of Enderby Land granulites and evidence for the redistribution of Sm and Nd during metamorphism. *Earth and Planetary Science Letters* 71, 46-58.
- OHTANI E. 1985. The primordial terrestrial magma ocean and its implication for stratification of the mantle. *Physics of the Earth and Planetary Interiors* 38, 70-80.
- RICHARDSON S.H., ERLANK A.J. and HART S.R. 1985. Kimberlite-borne garnet peridotite xenoliths from old enriched subcontinental lithosphere. *Earth and Planetary Letters* 75, 116-128.
- RINGWOOD A.E. 1982. Phase transformations and differentiation in subducted lithosphere: implications for mantle dynamics, basalt petrogenesis, and crustal evolution. *The Journal of Geology* 90, 611-643.

William F. McDonough and Malcolm T. McCulloch
 Research School of Earth Sciences, The Australian National University
 Canberra, A.C.T. 2601 Australia

Integrated petrologic, chemical and isotopic data for spinel-bearing lherzolite and harzburgite xenoliths from the Newer basalt field, southeastern Australia provide an internally consistent multistage model for the evolution of the subcontinental lithosphere. Whole rock isotopic compositions show exceedingly large variations including nodules from the same host basalt, with $^{87}\text{Sr}/^{86}\text{Sr}$ ranging from 0.7034 to 0.7084 and ϵ_{Nd} values ranging from +10.6 to -7.5. Constant Sr/Nd ratios of 15 for whole rocks and clinopyroxenes is consistent with the added incompatible element enriched component (component B) being a basaltic melt with intraplate chemical characteristics. The isotopic compositions of these peridotites indicate long-term, small-scale heterogeneities in the subcontinental lithosphere, and are in marked contrast to the near uniform isotopic compositions of the host alkali basalts ($^{87}\text{Sr}/^{86}\text{Sr} = 0.7038$ to 0.7041 and $\epsilon_{\text{Nd}} = +3.6$ to +2.9). The data are consistent with lithospheric mantle growth involving the underplating of refractory peridotite diapirs. A minimum of three evolutionary stages are identified: an early basalt depletion event, recording the initial development and stabilization of the lithospheric mantle, and subsequent enrichment episodes, documenting later reactivation events.

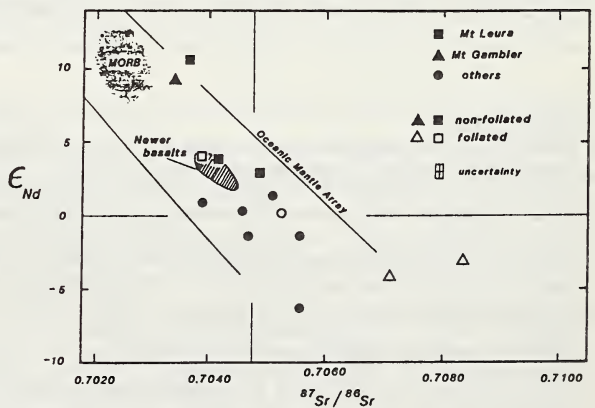
SAMPLES

Trace element and Sr and Nd isotopic compositions of whole rocks and mineral separates for 14 peridotite inclusions are combined with previously reported petrologic and geochemical data for these samples (Frey and Green, 1974; Nickel and Green, 1984). These lherzolite and harzburgite inclusions all contain, in decreasing order of abundances, olivine, orthopyroxene, clinopyroxene and spinel, and some also contain amphibole, phlogopite or apatite. Samples are coarse to medium grained, with porphyroclastic textures. Four samples are strongly foliated. More detailed petrographic descriptions are given in (Frey and Green, 1974; Nickel and Green, 1984).

Sr AND Nd ISOTOPIC COMPOSITIONS

The whole rock data shows the largest known variation in Sr and Nd isotopic compositions for spinel-bearing lherzolite and harzburgite xenoliths from a given basalt field (Fig. 1). Three samples from Mt. Gambier alone display nearly as large a range in isotopic compositions as found in the field. Combined with earlier isotope data (Chen and Frey, 1981) the Mt. Leura peridotites show an enormous variation in Nd isotope composition from $\epsilon_{\text{Nd}} = +10.6$ to -7.5. Most significantly, these isotopic heterogeneities occur within a single vent and reveal significant compositional diversity in the present day southeast Australian subcontinental lithosphere over a restricted vertical section, the spinel lherzolite stability field (e.g., some 40 to 70 kms depth).

FIGURE 1. $^{87}\text{Sr}/^{86}\text{Sr}$ versus ϵ_{Nd} values for whole rock spinel-bearing peridotite xenoliths from southeast Australia. Open symbols identify peridotites with a well defined foliated fabric. The field of Sr and Nd isotopic compositions for the Newer basalts includes tholeiitic and alkalic basalts from McDonough et al (1985).



The large variation in their Sr and Nd isotope compositions is in marked contrast to the limited range in isotope composition of the host alkalic basalts (McDonough et al, 1985), thus precluding significant host basalt contamination. Note that contamination by the host basalts would only reduce the total isotopic variation and therefore, the present spread would represent a minimum for the peridotite source region. Rb-Sr and Sm-Nd isotope compositions for the peridotites show considerable scatter (Fig. 2), although there is a positive trend in the $^{147}\text{Sm}/^{144}\text{Nd}$ versus $^{143}\text{Nd}/^{144}\text{Nd}$ data. Reference isochrons are provided in Fig. 2, although these isochrons are neither geologically nor statistically significant.

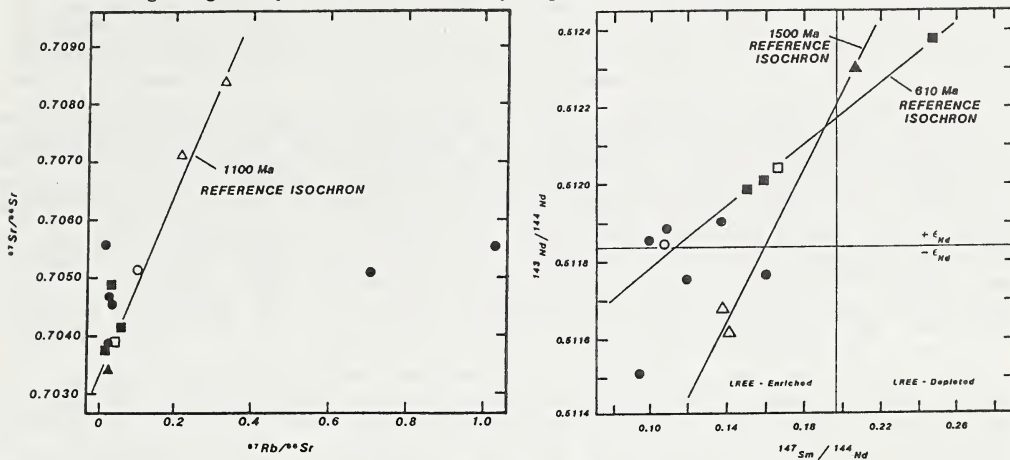


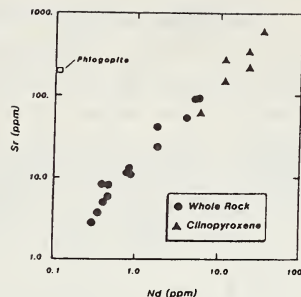
FIGURE 2. (a) $^{87}\text{Sr}/^{86}\text{Sr}$ versus $^{87}\text{Rb}/^{86}\text{Sr}$ and (b) $^{143}\text{Nd}/^{144}\text{Nd}$ versus $^{147}\text{Sm}/^{144}\text{Nd}$ whole rock variation for Australian peridotites. 1100 Ma Rb-Sr reference isochron is shown for three Mt. Gambier peridotites. Sm-Nd reference isochrons for three Mt. Gambier peridotites (1500 Ma), and four Mt. Leura peridotites (610 Ma) are shown, however all ages have no geological significance, see text. Symbols as in Fig. 1.

Mineral phases in a phlogopite lherzolite (84-413) are in gross Sr isotopic disequilibrium. The $^{87}\text{Rb}/^{86}\text{Sr}$ of the phlogopite is much higher than that of the clinopyroxene (and whole rock), whereas the clinopyroxene has a higher $^{87}\text{Sr}/^{86}\text{Sr}$ (0.70710) than the $^{87}\text{Sr}/^{86}\text{Sr}$ of phlogopite (0.70498); the whole rock has an intermediate $^{87}\text{Sr}/^{86}\text{Sr}$ value (0.70553). The low $^{87}\text{Sr}/^{86}\text{Sr}$ of the phlogopite indicates a recent addition of a low $^{87}\text{Sr}/^{86}\text{Sr}$ to this rock; it is possible that this addition is associated with the Pliocene-Recent basaltic magmatism in the region.

THE NATURE AND TIMING OF THE LREE-ENRICHED ADDED COMPONENT

Frey and Green (1974) suggested the major and compatible minor element characteristics of these peridotites (their component A) resulted from the extraction of a basaltic melt, whereas the incompatible element composition is dominated by a later added component (their component B) that is genetically unrelated to component A and was derived by a small degree (<5%) of melting in equilibrium with garnet. The Sr and Nd concentrations in these peridotites show an excellent correlation (Fig. 3), and allows us to place constraints on the nature and origin of this component. The average whole rock Sr/Nd ratio of 15 is similar to that found in the clinopyroxenes (14.5), and in marked contrast to that in phlogopite (1800). The averaged Sr/Nd ratio of these peridotites is similar to the primitive earth Sr/Nd ratio (17.1), primitive MORBs (10-15) and primitive intraplate basalts (15-20) and less than the ratio commonly measured for primitive island arc basalts (30-35). The added component B documented by Frey and Green (1974) and recorded by the Nd isotope system is suggested to be a LREE-enriched melt with intraplate basaltic characteristics, although a melt component derived by low degrees (<2%) of melting of the MORB source would have most of the necessary chemical characteristics. The isotopic composition of these peridotites are distinct from their host basalts, suggesting that the introduced melt component is generally unrelated to this intraplate magmatic event.

FIGURE 3. Sr (ppm) versus Nd (ppm) concentrations for whole rock and their clinopyroxene mineral separates for peridotite xenoliths from southeast Australia. A single phlogopite mineral separate clearly shows a markedly different Sr/Nd ratio.



Given that these peridotites are mixtures of at least 2 components, then traditional isochron diagrams cannot yield any significant age information. Assuming a two stage model, whereby the peridotites experienced one depletion event and one enrichment event, an age estimate for the LREE-enrichment event may be calculated using a T_{DM} model. T_{DM} model ages for these peridotites vary from 600 to 1370 Ma. These models yield only a gross age estimate for the timing of the enrichment event, as they assume only a single stage enrichment event. The phlogopite in peridotite 84-413 has a lower $^{87}\text{Sr}/^{86}\text{Sr}$ than the whole rock and coexisting clinopyroxene, indicating a recent addition that post-dates the earlier partial melt extraction and incompatible element enrichment event recorded in the clinopyroxene. It would take 60 Ma for the phlogopite to evolve to its present $^{87}\text{Sr}/^{86}\text{Sr}$ value if it was introduced from a depleted mantle source (i.e., $^{87}\text{Sr}/^{86}\text{Sr} = 0.7025$). If the component was derived from a less depleted mantle, that is a higher $^{87}\text{Sr}/^{86}\text{Sr}$ source, then the age of the phlogopite would be less than 60 Ma. Therefore, phlogopite generation occurred sometime during the Cenozoic, consistent with the observation that intraplate magmatism occurred throughout this period. An important result which comes from documenting a minimum of 3 evolutionary stages for the phlogopite-bearing peridotite is that it records an earlier mantle enrichment event which pre-dates the present alkaline volcanism.

EVOLUTION OF THE SUBCONTINENTAL LITHOSPHERE

Subcontinental lithospheric mantle accreted during interplate and intraplate magmatism would most likely be depleted peridotite, having a petrologic and chemical composition similar to component A as characterized by Frey and Green (1974). Such Mg-rich, refractory residuum is less dense than the ambient mantle and thus, intrinsically buoyant. The residual peridotite bodies produced during interplate or intraplate magmatism become permanently trapped beneath the continents and are incorporated into the lithosphere as a gravitationally stable, depleted lithospheric mantle. However, undepleted or less-depleted peridotite accreted directly from the asthenosphere during conductive cooling of the lithosphere would be denser and gravitationally unstable upon cooling. The early partial melting event identified in these peridotites documents the initial development and stabilization of the subcontinental lithosphere. Deciding whether the tectonic setting of the initial lithospheric growth stage was in an interplate or intraplate environment is not straightforward. Lithospheric growth may have occurred initially in either an oceanic or intracratonic setting, although Frey and Green (1974) have appealed to a mid-ocean ridge setting. Later incompatible element enrichment events, recorded in these peridotites, document reactivation episodes which have occurred in this lithosphere.

References

- Chen, C.Y. and Frey, F.A. (1981) Multi-stage geochemical events in the upper mantle: geochemical studies of spinel lherzolites Mount Leura, Australia. *EOS* 62, 415.
- Frey, F.A. and Green, D.H. (1974) The mineralogy, geochemistry and origin of lherzolite inclusions in Victorian basanites. *Geochim. Cosmochim. Acta* 38, 1023-1059.
- McDonough, W.F., McCulloch, M.T. and Sun, S-s. (1985) Isotopic and geochemical systematics in basalts from southeastern Australia and implications for the evolution of subcontinental lithosphere. *Geochim. Cosmochim. Acta* 49, 2051-2067.
- Nickel, K.G. and Green, D.H. (1984) The nature of the upper-most mantle beneath Victoria, Australia as deduced from ultramafic xenoliths. In Kornprobst, J. ed, *Kimberlites II: The Crust-Mantle Relationships* pp. 161-178. Elsevier, Amsterdam.

CARBONATED XENOLITHS FROM THE MACDOUGAL SPRINGS MICA PERIDOTITE DIATREME:
INFERENCES FOR UPPER MANTLE CONDITIONS IN NORTH-CENTRAL MONTANA

E.S. McGee and B.C. Hearn, Jr.

U.S. Geological Survey, Reston, VA USA

Carbonated garnet, spinel, and garnet-spinel harzburgites and lherzolites comprise the largest group of upper mantle xenoliths from the MacDougal Springs mica peridotite, located in the Missouri River Breaks area of north-central Montana. Primary and secondary silicate minerals in these xenoliths reveal that, in this region, the upper mantle has experienced a complex history of metasomatic and intrusive activity. These xenoliths represent a range of upper mantle assemblages across the transition: garnet lherzolite + garnet + spinel lherzolite + spinel lherzolite. Unaltered garnet cores, surrounded by clay + spinel alteration, give the garnet bearing xenoliths a distinctive appearance; similar clots in other xenoliths suggest the former presence of garnet. Compositions of primary and secondary spinel and phlogopite in some xenoliths reflect a range of conditions. Calcite and minor quartz have completely replaced the original olivine and orthopyroxene. Although the xenoliths are altered, fresh garnet, clinopyroxene, and spinel that remain reveal characteristics of the xenolith source region. Secondary minerals, especially those in clusters of fine-grained spinel + phlogopite ± diopside ± fine-grained clay or serpentine are varied in composition and are important because they provide clues about the fluids and the sequence of alteration.

82 upper mantle xenoliths were collected from a carbonate-rich altered breccia adjacent to a fresh, carbonate-rich mica peridotite. The xenoliths range from 2 to 10.5 cm, are ellipsoidal in shape, and are similar to the type B carbonated xenoliths from Sekameng (Nixon and Boyd 1973) but are more extensively carbonated. 25% contain garnet, 57% contain spinel, and 18% contain both garnet and spinel. Diopside makes up less than 5% by volume of most xenoliths; thus the suite is predominantly harzburgitic. Minerals are categorized as primary, secondary, or alteration phases. Primary minerals are medium to large (>1mm) and are usually isolated grains. Secondary minerals are smaller (<1mm) and commonly rim primary minerals or are clustered with other secondary minerals. Alteration minerals partially or completely replace mineral phases. Garnet and clinopyroxene are primary phases only; spinel and phlogopite are primary and secondary. Alteration phases are calcite, quartz, apatite, and clay or serpentine.

Alteration surrounds garnets and clinopyroxenes in garnet-bearing peridotites, but fresh cores remain. The garnets are pyrope, show little range in composition (Fig. 1), and are chromium rich (3.4-7.0 wt. % Cr₂O₃). No major compositional differences exist between garnets from garnet-only peridotites and garnets from garnet-spinel peridotites. Clinopyroxene compositions overlap and have similar iron contents in all three types of peridotites (Fig. 1); clinopyroxenes from spinel peridotites have the widest range of Ca/(Ca+Mg). Clinopyroxenes have significant chromium (1.56-3.29 wt. %), aluminum (0.70-3.77 wt. %), and sodium (1.08-2.99 wt. %). Clinopyroxenes from garnet peridotites are slightly richer in Cr₂O₃, Al₂O₃, and Na₂O than clinopyroxenes from spinel peridotites; clinopyroxenes from garnet-spinel peridotites are intermediate. Primary spinels are chromium rich (56.1-58.9 wt. % Cr₂O₃); Al₂O₃ and MgO are 8.5-10.1 wt. % and 12.4-13.2 wt. %, respectively. Primary spinels from garnet-spinel peridotites and from spinel peridotites are not significantly different. Primary phlogopite ranges up to 4mm in size; it has 2.7 wt. % FeO, 1 wt. % Cr₂O₃, and 0.75 wt. % TiO₂. Primary phlogopite is significant in the spinel peridotites.

Spinel is the more abundant and more compositionally variable of the secondary minerals. Chromium is 23.1 to 58.4 wt. %, and aluminum is 8.5 to 43.8 wt. %. Three distinct spinel compositions (Cr/(Cr+Al) = 0.25-0.40, 0.55-0.70, or 0.75-0.95) are represented in the secondary group (Fig. 2) but do not correlate with xenolith type. Secondary phlogopites are richer in TiO₂ (~3 wt. %) compared to primary phlogopites.

Xenolith textures are dominantly granular; thin serpentine veins enclose patches of calcite (± quartz) and preserve original grain outlines. Distinctive fine-grained spinel-rich clots differ in the garnet and spinel peridotites. Garnet-bearing xenoliths contain round 2-4 mm clots of brown clay; small spinels decrease in size from the

clot rim (0.5mm) to the core (<0.01 mm). These clots are partly or completely altered garnets, as some contain remnants of pyrope garnet. Small spinels rim the edges of the clots and are subsidiary to the predominant clay-serpentine; they are Al-rich and have a limited compositional range. Clinopyroxene and discrete phlogopite grains are rare in these clots and are restricted to the outer rim, next to the surrounding calcite.

Spinel peridotite clots are smaller (1-2mm), more diffuse, and coarser grained than garnet peridotite clots. Phlogopite and spinel are the predominant minerals; clinopyroxene, calcite, and apatite may also be present. Brown clay that is characteristic in the garnet peridotite clots is absent or negligible in the spinel peridotite clots, which resemble the pools of primary spinel + diopside + phlogopite that have been described in xenoliths from the Pipe 200 (Carswell et al., 1979) and the Bultfontein kimberlites (Delaney et al., 1980). Clot spinels in Maccougal Springs spinel peridotites are variable in size, randomly distributed, and compositionally variable; Cr-rich spinel coexists with Al-rich spinel, and in some instances Al-rich spinel mantles Cr-rich spinel. Phlogopite is nearly euhedral in some clusters, clay-serpentine is minimal in the clusters, and clinopyroxene, if present, is intergrown with spinel, phlogopite, and serpentine.

Calcite replaces olivine and orthopyroxene throughout the samples; with serpentine, it invades clinopyroxenes and it is intergrown in some phlogopite and spinel clots. Minor quartz forms clusters or strings of rounded grains or ragged patches in the center of some calcite grains. Fine-grained brown saponite(?) fills cracks throughout the xenoliths and surrounds primary phases, particularly the clinopyroxenes. In two spinel peridotites minor apatite is finely disseminated and associated with abundant quartz and calcite, or forms fine needles in a phlogopite-spinel clot.

DISCUSSION

Compositions of the primary minerals indicate that the xenoliths equilibrated over a range of temperatures, but because primary clinopyroxene compositions vary little and do not correlate with xenolith type, calculated temperatures for the three xenolith types overlap. Spinel peridotite equilibration temperatures (Lindsley and Dixon 1976, 20-kb thermometer) range most widely (750-1065 °C); garnet peridotite temperatures range the least (935-1080 °C). The overlap of the calculated temperatures and the similarity of the primary mineral phases in each of the three xenolith types suggest that, although the xenoliths are nominally three distinct rock types, they represent a continuum of upper mantle compositions and conditions. Pressures of equilibration can only be inferred because orthopyroxene was not preserved, but if a continental geotherm similar to the present day geotherm is assumed, the xenoliths were derived from depths of 66 to 150 km.

Textures and mineral compositions indicate that at least four events have altered all the xenoliths. The events occurred in the following order: 1) development of secondary spinels; 2) serpentinization along grain boundaries; 3) carbonation that replaced all olivine and orthopyroxene; and 4) development of clay between grains and within cracks. Phlogopite was present as a primary phase, but it may also have grown during one or more of these stages. Aluminum-rich spinels were formed either at or near the source of the peridotite xenoliths. Disequilibrium that triggered secondary spinel development may have been caused by the introduction of a K-rich fluid accompanied by secondary phlogopite growth. Alternatively, Al-rich spinels may have developed after the xenoliths were carried a short distance upward, during a partial intrusion of magma. Ascent of the xenoliths to the surface arrested secondary spinel development and was accompanied by very little alteration. After the xenoliths were carried to a shallow level, serpentine developed along grain boundaries as a water-rich fluid invaded and preserved original textures. Invasion of a carbonate rich fluid followed, completely replacing olivine and orthopyroxene without disrupting the serpentinized grain boundaries. Development of clay during the fourth stage of alteration may have begun while the carbonation took place and continued after the carbonation ceased, accentuating the alteration rims on garnets and clinopyroxenes. Garnet and spinel peridotites were affected by each of the alteration stages but clay alteration is enhanced in the garnet peridotites. The garnet peridotites may have been more susceptible to the last alteration.

The mica peridotite magma was probably the source of the altering fluids. The Macdougall Springs diatreme experienced a series of multiple intrusions and all of the xenoliths are from a breccia that borders the main pipe. Field evidence suggests this breccia was emplaced during the second intrusive event at the diatreme and this event was followed by at least two or three intrusions. McCallum (1976) observed increased alteration in kimberlite pipes that experienced sequential intrusive pulses. The Macdougall carbonated xenoliths were collected from an extensively altered breccia, indicating the influence of magmatic or late fluid activity. CaO and CO₂-enriched calcium-silicate veins in the pyroclastic fill of the main Macdougall Springs pipe and adjacent dike material indicate enhanced carbonate-fluid activity. These subsequent intrusions in adjacent portions of the diatreme probably affected or enhanced xenolith alteration. Varying volume and composition of the erupting magma are reflected in the alteration and metasomatism of the xenoliths.

REFERENCES

- CARSWELL D.A., CLARKE D.B. and MITCHELL R.H. 1979. The petrology and geochemistry of ultramafic nodules from Pipe 200, Northern Lesotho. In Boyd F.R. and Meyer H.O.A. eds, *The Mantle Sample: Inclusions in Kimberlites and Other Volcanics*, pp. 127-144. American Geophysical Union, Washington, DC.
- DELANEY J.S., SMITH J.V., CARSWELL D.A. and DAWSON J.B. 1980. Chemistry of micas from kimberlites and xenoliths--II. Primary- and secondary-textured micas from peridotite xenoliths. *Geochimica et Cosmochimica Acta* 44, 857-872.
- LINDSLEY D.H. and DIXON S.A. 1976. Diopside-enstatite equilibria at 850° to 1400°C, 5 to 35 kb. *American Journal of Science* 276, 1285-1301.
- MCCALLUM M.E. 1976. An emplacement model to explain contrasting mineral assemblages in adjacent kimberlite pipes. *Journal of Geology* 84, 673-684.
- NIXON P.H. and BOYD F.R. 1973. Carbonated ultrabasic nodules from Sekameng. In Nixon P.H. ed. *Lesotho Kimberlites*, pp. 190-196. Lesotho National Development Corporation, Maseru.

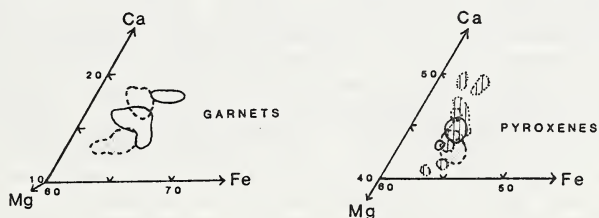


Fig. 1 Portions of Ca-Mg-Fe ternary for garnets and clinopyroxenes, by xenolith type. Solid line = garnet-only, gray = garnet + spinel, vertical lines = spinel-only.

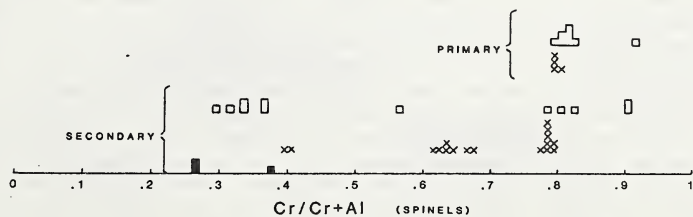


Fig. 2 Cr/Cr + Al in spinels by xenolith type. Solid squares = garnet-only, crosses = garnet + spinel, open squares = spinel-only.

Martin Menzies, Department of Geology, University of London (RHBNC), Egham,
Surrey TW20 OEX, England

Alexander Halliday, SURRC, East Kilbride, Glasgow G75 0QU, Scotland

Zenon Palacz, Earth Sciences, Open University, Milton Keynes MK7 6AA, England

Robert Hunter, Earth Sciences, Cambridge University, Cambridge CB2 2EW, England

Christopher Hawkesworth, Earth Sciences, Open University, Milton Keynes MK7 6AA,
England

INTRODUCTION

Controversy has arisen over the relative contribution of crust and mantle during the formation and evolution of Scottish igneous rocks emplaced in the Silurian-early Devonian and the Tertiary period. Whilst many studies have concentrated on an evaluation of the extent of contamination and the provenance of the crustal rocks presumed to have been involved, others have turned their attention to the polybaric history of the volcanic rocks including a detailed assessment of their source region. An inherent assumption in the majority of these ventures has been that the mantle beneath the N.W. Highlands of Scotland is relatively depleted and similar to the source of Atlantic MORB. This could prove to be a dangerous assumption since studies in S. Africa and Antarctica have revealed the presence of extremely heterogeneous lithospheric mantle. Although possibly underlain by relatively homogeneous MORB-OIB mantle this chemically complex lithospheric keel may modify asthenospheric magmas during their ascent to the surface or even act as an independent source for more unusual magmas.

LOCH ROAG XENOLITH DIKE

Peridotite and pyroxenite xenoliths found in a monchiquite dike on the island of Lewis, Scotland (Upon et al 1983) are enriched in barium, the light rare earth elements and in some instances niobium. Megacryst suites indicate the presence of a mineralogically complex upper mantle as they are characterised by apatite + mica + corundum + zircon + Nb rutile + anorthoclase. A time-integrated response to the low Sm/Nd and Rb/Sr ratios has resulted in an extremely variable Nd isotopic composition ($^{143}\text{Nd}/^{144}\text{Nd} = 0.51247-0.51097$) ($\epsilon_{\text{Nd}} = -3.4$ to -32.6) and a limited variation in Sr isotopic composition ($^{87}\text{Sr}/^{86}\text{Sr} = 0.70415-0.70636$) ($\epsilon_{\text{Sr}} = -5.0$ to $+26.4$). These data are very similar to Lewisian and Moianian metamorphic rocks and as such their isotopes could be thought of as "crustal" in character (fig.1). Furthermore these data overlap with that observed in garnet inclusions in megacrystic diamonds from kimberlites (Richardson et al 1984). and with lamproites - Group II Kimberlites (Fraser et al 1985). Model ages indicate that the pyroxenite-peridotite assemblage was affected by the influx of a LREE enriched, Rb depleted melt or fluid some 1.2 Ga ago. The remarkable similarity in isotopes and trace element characteristics (low Rb/Sr, low Rb/Ba) of the xenoliths and lamproites leads us to suggest that the melt responsible for this metasomatic enrichment was lamproitic. Hebridean mantle has evolved, locally, in a manner similar to that occurring below the S. African and N. American cratons.

EVIDENCE FOR CHEMICALLY ENRICHED LITHOSPHERIC MANTLE

Several investigators of Scottish volcanic rocks have commented on the need for "locally" heterogeneous mantle enriched in Ba, Sr, LREE with repositories for elements like P, Ta and Nb. Moreover, in a detailed study of Siluro-Devonian volcanism it was noted that volcanic rocks of the S.W. Highlands had systematically higher concentrations of Sr, K, Ba, P and the LREE in the more Ni-rich undifferentiated samples (Thirlwall 1982). A mantle source with a time integrated enrichment in incompatible elements would better explain these features than any model involving crustal contamination. A similarly unusual mantle contribution may account for the trace element and isotopic provinciality apparent in so many Scottish granitoids. The Scottish granitoids become enriched in Ba, Sr, LREE and impoverished in Rb and Th towards the northwest. Isotopically these rocks are more "Lewisian-like" indicative of either extensive contributions from the basement via assimilation and melting or some contribution to their chemistry from lithospheric mantle enriched in incompatible elements (Halliday et al 1986). Several independent lines of evidence appear to indicate that beneath the older crustal regions of N.W. Scotland the possibility exists for the presence of mantle that is

chemically enriched and has with time become isotopically distinct from the mantle tapped by magmas erupted in the Midland Valley of Scotland, or elsewhere in the North Atlantic volcanic province. Hence, the apparent regional chemical anomalies in the Scottish mantle defined by the enhanced trace element concentrations of Silurian-Devonian lavas and Palaeocene volcanic rocks of the British Tertiary province may result from the involvement of trace element enriched Hebridean lithospheric mantle like that found at Loch Roag.

CONCLUSION

Lithospheric mantle acts as a barrier to the passage of asthenospheric melts. Interaction between peridotite mantle and melts or fluids of variable chemical composition results in immediate chemical heterogeneity. The passage of time guarantees isotopic heterogeneity governed by the Sm/Nd and Rb/Sr ratios. Beneath the Archean of Scotland incompatible element enriched alkalic melts or fluids derived possibly from ancient subduction interacted with lithospheric mantle some 1.2 G yr ago. The resultant high concentrations of LREE in the wall rock and low Rb/Sr ratios produced isotopically unique lithosphere. This lay relatively undisturbed until in the Tertiary major tectonic changes due to the opening of the Atlantic led to disruption and possible involvement of this lithospheric keel in basaltic volcanism of the BTVP. The Hebridean mantle has recorded a variety of enrichment processes since the Archean resulting in the existence of enriched heterogeneous sub-Lewisian lithospheric mantle.

REFERENCES

- FRASER K.J., HAWKESWORTH C.J., ERLANK A.J., MITCHELL R.H. and SCOTT-SMITH B.H. 1985. Sr, Nd and Pb isotope and minor element geochemistry of lamproites and kimberlites. *Earth and Planetary Science Letters* 76, 1, 57-70
- HALLIDAY A.N., STEPHENS W.E., HUNTER R.U., MENZIES M.A., DICKIN A.P. and HAMILTON P.J. 1986. Isotopic and chemical constraints on the building of the Deep Scottish lithosphere. *Scottish Journal of Geology Special Issue* (in press).
- RICHARDSON S.H., GURNEY J.J., ERLANK A.J. and HARRIS J.W. 1984. Origin of diamonds in old enriched mantle. *Nature* 310, 198-202.
- THIRLWALL M.F. 1982. Systematic variation in chemistry and Nd-Sr isotopes across a Caledonian calc-alkaline volcanic arc: implications for source materials. *Earth and Planetary Science Letters* 58, 27-50.
- UPTON B.G.J., ASPEN P. and CHAPMAN N.A. 1983. The upper mantle and deep crust beneath the British Isles: Evidence from inclusion suites in volcanic rocks. *Journal Geological Society London* 140, 145-122.

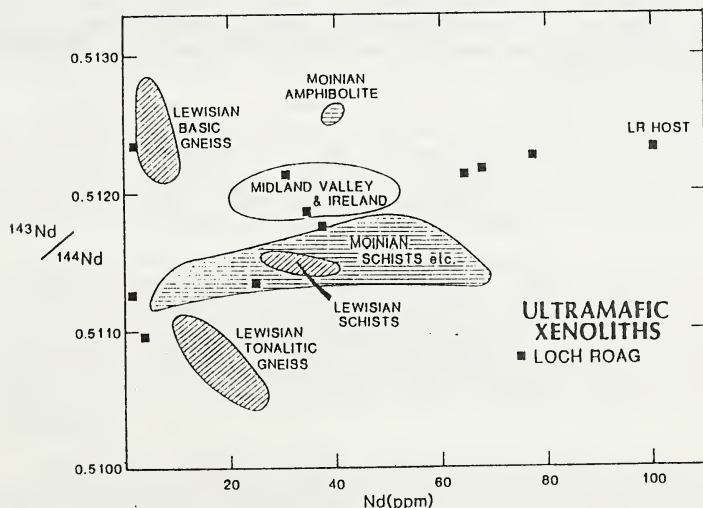


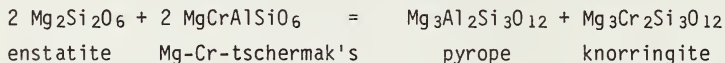
Fig.1 - Nd isotopic composition and relative abundance of Nd in Loch Roag xenoliths relative to crustal rocks.

K. G. Nickel

Max-Planck-Institut für Chemie, Saarstrasse 23, D-6500 Mainz, F.R.Germany

Experiments have been carried out in the system SMACCR from 900 to 1400°C and 15 to 35 kb. Equilibrium compositions for Al- and Cr-contents of both ortho- and clinopyroxene have been approached from different directions. The results allow an evaluation of the influence of Cr in the two pyroxenes and in garnet on solubilities of Al and Ca in pyroxenes. The behaviour of the quaternary solid solutions is thermodynamically complex.

Even in this simple, Na-free system clinopyroxene dissolves more Cr than orthopyroxene at a given condition, but Cr/Al exchange between ortho- and clinopyroxene or between pyroxenes and spinel is not sufficiently P- or T-dependent to be used for geothermobarometry. The Cr-solubility in orthopyroxene coexisting with garnet presents however an alternative to geobarometry based on Al-solubilities in orthopyroxene. The reaction



is similarly pressure- (and temperature-) dependent as conventional Al-barometry. Using recently developed non-ideality expressions for Ca-Mg mixing in garnets (Brey et al., 1986) and the cross-site interaction due to the reaction pyrope + uvarovite = grossular + knorringite (Nickel, 1986) values of $\Delta H^\circ = 15193$ cal, $\Delta S^\circ = -5.06$ cal/K and $\Delta V^\circ = -371$ cal/kb are obtained to satisfy the experimental data in the system SMACCR. Corrections for the influence of Fe on the reaction are checked with the aid of experiments in natural systems (Brey and Nickel, this volume). The use of independent barometric methods increases the precision of P-estimates for garnet-bearing nodules from kimberlite.

REFERENCES

- BREY, G.P. and NICKEL, K.G. (this volume). Experimental calibration of geothermobarometers in natural lherzolitic systems at high pressure.
- BREY, G.P., Nickel, K.G. and Kogarko, L. 1986. Garnet-pyroxene equilibria in the system CaO - MgO - Al₂O₃ - SiO₂ (CMAS): prospects for simplified ('T-dependent') lherzolite barometry and an eclogite barometer. *Contrib. Mineral. Petrol.* 92, 448-455.
- NICKEL, K.G. 1986. Phase equilibria in the system SiO₂ - MgO - Al₂O₃ - CaO - Cr₂O₃ (SMACCR) and their bearing on spinel/garnet lherzolite relationships. *N.Jb.Min. Abh.* 155 (2). In press.

MANTLE MAGMATIC EVENTS INDICATED BY ZONED OLIVINE AND PYROXENE
COMPOSITIONAL VARIATIONS IN A COMPOSITE MANTLE XENOLITH FROM
LASHAINE VOLCANO, TANZANIA

J.E. Nielson
U.S. Geological Survey

New information on the petrology and geochemistry of a composite mantle xenolith from Lashaine Volcano, Tanzania, indicates a diverse history for the mantle beneath eastern Africa. The xenolith is composed of websterite and olivine-rich wehrlite. In the wehrlite are preserved contrasting compositional gradients that reflect at least two igneous-metasomatic events in the mantle before entrainment of the xenolith by the host ankaramite lava.

The xenolith consists of olivine-rich spinel wehrlite in contact with spinel websterite. Both rock types are brecciated, but the wehrlite is more extensively disaggregated than the websterite. In one portion of the sample, a fragment of websterite is isolated in wehrlite (Pike et al., 1980). The wehrlite contains olivine porphyroclasts as large as 5.5 mm across that are surrounded by a finely comminuted matrix of irregular porphyroclastic olivine and clinopyroxene, and rare corroded spinel grains. Euhedral twinned and sector-zoned clinopyroxene neoblasts occur sparsely in the comminuted matrix, along with minute brown spinel neoblasts(?). The wehrlite originally was composed of about 90% olivine, 9% clinopyroxene, and a trace of spinel.

A textural transition zone, 4 mm wide, of clinopyroxene porphyroclasts as large as 2 mm across in a brecciated wehrlite matrix, separates the wehrlite from the websterite. The pre-brecciation even-grained mosaic texture of pyroxene (avg grain size, 1.5 mm) is preserved in the websterite. The modal composition of the websterite is 85% orthopyroxene, 10-12% clinopyroxene, and 3-5% euhedral black spinel grains. Clinopyroxene grain margins and some contacts between clinopyroxene and orthopyroxene appear spongy owing to partial melting.

The bulk composition of the websterite is markedly more Fe-rich (Mg-ratio, $Mg/(Mg + \Sigma Fe) = 0.75$) than that of the wehrlite (0.85). This wehrlite composition is in the middle of the range of variation for analyzed spinel-bearing peridotites (dominantly lherzolites) from Lashaine Volcano: the Mg-ratios of seven rocks in the U.S. Geological Survey (USGS) collection range from 0.71 to 0.92. Garnet or garnet+spinel peridotites from Lashaine are highly magnesian and have Mg-ratios between 0.91 and 0.94 (analyzed specimens in the USGS collection; see also data of Rhodes and Dawson, 1975).

In the composite xenolith the Fe content of clinopyroxene and small olivine grains decreases across the transition zone from websterite to wehrlite. A contrasting gradient of increasing Fe content from rims to cores occurs within olivine porphyroclasts in the wehrlite. Systematic electron microprobe (SEM-Q) analyses show that clinopyroxene porphyroclasts and neoblasts in the wehrlite have Mg-ratios of 0.87-0.84, whereas clinopyroxenes in the websterite have Mg-ratios of 0.82-0.80 (Fig. 1). In the transition zone both the Mg-ratios of clinopyroxenes and the Fe content of small olivine grains decrease with closer proximity to the websterite contact. Gradients also occur in the CaO, TiO₂, Na₂O, Al₂O₃, and Cr₂O₃ contents of clinopyroxene across the transition zone. Orthopyroxene is found only in the websterite, and has Mg-ratios similar to the clinopyroxenes. The scatter in Figure 1 is due to large inhomogeneities in the pyroxene grains.

Large and small olivine porphyroclasts in the wehrlite are reversely zoned. Normally the rims are relatively magnesian (Fo_{99.5} max), and the cores are Fe-rich (Fo₈₁ max). However, more complex zoning also occurs (Fig. 2). The zoning is not apparent either optically or in SEM images of X-ray spectra. Truncation of the zone boundaries by broken grain margins indicates that the zoning predated brecciation. Matrix olivines adjacent to the porphyroclasts have Fo contents that range from 85.2 to 89.3, like the relatively magnesian porphyroclast margins.

The compositional gradient in clinopyroxene grains between wehrlite and websterite is one of increasing Fe enrichment toward the websterite. This Fe enrichment, and the xenolith-in-xenolith texture of pyroxenite in peridotite (Pike et al., 1980), resemble the relations identified in other composite peridotite-pyroxenite xenoliths from basaltic lavas (Irving, 1980; Wilshire et al., 1985) and kimberlites (Harte et al., 1977). The websterite is interpreted to represent a relatively Fe-rich basaltic melt that intruded the more magnesian wehrlite. Reaction between this melt and the more magnesian wallrock converted minerals of the wehrlite in and near the contact zone to more Fe-rich compositions.

Formation of Mg-rich margins on zoned olivine grains is opposite to the trend that likely would have occurred from reaction between Fe-rich fluid from the websterite and more magnesian olivine grains of the wehrlite. The Mg-Fe olivine zoning is accordingly interpreted to have resulted from a

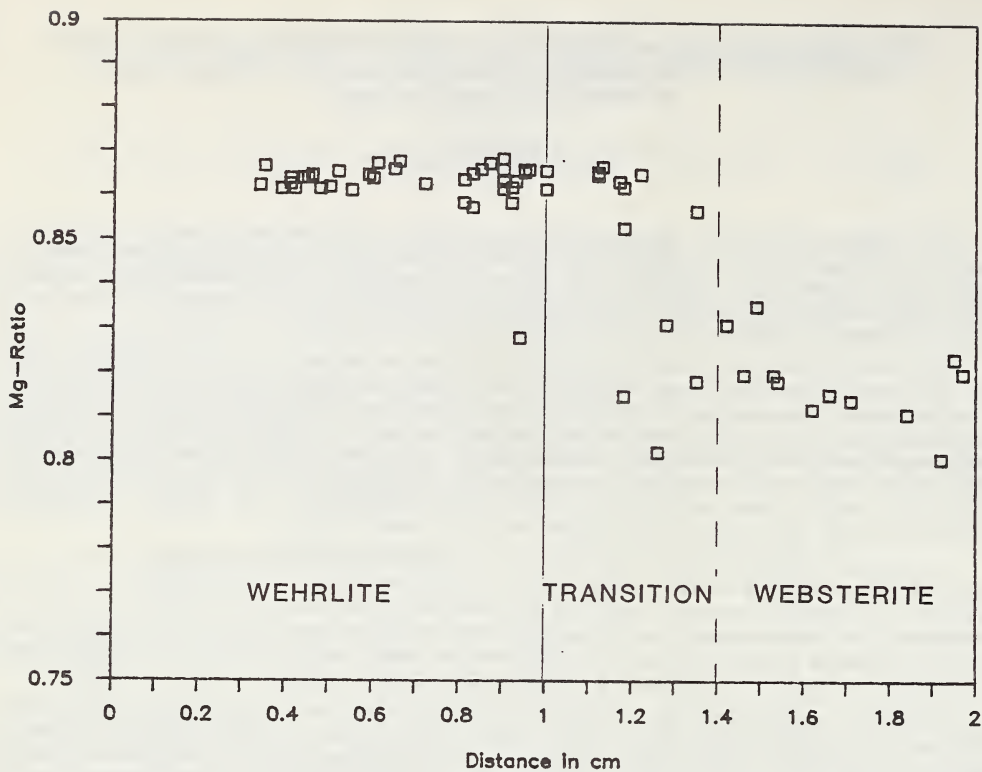


Figure 1. Variations of Mg and Fe content (Mg-ratio, $Mg/(Mg+\Sigma Fe)$) of clinopyroxene across a single probe mount (2.5 cm diam). Origin is at edge of wehrlite on probe mount; plane of projection is orthogonal to trend of wehrlite-websterite contact. Solid line is trace of contact between wehrlite and transition zone; dashed line is approximate contact of transition zone and websterite.

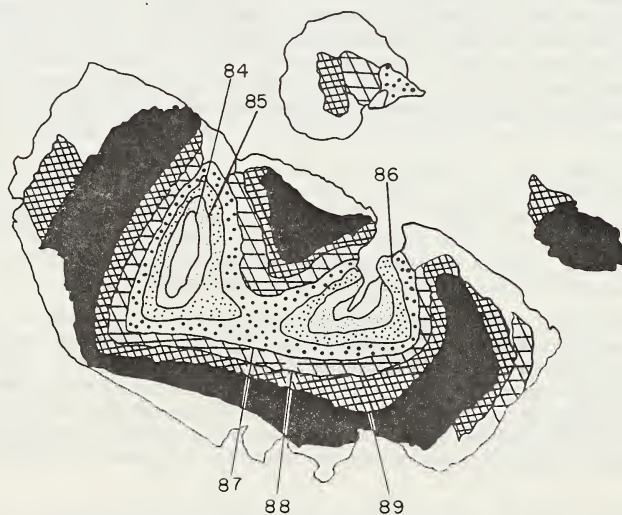


Figure 2. Zoned olivine porphyroblast, 5.0x2.5 mm. Contours in Fo content.

separate event that extracted Fe from the wehrlite. This event could have occurred if small amounts of relatively magnesian melt migrated through the wehrlite and websterite and caused depletion of Fe in the olivine grain margins. The absence of zoning in pyroxene, in contrast to the strong zonation of olivine, is generally consistent with data on relative rates of sub-solidus diffusion in olivine and pyroxene (e.g., Freer et al., 1982; Smith and Wilson, 1985) and on the dissolution of these minerals in basaltic liquids (Kuo and Kirkpatrick, 1985). Low rates of sub-solidus diffusion of Ca, Al, Mg, and Fe in pyroxenes are indicated by the absence of detectable reactions at high temperature (Freer et al., 1982). Conversely, the experiments by Kuo and Kirkpatrick (1985) suggest that olivine dissolves in basaltic melt more slowly than does clinopyroxene. The relation depends on several factors, including melt composition, mineral composition, and pressure. Experiments suggest that olivine should homogenize rapidly either by reaction with fluid or by sub-solidus diffusion (within a year, Smith and Wilson, 1985). Thus, zoning in olivine from Lashaine must have occurred in an event later than emplacement of the websterite.

From these data, I suggest that the Lashaine composite xenolith represents mantle peridotite wallrock that was intruded in more than one event by basaltic melts of contrasting compositions. In the first event minerals of the magnesian peridotite reacted with Fe-rich fluid that emanated from a basaltic intrusion as it crystallized to websterite. The compositional gradients created by this reaction would require very long periods of time to disappear by subsolidus diffusion between pyroxene grains, whereas the olivine compositions may have become homogenized very quickly, theoretically in less than a year (Smith and Ehrenberg, 1984).

The second event occurred an unknown time later (probably less than 1 Ma). In this event a more magnesian basaltic melt invaded the rocks and reacted with minerals in both the wehrlite and websterite. Minor inhomogeneities evident in the clinopyroxene porphyroclasts (Fig. 1) may have formed by reaction with this postulated magnesian melt. Olivine apparently dissolves in basaltic melts more readily than pyroxene and this difference may explain why the olivine margins were markedly depleted in Fe. However, because olivine should homogenize very quickly, the preservation of this zoning suggests that the second event occurred very shortly before eruption of the host lava. Both events predated brecciation of the rock association. The brecciation probably occurred as part of the eruptive process. The formation of clinopyroxene (and spinel?) neoblasts must have predated the eruption, but the relation between neoblast crystallization and the brecciation event is unclear.

REFERENCES

- Freer, R., Carpenter, M.A., Long, J.V.P., and Reed, S.J.B., 1982, "Null result" diffusion experiments with diopside: implications for pyroxene equilibria: *Earth and Planetary Science Letters*, v. 58, 285-292.
- Harte, B., Gurney, J., and Cox, K.G., 1977, Clinopyroxene-rich sheets in garnet-peridotite: xenolith specimens from the Matsoku kimberlite pipe, Lesotho: Second International Kimberlite Conference, Extended Abstracts Volume, no page number.
- Irving, A.J., 1980, Petrology and geochemistry of composite ultramafic xenoliths in alkalic basalts and implications for magmatic processes within the mantle: *American Journal of Science*, The Jackson Volume, v. 280-A, part 2, p. 389-426.
- Kuo, L. and Kirkpatrick, R.J., 1985, Dissolution of mafic minerals and its implications for the ascent velocities of peridotite-bearing basaltic magmas: *Journal of Geology*, v. 93, p. 691-700.
- Pike, J.E., Nielson, Meyer, C.E., and Wilshire, H.G., 1980, Petrography and chemical composition of a suite of ultramafic xenoliths from Lashaine, Tanzania: *Journal of Geology*, v. 88, p. 343-352.
- Rhodes, J.M. and Dawson, J.B., 1975, Major and trace element chemistry of peridotite inclusions from the Lashaine volcano, Tanzania: *Physics and Chemistry of the Earth*, v. 9, p. 545-557.
- Smith, D. and Ehrenberg, S.N., 1984, Zoned minerals in garnet peridotite nodules from the Colorado Plateau: implications for mantle metasomatism: *Contributions to Mineralogy and Petrology*, v. 86, p. 274-285.
- Smith, D. and Wilson, C.R., 1985, Garnet-olivine equilibration during cooling in the mantle: *American Mineralogist*, v. 70, p. 30-39.
- Wilshire, H.G., Meyer, C.E., Nakata, J.K., Calk, L.C., Shervais, J.W., Nielson, J.E., and Schwarzman, E.C., 1985, Mafic and ultramafic xenoliths from volcanic rocks of the western United States: U.S. Geological Survey Open-File Report 85-139, 505 p.

H. St. C. O'Neill¹, A. L. Jaques², C. B. Smith³ and J. Moon³

1. Research School of Earth Science, Australian National University, Canberra, ACT
2. Bureau of Mineral Resources, Canberra ACT
3. CRA Exploration Pty Limited, 21 Wynyard Street, Belmont WA

A suite of garnet peridotite xenoliths, some carrying diamonds at grades as high as the equivalent of 7.5 ct/tonne, has been recovered from the diamondiferous Argyle AK1 pipe, in northwestern Australia. Many of the xenoliths are altered but relicts of most primary phases have enabled estimates of the P-T equilibration history of the xenoliths. Significantly, all fall well within the diamond stability field in the mantle.

The xenoliths, which are rounded and range up to 7 cm diameter, have undergone varying degrees of alteration to talc, serpentine, and/or montmorillonite assemblages. Relict phases indicate that all are coarse textured garnet and chromite-garnet lherzolites and harzburgites containing a primary (P1) assemblage of olivine, enstatite, garnet, + diopside + rare picrochromite. In all cases the original garnet has been replaced by Al-spinel and Al-pyroxenes together with secondary calcite + serpentine + phlogopite + K-feldspar + illite. The Al-spinel and Al-pyroxenes (assemblage P2) typically forms very fine symplectic intergrowths, commonly radially oriented, at the core of the larger former garnets and are enveloped by coarser grained, euhedral to sub-skeletal spinel and pyroxene grains at the rim. Similar reaction coronas on garnets in peridotites from the Lashaine volcano and the Lesotho kimberlites have been described by Reid and Dawson (1972) and Lock and Dawson (1980) who attributed the corona formation to reaction of garnet and olivine to Al-pyroxenes and Al-spinel as a result of re-equilibration within the spinel lherzolite facies. However, in the Argyle nodules no relict garnet remains and the cores of many of the smaller former garnets are totally replaced by secondary silicates. These features, together with the highly irregular outlines of the former garnets and the quench-like form of many of the spinels and pyroxenes forming symplectic intergrowths in the larger former garnets, suggests that formation of the symplectite assemblage may have involved incongruent melting of the garnet followed by quenching of Al-rich spinels and pyroxenes from a melt as proposed by Hunter and Taylor (1982).

The P1 assemblage (Table 1) is characterised by uniformly magnesian compositions with olivine mg91-93 and pyroxenes mg92-94. The enstatites have exceptionally low Al₂O₃ (0.5-0.7%) and low CaO (0.8-1.1%), and significant Cr content (Table 1). The clinopyroxenes have high Cr (0.7-1.5% Cr₂O₃), and low Al₂O₃ (1.2-1.5%) and Na₂O (1%) contents; some contain significant K₂O. Ca/(Ca+Mg) ratios lie in the range 0.39-0.42. The picrochromites are extremely magnesian and Cr-rich (Cr/(Cr+Al) = 0.7-0.8). The highly refractory nature of this assemblage is typical of depleted peridotite and consistent with the high Mg/(Mg+Fe) ratios and very low Al₂O₃, CaO and Na₂O contents of their bulk rock compositions (Mg/(Mg+Fe) = 0.92, Al₂O₃ and CaO 1%, Na₂O = 0.03% or less).

In contrast, the P2 assemblage (Table 1) pyroxenes and spinels have high but variable contents of Al₂O₃ (up to 11% in opx, 10% in cpx). The Al-spinels show a very wide compositional range from more Al-rich cores to more Cr-rich rims (Cr/(Cr+Al) = 0.18-0.66).

Equilibration temperatures have been estimated for coexisting pyroxenes in both assemblages using the Ca solubility geothermometer of Bertrand and Mercier (1985). Pressures for assemblage P1 have been estimated using the garnet-orthopyroxene geobarometer of Nickel and Green (1985) and an assumed garnet composition with X_{Ca} = 0.15, X_{Cr} = 0.25 and Mg/Fe calculated from Fe-Mg partitioning between garnet and olivine (O'Neill and Wood, 1979). Uncertainties introduced by this assumed composition are small (2-3 kb), similar to the uncertainty attached to the geobarometer. Lower Ca and Cr contents will result in higher estimated pressures. Pressures for the P2 assemblage were estimated from the garnet-spinel transition (O'Neill, 1981).

Table 1 : Compositions of Phases in Argyle Xenolith (N24)

	ol	P1 opx	cpx	opx	P2 cpx	sp
SiO ₂	40.85	57.64	55.34	52.61	48.58	0.08
TiO ₂	nd	0.04	0.03	0.10	0.41	0.49
Al ₂ O ₃	nd	0.70	1.26	8.03	9.51	43.59
Cr ₂ O ₃	0.02	0.24	0.87	1.79	2.60	23.74
FeO	8.32	5.08	2.87	5.14	4.23	11.02
MnO	0.14	0.13	0.16	0.24	0.31	0.17
NiO	0.40	0.10	0.10	nd	nd	0.14
MgO	50.64	35.31	20.51	30.95	19.43	20.42
CaO	0.05	1.08	18.16	1.76	15.14	nd
Na ₂ O	nd	0.16	0.89*	nd	0.16	nd
Total	100.42	100.48	100.19	100.62	100.37	99.65
mg	91.6	92.6	92.7	91.5	91.2	76.8

*K₂O = 0.08%, nd = not detected

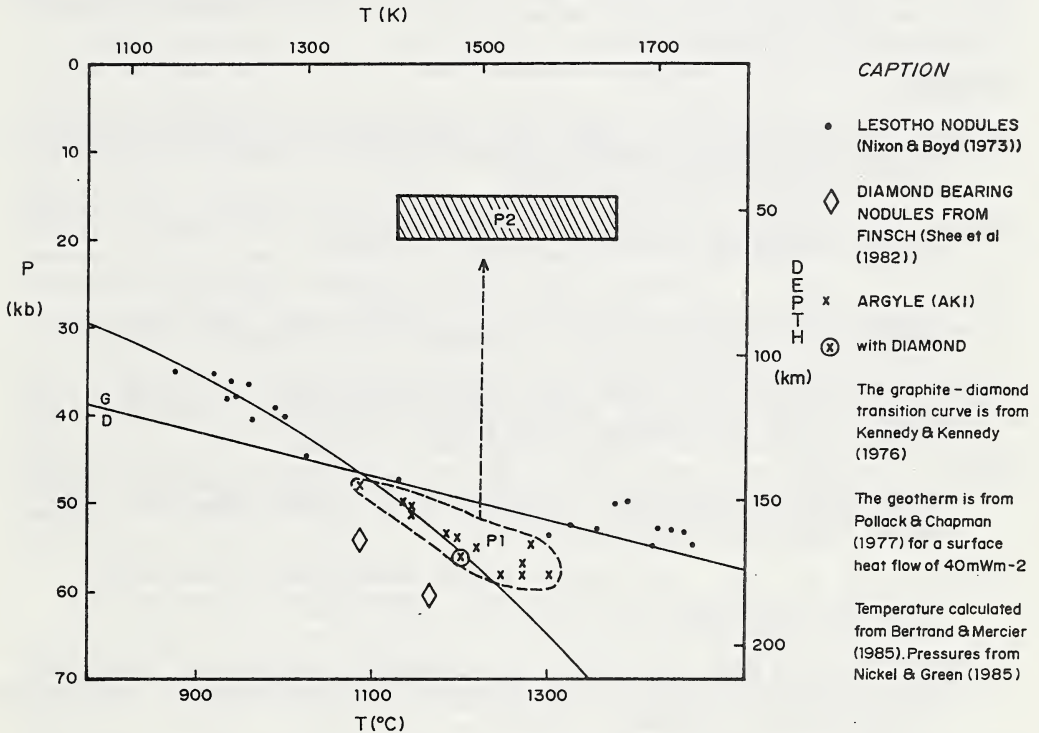


Fig. 1 P-T estimates for Argyle nodules

P-T estimates for the Argyle peridotite xenoliths are plotted in Fig. 1 together with estimates for two diamondiferous garnet lherzolites from the Finsch kimberlite (Shee et al, 1982) and for sheared and granular garnet lherzolites from the Lesotho kimberlites (Nixon and Boyd, 1973). The Argyle P1 assemblage and the diamondiferous Finsch peridotites fall well within the diamond stability field at pressures of 50-60 kb and temperatures of around 1200°C whereas the Lesotho lherzolites form two separate P-T fields both predominantly within the graphite stability field. Significantly, the lower temperature Lesotho xenoliths and the diamondiferous peridotites from Argyle and

Finsch all straddle the 40 mW m^{-2} continental (conductive) geotherm of Pollack and Chapman (1977) whereas the hotter Lesotho xenoliths are displaced towards a convective geotherm. Oxygen fugacities have been estimated for the chromite-bearing Argyle xenoliths using the olivine-orthopyroxene-spinel geosensor (O'Neill and Wall, in press) and lie within the wustite field below the magnetite-wustite and enstatite-magnesite-olivine-diamond buffer reactions.

Temperatures estimated for the P2 assemblage are similar to those of P1 whereas pressures are estimated at 20 kb or lower. This suggests that the P1 to P2 assemblage reaction is essentially one of decompression; the P-T estimates for the P2 assemblage lie close to the dry peridotite solidus.

The history of the Argyle xenoliths is therefore inferred to have been: (1) equilibration of refractory garnet lherzolite, depleted by prior melt extraction, well within the diamond stability field under a low geothermal gradient and reducing conditions where microdiamonds formed, (2) entrainment in a hot lamproite host magma, (3) ascent into the spinel peridotite stability field near the dry peridotite solidus causing reaction of garnet with olivine and incongruent (?) melting of the garnet, perhaps aided by metasomatic fluid from the host magma; subsequent quenching produced the Al-rich spinel and pyroxene, and (4) veining and alteration of the primary silicate phases and the inferred glass. The unusual complete elimination of the primary garnet in the xenoliths may reflect higher magmatic temperatures in the lamproite host than typically found in kimberlite.

REFERENCES

- BERTRAND, P. & MERCIER, J.-C. C., 1985. The mutual solubility of coexisting ortho- and clinopyroxene: toward an absolute geothermometer for the natural system? *Earth Planetary Science Letters* 76, 109-122.
- HUNTER, R. H. & TAYLOR, L. A., 1982. Instability of garnet from the mantle: Glass as evidence of metasomatic melting. *Geology* 10, 617-620.
- LOCK, N. P. & DAWSON, J. B., 1980. Garnet-olivine reaction in the upper mantle: evidence from peridotite xenoliths in the Letseng-la-Terae kimberlites, Lesotho. *Transactions of the Royal Society of Edinburgh: Earth Sciences* 71, 47-53.
- NICKEL, K. G. & GREEN, D. H., 1985. Empirical geothermobarometry for garnet peridotites and implications for the nature of the lithosphere, kimberlites and diamonds. *Earth and Planetary Science Letters* 73, 158-170.
- NIXON, P. H. & BOYD, F. R., 1973. Petrogenesis of the granular and sheared ultrabasic nodules suite in kimberlites. In Nixon, P. H. ed, *Lesotho Kimberlites*, 48-56. Lesotho National Development Corporation.
- O'NEILL, H. St. C., 1981. The transition between spinel lherzolite and garnet lherzolite, and its use as a geobarometer. *Contributions to Mineralogy and Petrology* 77, 185-194.
- O'NEILL, H. St. C. & WOOD, B. J., 1979. An experimental study of Fe-Mg partitioning between garnet and olivine and its calibration as a geothermometer. *Contributions to Mineralogy and Petrology* 70, 59-70.
- POLLACK, H. N. & CHAPMAN, D. S., 1977. On the regional variation of heat flow, geotherms and lithosphere thickness. *Tectonophysics* 38, 279-296.
- REID, A. M. & DAWSON, J. B., 1972. Olivine-garnet reaction in peridotites from Tanzania. *Lithos* 5, 115-124.
- SHEE, S. R., GURNEY, J. J. & ROBINSON, D. N., 1982. Two diamond-bearing peridotite xenoliths from the Finsch kimberlite, South Africa. *Contributions to Mineralogy and Petrology* 81, 79-87.

Suzanne Y. O'Reilly¹, W.L. Griffin² and B.D. Johnson¹

¹ School of Earth Sciences, Macquarie University, North Ryde,
NSW, 2113 Australia

² Mineralogisk-Geologisk Museum, Sars Gate, 1, 0562 Oslo, Norway

INTRODUCTION

Studies of the deep crust and uppermost mantle require the integration of petrologic and geophysical data to produce a geologically realistic model. Geophysicists need to incorporate into their modelling the petrologic constraints which are now available in considerable detail. The actual rock types present at depth, their relative proportions and stratigraphic relationships can be inferred from studies of xenolith suites and exposed terranes of tectonically-emplaced deep-seated sequences. Conversely, petrologic models must be consistent with the geophysical data including both field measurements (eg. seismic results) and laboratory measurements on the physical properties of the real rock types.

XENOLITH DATA AND GEOTHERMS

Xenolith-bearing basaltic and kimberlitic rocks are widespread on the earth's surface and hence give a statistically reasonable geographical sampling of the deep-seated rock types from all tectonic environments. We believe that the following traditional beliefs about the nature of the lower crust, Moho and upper mantle are challenged by the xenolith information. Geophysical models generally assume that the lower crust is andesitic, relatively homogeneous and that its thermal state can be described by a "continental geotherm". The Moho is commonly considered to be a sharp boundary both seismically and petrologically and to represent a discrete rock-type change from granulites to ultramafic rocks, this change being marked by an increase in compressional wave velocity (V_p) to about 8 km/sec. The upper mantle is generally modelled as homogeneous peridotite with $V_p >$ about 8 km/sec.

Xenolith suites reveal that the granulite- and eclogite- facies xenoliths which represent lower continental crustal material are overwhelmingly mafic (including plagioclase-rich types such as anorthositic) compositions (Griffin and O'Reilly, 1986a, 1986b, 1987). There are subordinate amounts of felsic meta-igneous rocks and very rare metasediments. Eclogite-facies rocks from the lower crust are restricted to some cratonic areas. Tectonically more active regions (e.g. eastern Australia) are characterized by granulite-facies lower crust, high geotherms and gradients in seismic velocity across broad (10-30 km) crust-mantle transition zones. P/T estimates on xenoliths, and exposed crustal sections, suggest that such gradients are due to interlayering of mafic rocks with felsic granulites in the lower crust, and with spinel lherzolite in the uppermost mantle.

A xenolith-derived geotherm for present-day southeastern Australia was constructed by O'Reilly and Griffin (1985) using geothermobarometry calculations on well-equilibrated mineral assemblages in xenoliths (mainly garnet websterites) from two young maars in western Victoria. P and T data from xenoliths from other basaltic provinces of various ages were then shown to plot on this geotherm. This geotherm gives a much higher T at any P than conventional continental or even oceanic geotherms. It has a strong curvature from about 10-30kb, indicating significant advective transfer of heat in the lower crust and upper mantle consistent with intrusions of basaltic magmas in those regions. This contrasts with the steady-state model conductive geotherm which has a shallower curvature at low pressures due to the assumption of simple conductive heat loss. This geotherm is higher than that of cratons (e.g. Western Australia). These differences in thermal state of contrasting continental lithosphere types are crucial in the interpretation of seismic data, especially when the lower crust is mafic.

MODEL FOR THE CRUST/MANTLE BOUNDARY

Using all the available xenolith information for eastern Australia it is possible

to construct a lower crust/upper mantle stratigraphy that is consistent with petrologic, P/T and geophysical data (Fig. 1). The crust/mantle boundary (CMB) occurs at about 25km which is the depth where ultramafic rocks (spinel lherzolites) start, and increase in proportion with depth. The black horizontal lines represent layers of mafic rocks which are frozen basaltic liquids or their cumulates (which may or may not have re-equilibrated to granulite or eclogite facies conditions). These decrease in proportion both up and down from the CMB. All lower crustal wall rocks are mafic to felsic granulites. The layers of mafic rocks represent repetitive basaltic under- and over-plating at the CMB by intrusive and tectonic processes.

Reversed seismic profiles for eastern Australia (Finlayson *et al.*, 1979) show that there is a gradient in V_p from about 25 km to 55 km where $\bar{V}_p =$ approx. 8 km/sec (Fig. 1) and thus represents the seismic Moho. 55 km is the predicted depth where the southeastern Australian geotherm crosses the spinel to garnet lherzolite boundary (Griffin *et al.*, 1984). Therefore it is suggested that in continental regions of high geothermal gradient, the seismic Moho represents the transition from spinel- to garnet- lherzolite rather than the CMB which represents the change from granulite to lherzolite wall rock.

Calculated (O'Reilly and Griffin, 1985) and measured (Bezant, 1985) V_p 's for real mantle rock types are consistent with this interpretation. These V_p values for spinel lherzolites are less than 8 km/sec for two main reasons: (i) the higher geothermal gradient lowers V_p and (ii) real mantle-derived spinel lherzolites generally contain significant (>40% pyroxene) which gives a lower V_p than peridotite which is usually used as the upper mantle rock type for modelling.

In order to address this problem, Bezant (1985) has devised a method for realistic estimation of V_p at 10 kb and 25°C for mafic and ultramafic rocks with different modes. Figure 2 illustrates the results for an olivine/clinopyroxene/orthopyroxene assemblage. This is based on the correlation of measured values of V_p (for three mantle-derived lherzolites) with those calculated using single crystal data (also based on laboratory measurements) for various modes. A temperature correction must be used for these values (e.g. Christensen, 1974) from T's derived by geothermometry calculations for the given mineral assemblage.

Another feature of seismic information are the zones with abundant horizontal reflectors (which we interpret as the mafic lenses) observed at depths of 15-35 km in many parts of the continental crust. These zones are usually described as "lower crust", with the seismically transparent zone below being "mantle". Despite demonstrations that the refraction Moho coincides with the base of such zones, this does not require that either the Moho, or the base of the layered zone, corresponds to the CMB. Where the uppermost mantle contains numerous subhorizontal lenses of mafic rocks (Fig. 1), this will appear as a layered zone on reflection profiles and will have a bulk density and V_p intermediate between "crust" and "mantle" values. Thus the "refraction Moho" and the "reflection Moho" must coincide in such areas, even though part of the layered zone would be regarded as "mantle" in the petrographic sense.

EFFECT OF GEOTHERMAL PROFILES ON SEISMIC INTERPRETATION

Figure 1 represents a lithospheric model for eastern Australia which is consistent with seismic evidence. In contrast, cratonic areas such as Western Australia usually show a shallower, sharper Moho. Such differences have been interpreted as due to contrasting types and thicknesses of crust. However, an important difference is the lower geothermal gradient of cratons. For mafic rocks, different thermal profiles are critical in determining whether or not the equilibrium mineral assemblage lies in the eclogite or the granulite facies, and hence in determining the V_p of these deep-seated regions.

The formation of the crust-mantle transition by magmatic under- and over-plating will inevitably be accompanied by an elevated, strongly curved geotherm like that for southeastern Australia. When the magmatic activity ceases, this geotherm will decay towards a conductive geotherm, like the Western Australian one, with a time constant on the order of 10 Ma.

With successive cooling, mafic assemblages convert from granulites to eclogites

With successive cooling, mafic assemblages convert from granulites to eclogites at shallower depths (Griffin and O'Reilly, 1987). This transition to eclogite results in an increase in V_p of 0.5 to 1.0 km/sec. The decrease in T will also raise the V_p of the other rock types, resulting in a maximum increase in V_p near the CMB. In terms of geophysical interpretation, the seismic Moho moves upward and becomes much more pronounced as a result of the cooling.

Useful petrological interpretation of geophysical data (especially seismic reflection and refraction surveys) requires knowledge of the local geothermal profile and of the effect of T on the stability of mineral assemblages at depth. The location of the CMB and its nature are critical to the solution of large-scale geological problems such as the nature of the evolution of the mantle, and mechanisms of crustal formation and growth throughout Earth's history. Neither petrologists nor geophysicists should allow considerations of these fundamental issues to become clouded and restricted by semantics such as traditional interpretations of the significance of terms like "Moho".

REFERENCES

- BEZANT, C. 1985. Geothermometry and seismic properties of upper mantle lherzolites from eastern Australia. **Unpub. Hons Thesis**, Macquarie University, Sydney.
- CHRISTENSEN, N.I. 1974. Compressional wave velocities in possible mantle rocks to pressures of 30 kilobars. **Journal of Geophysical Research** 79, 407-412.
- FINLAYSON, D.M., PRODEHL, C. and COLLINS, C.D.N. 1979. Explosion seismic profiles, and implications for crustal evolution in southeastern Australia. **BMR Journal of Australian Geology and Geophysics** 4, 243-252.
- GRIFFIN, W.L. and O'REILLY, S.Y. 1986a. The composition of the lower crust and the nature of the continental Moho - xenolith evidence. In Nixon, P.H. ed., **Mantle Xenoliths**, Wiley, London, in press.
- GRIFFIN, W.L. and O'REILLY, S.Y. 1986b. The lower crust in eastern Australia: xenolith evidence. **Journal of the Geological Society of London**, in press.
- GRIFFIN, W.L. and O'REILLY, S.Y. 1987. Is the Moho the crust-mantle boundary? **Geology**, in press.
- GRIFFIN, W.L., WASS, S.Y. and HOLLIS, J.D. 1984. Ultramafic xenoliths from Bullenmerri and Gnotuk maars, Victoria, Australia: petrology of a sub-continental crust-mantle transition. **Journal of Petrology** 25, 53-87.
- O'REILLY, S.Y. and GRIFFIN, W.L. 1985. A xenolith-derived geotherm for southeastern Australia and its geophysical implications. **Tectonophysics** 111, 41-63.

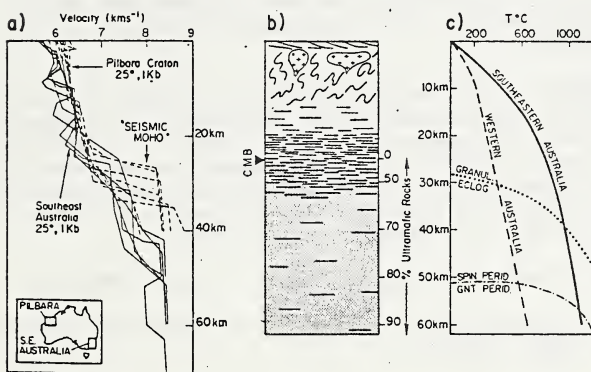


Fig. 1a: V_p profiles for southeastern Australia and the western Australian craton.

b: Petrologic model for the crust/mantle boundary (CMB) in non-cratonic regions.

c: Geotherms for southeastern Australia (xenolith-derived) and western Australia (extrapolated from heat flow).

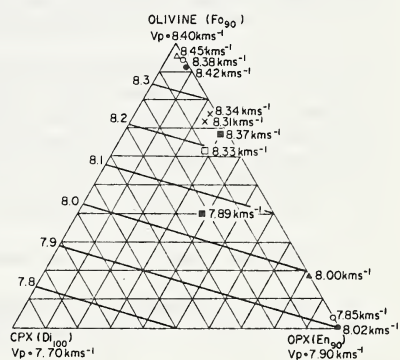


Fig. 2. Graphical estimation of V_p for oliv/opx/cpx modes at 25°C and 10 kb.

D. Phillips and T. C. Onstott

Department of Geological and Geophysical Sciences
Princeton University, Princeton, NJ 08544

Application of the $^{40}\text{Ar}/^{39}\text{Ar}$ dating technique to kimberlite geochronology often yields discordant spectra with ages that are older than the inferred time of kimberlite emplacement. The anomalously old dates have been attributed to the presence of 'excess' radiogenic argon, incorporated into mineral phases either prior to or during the intrusion of the kimberlite.

Detailed $^{40}\text{Ar}/^{39}\text{Ar}$ step-heating analyses have been performed on selected phlogopite samples from kimberlites of known age, to investigate the occurrence and isotopic composition of 'excess' argon components. These studies have also aided in the selection of sample material that is most likely to produce reliable geochronological information.

The Swartruggens Main Fissure, South Africa, is a kimberlite, which contains coarse phlogopite macrocrysts set in a fine-grained mica-rich groundmass. The matrix phlogopite yielded a plateau age of 145 ± 0.3 Ma, which is consistent with previously reported ages, ranging from 142 to 156 Ma (Fig. 1a). In contrast, the phlogopite macrocrysts are characterized by a discordant age spectra, and contain significant amounts of 'excess' radiogenic argon (Fig. 1b). It is suggested that the macrocrysts are xenocrystic, and have entrapped argon prior to crystallization of the kimberlite. Therefore, reliable eruption ages may be obtained on samples from which xenocrystic material can be eliminated. Similar results have been reported by Zartman et al. (1964) and Macintyre and Dawson (1976).

Phillips and Onstott (1986) recognized two distinct 'excess' argon components in phlogopite from the DK-7 kimberlite in southern Botswana. Similar components have since been recognized in phlogopite 'xenocrysts' from other kimberlites and phlogopite-bearing xenoliths. $^{40}\text{Ar}/^{39}\text{Ar}$ analyses of phlogopite separated from a garnet lherzolite nodule, from the Premier kimberlite yield ages that are greater than the established intrusion age of 1200 Ma (Allsopp and Kramers, 1977). The step-heating spectrum (Fig. 2) is suggestive of partial loss of 'excess' argon during cooling of the kimberlite.

The various argon components hosted by phlogopite are best distinguished using $^{36}\text{Ar}/^{40}\text{Ar}$ versus $^{39}\text{Ar}/^{40}\text{Ar}$ correlation diagrams. For the Premier phlogopite, four distinct components are recognized (Fig. 3):

- a) ^{36}Ar -rich (atmospheric) contaminating argon, accounting for the high $^{36}\text{Ar}/^{40}\text{Ar}$ ratios of the low temperature steps ($<800^\circ\text{C}$). The decrease in the $^{36}\text{Ar}/^{40}\text{Ar}$ ratio represents release of this component and increased degassing of radiogenic argon. Construction of a mixing line from the atmospheric ratio ($^{40}\text{Ar}/^{36}\text{Ar} = 295.5$) through the low temperature data points intersects the $^{39}\text{Ar}/^{40}\text{Ar}$ abscissa at a value corresponding to ± 1190 Ma. This is consistent with previously determined Rb-Sr dates. Therefore, despite the presence of 'excess' argon, age estimates may still be achieved, by this method.
- b) Radiogenic argon from the decay of ^{40}K subsequent to eruption of the kimberlite.
- c) 'Excess' radiogenic-rich argon, resulting in an increase in the $^{39}\text{Ar}/^{40}\text{Ar}$ ratio for the intermediate temperature steps ($800^\circ - 1100^\circ\text{C}$).
- d) 'Excess' radiogenic-poor argon released at the highest temperatures. The best-fit line through the three highest temperature data points represents a mixing line between decreasing quantities of radiogenic-rich and increasing amounts of radiogenic-poor argon. The intercept on the y-axis yields an $^{40}\text{Ar}/^{36}\text{Ar}$ ratio of 365 ± 40 .

The origin of the radiogenic-rich 'excess' argon component contained by the phlogopite is unclear. It may represent incomplete degassing of argon produced by in situ K-decay in the mantle, or contamination by a radiogenic-rich argon fluid phase, during residence in the mantle or during emplacement.

The radiogenic-poor 'excess' argon component may be trapped in the hydroxyl sites in phlogopite or in small undetected silicate inclusions (Phillips and Onstott, 1986). Regardless of the specific origin, it is suggested that this component may be representative of ambient argon isotopic compositions in the mantle lithosphere. Similar ratios were obtained on other kimberlitic phlogopites, with a range of values from 278 to 751 (Phillips and Onstott, 1986; and unpubl. data). These ratios are characteristic of an undegassed volatile source in the mantle (Allegre et al., 1983; Hart et al., 1985). As phlogopite is generally considered to be of metasomatic origin, it is suggested that the low $^{40}\text{Ar}/^{36}\text{Ar}$ ratios may be indicative of the metasomatising fluids. This implies derivation of the fluids from an undegassed source beneath the southern African lithosphere. Additional analyses on other kimberlite phases are in progress to assess further the validity of the above conclusions.

REFERENCES

- Allegre, C. J., Staudacher, T., Sarda, P., and Kurz, M., 1983. Constraints on evolution of the earth's mantle from rare gas systematics. *Nature* 303, 762-766.
- Allsopp, H. L. and Kramers, J. D., 1977. Rb-Sr and U-Pb age determinations on southern African kimberlite pipes. 2nd International Kimberlite Conference, Santa Fe, Extended Abstracts.
- Hart, R., Hogan, L., and Dymond, J., 1985. The closed system approximation for evolution of argon and helium in the mantle, crust and atmosphere. *Chemical Geology* 52, 45-73.
- Macintyre, R. M. and Dawson, J. B., 1976. Age and significance of some South African kimberlites. 4th European Colloquium on Geochronology and Cosmochronology, Isotope Geology, Amsterdam, Abstract, 66.
- Phillips, D. and Onstott, T. C., 1986. Application of $^{36}\text{Ar}/^{40}\text{Ar}$ versus $^{39}\text{Ar}/^{40}\text{Ar}$ correlation diagrams to the $^{40}\text{Ar}/^{39}\text{Ar}$ spectra of phlogopites from southern African kimberlites. *Journal of Geophysical Research* (in press).
- Zartman, R. E., Brock, M. R., Heyl, A. V. and Thomas, H. H., 1967. K-Ar and Rb-Sr ages of some alkalic intrusive rocks from central and eastern United States. *American Journal of Science*, 265, 848-870.

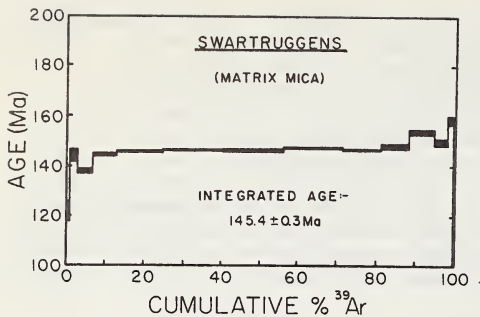


Figure 1a). Apparent age versus %³⁹Ar release for groundmass phlogopite from the Swartruggens Main Fissure. The spectra has a plateau age of 145±0.3 Ma, which is consistent with previous age determinations. The vertical width of the bars represent ±1S.D.

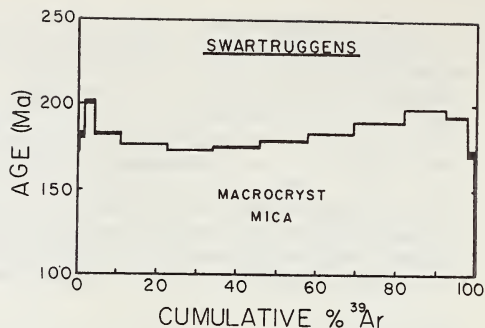


Figure 1b). Apparent age versus %³⁹Ar release for coarse-grained phlogopite 'xenocrysts' from the Swartruggens Main Fissure. The spectra is discordant and the anomalously high ages are indicative of the presence of 'excess' radiogenic argon.

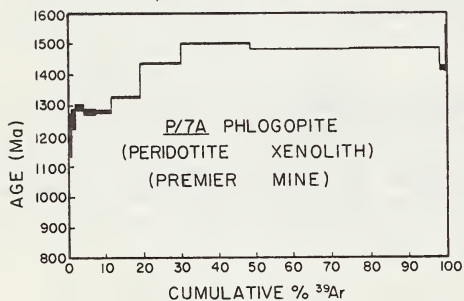


Figure 2. Apparent age versus %³⁹Ar release for phlogopite from a garnet lherzolite nodule from the Premier kimberlite. The general step-wise increase in age with temperature (and %³⁹Ar) is considered to result from partial diffusive loss of 'excess' radiogenic argon during cooling of the kimberlite.

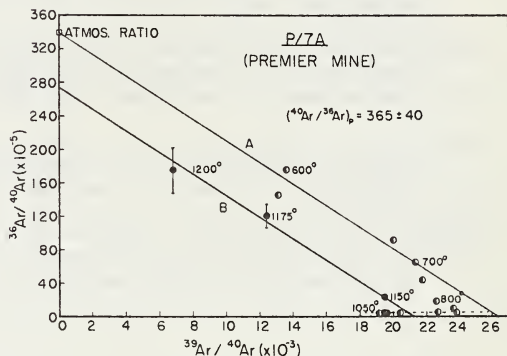


Figure 3. ³⁶Ar/⁴⁰Ar versus ³⁹Ar/⁴⁰Ar correlation plot for the Premier phlogopite separate. Line A is interpreted as a 'mixing' line between atmospheric contaminating argon and radiogenic argon. Line B is considered to represent mixing between radiogenic argon and a primitive mantle-derived component having an ⁴⁰Ar/³⁶Ar ratio of 365±40. The plotted error bars are ±1S.D.

XENOLITHS OF DIAMONDFEROUS PERIDOTITES
FROM UDACHNAYA KIMBERLITE PIPE, YAKUTIA

N.P.Pokhilenko, N.V.Sobolev

Institute of Geology and Geophysics, Siberian Division of the
Academy of Sciences of the USSR, Novosibirsk, USSR

The data obtained recently estimate the diamond age as 3.2-3.4 b.y. (Richardson et al., 1984) as compared with ages of diamondiferous kimberlites ranging from 20 to 1200 m.y., which directly indicates the xenogeneity of diamonds in kimberlites, and therefore the study of xenoliths of diamondiferous rocks is especially important.

Results of a study of xenoliths of diamondiferous peridotites (XDP) from the Udachnaya kimberlite pipe are given in this work. Our XDP collection from the Udachnaya pipe amounts to 18 specimens, i.e. more than a half of the total number of the findings of this type known at present (Sobolev et al., 1984). Sixteen xenoliths are composed of extremely depleted megacrystalline rocks where an olivine fraction accounts for more than 95% of volume. Six xenoliths are represented by paragenesis of olivine and pyrope; other six - by that of olivine, pyrope and chromite; three specimens are represented by paragenesis of olivine, pyrope, enstatite and chromite and one - by that of olivine, enstatite and chromite. One xenolith is composed of granular rock with deformation traces, it belongs to the paragenesis of ilmenite-pyrope lherzolite. And the last xenolith is composed of a rock the texture of which is intermediate between megacrystalline and granular rocks and refers to the paragenesis of pyrope harzburgite. Fresh olivine and enstatite are present in 17 and 2 specimens, respectively. A number of the diamond crystals found in XDP from the Udachnaya pipe varies from 1 to 7, their sizes being from 0.2 to 3 mm. The diamonds are practically colourless in all specimens. The predominant form of diamonds is octahedral and the presence of trigonal growth layers is typical of them.

The main results of the XDP mineral composition investigation by the microprobe analysis are given in Table. It shows that olivines from megacrystalline XDP are characterized by a rather low iron content, a stable chromium impurity, a negligible impurity of CaO, an average content of NiO being 0.36 wt% in a range of 0.31 to 0.39. The olivine from xenolith of diamondiferous ilmenite-pyrope lherzolite is characterized by higher values of iron content, chromium and calcium impurities. Pyropes in megacrystalline XDP are poor in iron and calcium and rich in chromium, which along with the extremely low content of titanium allows these to be clearly distinguished from pyropes of xenoliths of sheared lherzolites (Sobolev et al., 1984) and to be practically identified with pyropes included in diamonds of a similar paragenesis from the Udachnaya pipe. Chromites have very high contents of Cr_2O_3 and low, as compared with chromites from kimberlite concentrates, contents of titanium as well as magnetic component. Two enstatites studied from diamondiferous xenoliths of pyrope harzburgite and ilmenite pyrope lherzolite have marked differences in contents of TiO_2 (0.03 and 0.12 wt%), CaO (0.22 and 0.86 wt%), Na_2O (0.13 and 0.30 wt%) as well as iron content ($\text{Fe}/\text{Fe} + \text{Mg} = 5.9$ and 7.7%), which reflects the nature of their parageneses very well.

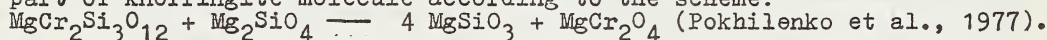
The comparative analysis of the results of the study of XDP minerals and the inclusion minerals of the same name in diamonds of a similar paragenesis from the Udachnaya pipe shows their similarity in compositions (see Table). This confirms the hypothesis that diamonds came into kimberlite in consequence of disintegration of ancient diamondiferous peridotites of the upper mantle (Boyd, Finnerty, 1980; Sobolev et al., 1984; Richardson et al., 1984; Haggerty, 1986). At the same time, there are

Table

		o l i v i n e			p y r o p e			c h r o m i t e	
		1 (15)	2 (61)	3	1 (15)	2 (89)	3	1 (10)	2 (87)
f	\bar{x}	6.99	6.97	8.8	14.9	14.2	16.4	47.6	40.7
	min	6.22	5.03		12.5	12.3		45.0	30.4
	max	8.11	8.12		16.1	16.5		51.0	55.3
Cr ₂ O ₃	\bar{x}	0.04		0.06	10.4	9.88	5.99	63.8	65.2
	min	0.02			7.1	4.93		61.7	61.9
	max	0.05			12.7	15.6		65.4	68.9
CaO	\bar{x}	0.007		0.042	2.38	2.67	5.41		
	min	0.003			0.88	0.68			
	max	0.011			4.29	6.54			
TiO ₂	\bar{x}				0.06	0.08	1.91	0.15	0.15
	min				0.02	0.01		0.02	0.01
	max				0.14	0.79		0.50	0.79
Al ₂ O ₃	\bar{x}							4.80	5.41
	min							3.60	1.58
	max							5.79	8.81

Notes: 1 - XDP of harzburgite-dunite paragenesis; 2 - inclusions in diamonds of harzburgite-dunite paragenesis of the Udachnaya pipe; 3 - xenolith of diamondiferous ilmenite-pyrope lherzolite, a number of the grains analyzed is given in parentheses.

evidences that diamondiferous rocks have undergone some evolution of parameters of equilibrium after the diamond formation. In particular, the high-temperature character of equilibrium of olivine-garnet associations found in diamonds from the Udachnaya pipe is observed steadily to be higher than equilibrium temperatures of analogous pairs in XDP from the same pipe (\bar{x} = 1010 °C and 920 °C, respectively) (Sobolev et al., 1984). In a series of XDP from the Udachnaya pipe related to harzburgite paragenesis, regular chromite-enstatite intergrowths were found which are spatially consistent with garnet extractions, this being interpreted as reaction disintegration resulted from the decompression of a certain part of khorringite molecule according to the scheme:



The facts observed, along with some others, may be explained by two reasons: 1) changes in thermal mode in different areas of the platform mantle within the period between the diamond formation and the time of diamond capture by kimberlite; 2) dynamical processes including significant displacements of mantle substance in vertical direction in kimberlite generation zones during and after diamond formation (Sobolev et al., 1984; Haggerty, 1986). To our opinion, these reasons, along with the fluid mode, determine the appearance of blocks of cold diamondiferous peridotites in central regions of cratons at relatively small depths, possibly, essentially higher than the level of diamond-graphite phase transition, their xenoliths being also found in the Udachnaya pipe.

REFERENCES

- BOYD F.R., FINNERTY A.A. 1980. Conditions of origin of natural diamonds of peridotite affinity. *Journal Geophysical Research*, 85, 6911-6918.
- HAGGERTY S.E. 1986. Diamond genesis in a multiply-constrained model. *Nature*, vol.320, No.6057, 34-38.
- POKHILENKO N.P., SOBOLEV N.V., LAVRENT'EV Yu.G. 1977. Xenoliths of diamondiferous ultramafic rocks from Yakutian kimberlites. *Ext. Abstr. vol.2nd International Kimberlite Conference, Santa Fe, USA.*

RICHARDSON S.H., GURNEY J.J., ERLANK A.J. and J.W.HARRIS, 1984. Origin of diamonds in old enriched mantle. Nature, vol.310, No.5974, 198-202.

SOBOLEV N.V., POKHILENKO N.P., YEFIMOVA E.S. 1984. Xenoliths of diamondiferous peridotites in kimberlites and the problem of diamond origin. (in Russian). Geology and Geophysics, No.12, 63-80.

COMPOSITION AND AGE OF THE LOWER CRUST IN NORTH QUEENSLAND

Roberta L. Rudnick, Ian S. Williams, S.R. Taylor and W. Compston
Research School of Earth Sciences, The Australian National Univ.
Canberra, A.C.T. 2601 Australia

Lower crustal xenoliths from Hill 32 in the McBride volcanic province, north Queensland, are compositionally diverse, contrasting with xenoliths from the more southerly Chudleigh province, which are young mafic cumulates. Protoliths for the Hill 32 xenoliths include mafic igneous rocks, mafic cumulates, mafic restites as well as felsic igneous rocks and sediments. High pressure mineral assemblages (> 8 Kb) and decompression melts suggest these are fragments of the present day lower crust, rather than near-surface granulite facies rocks. This is confirmed by U-Pb zircon ion probe ages which show that all xenoliths have undergone high-grade metamorphism at ~240 Ma, with little evidence of subsequent Pb loss. The lack of substantial uplift and erosion in this region, as evidenced by the preservation of voluminous 300 Ma felsic ash flows, suggests that all zircon-bearing xenoliths (from supracrustal to mafic inclusions) have formed part of the lower crust since this time. Proterozoic zircon ages in some of the xenoliths indicate a protracted history for these rocks. The chemical and geochronologic data for the xenoliths from the two volcanic provinces show that the lower crust in north Queensland consists of magmatically and tectonically interleaved mafic through supracrustal lithologies, which formed in discrete "orogenic" events from the Proterozoic through the Cenozoic.

INTRODUCTION

Young (< 5 Ma) alkali basalts in north Queensland carry numerous lower crustal xenoliths. The two volcanic provinces discussed here erupt in distinct tectonic settings: the Chudleigh province straddles the boundary of the Paleozoic Tasman fold belt and the Proterozoic Georgetown Inlier, whereas the McBride province is within the Georgetown Inlier. Crustal xenoliths from the Chudleigh province are exclusively mafic, but crustal xenoliths from Hill 32 range from felsic through mafic compositions, including metasedimentary lithologies. The Chudleigh lower crustal xenoliths are interpreted as genetically related cumulates from a basaltic melt (Rudnick et al., 1986), with correlations between major elements, trace elements and isotopic ratios reflecting simultaneous assimilation and fractional crystallization of the parental melt. The quality of the isotope-trace element correlations suggests that the xenoliths are less than 100 Ma old. This abstract deals with the composition, age and origin of the more diverse crustal xenolith suite from Hill 32.

MINERALOGY AND DEPTH OF ORIGIN

The mineralogy of the Hill 32 xenoliths is a function of their composition and P-T equilibration conditions. Unlike the Chudleigh province xenoliths, coronal textures are rare in this suite; most xenoliths are equigranular, and commonly minerals are compositionally zoned. Table 1 is a list of the mineralogy and thermobarometry determinations for the Hill 32 xenoliths. All appear to have equilibrated at high pressures (> 8 kb, where determined) and high temperatures (700-1000°C). Glass along grain boundaries, kelyphitic rims on garnets and anorthite rims on scapolite suggest the xenoliths experienced significant decompression and were rapidly transported from deep crustal levels by the host basalts.

COMPOSITION AND PETROGENESIS

The Hill 32 xenoliths are compositionally diverse and apparently unrelated to one another, so the origin of each must be considered separately. Individual compositions are a function of melt extraction, cumulate processes, and fractionation for the metaigneous xenoliths; weathering and erosion for the metasedimentary xenoliths, and high-grade metamorphism, which all xenoliths experienced. Metamorphic differentiation may be a particularly important process influencing the composition of these xenoliths because they are typically layered and small (most < 8 cm in diameter).

Fig. 1 shows REE patterns for the Hill 32 xenoliths. Intermediate xenoliths are metasediments, based upon their high $Al_2O_3/(Na_2O + CaO)$ ratios, and the presence of sillimanite in one of them. 83-157 has a REE pattern similar to PAAS, whereas the REE pattern of 85-101 exhibits an unusual HREE enrichment, probably due to preferential

sampling of garnet (Fig. 1a)(this xenolith is small and contains garnet-rich layers). Felsic xenoliths (83-160 and 83-162) have REE patterns similar to dacitic and granodioritic melts (Fig. 1b), consistent with their major element compositions. Mafic xenoliths 83-159 and 85-107 have $(La/Sm)_N > 1$ and positive Eu anomalies (Fig. 1c), and are either restites or cumulates from an intermediate to felsic magma. The abundant zircon in 85-107 (1600 ppm Zr) suggests it is a restite. The HREE enrichment and positive Eu anomaly in mafic xenolith 85-114 (Fig. 1c)(a large, unlayered xenolith), is probably due to removal of a partial melt rather than metamorphic differentiation. Garnet is not a liquidus phase in intermediate to mafic melts at crustal depths, so this xenolith is not a cumulate. Two mafic xenoliths with LREE depleted patterns (83-158 and 85-106; Fig. 1d) are interpreted to be clinopyroxene-rich cumulates. Finally, three xenoliths (85-100, 85-108 and 85-120) have major element and REE patterns typical of mafic, oversaturated melts (Fig. 1e), although the high Cr and Ni (1026 and 456 ppm, resp.) and low Al_2O_3 (11.3 %) in layered xenolith 85-100, suggests preferential sampling of metamorphic orthopyroxene.

TABLE 1. Mineralogy of McBride Provinces Lower Crustal Xenoliths

Sample	Mineralogy	Accessories	P-T
Metasedimentary			
83-157	Pe-Q-Gt-Opx-Ph	Rut-Cpx-Mt-Il-Ap-Zr	630°C ¹ , 8-10 Kb ²
85-101	Q-Po-Gt	Sil-Rut-Opx-Il	
Felsic			
83-160	Q-Pe-Cpx-Opx-Gt	Ph-Rut-Mt-Ap-Zr	780-860°C ¹ , 9-11 kb ²
83-162	Q-Kf-Gt	Rut-Mt-Il-Ap-Zr-Py	900-950°C ¹ , 8-16 Kb ²
Mafic			
83-158	Cpx-Gt-Pe-Opx	Amph-Il	940-1000°C ¹ 7-15 Kb ²
83-159	Cpx-Gt-Pe-Amph	Rut-Il-Zr	840-920°C ¹
85-100	Pl-Opx-Cpx-Amph	BiO-Ap-Zr	960-1000°C ¹
85-106	Gt-Cpx-Seap-Pe	Amph-Mt	890-1070°C ¹
85-107	Pe-Q-Gt-Cpx	Il-Ap-Amph-Zr	680-760°C ¹
85-108	Pl-Cpx-Q	Rut-Ap	810-860°C ¹
85-114	Cpx-Gt-Pe	Rut	830-910°C ¹
85-120	Pl-Opx-Cpx	Amph-Rut-Zr	860-910°C ¹

Minerals listed in order of relative abundances. ¹Ellis and Green (1980), ²Perkins and Newton (1982), ³Wells (1979), ⁴Harley and Green (1982). Amph = amphibole, Ap = apatite, BiO = biotite, Cpx = clinopyroxene, Gt = Garnet, Il = ilmenite, Kf = K-feldspar, Mt = magnetite, Opx = orthopyroxene, Pl = plagioclase, Ph = phlogopite, Py = pyrite, Q = quartz, Rut = rutile, Seap = seapolite, Sil = sillimanite, Zr = zircon.

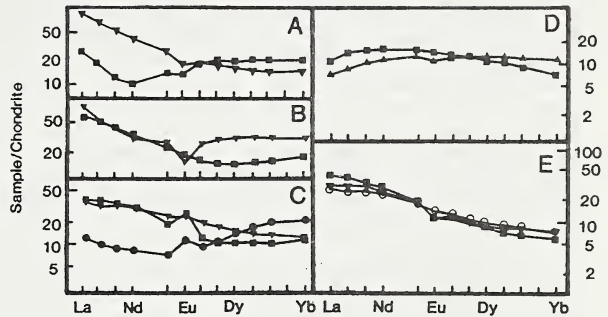


Fig. 1. REE patterns for McBride xenoliths. (A) metasedimentary (▼) = 83-157, (■) = 85-101; (B) felsic (■) = 83-160, (▼) = 83-162; (C) restitic (■) = 83-159, (▼) = 85-107, (●) = 85-114, (D) cumulate (▲) = 83-158, (■) = 85-106, and (E) possible melts (■) = 85-100, (○) = 85-108, (▼) = 85-120.

U-Pb ZIRCON CHRONOLOGY

The U-Th-Pb ages of zircons from 6 of the Hill 32 xenoliths have been measured on the SHRIMP ion microprobe. The following summarizes these data.

(1) Metasedimentary xenolith 83-157 contains zircons of two distinct morphologies: elongate, subhedral igneous zircons and round, high-grade metamorphic zircons. The igneous zircons fall into two age populations, both showing Pb loss at 240 Ma: one 2020 Ma zircon, and several zircons which define a chord between 1579 ± 6, (1 σ) and 245 ± 5 Ma. The round, metamorphic zircons are concordant at 240 ± 20 Ma.

(2) Granodioritic xenolith 83-162 has rounded zircons containing abundant CO₂ fluid inclusions in addition to apatite, feldspar and quartz. These zircons are discordant, with ²⁰⁶Pb/²³⁸U ages between 200 and 380 Ma. The highest, precisely measured ²⁰⁷Pb/²⁰⁶Pb age is 1650 ± 170 Ma, suggesting that, while most of these zircons grew during high-grade metamorphism (trapping CO₂ fluid inclusions), some may be Proterozoic.

(3) Rounded zircons in dioritic xenolith 83-160 mostly fall within uncertainty of concordia, and have ²⁰⁶Pb/²³⁸U ages between 200 to 350 Ma. It is not known whether this spread represents initial crystallization at 350 Ma with subsequent Pb loss, or continuous zircon crystallization over a 150 Ma period. One zircon is concordant at 2200 Ma, and may be an inherited grain.

(4) Mafic xenolith 83-159 has large, round zircons (up to 300 μm) which contain apatite inclusions. Some zircons are nearly concordant at 240 Ma, but most show the presence of much older components. The highest ²⁰⁷Pb/²⁰⁶Pb age measured was 1600 ± 35 Ma. The data do not define a single discordance line (MSWD = 6.8). As this rock formed either as a mafic cumulate or restite, the older zircons may be xenocrysts. All zircons appear to have lost Pb at ~240 Ma.

(5) Zircons in mafic xenolith 85-100 also show a spread in ages (>1200 to 250 Ma), but all analyses are concordant. The zircons are small, and generally rounded. As this xenolith formed as a mafic melt in which zircon would not be saturated, the range in ages suggests the zircons are xenocrystic. It is possible that the melting occurred about 400 Ma ago and that the zircons were affected by metamorphism at 240 Ma.

(6) Finally, mafic xenolith 85-107 contains an abundance of zircons of variable sizes and morphologies. Elongate, igneous zircons contain inclusions of acicular apatite, clinopyroxene, pyrrhotite and Fe-Ti oxides. In addition, many of these zircons are riddled with small (~10µm) felsic melt inclusions, with an immobile vapor bubble. Round, high-grade metamorphic zircons are also found in this sample. The $^{206}\text{Pb}/^{238}\text{U}$ ages of the two distinct morphological zircon types show complete overlap, from 240 to 340 Ma. The abundant igneous zircons, which crystallized from a felsic melt, were probably left behind in the residuum during partial melting.

In summary, the zircon ages for these 6 xenoliths show that all have undergone high-grade metamorphism at ~240 Ma. The lack of zircon ages less than about 200 Ma suggests that either recent (0 Ma) Pb loss has removed a small portion of the radiogenic Pb, or the zircons have remained closed to Pb loss after cooling below their blocking temperature at the close of the late Permian orogeny. It is possible that zircon Pb loss was inhibited by the continuous annealing of radiation damage to the zircon structure that would take place in lower crustal P-T conditions.

Some xenoliths formed during the late Permian event (e.g., mafic restite 85-107; dioritic xenolith 83-160), whereas others formed in the Proterozoic, and were metamorphosed at 240 Ma (83-157, 83-162). It is not possible to determine if the older xenoliths experienced one or multiple metamorphic events. It is more difficult to constrain the age of the mafic xenoliths with apparent xenocrystic zircons (83-159, 85-100), as there are no good criteria to distinguish metamorphic from igneous zircons in these samples. Because of the predominance of ages between 400 and 240 Ma in 85-100, this melt may have intruded the deep crust at ~400 Ma and been metamorphosed later. Similarly, 83-159 has many zircons falling between 350 and 200 Ma, suggesting intrusion of this melt during the early stages of the late Permian event.

The well determined age of 1575 Ma for the igneous zircons in metasediment 83-157 and the less precise age of 1670 ± 170 Ma for felsic xenolith 83-162 correspond to the timing of high-grade metamorphism and granite intrusion for the Georgetown Inlier (Black et al., 1979). Significant granite-forming events occurred during the Paleozoic at 400 Ma and 270-320 Ma (Black, 1980); the latter event is well represented in the xenolith suite, and the 400 Ma event is documented in one sample (85-100).

LOWER CRUSTAL HISTORY

The compositional and age data derived from these xenoliths can be used to construct a geological history for the lower crust. At least some of the lower crustal rocks formed during the Proterozoic at the earth's surface. These rocks were subsequently tectonically emplaced into the lower crust. The timing of this event is, as yet, poorly known, but may have accompanied the Paleozoic, granite-forming orogenies. Whatever the timing, this event did not involve double-thickening of the crust, because the rocks apparently remained in the lower crust for a considerable length of time (at least 300 Ma). The ~400 Ma granite-forming event did not appreciably affect the older rocks in this region, but one mafic xenolith may represent melt intruded into the crust at this time. The ~300 Ma granite-forming event clearly affected all of this portion of the lower crust. This event included addition of mafic, mantle-derived material to the crust and melting and metamorphism of older crust. The lack of significant erosion since ~300 Ma suggest that this orogeny was accompanied by minimal crustal thickening, but substantial heat input, most likely through intrusion of mantle-derived melts. The zircon-free mafic xenoliths within the suite may represent such material, or may be related to the Cenozoic basaltic volcanism, like the Chudleigh province xenoliths.

REFERENCES

- Black, L.P. 1980. Rb-Sr systematics of the Claret Creek ring complex and their bearing on the origin of Upper Palaeozoic igneous rocks in northeast Queensland. *J. Geol. Soc. Australia* 27, 157-166.
- Black, L.P., Bell, T.H., Rubenach, M.J. and Withnall, I.W. 1979. Geochronology of discrete structural-metamorphic events in a multiply deformed Precambrian terrain. *Tectonophysics* 54, 103-137.
- Rudnick, R.L., McDonough, W.F., McCulloch, M.T. and Taylor, S.R. (1986) Lower crustal xenoliths from Queensland, Australia: evidence for deep crustal assimilation and fractionation of continental basalts. *Geochim. Cosmochim. Acta* 50.

V. Sautter (1)
B. Harte (2)

- (1) Laboratoire de Géophysique, Université Paris-Sud, Bât. 510, 91405 Orsay.
(2) Grant Institute of Geology, University of Edinburgh, West Mains Road, Edinburgh EH9 3JW.

INTRODUCTION

The biminerallie xenolith JYG41 is striking for its high-alumina clinopyroxene crystals showing garnet exsolution lamellae. It has been described previously with respect to aspects of mineral chemistry by Harte and Gurney (1975) and with respect to the orientations of garnet lamellae within clinopyroxene by Desnoyers (1972). A model of development was considered (Harte and Gurney 1975) in which exsolution occurred over a range of temperatures as a result of a slow cooling from solidus (1400°C-35 Kbar) towards the normal mantle geotherm temperature at constant depth. The purpose of the present paper is to consider the possibility of an alternative model in which exsolution occurred isothermally and use this model to estimate the approximate value of Al diffusion coefficient in clinopyroxene.

RESUME OF TEXTURAL AND CHEMICAL DATA

On the (001) clinopyroxene plane, garnet lamellae show various size (1000µ to 10µ), shapes (discontinuous to continuous layers), spacing and orientations ($\{110\}$, $\{010\}$, $\{130\}$). Big lamellae (1000µ across) occurring parallel to $\{010\}$ form widely spaced (up to 1 cm), discontinuous layers. Medium to small lamellae (100µ to 10µ across) and parallel to $\{110\}$, $\{130\}$, closely spaced (100µ to 10µ) and form continuous lamellae. Simultaneous exsolution in $\{130\}$ and $\{110\}$ orientations is shown by single lamellae which pass from one orientation to the other.

At scalle of individual grains (included lamellae) garnet is homogeneous. However the grossular content of garnet grains is correlated with the size of garnet grains (1000µ across lamellae: Pyrope 33; Almandine 18; Grossular 44; 10µ across lamellae: Pyrope 26, Almandine 13; Grossular 60). Clinopyroxene shows strong compositional zoning, the main feature of which being a decrease of Al (and minor Fe) as Si and Mg increase towards garnet contacts (Fig. 1). The composition profiles are related to the size of garnet lamellae with gradients in Si and Al up to 100µ wide adjacent to 80µ thick garnet lamellae, and up to 10µ wide adjacent to 8µ thick garnet lamellae. Note that beyond these distances, original Al and Si compositions appear to be preserved (Fig. 1). Ca, unlike most of the elements, shows very flat profiles in the clinopyroxene. At all the interfaces Si and Al, which are stoichiometrically controlled in garnet, have also a fixed concentration in the pyroxene. Ca, Mg, Fe vary in such way in clinopyroxene and garnet that they are not related by crossed tie lines for these elements (Fig. 2). At the same time the $K_D^{P \times Gr}_{Fe \times Mg}$ maintains closely similar values at all interfaces. The interface Fe/Mg values give Grt. Cpx exchange temperature of c.a. 1050°C (Ganguly 1979) but are uncertain because of the large grossular component in the garnets.

REACTION MECHANISMS

Zoning in clinopyroxene is a result of unequal partitioning of Si/Al, Al/Mg during garnet growth depicted by the classical net transfer reaction 2 diopside + Al₂Mg-1 Si-1 = 2 grossular, 1 pyrope. Profiles within clinopyroxene wheras garnet are homogeneous

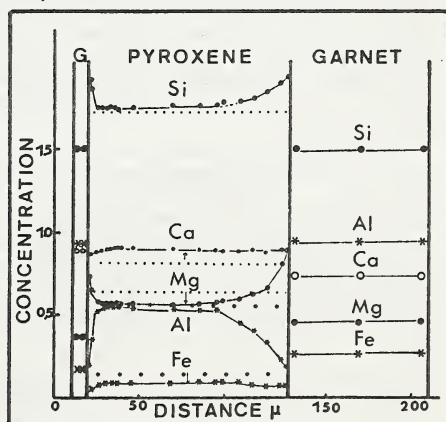


Fig. 1: Diffusion profiles in clinopyroxene adjacent to 8µ, 80µ thick garnets, parallel to $\{110\}$. Formulae calculated on the basis of 6 Oxy.: primary unexsolved pyroxene composition (Harte and Gurney 1975.)

REACTION MECHANISMS

Zoning in clinopyroxene is a result of unequal partitioning of Si/Al, Al/Mg during garnet growth depicted by the classical net transfer reaction $2 \text{diopside} + \text{Al}_2\text{Mg} - 1 \text{Si} - 1 = 2 \text{grossular} + 1 \text{pyrope}$. Profiles within clinopyroxene whereas garnet are homogeneous show that $D_{\text{Al}}^{\text{Px}} < D_{\text{Si}}^{\text{Px}} < D_{\text{Mg}}^{\text{Px}} < D_{\text{Ca}}^{\text{Px}}$.

Partitioning at the interface defines a state of local equilibrium consistent with diffusion controlled process. As we are concerned with multicomponent diffusion (Al₂Mg-1Si-1) the slowest species will be rate limiting. Homogenisation experiments (at high T and P; Sautter 1986) show clearly that garnet dissolution is possible because of an inwards Si diffusion from clinopyroxene whilst Al does not move outwards. Therefore D_{Al} will be rate limiting.

Although there is a correlation of the grossular content and size of garnet grains, there is no textural evidence to show a chronology of development of these lamellae. The correlation may indicate a relative chronology over a temperature range (Harte and Gurney 1975) but it is also possible that all lamellae nucleated simultaneously at one temperature, but showed varying nucleation density and amounts of subsequent growth partly as a function of clinopyroxene crystallography.

KINETICS MODELLING

The data of Richardson et Al. (1984) and Boyd et Al. (1985) indicate that the nodule may have formed in Archean times in a mantle with geotherm similar to present day shield areas. If we assume this and crystallisation of clinopyroxene from a magma initially at 1400°C, then the cooling interval of the clinopyroxene yielding garnet exsolution could be c.a. 400°C over a 3b.y. given kimberlite eruption at 100 M.y. For 1 km magmatic sheet at 1400°C, intruded into peridotite at 1050°C, the equation $T = T_0 + \frac{T_0 - T_s}{2} \text{erf} \frac{x}{2\sqrt{Kt}}$ (a = half layer thickness; $K = \text{thermal diffusivity} = 0.83 \times 10^2 \text{ km}^2/\text{s}$) gives a cooling duration of 0.005 M.y. By comparison with likely diffusion coefficients (from 10^{-10} to $10^{-22} \text{ cm}^2/\text{s}$) this cooling duration is effectively instantaneous. Therefore, as an alternative to the progressive cooling model, we shall consider a model in which all the exsolutions has occurred at 1050°C after a big overstep (400°C).

An internal kinetic model for exsolution reaction, where both diffusion and moving grain boundaries are involved, had been made to find the solution $C(x,t)$ of 2 Fick's law. Al diffusion in clinopyroxene being the rate limiting step, Al is the component used in the following calculations. Garnet symmetrical axis is chosen as the fixed system of reference (Fig. 2a: $X=0$) and we just consider a semi-infinite medium (clinopyroxene) next to half a garnet lamellae (Fig. 2b). In these cartesian coordinates, the flux of Al across clinopyroxene garnet interface ($X=X'$; Fig. 2b) is chosen parallel to $\{110\}$. The boundary ($X=X'$) conditions are as follows: $t=0 \quad X>0 \quad C=C_0$; $t>0 \quad x=x' \quad C=C_e$. The mass transfer problem is defined by interface velocity (v ; Fig. 2b) which decreases as garnet growths and Al diffusion distance which is proportional to garnet thickness (Fig. 1). This is equivalent to a heat transfer problem by conduction involving solidification of a liquid (-Stephan Problem: Ice crystallisation at the top of a lake). A transposition to our mass transfer problem gives a solution (Fig. 2c), obtained by scaling Al penetration depth and the width of garnet lamellae. Equation (Fig. 2c) contains two unknowns $D_{\text{Al}}^{\text{Px}}$ and t . As equilibrium (flat profile) had not been reached in JJG41, the time stay of almost 2.9 b.y. at 1050°C, constrains $D_{\text{Al}}^{\text{Px}}$ to an approximate value of $10^{-22} \text{ cm}^2/\text{s}$. With such a value, estimation of the time of development for various thickness of garnet lamellae had been done from the diffusion profiles in clinopyroxene (6.5 M.y. for 3u thick garnet; 50 M.y. for 80 u thick garnet).

An isothermal exsolution model is consistent with the diffusion profile for Al (Si,Mg) in clinopyroxene as well as being consistent with temperature of equilibration at garnet - clinopyroxene interface of a 1050°C. The constant composition of garnet lamellae is presumed to reflect the fact that diffusion rate, at least for 2^+ cations are fast enough to maintain equilibrium across the garnet. If the model provides no simple explanation for the correlation of lamellae thickness with grossular content it is nevertheless the most coherent way to justify textural relationships of these lamellae related to anisotropic properties of clinopyroxene.

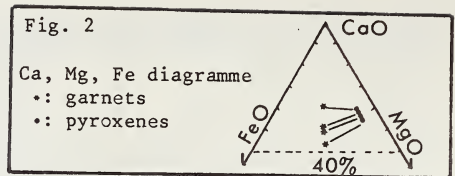
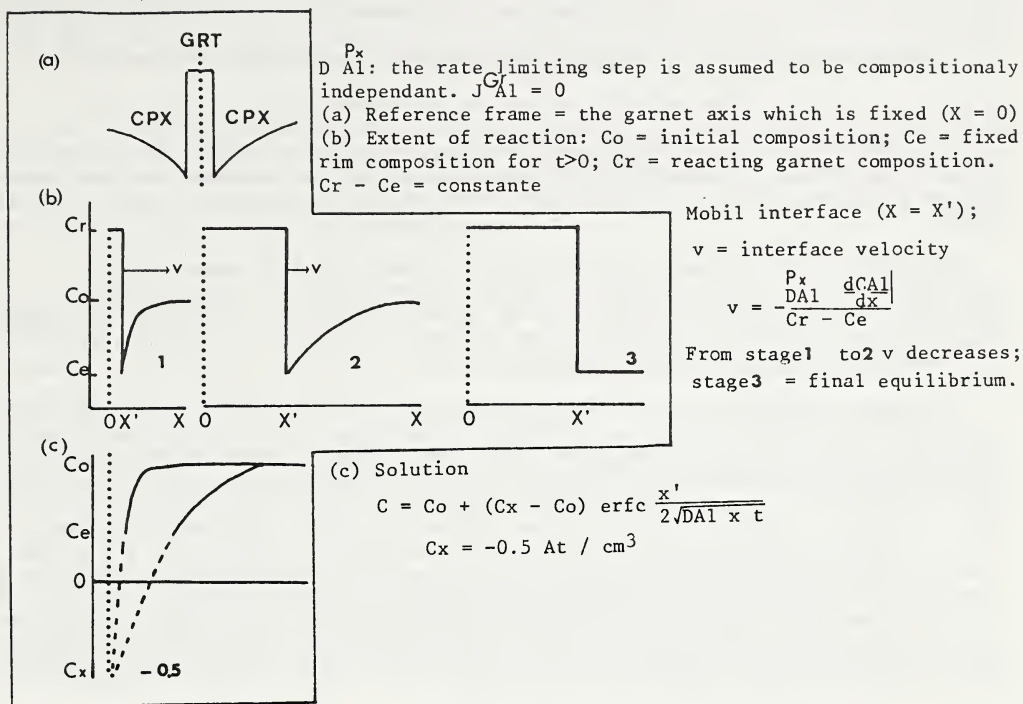


Fig. 3: Kinetics model (diffusion profiles C Al- X)



REFERENCES

Boyd, F.R., Gurney, J.J. and Richardson, S.M. 1985. Evidence for a 150- 200 km thick Archean lithosphere from diamond inclusion thermobarometry. *Nature*, 315, pp. 387. 389.

Desnoyers, M.C. 1972. Contribution à l'étude des exsolutions dans les pyroxènes des roches ultrabasiques. Doctoral thesis. University of Paris.

Ganguly, J. 1979. Garnet and clinopyroxene solid solutions, and geothermometry based on Fe-Mg distribution coefficient. *Geochim. Cosmo. Acta*, 43, pp. 1021. 1029.

Harte, B. and Gurney, J.J. 1975. Evolution of clinopyroxene and garnet in an eclogite module from Roberts Victor Kimberlite pipe. *Phys. Chem. Earth*, 9, pp. 367-387.

Sautter, V. 1986. Preliminary homogenisation experiments of garnets in clinopyroxene under H.P. conditions. Abstr. Experimental Mineralogy and geochemistry conf. France.

Richardson, S.H., Gurney, J.J., Erlank, A.J. and Harris J.W. 1984. Origin of diamonds in old enriched mantle. *Nature*, 310, pp. 198-202.

D. Schier and E. Jagoutz

Max-Planck-Institut für Chemie, Saarstrasse 23, D-6500 Mainz, F.R.Germany

The radioactive decay of La-138 to Ce-138 with a half-life of 112×10^9 y can be used for age determination but is especially interesting as an indicator for rare earth element fractionation, isotopic evolution and correlated geological processes (Tanaka, 1982).

The change of the valency from 3+ to 4+ by a temporary high oxygen fugacity is an outstanding feature of Ce (besides Eu) within the REE which may cause Ce anomalies. In meteorites and lunar rocks these anomalies reach 20% and more. Therefore the La-Ce system should be especially useful as an indicator of chemical processes involved in the genesis of crustal and mantle rocks.

We report here the first Ce isotopic data obtained for kimberlites. Three fresh South African kimberlites were analyzed for the radiogenic ratio Ce-138/Ce-142 (normalization ratio is Ce-136/Ce-142=0.01720) and compared with other terrestrial samples. The Jwaneng kimberlite (basaltic - Group I) has a significantly less radiogenic Ce-138/Ce-142 isotopic composition compared to the New Elands and Finsch kimberlites (micaceous - Group II) and to other terrestrial rocks. The measured differences for the isotopic composition of Ce between the two types of kimberlites reflect distinct mantle reservoirs with significant differences in Ce-138/Ce-142: the Group I kimberlite with Ce-138/Ce-142=0.02287955 \pm 44 clearly differs from the mean of the two Group II kimberlites which is Ce-138/Ce-142=0.0228261 \pm 12(26). The Group II kimberlites are identical within 1 σ . In terms of ϵ -deviation from the chondritic uniform reservoir (BCR-1: Ce-138/Ce-142=0.0228166) this is -9.2 \pm 1.9 ϵ for Group I and +4.2 \pm 0.5 ϵ for Group II kimberlites, a total variation of 13.4 \pm 2.4 ϵ .

New Elands and Finsch, Group II, may be derived from an enriched source as initial Sr and Nd isotopic ratios and high time-averaged Rb/Sr and Sm/Nd indicate, whereas Jwaneng, Group I, should come from an undifferentiated to slightly depleted source relative to bulk earth (Smith, 1983). For Group II this seems to be consistent with the isotopic data of Ce though the slightly radiogenic ratio Ce-138/Ce-142 compared to bulk earth and a "normal" Pb-206/Pb-204 ratio close to the geochron are more likely derived from a bulk-earth-like source region. In contrast the higher Pb-206/Pb-204 ratio of the Group I corresponds to a much less radiogenic Ce. This indicates anomalous time-averaged Pb/U and La/Ce ratios in the sources of Group I kimberlites significantly lower than in bulk earth. The measured La/Ce ratio of Jwaneng normalized to the chondritic value is 1.55; most terrestrial La/Ce ratios are between 0.5 and 2.0 (Schier, 1983). The calculated La/Ce ratio of the Group I source derived from the chondritic evolution line is dependent on its age and the measured radiogenic Ce of this Group I kimberlite: for 4.5 b.y. the La/Ce ratio of the source would be 0.42 and becomes zero at the minimum source age of 2.6 b.y. The corresponding range of the Sm/Nd ratio is much smaller, varying from 1.04 at 4.5 b.y. to 1.06 at 2.6 b.y. These calculated source ratios of Group I, required to generate the present-day Ce-138/Ce-142 and Nd-143/Nd-144 ratios, are unlikely caused by normal differentiation processes. Melting curves combined with the La/Ce-Sm/Nd correlation line of source ratios as a function of time should give more information about the generation of this kimberlites' source rock.

Starting from a chondritic reservoir for melting calculations, and provided that the La/Ce-Sm/Nd correlation line for the generation of the source represents all possible La/Ce and Sm/Nd ratios of the endproducts of melting as a function of time, it is apparent that a batch melting process cannot generate the source of the Group I kimberlite at any time, either as the residuum or as the melt. No batch melting curve, either for the liquid or the solid, intersects the La/Ce-Sm/Nd correlation line (see Fig.1). Agreement was found for continuous melting calculations (Langmuir, 1977) which showed that the possible range of Group I source ratios La/Ce and Sm/Nd result from a liquid (enriched in LREE) rather than the residue. It was postulated previously

(Wyllie, 1975) that fractional fusion can produce kimberlitic magmas. A corresponding calculation was performed as a 3% continuous melting of a chondritic source with total removal of the melt. The resulting liquid has the required La/Ce and Sm/Nd ratios 2.7 b.y. ago to generate the present-day Ce-138/Ce-142 and Nd-143/Nd-144 ratios, and could therefore serve as a 2.7 b.y. old source for cretaceous southern African kimberlites.

A second and much discussed event of melting of this original source occurred 90 m.y. ago (Smith, 1983) which again changed the La/Ce and Sm/Nd source ratios by enrichment of the LREE in the resulting liquid. The measured La/Ce and Sm/Nd ratios of the kimberlite represent the ratios in this liquid (Kramers, 1981). The radiogenic isotopic ratios of Ce and Nd are long-time-fractionated and should therefore reflect an original source feature of kimberlites.

REFERENCES

TANAKA T. and MASUDA A. 1982. The La-Ce geochronometer: a new dating method. *Nature* 300, 515-518.
 SMITH C.B. 1983. Pb, Sr and Nd isotopic evidence for sources in southern African Cretaceous kimberlites. *Nature* 304, 51-54.
 SCHIER D. 1983. Entwicklung eines Ionenaustausch-Trennverfahrens und massenspektrometrische Isotopiebestimmung des Cers (Seltene Erden) als Grundlage einer neuen radiometrischen Altersbestimmung, Diplomarbeit (unpubl.). MPI für Chemie, Mainz, 72.
 LANGMUIR C.H. et al 1977. Petrogenesis of basalts from the Famous Area mid-atlantic-ridge. *Earth and Planetary Science Letters* 36, 133-156.
 WYLLIE P.J. and HUANG W.-L. 1975. Peridotite, kimberlite, and carbonatite explained in the system CaO-MgO-SiO₂-CO₂. *Geology* 3, 621-624.
 KRAMERS J.D. et al. 1981. Can Kimberlites be generated from an ordinary mantle ? *Nature* 291, 53-56.

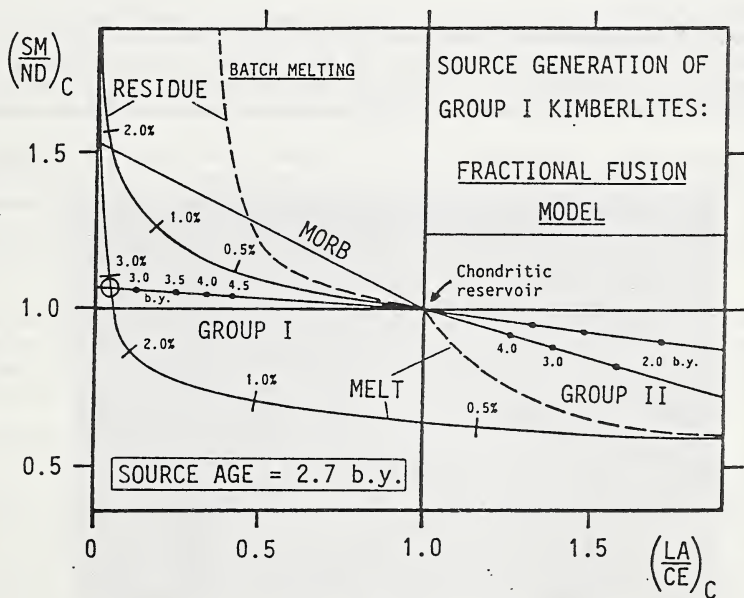


Figure 1.

INTERACTION OF METASOMATIC FLUIDS AND BASALTIC MELT WITH MANTLE XENOLITHS

Alfred Schneider

Geochemisches Institut, Universität Göttingen, D-3400 Göttingen, Federal Republic of Germany

Introduction

For the genesis of basaltic magmas three processes are under discussion:
 partial melting of primitive mantle rocks
 differentiation processes accompanied by crystal settling and
 partial melting of depleted mantle rocks, preceded by metasomatic processes.

Experimental petrology and almost the whole spectrum of geochemical methods have been applied to support the different hypotheses. Xenoliths of mantle rocks, transported by fast ascending magmas, i.e. kimberlites and basalts, are the favoured reference materials. They are also the basis of the results presented in this paper.

Source and relevance of samples

Cenozoic basalts of the Federal Republic of Germany are host rocks of peridotitic xenoliths from harzburgitic to lherzolitic composition. Their average composition is representative for continental spinel peridotitic xenoliths worldwide; they represent depleted mantle rocks (OEHM, SCHNEIDER, WEDEPOHL, 1983). Certain major and trace element compositions and Sr-isotope data of xenoliths indicate a metasomatic overprint preceding magma generation (WEDEPOHL, MENGEL, OEHM, 1984; MENGEL, KRAMM, WEDEPOHL, GOHN, 1985; HARTMANN, 1986).

The topic of this paper is

- to develop a model of the metasomatic process,
- to trace and localize it from the very first detectable chemical influence to the beginning of melting and magma separation in the xenoliths and
- to distinguish these features from reactions caused by the basaltic liquid, carrying the xenoliths to the surface.

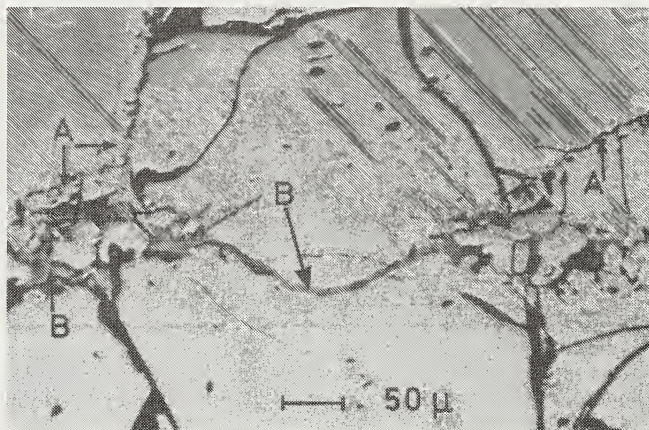


Fig. 1: Reaction rims around cpx (A) and melt (B), migrating along grain boundaries and mineral cracks.

Table 1: Average composition of glass, opx and rims of fluid inclusion tracks in opx (Microprobe analyses)

	A glass (n=66)	B opx core (n=3)	C opx fluid inclusion tracks (n=2)
SiO ₂	60.2	55.20	57.77
TiO ₂	1.6	0.02	0.06
Al ₂ O	18.7	3.54	4.31
ΣFeO	1.8	5.60	5.16
MnO	0.02	0.12	0.10
MgO	1.3	33.56	27.99
CaO	1.4	1.06	2.28
Na ₂ O	4.5*	0.13	1.52
K ₂ O	6.7	0.00	0.23
P ₂ O ₅	n.d.	<0.01	<0.02
SO ₃	n.d.	0.01	0.08
Cr ₂ O ₃	0.03	0.61	0.51
Total	96.25	99.86	100.03

- A: Average composition of glass from reaction rims, reaction domains and migration conduits.
 * minimum value due to losses by evaporation during electron bombardment
 B: orthopyroxene (core)
 C: Fingerprints from metasomatic fluids in fluid inclusion tracks of orthopyroxene (opx)
 Si, Al, Ca, Na, K, S contributed from the fluid phase

In the pathways of the degassed fluid inclusions the first fingerprints of a metasomatic fluid can be proven (Table 1). In a very small area around the open degassing pipes in an orthopyroxene Si, Al, Ca, K and Na are enriched, the latter by a factor of 10.

All the clinopyroxenes have reaction rims as shown in Fig. 1. The grain boundaries are corroded, some of the small cavities are filled with potassium- and sodium-rich glasses.

At grain boundary junctions reaction domains occur. Orthopyroxene, clinopyroxene and spinel are involved in solution processes. The matrix of these domains is also potassium-rich glass.

Starting from reaction rims or -domains, the melt migrates along grain boundaries and cracks, finally forming a tiny network, demonstrating the mobility of even very small amounts of melt. Minerals precipitated from this melt are:

Olivine - Clinopyroxene - Cr-rich Spinel - (Orthopyroxene) - Plagioclase (with K, Fe, Cr, Ti) - Apatite - Armalcolite - Picroilmenite - Calcite (from immiscible carbonate melt droplets) - Aegerine - Alkalihornblende (?) and secondary: - Smectite

The average composition of glass from reaction rims, reaction domains and migration channels (66 microprobe analyses) is given in Tab. 1. Whereas the content of K is comparatively constant, the variation of sodium is high, reflecting the interaction of the fluid phase with clinopyroxene and the crystallization of sodium-bearing minerals like clinopyroxene, aegerine and plagioclase from the melt.

The origin of glass in the xenoliths

These observations may not reflect a single-step process because during the rapid ascent the temperature of the xenoliths was raised to the temperature of the surrounding basalt magma. The observed melting may be caused only by this increase in temperature, but the structural relation in the involved microenvironments shows that a preceding metasomatic process in the mantle produced the extraordinary composition in these particular volumes. The concentration of Si, Al, K and Na cannot be contributed from the existing minerals, that are involved in these reactions, as a series of analyses of the minerals and their grain boundaries shows. They have to be transported by a metasomatic fluid phase.

In our case it can be proven, that minute amounts of isolated melt can not be directly related to preexisting crystals of phlogopite or amphiboles. Even if the secondary precipitated minerals and the change of composition of the involved veins of cpx, opx and spinel are recalculated the model doesn't fit.

Phlogopite and amphibole, as phases, formed by an early metasomatic process and melted because of the increased temperature induced by the surrounding basalt, is an insufficient picture, because in almost all samples, containing phlogopite this is in contact with melt, and it seems to be stable in these melt.

From these observations it is postulated that a fluid phase, transporting Si, Al, K and Na released primary melting and crystallization processes in depleted mantle environment under upper mantle conditions.

Experiments on the partial dissolution of peridotitic mineral associations under mantle conditions (SCHNEIDER and EGGLER, 1984) show appreciable dissolution of matter from the preexisting minerals in H₂O and H₂O + CO₂ as fluid phase (up to 11.8 weight % solute in fluid). Si, Al, Na and K are enriched in the solution, whereas there is a decrease of Fe, Mg and Ca compared to the composition of the peridotitic starting material. In our investigation all elements show exactly the same trend as predicted from the dissolution experiments.

The contact of the basaltic melt caused different reactions, including melting of peridotite minerals. Olivine becomes enriched in the fayalitic component. Spinel is gradually changed to magnetite, and the basaltic melt in contact with melt from the xenoliths is of different character. All that proves the differences in composition and oxygen fugacities of the melts.

References:

- MENGEL, K., KRAMM, U., WEDEPOHL, K.H., GOHN, E.: Sr isotopes in peridotite xenoliths and their basaltic host rocks from the northern Hessian Depression (NW Germany). *Contributions to Mineralogy and Petrology* **87**, 369-375 (1985)
- OEHM, J., SCHNEIDER, A., WEDEPOHL, K.H.: Upper mantle rocks from basalts of the northern Hessian Depression (NW Germany). *TMPM Tschermaks Mineralogisch-Petrographische Mitteilungen* **32**, 25-48 (1983)
- SCHNEIDER, M.E., EGGLER, D.H.: Composition of fluids in equilibrium with peridotite: Implications of alkaline magmatism-metasomatism. In J. Kornprobst: *Kimberlites I: Kimberlites and Related Rocks. Proceedings of the "Third International Kimberlite Conference" Vol. I.* Elsevier, Amsterdam-Oxford-New York-Tokyo 1984, p. 383
- WEDEPOHL, K.H., MENGEL, K., OEHM, J.: Depleted mantle rocks and metasomatically altered peridotite inclusions in Tertiary basalts from the Hessian Depression (NW-Germany). *Proc. 3rd Kimberlite Conf.* In: J. Kornprobst (ed.) *Kimberlites. II. The Mantle and Crust - Mantle Relationships*, pp. 191-201. Elsevier Science Publ., Amsterdam 1984
- HARTMANN, G.: *Chemische Zusammensetzung und Mineralbestand von Peridotit-Xenolithen mit unterschiedlicher metasomatischer Überprägung aus Basalten der Hessischen Senke.* Thesis, Göttingen 1986

Daniel J. Schulze

Department of Geological Sciences, Queen's University
Kingston, Ontario, Canada K7L 3N6

Xenocrysts of green garnet form a very minor fraction of the concentrate of the Kampfersdam kimberlite, Kimberley, R.S.A. Some are intergrown with clinopyroxene and/or spinel, thus providing an opportunity to better characterize the paragenesis of green garnets. With the exception of two green garnet-bearing wehrlite xenoliths from kimberlites in Yakutia, U.S.S.R. (Sobolev et al., 1973), such garnets are only known as xenocrysts in kimberlite (e.g. Hornung and Nixon, 1973; Clarke and Carswell, 1977; Scott and Skinner, 1979).

The Kampfersdam green garnets range from very deep blue-green to dark-purple with green tinges. They are rich in CaO (11.2-18.8 wt %) and Cr₂O₃ (9.5-13.3 wt %), and thus plot well above the trend of garnets from lherzolites (Fig. 2¹) noted by Sobolev et al. (1973). The lherzolite trend in Fig. 1 is approximated by garnets from Kimberley wehrlites, dark purple Kampfersdam xenocrysts, and Kao green garnets (Hornung and Nixon, 1973). The Kampfersdam green garnets overlap those from the Newlands kimberlites in South Africa (Clarke and Carswell, 1977) in their CaO and Cr₂O₃ values, but are generally lower in CaO than the Newlands examples. Green garnets from the Premier Mine in South Africa (Scott and Skinner, 1979) also overlap the Kampfersdam samples on Fig. 1., but extend to more Cr-rich values. One purple garnet from Kampfersdam plots in the green garnet field, but most of the dark purple garnets (without a green tinge) from this pipe plot on the lherzolite trend. The Mg/(Mg + Fe) values of the green garnets range from 0.763-0.860, somewhat higher than the Newlands examples (Fig. 2). Clinopyroxenes intergrown with the Kampfersdam green garnets are also magnesian, with Mg/(Mg + Fe) values of 0.914-0.969. They are quite calcic (Fig. 2), with values of Ca/(Ca + Mg) of 0.474-0.494, with one exception at 0.432, and their Cr₂O₃ range from 1.3-3.4 wt %. The intergrown spinels are similar to those from the green garnet wehrlites from Yakutia (Sobolev et al., 1973) and most coarse-textured garnet lherzolites, in terms of Mg/(Mg + Fe) (0.50-0.60) and Cr/(Cr + Al) (0.74-0.80).

Because the green garnets plot on the CaO-rich side of the lherzolite trend (Fig. 1), they could not have equilibrated with orthopyroxene, and are probably xenocrysts from disaggregated wehrlites. Two such green garnet-bearing wehrlites have been described by Sobolev et al. (1973) from the Dalnaya and Sytikanskaya pipes in Yakutia, U.S.S.R. Similar rocks have been inferred as the source of the very calcium-rich green garnets from the Newlands pipe by Clarke and Carswell (1977).

Four garnet-bearing, orthopyroxene-free wehrlites from Kampfersdam and the Kimberley dumps were also investigated (Figs. 1, 2). The garnets in these nodules, however, plot on the lherzolite trend, and the compositions of all phases are typical of the garnet peridotites from Kampfersdam and the Kimberley dumps (Boyd and Nixon, 1978).

In the absence of orthopyroxene, estimation of the pressure and temperature conditions of equilibration is restricted to calculation of temperature at an assumed pressure, using the garnet-clinopyroxene Fe-Mg exchange thermometer of Ellis and Green (1979). Even this estimation may be in error, in view of the very high calcium and chromium contents. Nevertheless, at an assumed pressure of 50 kb, eight composite xenocrysts yield a temperature range of 1040-1380°C, although only two of these are above 1200°C. Sodium content of the clinopyroxenes correlates positively with equilibration temperature. The four wehrlites yield a temperature range of 1125-1235°C, using the same method. As the compositions of the garnets in the latter indicate equilibration with both pyroxenes, however, it is valid to use pyroxene thermometry to calculate their equilibration temperatures. Using the 20 kb solvus of Lindsley and Dixon (1976), they yield a temperature range of 980-1080°C. This corresponds to the high-temperature end of the range for garnet peridotites from the Kimberley pipes (Boyd and Nixon, 1978), using the same thermometer. Considering the above assumptions and estimates, all that

can be realistically stated is that most of these composite xenocrysts probably equilibrated at temperatures comparable to the lower P-T nodules of the Kimberley suite, with the exception of the highest temperature xenocryst assemblage, which has a strikingly different garnet-clinopyroxene tie line orientation (Fig. 2).

Although Clarke and Carswell (1977) proposed that the green garnets from Newlands formed in very high temperature and pressure wehrlite cumulates (1600-2200°C, 200-250 km), there is no evidence in these nodules for such extreme conditions. It is suggested here that green Ca- and Cr-rich garnets may have originated in subducted serpentinites. Most occurrences, world-wide, of uvarovitic garnets are restricted to serpentinites (Deer et al., 1982), where they form by Ca- and Si-metasomatism (Ca released from pyroxenes during serpentinization) of chromite. Serpentinites are anomalously Ca-poor relative to most anhydrous peridotites, and the Ca enrichment associated with uvarovite formation must be very localized. During subduction and emplacement of a "cool" slab, temperatures would never rise above those of a steady-state geothermal gradient. The persistence of such low temperatures is essential for long term (billions of years for mantle rocks with Archean ages) preservation of both small scale inhomogeneities, such as the millimeter scale chemical variation described by Clarke and Carswell (1977), and large scale inhomogeneities. The latter are exemplified by the presence of both anomalously Ca-rich (green garnet wehrlite) and Ca-poor (low-Ca garnet harzburgite and dunite) peridotite bodies within an upper mantle that is virtually saturated in both pyroxenes. It should be noted that most single-pyroxene garnet peridotites, both wehrlites and harzburgites, are actually "closet lherzolites", in that their garnets plot on the lherzolite trend. This indicates that the rock equilibrated with both pyroxenes, although one may not be present in the sample. Real single-pyroxene garnet peridotites, such as green garnet wehrlites and low-Ca garnet harzburgites, are very rare.

Boyd, F.R., and Nixon, P.H. 1978. Ultramafic nodules from the Kimberley pipes, South Africa. *Geochimica et Cosmochimica Acta* 42, 1367-1382.

Clarke, D.B., and Carswell, D.A. 1977. Green garnets from the Newlands kimberlite, Cape Province, South Africa. *Earth and Planetary Science Letters* 34, 30-38.

Deer, W.A., Howie, R.A., and Zussman, J. 1982. *Rock-forming Minerals, Vol. 1A, Orthosilicates*, Longman, London.

Ellis, D.J., and Green, D.H. 1979. An experimental study of the effect of Ca upon garnet-clinopyroxene Fe-Mg exchange equilibria. *Contributions to Mineralogy and Petrology* 71, 13-22.

Hörnung, G., and Nixon, P.H. 1973. Chemical variations in the knorringite-rich garnets. In Nixon, P.H. ed., *Lesotho Kimberlites*, pp. 122-127, Cape and Transvaal, Cape Town.

Lindsley, D.H., and Dixon, S.A. 1976. Diopside-enstatite equilibria at 850°C to 1400°C, 5 to 35 kb. *The American Journal of Science* 276, 1285-1301.

Scott, B.H., and Skinner, E.M.W. 1979. The Premier kimberlite, Transvaal, South Africa, *Kimberlite Symposium II*, pp. 95-101, Cambridge.

Sobolev, N.V., Lavrent'ev, Yu. G., Pokhilenko, N.P., and Usova, L.V. 1973. Chrome-rich garnets from the kimberlites of Yakutia and their parageneses. *Contributions to Mineralogy and Petrology* 40, 39-52.

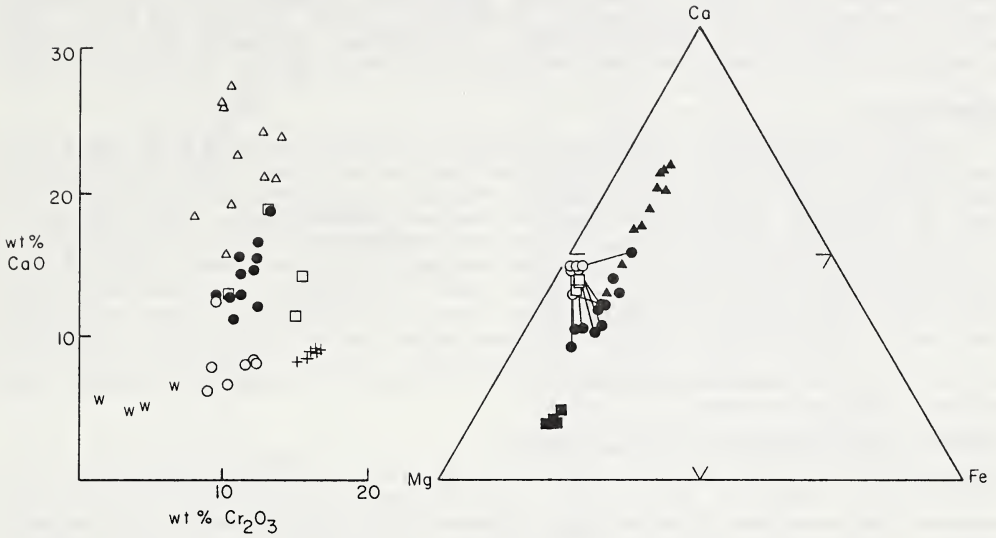


Fig. 1 (left). Plot of CaO vs. Cr₂O₃ for selected garnets. Filled circles = Kampfersdam green garnets, open circles = Kampfersdam dark purple garnets, open triangles = Newlands green garnets (Clarke and Carswell, 1977; Schulze, unpublished data), open squares = Premier green garnets (Scott and Skinner, 1979; Boyd, unpublished data), crosses = Kao green garnets (Hornung and Nixon, 1973), W = Kimberley wehrlite garnets.

Fig. 2 (right). Ca-Mg-Fe values (mole %) of selected garnets (filled symbols) and clinopyroxenes (open symbols). Circles = Kampfersdam green garnets and coexisting clinopyroxenes, squares = Kimberley garnet wehrlites (tie lines not shown), triangles = Newlands green garnets (Clarke and Carswell, 1977; Schulze, unpublished data).

**EVOLUTION OF SUB-CONTINENTAL MANTLE AND CRUST:
ECLOGITES FROM SOUTHERN AFRICA**

John W. SHERVAIS^{1,2}, Lawrence A. TAYLOR¹, Gunter W. LUGMAIR³, Robert N. CLAYTON⁴,
T. MAYEDA⁴, and Randy L. KOROTEV⁵.

1 Dept. of Geol. Sci., Univ. of Tennessee, Knoxville, TN 37996; 2 Present Address: Dept. of Geology, Univ. of So. Carolina, Columbia, SC 29208; 3 Dept. of Chem., Univ. of Calif. at San Diego, La Jolla, CA 92093; 4 Enrico Fermi Institute, Univ. of Chicago, Chicago, IL 60637; 5 Dept. of Earth & Planet. Sci., Wash. Univ., St. Louis, MO 63130.

INTRODUCTION

Eclogites are essentially biminerally garnet + clinopyroxene rocks with basaltic bulk compositions that crystallized (or re-crystallized) at relatively high pressures in the lower crust or upper mantle. Eclogites with omphacitic pyroxene and Ca, Fe-rich garnet found in blueschist terranes are thought to represent metamorphosed oceanic crust. In contrast, eclogite xenoliths in kimberlites and alkali basalts are more magnesian and are generally interpreted as high pressure cumulates that form dikes within the upper mantle. Eclogites that occur in kimberlites vary greatly in texture, mineral compositions, and isotopic characteristics, however, and there is increasing evidence that some of these nodules may also represent metamorphosed oceanic crust. In order to distinguish between these contrasting hypotheses, we have selected a suite of six African eclogites, from the collections of Dr. F.R. Boyd, for detailed petrologic, trace element, and isotopic study.

PETROLOGY AND GEOCHEMISTRY OF THE ECLOGITES

Petrography: The six eclogite xenoliths chosen are from four African kimberlites: three from Bellsbank (FRB-437-1, 438-2, 438-7), and one each from Kao, Lesotho (PHN-1850), Deutsche Erde, Namibia (DE-15), Vale do Queve, Angola (FRB-340). All consist of subequal proportions of garnet and clinopyroxene, with traces of rutile and phlogopite. FRB-437 samples also contain olivine (Fo92) and enstatite (En 95); FRB-340 contains plagioclase (An15) and sanidine (Or40-60). All have coarse granular or granoblastic textures.

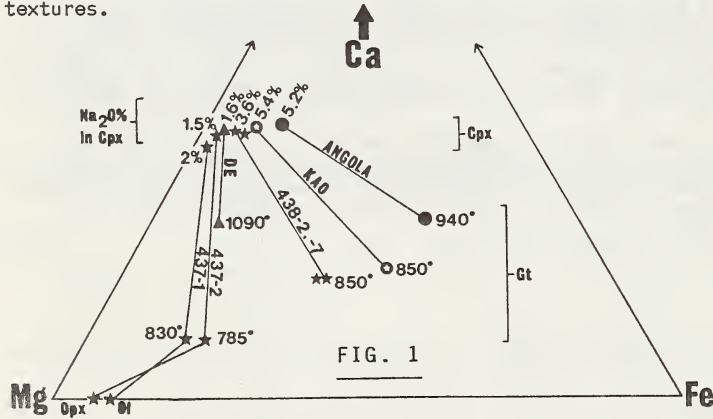
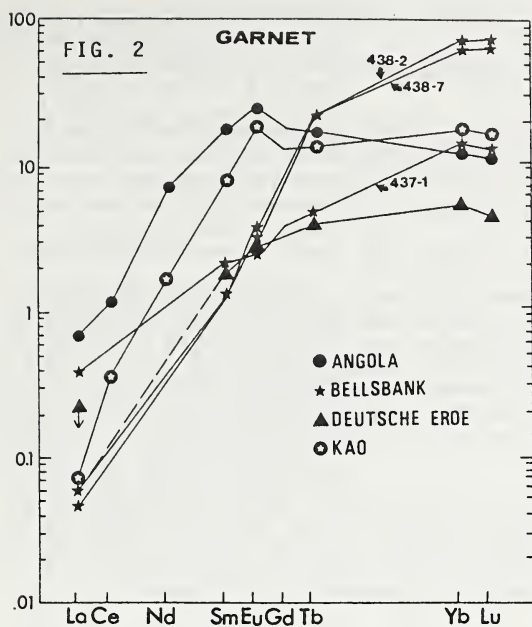


FIG. 1

Mineral Chemistry: Three groups of eclogite are recognized from major element compositions. **Group A (Kao and Angola):** High Fe/Mg ratios in both pyroxene and garnet (Pyroxene MG# = 77-84, Garnet MG#s = 36-46), K_D 's of 5-6, and jadeite-rich pyroxene ($Na_2O \approx 5.5\%$); **Group B (438-1, 438-7):** Intermediate Fe/Mg ratios (Pyroxene MG# = 86-89, Garnet MG# = 57-59), K_D 's of 4.8-5.8, moderate jadeite contents in pyroxene ($Na_2O \approx 3.75\%$); **Group C (437-1,2; DE-15):** Low Fe/Mg ratios (Pyroxene MG# = 95.0-95.5, Olivine Fo 92.5, Garnet MG# = 79-83), K_D 's of 3.5-5.0, and jadeite-poor pyroxene ($Na_2O \approx 1-2\%$).

These relationships are illustrated in Figure 1. The Trace element analyses by INAA of hand-picked mineral separates support the three groups defined above by major element chemistry and provide further constraints on their origin (Fig. 2). The most LREE-enriched pyroxenes are those of Group C, with Ce/Tb ratios of 600-1200 (30-70 x chondrite). Pyroxenes from the Group A and Group B eclogites have Ce/Tb ratios which range from 9-90 (0.5-5.3 x chondrite). Group A garnets have flat or slightly positive HREE slopes that turn down at Sm ($Yb/Sm = 0.7-2.2 \times$ chondrite) and distinct positive Eu anomalies (Figure 2). These characteristics strongly suggest recrystallization of a plagioclase enriched protolith. Group B garnets feature extreme depletion of the LREE and enrichment of the HREE ($Yb/Sm = 50-60 \times$ chondrite) which suggest a refractory origin for the Group B eclogites. Group C garnets have intermediate characteristics and feature smooth positive slopes from La to Yb ($Yb/Sm = 3-7 \times$ chondrite).



Whole Rock Geochemistry: All of the eclogites studied here are approximately "basaltic" in the sense that they contain 45-51% SiO_2 ; however, only the Group A eclogites could represent realistic liquid compositions. The other eclogites are too low in TiO_2 , and too high in CaO (DE), MgO (437-1,2), or MG\# ($=100 \cdot \text{Mg}/[\text{Mg}+\text{Fe}]$). Concentrations of the REE in whole rock samples of eclogite have been determined by modal recombination. The Group A eclogites have REE concentrations similar to 'normal' depleted MORB, but with a large positive Eu anomaly (Figure 3). This suggests that the Group A eclogites had anorthositic protoliths (Jagoutz *et al* 1985). The Group B eclogites and 437-1 have HREE slopes that are dominated by garnet and LREE enrichments that reflect modal pyroxene. DE-15-1 has a relatively unfractionated REE pattern with concentrations 2-3x chondrite.

Isotope Geochemistry: The results of our isotopic analyses are presented in Table 1. The Group B and C eclogites define a whole rock error-chron of 2.4 b.y. with an initial ϵ_{Nd} of +28. If these eclogites formed at this time, their precursor was

already highly differentiated (LREE depleted). De-coupling of the Sr and Nd systems is evident in the Group B eclogites. The high $^{87}\text{Sr}/^{86}\text{Sr}$ and low ϵ_{Nd} of these eclogites suggests hydrothermal exchange with a seawater. The isotopic composition of oxygen in the eclogites studied here is listed in Table 1. These data suggest that hydrothermal exchange with seawater is a required in the petrogenetic history of the Group B eclogites and that this process may have affected the progenitors of the Group A and Group C eclogites as well.

DISCUSSION

The data presented in the preceding sections show that the eclogites studied here can be divided into three distinct groups based on the major element composition of their silicate phases. We have shown further that these distinctions are supported by (a) whole rock major and trace element data, (b) trace element analyses of the silicate phases, (c) the isotopic composition of Sr and Nd in garnet and pyroxene, and (d) the isotopic composition of oxygen in the same phases. 100 The petrologic and geochemical characteristics of these groups are:

Group A (Kao and Angola): Group A eclogites are characterized by high Fe/Mg ratios ($\text{MG\#s} = 77-84$ Cpx; 36-46 Gt; 62-76 whole rock), jadeite-rich pyroxene ($\text{Na}_2\text{O} \approx 5.5\%$), extremely low Cr_2O_3 (< 0.1%), variable ϵ_{Nd} (-16 to +24) and $^{87}\text{Sr}/^{86}\text{Sr}$ (0.704-0.707), $\delta^{18}\text{O} = +4$ to +6, and positive Eu anomalies in garnet and possibly pyroxene; Plagioclase and sanidine may be present.

Group B (438-1,438-7): Group B eclogites are characterized by moderate to low Fe/Mg ratios ($\text{MG\#s} = 86-89$ Cpx; 57-59 Gt; 79-82 whole rock), moderately jadeite-rich pyroxene ($\text{Na}_2\text{O} \approx 3.75\%$), extremely low Cr_2O_3 (< 0.1%), high ϵ_{Nd} (+100 to +250) and $^{87}\text{Sr}/^{86}\text{Sr}$ (0.709-0.710), $\delta^{18}\text{O} = +3$ to +3.4, and extremely LREE-depleted/HREE-enriched garnets with no Eu anomalies.

Group C (437-1,437-2,DE-15-1): Group C eclogites are characterized by very low Fe/Mg ratios

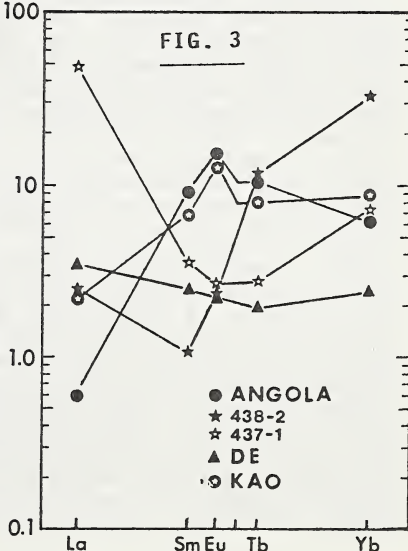


TABLE 1. Isotopic Data for African Eclogites.

Type	Sample	Phase	Sm ppm	Nd ppm	$^{143}\text{Nd}/^{144}\text{Nd}$	ϵ Nd	$^{87}\text{Sr}/^{86}\text{Sr}$	$\delta^{18}\text{O}$
"A"	KAO	Cpx	1.148	4.6820	0.512761	3.80	0.704264	4.72
		Gt*	1.351	1.1070	0.513781	23.70	----	4.12
		Gt**	1.543	1.2500	0.513421	16.68	----	4.03
"A"	Angola	Cpx	0.1736	0.6157	0.511771	-15.51	0.707376	---
		Gt	3.1160	4.659	0.512665	1.93	----	6.07
"B"	438-2	Cpx	0.1945	0.4380	0.518733	120.32	0.709359	3.42
		Gt	0.2257	0.1174	0.518923	124.02	----	3.25
"B"	438-7	Cpx	0.201	0.2410	0.524274	228.42	0.710022	---
		Gt	0.2137	0.0557	0.525428	250.93	----	3.04
"C"	437-1	Cpx	1.4660	22.140	0.511594	-18.96	0.704197	5.25
		Gt	0.3596	0.8358	0.512008	-10.89	----	5.02
"C"	DE	Cpx	0.5841	4.240	0.512853	5.60	0.703326	4.87
		Gt	0.3309	0.385	0.513382	15.92	----	4.76

* Garnet with rutile exsolution.

** Garnet without rutile exsolution.

(MG#s = 95-96 Cpx, 0px; 92-93 01; 79-83 Gt; 91-94 whole rock), low jadeite pyroxene ($\text{Na}_2\text{O} \approx 1-2\%$), $\text{Cr}_2\text{O}_3 = 0.1-1.0\%$ bulk, low ϵ Nd (-20 to +16) and $\delta^{18}\text{O} = +4.7$ to $+5.3$, and extremely LREE-enriched pyroxene. Olivine and enstatite are commonly present, Eu anomalies are absent.

The Group A and Group B eclogites defined here correlate well with the Roberts Victor Type A and Type B eclogites, resp., described by Jagoutz *et al* (1985) -- the similarity in our terminology is intentional. The close similarity between the groups defined here and correlative

eclogite types from the Roberts Victor kimberlite suggests that these eclogites formed by the same processes. The areal distribution of these eclogite groups -- from Angola in the North to Lesotho in the South) supports the hypothesis that these groups are fundamental petrologic units that have widespread petrogenetic significance.

PETROGENESIS

The Group A eclogites are the most easily interpreted. The positive Eu anomaly that is superimposed on both the garnet and pyroxene REE patterns is characteristic of plagioclase accumulation and requires an anorthositic protolith for these eclogites. The re-constructed whole rock REE patterns are similar to normal MORB, with flat HREE-MREE at approximately 10x chondrite and slightly depleted LREE (Figure 3). A Positive Eu anomaly is also superimposed on these whole rock patterns. The $^{87}\text{Sr}/^{86}\text{Sr}$ ratios are consistent with the ϵ Nd (-1.3 to +7.0) and lie on or near the trend of ocean island basalts in a Sr-Nd correlation diagram. Both eclogites contain jadeite-rich pyroxene, consistent with a "spilitized" protolith. We conclude that the Group A eclogites represent anorthositic ocean crust, as proposed by Jagoutz *et al* (1985) for Roberts Victor Type A eclogites. Our analyses suggest that anorthositic gabbro is the most likely protolith. The felsic portion of the crust contains less water than the overlying basaltic portion and is less affected by dehydration and partial melting.

The Group B eclogites are characterized by extremely depleted LREE and C Nd values 10x to 20x MORB. The high $^{87}\text{Sr}/^{86}\text{Sr}$ of these eclogites is not consistent with their strongly depleted LREE and high ϵ Nd, and cannot be a primary feature of the protolith. Similarly, the extremely low $\delta^{18}\text{O}$ of the Group B eclogites cannot form by mantle fractionation processes. Both the low $\delta^{18}\text{O}$ and high $^{87}\text{Sr}/^{86}\text{Sr}$ are consistent with high temperature seawater alteration of a basaltic protolith. The low concentrations of incompatible trace elements in the whole rocks and the extreme LREE-depleted/HREE-enriched character of the garnets, are most consistent with a refractory origin for the Group B eclogites. Because of its high water content, the mafic portion of the oceanic crust will be affected more strongly by dehydration and partial melting than the less hydrous felsic portion (= Group A eclogites).

The Group C eclogites are the only eclogites studied here whose geochemical characteristics are consistent with an origin as cumulate dike rocks in the upper mantle. They have high MG#s that are similar to the refractory peridotites thought to comprise most of the upper mantle, low concentrations of incompatible elements, and Sr-Nd systematics that are similar to ocean island basalts. The reconstructed REE patterns for these eclogites are consistent with the accumulation of pyroxene and garnet in these dikes, along with minor trapped liquid, and the values for K_{Sm} and K_{Nd} are consistent empirical pyroxene/garnet partition coefficients. The slightly low $\delta^{18}\text{O}$ values in these eclogites are inherited from the source region of the partial melts, which may correspond to the subducted ocean crust that formed eclogites of Groups A and B.

Reference: Jagoutz E., Dawson J., Hoernes S., Spettel B., Wänke H. 1985. Anorthositic oceanic crust in the Archean Earth. *The Early Earth*, LPI Tech Rept. 85-01, 40-41.

C.B. Smith¹, H.L. Allsopp², J.D. Kramers³, J.J. Gurney⁴ and E. Jagoutz¹

1 - Max Planck Institut für Chemie, Mainz, F.R.G., 2 - Bernard Price Institute for Geophysical Research, Johannesburg, R.S.A. (deceased), 3 - University of Zimbabwe, Harare, Zimbabwe, 4 - University of Cape Town, Rondebosch, R.S.A.

KIMBERLITE

Initial Sr, Nd and Pb isotopic compositions of southern African Jurassic-Cretaceous kimberlites define two distinctive varieties that must be derived from different types of upper mantle sources (Smith, 1983). Group I kimberlites, commonly referred to as "basaltic", generally lack appreciable mica and with some exceptions have consistent Nd isotopic compositions slightly higher than the bulk earth value. $^{87}\text{Sr}/^{86}\text{Sr}$ ratios are somewhat more variable ranging from about .7035 to .7050 in reasonably fresh hypabyssal samples. Pb isotopic compositions are more variable, spanning nearly the full range of oceanic island basalts (OIB). Group II kimberlites have high groundmass mica contents and tend to lack ilmenite, zircon and perovskite, minerals characteristic of Group I kimberlites, as well as having somewhat older emplacement ages (Smith et al., in press). In addition, inclusions of the Cr-poor subcalcic megacryst assemblage and high P-T sheared lherzolite xenoliths with isotopic characteristics suggestive of asthenospheric origins are apparently absent in Group II intrusives. The Group II kimberlites have radiogenic Sr ($^{87}\text{Sr}/^{86}\text{Sr} = .7075$ to greater than .710) and non-radiogenic Nd ($^{143}\text{Nd}/^{144}\text{Nd} = .5120$ to .5123, relative to .51264 in standard BCR-1), plotting in the enriched mantle quadrant of the Sr-Nd correlation diagram. Compared to Group I, Group II source rocks have had high time-averaged Rb/Sr and LREE enrichment, with minimum model source ages from Sm-Nd systematics being of the order of 600 million years. Pb isotopic compositions are considerably less radiogenic and less variable than Group I, OIB or most mid-ocean ridge basalts (MORB).

Major and trace element analyses of the samples analyzed for isotopic compositions confirm that Group I and Group II kimberlites are chemically distinctive, the K/Ti ratio alone serving as an efficient discriminator. Stepwise discriminant function analysis using isotopic character as the independent grouping variable identifies the combination of chemical features that best separate the two groups and successfully classifies a large number of kimberlites for which published data are available, as well as highlighting second order distinctions. Among other features, Group II kimberlites have significantly greater enrichment in SiO_2 and the most incompatible trace elements K, Rb, Ba, Pb and LREE compared to Group I. The latter have significantly higher abundances of Ti and Nb. Group I kimberlites can be subdivided into two gradational varieties that are not, from limited available data, correlative with isotopic character. Compared to IA, kimberlites of the IB subgrouping tend to have higher Fe/Mg and higher abundances of the high field strength incompatible elements (Zr, Y, Ti, P). In the data set analyzed, the IB kimberlites tend to be those situated at or outside the margins of the Kaapvaal Craton although a number of exceptions are known.

Since chemical differences between Groups I and II are correlated with isotopic character, it is likely that at least some of the chemical distinctions (particularly incompatible element abundances) reflect distinctions in source compositions. The isotopic evidence, in conjunction with apparent distribution of high P-T xenolith suites, suggests that Group I kimberlites are derived from asthenospheric plume sources similar to those from which OIB are produced (Kramers, 1977). In contrast, Group II kimberlites may originate within enriched portions of the subcontinental lithosphere that has been stabilized against convective disruption for a long period of time (Smith et al., in press). The geochemical evidence, though not inconsistent with this, is neither particularly supportive, however. Group I and Group II kimberlites have similar OIB-like incompatible element abundance patterns implying similar trace element incompatibility sequences in the sources. Both groups could be plume related although basalts with isotopic character similar to Group II kimberlites have not yet been documented from the ocean basins. le Roex (in press) has compared isotopic and geochemical signatures of southern African kimberlites with South Atlantic

ridge and plume basalts, and argues persuasively that the chemical signatures of the two kimberlite groups are extensions of the diverging chemical trends characteristic of DUPAL (Group II) and non-DUPAL (Group I) types of basalt sources.

ECLOGITE XENOLITHS FROM THE ORAPA KIMBERLITE

Eclogite xenoliths, many with accessory diamond, are the dominant nodule type in the Orapa kimberlite (Shee and Gurney, 1979) and likely represent the major source of diamond in the pipe. Sr and Nd isotopic compositions of clinopyroxene and garnet from a compositionally diverse suite of eclogite xenoliths are characterized by extreme variability, with $^{87}\text{Sr}/^{86}\text{Sr}$ ratios in clinopyroxene ranging from .7025 to .709 and corresponding variation in emplacement age corrected $^{143}\text{Nd}/^{144}\text{Nd}$ of .5128 to .5122, and in this regard are similar to Roberts Victor eclogites studied by Kramers (1979). In contrast to the Roberts Victor samples, Pb isotopic compositions are consistent and similar to modern MORB and do not provide age constraints. Isotopic character is to some degree correlated with major element chemistry for the compositional groupings thus far examined. Type 2 websterite group samples with Ca-poor magnesian garnet have clinopyroxenes with radiogenic $^{87}\text{Sr}/^{86}\text{Sr}$ (.705 to .709) and the least radiogenic $^{143}\text{Nd}/^{144}\text{Nd}$ (.5122 to .5125). Type 1 eclogites with higher Ca and Fe in garnets have less radiogenic $^{87}\text{Sr}/^{86}\text{Sr}$ (.7024 to .7066) and bulk earth or higher $^{143}\text{Nd}/^{144}\text{Nd}$ ratios. In the context of the subdivision of the type 1 eclogites by Shee and Gurney (1979), the Ca-rich subgroup has the least radiogenic Sr and most radiogenic Nd compared to main and Ca+Fe rich subgroups. Diamond eclogites are all type 1 samples, and have variable isotopic character consistent with variable subgrouping according to major element compositions of the garnets. Type 1 and type 2 clinopyroxenes differ considerably in their trace element contents, with type 1 pyroxenes having significantly lower Sr, Nd, Sm and Pb but higher Rb (in keeping with generally higher jadeite). Rb/Sr and Sm/Nd ratios tend to be anticorrelated with Sr and Nd isotopic compositions in type 1 pyroxenes, suggestive of mixing processes in parent liquids and not supportive of old ages for the eclogites themselves. Coexisting clinopyroxene and garnet were in Nd isotopic equilibrium at the time of kimberlite emplacement in all but one of the samples, thus precluding internal Sm-Nd age determinations from mineral pairs. A garnet-clinopyroxene apparent age of about 180 million years in one sample is marginally older than pipe emplacement.

Despite the lack of age constraints, the variable isotopic character of the samples analyzed so far indicate that the xenoliths do not likely comprise a related group of samples, and as concluded for the Roberts Victor assemblage, likely represent cumulates of melts derived from a variety of sources. Parents of type 2 eclogites must have had time-averaged enriched Rb/Sr and LREE character, suggestive of derivation from enriched lithospheric mantle sources. Type 1 eclogites could be derived from more primitive to depleted mantle, and in some cases could have had MORB as a parent.

MEGACRYSTS

Minerals of the Cr-poor subcalcic megacryst assemblage are abundant in Group I kimberlites in southern Africa and other localities worldwide. Although the origins of the assemblage have not been satisfactorily resolved, the constituent minerals are generally regarded to have crystallized at high pressures from a fractionating kimberlite-like liquid. Pb, Sr and Nd isotopic compositions of clinopyroxene megacrysts of this suite are distinctive, with $^{87}\text{Sr}/^{86}\text{Sr}$ = .7028 to .7032 throughout southern Africa except Orapa, where Sr in both Cr-poor and Cr-rich megacrysts is somewhat more primitive ($^{87}\text{Sr}/^{86}\text{Sr}$ = .7025). Nd isotopic compositions are marginally higher than bulk earth, and $^{206}\text{Pb}/^{204}\text{Pb}$ ratios are notably radiogenic except in one sample from Jwaneng. Isotopically, the Cr-poor megacrysts are generally dissimilar to megacrysts of other associations and to kimberlite in which they are entrained. Hence a cognate origin is possible only if kimberlite has been contaminated subsequent to megacryst crystallization. Isotopic compositions of Cr-poor clinopyroxenes are similar to the St. Helena type of oceanic basalt (e.g. White, 1985). The assemblage may thus have an important bearing on the origins of some oceanic basalts, and in kimberlites older than the age of the ocean basins may be useful in constraining the isotopic evolution of some OIB reservoirs.

REFERENCES

- KRAMERS J.D. 1977. Lead and strontium isotopes in Cretaceous kimberlites and mantle-derived xenoliths from southern Africa. *Earth Planet. Sci. Lett.* 34, 419-431.
- KRAMERS J.D. 1979. Lead, uranium, strontium potassium and rubidium in inclusion-bearing diamonds and mantle-derived xenoliths from southern Africa. *Earth Planet. Sci. Lett.* 42, 58-70.
- LE ROEX A.P. submitted to *Nature*. A geochemical correlation between source region signatures of southern African kimberlites and southern ocean hotspots.
- SHEE S.R. and GURNEY J.J. 1979. The mineralogy of xenoliths from Orapa, Botswana. In Boyd F.R. and Meyer H.O.A. eds, *Proc. 2nd Int. Kimberlite Conf.*, Vol. 2, pp. 37-49. American Geophys. Union, Washington, D.C.
- SMITH C.B. 1983. Pb, Sr and Nd isotopic evidence for sources of southern African kimberlites. *Nature* 304, 51-54.
- SMITH C.B., ALLSOPP H.L., KRAMERS J.D., HUTCHINSON G. and RODDICK J.C. in press. Emplacement ages of Jurassic-Cretaceous South African kimberlites by the Rb-Sr method on phlogopite and whole-rock samples. *Trans. Geol. Soc. S. Afr.* 88.
- SMITH C.B., GURNEY J.J., SKINNER E.M.W., CLEMENT C.R. and EBRAHIM N. in press. Geochemical character of southern African kimberlites: a new approach based on isotopic constraints. *Trans. Geol. Soc. S. Afr.* 88.
- WHITE W.M. 1985. Sources of oceanic basalts: radiogenic isotope evidence. *Geology* 13, 115-118.

C.B. Smith¹, J.J. Gurney², J.W. Harris³, D.N. Robinson⁴, S.R. Shee⁴ and E. Jagoutz¹

1 - Max Planck Institut für Chemie, Mainz, F.R.G., 2 - University of Cape Town, Rondebosch, R.S.A., 3 - University of Strathclyde, Glasgow, U.K., 4 - Anglo American Research Laboratories, Johannesburg, R.S.A.

Eclogite is an important source of diamond in many southern African kimberlites as evidenced by the not uncommon occurrence of diamond-bearing eclogite xenoliths as well as the abundance of eclogite paragenesis inclusions within diamonds. Despite the importance of the eclogite association, the isotopic character of silicate minerals co-existing with diamond in xenoliths or as inclusions within individual diamonds has not previously been investigated. Here we report Sr and Nd isotopic analyses of clinopyroxene and garnet in selected diamond-bearing eclogite xenoliths from the Excelsior, Orapa, Newlands and Roberts Victor kimberlites, and of eclogitic garnet inclusions from a single Finsch diamond.

DIAMONDIFEROUS ECLOGITE XENOLITHS

Of the samples analyzed, those from Orapa and the single Roberts Victor sample have been described (Robinson et al., 1984; Shee and Gurney, 1979; Hatton and Gurney, 1979) whereas the single Newlands sample and a suite of fourteen newly collected Excelsior samples have not previously been studied. With the exceptions of samples HRV247, a type 2 calcium-rich eclogite from Roberts Victor, and diamond-free graphite eclogite XM11 from Orapa (type 2, websterite association) all samples are type 1 eclogites (terminology of MacGregor and Carter, 1970; Robinson et al., 1984) with garnet and clinopyroxene characterized by somewhat elevated Na₂O and K₂O respectively in comparison to non-carbonaceous eclogite, consistent with high pressure origins. All samples are kyanite-free. Garnet compositions (Fig. 1) are diverse, though still somewhat restricted compared to the full compositional range of southern African diamond eclogites (Reid et al., 1976). The distribution of Mg and Fe between clinopyroxene and garnet indicates equilibration temperatures of between 1000 and 1200°C (calculated for P=50kb). Within these limits, however, the Excelsior samples are physically and chemically distinctive compared to diamond eclogite from other localities. Garnet in the Excelsior eclogites is markedly coarse-grained (up to 3 cm), with most samples being small and consisting dominantly of single garnet crystals with accessory octahedral diamond. Clinopyroxene is present in only minor amounts in five of the fourteen specimens and in some cases is less abundant than diamond. In comparison with the compositional variability characteristic of diamond eclogite from Roberts Victor and Orapa, all but two of the Excelsior samples have restricted compositional range (Fig. 1), strongly supportive of these rocks comprising a genetically related assemblage.

Despite the small size and somewhat altered nature of most samples, isotopic results on carefully cleaned and leached mineral separates cannot be explained by kimberlite contamination or alteration effects. ⁸⁷Sr/⁸⁶Sr ratios in clinopyroxenes of the type 1 samples and HRV247 are highly variable, ranging from .7026 to .7067 (Fig. 2), similar to the range in the Orapa samples alone. Clinopyroxene in the type 2 graphite eclogite from Orapa has the most radiogenic Sr, with ⁸⁷Sr/⁸⁶Sr = .7081. Nd isotopic compositions of clinopyroxenes and garnets are correspondingly variable, with emplacement age corrected ¹⁴³Nd/¹⁴⁴Nd varying from .5117 to .5129 (Fig. 2).

With the exception of the Newlands sample, JJG144, garnet and clinopyroxene were in Nd isotopic equilibrium at the time of kimberlite emplacement, consistent with lack of petrographic or chemical disequilibrium features in all samples except HRV247. Presuming that the samples are older than pipe emplacement, internal age determinations from mineral pairs are not possible. Samples from the Excelsior suite are most likely cogenetic from chemical evidence, but between-sample ages are also equivalent (within error) to the kimberlite emplacement age. Either these rocks are young, or more likely, isotopic equilibrium was maintained on the scale of their spatial separation in the upper mantle. In JJG144, however, an apparent clinopyroxene-garnet age is 440 m.a., compared to 115 m.a. for the kimberlite. The initial ¹⁴³Nd/¹⁴⁴Nd ratio of about .5110 is extremely low, particularly in view of relatively high

$^{87}\text{Sr}/^{86}\text{Sr} = .7043$. The eclogite (and/or the protolith) must have had a complex history, and indicates that preservation of upper mantle domains with isotopic character somewhat similar to that of peridotitic garnet inclusions in diamond (Richardson et al., 1984) need not necessarily require early encapsulation by diamond.

INCLUSIONS IN DIAMOND

Isotopic studies of silicate and sulphide inclusions in diamonds have convincingly demonstrated, with the possible exception of samples from the Premier kimberlite, that the inclusions and presumably the enclosing diamonds are much older than the host kimberlites (Kramers et al., 1979; Richardson et al., 1984). Typically small inclusion sizes and consequently low absolute trace element contents generally require that such work be performed on composite samples comprising tens to hundreds of diamonds. A potential problem with this approach is the possible presence of more than one inclusion population that may not be optically distinguishable (particularly in the case of sulphides). Through the efforts of De Beers Consolidated Mines, a collection of diamonds with uncharacteristically large inclusions has been assembled, and preliminary experiments on inclusions from a single diamond have proven successful.

A 2.3 carat yellow octahedral diamond from the Finsch kimberlite contained 35 eclogitic garnet inclusions with a total weight of 1.2 mg. The largest inclusion, about a cubic mm in size, is responsible for the greatest part of the sample weight. Inclusions were extracted by breaking the diamond in filtered air, and were rinsed with HCl prior to dissolution. Sm and Nd concentrations of 2.52 and 2.19 ppm respectively yield a high Sm/Nd ratio of 1.15 and consequently radiogenic Nd ($^{145}\text{Nd}/^{144}\text{Nd} = .51817 \pm 5$; 2 sigma error, small blank correction applied).

Assuming a single stage history and derivation from a chondritic reservoir, the model age is 1670 \pm 40 m.a. (Fig. 3; error from analytical uncertainties). If the parent reservoir is not chondritic, but still within the compositional limits of normal depleted or enriched upper mantle, the age calculation varies little because of the highly radiogenic Nd. The age, though much older than pipe emplacement (120 m.a.), is substantially younger than sulphide inclusions (greater than 2000 m.a.; Kramers, 1979) or peridotitic garnet inclusions (3300 m.a.; Richardson et al., 1984) in Finsch diamonds. It is thus not possible to relate in a single event formation of eclogitic and peridotitic inclusion suites represented by silicate samples analyzed to date. The sulphide inclusions analyzed by Kramers (1979) may represent an additional diamond forming event. The Proterozoic model age of the eclogitic garnet is similar to some of the older ages obtained in crustal rocks of the off-craton Namaqua and Bushmanland provinces, and it is tempting to speculate that eclogitic diamond inclusions of this age could represent upper mantle event(s) related to those crustal processes.

REFERENCES

- HATTON C.J. and GURNEY J.J. 1979. A diamond-graphite eclogite from the Roberts Victor Mine. In Boyd F.R. and Meyer H.O.A. eds, Proc. 2nd Int. Kimberlite Conf., Vol. 2, pp. 37-49. American Geophys. Union, Washington, D.C.
- KRAMERS J.D. 1979. Lead, uranium, strontium, potassium and rubidium in inclusion-bearing diamonds and mantle-derived xenoliths from southern Africa. *Earth Planet. Sci. Lett.* 42, 58-70.
- MACGREGOR I.D. and CARTER J.L. 1970. The chemistry of clinopyroxenes and garnets of eclogites and peridotite xenoliths from the Roberts Victor Mine, South Africa. *Phys. Earth Planet. Interiors* 3, 391-397.
- REID A.M., BROWN R.W., DAWSON J.B., WHITFIELD G.G. and SIEBERT J.C. 1976. Garnet and pyroxene compositions in some diamondiferous eclogites. *Contrib. Mineral. Petrol.* 58, 203-220.
- RICHARDSON S.H., GURNEY J.J., ERLANK A.J. and HARRIS J.W. 1984. Origin of diamonds in old enriched mantle. *Nature* 310, 198-202.
- ROBINSON D.N., GURNEY J.J. and SHEE S.R. 1984. Diamond eclogite and graphite eclogite xenoliths from Orapa, Botswana. In Kornprobst J. ed, Proc. 3rd Int. Kimberlite Conf., Vol. II, pp. 11-24. Elsevier, Amsterdam.
- SHEE S.R. and GURNEY J.J. 1979. The mineralogy of xenoliths from Orapa, Botswana. In Boyd F.R. and Meyer H.O.A. eds, Proc. 2nd Int. Kimberlite Conf., Vol. 2, pp. 37-49. American Geophys. Union, Washington, D.C.

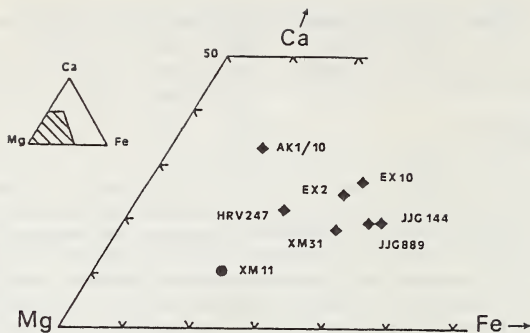


Figure 1. Garnet compositions in diamond eclogite.

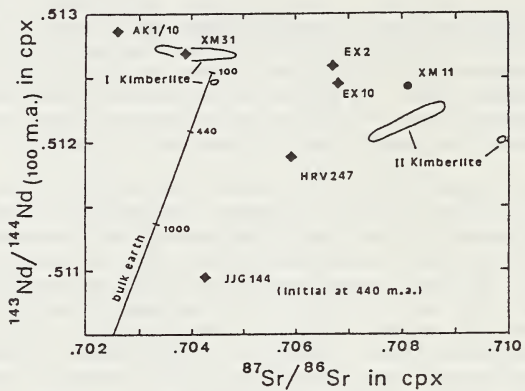


Figure 2. $^{87}\text{Sr}/^{86}\text{Sr}$ vs. initial $^{143}\text{Nd}/^{144}\text{Nd}$ in cpx from diamond eclogite.

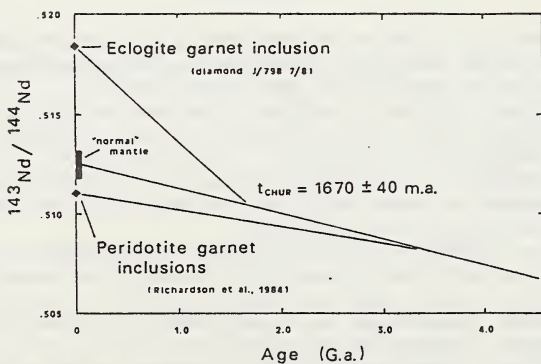


Figure 3. Model ages of Finsch diamond inclusions.

D. Smith¹ and F. R. Boyd²

1. Department of Geological Sciences, University of Texas, Austin, Texas, 78713
2. Geophysical Laboratory, Carnegie Institution of Washington, 2801 Upton Street, N. W., Washington, D.C., 2008, USA

The homogeneity of minerals in peridotite inclusions from kimberlites in southern Africa has been studied by high-precision electron probe analysis. Equilibration temperatures of the rocks examined span the range 710^o to 1460^oC. Most of the observed heterogeneities are attributable to one or more of the following processes: (1) metasomatism by an introduced fluid, in general probably a silicate melt; (2) mechanical mixing of phases from volumes with different mineral compositions; (3) changes in temperature and pressure prior to eruption. The observed heterogeneities provide keys not only to these processes but also to their timing. In rocks with calculated equilibration temperatures below 1100^oC, and in rocks with coarse textures regardless of equilibration temperature, heterogeneities commonly involve only Cr-Al zoning and related element variations in garnet; such Cr-Al variations are most apt to be responses to changes in temperature and pressure. More complex heterogeneities were analyzed in the inclusions with porphyroclastic textures and equilibration temperatures above 1100^oC; these are the rocks primarily considered here.

The most common heterogeneity detected in minerals of the high-temperature, sheared rocks is zoning in garnet; garnets have core-to-rim increases in Ti and decreases in Cr in more than half of such rocks examined (Table 1). Perhaps as common is rim enrichment in Na, and P, but it is more difficult to detect because absolute values are low. Garnets are zoned in Fe-Mg in 5 of the 13 samples. Well-developed Ti, Fe, and Cr gradients are illustrated in Figure 1. Such zoning has not yet been correlated with equilibration temperature, phase assemblage, or Fe enrichment in olivine. For instance, though garnet is apparently homogeneous in the rock studied with the highest equilibration temperature (1460^oC), other high-temperature rocks have garnet with pronounced zoning (Table 1 and Smith and Boyd, 1986). The steepest Ti and Cr gradients, essentially step changes, were observed in a rock (PHN2766/8, Table 1) with a relatively low calculated temperature (1100^oC) and magnesian olivine (Fa7). Pronounced zoning is present in garnets in both lherzolite (PHN1611) and garnetiferous dunite (FRB 450).

In each of three rocks, phases have heterogeneities in addition to zoning. In rock FRB76, for instance, two contiguous garnets, each with cross sections about 3 mm in diameter, have similar contents and gradients of Ti, Fe, and P but distinctly different core contents of Cr; the opposing gradients of Cr converge to a common value at the crystal rims (Fig. 1). The garnets appear first to have acquired distinct Cr contents in different environments, then to have been brought into proximity and rims equilibrated to a common composition and also enriched in Ti, Fe, and P. The hypothesis that garnets of contrasting compositions can be mixed together is supported by mineral associations in rock PHN 1611 (Table 1). In this rock, relatively magnesian and iron-rich volumes of peridotite are juxtaposed, apparently by deformation within tens of days of eruption of the host kimberlite (Smith and Boyd, 1986): garnets in the more magnesian volume are more chrome-rich.

Enrichment of Ti, Fe, P, and Na in garnet rims most plausibly is due to the introduction of these elements into the rocks by a fluid phase. Because most of the garnets with Ti zoning are in rocks with equilibration temperatures above 1100^oC, and because the extrapolated solidus temperature for peridotite in the presence of water and carbon dioxide is near 1100^oC at 40 kb (Olafsson and Eggler, 1983), the fluid probably was a silicate melt. Boullier and Nicolas (1973) noted that rocks appear to have been mixed together during deformation at the margins of some dikes in several crustal peridotite masses, and they hypothesized that mixtures of minerals might also occur in nodules with sheared textures. Textures of the porphyroclastic rocks may be related to the formation of conduits for erupting kimberlites (Mercier, 1979), and the metasomatism and mixing also may have occurred during conduit formation.

The high-temperature, porphyroclastic nodules may be samples of the asthenosphere, and hence understanding the evolution of the compositional contrast between these rocks and the lower-temperature, coarse nodules is important for models of mantle processes (e.g., Boyd, 1973; Nixon and Boyd, 1973). The higher-temperature rocks generally are distinctly more iron-rich than the nodules sampled from lower temperatures, as evidenced by olivine compositions and as summarized by Boyd (1986). Olivine compositions in peridotite are relatively insensitive to melt infiltration, due to the high modal abundance of the phase, its high magnesium plus iron content, and the melt-olivine distribution coefficients for Fe and Mg. Ti contents of garnets are more sensitive indicators of melt metasomatism. The metasomatism and mixing inferred from chemical heterogeneities in phases may have significantly increased the contents of Ti, Na, P, and some other elements in the high-temperature nodules; nonetheless, important compositional differences between the high and low-T suites, such as differences in Fe/Mg, probably predate the late-stage metasomatism and mixing.

REFERENCES

- BOYD F. R. 1973. A pyroxene geotherm. *Geochimica et Cosmochimica Acta* 37, 2533-2546.
- BOYD F. R. 1986. High- and low-temperature garnet peridotite xenoliths and their possible relation to the lithosphere-asthenosphere boundary. In Nixon P. H. ed, *Mantle Xenoliths*, Elsevier, in press.
- BOULLIER A. and NICOLAS A. 1973. Texture and fabric of peridotite nodules from kimberlite. In Nixon P. H. ed, *Lesotho Kimberlites*, pp. 57-66, Lesotho National Development Corporation, Maseru.
- MERCIER J.-C. C. 1979. Peridotite xenoliths and the dynamics of kimerlite intrusion. In Boyd F. R. and Meyer H. O. A. eds, *The Mantle Sample: Inclusions in Kimberlites and Other Volcanics*, pp. 197-212, American Geophysical Union.
- NIXON P. H. and BOYD F. R. 1973. Petrogenesis of the granular and sheared ultrabasic nodule suite in kimerlite. In Nixon P. H. ed, *Lesotho Kimberlites*, pp. 48-56, Lesotho National Development Corporation, Maseru.
- OLAFSSON M. and EGGLER D. H. 1983. Phase relations of amphibole, amphibole-carbonate, and phlogopite-carbonate peridotite: petrologic constraints on the asthenosphere. *Earth and Planetary Science Letters* 64, 305-315.
- SMITH D. and BOYD F. R. 1986. Compositional heterogeneities in a high-temperature herzolite nodule and implications for mantle processes. In Nixon P. H. ed, *Mantle Xenoliths*, Elsevier, in press.

TABLE 1: XENOLITHS WITH PORPHYROCLASTIC TEXTURES

T *	TiO ₂ garnet core-rim	Cr ₂ O ₃ garnet core-rim	% Fa olivine	Sample (Location)
1460	0.70	2.6	8.3	PHN 1596 (Thaba Putsoa)
1400 **	0.65 - 0.95	2.2 - 1.4	11.7 - 13.2	PHN 1611 (Thaba Putsoa)
1300	0.38 - 1.16	3.3 - 1.7	12	FRB 450 (Frank Smith)
1280 **	0.40 - 1.20	varied	9.2	FRB76 (Frank Smith)
1280	0.74	2.6	9.2	PHN 2001 (Mothae)
1220	0.43 - 0.63	6.1 - 5.8	7.5	PHN 2273 (Kao)
1220	0.44	3.2 - 2.8	9	FRB 1 (Monastery)
1220	0.24 - 0.52	6.6 - 6.0	9.6	PHN 4402 (Gibeon Townlands)
1200 **	0.21 - 0.25	varied	8.1	PHN 5555 (Abbotsford)
1100	0.25 - 0.60	7.2 - 4.5	7	PHN2766/8 (Bultfontein Floors)
990	0.04	6.65	7	PHN2766/4 (Bultfontein Floors)
970	0.02	4.85	7.5	FRB 351 (Bultfontein Floors)
940	0.02	4.54	7.4	JJG 1289 (Premier)

* Most temperatures are from two-pyroxene equilibria.

** These rocks preserve mineralogic evidence of mixing.

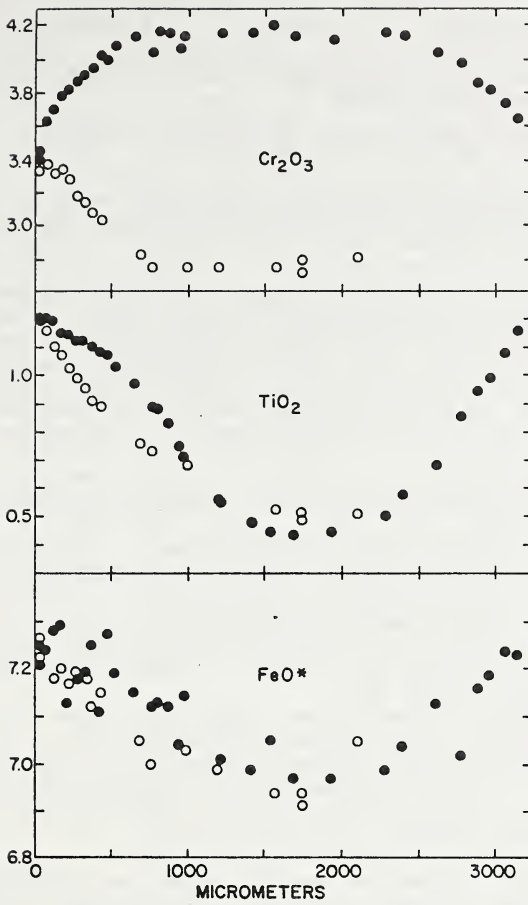


FIGURE 1: Compositional profiles for chrome, titania, and iron in two garnet crystals in rock FRB 76. In one cross section, the profile spans the diameter of a cross section (solid dots), while in the other crystal, the profile extends from interior to rim (open circles). The two crystals are close to one another in the fine-grained, olivine-rich matrix. Crystal rims are also enriched in phosphorus.

N.V.Sobolev¹, N.P.Pokhilenko¹, D.A.Carswell², A.S.Rodionov¹¹Institute of Geology and Geophysics, Siberian Division of the Academy of Sciences of the USSR, Novosibirsk, USSR²Department of Geology, Sheffield University, Sheffield, ENGLAND

The problem of origin of sheared lherzolite xenoliths (SLX) in kimberlites is one of the most important and disputable problems in the Upper Mantle petrology.

We have studied SLX collections from Udachnaya and Dalnaya Yakutian kimberlite pipes (Sobolev et al., 1984; Kharkiv et al., 1983). The SLXs as a rule are of oval, smoothed form, their sizes being ranged from the first cm to 57 cm along the long axis. All the studied SLXs belong to lherzolite paragenesis, ilmenite-bearing varieties often occur among them, chromite-bearing ones are more seldom. The texture of SLX rocks varies from fluidal-mosaic up to regular granular with subordinate development of mosaic areas.

The analysis of microprobe study results allows the following conclusions to be made:

1. SLX from both pipes are represented by two types
 - a) common sheared lherzolites with the range of equilibrium temperatures from 1150 to 1290 °C;
 - b) ilmenite-bearing SLX with lower temperatures of equilibrium (1080-1210 °C); the minerals of ilmenite-bearing SLX are enriched in iron on an average and contain a lower chromium admixture compared with common SLX.
2. Xenoliths of common granular lherzolites from both pipes are characterized by lower temperatures of equilibrium (890-1160 °C).
3. Some xenoliths with transitional textures between SLX and common granular rocks are discovered in both studied pipes. Compositional features of the minerals of these rocks are close to the minerals of SLX. Temperatures of equilibrium range within 1140 to 1260 °C.

Calculations of equilibrium parameters for SLX from the Udachnaya and Dalnaya pipes show that equilibrium points in P-T coordinates for CLX are between geotherms for heat flows in 40 and 50 mW/m²/s, being closer to the second geotherm, and refer to depths of 120-160 km, whereas equilibrium points of regular granular xenoliths from the same pipes occupy a position which is closer to or even lower sometimes than the geotherm for the flow in 40 mW/m²/s and are typical of depths of 70 to 170 km.

An important feature of SLX from Yakutian pipes is the presence of inhomogeneities of some types (Sobolev et al., 1984), the main ones being as follows:

- 1) zonality of garnets from the core to rim according to Cr₂O₃ content (maximum range of 8.5-1.1 wt% for common SLX and 6.4-0.9 wt% for ilmenite SLX); a conjugate increase in titanium content and iron content of garnet from the core to rim is noted;
- 2) a difference in compositions of clinopyroxenes from the ground mass of sheared lherzolites, the maximum range of variations being in magnitude of Ca/Ca+Mg ratios (43.7 - 41.3%, respectively) and Fe/Fe+Mg ratios (8.5 - 9.5%, respectively);
- 3) composition differences of minerals homogenous within a grain for different areas of SLX: a) garnets according to Cr₂O₃ contents (1.1 - 9.9 wt%), TiO₂ (1.12 - 1.61 wt%), FeO (8.47 - 10.6 wt%), a clear positive correlation being stated between chromium and titanium contents,

and negative one between iron and chromium contents; b) olivines according to iron contents from 9.1 to 12.4%.

When considering SXL genesis problems the main attention was paid to the specific character of their texture and especially to the depth nature of equilibrium. It permitted F.R.Boyd to connect their genesis with dynamic processes in the basement of moving platform plates. To our opinion, the mechanism of similar rock formation during intrusion of deep substance into upper levels in the form of diapirs is more real. It was shown that under conditions of upper mantle at temperatures more than 1100 °C coexisting minerals are reequilibrated rather quickly when changing P-T parameters. This feature strongly prevents from detection of traces of vertical displacement of deep rocks on the basis of mineralogical and petrological data. The data obtained can be related to changes of equilibrium P-T parameters resulted from vertical movements of mantle substance during the period immediately preceding to the kimberlite formation.

REFERENCES

- SOBOLEV N.V., POKHILENKO N.P., RODIONOV A.S. 1984. Inhomogeneities of the deep-seated inclusions in kimberlites as an indication of the processes of dynamic evolution in the upper mantle substance. Abstracts vol.5, 27th IGCC, Moscow, U.S.S.R., 399-401.
- KHARKIV A.D., POKHILENKO N.P., SOBOLEV N.V. 1982. Xenoliths of sheared lherzolites of large size from Udachnaya kimberlite pipe, Yakutia. (In Russian). Geology and Geophysics, No.1, 74-80.

SOLOVJEVA L.V.

Institute of the Earth's Crust, Siberian Branch of the USSR Ac.Sci.
Irkutsk, USSR

Several main types corresponding to certain stages of ancient metamorphic, magmatic and metasomatic processes, as well as more recent magmatic and metasomatic events, can be established in xenoliths from kimberlites of the Siberian platform among granular-types of ultrabasic nodules, presenting, according to majority of researches, mantle part of lithosphere (Sobolev, 1974; Dawson, 1980). The rocks suggesting ancient restite metamorphic origin are the most abundant among granular-type of xenoliths. These rocks are represented by spinel, spinel-garnet and garnet harzburgites, lherzolites. Sufficiently clear mineral orientation, sharp depletion of modal mineral composition in garnet (spinel) and clinopyroxene, impoverishment of bulk chemistry in basaltoid components are most specific to the above rocks. Large (1,5-4,0 cm) relict crystals of orthopyroxene with strongly deformed lamellar ingrowths of garnet (spinel) and clinopyroxene are occasionally found. Exsolution lamellae of these minerals would recrystallize into fine polygonal grains. The earlier stage of the rock existence evidently involved harzburgite restites (olivine+high-temperature orthopyroxene) subjected to cooling and intensive recrystallization with garnet (spinel) and clinopyroxene squeezing out to intergranular segregations. The shift of reaction in spinel-garnet paragenesis towards garnet formation after spinel is likely to indicate global cooling of the ancient mantle lithosphere subsequent to ancient crust formation.

Evidence of ancient premetamorphic magmatism has been established for rocks of pyroxenite-olivine-websterite serie. Large (2-15 cm) relict crystals of pyroxenes having laminar fabric (Fig.1) due to regularly aggregated plates of two pyroxenes, garnet or spinel lamellae allows their interpretation as exsolution texture in primary high temperature pyroxene. All the substitution stages of laminar pyroxenes by medium grain matrix of these oriented minerals+olivine are traced. The "hot" phase temperature obtained from calculated compositions of laminar pyroxenes ranges from 1260 to 1500°C (Fig.2). Garnet develops both around spinel lamellae in large crystals and around matrix spinel grain sometimes at the expense of matrix pyroxenes and those of laminar relict crystals (Fig.1). In scarce samples with contacts between lherzolites, harzburgites of restite type and websterites, pyroxenites both rocks being in contact are deformed and similar in composition of minerals which suggests the contact prior to the rock deformation and chemical equilibration of minerals at recrystallization. Differentiated pyroxenite-olivine websterite serie corresponds to peridotite and pyroxenite komatiites (Solovjeva, Vladimirov, 1984) in bulk chemistry and on the basis of P-T data occurs in all lithosphere. Yet hot orthopyroxene-olivine restites (Fig.3) were likely to be intruded by large magmatic chambers of protokomatiitic melts corresponding in general to Nisbet a. Walker LLLAMA model (1983) and ideas by Kirkley et al. (1984).

Mineral association with phlogopite, sulphides, apatite, graphite, amphibole and probably titanates of crichtonite series has been found in the rocks of harzburgite-lherzolite and websterite-pyroxenite series. It exhibits superposed character but texturally and chemically is equilibrated with main minerals. Apatite and graphite have been found in different samples of orthopyroxenites and websterites from "Udachnaya" pipe, where they together with phlogopite, garnet and clinopyroxene cement large exsolved crystals of pyroxenes. This stage of metasomatism in the lithospheric mantle is likely to follow its total cooling, entrainment into the crust or crystallization of protokomatiitic melts. This results in the lithosphere fragility allowing permeability by asthenospheric fluids of KREEP-type (Fig3). Three groups of rocks are conventionally allocated to more recent

postmetamorphic magmatites, basically, on the grounds of weak or no recrystallization evidence under stress conditions. Garnet lherzolites of probable magmatic type from Udachnaya pipe differ from those of restite type in such parameters as enrichment of rocks by garnet and clinopyroxene, cumulative banding, composition heterogeneity, presence of paragenetic phlogopite, more ferroginous composition of minerals, sulphide globules present, probably, former drops of sulphide liquid in siliceous one. High mag-



Fig.1. Curved plates of orthopyroxene(light) and clinopyroxene(grey) in lamellar crystal. Garnet(black) replaces orthopyroxene. X nicols, magn.30.

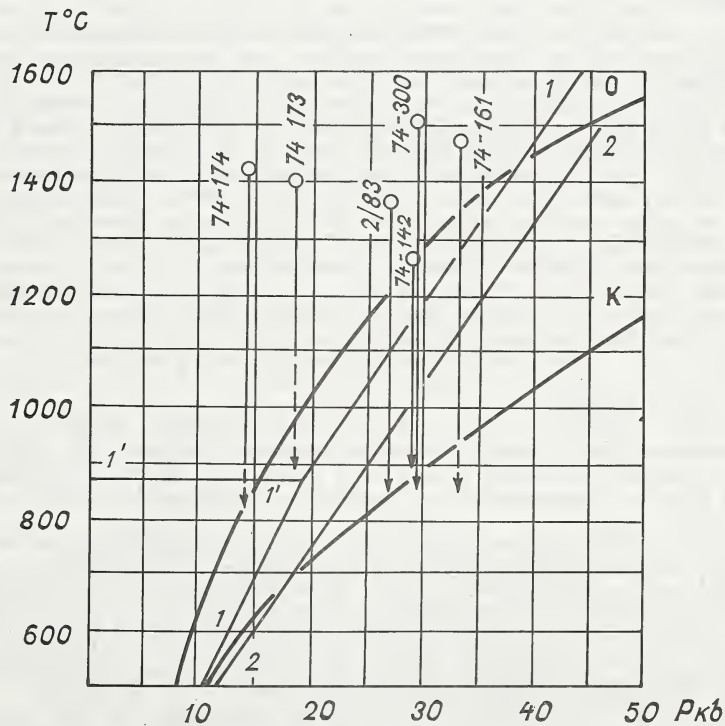


Fig.2. Evolution of large lamellar pyroxenes from pyroxenites, websterites from Obnazhennaya and Udachnaya pipes in P-T field. Circles - "hot" stage of homogeneous pyroxenes, arrows indicate decrease of temperature involving exsolution. O - oceanic geotherm; K - shield geotherm; I-I, I'-I', 2-2 - lines of spinel-garnet transitions (MacGregor, 1965; Ringwood, MacGregor, Boyd, 1964). Temperatures are estimated by pyroxene solvus (Davis & Boyd, 1966; Boyd & Nixon, 1975). Pressure - by Al_2O_3 isopleths (MacGregor, 1974).

nesian eclogite serie from the Mir pipe is also assumed to have magmatic origin. Samples with diamond, accessory phlogopite as well as those having porphyraceous texture (Solovjeva et al., 1980) are found among the above rocks. Rocks similar in bulk chemistry to some types of mica kimberlites (Solovjeva et al., 1984) presented by mica ilmenite and rutile pyroxenites can be considered as magmatic ones (Solovjeva et al., 1984). Metasomatism preceding protokimberlite formation likely associates with these magmatites.

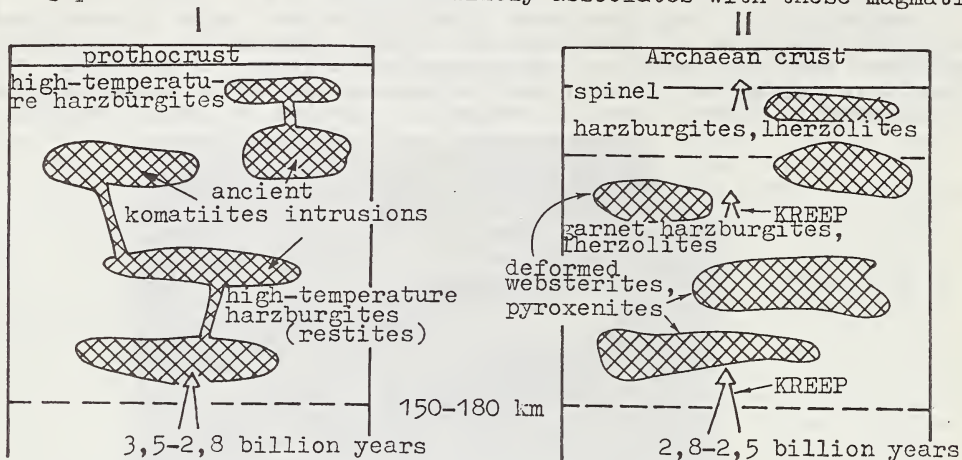


Fig.3. Evolution model of ancient lithospheric mantle. I - upper mantle extracted prothocrust is composed of "hot" harzburgite, intruded by komatiite melts. II - cooling and recrystallising lithospheric mantle becomes permeable for KREEP-type fluids.

References

- BOYD F.R. and NIXON P.H. 1975. Origins of the ultramafic nodules from some kimberlites of Northern Lesotho and the Monastery mine, South Africa. *Physics and Chemistry of the Earth* 9, 431-453.
- DAVIS B.T.C. and BOYD F.R. 1966. The join $Mg_2Si_2O_6$ - $CaMgSi_2O_6$ at 30 kilobars pressure and its applications to pyroxenes from kimberlites. *Journal of Geophysical Researches*, 1, # 14, 3567-3777.
- DAWSON J.B. 1980. Kimberlites and their xenoliths. Springer-Verlag, Berlin.
- KIRKLEY M.B., MCCALLUM M.E., EGGLER D.H. 1984. Coexisting garnet and spinel in upper mantle xenoliths from Colorado Wyoming kimberlites. In Kornprobst J. ed, *Kimberlites II: The mantle and crust-mantle relationships*, pp. 85-96. Elsevier, Amsterdam.
- MACGREGOR I.D. 1965. Stability fields of spinel and garnet peridotites in the synthetic system MgO - CaO - Al_2O_3 - SiO_2 . *Yearbook Carnegie Institute*, Washington, 64, 126-134.
- MACGREGOR I.D. 1974. The system MgO - Al_2O_3 - SiO_2 solubility of Al_2O_3 in enstatite for spinel and garnet peridotite system. *American Mineralogist* 59, 110-119.
- NISBET E.G., WALKER D. 1982. Komatiites and the structure of the Archaean mantle. *Earth and Planetary Science Letters* 60, 105-116.
- RINGWOOD A.E., MACGREGOR I.D., and BOYD F.R. 1964. Petrological constitution of the upper mantle. *Yearbook Carnegie Institute*, Washington, 63, 147-152.
- SOBOLEV N.V. 1974. Deep-seated inclusions in kimberlites and the problems of the upper mantle composition. Nauka, Novosibirsk.
- SOLOVJEVA L.V., VLADIMIROV B.M., BAGDASAROV E.A., VOLYANYUK N.Ya. 1980. The textures of clinopyroxene exsolution from porphyraceous eclogite from kimberlite pipe Mir. *Doklady Akademii Nauk SSSR*, 250, #3, 708-711.
- SOLOVJEVA L.V., VLADIMIROV B.M., ZAVYALOVA L.L., BARANKEVICH V.G. 1984. Deep-seated inclusions of a complex type from kimberlite pipe Udachnaya. *Doklady Akademii Nauk SSSR*, 277, # 2, 461-466.
- SOLOVJEVA L.V., VLADIMIROV B.M. 1984. Substance of the upper mantle beneath the Siberian platform. Abstracts for 27th International Geological Congress, V, 403.404. Moscow.

ULTRAMAFIC XENOLITHS FROM THE PALI-AIKE BASALTS: IMPLICATIONS FOR THE NATURE AND EVOLUTION OF THE SUBCONTINENTAL LITHOSPHERE BELOW SOUTHERN SOUTH AMERICA

Charles R. Stern, Kiyoto Futa, Sandra Saul, and Milka Alexandra Skewes

Department of Geological Sciences, University of Colorado, Boulder, CO 80309, U.S.A.

Type-I Cr-diopside ultramafic xenoliths found in the Pleistocene Pali-Aike alkali basalts, the southernmost units of the Patagonian plateau lavas of southern South America, include both garnet-free and garnet-bearing peridotites, the latter uncommon in alkali basalts (Skewes and Stern, 1979). Spinel occurs in both the garnet-free and the garnet-bearing xenoliths so that a division between spinel- and garnet-peridotite is not suitable for the Pali-Aike xenoliths. The xenoliths are lithologically diverse, consisting dominantly of lherzolites and harzburgites, but also including dunites and orthopyroxenites. All the Pali-Aike peridotites have coarse granular textures.

Olivine and orthopyroxene compositions in both garnet-free and garnet-bearing lherzolites are similar and range from between Fo_{90-87} and En_{87-85} . These minerals are more Mg-rich in garnet-free harzburgites, with olivine composition ranging between Fo_{92-90} and orthopyroxene compositions between En_{90-87} . In contrast, garnet-bearing harzburgites have more Fe-rich olivines, with compositions between Fo_{88-85} , and orthopyroxenes, with compositions between En_{85-83} . Garnet-orthopyroxenites, which typically occur as segregations within garnet-harzburgites, have even more Fe-rich orthopyroxenes, with compositions between En_{84-82} . Clinopyroxenes are Cr-diopsides. Garnets, which vary from 0-25 modal percent in lherzolites and harzburgites, and from 0-60 modal percent in orthopyroxenites, are Cr-pyropes with $Cr_2O_3=0.8-2.2$ weight percent. Cr contents are higher in garnets in lherzolites compared to either harzburgites or orthopyroxenites. Spinel compositions range from low Cr/high Al types to high Cr/low Al chromites. Garnet-bearing xenoliths contain only the latter type, but garnet-free xenoliths may contain either type but not both together. Mineral geothermometry indicates that the low Cr/high Al spinels occur in lower temperature xenoliths and the high Cr/low Al chromites occur in higher temperature xenoliths.

Pargasitic amphibole, with $K_2O=0.9-1.4$, $TiO_2=1.8-2.4$, and $Cr_2O_3=1.4-1.7$ weight percent, occurs as between 0-5 modal percent of unzoned grains equidimensional to other mineral grains in garnet-lherzolites. Phlogopite occurs as both disseminated grains and in veins. Disseminated phlogopite is pale in color and contains significant $Cr_2O_3=2.2$ weight percent, but little $TiO_2=0.6$ weight percent. Phlogopite in veins, occasionally with ilmenite, is dark orange due to high $TiO_2=5.3-7.0$ weight percent.

Bulk-rock chemistry of the xenoliths reflects mineral compositions. The garnet-lherzolites are fertile, having SiO_2 , TiO_2 , Al_2O_3 , FeO , MgO , and CaO similar to estimates of 'pyrolite'. However, K_2O is very low in all xenoliths except those cut by phlogopite veins. Harzburgites are infertile, with very low TiO_2 and Na_2O as well as K_2O , but garnet-bearing harzburgites have higher FeO , Al_2O_3 , and CaO than garnet-free harzburgites.

Temperatures of equilibration, determined using the two-pyroxene geothermometer of Wells (1977), range from 830-1080°C for garnet-free peridotites and from 1000-1150°C for garnet-bearing peridotites. With these temperatures, pressures of equilibration of garnet-bearing xenoliths determined with the geobarometer of Nickel and Green (1985) range from 18-24 kilobars, consistent with the stability of amphibole in some of these xenoliths. The coarse granular textures of the xenoliths, combined with these estimates of their pressure and temperature of equilibration, indicate that they were all derived from the continental lithosphere above the zone of generation of their alkali basalt host. The calculated temperature of 1150°C at a depth of 75 kilometers and the calculated geotherm of 10°C/km between 60-80 kilometers depth are higher than those determined from xenoliths suites found in cratonic regions of low heat flow, which is considered appropriate for the tectonically active area of back-arc magmatic activity in which the Pali-Aike basalts occur. Recrystallized-grain-size paleopiezometry has been used to estimate the differential stress levels for the mantle source of these xenoliths and this stress profile is similar in character to that determined for other continental extension zones (Douglas et al., 1985).

The data indicate that the upper part of the subcontinental lithosphere below southernmost South America consists dominantly of infertile garnet-free harzburgites at depths shallower than about 50 kilometers. At greater depths, between 50-70 km, fertile garnet-lherzolites occur along with infertile Mg-rich garnet-free harzburgites. The coexistence of these two lithologies is confirmed by their occurrence as compound xenoliths. Garnet-lherzolites dominate, and Mg-rich garnet-free harzburgites are absent from the deepest portion of the subcontinental lithosphere represented by the Pali-Aike xenoliths, at depths greater than 70 km. Infertile but Fe-rich garnet-harzburgites and orthopyroxenites also occur within the deeper portions of the lithosphere, at depths greater than 50 kilometers, and this part of the subcontinental lithosphere has been affected by modal metasomatism responsible for the emplacement of disseminated and vein phlogopite.

The Sr and Nd isotopic compositions of the fertile garnet-lherzolites range from $^{87}\text{Sr}/^{86}\text{Sr}=0.7027-0.7032$ and $^{143}\text{Nd}/^{144}\text{Nd}=0.5131-0.5128$, the lower Sr and higher Nd isotopic values being similar to mid-ocean ridge basalts. The isotopic compositions of the infertile garnet-free harzburgites range from $^{87}\text{Sr}/^{86}\text{Sr}=0.7034-0.7043$ and $^{143}\text{Nd}/^{144}\text{Nd}=0.5129-0.5127$ and these values are similar to ocean island basalts. Although all the xenoliths have isotopic compositions indicating time integrated depletion, compared to undifferentiated Bulk Earth, of Rb relative to Sr and Nd relative to Sm, their current $^{147}\text{Sm}/^{144}\text{Nd}$ ratios are similar to or less than Bulk Earth and range from 0.23-0.19 for the garnet-lherzolites and 0.16-0.13 for the garnet-free harzburgites. Vein phlogopite has $^{147}\text{Sm}/^{144}\text{Nd}=0.125$ and $^{143}\text{Nd}/^{144}\text{Nd}=0.51255$, but plots on the low $^{87}\text{Sr}/^{86}\text{Sr}$ side of the mantle array, with $^{87}\text{Sr}/^{86}\text{Sr}=0.7035$ despite having a very high Rb/Sr=3.

The lack of any phases with Sr and Nd isotopic compositions suggesting ancient enrichment events, such as have been reported from xenoliths derived from the Precambrian cratonic regions of Africa (Cohen et al., 1984), suggests that the accretion of the lithosphere below southern South America was a relatively recent event, consistent with the Phanerozoic age of the crustal rocks in this region (de Wit, 1977). The isotopic similarity of the Pali-Aike peridotites with oceanic basalts suggests that prior to being removed from large scale convective overturn and stabilized below the continental crust during the Phanerozoic this material was evolving along with the current suboceanic mantle system. It is probable that the formation of the main lithologic diversity observed in the Pali-Aike xenoliths took place during this pre-accretionary phase by heterogeneous removal of magma below an oceanic spreading center resulting in fertile unmelted garnet-lherzolites being mixed with infertile Mg-rich crystal residues. Fe-rich garnet-harzburgites and orthopyroxenites may be recrystallized crystal cumulates formed in magma conduits during this event.

A feature of the xenoliths that developed after this material had been stabilized below the continental crust is the observed decoupling of trace element composition and isotopic ratios. In those xenoliths in which no amphibole or phlogopite is observed, this effect may be explained by 'mantle metasomatism' which introduces large-ion-lithophile element enriched fluids into the mantle without modifying its mineralogy. This non-modal enrichment of the subcontinental mantle may be related to the modal metasomatism responsible for the emplacement of phlogopite veins, with disseminated phlogopite representing an intermediate stage of recrystallization and dispersal of such veins.

The emplacement of phlogopite veins apparently occurred only shortly before the xenoliths were transported to the surface in the Pali-Aike basalts, as indicated by their high Rb/Sr ratios and low $^{87}\text{Sr}/^{86}\text{Sr}$. These phlogopites are isotopically very distinct from the Pali-Aike basalts, but the isotopic composition of the basalts lie along a mixing curve for phlogopite + garnet-lherzolite. Modal metasomatism of the subjacent mantle may have been a precursor for the generation of the alkali basalts themselves. The isotopic composition of the phlogopites is similar to mixtures of oceanic basalts and sediments and the material responsible for the emplacement of these veins may have been derived by dehydration of subducted oceanic lithosphere. A great deal of ocean lithosphere has been subducted beneath the western margin of South America during the Phanerozoic and fluids derived by dehydration of this subducted material may rise continually through the asthenosphere into the overlying

subcontinental lithosphere or be emplaced only during episodes of low angle subduction such as may have occurred below southern South America just after the subduction of the Chile Rise in the Miocene.

References

- Cohen, R.S., O'Nions, R.K., and Dawson, J.B. 1984. Isotope geochemistry of xenoliths from East Africa: implications for the development of mantle reservoirs and their interaction. *Earth and Planetary Science Letters* 68, 209-220.
- De Wit, M.J. 1977. The evolution of the Scotia arc as the key to the reconstruction of Gondwanaland. *Tectonophysics* 37, 53-81.
- Douglas, B.J., Saul, S., Stern, C.R. 1985. Use of recrystallized grain size paleopiezometers to infer the state of stress in the mantle beneath southernmost South America. *EOS, Transactions of the American Geophysical Union* 66, 378.
- Nickel, K.G., and Green, D.H. 1985. Empirical geothermobarometry for garnet lherzolites and implications for the nature of the lithosphere, diamonds, and kimberlite. *Earth and Planetary Science Letters* 73, 158-170.
- Skewes, M.A., and Stern, C.R. 1979. Petrology and geochemistry of alkali basalts and ultramafic inclusions from the Pali-Aike volcanic field in southern Chile and the origin of the Patagonian plateau lavas. *Journal of Volcanology and Geothermal Research* 6, 3-25.
- Wells, P.R.A. 1977. Pyroxene thermometry in simple and complex systems. *Contributions to Mineralogy and Petrology* 62, 129-139.

S-S. Sun¹, A.L. Jaques¹, and M.T. McCulloch²

1. Bureau of Mineral Resources, GPO Box 378, Canberra, ACT, 2601.
2. Research School of Earth Sciences, Australian National University, PO Box 4, Canberra, ACT, 2600, Australia.

Previous studies of the isotopic characteristics of the Miocene olivine and leucite lamproites of the Fitzroy area of the West Kimberley have demonstrated the existence of ancient (>2000 Ma) mantle sources beneath the southwestern margin of the Kimberley Block (McCulloch et al., 1983; Fraser et al., 1985; Nelson et al., 1986). In this paper we report Sr and Nd isotopic data on a various suites of basic to ultrabasic intrusions ranging in age from early Proterozoic (~1900 Ma) to Miocene (20 Ma) from different parts of the Kimberley to assess the extent and timing of enrichment processes of the subcontinental lithosphere.

The Kimberley Block of Western Australia is bounded by the Halls Creek and King Leopold Mobile Zones which consist of early Proterozoic eugeo-synclinal sediments and volcanics which have been folded and metamorphosed to comparatively high grade, and intruded by granites and basic and ultrabasic rocks. Early to middle Proterozoic platform cover clastic sediments of the Kimberley Basin partly overlie the 1920-1815 Ma basement rocks of the mobile belts and elsewhere are presumed to be underlain by Archaean basement.

EARLY PROTEROZOIC MAFIC-ULTRAMAFIC ROCKS IN THE HALLS CREEK MOBILE ZONE

LREE-depleted, MORB-type Woodward Dolerite has initial $\epsilon_{Nd} = +5$ falling on the growth curve of the depleted convecting mantle. In contrast, LREE-enriched basalts and basic intrusives of the Hart Dolerite and Lamboo Complex showing depletion of Nb and Ti have $\epsilon_{Nd} = 0$ to -2 . These suites may be derived by either melting of ancient enriched mantle or interaction of magma derived from depleted convecting mantle with Archaean crust and/or lithosphere. Significantly, both imply the existence of Archaean crust and lithosphere in this area.

MID-PROTEROZOIC ARGYLE (AK1) LAMPROITES

The richly diamondiferous Argyle lamproite pipe (Atkinson et al., 1984) intrudes the mid-Proterozoic sediments of the Halls Creek Mobile Zone. The pipe is composed of three main lithologies: largely vitric, essentially monogenetic lapilli tuffs (NST = "non-sandy tuffs"); polygenetic lapilli ash tuffs and ash tuffs (ST = "sandy tuffs") with abundant accidental quartz; and olivine (-phlogopite) lamproite dykes (OPLD).

An emplacement age of 1178 Ma is estimated for the Argyle pipe by a Rb-Sr mineral isochron defined by phlogopite and the heavy mineral fraction (dominated by apatite) from an OPLD sample. The phlogopite has $^{87}\text{Sr}/^{86}\text{Sr} = 0.92114 \pm 6$ and $^{87}\text{Sr}/^{86}\text{Sr} = 12.701$. The heavy mineral fraction has $^{87}\text{Sr}/^{86}\text{Sr} = 0.70645 \pm 6$ and $^{87}\text{Rb}/^{86}\text{Sr} = 0.0114$. The sample has $^{87}\text{Sr}/^{86}\text{Sr}$ and ϵ_{Nd} initial ratios of 0.7063 and -5.3 respectively at 1178 Ma. Whole rock Rb-Sr isotope data of OPLD and clasts from "sandy-tuffs" are consistent with this age of 1178 Ma; whereas "non-sandy tuffs" of AK1 pipe give younger Rb/Sr ages which suggest a younger disturbance.

NST samples have ϵ_{Nd} values -3.6 to -4.0 at 1178 Ma consistently higher than ϵ_{Nd} values obtained for the OPLD (-4.6 to -5.3). One clast from a ST analyzed has an ϵ_{Nd} value similar to that of the OPLD. Nd isotope data suggest that OPLD and NST were derived from slightly different mantle sources or by a different magma generation processes such as different degree of partial melting and varying degrees of wall rock reaction. Sm-Nd model calculation suggest that these lamproites were derived from enriched mantle sources of probably early proterozoic or possibly late Archaean age.

LATE PROTEROZOIC CUMMINS RANGE CARBONATITE

The Cummins Range carbonatite (Andrew et al, this volume) is located some 350 km SW of Argyle at the intersection of the Halls Creek Mobile Zone and King Leopard Mobile Zone. A Rb-Sr mineral isochron based on an apatite-phlogopite pair gives an

age of 905 ± 2 Ma. Carbonatite samples analyzed have low but variable $^{87}\text{Sr}/^{86}\text{Sr}$ initial ratios ranging from 0.7028 to 0.7032 suggesting crustal contamination may be responsible as inferred from other studies of carbonatite intrusives. The three samples studied have similar ϵNd initial ratios (+1.6 to 2.4). These Nd and Sr isotope initial ratios are typical of carbonatites of world-wide occurrences and suggest that Cummins Range carbonatite is likely to be derived from ocean island basalt (OIB) type source originated from within the depleted convecting mantle.

LATE PROTEROZOIC MICACEOUS LAMPROPHYRE DYKES OF BOW HILL

Bow Hill lamprophyre dyke swarm (Atkinson et al., 1984; Fielding and Jaques, this volume) is located some 22 km west of the Argyle pipe. Preliminary Rb/Sr and Sr isotope data of whole rock samples with $^{87}\text{Sr}/^{86}\text{Sr}$ initial ratio (0.7057) defined by a clinopyroxene give an age of 900 Ma. Four Bow Hill samples analyzed have ϵNd initial ratios about +2.0. Similar to Cummins Range carbonatite.

MIOCENE (20 Ma) LAMPROITES OF THE WEST KIMBERLEY REGION

Lamproites from this region show a large range of variation in ϵNd and $^{87}\text{Sr}/^{86}\text{Sr}$ initial ratios: ϵNd from -7.4 to -18.9 and $^{87}\text{Sr}/^{86}\text{Sr}$ from 0.7104 to 0.7208 (McCulloch et al., 1983; Fraser et al., 1985; this study). On the ϵNd versus $^{87}\text{Sr}/^{86}\text{Sr}$ plot, olivine lamproites, chemically similar to micaceous kimberlites, define a field of ϵNd (-7.4 to -13.8) and $^{87}\text{Sr}/^{86}\text{Sr}$ initial ratios (0.7104 to 0.7123) which is distinct from the leucite lamproites ($\epsilon\text{Nd} = -10.2$ to -18.9 and $^{87}\text{Sr}/^{86}\text{Sr} = 0.7123$ to 0.7208). At the same ϵNd value leucite lamproites have higher $^{87}\text{Sr}/^{86}\text{Sr}$ initial ratios. Such difference could be interpreted in terms of mixing of two mantle components - mixture of enriched and depleted components within the non-convective lithosphere (e.g., McCulloch et al., 1983; Jaques et al., 1984) or mixing of the enriched lithosphere with the relatively depleted convecting mantle. In either model the olivine lamproites contain a larger amount of material from the depleted convecting mantle. Only minor isotopic heterogeneity was observed among samples from individual pipes except at Ellendale 7 where olivine lamproites ($\epsilon\text{Nd} = -7.6$ and $^{87}\text{Sr}/^{86}\text{Sr} = 0.7104$) and leucite lamproites ($\epsilon\text{Nd} = -15.4$ and $^{87}\text{Sr}/^{86}\text{Sr} = 0.7168$) occur in the same pipe.

DISCUSSION

The oldest exposed rock in the Kimberley Block is of early Proterozoic age (about 2000 Ma). However, Nd isotope data of Early Proterozoic mafic-ultramafic volcanics and clastic sediments from the Halls Creek Mobile Zone suggest the existence of Archaean continental crust and lithosphere in this region.

Chemical data of lamproites from Argyle and west Kimberley (Jaques et al., 1984; and this volume) suggest that these lamproites were derived from a strongly depleted refractory mantle source (poor in Al, Ca, Na, V, Y and Sc) which was subsequently enriched in incompatible elements.

Modelling of Sr, Nd and Pb isotope data of Miocene lamproites from west Kimberley (Fraser et al., 1985; Nelson et al., 1986) suggest that they were derived from ancient (>2000 Ma) enriched mantle sources or at least contained an ancient enriched component.

Calculation of the Sm-Nd evolutionary trajectories of the source regions for the Miocene lamproites at 1178 Ma (the age of the Argyle pipe) gives ϵNd (1178 Ma) values about +2 for the olivine lamproites with relatively high ϵNd (-7.8 at 20 Ma); whereas most other olivine and leucite lamproites ($\epsilon\text{Nd} = -12$ to -15 at 20 Ma) give ϵNd (1178 Ma) values of -3 to -5. These latter values are similar to the initial ratios of AK1 lamproites at that time, consequently mantle sources for lamproites of different ages from east and west Kimberley could have been formed at about the same time and by similar processes. Combined chemical and isotopic data of these lamproites can be best explained by reactivation of the enriched but formerly refractory continental lithosphere formed during early pre-cambrian.

The fundamentally different isotopic characters observed in the Cummins Range carbonatite and Bow Hill dykes of late Proterozoic ages indicate distinctly different magma sources to the lamproite magmas. Carbonatites are generally associated with

lithospheric rifting which could have lead to tapping of deeper convecting mantle as major magma sources.

In conclusion, we consider that the Kimberley craton has developed a thick refractory lithosphere in the early pre-cambrian following extensive subalkaline magma extraction. The timing of the initial enrichment of the subcontinental lithosphere since late Archaean is not well constrained, but it could be partly related to the rifting and magmatism associated with the formation of the early proterozoic Halls Creek Mobile Zone. Subsequent alkaline magmas represent small volume melts extracted from zones of enrichment in this refractory lithosphere at depth of diamond stability (lamproites) or result from direct input from the convecting mantle (carbonatites and Bow Hill lamprophyre). Enrichment of the lithosphere may be due to a number of processes including lithosphere subduction and/or mantle metasomatism and could have resulted from discreet events(s) or continuous processes since the Archaean.

ACKNOWLEDGEMENTS

We thank CRAE Pty Ltd and particularly C.B. Smith for samples used and interest in this study. S-S Sun and A.L. Jaques published with the permission of the Director, Bureau of Mineral Resources.

REFERENCES

- ATKINSON W.J., HUGHES F.E. and SMITH C.B. 1984. A review of the kimberlitic rocks of Western Australia. In Kronprobst J. ed., Kimberlites and Related Rocks, pp. 195-224.
- FRASER K.J., HAWKESWORTH C.J., ERLANK A.J., MITCHELL R.H. and SCOTT-SMITH B.H. 1985. Sr, Nd and Pb isotope and minor element geochemistry of lamproites and Kimberlites. Earth and Planetary Science Letters 76, 57-70.
- JAQUES A.L., LEWIS, J.D., SMITH C.B., GREGORY G.P., FERGUSON J., CHAPPELL B.W. and McCULLOCH M.T. 1984. The diamond-bearing ultrapotassic (lamproitic) rocks of the West Kimberley region, Western Australia. In Kronprobst J. ed., Kimberlites and Related Rocks, pp. 225-254.
- McCULLOCH M.T., JAQUES, A.L., NELSON D.R., and LEWIS J.D. 1983. Nd and Sr isotopes in Kimberlites and lamproites from Western Australia: an enriched mantle origin. Nature 302, 400-403.
- NELSON D.R., McCULLOCH M.T., and SUN S-S, 1986. The origins of ultrapotassic rocks as inferred from Sr, Nd and Pb isotopes. Geochimica Cosmochimica Acta 50, 231-246.

THE SOLUBILITY AND DIFFUSIVITY OF CARBON IN OLIVINE:
IMPLICATIONS FOR CARBON IN THE EARTH'S UPPER MANTLE

T. N. Tingle, H. W. Green, and A. A. Finnerty

Department of Geology, University of California, Davis, CA 95616 USA

Abundant evidence exists for the presence of carbon in the earth's upper mantle. The amount of C, the C-bearing phases extant and their distribution, and the effect of trace quantities of C on the physical properties of the mantle remain largely known. Voluminous CO₂ emissions from volcanoes (Barnes et al., 1978) and mid-ocean ridge basalts (Pineau and Javoy, 1983) bear mantle C isotopic signatures and thus indicate a present-day mantle C source. CO₂ inclusions in xenolith minerals (Roedder, 1965) are interpreted as CO₂ evolved from the magma during transport to the surface. Diamonds and graphite in kimberlite and peridotite xenoliths are further proof of C in the mantle, although radiometric ages on diamond inclusions > 3 Ga (Richardson et al., 1984) argue against these minerals as the present-day C source. The paucity of carbonate in mantle xenoliths contrasts with phase equilibrium studies indicating that carbonates, and not CO₂, should be stable in a peridotite mineralogy (Newton and Sharp, 1975; Egglar et al., 1979). Intrinsic oxygen fugacity measurements on mantle minerals indicate that the mantle is generally not reducing enough to stabilize CH₄ (Sato, 1984). Mathez et al. (1984) analyzed 15-100 ppm C in mantle peridotites from kimberlites and alkali basalts which they interpreted as CO₂ inclusions and condensed C on grain boundaries and cracks.

Olivine in some harzburgite and lherzolite nodules from South Africa contains abundant co-precipitates of a fluid phase and spinel (Green and Guegen, 1983). The volume fraction of bubbles (<0.1 μ) corresponds to a few hundred ppm CO₂, assuming the fluid is CO₂ and has a specific gravity of 1. The bubble precipitates contain an amorphous surface film and electron energy loss spectroscopy showed C associated with the sub-grain boundaries containing these bubbles (H.W.G. and P.J. Vaughan, unpublished data). Infrared spectroscopy (IR) on these crystals and fracture of the crystals under water indicate that these bubbles are now empty (R. Borch and H.W.G., unpublished data); IR did show some water-related species (Mackwell et al., 1985; Miller and Rossman, 1985) corresponding to a few ppm hydrogen. These observations indicate that the volatile species originally dissolved in the crystals contained C, and perhaps H. The decrease in the solubility of these species with decreasing pressure presumably led to the precipitation of fluid during ascent.

Freund and coworkers (Freund et al., 1980; Oberheuser et al, 1983; Knobel and Freund, 1986) claim C exists in solid solution in olivine from the mantle and further that the C species is highly mobile at low temperatures (<800 °K). In contrast, Mathez et al. (1986) also have analyzed C in mantle olivines using the same nuclear reaction technique as Oberheuser et al. (1983) and Knobel and Freund (1986) and find no C.

To pursue the significance of C dissolution in olivine, we have initiated an experimental program in which single crystals of San Carlos olivine are sealed in platinum capsules with ¹⁴C-labelled silver oxalate (CO₂) and oxalic acid (CO₂-H₂O). The specimens are then annealed at 0.1 GPa in an internally heated gas apparatus or at 3.0 GPa in a solid medium apparatus at temperatures from 1200-1600 °C. Carbon concentrations are determined by the beta track method (Tingle, 1986; Mysen and Seitz, 1975). After 100 hrs. at 1175 °C and 0.1 GPa, no C was observed in crystals exposed to either CO₂ or CO₂-H₂O, indicating that at low pressure, the solubility or the diffusivity of C in olivine is very low. At 3.0 GPa, the inferred solubility from experiments on coarse-grained powders using CO₂-H₂O is 100-150 wt. ppm C independent of temperature within experimental error. At 3.0 GPa and 1200 °C, C concentration gradients extending from the surfaces into the interiors of single crystals exposed to CO₂-H₂O for 2 and 14 days yield diffusivities of 10^{-8-10⁻⁹} mm²/sec. A single crystal exposed to pure CO₂ for 2 days at 1200 °C and 3.0 GPa showed no C uptake (D < 10⁻¹⁰ mm²/sec), indicating that either H₂O catalyzes the incorporation of C into the crystals or that the presence of elemental C is required for diffusion of C into the crystals (elemental C in the CO₂-H₂O experiments is

thought to be a consequence of hydrogen diffusion between the BN sample assembly and the capsule contents).

These experiments on C solubility and diffusion in olivine are consistent with observations on natural rocks in several respects. 1) Solubilities greater than 100 wt. ppm C are in rough agreement with deductions from mantle xenoliths (Green and Guegen, 1983). 2) The apparent insolubility of C in olivine at low pressure confirms the pressure dependence of the solubility (Green and Guegen, 1983). 3) High diffusivities of C and H in olivine predict that analyses of mantle-derived olivines will underestimate their concentrations in the mantle. Condensed C on grain boundaries and cracks (e.g. Mathez et al., 1984) may represent C dissolved in the crystals that exsolved during diapiric uprise in the mantle and eruption. 4) The significant solubility of both C and H in olivine establishes that the nominally volatile-free silicates of the mantle potentially constitute a large reservoir for fluids. This would explain the origin of present-day C associated with volcanism and resolve the paradox that the absence of carbonate in mantle xenoliths presents without excluding the possibility that carbonate minerals may exist in the mantle.

C diffusivities of 10^{-9} mm²/sec are similar to Fe-Mg interdiffusivities in olivine at 1200 °C reported by Buening and Buseck (1973). These diffusivities are rapid in their geologic context, but they contrast with the high mobilities attributed to solute C by Knobel and Freund (1986) who claim C can diffuse from the bulk to the surface of olivine crystals even at room temperature. Crystals of San Carlos olivine have been exposed to a thin film of ¹⁴C-bearing graphite (vapor-deposited) for two years at room temperature. If natural olivine contains C and this C species has a high mobility, as Oberheuser et al. (1983) and Knobel and Freund (1986) claim, then ¹⁴C atoms at the surface should mix spontaneously with "solute" C atoms producing ¹⁴C profiles into the crystals. Our failure to observe such profiles indicates that C is not mobile at room temperature and pressure in olivine.

REFERENCES

- BARNES, I., IRWIN, W.P. and WHITE, D.E. 1978. Global distribution of carbon dioxide discharges and major zones of seismicity. *U.S. Geol. Surv. Water Resour. Invest. Open-file Rep.* 78-39.
- BUENING, D.K and BUSECK, P.R. 1973. Fe-Mg lattice diffusion in olivine. *Jour. Geophys. Res.* 78, 6852-6862.
- EGGLER, D.H., KUSHIRO, I. and HOLLOWAY, J.R. 1979. Free energies of decarbonation reactions at mantle pressures: I. Stability of the assemblage forsterite-enstatite-magnesite in the system MgO-SiO₂-CO₂-H₂O to 60 kbar. *Amer. Mineral.* 64, 288-293.
- FREUND, F., KATHREIN, H., WENGLER, H., KNOBEL, R. and HEINEN, H. J. 1980. Carbon in solid solution in forsterite - a key to the untractable nature of reduced carbon in terrestrial and cosmogenic rocks. *Geochim. Cosmochim. Acta* 44, 1319-1333.
- GREEN, H.W., II and GUEGEN, Y. 1983. Deformation of peridotite in the mantle and extraction by kimberlite: A case history documented by fluid and solid precipitates in olivine. *Tectonophysics* 92, 71-92.
- KNOBEL, R. and FREUND, F. 1986. Carbon in mantle-derived olivine: A nuclear reaction study (submitted to *Jour. Geophys. Res.*).
- MACHWELL, S.J., KOHLSTEDT, D.L. and PATERSON, M.S. 1985. The role of water in the deformation of olivine single crystals. *Jour. Geophys. Res.* 90, 11,319-11,333.
- MATHEZ, E.A., DIETRICH, V.J. and IRVING, A.J. 1984. The geochemistry of carbon in mantle peridotites. *Geochim. Cosmochim. Acta* 48, 1849-1859.

- MATHEZ, E.A., BLACIC, J.D., BERRY, J. MAGGIORE, C. and HOLLANDER, M. 1986. Carbon in olivine: Results from nuclear reaction analysis (submitted to **Jour. Geophys. Res.**).
- MILLER, G.H. and ROSSMAN, G.R. 1985. The natural occurrence of hydrogen in olivine. **EOS** 66, 1135 (abstr.).
- MYSEN, B.O. and SEITZ, M.G. 1975. Trace element partitioning determined by beta track mapping: An experimental study using carbon and samarium as examples. **Jour. Geophys. Res.** 80, 2627-2635.
- NEWTON, R.C. and SHARP, W.E. 1975. Stability of forsterite + CO₂ and its bearing on the role of CO₂ in the mantle. **Earth Planet. Sci. Letters** 6, 239-244.
- OBERHEUSER, G., KATHREIN, H., DEMORTIER, G., GONSKA, H. and FREUND, F. 1983. Carbon in olivine single crystals analyzed by the ¹²C(d,p)¹³C method and by photoelectron spectroscopy. **Geochim. Cosmochim. Acta** 47, 1117-1129.
- PINEAU, F. and JAVOY, M. 1983. Carbon isotopes and concentrations in mid-ocean ridge basalts. **Earth Planet. Sci. Letters** 62, 239-257.
- RICHARDSON, S.H., GURNEY, J.J., ERLANK, A.J. and HARRIS, J.W. 1984. Origin of diamonds in old enriched mantle. **Nature** 310, 198-202.
- ROEDDER, E. 1965. Liquid CO₂ inclusions in olivine-bearing nodules and phenocrysts in basalts. **Amer. Mineral.** 50, 1746-1786.
- SATO, M. 1984. The oxidation state of the upper mantle: Thermochemical modeling and experimental evidence. **Proc. 27th Inter. Geol. Cong.** 11, 405-433.
- TINGLE, T.N. 1986. An evaluation of the carbon-14 beta track technique (submitted to **Geochim. Cosmochim. Acta**).

**A SUGGESTED ORIGIN OF MARID NODULES IN KIMBERLITES BY HIGH PRESSURE
CRYSTALLIZATION OF LAMPROITIC MAGMA.**

Frances G. Waters

Department of Geochemistry, University of Cape Town, Rondebosch,
Cape 7700, South Africa.

Chemical, mineralogical and isotopic studies have been made on the nodules of the MARID (Mica-Amphibole-Rutile-Ilmenite-Diopside) suite in southern African kimberlites. Dawson and Smith (1977) proposed that MARID rocks represent crystallization products of magmas in the higher parts of the upper mantle. With the underlying assumption that the MARID suite is indeed igneous in origin, this abstract discusses the possible relationships between MARID rocks and other ultrapotassic ultrabasic rocks.

Patchy, inhomogeneous distribution of all minerals and variable grain size within and between nodules is characteristic of MARID rocks. Phlogopite usually dominates with diopside and K-richterite being the other major minerals. All contain varying amounts of ilmenite, rutile and a variety of accessory minerals including apatite, which are usually only present as a few modal percent or are absent. Olivine is absent from these rocks and enstatite is found only in rare samples (one in this study). Many of the textures seen in MARID rocks are broadly analogous to those in the coarse pyroxenite body of the plutonic alkaline Phalaborwa Igneous Complex in South Africa.

MARID nodules have been analysed by XRF for major and trace elements. The textural characteristics already discussed and the small size of samples (long axis typically 10-15 cm) contribute towards the problem that individual bulk compositions cannot be representative of potential precursor melt compositions. Notwithstanding this limitation, the analyses obtained do provide an indication of the compositions and compositional ranges to be found in MARID rocks. Table 1 and Fig.1 present the compositions of four nodules which represent two common types of assemblage. AJE137 and BF05 have phlogopite >> diopside > K-richterite >>> ilmenite ~ rutile. AJE214 and 5 have > 70% K-richterite, with phlogopite > ilmenite, and minor rutile. AJE214 has ~ 15% ilmenite which is untypically high. The MARID rock analyses bear a striking resemblance to Mg-rich ultrapotassic rocks from various localities. In particular as shown in Table 1, the range of compositions exhibited by the lamproites from W. Australia that Jaques et al (1984) defined as ultrabasic (MgO>18%), is remarkably

Table 1. Whole rock analyses of MARID nodules and of selected rocks from the literature.

	AJE137	AJE214	BF05	5	ol-lamproites		bt.
					min	max	maf.
SiO ₂	45.57	42.65	44.28	45.94	40.10	42.80	42.6
TiO ₂	3.03	10.71	2.88	4.80	2.64	5.77	5.3
Al ₂ O ₃	6.55	1.32	7.13	1.51	3.30	4.51	8.3
Cr ₂ O ₃	0.15	0.17	0.15	0.09	0.08	0.25	0.2
Fe ₂ O ₃	7.53	11.59	7.29	7.56	7.57	9.34	8.9
MnO	0.06	0.10	0.06	0.07	0.11	0.14	-
MgO	21.08	20.24	20.91	20.52	19.04	26.90	15.8
CaO	5.74	6.11	5.37	6.24	4.06	5.61	10.7
Na ₂ O	0.91	2.01	0.62	2.22	0.36	0.63	0.8
K ₂ O	6.95	4.09	7.68	4.16	3.46	5.11	7.1
P ₂ O ₅	0.07	0.01	0.06	0.03	0.62	1.48	-
NiO	0.08	0.08	0.10	0.09	0.09	0.19	-
L.O.I.	3.09	1.71	3.99	3.87	5.90	8.72	-
H ₂ O-	0.14	0.16	0.18	0.19	0.95	2.32	-
Total	100.94	100.95	100.70	97.30	98.70	101.13	98.8

AJE137, BF05, AJE214 and 5 are MARID rocks.
Olivine-lamproites: range of 6 analyses with MgO>18 %
from W.Australia, Jaques et al (1984).
Synthetic biotite mafurite used by Edgar et al (1976).

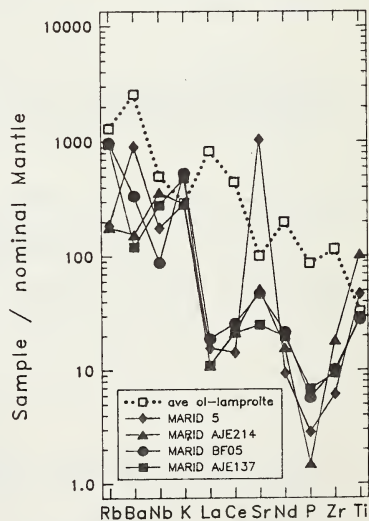


Fig.1 "Spidergram" comparing the compositions of MARID rocks with that of average olivine-lamproite for the same samples as reported in Table 1.

close to those of MARID samples. It is proposed that the compositional similarities and the textural appearance of MARID rocks strongly suggest that they represent the plutonic compositional equivalents of highly potassic volcanics of lamproite-type, crystallized at depth.

There have been a number of experimental studies on a variety of ultrapotassic rocks at a range of high temperatures, and pressures up to 40 kbar, in the presence of H₂O (+CO₂). Of them, the synthetic biotite mafurite used by Edgar *et al* (1976) shown in Table 1, is most similar to MARID rock compositions. At 30 kbar (likely maximum pressure of formation of MARID rocks), and 15% added H₂O, phlogopite, diopside and ilmenite crystallized. The compositions of these phases compare well for most elements with those in MARID rocks (see Fig.2). K-richterite was absent in this study but was present in other similar experiments, eg. on a melilite-nepheline leucitite by Gupta *et al* (1976).

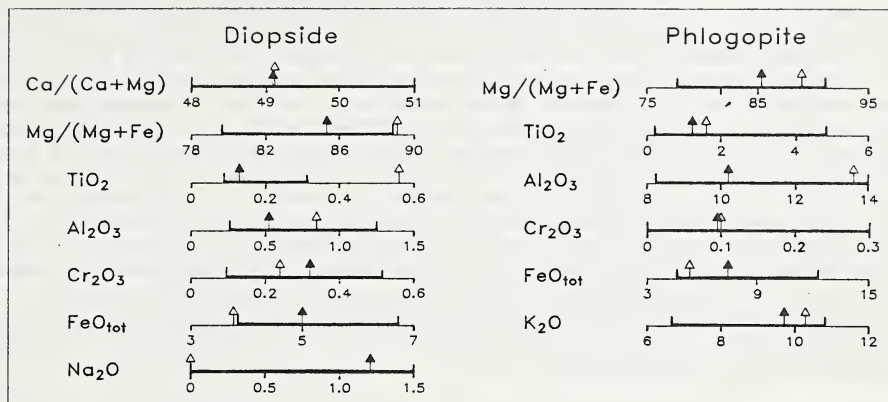


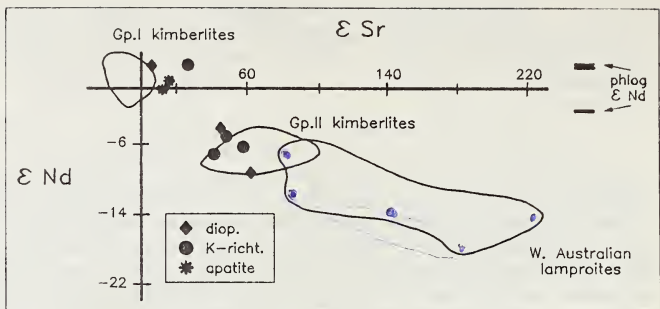
Fig.2 Comparison of average mineral compositions produced by Edgar *et al* (1976) at 30 kbar, 1100° C (open arrows), to those in MARID rocks (filled arrows). The range in MARID rocks is also shown (thick horizontal bars).

It is suggested that the principal differences in mineral assemblage and composition between MARID and lamproitic rocks result from crystallization of the latter at lower pressures. Experimental work on TiO₂ solubility in phlogopite (Tronnes *et al* 1985) for example, supports this view. They found that with increasing pressure, high Ti-phlogopite broke down to low Ti-phlogopite + rutile. Lamproitic phlogopite is TiO₂-rich (up to 10%), whereas primary MARID phlogopite in this study has an average concentration of 1.2% TiO₂, with rutile present in the rocks.

Incompatible trace element concentrations in MARID rocks are high. While lamproites have higher average concentrations of these elements, some MARID rocks have comparable concentrations, as shown in Fig.1. Very high REE concentrations are found in relatively rare apatite-rich MARID rocks, (not shown), but generally the REE and Zr contents are distinctly lower in MARID nodules. It is speculated that late stage aqueous fluids may have escaped from the crystallizing MARID magma carrying the bulk of the REE and the complement of other incompatible elements that had not been accommodated in MARID phases, metasomatizing the surrounding peridotite mantle. Faster crystallization under volcanic or hypabyssal lower temperature conditions would have prevented similar losses in lamproitic rocks. High (50 ppm) concentrations of Nd in diopsides indicate that MARID melts must originally have had high REE concentrations; using a K_d of 0.22, a parent melt of ~200 ppm Nd is indicated.

In Fig.3, Nd and Sr isotopic ratios on minerals separated from MARID rocks from this study and Kramers *et al* (1983) are compared to fields for W. Australian lamproites and southern African kimberlites (after Fraser *et al* 1985). There is a range in isotopic composition from mildly depleted to fairly enriched in the minerals, which lie along this shallow trend. It is suggested that this array in MARID minerals reflects a mixing process between original melt compositions with relatively depleted signatures like those of Group I kimberlites, and ancient enriched subcontinental lithosphere.

Fig.3 ϵ Sr- ϵ Nd correlation diagram for MARID minerals as compared to W. Australian lamproites and S. African kimberlites. Sources of data given in the text. ϵ Nd values of phlogopites shown on the right of diagram as ϵ Sr values not determined or out of range.



Although MARID-type rocks (mica-pyroxenites \pm amphibole) have been invoked as a source material for various ultrapotassic rocks in studies that have recognised their genetic connection, an alternative explanation which fits observations is that they are plutonic equivalents of these volcanics, and are regional parallels of MARID rocks. Gupta and Yagi (1976) reviewed a range of theories on the origin of highly potassic magmas, and concluded that they are most likely to be derived by partial melting of phlogopite-rich peridotite. While this may be in part correct as a source of lamproitic magmas in general, as well as MARID magmas, it is considered likely that the scavenging of incompatible elements from the surrounding enriched subcontinental lithosphere by the rising melts may play a further role in creating the extremely enriched nature of these rocks. Thus their compositional characteristics may not solely reflect those of their source material. It is also considered feasible that MARID melts could have originated as small volume asthenospheric melts which were substantially modified by scavenging as they rose, in the manner described above. The isotopic evidence for a mixing relationship with one end-member having a relatively depleted isotopic signature is more readily reconcilable with an ultimate source in the asthenosphere than in previously enriched peridotitic lithosphere.

MARID rocks may be the unique result of conditions prevailing beneath southern Africa. The stable cratonic setting in which they are found contrasts with the mobile belt/rift related settings in which most ultrapotassic rocks of similar composition occur. This may be why MARID magmas were less likely than equivalent magmas in other areas to have succeeded in penetrating the lithosphere to appear as lamproitic rocks, but crystallized at high pressures at depth instead, probably resorbing any diamonds that may accidentally have been incorporated.

REFERENCES:

- Dawson, J.B. and Smith J.V. 1977. The MARID (mica-amphibole-rutile-ilmenite-diopside) suite of xenoliths in kimberlite. *Geochimica Cosmochimica Acta*, 41, 309-323.
- Edgar, A.D., Green, D.H., and Hibberson, W.O. 1976. Experimental petrology of a highly potassic magma. *Journal of Petrology*, 17, 339-356.
- Fraser, K.J., Hawkesworth, C.J., Erlank, A.J., Mitchell, R.H., and Scott-Smith, B.H. 1985. Sr, Nd and Pb isotopic and minor element geochemistry of lamproites and kimberlites. *Earth and Planetary Science Letters*, 76, 57-70.
- Gupta, A.K. and Yagi, K. 1980. *Petrology and genesis of leucite-bearing rocks*. Springer, New York Heidelberg Berlin, pp252.
- Gupta, A.K., Yagi, K., Hariya, Y., and Onuma, K. 1976. Experimental investigations on some synthetic leucite rocks under water vapour pressures. *Proceedings of the Japanese Academy*, 52, 469-472.
- Jaques, A.L., Lewis, J.D., Smith, C.B., Gregory, G.P., Ferguson J., Chappell, B.W. and McCulloch, M.T. 1984. The diamond-bearing ultrapotassic (lamproitic) rocks of the West Kimberley region, Western Australia. In J. Kornprobst, (Ed.): *Kimberlites, 1: Kimberlites and related rocks*, Elsevier: Amsterdam, pp225-254.
- Kramers, J.D., Roddick, J.C.M. and Dawson, J.B. 1983. Trace element and isotopic studies on veined, metasomatic and "MARID" xenoliths from Bultfontein, South Africa. *Earth and Planetary Science Letters*, 65, 90-106.
- Tronnes, R.G., Edgar, A.D. and Arima, M. 1985. A high pressure-high temperature study of TiO_2 solubility in Mg-rich phlogopite: implications to phlogopite chemistry. *Geochimica Cosmochimica Acta*, 49, 2323-2329.

MANTLE/CRUSTAL XENOLITHS IN HAWAIIITE LAVAS: THE CIMA VOLCANIC FIELD, CALIFORNIA

H.G. Wilshire and J.S. Noller
U.S. Geological Survey

The Cima volcanic field in southeastern California is one of many isolated late Cenozoic basaltic volcanic fields in the Basin and Range province of the western U.S. Cima lavas are dominantly hawaiites like those in some other such fields (Best and Brimhall, 1974; Vaniman et al., 1982), but Cima differs from the other fields in having abundant mafic and ultramafic xenoliths in lavas of hawaiite composition. The xenoliths give direct information about complex events of melting and fractionation that occurred in the mantle before and during generation of hawaiite magmas, and about the nature of the mantle source of the hawaiites.

The Cima volcanic field comprises more than 50 vents and associated flows that were erupted over a period of at least 7 m.y. (Turrin and others, 1985). The tephra and flows are of small volume. Detailed studies (Breslin, 1982) of flows and tephra from two coalescing cones show substantial differences in the degree of silica saturation between the cones and show large ranges within a single flow in the ratios of molecular Mg/Mg+Fe (mg-ratio), 40-51, and normative an/an+ab (an-ratio), 22-45. The volcanic field as a whole has the chemical features of alkaline basaltic suites described by Thompson (1974) and Miyashiro (1978) as "straddle-types"; that is, the lavas vary from ne- to hy-normative (Fig. 1). There is no systematic relation between ages of lavas and either mg- or an-ratio. Similarly, there is no correlation between the presence of xenoliths and age, an- or mg-ratio (Fig. 2), or normative ne. A small number of analyzed lavas (Semken, 1984; Breslin, 1982) have MORB-like isotopic compositions ($\epsilon_{Nd} +9$ to $+10$; $\epsilon_{Sr} -21$ to -22), and LREE-enriched compositions.

We separated the xenoliths into four groups based on their mineralogy: (1) Cr-diopside group of spinel lherzolite and websterite; (2) Cr-diopside group rocks with introduced plagioclase; (3) green-pyroxene (not Cr-diopside) group of websterite, gabbro, and microgabbro; and (4) Al-augite group of clinopyroxenite, gabbro, and microgabbro. Common mineral assemblages and average mineral compositions are given in Table 1.

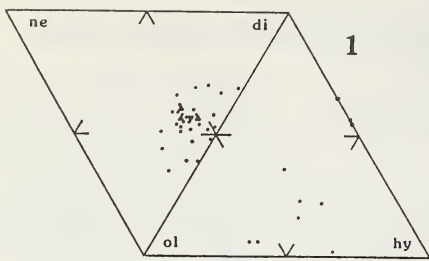
Rocks of the Cr-diopside group are refractory upper mantle lherzolites and websterites typical of basalt xenolith assemblages the world over. The rocks usually are medium grained with allotropic-granular textures and common strain lamellae in olivine. Porphyroclastic or tabular textures are less common.

Many rocks of the Cr-diopside group were invaded by mafic melts from which plagioclase crystallized. These rocks form the second group, in which plagioclase commonly forms thin, irregular stringers in peridotite or pyroxenite. The rocks generally have a hybrid texture of metamorphic peridotite with igneous felsic minerals. In some samples deformation and recrystallization to a mosaic or tabular texture followed crystallization of plagioclase.

Rocks of the green-pyroxene group include websterite, which commonly has high orthopyroxene/clinopyroxene ratios, and two-pyroxene gabbro and microgabbro. All of these rocks have igneous textures. Large orthopyroxene and clinopyroxene grains generally show well-developed lamellar or complex blebby exsolution. Clinopyroxenes of both websterite and gabbro have Al_2O_3 and Cr_2O_3 values intermediate between, but distinct from, those in rocks of the Cr-diopside and Al-augite group (Table 1).

Rocks of the Al-augite group comprise clinopyroxenite and one-pyroxene gabbro and microgabbro. Rare Al-augite gabbro has been deformed and recrystallized to granulite texture.

Composite xenoliths are common at Cima. All the mafic lithologies are found in contact with Cr-diopside peridotite and are clearly dike-like intrusions in the host peridotite. In addition, composite Al-augite pyroxenite-gabbro xenoliths occur. Reactions between dikes and wallrocks in composite xenoliths from this locality have been described (Wilshire and others, 1985). A feature not previously described is the abundant evidence of fractionation within many dikes. In one composite xenolith of peridotite and hornblende microgabbro, hornblende veins derived from gabbro penetrate the peridotite. Composite Al-augite pyroxenite/gabbro xenoliths contain plagioclase veins that extend from pyroxenite into gabbro. We interpret these veins as residual liquids that froze during a process of extraction from an early-crystallized pyroxene aggregate. Such a process would yield complementary pyroxenite and gabbro, as also shown by composite dikes with pyroxenite margins and gabbro cores that apparently resulted from initial crystallization of pyroxene at the dike margins.



Na₂O vs. mg-ratio

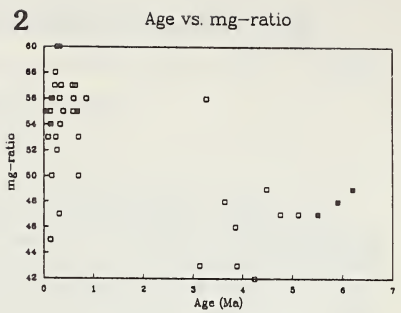


Fig. 1. Normative ne, ol, di, hy components of basalts

Fig. 2. Age vs. mg-ratio, basalts. Filled symbols, xenolith-bearing basalts.

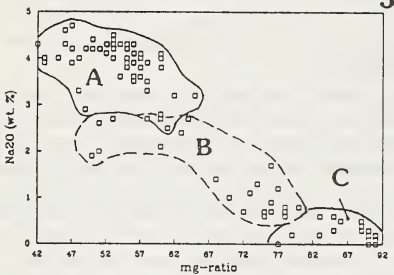


Fig. 3. Mg-ratio vs. Na₂O, basalts and xenoliths. Field A = basalt; field B = gabbro, microgabbro, pyroxenite; field C = Cr-diopside group, feldspathic peridotite.

Crosscutting relations between dikes indicate that Al-augite pyroxenite and gabbro are younger than Cr-diopside websterite. No direct evidence of the age relation between rocks of the green-pyroxene group and either the Cr-diopside websterite or Al-augite group has been found. However, the presence of gabbro and microgabbro in both green-pyroxene and Al-augite groups and the occurrence of representatives of both groups as composites with peridotite suggest that all these xenoliths were in close proximity in their source area. Thus, the xenolith assemblage probably represents a complex terrane of metamorphic peridotite and mafic intrusions rather than samples of stratified mantle and crust.

Striking faceted xenoliths having angular, polygonal shapes are common at Cima. The facets are interpreted (Nicolas and Jackson, 1982; Wilshire and others, 1985) as hydraulic fractures produced by high fluid pressures in the mantle. Some of the fracture systems were intruded by various mafic magmas and healed by crystallization before entrainment in lava. Unhealed fractures were planes of weakness along which the rocks fractured during excavation. Planar facets are found on representatives of all mafic and ultramafic xenoliths at Cima, including the microgabbros. Thus, even those lithologies that were emplaced as dikes in hydraulic fracture systems were themselves subjected to hydraulic fracturing after consolidation. This indicates a mantle history of periodic buildup of fluid pressures, followed by the injection and crystallization of melts. Repetition of the sequence causes hydraulic fracturing of earlier injections and produces crosscutting relations that are consistent with the eruption history at Cima, which is characterized by the episodic generation of small volumes of melt over long periods of time. The fact that old and young lavas in the field contain the same xenolith populations indicates that the magmatic episodes occurred in the same source area and that earlier products of intrusion were affected by later episodes of melt production.

Some bulk chemical parameters (Fig. 3) indicate an overall compositional coherence in the xenolith-host rock assemblage, which we believe indicates a genetic relationship between the host rock and the igneous xenoliths. We interpret the xenolith assemblage to represent batches of basaltic melts emplaced in the mantle near the crust boundary (as envisaged by Thompson, 1974 and Ewart et al., 1980). The parent melts are not represented in erupted magma. Differentiation of the parent led to formation of evolved hawaiite liquids. Separation of Ca-poor pyroxene formed the green-pyroxene group and produced liquids that trend toward more undersaturated compositions (Thompson, 1974). Separation of kaersutite and aluminous high-calcium pyroxene that formed the Al-augite group, produced liquids of hy-normative compositions (Vaniman et al., 1982).

Characteristic features of the Cima volcanic field are a long eruptive history of small volumes of lava and a wide variability of normative composition. These features may arise from production of small volumes of melt that differentiate in the mantle. Numerous melt batches emplaced in a restricted mantle area may have been isolated from each other and may have evolved in different directions. A long history of these events makes mixing of derivative magmas likely. Incomplete mixing may explain the observed wide chemical variations within a single flow (Breslin, 1982).

TABLE 1. XENOLITH MINERAL ASSEMBLAGES AND AVERAGE MINERAL COMPOSITIONAL DATA

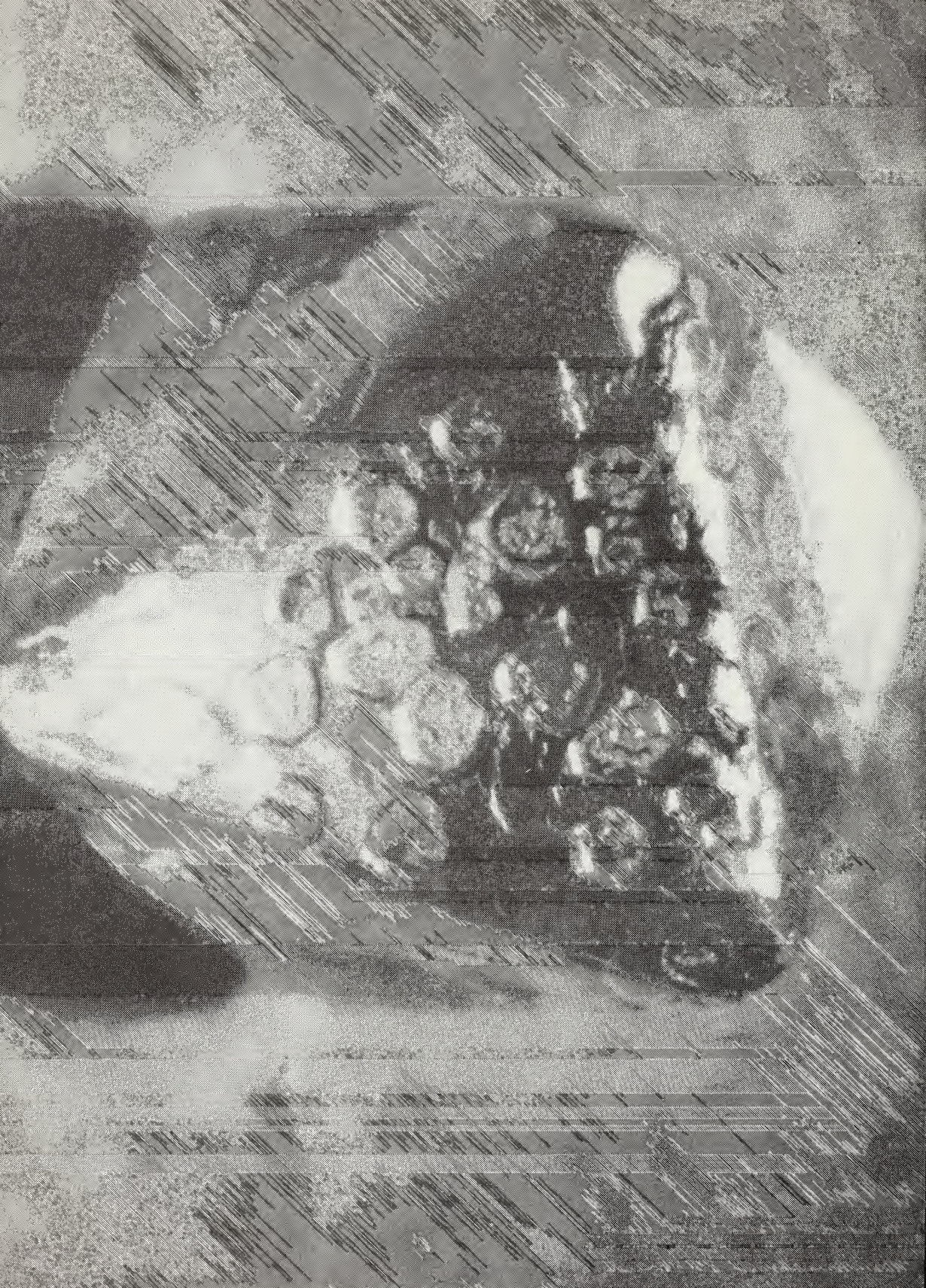
Xenoliths	Clinopyroxene and Orthopyroxene				Plagioclase			Olivine	Oxide	Oxides				
	Ca	Mg	Fe	TiO ₂	Al ₂ O ₃	Cr ₂ O ₃	An	Ab		Or	Fo	Mg	Cr	Ti
Crdiopsid Group														
Lherzollite	(Cpx + Opx + Ol + Oxide)													
Cpx	45-49	46-50	4-5	0.17-0.40	3.2-5.4	0.76-1.2	--	--	--	--	Mg-Al chromite	0.69	0.39	0.0
Opx	1-2	87-90	8-11	.06-.09	2.5-3.9	.39-.52	--	--	--	--	Spinel	.68-.71	.12-.46	0.03-.07
Ol	--	--	--	--	--	--	--	--	--	90-91	--	--	--	--
Websterite	(Cpx + Opx + Ol + Oxide)													
Cpx	46	44	10	.04	4.8	.88	--	--	--	--	--	--	--	--
Opx	1-2	82-89	9-16	.08	3.4	.45	--	--	--	--	--	--	--	--
Feldspathic Lherzollite (Cpx + Opx + Ol + Pc + Oxide)														
Cpx	44-46	47-49	5-8	.40-.81	5.4-6.5	.56-.75	--	--	--	--	--	--	--	--
Opx	1-2	81-89	9-18	.13-.27	2.7-4.0	.28-.43	--	--	--	--	Spinel	.60-.79	.14-.17	0.0
Pc	--	--	--	--	--	--	--	45-66	33-53	1-2	--	--	--	--
Ol	--	--	--	--	--	--	--	--	--	88-90	--	--	--	--
Green-pyroxene Group														
Websterite	(Cpx + Opx + Pc + Hbl + Oxide)													
Cpx	39-43	45-48	12-13	.90-1.4	5.5-6.2	.17-.37	--	--	--	--	--	--	--	--
Opx	3	72-79	18-25	.27-.30	2.7-3.0	.31-.36	--	--	--	--	Ilmenite	.26-.28	.40-.60	.96-.99
Pc	--	--	--	--	--	--	--	53-54	45-46	1	--	--	--	--
Gabbro	(Cpx + Opx + Pc + Ol + Oxide)													
Cpx	40-43	40-43	17	.50-1.2	2.6-5.6	.04-.06	--	--	--	--	--	--	--	--
Opx	2-4	70	26-28	.28-.32	2.4-3.0	.11-.17	--	--	--	--	Ilmenite	.28	.22	.99
Pc	--	--	--	--	--	--	--	48-55	44-51	1	--	Titanomagnesi-	--	--
Ol	--	--	--	--	--	--	--	--	--	67	--	ferrite	.64	0.0
Microgabbro	(Cpx + Opx + Pc + Ol + Oxide)													
Cpx	40	44	16	1.6	5.6	.05	--	--	--	--	Titanomagnete-	--	--	--
Opx	2	70	28	.41	2.9	.01	--	--	--	--	ulvospinel	.18	.09	.79
Pc	--	--	--	--	--	--	--	42	56	2	--	Titanomagnesi-	--	--
Ol	--	--	--	--	--	--	--	--	--	70	--	ferrite	.14	.10
Al-augite Group														
Pyroxenite	(Cpx + Pc + Hbl + Ol + Phlog. + Oxide)													
Cpx	44-46	43-46	8-13	1.1-1.5	5.4-8.4	.01-.04	--	--	--	--	Titanan-	--	--	--
Pc	--	--	--	--	--	--	59	40	1	--	hercynite	.31	.30	.63
Ol	--	--	--	--	--	--	--	--	--	70	--	Ilmenite	.25	.28
											Pleonaste	.60-.61	.0-.01	.01-.07
Gabbro	(Cpx + Pc + Ol + Hbl + Oxide)													
Cpx	44-45	43-44	12	1.1-1.6	5.4-8.7	.0-.40	--	--	--	--	Pleonaste	.59-.67	.0	.01-.07
Pc	--	--	--	--	--	--	48-61	37-50	2	--	Titanan-	.18	.0	.53
											ferropleonaste	--	--	--
Microgabbro	(Cpx + Pc + Ol + Hbl + Oxide)													
Cpx	40	43	17	1.6	5.6	.05	--	--	--	--	Ilmenite	.19	.20	.98
Pc	--	--	--	--	--	--	45	53	2	--	Titanomagnete-	.22	.15	.84
Ol	--	--	--	--	--	--	--	--	--	65	--	ulvospinel	--	--

REFERENCES

- Best, M.G. and Brimhall, W.H., 1974, Late Cenozoic alkalic basaltic magma in the western Colorado plateaus and the Basin and Range transition zone, U.S.A., and their bearing on mantle dynamics: Geological Society of America Bulletin, v. 85, p. 1677-1690.
- Breslin, P.A., 1982, Geology and geochemistry of a young cinder cone in the Cima volcanic field, eastern Mojave Desert, California: MS. thesis, University of California, Los Angeles, 119 p.
- Ewart, A., Baxter, K., and Ross, J.A., 1980, The petrology and petrogenesis of the Tertiary anorogenic mafic lavas of southern and central Queensland, Australia—Possible implications for crustal thickening: Contributions to Mineralogy and Petrology, v. 75, p. 129-152.
- Miyashiro, A., 1978, Nature of alkalic volcanic series: Contributions to Mineralogy and Petrology, v. 66, p. 91-104.
- Nicolas, A. and Jackson, M., 1982, High temperature dikes in peridotites: Origin by hydraulic fracturing: Journal of Petrology, v. 23, p. 568-582.
- Semken, S.C., 1984, A neodymium and strontium isotopic study of late Cenozoic basaltic volcanism in the southwestern Basin and Range province: MS. thesis, University of California, Los Angeles, 68 p.
- Thompson, R.N., 1974, Primary basalts and magma genesis: I. Skye, north-west Scotland: Contributions to Mineralogy and Petrology, v. 45, p. 317-341.
- Turrin, B.D., Dohrenwend, J.C., Drake, R.E., and Curtis, G.H., 1985, K-Ar ages from the Cima volcanic field, eastern Mojave Desert, California: Isochron/West, no. 44, p. 9-16.
- Vaniman, D.T., Crowe, B.M., and Gladney, E.S., 1982, Petrology and geochemistry of hawaiiite lavas from Crater Flat, Nevada: Contributions to Mineralogy and Petrology, v. 80, p. 341-357.
- Wilshire, H.G., Meyer, C.E., Nakata, J.K., Calk, L.C., Shervais, J.W., Nielson, J.E., and Schwarzman, E.C., 1985, Mafic and ultramafic xenoliths from volcanic rocks of the western United States: U.S. Geological Survey Open-file Report 85-139, 505 p.

V. DIAMONDS

All aspects of diamond research, including inclusions in diamonds.



1.25 ct OCTAHEDRON FROM ARGYLE ALLUVIAL DIAMOND DEPOSITS,
WESTERN AUSTRALIA

	Page
REVIEW PAPER	
Diamonds	363
J. J. GURNEY	
Growth history of natural diamond	368
V. V. BESKROVANOV	
Compositional evolution of syngenetic inclusions of ultrabasic association in Yakutian diamonds	371
G. P. BULANOVA	
Paragenesis and peculiarities of sulphides in diamonds and mantle xenoliths from kimberlites	374
G. P. BULANOVA and Z. V. SPETSIUS	
Oxidation of diamond at high temperature and 1 atm total pressure with controlled oxygen fugacity	377
F. A. CULL and H. O. A. MEYER	
The chemistry of concentrate minerals and diamond inclusions of the Dokolwayo Kimberlite, Swaziland	380
L. R. M. DANIELS and J. J. GURNEY	
On the existence of C-13 depleted carbon in the mantle, evidence from diamond studies	383
P. DEINES, J. W. HARRIS and J. J. GURNEY	
Nitrogen aggregation, inclusion equilibration temperatures and the age of diamonds	386
T. EVANS and J. W. HARRIS	
Mineral inclusions in diamonds from Koffiefontein Mine	389
J. J. GURNEY, J. W. HARRIS, R. S. RICKARD and P. CARDOSO	
Diamondiferous minerals from the Star Mine, South Africa	392
J. J. GURNEY and C. J. HATTON	
A comparison of characteristics of diamonds from the Orapa and Jwaneng kimberlite pipes in Botswana	395
J. W. HARRIS, J. B. HAWTHORNE and M. M. OOSTERVELD	
Systematic studies of nitrogen in diamonds from known sources	398
J. W. HARRIS and P. M. SPEAR	
Helium isotopic heterogeneity within single diamonds from the Orapa kimberlite pipe	401
M. D. KURZ and J. J. GURNEY	
A diamond-graphite eclogite from the Sloan 2 kimberlite, Colorado, USA	403
T. E. McCANDLESS and D. S. COLLINS	
Mineral inclusions in diamonds from the Monastery Kimberlite, South Africa	406
R. O. MOORE and J. J. GURNEY	
The occurrence of moissanite and ferro-periclase as inclusions in diamond	409
R. O. MOORE, M. L. OTTER, R. S. RICKARD, J. W. HARRIS and J. J. GURNEY	
Graphite pseudomorphs after diamond in the eclogite-peridotite massif of Beni Bousera, Morocco and a review of anomalous diamond occurrences	412
P. H. NIXON, G. R. DAVIES, V. V. SLODKEVICH and S. C. BERGMAN	
Mineral inclusions in diamonds from the Sloan diatremes, Colorado-Wyoming State Line kimberlite district, North America	415
M. L. OTTER and J. J. GURNEY	

	Page
Origin of diamonds of peridotitic and eclogitic parageneses S. H. RICHARDSON	418
Events reflected in the diamonds of some southern African kimberlites D. N. ROBINSON, J. A. SCOTT, A. VAN NIEKERK and V. G. ANDERSON	421
Do peridotite-suite diamonds form in subducted serpentinites? D. J. SCHULZE	424
Composition of crystalline inclusions and C-isotopic composition of Argyle and Ellendale diamonds A. L. JAQUES, J. W. SHERATON, A. E. HALL, C. B. SMITH, S-S. SUN, R. DREW and C. FOUDOULIS	426
Crystalline inclusions in alluvial diamonds from the Urals, USSR N. V. SOBOLEV, E. S. YEFIMOVA and E. I. SHERMANINA	429

Department of Geochemistry, University of Cape Town,
Rondebosch, South Africa.

Introduction

The most striking new information about diamonds in the past decade has been the evidence of their ancient origins first brought to notice by Kramers (1977) in a study of composited sulphide diamond inclusions for the Finsch, Kimberley and Premier Mines. Results with similar implications were reported by Takaoka and Ozima (1978), Melton and Giardini (1980), Evans and Qi (1982) and Ozima et al (1983, 1984). Very old ages for peridotitic garnet inclusions in diamonds from the cretaceous Finsch and Bultfontein kimberlite pipes were then demonstrated by Richardson et al (1984). Whilst these measurements are not yet sufficiently detailed to demonstrate that all diamonds are very old there is conversely less quantitative information to suggest that their formation can be contemporaneous with pipe emplacement.

Regional Diamond Distribution

In this light the confined distribution of primary diamond deposits to ancient crust and the similar if somewhat more diffuse spread of placer deposits seems to be of more fundamental importance than was formerly recognised.

Ages of Diamond Deposits

Diamond has been intermittently carried to the Earth's crust throughout a long period of the Earth's history with the oldest well documented diamonds being those found in the Witwatersrand conglomerates (\pm 2.6 billion years). Most of the younger diamondiferous deposits are also sedimentary, many being of quaternary age. The oldest well documented diamondiferous volcanic diatreme is the Premier Kimberlite in South Africa with a preferred age of 1250 m.y. (Welke et al 1974). The youngest are the diatremes at Ellendale, West Australia, with ages between 20 and 25 m.y. (Hall and Smith 1984). The volcanic emplacement of diamonds in the Earth's crust is also clearly episodic. Polar wandering curves provide some evidence of an association between this volcanism and plate motions (Hargraves and Onstott 1980). Most kimberlites are Phanerozoic and most placer deposits are Cenozoic but this is probably related to the effects of erosion and secondary weathering rather than to any increase in the rate of formation of diamond deposits with age of the earth.

Diamond Distribution within Kimberlite Clusters

It has been observed that if one kimberlite within a closely spaced petrographically and chemically linked group of kimberlites is diamondiferous then all the other kimberlites within that grouping will also carry diamonds. It is also clear that diamond grades may vary substantially from one occurrence to another. In many cases the diamond populations found in kimberlites within the same cluster have very similar overall characteristics of size shape and colour. Diamond paragenesis may also be similar but there is a recorded instance where the ratio of eclogitic to peridotitic diamonds in two diatremes from the same group are quite substantially different. There is evidence that the size distribution of diamonds within kimberlites in the same group may not be identical (Sutton 1928).

Diamond Distribution within Kimberlite Diatremes

Kimberlite pipes develop three characteristic morphological zones formed by different processes and reflected by predominantly epiclastic, tuffisitic and hypabyssal rocks respectively (Hawthorne 1975). Diamond concentrations within these three zones can fluctuate widely. The tuffisitic rocks show the greatest degree of homogenisation. The overall diamond distribution within and between the three zones does not show any simple well developed pattern. Individual intrusions may show a steadily declining

grade with depth whilst others do not show this feature. Changes in diamond recovery parameters, periods of "high grading", lack of concise records and the effects of geological processes all combine to prevent a really precise assessment of grade variations with depth (Clement 1982). Calculations for kimberlite mines over extended periods sometimes show roughly constant grades. On the other hand there is strong evidence from other occurrences that diamond content can decline quite rapidly with depth of mining and this appears to be most apparent when mining commenced in the epiclastic rocks. Pronounced long term increases in grade are unknown. In kimberlite dykes which presumably act as the feeders to major diatremes and are typically less than 1m wide, there is no evidence for consistent variations of grade with depth over mined sections in excess of 500 metres.

Diamond Distribution in Placer Deposits

The outstanding feature of alluvial diamond deposits is the improvement in average quality of the diamonds with distance from the primary source due apparently to the preferential breakage of inferior crystals. Alluvial diamonds do not show marked abrasion features but frequently many and sometimes all of the population are slightly worn (Robinson 1979). Breakage therefore presumably takes place chiefly by impact. Coastal diamonds having suffered wave damage show between two and three times more percussion marks than deposits inland (Robinson 1979). Industrial stones are very efficiently destroyed. No evidence is available about how many gem stones are broken by the same mechanisms.

Diamonds may be sorted by size and shape within a single deposit or dispersion train. Whilst this is usually a product of hydrodynamic processes in rivers and the sea it has been most impressively developed in an aeolian environment. Diamondiferous gravels in rivers and palaeo stream beds are usually of sub-economic grade. Diamonds are generally concentrated rapidly into a bed rock layer which is seldom very thick and frequently covered with overburden of finer grained sediments. Higher diamond contents are found in favourable trap sites and in some cases extreme enrichment combined with the high quality of the diamonds leads to the development of very rich deposits. This situation can be enhanced even further in the sea where grades in excess of 250 ct./c.m. of gravel have been reported and on sand sea deflation surfaces where significant diamond recoveries have been made by hand in the past. Throughout the world with some minor but no major exceptions lithified gravels are uneconomic to mine because of their low average grade and higher costs of mining.

Diamond Morphology

Diamonds with minor exceptions grow in the octahedral and cubic forms. The vast majority of natural diamond crystal surfaces show no growth features. The tetrahexahedroid is most commonly a shape produced by a major amount of resorption which must be a significant factor in controlling the diamond content of volcanic host rocks. There is an approximate correlation between diamond grade and the proportion of primary growth shapes in the diamonds from kimberlites in southern Africa. Diamonds in eclogite and peridotite xenoliths are characteristically well preserved and have clearly been protected from severe resorption. Diamond dissolution has been inferred to occur in the transporting magma. Lamination lines are often observed as positive features on the surfaces of resorbed diamonds. The deformation which produces these features and can make the diamonds pink or brown in colour is likely to have occurred in the mantle (Harris et al 1975, Robinson 1979).

Topographic studies of rare single crystal diamonds with minimal resorption features indicate that they grew by a spiral mechanism from a solution phase of low supersaturation through the incorporation of atomic growth units. It is thought highly improbable that they grew in metamorphic environments. Polycrystalline aggregates grew more quickly under rather higher supersaturation conditions (Sunagawa 1982).

Green spots can be caused on diamonds particularly in alluvial deposits by alpha particle damage. Experimental results show that these spots become brown at $+550^{\circ}\text{C}$. Brown spotted natural diamonds may therefore have passed through amphibolite facies metamorphic events (Vance et al 1973). However in detail occurrences of diamonds with brown spots cannot always be reconciled with such a sequence of events.

Diamonds

Diamonds have been classified into type 1 and type 2 on the basis of the presence or absence of detectable nitrogen (Robertson et al 1934). Type 1 diamonds represent about 98% of the total (Dyer et al 1965).

Type 1 diamonds can be subdivided on the basis of the aggregation states of nitrogen in the diamond lattice which in turn is related to temperature. Evans and Qi (1982) estimated that Type 1A diamonds remained in the upper mantle for periods in excess of 200 m.y. years at temperatures between 1000 and 1400°C, whilst the rare Type 1B diamond might have been present for as little as 50 y. if temperatures exceeded 1000°C.

Diamonds have a wide range of $\delta^{13}\text{C}$ values from +5 to -34 ‰. There is a marked mode between -5 and -6 ‰ (Harris 1986). Diamonds of both eclogitic and peridotitic parageneses contribute to this mode. Peridotitic diamonds have a restricted range of $\delta^{13}\text{C}$ values (Deines et al 1984), so that the isotopically light and heavy diamonds are either eclogitic or of unknown paragenesis. Since many of the latter are polycrystalline aggregates (Vinogradov 1966, Galimov and Kaminsky 1982) it can be inferred that they are likely to be eclogitic also. Studies of carbon isotopic variation within individual diamonds have found only minor $\delta^{13}\text{C}$ variations (Kaminsky et al 1978) except for diamonds from Zaire where variations of up to 5.2 ‰ have been reported (Swart et al 1983, Javoy et al 1984). Zairian diamonds show evidence for episodic growth in that clear diamond is frequently coated with fibrous diamond rich in impurities. At Roberts Victor a small data set available for eclogitic diamonds is bimodal suggesting two distinct environments of diamond crystallisation. One population has a primary mantle signature of $\delta^{13}\text{C}$ at approximately 5.6 ‰ and the other a $\delta^{13}\text{C}$ of approximately -15.5 ‰ is possibly related to the recycling of subducted lithosphere (Deines et al 1986).

The least radiogenic terrestrial helium isotope ratio which is 226 times the present day atmospheric ratio was measured in a diamond by Ozima and Zashu (1983). In this and subsequent work it has been inferred that some diamonds are nearly as old as the earth. At the same time a wide range in helium isotope ratios was measured in diamonds from both known and unknown sources. Amongst these and at the other extreme a framesite diamond with a $\delta^{13}\text{C}$ value of -29.7 ‰ contained extremely radiogenic helium leading to the suggestion that framesite formed in or from subducted crustal carbon.

Inclusions in Diamonds

Excluding sulphides which are a common inclusion in diamonds and in isolation do not have an obvious paragenesis peridotitic and eclogitic minerals are the only common primary inclusions in diamonds world wide, irrespective of source. Sulphides, olivine and orthopyroxene are the predominant peridotitic minerals with lesser abundances of garnet and chromite, rare clinopyroxene and very rare ilmenite, zircon, native iron and magnesio-wustite. Garnet, clinopyroxene and sulphides form the bulk of eclogitic inclusions with minor kyanite, rutile, corundum, coesite, ilmenite, sanidine, zircon and mica. Amphibole magnetite, apatite, ferro-periclase and moissanite have also been occasionally reported in diamonds, whilst inclusions of diamond in diamond bring the total number of minerals up to 22.

A similar number of epigenetic minerals have been reported.

Overall peridotitic inclusions predominate, but the eclogite/peridotite ratio has been shown to increase with larger sizes of diamond at one locality whilst at another variations of this ratio are even more complex. Both the peridotite and eclogite associations can show bimodal chemical characteristics suggesting that several diamond populations may be represented in the same kimberlite. The inclusions are generally interpreted to be syngenetic or occasionally protogenetic in origin and each isolated crystal or group of crystals is considered to be a closed system within the diamond. Numerous measurements including isotope ratios support this conclusion. Both parageneses are present at every locality so far studied in any detail. The relative proportions vary widely and are unrelated to the geochemical or isotopic signature of the host rock, to its age of emplacement or to the tectonic setting. In general

discrete mineral grains trapped inside the diamond are in equilibrium with each other. However this is not always true particularly where central inclusions in larger diamonds are compared with inclusions towards the margins of the host crystal (Bulanova 1985). The most graphic examples of this disequilibrium have been eclogitic. Examples of "crossed paragenesis" are extremely rare, but there are now at least four independent descriptions of eclogitic and peridotitic minerals having been found in the same diamond (Prinz et al 1975, Hall and Smith 1984, Otter and Gurney 1986, Moore and Gurney 1986). Some inclusions in diamonds have primitive isotope ratios which suggest archaean ages which are much older than the host diatreme. The peridotitic diamond inclusions have very refractory highly magnesian compositions but also show direct evidence of enrichment in light rare earth elements and alkalis which it has been suggested could have been present together with CO₂ in an interstitial fluid phase (Richardson et al 1984). The eclogitic diamond inclusions are characterised by trace amounts of sodium in garnet and potassium in clinopyroxene. The latter can only be expected at high pressures outside the stability field of phlogopite.

The calculation of equilibration conditions for co-existing mineral pairs in diamonds show that the majority of peridotitic inclusions formed within the diamond stability field under conditions that lie close to the predicted ambient shield geotherm and to the peridotite solidus. Calculated equilibration pressures correspond approximately to the highest pressures calculated for coarse grained garnet peridotite xenoliths from kimberlite. Eclogitic inclusions have similar ranges of equilibration temperature. Crystallisation for the majority of both the peridotitic and eclogitic diamond inclusions close to the base of the lithosphere at depths between 150 and 200 kilometres appear to be predicted.

A very few diamond inclusions could be derived from greater depths. Eclogitic garnets included in diamonds from the Monastery and Jagersfontein Mines show pyroxene solid solution and therefore appear to have a particularly deep origin. Rare inclusions of iron, moissanite, ferro-periclase and magnesio-wustite are additional possible ultra high pressure phases, all of which could be derived from the asthenosphere.

Diamond Indicator Minerals

Diamondiferous Type 1 and Type 2 kimberlites can usually be recognised by the presence of macrocrysts of high chrome chromites, subcalcic G10 garnets and high sodium eclogitic garnets, which appear to be related to the peridotitic and eclogitic parageneses defined by diamond inclusions. Rare examples where these indicator minerals are present and diamonds are absent could be due to the complete resorption of diamonds and may correlate with redox conditions of the transporting magma.

Diamondiferous Xenoliths

Diamondiferous eclogites, frequently with very high diamond contents, are found with sufficient frequency to be qualitatively compatible with the idea that diamonds of eclogitic provenance are entirely derived from disaggregated eclogite xenoliths.

Relationships between the compositions of the minerals in the xenoliths and the eclogitic inclusions in diamonds from the same volcanic source are complex and are not well understood. Diamondiferous eclogites show the sodium enrichment in garnet and potassium enrichment in clinopyroxene which is characteristic of the diamond inclusions. Several pieces of evidence suggest that eclogitic diamonds like peridotitic diamonds can be much older than the diatreme in which they are found.

Diamond bearing peridotites also occur but in contrast to the relative abundances of inclusions in diamonds, are much rarer than eclogite xenoliths. G10 garnets and high chrome chromites are so common in kimberlite by comparison to xenoliths containing minerals of the same composition and diamond peridotites are so rare that it has been suggested that diamondiferous peridotites self-destruct after sampling by the kimberlite due to decomposition of magnesite or to devolatilisation of a volatile rich interstitial fluid (Wyllie et al 1984, Boyd and Gurney 1982).

In a study based on southern African samples arguments have been advanced on chiefly isotopic grounds that there are two varieties of kimberlite. Group I have an asthenospheric origin. Group II are derived from sub-continental lithosphere (Smith 1983). This sub-division of two groups is not reflected in diamond paragenesis. All diatremes studied to date from both groups and indeed from lamproites contain diamonds with eclogitic and peridotitic mineral inclusions with widely variable apparently random relative proportions. Similar isotopic and trace element signatures to those seen in the kimberlites are generated in the south Atlantic by hotspots which can be recognised as having two "end member" types (Allegre and Turcotte 1985). One results from the up-welling of primordial mantle across an asthenosphere-mesosphere boundary and the second from a mesosphere boundary layer of recycled (subducted oceanic lithosphere) (Hofman and White 1982, Ringwood 1982) or of delaminated sub-continental lithosphere (McKenzie and O'Nions 1983). Extending the ideas of Duncan et al (1978) and Crough et al (1980) it has been suggested that both Group 1 and Group 2 kimberlites can be generated in the asthenosphere by hotspot activity. This would avoid having to derive spatially juxtaposed kimberlites of only slightly differing ages from two tectonically different source regions (le Roex 1986). Assuming a xenocrystic origin for diamonds then such a model will allow both kimberlite types to sample diamondiferous rocks from the same sources in the asthenosphere, lithosphere and perhaps most importantly the interface between the two which forms an integral part of the model proposed by Haggerty (1986).

References and Acknowledgments

It is impossible to acknowledge the contributions of more than a fraction of the researchers who in one way or another have a legitimate claim to having contributed through their hard work and ideas to this extended abstract. The vast majority are fully referenced in two excellent current reviews by H.O.A. Meyer and J.W. Harris in "Mantle Xenoliths" Ed. P.H. Nixon, Wiley and Sons (1986). Others will be found at the back of the Proceedings of the 3rd International Kimberlite Conference. Personal acknowledgments are due also to F.R. Boyd, J.B. Dawson, P. Deines, A.J. Erlank, S.E. Haggerty, J.W. Harris, B. Harte, J.B. Hawthorne, H. Helmstaedt, M. Kurz, R.O. Moore, M.L. Otter, R.S. Rickard, S.H. Richardson, C.B. Smith and N.V. Sobolev for all manner of contributions through what have in some cases been quite lengthy associations.

V.V.Beskrovanov

Institute of Geology, Yakut Branch,
Siberian Department, USSR Academy of
Sciences

Growth history of Type Ia and IIa diamonds of octahedral, rhombododecahedral, and cubic habits from Yakutia has been studied. 72 plane-parallel plates cut along the (110) and (100) of crystals different both in habit and type have been thoroughly investigated. To study their anatomy and following methods were: Lang's X-ray topography, polarizing optical method, UV-ray and cathode ray excited luminescence, UV-visible absorption in a narrow spectral range. Locally the plates and whole crystals were studied by IR- and UV-spectroscopy at room and nitrogen temperatures.

All the diamonds studied were inhomogeneous. Some crystals contained identical structural imperfections and impurities present in different amounts, while others included defects differing both in type and content. The former will be referred to as tentatively homogeneous (or simply homogeneous), while the latter - as inhomogeneous. The first group includes cubic Type Ia and Type Ia+IB crystals, as well as Type IIa and Type III diamonds. Type Ia octahedra and dodecahedra of the second group, in addition to zonal-sectorial inhomogeneity, have revealed 3 areas within their volume: central, intermediate and peripheral. The same areas in different crystals have similar physical and morphological properties. Different areas differ in these characteristics.

The central area is a small region within a genetic center of a crystal formed during the nucleation stage. Its properties are: a) high density of structural defects responsible for X-ray scattering and extremely high birefringence; b) yellow-green or orange photoluminescence; c) tendency towards sterility with regard to B2 defects and to a lesser extent with regard to N3 defects. Other properties of central area vary from crystal to crystal. Two crystals have revealed cubic-shaped central areas with physical properties characteristic of whole diamond cubes. The same properties are typical of 100 pyramids in sectorial crystals. Most common are Type III central areas. One specimen has shown a Type IIa central area containing 578 and SI systems in the photoluminescence spectrum.

The intermediate area is inhomogeneous and contains interbedded Type Ia and Type IIa zones. It is characterized by: a) alternating high and low birefringence zones, not luminescent or with blue luminescence; transparent and opaque at a definite UV-wavelength; b) higher

plate-type defect content along the (100); c) a step-like profile of octahedral growth zones.

The peripheral area has the following characteristics. It does not scatter X-rays; it has a low birefringence, if any at all; it does not luminesce and absorbs UV-light at 300 nm.

Type Ia flat-sided sharp-edged octahedra contain all the three areas mentioned. Type Ia and Type Ia+III coarse-layered octahedra contain the central and intermediate areas but lack the peripheral one. Tentatively homogeneous crystals show properties similar to those characteristic of one of the central area types in inhomogeneous crystals. A close similarity has been established between Type IIa central areas and Type IIa crystals, between Type III central areas and Type III crystals, between cubic-shaped central areas and cubic structured crystals. Two genetic types of rhombododecahedra have been established, in dodecahedra rectilinear octahedral zones are cut by a secondary rounded surface. In nearly flat-sided rhombododecahedra growth zones along the (110) have been first recognized in diamonds.

The data obtained suggest the following model for the evolution of conditions in which natural diamonds crystallized (schematic representation of the model is given in the figure). It is inferred that natural diamonds had a 3-stage growth history. The stages differed in their physical-chemical conditions, primarily in the degree of supersaturation of the crystallizing environment. At the early stage initiation and growth of the central area under high supersaturation occurred. Supersaturation provided high growth rate and largely normal growth mechanism. Diamonds that ceased their growth at the early stage belong to tentatively homogeneous crystals. These are Type Ia, Type IIa and Type III diamonds. It is at the early growth stage that a boart variety formed. The intermediate stage was marked by repeated changes in physical-chemical parameters of crystallization reflected in octahedral zoning of the intermediate area within crystals. Supersaturation was lower at the time than that at the early stage, growth rate and the proportion of normal growth lowered too. Diamonds that ceased their growth at this stage are represented by coarse-layered octahedra with blue luminescence. The final growth stage of natural diamonds occurred in stable near-equilibrium conditions. Crystals that ceased their growth at the final growth stage are flat-sided sharp-edged octahedra. Right on the scheme you can see reconstructed crystal forms, all occurring in nature as diamond habits. This accounts for a great variety of morphological and physical properties of natural diamond.

Relationship between the shape and properties of a diamond and its

size is well-known. The smaller diamond size, the lower proportion of non-luminescent sharp-edged octahedra and the greater amount of coarse-layered octahedra with blue luminescence. Small stones are largely cubic-shaped with yellow-green luminescence (Yurk et al., 1973). They are predominated by Type IIa and Type III diamonds. In terms of the hypothesis suggested this is explained by the fact that the role of the intermediate area and then of the central area successively increases with decreasing diamond size.

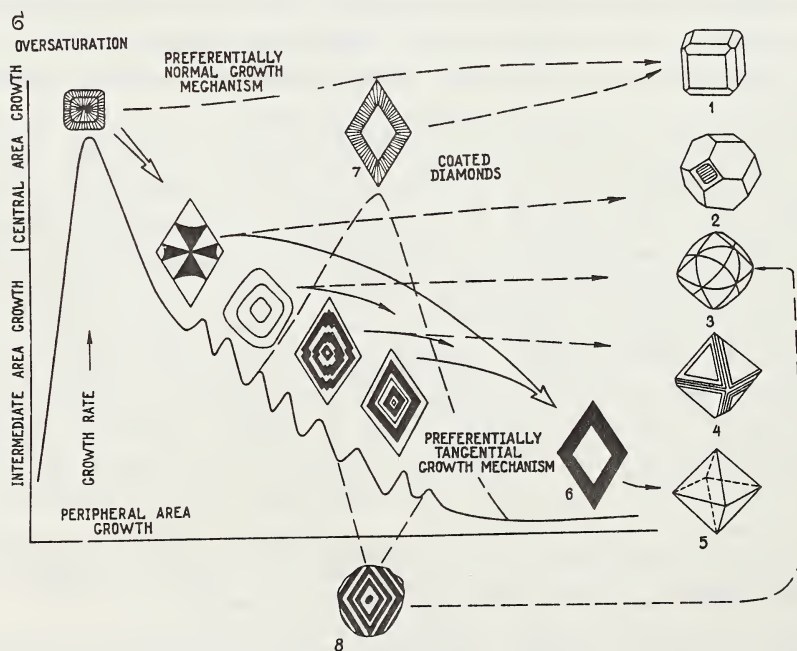
The evolution trend could be perturbed by supersaturation fluctuations. Sharp increases in supersaturation resulted in the coated diamond formation. The coat material properties are common to those of the central area material. As the coat thickened, the octahedral habit turned into the cubic one (Yu.L.Orlov, 1973). Decreasing supersaturation resulted in partial crystal dissolution, i.e. octahedra turned into dodecahedroids.

References.

Orlov, Yu.L. Mineralogy of diamond, M, Nauka, 223p.

Yurk, Yu.Yu., Karkarov, I.F., Polkanov, Yu.A., et al., 1973, Diamonds from sandy deposits of the Ukraine, Kiev, Naukova dumka, 167 p.

Tolansky, S., 1973, Distribution of Type I and Type II in South African diamonds, Diamond Res., pp. 28-31.



COMPOSITIONAL EVOLUTION OF SYNGENETIC
INCLUSIONS OF ULTRABASIC ASSOCIATION
IN YAKUTIAN DIAMONDS

G.P.Bulanova

Institute of Geology, Yakut Branch,
Siberian Department, USSR Academy of
Sciences

Syngenetic inclusions of ultrabasic association from growth zones of diamond crystals have been studied. The inclusions were exposed to the surface by progressive polishing technique. To study their composition JXA-50 A and Camebax-Micro microanalysers were used.

According to the precipitation sequence of diamond associated minerals the inclusions have been divided into 4 groups. These are seed-minerals and minerals from the central, intermediate and peripheral areas (made of small zones) of diamond crystals. Comparison was made between chemical compositions of inclusions from different areas within the same single diamond crystal and of those from the same areas in different crystals.

The following seed-inclusions have been recognised: olivine, enstatite, garnet, as well as ore minerals such as taenite, pyrrhotite, carbon iron and Zn-Fe spinel, representing inhomogenous fine mixtures of polycrystalline phases. Besides, in the initial growth centers of some single diamond crystals, monocrystalline graphite has been found.

Zonal distribution of inclusions was studied on olivines from I2 single crystal diamonds. Olivines from different areas within the same crystal have revealed normal zoning. Average FeO-content of olivines from different diamond crystals also increases from central areas (6.5 wt.%) through intermediate (6.8 wt.%) to peripheral ones (7.4 wt.%), which probably reflects high temperature conditions at the nucleation stage of single diamond crystals and some temperature drop during their subsequent growth.

One of the diamond studied in addition to olivine intermediate and peripheral areas, contained mineral pairs which can be used as geothermometers. Distribution of inclusions within diamond is schematical-

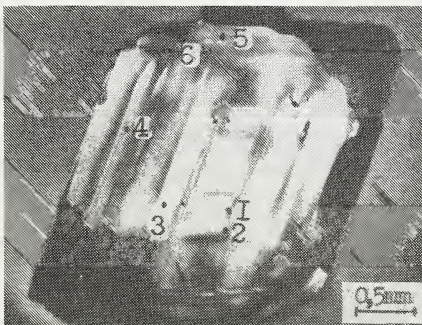


Fig. Zonally distributed inclusions in a diamond plate cut along the (100) of diamond I525; 1,2,3,4, 5 - olivines; 3 - garnet; 6 - three-phase inclusion: magnesite+enstatite+clinopyroxene.

ly represented in the figure, while their compositions are given in the table.

Composition of inclusions from diamond I525.

Compo- nents	central area		intermediate area			peripheral area		
	olivi- ne-1	olivi- ne-2	garnet -3	olivi- ne-4	olivi- ne-5	ensta- tite-6,1	clino- pyro- xene-6,2	magne- site- 6,3
SiO ₂	40,68	40,78	42,09	41,14	41,34	58,81	55,46	-
TiO ₂	0,03	-	0,05	-	0,03	0,07	0,07	-
Al ₂ O ₃	-	-	17,80	-	0,01	0,44	2,86	-
Cr ₂ O ₃	0,07	-	9,18	0,14	-	0,35	5,24	0,01
FeO	6,50*	6,36*	5,27	6,30*	6,59*	3,96	2,47	3,41
MnO	0,10	0,09	0,26	0,14	0,10	0,10	0,09	0,12
MgO	51,29	51,79	14,02	50,99	51,37	35,84	12,64	39,39
CaO	-	-	2,27	0,01	0,03	0,26	16,20	0,61
Na ₂ O	0,02	0,02	0,02	-	0,06	0,17	3,64	-
K ₂ O	-	-	0,01	0,01	0,02	0,01	0,07	-
CO ₂	-	-	-	-	-	-	-	56,6**
Total	98,69	94,04	100,98	98,74	99,53	99,00	98,74	100,00

* - average of 20 measurements; ** - calculated CO₂

Olivines from different areas insignificantly differ in their FeO-content. FeO - content of olivine 1 and olivine 5 is practically the same, it is somewhat lower in olivine 2 and olivine 4. Compositional peculiarities of garnet 3 enabled us to refer olivine 2 + garnet paragenesis 3 to the harzburgite-dunite one.

Inclusions 6 in the form of a single crystal 100x18 m in size from the outer zone of the crystal turned out to be three-phase when exposed to the surface. It is largely composed of enstatite; a narrow marginal zone is made of clinopyroxene, and another one made of magnesian-iron mineral with stoichiometry corresponding to magnesite. C-presence was supported by direct measurements of C K α - emission on a wavelength spectrometer.

By its mineral composition the association mentioned can be referred to the lherzolite one, but the harzburgite-dunite association is likely to contain very small amounts of clinopyroxene too. By its chemical composition clinopyroxene 6.2 corresponds to a ureyite-rich variety rarely occurring as diamond inclusion. It is more common in intergrowth with diamond and occurs rarely in ultrabasic xenoliths. Natural clinopyroxenes of similar composition are likely to belong to the magnesite-peridotite paragenesis. Magnesite has preserved in diamond sole-

ly due to its being entrapped by diamond and isolated from the environment, while in xenoliths it suffered secondary alteration.

Crystallization temperature of olivine 2 and garnet 3 from the intermediate area was estimated at 1190°C using O'Neill and Wood's geothermometer (1979), while that of the enstatite - clinopyroxene + magnesite association from the peripheral area was estimated at 1000°C using a two-pyroxene geothermometer by Wood and Banno (1973). Pressure was estimated at 50 kbar from the Al_2O_3 -content of enstatite co-existing with clinopyroxene.

Thus geothermometry in one diamond crystal supported data on temperature drop during the single diamond crystal growth obtained as a result of investigating zonal distribution of olivines in different diamonds.

Gradually increasing iron content of olivine inclusions with distance from the center of a host diamond is well accounted for by crystallization differentiation of the melt during the temperature drop in a closed magmatic system. Another reason for the melt evolution may be oxygen fugacity variations reflected in the composition of inclusions in diamonds. For example, central diamond zones contain phases indicating f_{O_2} that corresponds to the wustite-iron buffer, while in the peripheral area f_{O_2} roughly corresponds to the quartz-fayalite-magnetite buffer. The final growth stage of diamond crystals probably occurred in the conditions close to the diamond-carbonate monovariant equilibrium curve.

The finding of a magnesite inclusion syngenetic with diamond supports the possibility of kimberlite melt formation and diamond growth in natural conditions as a result of the realization of processes described by model systems (Ryabchikov, 1980; Wyllie, 1980).

References

Bulanova G.P., Varshavsky A.V., Leskova N.V., Nikishova L.V., 1984, Central inclusions as indicators of conditions of natural diamond nucleation. Tezisy dokladov na 27 sessii MGK, Moscow, T. Mineralogia, p.193.

Ryabchikov I.D., 1980, Nature of kimberlite magmas. Geologia rudnykh mestorozhdeniy, N 6, pp.18-26.

O'Neill M.S.C., Wood B.J., 1979, An experimental study of Fe-Mg-partitioning between garnet and olivine and its calibration as geothermometer. Contr. Mineral. Petrol., v.70, pp.59-70.

Wood B.J., Banno S., 1973, Garnet-orthopyroxene and orthopyroxene-clinopyroxene relationships in simple and complex systems. Contr. Mineral. Petrol., v.42, N 2, pp.109-124.

Wyllie P.J., 1980, The origin of kimberlite. Journal of Geophysical Research, v.85, N B-12, pp.6911-6918.

PARAGENESIS AND PECULIARITIES OF SULPHIDES
IN DIAMONDS AND MANTLE XENOLITHS FROM
KIMBERLITES

G.P.Bulanova, Z.V.Spetsius

Institute of Geology, Yakutian Branch,
Siberian Department, USSR Academy of
Sciences. Yakutniproalmaz.

Study of syngenetic inclusions in diamonds has revealed that in Yakutian stones sulphides are strongly predominant over oxide and silicate minerals. Microprobe analysis of sulphides in diamonds from several kimberlite pipes in Yakutia indicates that they mostly have a multiphase composition. The following assemblages are distinguished: pyrrhotite + pentlandite \pm chalcopyrite, pyrrhotite + m_{SS} , m_{SS} + pentlandite (or violarite - like phase) \pm jerfischerite, pyrrhotite + pyrite. Pyrrhotite is among the major phases that comprise the sulphide inclusions in diamonds.

In addition to diamonds, sulphide inclusions have also been found in all xeno- and phenocrysts of kimberlite rock minerals: olivine, ilmenite, garnet, and zircon. The sulphide nodules are usually multiphase with pyrrhotite predominating; Pentlandite and chalcopyrite are also present; some jerfischerite occurs in the ilmenite.

Studies of the sulphide parageneses in mantle xenoliths from Yakutian kimberlites have shown that they characteristically have a wide range of phase and chemical compositions. As indicated by mineragraphic investigation of various mantle xenoliths in Yakutian kimberlite pipes, the sulphide are most abundant in basic xenoliths represented by various types of eclogites, garnet websterites, and garnet pyroxenites. Quantitatively, the sulphides generally constitute tenths of a volume percent of the rock and very rarely up to 3-5 volume percent. In ultrabasic xenoliths, the sulphide content is much lower and does not exceed 0,5 volume percent. Sulphide inclusions occur in the grains of the rock-forming minerals and, more often, in the interstices between them; their size ranges from a few microns to one or, rarely, more mm.

We made microprobe analysis of 100 xenoliths of eclogites and rocks of similar composition, approximately one third of the xenoliths being diamondiferous. Most of the sulphide nodules are of multiphase character. The most common assemblage is pyrrhotite + pentlandite + chalcopyrite \pm pyrite, with pyrrhotite and pentlandite predominating. Less common are the multi- and monomineral sulphides: pyrite, chalcopyrite, jerfischerite, and m_{SS} containing 35-45 mass percent Ni: Some samples contained polydymite and native iron.

Peculiar features of the sulphide inclusions in diamonds and xenolith minerals, such as a partly rounded shape, looseness, and the charac-

ter of mineral phase interrelations indicate that they were originally droplets of a sulphide melt that crystallized later. Probably in the case of rapid cooling of an entrapped droplet provided the kimberlite material was erupted, m_{SS} could persist as a quench phase. In accord with experimental data, in the case of slow cooling the assemblages pyrrhotite + pentlandite + chalcopyrite, etc. were formed. Thus the resultant low-temperature sulphide assemblage has originally been a high-temperature m_{SS} . Therefore the abundance of the sulphides is at no variance with the high P-T parameters for the origin of diamonds and xenoliths. The interstitial sulphides are thought to have had similar origin and evolution except that they probably evolved under conditions of an open system and were affected to a larger degree by deep-seated metasomatism, a process common in the upper mantle rocks. Particularly, that jerrfischerite has resulted from a stage of mantle metasomatism is indicated by a secondary character of its relations with other sulphides, heterogeneity of its composition within the grains, its restriction to intensely metasomatized xenoliths, and other factors.

Comparison of the sulphides in diamonds with those in various mantle assemblages made on the basis of our and published data shows (see Table) that the diamond sulphides are most similar in abundance and presence of individual phases to the sulphides in eclogite xenoliths. The latter show no apparent specialization in their parageneses or composition and the sulphides from diamondiferous specimens exhibit no special features either.

Study of the sulphides in diamonds and mantle xenoliths shows that a sulphide system has played an important role, together with a silicate medium represented by two geochemical types (ultrabasic and eclogitic), in the origin of natural diamonds. The definition of the place and role of sulphide melt in diamond nucleation and crystallization is the target of further study.

Minor elements	Inclusions in diamonds	From ultrabasic xenoliths	From eclogites	Inclusions in			
				olivine	ilmenite	garnet	zircon
Pyrrhotite	Ni 0-7:0	0.09-0.6	0.07-10.47	3-12	1.8	3.99-8.35	4-18.38
	Co 0-0.65	0-0.1	0-2.50	0.11-0.22	-	0.06-0.38	0-0.73
	Cu 0-2.32	0-0.08	0-3.42	0-1.46	0.97	0-0.15	0-2.49
Pentlandite	Co 0.11-1.05	0-6.07	0-1.44	0.43-0.89	-	0.51-0.79	0-2.07
	Cu 0-1.51	0.05-1.76	0.05-5.15	0.08-0.15	3.29	0.11-0.36	0.07-1.19
Chalcopyrite	Ni 0.51-1.07	0.74-8.21	0-0.62	0.06-0.67	0.24	0.28-0.41	-
	Co 0-0.07	0.14	0-0.09	0.03-0.34	-	0-0.10	-
Pyrite	Ni 0.2-5.7	-	0.15-0.52	-	0-0.39	-	-
	Co 0.04-2.08	-	0.05-3.76	-	-	-	-
	Cu 0.6-3.24	-	0-0.76	-	0-0.05	-	-
Jerrisite	Ni 13.70-17.30	10.09-15.30	4.61-9.94	-	10.95-19.33	10.39-13.0	-
	Co 0-0.22	0.10-0.67	0.11-0.54	-	-	0.18-0.35	-
	Cl 1.89-5.55	0.44-2.15	4.70-19.87	-	0.08-7.80	3.55-6.96	-
	K 7.40-9.29	8.89-11.48	9.20-9.77	-	7.66-8.30	9.21-9.97	-

OXIDATION OF DIAMOND
AT HIGH TEMPERATURE AND 1 ATM TOTAL PRESSURE
WITH CONTROLLED OXYGEN FUGACITY

Frances A. Cull and Henry O. A. Meyer

Department of Earth and Atmospheric Sciences, Purdue University,
West Lafayette, IN 47907 U.S.A.

The presence of diamond in kimberlite is generally believed to be due to rapid ascent of a diamond-bearing magma from the mantle to the crust. The temperature of the magma plus the oxygen fugacity (f_{O_2}) and the residence time within the crust prior to intrusion at the surface all play a role in the retention or removal of diamond. Evidence for this is perhaps illustrated by the presence of some diamonds showing resorption features, the occurrence of non-octahedral forms of diamond and the development of trigons on diamond surfaces.

It is commonly accepted that mantle and crustal fluids can be represented in part by the system C-H-O (Wyllie, 1980). Within this system the important phases are CO_2 and H_2O and these can be conveniently discussed as a function of the oxygen they contain i.e. f_{O_2} . Evidence from coexisting iron-titanium oxides (Haggerty and Tompkins, 1983) and from a thermodynamic treatment of assemblages of olivine-orthopyroxene-ilmenite (Eggler, 1983) yield a f_{O_2} for diamond-bearing magmas in the range bounded by QFM and MW buffers.

In the study reported herein experiments were undertaken to determine a kinetic model for the rate of transformation of diamond at high temperature (900-1000°C) and controlled f_{O_2} approximately to the QFM-NNO buffers (i.e. $\log f_{O_2}$ 10^{-10} to 10^{-14}) through use of a CO- CO_2 gas mixture, and a calcia-zirconia solid electrolyte cell. In the majority of the experiments the diamonds used were almost perfect octahedra, about 1 mm on edge and approximately 2 to 3 mg in weight. Octahedrons were chosen for several reasons including the fact that the octahedron is considered to be a growth form and also that trigons develop on 111 faces. All the diamonds were clear, colorless and free of macroscopic inclusions. After weighing the diamonds were placed in a Pt capsule and suspended in the furnace at the required temperature and f_{O_2} . The capsule (+ diamond) were periodically quenched, the diamond reweighed and then returned in a new Pt capsule to the furnace. Individual diamonds were normally held at T and f_{O_2} for 12 to 48 hours between quenchings.

Examples of some results at 910° and 935°C and f_{O_2} of 10^{-10} and 10^{-12} atm are shown in figures 1 and 2. The rate constant, K, for each data set is given by the slope of the best fit line. In reality, this constant can only be called a pseudo-rate constant due to the fact that the diamonds that were used for these experiments were only of one size, and thus the possible influence of a change in surface area with degree of oxidation was not taken into account.

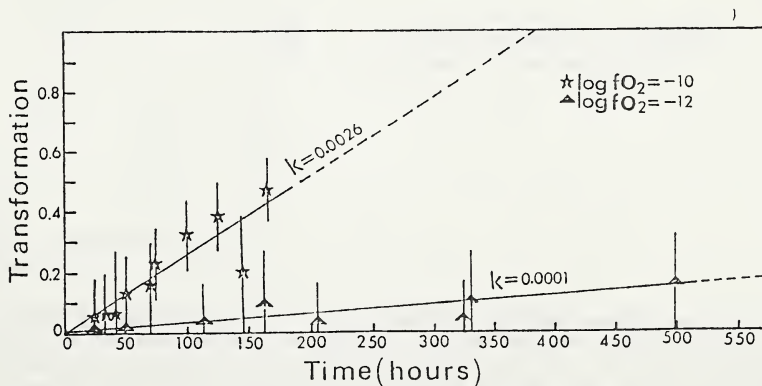


Figure 1. Temperature = 910°C.

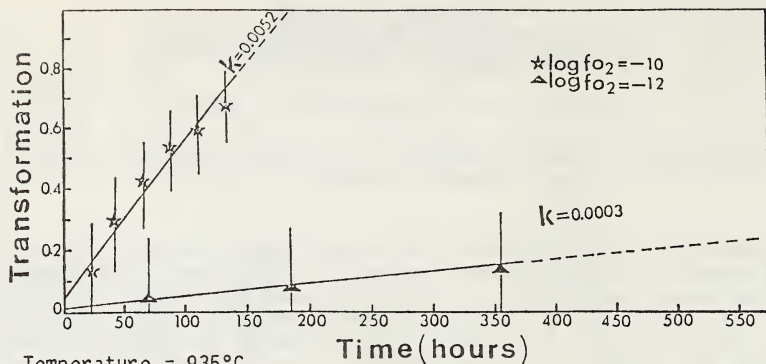
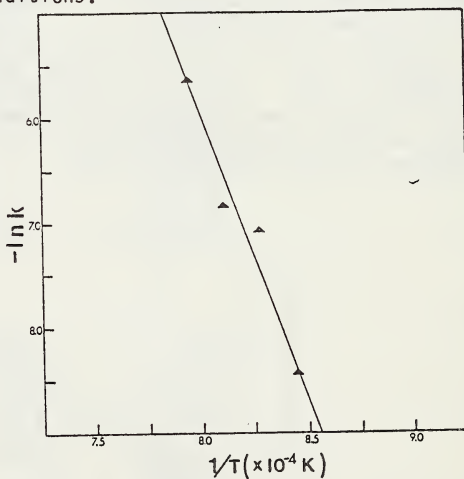


Figure 2. Temperature = 935°C.

A feature of the surface morphology of the diamonds during and subsequent to the runs was the development of negative trigons of varying depths and sizes. It was observed that an increase in all three factors under investigation, length of time for a run, temperature and f_{O_2} resulted in an increase in the size and frequency of the trigons that were produced. Of these three variables, f_{O_2} appeared to produce the greatest change in surface morphology. Diamonds treated at $f_{O_2} 10^{-12}$ atm showed the greatest resemblance to diamonds as they occur in nature.

The general pattern that can be discerned from the experiments that were performed during the course of this study is that an increase in temperature at a constant f_{O_2} produces an increase in the rate of the oxidation of diamond. Similarly, an increase in f_{O_2} at a constant temperature also resulted in an increased oxidation rate. Thus, the most rapid oxidation rates were observed for diamonds which were oxidized at higher temperatures and in the more oxidizing of the two environments. Of the two variables under investigation, examination of the rate of change of oxidation with temperature at a constant f_{O_2} reveals that at conditions corresponding to $\log f_{O_2} = -10$, the rate constant increased by a factor of 9 between 910° and 985°, while spanning a similar temperature range at $\log f_{O_2} = -12$ produced an increase in oxidation rate by a factor of 4.2. Thus, one may deduce that an increase in f_{O_2} resulted in an increase in oxidation rate such that the rate constant at $\log f_{O_2} = -10$ increased nearly twice as fast as did the rate constant at the less oxidizing conditions.

Figure 3. Arrhenius plot of data collected at $\log f_{O_2} = -12$.



If one assumes constant surface area, then the activation energies for the diamond oxidation reaction at the two f_{O_2} conditions, can be obtained from Arrhenius plots of the data ($\ln k$ vs. $1/T$, fig. 3). The resulting activation energies are 87.3 ± 4 kcal/mole at $\log f_{O_2} = -10$ and 102.6 ± 6 kcal/mole at $\log f_{O_2} = -12$. It is not clear what the significance of these numbers are if the surface area of the diamond during oxidation is

not taken to be constant. A possible way in which the oxidation of diamond may be viewed is as a solid state diffusion phenomenon. This is suggested by the high correlation of the data obtained with the Avrami equation ($\xi = 1 - \exp[-Kt^n]$, where ξ = volume transformed, K and n are rate constants, and t is time) for non-randomly distributed nuclei.

Based on the rate constants that can be extracted from the time vs. transformation plots, one can calculate an upper bound on how long a diamond in the size range of 2 to 3 mg could remain at a temperature and f_{O_2} in the range studied herein before disappearing completely. This period of time ranges from 23 days at 900°C to 1.2 days at 1000°C for an atmosphere of $\log f_{O_2} = -10$, and to 69 days at 900°C to 21 days at 1000°C for an atmosphere of $\log f_{O_2} = -12$. Given the rapid rate of transformation that a diamond undergoes in this temperature and f_{O_2} range, as is evidenced by the calculation above, one can hypothesize that a long residence of a diamond-bearing magma in a lower crustal environment of sufficiently high T and f_{O_2} would not be conducive to the preservation of micro diamond, and could cause total disappearance of such size material from the magma prior to intrusion into the upper crust.

However, it should be stressed that these values are only applicable to diamonds in the 2.0 to 3.0 mg size range. Attempting to extrapolate from these data so as to incorporate diamonds of all sizes brings one to the question of the role played by surface area in the rates reported above.

Closer scrutiny of the data reveals that while the percentage of weight lost by the diamond with time at a given T and f_{O_2} , increases dramatically with an increase in the degree of oxidation, the actual weight loss (in terms of mg/hr) remains in a limited range. Furthermore, preliminary data obtained for a diamond in the 50 mg size range (25X the smaller ones cited above) which was subject to a temperature of 935°C at $\log f_{O_2} = -10$ indicates that the weight loss per hour is essentially the same as that observed for smaller diamonds at the same conditions. This observation could be interpreted as suggesting that surface area has no major impact on the absolute rate of the oxidation of diamond, but does have an effect on the relative rate when diamonds of different sizes are compared.

References:

- EGGLER, D.H. 1983. Upper mantle oxidation state: evidence from ol-opx-ilmenite assemblages. *Geophys. Res. Letts.*, 10, 365-368.
- HAGGERTY, S.E. and TOMPKINS, L.A. 1983. Redox state of earth's upper mantle from kimberlite ilmenites. *Nature*, 303, 295-300.
- WYLLIE, P.J. 1980. The Origin of kimberlite. *J. Geophys. Res.*, 85, 6902-6910.

THE CHEMISTRY OF CONCENTRATE MINERALS AND DIAMOND INCLUSIONS
OF THE DOKOLWAYO KIMBERLITE, SWAZILAND

Leon R M Daniels* and J J Gurney

*Dokolwayo Diamond Mines, P O Box 1172, Manzini, Kingdom of Swaziland

Department of Geochemistry, University of Cape Town, Rondebosch 7700
South Africa

The Dokolwayo diatreme has the petrographic character of a Type II kimberlite (Smith, C.B. 1983) is diamondiferous and has a preferred emplacement age of 200 ± 5 m.y. (Allsopp, H.L. and Roddick, J.C. 1985) It therefore just predates the Stormberg volcanism which in the vicinity of Dokolwayo commenced at $+ 190$ m.y.

Probably due to the extensive secondary alteration in the near-surface kimberlite sampled to date, only a few highly altered mantle xenoliths have been found. This study is therefore confined to mantle derived megacryst and macrocryst garnets (55%) and chromites (45%) and most significantly of diamonds with mineral inclusions.

CHROME POOR GARNETS

The majority of the garnets ($\pm 60\%$) have chrome poor compositions and are confined to a restricted range of high Mg/Fe ratios. MgO is within the range of 15-22 wt %, FeO 7-15 wt % and CaO 2.8-6 wt %. Two more calcic compositions extending this range were reported in an extensive earlier study of Dokolwayo garnets (Hawthorne et. al. 1979) Na₂O lies in the range 0.04-0.022 wt % and shows a positive correlation with TiO₂. Both megacryst and macrocryst garnets with similar compositional ranges and trends as have been established for the Monastery (Jakob, W.R.O. 1977) and Lekkerfontein (Robey, J.V.A. 1980) Cr-poor discrete garnet megacrysts are present. These have not previously been reported from Type II kimberlites. In addition garnet macrocrysts with chemistry similar to Group II eclogites from Roberts Victor (Hatton, C.J. 1978) have also been identified.

CHROME RICH GARNETS

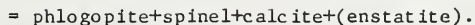
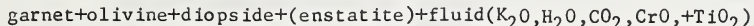
The chromiferous peridotitic macrocrysts are bimodal with respect to both CaO and TiO₂, suggesting at least three populations are present. These are inferred to be derived from disaggregated garnet harzburgites, coarse garnet lherzolite and high temperature deformed garnet lherzolite. The presence of the latter in Type II kimberlite has also not been suspected previously. The sub-calcic (G10) garnet population present (~1%) has been inferred to be derived from garnet harzburgite. It is consistent with the presence of diamonds in the kimberlite. (Gurney, J.J. 1984). Green garnets form a very minor part of the macrocryst suite.

Chromite Macrocrysts

The outstanding feature of the macrocryst chromites is the consistently high chrome content. More than 77% contain >60 wt % Cr₂O₃, with a highest determined concentration of 71,7 wt %. There is no correlation between the chromite compositions and grain size, texture or shape, although both euhedral and anhedral population groups are present. The presence of high chrome chromites is frequently observed in diamondiferous kimberlites, but this population is exceptional.

The unusually high Cr₂O₃ content (70-75 wt %) in meteoritic chromites, above the stoichiometric 67,9 %, has been suggested to be due to tetrahedrally coordinated chromium (Bunch, T.E. and Olsen, E. 1975) Divalent, tetrahedrally coordinated Cr²⁺ has been demonstrated for a kimberlitic spinel which was equilibrated at 1400°C and $f_{O_2} = 10^{-11.5}$ atm. (Mao, H.K. and Bell, P.M. 1974) The presence of Cr²⁺ in the mantle has been suggested by several authors. (Mao, H.K. and Bell, P.M. 1974; Meyer, H.O.A. and Boyd, F.R. 1972; Burns, R.G. 1975).

It is possible that the very high chrome chromites from Dokolwayo contain Cr^{2+} . It is envisaged that the macrocryst chromites are metasomatic in origin. A generalised reaction could be:



Diamond Inclusions

The diamond inclusions can be readily assigned to the eclogitic and peridotitic parageneses universally reported to be present at other localities. The eclogitic paragenesis predominates in contrast to most diamond sources (Gurney, J.J. et. al. 1978). and to other well described inclusion suites from Type II kimberlites (Gurney, J.J. et. al. 1979; Gurney, J.J. et. al. 1984) The peridotitic paragenesis suggests garnet harzburgite and garnet lherzolite as the source rocks for the diamonds.

Both the eclogitic inclusions and the sub-calcic (G10) peridotitic inclusions have distinctly different compositions compared to the macrocrysts. The eclogitic diamond inclusions have $\text{CaO} > 7 \text{ wt } \%$, $\text{FeO} > 14 \text{ wt } \%$ and $\text{MgO} < 12 \text{ wt } \%$. Na_2O ranges up to 0.52 wt %. The sub-calcic macrocrysts have $< 8 \text{ wt } \%$ Cr_2O_3 whilst the sub-calcic peridotitic inclusions have $\text{Cr}_2\text{O}_3 > 9 \text{ wt } \%$. The chromite inclusions have Cr_2O_3 content ranging from 62.0 - 66.2 wt %, Al_2O_3 content 4.7 - 8.5 wt % and TiO_2 0 - 0.32 wt %. On average they have distinctly lower TiO_2 than the macrocrysts (0.90 wt % ave.).

Such differences between the diamond inclusions and the macrocryst minerals preclude a simple single stage model for derivation of the diamonds from common xenoliths. The diamonds must be derived from disaggregation of xenoliths which are either very rare or which have re-equilibrated post-diamond formation. The latter infers that the diamonds with the inclusions are older than the diatreme as supported by several independent lines of evidence for some other localities (Kramers, J.D. 1979; Melton, C.E. and Giardini, A.A. 1980; Ozima, M., et. al. 1983; Richardson, S.H., et. al. 1984). It would appear that the local tectonic setting and the unusual age of emplacement of the Dokolwayo diatreme are not reflected in the diamond inclusion compositions which are similar to those reported from other localities world-wide.

The inferred presence of high temperature sheared peridotites and the presence of Cr-poor discrete garnet megacrysts in Dokolwayo is indicative of high temperature and pressure regimes implying a depth of derivation similar to that of Type I kimberlites.

REFERENCES

- Allsopp, H.L. and Roddick, J.C. 1985. Geol. Soc. S. Africa., **Special Publication**, 13.
- Bunch, T.E. and Olsen, E. 1975. *Geochim. Cosmochim. Acta* 36, 911-927.
- Burns, R.G. 1975. *Geochim. Cosmochim. Acta* 39, 857-864.
- Gurney, J.J. 1984. In: **Kimberlite occurrence and origin: a basis for conceptual models in exploration**. Eds. J.E. Glover, P.G. Harris. Univ. W. Australia, 143-166.
- Gurney, J.J., Harris, J.W., and Rickard, R.S. 1978. **Extended Abstracts Part I 18th Congress**. G.S.S.A. 164-166.
- Gurney, J.J., Harris, J.W., and Rickard, R.S. 1979. In: **Kimberlites, diatremes and diamonds: their petrology and chemistry**. Ed: F.R. Boyd, H.A.O. Meyer. A.G.U. 1-15.
- Gurney, J.J., Harris J.W., and Rickard, R.S. 1984. In: **Kimberlites II: the mantle and crust-mantle relationships**. Ed: J. Kornprobst. Elsevier. 25-32.
- Hatton, C.J. 1978. **Unpubl. Ph.D.** Univ. Cape Town, S. Afr.
- Hawthorne, J.B., Carrington, A.J., Clement, C.R., Skinner, E.M.W. 1979. In: **Kimberlites, diatreme and diamonds: their geology, petrology and chemistry**. Ed. F.R. Boyd, H.A.O. Meyer. A.G.U. 59-70.

- Jakob, J.V.A. 1980. Unpubl. M.Sc. Univ. Cape Town, S. Afr.
- Kramers, J.D. 1979. *Earth planet Sci. Lett.* 42, 58-70.
- Manton, W.I. 1968. *J. Petrol.* 9, 23-39.
- Mao, H.K. and Bell, P.M. 1974. *Carnegie Inst., Washington Yr. Bk.* 73, 332-341.
- Melton, C.E. and Giardini, A.A. 1980. *Geophys. Res. Letters* 7, 461-464.
- Meyer, H.A.O. and Boyd, F.R. 1972. *Geochim. Cosmochim. Acta* 36, 1255-1273.
- Ozima, M., Zashu, S. and Nitoh, O. 1983. *Geochim. Cosmochim. Acta* 47, 2217-2224.
- Richardson, S.H., Gurney, J.J., Erlank, A.J. and Harris, J.W. 1984. *Nature* 310, 198-202.
- Robey, J.V.A. 1980. Unpubl. Ph.D. Univ. Cape Town, S. Afr.
- Smith, C.B. 1983. *Nature* 304, 51-54.

ON THE EXISTENCE OF C-13 DEPLETED CARBON IN THE MANTLE,
EVIDENCE FROM DIAMOND STUDIES

P. Deines

Department of Geosciences
The Pennsylvania State University
University Park, PA 16802

J. W. Harris

Department of Applied Geology
University of Strathclyde
Glasgow G1 1X3

J. J. Gurney

Geochemistry Department
University of Cape Town
Rondebosch 7700
South Africa

The concept that primitive mantle carbon can be characterized by a single carbon isotope ratio around which relatively small variations occur can no longer be accepted without question.

Carbon isotope studies of intrusive and extrusive carbonatites and carbonate tuffs indicate that there is a north - south trending zone of carbonatites in East Africa, between the Eastern and Western Rift, which is characterized by average carbon isotopic compositions between -2.4 and -4.4 o/oo vs. PDB. Eastern and Western Rift carbonatites on the other hand show carbon isotopic compositions between -5 and -8 o/oo vs. PDB. Investigations of the carbon isotopic composition of well characterized diamonds have shown that there are small but significant differences in the mean ¹³C-content of diamonds suites from different diatremes. For example: Premier -4.87 ± 1.87 o/oo vs. PDB (n = 176), Finsch -5.99 ± 1.11 o/oo vs. PDB (n = 93), Dan Carl -3.34 ± 0.95 o/oo vs. PDB (n = 91), Koffiefontein -5.52 ± 2.07 o/oo vs. PDB (n = 56), New Elands -5.53 ± 0.69 o/oo vs. PDB (n = 18). In the sample suites from these kimberlites highly ¹³C depleted diamonds are absent or rare. A larger number of such specimens has been found, however, among samples from the Roberts Victor and the Orapa kimberlite.

In the sample suite from the Roberts Victor kimberlite diamonds with peridotitic inclusions show a narrow range -5.43 ± 0.94 o/oo vs. PDB (n = 65). Diamonds containing eclogitic inclusions can be subdivided on the basis of their carbon isotopic composition into two groups: Group-A, -15.52 ± 0.40 o/oo vs. PDB (n = 10); Group-B, -5.89 ± 0.39 o/oo vs. PDB (n = 3). Within each group the isotopic composition variation is rather small. Comparison of the chemical composition of clinopyroxenes from diamonds of Group-A and Group-B reveals significant differences. Clinopyroxenes from diamonds of Group-A are enriched in Al, Fe, and Mn and depleted in Si, Mg, and Ca compared to clinopyroxenes from Group-B diamonds. The latter are in composition similar to those of the clinopyroxenes from graphite-diamond eclogites. Corresponding compositional grouping are observed for the garnet inclusions. The difference in composition between the inclusions from the two groups is very much larger than the variations generally produced during igneous fractionation processes. Hence it is not likely that the two groups are related through a single such process.

Among the close to 200 garnets from eclogite xenoliths that have been analyzed by Hatton (1978) there is only one that has Fe and Mn enrichments that are similar to those observed in the inclusions in diamonds. This particular garnet occurs within a larger clinopyroxene. Since the enclosing clinopyroxene does not show a similar extreme enrichment in these two elements disequilibrium between host and inclusion is suggested. One might hence interpret the garnet inclusion in the clinopyroxene as a

relict of an earlier crystallization event in which the inclusions found in the Group-A diamonds were also formed.

As from the Roberts Victor kimberlite eclogites have been described that show unusual oxygen isotopic compositions it is of interest to investigate whether there is any reason to suggest that the unusual carbon and oxygen isotopic compositions might be related. The compositions of the garnets and clinopyroxenes from diamond inclusions have been compared in terms of ACF components with the bulk compositions of the eclogite xenoliths whose oxygen isotopic composition have been measured. It is found that the bulk compositions deduced from the inclusions in diamonds of a carbon isotopic composition of -15 o/oo vs. PDB are akin to compositions of eclogites that have oxygen isotopic compositions around 6 o/oo vs. SMOW (normal mantle). Bulk compositions deduced from graphite-diamond eclogites with carbon isotopic compositions of about -5 o/oo vs. PDB are similar to those of eclogites with oxygen isotopic compositions of about 3 o/oo vs SMOW (^{18}O depleted compared to normal mantle). More recently acquired data (McGregor private communications) indicate that clinopyroxenes depleted in ^{18}O with respect to normal mantle compositions have FeO and MnO contents that are generally lower than those of clinopyroxenes from eclogites of normal oxygen isotopic compositions and very much lower than those of the clinopyroxenes from ^{13}C -depleted diamonds. Hence the available data do not point to an association between the depletion in the heavy isotopes of carbon and oxygen in the eclogitic material from the Roberts Victor kimberlite.

The carbon isotopic composition of diamonds from the Orapa kimberlite shows a range from -2.5 to 22.5 o/oo vs. PDB ($n = 148$). Within this range one may distinguish 4 modes. Mode-1 (M1) occurs between -4 to -8.5 o/oo (75 samples), Mode-2 (M2) between -9 and -12.5 o/oo (10 samples), Mode-3 (M3) between -13 to -16.5 o/oo (21 samples), and Mode-4 (M4) between -16.5 to -20.5 o/oo (35 samples). There are insufficient data to establish whether there are additional modes at -2.5 to -3.5 o/oo (3 samples) or -21 to -22.5 o/oo (4 samples). The chemical composition of the inclusions may differ depending on the carbon isotopic composition of the host. For example 4 olivine samples coming from hosts belonging to M1 have a mean forsterite content of $92.72 \pm 0.45\%$ while an olivine from a host belonging to M4 has the lowest forsterite content (92.2) of the samples suite. Five orthopyroxenes ($\text{SiO}_2 = 55.03 \pm 0.66$, $\text{Al}_2\text{O}_3 = 0.56 \pm 0.18$, $\text{FeO} = 11.91 \pm 2.50$, $\text{MgO} = 30.19 \pm 1.70$) from hosts belonging to M4 have notably lower silica, alumina and magnesia and higher iron content than the pyroxene ($\text{SiO}_2 = 56.9$, $\text{Al}_2\text{O}_3 = 0.82$, $\text{FeO} = 4.62$, $\text{MgO} = 35.9$) from a host belonging to M1. In both cases the minerals from the ^{13}C depleted hosts show higher iron contents. No hosts belonging to M4 containing chromites were found, however 6 chromites from hosts belonging to M1 show lower alumina and higher titanium contents than a chromite from a diamond belonging to M2.

The most common inclusion mineral in the samples suite from Orapa is garnet. Within some of the carbon isotopic composition modes different garnet composition groups may be recognized; some of them may occur in several of the ^{13}C modes. One can distinguish a group of garnets whose compositions is very similar to that of the garnets in graphite and diamond eclogites (E); it occurs in modes M1, M2, M3, and M4. We may also distinguish a second group (P), occurring, only in M1 characterized by lower iron and higher chrome contents and compositionally akin to the peridotitic garnets frequently encountered among the Premier and Finsch kimberlite diamond inclusions and associated there with iron depleted olivines. In modes M3 and M4 a third compositional group of garnets can be distinguished, which has a lightly lower chrome and much higher iron content than the normal P-Type garnets. Several of the garnets belonging to this compositional group coexists with orthopyroxenes, one with clinopyroxene. The mean composition of five garnets ($\text{SiO}_2 = 40.25 \pm 0.54$, $\text{TiO}_2 = 0.73 \pm 0.26$, $\text{Al}_2\text{O}_3 = 19.63 \pm 1.39$, $\text{Cr}_2\text{O}_3 = 2.93 \pm 1.64$, $\text{FeO} = 14.29 \pm 2.80$, $\text{MnO} = 0.54 \pm 0.11$, $\text{MgO} = 16.82 \pm 1.83$, $\text{CaO} = 4.16 \pm 1.14$) from hosts belonging to M4 is very similar to the mean composition of garnets from three peridotite xenoliths from the Matsoku pipe which show the highest iron contents ($\text{SiO}_2 = 40.83 \pm 0.45$, $\text{TiO}_2 = 0.33 \pm 0.02$, $\text{Al}_2\text{O}_3 = 20.67 \pm 1.13$, $\text{Cr}_2\text{O}_3 = 2.94 \pm 1.63$, $\text{FeO} = 13.06 \pm 0.11$, $\text{MnO} = 0.38 \pm 0.2$, $\text{MgO} = 17.17 \pm 0.26$, $\text{CaO} = 4.38$; Cox et al., 1973). A corresponding similarity is found for the pyroxenes. A comparison of the whole rock compositions of these rocks with the various estimates that have been made for the composition of

primitive mantle indicates that they fall within the range of postulated mantle compositions.

We conclude that the association of ^{13}C depleted diamonds with garnets of compositions that are generally considered as representing most fertile mantle is evidence that ^{13}C depleted carbon is a primary constituent of the mantle underlying the Orapa Kimberlite. Very special circumstances would have to prevail in order that a subduction process would result in the very close correspondence in chemical composition between the garnets from highly ^{13}C depleted diamonds and those from the most fertile ultramafic xenoliths, in particular the combination of high Fe/Mg ratio with moderate chrome contents.

On the basis of the data for the Roberts Victor and Orapa diamonds we suggest that in the mantle regions exists which can show considerable ^{13}C depletion and which can be identified at two localities that are separated by about 1000 km. At a particular locality there can be characteristic chemical signatures associated with the ^{13}C depletion. The common chemical feature that has been observed at the Orapa and Roberts Victor kimberlite is a relative increase in the iron content of the minerals included in the ^{13}C depleted diamonds. Attempts to find a direct link between ^{13}C depletion and a subduction process have not been successful. In view of the general similarity of the carbon isotope distribution in diamonds and meteorites and the association of some of the highly ^{13}C depleted carbon with chemical compositions that are thought to be characteristic for undifferentiated mantle we propose that part of the isotope variability and ^{13}C depletion of diamonds is derived from inhomogeneities remaining from the original accretion of the Earth.

REFERENCES

- Cox, K.G., Gurney J.J. and Harte B. (1973) Xenoliths from the Matsoku Pipe; in: Lesotho Kimberlites. ed. P.H. Nixon, P. 76 - 100.
- Hatton C.J. (1978) The Geochemistry and Origin of Xenoliths from the Roberts Victor Mine. Unpublished Ph.D. Thesis Department of Geochemistry of the University Cape Town, 179 pp.

AND THE AGE OF DIAMONDS

T. Evans

Department of Physics, University of Reading,
Berkshire, RG6 2AB.

J.W. Harris

Department of Applied Geology, University of Strathclyde,
Glasgow, G1 1XJ.INTRODUCTION

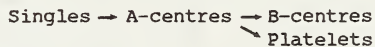
Most diamonds contain significant amounts of nitrogen as a major impurity and the commonest are termed Type I(a). The nitrogen is present in several distinct aggregation states. Pairs of nitrogen atoms are called A-centres, N₃ centres contain three nitrogen atoms and B-centres consist of four nitrogen atoms and a vacancy. Transmission electron microscopy as well as infrared absorption techniques also indicate that Type I(a) diamonds usually contain platelets present in the cube planes.

When synthetic diamonds containing nitrogen are grown (at about 1500°C and 5GPa), the nitrogen is incorporated in the diamond lattice as single substitutional atoms. In the same way, it is assumed that nitrogen atoms were similarly sited when natural diamond grew. If an extended period of residence in the Upper Mantle then follows, the nitrogen would diffuse to form the various types of aggregate. The amount of aggregation that occurs would depend upon the initial nitrogen concentration, the temperature that was encountered in the Upper Mantle and the time spent at that temperature before quenching by eruption to the Earth's surface.

The work presented here shows how the nitrogen aggregation characteristics obtained from infrared spectroscopy, can be linked through kinetic equations and activation energy values to either the temperature of equilibration or the geological age of a diamond.

THE AGGREGATION PROCESS, THE KINETICS AND INFRA-RED SPECTROSCOPY

Evans and Qi (1982) studied the aggregation process in the laboratory by heating synthetic diamonds containing dispersed nitrogen at temperatures between 1500°C and 2500°C under stabilizing pressures. All the types of nitrogenous aggregates that are found in Type I(a) natural diamonds were reproduced and a sequence of aggregation proposed.



Initially, single substitutional nitrogen aggregates to form A-centres with an activation energy of 5eV. The process obeys second order kinetics according to the formula.

$$\frac{dC}{dt} = -K C^2 \quad \text{where } K = A \exp \left[-\frac{E}{kT} \right] \quad \text{and } Kt = \frac{1}{C} - \frac{1}{C_0}$$

K = the rate constant; A = a constant; E = activation energy; C = the single nitrogen concentration after heating at the temperature T for time t; C₀ = the initial single nitrogen concentration. Values of K were determined at different temperatures.

The A-centres, in turn, aggregate to form B-centres and a side reaction is the formation of N₃ centres. Unfortunately, an activation energy for this process could not be determined in the laboratory owing to the unreliability of the temperature measurements above 2200°C, although using natural diamonds in heating experiments, some rates of aggregation were determined between about 2500°C and 2800°C.

Both the A- and B-centre nitrogen in Type I(a) diamond absorb infrared radiation in the so-called one phonon region between $7\mu\text{m}$ (wavenumber 1417cm^{-1}) and $10\mu\text{m}$ (wavenumber 1000cm^{-1}). A perfect diamond would be transparent in this region. Using the method described by Clark and Davey (1984) the absorption characteristics of Type I(a) diamond in this region can be decomposed into three spectra, named A and B, with a minor component D, the latter probably due to platelets (Woods 1986). The nitrogen concentrations in the A- and B-centres is found by using the formulae

$$\mu_{1282}^A = 300 N_A \quad \text{and} \quad \mu_{1282}^B = 80 N_B$$

where μ_{1282}^A and μ_{1282}^B equals the absorption coefficient in cm^{-1} due to the A- and B-centres respectively, at the wavenumber 1282cm^{-1} (equivalent to $7.8\mu\text{m}$) and N_A and N_B are the concentrations respectively of nitrogen atoms present in the A- and B-centres in atomic percent (Kaiser and Bond (1959), Evans and Qi (1982)). Thus the total nitrogen concentration can be determined. In addition the A/B ratio at 1282cm^{-1} can be obtained and this ratio is a measure of the conversion of nitrogen in A-centres to nitrogen in B-centres. For example, diamond with an A/B ratio of 1, has about 80% of A-centres aggregated to form B-centres.

RESULTS

Four diamonds were investigated. F13 and F39 are 'peridotitic' suite diamonds from the Finsch Mine (see Gurney *et al.* 1979); diamond XM48 was released from a common coarse-grained garnet lherzolite xenolith with that designation, also from Finsch (Shee *et al.* 1982) and the fourth diamond was recovered from a Type II eclogite xenolith XRV247 from Roberts Victor (Robinson (1977)).

For the Finsch diamonds, an equilibration temperature of 1130°C and a pressure of 5 to 5.3GPa was assigned (Shee *et al.* 1982) with a model age of 3300Ma (Richardson *et al.* 1984). For F39 these pieces of information were used in conjunction with the nitrogen aggregation results to determine an activation energy for the aggregation of A-centres to B-centres assuming that this aggregation process obeys second order kinetics. An A/B ratio at 1282cm^{-1} of 8.05 was measured from the decomposed infrared absorption spectrum and a nitrogen concentration of 0.02 at.% determined. An activation energy of 6.83eV was calculated. To see if this value is reasonable, a temperature of equilibration for F13 was determined. The infrared absorption spectrum gave an A/B ratio of 15.3 with nitrogen concentration of 0.015 at.%. Assigning a model age of 3300Ma and an activation energy of 6.83eV an equilibration temperature of 1120°C was obtained in good agreement to the proposed equilibration of 1130°C given by Shee *et al.* (1982).

A temperature of 1130°C was also determined for the equilibration of xenolith XM48 from Finsch (Shee *et al.* 1982). Thus the age of the diamond from XM48 could be compared to the 3300Ma age obtained for the 'peridotitic' diamond suite at that mine. From the infrared absorption spectrum an A/B ratio of 4.7 was measured with a nitrogen concentration of 0.097 at.%. Using the equilibration temperature of 1130°C a model age of 1100Ma was determined. (If a model age of 3300Ma was assigned, then an equilibration temperature of 1050°C would result which is rather a large discrepancy from the suggested 1130°C). Thus it appears that XM48 has a younger model age than such 'peridotitic' diamonds as F39 or F13.

For the Roberts Victor eclogite xenolith XRV247, an equilibration temperature of 1024°C at 3GPa or 1115°C at 6GPa was calculated using the method of Ganguly (1979) with a minimum theoretical temperature at the diamond-graphite intercept at 1062°C . Taking the method of Ellis and Green (1979) temperatures for the same pressures were 985°C and 1088°C respectively with the diamond-graphite intercept occurring at 1027°C . As there is no pressure calibration available there are two ways of considering the probable temperature. An average of the two minimum temperatures is 1045°C . On the other hand, if it is assumed that, as at Finsch, the diamond grew at a pressure of 5GPa the average temperature obtained by the two equilibration methods is 1069°C . The age of the eclogite xenoliths at Roberts Victor have been determined by Kramers (1979) as 2465Ma. Although HRV247 was not one of the xenoliths to be age-dated, it is likely to have an age of 2465Ma in view of the very wide selection process in which five of the six xenoliths chosen were Type II; similar to HRV247. From the infrared absorption spectrum an A/B ratio of 11.1 was obtained with a nitrogen concentration of 0.11 at.%. Using the age of 2465Ma and activation energy of 6.83eV , a calculated equilibration temperature of

1087°C was obtained. Thus it appears reasonable that the growth and equilibration took place at a pressure of slightly above 5GPa, say between 5.5 and 6.0GPa at a temperature of about 1090°C.

CONCLUSIONS

The examination of these four diamonds shows that it is reasonable to relate the aggregation of nitrogen in Type I(a) diamonds to geological information. Some caution, however, must be exercised in using this relationship. It is based upon the assumption that total nitrogen concentration can be obtained from infrared absorption data and that the A-centre to B-centre aggregation step obeys second order kinetics. There is mounting evidence that at later stages of the aggregation sequence further reaction, other than those described here, takes place and that some of the nitrogen becomes optically inactive. It is suggested that fairly reliable information about equilibration temperatures and/or geological ages can be obtained by considering the aggregation of nitrogen in diamond providing that the A/B ratio at 1282cm⁻¹ is greater than 2. This ensures that no optically inactive nitrogen is present and the aggregation process described above is appropriate. This limitation is not serious as a large majority of African diamonds have an A/B ratio of greater than 2.

REFERENCES

- CLARK, C.D. and DAVEY, S.T., 1984. One-phonon infrared absorption in diamond. *Journal of Physics*, C17, 1127-1140.
- DAVIS, G.L., 1977. The ages and uranium contents of zircons from kimberlites and associated rocks. *Extended Abstract*. 2nd International Kimberlite Conference, Santa Fe, Mexico.
- ELLIS, D.J. and GREEN, D.H., 1979. An experimental study of the effect of Ca upon garnet-clinopyroxene Fe-Mg exchange equilibria. *Contributions to Mineralogy and Petrology*, 71, 13-22.
- EVANS, T. and QI, Z., 1982. The kinetics of the aggregation of nitrogen atoms in diamond. *Proceedings Royal Society London*, A381, 159-178.
- GANGULY, J., 1979. Garnet and clinopyroxene solid solutions and geothermometry based on Fe-Mg distribution coefficient. *Geochimica Cosmochimica Acta*, 43, 1021-1029.
- GURNEY, J.J., HARRIS, J.W. and RICKARD, R.S., 1979. Silicate and oxide inclusions in diamonds from the Finsch kimberlite pipe. In: Boyd, F.R. and Meyer, H.O.A. (Eds.): *Kimberlites, Diatremes and Diamonds*. American Geophysical Union, pp. 1-15.
- KAISER, W. and BOND, W.L., 1959. Nitrogen a major impurity in common type 1 diamonds. *Physical Review*, 115, 857-863.
- KRAMERS, J.D., 1979. Lead, uranium, strontium, potassium and rubidium in inclusion-bearing diamonds and mantle-derived xenoliths from Southern Africa. *Earth and Planetary Science Letters*, 42, 58-70.
- RICHARDSON, S.H., GURNEY, J.J., ERLANK, A.J. and HARRIS, J.W., 1984. Origin of diamonds in old enriched mantle. *Nature*, 310, 198-202.
- ROBINSON, D.N., 1977. Diamond and graphite in eclogite xenoliths from kimberlite. *Extended Abstract*. 2nd International Kimberlite Conference, Santa Fe, Mexico.
- SHEE, S.R., GURNEY, J.J. and ROBINSON, D.N., 1982. Two diamond-bearing peridotite xenoliths from the Finsch kimberlite, South Africa. *Contributions to Mineralogy and Petrology*, 81, 79-87.
- WOODS, G.S., 1986. Platelets and the Infrared absorption of type 1a diamonds. *Proceedings Royal Society London*, A, In Press.

MINERAL INCLUSIONS IN DIAMONDS FROM KOFFIEFONTEIN MINE.

J.J. GURNEY, J.W.HARRIS¹, R.S. RICKARD, P. CARDOSO².

Department of Geochemistry, University of Cape Town, Rondebosch 7700,
South Africa.

¹Department of Applied Geology, University of Strathclyde,
Glasgow G1 1XJ, United Kingdom.

²De Beers Marine (Pty) Ltd. Olivetti House, Hertzog Blvd.
Cape Town, South Africa.

The composition of 78 mineral inclusions recovered from 54 Koffiefontein diamonds have been determined by electron microprobe. Based on these analyses and observations on 938 diamonds with mineral inclusions it is clear that sulphides are most common and that peridotitic minerals are much more abundant than their eclogitic counterparts. (see Table 1.) (This study does not deal with the sulphides any further).

The peridotitic and eclogitic inclusions at Koffiefontein have compositions which cover almost the full range found in inclusions world-wide. (Meyer H.O.A. 1986).

The peridotitic garnets (n=14) have a range in Mg/Mg+Fe from 84.0 to 92.6, in CaO from 3.5 to 8.7 wt%. The latter is rather lower than average. Four garnets plot on the hercynite trend. The olivines (n=15) have the normal Mg-rich compositions (Fo 91.6 - Fo 95.4). The Cr₂O₃ contents range up to a value of 0.15 wt%. CaO can also be high for a mantle olivine but both the inclusions with the highest CaO (0.13 and 0.16 wt%) occurred in diamonds with black fracture flaws so this could be related to secondary processes. The orthopyroxenes (n=12) are enstatites (En 92.6 - En 95.8) with a low CaO content (0.13 - 0.78 wt%) which decreases with increasing Mg/Mg+Fe ratio. Al₂O₃ ranges from 0.30 to 0.90 wt% with a single exception which co-exists with ferro-periclase and has an Al₂O₃ of 1.16 wt%. Cr₂O₃ ranges from 0.07 to 0.57 wt%. In the majority of cases (n=7) [Al+Cr-Na] at. prop. is restricted to the narrow range of 0.030 - 0.037 suggesting a limited amount of variation in garnet s.s. and therefore a modest crystallisation pressure interval. The single chromite has 63.3 wt% Cr₂O₃ and 0.1 wt% TiO₂. The chromiferous peridotitic clinopyroxenes have very high K₂O contents. (see Table 2). The assigned peridotitic paragenesis is strengthened by the presence of two inclusions of K-rich pyroxene with olivine in one diamond (K-18). The only other apparently peridotitic inclusions found in this study are four ferro-periclases which have been confirmed by X-ray diffraction and are described in detail elsewhere in this volume. (Moore et al.)

The eclogitic garnet inclusions have a wide range in CaO, MgO and particularly FeO. They are characterised by low Cr₂O₃ (nd - 0.85 wt%), minor TiO₂ (0.07 - 0.76 wt%) and Na₂O (up to 0.34 wt%), all of which are typical of diamond inclusions and Type I eclogite garnets. The eclogitic clinopyroxenes also show a wide range in compositions. They all have minor TiO₂ (0.13 - 0.42 wt%). Na₂O (1.4 - 4.6 wt%) and Al₂O₃ (2.7 - 7.9 wt%) are in a few cases low for eclogitic clinopyroxene diamond inclusions. (cf Meyer H.O.A. 1986). K₂O contents range up to 0.23 wt%.

In contrast to many other diamond inclusion suites the Koffiefontein mineral inclusions provide a number of examples of disequilibrium assemblages in single diamonds. In all three cases where two inclusions of the same mineral were recovered from one diamond the individual grains had different compositions. (see Table 3). In one case (K-37) two radically different garnets coexist with the same clinopyroxene generating tie lines with very different slopes. Since one more gar-cpx pair (K-16) generates a similar cross-cutting tie line it may be yet another instance of disequilibrium between co-existing phases.

Calculated equilibration conditions for co-existing mineral pairs are given in Table 4. Obviously diamonds with disequilibrium assemblages do not give valid answers. They are included in the Table to show the magnitude of the errors which can result from

this source. The minerals found, their relative abundances, and their compositions suggest garnet hartzburgite (gar,opx,olv), garnet lherzolite (gar,cpx,opx,olv) and eclogite parageneses for the diamonds with a very minor chromite hartzburgite field. The peridotitic parageneses predominate. This is a common association. The high K₂O contents of the peridotitic clinopyroxenes have never previously been reported. The presence of ferro-periclasite is also unusual and noteworthy because this mineral is stable at very high pressures, and may be an important phase in the lower mantle. Calculated equilibration temperatures for both peridotitic and eclogitic mineral pairs are so low that they are close to or below current estimates of the mantle solidus. Since crystallographic evidence strongly argues against a metamorphic origin for diamonds volatile induced small volume partial melting and/or metasomatic processes must be invoked.

Table 1. (A) Relative diamond inclusion abundances based on observations and analytical determinations from the Koffiefontein Mine.

<u>Sulphides</u>	<u>Perid.</u>	<u>Ecl.</u>	<u>graph.</u>	<u>Clouds</u>	<u>(Ec/Ec+Perid.)%</u>
397	277	22	66	176	7

(B) Relative proportions of peridotite silicate minerals in Koffiefontein diamonds.

<u>Observed Abundances</u>				<u>Calculated Proportions</u>			
<u>gar.</u>	<u>cpx.</u>	<u>colourless</u>	<u>ratio</u> *	<u>gar.</u>	<u>cpx.</u>	<u>opx.</u>	<u>olv.</u>
		<u>opx + olv</u>	<u>opx/olv</u>				
47	5	222	10:12	17.2	1.8	36.8	44.2

* Determined from 22 diamonds and 27 inclusions.

Table 2. Peridotitic clinopyroxenes in Koffiefontein diamonds.

	<u>K13</u>	<u>K14</u>	<u>K15</u>	<u>K18a</u>	<u>K18b</u>
SiO ₂	55.00	54.70	55.10	54.30	54.80
TiO ₂	.07	n.d.	n.d.	n.d.	n.d.
Al ₂ O ₃	2.14	1.55	1.37	.68	.72
Cr ₂ O ₃	3.66	.89	.75	2.44	2.34
FeO	1.75	2.40	2.69	1.91	2.28
MnO	.08	.09	.09	.08	.11
MgO	16.60	18.50	18.30	17.50	19.10
CaO	18.30	20.10	19.20	20.30	17.90
Na ₂ O	2.35	.45	1.22	.33	.30
K ₂ O	.04	.79	.31	1.57	1.68
Total	99.99	99.50	99.04	99.11	99.26

Table 3. Disequilibrium in Koffiefontein diamond inclusions.

	<u>K18a.</u>	<u>K18b.</u>	<u>K19a.</u>	<u>K19b.</u>	<u>K37a.</u>	<u>K37b.</u>
SiO ₂	54.30	54.80	38.70	39.20	40.70	38.00
TiO ₂	n.d.	n.d.	.07	.07	.38	.13
Al ₂ O ₃	.68	.72	22.40	22.40	22.40	21.60
Cr ₂ O ₃	2.44	2.34	n.d.	n.d.	.20	.04
FeO	1.91	2.28	24.00	21.30	16.20	22.90
MnO	.08	.11	.61	.38	.25	.42
MgO	17.50	19.10	9.63	10.60	15.40	7.36
CaO	20.30	17.90	4.13	5.45	4.05	8.00
Na ₂ O	.33	.30	.08	.20	.18	.07
K ₂ O	1.57	1.68				
Total	99.11	99.26	99.63	99.60	99.76	98.57

n.d. = not detected

Table 4.

Calculated conditions of equilibration for Koffiefontein
diamond inclusions.

<u>Diamond Number</u>	<u>Mineral Pair</u>	<u>T^oC</u>	<u>Method</u>	<u>Pkb.</u>	<u>Method</u>	<u>Probable paragenesis</u>
K10	Gar-Olv	940	OW 79	50	Assumed	Gar-Harz
K11	Gar-Olv	1180	OW 79	50	Assumed	Gar-Harz
K48	Gar-Olv	1157	OW 79	50	Assumed	Gar-Harz
K47	Gar-Opx	1086	MG 78	50	NG 85	Gar-Harz
K2	Gar-Opx	1156	MG 78	57	NG 85	Gar-Lherz
K9	Gar-Opx	1116	MG 78	49	NG 85	Gar-Lherz
K46	Gar-Opx	1014	MG 78	45	NG 85	Gar-Lherz
K13	Cpx only	1094	LD 76	-	None	Gar-Lherz
K14	Cpx only	1109	LD 76	-	None	Gar-Lherz
K15	Cpx only	1143	LD 76	-	None	Gar-Lherz
K8	Gar-Cpx	1016	EG 79	50	Assumed	Eclogite
K16*	Gar-Cpx	895	EG 79	50	Assumed	Eclogite
K41	Gar-Cpx	1221	EG 79	50	Assumed	Eclogite
K42	Gar-Cpx	1220	EG 79	50	Assumed	Eclogite
K43	Gar-Cpx	1231	EG 79	50	Assumed	Eclogite
K56	Gar-Cpx	1160	EG 79	50	Assumed	Eclogite

Disequilibrium Assemblages.

K18	Olv-Cpx	1033	LD 76	-	None	Gar-Lherz
K18	Olv-Cpx	1233	LD 76	-	None	Gar-Lherz
K37	Gar-Cpx	1189	EG 79	50	Assumed	Eclogite
K37	Gar-Cpx	860	EG 79	50	Assumed	Eclogite

* K16 tie line parallels K37 disequilibrium tie line, which cross cuts other tie lines. Possibly K16 gar-cpx pair are not in equilibrium either, providing an explanation for the very low calculated T.

EG 79 = Ellis and Green 1979

OW 79 = O'Neill and Wood 1979

LD 76 = Lindsley and Dixon 1976

MG 78 = Mori and Green 1978

NG 85 = Nickel and Green 1985

REFERENCES

- ELLIS D.J. and GREEN D.H. 1979. An experimental study of the effect of Ca upon garnet-clinopyroxene Fe-Mg exchange equilibria. *Contributions to Mineralogy & Petrology*, 71, 13-22.
- LINDSLEY D.H. and DIXON S.A. 1976. Diopside-enstatite equilibria at 850-1400°C, 5-35 kb. *American Journal of Science* 276, 1285-1301.
- MEYER H.O.A. 1986. (in press) Inclusions in diamond. *Mantle Xenoliths.* (ed. P.H. NIXON.) Wiley & Son.
- MORI T. and GREEN D.H. 1978. Laboratory duplication of phase equilibria observed in natural garnet lherzolites. *Journal Geology* 86, 83-97.
- NICKEL K.G. and GREEN D.H. 1985. Empirical geothermobarometry for garnet peridotites and implications for the nature of the lithosphere, kimberlites and diamonds. *Earth and Planetary Science Letters* 73, 158-170.
- O'NEILL H.S.C. and WOOD B.J. 1979. An experimental study of Fe-Mg partitioning between garnet and olivine and its calibration as a geothermometer. *Contributions to Mineralogy & Petrology* 70, 59-70.

J J Gurney* and C J Hatton

*Department of Geochemistry, University of Cape Town, Rondebosch 7700
South Africa

Bushveld Economic Research Unit, University of Pretoria, Pretoria 0001
South Africa

INTRODUCTION

Star Mine is located towards the eastern end of a series of East/West trending dykes and dyke enlargements situated approximately 15 km north east of Theunissen (O.F.S., Rep. S. Africa). The main 'Byrnes Dyke' is a micaceous kimberlite with an average diamond grade of not less than 0.4cts. per tonne which has proved economically viable and produces extremely good quality stones of excellent shape and colour. One characteristic of the production is the scarcity of yellow diamonds. This kimberlite occurrence has many similarities with the better described Bellsbank Fissure system. It has been classified petrographically as a Type II kimberlite and assigned a 124 m.y. (K/Ar) age by other workers. Garnet and chromite are significant components of the mantle derived heavy mineral fraction in the Byrnes kimberlite but ilmenite is very rare.

DIAMOND INCLUSIONS

Reconnaissance observations of the inclusions (in only 59 diamonds) suggest that peridotitic minerals predominate. There is a major component of chromites. Eclogitic mineral inclusions have been observed in minor amount.

DIAMONDIFEROUS MINERALS

Twenty-two small (<2cm) samples of silicate minerals which have diamonds embedded chiefly in their outer surfaces have been found at Star.

In contrast to the diamond inclusions, these macrocrysts have a predominantly eclogitic association: one consists of eclogitic garnet, clinopyroxene and diamond, and nineteen are eclogitic garnets with one or more diamonds protruding from each grain.

One specimen (JJG1250) is a peridotitic garnet with diamond and the last one remaining to be described (JJG1245) consists of a diamond embedded in a cluster of mica crystals.

The mineral compositions are given in Table I.

Nineteen of the twenty eclogitic garnets form a coherent main grouping in terms of chemical composition. The major variations can be expressed in terms of a negative correlation between calcium and magnesium within a narrow band of relatively constant iron contents. Similar garnets have been noted in diamond eclogites from Roberts Victor and the Crown Mine which like Star are north and east of Kimberley. Similar garnet compositions have also been reported in non-diamond bearing eclogite xenoliths at Premier Mine.

The field defined by the main Star grouping is outside the field of compositions of eclogitic garnets found in diamonds world-wide. It is also different to the fields defined by garnets in diamond eclogite from kimberlites in the Barkly West area, from Orapa, Botswana and particularly from Mir, U.S.S.R.

The single iron rich garnet in the sample suite described here (JJG1251) is well separated from the other garnets in the main trend and does fall within the diamond inclusion field.

All the eclogitic garnets have detectable sodium (up to 0.10 wt % Na₂O) and although titanium is lower than usual for diamond eclogite there is a linear (1:1)

Table I. Diamondiferous Minerals from Star Mine

Sample No	1232	1233	1234	1235	1236	1237	1238	1239
Oxide. Wt %	Gar.	Gar.	Gar.	Gar.	Gar.	Gar.	Gar.	Gar.
SiO ₂	42.0	41.0	41.4	41.0	41.3	41.4	41.4	40.7
TiO ₂	0.10	0.09	0.08	0.07	0.08	0.06	0.06	0.14
Al ₂ O ₃	24.1	23.6	23.8	23.8	23.9	23.7	23.6	23.3
Cr ₂ O ₃	0.09	0.10	0.11	0.08	0.08	0.11	0.11	0.01
FeO	9.86	7.80	8.98	6.77	8.41	9.50	7.41	10.6
MnO	0.19	0.18	0.17	0.12	0.17	0.18	0.13	0.17
MgO	18.4	12.7	14.8	13.7	14.6	16.6	14.7	12.5
CaO	6.56	15.3	11.6	14.8	12.6	8.68	12.4	13.2
Na ₂ O	0.06	0.09	0.06	0.08	0.05	0.04	0.06	0.09
K ₂ O	ND	ND	ND	ND	ND	ND	ND	ND
P ₂ O ₅	0.04	0.11	0.03	0.03	0.05	0.03	0.04	0.09
Total	101.4	101.0	101.0	100.4	101.2	100.3	99.9	100.8

Sample No	1240	1241	1242	1243	1244	1245	1246	1247
Oxide. Wt %	Gar.	Gar.	Gar.	Gar.	Gar.	Phlog	Gar.	Gar.
SiO ₂	40.9	41.1	41.2	41.1	40.7	39.5	41.1	41.1
TiO ₂	0.11	0.08	0.07	0.06	0.10	0.85	0.07	0.08
Al ₂ O ₃	23.3	23.7	23.9	23.9	23.5	16.2	24.0	23.6
Cr ₂ O ₃	0.03	0.03	0.07	0.08	0.13	0.36	0.05	0.07
FeO	7.53	9.36	9.89	7.71	8.27	3.97	10.4	8.31
MnO	0.14	0.18	0.23	0.13	0.18	0.04	0.19	0.18
MgO	12.4	14.1	17.6	12.3	14.6	24.3	16.0	15.0
CaO	15.1	11.5	6.46	15.7	12.1	0.03	9.07	12.3
Na ₂ O	0.04	0.08	0.06	0.10	0.06	0.19	0.08	0.07
K ₂ O	ND	ND	ND	ND	ND	10.5	ND	ND
P ₂ O ₅	ND	0.08	0.08	0.18	0.08	ND	0.10	ND
Total	99.5	100.2	99.6	101.2	99.7	95.9	101.1	100.7

Sample No	1248	1248	1249	1250	1251	1252	1253
Oxide. Wt %	Gar.	Cpx.	Gar.	Gar.	Gar.	Gar.	Gar.
SiO ₂	41.5	56.2	41.7	42.3	40.9	41.6	40.8
TiO ₂	0.13	0.14	0.08	0.02	0.04	0.08	0.08
Al ₂ O ₃	23.7	11.8	23.4	21.6	23.2	23.2	23.4
Cr ₂ O ₃	0.04	0.05	0.05	3.48	0.29	0.05	0.08
FeO	9.86	1.86	10.2	6.61	15.8	8.91	7.47
MnO	0.16	0.01	0.22	0.26	0.26	0.17	0.13
MgO	14.1	10.4	15.3	20.8	16.2	14.4	12.5
CaO	11.6	14.2	8.54	5.06	3.70	11.6	15.8
Na ₂ O	0.08	6.41	0.13	ND	0.09	0.05	0.06
K ₂ O	ND	0.02	ND	ND	ND	ND	ND
P ₂ O ₅	0.08	ND	0.02	0.02	0.02	0.04	0.06
Total	101.2	101.1	99.6	100.2	100.5	100.1	100.4

relationship between (Ti + P) and Na. In addition none of the garnets have excess silica therefore the trace levels of sodium in the garnets cannot be attributed to pyroxene solid solution as was the case for inclusions in diamonds from the nearby Monastery Mine.

CONCLUSIONS

The co-existing gar-cpx pair in sample JJG1248 gives an apparent equilibration temperature of 1100°C (EG79, 50 kb).

The single peridotitic garnet with diamonds (JJG1250) has a composition which suggests it is derived from disaggregated garnet lherzolite. In southern Africa diamondiferous garnet lherzolite has been described from Mothae and Finsch by others.

The origin of the phlogopite - diamond sample JJG1245 is not clear. However phlogopite is a rarely reported inclusion in diamond so it is possible that the association is primary.

The kimberlite at Star contains macrocrysts of garnet and fragments of eclogite with garnets which have the same compositions as the garnets with the diamonds listed in Table I. This suggests that disaggregation of eclogite is a common source of diamonds in the intrusion. However since most of the specimens described here have well developed kelyphite rinds on their rounded outer surfaces it is clear that the break up of the xenoliths occurs during or prior to emplacement of the kimberlite and is not related to the mining process. Sub-calcic G10 garnets and chromites with >62.5 wt % Cr₂O₃ are also found in the Star kimberlite. Their presence is usually diagnostic of the peridotitic diamond paragenesis. Several sets of observations therefore suggest the presence of both eclogitic and peridotitic diamonds at Star as has been reported at many other localities. It is not possible to define the relative importance of the two parageneses but the finding of twenty samples of diamondiferous eclogitic minerals suggests that disaggregation of eclogite provides an important component of the diamonds at this locality. In this respect it adds to a growing list of localities which are emphasising the importance of eclogite as a diamond source. (Orapa, Premier, Monastery, Bellsbank, Dokolwayo and Sloan).

The differences in compositions noted between most of the garnets described here and eclogitic garnet inclusions in diamonds world-wide is attributed to re-equilibration of the xenocrysts post-diamond crystallisation, and to the armouring effects of the host diamond in respect of the inclusions.

The regional trends in composition of xenocrystal and xenolithic eclogitic garnets noted earlier suggest that the diamondiferous eclogite bodies sampled by the kimberlites have had different post-diamond crystallisation histories.

A COMPARISON OF CHARACTERISTICS OF DIAMONDS

FROM THE ORAPA AND JWANENG KIMBERLITE PIPES IN BOTSWANA

J.W. Harris

Department of Applied Geology, University of Strathclyde,
Glasgow, G1 1XJ.

J.B. Hawthorne

Consulting Geologist Department, Anglo-American Corporation,
P.O. Box 61587, Johannesburg 2107, Republic of South Africa.

M.M. Oosterveld

Computer Services Department, De Beers Consolidated Mines Ltd.,
P.O. Box 616, Kimberley, Republic of South Africa.

INTRODUCTION

As part of a continuing research programme to define diamond populations from kimberlites and lamproites, the physical characteristics of the diamonds from the Jwaneng and Orapa mines in southwest and northeast Botswana, respectively, have been classified. As with previous investigations, the procedures used are those outlined by Harris *et al.* (1975) with additional physical properties discussed in Harris *et al.* (1984) also being applied. With one exception, the results are determined as a function of diamond size. In all, five characteristics are used to define the two diamond populations: crystal form, colour, ultraviolet fluorescence, levels of plastic deformation and, specifically in the -7+5 diamond sieve size classes (maximum circular sieve diameter ranging from 2.16 to 1.83mm), the syngenetic inclusion abundances.

CRYSTAL FORM

JWANENG 1982

FORM AS FUNCTION
OF SIZE

ORAPA 1983

FORM AS FUNCTION
OF SIZE

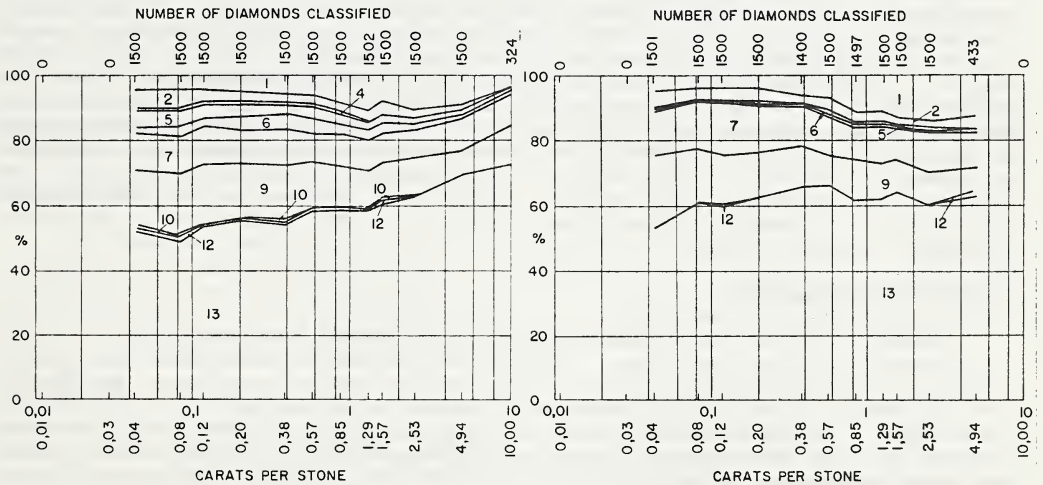


Fig. 1

1. octahedra; 2. dodecahedra; 4. cubo-octahedra; 5. cubo-dodecahedra; 6. cubes;
7. macles; 9. irregulars; 10. cubo-octa-dodecahedra; 12. tetrahexahedra;
13. polycrystalline aggregates. (For a full listing see Harris *et al.* (1984)).

At both mines aggregated diamonds comprise about 60% of the productions with cube or cube-related shapes constituting a significant minor form. The latter are

minor form. The latter are approximately four times more common (8%) at Jwaneng than Orapa. Other shape characteristics differ overall by less than 5%. A notable absence from both productions are flattened dodecahedra (see Fig. 1).

COLOUR

JWANENG 1982

COLOUR AS A FUNCTION OF SIZE

ORAPA 1983

COLOUR AS A FUNCTION OF SIZE

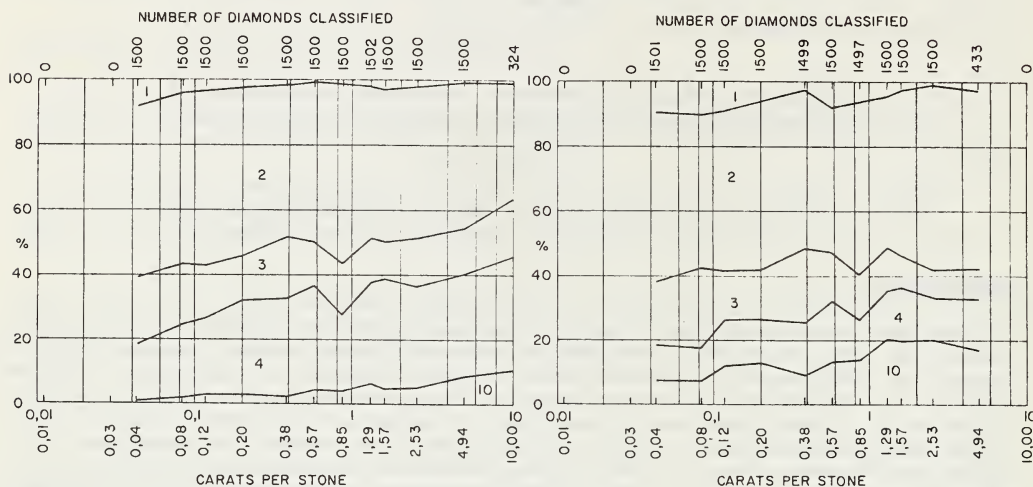


Fig. 2

1. colourless; 2. yellow; 3. brown; 4. transparent green-coated; 10. steel grey or grey. (For a full listing see Harris *et al.* 1984).

The similarity between the proportions of colourless yellow and brown diamonds at both mines is evident in Figure 2. With increasing diamond size, the proportion of colourless diamonds steadily decreases from just under 10% to about 2%. Yellow diamonds have an equal overall average of 50%. The 17% proportion of brown diamonds at Jwaneng varies insignificantly with diamond size but a steady decrease is seen at Orapa from 25% to 9%. Principal colour variations are the 10% overall differences between the proportions of transparent green coated and grey diamonds. With the former, levels are constant at Jwaneng but slightly increase with increasing diamond size at Orapa. These proportional differences reflect local variations in the movement of radioactive groundwaters through the epiclastic sediments above the diatremes from which the diamonds were recovered. The distinct proportional increase in steel grey and grey diamonds with increasing diamond size corresponds to the higher levels of bort or industrial diamonds at Orapa than Jwaneng.

ULTRAVIOLET FLUORESCENCE

Figure 3 shows distinct characteristics with diamonds from Jwaneng being 40% less fluorescent than those from Orapa. Light blue fluorescence predominates with yellow, orange and green fluorescence constituting less than 10% for both mines (see Fig. 3). The dominance of light blue fluorescence is related to the dominance of yellow diamonds (see before). The marked differences in fluorescence levels, however, suggests that at Jwaneng, nitrogen impurities in N3 centres (which mostly give rise to yellow diamonds) are also accompanied by high levels of nitrogen in A-centres, because the latter, quenches blue luminescence and thereby makes a stone non-fluorescent (Davies and Thomaz, 1979).

PLASTIC DEFORMATION

Over the major part of both productions plastic deformation levels are independent, of diamond size, averaging 8.05% (σ 1.19) at Jwaneng and 11.73% (σ 1.99) at Orapa. For both mines no specific relationship between diamond colour and plastic deformation was

found. The present values are the lowest so far recorded and, as elsewhere, show that deformation largely post-dates diamond formation (see Harris *et al.* (1984)).

JWANENG 1982

UV COLOURS AS A FUNCTION OF SIZE

ORAPA 1983

UV COLOURS AS A FUNCTION OF SIZE

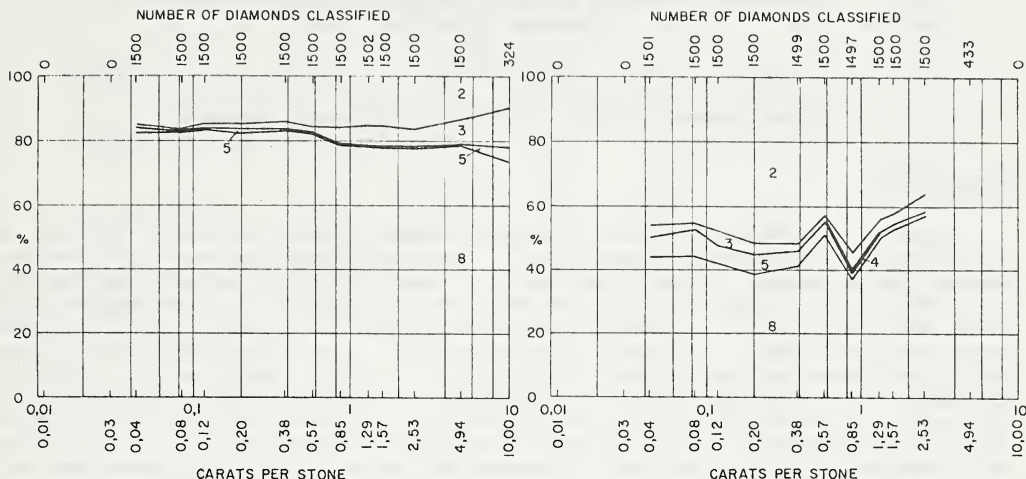


Fig. 3

2. light blue; 3. yellow; 4. green; 5. orange; 8. non-fluorescent.
 (For a full listing see Harris *et al.* (1983)).

SYNGENETIC INCLUSION ABUNDANCES

A visual evaluation of tens of thousands of diamonds from both mines shows a distinct difference in inclusion abundance as follows:-

Jwaneng: eclogitic 38.5%; peridotitic 41.9%; sulphides 19.8%

Orapa: eclogitic 65.4%; peridotitic 19.6%; sulphides 15.0%

For Orapa, the proportions have been slightly modified after analysis of the inclusions (Gurney *et al.* (1984)) and in view of the high 'eclogitic' content of Jwaneng similar changes may also occur when these inclusions are analysed.

CONCLUSIONS

Compared to diamond production in other parts of southern Africa, distinctive characters at Jwaneng and Orapa are; 1) high levels of a) aggregated and cube-shaped diamonds, b) transparent green coated stones and c) light blue fluorescent diamonds; 2) the low levels of plastic deformation; and 3) a dominant eclogitic inclusion suite at Orapa and equally high eclogitic and peridotitic paragenesis at Jwaneng.

REFERENCES

DAVIES, G. and THOMAZ, M.F. 1979. The N₃ centre Diamond Research, 79, 18-24.
 GURNEY, J.J., HARRIS, J.W. and RICKARD, R.S. 1984. Silicate and oxide inclusions in diamonds from the Orapa mine, Botswana. In: Kornprobts, J. (Ed.): Kimberlites, Vol. II: The mantle and crust-mantle relationships. Elsevier: Holland, pp. 3-9.
 HARRIS, J.W., HAWTHORNE, J.B., OOSTERVELD, M.M. and WEHMEYER, E. 1975. A classification scheme for diamond and a comparative study of South African diamond characteristics. In: Ahrens, L.H., Dawson, J.B. and Erlank, A.J. (Eds.): Physics and Chemistry of the Earth, Vol. 9. Pergamon: Oxford, pp.765-783.
 HARRIS, J.W., HAWTHORNE, J.B. and OOSTERVELD, M.M. 1984. A comparison of diamond characteristics from the De Beers Pool mines, Kimberley, South Africa. Annales Scientifiques de l' Universite de Clermont-Ferrand II, 74, 1-13.

FROM KNOWN SOURCES

J.W. Harris

Department of Applied Geology, University of Strathclyde,
Glasgow, G1 1XJ.

P.M. Spear

Diamond Research Centre, Maidenhead, Berkshire, SL6 6JW.

INTRODUCTION

Nitrogen is a major impurity in natural diamond with, occasionally, as much as 0.5at.% being present (Burgermeister 1979). In the one-phonon region of the spectrum, between $7\mu\text{m}$ (wavenumber 1417cm^{-1}) and $10\mu\text{m}$ (wavenumber 1000cm^{-1}), infrared spectroscopy most definitively identifies this element and a classification scheme is well established (Robertson *et al.* 1934). Two main types are recognised; Type I (nitrogen containing) and Type II (no detectable nitrogen). Type I diamonds are further sub-divided according to whether the nitrogen is single substitutional (Type Ib diamonds), or whether the nitrogen is aggregated within the carbon lattice (Type Ia diamonds). Nitrogen aggregation occurs principally in either the A-form (a nitrogen pair) or the B-form (a more complicated arrangement, but probably four nitrogen atoms and a vacancy). In addition, Type Ia diamonds may contain a so-called platelet peak and have N3 centres (triangles of nitrogen). With Type II diamonds the vast majority are subdivided into Type IIa but the rare Type IIb diamonds, which electrically conduct, have considerable importance as heat sinks (see Bibby 1982).

The amount of nitrogen within Type Ia diamonds can be determined by decomposing the infrared spectra (Davies 1981, Evans and Qi 1982). Both methods involve the absorption peak at $7.8\mu\text{m}$ (1282cm^{-1}) which is related to the total nitrogen present. With careful preparation, errors in nitrogen values range from $\pm 7\%$ for pure Type IaA diamonds to $\pm 25\%$ for pure Type IaB. As the majority of Type Ia diamonds have mixtures of both A- and B-centre nitrogen, but generally with Type IaA dominant, an average error of between 12 to 15% in the nitrogen value is likely. A measure of which centre is dominant is obtained from the ratio of the principal A- and B-peaks, the ratio for pure Type IaA being approximately 2.0 and for pure Type IaB being approximately 0.36.

The work reported here is an investigation into the prevalence, amount and aggregation state of nitrogen in representative inclusion-bearing diamonds from seven kimberlites in southern Africa and one lamproite from western Australia with the objective of determining inter-relationships.

RESULTS

Some general relationships are recorded in Table 1. Of the two diamond parageneses, 'eclogitic' diamonds are more commonly Type I, with the exception of Roberts Victor. With respect to Type II diamonds, they are: a) commonest in the 'peridotitic' paragenesis with the exception of Jagersfontein, b) rare in sulphide-bearing diamonds except at Jagersfontein. Nitrogen levels in 'peridotitic' diamonds (DeBeers Pool excepted) show a marked positive skewness with the vast majority having $<300\text{ppm}$. This skewness is independent of which inclusion paragenesis is dominant. A positive skewness, but with a much longer tail (up to 1700ppm) is also present among the 'eclogitic' diamonds at Koffiefontein, Jagersfontein, Roberts Victor and Argyle but not at the remaining mines, where the distribution is even over the same ppm values. With nitrogen in sulphide-bearing diamonds Jagersfontein and Argyle show positive skewness, but for the other mines nitrogen ranges evenly up to a maximum of 2100ppm .

In terms of the nitrogen aggregation states, no distinctions are apparent between the three recognised assemblages in the presently-available data set. Overall, diamonds from DeBeers Pool and Roberts Victor are the most dominantly Type IaA and

TABLE 1
 Inclusion-bearing diamonds: P = peridotitic; E = eclogitic; S = sulphide
 Diamond sizes range from 1.09mm (-2+1) to 2.46mm (-9+7)

SOURCE	Diamond Size	Approx. % inclusion abundance	Number studied	TYPE I	TYPE II	% of diamond with <300ppm N ₂
Premier	P -6+5	40	36	28	8 (22%)	83
	E -6+5	60	131	129	2 (2%)	24
Finsch	P -6+5	97	80	57	23 (29%)	88
	E -6+5	3	12	12	- -	20
Koffiefontein	P -6+5	31	38	28	10 (26%)	80
	E -6+5	2	22	21	1 (4%)	77
	S -6+5	66	62	60	2 (3%)	33
Jagersfontein	P -5+3		22	18	4 (18%)	86
	E to	No data	16	11	5 (31%)	75
	S -2+1		23	16	7 (30%)	61
Roberts Victor	P -6+5	78	62	48	14 (23%)	84
	E -6+5	12	14	4	10 (71%)	79
	S -6+5	10	20	19	1 (5%)	40
DeBeers Pool	P -6+5	88	58	56	2 (3%)	24
Orapa	P -6+5	20	22	20	2 (9%)	54
	E to	65	33	33	- -	25
	S -9+7	15	19	19	- -	16
Argyle	P -6+5	11	11	10	1 (9%)	64
	E to	76	76	76	- -	83
	S -9+7	13	14	14	- -	71

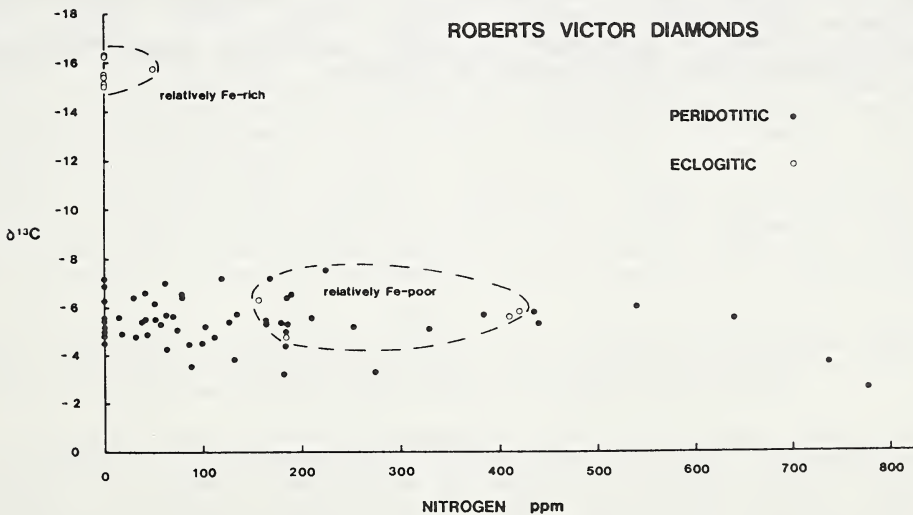


Fig. 1
 Nitrogen concentration versus $\delta^{13}\text{C}$ for inclusion-bearing diamonds Roberts Victor

Argyle the most dominantly Type IaB. For the remaining mines, nitrogen aggregations are broadly spread between Type IaA and Type IaB. The relationship between Type IaB diamonds and relatively low nitrogen levels can be clearly demonstrated at Argyle (see Table 1 and data in Harris and Collins 1985). Plots of ratios of principal absorption peaks also indicate that the path of nitrogen aggregation in diamond, as proposed by Brozel *et al.* (1978), is incorrect for the step from A- to B-centres.

Figure 1 is an example of how the nitrogen signatures from the mines studied can further help define the growth environment of diamond. The 'eclogitic' diamonds at Roberts Victor can be separated into two distinct sub-populations and, furthermore, the chemistry of the inclusions associated with these sub-populations indicate that one environment is more Fe-rich. The figure also illustrates the general lack of correlation between $\delta^{13}\text{C}$ and nitrogen concentration for the predominant 'peridotitic' diamond paragenesis.

CONCLUSION

From the data reported here, no distinctions between different diamond sources on the basis of nitrogen characteristics are apparent. So far, no single relationship correlates amount and/or aggregation state of nitrogen to diamond paragenesis. Combining nitrogen with $\delta^{13}\text{C}$ values from the same diamonds allows sub-populations within a particular paragenesis to be recognised. The role of nitrogen in mantle processes associated with diamond is, therefore, complex and a full elucidation of this element will require integrated studies of both carbon and nitrogen isotopes as well as work into phase systems such as C-H-N-O.

REFERENCES

- BIBBY, D.M. 1982. Impurities in Natural Diamond. *Chemistry and Physics of Carbon*, 18, 3-91.
- BROZEL, M.R., EVANS, T. and STEPHENSON, R.F. 1978. Partial dissociation of nitrogen aggregates in diamond by high temperature-high pressure treatments. *Proceedings Royal Society, London*, A361, 109-127.
- BURGERMEISTER, E.A. 1979. Thermal conductivities of diamonds with absorption at 3.22 μm . *Nature*, 279, 785-786.
- DAVIES, G. 1981. Decomposing the IR absorption spectra of diamonds. *Nature*, 290, 40-41.
- EVANS, T. and QI, Z. 1982. The kinetics of aggregation of nitrogen in diamond. *Proceedings Royal Society, London*, A381, 159-178.
- HARRIS, J.W. and COLLINS, A.T. 1985. Studies of Argyle diamonds. *Industrial Diamond Review*, 3/85, 128-130.
- ROBERTSON, D., FOX, J.J. and MARTIN, A.E. 1934. Two types of diamond. *Philosophical Transactions Royal Society London*, A232, 463-538.

Mark D. Kurz

Department of Chemistry
 Woods Hole Oceanographic Institution
 Woods Hole, Massachusetts 02543
 U.S.A.

John J. Gurney

Department of Geochemistry
 University of Capetown
 Rondebosch 7700
 South Africa

Helium measurements in igneous rocks and minerals have been extensively used in recent years to constrain the origin of mantle gases. Because the helium isotopic composition of a gas sample is generally a measure of the time-integrated $^3\text{He}/(^{\text{Th}} + ^{\text{U}})$ ratio of its source, high $^3\text{He}/^4\text{He}$ ratios can be used to infer the presence of a primitive or undegassed mantle source. Extremely high $^3\text{He}/^4\text{He}$ ratios in diamonds have been reported by Ozima and coworkers (1983) that place important constraints on the origin of diamond. The highest $^3\text{He}/^4\text{He}$ ratios that they observed (up to 290 x atmospheric), are significantly higher than any terrestrial igneous signature. In addition, they found a range in $^3\text{He}/^4\text{He}$ ratios of almost 10^{-4} in a suite of samples from various localities.

In an effort to understand the relationships between these data and the origin of diamond, we have performed detailed helium isotopic studies on a suite of large (1 carat) diamonds from a single kimberlite pipe (Orapa, Botswana). In order to determine the distribution of helium within the diamonds, we performed vacuum crushing experiments on a number of stones. Although significant amounts of helium are released by crushing (10^{-9} to 10^{-7} ccSTP/gram), in all cases this constituted less than 10 per cent of the total. Because crushing selectively releases gas from inclusions, we infer that most of the helium within diamond is contained by the diamond matrix.

Step heating experiments on small inclusion-free fragments indicate that individual diamonds contain dramatic internal variability with respect to $^3\text{He}/^4\text{He}$. The experiments were performed by heating the diamonds in two carefully controlled temperature steps (at 2000°C). In the first step, the diamonds are partially graphitized, and the helium released has quite low $^3\text{He}/^4\text{He}$ ratios (.05 to 3 times atmospheric). In the second step, the diamonds are completely graphitized, and extremely high $^3\text{He}/^4\text{He}$ ratios are observed (30 to 80 times atmospheric). The $^3\text{He}/^4\text{He}$ ratio released by this procedure can differ by up to a factor of 100 within a single diamond. We interpret these results to indicate that helium is zoned within the diamonds. The first graphitization step selectively releases the helium associated with defects, because graphitization begins at defects within the diamond. The later graphitization step releases helium from relatively defect free zones in the diamond. This explanation is supported by preliminary dissection experiments on single stones.

This behavior is observed in diamonds that contain peridotitic and eclogitic mineral inclusions, and the helium data does not at present differ between these two types. There appears to be some correlation to crystal form in that polycrystalline aggregates display lower $^3\text{He}/^4\text{He}$ ratios than the octahedral growth forms.

Although the recent discovery of cosmogenic helium in rocks (Kurz, 1986) provides a new mechanism for generating high $^3\text{He}/^4\text{He}$ ratios, this does not appear to be relevant to the present samples due to the depth of the kimberlite pipe. However, preliminary calculations suggest that the high $^3\text{He}/^4\text{He}$ ratios could be produced by $^6\text{Li}(n, \alpha)\text{T} \rightarrow ^3\text{He}$ within the mantle source, if Li contents are several ppm and the source region is enriched in Th and U.

The large helium isotopic variability within single diamonds has important implications. First, it suggests that much of the isotopic variability is caused by ingrowth of radiogenic ^4He , and that Th and U are zoned within single diamonds. Therefore, helium may possibly be used to date individual diamonds. In addition, if the explanation for the heterogeneity given here is correct, the highest $^3\text{He}/^4\text{He}$ ratios may be found in those diamonds with the fewest defects.

REFERENCES

- OZIMA M., ZASHU O. AND NITOH O. 1983. $^3\text{He}/^4\text{He}$ ratio, noble gas abundance and K-Ar dating of diamonds. *Geochimica et Cosmochimica Acta* 47, 2217-2224.
- KURZ, M. D. 1986. Cosmogenic helium in a terrestrial igneous rock. *Nature* 320, 435-439.

T. E. McCandless¹ and D. S. Collins²¹University of Cape Town, South Africa, ²United States Geological Survey, Denver, Colorado

Numerous kimberlites have produced peridotite and eclogite xenoliths with diamond present as a primary mineral. Most of these xenoliths come from South Africa and the USSR, although one diamondiferous peridotite comes from Australia, and one has been found in southern Wyoming, USA (Hall and Smith, 1984; McCallum and Eggler, 1976). In this study we examine in detail the first diamond-graphite eclogite reported in North America; from the Sloan 2 kimberlite in northern Colorado, USA (Collins, 1982).

Xenolith TP121 is a small subangular fragment, roughly two centimeters in diameter and weighing just over 32 grams. The rock is coarse-grained, with orange, subhedral garnets set in a matrix of mostly altered clinopyroxene. Texturally, it is a group I eclogite (MacGregor and Carter, 1970).

Four diamonds 1-2 mm in size are exposed at the surface of the eclogite. from 1-2 mm. Two are octahedra, with little or no effects of resorption. A third octahedron is slightly resorbed and has a graphite mass which wraps around the corner of the stone and curves into the altered clinopyroxene matrix. The fourth diamond is a fragment which is broken off at the surface of the nodule. Graphite comprises 5% of the rock, occurring as plates and masses up to 2 mm in size. The graphite has forms similar to those observed for primary graphite in eclogites from Orapa (Robinson et al, 1984).

Microprobe analysis of the eclogite in thin section indicates heterogeneity in the minerals. The garnets contain 46-55% pyrope, 30-33% almandine, and 14-20% grossular. Garnet grains taken from the nodule surface have higher grossular and almandine contents than those in thin section, with 44-45% pyrope, 34% almandine, and 22% grossular. The clinopyroxenes are omphacitic, with jadeite components from 35-42%, diopside-hedenbergite from 47-54%, and enstatite-ferrosilite from 8-10%. Pyroxenes taken from the nodule surface are higher in jadeite (41-43%) and lower in diopside-hedenbergite (44-46%) than grains in thin section. Values of 0.07-0.12% K₂O in the clinopyroxene and 0.09-0.11% Na₂O in the garnet classify the nodule as a group I eclogite, and are in the range for diamondiferous eclogites from other localities (McCandless and Gurney, this volume). K₂O in the clinopyroxene was found to vary with respect to crystal orientation, with the highest values produced from crystal surfaces at 90° to the z-axis. Secondary minerals include spinel and phlogopite after garnet, and a fine-grained diopside after omphacite. The diopside is depleted in K₂O, and is higher in diopside-hedenbergite (60-79%) and lower in jadeite (2-18%) than the fresh omphacites. Veins containing vermiculite, carbonate, an unidentified Ca-Al silicate, magnetite, and amphibole are also present, and have been introduced presumably from metasomatizing fluids or kimberlite magma.

Using the geothermometer of Ellis and Green (1979), for mineral compositions measured in the interior of the xenolith, temperatures from 1080-1140°C (average 1112°C) are obtained at 50 kb. This agrees with temperatures of 1088-1114°C at 50 kb, obtained from eclogitic inclusions in diamonds from the Sloan 1 kimberlite (Otter and Gurney, this volume). Temperatures calculated from garnet and pyroxene grains taken from the nodule surface are significantly higher, from 1144-1205°C (average 1174°C).

Extreme variability can be encountered during diamond eclogite formation, and involves fluctuations in temperature, pressure, and oxygen fugacity, occurring over long periods of time before the eclogites are finally brought to the surface in an ascending magma (Haggerty, 1986). Such processes are evident in the case of nodule TP121. The graphite crystals probably formed in a liquid, where their growth was not restricted by the presence of other solid phases. Diamonds also formed at this time. The eclogite was subsequently exposed to metasomatism and/or decompression melting, with spinel and phlogopite forming after garnet and diopside forming after omphacite. Veins of micaceous minerals, magnetite, and amphibole also developed. Higher temperatures obtained from the nodule surface indicate that the surface reequilibrated probably during transport in the kimberlite. Secondary phases produced by metasomatism were subsequently replaced by vermiculite and carbonate as a result of weathering processes.

Recent studies of mantle eclogites from Colorado-Wyoming kimberlites have shown a lack of group I eclogites (Ater, 1982; Ater et al., 1984). The diamond-graphite eclogite TP121 is a group I eclogite, both in textural and chemical characteristics (MacGregor and Carter, 1970; McCandless and Gurney, 1986). It is believed that metasomatism and/or decompression melting, coupled with abrasion in the kimberlite, and weathering since the Devonian, have made the group I eclogites from the xenolith suite in Colorado-Wyoming kimberlites very rare.

A metamorphic origin has been postulated for the Colorado-Wyoming eclogites, as group I eclogites were absent, and no differentiation trend could be recognized for the different chemical groups (Ater et al., 1984). Recalculated temperatures for the Colorado-Wyoming eclogites at 50kb show that several could have formed at conditions similar to those inferred for TP121 and for eclogitic inclusions in diamond (Fig. 1). These may be transitional to the group I eclogites which it is proposed formerly existed in the mantle. Hatton and Gurney (1986) have proposed a model for eclogites at Roberts Victor, in which group I eclogites formed from a volatile-induced differentiated magma, which in turn provided the heat and volatiles necessary to form a suite of undifferentiated group II eclogites from partial melting, metamorphism, and contamination of the overlying garnet lherzolite. Such a model, though on a smaller scale, may apply to the Colorado-Wyoming eclogites. It is not unreasonable that eclogites (and diamonds) may have formed under both metamorphic (Haggerty, 1986) or igneous (Sunagawa et al., 1984) conditions, and until further evidence of group I eclogites is found, such a model for eclogites from Colorado-Wyoming kimberlites must remain speculative.

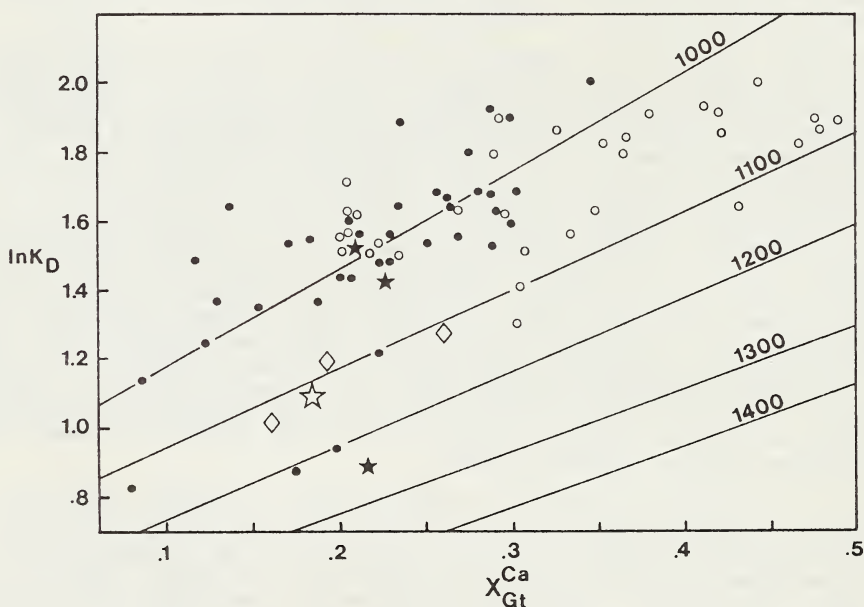


Figure 1. $\ln K_D$ versus X_{Ca}^{Gt} garnet at 50kb for diamond-graphite nodule TP121 (open star), eclogitic inclusions in diamonds (diamonds), and eclogites from Colorado-Wyoming kimberlites; including bimineralic (solid circles), kyanite-bearing (open circles), and graphite-bearing (solid stars). Data from this study; Otter and Gurney, 1986; Ater, 1982.

REFERENCES

- ATER, P. C. 1982. Petrology and geochemistry of eclogite xenoliths from Colorado-Wyoming kimberlites. M. S. Thesis, Colorado State University, Fort Collins, Colorado.
- ATER, P. C. EGGLER, D. H. and MCCALLUM M. E. 1984. Petrology and geochemistry of mantle eclogite xenoliths from Colorado-Wyoming kimberlites: recycled ocean crust? In Kornprobst, J. ed, Kimberlites II: The Mantle and Crust-Mantle Relationships. Elsevier, New York, pp.309-318.
- COLLINS, D. S. 1982. Diamond collecting in northern Colorado. The Mineralogical Record, 13, 4, pp.205-208.
- ELLIS, D. J. and GREEN, D. H. 1979. An experimental study of the effect of Ca upon garnet-clinopyroxene Fe-Mg exchange equilibria. Contributions to Mineralogy and Petrology, 71, pp. 13-22.
- HAGGERTY, S. E. 1986. Diamond genesis in a multiply-constrained model. Nature 320, 34-38.
- HALL, A. E. and SMITH, C. B. 1984. Lamproite diamonds: are they different? In Glover, J. E. and Harris, P. G., eds, Kimberlite Occurrence and Origin: Conceptual Models in Exploration. University Extension, University of Western Australia, 167-212.
- HATTON, C. J. and GURNEY, J. J. 1986. Roberts Victor eclogites and their relation to the mantle. In Nixon, P. H. , ed., Mantle Xenoliths, John Wiley.
- MACGREGOR I. D. and CARTER, J. L. 1970. The chemistry of clinopyroxenes and garnets of eclogite and peridotite xenoliths from the Roberts Victor mine, South Africa. Physics of the Earth and Planetary Interiors, 3, pp. 391-397.
- MCCALLUM, M. E. and EGGLER, D. H. 1976. Diamonds in an upper mantle peridotite nodule from kimberlite in southern Wyoming. Science 192, 673-684.
- ROBINSON, D. N., GURNEY, J. J., and SHEE, S. R. 1984. Diamond eclogite and graphite eclogite xenoliths from Orapa, Botswana. In Kornprobst, J. Ed., Kimberlites II: The Mantle and Crust-Mantle Relationships, Developments in Petrology IIB, Elsevier, New York, pp. 11-24.
- SUNAGAWA, I., TSUKAMOTO, K. and YASUDA, T. 1984. Surface microtopographic and x-ray topographic study of octahedral crystals of natural diamond from Siberia. In Sunugawa, I. ed, Materials Science of the Earth's Interior. pp.331-349. D. Reidel Publishing Company.

Department of Geochemistry, University of Cape Town, Rondebosch, South Africa.

PHYSICAL CHARACTERISTICS OF THE DIAMONDS

The general quality of Monastery diamonds is extremely poor. A size analysis based on 4600 carats of general mine production revealed the diamonds to display a gaussian size distribution with a mode in the size range $-11 +9$ (~3mm). A large proportion of the diamonds are almost devoid of primary crystal form, and the majority exhibit some form of breakage surface often accompanied by the effects of severe resorption. The diamonds are colourless or shades of brown in approximately equal proportions. Yellow diamonds are conspicuously absent. A wide variety of surface features are represented, with trigons, hexagonal etch pits, corrosion sculptures and shallow depressions being the most common.

MINERAL INCLUSIONS

A sample of 131 inclusion-bearing diamonds have been categorised as eclogitic, peridotitic and miscellaneous, the latter category comprising inclusions of uncertain paragenesis as well as sulphide inclusions.

Miscellaneous Inclusions

The majority of the fifty inclusions assigned to this category are accounted for by sulphide (30) and Fe-oxide (14) inclusions. Other phases represented include plagioclase (1), zircon (1), phlogopite (1) and moissanite (3). Minerals represented under the broad term of Fe-oxide include magnetite (9), spinel (6), hematite (6), ilmenite (1) and magnesio-wustite (1). The high incidence of black spots and impurities in Monastery diamonds made correlation between the inclusions observed within the diamond with iron-oxide inclusions liberated upon diamond destruction extremely difficult. In many cases, it was not possible to claim with confidence that a particular inclusion was derived from a primary setting within the diamond. A small number of magnetite inclusions were however found in association with primary sulphide inclusions. Furthermore, the primary nature of a small proportion of monomineralic magnetite inclusions was beyond dispute. In view of the lack of any compelling evidence in support of a primary origin for the spinel, hematite and ilmenite inclusions, they are considered to be epigenetic. The plagioclase ($An_{68.3} Ab_{31.0} Or_{0.7}$) and phlogopite inclusions were both recovered from diamonds hosting eclogitic inclusions but neither were observed within the diamonds prior to their destruction. A single zircon of primary nature was recovered and identified by means of qualitative microprobe techniques. The magnesio-wustite and three moissanite (SiC) inclusions are discussed in an accompanying paper (Moore et al., this volume).

Peridotitic Paragenesis

Inclusions of peridotitic affinity are poorly represented. The majority of olivines (5 out of 6) exhibit a restricted compositional range ($For_{90.0}$ to 91.6), the sixth is $For_{94.9}$. A single peridotitic clinopyroxene is a chrome diopside with 2.00 wt.% Cr_2O_3 , 1.69 wt.% Al_2O_3 and 20.34 wt.% CaO. The one peridotitic garnet recovered coexists with an olivine ($For_{91.6}$). Distinguishing features of the garnet composition include high levels of SiO_2 and TiO_2 (43.77 wt.% and 0.51 wt.% respectively) as well as slight enrichments in FeO and CaO (7.23 wt.% and 3.66 wt.% respectively) compared to characteristic "G10" garnets of the harzburgitic paragenesis. The pair yields a calculated equilibration temperature (O'Neill and Wood, 1979) of 1173°C (for $P = 50$ kbars). A temperature estimate based on the Ca/(Ca+Mg) ratio of the Cr-diopside inclusion (Lindsley and Dixon, 1976) is 1002°C.

Eclogitic Paragenesis

Fifty-six eclogitic garnets fall into two distinct populations. One group of 10 (Group A) have compositions similar to other localities. They contain detectable

quantities of Na₂O (0.04 to 0.25 wt.%) and widely ranging concentrations of MgO, FeO and CaO. Furthermore, most are chemically indistinguishable from the garnets in Group I eclogite nodules at Monastery. The second group of 46 (Group B) form a related suite of compositions that appear to reflect the effects of pyroxene solid solution in the garnets (Moore and Gurney, 1985). Extreme concentrations of Si and Al range to as high as 47.43 wt.% SiO₂ and as low as 11.29 wt.% Al₂O₃. Sodium is also present in extremely high concentrations, ranging to 1.03 wt.% Na₂O. Since the solid solution of pyroxene in garnet is a predominantly pressure dependent reaction (Ringwood, 1967), it has been suggested that the Group B garnets have an extremely deep origin (Moore and Gurney, 1985). Eclogitic clinopyroxenes (N=15) display a wide range in chemical composition. The majority are chemically indistinguishable from eclogitic clinopyroxenes included in diamond from other localities. Three have anomalously high Al₂O₃ concentrations (11.83 to 12.46 wt%) in combination with low Na₂O contents (0.78 to 2.49 wt.%) indicating the presence of the Ca-tschermakite molecule. The clinopyroxenes from eclogite nodules at Monastery exhibit restricted compositions within the range displayed by the clinopyroxene inclusions. The possibility exists that some of the diamonds hosting Group A garnets as well as a minority of clinopyroxene bearing diamonds have been derived by disaggregation of diamondiferous Type I eclogite. However, this do not represent the major source of eclogitic diamonds at Monastery. Two orthopyroxenes are highly aluminous (4.1 and 11.8 wt.% Al₂O₃) and have Mg/(Mg+Fe) ratios of 0.83 and 0.85 respectively. Both orthopyroxenes were observed to coexist with phases of eclogitic affinity indicating that the garnet websterite association reported for inclusions in diamonds from Orapa (Gurney et al. 1984) is also present at Monastery. Two inclusions of SiO₂ have been recovered. Their primary nature within the host diamonds argues in favour of them being coesite rather than quartz. A single primary corundum inclusion hosting only TiO₂ (3.05 wt.%) as an impurity has also been recovered.

Seven cases of individual diamonds yielding multiple inclusions of the same phase which display dramatic differences in composition have emerged in this study. In five of the diamonds, garnet is the responsible phase, while two cases involving eclogitic clinopyroxene have also been detected. The compositional discrepancies far exceed statistical analytical error, with variances of 30 relative percent being common. Episodic diamond growth (Meyer, 1985) within an environment of rapidly changing chemical composition is favoured as the most likely mechanism to account for the compositional variations.

Coexisting mineral phases useful for geothermobarometric calculations were found to be extremely rare in this study. Compounding this problem was the fact that in two of the diamonds hosting coexisting pairs, one of the phases was represented by two inclusions which displayed chemical disequilibrium. Moreover, two of the garnet-clinopyroxene pairs are represented by group B garnets. The temperatures calculated from these pairs are considered to be geologically meaningless because the presence of pyroxene in solid solution in these garnets violates the basic assumptions of the geothermometers. Two clinopyroxene-orthopyroxene pairs of eclogitic affinity yield calculated equilibration temperatures (Lindsley and Dixon, 1976; 20 kbars) in the region of 1415°C. The high Al content of the orthopyroxenes is consistent with a high temperature origin.

One diamond was found to host an olivine (Fog_{4.9}) and a group B eclogitic garnet. This phenomenon has now been observed by three other authors (Prinz et al., 1975; Hall and Smith, 1984 and Otter and Gurney, this volume), and it is considered that genuine cases of mixed paragenesis diamonds do occur.

The formation pressures indicated by the group B garnets are in the range 60 to approximately 140 kbars (estimated from the experimental data Akaogi and Akimoto, 1979 and Irifune et al., 1986). These diamonds thus provide an important sampling of the deep upper mantle or transition zone, the structure and composition of which is currently under debate (see review by Anderson and Bass, 1986). If the Group B diamonds were formed in a lithospheric environment then ultra-deep subcontinental root zones are implied (e.g. Jordan, 1981). However, these diamonds could have been derived from an asthenospheric source. Recent plate tectonic reconstruction models have indicated a possible correlation between South Atlantic hotspots and the Cretaceous kimberlites within southern Africa (e.g. Crough et al., 1980; Duncan, 1981). Furthermore, le Roex (Nature, submitted) has recently demonstrated chemical correlations between both Group I and II kimberlites and the South Atlantic hotspots, implying asthenospheric source

regions for both groups. The possibility thus exists that Group B diamonds have formed in association with a rising diapir directly related to hotspot activity. The ultimate source of the diapir could be:

- (i) a megalith of accumulated recycled (subducted) oceanic lithosphere positioned at the base of the upper mantle (Ringwood, 1982) or convectively downrafted subcontinental lithosphere as envisaged by McKenzie and O'Nions (1983).
- (ii) primordial or near primordial mantle upwelled from the mesosphere (Morgan, 1971). Assuming the Monastery kimberlite (a Group I kimberlite, Smith, 1983) itself represents a product of the same hotspot, then a near primordial source would be the most applicable since it would be consistent with the geochemical characteristics of Group I kimberlite (le Roex, op cit).

REFERENCES

- AKAOGI, M. and AKIMOTO, S. 1979. High pressure phase equilibria in a garnet lherzolite, with special reference to Mg^{2+} - Fe^{2+} partitioning among constituent minerals. **Physics of the Earth and Planetary Interiors**, 19, 31-51.
- ANDERSON, D.L. and BASS, J.D. 1986. Transition region of the Earth's upper mantle. **Nature**, 320, 321-328.
- CROUCH, S.T., MORGAN, W.J. and HARGRAVES, R.B. 1980. Kimberlites: their relation to mantle hotspots. **Earth and Planetary Science Letters**, 50, 260-274.
- DUNCAN, R.A. 1981. Hotspots in the southern oceans - an absolute frame of reference for motion of the Gondwana continents. **Tectonophysics**, 74, 29-42.
- GURNEY, J.J., HARRIS, J.W., RICKARD, R.S. 1984. Silicate and oxide minerals in diamonds from the Orapa Mine, Botswana. In: J. Kornprobst, (Ed.), **Kimberlites II: The Mantle and Crust-Mantle Relationships**, pp. 3-9, Elsevier, Amsterdam.
- HALL, A.E. and SMITH, C.B. 1984. Lamproite diamonds - are they different? In: Grove, J.E. and Harris, P.G., (Eds.) **Kimberlite Occurrences and Origin: A Basis for Conceptual Models in Exploration**, pp. 167-212, University of Western Australia.
- IRIFUNE, T., SEKINE, T., RINGWOOD, A.E. and HIBBERSON, W.O. 1986. The eclogite-garnetite transformation at high pressure and some geophysical implications. **Earth and Planetary Science Letters**, 77, 245-256.
- JORDAN, T.H. 1981. Continents as a chemical boundary layer. **Philosophical Transactions of the Royal Society of London**, A301, 359-373.
- LINDSLEY, D.H. and DIXON, S.A. 1976. Diopside-enstatite equilibria at 850 to 1400°C, 5 to 35 kbars. **American Journal of Science**, 276, 1285-1301.
- McKENZIE, D. and O'NIONS, R.K. 1983. Mantle reservoirs and ocean island basalts. **Nature**, 301, 229-231.
- MEYER, H.O.A. 1985. Genesis of Diamond: A mantle saga. **American Mineralogist**, 70, 344-355.
- MOORE, R.O. and GURNEY, J.J. 1985. Pyroxene solid solution in garnets included in diamond. **Nature**, 318, 553-555.
- MORGAN, W.J. 1971. Convection plumes in the lower mantle. **Nature**, 230, 42-43.
- O'NEILL, H.C. and WOOD, B.J. 1979. An experimental study of Fe-Mg partitioning between garnet and olivine and its calibration as a geothermometer. **Contributions to Mineralogy and Petrology**, 70, 59-70.
- PRINZ, M., MANSON, D.V., HLAVA, P.F., and KIEL, K. 1975. Inclusions in diamonds: garnet lherzolite and eclogite assemblages. **Physics and Chemistry of the Earth**, 9, 797-815.
- RINGWOOD, A.E. 1967. The pyroxene-garnet transformation in the Earth's mantle. **Earth and Planetary Science Letters**, 2, 255-263.
- RINGWOOD, A.E. 1982. Phase transformations and differentiation in subducted lithosphere: implications for mantle dynamics, basalt petrogenesis, and crustal evolution. **Journal of Geology**, 90, 611-643.
- SMITH, C.B. 1983. Pb, Sr and Nd isotopic evidence for sources of southern African Cretaceous kimberlites. **Nature**, 304, 51-54.

R.O. MOORE; M.L. OTTER; R.S. RICKARD; J.W. HARRIS*; J.J. GURNEY

Department of Geochemistry, University of Cape Town, South Africa.

*Department of Applied Geology, University of Strathclyde, Glasgow.

MOISSANITE

Moissanite (SiC) has been reported from a wide variety of geological environments, including a number Soviet kimberlites (e.g. Marshintsev et al., 1984). However, the validity of the numerous documentations of "natural" SiC have been seriously questioned by a number of authors. Milton and Vitaliano (1984) believe that not a single report convincingly proves its existence in nature and that contamination from industrial sources represents the real source.

Moissanite has been found for the first time as a primary inclusion in diamonds from the Monastery kimberlite in South Africa and the Sloan diatremes in the U.S.A. A total of six inclusions of this phase (three from each of the above localities) were observed to be primary within their host before the diamond was broken for inclusion recovery. It is emphasised that the moissanite inclusions reported here were mounted directly in epoxy resin without coming into contact with carborundum abrasives.

The inclusions range in size from 40 to 125 μm and are a pale green translucent colour. Their morphologies were not well characterised, but curved, possible cubo-octahedral, crystal faces are evident on one inclusion from Sloan (A90), whilst one of the Monastery inclusions (Cl6-01) has a distinctive flattened disc shape. This inclusion was analysed by X-ray diffraction (XRD) techniques using a 57.4mm Gandolfi camera, and the results are tabulated in Table 1. Only the largest inclusion has been analysed. The remaining inclusions were identified by semi-quantitative microprobe techniques which together with careful qualitative scans over the full spectrum of elements detectable on the microprobe indicated them to be pure SiC (~67%Si; ~33%C).

Although the general structure of silicon carbide is relatively simple (essentially long chains of SiC tetrahedra), detailed structures may be extremely complex due to one dimensional disorder or polytypism (Shaffer, 1969). Over 75 polymorphs have been identified in the literature. The XRD analysis of the moissanite inclusion does not perfectly match any of the nine polymorphs for which detailed XRD data was available to the authors (Shaffer, 1969). However, specific peaks from the 2H and 6H polymorphs correspond with a large number of the inclusion reflections. It is possible that the moissanite inclusion represents a mixture of more than one SiC polymorph, or more likely, that it represents a polymorph for which XRD data was not available to the authors.

Mineral associations were observed at both localities. At Monastery, two of the moissanite inclusions were liberated from diamonds hosting eclogitic garnets showing the effects of pyroxene solid-solution in garnet (Moore and Gurney, 1985; Moore and Gurney, this volume), whilst the third occurred as a discrete monomineralic inclusion. At Sloan, however, one moissanite inclusion was liberated from a diamond hosting a diopside of peridotitic affinity, while another formed the crystalline eye to a sulphide (?) rosette feature. The third occurred as a single inclusion within its host diamond. Table 2 lists microprobe analyses of mineral inclusion phases found in association with moissanite.

Some interesting observations can be made from the associated mineral inclusions. At Monastery, the two garnet inclusions imply a high pressure origin for their host diamonds. Crude estimates evaluated from the experimental data of Akaogi and Akimoto, (1979) are 110 and 140 kbars for diamonds A4-03 and A1-15 respectively. These pressures represent absolute maxima, as a combination of bulk compositional effects as well as the reported overestimate of pressure calibrations in the experimental data (Irifune et al., 1986) will lower these estimates by approximately 40 kbars to 70 and 100 kbars respectively. At Sloan, where moissanite is found in association with the peridotitic paragenesis, high temperatures and pressures of formation are again implied. However, it is emphasised that equilibration conditions are not tightly constrained due to the

rarity of coexisting mineral pairs (see Otter and Gurney, this volume). A single garnet-olivine pair yields an O'Neill and Wood (1979) temperature of 1370°C (50 kbars assumed). Furthermore, the single diopside found in association with moissanite yields a Lindsley and Dixon (1976) (20 kbars) temperature of 1224°C. Pressure estimates following Nickel and Green (1985) for four orthopyroxenes range between 58 and 73 kbars if one assumes a temperature of 1370°C and/or between 52 and 65 kbars if one adopts the lower temperature option of 1224°C.

The common factor which has emerged between the Monastery and Sloan moissanite occurrences is the high temperatures and pressures of equilibration. Furthermore, our observations indicate that moissanite is not restricted to either peridotitic or eclogitic paragenesis diamonds (the same is observed for sulphide inclusions). Data on the physical (P,T, f_{O_2}) and chemical conditions favoured by moissanite is insufficient to justify speculation as to its significance to diamond formation and mantle petrology. However, the occurrence of moissanite as a primary inclusion in diamond implies an extremely reducing environment for diamond growth. This is consistent with the common occurrence of sulphide inclusions as well as the rare reports of metallic iron in diamonds (Meyer, 1986).

FERRO-PERICLASE AND MAGNESIO-WUSTITE

Two types of Fe-Mg oxide minerals have been found as inclusions in diamond. The first, which is represented by a single inclusion from a Monastery diamond has been termed magnesio-wustite (FeO = 93.01 wt.% and MgO = 7.29 wt.%, Table 3). The second type represented by 5 inclusions (4 from Koffiefontein; 1 from Sloan) have been called ferro-periclase. The latter have MgO contents which range between 76.04 and 78.74 wt.% and FeO between 19.41 and 21.55 wt.% (Table 3). The terminology adopted in this report differs from that used by Scott Smith et al. (1984) who report the occurrence of two magnesio-wustites (ferro-periclase in our terminology) as inclusions in diamonds from kimberlites near Orroroo.

The inclusions are all in the region of 70 μ m in maximum dimension with ferro-periclase being dark orange to brown in colour, translucent and isotropic. The magnesio-wustite is black and opaque. One of the four ferro-periclase inclusions from Koffiefontein coexists with an enstatite (Table 3), implying a peridotitic association.

Periclase in association with magnetite has been reported from an Arkansas diamond (Newton et al., 1977), who suggested that it represents an original magnesite inclusion which decomposed upon diamond combustion in the inclusion recovery process. The inclusions discussed here have all been liberated by mechanical breakage, which renders this potential origin inappropriate. The association of a ferro-periclase inclusion with orthopyroxene raises the possibility that it may be formed by the desilicification of enstatite. Scott Smith et al. (1984) reject such a mechanism since enstatites of typical mantle compositions (Mg/Mg+Fe ~0.94) would be unlikely to produce the ferro-periclase compositions (Mg/Mg+Fe ~0.86) observed both at Koffiefontein and Orroroo by this simple reaction.

Indications are therefore that these oxide phases represent primary inclusions. Experimental work by Liu (1975) suggests that at 250 kbars Mg_2SiO_4 (olivine with a spinel structure) transforms to pyroxene with a perovskite structure plus MgO with a cubic structure. Scott Smith et al. (op cit) point out that if the enstatite and ferro-periclase found in the Koffiefontein diamond crystallised in equilibrium at 1000°C, pressures in excess of 200 kbars are implied by the experimental data of Yagi et al. (1979). Another consideration is that these oxide phases would require extremely reducing conditions of formation which are not readily apparent in the well documented regions of the upper mantle. It is therefore possible that the ferro-periclase and magnesio-wustite inclusions in fact represent ultra-high pressure phases. Le Roex (Nature, submitted) has recently demonstrated chemical correlations between southern African kimberlites and South Atlantic hotspots. Moore and Gurney (this volume) drew attention to the possibility that a rising diapir(s) related to hot-spot activity could serve as a potential mechanism for the sampling of diamonds from extreme depths in the mantle. This suggestion could also be applied to the ferro-periclase, magnesio-wustite and even the moissanite inclusions described here.

REFERENCES

- AKAOGI M. and AKIMOTO S. 1979. High pressure phase equilibria in a garnet lherzolite, with special references to Mg^{2+} - Fe^{2+} partitioning among constituent minerals. *Physics of the Earth and Planetary Interiors* 19, 31-51.
- IRIFUNE T., SEKINE T., RINGWOOD A.E. AND HIBBERSON W.O. 1986. The eclogite-garnetite transformation at high pressure and some geophysical implications. *Earth and Planetary Science Letters* 77, 245-256.
- le ROEX A.P. 1986. A geochemical correlation between source region signatures of southern African kimberlites and South Atlantic hotspots. submitted to *Nature*.
- LINDSLEY D.H. and DIXON S.A. 1979. Diopside-enstatite equilibria at 850-1400°C, 5-35 kb. *American Journal of Science* 276, 1285-1301.
- LUI L. 1975. Post-oxide phases of olivine and pyroxene and the mineralogy of the mantle. *Nature* 258, 510-512.
- MARSHINTSEV V.K., SHCHELCHKOVA S.G., ZOL'NIKOV G.V. and VOSKRESENSKAYA V.B. 1967. New data on moissanite from kimberlites in Yakutia. *Geologiya Geofizika* 12, 22-31.
- MEYER H.O.A. 1986. Inclusions in diamond. In Nixon P.H. ed, *Mantle Xenoliths*, Wiley & Son, in press.
- MILTON C. and VITALIANO D. 1984. Moissanite, SiC, a non-existent mineral. XXVII International Geological Congress, Moscow.
- MOORE R.O. and GURNEY J.J. 1985. Pyroxene solid solution in garnets included in diamond. *Nature* 318, 553-555.
- NEWTON M.G., MELTON C.E. and GIARDINI A.A. 1977. Mineral Inclusions in an Arkansas diamond. *American Mineralogist* 62, 583-586.
- NICKEL K.G. and GREEN D.H. 1985. Empirical geothermobarometry for garnet peridotites and implications for the nature of the lithosphere, kimberlites and diamonds. *Earth and Planetary Science Letters* 73, 158-170.
- O'NEILL H.S.C. and WOOD B.J. 1979. An experimental study of Fe-Mg partitioning between garnet and olivine and its calibration as a geothermometer. *Contributions to Mineralogy and Petrology* 70, 59-70.
- SCOTT SMITH B.H., DANCHIN R.V., HARRIS J.W. and STRACKE K.J. 1984. Kimberlites near Orroroo, South Australia. In Kornprobst J. ed, *Kimberlites I: Kimberlites and Related Rocks*, pp.121-142. Elsevier, Amsterdam.
- SHAFFER P. 1969. A Review of the structure of silicon carbide. *Acta Crystallographica* B25, 477-488.
- YAGI T., BELL P.M. and MAO H.K. 1979. Phase relations in the system MgO - FeO - SiO_2 between 150 and 700 kbar at 1000°C. *Carnegie Institute of Washington Yearbook* 78, 614-618.

TABLE 1
XRD Analysis of Moissanite Cl6-01
(d-spacings/intensity)

4.01/5	2.54/5	2.37/5	2.08/2	1.58/1	1.44/3	1.11/1	1.00/2	.986/1	.955/2	.900/3
2.60/8	2.49/10	2.30/5	1.69/1	1.53/6	1.39/3	1.05/1	.992/1	.976/2	.933/2	

TABLE 2
Phases coexisting w/ Moissanite

TABLE 3
Magnesio-Wustite, Ferro-Periclase & Coexisting Phases

	Monastery			Sloan		Koffiefontein				
	A4-03	A1-15	A78	A1-40	A100	K30	K33	K34	A262	A262
	GAR	GAR	CPX	MG-WUS	FE-PER	FE-PER	FE-PER	FE-PER	FE-PER	OPX
SiO ₂	42.1	46.3	54.7	ND	ND	0.08	0.09	0.13	ND	57.1
TiO ₂	1.21	1.05	0.05	0.17	ND	ND	ND	ND	ND	0.03
Al ₂ O ₃	18.3	13.6	0.99	0.17	0.10	ND	ND	0.07	ND	1.16
Cr ₂ O ₃	0.02	1.20	1.29	ND	0.84	0.49	0.52	0.67	0.57	0.36
FeO	14.7	9.07	2.72	93.0	19.4	21.7	20.5	20.3	19.8	3.33
MnO	0.27	0.23	0.11	0.32	0.32	0.15	0.16	0.17	0.19	0.11
MgO	10.3	23.6	19.9	7.29	78.7	77.3	76.8	76.9	78.1	36.9
CaO	11.9	5.16	18.9	ND	0.04	ND	0.05	0.03	ND	0.12
Na ₂ O	1.08	0.14	0.65	-	0.07	0.29	0.25	0.20	0.30	ND
K ₂ O	-	-	0.20	-	ND	ND	0.06	ND	-	ND
NiO	-	-	-	-	-	-	-	-	1.41	-
Total	99.88	100.35	99.51	100.95	99.47	100.01	98.40	98.40	100.37	99.11

ND = not detected; - = not analysed .

GRAPHITE PSEUDOMORPHS AFTER DIAMOND IN THE ECLOGITE-PERIDOTITE MASSIF OF BENI BOUSERA,
MOROCCO, AND A REVIEW OF ANOMALOUS DIAMOND OCCURRENCES

P. H. Nixon, G. R. Davies, V. V. Slodkevich⁺ and S. C. Bergman⁺⁺

Dept. of Earth Sciences, The University of Leeds, Leeds LS2 9JT, UK.

⁺All-Union Geological Research Institute, Sredny pr., 74, 199178 Leningrad, USSR.

⁺⁺ARCO Resources Technology, Exploration and Production Research Center, PRC 3005,
P.O. Box 2819, Dallas, Texas 75221, USA.

Abnormal and unexplained reported occurrences of diamonds or its pseudomorphs can be categorised as follows (selected references only):

- 1A. Those occurring in deep-seated lithospheric rocks, including ophiolites and orogenic ultrabasic rocks that may have suffered subduction and subsequent emplacement as a diapir and/or tectonic wedge, exemplified by Cr spinel dunite/harzburgite/lherzolite e.g. Tibet (Fang Chingson and Bai Wenji, 1981); Koryak Mountains, eastern USSR (Shilo et al., 1981), Kamenushinsk massif, Urals (Sarsádsikh, 1973), Armenia ultramafites (Gevorkyan et al., 1976). Tulameen, British Columbia (Camsell, 1911).
- 1B. Graphite pseudomorphs after diamond in deep-seated lithospheric rocks of the above category exemplified by eclogites in Beni Bousera (see below).
- 2A. Sedimentary diamond (placer) deposits closely associated with 1A situation for which a conventional volcanic origin has not been proved e.g. diamond deposits of SE Kalimantan and the occurrences of Thailand; serpentinites of NSW and NW Tasmania (Twelvetrees, 1914), ultrabasics of Alaska, Oregon, California, Carolina, Georgia, Alabama in U.S.A. etc.
- 2B. Sedimentary diamond deposits of unknown or controversial origin not included in 2A e.g. those of Venezuela; Copeton NSW, Brunette Downs NT, Australia.
- 2C. Regionally metamorphosed sedimentary diamond deposits, e.g. Birrimian schists of West Africa.
3. Regionally metamorphosed kimberlitic/lamproitic rocks e.g. at Mitzic, Gabon, (Bardet, 1973).
- 4A. Diamonds in non kimberlitic/lamproitic volcanic rocks representing contamination from diamond bearing gravels and other crustal sources e.g. dolerite at Oakey Creek, Copeton; Icha alkali basalt volcano, Kamchatka (Kaminskii et al. 1981).
- 4B. Microdiamonds of probable metastable origin in non kimberlitic/lamproitic volcanic rocks.
5. Extra terrestrial origins; meteoritic and shock-impact diamonds, e.g. as postulated for diamonds in Neogene placers of the Dnieper region, Ukraine (Kaminskii et al., 1979).

This paper is concerned with diamonds associated with orogenic ultrabasic massifs of non volcanic origin. They are emplaced close to active plate margins and most recognised examples are Phanerozoic. Host rocks are typically Cr spinel depleted peridotites (dunites, harzburgites) and many are interpreted as ophiolites, i.e. ocean lithosphere. Accompanying high pressure 'indicator' minerals particularly pyrope-rich garnet are not common and indeed it is more usual to find almandine-rich garnet and such minerals as corundum (which however is an indicator in some assumed kimberlite derived diamond alluvials e.g. in Sierra Leone) platinoid metals, rutile, staurolite and florencite (Kaminskii, 1980).

The modern case for orogenic diamonds fostered mainly by Kaminskii and coworkers, although largely based on circumstantial 'alluvial' evidence (group 2A) is most persuasive when related to primary host peridotites of Armenia, Koryak Mountains and Tibet notwithstanding the strong reservations of V.S. Sobolev (Kaminskii, 1980). The discovery of coesite in pyrope-bearing 'alpine schists' (Chopin, 1984) illustrates that crustal rocks can be subducted to great depths, in this case 90km, which after all is only a fraction of the depth of some Benioff zones. A major task is to discover how many deep lithospheric rocks exposed in orogenic or mobile belts have previously been at depths at which coesite (ca. 90 km) or diamond (ca. 150 km) could crystallise, and how these rocks rose quickly to the surface without undue retrogressive effects.

This layered peridotite and garnet pyroxenite complex and associated thermally metamorphosed gneisses, together with others, notably the Ronda complex, form part of the Betico-Rifean orogenic belt in the western Mediterranean (Kornprobst and Vielzeuf, 1984, and references therein) (Fig. 1).

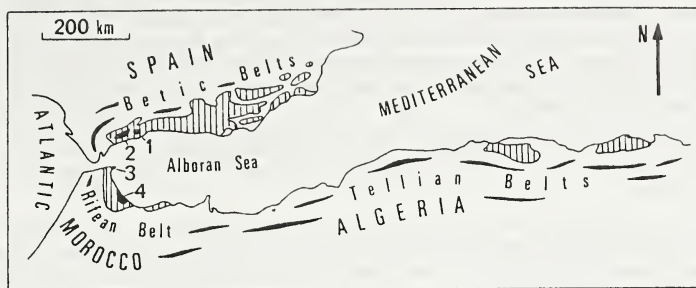


Figure 1. Ultramafic/granulitic associations in the Betico-Rifean belt; southern Spain: 1 - Ronda, 2 - Ojen; Northern Morocco : 3 - Ceuta, 4 - Beni Bousera (Kornprobst and Vielzeuf, 1984).

Kornprobst and Vielzeuf (1984) have described early magmatic parageneses including garnet and corundum pyroxenites, resembling grosspyrite xenoliths in kimberlites, which crystallised at pressures equivalent to 90 km. Locally, coarse somewhat tectonised banded inequigranular pyroxenites, garnet clinopyroxenites (eclogites) and garnetites contain graphite octahedral pseudomorphs of diamond up to 7mm. across (similar in size to the silicate minerals) and constituting up to 15% of the rock (Slodkevich, 1982). The garnets have spinel bearing coronas; they also occur as inclusions in the graphite. They are mainly py (39-50) alm (32-45) and gross (6-13) with no definite high pressure Si excess yet proved. The clinopyroxenes are omphacites (up to 18% jadeite) with small amounts of Cr₂O₅ (< 0.4 wt%). A small acid resistant residue is currently being examined.

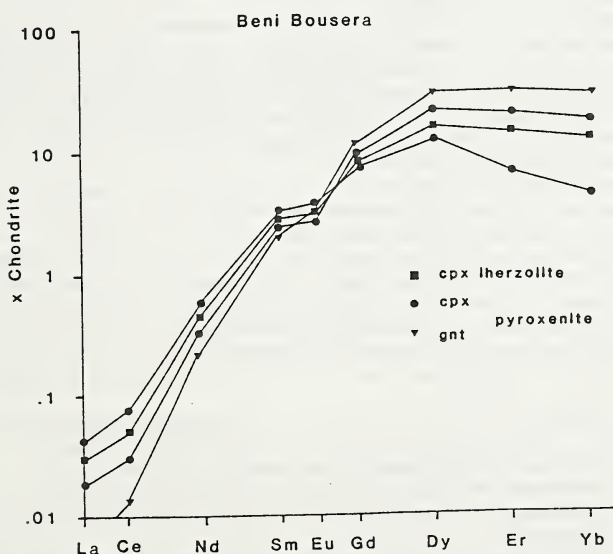


Figure 2. REE patterns of clinopyroxenes and garnets in a spinel lherzolite and graphite-bearing garnet pyroxenite (eclogite) from Beni Bousera.

REE element analysis of cpx and gt, of the graphite bearing pyroxenites and the associated spinel lherzolites, which locally also contain (amorphous) graphite, indicate that both have undergone several partial melting events in the garnet stability field ($(Yb)_N = 20$, $(La)_N = 0.03$, $Sm/Nd > 2.0$. (Fig. 2). The relatively unradiogenic $^{143}Nd/^{144}Nd$ ratios of the minerals, 0.5131-0.5132 show that there has been less than 100 Ma since the rocks suffered their last depletion/melting event. Unradiogenic Pb isotope ratios $^{206}Pb/^{204}Pb = 166$ suggest derivation from a long term depleted MORB-like reservoir. However, $^{207}Pb/^{204}Pb$ and $^{208}Pb/^{204}Pb$ ratios are comparatively radiogenic (15.2 and 35.7 respectively). These data in conjunction with the radiogenic $^{87}Sr/^{86}Sr$ ratios 0.7045-0.705 imply that some crustal/seawater interaction has occurred in the history of these rocks. $\delta^{13}C$ analyses of the graphite pseudomorphs (Slodkevich, 1982) yield high (depleted) values of -19.1 to -22.9 (10 analyses) and -15.5 (1 anal.) suggesting a possible biogenic component.

We interpret the data to indicate the following sequence of events in the context of the Rifean Orogenic Belt and the northward motion of Africa beneath the edge of the European Plate:

Subduction of hydrothermally altered oceanic lithosphere to 150-200 km at which depths (depending on cold slab geotherm considerations) crustal carbon could crystallise as diamond in the deep eclogite facies environment. The degree of depletion during subduction is uncertain.

A heating event of young age and thought to be associated with the Mesozoic (Lias to Senonian) lithospheric extension stage of Kornprobst and Vielzeuf (1984) caused diapiric upwelling of mantle peridotites and eclogite. Segregations of partial melts and crystallisation of diamond took place locally.

The ascent of the diapir (associated with the Betico-Rifean oceanic transform - in the early Tertiary, a compression zone) caused extensive thermal metamorphism of crustal rocks (Kornprobst and Vielzeuf, 1984). The diamonds reverted to graphite but are not significantly deformed.

We thank Dearn C. Lee for comments and assistance.

SELECTED REFERENCES

- Bardet, M.G. 1973. Metakimberlites. Extended. abst. Int. Kimberlite Conf. Cape Town, 15-17.
- Camsell, C.A. 1911. A new diamond locality in the Tulameen District, British Columbia. *Econ. Geol.*, 6, 604-611.
- Chopin, C. 1984. Coesite and pure pyrope in high grade blue schists of the Western Alps: a first record and some consequences. *Contrib. Mineral. Petrol.* 86, 107-118.
- Fang, Chingson and Bai Wenji, 1981. The discovery of alpine-type diamond-bearing ultrabasic intrusion in Xizang (Tibet). *Geol. Review*, 27, 455-457 (in Chinese).
- Gevorkyan, R.G., Kaminskii, F.V., Lunev, B.S., Osovetskii, B.M. Khachatryan, N.D. 1976. New occurrences of diamonds in Armenian ultramafics. *DAN ArmSSR* 63, No. 3
- Kaminskii, F.V., Galimov, E.M., Ivanovskaya, I.N., Kiribilita and Polkanov, Yu, A. 1979. Isotopic distribution in carbon of small diamonds from the Ukraine. *Dokl. ACad. Nauk., SSSR*, 236, 174-175.
- Kaminskii, F., V. 1980. The Authenticity and Regularity of Occurrences of Diamonds in Alkaline-Basaltoid and Ultrabasic (other than Kimberlite) Rocks. *Zapiski Vsesoyuznogo Mineralogicheskogo Obshchestva*, 4, 488-493.
- Kaminskii, F.V., Patoka, M.G. and Sheymovich, V.S. 1981. Geologic and tectonic position of diamond-bearing basalts of Kamchatka. *Dokl. Akad. Nauk SSSR*, 246, 55-58
- Kornprobst, J. and Vielzeuf, D. 1984. Transcurrent crustal thinning: a mechanism for the uplift of deep continental crust/upper mantle associations. In *Developments in Petrology* 11B "Kimberlites", Elsevier, pp. 347-351.
- Sarsadskikh, N.N. 1973. Regional and local properties of the distribution of endogenic deposits of diamonds. "Nedra".
- Shilo, N.A., Kaminskii, F.V., Palandzhyan, S.A. Til'man, S.M., Tkachenko, Lavrova, L.D. and Shepeleva, 1981. First diamond finds in alpine-type ultramafic rocks of the northeastern USSR. *Dokl. Acad. Nauk.*, 241, 179-182.
- Slodkevich, V.V. 1982. Graphite octahedra at Beni Bousera, N. Morocco, associated with garnet-clinopyroxene layered complex. *Zapiski Vses. Mineralog. ob-va*, 13-33 (in Russian)
- Twelvetrees, W.H. 1914. The Bald Hill osmiridian field, Tasmania *Geol. Surv. Bull.* 17.

MINERAL INCLUSIONS IN DIAMONDS FROM THE SLOAN DIATREMES,
COLORADO-WYOMING STATE LINE KIMBERLITE DISTRICT, NORTH AMERICA

M.L. Otter and J.J. Gurney

Department of Geochemistry, University of Cape Town, South Africa

Of 153 diamonds from the Sloan diatremes in the Colorado-Wyoming kimberlite district, comprising the bulk of the inclusion-bearing stones recovered during prospecting operations, 80 released primary inclusions which, for the most part, fall into the broadly defined eclogitic and peridotitic parageneses found worldwide. The eclogitic minerals predominate (Ecl./Ecl.+Per. ratio = 0.74). The paragenetic division of the inclusions is reflected by differences in the physical characteristics of their diamond hosts.

THE DIAMONDS

The physical characteristics of the diamonds have been described with emphasis on primary features. In general, the Sloan inclusion-bearing diamonds are similar to the 78 State Line diamonds described by McCallum et al. (1979). The dominant primary morphology is the octahedron (71%) followed by aggregates (18%), triangular macles (10%) and unassignable fragments (1%). The largest diamond weighed 0.65 carat, but most weighed less than 0.03 carat. Triangular growth plates are common and sharp-edged, smooth-faced, unresorbed crystals are also present, but most of the diamonds exhibit resorption features such as negative trigonal pits, shield-shaped laminae and rounded tetrahahedroidal crystal faces. When classified according to their degree of resorption (D.N. Robinson, pers. comm.), it was found that the smaller crystals tend to be better preserved, a trend also noted by McCallum et al. (1979). This runs contrary to the trend observed on samples of larger southern African diamonds by Harris et al. (1975), a discrepancy which is probably related to the size ranges investigated.

The diamond characteristics are related to inclusion paragenesis. A high proportion of the macles and aggregates are peridotitic, while the eclogitic diamonds are mostly octahedra. In addition, all of the peridotitic diamonds weigh under 0.02 carat, while the eclogitic diamonds include many crystals heavier than 0.03 carat. Interestingly, McCallum et al. (1979) found a much higher percentage of aggregates in their sample which was dominated by diamonds weighing less than 0.01 carat. These are interpreted as primary trends related to differences in carbon super-saturation of the growth environments. According to observations on diamond growth by Sunagawa (1984), the peridotitic diamonds at Sloan crystallised under conditions of slightly higher super-saturation than the eclogitic diamonds. The peridotitic diamonds tend to be better preserved, which reflects the inverse mass vs. resorption relationship. Diamonds of both parageneses exhibit resorption and/or features consistent with a xenolithic association which is not surprising since both a diamond peridotite (McCallum and Egger, 1976) and a diamond-graphite eclogite (McCandless and Collins, this volume) have been recovered in the State Line district. Sharp edged, smooth faced, unresorbed crystals also occur in both parageneses, although they are most abundant in the smaller, peridotitic diamonds. The better preservation of the smaller diamonds may be a consequence of protection within a xenolith during a resorption event. The smaller diamonds which are exposed to the resorbing medium may dissolve completely, while those which are protected survive, obviously with better preservation. Diamonds exhibiting no resorption must have been totally shielded or, alternatively, have crystallised after the resorption event ceased. At Sloan, it seems likely that such unresorbed morphologies are a consequence of more efficient shielding from the resorbing medium within a xenolith.

INCLUSION MINERALOGY

The inclusions were assigned into their respective paragenetic suites based on garnet, clinopyroxene, olivine, orthopyroxene and their coexisting phases. The eclogitic minerals include sulphide(23), pyrope-almandine garnet(25), omphacitic clinopyroxene(15), rutile(12), coesite(3), corundum(2) and sanidine(1). The peridotitic minerals are olivine(14), orthopyroxene(4), moissanite(3), Cr-dioptase(1), pyrope garnet(1) and ferro-periclaise(1). Zircon was also recovered, but is left unclassified.

Eleven of the 23 diamonds containing sulphide are eclogitic. No sulphides were recovered from diamonds releasing peridotitic minerals although sulphide(?) rosette features were visually identified in three peridotitic stones. For these reasons, it is assumed that most of the sulphides recovered are eclogitic. Based on a visual inspection of over 2000 stones, sulphide is probably the most abundant mineral inclusion in Sloan diamonds. Rutile, coesite, corundum and sanidine coexisted only with eclogitic minerals. One coesite occurs as an inclusion within a pyrope-almandine garnet. A moissanite coexisted with the chrome-diopside and is, therefore, classified as peridotitic. The ferro-periclasite is assigned to the peridotitic suite based on its coexistence with enstatite in a diamond from Koffiefontein mine (Richard et al., this volume). Moissanite and ferro-periclasite are discussed more comprehensively by Moore et al. (this volume). In one Sloan diamond, an olivine coexisted with a pyrope-almandine garnet! Three other cases of mixed parageneses in a single diamond have been reported (Prinz et al., 1975; Hall and Smith, 1984; Moore and Gurney, this volume). This implies a close, spatial relationship between the two paragenetic diamond growth environments at the specific localities.

INCLUSION CHEMISTRY

The chemical analyses of important inclusion minerals are presented in Table I. The eclogitic minerals in Sloan diamonds are, with minor differences, typical of those found in diamonds worldwide. The pyrope-almandine garnets have a wide range in Mg/Mg+Fe (.36-.65), but tend to be more iron-rich than those from other localities. Otherwise, these garnets are chrome-poor (≤ 15 wt.% Cr_2O_3), rich in titanium (.28-.76 wt.% TiO_2) and contain trace levels of sodium (.10-.25 wt.% Na_2O). The omphacitic clinopyroxenes are enriched in both the jadeite component (18-57%) and in potassium (0.1-1.2 wt.% K_2O). Using the method of Ellis and Green (1979), assuming all iron as Fe^{2+} and 50 kbar, the three eclogitic garnet/cpx pairs, in diamonds A37, A73 and 1-10, give equilibration temperatures of 1088°C, 1102°C and 1114°C respectively. Diamond 1-15 released garnet with two compositionally different omphacites. The temperatures calculated for the two possible garnet/cpx pairs are 989°C and 1256°C. Coesite and sanidine are essentially pure phases. Many of the rutiles had minor iron and aluminium contents possibly because of alteration. The two corundums contain 1.1 and 2.0 wt.% TiO_2 . The sulphides are predominantly pyrrhotite, usually with minor pentlandite exsolution blebs. One of these coexisted with a chalcopyrite. Rutile, quartz, corundum and sanidine, in addition to kyanite and sphene, are common accessory minerals in State Line eclogites (Ater et al., 1984), but Na-rich garnets and K-rich clinopyroxenes are rare, having been reported only in the single diamond-graphite eclogite from Sloan (McCandless and Collins, this volume). The lack of sulphide in Sloan eclogites accents the differences between the eclogitic inclusions and most of the eclogites found at Sloan. The eclogitic inclusions and the diamond-graphite xenolith are probably genetically related and both can be linked to Type I eclogites (McCandless and Gurney, this volume).

The Sloan group of peridotitic inclusions are chemically similar to those minerals found in garnet lherzolites in the area (Kirkley, 1981). The single pyrope garnet is calcium saturated and the olivines are all Fo 92 with up to .14 wt.% Cr_2O_3 . Using O'Neill and Wood (1979), the single garnet/olivine pair in diamond A12 gives a temperature of 1374°C at an assumed pressure of 50 kbar. The orthopyroxenes (Mg/Mg+Fe=.93) are distinguished by unusually high calcium concentrations (1.0-1.4 wt.% CaO). Two of the orthopyroxenes coexisted with olivines (Diamonds A34 and A64) which are compositionally similar to the olivine which coexisted with the pyrope garnet. Assuming the orthopyroxenes also equilibrated with that garnet, pressures calculated using Nickel and Green (1985), range from 58-73 kbar. The Cr-diopside, which coexisted with moissanite in diamond A78, is unusual with .20 wt.% K_2O . It yields an equilibration temperature of 1224°C using Lindsley and Dixon (1976, 20 kbar). The peridotitic inclusions appear to be of a deeper origin than those reported from most other localities, but this is based largely on the one pyrope garnet, which perhaps should not be considered representative of the peridotitic inclusion population as a whole. Nevertheless, the further occurrence of Ca-enriched orthopyroxene, moissanite and ferro-periclasite is consistent with higher pressures.

REFERENCES

- ATER P.C, EGGLER D.H. AND McCALLUM M.E. 1984. Petrology and geochemistry of mantle eclogite xenoliths from Colorado-Wyoming kimberlites: Recycled Ocean Crust? In Kornprobst J. ed, **Kimberlites II: The Mantle and Crust-Mantle Relationships**, pp.309-318. Elsevier, Amsterdam.
- ELLIS D.J. and GREEN D.H. 1979. An experimental study of the effect of Ca upon garnet-clinopyroxene Fe-Mg exchange equilibria. **Contributions to Mineralogy and Petrology** 71, 13-22.
- HALL A.E. and SMITH C.B. 1984. Lamproite diamonds--are they different? **Publications of the Geology Department & University Extension**, University of Western Australia 8, 167-212.
- HARRIS J.W., HAWTHORNE J.B., OOSTERVELD M.M. and WEHMEYER E. 1975. A classification scheme for diamond and a comparative study of South African diamond characteristics. **Physics and Chemistry of the Earth** 9, 765-783.
- KIRKLEY M.B. 1980. Peridotite xenoliths in Colorado-Wyoming kimberlites. M.Sc. Thesis, Colorado State University, Fort Collins. Unpublished.
- LINDSLEY D.H. and DIXON S.A. 1976. Diopside-enstatite equilibria at 850-1400°C, 5-35 kb. **American Journal of Science** 276, 1285-1301.
- McCALLUM M.E. and EGGLER D.H. 1976. Diamonds in an upper mantle peridotite nodule from kimberlite in southern Wyoming. **Science** 192, 253-256.
- McCALLUM M.E., MABARAK C.D. and COOPERSMITH H.G. 1979. Diamonds from kimberlites in the Colorado-Wyoming State Line district. In Boyd F.R. and Meyer H.O.A. eds, **Kimberlites, Diatremes and Diamonds: Their Geology, Petrology and Geochemistry**, pp. 42-58. American Geophysical Union, Washington, D.C.
- NICKEL K.G. and GREEN D.H. 1985. Empirical geothermobarometry for garnet peridotites and implications for the nature of the lithosphere, kimberlites and diamonds. **Earth and Planetary Science Letters** 73, 158-170.
- O'NEILL H.S.C. and WOOD B.J. 1979. An experimental study of Fe-Mg partitioning between garnet and olivine and its calibration as a geothermometer. **Contributions to Mineralogy & Petrology** 70, 59-70.
- PRINZ M., MANSON D.V., HLAVA P.F. and KEIL K. 1975. Inclusions in diamonds: garnet lherzolite and eclogite assemblages. **Physics and Chemistry of the Earth** 9, 797-815.
- SUNAGAWA I. 1984. Morphology of natural diamond crystals. In Sunagawa I. ed, **Materials Science of the Earth's Interior**, pp.303-330. Terra Scientific Publishing Company, Tokyo.

TABLE I

	A37		A73		1-10		1-15			A12		A34	A64	A78
	GAR	CPX	GAR	CPX	GAR	CPX	GAR	CPX	CPX	GAR	OLV	OPX	OPX	CPX
SiO ₂	38.6	55.7	40.4	55.4	40.0	54.4	40.9	55.2	55.5	41.1	40.7	57.9	57.5	54.7
TiO ₂	0.44	0.46	0.29	0.37	0.49	0.33	0.65	0.60	0.53	0.14	ND	ND	ND	0.05
Al ₂ O ₃	22.2	9.77	22.5	9.92	22.2	5.58	22.4	6.33	4.30	17.3	0.04	0.49	0.86	0.99
Cr ₂ O ₃	ND	ND	0.06	0.06	ND	ND	ND	ND	ND	8.64	0.10	0.41	0.44	1.29
FeO	19.5	5.49	14.0	3.12	17.9	6.74	15.0	7.00	4.62	5.90	8.20	4.57	4.79	2.72
MnO	0.40	0.07	0.34	ND	0.59	0.16	0.47	0.20	0.10	0.24	0.12	0.12	0.10	0.11
MgO	8.71	8.81	14.6	10.4	12.7	13.4	16.5	14.2	16.0	20.5	50.7	34.6	34.2	19.9
CaO	9.61	13.6	7.55	14.3	6.06	15.8	3.49	12.5	16.5	6.00	0.12	1.14	1.36	18.9
Na ₂ O	0.19	5.53	0.16	5.12	0.14	3.29	0.18	3.80	2.62	ND	-	0.04	0.06	0.65
K ₂ O	-	0.78	-	0.55	-	0.43	-	0.25	0.11	-	-	ND	ND	0.20
NiO	-	-	-	-	-	-	-	-	-	-	0.20	-	-	-
Total	99.65	100.2	99.90	99.24	100.1	100.1	99.59	100.1	100.3	99.82	100.2	99.27	99.31	99.51

S.H. Richardson

Laboratoire de Géochimie et Cosmochimie, Institut de Physique du Globe
4, Place Jussieu, 75252 Paris Cedex 05, France

Syngenetic mineral inclusions in diamonds provide the best means for determining their age and origin. Among such inclusions, the peridotitic paragenesis of olivine, orthopyroxene and purple subcalcic chrome-pyropo garnet is on average far more abundant than the eclogitic paragenesis of orange pyropo-almandine garnet and pale green omphacitic clinopyroxene.

Subcalcic garnet inclusion bearing diamonds and related heavy mineral concentrate garnets from the ~100 Ma old Kimberley and Finsch kimberlites in southern Africa were previously shown to have originated in residual yet trace element enriched lithosphere beneath the Kaapvaal craton ~3300 Ma ago (Richardson et al 1984). Comparable Sm-Nd and Rb-Sr isotopic data have been obtained for subcalcic garnets in two diamondiferous megacrystalline harzburgite-dunite xenoliths (Uv402 & Uv727) and a similar albeit modally non-diamondiferous specimen (Uv49/76) in the suite described by Pokhilenko et al (1977) from the ~350 Ma old Udachnaya kimberlite in Yakutia. These data (Fig.1) are consistent with a similar origin and Archaean age for diamonds of peridotitic paragenesis from the Siberian and Kaapvaal cratons. The significant xenolith preservation potential of the Udachnaya specimens relative to their disaggregated southern African counterparts may be attributed to minor physico-chemical differences possibly correlated with the time-integrated Rb/Sr ratio of their enriched lithospheric hosts. Thus, the dominant peridotitic diamonds and their host rocks have been stored in the subcontinental lithosphere at depths of 150-200 km and temperatures of 900-1200°C (Boyd & Finnerty 1980; Boyd et al 1985) for more than 3000 Ma, surviving convective disruption and remaining available for episodic sampling by kimberlite.

At a few localities such as the Premier kimberlite in southern Africa and the Argyle lamproite in northwest Australia diamonds of eclogitic paragenesis predominate, allowing recovery of sufficient material for complementary isotopic analysis. At Argyle and with greater difficulty at Premier, a distinction within the eclogitic garnet inclusion population can be made between deep orange garnet, which may be paired with pale green clinopyroxene, and pale orange garnet which has no obvious clinopyroxene complement. Deep orange garnet and pale green clinopyroxene inclusions in Premier diamonds yield a Sm-Nd isochron age of 1150 ± 60 Ma (Fig. 2). This coincides with the preferred host kimberlite age of 1180 ± 30 Ma (Smith 1983; Jones 1984) as well as a model Pb age of ~1200 Ma for sulphide inclusions in Premier diamonds (Kramers 1979). The corresponding result for the same eclogitic inclusion mineral pair in Argyle diamonds is 1580 ± 60 Ma (Fig. 2). This age is a few hundred Ma greater than the host lamproite emplacement age of ~1130 Ma (Skinner et al 1986) and closer to the ~1800 Ma age of stabilization of the surrounding Halls Creek mobile zone (Atkinson et al 1984). While this indicates that Argyle eclogitic diamonds are xenocrysts in the host lamproite, it does not preclude an original phenocrystal relationship with related small-volume mantle magmatism ~500 Ma earlier and subsequent lithospheric storage. In contrast, there is no resolvable time difference between Premier eclogitic diamond crystallization and host kimberlite emplacement. Eclogitic diamond inclusion chemistry, ages and precursor isotopic signatures indicate a second genetically distinct origin of diamonds apparently related in time and space to mantle magmatism of kimberlitic or lamproitic affinity.

ACKNOWLEDGMENTS

I wish to thank De Beers Consolidated Mines Ltd. and in particular J.B. Hawthorne, J.W. Harris, J. Scott, A. van Niekerk and V. Anderson for diamond specimens and support; N.P. Pokhilenko and A.J. Erlank for xenolith specimens; S.R. Hart for analytical facilities at MIT and C.J. Allegre for support at IPG.

REFERENCES

- ATKINSON W.J., HUGHES F.E. and SMITH C.B. 1984. A review of the kimberlitic rocks of Western Australia. In Kornprobst J. ed, Kimberlites I : Kimberlites and Related Rocks, pp. 195-224. Elsevier, Amsterdam.
- BOYD F.R. and FINNERTY A.A. 1980. Conditions of origin of natural diamonds of peridotite affinity. *Journal of Geophysical Research* 85, 6911-6918.
- BOYD F.R., GURNEY J.J. and RICHARDSON S.H. 1985. Evidence for a 150-200-km thick Archaean lithosphere from diamond inclusion thermobarometry. *Nature* 315, 387-389.
- JONES R.A. 1984. Geochemical and isotopic studies of some kimberlites and included ultrabasic xenoliths from southern Africa. Ph.D. thesis, University of Leeds.
- KRAMERS J.D. 1979. Lead, uranium, strontium, potassium and rubidium in inclusion-bearing diamonds and mantle-derived xenoliths from southern Africa. *Earth and Planetary Science Letters* 42, 58-70.
- POKHILENKO N.P., SOBOLEV N.V. and LAVRENT'EV Yu.G. 1977. Xenoliths of diamondiferous ultramafic rocks from Yakutian kimberlites. Extended Abstracts, Second International Kimberlite Conference, Santa Fe, New Mexico.
- RICHARDSON S.H., GURNEY J.J., ERLANK A.J. and HARRIS J.W. 1984. Origin of diamonds in old enriched mantle. *Nature* 310, 198-202.
- SMITH C.B. 1983. Rubidium-strontium, uranium-lead and samarium-neodymium isotopic studies of kimberlite and selected mantle-derived xenoliths. Ph.D. thesis, University of the Witwatersrand.
- SKINNER E.M.W., SMITH C.B., ALLSOPP H.L., SCOTT-SMITH B.H. and DAWSON J.B. 1986. Proterozoic kimberlites and lamproites and a preliminary age for the Argyle lamproite pipe, Western Australia. *Transactions of the Geological Society of South Africa* 88, in press.

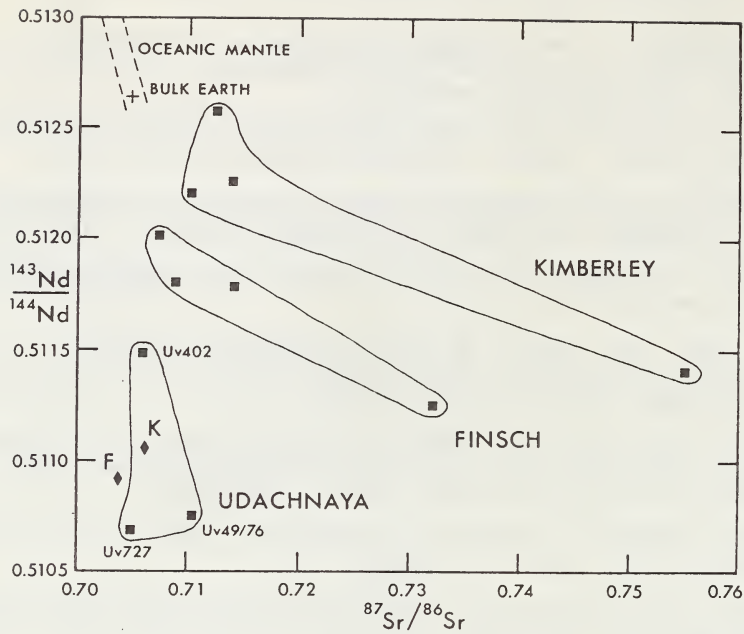


Fig. 1 Nd-Sr isotope correlation diagram for subcalcic garnets in diamondiferous harzburgite-dunite xenoliths from the Udachnaya kimberlite. Data for similar peridotitic garnets in Kimberley (K) and Finsch (F) diamond inclusions (diamond symbols) and heavy mineral concentrates (squares) are from Richardson et al (1984).

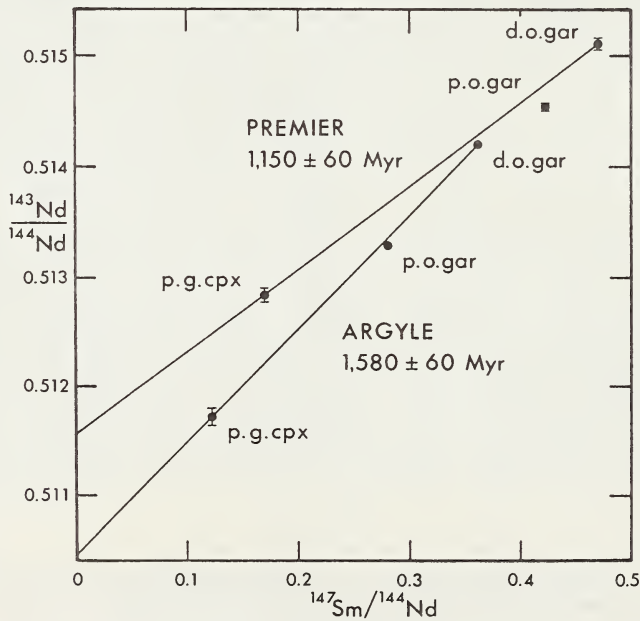


Fig. 2 Sm-Nd isochron diagram for eclogitic garnet and clinopyroxene inclusions in Argyle and Premier diamonds. Ages are for deep orange garnet - pale green clinopyroxene pairs.

D.N. Robinson*, J.A. Scott**, A. Van Niekerk** and V.G. Anderson**

*Anglo American Research Laboratories, P.O. Box 106, Crown Mines, 2025, South Africa.

**CSO Valuations (Pty) Limited, P.O. Box 633, Kimberley, 8300, South Africa.

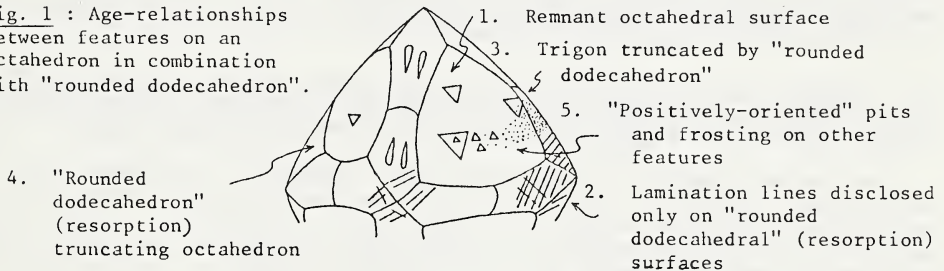
INTRODUCTION

Observations made of diamond samples (all of 0.15 to 0.35-carat diamonds, to facilitate comparisons) from fifteen Southern African kimberlite localities are reported.

THE SEQUENCE OF EVENTS IN EVIDENCE

Age relationships are apparent between many diamond features (Fig.1). The processes responsible for some of these features are tolerably well understood. For example, lamination lines have been shown to reflect plastic deformation (Urusovskaya and Orlov, 1964), the "rounded dodecahedral" form results from partial resorption (e.g. Moore and Lang, 1974) and various octahedral surface pits manifest etching at different combinations of temperature and oxygen fugacity (e.g. Yamaoka et al., 1980). In addition, the xenocrystic origin of kimberlitic diamonds has been confirmed by Richardson et al. (1984), who also demonstrated the very considerable interval which may elapse between diamond crystallization and incorporation into kimberlite. Thus, a sequence of events which have affected diamonds can be recognized. This sequence includes crystallization, residence at high T and P, plastic deformation, resorption (and associated etching), mechanical damage and further etching.

Fig. 1 : Age-relationships between features on an octahedron in combination with "rounded dodecahedron".

SAMPLE CHARACTERISTICS AND THEIR INTERPRETATION

The abundances of some features are given in the appended table. Grey/black diamonds are common at Palmietgat but are scarce, elsewhere, to a degree which is uniform within any particular kimberlite province. This distribution can reflect that present within the zone of mantle sampled by kimberlites. By contrast, the content of brown diamonds varies considerably within individual provinces (e.g. Kimberley, Jwaneng) and even within a composite pipe (e.g. Premier Mine). These variations suggest a secondary origin for the brown colour. They also require that associated kimberlites with differing proportions of brown diamonds were emplaced separately from wherever the differences originated.

Primary growth forms of diamond are the octahedron and, at lower temperatures, the cube (Bovenkerk, 1961). Octahedra dominate, to the virtual exclusion of cubes (as main form), at most localities. Of the three exceptions, two (Jwaneng) are a few kilometres apart while none are close to any of the octahedron-dominated (relative to cube) localities. Therefore, variations in cube content may reflect lateral variations within diamond-bearing mantle, rather than relatively shallow sampling by kimberlite.

The "rounded dodecahedron" (i.e. tetrahexahedroid) is always the predominant, main crystal form. Haggerty (1986) considers the resorption responsible for this form to occur during diamond residence in the mantle. That it actually occurs within transporting kimberlite magma is indicated, however, by the relatively unresorbed nature

of any diamonds in xenoliths (e.g. Shee et al., 1982) by occurrences of pseudo-hemimorphic crystals (more resorbed at one side than the other) and by the range, in every sample, from nearly sharp-edged octahedra, through intermediate (combined) forms to pure "rounded dodecahedra". Thus, a model is favoured whereby the degree to which individual diamonds get resorbed is determined largely by the level (during kimberlite-magma ascent) at which they are liberated from enclosing xenoliths or xenocrysts. This model, unlike Haggerty's (op. cit.) hypothesis, also allows the widely differing proportions of preserved growth forms in closely associated kimberlites (e.g. Bultfontein compared with other Kimberley bodies) to be readily explained.

"Rounded dodecahedra" are as common in samples from dykes and diatreme root zones as in higher-level samples. The resorption must be practically complete before kimberlite magma becomes involved in diatreme formation.

The majority of the diamonds in most samples show evidence (lamination lines) of having undergone plastic deformation. Such deformation requires deviatoric stress, hence an essentially solid environment, and (De Vries, 1975) temperatures above 900°C which are coupled to high pressures. Only in the mantle are such conditions likely to be realized. Mantle-derived xenoliths in kimberlites could be deformed as a consequence (Mercier, 1979) of stress in aureoles about developing kimberlite conduits. Should diamond also be deformed in such aureoles, kimberlite magma would have to be responsible for the resorption which follows.

Lamination lines are much more common on brown than other diamonds. This suggests that plastic deformation is responsible for much of the brown colour. An additional factor (high temperature?) may also be involved as indicated by the data for Premier Mine (where brown diamonds are relatively scarce in the Brown Kimberlite, even though lamination lines are at least as common as in the other two kimberlites). It is possible that this factor operates subsequently to the deformation. Otherwise, associated kimberlites which contain differing proportions of brown diamonds will need to have been emplaced separately from the mantle.

Breakage is very common in all of the samples examined in this study. This includes samples from dykes so most breakage must pre-date diatreme formation. Few breakage surfaces are modified by resorption but they are generally etched.

Two merging groups of late-stage etch features are developed upon "rounded dodecahedral" surfaces. The first group includes microdisk patterns, corrosion sculpture and shallow depressions, while the second group consists of frosting (coarse and fine). On crystals exhibiting the first group of features, any remnant octahedral faces exhibit only the trigons also produced during resorption. Frosting, on the other hand, extends onto octahedral faces as a myriad of hexagonal pits or trigonal pits in the "positive" orientation. Yamaoka et al. (op. cit.) demonstrates that cooler and/or more oxidizing conditions are required for these pits than for trigons and the resorption forms.

The first group of late-stage etch features is particularly common in samples from hypabyssal-facies and the deeper parts of some diatreme-facies kimberlites. Etch-pit development could have continued after emplacement during relatively slow cooling. Frosting tends to be more common in samples from diatreme-facies kimberlites. This can reflect brief etching associated with a sudden increase in fO_2 just prior to quenching. Both groups of late-stage etch features are relatively scarce in the sample from epiclastic kimberlite. Some samples from hypabyssal and diatreme-facies kimberlites are also poor in diamonds exhibiting either group of features.

CONCLUSIONS

Essentially the same sequence of events is evident in the diamonds of all the kimberlites considered. The frequencies of occurrence of certain features, e.g. grey/black colour, can reflect the situation in underlying mantle but this is not the case for brown colour or for the "rounded dodecahedral" form. Brown colour is associated with plastic deformation which probably occurred during the initial ascent of kimberlite magma. Such magma subsequently produced "rounded dodecahedra" by partial resorption of growth forms. The development of late-stage etch features extends to the final phases of kimberlite emplacement.

REFERENCES

Bovenkerk H.P. 1961. Some observations on the morphology and physical characteristics of synthetic diamond. *American Mineralogist* 46, 952-963.

De Vries R.C. 1975. Plastic deformation and "work-hardening" of diamond. *Materials Research Bulletin* 10, 1193-1200.

Haggerty S.E. 1986. Diamond genesis in a multiply-constrained model. *Nature* 320, 34-38.

Mercier J.C.C. 1979. Peridotite xenoliths and the dynamics of kimberlite intrusion. In : *The Mantle Sample : Inclusions in Kimberlites and other Volcanics* (editors F.R. Boyd and H.O.A. Meyer), 197-212. American Geophysical Union.

Moore M and Lang A.R. 1972. On the origin of the rounded dodecahedral habit of natural diamond. *Journal of Crystal Growth* 26, 133-139.

Richardson S.H., Gurney J.J., Erlank A.J. and Harris J.W. 1984. Origin of diamonds in old enriched mantle. *Nature* 310, 198-202.

Shee S.R., Gurney J.J. and Robinson D.N. 1982. Two diamond-bearing peridotite xenoliths from the Finsch Kimberlite, South Africa. *Contributions to Mineralogy and Petrology* 81, 79-87.

Urusovskaya A.A. and Orlov Yu. L. 1964. Nature of plastic deformation of diamond crystals. *Doklady Akademii Nauk SSSR* 154, 112-115.

Yamaoka S., Kanda H. and Setaka N. 1980. Etching of diamond octahedrons at high temperatures and pressures with controlled oxygen partial pressure. *Journal of Materials Science* 15, 332-336.

Table giving the percentages of the diamonds which exhibit particular features. (N = number of diamonds. Facies T = diatrema, 1 = upper and 2 = lower portion, H = hypabyssal, R = root zone, D = dyke, Tr = transitional or mixed T/H, E = epiclastic).

	N	Colour		Main Form		Shape		Surface Texture						Facies		
		Yellow-col.	Brown	Grey/black	Octahedron	"Rnd. dodec."	Cube	Broken	Pseudohemi.	Lam. lines	Microdisks	Corrosion	Shallow dep.		Coarse frost	Fine frost
Dokolwayo	301	81	18	1	6	94	0	54	tr	55	2	1	4	24	30	T1
Dullstroom	72	79	19	1	4	94	0	75	0	51	6	1	11	6	0	HD
Palmietgat	299	9	11	46	2	95	1	76	tr	46	3	24	31	1	4	T2
Premier Brown K	300	70	30	1	4	95	0	70	1	73	0	5	16	13	21	T2
Grey K	300	36	63	1	11	86	0	67	3	65	5	9	25	3	6	T2
Black K	300	34	65	1	7	89	0	68	2	59	3	15	31	8	16	Tr
Helam	246	69	24	7	11	51	22	44	0	38	1	0	4	0	tr	HD
Kamfersdam	300	29	71	0	11	86	0	68	3	64	tr	1	2	tr	1	Tr
De Beers	161	63	37	0	7	89	0	60	1	63	3	6	28	12	10	HR
Dutoitspan E Plug	253	54	44	2	10	88	0	71	2	58	5	25	30	5	8	HR
Bultfontein	300	57	38	2	21	76	1	75	tr	54	tr	2	2	2	2	Tr
Wesselton W2	290	51	45	2	4	96	0	62	tr	57	2	12	34	0	1	HR
W3	300	47	51	2	3	95	0	73	0	61	1	43	50	1	1	HR
W5	94	69	31	0	4	95	0	69	1	51	0	2	3	0	0	T2
W7	160	44	55	1	4	95	0	69	0	54	1	5	11	2	18	Tr
Finsch K-F1	307	45	53	2	6	94	tr	62	tr	73	3	2	9	3	3	T1
K-F6	102	54	46	0	11	89	0	65	1	48	0	2	4	2	6	HD
Makganyene	332	44	54	2	2	98	0	51	1	62	12	1	11	1	tr	Tr
Peizer	108	19	81	0	6	94	0	64	0	69	4	10	45	5	10	HR
Jwaneng DK2	300	86	14	1	16	62	19	57	1	22	1	1	3	0	1	F
DK7	299	53	46	tr	32	55	8	66	4	36	2	1	1	1	2	Tr

Daniel J. Schulze

Department of Geological Sciences, Queen's University
Kingston, Ontario, Canada K7L 3N6

Based on the abundance and composition of silicate and oxide inclusions in natural diamonds, most diamonds are thought to represent xenocrysts derived by disaggregation of dunites or harzburgites that contain low-calcium garnet and chromite. Although current models explaining the origin of such Ca-poor ultrabasic rocks involve magmatic depletion through high degrees of partial melting (e.g., Boyd and Gurney, 1982), virtually Ca-free ultrabasic rocks are also produced by thorough serpentinization of peridotite. Subduction of oceanic serpentinites, and subsequent prograde metamorphism to garnet peridotite facies would, therefore, result in low-calcium garnet harzburgites, the host rocks of most diamonds in the upper mantle.

To test this hypothesis, an ACF diagram has been constructed (Fig. 1), corresponding to equilibration conditions of approximately 1100°C and 55-60 kb. The data used in the construction of this figure were taken from diamondiferous garnet lherzolites and peridotite-suite minerals included in diamonds from the Finsch pipe in South Africa (Shee et al., 1982; Gurney et al., 1979; Tsai et al., 1979). These data were chosen because they represent the best documentation of diamond-related minerals from a single pipe. By plotting serpentinite bulk chemical analyses in this diagram, the serpentinites are effectively recast into approximate proportions of the various minerals that are stable under these conditions.

The results of this exercise are shown in Fig. 1. Of the 57 published analyses of serpentinites taken from the literature, the majority (44) are compositionally equivalent to harzburgites in which low-calcium garnet is stable. The Mg/(Mg + Fe) values of these 44 rocks range from 0.88-0.98. Exclusion of the vein serpentinites (Mg/(Mg + Fe) >0.97), however, results in an approximately bimodal distribution with a major peak at ~0.940 and a broader peak at ~0.915. These data correlate well with the Mg/(Mg + Fe) values of olivine inclusions in diamonds (J.J. Gurney, unpublished data), which have a perfect bimodal distribution with maxima near 0.920 and 0.945.

Elemental carbon is not uniformly distributed within the upper mantle but, excluding the eclogite suite, is preferentially associated with the low-Ca ("depleted") peridotite association. Diamond-bearing low-Ca garnet dunites and harzburgites are more abundant than are diamondiferous garnet lherzolites, just as peridotite-suite garnets included in diamonds are generally calcium-poor, and not of lherzolite affinity. Furthermore, a high percentage of diamond-free low-Ca garnet harzburgites contain graphite (Nixon et al., in press), whereas it is rare in garnet lherzolites. Therefore, the process that produces the Ca-poor characteristics of the peridotite must be related to the introduction of carbon. Most current hypotheses of formation of peridotite-suite diamonds do not explain the carbon source, although Haggerty (1986) states that the Ca-poor peridotites are more reducing than are the abundant garnet lherzolites, thus reducing CO₂ or oxidizing CH₄ when these volatiles are introduced into the peridotite. In the present model, graphite is formed during the serpentinization process, as documented by Pasteris (1981). The ultimate source for carbon is uncertain, but could be methane-bearing fluids, CO₂ fluid inclusions in olivine or pyroxene, or elemental carbon present in the fresh olivine. It is clear, however, that the carbon that could eventually form as diamond originates in the process of serpentinization, as does the chemical signature of the Ca-deficient host peridotite.

Boyd and Gurney (1982) proposed that the apparent restriction of both diamonds and low-calcium garnet xenocrysts to stable Archean cratons was due to the fact that generation of komatiitic magmas during the Archean was responsible for the calcium-depleted residual harzburgites, in which diamond subsequently formed. Archean ages for Ca-poor garnets and diamonds were demonstrated by Richardson et al. (1984). In the subducted serpentinite model, the apparent geographic restriction of these phases would be due to high convergence rates in the Archean that would promote shallow subduction

of the partially serpentinized oceanic lithosphere. Repeated episodes of shallow subduction (underthrusting) would be primarily responsible for the formation of the relatively cool, subcratonic lithosphere (Helmstaedt and Schulze, this volume), a process analogous to "dealing onto the bottom of the deck". This would allow for emplacement of metaserpentinites at relatively low temperatures, thus avoiding partial melting that might destroy both the low-calcium nature of the peridotites and their diamonds by heating and metasomatic hybridization. This origin and emplacement mechanism would also account for the lack of evidence for a high temperature protolith of the low-Ca peridotites, as required by komatiite residue models. Emplacement beneath Archean cratons would protect the metaserpentinites from tectonism and magma production during subsequent orogenesis that occurred in adjacent mobile belts.

- Boyd, F.R., and Gurney, J.J. 1982. Low-calcium garnets: Keys to craton structure and diamond crystallization. *Carnegie Institution of Washington Year Book*, 261-267.
- Gurney, J.J., Harris, J.W., and Rickard, R.S. 1979. Silicate and oxide inclusions in diamonds from the Finsch kimberlite pipe. In Boyd, F.R., and Meyer, H.O.A. eds., *Kimberlites, Diatremes, and Diamonds: Their Geology, Petrology, and Geochemistry*, pp. 1-15, A.G.U., Washington.
- Haggerty, S.E. 1986. Diamond genesis in a multiply-constrained model. *Nature* 320, 34-38.
- Nixon, P.H., van Carlsteren, P., Boyd, F.R., and Hawkesworth, C.J. in press. Harzburgites with garnets of diamond facies from southern African kimberlites. In Nixon, P.H. ed., *Mantle Xenoliths*, Wiley, London.
- Pasteris, J.D. 1981. Occurrence of graphite in serpentinized olivine in kimberlite. *Geology* 9, 356-359.
- Richardson, S.H., Gurney, J.J., Erlank, A.J., and Harris, J.W. 1984. Origin of diamonds in an old enriched mantle. *Nature* 310, 198-202.
- Shee, S.R., Gurney, J.J., and Robinson, D.N. 1982. Two diamond-bearing peridotite xenoliths from the Finsch kimberlite, South Africa. *Contributions to Mineralogy and Petrology* 81, 79-87.
- Tsai, H.M., Meyer, H.O.A., Moreau, J., and Milledge, H.J. 1979. Mineral inclusions in diamond: Premier, Jagersfontein, and Finsch kimberlites, South Africa, and Williamson Mine, Tanzania. In Boyd, F.R., and Meyer, H.O.A. eds., *Kimberlites, Diatremes, and Diamonds: Their Geology, Petrology, and Geochemistry*, pp. 16-26, A.G.U., Washington.

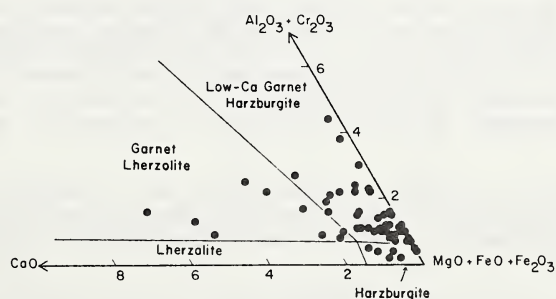


Fig. 1. Serpentinite bulk compositions plotted in an ACF diagram, applicable to equilibration conditions of approximately 1100°C and 55-60 kb.

COMPOSITION OF CRYSTALLINE INCLUSIONS AND C-ISOTOPIC
COMPOSITION OF ARGYLE AND ELLENDALE DIAMONDS

A. L. Jagues¹, J. W. Sheraton¹, A. E. Hall²,
C. B. Smith², S. S. Sun¹, R. Drew¹ & C. Foudoulis³

1. Bureau of Mineral Resources, GPO Box 378, Canberra ACT
2. CRA Exploration, Pty Limited, 21 Wynyard Street, Belmont, WA
3. Department of Geology, Australian National University, PO Box 4, Canberra ACT

This study continues the work reported by Hall and Smith (1984). Further data on syngenetic inclusion abundances at Argyle has been given by Harris and Collins (1985).

Ellendale diamonds contain approximately equal proportions of peridotitic and eclogitic inclusions. The peridotitic suite includes olivine, chrome-pyropo, chrome-diopside, enstatite and chrome spinel. The eclogitic suite is dominated by orange garnet but clinopyroxene, coesite and rutile are also present. Sulphides occur in both parageneses.

Inclusions in the Argyle diamonds are dominantly of eclogitic paragenesis of which orange garnet is the major syngenetic inclusion, with lesser clinopyroxene, coesite, kyanite, rutile and sulphide. Very rare ilmenite and moissanite were recovered. Peridotitic inclusions are dominantly olivine with rare purple chrome-pyropo and enstatite. Sulphide (chiefly pyrrhotite) also occurs in some peridotitic suites but can also occur solely associated with graphite. K-feldspar, determined by X-ray analysis to be orthoclase rather than sanidine, is a widespread inclusion. Although commonly having crystalline shape similar to the syngenetic inclusions it is assigned to the epigenetic suite as it is invariably rimmed by phlogopite or mixtures of other sheet silicates. Other epigenetic inclusions, also widespread, include abundant graphite together with phlogopite, talc, calcite, quartz, haematite, chlorite, anatase, sphene, rutile, kaolin and very rare priderite.

The Argyle eclogitic suite exhibits a wide range in Ca-Mg-Fe as shown by co-existing garnet and clinopyroxene (Fig. 1). Garnets range from relatively Ca-poor, pyropo-almandine (6 wt % CaO) through more calcium- and iron-rich varieties to rare grossular-rich garnet (17-18 wt % CaO). Ellendale eclogitic garnets have a more restricted range in Ca-Mg-Fe generally containing less than 10 wt % CaO. A characteristic of the Argyle eclogitic garnets is the very high Na contents, commonly 0.45-0.55 wt %, but range up to 0.71 wt %. These high Na contents are attended by high P and Ti (up to 0.39 wt % P₂O₅, 1.45 wt % TiO₂) but in contrast to the observations of Bishop et al (1976) in a number of the higher Na garnets Na exceeds P + Ti. In the most Na-rich garnets Si contents closely approximate ideal garnet stoichiometry and are unlike the Na-rich garnets with excess Si described by Moore and Gurney (1985). In contrast Ellendale eclogitic garnets are generally low in Na (<0.2 wt %) but can range up to 0.5 wt %. With no excess Na there is a balance with the P and Ti in the structural formula. There is also no excess Si implying no pyroxene component in the garnet.

The Argyle clinopyroxenes have very high jadeite components (up to 9.5 wt % Na₂O, 19 wt % Al₂O₃) and extremely high K₂O contents (up to 1.3 wt %). These are the highest K levels reported in pyroxene and indicate formation under very high pressure. There is little correlation between Na and K contents (Fig. 2). The clinopyroxenes from the Ellendale inclusions are more Mg-rich and have a lower jadeite component (<7 wt % Na₂O) and lower K₂O (<0.5 wt %) values than the Argyle inclusion clinopyroxenes.

The peridotitic inclusions from both Argyle and Ellendale are characterised by refractory compositions, i.e. high olivine with mg₉₂₋₉₄ and Cr-rich pyropo (up to 15% Cr₂O₃). Alumina contents in enstatite are particularly low, as observed by Hall and Smith (1984).

Comparison of the C-isotopic compositions of Argyle and Ellendale inclusion-bearing diamonds shows that most of the Ellendale stones, both peridotitic and eclogitic, and the Argyle diamonds with peridotitic inclusions have small negative

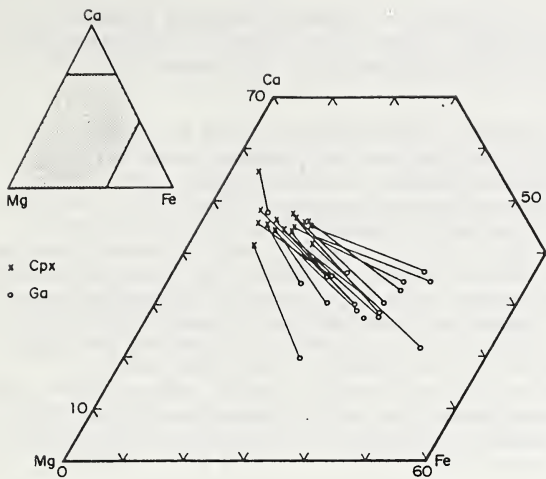


Fig. 1

Ca-Fe-Mg diagram for co-existing garnet and clinopyroxene inclusions from Argyle diamonds.

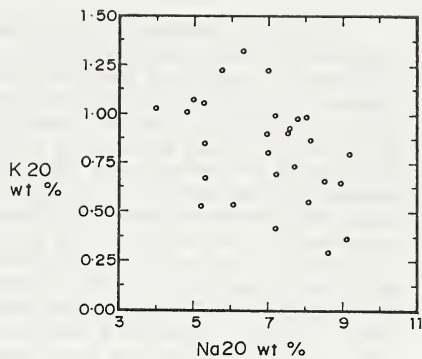


Fig. 2

Variation of Na₂O with K₂O in clinopyroxenes from Argyle diamonds.

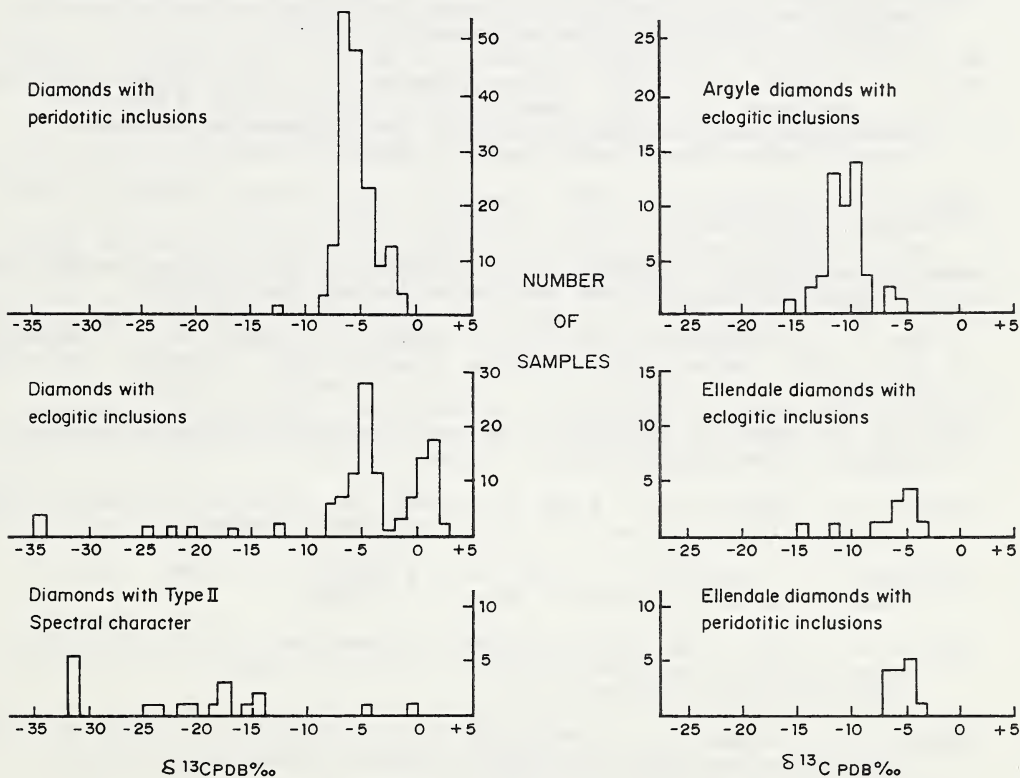


Fig. 3

Carbon isotopic compositions of inclusion-bearing diamonds from Argyle and Ellendale compared with inclusion-bearing stones elsewhere (data from Sobolev et al. (1979), Sobolev (1984), Deines et al. (1984)) and diamonds with Type II spectral character (Milledge et al., 1983).

$\delta^{13}\text{C}$ values (-4 to -6 ‰PDB) similar to the bulk of inclusion-bearing diamonds elsewhere (Fig. 3). The majority of the Argyle stones with eclogitic inclusions have significantly lighter C isotopic compositions lying mostly in the range -9 to -12 ‰PDB.

At Argyle an association of stone morphology and inclusion type has been recognised. Sharp edged octahedra with etched and frosted surfaces contained only peridotitic inclusions and have a restricted range of isotopic compositions. These diamonds resemble the diamonds recovered from peridotite nodules from Argyle (Hall and Smith, 1984). Two distinct sources for the Argyle diamonds are therefore suggested. The octahedral (and associated forms) formed during a relaxed (low) geothermal gradient in Archaean (?) refractory, reduced peridotite comprising much of the lower lithosphere beneath the Kimberley craton which is inferred to be the residue of Precambrian magma extraction (Richardson et al, 1984). The bulk of the diamonds - rounded, resorbed dodecahedra - are of eclogitic paragenesis and it is tentatively suggested that these are derived from recycled crustal material and are younger in age than those of peridotitic paragenesis. This recycled crustal material may be the same as or related to the ancient (>2 By) enriched component identified in the lamproites (Nelson et al, 1986). A dual or multiple origin for the Argyle diamonds is consistent with the very wide range in $^3\text{He}/^4\text{He}$ and other noble gas ratios reported by Honda et al (1985).

REFERENCES

- BISHOP, F. C., SMITH, J. V. & DAWSON, J. B., 1976. Na, P and Ti and co-ordination of Si in garnet from peridotite and eclogite xenoliths. *Nature* 260, 696-697.
- DEINES, P., GURNEY, J. J. & HARRIS, J. W., 1984. Associated chemical and carbon isotopic composition variations in diamonds from Finsch and Premier kimberlite, South Africa. *Geochimica Cosmochimica Acta* 48, 325-342.
- HALL, A. E. & SMITH, C. B., 1984. Lamproite diamonds - are they different. In Glover, J. E. and Harris, P. G. eds. *Kimberlite Occurrence and Origin: A Basis for Conceptual Models in Exploration*, 167-212. Geology Department and University Extension, University of Western Australia, Publication No. 8.
- HARRIS, J. W. & COLLINS, A. T., 1985. Studies of Argyle diamonds. *Industrial Diamond Review* 3/85, 128-130.
- HONDA, M., McCONVILLE, P., REYNOLDS, J. H. & ROEDDER, E., 1986. Solar-like noble gases in terrestrial diamond. *Lunar and Planetary Science XVII*, 348-349.
- MILLEDGE, H. J., MENDELSSOHN, M. J., SEAL, M., ROUSE, J. E., SWART, P. K. & PILLINGER, C. T., 1983. Carbon isotopic variation in spectral type II diamonds. *Nature* 303, 791-792.
- MCORE, R. O. & GURNEY, J. J., 1985. Pyroxene solid solution in garnets included in diamond. *Nature* 318, 553-555.
- NELSON, D. R., McCULLOCH, M. T. & SUN, S-S., 1986. The origins of ultrapotassic rocks as inferred from Sr, Nd and Pb isotopes. *Geochimica Cosmochimica Acta* 50, 231-245.
- RICHARDSON, S. H., GURNEY, J. J., ERLANK, A. J. & HARRIS, J. W., 1984. Origin of diamonds in old enriched mantle. *Nature* 310, 198-202.
- SOBOLEV, M. V., 1977. Deep-seated inclusions in kimberlites and the problem of the composition of the upper mantle (Brown, D. W. transl, Boyd, F. R. ed), American Geophysical Union, Washington, D.C.
- SOBOLEV, N. V., GALIMOV, E. M., IVANOVSKAYA, N. N. & YEFIMOVA, E. S., 1979. Isotopic composition of the carbon from diamonds containing inclusions (in Russian). *Doklady Akad Nauk USSR* 249, 1217-1220.

N. V. Sobolev¹, E. S. Yefimova¹ and E. I. Shemanina²

1. Institute of Geology & Geophysics, Siberian Division
of Academy of Science, Novosibirsk, USSR

2. All-Union Geological Institute (VSEGEI), Leningrad, USSR

Diamonds from alluvial sources of the northern Urals have been known since 1829 but no kimberlites have yet been found there. Most of the finds are located within the area of the Vishera River. Most of the diamonds are represented by rounded dodecahedra typical of alluvial deposits of Brazilian type.

Protogenetic and/or syngenetic inclusions have been recovered from more than 200 diamonds of variable size. The included minerals are olivine, chromite, chrome pyrope, chrome diopside, enstatite, Mg-Fe-garnet, omphacite, kyanite, coesite, rutile, sulphides.

The majority of the primary inclusions have an eclogitic suite affinity. Garnets of that type are the most common inclusions. They are represented by a wide series of compositions with Fe/Fe+Mg ratios mainly ranging from 30% to 60% and of Ca-component contents varying from 10 to 55 mol % but mostly lying between 20 and 35 mol %.

Clinopyroxenes of the eclogitic suite contain from 2.13 up to 9.59% Na₂O, i.e. from 14 to 72% of jadeite. A stable impurity of K₂O (up to 0.38 wt %) is fixed in them. In addition to these major minerals, coesite, kyanite, rutile and low Ni sulphides have been found. The most interesting polymineralic inclusion found in the single diamond is a garnet-coesite intergrowth.

Ultramafic suite inclusions are represented by high chrome pyrope (up to 15.6 wt % Cr₂O₃), forsteritic olivine, enstatite, chromite (more than 62 wt % of Cr₂O₃) and chrome diopside.

The studies of carbon isotopic composition have been undertaken by E. M. Galimov on about 90 diamonds, most of which contain inclusions. Fifteen diamonds of the ultramafic suite show small negative $\delta^{13}\text{C}$ ratios typical of diamonds from this type of all known localities (from -7.94 up to -2.10 ‰). Eclogitic suite diamonds based on study of more than 70 crystals have a wide range of $\delta^{13}\text{C}$ (from -22.20 up to -4.16 ‰) which is a typical feature of most known eclogitic suite diamonds.

The abundances of syngenetic inclusions in the diamonds from the Urals indicate a predominance of the eclogitic suite diamonds. The evaluation of more than 200 diamonds with inclusions of primary minerals indicate the following percentage; 75% eclogitic and 25% peridotitic. All sulphides analysed (about 10) are related to the eclogitic suite.

VI. DIAMOND EXPLORATION

Exploration for primary and alluvial deposits of diamonds, including: concepts, exploration technology, evaluation procedures and case histories.



HEAVY MINERAL GRAVEL SAMPLING IN THE KIMBERLEY,
WESTERN AUSTRALIA

	Page
REVIEW PAPER	
A review of diamond exploration philosophy, practice, problems and promises Warren J. ATKINSON	435
Preliminary study of soil bacterial populations over and adjacent to three kimberlite diatremes P. O. ALEXANDER	440
Discovery of the George Creek, Colorado kimberlite dikes J. A. CARLSON and S. W. MARSH	443
Geology and exploration of the Rose lamproite, South East Kansas, USA H. G. COOPERSMITH and R. H. MITCHELL	446
The Argyle AK1 diamond size distribution: the use of fine diamonds to predict the occurrence of commercial size diamonds A. S. DEAKIN and G. L. BOXER	448
Geology of the Argyle alluvial diamond deposits A. S. DEAKIN, G. L. BOXER, A. E. MEAKINS, E. HAEBIG and J. H. LEW	451
A geophysical case history of the AK1 lamproite pipe G. J. DREW	454
Morphology of kimberlite minerals: its usage for predicting and searching for diamond deposits V. K. GARANIN, G. P. KUDRYAVTSEVA, T. V. POSUKHOVA and V. P. AFANASJEV	457
Collection and treatment of diamond exploration samples P. G. GREGORY and D. R. WHITE	460
Origin of the Casuarina alluvial diamonds, Western Australia M. J. GUNN, A. C. EDWARDS, D. A. PATERSON, W. H. RINGENBERGS and G. E. WILLIAMS	463
Geochemical expression of some West Australian kimberlites and lamproites A. E. HAEBIG and D. G. JACKSON	466
Alkaline diatremes in the Hudson Bay lowlands, Canada, exploration methods, petrology and geochemistry A. J. A. JANSE, I. F. DOWNIE, L. E. REED and I. G. L. SINCLAIR	469
Spectral reflectance features of kimberlites and carbonatites; the key to remote sensing for exploration M. J. KINGSTON	472
Trace element detection in individual mineral grains D. C. LEE, A. VAN RIESSEN and K. W. TERRY	475
The alluvial diamonds of the Western Transvaal South Africa T. R. MARSHALL	478
The efficiency of fluvial trap sites to concentrate kimberlitic minerals: An experimental sampling programme M. T. MUGGERIDGE	481
Prospective relationships between diamonds, volcanism and tectonism in Australia F. L. SUTHERLAND, L. R. RAYNOR, J. D. HOLLIS and P. A. TEMBY	484

Warren J. Atkinson

CRA Exploration Pty Limited, 21 Wynyard Street, Belmont, Western Australia

INTRODUCTION

Since inception in the post-war period the introduction of well-funded, scientifically based surveys of large areas for diamond has more than doubled the global supply of natural stones to the market. Pre-war production is mainly attributed to the historical and "prospector" period, albeit often very skilled and systematic, but lacking the funding and technology to advance the search for resources into geologically favourable areas that were relatively inaccessible by virtue of isolation, climate or surficial cover, and which required scientifically based concepts for area selection and an improved technological approach to explore them.

Significant modern discoveries have been primary deposits, pipes, generally at the expense of major new alluvial supplies reflecting:

- (i) recognition that large primary deposits can represent long-life mines, amenable to large scale mining methods, with secure consistent production warranting the exploration funding required;
- (ii) that alluvials, by virtue of their nature, had been more readily discovered by direct prospector recognition of diamond, in contrast to the indirect and more difficult exploratory methods required for pipes.

This major increase in exploration-initiated pipe production has, most significantly, been marked by the development of new production centres. These are away from countries where the major fields were initially alluvial producers, discovered in past centuries or early in the 20th, and where pipe discoveries generally followed as a result of follow-up of alluvial/elluvial dispersion trains. In contrast the most marked effect of modern exploration has been the rapid rise of countries that hitherto were nil or insignificant producers of diamond but are now major producers, notably of course the USSR and Botswana and latterly Australia.

In respect of the last the selection of the present venue of the 4th IKC is endorsement of very recent exploration that:

- has extended the occurrence of large economic pipe mines to a third continent;
- will increase production of natural diamond by 40 to 50 percent this year;
- has confirmed lamproite as an alternative primary source to kimberlite for economic concentrations of diamond;
- increased the world's portfolio by some 150 additional kimberlite, lamproite and related rock occurrences of all sizes that are available for study both by academia to further our understanding of the mantle, and also by the exploration industry for the ongoing advancement of exploration techniques.

The rapidity with which increased production from new countries has been achieved by modern exploration, an occurrence not restricted to diamonds, raises of course the inherent question of where will it end if exploration continues at its post-war rate - a "problem" or a "promise", for which the answer can only lie with expanding markets, elimination of uneconomic producers, or a combination of this and controlled supply to the market place.

THE EXPLORATION PROCESS

Exploration for diamonds is an industry, or national response to demand for more of a particular product than existing mines can supply at an economic price. It comprises "risk" that unsuccessful exploration will result in a loss of money or other resources, and "reward", i.e. an economic mine producing profit, or alternatively, a

product that a nation, for example, cannot afford to import, or for security purposes, requires to be produced internally. There are other commercial constraints, in a free enterprise economy; access to land, secure title to discoveries, and realistic rules for commercial development and mining must be in place.

The exploration process comprises therefore:-

- (i) commercial factors
 - need and market
 - access to land and commercially acceptable rules for exploration and exploitation;
 - adequate risk funding
- (ii) technical factors
 - area selection - development of advanced concepts for emplacement and preservation of economic sized pipes and grades (value) so that practical areas of prospective ground, giving the greatest probability for economic discovery, are selected. Area selection techniques need major improvement.
 - search technology - it is increasingly recognised that major exploratory successes are achieved by indirect exploration for large primary sources in areas where prospector discovery was precluded by other factors, e.g. lack of exposed alluvials, surficial overburden, isolation, climate, etc. This has required adaption of existing techniques, remote sensing, indicator sampling, direct diamond detection, geophysics, etc. to progressively varying geological, geomorphological, climatic and other regimes. This is an ongoing process with vast scope for improvements of existing practices and developments of new technology.
- (iii) human factors
 - the right people, trained, field orientated, observant, inquisitive and motivated.
 - risk tolerant management committed to success.

Area Selection

The empirical study by Clifford (1967) showed that diamondiferous kimberlites are restricted to areas cratonised by 1500 My. Suggested association of West African kimberlites with the passage of the continent over hot spots has drawn attention to the alignment of kimberlite and the use of linears during exploration area selection. Diamondiferous lamproites are associated with rift zones (Luangwa Valley, Zambia; Prairie Creek, Arkansas; Ellendale, Western Australia) and transcurrent faulting developed along Proterozoic mobile zones (Ellendale and Argyle, Western Australia). These Western Australian mobile zones were stabilised by 1800 My, hence Clifford's view also applies to lamproites and is still useful in area selection.

Establishment of the prospective age of kimberlite helps target exploration areas both for alluvials and primary sources, e.g. the discovery of the Triassic Dokolwayo pipe intruding an inlier of basement granite surrounded by overlying Upper Karroo sediments (Hawthorne et al, 1979). In this case diamonds and indicators in the Karroo sediments provided the lead towards location of the pipe.

The geomorphological environment determines the degree of preservation of the kimberlites (Gold, 1984), uplifted areas being subjected to erosion and rapid removal of the upper levels of the diatremes. Good stream drainage may be present in such uplifted areas, and stream sampling for kimberlite indicator minerals may be an effective search technique, but if the kimberlites preserved have been eroded down to stringers or thin dykes they are of relatively low commercial value (eg. North Kimberley, Western Australia; Sierra Leone). Adjacent low lying ground is subject to deposition rather than erosion. There is a better chance of preservation of the upper levels of diatremes (e.g. West Kimberley lamproites), but they may be buried by overlying sediments. Stream drainage on plains country may be poor and indicator mineral searches may have to be carried out by the grid loaming technique.

The nature of alluvial diamond deposits is related not only to areas of deposition and manner of concentration, but also to climate. Rapid stream deposition under an

arid climate may result in little concentration, with grades tailing off rapidly downstream (e.g. Argyle). In contrast, tropical humid climates with attendant chemical weathering cause breakdown of the less resistant components in the alluvials, with consequent upgrading of the diamond content (Hall et al, 1985; Thomas et al, 1985). Such alluvials may produce ore deposits further from their primary diamond source (eg. Tertiary alluvial terraces in South Africa). Where concentration factors are extreme, such as on the marine beaches of Namibia (Hallam, 1964) payable alluvials may be found at extreme distances from source. A further effect of transportation is improvement in the quality of the stones preserved, the more fractured and easily broken stones being eliminated. On the other hand average diamond sizes decrease downstream (Sutherland, 1985), though local sorting effects can cause reversals in the trend.

Search Technology

Prospectors traditionally fossicked in river gravels for diamonds, and from this approach has stemmed the indicator mineral search techniques using kimberlite minerals as pathfinders.

The chemistry of minerals from kimberlite and lamproite, from mantle nodules within these rocks and from diamond inclusions, has been characterised by extensive analysis (eg. Dawson and Stephens, 1977; Sobolev, 1977). This characterisation not only enables chemical confirmation that suspected indicator minerals obtained in a field sampling programme have indeed emanated from a kimberlite, but also allows estimation of the diamond potential of the kimberlite source. Hence newly found clusters of kimberlite can be ranked in order of priority for evaluation of diamond content by bulk sampling (Gurney, 1984; Sobolev et al, 1984).

Field methods of processing samples involve gravity separation of the heavy minerals by gold pan or jig, and visual observation of the concentrate to identify the kimberlite indicator minerals. Such practice is effective where the minerals are coarse grained (+1mm) and numerous, but where success may be represented by recovery and recognition of 1 single indicator mineral grain of, say, 0.4mm size in a whole sample, greater efficiency of laboratory processing is a requisite.

Where river drainage exists, indicator minerals from kimberlite are released by weathering and move by soil creep or sheet wash into the nearby streams. Downstream transportation of these minerals provides a train leading back to the kimberlite. In Yakutia, USSR, the cold climate inhibits chemical weathering and olivine grains -1.0 + 0.5mm travel up to 100 km from kimberlites without significant wear (Afanasev et al, 1984). In Africa and Australia, in warmer climates with marked seasonal rainfall, indicator minerals have been found to travel from 20 km or more for 0.4mm size grains to only 1 or 2 km for 1.0mm size grains dependant on stream gradient and stream flux (Bardet, 1973; Mosig, 1980). As the indicators are heavy they concentrate en route in natural trap sites, eg. above rock bars, in crevices in bedrock, in gravel point bars often on the inside of meanders. In exploration small samples of this gravel, typically 8 - 40 kg in size, are collected at reconnaissance intervals of 3 to 15 km along the streams, a typical coverage of say, 1 sample per 50 sq km (Atkinson et al, 1984). Where kimberlite indicators are found then follow up gravel sampling is undertaken at closer intervals until the source area is defined. This technique has been responsible for the discovery of the economic Mir and Udachnya kimberlite pipes in USSR, and the Ellendale and Argyle lamproite pipes in Western Australia. In north America, gravels from eskers have been sampled in similar manner.

In regions which lack effective drainage the loam sampling technique is used and consists of collecting the top 1cm of soil in which wind deflation has concentrated the heavy minerals. Initial reconnaissance work may be widely spaced, eg. 13.5 kg samples on a 1.6 km square grid as described by Bardet (1973) for exploration in Tanzania. Follow up work requires more detailed sampling to locate individual pipes, often characterized by anomalous haloes of indicators spread over some six times the area of the pipe.

Bulk sampling of one to several cubic metres of gravel or rock is required if diamonds are sought directly during prospecting operations. This method is normally used in the search for alluvial deposits (eg in west Africa, Bardet 1973), particularly

those far from source. The method can also give information on the presence of diamonds in a stream catchment where indicator minerals are already known, and hence provide encouragement to continue searching for the primary kimberlite host. The disadvantage of the method is the high cost of bulk sampling, and the attendant need for concentrating machinery (unless an abundant supply of cheap labour is at hand) which restricts prospecting mobility. The method is not readily applicable to arid areas and to regions without stream drainage.

Air photo interpretation is of wide value in diamond exploration, providing information on regional structure and geomorphology during area selection, and being used as a mapping tool in association with field work when delineating alluvials or prospecting for kimberlite. Many pipes and dykes have been located in southern and central Africa where they gave rise to vegetational features, circular depressions or mounds, or tonal differences visible on air photos (Mannard, 1968; Edwards and Howkins, 1966).

Landsat imagery pixels are too coarse to detect individual kimberlites (Nixon, 1980), but such imagery has been used in regional structural analysis of kimberlite provinces (Woodzick and McCallum, 1984). The airborne multispectral systems being developed today have much greater resolution, can detect the signature of specific clay minerals and therefore have the potential to locate kimberlite weathering products. Future developments of this method may become important in diamond prospecting.

Geophysics has been used in kimberlite exploration since the 1930s, but early use was generally confined to delineation of pipes rather than exploration for them, due to the available technology of the day. Magnetic gravimetric and resistivity contrasts between kimberlite and country rock have been employed to locate pipe boundaries and provide information on the size and depth extent of pipes. All early surveys were conducted on the ground using relatively cumbersome equipment making regional coverage very difficult and time consuming. USSR scientists were the first to use airborne magnetic surveys extensively in kimberlite exploration, many of the pipes in Yakutia being found by this method. Since the 1970s, geophysical surveys, particularly airborne methods, have focussed on kimberlite exploration rather than delineation. The greatly improved technology and understanding of airborne magnetometry and radiometric systems, plus the advent of digital recording, has made these the most popular methods. In Australia alone it is estimated that some 200,000 line km of such airborne surveys are conducted each year in diamond exploration. Airborne electrical methods such as INPUT are also effective, but it is aeromagnetics that have been responsible in the late seventies for finding most of the pipes in the West Kimberley, Australia and in central Botswana.

Kimberlites and lamproites are enriched both in elements of ultramafic affinity (eg. Mg, Co, Ni, Cr, Cu) and in "incompatible" elements (eg. LREE, Ba, Sr, Rb, P, NG) (Dawson, 1967; Smith, 1984) which gives these rocks a characteristic identification signature. This signature is used in two ways: 1. in pathfinder regional stream and soil surveys seeking to locate kimberlites suspected to occur nearby (Gregory and Tooms, 1969); 2. as support towards the identification of rocks from weathered outcrop or drill cuttings. Stream and soil geochemistry is of limited use because the detectable halo of chemical dispersion around kimberlites rarely exceeds a few tens of metres in soil, or a few hundreds of metres in streams. Chemical analysis for rock identification is cheap and effective and particularly useful where extensive oxidation and weathering of kimberlitic rocks renders their identification very difficult by optical or petrological methods in the field or laboratory.

EVALUATION OF DIAMOND DEPOSITS

Evaluation of diamond deposits requires determination of the volume of ore reserves by conventional drilling and pitting methods, plus calculation of the in-situ worth of the ground. This worth (revenue) is related to both grade (ct/t or ct/m³) and quality of the diamonds. The relative rarity of diamond in an economic deposit, from 0.01 to 3.5 ppm (Atkinson et al, 1984), combined with the need for a parcel of at least 5000 ct for valuation (Sutherland and Dale, 1984), shows why bulk sampling operations involving treatment of several hundred to several thousand m³ are required during evaluation work.

Diamond size distributions are lognormal in alluvial deposits (Sichel, 1972) and in lamproite and kimberlite (Hall and Smith, 1984), and special techniques based on classical statistics have been devised for grade and revenue calculations (Oosterveldt, 1972). Recent ore reserve estimations for the Argyle diamond deposits (Boxer et al, 1985) used both classical and geostatistical methods of calculation, and found good agreement between the methods.

PROBLEMS AND PROMISES

The discovery of diamond-bearing lamproites at Ellendale (Atkinson et al, 1984) and Argyle (Atkinson et al, 1985) has revealed a new primary source rock as a target for diamond exploration, and raises the query as to what other mantle-derived igneous rocks may also be diamondiferous.

Diamondiferous lamproites contain the same indicator minerals such as pyrope, chrome diopside and picroilmenite (the latter is rare in lamproite) that also characterise kimberlites, but they are not as abundant and usually finer grained. The megacryst suite of indicators (Nixon and Boyd, 1973), large picroilmenites, Ti-rich garnet and diopside, zircon, etc, appears to be absent. Other minerals such as priderite, richterite, can be used as indicators of lamproite (Atkinson et al, 1984).

Alluvial diamond localities without such indicators have traditionally been viewed as far removed from any primary source rock. Diamond, because of its hardness and inertness to chemical weathering, survives both long distance of travel and recycling through the sedimentary record. Local reconcentration may give rise to alluvial ore deposits such as the Namibian marine terraces. Elsewhere a wide geographical dispersion of occasional diamond may occur, such as those being reworked from the Roraima Series sediments in Venezuela. Indicator minerals such as garnet, chrome diopside and picroilmenite are not as resistant to chemical weathering and abrasion, especially under tropical climates. Hence the presence of indicators within the sedimentary column suggests a local source, though it may still be blind.

The discovery of diamond in lamproite accompanied by relatively few classical indicator minerals now shows that alluvial diamond deposits with a virtual absence of indicators such, as at Argyle, can exist close to primary source. This throws into question the distant primary source invoked for many of the world's alluvial diamond localities.

ACKNOWLEDGEMENTS

Lack of space prohibits full reference to all researchers and explorationists whose ideas and work are reflected in this abstract. A useful exploration bibliography is provided by Glover and Phillips (1980) in "Kimberlite and diamonds; publication No. 5, Geology Department and the Extension Service, University of Western Australia, and Gregory (1984) has included more recent references in his paper, "Exploration for Primary Diamond Deposits, with Special Emphasis on the Lennard Shelf, WA" in the Canning Basin, WA: Proceedings of the Geol. Soc. Aust./Pet. Expl. Soc. Aust. Symposium, Perth. Special thanks for discussions and comment during preparation of this paper are given to Messrs C. B. Smith, R. Ramsay, G. J. Drew and R. G. Spencer.

PRELIMINARY STUDY OF SOIL BACTERIAL POPULATIONS OVER AND ADJACENT TO THREE KIMBERLITE DIATREMES

P.O. Alexander
Department of Applied Geology
The University, Sagar
M.P., 470003, India

Geophysical methods are less sensitive for the purpose of locating small kimberlitic bodies. The quality of diamonds that may be contained in kimberlites apparently bears little relation to their size. Searching out smaller kimberlite pipes should be rewarding, therefore, for increasing diamond potential in view of the possibility that most of the larger kimberlites of the world seem to have already been found. Geochemical and botanical methods of prospecting (Alexander and Shrivastava, 1964; Litinskiy, 1964) have been shown to delineate even smaller diatremes but not without limitations.

Research activity in the field of organic matter, biological systems and mineral exploration is on the increase (Updegraff, 1983). Of all the living organisms, bacteria are by far the most versatile, making roughly 50% of the biomass. They survive at far greater depth than other organisms. It is logical that they will reflect the geochemical environment in which they live. Study of their kind and relative abundance over and around the mineralised ground therefore, should constitute an exploration tool. Geomicrobiological prospecting for oil and gas fields has been helpful in the Soviet Union and other places for a long time but its application for prospecting metallic deposits has only recently been attempted (Parduhn and Watterson et al., 1984; Watterson et al., 1984). The present work aims to suggest soil bacterial populations as an additional tool for locating even kimberlitic bodies that may be devoid of characteristic vegetation cover for one reason or the other.

A total of 53 soil samples collected in traverses over and adjacent to undisturbed portions of three kimberlitic pipes were analysed for their total streptomycetes, total *Bacillus* species (ssp) and *Bacillus cereus* (159 data points) at the Geomicrobiology laboratory of the Exploration Geochemistry section, USGS, Denver, Colorado. The geometric mean of *B. cereus* counts in soil samples over a small kimberlite pipe with a thin soil cover near Boulder, Colorado was 13 times higher

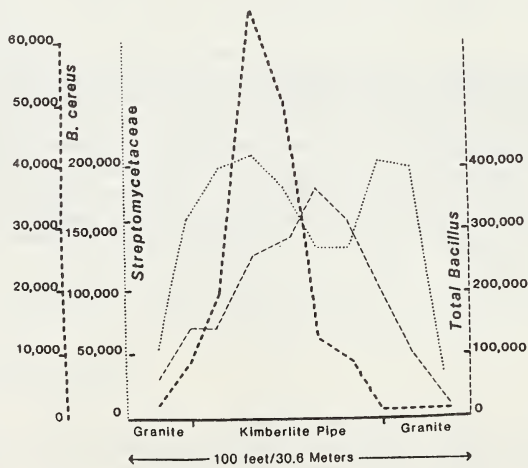


Fig. 1. Streptomycetes, *Bacillus cereus* and total *Bacillus* counts for each gram of soil across Green Mountain Kimberlite, Colorado, USA.

than the geometric mean of counts in soil over adjacent granitic rock (Fig. 1). Streptomyces counts and total Bacillus spp. were also more than two standard deviations higher over the pipe. B. cereus was significantly enriched over Sloan-1 pipe near the Colorado-Wyoming border, northwest of Fort-Collins, Colorado, and total Bacillus counts were 11 times higher than over adjacent country rock; streptomyces counts were more than two standard deviations higher over the pipe.

Counts of the three microbial groups in soil over and adjacent to the Hinota pipe of Central India were the same or even lower than in the sandy soil outside the pipe rock (Fig. 2). This finding appears consistent with the observed

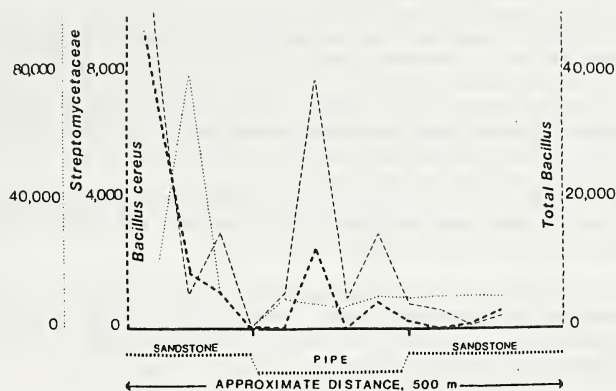


Fig. 2. Streptomyces, Bacillus cereus and total Bacillus counts for each gram of soil across Hinota Kimberlite pipe, Central India.

erosion and considerable infilling of this pipe with the surrounding sandy soil. However, B. cereus and streptomyces counts in termite mounds (apparently deriving their material from a much deeper source) over this pipe showed appreciable (7- and 34 times respectively) enrichments compared to those on adjacent sandstone.

Ecological reasons underlying these anomalies have not been investigated to date, but may be related in part to the increased availability of potassium, phosphate, and other inorganic nutrients thought to be responsible for observed botanical anomalies in kimberlitic derived soils in many parts of the world (Alexander, 1983).

Bacterial populations can be determined more quickly and inexpensively than elemental analyses. Pipe/background contrasts under the present study (Table 1) also appear to be reasonably good except for the Hinota pipe of Central India

Table 1. Kimberlite/background ratios for Total Bacillus, Bacillus cereus and streptomyces

Bacteria	Green Mountain Colorado	Sloan-1 Colorado	Hinota, Central India	
			Pipe	'Termite mound
Total <u>Bacillus</u>	1.8	11	1.1	0.5
<u>Bacillus cereus</u>	13.1	3.2	0.3	7.3
Streptomyces	1.5	1.9	0.6	34

which has appreciable infilling of soils derived from other sources. It is believed that a more detailed geomicrobial approach to kimberlite prospecting in different lithologic and climatic settings would be a rewarding study, and has the potential for becoming a supplementary tool for diamond prospecting.

REFERENCES

- Alexander P.O. 1983. Looking for Diamonds? Try Geobotany. De Beers Industrial Diamond Quarterly, London, Vol. 3, No. 36 pp. 33-38.
- Alexander P.O. and Shrivastava V.K. 1984. Geobotanical expression of a blind Kimberlite pipe, Central India. In Kornprobst J. ed., Kimberlites Vol. 1, pp. 33-40. Elsevier, Amsterdam.
- Litinskiy V.A. 1964. Application of metallometry and kappametry in prospecting for kimberlites. Internat. Geol. Rev. Vol. 6, pp. 2027-2035.
- Parduhn N.L. and Watterson, J.R. 1984. Preliminary studies of Bacillus cereus distribution near a gold vein and a disseminated gold deposit, U.S. Geological Survey Open-File Report 84-509, 6p.
- Updegraff D.M. 1983. Geomicrobiological prospecting: past and future. In Abstracts, Organic Matter, Biological systems and Mineral Exploration, a workshop and colloquium, UCLA, Feb. 14-18.
- Watterson J.R., Nagy L.A. and Updegraff D.M. 1984. Penicillin resistance in soil bacteria is an index of soil metal content near a porphyry copper deposit and near a concealed massive sulfide deposit. U.S. Geological Survey Open-File Report 84-016, 27 p.

J.A. Carlson and S.W. Marsh

Long Lac Mineral Exploration (Texas), Inc.

Extensive heavy mineral sampling, detailed geophysical surveys and exploratory trenching resulted in discovery of the George Creek kimberlite dikes. The George Creek kimberlites are situated within the northeastern Colorado Front Range, approximately 22 kilometers northwest of the reported Sloan kimberlites (Fig. 1).

The regional geology consists predominantly of metasedimentary and metavolcanic rocks of Proterozoic age that have been severely deformed and extensively intruded by late Precambrian plutonic rocks. The metamorphic host rocks are mainly schist and gneiss units formed from a sedimentary and volcanic suite deposited between 1.8 and 2.5 b.y. ago (Peterson and Hedge, 1968). The thick sequence was deformed into large isoclinal folds and then weakly metamorphosed prior to 1.75 b.y. ago. At about 1.75 b.y., these rocks were intruded by the Rawah Granite Complex, subjected to two episodes of folding and strongly metamorphosed producing amphibolite facies rocks having east-west and northeast trending foliations. At about 1.4 b.y. ago, Silver Plume granites and related rocks were emplaced with associated translational deformation.

Regional stream sediment sampling revealed a typical kimberlitic mineral suite comprising subangular to angular peridotitic and eclogitic garnets and trace quantities of chrome diopsides, altered magnesian ilmenites and spinels. Peridotitic garnets from the George Creek exploration samples are characterized by ilherzolitic (G9) and high chrome - low calcium (G10) harzburgitic compositions (Dawson and Stephens, 1976).

Detailed soil sampling along a north-south grid system defined an erratic northeastern trend suggesting the presence of nearly linear kimberlite intrusives. A comprehensive geophysical programme was initiated to delineate probable kimberlitic sources. The VLF (very low frequency) method defined several northeast and east-west trending linear conductive zones. The in-phase profiles are symmetrical indicating that the conductive bodies are steeply dipping. Exploration trenching confirmed the presence of at least three separate kimberlite intrusions within northeast trending conductivity regions delineated by the VLF method. Magnetic surveys did not discriminate kimberlite dikes in the George Creek area because large scale amplitude variations of the magnetic field likely overshadowed local magnetic effects caused by the relatively narrow, highly weathered linear kimberlite features.

The kimberlite intrusions (Fig. 1), comprise northeast trending en echelon dikes ranging in length from several hundred meters to 1 kilometer and in width from several centimeters to about 4 meters. Kimberlite creep zones are present but irregular along much of the K-1 and K-2 dikes. Creep zones are reddish-brown in colour, range in thickness from several centimeters to 1 meter and extend downslope several tens of meters from the kimberlites. The kimberlites are essentially massive, distinctly macrocrystic and contain minor amounts of megacrysts, eclogites and serpentized peridotitic nodules. The dikes have apparent dips of 70° NW to nearly vertical, show little or no surface expression and are covered by 1 to 5 meters of colluvium. Contacts of the kimberlite dikes with the enclosing amphibolite grade gneisses are typically sharp and narrow. Minor serpentine and carbonate veinlets (1 to 3 cm wide) extend outward up to 1 meter into the gneiss in places along K-1 but are not characteristic of the K-2 and K-3 kimberlites (Fig. 1).

The George Creek dikes are classified as hypabyssal macrocrystic phlogopite kimberlites according to Clement et al. (1984). The kimberlites have distinct inequigranular textures characterized by macrocrysts and microcrysts set in an essentially microporphyritic groundmass. Olivine and phlogopite occur in at least two generations with olivine being the dominant mineral in both macrocryst and

microcryst populations. The macrocrysts (2 mm to 1 cm) and microcrysts (1 to 2 mm) include serpentinized olivine pseudomorphs, chloritized phlogopites, kelyphitized garnets, magnesian ilmenites commonly with spinel and perovskite mantles and trace chrome diopsides. Deformation is evidenced by strained and kinked phlogopites, shattered garnets and subparallel tensional fractures within the macrocrysts. Primary groundmass minerals include phlogopite, serpentine (typically replaced by carbonate or silica), altered ilmenite and spinel, perovskite and apatite. The primary differences between the kimberlites are variations in their alteration and deformation characteristics.

The K-1 dike is classified as a carbonatized phlogopite kimberlite. Carbonates typically rim the macrocrysts, occur along crystallographic fractures in the macrocrysts and(or) have been introduced along tensional fractures in the macrocrysts. Groundmass carbonate is relatively abundant and has apparently replaced groundmass olivines and serpentine.

The K-2 and K-3 dikes (Fig. 1) are classified as silicified phlogopite kimberlites. The K-2 dike has a flow texture defined by the preferred alignment of altered and internally distorted ferromagnesian pseudomorphs. The K-3 kimberlite has a vuggy appearance due to the partial dissolution of microcrysts and macrocrysts. Relict olivine pseudomorphs in the K-3 dike are defined by their silicified oxide-rich anhedral to subhedral crystal outlines and void cores. Silica in both kimberlites has apparently replaced serpentines and to a lesser degree groundmass phlogopites. Prismatic and acicular groundmass apatites are more abundant in the K-2 and K-3 intrusions than in the K-1 kimberlite.

The kimberlite intrusions have been subjected to highly oxidizing conditions (M. McCallum, personal communication, 1986). Numerous primary ilmenites in the George Creek dikes have been converted to pseudobrookites and have textures similar to those described by Haggerty (1976) in the advanced oxidation stage of basaltic ilmenites. The pseudobrookites are commonly enriched in both chrome and(or) magnesium reflecting original kimberlitic ilmenite compositions. This feature is significant because pseudobrookite enriched in chrome and magnesium can be utilized as an additional kimberlite exploration indicator mineral in the George Creek region. Spinels in the George Creek kimberlites display atoll-type structures and are dominantly altered to titanomaghemites, perovskites and maghemites. Chrome spinels also occur in the kimberlites.

Whole rock geochemistry results of surficial kimberlite samples indicate that late-stage alteration processes (serpentinization, carbonatization, silicification and oxidation) apparently redistributed the more mobile major and compatible trace elements in the George Creek kimberlites. The incompatible trace elements which are less mobile and dominantly restricted to late-stage groundmass phases (Dawson, 1980; Mitchell, 1986) apparently discriminate the George Creek kimberlites. Dawson (1980) states that perovskite and apatite are the dominant host minerals for La and Th. Higher La and Th concentrations in the K-2 and K-3 dikes suggest that the two intrusions are enriched in perovskite and apatite relative to the K-1 dike. Perovskites, ilmenites and zircons in kimberlites are dominant host phases for Nb, Ta and Zr (Mitchell, 1986). The K-2 and K-3 dikes are enriched in Nb, Ta and Zr relative to the K-1 dike.

The George Creek K-1 diamond population is characterized by a high proportion of aggregates (23.5% in the -11+9 size range) relative to most reported diamondiferous kimberlites in Southern Africa (Whitelock, 1973; Robinson, 1979; Harris, et al., 1984). Orapa is the exception containing approximately 37% aggregates in the -11+9 size range (Robinson, 1979). Variations in diamond morphology with increasing stone size include higher proportions of aggregates and lower percentages of tetrahedra.

The diamond population is typified by a very high proportion of colourless stones (89.6% in -11+9 sieve class). The percentage of coloured diamonds appears to decrease with increasing size. Yellow and brown diamonds dominate within the coloured categories and comprise approximately 15 percent of the -9+7 size category.

Discovery of the George Creek kimberlite dikes was the culmination of detailed heavy mineral sampling, geophysical surveys and exploratory trenching. The intrusions are classified as hypabyssal macrocrystic phlogopite kimberlites and differ according to alteration, deformation and trace element chemistries. Diamond studies indicate that the George Creek kimberlites are typified by high proportions of colourless stones and crystal aggregates compared to most reported diamondiferous kimberlites.

References

Clement, C.R., Skinner, E.M.W. and Scott-Smith, B.H., 1984. Kimberlite redefined. *Journal of Geology* 92, pp. 223-228.

Dawson, J.B., 1980. Kimberlites and their xenoliths. 250 pp. Springer-Verlag, Berlin, New York.

Dawson, J.B. and Stephens, W.E., 1975. Statistical classification of garnets from kimberlite and associated xenoliths. *Journal of Geology* 83, pp. 589-607.

Haggerty, S.E., 1976. Opaque mineral oxides in terrestrial igneous rocks. In Rumble, D. ed., *Reviews in Mineralogy - Oxide minerals*, Mineralogy Society of America 3, pp. 101-176.

Harris, J.W., Hawthorne, J.B. and Oosterveld, M.M., 1984. A comparison of diamond characteristics from the DeBeers Pool Mines, Kimberly, South Africa. *Annales Scientifiques Université Clermont-Ferrand II*, pp. 1-13.

Mitchell, R.H., 1986. Kimberlites mineralogy, geochemistry and petrology. 442 pp. Plenum Publishing Corporation, New York.

Peterman, Z.E., Hedge, C.E. and Braddock, W.A., 1968. Age of Precambrian events in the northeastern Front Range, Colorado: *Journal of Geophysical Research* 73, pp. 2277-2296.

Robinson, D.N., 1979. Surface textures and other features of diamonds. PhD Thesis, University of Capetown, unpublished.

Whitelock, T.K., 1973. Morphology of the Kao Diamonds. In Nixon, P.H. ed., *Lesotho Kimberlites* pp. 128-140. Lesotho National Development Corporation Maseru.

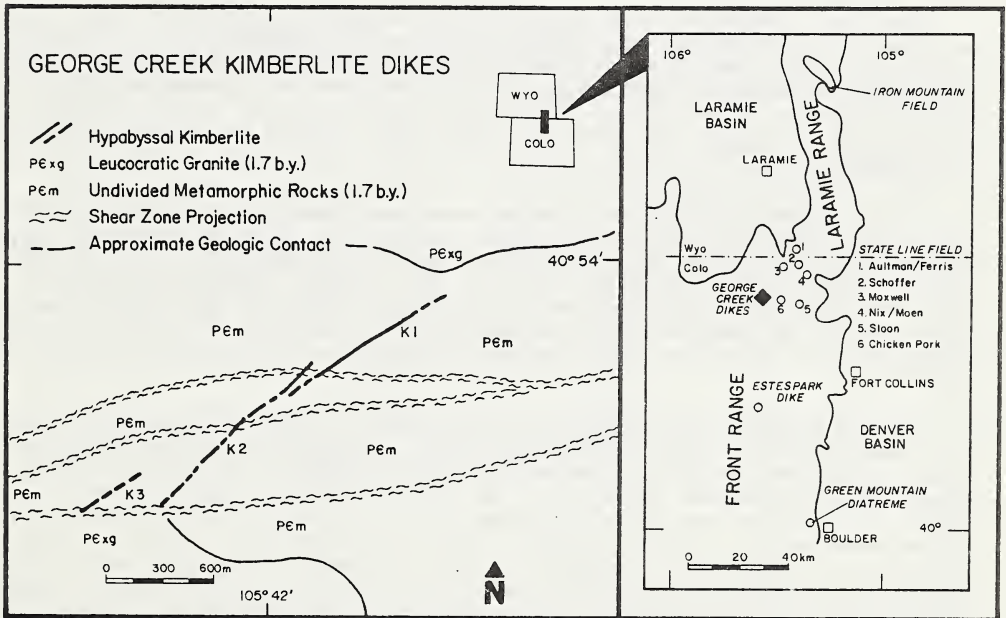


Figure 1: Location of the George Creek kimberlite dikes, Colorado, U.S.A.

GEOLOGY AND EXPLORATION OF THE ROSE LAMPROITE
SOUTHEAST KANSAS, U.S.A.

Howard G. Coopersmith^{1,3} and Roger H. Mitchell²

¹Cominco American Incorporated, Fort Collins, Colorado, U.S.A.

²Geology Department, Lakehead University, Thunder Bay, Canada

³Present address: 425 E. Elizabeth, Fort Collins, Colorado 80524

Lamproite occurrences at Hill's Pond (Silver City) and Rose Dome in Woodson County, Kansas have been known since 1880 as geologic curiosities. In the 1950's these localities were first described as intrusive peridotites, and later as kimberlites. Recent studies document that these rocks have lamproite affinities (Merrill et al. 1977, Cullers et al. 1985, Mitchell, 1985).

Hill's Pond occurs as an elongate plug-like body with sill extensions to the south. The plug has dimensions of approximately 1700m by 250m, while the near surface sills are encountered over a 1400m by 2000m area. Petrographically the intrusion is a Ti-K-richterite diopside madupitic lamproite containing strongly zoned (8.0-1.0% Al₂O₃; 6-13% FeO_T) poikilitic groundmass Ti-phlogopite. Ti-poor chromites are the common opaque phases. As indicated by the petrology and mineral chemistry the intrusion history at Hill's Pond produced evolved lamproites of poor diamond-bearing potential.

The Rose lamproite occurrence is located approximately 7km northeast of Hill's Pond. Due to lack of outcrop and core samples this site was previously poorly studied. Based on a probable diatreme nature and initial mineralogical study the Rose lamproite was selected for detailed exploration for diamond.

The Rose lamproite occurs astride an elongate structural dome in an area of relatively flat lying Pennsylvanian sedimentary rocks. At the surface the lamproite is intrusive into the Stanton Limestone and the overlying Weston Shale. Some sill formation is apparent along this contact (Franks et al. 1971). K-Ar ages of phlogopite from Rose and Hill's Pond are 88-91 my (Zartman et al. 1967) which are geologically reasonable.

Orientation exploration studies were performed over the Hill's Pond and Rose lamproites. An aeromagnetic survey was flown with a line spacing of approximately 800m. Ground studies included magnetics, conductivity, soil geochemistry and heavy minerals. As the Rose lamproite generally does not outcrop, these indirect techniques were used for mapping with confirmation by shallow auger drilling. Sill and dike-like bodies were found over a 2km by 1km area and one centrally located diatreme was identified.

Ground geophysics detected the diatreme at Rose as a magnetic high and several of the near surface sills as conductivity highs. Soil geochemistry showed Ni and Nb anomalies corresponded well to the lamproite. Other useful elements include Ti, Ba, Zr, Cr and La. Heavy minerals in soils included chrome spinel, lesser phlogopite, pyrope, pyroxene, olivine, amphibole, crustal garnet, rutile?, priderite?, barite, chlorite and lithic fragments of lamproite. Heavy minerals displayed wider dispersion than the soil chemistry and the lamproite itself. Shallow auger drilling confirmed mapping, and geophysical and geochemical targets.

The Rose lamproites include rocks of highly fragmental diatreme facies, fragmental hypabyssal breccias and fine-grained magmatic hypabyssal types. Extensive alteration and weathering preclude satisfactory petrographic study, although pseudomorphs after olivine and relict

phlogopite phenocrysts can be seen in some samples. Despite alteration select subsurface samples show major oxide and trace element compositions similar to diamondiferous lamproites from elsewhere.

Spinel from heavy mineral concentrates are Ti-poor magnesian aluminous chromites, aluminous magnesian chromites and Fe₂O₃-rich spinels representing members of the pleonaste-magnesiochromite-magnetite-magnesioferrite series. Garnets include Cr-pyrope, sub-calcic Cr-pyrope, almandines and spessartites.

The study indicates that the Rose lamproites are relatively unevolved as compared with the Hill's Pond lamproites and therefore are of greater diamond potential. Testing of bulk samples obtained from trenching of the diatreme however produced no diamonds.

The Rose and Hill's Pond lamproites define a province of Cretaceous ultrapotassic mantle-derived magmas emplaced along the southern margin of the North American craton. The diamondiferous Prairie Creek district of similar age is 450 km to the southeast along this margin. The Tuttle Creek kimberlite district, also of similar age, is 300 km north (on craton) along the Midcontinent Rift.

ACKNOWLEDGMENTS

We thank Cominco American Incorporated for their support of this project and for permission to publish. Field work and sample studies were greatly enhanced through the help of P.B. Hubbard, M.L. Hobbs and P.M. Huntley. S.C. Bergman provided microprobe analyses. RHM's work was conducted in part while on sabbatical at the Department of Earth Sciences, University of Cambridge.

REFERENCES

- CULLERS R.L., RAMAKRISHNAN S., BERENDSEN P. and GRIFFIN T. 1985. Geochemistry and petrogenesis of lamproites, Late Cretaceous age, Woodson County Kansas, U.S.A. *Geochimica et Cosmochimica Acta* 49, 1333 - 1402.
- FRANKS P.C., BICKFORD M.E. and WAGNER H.C. 1971. Metamorphism of Precambrian granitic xenoliths in a mica peridotite at Rose Dome, Woodson County, Kansas: Part 2, Petrologic and mineralogic studies. *Geological Society of America Bulletin* 82, 2869 - 2890.
- MERRILL R.B., BICKFORD M.E. and IRVING A.J. 1976. The Hill's Pond peridotite, Woodson County, Kansas: a richterite-bearing Cretaceous intrusive with kimberlite affinities. Extended Abstracts. Second International Kimberlite Conference. Santa Fe, New Mexico.
- MITCHELL R.H. 1985. A review of the mineralogy of lamproites. *Transactions Geological Society of South Africa*. In press.
- ZARTMAN R.E., BROCK M.R., HEYL A.V. and THOMAS H.H. 1967. K-Ar and Rb-Sr ages of some alkaline intrusive rocks from central and eastern United States. *American Journal of Science* 267, 297 - 309.

ARGYLE AK1 DIAMOND SIZE DISTRIBUTION; THE USE OF FINE DIAMONDS TO PREDICT THE OCCURRENCE OF COMMERCIAL SIZE DIAMONDS

A.S. Deakin, G.L. Boxer

Argyle Diamond Mines Pty. Limited

INTRODUCTION

In the detailed evaluation of diamondiferous diatremes, several problems are encountered when attempting to obtain samples for use in carats per tonne (ct/t) grade estimation.

- Samples must be large to obtain sufficient diamonds, which are therefore costly both in excavation and sample processing stages.
- Many samples have to be taken to assess the spatial variation in grade.
- Samples must be taken at depth in hard rock in such a manner that diamonds are not broken.

At AK1, samples for grade determination were obtained by taking large diameter cores (LDC's) of 200mm diameter. This is an expensive process costing over A\$1000 per metre. The possibility of using fine diamonds (microdiamonds) - diamonds smaller than those recovered by normal plant processing - to predict the occurrence of larger, commercial size stones (macrodiamonds) was therefore investigated. The extremely high grade and small mean stone size of the Argyle pipe offered the opportunity of establishing a reliable statistical relationship between numbers of macrodiamonds and microdiamonds.

LOCATION AND GEOLOGY

AK1 is a diamondiferous Precambrian age olivine-lamproite diatreme of 50 hectares surface area located at 128° 23'E, 16° 43'S in the East Kimberley region of Western Australia. The pipe is 2km long, averages 250m in width and exhibits a complex series of disrupted and faulted pyroclastics. Two main tuff types are recognised; the "sandy tuff" forming the major part of the pipe consisting of lamproite lapilli set in a matrix of ash and quartz sand, and the "non-sandy tuff" situated in the 450m wide northern bowl of the pipe and representing a later stage quartz-free intrusion. Minor magmatic lamproite dykes occur predominantly in the south of the pipe. Its detailed geology is described by Atkinson et al. (1984).

METHOD

Initial sampling of AK1 indicated that highest grades occurred in the southern half of the pipe in the sandy tuff. Consequently, evaluation work centred on this area and LDC's were taken on a 50m square grid to a maximum depth of 200m. The cores were divided into 20m sample lengths and processed through a 10tph HMS plant using 12mm and 6mm crushes and a 0.5mm lower screen size. Due to the high grade at AK1, averaging 6.8ct/t in the grid drilled area, sufficient diamonds were recovered per sample to approximate the target population. This contrasts with most economic diamondiferous pipes where grades are much lower, typically 0.1 - 0.5ct/t, and where only a limited number of diamonds, if any, are recovered per sample.

The AK1 recovered (macrodiamond) size distribution was 3 parameter lognormal with a mean of 0.032 carats per stone (ct/st), and showed little variation between samples. It was noted that a constant ratio in terms of stone numbers existed between any two sieve sizes within the recovered size range, and it was argued that if a similar, constant ratio existed between even smaller diamonds and the macrodiamonds, a method could be established to predict the occurrence of commercial size diamonds from microdiamonds.

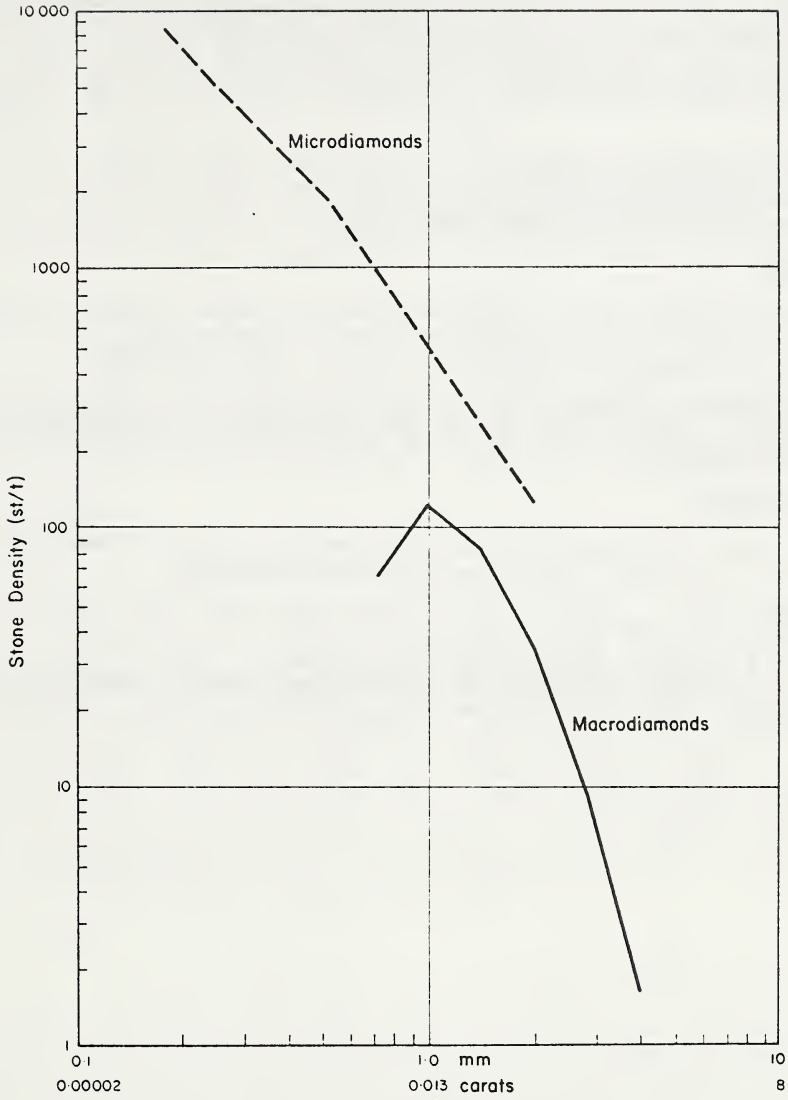


Fig. 1. Stone density plot of microdiamonds and macrodiamonds for 1 tonne of 10ct/t grade lamproite

Sub samples of LDC's were taken in 20kg size and acid digested to release microdiamonds down to 0.15mm size. The resulting natural stone size distribution confirmed that stone numbers continued to increase with decreasing stone size (fig. 1).

Size intervals were selected in the microdiamond and macrodiamond size ranges. A relatively constant stone number ratio existed between the two intervals. Grade (ct/t) is a function of stone size (ct/st) and stone density (stones per tonne, st/t). Recoverable macrodiamond grade could therefore be estimated using the microdiamond stone density, the microdiamond - macrodiamond stone number ratio and the known mean stone size of the macrodiamond population by;

$$\text{Recoverable grade (ct/t)} = \frac{M}{R} \cdot S$$

where:

M = microdiamond density (st/t)

R = microdiamond-macrodiamond ratio

S = known macrodiamond mean stone size (ct/st)

CONCLUSION

The microdiamond method of grade determination reduces the need to take large samples, resulting in lower expenditure on detailed evaluation; smaller, conventional size cores can be used at a cost of around A\$100/metre.

The method may be used in the evaluation of deeper levels of AK1, production grade control, mine planning, and may have application to other diamondiferous diatremes elsewhere.

ACKNOWLEDGEMENTS

This paper is presented with the kind permission of Argyle Diamond Mines, CRA Exploration, and Ashton Exploration Joint Venture management.

REFERENCES

Atkinson, W.J., Smith, C.B., and Boxer, G.L., 1984

The discovery and geology of the Argyle diamond deposits, Kimberley, Western Australia. Aust. Inst. Min. Met., Annual Conference, Darwin, Australia.

A.S. Deakin¹, G.L. Boxer¹, A.E. Meakins², E. Haebig², J.H. Lew²

(1) Argyle Diamond Mines Pty. Limited, (2) CRA Exploration Pty. Limited

LOCATION AND REGIONAL GEOLOGY

The Argyle alluvial diamond deposits are associated with the AK1 pipe, a lamproite diatreme of 50 hectares surface area located in the Halls Creek Mobile Zone 120km south of the town of Kununurra in the Kimberley region of Western Australia.

The pipe forms a 200m deep valley in the northerly dipping Proterozoic sediments of the Matsu Range. Smoke Creek and Gap Creek, a tributary of Limestone Creek, originate in the range and flow across the surrounding plains into Lake Argyle 35km distant (fig. 1). Diamonds derived by erosion of the pipe are found in both drainages. Coarse diamondiferous scree deposits cover the surface of the pipe.

DISCOVERY

In August 1979 diamonds were recovered from 40kg-sized gravel samples taken in Smoke Creek as part of a regional drainage sampling programme carried out by the Ashton Joint Venture. Follow-up work led to the recognition of the Smoke Creek alluvial deposits and the AK1 diatreme one month later (Atkinson et al, 1984). The Limestone Creek deposit was identified in 1981 after further sampling.

ALLUVIAL GEOLOGY

Smoke Creek

The economic Upper Smoke Creek deposit occurs directly to the north of the pipe and comprises coarse, poorly sorted, massively bedded modern floodplain deposits situated upstream of a gap in the hills formed of the Devonian Ragged Range Conglomerate, and underlain by Cambrian Antrim Plateau Volcanics.

Downstream of the gorge are located the lower grade Lower Smoke Creek deposits where three deposit types are recognised; modern floodplain deposits, Pliocene low terrace gravels and a high level lateritised terrace of Miocene age. The floodplain gravels, up to 4m in thickness, form a broad, sinuous and partly braided tract. The low terrace gravels occur as terrace remnants 4m above the floodplain and exhibit incipient lateritisation. A 2m thick lateritised and lightly cemented gravel comprises the high terrace which occurs 8m above the floodplain and forms the high ground flanking Smoke Creek.

Limestone Creek

Directly to the east of the pipe are situated the Limestone Creek deposits where modern floodplain, low terrace and lag gravels occur derived from the partial erosion of a lateritised and partly duricrusted Pliocene age piedmont fan. The deposits range to 3.5m in thickness and blanket the undulating granitic rocks of the Lower Proterozoic Lamboo Complex (fig. 2). The fan splays south east from the foot of Matsu Range and may be subdivided into proximal facies with coarse, angular and poorly sorted detrital sediments, and distal facies with subrounded clasts, reasonable sorting and interdigitation of gravel with sand lenses (Meakins, 1983). With increasing distance from source the fan deposits grade into coarse channel fill gravels which occur as remnant terraces along the creek.

The alluvial deposits have little or no overburden near source with increasing sand and silt overburden in the lower reaches of the creeks.

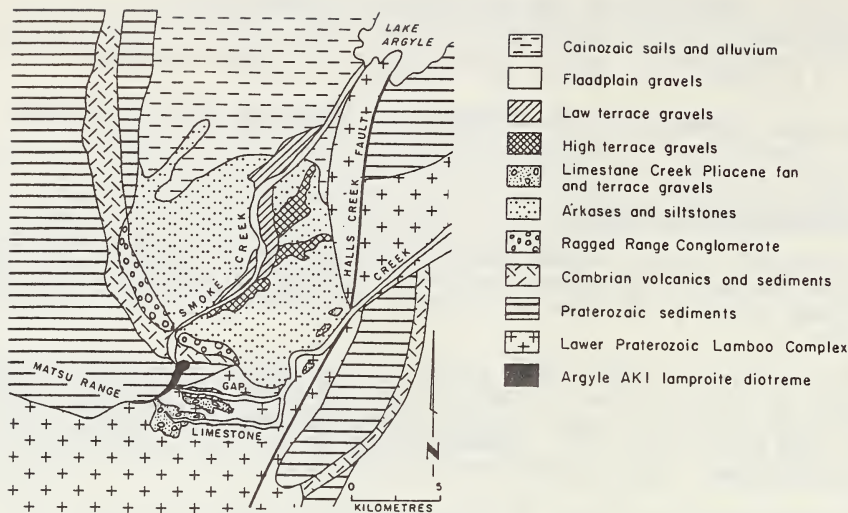


Fig. 1. Argyle diamond deposits, geology and geographic distribution

Age determination of the deposits is based on the geomorphological relationships of the terraces, supported by Mössbauer spectroscopic investigations of the relative degree of development of crystallinity, and hence of age, shown by iron-oxide pisolites and ferruginous cement in the gravels.

Diamond Size Distributions

Each geologically homogeneous economic deposit type has its characteristic lognormal size distribution and price per carat. Mean stone sizes range from 0.08 carats per stone (ct/st) to 0.24 ct/st. The high level terrace and lag gravels contain the larger diamond populations. The alluvial diamonds have larger mean stone sizes and higher value compared to diamonds from the pipe. Quality is also better due to elimination of the weaker and more fractured pipe diamonds during alluvial transportation.

DIAMOND DISTRIBUTION

Spatial Variations

In contrast to many of the classic African alluvial diamond deposits, the economic Argyle alluvials are only marginally removed from, and poorly enriched in relation to the primary source. This is a reflection of the steep gradient in the source area, the abrupt change in creek gradient at the surrounding plains, and the semi-arid environment with sporadic but intense rainfall.

Their high grades are derived from the high grade of the AK1 pipe which averages 5 carats per tonne (ct/t) grade at surface.

The Upper Smoke Creek gravels average 4.6 ct/t with a mean stone size of 0.08 ct/st. Grades decrease laterally from the creek channel (5-10 ct/t) to the edge of the floodplain (1-2 ct/t). With increasing distance from source there is a steady decrease in grade due to dilution and a decrease in diamond size. At 20km from the pipe grades in the floodplain gravels are reduced to 0.05 ct/t and mean stone size to 0.05 ct/st.

Vertical Variations

In all deposit types diamonds occur throughout the gravel profile but with a

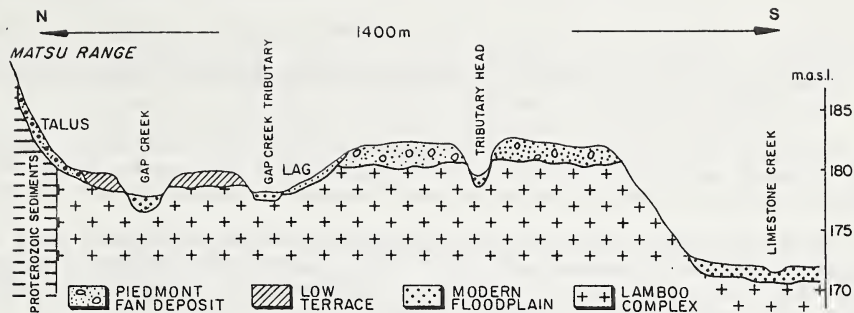


Fig. 2. Schematic cross-section of Limestone Creek deposit 1.5 km downstream of AK1 pipe.

distinct increase in number and size towards the base. In Lower Smoke Creek floodplain gravels directly below the gap, grade increases from 0.97 ct/t in the upper gravel layers to 1.80 ct/t in the basal 1m of gravel resting on bedrock. Similarly average stone size and stone density (stones per tonne [st/t]) increase from 0.08 ct/st to 0.12 ct/st, and from 12 st/t to 15 st/t respectively. This vertical sorting of diamonds is related to the clast size of the gravels which generally increases with depth.

INDICATOR MINERALS

In the alluvials the normal suite of kimberlitic indicator minerals; picroilmenite, pyrope garnet and chrome diopside, is absent, reflecting the mineralogy of the primary AK1 lamproite.

The location of these rich diamond deposits in a mobile zone and the absence of typical indicator minerals have important implications for regional diamond exploration.

THE DIAMONDS

The diamonds are predominantly of industrial quality with a 10% gem content and have an average price of US\$9 per carat. Production from the Argyle alluvials since the start of alluvial mining in January 1983 to December 1985 totalled 17 million carats, 11% of world natural diamond production.

ACKNOWLEDGEMENTS

This paper is presented with the kind permission of Argyle Diamond Mines, CRA Exploration, and Ashton Exploration Joint Venture management.

REFERENCES

- Atkinson, W.J., Smith, C.B., and Boxer, G.L., 1984
The discovery and geology of the Argyle diamond deposits, Kimberley, Western Australia. Aust. Inst. Min. Met., Annual Conference, Darwin, Australia.
- Meakins, A., 1983, Geology and genesis of the Argyle alluvial diamond deposits, Kimberley region, Western Australia. Abstracts volume, Australian Regional Meeting, Association of Exploration Geochemists, May 1983, Perth, pp. 54-56.

G. J. Drew

CRA Exploration Pty Limited, 21 Wynyard Street, Belmont, Western Australia

Following the discovery of the AK1 lamproite pipe in October 1979 (Atkinson et al, 1984), several geophysical surveys were undertaken over the pipe to determine the most effective method(s) for locating additional lamproites in the surrounding area.

In January 1980, a small detailed aeromagnetic/radiometric survey was flown by Geometrics Ltd, over the immediate area of AK1. Survey specifications included north-south flight lines and a line spacing of 250 metres. Examination of the results showed a low amplitude (5 nT) magnetic response coincident with the northern margin of the pipe (Figure 1).

This led to the commissioning of a larger airborne survey (15000 line km) in July 1980, to explore the ground surrounding AK1, now under title to the Ashton Joint Venture. Geometrics were again awarded the contract. Both magnetic and radiometric data were collected using a line spacing of 300 metres and NW-SE flight lines. The line direction was changed from that of the initial test survey to account for regional strike and to try and minimise the effects of rugged topography. This survey, however, failed to detect the magnetic response located by the original survey (Figure 2).

Detailed helicopter-borne and ground magnetic surveys were subsequently completed along traverses orthogonal to the strike of the pipe to better elucidate its magnetic signature. Results again showed the general lack of magnetic response over the pipe but did confirm the presence of a low amplitude anomaly at its northern end (Figure 3). Ground coverage was severely limited by the harsh topographical relief. Detailed modelling of this feature predicted depths ranging from 100 to 150 metres, a southerly dip which was in contrast to the northerly dipping stratigraphy, and magnetic susceptibilities between 200 and 600 x 10⁻⁵ SI units, typical of a lamproite source.

Drilling however, failed to intersect magnetic lamproite before the holes were terminated in footwall sediments of the Lissadell Formation. Drilling depths ranged from 100 to 140 metres. Magnetic susceptibility measurements on the core yielded values less than 50 x 10⁻⁵ SI units for the lamproite. It was therefore concluded that the magnetic source must emanate from within the sedimentary sequence (possibly a raft of Lissadell Iron Formation) and not from lamproite as was originally thought. More recent thinking, however, based on a better understanding of the pipes structural setting, may suggest the above conclusion needs further consideration.

Modelling of a weak magnetic response along the western contact, successfully predicted a steep westerly dip to the pipe, which at the time was not regarded as geologically feasible (see cross sections in Boxer et al, this volume).

Examination of the radiometric data failed to locate a recognisable response over the pipe. Average potassium contents for the lamproite were found to vary from 3 to 6 percent.

Electrical methods were also tested over the pipe both in the air and on the ground. A trial INPUT survey flown in late 1980 by Geoterrax Ltd., detected a weak 4-channel anomaly (figure 4) over the northern end of the pipe where the pipe width is greatest (500 metres) and the topographical relief smallest. Excessive flying altitude due to the rugged terrain helped to minimise INPUT responses elsewhere over the pipe.

An EM 34 survey using vertical coplanar coils and a coil separation of 20 metres was subsequently undertaken (Figure 5). Apparent resistivities over the lamproite were found to range from 40 to 100 ohm-metres, the more conductive section coinciding with non-sandy tuff, whilst values greater than 200 ohm-metres were encountered over the surrounding Lissadell Formation. A limited Sirotem survey confirmed the low near surface resistivities but indicated the fresh lamproite (sandy tuff) was much more

resistive (Figure 6). Results of the EM 34 survey helped to delineate pipe contacts during the early phases of exploration.

Downhole geophysical logging, measuring density, natural radiation and resistance was undertaken in selected drill holes as an aid to geological logging. Variations in density and resistance were found to correlate with altered zones associated with fracturing, whilst there was little recorded variation in the natural gamma log. Efforts to correlate these parameters with such things as diamond grade were unsuccessful.

REFERENCES

- ATKINSON, W. J., HUGHES, F. E. & SMITH, C. B., 1984. A review of the kimberlitic rocks of Western Australia; in Kornprobst, J. (Ed), Kimberlites. 1: Kimberlites and Related Rocks, pp.195-224, Elsevier, Amsterdam.
- BCXER, G. L., LORENZ, V. & SMITH, C. B., 1986. The geology and volcanology of the Argyle (AK1) lamproite diatreme. This volume.

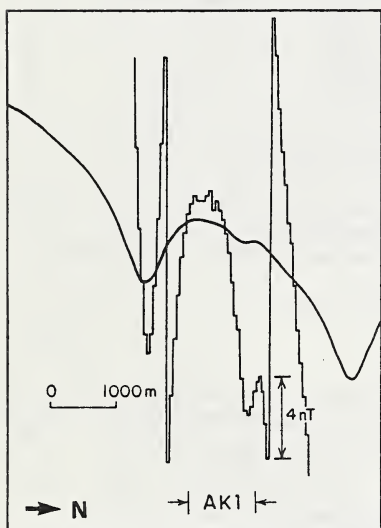


Fig. 1 Aeromagnetic Profile
January 1980 Survey

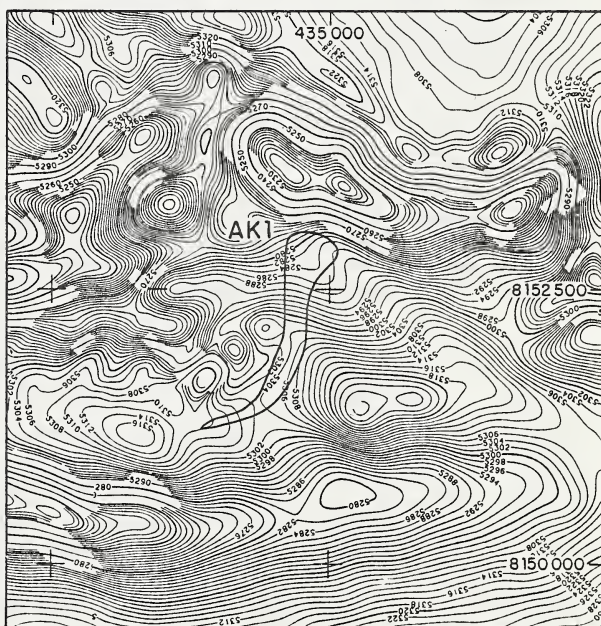


Fig. 2 Aeromagnetic Contours August 1980 Survey

MORPHOLOGY OF KIMBERLITE MINERALS: ITS USAGE
FOR PREDICTING AND SEARCHING THE DIAMOND DEPOSITS

V.K.Garanin, G.P.Kudryavtseva, T.V.Posukhova and V.P.Afanasjev

Department of Geology, Moscow State University, USSR

The morphology of kimberlite minerals, is very diverse which is due to their formation under impacts of various abyssal and exogenous morphogenetic factors. Being easily accessible to investigation, it provides ample information for predicting and searching the diamond deposits.

The morphological features of kimberlite minerals fall into two groups: 1 - those insignificantly varying during the formation of placer aureoles and permitting reconstruction of the original mineral, features specific for each individual source; 2 - those strongly and regularly varying during the formation and following existence of placer aureoles and functionally dependent upon the distance from their sources - for the placer aureoles formed in continental environments.

The first group of features allows typification of bedrock sources, i.e. referring the minerals of placer aureoles to specific kimberlite bodies. It comprises: the morphology of pyrope grains (oval-shaped, angular-oval, fragmentary, block-shaped, oval-shaped with scale-like, crescent-like and cirque-like gorges on the surfaces that are due to postmagmatic corrosive splitting); inclusions in pyropes and the total amount of grains with inclusions; pyrope colours; the morphology of microilmnite grains (the presence or absence of fine-prained shells on their surface); the character of faceting of chromespinel grains. As a rule, kimberlite bodies are typified with respect to several above-listed features, specific to each of them.

The second group includes more stable primary features, as well as the specific exogenous ones, permitting the estimation of the relative remoteness of the bedrock sources: the proportion of pyropes with the dislocational and cuboidal type of hypergenous corrosion; the share of microilmnite with the structures of solid solution decay and recrystallization; the presence of signs of mechanical wear, and the degree of its manifestation; the presence or absence of primary reactional formations, such as kelyphitic and subkelyphitic shells, chlorite incrustations on pyropes and kimberlite selvage in contrasting microilmnite relief.

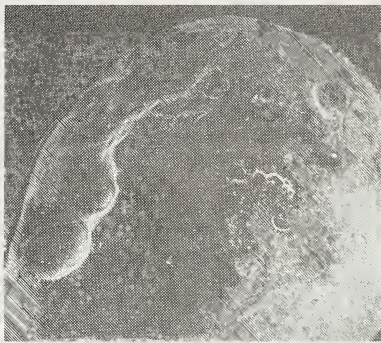
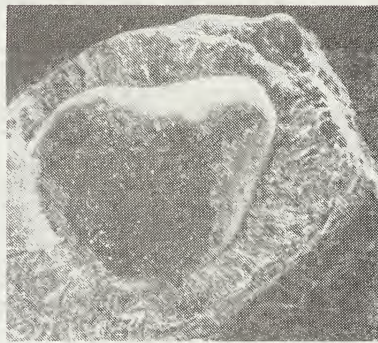
The morphology of kimberlite minerals is instrumental in deciphering the history of formation of placer aureoles and their development, permitting to establish their genesis: "primary" if they were formed by direct washing-out of kimberlites, and "redeposited" if the bedrock source was buried beneath younger deposits containing associated minerals of diamond.

The genetic approach to the morphology of kimberlite minerals is particularly important since it permits the estimation of the potentials of the placer-mineralogical technique and the tactics of exploration work in different geological environments. For primary aureoles the discovery of the kimberlite body is secured by tracing direct-ablation minerals along the stray flux. For the aureoles of a redeposited kimberlite washout products synchronous to sedimentation there is possible in principle only prognostication of more or less limited areas in which the search for buried deposits must be conducted by alternative methods (geophysical, drilling after a congested grid for possible direct undercutting). A particularly important sign of redeposited character of a concentrate aureole proves to be a mass manifestation on minerals of hypergenous alterations acquired during crust-forming epoch preceding sedimentation. Furthermore, in certain cases there is observed a great incompatibility between mineralogical features of concentrate aureoles and the facial pattern of the enclosing deposits. Thus, for a number of aureoles occurring in the Upper Paleozoic conti-

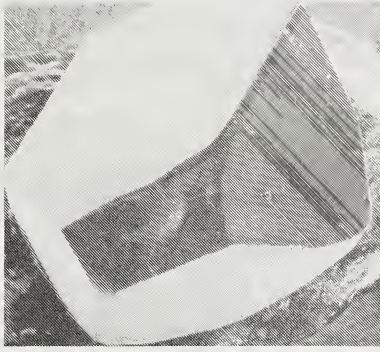
mental deposits in the Tunguska syncline eastern framing the morphological features of kimberlite minerals (in the first place, extreme mechanical wear), the composition of their association (predominantly diamond-pyrope with a far-reaching granulometric grading) point to the original formation of aureoles under the coastal-marine conditions in the Middle Paleozoic and their redeposited character in the Upper Paleozoic deposits.

It should be emphasized that now the best instrument for morphological examination of kimberlite minerals is the scanning electron microscope (SEM) which makes possible the high-quality photography of minerals under a wide range of magnifications and with the sharpness that can not be achieved by optical instruments.

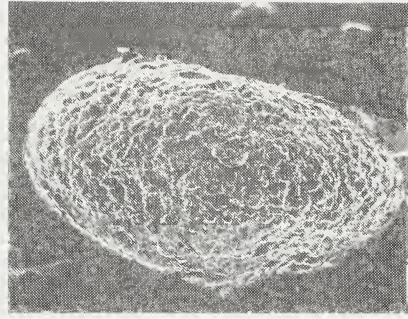
The secondary electron images of the grains of garnets, ilmenites and spinels, as shown in Figure I, illustrate the potentials of SEM-techniques for examination the minerals associated with diamonds.

a, 75^xb, 75^xc, 350^xd, 350^x

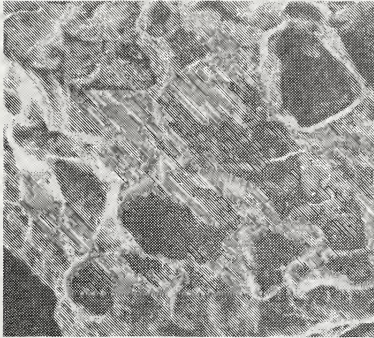
(Figure I)



e, 75^x



f, 35^x



g, 150^x



h, 1500^x

Fig.I. Morphological features of kimberlite minerals:
a - oval-shaped pyrope grain with cirque-like gouges; b - kelyphitic shell on a pyrope grain and sub-kelyphitic surface of garnet; c - inclusion of chromspinel in pyrope; d - inclusion of rutile in pyrope; e - crystal-shaped chrome spinel grain; f - ilmenite with fine-grained shell on their surface; g - recrystallisation structures in ilmenite; h - exsolution texture with platy intergrowth of chrome spinels in ilmenite

G.P. Gregory* and D.R. White**

* Formerly BP minerals australia,
Now Australian Ores and Minerals Limited.
**Formerly BP minerals australia

INTRODUCTION

Exploration for primary diamond deposits in many areas is based on the results obtained from drainage or loam samples. Because macrodiamonds (diamonds plus 0.5mm in size) are very rare, even in economic deposits, search is often made for more common pathfinder minerals, typically microilmennite, pyrope garnet, microdiamonds (diamonds less than 0.5mm size), magnesiochromite and chrome diopside though other minerals may be important in some areas. However, even these pathfinder minerals usually occur in very low concentrations, perhaps only one or two grains per sample, and thus collection and treatment of samples must be meticulous if success in exploration is to be achieved.

This paper outlines the drainage sampling and treatment procedure used by BP minerals australia / Seltrust Mining during their Australian diamond exploration programme from 1978 to 1983. Two main sampling methods are used viz. "Diamond Sampling" and "Pathfinder Sampling". The former is mainly used in the search for diamondiferous olivine lamproites where typical pathfinder minerals are rare or absent and the latter mainly used to explore for diamondiferous kimberlites.

DIAMOND SAMPLING

Collection Of Samples

The purpose of diamond sampling is to detect whether or not a drainage catchment, or part of a catchment, contains macrodiamonds. In this regard a single macrodiamond could constitute an anomaly and would be investigated. Samples are collected at a density of 100 tonnes of unscreened sediment per 1000 square kilometres of drainage catchment, with a minimum size of 15 tonnes (one truck load). A theoretical sample site is first chosen based on the size of catchment, drainage characteristics, geology, topography, access and logistics. This general site, and possible alternatives, is then field checked for suitability and an actual sample position identified. The best sample positions are:- large potholes; near the base of large waterfalls; in the lee of rock bars; gravel filled depressions in drainage channels. Boulder bars are taken as a last resort. Excavation of the sample is achieved using a back hoe and the sample is then trucked to a field treatment plant established nearby. Considerable effort is made to clean out the bottom of the sample site. Where bedrock is soft approximately 150 mm depth of this is excavated and forms part of the sample. Where bedrock is hard, it is cleaned mechanically as best as possible. Dry sample sites are finished using a broom and a shovel.

Treatment Of Samples

Diamond samples are first concentrated in the field. Where water is plentiful, access easy and logistical parameters acceptable, samples are treated using a Mitchell Cotts Mk3 heavy media plant. Where water is scarce, access difficult and sites scattered, a portable, trommel-quadruple yuba jig plant is used. The size range of the concentrate obtained from the heavy media plant is minus 12 mm plus 0.5 mm whilst the trommel - jig plant yields concentrate of minus 6 mm plus 0.5 mm size. Test markers at SG 3.5 are added routinely to both circuits and the usual recovery is 100%.

Ongoing treatment of the concentrate is carried out in the laboratory. Field concentrate is first dried using a gas fired rotary drier of 0.5 tph capacity which discharges directly onto a 4 deck Kason screen. The plus 4 mm fraction is observed without further treatment. The minus 4 plus 2.5 mm fraction and the minus 2.5 mm fraction is further upgraded using a Pleitz jig and then observed. The minus 1 mm plus 0.5 mm fraction is batch fed through a scalper to remove highly magnetic minerals and then to a custom made high intensity Mecal induced roll magnetic separator. Diamonds are concentrated in the non magnetic fraction whilst weakly magnetic minerals, including most of the laterite, are removed in the magnetic fraction. Two passes may be necessary. The

non magnetic fractions are upgraded using tetrabromoethane at SG 2.95. The sink fraction is treated on a Readings pilot roll magnetic separator to remove any weakly magnetic minerals remaining and then observed. This circuit will not separate magnetic diamonds minus 1.0 mm in size and where these are suspected, or important, a grease table can be used in lieu of magnetic separation.

PATHFINDER SAMPLING

Collection Of Samples

The purpose of pathfinder sampling is to detect pathfinder minerals dispersed from kimberlitic rocks. The main pathfinder minerals have been listed above and often a single grain of any one of them could constitute an anomaly. On a reconnaissance survey, pathfinder drainage samples are collected at a density of about 6 kg of minus 2.5 mm sediment per square kilometre with a minimum size of 25kg and a normal range of 25 to 200 kg. It is critical that samples be collected from good trap sites. The best sites are crevices or open joints trending near normal to the drainage. Boulder bars, basal gravel accumulations, the lee of rock bars, under tree roots and in the lee of islands vary from good to moderate sites generally in the order listed. Pot holes are not good trap sites as pathfinder minerals may be destroyed by attrition. Only in very special circumstances is it worth taking a sample from the well sorted sand choked streams so common in many parts of Australia.

Samples are screened in the field at 2.5 mm, the minus 2.5 mm fraction being stored in ultraviolet resistant polythene bags for despatch to the laboratory. Damp or wet samples, and samples over 100 kg, are generally wet screened in the field. This is achieved using a Cheers hanging screen suspended over a polythene dustbin; water is pumped from a nearby source and sprayed over the sample with a garden hose. Excess water is decanted from the sample. The main advantage of wet screening is that it provides a much cleaner sample and removes unwanted salt and gypsum.

Treatment Of Samples

Treatment of pathfinder samples in the laboratory is based on jigging, tableing, heavy media separation, magnetic separation, alkali fusion and observation. The general circuit is described below but may be modified in detail depending on the size, composition and purpose of individual samples.

All samples are dried and screened at 1.0 mm, 0.5 mm and 0.25 mm on arrival at the laboratory using a Cheers hanging screen. The minus 2.5 mm plus 1.0 mm fraction is treated using a Pleitz jig and the jig "eye" observed for diamonds and pathfinder minerals. The eye is subsequently upgraded using tetrabromoethane (TBE) at SG 2.95 and the concentrate observed again. The minus 1 mm plus 0.5 mm and minus 0.5 mm plus 0.25 mm fractions are soaked for 24 hours in water containing Calgon. The wet sample is fed to a conical hopper containing a compressed air driven stirrer where it is mixed with water laced with Calgon. The resulting slurry, at a pulp density of about 50%, is discharged directly onto a laboratory sized Wilfley table with a fibreglass sand deck. Middlings are recirculated and tails are discharged to waste.

Wilfley concentrate is dried and upgraded using tetrabromoethane at SG 2.95. The finer fraction being left overnight to reach equilibrium.

Coarse (plus 0.5 mm) TBE concentrate is scalped using a Readings pilot roll magnetic separator to remove highly magnetic minerals and then passed several times through a Rapid rotary disc magnetic separator. This produces a magnetic fraction containing any picroilmenite and magnesiochromite, a non magnetic fraction containing any pyrope and macrodiamonds and a middle fraction (the greatest bulk) which is of no interest.

Both the magnetic and non magnetic fractions obtained above are further upgraded using a Readings high tension separator, if necessary, before being observed. As a final check for small diamonds, the observed minus 1mm plus 0.5 mm fraction is sent to the alkali fusion circuit described below.

Fine TBE concentrate (minus 0.5 mm plus 0.25 mm) is mixed with approximately 6 times its own volume of sodium peroxide and fused in a zirconia crucible at 600°C for 20 minutes in a muffle furnace. The fused product is digested in dilute HCl and the residue

observed for microdiamonds.

Observing consists of examining every single grain of the appropriate concentrate usually under a binocular microscope. It is a slow tedious job and one that can neither be hurried or circumvented. It represents the final stage in the analytical process and whilst checks can, and are, carried out it is impractical to do this with every sample. In consequence the correct choice of personnel to carry out this work is critical.

The composition of pathfinder minerals is determined using electron probe microanalysis and microdiamonds are confirmed using a scanning electron microscope.

PROBLEM AREAS

Whilst it is important that all the work be carried out meticulously, some areas are more prone to problems than others. Attention is particularly drawn to the following points:

All equipment must be cleaned between samples. Especial attention must be paid to screens, cabinets and brushes which are all difficult to clean and may contain mineral grains from previous samples.

Microdiamonds are hydrophobic and tend to float on the surface of water. The circuit described has been developed following a variety of tests and obtained a normal microdiamond recovery of 85 to 100%. Short circuiting the described procedure may result in loss of microdiamonds. For example tests on dry samples fed directly to the Wilfley table gave recoveries of 0 to 46% whilst tests on Calgon soaked samples which had not been passed through the stirrer gave recoveries of 50 to 80%.

Diamonds work down crevices in rock. It is essential that, during collection of the field samples, crevices and joints be thoroughly cleaned out.

Because of the need to carry out all aspects of the work accurately, and because errors may be difficult to identify and check, it is essential that only competent and trusted staff be used for collection and treatment of samples.

Accurate labelling of samples is essential to avoid mix up of sample numbers. This potential problem can be minimised by using a numbered aluminum tag at the collection stage and which accompanies the sample throughout treatment.

CONCLUDING REMARK

The circuit described above has been developed and found effective in Australia. Whilst it is probably applicable in other areas, orientation tests should be carried out to ensure this is the case.

ACKNOWLEDGMENT

BP minerals australia are thanked for permission to use the data given in this paper.

M. J. Gunn¹, A.C. Edwards¹, D.A. Paterson², W.H. Ringenbergs¹, G.E. Williams¹¹The Broken Hill Proprietary Co. Ltd. ²Goldsmith & Co. Pty. Ltd., Adelaide.

The Casuarina area lies to the east of the North Kimberley Kimberlite Province (Jaques *et al.*, 1986), and was intensively explored for diamondiferous kimberlite pipes during the period 1980 - 1984. The regional geology consists of shallowly south-dipping and gently folded sediments and basic volcanics of the Lower Proterozoic Kimberley Group, elsewhere intruded by kimberlite (Skerring, Hadfields, etc.), lamproite (Pteropus Creek) and dolerite, and in places veneered by Tertiary laterite. Regional metamorphism approaches lower greenschist facies. There are no known kimberlite or lamproite intrusions within the Casuarina area.

Diamond exploration consisted of a number of phases of sampling, which followed-up results from aeromagnetic and photo-interpretation studies as well as from regional stream sediment surveys. Within the 600 square kilometres of the Casuarina area (Fig. 1), approximately 350 separate sites were sampled, using sample sizes from 8 kilogrammes up to 50 tonnes. The samples characteristically contained very small amounts of heavy minerals. A total of 154 diamonds aggregating 12.88 carats and 49 picroilmenites was recovered, as well as anomalous minerals such as zircons regarded as kimberlitic, manganese-rich ilmenite, xenotime and tektites. All the diamonds were found in stream samples, sometimes, but not always, associated with picroilmenite.

It is assumed, with some justification, that the diamonds were brought up from the mantle by kimberlite or lamproite intrusions. Erosion has removed the diamonds and deposited them ultimately in the creeks in the Casuarina area. The question is, do the diamonds come from outcropping intrusions near or within the Casuarina area, or do they have a more complicated history involving several cycles of erosion and deposition?

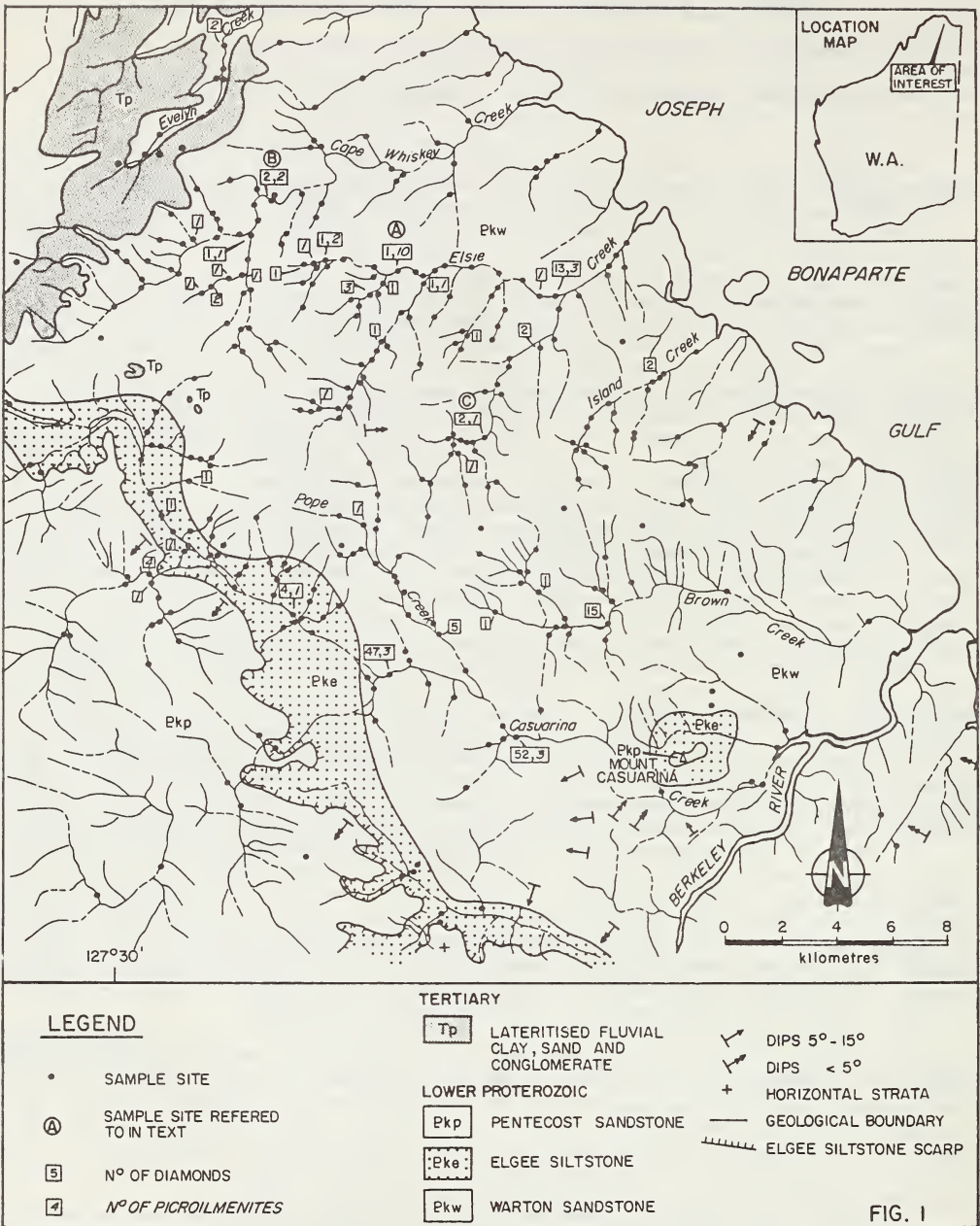
Geomorphological studies of the Kimberley region have identified a northward tilted high level dissected peneplain surface of presumed Mesozoic age, developed on Proterozoic formations, and which in the north is blanketed by lateritised alluvial deposits (boulder conglomerates, sands, clays) of presumed early Tertiary age. Palaeocurrents in Tertiary alluvium are directed northward to northeastward, a similar direction to the present day consequent streams. This evidence allows the possibility that a primary source of the Casuarina diamonds lies many kilometres to the southwest, and that the lateritised and ferricreted Tertiary gravels may be a secondary source.

The more recent geomorphological history of the Casuarina area is dominated by gentle doming and scarp retreat. The diamond bearing streams all occur on or immediately above Warton Sandstone bedrock. The overlying Elgee Siltstone is not resistant to erosion, and the southward retreat of the Elgee siltstone scarp, capped by Pentecost Sandstone, has allowed the major drainage to be captured and successively occupy the present positions of Cape Whisky, Elsie, Island, Brown and Casuarina Creeks. Thus, any diamond source in the catchment area may have contributed diamonds to these now-smaller drainages, at different times in the past.

The stream bedload in modern drainages is bimodal, consisting of sandstone-boulders and sand. During normal wet season runoff, only the top of sand and gravel bars moves about or is winnowed. It is apparent that the threshold of stream energy, above which the boulders start to move, may occur only once every several decades or more. A small increase in stream energy would cause virtually all the boulders to start moving, destroying the trap site and redistributing any diamond-bearing concentrate. This may provide an explanation for the small amounts of concentrate in the samples and the perceived concentration of diamonds in the tops of gravel traps.

Studies of the diamonds themselves have not produced definite conclusions as to their origin. The diamonds range in size from 0.5092 carats down to 0.0042 carats. There is a clustering of diamonds around the 0.03 carats weight. This skewed distribution and the lack of large stones suggests a mature alluvial diamond population. Although few of the diamonds exhibit features that can be ascribed to transportation, this may not be unexpected considering their small size.

The diamonds can be classified into groups based on crystal form. A majority (61%) of the diamonds have a growth-modified octahedral habit. A smaller fraction (35%) have rounded dodecahedral to irregular and complex forms showing features characteristic of resorption and magmatic corrosion. Approximately 4% show highly pitted and striated cubic forms. Diamonds in the centre of the Casuarina area, that is the headwaters of



Pope Creek, Brown Creek and the southern branch of Elsie Creek, are almost exclusively octahedral stones, whereas rounded dodecahedral stones are more common in the western part of the area. These two populations are believed to be distinct and real.

Diamonds can be classified according to their body colour. However, for 56% of the Casuarina diamonds, surface features mask any internal colouration. Of the remainder, 60% are brown, 32% are yellow and 7% are colourless. The distribution of these coloured stones appears to be random.

Diamonds can also be classified into groups based on combinations of features which appear to be characteristic of diamonds from known kimberlite intrusions. Although the Argyle diatreme is not a kimberlite and is 270 km to the south-southeast, it is richly diamondiferous and its diamonds show a characteristic set of features, including

granular surfaces, rounded hexagonal to oval pits, and black inclusions. Of the Casuarina diamonds, however, only 6% can be classified as 'Argyle-like', and significantly have no green or brown spots. No diamonds were recognised as being similar to those from Ellendale.

The most remarkable and perhaps most significant feature of the Casuarina diamonds is the presence, on 75% of the stones, of green and/or brown spots. Vance *et al.* (1973) proposed that green spots are crystal lattice distortions in the surface skin (20 microns) of diamonds, caused by alpha particle radiation from contact with a radioactive mineral, and that brown spots are former green spots that have been annealed by heating to elevated temperatures. Green spotted Casuarina diamonds have been heated to temperatures above 540°C for 24 hours, and the spots turn brown, whilst temperatures below this appear to have no effect over periods of a few days.

Some of the Casuarina diamonds (6%) have both green and brown spots. It is also common for a single stone to have more than 25 discrete coloured spots. Colours range from green through dark green to nearly black, and from pale orange to dark brown. The colour of an individual spot is generally lightest on the outside, becoming darker towards the centre. However, there are some spots that exhibit distinct rings of colour intensity (bull's eyes). A few of the spots have what can only be described as tails, and in rare instances, the tails of green spots are brown. These green and brown spotted diamonds may have had a complex history involving residence at an alluvial site where extended periods of contact with small radioactive mineral grains produced some green spots. Subsequent heating, either by metamorphism, or proximity to an igneous intrusion, turned all the spots brown. Continued contact with radioactive grains produced a second crop of green spots. However, the large number of spots per diamond implies an unreasonably high concentration of radioactive minerals. Alternative and less well researched explanations of the spots include: a) the inclusion of radioactive particles in the diamond during crystal growth, b) explosive pressure release of fluid inclusions, c) ionic diffusion of elements, such as iron, into the diamond surface during intense lateritisation.

Magnesium-rich ilmenites are common in the kimberlites and some of the creeks of the North Kimberley Kimberlite Province, but rare in the Casuarina area. A total of 223 grains were analysed by electron microprobe, and the results subjected to cluster analysis. This work indicated a distinct correlation between cluster groups and particular drainages in the kimberlite province, consistent with there being a number of primary sources. Within the Casuarina area however, the small number of ilmenites found makes statistical treatment difficult. The most compelling evidence that these indicator minerals were derived from nearby primary sources is the presence of eight grains from one cluster group in sample A (Fig. 1), when only ten grains were found in that sample. When compared with the scatter of compositions that is present within the Casuarina area, it appears unlikely that this concentration was fortuitous.

There are too few ilmenite grains to indicate well-developed trains showing increasing wear with down-stream distance. A microscopic study of the picroilmenites demonstrated that most appear to be fresh to fresh-worn. Few worn grains occur. Two very fresh picroilmenites still retaining a substantial portion of a thick leucocoxene skin were found, one each at sample sites B and C. These are believed to have come from a primary source within a few kilometres. Several polycrystalline aggregates have been found, which also implies only limited fluvial transport. These data strongly suggest that there are a number of small kimberlite dykes within the Casuarina area.

The results of all these studies suggest that there are kimberlitic intrusions within the Casuarina area. These are likely to be small dykes and have either no diamonds, or diamonds which may have similar features to those from Argyle. The majority of the diamonds, particularly the spotted stones, are probably not derived from a local primary source. The most likely source area lies some considerable distance to the southwest. The Drysdale River may once have continued its north-northeasterly course from the centre of the Kimberley Plateau, via the sand-choked and weakly diamond-bearing Beta Creek to the area now drained by Casuarina Creek, where extensive early Cenozoic gravels were deposited. The lack of abrasion of the diamonds, and the distribution of crystal forms appears not to support this explanation, however the other evidence, particularly the preponderance of spotted stones suggests that an unknown primary source of many Casuarina alluvial diamonds lies closer to the diamondiferous intrusions of the East or West Kimberley lamproite provinces.

- JAQUES, A.L., LEWIS, J.D. and SMITH, C.B., 1986: The kimberlites and lamproites of Western Australia. Geological Survey of Western Australia Bulletin No. 132.
VANCE, E.R., HARRIS, J.W. and MILLEDGE, H.J., 1973: Possible origins of Alpha-damage in diamonds from kimberlite and alluvial sources. *Min. Mag.* Vol. 39 p349-360.

A. E. Haebig and D. G. Jackson

CRA Exploration Pty Limited, 21 Wynyard Street, Belmont, Western Australia

INTRODUCTION

Geochemical analyses of soil and drill spoil samples have been used during diamond exploration in Western Australia to identify overburden-covered diatremes, dykes and sills of kimberlite, lamproite and related rocks (hereafter termed "kimberlitic" rocks where referred to collectively).

The elements chosen for analysis reflect the characteristic kimberlitic association of enrichment in elements of ultramafic affinity combined with high values for incompatible elements (Dawson, 1967). This association is as characteristic of lamproite as it is of kimberlite (Smith, 1984). Elements most widely used were chromium, cobalt and nickel as representatives of the ultramafic suite and niobium as an incompatible element. However, orientation surveys have shown that markedly anomalous values of magnesium, titanium, phosphorous, barium, strontium, lanthanum and cerium are also developed in soils over kimberlitic source rocks.

Emission spectroscopy was widely used as an analytical method and is sensitive enough for analysis of drill spoil of ultrabasic rocks and their weathering products. For soil geochemistry a combination of emission spectroscopy (Ni/Co) and XRF (Cr, Nb) has been used to increase the sensitivity, especially for niobium analysis (the detection limit for Nb was 20 ppm by emission spectroscopy and 3 ppm by XRF, whereas 15 ppm Nb can represent a soil anomaly over a lamproitic/kimberlitic body). High Ni-Co-Cr contents (hundreds of ppm) identify a soil or drill sample as derived from a basic or ultrabasic source rock. If the Nb level is also raised (15 ppm to several hundred ppm) a kimberlitic source rock is indicated. Niobium anomalies can be found in soils over siltstones and shales; Ni-Co-Cr levels then remain low.

EXAMPLES OF APPLICATION

The Skerring kimberlite (King George River area, North Kimberley) measures approximately 600m in length and 7 to 75 metres in width as defined by prospect pits and intrudes Proterozoic shale country rock. It is a micaceous peridotite body containing abundant picroilmenite megacrysts, chrome and titanian pyrope and has been likened to classical kimberlite of South African type (Atkinson et al, 1984; Jaques et al, 1986). It is lateritised and silicified at surface and forms a slight topographic ridge. Due to downslope creeping of soil and debris the width as indicated by soil geochemistry is considerably larger than the actual width of the body. The soil geochemical response in order of times background was: Cr 6, Nb more than 4, Ni 4, Co 3, Mg 2. The samples were -80# (180) and taken from a depth of 10-15 cm.

The lamproites of the West Kimberley (Prider, 1960; Jaques et al, 1984) range from basic to ultrabasic in composition, i.e. from leucite lamproite, composed essentially of leucite+phlogopite+diopside+richterite and with modal olivine content typically 5 Wt % and SiO₂ 50 Wt %, to marked undersaturated olivine lamproite in which modal olivine is 20% (typically 30%). Whereas some of the leucite lamproites form fresh outcrops at surface and give rise to topographic highs, the olivine lamproites rarely do so, the olivine is frequently altered to talc and the rock rapidly weathers to form montmorillonite-rich clays. The olivine lamproites often form slight topographic depressions. The soil and weathering products are retained inside the depression if no connection to the drainage exists. At Big Spring, 5 lamproite bodies intruded Devonian limestones and Proterozoic granodiorite. The largest body has a surface area of 10 ha. The -80# (180) fraction of grid loam samples was analysed by emission spectroscopy. Anomalous values ranged from:

2 to 11 times background for Ni, average 6 times
2 to 12 times background for Cr, average 5 times

1.5 to 4 times background for Co, average 2.5 times

Niobium was not analysed for. A stream sample collected near a lamproitic breccia outcrop yielded 13, 5 and 7 times background for Ni, Co and Cr. Only 200m downstream and outside of the pipe the values had dropped to 1.7, 1.7 and 1.4 times background.

The Ellendale lamproites in the West Kimberley intrude Devonian and Permian limestones, calcarenites, siltstones and sandstones. They often form depressions, and the geochemical response occurs only immediately over the diatreme. Values recorded from Ellendale 9 olivine lamproite were:

Soil: Background Ni 25 ppm Anomaly : average 5 times background
Nb 20 ppm average 4 times background

Auger Drilling : Ni 150 ppm Anomaly : average 5 times background
Nb 20 ppm average 7.5 times background

All auger holes bottomed in weathered ultrabasics or sandstone. The soil geochemistry results show the position of the boundary of the diatreme quite clearly. Values drop from as high as 10 times background to background inside 50m (i.e. 1 sample interval). The soil geochemistry values over the 81 Mile Vent leucite lamproite are virtually identical to those over the Ellendale No. 9 olivine lamproite. Soil geochemistry is effective in areas with overburden to 7m and more. At Ellendale No. 7 olivine lamproite, which is covered by 4 to 8 m (average 7m) of transported aeolian sand, nickel averages 3 times background, cobalt 1.2 times, chromium 4.5 times and niobium twice. The boundary is as sharp as at No. 9, i.e. there appears to be no "mushroom effect". At Ellendale 6 leucite lamproite where aeolian sand overburden averages 14m depth no surface geochemical anomaly could be detected.

At Wandagee in the Carnarvon Basin, breccia diatremes with kimberlitic affinities are associated with olivine picrite sills (Atkinson et al, 1984). The diatremes carry chrome pyrope, chrome diopside, rare picroilmenite macrocrysts, and very rare microdiamond. Juvenile clasts in the diatremes are olivine-rich, sometimes contain phlogopite, but are too altered to determine their full petrographic affinities. Geochemically the diatremes are generally similar to kimberlite, but niobium values are noticeably low. During exploration at Wandagee the -40# size fraction of grid loam samples was analysed by AAS and XRF for Ni, Co, Mg, Cr and Nb. For pipe M89 nickel and magnesium anomalies occur over the pipe and to the west. Chromium is centred on the pipe, niobium and cobalt do not show any correlation with the pipe. Nb anomalies of 2.5 times background occur to the NW and SW of the pipe, Co shows 2 depletion anomalies to the E and W of the pipe.

DISCUSSION

Geochemical analysis of samples of soil and sand overburden over West Australian kimberlitic pipes has shown that anomalous values of ultramafic-association elements and of incompatible elements occur immediately above the pipes. Where the pipes are marked by a topographic hollow at surface, or where the ground is flat, there is little lateral dispersion of the geochemical anomaly and the pipe contacts are sharply defined. Where there is sloping ground the anomaly will extend downslope, but only for distances less than the diameter of the pipe. These results parallel those obtained overseas, e.g. Yakutia (Litinskiy, 1964), Mali (Alcard, 1959), even to the magnitude of the anomalies, i.e. typically some 2 to 7 times background values for Cr, Ni, Co, Nb.

The Western Australian results show that similar geochemical anomalies characterise leucite and olivine lamproite as well as kimberlite. Even where transported sand overburden as thick as 7 metres covers the pipe, a geochemical anomaly can be found at surface. However, the limited lateral dispersion of the soil geochemical anomalies has meant that the method has not been as effective as an exploration method for kimberlite as have heavy mineral indicator or geophysical techniques, although the characteristic geochemical signature helps to identify weathered rock samples from outcrop or borehole spoil.

REFERENCES

ALCARD, P., 1959. The application of geochemical methods (Cr and Ni) to prospecting for kimberlite pipes, *Annales des Mines*, p.103-110.

ATKINSON, W. J., HUGHES, F. E. & SMITH, C. B., 1984. A review of the kimberlitic rocks of Western Australia; in Kornprobst, J. (Ed), *Kimberlites. 1: Kimberlites and Related Rocks*, pp.195-224, Elsevier, Amsterdam.

DAWSON, J. B., 1967. Geochemistry and origin of kimberlite. In *ultramafic and unrelated rocks*, Ed. P. J. Wyllie, Wiley, New York, pp.269-278.

LITINSKIY, V. A., 1964. Application of metallometry and kappametry in prospecting for kimberlite bodies. *Internat. Geol. Rev.*, 6, pp.2027-2035. (Geochemical and magnetic methods of prospecting).

JAIQUES, A. L., LEWIS, J. D., SMITH, C. B., FERGUSON, J., CHAPPELL, B. W. & McCULLOCH, M. T., 1984. The diamond-bearing ultrapotassic (lamproitic) rocks of the West Kimberley region, Western Australia; In Kornprobst, J. (Ed), *Kimberlites. 1: Kimberlites and Related Rocks*, pp.225-254, Elsevier, Amsterdam.

PRIDER, R. T., 1960. The leucite lamproites of the Fitzroy Basin, Western Australia. *J. Geol. Soc. Australia*, Vol.6, pp.71-118.

SMITH, C. B., 1984. What is a kimberlite, in Glover, J. E., and Harris, P. G. (Eds), *Kimberlite Occurrence and Origin: a basis for conceptual models in exploration*, pp.1-18, Publication No. 8, Geology Dept., and University Extension, University of Western Australia.

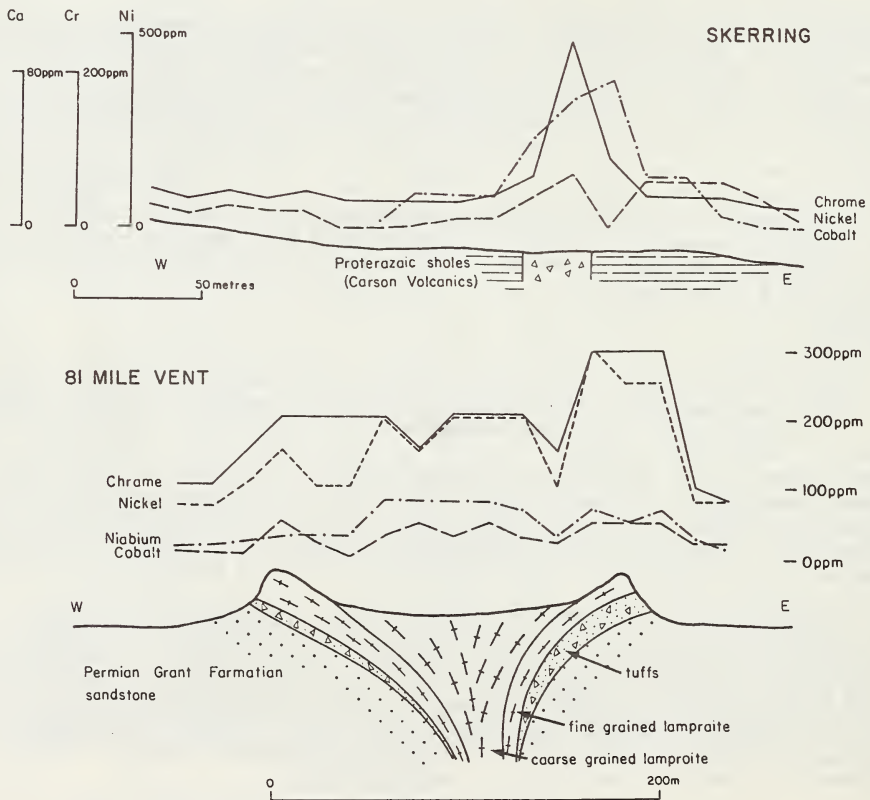


Fig. 1 Cross sections and geochemical profiles for Skerring Pipe and 81 Mile Vent

ALKALINE DIATREMES IN THE HUDSON BAY LOWLANDS, CANADA
EXPLORATION METHODS, PETROLOGY AND GEOCHEMISTRY

A.J.A. Janse, Mintel Pty. Ltd., Carine, Western Australia
I.F. Downie, L.E. Reed and I.G.L. Sinclair, Selco Division,
BP Resources Canada Limited, Toronto, Canada

LOCALITY AND GEOLOGY

A kimberlite exploration programme in the Hudson Bay Lowlands of Northern Ontario resulted in the discovery, in 1980, of a group of alkaline, ultrabasic diatremes with kimberlitic affinities. The programme was conducted by Selco Mining Corporation in partnership with Esso Minerals Canada. The Lowlands form a large area of relatively flat, poorly drained land along the southwestern shore of Hudson Bay and the western shore of James Bay (Fig.1) which extends inland for some 300 km and has an elevation ranging from zero to about 200m. At their southern margin, the Lowlands are underlain by rocks and unconsolidated deposits ranging in age from Archean to Recent.

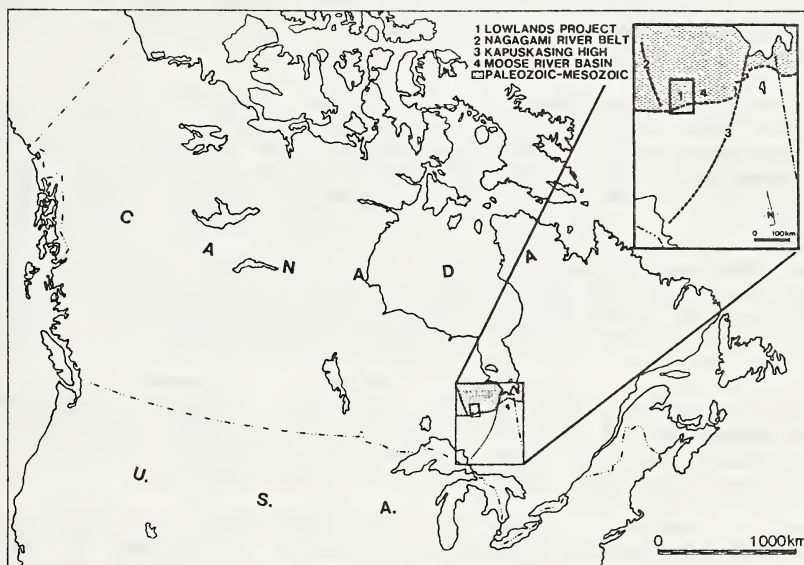


Fig. 1: Location of Lowlands Project.

The project area is located some 30 km north of Hearst, Ontario. Archean crystalline rocks, belonging to the Superior Province of the Canadian Shield, slope northwards beneath a cover of Paleozoic carbonates and clastic sediments up to 800m thick. The Paleozoic rocks are in turn overlain by glacial and recent deposits varying in thickness from 25m to more than 150m. The nature of this cover renders prospecting for kimberlites by conventional heavy mineral sampling impractical. Therefore, the exploration method used in this project was low-level airborne magnetic surveying, followed, where appropriate, by detailed ground geophysics and drilling.

The selection of the particular area to be flown was based on general geotectonic principles with reference being made to all available published geophysical and geological data. Important considerations were the presumed downwarping of the crystalline basement at the margin of the Lowlands some 20 km to the south, the presence of local flexures in the basement, primarily the sharply depressed Moose River Basin just to the east, and the avoidance of major groups of alkaline complexes, such as

the Nagagami River Belt to the west. The presence of overlying, undisturbed Paleozoic sedimentary rocks was considered a favourable factor; firstly, because such rocks filter out magnetic 'noise' from the basement rocks so that anomalies due to younger intrusions are more easily identified; and secondly, because the presence of these rocks may mean that post-Paleozoic erosion has not been profound enough to remove Mesozoic or younger intrusions.

GEOPHYSICS

Magnetometer surveying has been employed in the search for kimberlites in a number of places in the world. New aeromagnetic surveys were required in the study area as the existing magnetic coverage flown for the Canadian government was not sufficiently detailed (800m line separations), and not at a low enough terrain clearance (300m) to be effective in detecting the target bodies. Surveys were flown using fluxgate magnetometers in tail stinger assemblies on fixed wing aircraft. The total field magnetometer data is accurate to one nano-Tesla (nT). The sensors were flown at an elevation of 60m, at a flight line interval of 250m, in a north-south direction. The line spacing chosen was such that most, if not all, bodies of economically significant size (greater than 200m) would be detected as long as they were magnetic. It was recognized that not all kimberlites demonstrate significant magnetism, but it was felt that a sufficient number in any kimberlite field would be magnetic to make possible the detection of the field. The flying elevation was chosen to be as low as was considered safe.

The earliest survey results observed magnetic responses of a few tens to a few hundred nT. It is known that the Paleozoic rocks in this area are not magnetic, and that the magnetic rocks of the Precambrian basement generally lie several hundred metres below the ground surface. The observed magnetic responses were very distinctive, and suggested the kind of anomalous response one would expect from pipe-like bodies with tops 20 to 50m below the ground surface. Identification of these targets was carried out using line profiles and contour maps of the survey data. Estimations of source depths were made using Peter's half-slope method. While more sophisticated computer-based modelling interpretation techniques were available, it was realized that the "rule of thumb" method identified the targets quickly and simply. However, some processed products, such as apparent susceptibility and regional/residual filters were generated. These enhanced not only the responses from the target bodies but also enhanced the high frequency elements of the basement responses, degrading the resolution of the target bodies. The natural separation of responses between shallow intrusives and the deep basement by the magnetically neutral Paleozoic rocks, provided the best filter of the data. Accordingly, the total field data rather than processed data were used for the anomaly selection.

Over 130 anomalous responses were identified across an area about 70 km long by 30 km wide. The long axis is in a north-northeasterly direction. The responses appear to cluster in two large areas with groups of anomalies lying along lines which tend to identify with linear events in the basement as seen by the magnetics. Evidently there is some control by the basement structure over the emplacement of the shallow magnetic bodies. Circular and oval responses predominate although a few elongate or dyke like features are evident. The horizontal dimensions of the source bodies, indicated by the airborne responses, range from less than 100m to over 1 km. Diameters of a few hundred metres are most frequently observed.

Selected anomalies were followed up on the ground using total field proton precession magnetometers accurate to one nT. Readings were taken at 25m intervals along north-south lines 100m apart across the anomalous areas. The ground responses generally support the airborne interpretation, but with greater detail and spatial precision. Again, simple "rules of thumb" were used for depth, location and shape information. Ground data over a number of the bodies suggest they contain some remanent magnetism with a magnetic pole orientation toward the north-west. This would be consistent with an age of emplacement (or at least the last thermal event) in the mid to late Mesozoic.

Drill targets were selected on the basis of the ground magnetic responses. The amplitude was not considered significant in the selection of drill targets, so that

among the bodies sampled, a range of anomalous responses was identified. Ground responses were a few hundred to a few thousand nT. Subsequent to drilling, magnetic susceptibility measurements on the core indicated a range of response from 0.1 to 1.6×10^{-3} cgs units. The surface and airborne magnetometer readings were entirely consistent with these levels of magnetism in the rocks.

PETROLOGY AND GEOCHEMISTRY

The targets drilled proved to be a suite of heavily serpentinized, alkaline intrusions. Although there is considerable overlap in their mineralogy, texture and chemistry, the rocks can conveniently be divided into three groups, viz: ultramafic tuff breccias, massive alnoites, and carbonatites. Thirty-four of the forty-five intrusions drilled fall in the first group, four in the second, and seven in the third.

The tuff breccias characteristically contain an abundance of autoliths and crustal xenoliths as well as scattered xenocrysts and macrocrysts of garnet, olivine, clinopyroxene and ilmenite. Their matrices consist of serpentine and subordinate carbonate in which are scattered fine spinels and perovskite grains. There are two varieties of autoliths: sub-rounded to sub-angular pellets of heavily serpentinized, microporphyritic ultramafic rock, and nucleated autoliths. The nuclei of the latter are composed of grains of clinopyroxene, mica or serpentinized olivine. The bulk chemistry of these rocks is similar to that of kimberlites, except for their generally lower MgO and higher CaO contents. Trace element analyses shows them to be deficient in chromium and nickel relative to most kimberlites. Microprobe analyses of selected grains of garnet, pyroxene, spinel, mica and ilmenite show that, with rare exceptions, their compositions lie outside the ranges considered to be typical of kimberlites. The relatively high CaO/MgO ratio exhibited by these rocks, reflected by the common occurrence of calcite in their matrices, suggests that they be tentatively classed as aillikites.

The rocks identified as alnoites are similar in mineralogy and chemistry to the tuff breccias, but they are much more massive in appearance and do not contain the abundant autoliths and xenoliths observed in the breccias. The occasional presence of melilite, or pseudomorphs after melilite suggests their classification as alnoites.

The carbonatites range in composition from pure varieties containing less than five per cent SiO_2 , through to alnoitic types, which contain minor amounts of melilite (or pseudomorphs after melilite), and have SiO_2 contents of around twenty per cent. They contain scattered grains of clinopyroxene, spinels, phlogopite, olivine, garnet, hornblende, apatite, barite and a niobium-rich variety of perovskite. Spatially, the carbonatites tend to occur in a cluster more or less in the centre of this suite of intrusions - a pattern reminiscent of the relationships between carbonatites and alnoitic rocks in many other alkalic/carbonatite complexes.

REE analyses were conducted on six samples of the Lowlands intrusions. Chondrite plots for samples of the tuff breccias and alnoites are similar to those obtained from two samples of South African kimberlites, suggesting some similarities in petrogenetic history. Samples of the carbonatites have the intense LREE enrichment typical of the genre.

The tuff breccias are too heavily serpentinized to yield mineral samples suitable for age-dating, but K-Ar ages of $152 \pm 3\text{Ma}$ and $180 \pm 9\text{Ma}$ were obtained, by Teledyne Isotopes Ltd. using mica concentrates from two of the massive alnoites. These ages are consistent with the geological setting of the intrusions.

CONCLUSION

Kimberlites were not discovered as a result of this project. However, it was demonstrated that alkaline diatremes can be located under heavy glacial cover, by the combined application of geological reasoning and sophisticated geophysical techniques.

SPECTRAL REFLECTANCE FEATURES OF KIMBERLITES AND CARBONATITES:
THE KEY TO REMOTE SENSING FOR EXPLORATION

Marguerite J. Kingston
United States Geological Survey
Reston, Virginia 22092

Recent advances in the spectral and spatial resolution of airborne and spaceborne multispectral scanning devices provide new opportunities for using remote sensing techniques in kimberlite and carbonatite exploration. To evaluate their remote sensing potential, laboratory diffuse reflectance spectra were recorded in the 0.4- μm to 2.5- μm wavelength range for naturally weathered surfaces of kimberlites from southern Africa and for carbonatites from South Africa and North America. Mineralogy was confirmed by petrographic and/or x-ray diffraction analysis.

Characteristic absorption features of minerals are derived from either electronic or vibrational processes. The principal electronic processes result from energy level transitions in a crystal field or from the formation of valence and conduction energy bands. In the near-infrared range, vibrational processes yield overtones and combination tones of the fundamental modes of anion groups and water.

The spectrum of a relatively fresh dark kimberlite, fine grained hardebank (sample 1, Figure 1), contrasts with that of a weathered light green kimberlite (sample 2). Spectral contrast is reduced by the presence of finely disseminated opaque minerals so that features are often obscured in dark kimberlite samples.

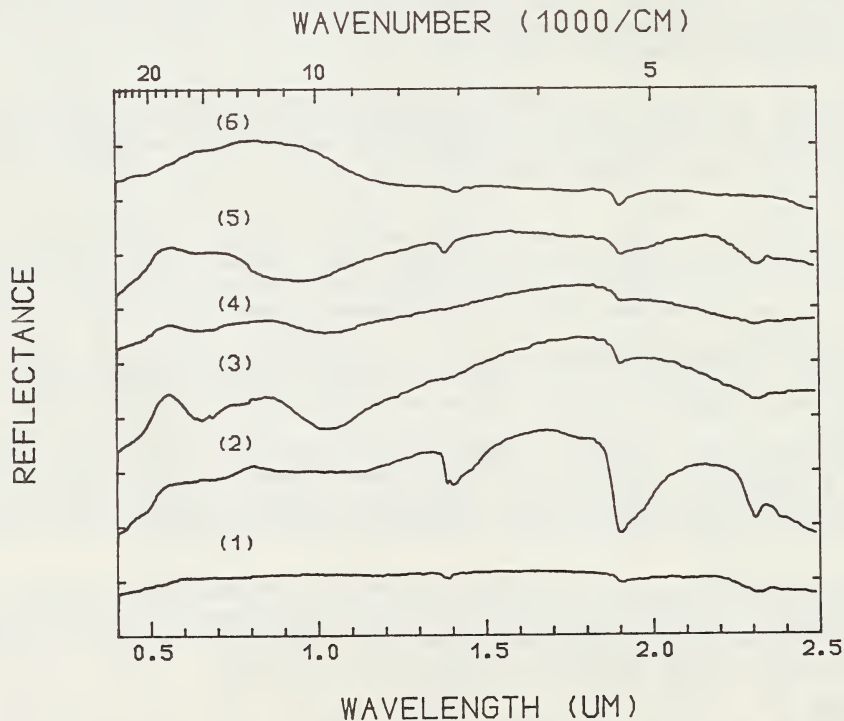


Fig. 1. Sample (1); kimberlite "hardebank", Doornkloof Mine, South Africa (2); kimberlite, Williamson Mine, South Africa (3); "Granny Smith" nodule (Ti-Cr diopside), Kampfersdam, South Africa (4); Cr-diopside nodule, Kampfersdam, South Africa (5); Lherzolite, Monestery Mine, South Africa (6); garnet-rich nodule, Orapa, Botswana. Spectra are displaced vertically.

Bands near 1.4 μm are due to the first overtone of the hydroxyl fundamental; the presence of bands at both 1.4 μm and 1.9 μm is diagnostic of water. Features near 2.32 and 2.38 μm are caused by MgOH stretching and bending modes. The spectrum of sample (1) is common to many kimberlites and absorption bands can be attributed to a small amount of serpentine. Features exhibited by the sample (2) spectrum can be assigned to saponite, a weathering product of olivine and pyroxene. The broad band centered near 1.0 μm is due to ferrous iron in a spin allowed transition in the octahedral field. Weak features between 0.4 μm to 0.5 μm are caused also by crystal field transitions of ferrous iron. Magnesium olivine strongly predominates in kimberlites, but the presence of only a small amount of iron will produce these features.

The features near 0.45 μm and 0.65 μm as displayed in the spectrum of sample (3), the "Granny Smith" nodule (Ti-Cr diopside), are due to ferrous iron but chromium also contributes to these absorption bands. The spectrum of sample (4), chrome-diopside, has a similar shape. These spectra display broad iron bands near 1.0 μm , due to ferrous iron of diopside which occurs in the $M_{(1)}$ octahedral site. The minima of the ferrous iron feature in the lherzolite, sample (5), is shifted to a shorter wavelength due to iron occupancy of the $M_{(2)}$ site of enstatite (Burns, 1970). Typically garnet-rich samples (sample 6) display a broad iron feature centered near 1.28 μm not 1.0 μm , due to eight fold co-ordinated ferrous iron in pyrope (Bancroft et al., 1967). Serpentinization and/or kelyphitization is the cause of the OH, MgOH and H_2O bands. As garnet and chrome-diopside are both indicator minerals in kimberlite prospecting, their spectral properties may be significant in exploration, especially in aerial surveys of desert regions.

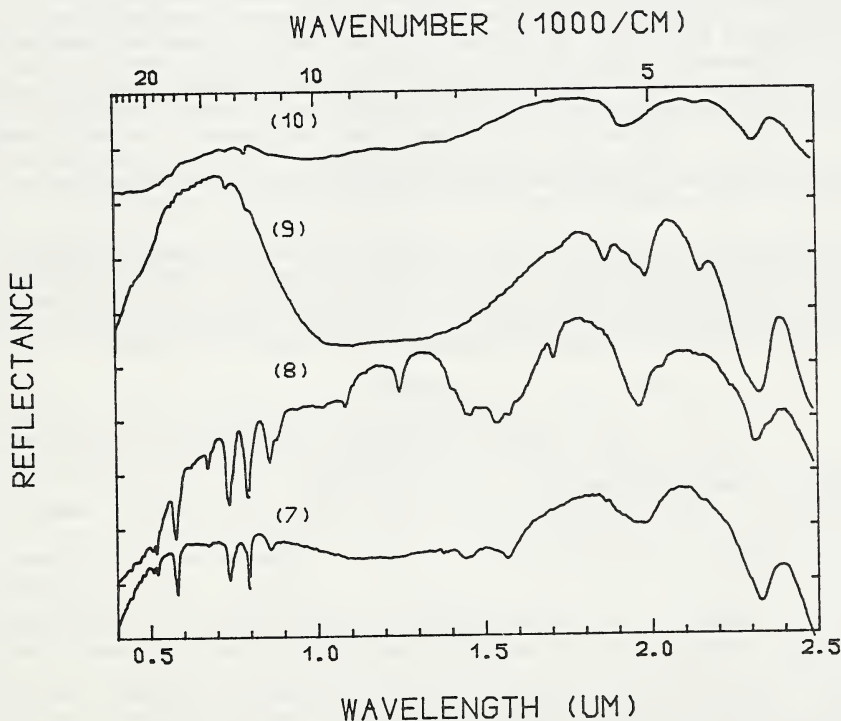


Fig. 2, Sample (7); sövite, Bear Paw Mountains, Montana, USA (8); sövite, Mountain Pass, California, USA (9); rauhaugite, McCloskey's Field, Quebec, Canada (10); rauhaugite, Glenover Complex, South Africa. Spectra are displaced vertically.

Carbonatites may have a higher reflectivity and may display more intense absorption bands than kimberlites. Near-infrared features of carbonatites are due to carboxyl-group vibrational processes, with the 2.34- μm band at a slightly longer wavelength than the 2.32 μm MgOH feature. Some samples display a series of sharp, narrow bands between 0.5 μm and 0.9 μm caused by electronic transitions of neodymium (Rowan et al, in press). In sovite sample (7) (Figure 2), enriched in the mineral burbankite, neodymium causes the bands at 0.52, 0.58, 0.74, 0.80 and 0.87 μm . Carbonatites containing as little as 100 ppm neodymium display these bands, if they are not obscured by spectrally opaque minerals. Whole rock analysis of the McCloskey's Field, Quebec, coarse-grained carbonatite (sample 8) gives 180 ppm neodymium. Except for samarium other rare earth elements do not exhibit absorption bands, because of their unsuitable electronic configuration and/or low concentrations. The spectrum of sample (8) (20% bastnaesite) displays not only neodymium features but also prominent bands between 1.0 μm and 1.7 μm due to samarium. A broad double absorption band centered near 1.0 μm and 1.25 μm is conspicuous in some rauhaugite samples and is due to ferrous iron substituting in the dolomite lattice, (sample 9). The presence of this feature in rock spectra in combination with carboxyl and neodymium bands is diagnostic of carbonatite. Finely disseminated magnetite in carbonatite will quench the rare earth, ferrous iron and carboxyl spectral features as demonstrated in the South African rauhaugite spectrum (sample 10).

We have successfully used a portable spectrometer in field studies at the Iron Hill, Colorado carbonate complex to map the distribution of rare-earth-rich phases on the basis of observation of neodymium absorption bands. Remote exploration of kimberlites and carbonatites however is dependent on the occurrence of spectral and spatial contrast with country rock. Distinctively shaped discordant bodies in the appropriate tectonic setting should be identifiable. Serpentine-rich kimberlites that intrude basalt, granite or most sedimentary rock can be spectrally discriminated. Differences in soil development due to contrasting weathering resistance between kimberlite and country rock will result in remotely detectable vegetation differences. Carbonatite may be remotely discriminated because the frequently associated alkalic igneous rocks are spectrally featureless. An airborne high-resolution spectroradiometer has distinguished both carbonate and neodymium spectral features in flights over the Mountain Pass, California carbonatite complex (Kingston and Rowan, 1986). Flightlines that recorded intense neodymium absorption spectra were juxtaposed on those recording anomalous carbonate features and were used to outline the rare-earth-enriched sectors of the carbonatite complex.

A new generation of high-resolution airborne imaging spectrometers offers substantial potential for exploration. The NASA imaging spectrometer will soon be operational, acquiring data from a U-2 aircraft in 160 spectral channels from 0.4 to 2.5 μm , and having a ground resolution of 15 m. Spectral features of iron, hydroxyl, carboxyl and rare earth elements will be detectable at this resolution.

REFERENCES

- Bancroft, G.M., Maddock, A.G., and Burns, R.G., 1967, Application of the Mossbauer effect to silicate mineralogy I. Iron silicates of known structure. *Geochemical et Cosmochimica Acta* 31, p. 2219-2246.
- Burns, R.G., 1970, *Mineralogical applications of crystal field theory*: Cambridge University Press, p. 87-94.
- Hunt, G.R., Salisbury, J.W., and Lerhoff, C.J., 1971, Visible and near infrared spectra of minerals and rocks: III oxides and hydroxides: *Modern Geology* 2, p. 195-205.
- Kingston, M.J., and Rowan, L.C., 1986, Spectral characteristics of carbonatites: A potential exploration tool. Geological Association of Canada abstracts with program. 2, p. 89.
- Rowan, L.C., Kingston, M.J., and Crowley, J.C., in press, Spectral reflectance of carbonatites and related alkalic igneous rocks: Selected samples from four North American localities. *Economic Geology*.

D.C. Lee, A.van Riessen*, K.W. Terry*

Ashton Mining Limited
100 Jersey Street
Jolimont 6014
Western Australia

*School of Physics and Geosciences
Western Australian Institute of Technology
Kent Street
Bentley WA 6102

TECHNIQUE

The conventional method of x-ray analysis in the scanning electron microscope (SEM) is to excite the sample with a beam of electrons and to detect emitted x-rays with a lithium drifted silicon (Si (Li)) detector. Such a system has a maximum sensitivity at around 3.5 keV but drops rapidly for higher energy photons.

Improved sensitivity of elements emitting higher energy photons can be achieved by exciting the sample with x-ray radiation. The technique adopted is to direct the electron beam onto a thin metal foil and use the x-rays transmitted through the foil to excite the sample. The consequence of irradiating a sample with an x-ray beam is that one of three mechanisms can take place between the photon and sample. If the sample absorbs a photon with an energy greater than an absorption edge of one of the elements present in the sample, then characteristic photons may be emitted (i.e. x-ray fluorescence). The other two mechanisms that can take place when a sample is irradiated with an x-ray beam are Rayleigh and Compton scattering.

Energy dispersive spectra obtained from the x-ray excited technique consist of characteristic peaks of the sample (fluorescence) superimposed upon a background caused by the combination of Rayleigh and Compton scattering of the primary x-ray beam. The amount of general background can be minimised with the use of a monoenergetic incident x-ray beam. However, in practice there is always some continuum associated with the characteristic line of the incident beam. This undergoes both Rayleigh and Compton scattering and hence gives rise to the general background of the emitted spectrum from the sample. The rest of the background arises from the Rayleigh scattering of the incident monoenergetic x-ray beam, and this beam's Compton scattering which manifests itself as a broader maximum in the background immediately below the Rayleigh peak. In addition there occurs a Compton scattering of detected photons within the lithium drifted silicon detector that results in an increase in background at low energies.

In the design of the thin foil device there are basically four variables that need to be considered, namely, accelerating voltage, foil type, foil thickness and x-ray spot size.

Accelerating Voltage. Excitation of the sample is due to both the characteristic and continuum x-ray photons originating from the foil. The intensity of the primary characteristic lines increases as the 1.67 power of the accelerating voltage of the electron beam while the intensity of the continuum increases linearly. To maximise the x-ray flux impinging on the sample the highest accelerating voltage available should be selected.

Foil Type. For optimum conditions for the x-ray excited technique a foil type should be selected such that its characteristic radiation is slightly more energetic than the critical excitation energy of the element being detected.

Foil Thickness. The fact that the continuum plays an important part in causing secondary fluorescence means that the foil need only be thick enough to prevent electron penetration. Thick foils do extend the very low background region to higher energies but at the expense of primary x-ray flux. Consequently, in order to maximise the counting statistics for reasonable counting time, the thinnest possible foil is desirable.

X-ray Spot Size. The size of the x-ray beam from the foil, impinging on the sample, is determined by collimator length and diameter as well as collimator to sample distance. For the geometry selected (0.6mm diameter collimator, 6mm collimator length and 7.75mm between collimator and sample) an x-ray spot size at the sample of 1.5mm in diameter is obtained. However, the sample is normally tilted towards the x-ray detector so an elliptical spot is formed with a long axis of approximately 2.5mm. The spot size used in this project was found to be satisfactory for most grains. Where grain size was less than the spot size, a correction factor was used on the data collected from the thin foil generated spectra.

Spot size of the x-ray beam also controls minimum detection limits. As spot size is increased, so does the quantity of x-ray flux impinging on the sample, with the

result that minimum detection limits are improved. The restricted size of grains supplied in this project prevented the use of larger spot sizes.

Advantages of X-ray Excited XRF. The strength of the thin foil technique stems partly from the ability to select operational conditions which optimise minimum detection limits for a range of elements. Foil type and thickness as well as accelerating potential all contribute to the final sensitivity. Used in conjunction with electron excited results, the thin foil technique considerably expands the capability of the SEM/EDS system for a modest outlay.

A comparison of electron excited and x-ray excited XRF in a SEM has shown that the two methods are complementary. The electron technique is more sensitive to low atomic number elements while the x-ray technique is more sensitive to high atomic number elements. In addition the minimum detection limits have been reduced to better than 20ppm for certain elements using the x-ray excited method.

The x-ray excited technique differs from electron microprobe analysis in that the whole surface of a polished cross-section of a mineral grain is analysed. There is a considerable depth of penetration by the x-rays used to excite the mineral grain and information on trace element content of a relatively large volume of a mineral grain is obtained by this technique. It would be very time consuming and difficult to generate the same information about a single grain by use of an electron microprobe.

EXPERIMENTAL DETAILS.

The approach in the project detailed below has been to analyse mineral grains quantitatively for the major and minor elements together with a qualitative assessment of the trace elements. This has been achieved using a scanning electron microscope equipped with an energy dispersive x-ray spectrometer. Results from conventional electron excited XRF were supplemented with those obtained from the x-ray excited XRF method.

Electron Excited XRF. The elemental analyses were carried out using a JEOL JSM 35C scanning electron microscope equipped with a United Scientific lithium drifted silicon detector and associated electronics. The spectra were accumulated in a Tracor Northern TN 1705 multi-channel analyser (MCA). The adopted procedure for elemental analysis was to use 20kV and 5×10^{-10} amps at normal incidence onto a $40 \times 40 \mu\text{m}$ raster on a polished sample and a detector take-off angle of 35° . A typical count rate of 5 kcps was obtained. The spectra were collected in the MCA for 50 s live time and were then transferred to a Sirius 1 microcomputer for subsequent processing. The elemental analysis was then computed using the peak integration with background subtraction (PIBS) technique of Ware (1981). The current program provides for an elemental analysis for Na, Mg, Al, Si, P or Zr, Cl, S, K, Ca, Ti, V, Fe, Mn and Zn expressed as oxides and has a sensitivity down to approximately 0.1%.

X-ray Excited XRF. The x-ray excited method adopted was to focus the 39 keV, $1 \mu\text{A}$ electron beam onto a silver or molybdenum foil of $5 \mu\text{m}$ thickness which acts as a transmission x-ray target. The resultant collimated primary x-ray beam impinging on the sample consisted of the characteristic peaks together with the continuum that had been self-filtered by the foil. The incident primary x-ray beam caused secondary x-ray fluorescence in the sample so that characteristic x-rays of the elements in the sample were subsequently detected by the Si(Li) detector.

Although better minimum detection levels were achieved compared with electron excited XRF, considerably longer counting times (typically 200s) were required to accumulate sufficient counts. Integrated peak minus background counts from the central seven channels of each peak in the x-ray spectra provided semi-quantitative information regarding the amount of a particular element present in the sample.

APPLICATION.

This project with the thin foil device attached to a scanning electron microscope was aimed at finding a practical method of detecting some of the trace elements in mineral grains from kimberlitic sources. A reasonably large number of grains have been analysed in a relatively short time to build up a data base.

A total of 310 grains were selected from kimberlitic and non-kimberlitic rock types: chrome diopside, chromite, garnet, ilmenite, olivine and zircon. The major and minor elemental contents were obtained by using electron excited XRF in the SEM while the x-ray excitation method was used to determine the trace elements.

One set of significant data is that, for the garnets, it can be seen that Cr, Zn and Y are present in higher amounts for the kimberlitic garnets than in the non-kimberlitic samples. The result is of considerable interest as the garnet types chosen for study cannot otherwise be distinguished as either kimberlitic or non-kimberlitic. The reason for the difference in trace element content of almandine garnets from kimberlite and common almandine garnets is not established. It may be a result of late

stage metasomatism i.e. diffusion of trace elements from kimberlite magma into mineral grains derived from the earth's crustal zones.

The separation of two samples of eclogitic pyrope into kimberlitic and non-kimberlitic groups is a potentially useful result and worthy of further work to establish whether this would be reliable in exploration.

High trace amounts of Cr, Zr, and Nb in kimberlitic ilmenite distinguish it from the ilmenites in alkali basalts. This is the most useful result of the study and means that some of the micro-ilmenite grains encountered in exploration programmes can be eliminated as of no interest if trace amounts of Nb, Zr, and Cr cannot be detected in them. A large range of ilmenite grains was included in this study and the results are more reliable than for the other mineral types.

Results on the first two groups of olivine grains were not encouraging and no further work was undertaken. Trace element work on zircon grains was also not encouraging and the expected low uranium levels in kimberlitic zircons relative to non-kimberlitic grains could not be confirmed by the x-ray technique.

The data has been assessed using the DISCRIMINANT procedure of SPSS. Initially the grains of each mineral type were classified as being from kimberlitic or non-kimberlitic rock sources. The DISCRIMINANT procedure was then run for each mineral type using the subsets of the trace element variables, the oxide variables, and a combination of all the variables. The success rates of predicting the rock source of a grain using the trace element variables are in excess of 90% for the suite of garnet and ilmenite grains. Lower success rates occur for the other grains. Success rates of greater than 90% are obtained for chrome diopsides, garnets and ilmenite grains when the subset of oxide variables are used. When the two sets of variables are combined impressive prediction accuracies of 100%, 98% and 100% are obtained for chrome diopside, garnet and ilmenite grains respectively.

The use of x-ray excitation of individual mineral grains within a SEM has revealed significant differences in elemental content. When this data is combined with major and minor elemental data it has been possible to predict for three mineral types whether the grains come from a kimberlitic or non-kimberlitic rock source. It should be emphasised that only a limited number of mineral grains have been analysed. A larger programme of work is desirable in order to determine whether these differences are maintained for these mineral types from all kimberlitic and non-kimberlitic rock sources.

Reference:

- WARE, N.G. 1981. Computer Programs and Calibration with the PIBS Technique for Quantitative Electron Probe Analysis using a Lithium-Drifted Silicon Detector. Computers and Geosciences 7. pp 167-184.

T. R. Marshall

Economic Geology Research Unit, University of the Witwatersrand
Johannesburg, South Africa

Alluvial diamonds are distributed over an extensive area of the western and south-western Transvaal (Fig. 1). Within the region, three major fields are developed : (i) the Lichtenburg-Bakerville Field, developed on the dolomite plain in the north; (ii) the Ventersdorp-Klerksdorp-Potchefstroom Field to the northeast; and (iii) the Christiana-Schweizer-Reneke-Wolmaransstad Field in the southwest. Scattered between and around these fields, as far as Mafikeng, are numerous small and sporadic patches of diamondiferous gravels. The diamond-bearing gravels appear to be confined to the Vaal-Harts interfluvium, the dolomite plain, and the present channels of the Vaal River and its right-bank tributaries, between Potchefstroom and Christiana. The total area embraced is of the order of 25 000 sq. km, having a southwest-northeast length of 300 km, and a maximum width of 170 km. Between 1904 and 1984, a total of 14,4 million carats were recovered from the gravels, valued at R141,6 million (Table I). The average realized value of the diamonds was thus R9,83 per carat. For comparison, the Big Hole of the Kimberley pipe yielded, after 44 years of mining, 14,5 million carats, valued at R100,0 million, and averaging R6,90 per carat. On surface, this pipe measured 490 x 450 m, and covered an area of 0,15 sq. km (15,4 ha). Mining terminated at a depth of 1098 m, after 25,4 million metric tonnes of kimberlite had been excavated.

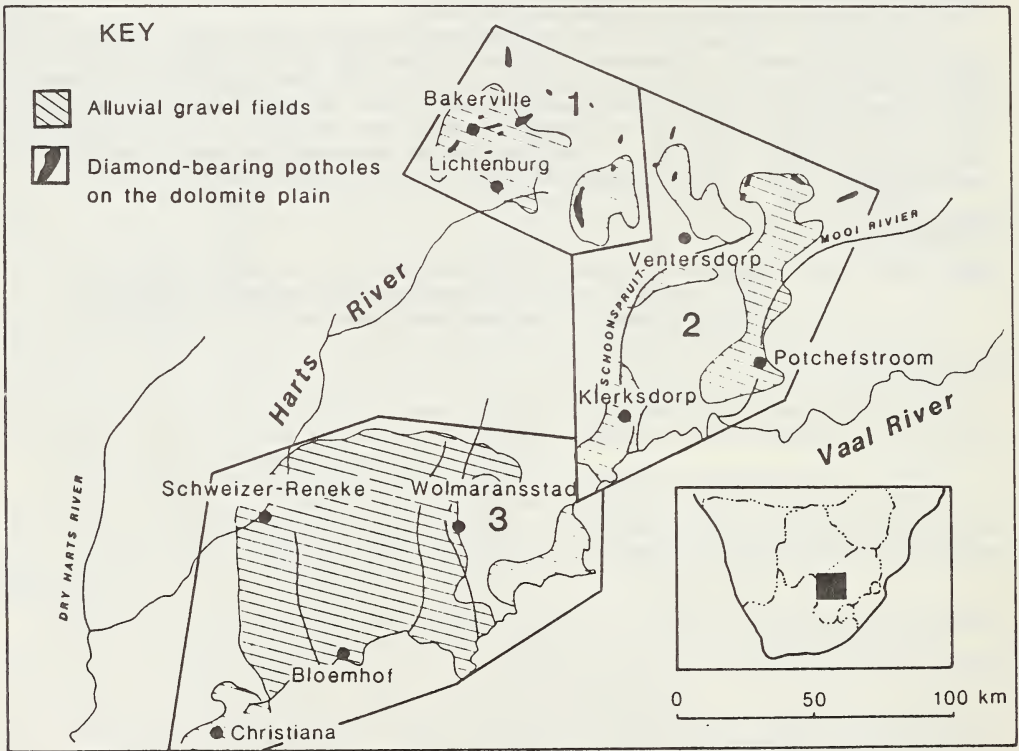


Figure 1 : Locality of the diamond-bearing alluvial gravels of the Western Transvaal, showing the Northern (Bakerville-Lichtenburg) Field (1), the Eastern (Ventersdorp-Potchefstroom-Klerksdorp) Field (2), and the Southern (Christiana-Schweizer-Reneke-Wolmaransstad) Field (3).

TABLE I
ALLUVIAL DIAMOND PRODUCTION (1904-1984)

FIELD	TOTAL PRODUCTION (CARATS)	TOTAL VALUE (RANDS)	AVE. VALUE (R/CARAT)
Lichtenburg-Bakerville (Northern Field)	9 766 224,21	52 185 860	5,34
Christiana-Bloemhof- Wolmaransstad (Southern Field)	1 961 747,74	66 614 577	33,96
Ventersdorp-Klerksdorp- Potchefstroom (Eastern Field) and scattered occurrences	2 674 080,66	22 835 527	8,54
TOTAL	14 402 052,61	141 635 864	9,83

The Gravel Deposits

On the dolomite plain the diamondiferous gravels occur both in potholes and terraces in what appears to be palaeo-river courses (du Toit, 1951). Here, the gravels are dominated by cherty and dolomitic angular detritus, similar to that found on the present-day surrounding deflation surfaces. The diamonds, however, are associated with the rubefied, colluvially-reworked portions of the gravels that contain abundant proportions of mulberry-wash (small manganiferous concretions). In the southern and eastern alluvial fields, the gravels are found on Palaeozoic terraces, on terraces associated with the Tertiary Vaal drainage system, and in and along the present stream channels. The oldest gravels, occurring on exhumed pre-Karoo terraces, represent remnants of original fluvial gravels of a high-competence river (the ancestral-Vaal) and of predominantly colluvial gravels veneered across generally planar segments of the Palaeozoic surface, indicative of a long period of continuing erosion (Helgren, 1979). The younger gravel deposits are confined almost exclusively to the terraces and channels associated with the Quaternary Vaal-Harts drainage lines. These gravels are often highly calcretized, once again indicating extended periods of subaerial exposure. An analysis of the pebbles has indicated that the gravels have been derived from both local and extrabasinal sources (Helgren, 1979) :

(a) material derived from extrabasinal sources includes striated clasts of Waterberg and Transvaal material obviously derived from the northern Transvaal, pebbles from eastern Botswana (found only in the London Run between Schweizer-Reneke and Bloemhof), and fine bedload identical to that found in all rivers which drain the high Lesotho plateaux;

(b) locally, material has been derived from the Karoo rocks (shales and dolerite), from the Ventersdorp lavas, from the reworking of the older gravel deposits, and from the detritus on the dolomite plain; furthermore the nearby Dwyka tillite and dropstone beds have been eroded to produce the extraneously derived, striated Waterberg and Transvaal pebbles mentioned above.

Apart from the small amounts of material emanating from eastern Botswana and the fine bedload originating on the Lesotho highlands, all the other clasts have been eroded from local material. This is also obvious from the sub-angular nature of many of the gravel clasts.

The Diamonds

The Lichtenburg-Bakerville Field, between 1926 and 1984, yielded 9,7 million carats (68 per cent of the alluvial diamonds of the western Transvaal), with an average value of only R5,34 per carat. In contrast, the Southern Field has contributed 14 per cent of the diamonds, but, with an average value of R33,96 per carat, has realized over R66,6 million. This difference may be attributed to the differing nature of the processes responsible for the concentration of the gravels in the two fields and to an abundance of pure, snowy-white brilliant stones and blue-white cleavages found in the Southern Field

(Wagner, 1914). A review of the literature concerning the diamonds themselves indicates that the majority of these are of unknown origin. Some of the diamonds, however, are traceable : the pale green diamonds found only in the Schoonspruit are derived from the Witwatersrand uraniferous conglomerates of the Klerksdorp Goldfield (Wagner, 1914); those diamonds that show distinct signs of glacial attrition were initially transported from the northern Transvaal by the Dwyka glaciers and were subsequently eroded from the tillite deposits (Harger, 1909); and some of the diamonds have been reported as having similar characteristics to those found in the pipes of the Orange Free State (Wagner, 1914).

Discussion

Earlier theories (Stratten, 1979) have hypothesized that the gravels and the associated diamonds were derived from kimberlite intrusions in eastern Botswana and the northwestern and northern Transvaal. However, it has been shown that almost all the gravel is of local origin, and the implication is that the diamonds are as well. Further, studies of erosion surfaces in the area indicate that the Cretaceous landscape was lowered by relatively-humid fluvial processes (accompanied by extensive laterite development), followed by semi-arid deflation and calcretization of the subsequently formed mid-Tertiary erosion surfaces. Under such circumstances the dominant surface processes would lower the surface vertically, allowing any gravels to accrue as lag accumulation. Structural studies in progress (D.A. Pretorius, pers. comm., 1986) show that the exposed basement granite between Lichtenburg and Wolmaransstad is the result of a structural culmination. On the northeastwards extension of the upwarp axis occur the diamondiferous kimberlites of Swartruggens and the Pilanesberg and, on the south-westward extension, the fissures and pipes of Barkly West and Kimberley. It is suggested that other diamond-bearing kimberlites were emplaced along the upwarp between Swartruggens and Barkly West (along the Vaal-Harts interfluvium) and the accentuated uplift of the structural culmination in this area led to the complete erosion of these bodies. The extended period of erosion that followed allowed for the development of the lateritic horizons and the destruction of the pyrope garnets and other kimberlitic indicator minerals that are obviously lacking in the gravel deposits and soil profiles today. Later reactivation of the structural culmination resulted in the reworking of the older gravel deposits into the Pliocene-to-Recent stream channels adjacent to the palaeotopographic high, and in the depression of the lateritized surface both to the north (Kalahari basin) and to the south (western Orange Free State) of it.

Morphotectonic analysis of the mid-Tertiary landscape in the Orange Free State indicates that it was drained by a large, east-west flowing river, situated to the north of Kimberley. The gravels of this river have been downwarped, along with its associated erosion surface, and are buried beneath cultivated farmlands. It is suggested that the gravels of this river were derived from the same deflation surface as gave rise to the diamondiferous deposits of the western Transvaal and, therefore, should contain the same basal, diamond-bearing, older gravel units.

The new model that is thus proposed for the development of the alluvial diamondiferous gravels of the western Transvaal suggests that the source of the diamonds was kimberlite intruded into the area now underlain by the gravels and that the optimum concentration of the alluvial diamonds is a product of maximum tectonic uplift and the consequent erosion of *in situ* diamondiferous kimberlites.

References

- DU TOIT A.L. 1951. The diamondiferous gravels of Lichtenburg. Geological Survey of South Africa Memoir 44, 58 pp.
- HARGER H.S. 1909. The occurrence of diamonds in Dwyka conglomerate and amygdaloidal lavas; and the origin of the Vaal River diamonds. Transactions of the Geological Society of South Africa, XII, 139-158.
- HELGREN D.M. 1979. River of Diamonds. Univ. Chicago. Dept. Geog. Res. Paper 185, 399 pp.
- STRATTEN T. 1979. The origin of the diamondiferous gravels of the Southwestern Transvaal. Geological Society of South Africa Special Publication 6, 219-228.
- WAGNER P.A. 1914. The Diamond Fields of South Africa. The Transvaal Leader, Johannesburg, 347 pp.

THE EFFICIENCY OF FLUVIAL TRAP SITES TO CONCENTRATE KIMBERLITIC MINERALS: AN EXPERIMENTAL SAMPLING PROGRAMME

M. T. Muggerridge

Department of Geology, University of Western Australia, Nedlands, WA 6009, Australia

The selection of optimum river-bed trap sites for heavy minerals associated with kimberlites, lamproites or other potential diamond host rocks is based largely on theoretical predictions about fluvial processes, combined with cumulative prospecting experience spanning several decades. There is relatively little published information on heavy-mineral distribution within the fluvial environment, and a particular paucity of data relating specifically to diamond-indicator minerals. This paper discusses a small-scale experiment carried out to test the validity of traditional stream-gravel sampling methods used for diamond prospecting.

A sampling location was selected in the Kimberley Region of Western Australia (Fig. 1). Apart from the highly diamondiferous Argyle lamproite (AK1), this Region hosts a large range of other lamproites, some also diamondiferous, as well as a few, mainly barren, kimberlites. A comprehensive network of rivers, active on a seasonal basis, cuts the central craton and its flanking mobile zones, generally providing excellent conditions for stream-sampling operations. Within this environment there were a number of constraints on the selection of the location for the experiment. It was essential to choose a river site where gravels would yield a sufficient quantity of kimberlitic indicator minerals to permit a viable statistical study of their distribution. Moreover, it was important to conduct the experiment within a restricted length of river to minimize bias in results caused by variations in the creek load and distance from the kimberlitic source(s). The test locality had also to include a variety of stream-bed environments to provide a suitable range of trap sites. The location chosen on the Wilson River (16°49'S, 127°50'E) embraces the abovementioned criteria. Previous sampling during regional exploration had indicated moderate quantities of picroilmenite and traces of pyrope-garnet in the gravels at this point. The Devils Elbow kimberlite dykes of the East Kimberley Kimberlite Province lie around 15 kilometres upstream.

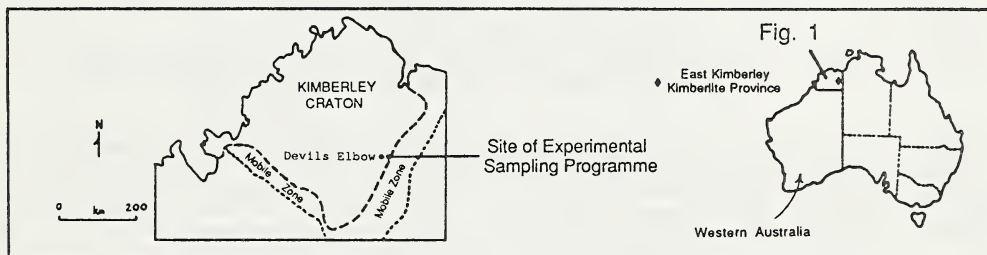


Fig. 1 Sampling Location: Kimberley Region, Western Australia

Twelve samples were collected from sites up to 200 metres apart, but generally much closer. Each site was classified in the field into one of five categories, from "good" through to "poor", based on a set of standard river-bed conditions for assessing the quality of a diamond prospecting sample (Fig. 2). All samples initially had the same volume (equivalent to 10.8 ± 0.2 litres) and consisted of the minus 4 millimetre fraction screened on site. Sample weights, and volumes in the later processing stages, of the heavy-mineral fractions were recorded during the successive steps of laboratory processing in order to monitor relative weights and increasing sample densities during heavy-mineral concentration to achieve final densities exceeding 2.95. Table 1a shows, for each sample, the initial field-assessed trap-site ratings, and the results for each stage of laboratory processing, listed in sample-number sequence. Final ratings, based on the number of picroilmenite grains present in each sample, are also shown. Studies of final heavy-mineral concentrates provided counts of kimberlitic indicator-mineral grains and percentage estimates of phases occurring in the accompanying detrital suite.

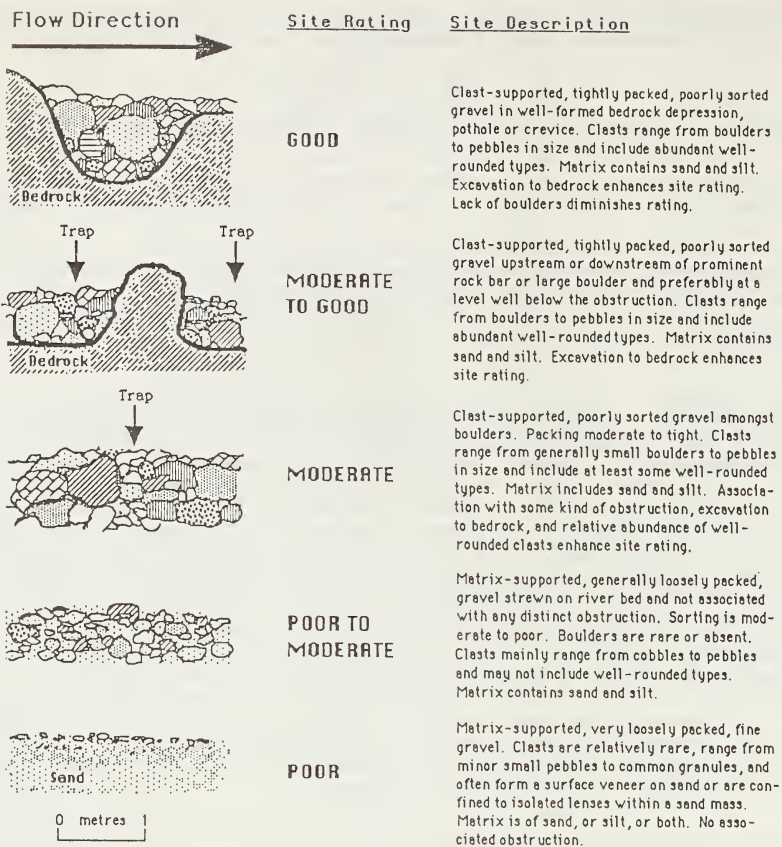


Fig. 2 Broad Field Classification of Heavy-Mineral Trap Sites. Diagrams are of River-Bed Cross Sections Parallel to Main Water Flow Direction.

Table 1b contains a brief description of each trap site, with samples listed in sequence of declining initial trap-site ratings. Their corresponding amended ratings, based on microilmenite grain counts, are also shown. Although there are some interesting exceptions, the results show that field site-ratings based on conventional concepts are reasonably accurate. There is strong evidence to show that the commonly adopted traditional practice of sampling the deepest part of the main, active flow-channel is of prime importance. A common belief when collecting uniform-size diamond prospecting samples is that relatively heavy ones, assuming all wet or all dry conditions, signify the best traps. The results in Table 1c, listed according to diminishing final site ratings, demonstrate this concept to be very misleading. In this experiment, the initially least dense samples generally became the most dense after heavy-mineral concentration, and tend to correlate with the more effective trap sites. Where poor sampling conditions prevail, choice is often restricted to a sample site located by a midstream obstacle, such as a rock bar or tree trunk, and a trap amongst loose, extremely fine gravel (less than 1 cm diameter) strewn on the river-bed surface with no nearby obstruction. The results suggest that the former is more likely to trap kimberlitic minerals, even if the site has no obvious gravel. A study of the distribution of heavy minerals in different grain size-fractions provides further insight into the most favourable conditions for trapping kimberlitic species.

In summary, mineralogical information derived from a set of experimental, diamond-prospecting samples, combined with detailed descriptions, including observations of sorting and packing, of their river-bed locations provide a basis for reviewing trap-site selection for kimberlitic indicator minerals.

Table 1a Laboratory Processing Results

SN	Field	A	IW	B	ID	C	WT	D	W2	E	WF	F	TB	G	FD	H	NP	I	Final
1	GOOD	2	23.8	9	2.2	9	7.5	3	4.0	2	1.7	4	74.2	11	3.7	5	25	4	MODERATE TO GOOD
2	MODERATE TO GOOD	3	22.0	11	2.0	11	6.3	8	4.0	2	2.0	2	229.4	3	3.9	2	43	3	MODERATE TO GOOD
3	MODERATE TO GOOD	5	19.7	12	1.8	12	3.3	12	1.6	12	0.9	6	155.0	4	4.1	1	47	2	MODERATE TO GOOD
4	GOOD	1	27.0	7	2.5	7	5.1	8	1.7	8	0.8	7	95.6	7	3.8	4	59	1	GOOD
5	MODERATE	6	23.3	10	2.2	9	6.9	4	3.5	5	1.7	4	95.5	8	3.2	11	4	6	POOR TO MODERATE
6	POOR TO MODERATE	8	30.4	5	2.8	3	4.3	9	1.7	8	0.7	8	81.2	10	3.6	7	4	8	POOR TO MODERATE
7	POOR	11	30.0	6	2.8	3	8.4	2	6.5	1	3.9	1	112.4	6	3.1	12	0	12	POOR
8	POOR	10	31.9	1	2.9	1	4.2	10	1.7	8	0.7	8	89.7	9	3.4	10	2	10	POOR
9	POOR TO MODERATE	9	30.6	4	2.8	3	6.1	7	4.0	2	1.3	5	279.9	2	3.5	8	4	6	POOR TO MODERATE
10	MODERATE TO GOOD	4	31.0	2	2.9	1	3.9	11	1.7	8	0.8	7	115.3	5	3.9	2	3	9	POOR TO MODERATE
11	MODERATE	7	24.7	8	2.3	8	6.4	5	2.7	7	1.9	3	351.7	1	3.5	8	18	5	MODERATE
12	POOR	12	30.8	3	2.8	3	8.8	1	3.5	5	0.8	7	72.8	12	3.7	5	1	11	POOR

Table 1c Sample Density Comparisons

SN	Final	I	IW	B	ID	C	FD	H
4	GOOD	1	27.0	7	2.5	7	3.8	4
3	MODERATE TO GOOD	2	19.7	12	1.8	12	4.1	1
2	MODERATE TO GOOD	3	22.0	11	2.0	11	3.9	2
1	MODERATE TO GOOD	4	23.8	9	2.2	9	3.7	5
11	MODERATE	5	24.7	8	2.3	8	3.5	8
5	POOR TO MODERATE	6	23.3	10	2.2	9	3.2	11
9	POOR TO MODERATE	8	30.6	4	2.8	3	3.5	8
6	POOR TO MODERATE	8	30.4	5	2.8	3	3.6	7
10	POOR TO MODERATE	9	31.0	2	2.9	1	3.9	2
8	POOR	10	31.9	1	2.9	1	3.4	10
12	POOR	11	30.8	3	2.8	3	3.7	5
7	POOR	12	30.0	6	2.8	3	3.1	12

Table 1b Sample Trap-Site Ratings and Descriptions

SN	Field	A	Description	% BP	X	NP	I	Final
4	Good	1	Very tightly packed, poorly sorted gravel amongst large local granitic boulders near rock outcrop. Site at deepest point in main channel. Bedrock reached during excavation and sample material removed to this depth. Sample sites Nos 1-3 a few metres away.	85	1	59	1	Good
1	Good	2	Tightly packed, poorly sorted gravel amongst local granitic boulders and bedrock. Deep point in main channel. Fairly high mud content at base probably reflects bedrock weathering. Bedrock reached and sample material removed to this depth. Sample sites Nos 2-4 a few metres away.	85	1	25	4	Moderate to Good
2	Moderate to Good	3	Similar to sample No.1, but site amongst boulders only (no bedrock). Bedrock not reached during excavation. Sample sites Nos 1, 3 and 4 a few metres away.	85	1	43	3	Moderate to Good
10	Moderate to Good	4	Good wedge-shaped trap on downstream side of small rock bar. Loose sand only on top but, below this, poorly sorted, fairly tightly packed gravel. Fairly low point in main channel but not as low as site for No. 4. Bedrock reached and sample excavated to this depth.	75	5	3	9	Poor to Moderate
3	Moderate to Good	5	Same type of site as No. 2 but at deeper point in main channel. Tree roots also present. Bedrock not reached during excavation but suspected close due to relative position and excavation depth of nearby sample site No.1, and increase of clay towards bottom of hole.	85	1	47	2	Moderate to Good
5	Moderate	6	Site near the northern bank approaching or in flood-level zone at much higher level than site Nos 1-4. Rather loosely packed, poorly sorted gravel of pebbles and cobbles up to 10 cm diameter in good wedge-shaped bedrock trap. Sample hole very deep, but bedrock not reached.	65	6	4	6	Poor to Moderate
11	Moderate	7	Similar to site No. 9 but material more tightly packed, amongst a few boulders. Site at a fairly low point in main channel. Packing in trap became tighter with depth of sample hole. Bedrock not reached during excavation.	60	7	18	5	Moderate
6	Poor to Moderate	8	Site a few metres away from that of No. 5 at same height near or at flood level. A small saucer-shaped bedrock trap with very loosely packed pebble gravel, clasts up to 3 cm diameter, mainly 1 cm or less. Sample hole closely approached, but did not reach, bedrock.	50	8	4	6	Poor to Moderate
9	Poor to Moderate	9	Site on downstream side of bouldery area consisting of large local granitic boulders and bedrock. No distinct trap at site. Sample consisted of essentially matrix-supported gravel with very loosely packed pebbles up to 6 cm diameter, mainly 2-3 cm. Bedrock not reached during excavation.	45	9	4	6	Poor to Moderate
8	Poor	10	Similar to site No. 7 but gravel coarser, up to 1 cm diameter. Sampled material consisted of a thin surface scrape of fine, matrix-supported gravel overlying sand in a mini-channel. Gravel not present in sand below about 1 cm from surface. Bedrock not reached during excavation.	8	10	2	10	Poor
7	Poor	11	No trap. Sampled material consisted of a thin surface scrape of fine, matrix-supported gravel (granules up to 3mm diameter) overlying sand near prominent bend in river. Site fairly low in main channel. Sand contains some granules to 3 cm depth. Bedrock not reached during excavation.	5	11	0	12	Poor
12	Poor	12	Small, wedge-shaped bedrock trapon downstream side and at base of steep outcrop. Material at site almost entirely sand with rare granules, chiefly granitic (derived locally). Possibly material would become coarser below surface sand. Bedrock not reached during excavation.	1	12	1	11	Poor

Abbreviations

SN	Sample number	F	Index for WF: Heaviest of the 2 - 0.4 mm HM fractions (1) to lightest (12)
Field	Field trap-site ratings (Initial ratings) based on standard assessment criteria	TB	Weight (g) of ~ 2 mm HM fraction ("sinks") after immersion in tetrabromoethane (TBE): TBE density = 2.95.
A	Index for Field: Best Initial rating (1) to worst (12)	G	Index for TB: Heaviest of the HM TBE "sinks" fractions (1) to lightest (12)
IW	Initial dry sample weight (kg)	FD	Final density, of the HM TBE "sinks" fraction.
B	Index for IW: Initially heaviest sample (1) to lightest (12)	H	Index for FD: Most dense of the "sinks" fractions (1) to least dense (12)
ID	Initial density (based on standard initial sample volume of 10.8 litres)	NP	Number of picrolimnetic grains recovered from 2 - 0.4 mm HM TBE "sinks" fraction: This determines the revised trap-site ratings ("Final").
C	Index for ID: Initially most dense (1) to least dense (12)	I	Index for NP: Greatest number of picrolimnetic grains (1) to smallest (12)
WT	Weight (kg) of heavy-mineral (HM) fraction after Wilfley Tabling	Final	Revised trap-site ratings based on number of picrolimnetic grains in 2 - 0.4 mm HM TBE "sinks" fraction.
D	Index for WT: Heaviest after Wilfley Tabling (1) to lightest (12)	% BP	In situ field estimate of percentage of gravel (including boulders) to sand in trap-site.
W2	Weight (kg) of minus 2 mm HM fraction after Wilfley Tabling	X	Index for % BP: Highest percentage of gravel (1) to lowest (12)
E	Index for W2: Heaviest of the minus 2 mm HM fractions (1) to lightest (12)		
WF	Weight (kg) of 2 - 0.4 mm HM fraction after Wilfley Tabling; Fraction used for subsequent studies.		

PROSPECTIVE RELATIONSHIPS BETWEEN DIAMONDS,
VOLCANISM AND TECTONISM IN AUSTRALIA

F.L. Sutherland,¹ L.R. Raynor,² J.D. Hollis,¹ P.A. Temby.³

1. Division of Earth Sciences, The Australian Museum, 6-8 College St., Sydney, Australia. 2000.
2. Dept. of Geology & Geophysics, University of Sydney, Sydney, Australia. 2007.
3. Blue Circle Southern Cement, P.O. Box 1571, Sydney, Australia. 2001.

There are several regional occurrences of diamonds across Australia (Jaques et al. 1984). These include:-

- a) an eastern highlands Palaeozoic-orogenic belt, where there was considerable Mesozoic-Cainozoic volcanism.
- b) central epicratonic belts, associated with Mesozoic kimberlites and kimberlitic lamprophyres.
- c) western-northern cratons, characterised by leucite lamproites and kimberlitic lamproites of several ages (Precambrian-Tertiary).

Other occurrences, mostly detrital, have unproven provenance (e.g. in Tertiary gravels, Nullagine, W.A.; Triassic conglomerates, S.A. and fields strewn across northern Australia).

HOSTS AND SOURCES

Confirmed diamond hosts are diverse and some are unusual. Direct evidence for the eastern hosts is scarce, but diamonds are known from Mesozoic (?) tholeiitic dykes (Copeton) and also appear to be derived from a Tertiary nepheline mugearite intrusion near Walcha (Sutherland et al. 1985). Alluvial 'kimberlitic' zircons (low U, 21ppm) giving early Tertiary-late Cretaceous fission track ages (41-66 Ma) are present in some eastern gemfields (New England, Anakie).

Diamond distribution in eastern Australia can be viewed as a 'background' of low concentrations on which is superimposed some restricted regions of 'anomalous' higher concentrations. Some of the background diamonds may be recycled from Palaeozoic sediments of the Lachlan Fold Belt, as studies show a dominance of northerly current directions in these beds, with possible derivation of large amounts of sediments from Antarctica. If these diamonds came from Antarctica or other adjacent cratons, they should be able to survive to or beyond upper greenschist facies (c.400°C, 2-10kb) typical of this fold belt. However, this model is incapable of accounting for the more concentrated diamond 'anomalies' whose specific features and preservation of detail suggest local sources (Copeton, Bingara, Cudgewong, Beechworth).

The Copeton and Walcha diamonds are unusual in their inclusions (grossular garnet, abundant coesite) and anomalously heavy C isotope compositions (Sobolev 1984 and pers.comm.), in keeping with an orogenic 'subduction' source.

REGIONAL SETTING

The occurrences of Australian diamonds can be examined in relation to intraplate volcanism and tectonism (Sutherland, 1985). Migration patterns appear to characterise much of the late Mesozoic-Cainozoic and possibly late Palaeozoic-early Mesozoic volcanism. This migration offers important clues in targetting potential diamondiferous areas; its features are:-

- 1) migrations are irregularly spaced in place and time,
- 2) they seem to originate from rift-spreading zones,
- 3) episodes within them tend to be localised on structural weaknesses,
- 4) individually they commonly show an overall decay in volcanic intensity with time,
- 5) regions of multiple migrations typically record high palaeogeotherms in mantle/lower crustal xenoliths,

- 6) migrations show variations in parental alkaline magmas which reflect underlying mantle heterogeneity,
- 7) migrations seems to add metasomatic elements to the mantle,
- 8) peaks in the migrational activity appear to coincide with periods of maximal regional tension.

Certain combinations of these factors may generate deep undersaturated volatile-rich magmas capable of transporting diamonds from 'diamond windows' (Nickel and Green, 1985) or from 'kimberlitic' material introduced into higher mantle levels. Conditions favouring diamond transport in one region, may be unfavourable in another region at any one time.

PROSPECTIVE CONDITIONS

The rift-spreading hot spot model proposed for much of the late Palaeozoic to Cainozoic volcanism in Australia would favour ascent of diamondiferous undersaturated magmas,

- a) over small weak hot spots,
- b) during initial or dying stages of stronger hot spots,
- c) within periods of cooler geotherms between migrations over hot spots,
- d) in later migrations, over mantle metasomatized by earlier migrations,
- e) in traverses of mantle metasomatized by old events, including subduction.

Hot spot traces, sometimes changing direction, can be traced on the Australian continent for periods of up to 65-150 Ma. These provide a variability of conditions, which could yield some discrete diamondiferous eruptions. Changes in Australia's plate speed over hot spots may also play a role in production of kimberlitic magmas and diamond transport.

Indications are that particular periods in the cratonic areas provide better prospects for economic diamond deposits than in the younger orogenic belts. Certain periods of activity and places that offer more potential for diamond exploration can be suggested. These would avoid peaks of multiple volcanic/intrusive episodes, which maintain hot geotherms for extended periods (Griffin et al. 1986).

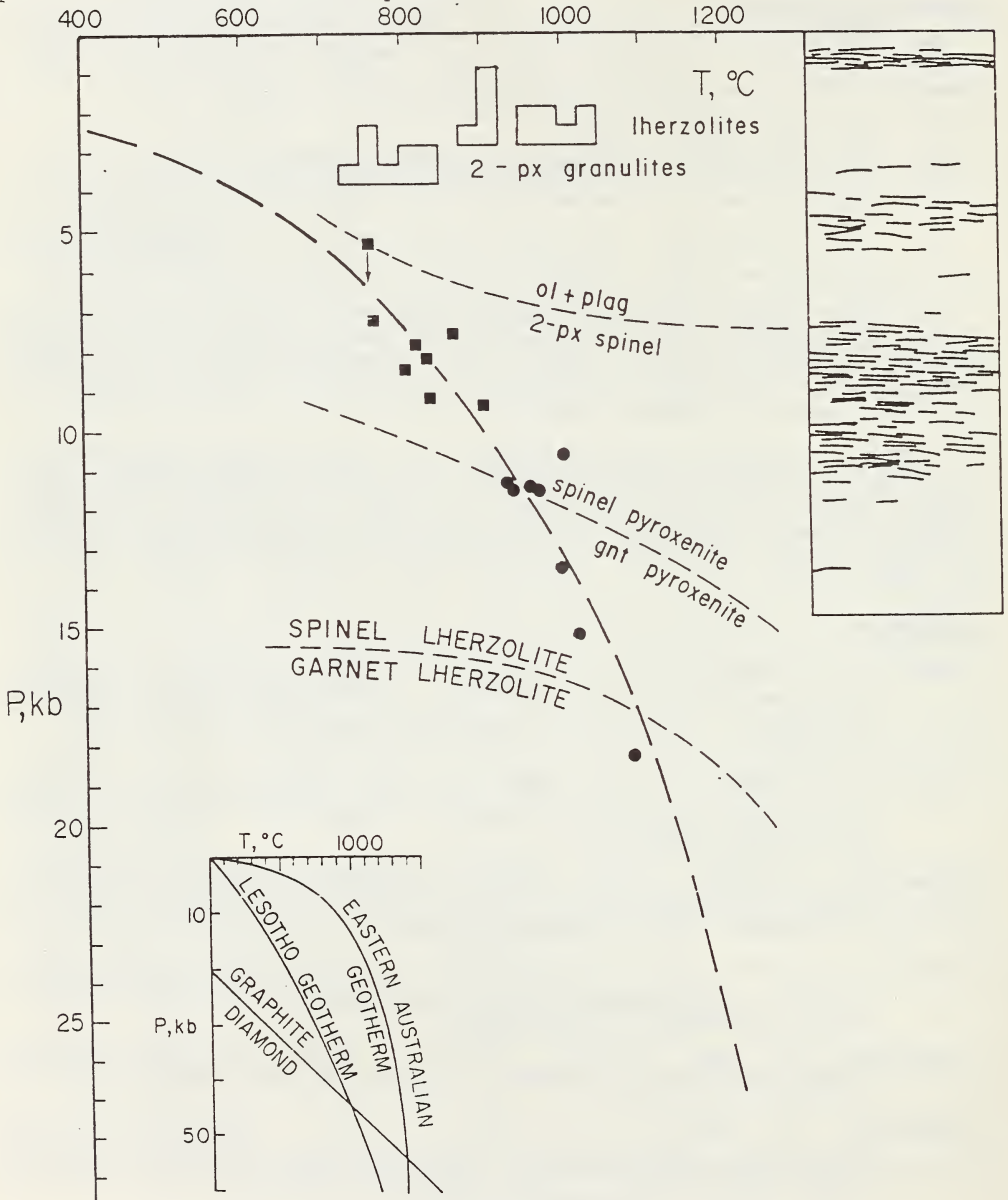
REFERENCES

- GRIFFIN, W.L., SUTHERLAND, F.L. and HOLLIS, J.D. 1986. The crust-mantle transition beneath east-central Queensland: Correlation of xenolith petrology and seismic data. Journal of Volcanology and Geothermal Research, in submission.
- JAQUES, A.L., FERGUSON, J. and SMITH, C.B. 1984. Kimberlites in Australia. Publications of the Geology Department and University Extension, University of Western Australia 8, 227-274.
- NICKEL, K.G. and GREEN, D.H. 1985. Empirical geothermobarometry for garnet peridotites and implications for the nature of the lithosphere, kimberlites and diamonds. Earth and Planetary Science Letters 73, 158-170.
- SOBOLEV, N.V. 1984. Crystalline inclusions in diamonds from New South Wales, Australia. Publications of the Geology Department and University Extension, University of Western Australia 8, 213-226.
- SUTHERLAND, F.L. 1985. Regional controls in eastern Australian volcanism. Publications of the Geological Society of Australia, NSW Division 1, 13-32.
- SUTHERLAND, F.L., HOLLIS, J.D. and RAYNOR, L.R. 1985. Diamonds from nepheline mugearite? A discussion of 'Garnet websterites and associated ultramafic inclusions from a nepheline mugearite in the Walcha area, New South Wales, Australia' Mineralogical Magazine 49, 748-751.

Figure

Typical geotherm for eastern Australia (Griffin et al. 1986), constructed from P,T data derived from lower crustal-upper mantle xenoliths in regions of multiple basaltic volcanism (35-55 Ma to present). The geotherm is based on garnet granulites (squares) and garnet websterites (dots) and the histograms (boxes) represent T determinations on granulites and spinel lherzolites. The seismic crust-mantle profile (vertical rectangle) is scaled to a depth of 48 km, in equivalence to the pressure scale. The relationships of the hot Australian geotherm to the Lesotho African geotherm and diamond/graphite stability fields is shown in inset.

Note that time-space domain associated with such a geotherm has little potential for diamond transport, but that domains of restricted volcanism interspersed with or outside them have potential.



**GEOLOGICAL SOCIETY OF AUSTRALIA
(W.A. DIVISION)
SPECIAL INVITED LECTURE**

**The constitution and evolution of the mantle
A.E. Ringwood**

**Professor Ringwood's lecture will be delivered on
11 August 1986 at a special meeting of the Western
Australian Division of the Geological Society of
Australia, held in conjunction with the Fourth
International Kimberlite Conference.**

THE UNIVERSITY OF CHICAGO
DEPARTMENT OF CHEMISTRY

PHYSICAL CHEMISTRY
LECTURE NOTES

BY
PROFESSOR [Name]

CHICAGO, ILLINOIS
19[Year]

A.E. Ringwood

Australian National University

COMPOSITION

The bulk chemical composition of the upper mantle beneath the ocean basins can be estimated on the basis of petrological relationships between various classes of basaltic magmas and residual peridotites, interpreted in the light of geochemical and experimental petrology data. Several techniques of deriving this composition, 'pyrolite', have been employed. These include the complementary relationships between MORBs, komatiites and their residual harzburgites and dunites. Another approach is based upon the recognition of particular peridotites which have experienced only minor losses of magmatic liquids and which remain geochemically fertile in their capacity to produce basaltic magmas by more advanced degrees of partial melting.

Estimates of the pyrolite composition obtained by these methods are in good agreement. They are characterized by near-chondritic ratios of many lithophile involatile elements such as Ca, Al, Ti, Zr, Hf, Sc, Y, heavy and intermediate REE. Highly incompatible elements such as light REE, U, Th, and Ba are substantially depleted compared to chondritic abundances. These depletions are believed to have arisen via the extraction from pyrolite throughout geological time of small amounts of highly alkalic liquids strongly enriched in incompatible elements. It seems possible that at an early stage of the Earth's history, these incompatible elements were originally present in pyrolite in chondritic relative abundances. The pyrolite composition in turn can be related to the primordial abundances of elements as displayed by Cl chondrites, via processes which involve loss of volatiles and partial reduction of oxidised iron and nickel to the metallic state. Significant amounts of silica must also be removed in order to preserve this close relationship. Alternative interpretations propose that silica was removed as a volatile species in the solar nebula prior to accretion, or that the silica deficit in the upper mantle is compensated by excess silica in the lower mantle, so that the Mg/Si ratio of the bulk mantle is similar to that of Cl chondrites.

The pyrolite bulk composition prevails in the upper mantle beneath ocean basins. However the upper mantle layer immediately underlying stable continental regions differs from pyrolite in several important respects. Its composition is obtained from analyses of mantle xenoliths brought to the surface in kimberlites and alkali basalts and is characterised by marked depletions in Ca, Al, Na and Fe as compared to pyrolite. These depletions were caused by previous extraction of basaltic magmas. The distribution of incompatible elements in this layer is extremely heterogeneous, testifying to a complex, multi-stage history of prior melt extractions, melt additions and metasomatism. Many localised regions are enriched in incompatible elements and are capable of yielding specialised varieties of basaltic magmas when subjected to small degrees of partial melting. The sub-continental mantle is significantly less dense than pyrolite under equivalent P,T conditions and hence is gravitationally stabilized, forming a long-lived chemical boundary layer. The thickness of this layer varies widely, but probably extends at least to 200 km in some regions. When continents and sub-continental lithosphere are rifted to form new ocean basins, MORB basalts are erupted along the new oceanic ridges, strongly implying that upper mantle of pyrolite composition extends continuously beneath the 'depleted' sub-continental chemical boundary layer.

The copious volumes of MORBs and komatiites which have been erupted during and since the Archaean implies that the pyrolite composition has predominated in basaltic source regions of the upper mantle throughout geological time. The near-chondritic ratios of many involatile lithophile elements in pyrolite provide an important boundary condition for geochemical earth models and place severe limitations upon hypotheses which invoke large-scale melting of the mantle early in the Earth's history. If large-scale melting did occur, subsequent mixing processes via solid state convection must have been extraordinarily effective in re-establishing the degree of homogeneity

in pyrolite (over scales of a few kilometers) which is recognized today. Recent high pressure experiments have shown that the temperature interval between the solidus and liquidus of pyrolite narrows considerably at pressures of 12-15 GPa. This has been interpreted to imply that upper mantle pyrolite was itself produced by partial melting of more primitive material at greater depths. However, the thermodynamic basis for this inference is non-unique. Experimental studies show that majorite garnet would be the principal residual phase in the source region where partial melting is inferred to have occurred (400-600 km). This would probably have caused substantial relative fractionations of Ca, Al, Ti, Zr, Sc and heavy REE to a degree which makes it very difficult to explain the near-chondritic relative abundances of these elements in pyrolite.

CONSTITUTION

The phase transformations which are experienced by pyrolite and other relevant mantle compositions such as harzburgite and eclogite are reviewed in some detail. The olivine component of pyrolite transforms sharply to the $\beta\text{-Mg}_2\text{SiO}_4$ structure near 400 km, whilst pyroxene dissolves in the garnet structure over a broad interval between 350-450 km. At a depth of about 550 km, the beta phase transforms to spinel and so the stable mineral assemblage between 550-670 km consists of spinel + garnet. Near 670 km, spinel disproportionates to MgSiO_3 , perovskite + magnesiowüstite, whilst the transformation of garnet, mainly to perovskite-related phases, occurs over a broad depth interval between 650-750 km. The phase transformations experienced by harzburgite between 500-670 km are substantially different to those of pyrolite because of the lower Ca and Al contents of harzburgite. These differences have significant geodynamic implications and are discussed later. Basaltic compositions transform successively from basalt/amphibolite to eclogite to garnetite and finally to perovskitite. Recent experimental data show that the transition of eclogite to garnetite is complete by 450 km and contradict arguments that the mantle between 450-600 km is composed of 'piclogite'.

Despite many decades of effort by seismologists, appreciable uncertainties remain in the distributions of P and S wave velocities with depth. It is important that these uncertainties be considered when attempts are made to use seismic velocity distributions as constraints on petrological models. There is a clearly-defined low velocity zone beneath ocean basins, extending approximately from 70-150 km, which is widely attributed to the occurrence of a small degree of partial melting. A less well-defined low velocity zone for S waves can be recognised beneath stable continental regions. Some but not all sub-continental profiles show evidence for a sharp increase of velocity near 200 km which is difficult to explain in terms of known phase changes or plausible changes in chemistry and mineralogy. It is possible that the "200 km discontinuity" is caused by a high degree of velocity-anisotropy in a layer near this depth, which may mark a zone where the sub-continental tectosphere is mechanically decoupled from underlying mantle.

Seismic profiles display large velocity discontinuities at depths near 400 and 670 km. The capacity of pyrolite and related compositions to explain the seismic velocity distributions is examined below. The transition of olivine and pyroxene to $\beta\text{-Mg}_2\text{SiO}_4$ plus garnet provides a quantitative explanation of the velocity changes associated with the 400 km discontinuity within the limits of error of the seismic velocity determinations. Likewise, seismic velocities in the region between 400-670 km are consistent with this region being of pyrolite composition and crystallizing as an assemblage of $\beta, \gamma(\text{Mg, Fe})_2\text{SiO}_4$, spinel + garnet. The depth of the 670 km seismic discontinuity corresponds closely to the pressure at which spinel disproportionates to MgSiO_3 , perovskite plus $(\text{Mg, Fe})\text{O}$ magnesiowüstite. Considerable controversy exists as to whether this transformation, together with a related transformation of garnet to perovskite, is capable of providing an adequate explanation of the 670 km discontinuity and the properties of the lower mantle, or whether in addition, a major change in chemical composition occurs at this depth, e.g. an increase in SiO_2 and a decrease in FeO . Recent experimental data have shown that the spinel to perovskite plus magnesiowüstite transformation is sharper than previously realized and is probably capable of explaining the sharpness of the 670 km discontinuity. Moreover the elastic properties and density of the lower mantle are readily explained within their observational uncertainties by a pyrolite composition crystallizing as an assemblage of perovskites plus magnesiowüstite.

It is concluded that a substantial change in chemical composition at the 670 km discontinuity is neither required nor implied by available geophysical data. Whilst a substantial change in chemical composition cannot be excluded, it would represent a somewhat arbitrary assumption. An essentially isochemical interpretation of the 670 km discontinuity is favoured by other sources of evidence, which, whilst not compelling, are nevertheless strongly suggestive. These include (1) the close geochemical relationship of upper mantle pyrolite to a chondrite-derived composition suggests that the pyrolite composition is essentially primitive and is unlikely to have been formed by differentiation of even more primitive parental material in the lower mantle, (2) recent seismic evidence suggests that subducted slabs may penetrate deeply below the 670 km discontinuity to an extent which implies continuing and extensive interchange of material between upper and lower mantle, (3) it would be highly coincidental for the depth of a gross change in mantle chemical composition to be identical with the depth of which $(\text{Mg,Fe})_2\text{SiO}_4$ spinel happens to transform to perovskite plus magnesiowüstite.

GEOCHEMICAL AND DYNAMICAL EVOLUTION

The geochemical evolution and dynamical behaviour of the mantle are strongly influenced by the petrological differentiation of pyrolite at mid-oceanic spreading centres to form new oceanic lithosphere. This consists of a basaltic crust underlain by harzburgite and further underlain by pyrolite which has experienced depletion only of highly incompatible elements. When this differentiated lithosphere is ultimately consumed at trenches, the gravitational body forces driving subduction are concentrated mainly in the upper cool, dense and brittle layers of basalt and harzburgite. The density contrast between the lower layer of depleted pyrolite and surrounding mantle is small and so this layer experiences a correspondingly small body force. Because of its relatively ductile nature, depleted pyrolite is continually eroded from the base of the sinking plate and resorbed into the convective system which circulates within the upper mantle. Mixing of depleted pyrolite into the upper mantle generates source regions for mid-oceanic (MORB) basalts which are produced during subsequent partial melting episodes. Chemical and isotopic characteristics of MORB's can be explained on the basis of this model.

The slab which sinks to the 670 km seismic discontinuity is comprised mainly of former basalt and harzburgite. These differentiated layers undergo a significantly different series of phase transformations to those experienced by mantle pyrolite. Former basaltic crust remains $0.1 - 0.2 \text{ g/cm}^3$ denser than surrounding pyrolite above and below the discontinuity. However former harzburgite becomes appreciably buoyant relative to pyrolite below 670 km. As a result of this inhomogeneous density distribution, a bending couple is applied to the tip of the slab at 670 km, causing it to buckle. This process is magnified by the high viscosity in the slab arising from its lower temperature than surrounding mantle. In consequence, the descending slab piles up and forms a large melange or "megalith" of mixed, former harzburgite and oceanic crust. The megalith has a mean density similar to surrounding mantle below 670 km and accumulates as an ovoid body in the lower mantle, beneath the intersection of the slab with the 670 km discontinuity. Its cross-sectional dimensions may exceed 500 km.

BASALT PETROGENESIS

The integrity of the megalith is maintained initially by its high viscosity relative to surrounding mantle. However, after the cessation of subduction, on timescales exceeding 10^8 y., conduction of heat from the surrounding mantle raises the temperatures of the outer shell of the megalith. Partial melting of entrained oceanic crust ensues. The resultant liquids extract incompatible elements from the former crust and react with former harzburgite, causing the latter to become fertile in the sense of its future capacity to produce basaltic magmas. With further heating, the viscosity of the outer shell of the megalith is reduced and large blocks of former oceanic crust (now depleted in incompatible elements by partial melting) sink into the lower mantle. Newly fertile, thermally equilibrated, former harzburgite is now buoyant relative to the lower mantle, and flows upwards, spreading out to form a layer at depths of 500-670 km, which is gravitationally stable. After an extended residence time in this layer (0.5 - 2.0 b.y.), diapirs of fertilized former harzburgite ascend into the upper mantle. Large diapirs rise comparatively rapidly and experience small

degrees of partial melting to produce alkalic, and in some cases, 'enriched' tholeiitic magmas. These diapirs possess sufficient energy to penetrate the lithosphere and are responsible for intraplate hot-spots beneath oceans and continents, with their associated volcanism. Small diapirs of fertilized former harzburgite ascend much more slowly from the 500-670 km source region, and do not experience partial melting. Where they ascend beneath continents, the smaller diapirs become incorporated into the sub-continental lithosphere which grows by accretion from this source. Ascending small diapirs beneath oceans become trapped in the sub-oceanic lithosphere. When subjected to later episodes of partial melting these geochemically enriched local source regions contribute to the chemical and isotopic diversity of oceanic basaltic magmas.

The above model implies that a significant relationship exists between the petrogenesis of intraplate basaltic magmas (mainly alkalic) and that of calcalkaline magmas erupted above subduction zones. In both cases, the incompatible element characteristics and isotopic systematics of the respective source regions are believed to have been inherited from a liquid extracted at depth from subducted former oceanic crust and transferred to depleted former peridotite. The essential differences are that in the case of calcalkaline magmas, the process occurred at shallow depths (80-150 km) shortly after subduction, whereas, in the case of intraplate basalts, the process occurred at depths of 650-1000 km, and the enriched sources were stored in the mantle for 0.5 - 2.0 b.y. prior to eruption of magmas at the surface.

V. P. AFANASJEV graduated from the Geological Department from Lvov States University in 1969. He gained degree of candidate of geological-mineralogical sciences in 1982 for his work devoted to the silicate and oxide minerals of kimberlites. He is working in Mirny City.

M. J. ALDRICH received his Ph.D. in structural geology from the University of New Mexico in 1972. After teaching at Allegheny College and North Carolina State University he moved to Los Alamos National Laboratory. He is currently an Associate Group Leader and is working on the Tertiary tectonics and magmatism of the southwestern U.S.

P. O. ALEXANDER Fullbright Fellow in Earth Sciences, 1985. Gained his M. Tech (1966) in Applied Geology from India, M.Sc. (1976) in Geochemistry from Leeds University, and was awarded Ph.D. in India for his geochemical/geochronological studies on Deccan Traps. Currently, Reader in Geochemistry at Saugar University. Involved in Applied Geochemical research including kimberlite exploration studies.

Hugh L. ALLSOPP Prior to his untimely death in March 1986, Prof. Allsopp was Head of the Isotope Division in the Bernard Price Institute of Geophysical Research at the University of the Witwatersrand. He graduated with B.Sc. and M.Sc. degrees from the University of Natal and a Ph.D. from the University of Bristol.

H. E. F. AMUNDSEN is a graduate student in geochemistry at the Mineralogical-Geological Museum, University of Oslo, Norway. He is working on the petrology and geochemistry of mantle-derived xenoliths and metasomatic processes.

V. G. ANDERSON is a senior diamond sorter with CSO Valuations (Pty) Ltd, Kimberley.

R. L. ANDREW graduated from the University of Glasgow in 1970 when he was appointed to the RTZ Group as exploration geologist working in Britain and in Burma. In 1973 he joined the Palabora Mining Co. Ltd. in South Africa and later worked as project geologist with the Hunting Group in Johannesburg. He was awarded a Ph.D. degree in 1979 for research into gossan evaluation at Imperial College, London and has undertaken consulting work in South Africa and in Saudi Arabia. He is currently a Chief Geologist with CRA Exploration Pty Limited in Western Australia.

M. ARIMA obtained his B.A. (1972), M.Sc. (1974) and D.Sc. (1977) from Hokkaido University in geology. He has worked for the Japanese Science Council as a post-doctoral fellow and research associate at the University of Western Ontario and is now assistant professor at the University of Yokohama. His interests are in igneous and metamorphic rocks.

Frank ARNOTT graduated B.Sc. (Hons) from Rhodes University in 1974 and M.Sc. from the University of Witwatersrand in 1981. He joined Stockdale Prospecting Ltd., Australia in 1980.

Warren J. ATKINSON graduated B.Sc. from Melbourne University in 1957 and gained his Ph.D. from Imperial College, London in 1967 for work in Applied Geochemistry. He has worked as an exploration geologist for the CRA Group mainly in Australia and the Pacific Islands since graduation and is currently Group Geologist with responsibility for mineral exploration in Western Australia, South Australia and the Northern Territory, including the Ashton Exploration Joint Venture for diamonds. He is a member of the GSA, AusIMM and an Executive Councillor of The Chamber of Mines of Western Australia (Inc).

D. K. BALDWIN received her honours B.Sc. degree in geology from the University of Western Ontario in 1985. She has done research on assessment of an igneous pluton as a nuclear waste disposal site. Since graduation she has been employed as a research associate in experimental petrology at the University of Western Ontario.

Dave R. BELL graduated (B.Sc. Hons) from the University of Cape Town in 1981. He is currently reading for a Ph.D. at the California Institute of Technology, Pasadena.

G. W. BERG graduated in Geochemistry from the University of Cape Town in 1962. After post graduate research at the Universities of Cape Town, Edinburgh and Chicago he entered metallurgical research as a mineralogist. Since 1979 he has lectured in petrology at the University of Port Elizabeth.

V. V. BESKROVANOV born in 1948, physicist, graduated from the Physics Department of the Yakutsk State University in 1971, Research associate, Laboratory of Crystallography,

Geological Institute, Yakutian Branch of the Siberian Department, USSR Academy of Sciences. Studies the internal structure and physical properties of natural diamonds.

R. S. BORCH received his B.S. degree in Geology from the University of California, Davis in 1983. He currently is a Ph.D. candidate at Davis investigating the effect of dissolved volatiles on the high-pressure rheology of olivine. He is a member of the American Geophysical Union.

G. BOXER graduated in Geology from the Royal Melbourne Institute of Technology in 1973. He has worked in South Africa and Eire. He has been employed with CRA Exploration since 1978 on diamond exploration in the West and East Kimberley and has been on site at the Argyle project since October 1979.

John W. BRISTOW completed B.Sc. Honours (1974) and M.Sc. (1976) degrees at the University of Natal and a Ph.D. (1980) at the University of Cape Town. He was a Post-doctoral Research Fellow at the University of New Mexico in 1981/82 and is presently a Senior Geologist in the Research Unit, Geology Department, De Beers Consolidated Mines Limited, Kimberley.

C. G. BRODIE completed a B.Sc. at the University of Otago in 1979 and was awarded an M.Sc. from the same university in 1985 for his study of nodule-bearing lamprophyres in the Haast Pass area. He is currently an exploration geologist for LandMark Resource Consultants Ltd.

Rod BROWN graduated in 1985 with a B.Sc. Hons. (Geology) at Rhodes University in Grahamstown.

G. P. BULANOVA born in 1946, mineralogist, graduated from the A. A. Zhdanov Leningrad State University in 1970. Senior research associate, Cand. Sc. (Geol. and Mineral.), Laboratory of Crystallography, Geological Institute, Yakutian Branch of the Siberian Department, USSR Academy of Sciences. Deals with inclusions in natural diamonds.

J. A. CARLSON gained his B.Sc. at West Virginia University in 1979, and was awarded an M.Sc. in 1983 from Colorado State University for his work on the exploration and delineation of State Line kimberlites. He has since worked for Superior Oil's diamond exploration programmes and is currently Geologist for Long Lac Mineral Exploration (Texas) Inc.

B. W. CHAPPELL gained his B.Sc. (Hons) in 1959 and M.Sc. in 1959 from the University of New England, and his Ph.D. in 1966 from the Australian National University. His research centres on granites and chemical fractionation within the Earth's crust. He is a Reader at the Department of Geology, Australian National University. He is a member of the Geochemical Society, the Geological Society, the Mineralogical Society, the Mineralogical Society of America, the Geological Society of America, the Geological Society of Australia, and the Mineralogical Association of Canada.

R. W. CHARLES received his Ph.D. from the Massachusetts Institute of Technology in 1972. He came to Los Alamos National Laboratory in 1974 after a Post-Doctoral position at the Geophysical Laboratory. He is currently an Associate Group Leader and works primarily on rock-water interactions and experimental petrology.

C. Roger CLEMENT graduated from Rhodes University, Grahamstown and has a Ph.D. for work on kimberlites from the University of Cape Town. He is currently Chief Geologist, De Beers Consolidated Mines Ltd.

E. (Libby) A. COLGAN graduated B.Sc. (Hons) 1977 at the University of Rhodesia. She is currently a Senior Geologist in the Kimberlite Petrological Unit, Geology Department, De Beers Consolidated Mines Limited, Kimberley.

Donley S. COLLINS B.A. in Psychology and Geography, BS in Geology. Currently a research geologist for the Branch of Geologic Risk Assessment, U.S. Geological Survey.

W. COMPSTON was awarded a Ph.D. in 1956 from the University of Western Australia with a thesis on stable isotope variations in marine carbonates. Currently he is Professional Fellow in the Research School of Earth Sciences, Australian National University, and leads a group researching in situ U-Pb dating of minerals and other isotope studies with the ion microprobe SHRIMP. He was elected Fellow of the Australian Academy of Science in 1971 and Honorary Fellow of the Geological Society of America in 1976.

A. F. COOPER graduated B.Sc. at Sheffield in 1966 and was awarded a Ph.D. from the University of Otago in 1970 for work on metamorphism and structure of the Haast Schists and the petrology of a post-metamorphic lamprophyre dyke swarm. At present he is

Senior Lecturer at Otago with research interests in metamorphic and igneous rocks of South Island, New Zealand.

Howard G. COOPERSMITH graduated in Geology at Colorado State University in 1975. Post-graduate work concentrated on kimberlite exploration. Employed by Cominco American Incorporated 1975 to 1986, he has managed various aspects of diamond prospecting, exploration and evaluation. Currently an independent consultant, he is a member of the Mineralogical Society of America and the Society of Economic Geologists.

Frances A. CULL graduated with a B.A. in Chemistry from Case Western Reserve University, Ohio in 1982 and obtained a MS degree from Purdue University in December 1985 for her work on the oxidation kinetics of diamond.

R. (Bobby) V. DANCHIN graduated B.Sc. in 1963 from the University of Witwatersrand and B.Sc. (Hons), M.Sc. and Ph.D. from the University of Cape Town from 1964 to 1970. He joined Anglo American Research Laboratories in 1971 and in 1980 moved to Stockdale Prospecting Ltd., Australia.

Leon R. M. DANIELS, B.Sc. Hons (UCT) 1980. Kimberlite exploration in southern and central Botswana in Kalahari desert and ground geophysics, soil sampling, geochemistry and drilling. Modelling of plus 200ha sedimentary kimberlite basin. Since July 1983, evaluation, development and mining of Dokolwayo kimberlite, Swaziland. Special research interest: macrocryst kimberlitic chromites, green garnets. Hobbies and Sport: sailing, reading, travelling.

J. B. DAWSON graduated from the University of Leeds in 1957 and was awarded his Ph.D. from the same University in 1960 for his work on Basutoland kimberlites. A period of service with the Tanganyika Geological Survey working on Rift Valley tectonics and volcanoes (including the active carbonatite volcano, Oldonyo Lengai) was followed by a two-year period at Dalhousie University, Halifax, Nova Scotia. In 1964 he joined the University of St. Andrews, Scotland, where he was successively lecturer, Reader and Professor of Petrology; he was awarded his D.Sc. from St. Andrews in 1971 for his continuing work on the kimberlites and carbonatites in eastern and southern Africa. In 1978 he was appointed to the Sorby Chair at the University of Sheffield. He is currently a member of the British National Committee for Geology, and Foreign Secretary of the Geological Society of London.

A. S. DEAKIN B.Sc., Geology, U.C. Swansea, 1971. M.Sc., D.I.C., Petroleum Geology, Imperial College, 1974. He has worked for several major diamond exploration and mining companies in Zambia, Sierra Leone and Angola. He joined Argyle Diamond Mines Pty. Ltd., in 1981 and is presently Mine Geologist at the AKI lamproite open pit mine in Western Australia.

Peter DEINES studied Geology at the Rheinische Friedrich-Wilhelms-Universität, Bonn, Germany, received his M.S. (1964) and Ph.D. (1967) degrees, both from the Pennsylvania State University and is currently Professor of Geochemistry and Program Chairman of the Geochemistry and Mineralogy Program of the Department of Geosciences at the Pennsylvania State University. He is a member of the Geochemical Society, and the American Association for the Advancement of Science, a Fellow of the Mineralogical Society of America and serves presently as Treasurer of the Geochemical Society.

I. F. DOWNIE obtained a B.Sc. from the University of Toronto and was employed in base metal exploration in eastern Canada until 1979; since then has been involved in diamond exploration. He is a Member of the Association of Professional Engineers of Ontario and of the CIMM.

R. DREW is a Senior Technical Officer in the stable isotope laboratory of the Bureau of the Mineral Resources, Canberra. His background qualifications are in electronics and analytical chemistry.

G. J. DREW graduated from the University of Adelaide with B.Sc. (Hons) in 1970. He has worked extensively in South Africa, Canada and Western Australia as an exploration geophysicist in searches for base and precious metals. Since 1980 he has been Principal Geophysicist with CRA Exploration in the Western Region of Australia. He is a member of AusIMM, ASEG and SEG.

R. K. DUNCAN completed a B.Sc. at Melbourne University in 1971 and subsequently worked in mineral exploration with Utah Development Company in Australia and West Africa. He joined Union Oil in 1983 to continue exploration of the Mt Weld Carbonatite and is assisting CSBP and Farmers with phosphate development on the property. He is currently Secretary to the W A Branch of the Australian Institute of Geoscientists.

A. D. EDGAR graduated from McMaster University with a B.A. in geology and chemistry and M.Sc. in geology. He obtained a Ph.D. in experimental petrology from Manchester University in 1963. He is currently Professor of Geology at the University of Western Ontario. His interests are in lamproites, kimberlites and alkaline rocks.

A. C. EDWARDS graduated in geology from Melbourne University in 1968. After four years in industry he joined the staff of the Broken Hill college of the University of New South Wales and was awarded a Ph.D. in 1980. He joined BHP in 1979 and is currently a member of the Research and Project Development Group.

A. J. ERLANK received all his degrees from the University of Cape Town and is currently Professor and Head of the Geochemistry Department at UCT. A former Fellow of the Carnegie Institution of Washington, he has also spent extended periods as visiting scientist at Oxford and the Institut de Physique du Globe in Paris.

T. EVANS graduated in physics, University of Bristol and obtained his Ph.D. and D.Sc. from the same university in 1955 and 1976 respectively. Joined the Physics Department at University of Reading in 1958 and was made a personal professor in 1968. He is at present Head of the Physics Department at Reading.

Stephen W. FIELD, B.S., Pennsylvania State University 1980, M.S. University of Massachusetts 1985. Currently working on his Ph.D. at the University of Massachusetts.

D. C. FIELDING graduated from Cape Town University with a B.Sc. (Hons) in geology in 1973 and gained an M.Sc. (Mineral Exploration) at Imperial College, London in 1978. He has since worked for Falconbridge in Southern Africa and is currently engaged in diamond exploration in Australia with CRA.

Anthony A. FINNERTY obtained his Ph.D. at the University of California at Los Angeles in 1976. Following a post-doctoral fellowship at the Carnegie Institution of Washington Geophysical Laboratory, he worked on problems related to the petrology of planetary interiors at NASA's Jet Propulsion Laboratory. Joining the faculty of the Department of Geology at University of California at Davis in 1982, he now pursues petrologic investigations of the interior of his favourite planet through study of mantle xenoliths.

Stephen F. FOLEY gained his B.Sc. from Southampton University in 1979 and his M.Sc. from Memorial University of Newfoundland in 1982 for work on alkaline and ultramafic lamprophyres in Labrador. He is currently completing his Ph.D. at the University of Tasmania on experimental studies of lamproite genesis, and will continue in experimental petrology at the Max-Planck-Institut in Mainz from September 1986.

C. FOUDOULIS gained his B. Applied Sc. (Geology) from the Canberra College of Advanced Education in 1982. He is a Senior Technical Officer in the X-ray diffraction laboratory at the Department of Geology, Australian National University.

K. J. FRASER gained her B.Sc. at the University of Edinburgh in 1983 and is currently in the final year of her Ph.D. on the geochemistry of kimberlites and lamproites from South Africa, North America and Australia.

K. FUTA received a B.S. and in 1974 an M.S. in inorganic chemistry from the University of Wyoming. He received an M.S. in geological sciences from the University of Colorado in 1985. He currently works as a chemist in the Isotope Branch of the U.S. Geological Survey in Denver, Colorado.

V. K. GARANIN graduated from the Geological Department at Moscow States University in 1970, gained the degree of candidate of geological-mineralogical sciences at the same university for his work on the mineralogy of ilmenite of kimberlites and carbonatites. He is chief of the diamond laboratory, Mineralogical Department of the Geological Faculty. He is a member of the Union Mineralogical Society.

Michael O. GARCIA received his Ph.D. degree in geology from University of California at Los Angeles in 1976. He is currently an Associate Professor with the Geology-Geophysics Department and the Hawaii Institute of Geophysics at the University of Hawaii. His primary research interests are: Origin and evolution of Hawaiian magma; and volatiles in magmas and their mantle sources.

Owen G. GARVIE graduated with a B.Sc. (Hons) degree from the University of Natal and an M.Sc. in geology from the University of Cape Town. He is presently a Divisional Mineralogist at the Anglo American Research Laboratories in Johannesburg.

H. W. GREEN received his Ph.D. in Experimental Rock Deformation from University of California at Los Angeles in 1968. He was a post-doctoral research associate in Metallurgy and Materials Science at Case Western Reserve University before moving to Davis in 1970. He presently is Professor of Geology and Department Chairman. He is a member of the American Geophysical Union and the Mineralogical Society of America.

G. P. GREGORY graduated in mining geology at Imperial College, London in 1965. He was awarded a Ph.D. from the same university for his work on secondary dispersion patterns related to kimberlites in North America. From 1970 to 1985 he was employed by the Selection Trust/BP Group to explore for diamonds, gold and base metals in North America, Europe, South Africa, Sierra Leone and Australia. He is currently a Director of Australian Ores & Minerals Limited.

William L. GRIFFIN received his B.Sc. (1962) and M.Sc. (1964) from Stanford University and his Ph.D. (1967) from the University of Minnesota. He is currently Professor of Geochemistry at the Mineralogical-Geological Museum of the University of Oslo, Norway, with responsibility for the National Lab for Geologic Mass-spectrometry. From October 1986 he will be Principal Research Scientist with the Division of Mineral Physics and Mineralogy, CSIRO, North Ryde, NSW 2113, Australia.

M. J. GUNN graduated in Geology and Chemistry at Nottingham in 1965. He has since worked for the The Broken Hill Proprietary Co. Ltd. and is currently Principal Geologist Operations, Western Australia. He is a member of the Geological Society of Australia, the Society of Economic Geologists and past-Chairman of the Australasian Institute of Mining & Metallurgy (NW Queensland Branch).

J. J. GURNEY graduated with an Honours degree in Chemistry at the University of Cape Town in 1962 and was awarded a Ph.D. in Geochemistry from the same University in 1968. He is currently an Associate Professor in Cape Town where he has an active kimberlite research group.

E. HAEBIG graduated in Geology at the University of Stuttgart, Germany in 1966. Since 1968 he has worked for CRA Exploration Pty. Ltd., and is currently geologist in charge of diamond exploration for the Ashton Joint Venture in the far north of Western Australia.

Stephen E. HAGGERTY, Professor of Geology, University of Massachusetts, Ph.D., Royal School of Mines, London.

Anne HALL graduated with a B.Sc. from the University of Otago (NZ) in 1968. She has been involved in diamond exploration in Western Australia since 1974 initially with Tanganyika Holdings and since 1976 with CRA Exploration where she is currently Principal Mineralogist. She is a member of the Geological Society of Australia and the Australasian Institute of Mining and Metallurgy.

D. C. HALL received his B.Sc. from the University of Toronto in 1982, and his M.Sc. from the Queen's University in 1985. He is currently enrolled in the doctoral programme at Queen's, studying the diatreme breccias in southeastern British Columbia, Canada. He is part Vice-president (Coffee) of the Queen's Geology Journal Club.

A. HALLIDAY gained his B.Sc. (1973) and Ph.D. (1979) from the University of Newcastle UK. He was a research assistant at the Scottish Universities Research and Reactor Centre East Kilbride Scotland until 1981. Since then he has been a lecturer at SURRC. From September 1986 he will take up an appointment at Ann Arbor Michigan USA.

J. W. HARRIS graduated in geology, University of Liverpool and obtained his Ph.D., University of London in 1968. After five years post-doctoral research in London, joined DeBeers Industrial Diamond Division in Johannesburg before becoming, in 1975, Research Fellow at the Geology Department, University of Edinburgh. Since 1980 he has been Senior Research Fellow in the Department of Applied Geology, University of Strathclyde.

B. HARTE gained his B.A., M.A., Ph.D. at Cambridge, England in 1962 and 1966 respectively. He was appointed Assistant Lecturer at Edinburgh University in 1965 and is currently Reader in Geology at Edinburgh. He was a Guest Investigator at the Geophysical Laboratory, Washington, in 1974-75; Invited Lecturer at Cape Town University in 1979; visiting Associate Professor at Yale University, New Haven, in 1982; Chairman of Metamorphic Studies of the Mineralogical Society and the Geological Society of London in 1983-85; and appointed a fellow of the Royal Society of Edinburgh in 1986.

C. J. HAWKESWORTH graduated from Trinity College Dublin in 1970 and was awarded his D.Phil from Oxford University for structural and geochemical studies in the Austrian Alps. After post doctoral positions at Oxford and Leeds he is now a Senior Lecturer in Isotope Geology at the Open University and chairman of the Petrogenesis Research Group. He is also an editor of Earth and Planetary Science Letters and Terra Cognita.

J. B. HAWTHORNE graduated in geology at Rhodes University, Grahamstown in 1956. He has since worked almost exclusively on diamond and kimberlite exploration in central and southern Africa. He is currently a consulting geologist to DeBeers and Chichester Diamond Services, London. He is a member of the Geological Society of South Africa and a fellow of the Geological Society of London.

B. Carter HEARN Jr received the Ph.D. degree in Geology from Johns Hopkins University, Baltimore in 1959. He has worked for the US Geological Survey since 1957, and is currently working on Montana, Michigan, and other US kimberlites and their xenoliths, and on upper mantle xenoliths from eastern China.

H. HELMSTAEDT received his Ph.D. in 1968 from the University of New Brunswick. After a year as a post-doctoral fellow at the Lamont-Doherty Geological Observatory, he spent three years each at the Geological Survey of Canada and McGill University before joining Queen's University where he is a Professor of Geology. In addition to ultramafic xenoliths and kimberlites, his major research interests lie in the tectonic evolution of Archaean greenstone belts in the Slave Province of the Canadian Shield.

W. O. HIBBERSON graduated in geology at the Canberra College of Advanced Education in 1975 and is currently Senior Technical Officer in the Research School of Earth Sciences at A N U. He has worked extensively with D H Green and A E Ringwood on a wide range of problems in experimental petrology and is co-author of 20 papers in this field.

B. E. HOBBS received his Ph.D. in Geology from the University of Sydney in 1962. He remained on the faculty there until 1967, when he became a Fellow of the Australian National University. In 1971 he became the Chairman and Professor of Geology at Monash University, where he remained until 1984 when he became the Chief Research Scientist for the Geomechanics Division of CSIRO.

J. J. HOPS gained her B.Sc. (Hons) at the University of Cape Town in 1983. She is currently completing her M.Sc. at the same university, working on megacrysts and deformed peridotite nodules from the Jagersfontein kimberlite pipe.

S. HU graduated from Beijing College of Geology in 1961, receiving a post-graduate qualification from the same institution in 1965. He has studied the Tanlu Fault Zone since 1962, and in 1966 became involved in diamond prospecting. Since 1981 he has been Chief Geologist of the No. 7 Geological Brigade in Meng Yin, and, more recently, of the Sino-British Cooperation Brigade.

R. H. HUNTER took B.Sc. and Ph.D. degrees at Durham, England in 1977 and 1980. From 1980 to 1982 he was a Postdoctoral Research Associate at the University of Tennessee, and then a Postdoctoral Research Fellow at the University of Edinburgh from 1982 to 1984. He is currently a Postdoctoral Research Associate at the University of Cambridge.

T. IRIFUNE graduated in Geophysics at Kyoto University in 1978, and was awarded a Ph.D. in 1984 from Hokkaido University for his work on the high-pressure experimental study of Cr-garnet and structure of garnet melt. He is now working as a post-doctoral fellow at the Research School of Earth Sciences, the Australian National University.

Tony IRVING was born in Sydney, received his Ph.D. at Australian National University in 1972, and subsequently has lived in the US. His major research interests over the last 18 years have been the geochemical evolution of mantle xenoliths and alkalic magmas.

E. ITO graduated in the faculty of technology at Shizuoka University in 1965. He was awarded a Ph.D. in 1979 from the University of Tokyo (Geophysics) for his researches on ultrahigh pressure studies on geophysically important silicates. He was a graduate student of the late Prof. Kawai at Osaka University and established a laboratory for ultrahigh pressure experiments at the Institute for Study of the Earth's Interior in Misasa in the last 15 years. He is currently associate professor in geophysics section of the ISEI and is working on mineralogy and chemistry of deep Earth's interior.

M. ITO graduated in petrology from the Faculty of Science, Nagoya University, of Japan in 1959. He is Associated Professor in Geology and Mineralogy at the Laboratory of Geology, College of General Education, Nagoya University, and is making petrological studies of western Kenya kimberlites and the Fe-Mg carbonate hydroxide hydrate minerals in serpentinites from Japan.

D. G. JACKSON graduated from the Western Australian Institute of Technology with an Associateship in Applied Geology in 1973. He worked with Hamersley Iron in the Pilbara region of Western Australia from 1974 to 1979, and then transferred to CRA Exploration participating in diamond exploration in Western Australia until 1985. He is currently Principal Geologist involved in a multi-commodity project in the Pilbara.

Bruce C. JAGO obtained an H.B.Sc. (1980) and M.Sc. (1982) from Lakehead University. Since then he has worked, in industry, exploring for base and precious metals in Canada, for diamonds in Venezuela and as a Lecturer in Geology at Lakehead University. Currently he is working toward a Ph.D. at University of Toronto and is studying experimentally, alkali-rich carbonate systems.

Emil JAGOUTZ graduated in Physics at the University of Mainz in 1976 and was awarded a Ph.D. in 1981 from the same university for his work on ultramafic rocks. He is currently Research Assistant at the Max-Planck-Institut für Chemie, Mainz, Department of Cosmochemistry with responsibilities for isotopic analysis.

A. J. A. JANSE graduated from the University of Leiden in 1955 and obtained a Ph.D. from the University of Leeds in 1964. For many years he was involved in diamond exploration with the Selection Trust Group and is now Managing Director of Mintel Pty. Ltd. Dr. Janse is a Fellow of the Geological Society of London and a member of the IMM, CIMM and GAC.

A. L. JQUES gained his B.Sc. (Hons) at the University of Western Australia in 1972 and was awarded a Ph.D. in 1980 from the University of Tasmania. He is currently a Senior Research Scientist in the Division of Petrology and Geochemistry, Bureau of Mineral Resources, Canberra. He is currently researching Australian lamproites, kimberlites and diamonds. He is a member of the Geological Society of Australia.

B. David JOHNSON graduated from Durham University with a B.Sc. in geology followed by an M.Sc. in geophysics. He then moved to Hobart where he completed a Ph.D. studying the crustal structure of Tasmania. Since that time he has been lecturing at the University of New South Wales and at Macquarie University, where he is currently Senior Lecturer. His research interests include potential field modelling techniques, plate tectonic synthesis and computer graphic techniques. He is an active member of ASEG, SEG, EAEG, AGU, IAMG, ACGA and helped to organise the ICOGEO conferences and establish the ASEG.

Joe J. JOYCE graduated with a B.Sc. (Hons) from Sheffield in 1970 and joined Stockdale Prospecting Ltd., Australia. He is currently on secondment to the Geology Department, Anglo American Corporation Limited, Johannesburg.

I. D. KERR completed his B.Sc. (Hons) at Queensland University in 1976. From 1977 to 1983 he worked as a Project Geologist in diamond exploration throughout Western Australia for CRA Exploration Pty. Limited. Transferred to CRAE Broken Hill in 1984, he is now a self-employed contract geologist in the Broken Hill district. Member GSA since 1975.

Marguerite KINGSTON was educated at Dunbarton College, the University of San Francisco and George Washington University, receiving advanced degrees in chemistry and geology. Since 1980, she has been with the Remote Sensing section of the U.S. Geological Survey. She is currently secretary of the Geological Society of Washington.

Peter D. KINNY was born in Melbourne, Australia. He graduated from the University of Sydney in 1978 with first class honours in Geology and Geophysics. He is currently completing a Ph.D. in Isotope Geochemistry at the Research School of Earth Sciences, A.N.U., Canberra. He needs a job.

M. B. KIRKLEY obtained her B.Sc. (1978) and M.Sc. (1980) from Colorado State University where she studied the peridotite xenoliths from Colorado and Wyoming kimberlites. The following three years were spent in base and precious metals exploration. She is presently concluding her research on stable isotopes in kimberlite carbonates in expectation of being granted a Ph.D. from the University of Cape Town.

S. I. KOSTROVITSKY graduated in Geology at Polytechnical Institute, Irkutsk in 1962 and in Mathematics at State University, Irkutsk in 1972. He was awarded a Ph.P. in 1973 for his work in mechanism of kimberlite pipe formation. He is a Senior Geologist at the Institute of the Earth's Crust, USSR Academy of Science. He is working on a kimberlite substance.

Jan D. KRAMERS. As an undergraduate he attended the University of Berne, Switzerland. He completed a Ph.D. in Economic Geology at the same university in 1973. He

subsequently completed post doctorate at Leeds and the University of Witwatersrand. Since 1981 he has been a Lecturer at the University of Zimbabwe in Harare.

G. P. KUDRYAVTSEVA graduated from the Geological Department at Moscow States University in 1970 where she gained of candidate and degree of Doctor of geological-mineralogical sciences for her work on the nature of magnetism in minerals in 1985. She is currently Reader in Mineralogy at the same University and is a member of the Union Mineralogical Society.

Mark D. KURZ received a BS in chemistry from the University of Wisconsin (1976) and Ph.D. from the Massachusetts Institute of Technology/Woods Hole Oceanographic Institution Joint Program (1982). He is currently an Assistant Scientist at Woods Hole Oceanographic Institution.

A. W. LAUGHLIN received his Ph.D. in economic geology/geochemistry from the university of Arizona in 1969. After teaching four years at Kent State University, Ohio, he moved to Los Alamos National Laboratory in New Mexico. He is currently an Associate Group Leader and is working on Tertiary tectonics and magmatism of the southwestern U.S.

D. C. LEE graduated with B.Sc. (Physics) from the University of Western Australia in 1967. He began his association with the mining industry whilst working with the Chamber of Mines in South Africa. He joined Kalumburu Joint Venture (the forerunner of the Ashton Joint Venture) with Tanganyika Holdings in 1975. He is currently working with Ashton Mining Limited, based in their exploration laboratory in Perth, WA.

J. H. LEW gained his B.Sc. (Hons) in Geology at Monash University in 1980. He then joined CRA Exploration, working on the evaluation of the Argyle AKI lamproite and its associated alluvials. Subsequently he was involved in diamond exploration in Western Australia, and is presently responsible for CRA Exploration's gold programme in Reefton, New Zealand.

P. E. LONEY graduated from the University of Birmingham with a B.Sc. in 1961 and from the University of Leeds with a Ph.D. in 1970. Since 1961 he has worked in several countries in Africa and is now Exploration Manager for De Beers Prospecting Botswana (Pty) Ltd.

V. LORENZ studied in Mainz, Zurich and Cambridge and received his Dr. Rer. Nat. at Mainz University in 1968. His main interests are physical volcanology, especially explosive volcanism of maars and diatremes and geodynamics. He is currently professor in geology at Mainz University, F. R. Germany.

Hans LUCAS obtained a B.Sc. from the University of Adelaide in 1975 with majors in Geochemistry and Physical and Inorganic Chemistry. He obtained a Diploma of Education in 1977 while teaching Earth Science in South Australia. In 1980 he joined CRA Exploration in Western Australia and is currently involved in the diamond exploration programme.

Robert A. MAHIN received his B.S. from Purdue University in 1983 and a B.A. in 1984. He is currently enrolled for graduate study towards an M.S. degree at the University of Utah, Salt Lake City.

S. W. MARSH was granted his B.Sc. from Saint Mary's University, Nova Scotia, Canada in 1974. He has since worked as a geologist on diamond exploration programmes for Anglo-American Corporation of South Africa Limited, Falconbridge Canada Limited and The Superior Oil Company. He is currently a geologist with Long Lac Mineral Exploration (Texas) Inc.

T. R. MARSHALL graduated in both geology and geomorphology from the University of the Witwatersrand in 1984. She is currently employed by the Economic Geology Research Unit (University of the Witwatersrand) and is completing a Masters degree on morphotectonic analysis and landscape development in Southern Africa.

Manfred R. MARX is a graduate of the University of Cape Town. He joined De Beers Botswana in 1966. After 5 years' secondment to Anglo he joined Stockdale Prospecting Limited, Australia in 1976 where he is currently employed.

D. P. MATTEY graduated from Cambridge in 1974 and was awarded a Ph.D. in 1980 by the University of London. He is currently a Research Fellow in the Department of Earth Sciences at the Open University studying stable isotope compositions of diamonds and mantle fluids.

Mike MAYHEW graduated from Ohio State University in mathematics and then received a Ph.D. in marine geophysics from Columbia University. He became a Senior Resident Research Associate at the NASA Goddard Space Flight Center where he pioneered the inversion work on satellite data and played a role in the MAGSAT planning stages. He has since continued his association with NASA and MAGSAT both as a consultant and more recently as a Program Director (Experimental and Theoretical Geophysics) at the National Science Foundation in Washington. He is an active member of AGU, AAAS, the Potomac Geophysical Society, and the Geological Society of Washington.

Peter MAZZONE, B.S., Illinois State University, 1981, M.S., Miami University, 1983. Currently working on his Ph.D. at the University of Massachusetts.

I. S. McCALLUM received his Ph.D. from the University of Chicago in 1968. He is presently a Professor in the Department of Geological Sciences at the University of Washington, Seattle. In addition to research on the potassic rocks of the Highwood Mountains, he has worked extensively on the Stillwater Complex. He is a member of American Geophysical Union and editor of the Journal of Petrology.

M. E. McCALLUM, A. B. Middlebury College 1956, MS, University of Tennessee 1958, Ph.D., University of Wyoming, 1964. Currently Professor of Mineralogy and Geochemistry at Colorado State University, Fort Collins. Part-time research geologist with U.S. Geological Survey since 1956. Research studies include geochemistry and petrology of Colorado-Wyoming kimberlites (and diamonds), precious and base metal evaluations of Precambrian terranes on Colorado and Wyoming, and diamond placers in northern South America.

T. E. McCANDLESS obtained his B.Sc. in 1978 and M.Sc. in 1982 from the University of Utah, Salt Lake City. From 1981-1985 he was involved in diamond exploration in North America with Superior Oil. He is currently a research scientist in geochemistry at the University of Cape Town, South Africa.

D. M. McCONCHIE gained his M.Sc. in geology at the University of Canterbury, New Zealand in 1978 and was awarded a Ph.D. in 1986 by the University of Western Australia for his work on Proterozoic banded iron formations in the Pilbara of W. A. He is currently employed as a research officer at the University of W. A. to work on heavy metals in marginal marine environments.

M. T. McCULLOCH gained his B.Sc. and M.Sc. at the Western Australian Institute of Technology in 1973 and 1975 respectively. He was awarded a Ph.D. in 1980 from the California Institute of Technology for his work on the application of Sm-Nd isotopic systematics to crustal growth. He is currently a Fellow in the Geochronology and Isotope Geochemistry Group of the Research School of Earth Sciences at the Australian National University and is working on the isotope geochemistry of mantle xenoliths.

W. F. McDONOUGH received a B.A. in Anthropology from the University of Massachusetts and a M.S. in Geochemistry from Sul Ross State University. After a fellowship at the Lunar and Planetary Institute, he began a Ph.D. program at the Research School of Earth Sciences, The Australian National University.

Elaine S. McGEE received a B.S. degree from the University of Michigan (1975) and an M.S. degree from SUNY Stony Brook (1977). She has worked at the U.S. Geological Survey, studying upper mantle xenoliths from kimberlitic diatremes, since 1978. She is a member of the Mineralogical Society of America and of the American Geophysical Union.

A. E. MEAKINS gained her B.Sc. at Sydney University. She worked for consultant micropalaeontologists, Paltech Pty. Ltd., then joined CRA Exploration Pty. Ltd. in 1980. She undertook the evaluation of the Limestone Creek alluvial diamond deposits. Since 1983 she has been involved in base and precious metal exploration in the Pilbara Region of Western Australia and is studying externally for an M.Sc. in Exploration Geology at James Cook University.

K. MENGEL graduated from the University of Gottingen (W-Germany) in Mineralogy in 1977 and was awarded a Ph.D. in 1981. He is currently working there on the petrology and geochemistry of the upper mantle and the lower crust.

M. MENZIES gained his B.Sc. (Aberdeen UK) in 1971 and his Ph.D. (Cambridge UK) in 1974. Seven years as a research fellow in the USA was followed by a period at the Open University UK. Since 1985 he has been a lecturer at the Department of Geology, Royal Holloway and Bedford New College, University of London, England.

Henry O. A. MEYER was awarded a B.Sc. in 1959, and a Ph.D. in 1962 from University College, London for his work on evaporite deposits in NW England. After spending five

years studying the physics and chemistry of diamond with Dame Kathleen Lonsdale he moved to the Geophysical Lab., Washington and subsequently was a Senior Research Fellow at NASA. He is currently Professor of Mineralogy at Purdue University, as well as Secretary, Mineralogical Society of America and on the Executive Committee, American Geological Institute.

E. A. K. MIDDLEMOST was awarded a Ph.D. in 1963. He has published papers on the petrology and geochemistry of rocks from Australia, the Canary Islands, India, Namibia, Norway and South Africa. Recently he has published a book entitled "Magmas and Magmatic Rocks". He is currently a senior lecturer in petrology at the University of Sydney.

R. H. MITCHELL graduated with the degrees of B.Sc. (1964) and M.Sc. (1966) in Geology from Manchester University, England, and was awarded a D.Sc. by that University in 1978. He gained his Ph.D. in 1969 at McMaster University, Hamilton, Ontario. Currently he is Professor and Chairman of Geology at Lakehead University, Thunder Bay, Ontario. Research interests include the geochemistry and petrology of alkaline rocks and the upper mantle, especially kimberlites, lamproites, lamprophyres and nepheline-bearing volcanic and plutonic rocks.

J. MOON joined CRA Ltd in 1964 and worked on the analysis of Queensland beach sands. He transferred to CRA Exploration in 1968 as a chemical analyst for base metals at Bougainville Island, Goroka and Honiara. He ran the floating laboratory aboard the ship "Craystar" during exploration in the Solomon Islands and the Indonesian Archipelago before coming to Perth in 1980 as Superintendent of the CRAE microdiamond laboratory.

Andrew MOORE obtained a Ph.D. at the University of Cape Town in 1979. This was followed by six years working on kimberlite exploration programmes in Botswana. Currently involved in the evaluation of a kuroko-type massive sulphide deposit in north-eastern Turkey.

R. O. MOORE gained his B.Sc. (Hons) degree in geochemistry at the University of Cape Town in 1981. He is currently working towards a Ph.D. degree at the same institution under the supervision of Prof. J. J. Gurney. His thesis involves an investigation of the kimberlites, diamonds and mantle xenolith suite at Monastery Mine.

Maureen T. MUGGERIDGE gained her B.Sc. in Geology and Computer Science at St Andrews University, Scotland in 1971. She has subsequently worked in diamond exploration, especially in the fields of regional exploration and mineralogy. She is currently a post-graduate student at the University of Western Australia engaged in research related to kimberlites.

C. E. NEHRU received his M.A. from Columbia University, New York, USA, M.Sc. and Ph.D. (1963) from the University of Madras, India, in mineralogy and petrology. He is currently Chairman and Professor of Geology at Brooklyn College, City University of New York. He is a Fellow of the Geological Societies of America and India, and member of the Mineralogical Society, Geochemical Society and Meteoritical Society. Most of his publications are on terrestrial and lunar rocks and meteorites.

David R. NELSON is a former student of the Universities of Tasmania and Melbourne and is currently undertaking a Ph.D. degree at the Research School of Earth Sciences, Australian National University.

J. E. NELSON holds an A.B. degree in Geology from George Washington University (1965), M.S. in Geochemistry from the University of Michigan (1968) and Ph.D. in Geology from Stanford University (1974). She has studied ophiolite bodies in the eastern and western US, and ultramafic xenoliths and Tertiary volcanic assemblages in the western US. She has been employed since 1977 by the US Geological Survey.

Peter H. NIXON D.Sc., Ph.D., FIMM, obtained his degrees at Leeds University, UK. He has since worked as a geologist/petrologist/mining geologist with the Uganda Geological Survey (9 years) and Lesotho Geological Survey and Mines Department (5 years). He was Professor of Geology, University of Papua New Guinea (5 years) and is currently Reader in Mantle Geology at Leeds University, and a Diamond Exploration consultant. Editor of Lesotho Kimberlites (1973) and Mantle Xenoliths (in press).

Hugh O'BRIEN received his B.S. from the University of Minnesota in 1982 and his M.S. from the University of Washington in 1985. He has spent the past three summers working in the Highwood Mountains in Montana and is currently working on his Ph.D. involving the petrogenesis of the north-central Montana alkalic province. He is a member of American Geophysical Union, Mineralogical Society and Geological Society of America.

T. C. ONSTOTT earned a B.Sc. in geophysics at California Institute of Technology in 1976, an M.A. and Ph.D. in geology at Princeton University in 1978 and 1980, respectively. Following a joint postdoctoral appointment at the University of Toronto and Princeton University, he joined the faculty at Princeton University in 1986. His fields of interest lie in Precambrian tectonic evolution and crystal chemical controls on argon diffusion.

Suzanne Y. O'REILLY graduated from Sydney University with B.Sc. Hons (1967) and Ph.D. (1972). She taught at Sydney University (1967-1970) and at Macquarie University (Sydney) from 1971 where she is currently Associate Professor. Research, (including visiting programmes at the British Museum of Natural History, the Smithsonian Institute and the Geological Museum of Oslo) is centred on mantle/crust evolution using geochemical, tectonic and geophysical data.

M. L. OTTER completed a B.A. in geology at Humboldt State University (Arcata, California) in 1979. After a brief period of interpreting offshore geophysical records with the US Geological Survey, Marine Branch, Woods Hole, Massachusetts, he found employment as a research assistant for Dr. H. J. B. Dick in Petrology and Geochemistry at the Woods Hole Oceanographic Institution. He is presently completing an M.Sc. on mineral inclusions in diamonds from the Sloan kimberlites, Colorado, under Professor J. J. Gurney at the University of Cape Town.

M. M. OOSTERVELD, M.Sc. in mining engineering, Technical University, Delft, Netherlands. He has 25 years experience in diamond exploration, in particular, the evaluation of diamond deposits. He is currently ore evaluation consultant to DeBeers Consolidated Mines Limited.

Z. PALACZ completed his B.Sc. at Birmingham UK in 1979 and his Ph.D. at Leeds UK in 1983. Since then he has been a research fellow at the Open University UK.

D. A. PATERSON graduated in applied geology at the South Australian Institute of Technology, Adelaide in 1973 and in 1984 completed the graduate Diploma in Business Administration at the same institution. Current employment as 'Investment Adviser Resources' with Adelaide stockbrokers Goldsmith & Co. Pty. Ltd. follows nine years practical experience in the Australasian mining and exploration industries. He is a member of the Geological Society of Australia, the Australasian Institute of Mining and Metallurgy and the Securities Institute of Australia.

D. PHILLIPS gained his B.Sc. at Rhodes University, South Africa in 1982, and was awarded an M.Sc. in 1985. He is currently enrolled as a graduate student at Princeton University and is working on argon isotopic systematics of mantle xenoliths from southern African kimberlites.

N. P. POKHILENKO gained his B.Sc. at Novosibirsk State University in 1970, and was awarded a D.Sc. in 1974. He is the Head of the Laboratory of the Institute of Geology and Geophysics, Siberian Division of the USSR Academy of Science.

T. V. POSUKHOVA graduated from the Geological Department at Moscow State University in 1974 where she gained the degree of candidate of geological-mineralogical sciences for her work on the mineralogy of gold-silver deposits in the Far East of the USSR. She is working at the same university and is a member of the Union Mineralogical Society.

Alicia A. PRESTI received her MS in petrology from the University of Hawaii in 1982. She is currently working for Mobil Oil Company in Texas as a geophysicist.

D. A. PRETORIUS is a graduate in mining geology from the University of the Witwatersrand, by which institution he has been awarded also a M.Sc. and a Ph.D. degree. He has been the Director of the Economic Geology Research Unit since 1959, where his research activities have concentrated on diamonds in Southern Africa and Witwatersrand gold mineralization. He is an Honorary Life Member of the Geological Society of South Africa and an Honorary Fellow of the Geological Society of America.

Rob RAMSAY graduated from the University of Adelaide with a B.Sc. (Hons) in 1979. He has worked for CRA Exploration in Western Australia as a mineralogist in diamond exploration since 1980 and is currently completing a part-time M.Sc. at the University of Western Australia.

R. A. RANKIN was brought up in Kenya and gained his B.Sc. at the University of Capetown in 1980 before working in mineral exploration in South Africa. He emigrated to Australia in 1983 where he worked as a hydrologist before joining Union Oil in 1984. He is a member of the Geological Society of South Africa, Geological Society of Australia and Australasian Institute of Geoscientists and currently resides in Townsville.

A. K. REDDY took Master of Science Degree in Geology at Osmania University, Hyderabad, India in 1964, and was awarded a Ph.D. in 1985 from the same university for his work on the petrological studies of kimberlite rocks of S. India. He is currently a Senior Geologist working with the Geological Survey of India, since 1970.

L. E. REED graduated from the University of Waterloo, Canada, in 1964 with a B.Sc. in Engineering Physics. Laurie has worked on diamond and metallic mineral exploration in a number of countries. He is currently Chief Geophysicist for Selco Div., BP Resources Canada. He is a member of the SEG, EAEG, AGU, GAC, CIMM and is a past president of KEGS, the Canadian Exploration Geophysical Society.

A. M. REID graduated from the University of St. Andrews and has a M.Sc. from the University of Western Ontario and a Ph.D. from the University of Pittsburgh. He is currently Phillipson-Stow Professor of Mineralogy and Geology at the University of Cape Town.

S. H. RICHARDSON received a B.Sc. at the University of Cape Town in 1977 and a Ph.D. at the Massachusetts Institute of Technology in 1984 with a dissertation on the isotope geochemistry of mantle-derived basalts, peridotites and diamonds. He is currently a postdoctoral research fellow in isotope geochemistry at the Institut de Physique du Globe in Paris.

R. S. RICKARD worked for Cambridge Instruments from 1959-1973 on the design developments sales and service of microprobes. Since 1973 he has been in charge of the electron microprobe laboratory in the Geochemistry Department at the University of Cape Town. He is an M.I.S.E. and A.I.E.E.

W. J. RINGENBERGS graduated with geology majors from the University of Adelaide in 1976 and was involved in the Ashton Project while employed as a mineralogist by Tanganyika Holdings and Conzinc Riotinto Australia. He gained a graduate Diploma of Environmental Studies from the University of Adelaide in 1981 and has since been employed as a petrologist at the BHP Melbourne Research Laboratories.

A. E. RINGWOOD gained his Ph.D. in 1956 from the University of Melbourne where he investigated the olivine-spinel transformation in the Earth's mantle. After a period at Harvard where he worked as a post-doctoral fellow with Francis Birch, he took an appointment in 1959 at the Australian National University where he has since remained. He is currently Professor of Geochemistry at the ANU and was Director of the Research School of Earth Sciences during the period 1978-83.

Jock V. A. ROBEY graduated B.Sc. (Hons), M.Sc. from the Rhodes University in 1976 and Ph.D. in the Department of Geochemistry, University of Cape Town in 1981. He is currently employed as a Senior Geologist in the Geology Department, De Beers Consolidated Mines Ltd., Kimberley.

Derek N. ROBINSON graduated B.Sc. (Hons) 1964 and M.Sc. 1970 at the University of Natal. He was awarded a Ph.D. at the University of Cape Town in 1980. He is currently a Senior Research Fellow at the Anglo American Research Laboratories, Johannesburg.

N. M. S. ROCK gained his M.A. and Ph.D. at Cambridge in 1978, for work on alkaline rocks from Portugal and East Africa. After nearly 10 years with the British Geological Survey, he recently joined the University of Western Australia, specialising in numerical geology and computing applications. He belongs to the Edinburgh Geological Society.

A. S. RODIONOV gained his B.Sc. at Novosibirsk State University in 1975, and was awarded a D.Sc. in 1981. He is a senior research worker of the Institute of Geology and Geophysics, Siberian Division of the USSR Academy of Science.

N. W. ROGERS graduated from London University in 1974, received an M.Sc. from Leeds University in 1975 and a Ph.D. from London University for his work on trace element analysis of kimberlites and associated rocks and xenoliths in 1979. He is currently responsible for the INAA research group at the Open University tackling a range of geochemical problems from the genesis of ultrapotassic rocks to chemical remobilisation during orogenesis.

R. L. RUDNICK received her B.S. degree from Portland State University, and an M.S. from Sul Ross State University, Alpine, Texas in 1982, after which she spent a year at the Lunar and Planetary Institute, Houston. She is currently in a Ph.D. program at the Research School of Earth Sciences, Australian National University, Canberra studying the lower continental crust.

S. SAUL received a B.S. in geology from the University of Illinois Circle Campus in Chicago in 1982. She worked for Digicon Geophysical Company Inc. as a data processor and is currently working towards a M.S. at the University of Colorado.

V. SAUTTER graduated in Petrography at University of Paris 6 in 1980 and was awarded a Doctoral thesis in 1983 from the Museum d'Histoire National d'Histoire Naturelle de Paris for her work on Eclogite-Amphibolite transition. After a post doctoral year at the Grant University of Edinburgh she is currently researcher in Mineralogy at the University of Paris Sud and is working on diffusion within clinopyroxene.

C. M. SCARFE gained his B.Sc. at the University of Durnham in 1964, and was awarded a Ph.D. at the University of Leeds in 1972 for his work on physico-chemical properties of magmatic silicate melts. He is currently professor in the geology department of the University of Alberta and is working on experimental petrology on igneous rocks. He has stayed a month each in 1984 and 1985 at the Institute for Study of the Earth's Interior, Misasa, Japan and collaborated with E. Takahashi in the melting study of mantle peridotite at very high pressure.

D. SCHIER graduated in Physics at Johannes-Gutenberg- Universitat, Mainz, in 1984. Graduate studies at Max-Planck-Institut fur Chemie, Mainz, are centred on the development and application of La-Ce isotopic systematics to terrestrial rocks, with the Ph.D. for this work expected in 1987.

D. J. SCHULZE received his Ph.D. from the University of Texas at Dallas in 1982, and went on to do post-doctoral work at the University of Chicago and the Geophysical Laboratory. He is currently an assistant professor at Queen's University, and holds memberships in the American Geophysical Union, Geological Association of Canada, and the Mineralogical Society of America. In his spare time he enjoys competitive beer brewing and chili cooking.

Jenny A. SCOTT heads the geological section of CSO Valuations (Pty) Ltd, Kimberley.

B. H. SCOTT SMITH graduated from the University of Edinburgh (B.Sc. (Hons) in 1972 and Ph.D. in 1977). From 1977 to 1981 she was a research mineralogist in the Kimberlite Research Unit of the Anglo American Research Laboratories. Since 1982 she has been a private consultant working in the field of petrology of kimberlites and related rocks.

Patricia B.S. SHEE (nee Cangley) graduated B.Sc. from Rhodes University in 1981. She was formerly employed as a Research Assistant in the Geology Department, De Beers Consolidated Mines Limited, Kimberley.

Simon R. SHEE graduated B.Sc. (Hons) 1974, M.Sc. 1978 and Ph.D. 1986 from the University of Cape Town. He is currently a Principal Research Mineralogist at the Anglo American Research Laboratories, Johannesburg.

John W. SHERVAIS received his Ph.D. from the University of California (Santa Barbara) in 1979 and has done post-doctoral research at the Institut fur Petrographie und Mineralogie (ETH-Zurich) and the University of Tennessee. He is currently Assistant Professor of Petrology and Geochemistry at the University of South Carolina.

I. G. L. SINCLAIR obtained a B.Sc. from the University of Edinburgh in 1956 and a Ph.D. from the University of St. Andrews in 1964. He worked with the Geological Survey of Jamaica until joining Selco in 1967. Dr. Sinclair is a Fellow of the Geological Societies of London and of Canada and a Registered Professional Engineer in Ontario.

M. A. SKEWES obtained her Titelo de Geologo from the University of Chile, Santiago, in 1980, and an M.S. from the University of Colorado in 1984. She is currently studying for a Ph.D. from the University of Colorado while working as a private consultant specializing in ore petrology and fluid inclusion studies.

E. Michael W. SKINNER graduated from Rhodes University B.Sc. 1966, Hons 1970. He is at present based in Kimberley as Head of the Kimberlite Petrology Unit, Geology Department, De Beers Consolidated Mines Limited.

Chris B. SMITH graduated with B.Sc. (Hons) from the University of Bristol in 1960. He worked as a diamond explorationist and gold mine geologist in central and southern Africa and, since 1970, in searches for mineral sand and diamond deposits in Australia. He is currently Chief Geologist (Diamond Research) with CRAE Exploration Pty. Ltd. in Western Australia, and is a member of the Min. Soc., GSA and the AusIMM.

Craig B. SMITH obtained his B.Sc. from the University of Illinios in 1974, his M.Sc. from Colorado State University in 1977, and his Ph.D. from the University of the

Witwatersrand in 1983. Following a one year postdoctoral fellowship at the University of Cape Town in 1984, he currently holds a postdoctoral fellowship at the Max Planck Institute für Chemie in Mainz.

H. S. SMITH graduated with a B.Sc. (1971) in geology from the University of the Witwatersrand, Johannesburg and gained his Ph.D. (1980) from the University of Cape Town for his work on the geochemistry of komatiites from the Barberton greenstone belt. He is currently a research officer in the Geochemistry Department at Cape Town working on the stable isotope geochemistry of rocks and minerals from South Africa.

D. SMITH received his Ph.D. from the California Institute of Technology in 1969 for his study of a diabase-granophyre complex in Arizona. While a post-doctoral fellow at the Geophysical Laboratory, he investigated pyroxenes and basalts. He is now a professor at the University of Texas; current interests include kinetics, volcanism, and the evolution of the mantle and crust.

H. S. SMITH graduated with a B.Sc. (1971) in geology from the University of the Witwatersrand, Johannesburg and gained his Ph.D. (1980) from the University of Cape Town for his work on the geochemistry of komatiites from the Barberton greenstone belt. He is currently a research officer in the Geochemistry Department at Cape Town working on the stable isotope geochemistry of rocks and minerals from South Africa.

N. V. SOBOLEV gained his B.Sc. at Lvov State University in 1958, and was awarded a D.Sc. in 1963, Prof. in 1971. He is an Associate Member of the USSR Academy of Science, Deputy Director of the Institute of Geology and Geophysics, Siberian Division of the USSR Academy of Science. He is the Counsellor of the IMA.

L. V. SOLOVJEVA graduated in geology at Leningrad State University in 1958. She has worked since at the Institute of the Earth's Crust, Irkutsk and was awarded a Ph.D. in 1973 for her work on minor intrusions in Eastern Zabaikalje. Currently she is a Senior Research worker dealing with deep seated xenoliths from kimberlites of the Siberian platform.

P. M. SPEAR graduated in physics, University of Manchester in 1981 and obtained his Ph.D., Kings College, University of London 1985. Currently he is a Research Scientist at Diamond Research Centre, Maidenhead, Berkshire.

Z. V. SPETSIUS born in 1945, geochemistry geologist, graduated from the M. V. Lomonosov Moscow State University in 1974. Senior research associate, Laboratory of Geological and Mineralogical Methods of Research, Yakutniiproalmaz Institute, Mirnyi. Deals with mantle-derived xenoliths in kimberlite pipes.

C. R. STERN received a B.S., M.S., and in 1973 a Ph.D. from the University of Chicago. He has been a Research Associate at Lamont-Doherty Geological Observatory, Assistant Professor at Cornell University, Visiting Professor at the University of Chile, and is currently Associate Professor at the University of Colorado.

Shen-Su SUN graduated from National Taiwan University in 1966 and gained his Ph.D. in 1973 from Columbia University majoring in Geochemistry. He has been mainly working on study of mantle derived magmas including Archaean komatiites and young oceanic basalts. Recently, he also studied granite genesis. He is currently a Principal Research Scientist at the Bureau of Mineral Resources, Canberra.

D. P. SVISERO graduated in geology at the University of Sao Paulo in 1964, and was awarded a Ph.D. in 1971 from the same university for his work on Brazilian diamonds. He became Professor of Mineralogy in 1978 and is currently working on diamonds, kimberlites and related subjects.

E. TAKAHASHI gained his B.Sc. at the University of Tokyo (Geophysics Institute) in 1974, and was awarded a Ph.D. in 1979 from the same University (Geology Institute) for his work on petrology of upper mantle derived xenoliths in Japan. He is currently assistant professor in the geophysics section of the Institute for Study of the Earth's Interior and is working on the petrology and origin of mantle peridotite. He is also interested in generation of basaltic magmas in the upper mantle.

Lawrence A. TAYLOR received his Ph.D. in Geology/Material Science from Lehigh University (Bethlehem, PA) in 1968 and has done post-doctoral research at the Geophysical Laboratory of the Carnegie Institute of Washington and the Max Planck Institut für Kernphysik (Heidelberg). He is currently Professor of Geochemistry and Petrology at the University of Tennessee.

S. R. TAYLOR, M.A., D.Sc. (Oxford), M.Sc. (N.Z.), Ph.D. (Indiana), Hon. F.G.S., F.A.A., is a Professorial Fellow at the Research School of Earth Sciences, Australian National University, Canberra. He has published 5 books and 170 research papers on lunar and terrestrial geochemistry.

Wayne R. TAYLOR gained his B.Sc. (Hons) at Auckland University, N.Z. in 1980. His Ph.D. on the role of C-O-H fluids in upper mantle processes was awarded by the University of Tasmania in 1985. At present he is post-doctoral fellow in experimental petrology at the University of Tasmania where he is currently working on melting studies in the system peridotite-C-O-H and aspects of aluminosilicate melt structure.

K. W. TERRY graduated with a B.Sc. (Hons) in 1961 from London University and a Ph.D. in 1965 from the University of Wales. He has since worked at the Western Australian Institute of Technology where he is currently a Senior Lecturer in Physics. His interests are in the micro structure of materials, including minerals, and scanning electron microscopy techniques. He is Chairman of the WA Ceramic Association and the EM Users Group of WA.

T. N. TINGLE received his B.Sc. degree in Geology from the University of North Carolina and his M.S. in Experimental Petrology from the University of California, Davis. He currently is a Ph.D. candidate at Davis investigating the solubility and diffusivity of carbon in olivine. He is a member of the American Geophysical Union, Mineral Society of America and the Geochemical Society.

P. VAN CALSTEREN gained his M.Sc. in geology at Leiden State University, The Netherlands, followed by a Ph.D. in 1977. Since 1980 he has been at the Department of Earth Sciences, Open University with responsibilities in the Solid Source Mass Spectrometry laboratory and involved in research, mainly the generation and evolution of the continental lithosphere.

Annelie VAN NIEKERK is a senior diamond sorter with CSO Valuations (Pty) Ltd, Kimberley.

A. VAN RIESSEN gained his BAppSc in 1972 and an MAppSc in 1979 from Western Australian Institute of Technology. He is currently a lecturer in Physics in the School of Physics and Geosciences at WAIT, with special interests in developing techniques for the scanning electron microscope.

B. M. VLADIMIROV graduated from the Irkutsk College of Mines and since he has worked at the Institute of the Earth's Crust of the Soviet Academy of Sciences in Irkutsk. For two years he was studying kimberlites in West Africa. His scientific interests are in kimberlites and kimberlite-like rocks of the Siberian platform. Since 1971 he has been the Chief of Laboratory of Geology and Magmatism of ancient platforms.

E. C. WALKER obtained his B.Sc. degree in geology from Brock University. He is currently a Ph.D. student at the University of Western Ontario working on high pressure-temperature relations of the Prairie Creek, Arkansas olivine lamproite.

Guodong WAN graduated in 1960 from Chengdu Geological College. She has since specialized in diamond geology, and participated in the discovery of the Meng Yin kimberlites. She was, for some time, head of the Comprehensive Research Group of the No. 7 Geological Brigade. Since 1983 she has concentrated on the technical management of prospecting for diamonds and other minerals in Shandong.

Peter J. WASILEWSKI received his Ph.D. from the University of Tokyo after studying under Professor Takesi Nagata. He has since been acquiring a large suite of crustal and upper mantle rocks and carried out a comprehensive study of their magnetic properties at his laboratory at Goddard. He is also interested in the magnetic properties of dinosaur bones, lodestone and meteorites.

F. G. WATERS gained her B.Sc. Hons. in geochemistry at the University of Cape Town in 1981. She is currently working towards a Ph.D. degree at U.C.T. investigating various geochemical aspects of metasomatised peridotite and MARID xenoliths from southern African kimberlites, under the supervision of Prof. A.J. Erlank.

D. R. WHITE was metallurgical assistant at the Kwinana Bauxite Refinery, Western Australia from 1963 to 1972 and subsequently laboratory supervisor for Jennings Mining to 1973. He joined the laboratory staff of Tanganyka Holdings in 1973 and became Manager of the Seltrust Mining/BP Minerals diamond laboratory in 1978 until its closure in 1985.

G. C. WILLETT gained his B.Sc. and M.Sc. at the University of Sydney in 1967 and 1978 respectively. In the intervening years he was an exploration geologist with Union

Miniere and Union Carbide. Subsequently he has worked for Union Oil as Senior Geologist in speciality metal exploration. He is currently a member of ANZAAS, Geological Society of Australia, AusIMM and a committee member of SMEDGE.

G. E. WILLIAMS gained his M.Sc. at the University of Melbourne in 1963 and Ph.D. in sedimentology at Reading, U. K. in 1966. Postdoctoral research at the University of Adelaide until 1970 was followed by four years in the petroleum industry. He joined BHP in 1975 and is currently Principal Research Geologist. He is a member of the Geological Societies of Australia and America and of the American Geophysical Union.

I. S. WILLIAMS graduated from the Australian National University with a B.Sc. in Geology in 1974. He subsequently gained a Ph.D. from the same university in 1978 for work on Rb-Sr and U-Pb isotopes in granites of southeastern Australia. He is presently doing research at the Research School of Earth Sciences, Australian National University, on U-Pb geochronology, particularly using zircons, by ion microprobe.

H. G. WILSHIRE has a Ph.D. from the University of California, Berkeley, 1956. He is currently a research geologist, US Geological Survey, where he studies environmental geological and upper mantle/ lower crustal problems.

P. J. WYLLIE gained his B.Sc. and Ph.D. in Geology from the University of St. Andrews in Scotland. He is currently Chairman, Division of Geological and Planetary Sciences, California Institute of Technology. He is past-President of the Mineralogical Society of America, and Vice President of the International Mineralogical Association.

Peiyuan ZHANG graduated from Chengdu College of Geology in 1960. Since then he has been involved in diamond prospecting. He is currently a Deputy Division Chief in a department of the Ministry of Geology and Mineral Resources, and is in charge of diamond prospecting in China.

Jianxiong ZHOU graduated from the Chinese Academy of Geological Sciences in Beijing as post-graduate in 1967. He has been working in CAGS and is currently Vice Chief of the Division of Mineral Physics. He is also a council member of the Scientific and Technique Committee of Ministry of Geology and Resources.

V. N. ZYRYANOV graduated from the Geology department of Alma-Ata University in 1958. In 1965 he took his Ph.D. and in 1979 defended his doctoral thesis (corresponds to professorship). At present he works at the Institute of Experimental Mineralogy, USSR Ac. Sci. as Senior Research Associate, Professor of Petrology. His recent attention has been devoted to experimental studies on the "Origin of lamproites".

AUTHOR INDEX

SECTION	NAME	PAGE	SECTION	NAME	PAGE
VI	Afanasjev, V. P.	457	VI	Deakin, A. S.	451
III	Aldrich, M. J.	187	V	Deines, P.	383
VI	Alexander, P. O.	440	VI	Downie, I. F.	469
II	Allsopp, H. L.	109	VI	Drew, G. J.	454
II	Allsopp, H. L.	112	V	Drew, R.	426
II	Allsopp, H. L.	115	I	Dubessy, J.	93
IV	Allsopp, H. L.	329	I	Duncan, R. K.	97
III	Amundsen, H. E. F.	160	III	Edgar, A. D.	170
V	Anderson, V. G.	421	VI	Edwards, A. C.	463
I	Andrew, R. L.	12	II	Eggler, D. H.	155
I	Arima, M.	15	IV	Erlank, A. J.	232
III	Arima, M.	170	IV	Erlank, A. J.	235
II	Arnott, F.	127	V	Evans, T.	386
II	Arnott, F.	142	III	Falloon, T. J.	181
V	Atkinson, W. J.	435	II	Fanning, C. M.	136
III	Baldwin, D. K.	170	IV	Field, S. W.	235
I	Barnett, R. L.	15	I	Fielding, D. C.	24
IV	Beery, J.	273	IV	Finnerty, A. A.	238
I	Bell, D. R.	90	IV	Finnerty, A. A.	349
III	Bell, D. R.	170	III	Foley, S. F.	173
I	Berg, G. W.	18	V	Foudoulis, C.	426
V	Bergman, S. C.	412	III	Fraser, K. J.	176
V	Beskrovanov, V. V.	368	IV	Futa, K.	343
IV	Blacic, J. D.	273	III	Garanin, V. K.	178
IV	Borch, R.	244	VI	Garanin, V. K.	457
I	Boxer, G.	48	IV	Garcia, M. O.	241
I	Boxer, G. L.	21	II	Garvie, O. G.	109
VI	Boxer, G. L.	448	III	Green, D. H.	181
VI	Boxer, G. L.	451	III	Green, D. H.	193
IV	Boyd, F. R.	335	III	Green, D. H.	211
III	Brey, G. P.	163	IV	Green, H. W.	244
III	Brey, G. P.	181	IV	Green, H. W.	349
IV	Brey, G. P.	228	VI	Gregory, P. G.	460
IV	Bristow, J. W.	267	II	Griffin, W. L.	127
I	Bristow, J. W.	90	IV	Griffin, W. L.	247
II	Bristow, J. W.	109	IV	Griffin, W. L.	303
II	Bristow, J. W.	112	VI	Gunn, M. J.	463
II	Bristow, J. W.	142	I	Gupta, A. K.	27
III	Brodie, C. G.	164	I	Gurney, J. J.	57
II	Brown, R.	109	IV	Gurney, J. J.	256
V	Bulanova, G. P.	371	IV	Gurney, J. J.	282
V	Bulanova, G. P.	374	IV	Gurney, J. J.	329
V	Cardoso, P.	389	IV	Gurney, J. J.	332
VI	Carlson, J. A.	443	IV	Gurney, J. J.	363
IV	Carswell, D. A.	338	V	Gurney, J. J.	380
I	Chappell, B. W.	51	V	Gurney, J. J.	383
I	Chappell, B. W.	54	V	Gurney, J. J.	389
III	Charles, R. W.	187	V	Gurney, J. J.	392
IV	Clayton, R. N.	326	V	Gurney, J. J.	401
III	Clement, C. R.	167	V	Gurney, J. J.	406
II	Colgan, E. A.	115	V	Gurney, J. J.	409
V	Collins, D. S.	403	V	Gurney, J. J.	415
IV	Compston, W.	267	VI	Haebig, A. E.	451
IV	Compston, W.	312	VI	Haebig, A. E.	466
II	Condliffe, E.	133	I	Haggerty, S. E.	48
III	Cooper, A. F.	164	I	Haggerty, S. E.	69
VI	Coopersmith, H. G.	446	IV	Haggerty, S. E.	232
V	Cull, F. A.	377	IV	Haggerty, S. E.	235
II	Danchin, R. V.	142	IV	Haggerty, S. E.	250
V	Daniels, L. R. M.	380	IV	Haggerty, S. E.	279
IV	Davies, G. R.	229	IV	Hall, A. E.	270
V	Davies, G. R.	412	V	Hall, A. E.	426
I	Dawson, J. B.	107	I	Hall, D. C.	30
VI	Deakin, A. S.	448	IV	Halliday, A.	294

SECTION	NAME	PAGE	SECTION	NAME	PAGE
IV	Harris, J. W.	332	VI	Kudryavtseva, G. P.	457
V	Harris, J. W.	383	V	Kurz, M. D.	401
V	Harris, J. W.	386	III	Laughlin, A. W.	187
V	Harris, J. W.	389	VI	Lee, D. C.	475
V	Harris, J. W.	395	VI	Lew, J. H.	451
V	Harris, J. W.	398	IV	Lloyd, F. E.	229
V	Harris, J. W.	409	I	Loney, P. E.	87
III	Harte, B.	184	I	Lorenz, V.	21
III	Harte, B.	224	III	Lorenz, V.	205
IV	Harte, B.	256	I	Lovering, J.	27
IV	Harte, B.	315	I	Lucas, H.	48
V	Hatton, C. J.	392	I	Lucas, H.	54
III	Hawkesworth, C. J.	176	I	Lucas, H.	60
IV	Hawkesworth, C. J.	232	IV	Lucas, H.	270
IV	Hawkesworth, C. J.	253	IV	Lugmair, G. W.	326
IV	Hawkesworth, C. J.	294	IV	Maggiore, C.	273
V	Hawthorne, J. B.	395	I	Mahin, R. A.	66
I	He, G.	36	VI	Marsh, S. W.	443
I	He, G.	39	VI	Marshall, T. R.	478
I	Hearn, B. C.	33	II	Marx, M. R.	142
IV	Hearn, B. C.	291	IV	Mathez, E. A.	273
I	Helmstaedt, H.	30	IV	Mattey, D.	276
II	Helmstaedt, H.	118	IV	Mayeda, T.	326
IV	Hibberson, W. O.	259	II	Mayhew, M. A.	127
IV	Hobbs, B. E.	244	IV	Mazzone, P.	279
IV	Hollander, M.	273	III	McCallum, I. S.	199
VI	Hollis, J. D.	484	I	McCallum, M. E.	63
IV	Hops, J. J.	256	IV	McCandless, T. E.	282
II	Hu, S.	121	V	McCandless, T. E.	403
IV	Hunter, R.	294	I	McConchie, D. M.	60
IV	Irifune, T.	259	III	McConchie, D. M.	190
III	Irving, A. J.	199	III	McCulloch, M. T.	196
IV	Irving, A. J.	262	IV	McCulloch, M. T.	285
III	Ito, E.	208	IV	McCulloch, M. T.	288
II	Ito, M.	124	IV	McCulloch, M. T.	346
VI	Jackson, D. G.	466	IV	McDonough, W. F.	288
I	Jago, B. C.	42	IV	McGee, E. S.	291
IV	Jagoutz, E.	265	VI	Meakins, A. E.	451
IV	Jagoutz, E.	318	III	Mengel, K.	193
IV	Jagoutz, E.	329	IV	Menzies, M.	294
IV	Jagoutz, E.	332	IV	Menzies, M. A.	276
VI	Janse, A. J. A.	469	I	Meyer, H. O. A.	66
I	Jaques, A. L.	12	I	Meyer, H. O. A.	69
I	Jaques, A. L.	24	I	Meyer, H. O. A.	75
I	Jaques, A. L.	27	II	Meyer, H. O. A.	145
I	Jaques, A. L.	45	V	Meyer, H. O. A.	377
I	Jaques, A. L.	48	I	Middlemost, E. A. K.	72
I	Jaques, A. L.	51	I	Mitchell, R. H.	9
I	Jaques, A. L.	54	I	Mitchell, R. H.	42
IV	Jaques, A. L.	300	I	Mitchell, R. H.	75
IV	Jaques, A. L.	346	VI	Mitchell, R. H.	446
V	Jaques, A. L.	426	IV	Moon, J.	300
II	Johnson, B. D.	127	I	Moore, A. E.	78
IV	Johnson, B. D.	303	V	Moore, R. O.	406
II	Joyce, J.	142	V	Moore, R. O.	409
I	Kerr, I. D.	54	I	Muggeridge, M. T.	60
I	Kerrich, R.	15	II	Muggeridge, M. T.	130
VI	Kingston, M. J.	472	VI	Muggeridge, M. T.	481
IV	Kinny, P. D.	267	I	Nehru, C. E.	81
I	Kirkley, M. D.	57	III	Nelson, D. R.	196
I	Knutson, J.	12	III	Nickel, K. G.	181
III	Kogarko, L.	163	IV	Nickel, K. G.	228
IV	Korotev, R. L.	326	IV	Nickel, K. G.	296
II	Kramers, J. D.	109	IV	Nielson, J. E.	297
IV	Kramers, J. D.	329	II	Nixon, P. H.	133
III	Krot, A. N.	178	V	Nixon, P. H.	412
III	Kudryavtseva, G. P.	178	IV	Noller, J. S.	355

SECTION	NAME	PAGE	SECTION	NAME	PAGE
III	O'Brien, H. E.	199	III	Skinner, E. M. W.	202
IV	O'Neill, H. St. C.	300	V	Slodkevich, V. V.	412
IV	Onstott, T. C.	306	I	Smith, Chris B.	21
V	Oosterveld, M. M.	395	I	Smith, Chris B.	93
II	O'Reilly, S. Y.	127	II	Smith, Chris B.	136
IV	O'Reilly, S. Y.	247	III	Smith, Chris B.	190
IV	O'Reilly, S. Y.	303	III	Smith, Chris B.	205
V	Otter, M. L.	409	IV	Smith, Chris B.	270
V	Otter, M. L.	415	IV	Smith, Chris B.	300
IV	Palacz, Z.	253	V	Smith, Chris B.	426
IV	Palacz, Z.	294	II	Smith, Craig B.	109
VI	Paterson, D. A.	463	II	Smith, Craig B.	112
IV	Phillips, D.	306	IV	Smith, Craig B.	329
II	Pidgeon, R. T.	136	IV	Smith, Craig B.	332
IV	Pillinger, C. T.	276	IV	Smith, D.	335
IV	Pokhilenko, N. P.	309	I	Smith, H. S.	57
IV	Pokhilenko, N. P.	338	I	Sobolev, A. V.	93
VI	Posukhova, T. V.	457	I	Sobolev, N. V.	93
IV	Presti, A. E.	241	IV	Sobolev, N. V.	270
II	Pretorius, D. A.	139	IV	Sobolev, N. V.	309
IV	Ramsay, R.	270	IV	Sobolev, N. V.	338
I	Rankin R. A.	97	V	Sobolev, N. V.	429
VI	Raynor, L. R.	484	IV	Solovjeva, L. V.	340
I	Reddy, A. K.	81	I	Solovyeva, L. V.	95
VI	Reed, . R..	469	V	Spear, P. M.	398
III	Reid, A. M.	167	V	Spetsius, Z. V.	374
I	Richards, M. N.	12	IV	Stern, C. R.	343
V	Richardson, S. H.	418	I	Sun, S-S.	51
V	Rickard, R. S.	389	I	Sun, S-S.	54
V	Rickard, R. S.	409	IV	Sun, S-S.	346
VI	Ringenbergs, W. H.	463	V	Sun, S-S.	426
III	Ringwood, A. E.	196	VI	Sutherland, F. L.	484
IV	Ringwood, A. E.	259	I	Svisero, D. P.	69
	Ringwood, A. E.	489	II	Svisero, D. P.	145
II	Robey, J. V. A.	142	III	Takahashi, E.	208
IV	Robinson, D. N.	332	IV	Taylor, L. A.	326
V	Robinson, D. N.	421	IV	Taylor, S. R.	312
I	Rock, N. M. S..	84	III	Taylor, W. R.	211
IV	Rodionov, A. S.	338	VI	Temby, P. A.	484
IV	Rogers, N. W.	253	VI	Terry, K. W.	475
IV	Rudnick, R. L.	312	IV	Tingle, T. N.	349
IV	Saul, S.	343	I	Townend, R.	12
IV	Sautter, V.	315	IV	Van Calsteren, P.	253
III	Scarfe, C. M.	208	V	Van Niekerk, A.	421
IV	Schier, D.	318	VI	Van Riessen, A.	475
IV	Schneider, A.	320	I	Vladimirov, B. M.	95
I	Schulze, D. J.	30	III	Walker, E. C.	170
II	Schulze, D. J.	118	II	Wan, G.	121
IV	Schulze, D. J.	323	II	Wan, G.	148
V	Schulze, D. J.	424	II	Wasilewski, P. J.	127
V	Scott, J. A.	421	IV	Waters, F.	352
I	Scott-Smith, B. H.	87	IV	Waters, F. G.	232
I	Shanguan, Z.	39	VI	White, D. R.	460
I	Shee, P. B. S.	90	I	Willett, G. C.	97
I	Shee, S. R.	90	VI	Williams, G. E.	463
II	Shee, S. R.	112	IV	Williams, I. S.	267
III	Shee, S. R.	170	IV	Williams, I. S.	312
IV	Shee, S. R.	332	IV	Wilshire, H. G.	355
V	Sheraton, J. W.	426	III	Wyllie, P. J.	214
V	Shermanina, E. I.	429	I	Yagi, K.	27
IV	Shervais, J. W.	326	V	Yefimova, E. S.	429
VI	Sinclair, I. G. L.	469	II	Zhang, P.	121
IV	Skewes, M. A.	343	I	Zhao, Y.	36
I	Skinner, E. M. W.	87	I	Zhao, Y.	39
II	Skinner, E. M. W.	112	I	Zhou, J.	100
III	Skinner, E. M. W.	170	III	Zyryanov, V. N.	217

